

Francisco Pereira · Penousal Machado  
Ernesto Costa · Amílcar Cardoso (Eds.)

LNAI 9273

# Progress in Artificial Intelligence

17th Portuguese Conference  
on Artificial Intelligence, EPIA 2015  
Coimbra, Portugal, September 8–11, 2015, Proceedings



Springer

**LNAI Series Editors**

Randy Goebel

*University of Alberta, Edmonton, Canada*

Yuzuru Tanaka

*Hokkaido University, Sapporo, Japan*

Wolfgang Wahlster

*DFKI and Saarland University, Saarbrücken, Germany*

**LNAI Founding Series Editor**

Joerg Siekmann

*DFKI and Saarland University, Saarbrücken, Germany*

More information about this series at <http://www.springer.com/series/1244>

Francisco Pereira · Penousal Machado  
Ernesto Costa · Amílcar Cardoso (Eds.)

# Progress in Artificial Intelligence

17th Portuguese Conference  
on Artificial Intelligence, EPIA 2015  
Coimbra, Portugal, September 8–11, 2015  
Proceedings



Springer

*Editors*

Francisco Pereira  
ISEC - Coimbra Institute of Engineering  
Polytechnic Institute of Coimbra  
Coimbra  
Portugal  
  
Penousal Machado  
CIUSC, Department of Informatics  
Engineering  
University of Coimbra  
Coimbra  
Portugal

Ernesto Costa  
CIUSC, Department of Informatics  
Engineering  
University of Coimbra  
Coimbra  
Portugal  
  
Amílcar Cardoso  
CIUSC, Department of Informatics  
Engineering  
University of Coimbra  
Coimbra  
Portugal

ISSN 0302-9743

ISSN 1611-3349 (electronic)

Lecture Notes in Artificial Intelligence

ISBN 978-3-319-23484-7

ISBN 978-3-319-23485-4 (eBook)

DOI 10.1007/978-3-319-23485-4

Library of Congress Control Number: 2015947099

LNCS Sublibrary: SL7 – Artificial Intelligence

Springer Cham Heidelberg New York Dordrecht London

© Springer International Publishing Switzerland 2015

This work is subject to copyright. All rights are reserved by the Publisher, whether the whole or part of the material is concerned, specifically the rights of translation, reprinting, reuse of illustrations, recitation, broadcasting, reproduction on microfilms or in any other physical way, and transmission or information storage and retrieval, electronic adaptation, computer software, or by similar or dissimilar methodology now known or hereafter developed.

The use of general descriptive names, registered names, trademarks, service marks, etc. in this publication does not imply, even in the absence of a specific statement, that such names are exempt from the relevant protective laws and regulations and therefore free for general use.

The publisher, the authors and the editors are safe to assume that the advice and information in this book are believed to be true and accurate at the date of publication. Neither the publisher nor the authors or the editors give a warranty, express or implied, with respect to the material contained herein or for any errors or omissions that may have been made.

Printed on acid-free paper

Springer International Publishing AG Switzerland is part of Springer Science+Business Media  
([www.springer.com](http://www.springer.com))

## Preface

The Portuguese Conference on Artificial Intelligence is returning to Coimbra, 18 years after its previous edition in this city. UNESCO recently recognized the University of Coimbra, as well as some areas of the city, as a world heritage site, acknowledging its relevance in the dissemination of knowledge throughout the fields of arts, sciences, law, architecture, urban planning, and landscape. It is therefore the ideal period to welcome back the conference to Coimbra.

EPIA events have a longstanding tradition in the Portuguese Artificial Intelligence (AI) community. Their purpose is to promote research in AI and the scientific exchange among researchers, practitioners, scientists, and engineers in related disciplines. The first edition took place in 1985 and since 1989 it has occurred biennially as an international conference. Continuing this successful tradition, the 17th Portuguese Conference on Artificial Intelligence (EPIA 2015) took place on the campus of the University of Coimbra, Coimbra, Portugal (<http://epia2015.dei.uc.pt>), September 8–11, 2015.

Following the organization of recent editions, EPIA 2015 was organized as a series of thematic tracks. Each track was coordinated by an Organizing Committee and includes a specific international Program Committee, composed of experts in the corresponding scientific area. Twelve thematic tracks were selected for EPIA 2015: - Ambient Intelligence and Affective Environments (AmIA) - Artificial Intelligence in Medicine (AIM) - Artificial Intelligence in Transportation Systems (AITS) - Artificial Life and Evolutionary Algorithms (ALEA) - Computational Methods in Bioinformatics and Systems Biology (CMBSB) - General Artificial Intelligence (GAI) - Intelligent Information Systems (IIS) - Intelligent Robotics (IROBOT) - Knowledge Discovery and Business Intelligence (KDBI) - Multi-Agent Systems: Theory and Applications (MASTA) - Social Simulation and Modelling (SSM) - Text Mining and Applications (TEMA).

For this edition, 131 submissions were received. All papers were reviewed in a double-blind process by at least three members of the corresponding track Program Committee. Some of the submissions were reviewed by up to 5 reviewers. Following the revision process, 45 contributions were accepted as full regular papers. This corresponds to a full paper acceptance rate of approximately 34 %. Additionally, 36 other contributions were accepted as short papers. Geographically, the authors of accepted contributions belong to research groups from 18 different countries – Algeria, Austria, Brazil, the Czech Republic, Egypt, France, India, Italy, the Netherlands, Norway, Poland, Portugal, Russia, Spain, Sweden, the UK, and the USA –, confirming the attractiveness and international character of the conference.

We express our gratitude for the hard work of the track chairs and the members of the different Program Committees, as they were crucial for ensuring the high scientific quality of the event. This conference was only possible thanks to the joint effort of many people from different institutions. The main contributions came from the

University of Coimbra, the Polytechnic Institute of Coimbra, and the Centre for Informatics and Systems of the University of Coimbra. We would also like to thank the members of the Organizing Committee: Anabela Simões, António Leitão, João Correia, Jorge Ávila, Nuno Lourenço, and Pedro Martins. Acknowledgment is due to SISCOG – Sistemas Cognitivos S.A., Feedzai S.A., Thinkware S.A., iClio, FBA., and FCT – Fundação para a Ciência e a Tecnologia for the financial support. A final word goes to Easychair, which greatly simplified the management of submissions, reviews, and proceedings preparation, and to Springer for the assistance in publishing the current volume.

July 2015

Francisco Pereira  
Penousal Machado  
Ernesto Costa  
Amlcar Cardoso

# **Organization**

The 17th Portuguese Conference on Artificial Intelligence (EPIA 2015) was co-organized by the University of Coimbra, the Polytechnic Institute of Coimbra, and the Centre for Informatics and Systems of the University of Coimbra.

## **Conference Co-chairs**

Francisco Pereira Penousal Machado	Polytechnic Institute of Coimbra, Portugal University of Coimbra, Portugal
---------------------------------------	---

## **Program Co-chairs**

Ernesto Costa Francisco Pereira	University of Coimbra, Portugal Polytechnic Institute of Coimbra, Portugal
------------------------------------	---

## **Organization Co-chairs**

Amílcar Cardoso Penousal Machado	University of Coimbra, Portugal University of Coimbra, Portugal
-------------------------------------	--

## **Proceedings Co-chairs**

João Correia Pedro Martins	University of Coimbra, Portugal University of Coimbra, Portugal
-------------------------------	--

## **Program Committee**

### **AmIA Track Chairs**

Paulo Novais Goreti Marreiros Ana Almeida Sara Rodriguez Gonzalez	University of Minho, Portugal Polytechnic of Porto, Portugal Polytechnic of Porto, Portugal University of Salamanca, Spain
--	---

### **AmIA Program Committee**

Antonio Fernández Caballero	University of Castilla-La Mancha, Spain
Amílcar Cardoso	University of Coimbra, Portugal
Andrew Ortony	Northwestern University, USA
Angelo Costa	University of Minho, Portugal
Antonio Camurri	University of Genoa, Italy
Boon Kiat Quek	National University of Singapore
Carlos Bento	University of Coimbra, Portugal

Carlos Ramos	Polytechnic of Porto, Portugal
César Analide	University of Minho, Portugal
Dante Tapia	University of Salamanca, Spain
Davide Carneiro	University of Minho, Portugal
Diego Gachet	European University of Madrid, Spain
Eva Hudlicka	Psychometrix Associates Blacksburg, USA
Florentino Fdez-Riverola	University of Vigo, Spain
Javier Jaen	Polytechnic University of Valencia, Spain
Javier Bajo	Polytechnic University of Madrid, Spain
José M. Molina	University Carlos III of Madrid, Spain
José Machado	University of Minho, Portugal
José Neves	University of Minho, Portugal
Juan M. Corchado	University of Salamanca, Spain
Laurence Devillers	LIMS-CNRS, France
Lino Figueiredo	Polytechnic of Porto, Portugal
Luís Macedo	University of Coimbra, Portugal
Ricardo Costa	Polytechnic of Porto, Portugal
Rui José	University of Minho, Portugal
Vicente Julian	Polytechnic University of Valencia, Spain

### AIM Track Chairs

Manuel Filipe Santos	University of Minho, Portugal
Filipe Portela	University of Minho, Portugal

### AIM Program Committee

Allan Tucker	Brunel University, UK
Álvaro Silva	Abel Salazar Biomedical Sciences Institute, Portugal
Andreas Holzinger	Medical University Graz, Austria
António Abelha	University of Minho, Portugal
Antonio Manuel de Jesus Pereira	Polytechnic Institute of Leiria, Portugal
Barna Iantovics	Petru Maior University of Tîrgu-Mureş, Romania
Beatriz de la Iglesia	University of East Anglia, UK
Cinzia Pizzi	Università degli Studi di Padova, Italy
Danielle Mowery	University of Utah, USA
Do Kyoon Kim	Pennsylvania State University, USA
Giorgio Leonardi	University of Piemonte Orientale, Italy
Gören Falkman	University of Skövde, Sweden
Hélder Coelho	University of Lisbon, Portugal
Helena Lindgren	Umeå University, Sweden
Inna Skarga-Bandurova	East Ukrainian National University, Ukraine
José Machado	University of Minho, Portugal
José Maia Neves	University of Minho, Portugal
Luca Anselma	University of Turin, Italy

Michael Ignaz Schumacher	University of Applied Sciences Western Switzerland
Miguel Angel Mayer	Pompeu Fabra University, Spain
Mohd Khanapi Abd Ghani	Technical University of Malaysia, Malaysia
Panagiotis Bamidis	Aristotelian Univ. of Thessaloniki, Greece
Pedro Gago	Polytechnic Institute of Leiria, Portugal
Pedro Pereira Rodrigues	University of Porto, Portugal
Rainer Schmidt	Institute for Biometrics and Medical Informatics, Germany
Ricardo Martinho	Polytechnic Institute of Leiria, Portugal
Rui Camacho	University of Porto, Portugal
Salva Tortajada	Polytechnic University of Valencia, Spain
Shabbir Syed-Abdul	Taipei Medical University, Taiwan
Shelly Sachdeva	Jaypee Institute of Information Technology, India
Szymon Wilk	Poznan University of Technology, Poland
Ulf Blanke	Swiss Federal Institute of Technology in Zurich, Switzerland
Werner Ceusters	University of New York at Buffalo, USA

### AITS Track Chairs

Rui Gomes	Universidade de Coimbra, Portugal
Rosaldo Rossetti	Universidade do Porto, Portugal

### AITS Program Committee

Achille Fonzone	Edinburgh Napier University, UK
Agachai Sumalee	Hong Kong Polytechnic University, Hong Kong
Alberto Fernandez	Universidad Rey Juan Carlos, Spain
Ana Almeida	Instituto Politécnico do Porto, Portugal
Ana L.C. Bazzan	Universidade Federal do Rio Grande do Sul, Brazil
Constantinos Antoniou	National Technical University of Athens, Greece
Cristina Olaverri-Monreal	AIT Austrian Institute of Technology GmbH, Austria
Eduardo Camponogara	Universidade Federal de Santa Catarina, Brazil
Giovanna Di Marzo Serugendo	University of Geneva, Switzerland
Gonçalo Correia	Delft University of Technology, Netherlands
Harry Timmermans	Eindhoven University of Technology, Netherlands
Hussein Dia	Swinburne University of Technology, Australia
José Telhada	Universidade do Minho, Portugal
Kai Nagel	Technische Universität Berlin, Germany
Luís Moreira Matias	NEC Europe Ltd, Germany
Luís Nunes	ISCTE Instituto Universitário de Lisboa, Portugal
Oded Cats	Delft University of Technology, Netherlands
Sascha Ossowski	Universidad Rey Juan Carlos, Spain
Shuming Tang	Chinese Academy of Sciences, China
Tânia Fontes	Universidade do Porto, Portugal

### ALEA Track Chairs

Mauro Castelli	NOVA IMS, Universidade Nova de Lisboa, Portugal
Leonardo Vanneschi	NOVA IMS, Universidade Nova de Lisboa, Portugal
Sara Silva	University of Lisbon, Portugal

### ALEA Program Committee

Alberto Moraglio	University of Exeter, UK
Alessandro Re	NOVA IMS, Universidade Nova de Lisboa, Portugal
Anabela Simes	Instituto Politecnico de Coimbra, Portugal
Antonio Della-Cioppa	Università degli Studi di Salerno, Italy
António Gaspar-Cunha	University of Minho, Portugal
Arnaud Liefooghe	Université de Lille, France
Carlos Cotta	Universidad de Málaga, Spain
Carlos Fernandes	Instituto Superior Técnico, Lisboa, Portugal
Carlos Gershenson	Universidad Nacional Autónoma de México, Mexico
Carlotta Orsenigo	Politecnico di Milano, Italy
Christian Blum	University of the Basque Country, Spain
Ernesto Costa	University of Coimbra, Portugal
Fernando Lobo	University of Algarve, Portugal
Helio Barbosa	Laboratório Nacional de Computação Científica, Brazil
Ivanoe De-Falco	National Research Council, Italy
Ivo Gonçalves	University of Coimbra, Portugal
James Foster	University of Idaho, USA
Jin-Kao Hao	University of Angers, France
Leonardo Trujillo	Instituto Tecnológico de Tijuana, Mexico
Luca Manzoni	University of Milano-Bicocca, Italy
Luis Correia	University of Lisbon, Portugal
Luís Paquete	University of Coimbra, Portugal
Marc Schoenauer	INRIA, France
Mario Giacobini	University of Turin, Italy
Pedro Mariano	University of Lisbon, Portugal
Penousal Machado	University of Coimbra, Portugal
Rui Mendes	University of Minho, Portugal
Stefano Beretta	University of Milano-Bicocca, Italy
Stefano Cagnoni	University of Parma, Italy
Telmo Menezes	Centre National de la Recherche Scientifique, France

### CMSB Track Chairs

Rui Camacho	Universidade do Porto, Portugal
Miguel Rocha	Universidade do Minho, Portugal
Sara Madeira	Instituto Superior Técnico, Portugal
José Luís Oliveira	Universidade de Aveiro, Portugal

## CMBSB Program Committee

Francisco Couto	University of Lisbon, Portugal
Susana Vinga	IDMEC-LAETA, IST-UL, Portugal
Marie-France Sagot	INRIA Grenoble Rhône-Alpes and Université de Lyon 1, France
Alexessander Couto Alves	Imperial College London, UK
Alexandre P. Francisco	Technical University of Lisbon, Portugal
Vítor Santos Costa	Universidade do Porto, Portugal
Mário J. Silva	Universidade de Lisboa, Portugal
Fernando Diaz	University of Valladolid, Spain
Sérgio Matos	Universidade de Aveiro, Portugal
Paulo Azevedo	Universidade do Minho, Portugal
Rui Mendes	Universidade do Minho, Portugal
Inês Dutra	Universidade do Porto, Portugal
Nuno A. Fonseca	European Bioinformatics Institute, UK
Florentino Fdez-Riverola	University of Vigo, Spain
André Carvalho	USP, Brazil
Alexandra Carvalho	IT/IST, Portugal
Arlindo Oliveira	IST/INESC-ID and Cadence Research Laboratories, Portugal
Ross King	University of Manchester, UK
Luís M. Rocha	Indiana University, USA

## GAI Track Chairs

Francisco Pereira	Polytechnic Institute of Coimbra, Portugal
Penousal Machado	University of Coimbra, Portugal

## GAI Program Committee

Adriana Giret	Universitat Politècnica de València, Spain
Alexandra Carvalho	Technical University of Lisbon, Portugal
Amal El Fallah	Pierre-and-Marie-Curie University, France
Amílcar Cardoso	University of Coimbra, Portugal
Andrea Omicini	University of Bologna, Italy
Arlindo Oliveira	INESC-ID, Portugal
Carlos Bento	University of Coimbra, Portugal
Carlos Ramos	Polytechnic Institute of Porto, Portugal
César Analide	University of Minho, Portugal
Eric de La Clergerie	INRIA, France
Ernesto Costa	University of Coimbra, Portugal
Eugénio Oliveira	University of Porto, Portugal
Frank Dignum	Utrecht University, Netherlands
Gal Dias	University of Caen, France
Hélder Coelho	University of Lisbon, Portugal
Irene Rodrigues	University of Évora, Portugal

João Balsa	University of Lisbon, Portugal
João Gama	University of Porto, Portugal
João Leite	New University of Lisbon, Portugal
John-Jules Meyer	Utrecht University, Netherlands
José Cascalho	University of Azores, Portugal
José Neves	University of Minho, Portugal
José Gabriel Pereira Lopes	New University of Lisbon, Portugal
José Júlio Alferes	New University of Lisbon, Portugal
Juan Corchado	University of Salamanca, Spain
Luís Antunes	University of Lisbon, Portugal
Luís Cavique	University Aberta, Portugal
Luís Seabra Lopes	University of Aveiro, Portugal
Luís Correia	University of Lisbon, Portugal
Luís Macedo	University of Coimbra, Portugal
Michael Rovatsos	University of Edinburgh, UK
Miguel Calejo	APPIA, Portugal
Paulo Cortez	University of Minho, Portugal
Paulo Gomes	University of Coimbra, Portugal
Paulo Moura Oliveira	University of Trás-os-Montes and Alto Douro, Portugal
Paulo Urbano	University of Lisbon, Portugal
Pavel Brazdil	University of Porto, Portugal
Pedro Barahona	New University of Lisbon, Portugal
Pedro Henriques	University of Minho, Portugal
Pedro Mariano	University of Lisbon, Portugal
Rui Camacho	University of Porto, Portugal
Salvador Abreu	University of Évora, Portugal

### IIS Track Chairs

Álvaro Rocha	University of Coimbra, Portugal
Luís Paulo Reis	University of Minho, Portugal
Adolfo Lozano	University of Extremadura, Spain

### IIS Program Committee

Fernando Bobillo	University of Zaragoza, Spain
Tossapon Boongoen	Royal Thai Air Force Academy, Thailand
Carlos Costa	IUL-ISCTE, Portugal
Hironori Washizaki	Waseda University, Japan
Vitalyi Talanin	Zaporozhye Institute of Economics & Information Technologies, Ukraine
Mu-Song Chen	Da-Yeh University, Taiwan
Garyfallos Arabatzis	Democritus University of Thrace, Greece
Khalid Benali	Université de Lorraine, France
Salama Mostafa	UNITEN, Malaysia
Fernando Ribeiro	Polytechnic Institute of Castelo Branco, Portugal
Pedro Henriques Abreu	University of Coimbra, Portugal

Radouane Yafia Ibn	Zohr University, Morocco
Maria José Sousa	Universidade Europeia, Portugal
Mijalce Santa	Ss Cyril and Methodius University, Macedonia
Sławomir Źółkiewski	Silesian University of Technology, Poland
Kuan Yew Wong	Universiti Teknologi Malaysia, Malaysia
Alvaro Prieto	University of Extremadura, Spain
Roberto	University of Extremadura, Spain
Rodriguez-Echeverria	
Yair Wiseman	Bar-Ilan University, Israel
Babak Rouhani	Payame Noor University, Iran
Hing Kai Chan	University of Nottingham Ningbo China, China
José Palma	University of Murcia, Spain
Manuel Mazzara	Innopolis University, Russia
Brígida Mónica Faria	Polytechnic Institute of Porto, Portugal

### IROBOT Track Chairs

Luís Paulo Reis	University of Minho, Portugal
Nuno Lau	University of Aveiro, Portugal
Brígida Mónica Faria	Polytechnic Institute of Porto, Portugal
Rui P. Rocha	University of Coimbra, Portugal

### IROBOT Program Committee

António J.R. Neves	University of Aveiro, Portugal
Antonio P. Moreira	University of Porto, Portugal
Armando Sousa	University of Porto, Portugal
Carlos Cardeira	University of Lisbon, Portugal
Cristina Santos	University of Minho, Portugal
Filipe Santos	INESC TEC, Portugal
João Fabro	Federal University of Technology-Parana, Brazil
Josémar Rodrigues de Souza	Bahia State University, Brazil
Luís Correia	University of Lisbon, Portugal
Luís Mota	Lisbon University Institute, Portugal
Manuel Fernando Silva	Polytechnic Institute of Porto, Portugal
Nicolas Jouandeau	Paris 8 University, France
Paulo Goncalves	Polytechnic Institute of Castelo Branco, Portugal
Paulo Urbano	University of Lisbon, Portugal
Pedro Abreu	University of Coimbra, Portugal
Rodrigo Braga	Federal University of Santa Catarina, Brazil

### KDBI Track Chairs

Paulo Cortez	University of Minho, Portugal
Luís Cavique	Open University, Portugal
João Gama	University of Porto, Portugal

Nuno Marques  
Manuel Filipe Santos

New University of Lisbon, Portugal  
University of Minho, Portugal

### KDBI Program Committee

Agnès Braud	Univ. Robert Schuman, France
Albert Bifet	University of Waikato, New Zealand
Aline Villavicencio	UFRGS, Brazil
Alípio Jorge	University of Porto, Portugal
Amílcar Oliveira	Open University, Portugal
André Carvalho	University of São Paulo, Brazil
Armando Mendes	University of the Azores, Portugal
Bernardete Ribeiro	University of Coimbra, Portugal
Carlos Ferreira Gomes	Institute of Eng. of Porto, Portugal
Elaine Faria	Federal University of Uberlandia, Brazil
Fátima Rodrigues	Institute of Eng. of Porto, Portugal
Fernando Bação	New University of Lisbon, Portugal
Filipe Pinto	Polytechnical Inst. Leiria, Portugal
Gladys Castillo	Choose Digital, USA
José Costa	UFRN, Brazil
Karin Becker	UFRGS, Brazil
Leandro Krug Wives	UFRGS, Brazil
Luís Lamb	UFRGS, Brazil
Manuel Fernandez Delgado	University of Santiago Compostela, Spain
Marcos Domingues	University of São Paulo, Brazil
Margarida Cardoso	ISCTE-IUL, Portugal
Mark Embrechts	Rensselaer Polytechnic Institute, USA
Mohamed Gaber	University of Portsmouth, UK
Murate Testik	Hacettepe University, Turkey
Ning Chen	Institute of Eng. of Porto, Portugal
Orlando Belo	University of Minho, Portugal
Paulo Gomes	University of Coimbra, Portugal
Pedro Castillo	University of Granada, Spain
Phillipe Lenca	Télécom Bretagne, France
Rita Ribeiro	University of Porto, Portugal
Rui Camacho	University of Porto, Portugal
Stéphane Lallich	University of Lyon 2, France
Yanchang Zhao	Australian Government, Australia

### MASTA Track Chairs

Ana Paula Rocha	Porto University, Portugal
Pedro Henriques Abreu	Coimbra University, Portugal
Jomi Fred Hubner	Universidade Federal de Santa Catarina, Brazil
Jordi Sabater Mir	IIIA-CSIC, Spain
Luís Moniz	Lisbon University, Portugal

**MASTA Program Committee**

Alessandra Alaniz Macedo	São Paulo University, Brazil
António Castro	LIACC, Portugal
António Carlos da Rocha Costa	Universidade Federal do Rio Grande, Brazil
Brígida Mónica Faria	Polytechnic Institute of Porto, Portugal
Carlos Carrascosa	Universidad Politecnica de Valencia, Spain
César Analide	Minho University, Portugal
Daniel Castro Silva	LIACC-Porto University, Portugal
Didac Busquets	Imperial College London, UK
Eugénio Oliveira	LIACC-Porto University, Portugal
Felipe Meneguzzi	Pontifícia Universidade Católica do Rio Grande do Sul, Brazil
Francisco Grimaldo	Universidad de Valencia, Spain
Frank Dignum	Utrecht University, Netherlands
Hélder Coelho	Lisbon University, Portugal
Henrique Lopes Cardoso	LIACC-Porto University, Portugal
Jaime Sichmann	São Paulo University, Brazil
Javier Carbó	Universidad Carlos III, Spain
Joana Urbano	Instituto Superior Miguel Torga, Portugal
João Balsa	Lisbon University, Portugal
Laurent Vercouter	Ecole Nationale Supérieure des Mines de Saint-Etienne, France
Luís Correia	Lisbon University, Portugal
Luís Macedo	Coimbra University, Portugal
Luís Paulo Reis	LIACC-Minho University, Portugal
Manuel Filipe Santos	Minho University, Portugal
Maria Fasli	University of Essex, UK
Michael Schumacher	University of Applied Sciences, Western Switzerland
Márcia Ito	São Paulo Faculty of Technology, Brazil
Nicoletta Fornara	University of Lugano, Switzerland
Nuno Lau	Aveiro University, Portugal
Olivier Boisser	ENS Mines Saint-Etienne, France
Pablo Noriega	IIIA-CSIC, Spain
Paulo Trigo	Superior Institute of Engineering of Lisbon, Portugal
Paulo Urbano	Lisbon University, Portugal
Rafael Bordini	Pontifícia Universidade Católica do Rio Grande do Sul, Brazil
Ramón Hermoso	University of Zaragoza, Spain
Rosaldo Rossetti	Porto University, Portugal
Virginia Dignum	Delft University of Technology, Netherlands
Viviane Torres Da Silva	Universidade Federal Fluminense, Brazil
Wamberto Vasconcelos	University of Aberdeen, UK

### SSM Track Chairs

Luís Antunes	Universidade de Lisboa, Portugal
Graçaliz Pereira Dimuro	Universidade Federal do Rio Grande, Brazil
Pedro Campos	Universidade do Porto, Portugal
Juan Pavón	Universidad Complutense de Madrid, Spain

### SSM Program Committee

Frédéric Amblard	Univ. Toulouse 1, France
Pedro Andrade	INPE, Brazil
Tânya Araújo	ISEG, Portugal
Robert Axtell	George Mason Univ., USA
João Balsa	Univ. Lisbon, Portugal
Ana Bazzan	UFRGS, Brazil
François Bousquet	CIRAD/IRRI, Thailand
Amílcar Cardoso	University of Coimbra, Portugal
Cristiano Castelfranchi	ISTC/CNR, Italia
Shu-Heng Chen	National Chengchi Univ., Taiwan
Claudio Cioffi-Revilla	George Mason Univ., USA
Hélder Coelho	Univ. Lisbon, Portugal
Rosaria Conte	ISTC/CNR Rome, Italy
Nuno David	ISCTE, Portugal
Paul Davidsson	Blekinge Inst. Technology, Sweden
Guillaume Deffuant	Cemagref, France
Alexis Drogoul	IRD, France
Julie Dugdale	Lab. d'Informatique Grenoble, France
Bruce Edmonds	Centre for Policy Modelling, UK
Nigel Gilbert	Univ. Surrey, UK
Nick Gotts	Macaulay Inst., Scotland, UK
David Hales	The Open Univ., UK
Samer Hassan	Univ. Complutense Madrid, Spain
Rainer Hegselmann	Univ. Bayreuth, Germany
Wander Jager	Univ. Groningen, Netherlands
Adolfo Lópes Paredes	Univ. Valladolid, Spain
Pedro Magalhães	ICS, Portugal
Scott Moss	Centre for Policy Modelling, UK
Jean-Pierre Muller	CIRAD, France
Akira Namatame	National Defense Academy, Japan
Fernando Neto	Univ. Pernambuco, Brazil
Carlos Ramos	GECAD – ISEP, Portugal
Juliette Rouchier	Greqam/CNRS, France
David Sallach	Univ. Chicago, USA
Keith Sawyer	Washington Univ. St. Louis, USA
Carles Sierra	IIIA, Spain
Elizabeth Sklar	City Univ. New York, USA

Keiki Takadama	Univ. Electro-communications, Japan
Oswaldo Teran	Univ. Los Andes, Venezuela
Takao Terano	Univ. Tsukuba, Japan
Jan Treur	Vrije Univ. Amsterdam, The Netherlands
Klaus Troitzsch	Univ. Koblenz, Germany
Harko Verhagen	Stockholm Univ., Sweden

**TEMA Track Chairs**

Joaquim F. Ferreira da Silva	NOVA LINCS FCT/UNL, Portugal
Gabriel Pereira Lopes	NOVA LINCS FCT/UNL, Portugal
Hugo Gonçalo Oliveira	CISUC, University of Coimbra, Portugal
Vitor R. Rocio	Universidade Aberta, Portugal
Gaël Dias	University of Caen Basse-Normandie, France

**TEMA Program Committee**

Adam Jatowt	Kyoto University, Japan
Adeline Nazarenko	University of Paris 13, France
Aline Villavicencio	Universidade Federal do Rio Grande do Sul, Brazil
Antoine Doucet	University of Caen, France
António Branco	Universidade de Lisboa, Portugal
Béatrice Daille	University of Nantes, France
Belinda Maia	Universidade do Porto, Portugal
Brigitte Grau	LIMSI, France
Bruno Cremilleux	University of Caen, France
Christel Vrain	Université d'Orléans, France
Eric de La Clergerie	INRIA, France
Gabriel Pereira Lopes	NOVA LINCS FCT/UNL, Portugal
Gaël Dias	University of Caen Basse-Normandie, France
Gracinda Carvalho	Universidade Aberta, Portugal
Gregory Grefenstette	CEA, France
Hugo Gonalo Oliveira	CISUC, University of Coimbra, Portugal
Isabelle Tellier	University of Orléans, France
Joaquim F. Ferreira da Silva	NOVA LINCS FCT/UNL, Portugal
João Balsa	Universidade de Lisboa, Portugal
João Magalhães	Universidade Nova de Lisboa, Portugal
Lluís Padró	Universitat Politècnica de Catalunya, Spain
Lucinda Carvalho	Universidade Aberta, Portugal
Manuel Vilares Ferro	University of Vigo, Spain
Marc Spaniol	University of Caen Basse-Normandie, France
Marcelo Finger	Universidade de São Paulo, Brazil
Maria das Graças Volpe Nunes	Universidade de São Paulo, Brazil
Mark Lee	University of Birmingham, UK
Nuno Mamede	Universidade Técnica de Lisboa, Portugal
Nuno Marques	Universidade Nova de Lisboa, Portugal

Pablo Gamallo	Universidade de Santiago de Compostela, Spain
Paulo Quaresma	Universidade de Évora, Portugal
Pavel Brazdil	University of Porto, Portugal
Pierre Zweigenbaum	CNRS-LIMSI, France
Spela Vintar	University of Ljubljana, Slovenia
Vitor R. Rocio	Universidade Aberta, Portugal

## Additional Reviewers

Aching, Jorge	García-Magariño, Iván	Ramos, Ana
Adamatti, Diana Francisca	Gonçalves, Eder Mateus	Rocha, Luis
Adedoyin-Olowe, Mariam	Gorgonio, Flavius	Rodrigues, Filipe
Andeadis, Pavlos	Kheiri, Ahmed	Santos, António Paulo
André, João	Lopes Silva, Maria	Sarmento, Rui
Barbosa, Raquel	Amélia	Serrano, Emilio
Billa, Cleo	Magessi, Nuno	Shatnawi, Safwan
Cardoso, Douglas	Mota, Fernanda	Soulas, Julie
Ferreira, Carlos	Nibau Antunes, Francisco	Souza, Jackson
Flavien, Balbo	Nunes, Davide	Trigo, Luis
Francisco, Garijo	Paiva, Fábio	
Fuentes-Fernández, Rubén	Pasa, Leandro	
	Pinto, Andry	

# Contents

## Ambient Intelligence and Affective Environments

Defining Agents' Behaviour for Negotiation Contexts . . . . .	3
<i>João Carneiro, Diogo Martinho, Goreti Marreiros, and Paulo Novais</i>	
Improving User Privacy and the Accuracy of User Identification in Behavioral Biometrics . . . . .	15
<i>André Pimenta, Davide Carneiro, José Neves, and Paulo Novais</i>	
Including Emotion in Learning Process . . . . .	27
<i>Ana Raquel Faria, Ana Almeida, Constantino Martins, Ramiro Gonçalves, and Lino Figueiredo</i>	
Ambient Intelligence: Experiments on Sustainability Awareness . . . . .	33
<i>Fábio Silva and Cesar Analide</i>	

## Artificial Intelligence in Medicine

Reasoning with Uncertainty in Biomedical Models . . . . .	41
<i>Andrea Franco, Marco Correia, and Jorge Cruz</i>	
Smart Environments and Context-Awareness for Lifestyle Management in a Healthy Active Ageing Framework . . . . .	54
<i>Davide Bacci, Stefano Chessa, Claudio Gallicchio, Alessio Micheli, Erina Ferro, Luigi Fortunati, Filippo Palumbo, Oberdan Parodi, Federico Vozzi, Sten Hanke, Johannes Kropf, and Karl Kreiner</i>	
Gradient: A User-Centric Lightweight Smartphone Based Standalone Fall Detection System . . . . .	67
<i>Ajay Bhatia, Suman Kumar, and Vijay Kumar Mago</i>	
Towards Diet Management with Automatic Reasoning and Persuasive Natural Language Generation . . . . .	79
<i>Luca Anselma and Alessandro Mazzei</i>	
Predicting Within-24h Visualisation of Hospital Clinical Reports Using Bayesian Networks . . . . .	91
<i>Pedro Pereira Rodrigues, Cristiano Inácio Lemes, Cláudia Camila Dias, and Ricardo Cruz-Correia</i>	

On the Efficient Allocation of Diagnostic Activities in Modern Imaging Departments . . . . .	103
<i>Roberto Gatta, Mauro Vallati, Nicola Mazzini, Diane Kitchin, Andrea Bonisoli, Alfonso E. Gerevini, and Vincenzo Valentini</i>	
Ontology-Based Information Gathering System for Patients with Chronic Diseases: Lifestyle Questionnaire Design . . . . .	110
<i>Lamine Benmimoune, Amir Hajjam, Parisa Ghodous, Emmanuel Andres, Samy Talha, and Mohamed Hajjam</i>	
Predicting Preterm Birth in Maternity Care by Means of Data Mining . . . . .	116
<i>Sónia Pereira, Filipe Portela, Manuel F. Santos, José Machado, and António Abelha</i>	
Clustering Barotrauma Patients in ICU—A Data Mining Based Approach Using Ventilator Variables . . . . .	122
<i>Sérgio Oliveira, Filipe Portela, Manuel F. Santos, José Machado, António Abelha, Álvaro Silva, and Fernando Rua</i>	
Clinical Decision Support for Active and Healthy Ageing: An Intelligent Monitoring Approach of Daily Living Activities . . . . .	128
<i>Antonis S. Billis, Nikos Katzouris, Alexander Artikis, and Panagiotis D. Bamidis</i>	
Discovering Interesting Trends in Real Medical Data: A Study in Diabetic Retinopathy . . . . .	134
<i>Vassiliki Somaraki, Mauro Vallati, and Thomas Leo McCluskey</i>	
<b>Artificial Intelligence in Transportation Systems</b>	
A Column Generation Based Heuristic for a Bus Driver Rostering Problem . . . . .	143
<i>Vítor Barbosa, Ana Respício, and Filipe Alvelos</i>	
A Conceptual MAS Model for Real-Time Traffic Control . . . . .	157
<i>Cristina Vilarinho, José Pedro Tavares, and Rosaldo J.F. Rossetti</i>	
Prediction of Journey Destination in Urban Public Transport . . . . .	169
<i>Vera Costa, Tânia Fontes, Pedro Maurício Costa, and Teresa Galvão Dias</i>	
Demand Modelling for Responsive Transport Systems Using Digital Footprints . . . . .	181
<i>Paulo Silva, Francisco Antunes, Rui Gomes, and Carlos Bento</i>	

**Artificial Life and Evolutionary Algorithms**

A Case Study on the Scalability of Online Evolution of Robotic Controllers . . . . .	189
<i>Fernando Silva, Luís Correia, and Anders Lyhne Christensen</i>	
Spatial Complexity Measure for Characterising Cellular Automata Generated 2D Patterns . . . . .	201
<i>Mohammad Ali Javaheri Javid, Tim Blackwell, Robert Zimmer, and Mohammad Majid Al-Rifaie</i>	
Electricity Demand Modelling with Genetic Programming . . . . .	213
<i>Mauro Castelli, Matteo De Felice, Luca Manzoni, and Leonardo Vanneschi</i>	
The Optimization Ability of Evolved Strategies . . . . .	226
<i>Nuno Lourenço, Francisco B. Pereira, and Ernesto Costa</i>	
Evolution of a Metaheuristic for Aggregating Wisdom from Artificial Crowds . . . . .	238
<i>Christopher J. Lowrance, Omar Abdelwahab, and Roman V. Yampolskiy</i>	
The Influence of Topology in Coordinating Collective Decision-Making in Bio-hybrid Societies . . . . .	250
<i>Rob Mills and Luís Correia</i>	
A Differential Evolution Algorithm for Optimization Including Linear Equality Constraints . . . . .	262
<i>Helio J.C. Barbosa, Rodrigo L. Araujo, and Heder S. Bernardino</i>	
Multiobjective Firefly Algorithm for Variable Selection in Multivariate Calibration . . . . .	274
<i>Lauro Cássio Martins de Paula and Anderson da Silva Soares</i>	
Semantic Learning Machine: A Feedforward Neural Network Construction Algorithm Inspired by Geometric Semantic Genetic Programming . . . . .	280
<i>Ivo Gonçalves, Sara Silva, and Carlos M. Fonseca</i>	
Eager Random Search for Differential Evolution in Continuous Optimization . . . . .	286
<i>Miguel Leon and Ning Xiong</i>	
Learning from Play: Facilitating Character Design Through Genetic Programming and Human Mimicry . . . . .	292
<i>Swen E. Gaudl, Joseph Carter Osborn, and Joanna J. Bryson</i>	
Memetic Algorithm for Solving the 0-1 Multidimensional Knapsack Problem . . . . .	298
<i>Abdellah Rezoug, Dalila Boughaci, and Mohamed Badr-El-Den</i>	

Synthesis of In-Place Iterative Sorting Algorithms Using GP: A Comparison Between STGP, SFGP, G3P and GE . . . . .	305
<i>David Pinheiro, Alberto Cano, and Sebastián Ventura</i>	
<b>Computational Methods in Bioinformatics and Systems Biology</b>	
Variable Elimination Approaches for Data-Noise Reduction in 3D QSAR Calculations . . . . .	313
<i>Rafael Dolezal, Agata Bodnarova, Richard Cimler, Martina Husakova, Lukas Najman, Veronika Racakova, Jiri Krenek, Jan Korabecny, Kamil Kuca, and Ondrej Krejcar</i>	
Pattern-Based Biclustering with Constraints for Gene Expression Data Analysis . . . . .	326
<i>Rui Henriques and Sara C. Madeira</i>	
A Critical Evaluation of Methods for the Reconstruction of Tissue-Specific Models . . . . .	340
<i>Sara Correia and Miguel Rocha</i>	
Fuzzy Clustering for Incomplete Short Time Series Data . . . . .	353
<i>Lúcia P. Cruz, Susana M. Vieira, and Susana Vinga</i>	
<b>General Artificial Intelligence</b>	
Allowing Cyclic Dependencies in Modular Logic Programming . . . . .	363
<i>João Moura and Carlos Viegas Damásio</i>	
Probabilistic Constraint Programming for Parameters Optimisation of Generative Models . . . . .	376
<i>Massimiliano Zanin, Marco Correia, Pedro A.C. Sousa, and Jorge Cruz</i>	
Reasoning over Ontologies and Non-monotonic Rules . . . . .	388
<i>Vadim Ivanov, Matthias Knorr, and João Leite</i>	
On the Cognitive Surprise in Risk Management: An Analysis of the Value-at-Risk (VaR) Historical . . . . .	402
<i>Davi Baccan, Elton Sbruzzi, and Luis Macedo</i>	
Logic Programming Applied to Machine Ethics . . . . .	414
<i>Ari Saptawijaya and Luís Moniz Pereira</i>	
<b>Intelligent Information Systems</b>	
Are Collaborative Filtering Methods Suitable for Student Performance Prediction? . . . . .	425
<i>Hana Bydžovská</i>	

**Intelligent Robotics**

A New Approach for Dynamic Strategic Positioning in RoboCup Middle-Size League . . . . .	433
<i>António J.R. Neves, Filipe Amaral, Ricardo Dias, João Silva, and Nuno Lau</i>	
Intelligent Wheelchair Driving: Bridging the Gap Between Virtual and Real Intelligent Wheelchairs . . . . .	445
<i>Brígida Mónica Faria, Luís Paulo Reis, Nuno Lau, António Paulo Moreira, Marcelo Petry, and Luís Miguel Ferreira</i>	
A Skill-Based Architecture for Pick and Place Manipulation Tasks . . . . .	457
<i>Eurico Pedrosa, Nuno Lau, Artur Pereira, and Bernardo Cunha</i>	
Adaptive Behavior of a Biped Robot Using Dynamic Movement Primitives . . . . .	469
<i>José Rosado, Filipe Silva, and Vítor Santos</i>	
Probabilistic Constraints for Robot Localization . . . . .	480
<i>Marco Correia, Olga Meshcheryakova, Pedro Sousa, and Jorge Cruz</i>	
Detecting Motion Patterns in Dense Flow Fields: Euclidean Versus Polar Space . . . . .	487
<i>Andry Pinto, Paulo Costa, and Antonio Paulo Moreira</i>	
Swarm Robotics Obstacle Avoidance: A Progressive Minimal Criteria Novelty Search-Based Approach . . . . .	493
<i>Nesma M. Rezk, Yousra Alkabani, Hassan Bedour, and Sherif Hammad</i>	

**Knowledge Discovery and Business Intelligence**

An Experimental Study on Predictive Models Using Hierarchical Time Series . . . . .	501
<i>Ana M. Silva, Rita P. Ribeiro, and João Gama</i>	
Crime Prediction Using Regression and Resources Optimization . . . . .	513
<i>Bruno Cavadas, Paula Branco, and Sérgio Pereira</i>	
Distance-Based Decision Tree Algorithms for Label Ranking . . . . .	525
<i>Cláudio Rebelo de Sá, Carla Rebelo, Carlos Soares, and Arno Knobbe</i>	
A Proactive Intelligent Decision Support System for Predicting the Popularity of Online News . . . . .	535
<i>Kelwin Fernandes, Pedro Vinagre, and Paulo Cortez</i>	
Periodic Episode Discovery Over Event Streams . . . . .	547
<i>Julie Soulas and Philippe Lenca</i>	

Forecasting the Correct Trading Actions . . . . .	560
<i>Luís Baía and Luís Torgo</i>	
CTCHAID: Extending the Application of the Consolidation Methodology . . . . .	572
<i>Igor Ibarguren, Jesús María Pérez, and Javier Muguerza</i>	
Towards Interactive Visualization of Time Series Data to Support Knowledge Discovery . . . . .	578
<i>Jan Géryk</i>	
Ramex-Forum: Sequential Patterns of Prices in the Petroleum Production Chain . . . . .	584
<i>Pedro Tiple, Luís Cavique, and Nuno Cavalheiro Marques</i>	
Geocoding Textual Documents Through a Hierarchy of Linear Classifiers . . . . .	590
<i>Fernando Melo and Bruno Martins</i>	
A Domain-Specific Language for ETL Patterns Specification in Data Warehousing Systems. . . . .	597
<i>Bruno Oliveira and Orlando Belo</i>	
Optimized Multi-resolution Indexing and Retrieval Scheme of Time Series . . . . .	603
<i>Muhammad Marwan Muhammad Fuad</i>	
<b>Multi-agent Systems: Theory and Applications</b>	
Minimal Change in Evolving Multi-Context Systems. . . . .	611
<i>Ricardo Gonçalves, Matthias Knorr, and João Leite</i>	
Bringing Constitutive Dynamics to Situated Artificial Institutions . . . . .	624
<i>Maiquel de Brito, Jomi F. Hübler, and Olivier Boissier</i>	
Checking WECTLK Properties of Timed Real-Weighted Interpreted Systems via SMT-Based Bounded Model Checking. . . . .	638
<i>Agnieszka M. Zbrzezny and Andrzej Zbrzezny</i>	
SMT-Based Bounded Model Checking for Weighted Epistemic ECTL . . . . .	651
<i>Agnieszka M. Zbrzezny, Bożena Woźna-Szcześniak, and Andrzej Zbrzezny</i>	
Dynamic Selection of Learning Objects Based on SCORM Communication . . . . .	658
<i>João de Amorim Junior and Ricardo Azambuja Silveira</i>	
Sound Visualization Through a Swarm of Fireflies . . . . .	664
<i>Ana Rodrigues, Penousal Machado, Pedro Martins, and Amílcar Cardoso</i>	

**Social Simulation and Modelling**

Analysing the Influence of the Cultural Aspect in the Self-Regulation of Social Exchanges in MAS Societies: An Evolutionary Game-Based Approach . . . . .	673
<i>Andressa Von Laer, Graçaliz P. Dimuro, and Diana Francisca Adamatti</i>	
Modelling Agents' Perception: Issues and Challenges in Multi-agents Based Systems . . . . .	687
<i>Nuno Trindade Magessi and Luís Antunes</i>	
Agent-Based Modelling for a Resource Management Problem in a Role-Playing Game . . . . .	696
<i>José Cascalho and Pinto Mabunda</i>	
An Agent-Based MicMac Model for Forecasting of the Portuguese Population . . . . .	702
<i>Renato Fernandes, Pedro Campos, and A. Rita Gaio</i>	

**Text Mining and Applications**

Multilingual Open Information Extraction . . . . .	711
<i>Pablo Gamallo and Marcos Garcia</i>	
Classification and Selection of Translation Candidates for Parallel Corpora Alignment . . . . .	723
<i>K.M. Kavitha, Luís Gomes, José Aires, and José Gabriel P. Lopes</i>	
A SMS Information Extraction Architecture to Face Emergency Situations . . . . .	735
<i>Douglas Monteiro and Vera Lucia Strube de Lima</i>	
Cross-Lingual Word Sense Clustering for Sense Disambiguation . . . . .	747
<i>João Casteleiro, Joaquim Ferreira da Silva, and Gabriel Pereira Lopes</i>	
Towards the Improvement of a Topic Model with Semantic Knowledge . . . . .	759
<i>Adriana Ferrugento, Ana Alves, Hugo Gonçalo Oliveira, and Filipe Rodrigues</i>	
RAPPORT — A Portuguese Question-Answering System . . . . .	771
<i>Ricardo Rodrigues and Paulo Gomes</i>	
Automatic Distinction of Fernando Pessoa's Heteronyms . . . . .	783
<i>João F. Teixeira and Marco Couto</i>	
Social Impact - Identifying Quotes of Literary Works in Social Networks . . . . .	789
<i>Carlos Barata, Mónica Abreu, Pedro Torres, Jorge Teixeira, Tiago Guerreiro, and Francisco M. Couto</i>	

Fractal Beauty in Text . . . . .	796
<i>João Cordeiro, Pedro R.M. Inácio, and Diogo A.B. Fernandes</i>	
How Does Irony Affect Sentiment Analysis Tools? . . . . .	803
<i>Leila Weitzel, Raul A. Freire, Paulo Quaresma, Teresa Gonçalves, and Ronaldo Prati</i>	
<b>Author Index . . . . .</b>	<b>809</b>

# **Ambient Intelligence and Affective Environments**

# Defining Agents' Behaviour for Negotiation Contexts

João Carneiro<sup>1()</sup>, Diogo Martinho<sup>1</sup>, Goreti Marreiros<sup>1</sup>, and Paulo Novais<sup>2</sup>

<sup>1</sup> GECAD – Knowledge Engineering and Decision Support Group, Institute of Engineering,  
Polytechnic of Porto, Porto, Portugal  
[{jomrc,1090557,mgt}@isep.ipp.pt](mailto:{jomrc,1090557,mgt}@isep.ipp.pt)

<sup>2</sup> CCTC – Computer Science and Technology Center, University of Minho, Braga, Portugal  
[pjon@di.uminho.pt](mailto:pjon@di.uminho.pt)

**Abstract.** Agents who represent participants in the group decision-making context require a certain number of individual traits in order to be successful. By using argumentation models, agents are capable to defend the interests of those who they represent, and also justify and support their ideas and actions. However, regardless of how much knowledge they might hold, it is essential to define their behaviour. In this paper (1) is presented a study about the most important models to infer different types of behaviours that can be adapted and used in this context, (2) are proposed rules that must be followed to affect positively the system when defining behaviours and (3) is proposed the adaptation of a conflict management model to the context of Group Decision Support Systems. We propose one approach that (a) intends to reflect a natural way of human behaviour in the agents, (b) provides an easier way to reach an agreement between all parties involved and (c) does not have high configuration costs to the participants. Our approach will offer a simple yet perceptible configuration tool that can be used by the participants and contribute to more intelligent communications between agents and makes possible for the participants to have a better understanding of the types of interactions experienced by the agents belonging to the system.

**Keywords:** Group decision support systems · Ubiquitous computing · Affective computing · Multi-Agent systems · Automatic negotiation

## 1 Introduction

Rahwan et al. (2003) defined negotiation as “a form of interaction in which a group of agents, with conflicting interests and a desire to cooperate, try to come to a mutually acceptable agreement on the division of scarce resources” [1], Hadidi, Dimopoulos, and Moraitis (2011), defined negotiation as “the process of looking for an agreement between two or several agents on one or more issues” [2] and El-Sisi and Mousa (2012) defined as “a process of reaching an agreement on the terms of a transaction such as price, quantity, for two or more parties in multi-agent systems such as E-Commerce. It tries to maximize the benefits to all parties” [3]. It is possible to verify in the literature a consensus regarding to the main approaches to deal with negotiation: game theory, heuristics and argumentation [1-3]. It is a known fact that game

theoretic and heuristic based approaches evolved and turned more complex. With this development they have been used in a wide range of applications. However they share some limitations. In the majority of game-theoretic and heuristic models, agents exchange proposals, but these proposals are limited. Agents are not allowed to exchange any additional information other than what is expressed in the proposal itself. This can be problematic, for example, in situations where agents have limited information about the environment, or where their rational choices depend on those of other agents. Another important limitation is that agent's utilities or preferences are usually assumed to be completely characterized prior to the interaction. Thus, to overcome these limitations, argumentation-based negotiation appeared and turned one of the most popular approaches to negotiation [4], it has been extensively investigated and studied, as witnessed by many publications [5-7]. The main idea of argumentation-based negotiation is the ability to support offers with justifications and explanations, which play a key role in the negotiation settings. So, it allows the participants to the negotiation not only to exchange offers, but also reasons and justifications that support these offers in order to mutually influence their preference relations on the set of offers, and consequently the outcome of the dialogue.

It is simple to understand the parallelism between this approach and group decision-making. The idea of a group of agents exchanging arguments in order to achieve, for instance, a consensus, in order to support groups in decision-making process is easy to understand [8]. However the complexity of this process must not be underestimated, if considering a scenario where an agent seeks to defend the interests of who it represents and at the same time be part of a group that aims to reach a collective decision towards a problem for their organization [9, 10]. Not only are those agents simultaneously competitive and cooperative but also represent human beings. Establishing some sort of dialog, as well as the different types of arguments that can be exchanged by agents is only the first step towards the problem resolution. One agent that represents a decision-maker involved in a process of group decision-making may show different levels of experience and knowledge related with the situation and should behave accordingly. Literature shows that there are works on the subject [10-13], however it should be noted the existence of some flaws in terms of real world applicability of certain models. Some require high configuration costs that will not suit the different types of users they are built for and others show flaws that in our opinion are enough to affect the success of a Group Decision Support System (GDSS).

In this work it will be presented the most relevant models that allow inferring or configuring a behaviour style for a group decision-making context. It is also proposed a set of rules for which a behaviour model must follow without jeopardizing the entire GDSS and finally it is proposed an approach made through the modification of one existing model to the context of GDSS.

The rest of the paper is organized as follows: in the next section is presented the literature review. Section 3 presents our approach, where we identify different types of behaviours, defined with the use of an existing model and presented the set of rules that we believe that are the most important to allow defining types of behaviours for the agents in a way that does not compromise the system. In section 4 it will be discussed and debated how our approach can be applied to the context of GDSS and its differences compared

with other existing approaches. Finally, some conclusions are taken in section 5, along with the work to be done hereafter.

## 2 Literature Review

The concern for identifying and understanding particular behavioural attitudes has led to many investigations and studies throughout the last decades with emphasis on proposing models and behaviour styles that can relate to the personality of the negotiator.

Carl Jung (1921), was the first to specify a model to study different psychological personality types based on four types of consciousness (sensation, intuition, thinking and feeling) that could in turn be combined with two types of attitudes (extraversion and introversion) and that way identify eight primary psychological types [14].

In 1962, Myers Briggs, developed a personality indicator model (The Meyers-Briggs Type Indicator) based on Jung's theories [15]. This indicator is used as a psychometric questionnaire and allows people to understand the world around them and how they behave and make decisions based on their preferences [16]. This model was useful in order to identify different styles of leadership, which were later specified in Keirsey and Bate's publication [17], in 1984, as four styles of leadership:

- Stabilizer: tends to be very clear and precise when defining objectives and organizing and planning tasks in order to achieve them. Stabilizer leaders are also reliable and trustworthy due to the fact they show concern for other worker's necessities and problems. They are able to increase the motivation of their workers by setting tradition and organization as an example of success;
- Catalyst: the main focus is to develop the quality of own work and the one provided by their staff. They serve the facilitator's role by bringing the best out of other people, and motivate other workers with their own enthusiasm and potential;
- Trouble-shooter: as the name suggests, focus on dealing and solving problems. They show great aptitude for solving urgent problems by being practical and immediate. They bring people together as a team by analysing what needs to be done and informing exactly what to do as quickly as possible;
- Visionary: visionaries act based on their own intuition and perception of the problems in order to make decisions. They have a mind projected for the future and plan idealistic scenarios and objectives which may not always be achievable.

Related to vocational behaviour, Holland [18], in 1973 proposed a hexagonal model (RIASEC model) where he differentiates six types of personality mainly used in careers environments and to guide through the individual's choice of vocation. Those types are defined as:

- Realistic: realistic individuals value things over people and ideas. They are mechanical and athletic, and prefer working outdoors with tools and objects;
- Investigative: investigative individuals have excellent analytic skills. They prefer working alone and solving complex problems;
- Artistic: artistic individuals show a deep sense of creativity and imagination. They prefer working on original projects and value ideas over things;

- Social: social individuals have high social aptitude, preferring social relationships and helping other people solving their problems. They prefer working with people over things;
- Enterprising: enterprising individuals show great communication and leadership skills, and are usually concerned about establishing direct influence on other people. They prefer dealing with people and ideas over things;
- Conventional: conventional individuals value order and efficiency. They show administrative and organization skills. They prefer dealing with numbers and words over people and ideas.

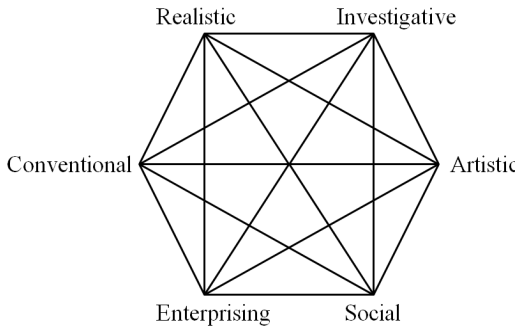


**Fig. 1.** Representation of Holland's hexagon model, adapted from [18]

It is important to note the distribution of these personalities in Holland's hexagon where personalities next to each other are the most similar while personalities facing against each other are the least similar (see Fig. 1).

Conflict management has always been an important area of decision-making, since it is very rare to find situations in group discussion where conflict is not present. In 1975, Thomas and Kilmann [19], also based on Jung's studies and a conflict-handling mode proposed by Blake and Mouton [20], suggested a model for interpersonal conflict-handling behaviour, defining five modes: competing, collaborating, compromising, avoiding and accommodating, according to two dimensions: assertiveness and cooperativeness. As seen in Fig. 2, both assertiveness and cooperativeness dimensions are related to integrative and distributive dimensions which were discussed by Walton and McKersie in 1965 [21]. Integrative dimensions refer to the overall satisfaction of the group involved in the discussion while distributive dimension refers to the individual satisfaction within the group. It is possible to see that the thinking-feeling dimension maps onto the distributive dimension while the introversion-extraversion dimension maps onto the integrative dimension. It is easy to understand this association by looking at competitors as the ones who seek the highest individual satisfaction, collaborators as the ones who prefer the highest satisfaction of the entire group. On the other hand avoiders do not worry about group satisfaction and accommodators do not worry about individual satisfaction. They also concluded that the thinking-feeling dimension did not move towards the integrative dimension, and also that the introversion-extraversion did not move towards the distributive dimension.

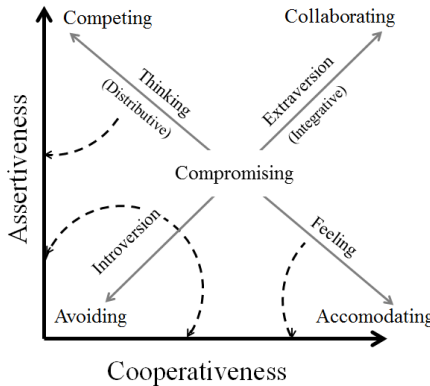


**Fig. 2.** Thomas and Kilmann's model for interpersonal conflict-handling behaviour, adapted from [19]

In 1992, Costa and McCrae [22] proposed a set of thirty traits extending the five-factor model of personality (OCEAN model) which included six facets for each of the factors. These traits were used in a study made by Howard and Howard [23] in order to help them separate different kinds of behaviour styles and identify corresponding themes. A theme is defined as “a trait which is attributable to the combined effect of two or more separate traits”. Those styles and themes are based on common sense and general research, and some of them have already been mentioned before in this literature review, however it is also important to refer to other relevant styles that were suggested such as the Decision and Learning styles. Decision style includes the Autocratic, Bureaucratic, Diplomat and Consensus themes while Learning style includes the Classroom, Tutorial, Correspondence and Independent themes.

In 1995, Rahim and Magnier [24] created a meta-model of styles for handling interpersonal conflict based on two dimensions: concern for self and concern for the other. This was the base for the five management styles identified as obliging, avoiding, dominating, integrating and compromising as will be explained in detail in the Section 3.

### 3 Methods

It is really important to define correctly the agent's behaviour in order to not jeopardize the validation of the entire GDSS. Sometimes, in this area of research, there is an exhaustive concern to find a better result and because of that, other variables may be forgotten which can make impossible the use of a certain approach in those situations. For example: Does it make sense for a decision-maker or a manager from a large company, with his super busy schedule have the patience/time to answer (seriously) to a questionnaire of 44 questions like “the Big Five Inventory” so that he can model his agent with his personality? Due to reasons like this we have defined a list with considerations to have when defining types of behaviours for the agents in the context here presented. The definition of behaviour should:

1. Enhance the capabilities of the agents, i.e., make the process more intelligent, more human and less sequential, even though it may not be visible in the conceptual model it must not be possible for the programmer to anticipate the sequence of interactions just by reading the code;
2. Be easy to configure (usability) or not need any configuration at all from the user (decision-maker);
3. Represent the interests of the decision-makers (strategy used), so that agent's way of acting meets the interests defined by the user (whenever possible);
4. Not be the reason for the decision-makers to give up using the application, i.e., in a hypothetical situation, a decision-maker should not "win" more decisions just because he knows how to manipulate/configure better the system;
5. Be available for everyone to benefit from it. Obviously all decision-makers face meetings in different ways. Their interests and knowledge for each topic is not always the same. Sometimes it may be of their interest to let others speak first and only after gathering all the information, elaborate a final opinion on the matter. Other times it may be important to control the entire conversation and try to convince the other participants to accept out opinion straightaway.

By taking into account all these points, we propose in this article a behaviour model for the decision-making context based on conflict styles defined by Rahim and Magner (1995) [24]. The styles defined are presented in Fig. 3 and have been adapted to our problem. Rahim and Magner reckons the existence of 5 types of conflict styles: integrating, obliging, dominating, avoiding and compromising. In their work, they suggested these styles in particular to describe different ways of behave in conflict situations. They defined these styles according to the level of concern a person has for reaching its own goal and reaching other people's objectives. This definition goes along exactly with what we consider that the agents that operate in a GDSS context should be, when we say that they are both cooperative and competitive simultaneously. Therefore this model ends up describing 5 conflict styles which support what we think that is required for the agents to have a positive behaviour in this context. It also has the advantage of being a model easy to understand and to use.

In our approach, the configuration of agent's behavior made by the decision-maker, will be done through the selection of one conflict style. The main idea is to define the agent with the participant's interests and strategies. For that, the definition of each conflict style should be clear and understandable for the decision-maker. The decision-maker can define in his agent different conflict styles throughout the process. For example, a decision-maker who is included in a decision process and has few or even no knowledge about the problem during the early stage of discussion. For that situation he may prefer to use an "avoiding" style and learn with what other people say, gather arguments and information that will support different options and that way learn more about the problem. In a following stage, when the decision-maker already has more information and knowledge about the problem, he may opt to use a more active and dominating style in order to convince others towards his opinion. Like mentioned before, there are many factors that can make the decision-maker face a meeting in different ways: interest about a topic, lack of knowledge about a topic, reckons the participation of more experienced people in the discussion, etc.

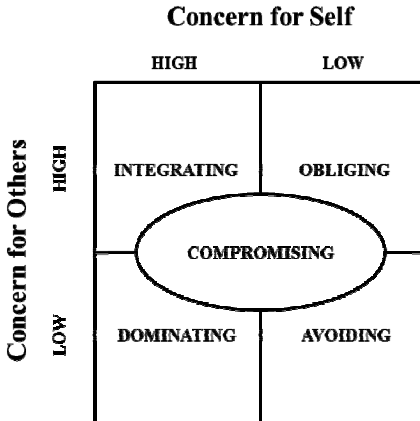


**Fig. 3.** Conflict Style, adapted from [24]

The different types of behaviour defined and that can be used by the agents are:

- Integrating (IN): This style should be selected every time the decision-maker considers that satisfying his own objectives is as important as satisfying the other participants' objectives. By choosing this conflict style, the agent will seek and cooperate with other agents in order to find a solution that is satisfactory to all the participants;
- Obliging (OB): This style should be selected if the decision-maker prefers to satisfy other participant's objectives instead of satisfying his own objectives. For example, in a situation where the decision-maker does not have any knowledge about the discussion topic;
- Dominating (DO): This style should be selected when the decision-maker only wants to pursue his own objectives and do everything in his power to achieve them. For example, in a situation where the decision-maker is absolutely sure that his option to solve the problem is the most benefic. By using this style, the agent will be more dominant and will try to persuade the maximum possible agents. With this style the agent will prefer to risk everything to achieve his objectives even if that means he might end up at disadvantage because of that;
- Avoiding (AV): This style should be selected when the decision-maker does not have any interest in achieving either his own and other participants' objectives. For example, when the decision-maker has been include in a group discussion for which he does not have any sort of interest;
- Compromising (CO): This style should be selected when the decision-maker has a moderate interest in the topic and at the same time he also has a certain interest to achieve his own and other participants' objectives.

## 4 Discussion

Many approaches have been suggested in the literature which define/model agents with characteristics that will differentiate them from each other and as result will also

show different ways of operating [11-13, 25-27]. However, even if many of those publications might be interesting for an academic context, they still show some issues that must be addressed. These issues that we will analyze are related to the context of support to group decision-making and also to competitive agents which represent real individuals. There are several approaches in literature for (1) agents that are modeled according to the real participant personality (decision-maker) which they represent and (2) modeled with different intelligence levels (abilities) [10, 12]. One of the most used technics in literature is “The Big Five Inventory” questionnaire that allows to obtain values for each one of the personality traits defined in the model of “The Big Five” (openness, conscientiousness, extraversion, agreeableness and neuroticism) [11, 26, 28]. Theoretically, we can think that the way agents operate, which is similar to real participant because it is modeled with “the same personality” is perfect. However, defining an agent with a conflict style based on the values of personality traits may not be the right way to identify the decision-maker. What makes a human act in a particular way is the result of much more than just its personality, it is a set of factors such as: personality, emotions, humor, knowledge, and body (physic part), and it can also be considered other factors such as sensations and the spiritual part [29]. Another relevant question is the fact this type of approach allows that certain agents have advantage over other agents. Many may say and think that this occurrence is correct, because close to what happens in real life, there are decision-makers that are more apt and therefore have advantage over other decision-makers. However the questions that arise are the following: Would a product like this used by decision-makers that knew they would be at disadvantage by using this tool? Would it be possible to sell a product that does not guarantee equality between its future users? It is also important to discuss another relevant analysis point which is the fact that this type of approach, in some situations, might provide less intelligent and more sequential outputs.

The study of different types of behaviour in agents has been represented in literature by a reasonable number of contributions. However, it is a subject that most of the times offers validation problems. Although there are proposals with cases of study aiming to validate this subject, that validation is somewhat subjective most of the times. Even when trying to mathematically formulate the problem so that it becomes scientifically “proven”, that proof may often feel forced. A reflection of this problem is the difference between the practiced approaches for social and exact sciences. It is clear for us, as computer science researchers that it is not our goal to elaborate a model for behavioural definition to use in specific scenarios. Instead, we will use a model defined and theoretically validated by others who work in areas that allow them to have these skills. However, the inclusion of intelligence in certain systems is growing at a blistering pace and some of the systems would not make sense nor would succeed without this inclusion. This means that it become more of common practice to adapt certain models that have not been designed specifically for the context for which they will be used. Because of that the evolution of the presented approaches will happen in an empirical way.

Another relevant condition is related with how most of the works are focused on very specific topics which may prevent a more pragmatic comparison of the various approaches. Even if in some situations the use of a specific technic (such as “The Big

Five Inventory") might make sense, in others, and even though it may scientifically provide a case of study with brilliant results, it can be responsible for jeopardizing the success of the system. Our work aims to support each participant (decision-maker) in the process of group decision-making. It is especially targeted for decision support in ubiquitous scenarios where participants are considered people with a very fast pace of life, where every second counts (top managers and executives). In our context the system will notify the participant whenever he is added in a decision process (for instance, by email), and after that every participant can access the system and model his agent according to his preferences (alternatives and attributes classification), as well as how he plans to face that decision process (informing the agent about the type of behaviour to have), always knowing that there are no required fields in the agent setup. This way provides more freedom for the user to configure (depending on his interest and time) his agent with detail or with no detail at all. As can be seen in this context (and referred previously) the agents must be cooperative and competitive. They are cooperative because they all seek one solution for the organization they belong to, and competitive because each agent seeks to defend the interests of its participant and persuade other agents to accept his preferred alternative. For us this means that if an agent is both cooperative and competitive then it cannot exhibit behaviour where it is only concerned in achieving its objectives and vice versa.

## 5 Conclusions and Future Work

The use of agents to represent/support humans as well as their intentions in negotiation context is relatively common practice in literature. There are several approaches which based on relationships allow agents to judge different levels for trust, credibility, intelligence, etc. Specifically looking at support to group decision-making context, a few approaches have appeared and propose modelling agents based on a number of characteristics that will allow them to operate in a way similar to how the decision-maker would in real life. If in one hand the modelling of an agent with certain human characteristics makes sense since it allows to define different types of behaviours and strategies according to the objectives of the decision-maker, on the other hand even if some of those approaches may seem intellectually interesting and complex, they affect the system where they belong due to many reasons, as for instance: illusory intelligence creation, unbalanced agent capabilities, high configuration costs and weak representation of what in practice the decision-maker would want the agent operating model to be.

In this paper we presented (1) a study about the most important models that can be used to infer different types of behaviours that can be adapted and used in this context, (2), a set of rules that must be followed and that will positively affect the system when defining behaviours and (3) is proposed the adaptation of a conflict management model in the context of GDSS. Furthermore we included a new approach of how to look at this problem, and alert to the negative impact some other approaches might

have in the system where they are used. Our approach intends to provide a more perceptible and concrete way for the decision-maker to understand the five types of behaviour that can be used to model the agent in support to group decision-making context where each agent represents a decision-maker. We believe that with our approach it will be simpler for agents to reach or suggest solutions since they are modeled with behaviours according to what the decision-maker wants. This makes it easier to reflect in the agent the concern to achieve the decision-maker's objectives or the objectives belonging to other participants in the decision process. With this approach the agents follow one defined type of behaviour that also works as a strategy that can be adopted by each one of the decision-makers.

As for future work we will work in the specific definition of each type of behaviour identified in this work. We intend to describe behaviours according to certain facets proposed in the Five Factor Model and also study tendencies for each type of behaviour to make questions, statements, and requests. At later stage we will integrate this model in the prototype of a group decision support system which we are developing.

**Acknowledgements.** This work is part-funded by ERDF - European Regional Development Fund through the COMPETE Programme (operational programme for competitiveness) within project FCOMP-01-0124-FEDER-028980 (PTDC/EEISII/1386/2012) and by National Funds through the FCT - Fundação para a Ciência e a Tecnologia (Portuguese Foundation for Science and Technology) with the João Carneiro PhD grant with the reference SFRH/BD/89697/2012.

## References

1. Rahwan, I., Ramchurn, S.D., Jennings, N.R., Mcburney, P., Parsons, S., Sonenberg, L.: Argumentation-based negotiation. *The Knowledge Engineering Review* **18**, 343–375 (2003)
2. Hadidi, N., Dimopoulos, Y., Moraitis, P.: Argumentative alternating offers. In: McBurney, P., Rahwan, I., Parsons, S. (eds.) ArgMAS 2010. LNCS, vol. 6614, pp. 105–122. Springer, Heidelberg (2011)
3. El-Sisi, A.B., Mousa, H.M.: Argumentation based negotiation in multiagent system. In: 2012 Seventh International Conference on, Computer Engineering & Systems (ICCES), pp. 261–266. IEEE (2012)
4. Marey, O., Bentahar, J., Asl, E.K., Mbarki, M., Dssouli, R.: Agents' Uncertainty in Argumentation-based Negotiation: Classification and Implementation. *Procedia Computer Science* **32**, 61–68 (2014)
5. Mbarki, M., Bentahar, J., Moulin, B.: Specification and complexity of strategic-based reasoning using argumentation. In: Maudet, N., Parsons, S., Rahwan, I. (eds.) ArgMAS 2006. LNCS (LNAI), vol. 4766, pp. 142–160. Springer, Heidelberg (2007)
6. Amgoud, L., Vesic, S.: A formal analysis of the outcomes of argumentation-based negotiations. In: The 10th International Conference on Autonomous Agents and Multiagent Systems, vol. 3, pp. 1237–1238. International Foundation for Autonomous Agents and Multiagent Systems (2011)

7. Bonzon, E., Dimopoulos, Y., Moraitsis, P.: Knowing each other in argumentation-based negotiation. In: Proceedings of the 11th International Conference on Autonomous Agents and Multiagent Systems, vol. 3, pp. 1413–1414. International Foundation for Autonomous Agents and Multiagent Systems (2012)
8. Kraus, S., Sycara, K., Evenchik, A.: Reaching agreements through argumentation: a logical model and implementation. *Artificial Intelligence* **104**, 1–69 (1998)
9. Faratin, P., Sierra, C., Jennings, N.R.: Negotiation decision functions for autonomous agents. *Robotics and Autonomous Systems* **24**, 159–182 (1998)
10. Rahwan, I., Kowalczyk, R., Pham, H.H.: Intelligent agents for automated one-to-many e-commerce negotiation. In: Australian Computer Science Communications, pp. 197–204. Australian Computer Society Inc. (2002)
11. Santos, R., Marreiros, G., Ramos, C., Neves, J., Bulas-Cruz, J.: Personality, emotion, and mood in agent-based group decision making (2011)
12. Kakas, A., Moraitsis, P.: Argumentation based decision making for autonomous agents. In: Proceedings of the Second International Joint Conference on Autonomous Agents and Multiagent Systems, pp. 883–890. ACM (2003)
13. Zamfirescu, C.-B.: An agent-oriented approach for supporting Self-facilitation for group decisions. *Studies in Informatics and control* **12**, 137–148 (2003)
14. Jung, C.G.: Psychological types. *The collected works of CG Jung* **6**(18), 169–170 (1971). Princeton University Press
15. Myers-Briggs, I.: The Myers-Briggs type indicator manual. Educational Testing Service, Princeton (1962)
16. Myers, I.B., Myers, P.B.: Gifts differing: Understanding personality type. Davies-Black Pub. (1980)
17. Bates, M., Keirsey, D.: Please Understand Me: Character and Temperament Types. Prometheus Nemesis Book Co., Del Mar (1984)
18. Holland, J.L.: Making vocational choices: A theory of vocational personalities and work environments. *Psychological Assessment Resources* (1997)
19. Kilmann, R.H., Thomas, K.W.: Interpersonal conflict-handling behavior as reflections of Jungian personality dimensions. *Psychological reports* **37**, 971–980 (1975)
20. Blake, R.R., Mouton, J.S.: The new managerial grid: strategic new insights into a proven system for increasing organization productivity and individual effectiveness, plus a revealing examination of how your managerial style can affect your mental and physical health. Gulf Pub. Co. (1964)
21. Walton, R.E., McKersie, R.B.: A behavioral theory of labor negotiations: An analysis of a social interaction system. Cornell University Press (1991)
22. Costa, P.T., MacCrae, R.R.: Revised NEO Personality Inventory (NEO PI-R) and NEO Five-Factor Inventory (NEO FFI): Professional Manual. Psychological Assessment Resources (1992)
23. Howard, P.J., Howard, J.M.: The big five quickstart: An introduction to the five-factor model of personality for human resource professionals. ERIC Clearinghouse (1995)
24. Rahim, M.A., Magner, N.R.: Confirmatory factor analysis of the styles of handling interpersonal conflict: First-order factor model and its invariance across groups. *Journal of Applied Psychology* **80**, 122 (1995)
25. Allbeck, J., Badler, N.: Toward representing agent behaviors modified by personality and emotion. *Embodied Conversational Agents at AAMAS* **2**, 15–19 (2002)
26. Badler, N., Allbeck, J., Zhao, L., Byun, M.: Representing and parameterizing agent behaviors. In: *Proceedings of Computer Animation, 2002*, pp. 133–143. IEEE (2002)

27. Velásquez, J.D.: Modeling emotions and other motivations in synthetic agents. In: AAAI/IAAI, pp. 10–15. Citeseer (1997)
28. Durupinar, F., Albeck, J., Pelechano, N., Badler, N.: Creating crowd variation with the ocean personality model. In: Proceedings of the 7th International Joint Conference on Autonomous Agents and Multiagent Systems, vol. 3, pp. 1217–1220. International Foundation for Autonomous Agents and Multiagent Systems (2008)
29. Pasquali, L.: Os tipos humanos: A teoria da personalidade. *Differences* **7**, 359–378 (2000)

# Improving User Privacy and the Accuracy of User Identification in Behavioral Biometrics

André Pimenta<sup>(✉)</sup>, Davide Carneiro, José Neves, and Paulo Novais

Algoritmi Centre, Universidade Do Minho, Braga, Portugal  
`{apimenta,dcarneiro,jneves,pjon}@di.uminho.pt`

**Abstract.** Humans exhibit their personality and their behavior through their daily actions. Moreover, these actions also show how behaviors differ between different scenarios or contexts. However, Human behavior is a complex issue as it results from the interaction of various internal and external factors such as personality, culture, education, social roles and social context, life experiences, among many others. This implies that a specific user may show different behaviors for a similar circumstance if one or more of these factors change. In past work we have addressed the development of behavior-based user identification based on keystroke and mouse dynamics. However, user states such as stress or fatigue significantly change interaction patterns, risking the accuracy of the identification. In this paper we address the effects of these variables on keystroke and mouse dynamics. We also show how, despite these effects, user identification can be successfully carried out, especially if task-specific information is considered.

**Keywords:** Mental fatigue · Machine learning · Computer security · Behavioral biometrics · Behavioral analysis

## 1 Introduction

In the last years there has been a significantly increase in jobs that are mentally stressful or fatiguing, in expense of otherwise traditional physically demanding jobs [1]. Workers are nowadays faced not only with more mentally demanding jobs but also with demanding work conditions (e.g. positions of high responsibility, competition, risk of unemployment, working by shifts, working extra hours). This results in the recent emergence of stress and mental fatigue as some of the most serious epidemics of the twenty first century [2, 3]. In terms of workplace indicators, this has an impact on human error, productivity or quality of work and of the workplace. In terms of social or personal indicators, this has an impact on quality of life, health or personal development. Moreover, there is an increase in the loss of focus that leads people to be unaware of risks, thus lowering the security threshold.

Recent studies show the negative impact of working extra hours on productivity [4, 5]: people work more but produce less. Stressful milieus just add to the

problem. The questions is thus how to create the optimal conditions to meet productivity requirements while respecting people's well-being and health. Since each worker is different, what procedures need to be implemented to measure the level of stress or burnout of each individual worker? And their level of productivity? The mere observation of these indicators using traditional invasive means may change the worker's behavior, leading to biased results that do not reflect his actual state. Directly asking, through questionnaires or similar instruments, can also lead to biased results as workers are often unwilling to share feelings concerning their workplace with their coworkers.

Recent approaches for assessing and managing fatigue have been developed that look at one's interaction patterns with technological devices to assess one's state (e.g. we type at a lower pace when fatigued). Moreover, the same approaches can be used to identify users (e.g. each individual types in a different manner). This field is known as behavioral biometrics. In this paper we present a framework for collecting from users in a transparent way, that allows to perform tasks commonly associated to behavioral biometrics. Moreover, this framework respects user privacy. Finally, we show how including the user's state and information about the interaction context may improve the accuracy of user identification. The main objective of this work is to define a reliable and non-intrusive user identification system for access control.

## 1.1 Human-Computer Interaction

Currently there is a very large community of computer users. In fact, most of the jobs today require some type of computer usage [6]. Moreover, with services like home banking, tech support services and social networks, people start to interact more with computers than with other persons, even to take care of important aspects of their lives.

There is thus a new form of communication in which computers serve as intermediaries. Therefore, the perception of a conversation between human beings is somewhat lost. By using a computer, the people involved cannot perceive one of the most important aspects in communication which is body language. Other important aspects include speech, intonation or facial expressions, just to mention a few. To overcome this loss of information computer systems must adopt new processes to better perceive the human being [7].

In fact, Humans tend to show their personality or their state through their actions, even in an unconscious way. Facial expressions and body language, for example, have been known as a gateway for feelings that result in intentions. The resultant actions can be traced to a certain behavior. Therefore, it is safe to assume that a human behavior can be outlined even if the person does not want to explicitly share that information.

Human behavior can also be deemed complex as it is driven by internal and external factors, such as personality, culture, education, social roles, life experiences, among others. Accurately evaluating a behavior requires constant observation of all the elements that are able to provide useful information. Nonetheless, with our evolved social skills, we are often able to conceal certain emotions or

shielding them with others. Thus, multi-modal approaches should be considered for increased accuracy (e.g. relying solely on visual emotion recognition may be less accurate than including additional aspects such as tone of voice or speech rhythm). An potentially interesting process is to consider involuntary actions, that cannot consciously controlled by the individual. This often includes movement and posture, hand gestures, touches and interaction with objects the environment, among others. Therefore, it can be stated that the observation and evaluation of behaviors must consider not only the displayed emotions and actions, but also the nature of the interaction with the environment.

One particularly interesting source of these unconscious behaviors is our interaction with computers and other technological devices. In fact, we don't think about controlling the rhythm at which we type on a keyboard or the way we move the mouse when we become fatigued or stress, although we might want to hide our state from our colleagues or superiors. But the truth is that our interaction does change, as we have established in previous work [8,9]. Under different states we use the mouse and the keyboard differently. Moreover, we also interact differently with the smartphone. The case of the smartphone is still more interesting as it provides a range of sensors that are not available on other platforms and can provide very valuable information about interaction patterns, including a touch screen (that provides information about touches, their intensities, their area or their duration), gyroscopes, accelerometers, among others.

Human-Computer Interaction thus becomes a very promising field when it comes to reliable sources of information for characterizing one's state following behavioral approaches, the main advantage being that the individual generally does not or cannot consistently change such precise and fine-grained behaviors. Thus, while one can, to some extent, fake facial expressions and transmit a chosen emotion or state, doing so successfully through these behaviors results much harder.

## 2 Security Systems

As stated before, with the increase of Human-computer Interaction and the development of social-networking, people rapidly increased the rate at which they share information, even when it is sensitive personal information. Some of the current concerns are thus privacy, security and data protection.

Deemed as the most profitable crime of modern times, information theft is increasing at an alarming rate, the corporate sector being the most affected. This type of crime frequently includes the theft of personal data and often does a large damage in a person's life, as well as in companies. One way to improve security is to build robust authentication systems which prevent unauthorized access to machines. These systems may range from password-based authentication, in the simplest cases, to biometry systems in the most complex ones.

One of the possible ways to increase security in the context of user identification is to consider the user' behavior when interacting with a technological

device. As each individual has a particular way to walk, talk, laugh or do anything else, each one of us has also their own interaction patterns with technological devices. Moreover, most of the applications we interact with have a specific flow of operation or require a particular type of interaction, restricting or conditioning the user's possible behaviors to a smaller set. Maintaining a behavioral profile of authorized users may allow to identify uncommon behaviors on the current user that may indicate a possible unauthorized user. This is even more likely to work when behavioral information for particular applications is used.

Such systems are known as Behavioural Biometrics: they rely on the users' behavioral profiles to establish the behavior of authorized users. Whenever, when analyzing the behavior of the current user, a moderate behavioral deviation is detected from the known profiles, the system may take action such as logging off, notifying the administrator or using an alternative method of authentication.

Such systems can also include behaviors other than the ones originated from keyboard and mouse interaction patterns [10]. In fact, any action performed on the technological device can be used as threat detection. For example, if the system console is started and the authorized user of the device never used the console before, a potential invasion may be taking place. Similar actions can be taken on other applications or even on specific commands (e.g. it is unlikely that a user with a non-expert profile suddenly starts using advanced commands on the console).

To implement behavioral biometrics, distinct procedures that can be adopted, such as:

- Biometric Sketch: this method uses the user drawings as templates for comparison [11, 12]. The system collects patterns from the user drawing and compares it to others in a database. Singularity is assured by the number of possible combinations. The downside is that the drawings must be very precise, which in most of the cases is quite difficult, even more by using a standard mouse to draw.
- GUI Interaction: this technique uses the interaction of the user with visual interfaces of the applications and compares it to the model present in the database. For every application that the user interacts with, a model must be present. Thus, both the model and the application must be saved in the database. This method requires that every action per application is saved, resulting in a large amount of information to be maintained. Moreover, each new application or update must be trained and modeled. Therefore, this method is very strict and complex to implement and maintain.
- Keystroke Dynamics: this method uses the keyboard as input and is based on the user's typing patterns. It captures the keys pressed, measuring time and pressing patterns, extracting several features about the typing behavior. This is a well established method, as it relies solely on the user's interaction, allowing to create simple and usable models.
- Mouse Dynamics: this method consists in capturing the mouse movement and translating it into a model. All the interactions are considered, such as movement and clicking. This method is similar to the GUI Interaction method but simpler; although it suffers the same context problem. The main

purpose of this method is to accompany the Keystroke Dynamics, providing additional data to the main model, thus increasing accuracy and decreasing false positives.

- Tapping: this method focuses on the pulse wave resulting from a touch sensor. The pulse duration and tapping interval are the proprieties considered for the analysis. The way a user acts with a smartphone or computer can be monitored, and a model can be extracted. Conceptually, it is a solid method, as tapping follows the same concept of the keystroke dynamics, but in reality the usage context must also be considered, as tapping changes according to the application being used.

In this work, Keystroke Dynamics and Mouse Dynamics are chosen as inputs. Their broader features and availability are the traits that suit the aim of the intended system. They are application independent and operating system independent, and are nowadays the most common input method when interacting with computers.

### 3 The Framework

The framework developed in the context of this work is a unified system, composed of two main modules: fatigue monitoring and security. The process of monitoring is implemented using an application that captures the keyboard and mouse inputs transparently. The features used are the same in both systems and are defined in more detail in [13]. The features extracted from the keyboard are:

- Key down time: total time that a key is pressed
- Time between keys: time between a key being released and the following key being pressed
- Writing speed: the rhythm at which keys are pressed
- Errors per key: quantification of the use of the backspace and delete keys

And the features extracted from the mouse are:

- Distance of the mouse to the straight line: the sum of the distances between the pointer and the line defined by each two consecutive clicks
- Mouse acceleration: the acceleration of the mouse
- Mouse velocity: the velocity of the mouse
- Average distance of the mouse to the straight line: the average distance at which the mouse pointer is from the line that is defined by each two consecutive clicks
- Total excess of distance: the distance that the mouse travels in excess between each two consecutive clicks
- Average excess of distance: the distance that the mouse travels in excess divided by the shortest distance between each two consecutive clicks
- Time between clicks: the time between each two consecutive clicks
- Distance during clicks: distance traveled by the mouse while performing a click

- Double click duration: the time between two clicks in a double click event
- Absolute sum of angles: the quantification of how much the mouse turns, regardless of the direction of the turn, between each two consecutive clicks
- Signed sum of angles: the quantification of how much the mouse turns, considering the direction of the turn, between each two consecutive clicks
- Distance between clicks: the distance traveled between each two consecutive clicks

The data gathered may be processed differently to extract the information related to each scope of the framework (fatigue monitoring and stress). An integrated system is beneficial due to the jointly nature of the data and to the fact that only one application is present locally, thus having a low footprint on computer resources. Furthermore, these are two areas that are intrinsically connected, and one can affect the other. Their joint analysis is fundamental to the achievement of the proposed objectives.

### 3.1 Providing Security and Safety in the Monitoring System

The use of Keystroke Dynamics and Mouse Dynamics for detecting behavior is extremely useful, especially since it allows the creation of non-intrusive and non-invasive systems.

However the use of behavioral biometrics, in particular the use of keystroke dynamics, can pose some risks to the data security and privacy of the user, especially when the data obtained from the mouse and keyboard are processed by remote or 3rd party Web Services. For this reason, and to ensure the users' privacy and data security, data must be encrypted. The most sensitive data is indeed the information about which key was pressed. However, this specific information is mostly irrelevant for behavior analysis, i.e., we are not interested in *which* keys the user presses but on *how* the user presses them.

We therefore propose the collection of events created by the mouse and the keyboard in the following way:

- MOV, timestamp, posX, posY - an event describing the movement of the mouse, in a given time, to coordinates (posX, posY) in the screen;
- MOUSE\_DOWN, timestamp, [Left—Right], posX, posY - this event describes the first half of a click (when the mouse button is pressed down), in a given time. It also describes which of the buttons was pressed (left or right) and the position of the mouse in that instant;
- MOUSE\_UP, timestamp, [Left—Right], posX, posY - an event similar to the previous one but describing the second part of the click, when the mouse button is released;
- MOUSE\_WHEEL, timestamp, dif - this event describes a mouse wheel scroll of amount dif, in a given time;
- KEY\_DOWN, timestamp, encrypted key - identifies a given key from the keyboard being pressed down, at a given time;
- KEY\_UP, timestamp, encrypted key - describes the release of a given key from the keyboard, in a given time;

In this approach, the encrypted key replaces the information about the specific key pressed. It is therefore still possible, while hiding what the user wrote, to extract the previously mentioned features, thus guaranteeing the user's privacy. The encryption of the pressed keys is carried out through the generation of random key encryptions at different times. This is done as depicted in Algorithm 1, which exemplifies the developed approach for the case of the key down time feature. An example of the result of the algorithm is depicted in Table 1, where a record with and without encryption is depicted for different keys.

```

Data: Keyboard Inputs
Result: List of KeyDownTime records
while Keyboard Inputs have records do
    Get timestamp of a KEY_DOWN ;
    Get code of a KEY_DOWN ;
    while Keyboard Inputs have records do
        Get timestamp of a KEY_UP ;
        Get code of a KEY_UP ;
        if KEY_DOWN code and KEY_UP code are the same then
            Save the difference between KEY_UP timestamp and KEY_DOWN
            timestamp;
        end
    end
end

```

**Algorithm 1.** Key down time algorithm

**Table 1.** Example of a keyboard log with and without encryption.

No Encryption	Random Encryption Key 1
KD,63521596046072,A	KD,63521596046072,1COc0qNOOk=
KU,63521596046165,A	KU,63521596046165,1COc0qNOOk=
KD,63521596057943,v	KD,63521596057943,sMA0Wu0n3k=
KU,63521596058037,v	KU,63521596058037,sMA0Wu0n3k=
KU,63521596058084,a	KU,63521596058084,hb0s0lHEF8+sA==
KU,63521596058037,v	KU,63521596058037,sMA0Wu0n3k=

Hiding user input is just one part of the solution for the issue of user security. The other is to prevent intrusions. In this scope, behavioral biometrics security systems can run in two different modes [14]: identification mode and verification mode. In this system we use the identification mode instead of the verification mode to ensure a constant user identification in the monitoring system.

The identification mode is the process of trying to discover the identity of a person by examining a biometric pattern calculated from biometric data of

the person. In this mode the user is identified based on information previously collected from keystroke dynamics profiles of all users. For each user, a biometric profile is built in a training phase. When in the running phase, the usage pattern being created in real-time is compared to every known model, producing either a score or a distance that describes the similarity between the pattern and the model. The system assigns the pattern to the user with the most similar biometric model. Thus, the user is identified without the need for extra information.

## 4 Case Study

The system was analyzed and tested in four different ways. As a first step we used the records of 40 users registered in the monitoring system to train different models. The created models were then validated through 150 random system usage records, taken from the system in order to validate the models created. In a second step models were created using the type of task to be performed in addition to the biometric information, and in the third step, models were trained using the user's fatigue state. We finally created models that, in addition to using biometric data, also used the type of task and the user's mental state at the time of registration. Both the type of task as the user's mental state are provided by the monitoring system.

The participants, forty in total (36 men, 4 women) which are registered in the monitoring system. Their age ranged between 18 and 45. The following requirements were established to select, among all the volunteers, the ones that participated: (1) familiarity and proficiency with the use of the computer; (2) use of the computer on a daily basis and throughout the day; (3) owning at least one personal computer.

### 4.1 Results and Discussion

After training different models (Naive Bayes, KNN, SVM and Random Forest) with data from different users on the system, different degrees of accuracy have been obtained in user identification, as depicted in Figure 1. It is also possible to observe that the type of task and the level of fatigue have influence on the process of identifying the user, since these factors effectively influence interaction patterns. Taking this information into consideration allows the creation of more accurate models.

The type of task being carried out during the monitoring of the interaction patterns is particularly important, mainly due to the very nature of the task, as well as the set of tools available to perform the task. Figure 2 shows the values of features Key Down Time and Average Excess of Distance for five different types of applications: Chat, Leisure, Office, Reading and Programming. The way each different application conditions the interaction behavior is explicit. Such information must, therefore, absolutely be considered while developing behavioral biometrics system based on input behavior. Table 2 further supports this claim showing that data collected in different types of applications has statistically

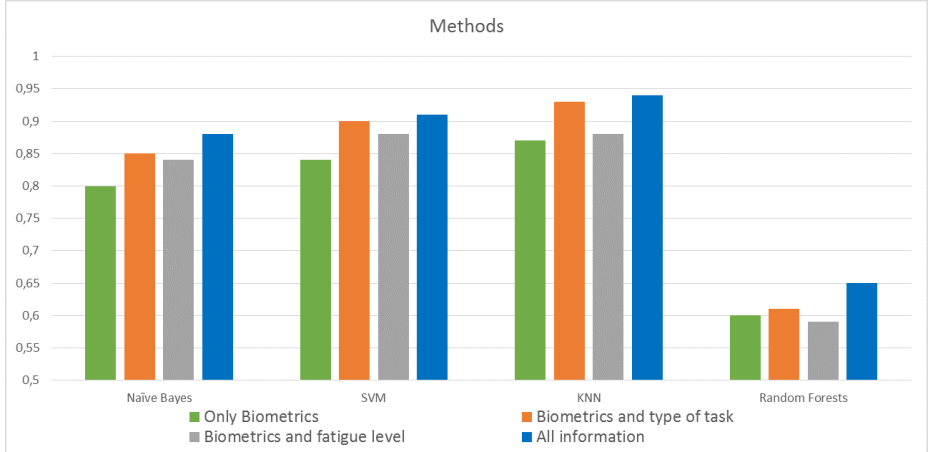


**Fig. 1.** Accuracy of the different algorithms and inputs considered for user authentication.

**Table 2.** *p*-values of the Kruskal-Wallis test when comparing the data organized according to the types of application and to the level of fatigue. In the vast majority of the cases, the differences between the different groups are statistically significant.

Features	Applications	Fatigue
Writing Velocity	4.4e-15	0.43
Time Between Keys	<2.2e-16	<2.2e-16
Key Down Time	<2.2e-16	3.8e-14
Distance of the Mouse to the SL	0.01	<2.2e-16
Mouse acceleration	<2.2e-16	1.3e-09
Average Distance of the Mouse to the SL	0.03	<2.2e-16
Mouse velocity	<2.2e-16	<2.2e-16
Average Excess of Distance	0.04	1.6e-08
Time Between Clicks	<2.2e-16	<2.2e-16
Distance During Clicks	<2.2e-16	0.05
Total Excess of Distance	0.22	<2.2e-16
Double Click Duration	1.0e-4	<2.2e-16
Absolute Sum of Angles	8.1e-3	2.5e-13
Signed Sum of Angles	0.91	<2.2e-16
Distance between clicks	0.06	<2.2e-16

significant differences for most of the features. The same happens for different levels of fatigue.

Another extremely important aspect in user identification is the influence of mental states on interaction patterns. Previous studies by our research team [8, 15] show that individuals under different states of stress, fatigue, high/low mental workload or even mood evidence significant behavior changes that impact interaction patterns with devices. They do, consequently, influence behavioral

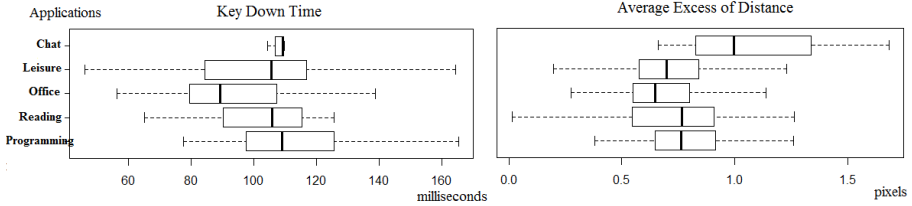


**Fig. 2.** Differences in the distributions of the data when comparing interaction patterns with different applications, for two interaction features.

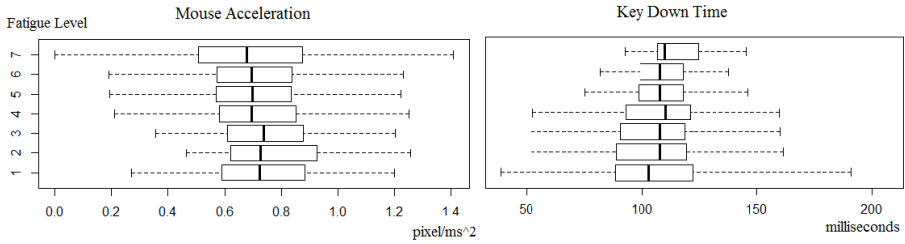


**Fig. 3.** Effects of different levels of fatigue on the interaction patterns, depicted for two different features.

biometric features. Figure 3 depicts this influence for two interaction features. Numbers in the y-axis represent the level of fatigue as self-reported by the individual using the seven-point USAFSAM Mental Fatigue Scale questionnaire [16]. Each value represents the following state:

1. Fully alert. Wide awake. Extremely peppy.
2. Very lively. Responsive, but not at peak.
3. Okay. Somewhat fresh.
4. A little tired. Less than fresh.
5. Moderately tired. Let down.
6. Extremely tired. Very difficult to concentrate.
7. Completely exhausted. Unable to function effectively. Ready to drop.

It is therefore possible to see how increased levels of fatigue result in generally less efficient interactions of the participants with the computer. For example, a higher value of the Mouse Acceleration depicts a more efficient interaction behavior in which the user is moving the mouse. The same happens with Key Down Time, where a shorter time corresponds to a more efficiency in the use of the keyboard.

This conclusion justifies the need for the inclusion of mental states on behavioral biometrics approaches and explains the increased accuracy of the presented approach concerning user identification when all modalities are used jointly: interaction patterns, user state and type of application, as depicted previously in Figure 1.

## 5 Conclusions and Future Work

This paper describes a non-invasive and non-intrusive approach to the field of behavioral biometrics. Specifically, we described a system that, transparently, acquires interaction features from keystroke dynamics and mouse dynamics, with the purpose of user identification. We analyzed the significant effect that mental states have on interaction patterns, particularly fatigue, to conclude that these aspects must be considered when developing identification systems based on interaction patterns. Likewise, we also show how user interaction significantly changes according to the application being used.

These notions support the claim put forward in this paper that accurate user identification approaches based on behavioral biometrics must absolutely include these aspects when building user profiles. That much is evidenced by our results. In all four classification algorithms used for user identification, the cases in which all these types of information are used together outperform the others.

Moreover, the proposed approach is also concerned with user privacy. Specifically, it is based not on *what* the user inputs but on *how* the user inputs. To this end it conceals each key under an encryption key that prevents remote services from knowing what the user typed. The data gathered from users thus respects their privacy while allowing to extract the necessary features for the system to carry out its task, i.e., to detect unauthorized accesses.

In future work we will focus on including additional user features, namely in what concerns user state. Specifically, we will include information regarding the user's level of stress, which we have already determined in previous work to significantly influence interaction patterns with technological devices. In the long-term we will include more potentially interesting features, namely the user's mood. It is our conviction that this kind of information, when available, can significantly increase the accuracy of user identification in behavioral biometrics approaches.

**Acknowledgments.** This work is part-funded by ERDF - European Regional Development Fund through the COMPETE Programme (operational programme for competitiveness) and by National Funds through the FCT (Portuguese Foundation for Science and Technology) within project FCOMP-01-0124-FEDER-028980 (PTDC/EEI-SII/1386/2012) and project PEst-OE/EEI/UI0752/2014.

## References

1. Tanabe, S., Nishihara, N.: Productivity and fatigue. *Indoor Air* **14**(s7), 126–133 (2004)
2. Miller, J.C.: Cognitive Performance Research at Brooks Air Force Base, Texas, 1960–2009. Smashwords, March 2013

3. Wainwright, D., Calnan, M.: Work stress: the making of a modern epidemic. McGraw-Hill International (2002)
4. Folkard, S., Tucker, P.: Shift work, safety and productivity. *Occupational Medicine* **53**(2), 95–101 (2003)
5. Rosekind, M.R.: Underestimating the societal costs of impaired alertness: safety, health and productivity risks. *Sleep Medicine* **6**, S21–S25 (2005)
6. Beauvisage, T.: Computer usage in daily life. In: Proceedings of the SIGCHI conference on Human Factors in Computing Systems, pp. 575–584. ACM (2009)
7. Pantic, M., Rothkrantz, L.J.: Toward an affect-sensitive multimodal human-computer interaction. *Proceedings of the IEEE* **91**(9), 1370–1390 (2003)
8. Pimenta, A., Carneiro, D., Novais, P., Neves, J.: Monitoring mental fatigue through the analysis of keyboard and mouse interaction patterns. In: Pan, J.-S., Polycarpou, M.M., Woźniak, M., de Carvalho, A.C.P.L.F., Quintián, H., Corchado, E. (eds.) HAIS 2013. LNCS, vol. 8073, pp. 222–231. Springer, Heidelberg (2013)
9. Carneiro, D., Castillo, J.C., Novais, P., Fernández-Caballero, A., Neves, J.: Multi-modal behavioral analysis for non-invasive stress detection. *Expert Systems with Applications* **39**(18), 13376–13389 (2012)
10. Lee, P.M., Chen, L.Y., Tsui, W.H., Hsiao, T.C.: Will user authentication using keystroke dynamics biometrics be interfered by emotions?-nctu-15 affective keyboard typing dataset for hypothesis testing
11. Al-Zubi, S., Brömmе, A., Tönnies, K.D.: Using an active shape structural model for biometric sketch recognition. In: Michaelis, B., Krell, G. (eds.) DAGM 2003. LNCS, vol. 2781, pp. 187–195. Springer, Heidelberg (2003)
12. Brömmе, A., Al-Zubi, S.: Multifactor biometric sketch authentication. In: BIOSIG, pp. 81–90 (2003)
13. Pimenta, A., Carneiro, D., Novais, P., Neves, J.: Analysis of human performance as a measure of mental fatigue. In: Polycarpou, M., de Carvalho, A.C.P.L.F., Pan, J.-S., Woźniak, M., Quintian, H., Corchado, E. (eds.) HAIS 2014. LNCS, vol. 8480, pp. 389–401. Springer, Heidelberg (2014)
14. Shanmugapriya, D., Padmavathi, G.: A survey of biometric keystroke dynamics: Approaches, security and challenges (2009). arXiv preprint [arXiv:0910.0817](https://arxiv.org/abs/0910.0817)
15. Rodrigues, M., Gonçalves, S., Carneiro, D., Novais, P., Fdez-Riverola, F.: Keystrokes and clicks: measuring stress on E-learning students. In: Casillas, J., Martínez-López, F.J., Vicari, R., De la Prieta, F. (eds.) Management Intelligent Systems. AISC, vol. 220, pp. 119–126. Springer, Heidelberg (2013)
16. Samn, S.W., Perelli, L.P.: Estimating aircrew fatigue: a technique with application to airlift operations. Technical report, DTIC Document (1982)

# Including Emotion in Learning Process

Ana Raquel Faria<sup>1(✉)</sup>, Ana Almeida<sup>1</sup>, Constantino Martins<sup>1</sup>,  
Ramiro Gonçalves<sup>2</sup>, and Lino Figueiredo<sup>1</sup>

<sup>1</sup> GECAD - Knowledge Engineering and Decision Support Research Center Institute of Engineering, Polytechnic of Porto (ISEP/IPP), Porto, Portugal  
`{arf, amn, acm, lbf}@isepp.ipp.pt`

<sup>2</sup> Universidade de Trás-Os-Montes E Alto Douro, Vila Real, Portugal  
`ramiro@utad.pt`

**Abstract.** The purpose of this paper is to propose new architecture that includes the student's, learning preferences, personality traits and emotions to adapt the user interface and learning path to the students need and requirements. This aims to reduce the difficulty and emotional stain that students encounter while interacting with learning platforms.

**Keywords:** Learning styles · Student modeling · Adaptive systems · Affective computing

## 1 Introduction

Human to human communication depends on the interpretation of a mix of audio-visual and sensorial signals. To simulate the same behaviour in a human-machine interface the computer has to be able to detect affective state and behaviour alterations and modify its interaction accordingly. The field of affective computing develops systems and mechanisms that are able to recognize, interpret and simulate human emotions [1] so closing the gap between human and machine. Affective Computing concept was introduced by Rosalind Picard in 1995 as a tool to improve human-machine interfaces by including affective connotations.

Emotion plays an important role in the decision process and knowledge acquisition of an individual. Therefore, it directly influences the perception, the learning process, the way people communicate and the way rational decisions are made. So the importance of understanding affects and its effect on cognition and in the learning process. To understand how the emotions influence the learning process several models were developed. Models like Russell's Circumplex model [2] are used to describe user's emotion space and Kort's learning spiral model [3] are used to explore the affective evolution during learning process.

In a traditional learning context the teacher serves as a facilitator between the student and his learning material. Students, as individuals, differ in their social, intellectual, physical, emotional, and ethnic characteristics. Also, differ in their learning rates, objectives and motivation turning, their behaviour rather unpredictable. The teacher has to perceive the student state of mind and adjust the teaching process to the student's needs

and behaviour. In a learning platform this feedback process does not take place in real time and, sometimes it is not what the student requires to overcome the problem at hand. This overtime can become a major problem and cause difficulties to the student learning process. A possible solution to this problem could be the addition of mechanisms, to the learning platforms, that enable computers to detect and interfere when the student requires help or motivation to complete a task. The major difficulties of this work will be the detection of these situations and how to interfere. The method of detection cannot be too intrusive, because that would affect the student behaviour in a negative way that would cause damage to his learning process. Another important issue is the selection of the variable to monitor. This can include the capture of emotions, behaviour or learning results among others. Finally, determining which will be the computer intervention when a help situation is detected in order to reverse the help situation.

## 2 EmotionTest Prototype

In order to prove that emotion can have influence in the learning process. A prototype (EmotionTest) was developed, a learning platform that takes into account the emotional aspect, the learning style and the personality traits, adapting the course (content and context) to the student needs. The architecture proposed for this prototype is composed of 4 major models: the Application Model, Emotive Pedagogical Model, Student Model, and Emotional Model [4], as shown in the figure bellow.

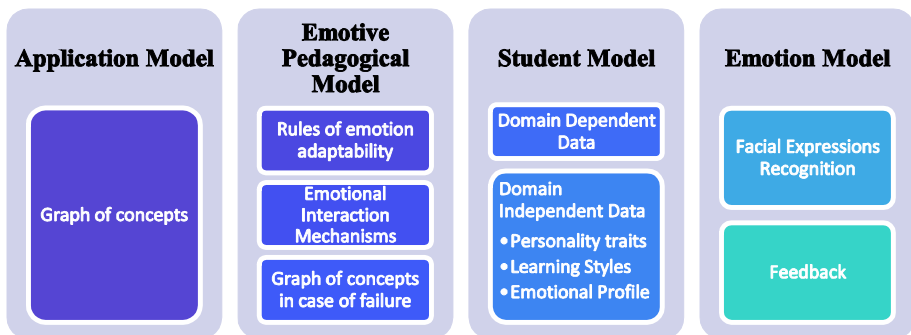


**Fig. 1.** Architecture

The student model consists in the user information and characteristics. This includes personal information (name, email, telephone, etc.), demographic data (gender, race, age, etc.), knowledge, deficiencies, learning styles, emotion profile, personality traits, etc. This information is used by the student model to better adapt the prototype to student [4].

The emotion model gathers all the information the facial emotion recognition software and feedback of the students. Facial Expression Recognition allows video analysis of images in order to recognise an emotion. This type of emotion recognition was

chosen because it was the least intrusive with the student activities. The emotion recognition is achieved by making use of an API entitled ReKognition [5]. This API allows detection of the face, eyes, nose and mouth and if the eyes and mouth are open or close. In addition specifies the gender of the individual and an estimate of age and emotion. In each moment a group of three emotions is captured. For each emotion is given a number that shows the confidence level of the emotion captured.

The application model is composed by a series of modules contain different subjects. The subject consist in a number steps that the student has to pass in order to complete is learning program. Usually each subject is composed by a Placement test in order to access and update the student level of knowledge. Followed by the subject content in which the subject is explained and follow by the subject exercises and final test. The first step is the subject's Placement Test (PT) that can be optional. This is designed to give students and teachers a quick way of assessing the approximate level of student's knowledge. The result of the PT is percentage PTs that is added to the student knowledge ( $K_s$ ), on a particular subject, and places the student at one of the five levels of knowledge  $k_{pt} = \sum_{i=0}^5 exercise_i$ . If the PT is not performed  $K_{sp}$  will be equal to zero and the student will start with any level of knowledge. The Subject Content (SC) contains the subject explanation. The subject explanation depends on the stereotype. Each explanation will have a practice exercise. These exercises will allow the students to obtain points to perform the final test of the subject. The student needs to get 80% on the Total $K_{sc}$  to undertake the subject test. The Subject Test (ST) is the assessment of the learned subject. This will give a final value  $K_{st}$  that represents the student's knowledge on the subject,  $k_{st} = \sum_{i=0}^5 exercise_i$ . Only if the  $k_{st}$  is higher than 50% it can be concluded that the student has successfully completed the subject. In this case the values of the  $K_{sp}$  and  $K_{st}$  are compared to see if there was an effective improvement on the student's knowledge. This is represented in the following diagram [6].

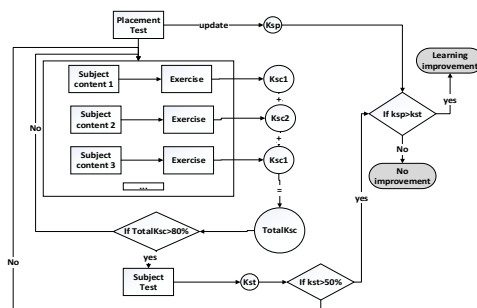


**Fig. 2.** Representation diagram

The last model is the emotive pedagogical model that is composed by three sub-models: the rules of emotion adaptability, the emotional interaction mechanisms and the graph of concepts in case of failure.

The Rules of Emotion Adaptability manage the way the subject content is presented. The subject content is presented according the student's learning preference

and personality. This way information and exercises are presented in a manner more agreeable to the student helping him to comprehend the subject at hand.

The subject content and subject exercises are presented according the learning style and personality of the student. The emotional interaction mechanisms consist in the trigger of an emotion interaction when is captured an emotion that need to be contradicted in order to facilitate the learning process. The emotions to be contradicted are: anger, sadness, confusion and disgusted. The interaction can depend on the personality and on the learning style of the student. Finally the graph of concepts in case of failure this indicates the steps to be taken when a student fails to pass a subject. The graph of concepts in case of failure represents the steps to be taken when fail to surpass a subject. To be approved in a subject the whole the tasks must be completed, and only with a subject completed it is possible to pass to the next. Inside of a subject the student has to complete the placement test, the subject content plus exercises with a grade equal or higher than 80% and the subject test with approval with a grade higher than 50% to complete the subject. In case of failure it has to go back to the subject content and repeat all the steps [6].

### **3 Data Analysis**

To test the performance of the developed prototype some experiences were carried out with students from two ISEP Engineering courses: Informatics Engineering and Systems Engineering. The total number of students involved in these tests was 115 with ages between 17 and 42 years old. This group of students was composed of 20% female (n=23) and 80% male (n=92), the participants were mainly from the districts of Oporto, Aveiro and Braga.

To assess validity of the prototype the students were divided in two groups, v1 and v2. Group v1 tested the prototype with emotional interaction and group v2 without any emotional interaction.

Group v1 had to accomplish a diagnostic test (in paper) to help grade the student initial knowledge level, followed by the evaluation of the prototype with the emotional interaction and learning style. This would include, the login into the prototype, at this moment is when the initial data is begins to be collected for the student model. By accessing the school's Lightweight Directory Access Protocol (LDAP) one was able to gather the generic information of the students (like name, email and other). After login the students were required to answer two questionnaires (TIPI, VARK) build into the prototype. This allows the prototype to known the student's personality traits and learning preferences. Afterward the student could assess the learning materials and exercises. From the moment the student login his emotion state has been monitor and saved and every time that is detected an emotion that triggers an intervention it would appear on the screen. After this evaluation the students had to complete a final test (in paper) to help grade the student final knowledge level [7].

Group v2 had to accomplish diagnostic test (in paper) to help grade the student initial knowledge level, followed by the prototype evaluation without any emotional interaction. This evaluation is in all similar to group v1, but with one big difference. Even though the emotional state is monitor, when is detected an emotion that triggers

an intervention it would not appear on the screen. After this test the students had to complete a final test (in paper) to help grade the student final knowledge level [7].

Analyzing the data of evaluation test, for group v3 for diagnostic test it has a mean of 45,7% ( $SD = 40,3$ ) and for the final test a mean of 85,7% ( $SD = 12,2$ ) and for group v4 for diagnostic test it has a mean of 37,1% ( $SD = 29,2$ ) and for the final test a mean of 61,4% ( $SD = 33,7$ ). The data gathered did not have a normal distribution so the two groups were compared using a non-parametric test Mann-Whitney. The diagnostic test has a Mann-Whitney  $U = 83,0$  and for a sample size of 14 students. For this analysis it was found a P value of 0,479 which indicates that it doesn't have any statistical difference which is understandable because it was assumed that all students had more or less the same level of knowledge. The final test it has a Mann-Whitney  $U = 54,0$  and for an equal sample size of the diagnostic test. For this analysis it was found a P value of 0,029 in this case the differences observed are statistical different. In addition, a series of tests were made to compare the means values of the students by group and by learning preference, by group and personality and by group and emotional state. The objective of running these tests was to find out if learning preference, personality and emotional state had any influence on the outcome of the final test. In relation to the first two tests, by learning preference and by personality, no statistically significant differences were found in the data. Therefore it cannot be concluded that learning preference and personality in each group had any influence in the final test outcome. To prove this assumption it is needed a larger sample size. For the question "if the emotional state had any influence in the in the final test", the differences observed were statistical significant [7].

## 4 Conclusion

In conclusion, with this work was attempted to answer several questions. The central question that guided this work was: "Does a learning platform that takes into account the student's emotions, learning preferences and personality improve the student's learning results?"

The gathered data from the performed test showed that there is a statistical difference between students' learning results while using two learning platforms: one learning platform that takes into account the student's emotional state and the other platform that does not have that in consideration. This gives an indication that by introducing the emotional component, the students' learning results can possibly be improved. Another question was: "Does Affective computing technology help improving a student learning process?"

In answering positively to the central question, this question is partly answered. As results showed, the students' learning results can be improved by adding an emotional component to a learning platform; also the use of Affective Computing technology to capture emotion can enhance this improvement. The use Affective Computing allows the capture of the student's emotion by using techniques that don't inhibit the student's actions. Also, it can be used one or more techniques simultaneously to help verify the accuracy of the emotional capture. The last question was: "What are the stimuli that can be used to induce or change the student state of mind in order to improve the learning process?"

First, the results indicate that the platform with an emotional component had an overall set of more positive emotions than the platform without this component. Showing that, the stimuli produced in the platform with an emotional component was able to keep the students in a positive emotional state and motivated to do the tasks at hand, this did not happen in the platform without this component.

Second the results demonstrated that the platform with an emotional component not only got the set of more positive emotions among the students, but also obtained an improvement in the students learning results.

**Acknowledgments.** This work is supported by FEDER Funds through the “Programa Operacional Factores de Competitividade - COMPETE” program and by National Funds through FCT “Fundação para a Ciência e a Tecnologia” under the project: FCOMP-01-0124-FEDER-PEst-OE/EEI/UI0760/2014.

## References

1. Picard, R.W., Papert, S., Bender, W., Blumberg, B., Breazeal, C., Cavallo, D., Machover, T., Resnick, M., Roy, D., Strohecker, C.: Affective learning - a manifesto. *BT Technol. J.* **22**(4), 253–268 (2004)
2. Russell, J.A.: A circumplex model of affect. *J. Pers. Soc. Psychol.* **39**(6), 1161–1178 (1980)
3. Kort, B., Reilly, R., Picard, R.W.: An affective model of interplay between emotions and learning: re-engineering educational pedagogy-building a learning companion. In: Proc. - IEEE Int. Conf. Adv. Learn. Technol. ICALT 2001, pp. 43–46 (2001)
4. Faria, A., Almeida, A., Martins, C., Lobo, C., Gonçalves, R.: Emotional Interaction Model For Learning. In: INTED 2015 Proc., pp. 7114–7120 (2015)
5. orbe.us | ReKognition - Welcome to Rekognition.com (2015) (Online). <http://rekognition.com/index.php/demo/face> (accessed: 26-Jul-2014)
6. Faria, A.R., Almeida, A., Martins, C., Gonçalves, R.: Emotional adaptive platform for learning. In: Mascio, T.D., Gennari, R., Vittorini, P., de la Prieta, F. (eds.) *Methodologies and Intelligent Systems for Technology Enhanced Learning*. AISC, vol. 374, pp. 9–16. Springer, Heidelberg (2015)
7. Faria, R., Almeida, A., Martins, C., Gonçalves, R.: Learning Platform. In: 10th Iberian Conference on Information Systems and Technologies – CISTI 2015 (2015)

# Ambient Intelligence: Experiments on Sustainability Awareness

Fábio Silva<sup>(✉)</sup> and Cesar Analide

Algoritmi Centre, University of Minho, Braga, Portugal  
`{fabiosilva, analide}@uminho.pt`

**Abstract.** Computer systems are designed to help solve problems presented to our society. New terms such as computational sustainability and internet of things present new fields where traditional information systems are being applied and implemented on the environment to maximize data output and our ability to understand how to improve them. The advancement of richer and interconnected devices has created opportunities to gather new data sources from the environment and use it together with other pre-existent information in new reasoning processes. This work describes a sensorial platform designed to help raise awareness towards sustainability and energy efficient systems by exploring the concepts of ambient intelligence and fusion of data to create monitoring and assessment systems. The presented platform embodies the effort to raise awareness of user actions on their impact towards their sustainability objectives.

**Keywords:** Ambient intelligence · Pervasive systems · Sustainability · Energy efficiency

## 1 Introduction

The advent of computer science and its evolution led to the availability of computational resources that can better assess and execute more complex reasoning and monitoring of sustainability attributes. This led to the creation of the field of computational sustainability (Gomes, 2011). Coupled with sustainability is energy efficiency which is directly affected by human behaviour and social aspects such as human comfort. Fundamentally, efficiency deals with the best strategy to obtain the objectives that are set, however, when the concept of sustainability is added, several efficient plans might be deemed unsustainable because they cannot be maintained in the future.

While efficiency is focused on optimization, sustainability is mostly concerned on restrictions put in place to ensure that the devised solution does not impair the future. Not only, context hardens the problem but also the possibility of missing information which might occur due to same unforeseen event that jeopardizes an efficient solution. To tackle such event, computational systems are able to maintain sensory networks over physical environments to acquire contextual information so it can validate the conditions for efficient planning but also acquire information and, as a last resort, act upon the physical environment.

## 2 Related Work

The term computational sustainability is used by researchers such as Carla Gomes (Gomes, 2011) to define the research field where sustainability problems are addressed by computer science programs and models in order to balance the three dimensions of sustainability: economic, ecologic and social dimensions.

It is accepted that the world ecosystem is a complex sustainability problem, affected by human and non-human actions. Despite the use of statistical and mathematical models for the study of sustainability and computational models to address problems of environmental and societal sustainability, the term computational sustainability appeared around 2008. Nevertheless, the pairing between computer science and the study of sustainability is as old as the awareness of sustainability and as long as computing was available. It is a fact that, as computational power capacity increased over time, so did the complexity and length of the models used to study sustainability. The advent and general availability of modern techniques from artificial intelligence and machine learning allowed better approaches to the study of each dimension of sustainability and their overall impact for sustainability.

The types of sensors used in the environment may be divided into categories to better explain their purpose. In terms of sensing the environment, sensors can be divided into sensors that sense the environment or users and their activities. Generally, an ambient might be divided in sensors and actuators. Sensors monitor the environment and gather data useful for cognitive and reasoning process. On the other hand, actuators take action upon the environment performing actions such as thermostats to control the temperature, lightning switches or other appliances.

Different methodologies and procedures exist to keep track of human activities and to make prediction based on previous and current information gathered in these environments. Common approaches with machine learning techniques involve the use of neural networks, classification techniques, fuzzy logic, sequence discovery, instance based learning and reinforced learning as in (Costa, Novais &, Simões, 2014).

An approach to this problem using fuzzy logic algorithms is proposed by Hagras et al (Hagras, Doctor, Callaghan, & Lopez, 2007). Sequence discovery approach is at the heart of learning algorithm in (Aztiria, Augusto, Basagoiti, Izaguirre, & Cook, 2012), which demonstrates a system that can learn user behavioural patterns and take proactive measures accordingly.

The work presented considers the use of these types of sensor to assess and reason about sustainability and indicator design. This information will then be used to reason about user behaviour and their accountability.

## 3 Platform Engine

The focus of this project is, more than developing new procedures or algorithms to solving problems, putting these innovations on the hand of the user, with a clear purpose: that these innovative tools should be guided to assist people in the context of energetic sustainability.

### 3.1 Network Design

The PHESS platform supports heterogeneous devices by implementing middleware upon groups of devices to control data and information acquisition. Local central servers are viewed as decentralized by the platforms which access them to obtain data and implement their plans through the local network actuators.

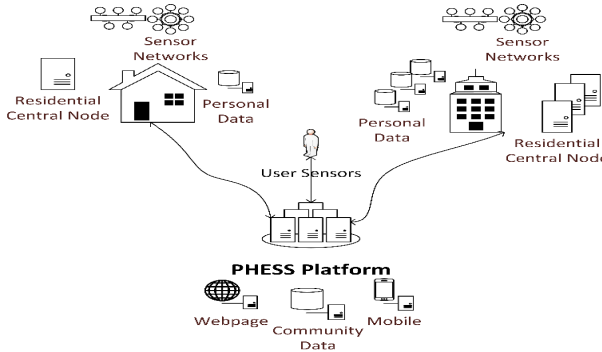


**Fig. 1.** Generic PHESS platform configuration.

Figure 1, details a generic composition of two different environment scenarios with users and their connection to PHESS platform. This residential central node is responsible for the middleware to connect local sensor networks to the PHESS platform using dedicated protocols for data acquisition and storing information.

The data gathered is summarized locally according to time and user presence models and synchronized with the central PHESS platform. It is also responsible for creating different user and environment profiles. Notifications are generated by the central PHESS platform to the project webpage or mobile application.

### 3.2 Data Fusion

The process of data fusion is handled by local central nodes where data is submitted to data fusion process according to the number of overlapping and complementing sensors. In this regard, there are strategies that can be followed according to the context and nature of the fusion process.

The first one is a weighted average of values, for the same type of sensors in the same context to get an overview of an attribute with multiple sensors to reduce measurement errors. The weights are defined manually by the local administrator. More sophisticated fusion is employed with complementary sensors which according to some logic defined into the system measure an attribute by joining efforts such as user presence with both RFID reader and wireless connection of personal devices such as smartphones. The last resource is the use of heterogeneous data to create attributes with some level of knowledge from the start. An example is the assessment of thermal comfort using default indicator expressed as mathematical formulae such as the PMV

index (Fanger, 1970) for instance. Other application is the definition of sustainable indicators according to custom mathematical formulae in the platform that shall process some attributes in the system to make their calculation.

The configuration of data fusion steps, the selection of sensors and streams of data is made on the initial step of the system by the local administrator. According to each area of interest and with specialized knowledge obtained by experts it is possible to monitor relevant information to build sustainable indicators.

### 3.3 Sustainability Indicators Generation

Indicators evaluate sustainability in terms of three main groups, namely economic, environmental and social. However, due to their impact, some indicators can be designed to influence more than one dimension of sustainability. For this reason it was chosen to have these indicators as the general analysis of sustainable principles instead of sustainability dimensions. In order to be directly comparable indicators are defined to use the same scale, and are based on the notion of positive and negative impact. The values of each indicator range from -1 to 1 and can be interpreted as unsustainable for values below zero and sustainable from there upwards.

Indicator definition is another configurable space inside the PHESS platform where monitoring indicators are defined using values from sensors and sensor fusion, and customized with mathematical formulas. All these indicators are calculated either locally, i.e., in a room basis, or they are evaluated for the entire setting which sums assessment of all different rooms. In this way, even if the environment is considered sustainable, the user may still assess changes in premises with low supportable standards. Environments are generally hosts to of many different users, which influence it with their behaviours, actions and habits. Tracking user activities is something that can be used to infer and establish cause and effect relationships. The PHESS system uses different dynamics to produce accountability reports on user actions based on environment and personal monitoring coupled user presence detection. Areas unoccupied, are considered the responsibility of all people present in the environment, so that the coverage of the entire environment is assured by its occupants. In cases where the local context and local sensor values are indistinguishable based on location them, user accountability takes in consideration only user presence in the environment. The richer the environment is in sensor data acquisition the richer results and analysis is.

## 4 Case Study and Results

As a case study, results from five days in an environment are presented. In this case a home environment with a limited set of sensors, and a smartphone as a user detection mechanism. User notifications are made by actuator modules which push notifications to users in order to alert them based on notification schemes and personal rules. Sensors include electrical consumption, temperature, humidity, luminosity and presence sensing through smartphones and an indicator based on the sensation of temperature PMV used in thermal comfort studies (Rana, Kusy, Jurdak, Wall, & Hu, 2013).

The indicators are designed in the platform in order to perceive energy efficacy and as such the case scenario uses electricity to do this analysis. Therefore, a list of sample indicator was defined using data fusion available through PHESS modules. A sample of four indicators were defined and their expression is as follows:

- Unoccupied consumption – measures the deviation of consumption when no user is present in the environment from a user inputted objective.
- Activity based consumption - measures the deviation of consumption during the period of 1 hour from the objective value set by the user, in this case;
- Total consumption: measures the deviation of total consumption during the period of a day based on a default value defined for consumption;
- Comfort Temperature – based on the PMV comfort indicator obtained through data fusion process which is calculated by PHESS platform;
- Comfort Humidity – based on comfort values that define the normal range of values humidity in indoor environments.

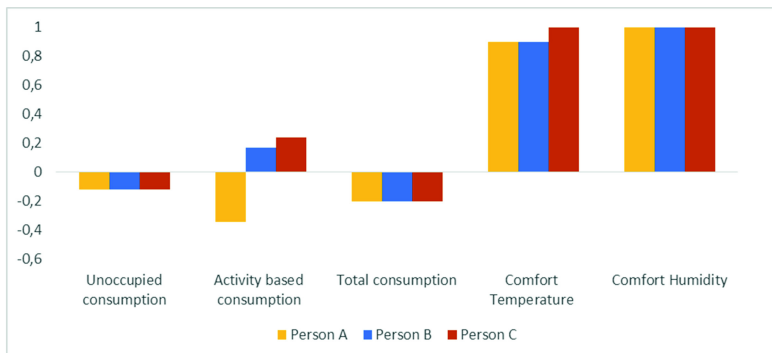


**Fig. 2.** Indicator values from the PHESS platform

As seen in figure 3, with the graphical representation of the indicators it is possible to analyse the behaviour of an environment based on user inputted indicators. These indicators are represented in the scale -1 to 1 as stated in section 3.4. While comfort values are being respected, consumption based indicator shows that the values set for the system are not yet being followed. As a result, indicators towards consumption analysis are performing below the accepted margin.

Accountability is based on the notion of user impact on the system. Results indicate a higher consumption when the environment is not occupied which demonstrates that the environment configuration has more impact than user actions. The person the longest in the environment each day has more impact towards the total consumption which is inputted to user actions.

This analysis allows the system to identify people with most impact on the system based on the attributes and indicators defined. There is the need to adapt each indicator set to the objectives and the areas to improve, but the generic platform allows for this configuration based on the layers of the PHESS platform.

## 5 Conclusions

Computational sustainability, although a new and interesting topic of research to the academic community, still presents a number of difficult challenges. The platform presented is the combination of modules which take inspiration from ambient intelligence and information systems to provide analysis and assessment of environment and their users, to identify and provide real time analysis of concepts based on sustainability and efficiency. Results indicate that modest configurations can yield meaningful results that may be used to take actions on the environment and user behaviour. The process of data fusion and indicator design are responsible to thoroughly analyse key situation of environment and user behaviour so they expression appears meaningful to produce not only user reports but also user suggestions.

With the mainstream use of interconnected appliances the possibilities for automatic actuation are increasing, mainly with the new internet of things standards being proposed by major companies. The PHESS project aim to increase its support by adding new features to their middleware layer and allow actuation in conjunction with sensorization. Moreover, it is expected to support multi environments for each user, increasing accountability to user behaviours regardless of location.

**Acknowledgements.** This work is part-funded by ERDF - European Regional Development Fund through the COMPETE Programme (operational programme for competitiveness) and by National Funds through the FCT (Portuguese Foundation for Science and Technology) within project FCOMP-01-0124-FEDER-028980 (PTDC/EEI-SII/1386/2012) and project PEst-OE/EEI/UI0752/2014.. Additionally, it is also supported by a doctoral grant, with the reference SFRH/BD/78713/2011, issued by FCT.

## References

1. Aztiria, A., Augusto, J.C., Basagoiti, R., Izaguirre, A., Cook, D.J.: Discovering frequent user-environment interactions in intelligent environments. *Personal and Ubiquitous Computing* **16**(1), 91–103 (2012)
2. Fanger, P.O.: Thermal comfort: Analysis and applications in environmental engineering. Danish Technical Press (1970)
3. Gomes, C.P.: Computational sustainability. In: Gama, J., Bradley, E., Hollmén, J. (eds.) IDA 2011. LNCS, vol. 7014, p. 8. Springer, Heidelberg (2011). <http://citeseerx.ist.psu.edu/viewdoc/download?doi=10.1.1.158.2293&rep=rep1&type=pdf>
4. Hagras, H., Doctor, F., Callaghan, V., Lopez, A.: An Incremental Adaptive Life Long Learning Approach for Type-2 Fuzzy Embedded Agents in Ambient Intelligent Environments. *IEEE Transactions on Fuzzy Systems* **15**(1), 41–55 (2007)
5. Rana, R., Kusy, B., Jurdak, R., Wall, J., Hu, W.: Feasibility analysis of using humidex as an indoor thermal comfort predictor. *Energy and Buildings* **64**, 17–25 (2013). doi:10.1016/j.enbuild.2013.04.019
6. Costa, A., Novais, P., Simões, R.: A Caregiver Support Platform within the Scope of an AAL Ecosystem. *Sensors* **14**(3), 654–5676 (2014). MDPI AG, ISSN: 1424-8220

# **Artificial Intelligence in Medicine**

# Reasoning with Uncertainty in Biomedical Models

Andrea Franco, Marco Correia, and Jorge Cruz<sup>(✉)</sup>

NOVA Laboratory for Computer Science and Informatics,  
DI/FCT/UNL, Caparica, Portugal  
[jcrc@fct.unl.pt](mailto:jcrc@fct.unl.pt)

**Abstract.** The use of mathematical models in biomedical research largely developed in the second half of the 20th century. However, their translation to clinically useful tools has proved challenging. Reasoning with deep biomedical models is computationally demanding as parameters are typically subject to nonlinear relations, dynamic behavior, and uncertainty. This paper proposes a new approach for assessing the reliability of the conclusions drawn from these models given the underlying uncertainty. It relies on probabilistic constraint programming for a sound propagation of uncertainty from model parameters to results. The advantages of the approach are illustrated on an important problem in the obesity research field, namely the estimation of free-living energy intake in humans. Based on a well known energy intake model, our approach is able to correctly characterize the provided estimates given the uncertainty inherent to the model parameters.

**Keywords:** Biomedical models · Constraint programming · Energy intake

## 1 Introduction

Mathematical models are extensively used in many biomedical domains for supporting rational decisions. A mathematical model describes a system by a set of variables and constraints that establish relations between them. Uncertainty and nonlinearity play a major role in modeling most real-world continuous systems. A competitive framework for decision support in continuous domains must provide an expressive mathematical model to represent the system behavior and be able to perform sound reasoning that accounts for the uncertainty and the effect of nonlinearity.

Given the uncertainty, there are two opposite attitudes for reasoning with scenarios consistent with the mathematical model. Stochastic approaches [1] reason on approximations of the most likely scenarios. They associate a probabilistic model to the problem thus characterizing the likelihood of the different scenarios. In contrast, constraint programming approaches [2] reason on safe enclosures of all consistent scenarios. Rather than associate approximate values

to real variables, intervals are used to include all their possible values. Model-based reasoning and what-if scenarios are adequately supported through safe constraint propagation techniques, which only eliminate combinations of values that definitely do not satisfy model constraints.

In this work we use a probabilistic constraint approach that combines a stochastic representation of uncertainty on the parameter values with a reliable constraint framework robust to nonlinearity. Similarly to stochastic approaches it associates an explicit probabilistic model to the problem, and similarly to constraint approaches it assumes reliable bounds for the model parameters. The approach computes conditional probability distributions of the model parameters, given the uncertainty and the constraints.

The potential of our approach to support clinical practice is illustrated in a real world problem from the obesity research field. The impact of obesity on health, at both individual and public levels, is widely documented [3–5]. Despite this fact, and the availability of nutritional recommendations and guidelines to the general audience, the prevalence of overweight and obesity in adults and children increased dramatically in the last 30 years [6]. According to the World’s Health Organization, the main cause for the “obesity pandemics” is the energy unbalance caused by an increased calorie intake associated to a lower energy expenditure as a result of a sedentary lifestyle.

Many biomedical models use the energy balance approach to simulate individual body weight dynamics, e.g. [7,8]. Change of body weight over time is modeled as the rate of energy stored (or lost), which is a function of the energy intake (from food) and the energy expended. However, the exact amount of calories ingested, or energy intake, is difficult to ascertain as it is usually obtained through methods that underestimate its real value, such as self-reported diet records [9].

The inability to rigorously assess the energy intake is considered by [10] the “fundamental flaw in obesity research”. This fact hinders the success and adherence to individual weight control interventions [11]. Therefore the correct evaluation of such interventions will be highly dependent on the precision of energy intake estimates and the assessment of the uncertainty inherent to those estimates. In this paper we show how the probabilistic constraint framework can be used in clinical practice to correctly characterize such uncertainty given the uncertainty of the underlying biomedical model.

Next section overviews the energy intake problem and introduces a biomedical model used in clinical practice. Section 3 addresses constraint programming and its extensions to differential equations and probabilistic reasoning. Section 4 shows how the problem is cast into the probabilistic constraint framework. Section 5 discusses the experimental results and the last section summarizes the main conclusions.

## 2 Energy Intake Problem

The mathematical models that predict weight change in humans are usually based on the energy balance equation:

$$R = I - E \quad (1)$$

where  $R$  is the energy stored or lost (kcal/d),  $I$  is the energy intake (kcal/d) and  $E$  is the energy expended (kcal/d).

Several models have been applied to provide estimates of individual energy intake [12,13]. Our paper focus on the work of [12] which developed a computational model to determine individual energy intake during weight loss. This model, herein designated EI model, calculates the energy intake based on the following differential equation:

$$cf \frac{dF}{dt} + cl \frac{dFF}{dt} = I - (DIT + PA + RMR + SPA) \quad (2)$$

The left hand side of equation (2) represents the change in body's energy stores,  $R$  in equation (1), and is modeled through the weighted sum of the changes in Fat mass ( $F$ ) - the body's long term energy storage mechanism - and Fat Free mass ( $FF$ ) - proxy for protein content used for energy purposes.

Differently from other models, that express the relationship between  $F$  and  $FF$  using logarithmic eq. (3) [14], or linear approximations [15], the EI model uses a fourth-order polynomial for estimating  $FF$  as a function of  $F$ , the age of the subject  $a$ , and its height  $h$  eq. (4),

$$FF^{log}(F) = d_0 + d_1 \log F \quad (3)$$

$$FF^{poly}(F, a, h) = (c_0 + c_1 F + c_2 F^2 + c_3 F^3 + c_4 F^4)(c_5 + c_6 a)(c_7 + c_8 h) \quad (4)$$

The rate of energy expended,  $E$  in equation (1), is the total amount of energy spent in several physiological processes: Diet Induced Thermogenesis ( $DIT$ ) - energy required to digest and absorb food; Physical Activity ( $PA$ ) - energy spent in volitional activities; Resting Metabolic Rate ( $RMR$ ) - minimal amount of energy used to sustain life and; Spontaneous Physical Activity ( $SPA$ ) - energy spent in spontaneous activities.

The EI model uses data from the 24-week CALERIE phase I study [16], in particular body weight for one female subject of the caloric restriction group. During the experiment, participants had their weight monitored every two weeks. Those weight measures are used to estimate the real energy intake for that particular individual.

### 3 Constraint Programming

A constraint satisfaction problem is a classical artificial intelligence paradigm characterized by a set of variables and a set of constraints that specify relations among subsets of these variables. Solutions are assignments of values to all variables that satisfy all the constraints. Constraint programming [2] is a form of declarative programming which must provide a set of constraint reasoning algorithms that take advantage of constraints to reduce the search space, avoiding

regions inconsistent with the constraints. These algorithms are supported by specialized techniques that explore the specificity of the constraint model such as the domain of its variables and the structure of its constraints.

Continuous constraint programming [17, 18] has been widely used to model safe reasoning in applications where uncertainty on the values of the variables is modeled by intervals including all their possibilities. A Continuous Constraint Satisfaction Problem (CCSP) is a triple  $\langle X, D, C \rangle$  where  $X$  is a tuple of  $n$  real variables  $\langle x_1, \dots, x_n \rangle$ ,  $D$  is a Cartesian product of intervals  $D(x_1) \times \dots \times D(x_n)$  (a box), where each  $D(x_i)$  is the domain of variable  $x_i$  and  $C$  is a set of numerical constraints (equations or inequalities) on subsets of the variables in  $X$ . A solution of the CCSP is a value assignment to all variables satisfying all the constraints in  $C$ . The feasible space  $F$  is the set of all CCSP solutions within  $D$ .

Continuous constraint reasoning relies on branch-and-prune algorithms [19] to obtain sets of boxes that cover exact solutions for the constraints (the feasible space  $F$ ). These algorithms begin with an initial crude cover of the feasible space (the initial search space,  $D$ ) which is recursively refined by interleaving pruning and branching steps until a stopping criterion is satisfied. The branching step splits a box from the covering into sub-boxes (usually two). The pruning step either eliminates a box from the covering or reduces it into a smaller (or equal) box maintaining all the exact solutions. Pruning is achieved through an algorithm that combines constraint propagation and consistency techniques based on interval analysis methods [20].

In the biomedical context, constraint technology seems to have the potential to bridge the gap between theory and practice. The declarative nature of constraints makes them an adequate tool for the explicit representation of any kind of domain knowledge, including “deep” biophysical modeling. The constraint propagation techniques provide sound methods, with respect to the underlying model, that can be used to support practical tasks (e.g. diagnosis/prognosis may be supported through propagation on data about the patient symptoms/diseases). In particular, the continuous constraint framework seems to be the most adequate for representing the nonlinear relations on continuous variables, often present in biophysical models. Additionally, the uncertainty of biophysical phenomena may be explicitly represented as intervals of possible values and handled through constraint propagation.

However, the direct application of classical constraint programming to biomedical models suffers from two major pitfalls. System dynamics which is often modeled through differential equations cannot be explicitly represented by these approaches and integrated within the constraint model. Moreover, the interval representation of uncertainty may be too conservative and inadequate to distinguish between consistent scenarios based on their likelihood which may be crucial to the development of effective tools. This work is based on extensions to constraint programming for handling both problems and provide sound propagation of uncertainty from model parameters to results.

### 3.1 Differential Equations

The behavior of many systems is naturally modeled by a system of first order Ordinary Differential Equations (ODEs), often parametric. ODEs are equations that involve derivatives with respect to a single independent variable,  $t$ , usually representing time. A parametric ODE system, with parameters  $p$ , represented in vector notation as:

$$y' = f(p, y, t) \quad (5)$$

is a restriction on the sequence of values that  $y$  can take over  $t$ . A solution, for a time interval  $T$ , is a function that satisfies equation (5) for all values of  $t \in T$ .

Since (5) does not fully determine a single solution (but rather a family of solutions), initial conditions are usually provided with a complete specification of  $y$  at some time point  $t$ . An Initial Value Problem (IVP) is characterized by an ODE system together with the initial condition  $y(t_0) = y_0$ . A solution of the IVP with respect to an interval of time  $T$  is the unique function that is a solution of (5) and satisfies the initial condition.

Parametric ODEs are expressive mathematical means to model system dynamics. Notwithstanding its expressive power, reasoning with such models may be quite difficult, given their complexity. Analytical solutions are available only for the simplest models. Alternative numerical simulations require precise numerical values for the parameters involved, often impossible to gather given the uncertainty on available data. This may be an important drawback since small differences on input values may cause important differences on the output produced.

Interval methods for solving differential equations with initial conditions [20] do verify the existence of unique solutions and produce guaranteed error bounds for the solution trajectory along an interval of time  $T$ . They use interval arithmetic to compute safe enclosures for the trajectory, explicitly keeping the error term within safe bounds.

Several extensions to constraint programming [21] were proposed for handling differential equations based on interval methods for solving IVPs. An approach that integrates other conditions of interest was proposed in [22] and successfully applied to support safe decisions based on deep biomedical models [23].

In this paper we use an approach similar to [21] that allows the integration of IVPs with the standard numerical constraints. The idea is to consider an IVP as a function  $\Phi$  where the first argument are the parameters  $p$ , the second argument is the initial condition that must be verified at time point  $t_0$  (third argument) and the last argument is a time point  $t \in T$ . A relation between the values at two time points  $t_0$  and  $t_1$  along the trajectory is represented by the equation:

$$y(t_1) = \Phi(p, y(t_0), t_0, t_1) \quad (6)$$

Using variables  $x_0$  and  $x_1$  to represent  $y(t_0)$  and  $y(t_1)$ , equation (6) is integrated into the CCSP as a constraint  $x_1 = \Phi(p, x_0, t_0, t_1)$  with specialized constraint propagators to safely prune both variable domains based on a validated solver for IVPs [24].

### 3.2 Probabilistic Constraint Programming

In classical CCSPs, uncertainty is modeled by intervals that represent the domains of the variables. Constraint reasoning reduces uncertainty providing a safe method for computing a set of boxes enclosing the feasible space. Nevertheless this paradigm cannot distinguish between different scenarios and all combination of values within such enclosure are considered equally plausible. In this work we use probabilistic constraint programming [25] that extends the continuous constraint framework with probabilistic reasoning, allowing to further characterize uncertainty with probability distributions over the domains of the variables.

In the continuous case, the usual method for specifying a probabilistic model assumes, either explicitly or implicitly, a full joint probability density function (p.d.f.) over the considered random variables, which assigns a probability measure to each point of the sample space  $\Omega$ . The probability of an event  $\mathcal{H}$ , given a p.d.f.  $f$ , is its multidimensional integral on the region defined by the event:

$$P(\mathcal{H}) = \int_{\mathcal{H}} f(\mathbf{x}) d\mathbf{x} \quad (7)$$

The idea of probabilistic constraint programming is to associate a probabilistic space to the classical CCSP by defining an appropriate density function. A probabilistic constraint space (PC) is a pair  $\langle \langle X, D, C \rangle, f \rangle$ , where  $\langle X, D, C \rangle$  is a CCSP and  $f$  is a p.d.f. defined in  $\Omega \supseteq D$  such that:  $\int_{\Omega} f(\mathbf{x}) d\mathbf{x} = 1$ .

A constraint (or set of constraints) can be viewed as an event  $\mathcal{H}$  whose probability can be computed by integrating the density function  $f$  over its feasible space as in equation (7). In general these multidimensional integrals cannot be easily computed, since they may have no closed-form solution and the event may establish a complex nonlinear integration boundary. The probabilistic constraint framework relies on continuous constraint reasoning to get a tight box cover of the region of integration  $\mathcal{H}$  and compute the overall integral by summing up the contributions of each box in the cover. Generic quadrature methods are used to evaluate the integral at each box.

In this work Monte Carlo methods [26] are used to estimate the value of the definite multidimensional integrals at each box. As long as the function is reasonably well behaved, the integral can be estimated by randomly selecting  $N$  points in the multidimensional space and averaging the function values at these points. Consider  $N$  random sample points  $x_1, \dots, x_N$  uniformly distributed inside a box  $B$ . The contribution of this box to the overall integral on the region of integration  $\mathcal{H}$  is approximated by:

$$\int_{B \cap \mathcal{H}} f(\mathbf{x}) d\mathbf{x} \approx \frac{\sum_{i=1}^N 1_{\mathcal{H}}(\mathbf{x}_i) f(\mathbf{x}_i)}{N} \text{vol}(B) \quad (8)$$

where  $1_{\mathcal{H}}$  is the indicator function<sup>1</sup> of  $\mathcal{H}$ . This method displays  $\frac{1}{\sqrt{N}}$  convergence, i.e., by quadrupling the number of sampled points the error is halved, regardless of the number of dimensions.

---

<sup>1</sup>  $1_{\mathcal{H}}(\mathbf{x}_i)$  returns 1 if  $\mathbf{x}_i \in \mathcal{H}$  and 0 otherwise.

The advantages from this close collaboration between constraint pruning and random sampling were previously illustrated in ocean color remote sensing studies [27] where this approach achieved quite accurate results even with small sampling rates. The success of this technique relies on the reduction of the sampling space where a pure non-naive Monte Carlo (adaptive) method is not only hard to tune but also impractical in small error settings.

## 4 Probabilistic Constraints for Solving the EI Problem

Let  $t$  be the number of days since the beginning of treatment of a given subject,  $F(t)$  the Fat Mass at time  $t$ ,  $w(t)$  the weight observed at time  $t$ , and  $I$  the subject's energy intake, which is assumed to be a constant parameter between consecutive observations [12]. The energy balance equation and total body mass are related through the model:

$$F'(t) = g(I, F(t), t) \quad (9)$$

$$w(t) = FF(a, h, F(t)) + F(t) \quad (10)$$

where  $g$  is obtained by solving equation (2) with respect to  $F'(t)$ .

### 4.1 CCSP Model

Let  $i \in \{0, \dots, n\}$  denote the  $i$ 'th observation since beginning of treatment, occurred at time  $t_i$ , and let  $F_i$  and  $w_i$  be respectively the fat mass and the weight of the patient at time  $t_i$  (with  $t_0 = 0$ ). The EI model may be formalized as a CCSP  $\langle X, \mathbb{IR}^{2n+1}, C \rangle$  with a set of variables  $X = \{F_0\} \cup_{i=1}^n \{F_i, I_i\}$  representing the fat mass  $F_i$  at each observation and the energy intake  $I_i$  between consecutive observations (at  $t_{i-1}$  and  $t_i$ ), and a set of constraints  $C = \{b_0\} \cup_{i=1}^n \{a_i, b_i\}$  enforcing eqs. (9, 10):

$$\begin{aligned} a_i &\equiv [F_i = \Phi(I_i, F_{i-1}, t_{i-1}, t_i)] \\ b_i &\equiv [w_i = FF(a, h, F_i) + F_i] \end{aligned}$$

Recall that solving the above CCSP means finding the values for  $F_0$  and the variables  $F_i, I_i$  ( $1 \leq i \leq n$ ) that satisfy the above set of constraints.

### 4.2 Probabilistic CCSP Model

Uncertainty inherent to  $FF$  estimation may be integrated into the above CCSP model by considering that the true value of  $FF$  is the model given  $FF^M$  plus an associated error term  $\epsilon_i \sim \mathcal{N}(\mu = 0, \sigma_\epsilon)$ ,

$$FF(a, h, F_i) = FF^M(a, h, F_i) + \epsilon_i$$

and we may rewrite the set of  $b_i$  constraints of the CCSP model as follows,

$$b_i \equiv [w_i = FF^M(a, h, F_i) + \epsilon_i + F_i]$$

Additionally, to keep the errors within reasonable bounds, bounding constraints are considered for each observation:  $3\sigma_\epsilon \leq \epsilon_i \leq 3\sigma_\epsilon$ , thus ignoring assignments whose contribution to the total error is less than 0.1%.

Note that a solution to the new (probabilistic) CCSP, i.e. an assignment of values to  $F_0$  and the variables  $F_i$ ,  $I_i$  ( $1 \leq i \leq n$ ), determines the possible combinations of values for the errors  $\epsilon_0, \dots, \epsilon_n$ .

If we assume that the  $FF$  model errors over the  $n + 1$  distinct observations are independent, then each solution has an associated probability density value given by the joint p.d.f.  $f$ ,

$$f(\epsilon_0, \dots, \epsilon_n) = \prod_{i=0}^n f_i(\epsilon_i) \quad (11)$$

where  $f_i$  is the normal distribution associated with the error  $\epsilon_i$ .

Instead of considering independence between model errors from consecutive observations, a more realistic alternative, explicitly represents the deviation between error  $\epsilon_i$  and the previous error  $\epsilon_{i-1}$  as a normally distributed random variable  $\delta_i \sim \mathcal{N}(\mu = 0, \sigma_\delta)$ , resulting in the following joint p.d.f.  $f$ ,

$$f(\epsilon_0, \dots, \epsilon_n, \delta_1, \dots, \delta_n) = \prod_{i=0}^n f_i(\epsilon_i) \prod_{i=1}^n h_i(\delta_i) \quad (12)$$

where  $f_i$  and  $h_i$  are the normal distributions associated with the errors  $\epsilon_i$  and  $\delta_i$  respectively. The deviations are introduced in the model by considering constraints  $\delta_i = \epsilon_i - \epsilon_{i-1}$  ( $1 \leq i \leq n$ ) determining their values from the  $\epsilon_i$  values.

A naive approximate algorithm for solving both alternative CCSP models could be simply to perform Monte Carlo sampling in the space defined by  $D(F_j) \times D(I_1) \times \dots \times D(I_n)$ , with  $j \in \{1, \dots, n\}$ . Note that, given the constraints in the model, each sampled point determines the values of all variables  $F_i$  and  $\epsilon_i$  (and  $\delta_i$ ). From the values assigned to  $\epsilon_i$  (and  $\delta_i$ ), eq. 11 (or 12) can be used to compute an estimate of its probability, as shown in (8).

With this approach, accurate results are hard to obtain for increasing number of observations due to the huge size of sampling space  $O(|D|^{n+1})$ . Instead, we developed an improved technique that is able to drastically reduce both the exponent  $n$  and the base  $|D|$  of this expression, as described in the following section.

### 4.3 Method

The main idea is to avoid considering all variables simultaneously but instead to reason only with a small subset that changes incrementally over time. For each observation  $i$ , we can compute the probability distributions of the variables of interest given the past knowledge already accumulated.

We start by computing the probability distribution of  $F_0$  given the initial weight  $w_0$  subject to the constraint  $b_0$  and the bounding constraints for  $\epsilon_0$ . This

distribution, denoted  $P^{\boxplus}(F_0)$ , is discretized on a grid over  $D(F_0)$  computed through probabilistic constraint reasoning integrated with Monte Carlo sampling as described in section 3.2. Specifically, given a point  $\dot{F}_0$  sampled from  $D(F_0)$ , value  $\dot{\epsilon}_0$  is determined by the constraint  $b_0$ , and its p.d.f. value is  $f(\dot{F}_0) = f_0(\dot{\epsilon}_0)$ .

The joint probability of  $F_1, I_1$  is computed by considering the constraints associated with observation 1, the observed weight  $w_1$ , and  $P^{\boxplus}(F_0)$ . The method is similar: the grid  $P^{\boxplus}(F_1, I_1)$ , discretized over  $D(F_1) \times D(I_1)$  is computed using probabilistic constraint reasoning; and Monte Carlo sampling is performed over this space region.

Given a point  $(\dot{F}_1, \dot{I}_1)$ , sampled from  $D(F_1) \times D(I_1)$ , the values  $\dot{F}_0$  and  $\dot{\epsilon}_1$  are determined by constraints  $a_1$  and  $b_1$ , and accordingly to equation (11), its p.d.f. value should be  $f(\dot{\epsilon}_0, \dot{\epsilon}_1) = f_0(\dot{\epsilon}_0)f_1(\dot{\epsilon}_1)$ . However, we replace the computation of  $f_0(\dot{\epsilon}_0)$  with the value of the discretized probability  $P^{\boxplus}(\dot{F}_0)$  computed in the previous step providing an approximation that converges to the correct value when the number of grid subdivisions goes to infinity:  $f(\dot{F}_1, \dot{I}_1) \approx P^{\boxplus}(\dot{F}_0)f_1(\dot{\epsilon}_1)$ . If the alternative equation (12) is used,  $\dot{\delta}_1$  is also computed from the constraints and the respective p.d.f. approximation is:  $f(\dot{F}_1, \dot{I}_1) \approx P^{\boxplus}(\dot{F}_0)f_1(\dot{\epsilon}_1)h_1(\dot{\delta}_1)$ .

Finally, the computed  $P^{\boxplus}(F_1, I_1)$  is marginalized to obtain  $P^{\boxplus}(F_1)$ , and the process is iterated for the remaining observations.

## 5 Experimental Results

This section demonstrates how to the previously described method may be used to improve the applicability of the EI model by complementing its predictions with measures of confidence. The algorithm was implemented in C++ and used for obtaining the probability distribution approximations  $P^{\boxplus}(F_i, I_i)$  at each observation  $i \in \{1, \dots, 12\}$  of a 45 year-old woman over the course of the 24-week trial (CALERIE Study phase I). The runtime was about 2 minutes per observation on an Intel Core i7 @ 2.4 GHz.

Fat Free mass is estimated using two distinct models:  $FF^{poly}$  (eq. 4), and  $FF^{log}$  (eq. 3). Both of these models were initially fit to a set of 7278 north american women resulting in the corresponding standard deviation of the error,  $\sigma_{\epsilon}^{poly} = 3.35$  and  $\sigma_{\epsilon}^{log} = 5.04$ . This data set was collected during NHANES surveys (1994 to 2004) and is available online at the Centers for Disease Control and Prevention website [28].

We considered also different assumptions regarding independence of the error: the uncorrelated error model (11), and a correlated error model (12) with a small  $\sigma_{\delta} = 0.5$ . Note that, due to current data access restrictions, this latter value is purely illustrative.

The following techniques could be used for assessing propagation of uncertainty.

### 5.1 Joint Probability Distributions

The direct visual inspection of the joint probability distributions of  $F_i$  and  $I_i$  conveys important information about the relation between these parameters.

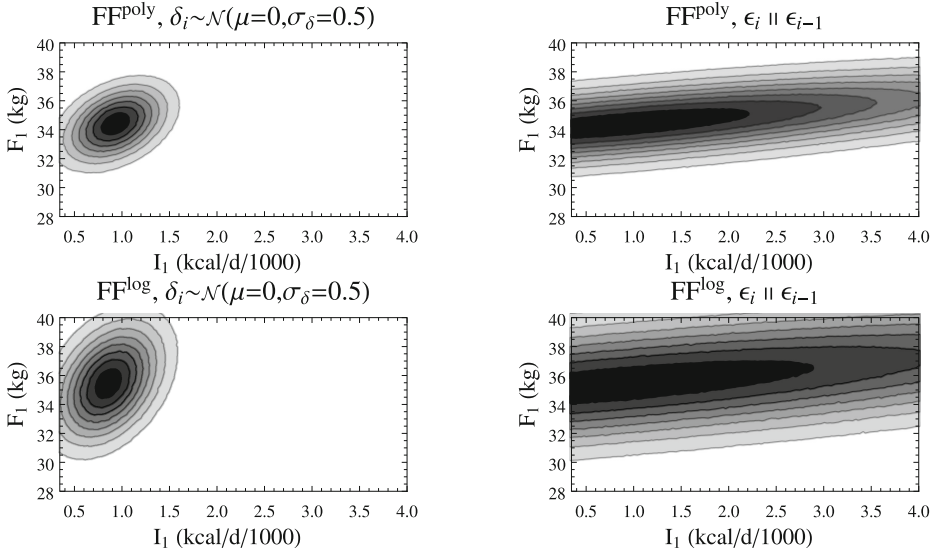


**Fig. 1.** Probabilities of fat mass ( $F$ ) and intake ( $I$ ) on the first clinical observation ( $t = 14$ ). Top and bottom rows shows results for different  $FF$  models. Left and right columns correspond to different assumptions regarding independence of model errors.

In figure 1 we plot the obtained results regarding the first observation  $i = 1$  for each combination of  $FF$  model and error correlation. The following is apparent from these plots: a) Uncertainty on  $F$  is positively correlated with uncertainty on  $I$ ; b) The assumption of independence between model errors on consecutive weeks drastically affects the predicted marginal distribution of  $I$  (compare horizontally); c) The improved accuracy of  $FF^{poly}$  model (note that  $\sigma_\epsilon^{poly} < \sigma_\epsilon^{log}$ ) reflects in slightly sharper  $F$  estimates, but does not seem to impact the estimation of  $I$  (compare vertically).

## 5.2 Marginal Probability Distributions with Confidence Intervals

To perceive the effect of the uncertainty on the estimated variables over time, it is useful to marginalize the computed joint probability distributions. Figure 2 shows the estimated  $F_i$ , and  $I_i$  over time, for each of the error correlation assumptions. Since the results concerning the  $FF^{poly}$  model are very similar to those obtained for  $FF^{log}$ , and for space economy reasons, we focus only on the former.

Each box in these plots depicts the most probable value (marked in the center of the box), the union hull of the 50% most probable values (the rectangle), and the union hull of the 82% most probable values (the whiskers). Additionally, each plot overlays the estimates obtained from the algorithm published by the author of the EI model [7].

The presented results show that the previous conclusions for the case of  $i = 1$  extend for all remaining observations. Additionally, an interesting phenomena occurs in the case of correlated error: the uncertainty in the estimation of  $F$  decreases slightly over time. This is most probably the consequence of having, at each new observation, an increasingly constrained problem for which the size of the solution space is consequently increasingly smaller. At least in the case of  $F$ , more information seems to lead to significantly better estimations. This can not occur if the errors are independent, as is indeed confirmed in the plots.

Finally, our results show that in some cases the most probable values obtained by [7] are crude approximations to their own proposed model.

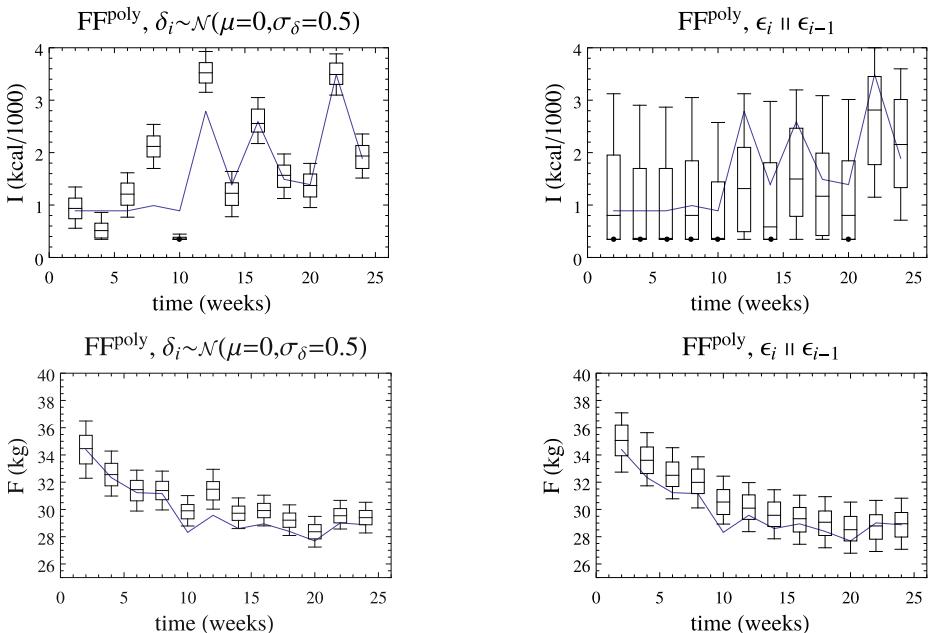


**Fig. 2.** Most probable intervals for the values of  $I$  (top row) and  $F$  (bottom row) over time using the  $F^{poly}$  model. Left and right columns correspond to different assumptions regarding independence of model errors. The continuous line plots estimates obtained in [12].

### 5.3 Best-Fit

Although the presented algorithm is primarily intended for characterizing uncertainty in model predictions, it is nevertheless a sound method for obtaining the predictions themselves. Indeed, as the magnitude of the error in the model parameters decreases ( $\sigma_\epsilon$  in our example), the obtained joint probability distributions will converge to the correct solution of the model.

## 6 Conclusions

The standard practice for characterizing confidence on the predictions resulting from a complex model is to perform controlled experiments. In the biomedical field, this often translates to closely monitoring distinct groups of subjects over large periods of time, and assessing the fitness of the model statistically. While the empirical approach has its own advantages, namely that it does not require a complete understanding of the implications of the individual assumptions and approximations made in the model, it has some important shortcomings. Depending on the medical field, controlled experiments are not always practical, do not convey enough statistical significance, or have associated high costs.

Contrary to the empirical, black-box approach, this paper proposes to characterize the uncertainty on the model estimates by propagating the errors stemming from each of its parts. The described technique extends constraint programming to integrate probabilistic reasoning and constraints modeling dynamic behaviour, offering a mathematically sound and efficient alternative.

The application field of the presented approach is quite broad: it targets models which are themselves composed of other, possibly identically complex (sub)models, for which there is a known characterization of the error. The selected case-study is a good example: the EI model is a fairly complex model including dynamic behaviour and nonlinear relations, and integrates various (sub)models with associated uncertainty. The experimental section illustrated how different choices for one of these (sub)models, the *FF* model, impacts the error of the complete EI model.

Probabilistic constraint programming offers modeling and reasoning capabilities that go beyond the traditional alternatives. This approach has the potential to bridge the gap between theory and practice by supporting reliable conclusions from complex biomedical models taking into account the underlying uncertainty.

## References

1. Halpern, J.Y.: *Reasoning about Uncertainty*. MIT Press (2003)
2. Rossi, F., Beek, P.V., Walsh, T. (eds.): *Handbook of Constraint Programming. Foundations of Artificial Intelligence*. Elsevier Science (2006)
3. Swinburn, B.A., et al.: The global obesity pandemic: shaped by global drivers and local environments. *The Lancet* **378**(9793), 804–814 (2011)
4. Leahy, S., Nolan, A., O’Connell, J., Kenny, R.A.: Obesity in an ageing society implications for health, physical function and health service utilisation. Technical report, The Irish Longitudinal Study on Ageing (2014)
5. Lehnert, T., Sonntag, D., Konnopka, A., Heller, S.R., König, H.: Economic costs of overweight and obesity. *Best Pract Res Clin Endoc. Metab.* **27**(2), 105–115 (2013)
6. Ng, M., et al.: Global, regional, and national prevalence of overweight and obesity in children and adults during 1980–2013: a systematic analysis for the global burden of disease study 2013. *The Lancet* **384**(9945), 766–781 (2014)

7. Thomas, D., Martin, C., Heymsfield, S., Redman, L., Schoeller, D., Levine, J.: A simple model predicting individual weight change in humans. *J. Biol. Dyn.* **5**(6), 579–599 (2011)
8. Christiansen, E., Garby, L., Sørensen, T.I.: Quantitative analysis of the energy requirements for development of obesity. *J. Theor. Biol.* **234**(1), 99–106 (2005)
9. Hill, R., Davies, P.: The validity of self-reported energy intake as determined using the doubly labelled water technique. *Brit. J. Nutr.* **85**, 415–430 (2001)
10. Winkler, J.T.: The fundamental flaw in obesity research. *Obesity Reviews* **6**, 199–202 (2005)
11. Champagne, C.M., et al.: Validity of the remote food photography method for estimating energy and nutrient intake in near real-time. *Obesity* **20**(4), 891–899 (2012)
12. Thomas, D.M., Schoeller, D.A., Redman, L.M., Martin, C.K., Levine, J.A., Heymsfield, S.: A computational model to determine energy intake during weight loss. *Am. J. Clin. Nutr.* **92**(6), 1326–1331 (2010)
13. Hall, K.D., Chow, C.C.: Estimating changes in free-living energy intake and its confidence interval. *Am. J. Clin. Nutr.* **94**, 66–74 (2011)
14. Forbes, G.B.: Lean body mass-body fat interrelationships in humans. *Nutr. Rev.* **45**, 225–231 (1987)
15. Thomas, D., Ciesla, A., Levine, J., Stevens, J., Martin, C.: A mathematical model of weight change with adaptation. *Math. Biosci. Eng.* **6**(4), 873–887 (2009)
16. Redman, L.M., et al.: Effect of calorie restriction with or without exercise on body composition and fat distribution. *J. Clin. Endocrinol. Metab.* **92**(3), 865–872 (2007)
17. Lhomme, O.: Consistency techniques for numeric CSPs. In: Proc. of the 13th IJCAI, pp. 232–238 (1993)
18. Benhamou, F., McAllester, D., van Hentenryck, P.: CLP(intervals) revisited. In: ISLP, pp. 124–138. MIT Press (1994)
19. Hentenryck, P.V., Mcallester, D., Kapur, D.: Solving polynomial systems using a branch and prune approach. *SIAM J. Num. Analysis* **34**, 797–827 (1997)
20. Moore, R.: Interval Analysis. Prentice-Hall, Englewood Cliffs (1966)
21. Goldsztejn, A., Mullier, O., Eveillard, D., Hosobe, H.: Including ordinary differential equations based constraints in the standard CP framework. In: Cohen, D. (ed.) CP 2010. LNCS, vol. 6308, pp. 221–235. Springer, Heidelberg (2010)
22. Cruz, J.: Constraint Reasoning for Differential Models. Frontiers in Artificial Intelligence and Applications, vol.126. IOS Press (2005)
23. Cruz, J., Barahona, P.: Constraint reasoning in deep biomedical models. *Artificial Intelligence in Medicine* **34**(1), 77–88 (2005)
24. Nedialkov, N.: Vnode-lp a validated solver for initial value problems in ordinary differential equations. Technical report, McMaster Univ., Hamilton, Canada (2006)
25. Carvalho, E.: Probabilistic Constraint Reasoning. PhD thesis, FCT/UNL (2012)
26. Hammersley, J., Handscomb, D.: Monte Carlo Methods. Methuen London (1964)
27. Carvalho, E., Cruz, J., Barahona, P.: Probabilistic constraints for nonlinear inverse problems. *Constraints* **18**(3), 344–376 (2013)
28. National health and nutrition examination survey. <http://www.cdc.gov/nchs/nhanes.htm>

# Smart Environments and Context-Awareness for Lifestyle Management in a Healthy Active Ageing Framework

Davide Bacciu<sup>1</sup>, Stefano Chessa<sup>1,2(✉)</sup>, Claudio Gallicchio<sup>1</sup>, Alessio Micheli<sup>1</sup>, Erina Ferro<sup>2</sup>, Luigi Fortunati<sup>2</sup>, Filippo Palumbo<sup>2</sup>, Oberdan Parodi<sup>2</sup>, Federico Vozzi<sup>2</sup>, Sten Hanke<sup>3</sup>, Johannes Kropf<sup>3</sup>, and Karl Kreiner<sup>4</sup>

<sup>1</sup> Department of Computer Science, University of Pisa, Largo Pontecorvo 3, Pisa, Italy

<sup>2</sup> CNR-ISTI, PISA CNR Research Area, via Moruzzi 1, 56126 Pisa, Italy

[stefano.chessa@unipi.it](mailto:stefano.chessa@unipi.it)

<sup>3</sup> Health and Environment Department, AIT Austrian Institute of Technology GmbH, Vienna, Austria

<sup>4</sup> Safety and Security Department, AIT Austrian Institute of Technology GmbH, Vienna, Austria

**Abstract.** Health trends of elderly in Europe motivate the need for technological solutions aimed at preventing the main causes of morbidity and premature mortality. In this framework, the DOREMI project addresses three important causes of morbidity and mortality in the elderly by devising an ICT-based home care services for aging people to contrast cognitive decline, sedentariness and unhealthy dietary habits. In this paper, we present the general architecture of DOREMI, focusing on its aspects of human activity recognition and reasoning.

**Keywords:** Human activity recognition · E-health · Reasoning · Smart environment

## 1 Introduction

According to the University College Dublin Institute of Food and Health, three are the most notable health promotion and disease prevention programs that target the main causes of morbidity and premature mortality: malnutrition, sedentariness, and cognitive decline, conditions that particularly affect the quality of life of elderly people and drive to disease progression. These three features represent the target areas in the DOREMI project. The project vision aims at developing a systemic solution for the elderly, able to prolong the functional and cognitive capacity by stimulating, and unobtrusively monitoring the daily activities according to well-defined “Active Ageing” lifestyle protocols. The project joins the concept of prevention centered on the elderly, characterized by a unified vision of being elderly today, namely, a promotion of the health by a constructive interaction among mind, body, and social engagement.

---

This work has been funded in the framework of the FP7 project “Decrease of cOgnitive decline, malnutRition and sedEntariness by elderly empowerment in lifestyle Management and social Inclusion” (DOREMI), contract N.611650.

To fulfill these goals, food intake measurements, exergames associated to social interaction stimulation, and cognitive training programs (cognitive games) will be proposed to an elderly population enrolled during a pilot study. The DOREMI project is going further with respect to the current state of the art by developing, testing, and exploiting with a short-term business model impact a set of IT-based (Information Technology) services able to:

- Stimulate elderly people in modifying dietary needs and physical activity according to the changes in age through creative, personalized, and engaging solutions;
- Monitor parameters of the elderly people to support the specialist in the daily verification of the compliance of the elderly with the prescribed lifestyle protocol, in accordance with his/her response to physical and cognitive activities.
- Advise the specialist with different types and/or intensities of daily activity for improving the elderly health, based on the assigned protocol progress assessment.
- Empower aging people by offering them knowledge about food and physical activity effectiveness, to let them become the main actors of their health.

To reach these objectives, the project builds over interdisciplinary knowledge encompassing health and artificial intelligence, the latter covering aspects ranging from sensing, machine learning, human-machine interfaces, and games. This paper focuses on the machine learning contribution of the project, which applies to the analysis of the sensor data with the purpose of identifying users' conditions (in terms of balance, calories expenditure, etc.) and activities, detecting changes in the users' habits, and reasoning over such data. The ultimate goal of this data analysis is to support the user who is following the lifestyle protocol prescribed by the specialist, by giving him feedbacks through an appropriate interface, and by providing the specialist with information about the user lifestyle. In particular, the paper gives a snapshot of the status of the project (which just concluded the first year of activity) in the design of the activity recognition and reasoning components.

## 2 Background and State of the Art on Machine Learning

Exploratory data analysis (EDA) analyzes data sets to find their main features [1], beyond what can be found by formal modeling or hypothesis testing task. When dealing with accelerometer data, features are classified in three categories: time domain, frequency domain, and spatial domain [2]. In the time domain, we use the standard deviation in a frame, which is indicative of the acceleration data and the intensity of the movement during the activity. In the frequency domain, frequency-domain entropy helps the distinction of activities with similar energy intensity by comparing their periodicities. This feature is computed as the information entropy of the normalized Power Spectral Density (PSD) function of the input signal without including the DC component (mean value of the waveform). The periodicity feature evaluates the periodicity of the signal that helps to distinguish cyclic and non-cyclic activities. In the spatial domain, orientation variation is defined by the variation of the gravitational

components at three axes of the accelerometer sensor. This feature effectively shows how severe the posture change can be during an activity.

Other EDA tasks of the project concern unsupervised user habits detection aimed at finding behavioral anomalies, by retrieving heterogeneous and multivariate timeseries of sensor data, over long periods. In the project, these tasks are unsupervised to avoid obtrusive data collection campaign at the user site. For this reason, we focus on motif search on sensory data collected in the test by exploiting the results obtained in the field of time series motifs discovery [3,4]. Time series motifs are approximately repeated patterns found within the data. The approach chosen is based on *stigmergy*. Several works used this technique in order to infer motifs in time series related to different fields, from DNA and biological sequences [5,6] to intrusion detection systems [7].

Human activity recognition refers to the process of inferring human activities from raw sensor data [8], classifying or evaluating specific sections of the continuous sensors data stream into specific human activities, events or health parameters values. Recently, the need for adaptive processing of temporal data from potentially large amounts of sensor data has led to an increasing use of machine learning models in activity recognition systems (see [9] for a recent survey), especially due to their robustness and flexibility. Depending on the nature of the treated data, of the specific scenario considered and of the admissible trade-off among efficiency, flexibility and performance, different supervised machine learning methods have been applied in this area.

Among others, Neural Network for sequences, including Recurrent Neural Networks (RNNs) [10], are considered as a class of learning models suitable for approaching tasks characterized by a sequential/temporal nature, and able to deal with noisy and heterogeneous input data streams. Within the class of RNNs, the Reservoir Computing (RC) paradigm [11] in general, and the Echo State Network (ESN) model, [12,13] in particular, represent an interesting efficient approach to build adaptive non-linear dynamical systems. The class of ESNs provides predictive models for *efficiently* learning in sequential/temporal domains from heterogeneous sources of noisy data, supported by theoretical studies [13,14] and with hundreds of relevant successful experimental studies reported in literature [15]. Interestingly, ESNs have recently proved to be particularly suitable for processing noisy information streams originated by sensor networks, resulting in successful real-world applications in supervised computational tasks related to AAL (Ambient Assisted Living) and human activity recognition. This is also testified by some recent results [16,17,18,19,20], which may be considered as a first preliminary experimental assessment of the feasibility of ESN to the estimation of some relevant target human parameters, although obtained on different and broader AAL benchmarks.

At the reasoning level, our interest is for hybrid approaches founded on static rules and probabilistic methods. Multiple-stage decisions refer to decision tasks that consist of a series of interdependent stages leading towards a final resolution. The decision-maker must decide at each stage what action to take next in order to optimize performance (usually utility). Some examples of this sort are working towards a degree, troubleshooting, medical treatment, budgeting, etc. Decision trees are a useful mean for representing and analyzing multiple-stage decision tasks; they support decisions learned from data, and their terminal nodes represent possible consequences [21].

Other popular approaches, which have been used to implement medical expert systems, are Bayesian Networks [22] and Neural Networks [23], but they require many empirical data to train the algorithms and are not appropriate to be manually adjusted. On the other hand, in our problem the decision process must be transparent and mainly requires static rules based on medical guidelines provided by the professionals. Thus, the decision trees are the best solution since they provide a very structured and easy to understand graphical representation. There also exist efficient and powerful algorithms for automated learning of the trees [24,25,26]. A decision tree is a flowchart-like structure in which an internal node represents the test on an attribute, each branch represents a test outcome and each leaf node represents a class label (decision taken after computing all attributes). A path from root to leaf represents classification rules. Decision trees give a simple representation for classifying examples. In general, as for all machine learning algorithms, the accuracy of the algorithms increases with the number of sample data. In applications in which the number of samples is not large, a high number of decisions could lead to problems. In these cases, a possible solution is the use of a Hybrid Decision Tree/Genetic Algorithm approach as suggested in [27].

### 3 Problem Definition and Requirements

Our main objective is to provide a solution for prolonging the functional and cognitive capacity of the elderly by proposing an “Active Ageing” lifestyle protocol. Medical specialists monitor the progress of their patients daily through a dashboard and modify the protocol for each user according to their capabilities. A set of mobile applications (social games, exer-games, cognitive games and diet application) feedback the protocol proposed by the specialist and the progress of games to the end user. The monitoring of each user is achieved by means of a network of sensors, either wearable or environmental, and applications running on personal mobile devices. The human activity recognition (HAR) measures characteristics of the elderly lifestyle in the physical and social domains through non-invasive monitoring solutions based on the sensor data. Custom mobile applications cover the areas of diet and cognitive monitoring. In the rest of this section, we present the main requirements of the HAR.

By leveraging environmental sensors, such as PIRs (Passive InfraRed) and a localization system, the HAR module profiles user habits in terms of daily ratio of room occupancy and indoor/outdoor living. The system is also able to detect changes in the user habits that occur in the long-term. By relying on accelerometer and heartbeat data from a wearable bracelet, the HAR module provides time-slotted estimates, in terms of calories, of the energy expenditure associated with the physical activities of the user. Energy consumption can result from everyday activities and physical exercises proposed by the protocol. The system also computes daily outdoor covered distance, the daily number of steps and detects periods of excessive physical stress by using data originated by the accelerometer and the heartbeat in the bracelet. Finally, a smart carpet is used to measure the user weight and balance skills, leveraging a machine learning classification model based on the BERG balance assessment test.

The HAR assesses the social interactions of the user both indoor and outdoor. In particular, in the indoor case, HAR estimates a quantitative measure of the social interactions based on the occurrence and duration of the daily social gatherings at the user house. Regarding the outdoor socialization, the system estimates the duration of the encounters with other users by detecting the proximity of the users' devices.

The Reasoner uses the data produced by the HAR, the diet, and the games applications to provide an indicator of the user protocol compliance and protocol progress in three areas: social life, physical activity and related diet, cognitive status. These indicators, along with the measured daily metrics and aggregate data, support medical specialists on providing periodical changes to the protocol (i.e.: set of physical activities and games challenges, diet). The Reasoner is able to suggest changes to the user protocol by means of specialist-defined rules.

The HAR module and the Reasoner are, therefore, core system modules, bridging the gap between sensors data, medical specialists, and the end user.

## 4 An Applicative Scenario

We consider a woman in her 70s, still independent and living alone in her apartment (for the sake of simplicity, we give her the name of Loredana). She is a bit overweight and she starts forgetting things. Recently, the specialist told her that she is at risk for cardiovascular disease, due to her overweight condition, and that she has a mild cognitive impairment. For this reason, Loredana uses our system as a technological support to monitor her life habits and to keep herself healthier and preventing chronic diseases. In a typical day, Loredana measures her weight and balance by means of a smart carpet, which collects data for the evaluation of her BERG scale equilibrium and her weight. The data concerning the balance is used to suggest a personalized physical activity (PA) plan, while the data about the weight give indications about the effectiveness of the intervention in terms of a personalized diet regimen and PA plan. During the day, Loredana wears a special bracelet, which measures (by means of an accelerometer) her heart rate, how much she walked, and how many movements she did with physical exercises. These data are used, by the system developed in the project, to assess her calories expenditure and to monitor the execution of the prescribed physical exercises. The bracelet is also used to localize her both indoor (also collecting information about the time spent in each room) and outdoor (collecting information about distance covered). Furthermore, the bracelet detects the proximity of Loredana with other users wearing the same bracelet, while machine-learning classification models based on environmental sensors deployed at home (PIRs and door switches) detect the presence of other people in her apartment to give indication about the number of received visits. These data are used as an indicator of her social life.

Loredana also uses a tablet to interact with the system, with which she performs cognitive games and inserts data concerning her meals, which are converted by the system (under the supervision of her specialist) in daily Kcalories intake and food composition. She is also guided through the daily physical exercises and games that are selected by the system (under the supervision of her specialist) based on the evolution

of her conditions (in terms of balance, weight, physical exercises etc.). All the data collected during the day are processed at night to produce a summary of the Loredana lifestyle, with the purpose of giving feedbacks to Loredana in terms of proposed physical activity, and presenting the condition of Loredana to the specialist on a daily basis.

## 5 Activity Recognition and Reasoning

### 5.1 High Level Architecture and Data Flows

The high-level system architecture is presented in Fig. 1, highlighting the data flow originated at a pilot site (in terms of sensor data), through the data processing stages (preprocessing, activity recognition and reasoner subsystems), and then back to the user (in terms of feedbacks) and to the specialist (in terms of information about the user performance).

In particular, Fig. 1 shows that the data processing system contains five main subsystems running on the server (the grey rectangles in the figure), three databases (RAW, HOMER [28] and KIOLA [29]), plus a middleware that uploads the sensors' data in the RAW database, whose description is out of the scope of this paper. At night, a synchronization mechanism (shown as a clock in Fig. 1), sequentially activates these five subsystems. In turn, these subsystems pre-process data (pre-processing subsystem in the Fig. 1), configure the predictive activity recognition tasks (task configurator subsystem), process the daily pre-processed data through the predictive human activity recognition subsystem (HAR subsystem), perform the exploratory data analysis (EDA subsystem), and refine and aggregate the results of these stages (Reasoner subsystem).

Along with the sensors' data, the RAW DB also stores the intermediate data produced by the pre-processing subsystem. The HOMER DB stores configuration information (e.g. regarding sensors deployment) that is used by the task configurator to retrieve the tuning parameters for the different pilot sites. The refined data produced by the HAR and EDA subsystems is then stored in the KIOLA DB, where the Reasoner reads them. The Reasoner outputs feedbacks for the user in terms of suggestions about her lifestyle, and data about her compliance to the suggested lifestyle protocol for the specialist (or caregiver) through the dashboard.

The data processing stages deal with three flows of data, related to the user diet, social relationships, and sedentariness, respectively. The dietary data flow relies on data produced by the smart carpet (pressure data and total weight), the bracelet (heart rate and accelerometers data), and data about the food composition provided by the user himself through an interface on his tablet. In particular, the data produced by the bracelet pass through the HAR subsystem that estimates the user physical activity. The data flow about the user's social relationships relies on a number of environmental sensors, which detect the contacts of the user with other people. To this purpose, the HAR and EDA subsystems detect the user encounters and the proximity of the user with other people by fusing information produced by presence sensors, user's localization and door switches. This data flow also relies on the user's mood

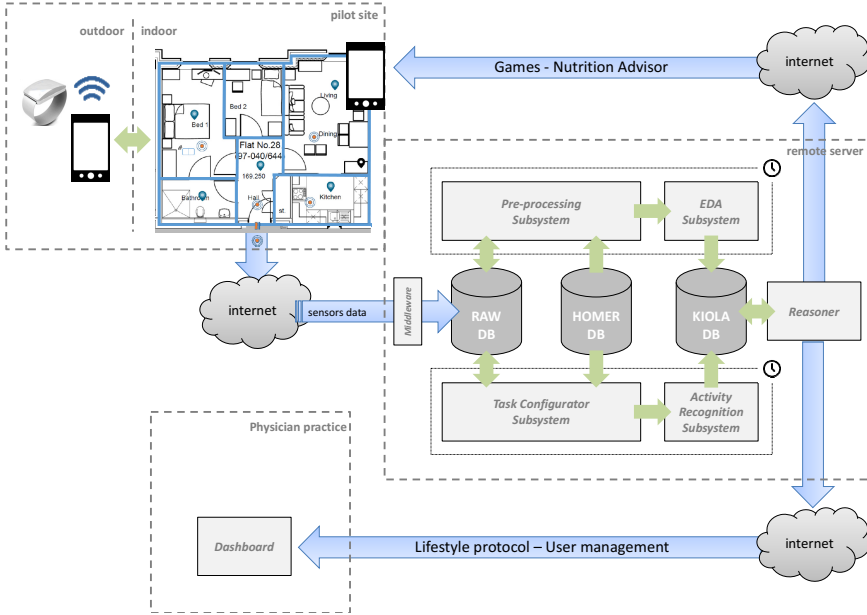


**Fig. 1.** High-level architecture and deployment of a typical installation, with data flowing from a pilot site to the remote Activity Recognition and Reasoning system.

information, which the user himself asserts daily through an app on his tablet. Finally, the sedentariness data flow exploits data produced by the bracelet (heart rate, user's localization, movements, and step count), the smart carpet, and data about the use of the application that guides the user through the daily physical activity. The HAR subsystem processes the data of the smart carpet to assess the user balance according to the BERG scale. The HAR and EDA subsystems also process data from the bracelet to assess the intensity of the physical effort.

The Reasoner fuses all these data flows at a higher level than that of HAR and EDA. In a first step, it exploits rules extracted from clinical guidelines to compute specific parameters for each of the three data flows. For example, it uses the physical activity estimation in the sedentariness data flow to assess the compliance of the user to the prescribed lifestyle protocol (as the medical expert defines it). In the second step, the Reasoner performs a cross-domain reasoning on top of the first step, allowing a deeper insight in the well-being of the patient. Note that the empirical rules needed to define the second-level reasoning protocol are yet not available, as they are the output of medical studies on the data collected from the on-site experimentation that will be concluded in the next year of the project activity. Hence, at this stage of the project, the second level reasoning is not yet implemented.

Note that the Reasoner subsystem operates at a different time-scale with respect to the HAR and EDA subsystems. In fact, the aim of HAR and EDA is the recognition of short-term activities of the user. These can be recognized from a sequence of input sensor information (possibly pre-processed) in a limited (short-term) time window.

All short-term predictions generated across the day are then forwarded to the Reasoner for information integration across medium/long time scales. Medium term reasoning operates over 24h periods (for example, to assess the calories assumption/consumption balance in a day). Long-term reasoning, on the other hand, shows general trends by aggregating information on the entire duration of the experimentation in the pilot sites (for example to offer statistical data about the user, which the medical experts can use to assess the overall user improvement during the experimentation).

## 5.2 Human Activity Recognition and Exploratory Data Analysis Subsystems

The goal of the activity recognition subsystems (HAR and EDA) is to evaluate the user parameters (referred to as *predictions*) concerning his short-term activities performed during the day. It exploits the *activity recognition configuration*, which is the result of an off-line configuration phase aimed at finding the final setting for the pre-processing and for the activity recognition subsystems (both HAR and EDA) that are deployed to implement the activity recognition tasks.

The EDA subsystem analyses pre-processed data in order to profile user's habits, to detect behavioral deviations of the routine indoor activities, and to provide aggregated values useful to the Reasoner in the sedentariness area, such as user habits, daily outdoor distance covered, daily steps and information about outdoor meetings with other users. The actual nature of the data streams processed by the EDA depends on the particular sensors originating them. For example, in the case of BERG score prediction concerning the user balance, the data produced by the smart carpet have a high and variable frequency (~100 Hz). These data are normalized and broken into fixed frequency time series segments of 200 ms, from which the preprocessing stage extracts statistical features consisting in mean, standard deviation, skewness and kurtosis. The resulting features time series, presenting a lower frequency of 5 Hz, are the input of the EDA subsystem. A similar pre-processing stage is applied to data coming from the other sensors.

The unsupervised models used for the EDA do not rely on a long-term, invasive and costly ground truth collection and annotation campaigns, which may be not acceptable by the users. Rather, EDA is designed to detect symptoms of chronic diseases (which are most relevant for the project purposes), characterized by a gradual, long-term deviation from the user typical behavior, or by critical trends in the user's vital parameters. For example, EDA features a module for the detection of abnormal deviations in the user habits (based on motif discovery and stigmergy algorithms) that relies on the locations of the user (at room-level) during his daily living activities.

Concerning the HAR subsystem, its internal architecture is shown in Fig. 2. It is composed of two main subsystems, which are the task configurator and the activity recognition subsystem. The former handles the retrieval of configuration information and pre-processed data for the tasks addressed in the system and forwards it to the latter subsystem, which is responsible for performing the actual activity recognition tasks. The core of the activity recognition system is given by the HAR scheduler (which activates the activity recognition tasks when all sensor information is consolidated and pre-processed in the RAW DB), and by the pool of activity recognition

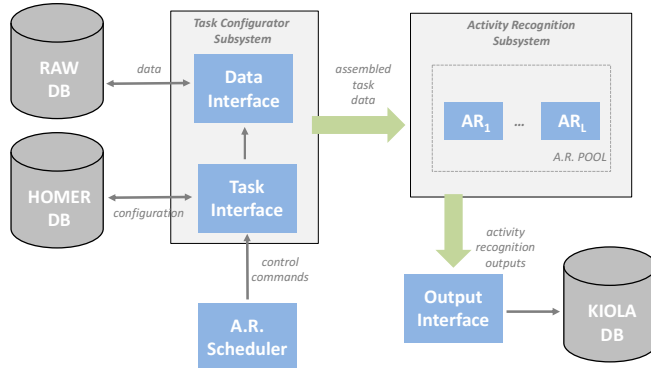


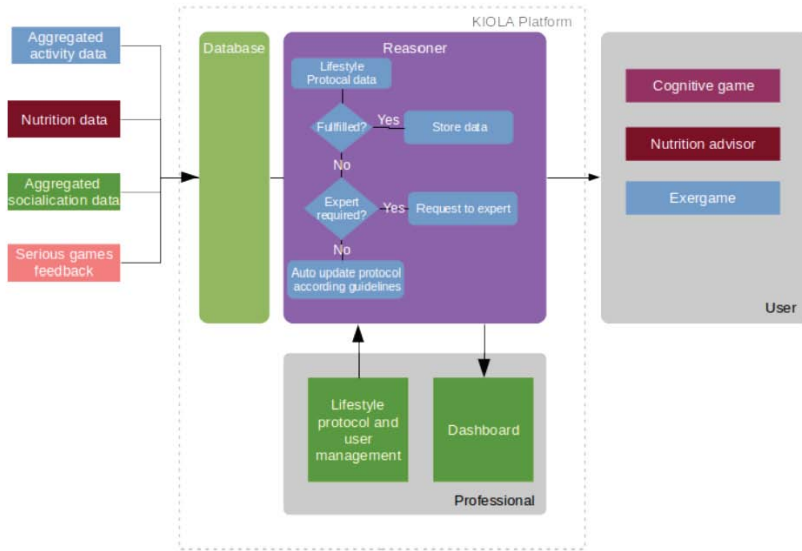
**Fig. 2.** Detailed architecture of the supervised HAR system

components (based on predictive learning models), one for each specific task. These components implement the trained predictive learning model obtained from a preliminary validation phase, and they produce their predictions by computing the outputs of the supervised learning model in response to the input data.

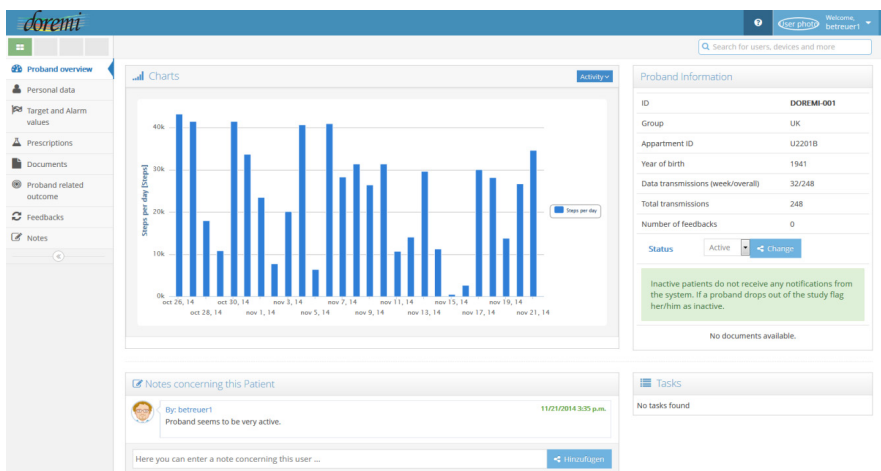
### 5.3 Reasoning Subsystem and Dashboard

Fig. 3 shows the Reasoner, the high-level database and the dashboard with the other system components. The high-level database receives the data from three sources: the activity recognition subsystem (data about physical activity, calories consumption, balance, user sociality etc.), the diet application on the tablet (nutritional data inserted by the users themselves), and the application for serious games on the tablet (statistics about the performance of the user in cognitive games).

The Reasoner compares all these data with the clinical protocol the person should follow based on the pre-sets from the medical experts. To this purpose, it adopts a rule based with hierarchical decision trees, where the rules will be created according to the actual medical guidelines. Based on this, a general overview, as well as some calculated data relations, is presented to the specialist's dashboard. The Reasoner settings can be modified by the medical experts to change the protocol according to a certain user behavior (for example he can change the food composition or reduce the overall caloric intake), or the Reasoner itself may adapt the protocol according to pre-defined rules, when some known conditions occur. For example, an improvement in the physical activity assessed by the heart rate response to exercise may result in a progressive increase in the intensity of proposed exercises. The Reasoner gives feedbacks to the user by means of applications on the user tablet (namely, the nutritional and physical activity advisors and the cognitive games).



**Fig. 3.** Architecture of the Reasoner and its relationship with the other system components



**Fig. 4.** Personal dashboard showing activity data of an end-user

The reasoning module and the dashboard are integrated in the KIOLA modular platform, suitable for clinical data and therapy management. It is built on top of the open-source web-framework Django<sup>1</sup> and uses PostgreSQL 9.4 as primary data storage. KIOLA has two groups of components: *core components* (that provide data

<sup>1</sup> <http://www.djangoproject.com>

models for receiving and storing external sensor data, rule-based reasoning on observations, and messaging services to communicate results of the reasoning to external systems), and *frontend components* (a dashboard for the specialists, an administrative interface, and a search engine for all data stored in KIOLA). In particular, the dashboard provides specialists with the possibility to review and adjust clinical protocols online, and it is designed for both mobile devices and computers. The dashboard can provide either an overview of all end-users to which the specialist has access, or a detailed view of a specific end-user. Charts are used to visualize all observations in the area of social, physical games, and dietary data (see Fig. 4). A task module on the dashboard is also used to notify specialists when the reasoning system suggests an adoption of the clinical protocol. Here, the specialist can then approve or disapprove the recommendation, and he can tune the parameters of the protocol by himself.

## 6 Conclusions

The DOREMI project addresses three important causes of morbidity and mortality in the elderly (malnutrition, sedentariness and cognitive decline), by designing a solution aimed at promoting an active aging lifestyle protocol. It envisages to provide an ICT-based home care services for aging people to contrast cognitive decline, sedentariness and unhealthy dietary habits. The proposed approach builds on activity recognition and reasoning subsystems, which are the scope of this paper. At the current stage of the project such components are being deployed, and they will be validated in the course of the year by means of an extensive data collection campaign aimed at obtaining the annotated datasets. These datasets, that are currently being collected over a group of elderly volunteers in Pisa, in view of the experimentation in the pilot sites planned by the beginning of 2016.

## References

1. Tukey, J.W.: Exploratory data analysis, pp. 2–3 (1977)
2. Long, X., Yin, B., Aarts, R.M.: Single-accelerometer-based daily physical activity classification. In: Engineering in Medicine and Biology Society, EMBC 2009. Annual International Conference of the IEEE. IEEE (2009)
3. Fernández-Llatas, C., et al.: Process Mining for Individualized Behavior Modeling Using Wireless Tracking in Nursing Homes. Sensors **13**(11), 15434–15451 (2013)
4. der Aalst, V., Wil, M.P., et al.: Workflow mining: A survey of issues and approaches. Data & Knowledge Engineering **47**(2), 237–267 (2003)
5. Yang, C.-H., Liu, Y.-T., Chuang, L.-Y.: DNA motif discovery based on ant colony optimization and expectation maximization. In: Proceedings of the International Multi Conference of Engineers and Computer Scientists, vol. 1 (2011)
6. Bouamama, S., Boukerram, A., Al-Badarneh, A.F.: Motif finding using ant colony optimization. In: Dorigo, M., Birattari, M., Di Caro, G.A., Doursat, R., Engelbrecht, A.P., Floreano, D., Gambardella, L.M., Groß, R., Şahin, E., Sayama, H., Stützle, T. (eds.) ANTS 2010. LNCS, vol. 6234, pp. 464–471. Springer, Heidelberg (2010)

7. Cui, X., et al.: Visual mining intrusion behaviors by using swarm technology. In: 2011 44th Hawaii International Conference on System Sciences (HICSS). IEEE (2011)
8. Bao, L., Intille, S.S.: Activity Recognition from User-Annotated Acceleration Data. In: Ferscha, A., Mattern, F. (eds.) PERVASIVE 2004. LNCS, vol. 3001, pp. 1–17. Springer, Heidelberg (2004)
9. Lara, O.D., Labrador, M.A.: A survey on human activity recognition using wearable sensors. *Communications Surveys & Tutorials, IEEE* **15**(3), 1192–1209 (2013)
10. Kolen, J., Kremer, S. (eds.): A Field Guide to Dynamical Recurrent Networks. IEEE Press (2001)
11. Lukoševicius, M., Jaeger, H.: Reservoir computing approaches to recurrent neural network training. *Computer Science Review* **3**(3), 127–149 (2009)
12. Jaeger, H., Haas, H.: Harnessing nonlinearity: Predicting chaotic systems and saving energy in wireless communication. *Science* **304**(5667), 78–80 (2004)
13. Gallicchio, C., Micheli, A.: Architectural and markovian factors of echo state networks. *Neural Networks* **24**(5), 440–456 (2011)
14. Tino, P., Hammer, B., Boden, M.: Markovian bias of neural based architectures with feedback connections. In: Hammer, B., Hitzler, P. (eds.) Perspectives of neural-symbolic integration. SCI, vol. 77, pp. 95–133. Springer-Verlag, Heidelberg (2007)
15. Lukoševičius, M., Jaeger, H., Schrauwen, B.: Reservoir Computing Trends. *KI - Künstliche Intelligenz* **26**(4), 365–371 (2012)
16. Bacciu, D., Barsocchi, P., Chessa, S., Gallicchio, C., Micheli, A.: An experimental characterization of reservoir computing in ambient assisted living applications. *Neural Computing and Applications* **24**(6), 1451–1464 (2014)
17. Chessa, S., et al.: Robot localization by echo state networks using RSS. In: Recent Advances of Neural Network Models and Applications. Smart Innovation, Systems and Technologies, vol. 26, pp. 147–154. Springer (2014)
18. Palumbo, F., Barsocchi, P., Gallicchio, C., Chessa, S., Micheli, A.: Multisensor data fusion for activity recognition based on reservoir computing. In: Bottia, J.A., Álvarez-García, J.A., Fujinami, K., Barsocchi, P., Riedel, T. (eds.) EvAAL 2013. CCIS, vol. 386, pp. 24–35. Springer, Heidelberg (2013)
19. Bacciu, D., Gallicchio, C., Micheli, A., Di Rocco, M., Saffiotti, A.: Learning context-aware mobile robot navigation in home environments. In: 5th IEEE Int. Conf. on Information, Intelligence, Systems and Applications (IISA) (2014)
20. Amato, G., Broxvall, M., Chessa, S., Dragone, M., Gennaro, C., López, R., Maguire, L., McGinnity, T., Micheli, A., Renteria, A., O'Hare, G., Pecora, F.: Robotic UBIQUITOUS COGNITIVE network. In: Novais, P., Hallenborg, K., Tapia, D.I., Rodriguez, J.M. (eds.) Ambient Intelligence - Software and Applications. AISC, vol. 153, pp. 191–195. Springer, Heidelberg (2012)
21. Lavrac, N., et al.: Intelligent data analysis in medicine. *IJCAI* **97**, 1–13 (1997)
22. Chae, Y.M.: Expert Systems in Medicine. In: Liebowitz, J. (ed.) The Handbook of applied expert systems, pp. 32.1–32.20. CRC Press (1998)
23. Gurgen, F.: Neuronal-Network-based decision making in diagnostic applications. *IEEE EMB Magazine* **18**(4), 89–93 (1999)
24. Anderson, J.R., Machine learning: An artificial intelligence approach. In: Michalski, R.S., Carbonell, J.G., Mitchell, T.M. (eds.) vol. 2. Morgan Kaufmann (1986)
25. Hastie, T., et al.: The elements of statistical learning, vol. 2(1). Springer (2009)
26. Murphy, K.P.: Machine learning: a probabilistic perspective. MIT Press (2012)

27. Carvalho, D.R., Freitas, A.A.: A hybrid decision tree/genetic algorithm method for data mining. *Information Sciences* **163**(1), 13–35 (2004). [EDA1] Tukey, J.W.: Exploratory data analysis, pp. 2–3 (1977)
28. Fuxreiter, T., et al.: A modular platform for event recognition in smart homes. In: 12th IEEE Int. Conf. on e-Health Networking Applications and Services (Healthcom), pp. 1–6 (2010)
29. Kreiner, K., et al.: Play up! A smart knowledge-based system using games for preventing falls in elderly people. *Health Informatics meets eHealth (eHealth 2013)*. In: Proceedings of the eHealth 2013, OCG, Vienna, pp. 243–248 (2013). ISBN: 978-3-85403-293-9

# Gradient: A User-Centric Lightweight Smartphone Based Standalone Fall Detection System

Ajay Bhatia<sup>1</sup>(✉), Suman Kumar<sup>2</sup>, and Vijay Kumar Mago<sup>3</sup>

<sup>1</sup> Punjab Technical University, Jalandhar, India

[prof.ajaybhatia@gmail.com](mailto:prof.ajaybhatia@gmail.com)

<sup>2</sup> Troy University, Troy, AL 36082, USA

[skumar@troy.edu](mailto:skumar@troy.edu)

<sup>3</sup> Department of Computer Science, Lakehead University,

Thunder Bay, ON, Canada

[vmago@lakeheadu.ca](mailto:vmago@lakeheadu.ca)

**Abstract.** A real time pervasive fall detection system is a very important tool that would assist health care professionals in the event of falls of monitored elderly people, the demography among which fall is the epidemic cause of injuries and deaths. In this work, *Gradient*, a user centric and device friendly standalone smartphone based fall detection solution is proposed. Our solution is standalone and user centric as it is portable, cost efficient, user friendly, privacy preserving, and requires only technologies which exists in cellphones. In addition, *Gradient* is light weight which makes it device friendly since cellphones are constrained by energy and memory limitations. Our work is based on accelerometer sensor data and the data derived from gravity sensors, a recently available inbuilt sensor in smartphones. Through experimentation, we demonstrate that *Gradient* exhibits superior accuracy among other fall detection solutions.

**Keywords:** Fall detection · Accelerometer · Gravity · Sensors · Android app

## 1 Introduction

Advances in health care services and technologies, and decrease in fertility rate (especially in developed countries) are bringing major demographic changes in aging. Currently, around 10% world population is aged over 65 and it is estimated that this demography will see a 10 times increase in next 50 years [1]. It is observed that fall is the major contributor to the growing rates of mortality, morbidity of aging population, and complications induced by fall contribute to the increase in higher health care cost also [2]. According to U.S. Census Bureau, 13% of the population is over 65 years old, out of which 40% homely old-age adults fall atleast once a year and 1 in 40 is hospitalised. Those who are hospitalised have 50% of chance to be alive a year later. Fall is a major health

threat to not only independently living elders [3] but also to community-dwelling ones where fall rate is estimated to be 30% to 60% annually [4]. Elders who suffer from visual impairment, urinary incontinence, and functional limitations are at increased risk of recurrent falls [5]. Therefore, pervasive fall detection systems that meet the needs of aging population is a necessity especially since increase of aging population and estimated decrease in health care professionals demand for technology assisted intelligent health care solutions [6].

Considerable efforts have been made to design fall detection solutions for elderly populations, see [7] for a comprehensive list of solutions proposed by researchers. As more of society is relying on smartphones because of its ubiquitous nature of internet connectivity and computing, smartphone based fall-detection assisted health monitoring and emergency response system is highly desired by elderly population. In fact, recent trend suggests that smartphones are reducing the need for wearing watches, the most common wearable gadget in previous centuries [8] making smartphones the most commonly carried device by people. Naturally, effective smartphone based fall-detection solutions that do not require any infrastructure support external to smartphones are more fitting the needs of elderly population.

In this work, we aim to design a smartphone based standalone fall detection system that is portable, cost efficient, user friendly, privacy preserving [9], and requiring only existing cellphone technology. In addition, such solution must exhibit low memory and low computational overhead which is only fitting since cellphones are constrained by limited energy and limited memory. Clearly, this motivates the design approaches centering around existing sensing technology available in cellphones. Among sensor data, accelerometer sensor is considered to be accurate [10] and therefore, a natural choice for design of such system. In fact, accelerometer and orientation sensor combination based solutions are proposed in past researches, for example, iFall [11] are some of the most notable solutions that meet the design requirements mentioned above. However, through experimentation, we show that smartphone fall detection solutions that involve accelerometer data supplemented with orientation sensor data are not very accurate. Therefore, to meet the above requirements, we propose a novel fall detection mechanism that utilizes gravity sensor data and accelerometer data. Experimental comparision shows that the proposed approach is superior as compared to its peers. In our work, Android operating system platform is used for experimentation and implementation purposes.

This paper is organized as follows: in Section 2, we discuss recent and landmark research work in this area. Section 3 discusses an Android based application for data acquisition and our proposed fall detection method. In Section 4, *alpha test* is performed on Gradient using simulated data. Finally, summary and possible future work are discussed in section 5.

## 2 Related Work

Various studies have been carried out on fall detection using wearable sensors and mobile phones. We divide the fall detection systems in two categories:

## 2.1 User-Centric and Device-Friendly

The first accelerometer data driven fall detection system was proposed in [12]. Their system detects a fall when there is a change in body orientation from upright to lying that occurs immediately after a large negative acceleration. This system design later becomes a reference point for many fall detection algorithms using accelerometers.

A popular Android phone application, iFall [11], is developed for fall monitoring and response. Data acquired from the accelerometer with the help of application is evaluated with several threshold based algorithms to determine a fall. Basic body metrics like height and weight, along with level of activity are used for estimating the threshold values. An alert notification system, SMS and emergency call is developed in moderate to critical situations and emergency.

A threshold based fall detection algorithm is proposed in [13]. The algorithm works by detecting dynamic situations of postures, followed by unintentional falls to lying postures. The thresholds calculated and obtained from the collected data are compared with the linear acceleration and the angular velocity sensor data for detecting the fall. After the fall is detected, a notification is sent to make an alert about the fall. The authors used gyroscope for data acquisition. The gyroscope data is not efficient in detecting the fall accurately therefore making the proposed system not a good choice for monitoring the fall. In [14], accelerometer and gyroscope sensors are used together to detect fall in elderly population. Further gravity and angular velocity is extracted from the data to detect fall. Using gravity and angular velocity not only detect a fall but also the posture of the body during fall is detected. Authors experimented the system to know the false positive and false negative fall detection. Also, false fall positions were used in study to know the impact and efficiency of the algorithm. The approach used to detect the fall in their proposed study is too simple to be adopted for detecting *quick* falls using accelerometer data. That is why, the system performs poorly in differentiating *jumping into bed* and *falling against wall* with seated posture.

In [15], a smartphone-based fall detection system using a threshold-based algorithm to distinguish between activities of daily living and falls in real time is proposed. By comparative analysis of threshold levels for acceleration, in order to get the best sensitivity and specificity, acceleration thresholds were determined for early pre-impact alarm ( $4.5\text{-}5 \text{ m/s}^2$ ) and post-fall detection ( $21\text{-}28 \text{ m/s}^2$ ) under experimental conditions. The experimental thresholds calculated are helpful for further study in this area of research. But accelerometer alone is not sufficient for detecting the fall effectively.

## 2.2 External Infrastructure Based

The paper [16] describes a fall detection sensor to monitor the subject safely and accurately by implementing it in a large sensor network called SensorNet. Initial approaches such as conjoined angle change and magnitude detection algorithm were unsuccessful. Another drawback of this approach involves inefficiency of

complex fall detection in which the user did not end up oriented horizontally with the ground. The fall-detection board designed was able to detect 90% of all falls with 5% false positive rate.

The Ivy project [17] used low-cost and low-power wearable accelerometer on wireless sensor network to detect the fall. The threshold on the peak values of the accelerometer were estimated along orientation angular data to detect the fall. The authors found that the intensity and acceleration of fall is far different from other activities. The main drawback of this proposed system is that it only works well for an indoor environment because of its dependance on a fixed network to relay events. In the study [18], accelerometer sensor is used to detect wearer's posture, activity and fall in wireless sensor network. The activity is determined by the *alternating current* component and posture is determined by the *direct current* component of the accelerometer signal. Fall detection rate of the proposed system is 93.2%. The paper lacks in explaining the actual algorithm. Moreover the complexity and cost involved in designing the system makes it less suitable for fall-detection in real life scenario.

In [19], authors proposed a fall detection system which uses two sets of sensors, one with an accelerometer and a gyroscope and the other with only an accelerometer. They used sensor data to calculate angular data and their system outperforms the earlier known systems as the system is able to detect fall with an average lead-time of 700 milliseconds before the impact to ground occurs. The major drawback of the system is that the subject has to wear torso and thigh sensors and this tends to be cumbersome for subjects. Also, the system is not capable to record data in real-life situations.

### 3 Methods

In this section, first, principle behind previous researches that utilize orientation sensor based design approaches is discussed, then we describe gravity sensor based approach that forms the principle and basis of our proposal. We further show that gravity sensor based design is more accurate and becomes a natural choice for user-centric and device friendly fall detection solution approaches.

#### 3.1 Design Principle: Orientation Sensor

A gyroscope can be used to either measure, or maintain, the orientation of a device. In comparison with an accelerometer, a gyroscope measures the orientation rather than linear acceleration of the device. Analyzing accelerometer and orientation data to detect fall is the core of several fall detection systems. Orientation sensor which in most cases is the combination of gyro sensor magnetometer supplements the aim to provide accurate orientation data. We further explain the idea behind this approach.

Tri-axial orientation is represented in Figure 1(a)) where  $\theta$ ,  $\phi$ , and  $\psi$  are azimuthal angle ( $0^0$  is north), pitch angle ( $0^0$  is flat on its back from positive Y, east) and roll angle ( $0^0$  is flat on its back from positive Z, downward) respectively.

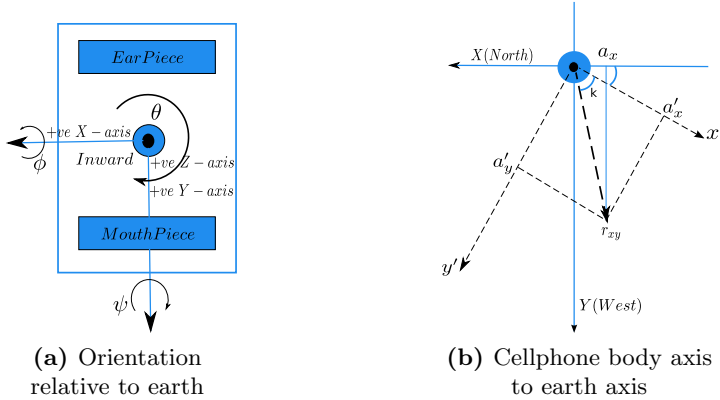


**Fig. 1.** Orientation of cellphone relative to real world axis system

Consider the example in Figure 1(b), where axis system is rotated around z axis by  $\theta$ . The rotated axis are shown as  $X'$  and  $Y'$ .  $X'$  and  $Y'$  are axis coordinates relative to phone. Contribution of this rotation to the X component of fixed axis (X and Y) is given as:  $a_x = r_{xy} \cos(\theta + k)$ , where  $a'_x$  and  $a'_y$  are  $X'$  and  $Y'$  components of acceleration vector and  $k$  is the angle acceleration vector makes width the  $X'$  axis. Combining the effect of azimuth, roll and pitch, we get following matrix:

$$M = \begin{bmatrix} \cos(\psi).\cos(\phi) & -\sin(\psi).\cos(\theta) & \sin(\psi).\sin(\theta) \\ \sin(\psi).\cos(\phi) & \cos(\psi).\cos(\theta) & -\cos(\psi).\sin(\theta) \\ -\sin(\psi) & \cos(\phi).\sin(\theta) & \cos(\phi).\cos(\theta) \end{bmatrix} + \begin{bmatrix} 0 & \cos(\psi).\sin(\phi).\sin(\theta) & \cos(\psi).\sin(\phi).\cos(\theta) \\ 0 & \sin(\phi).\sin(\theta) & \sin(\psi).\sin(\phi).\cos(\theta) \\ 0 & 0 & \cos(\phi).\cos(\theta) \end{bmatrix} \quad (1)$$

Relation between body axis ( $[x', y', z']$ ) and earth axis ( $[x, y, z]$ ) is given as

$$[a_x \quad a_y \quad a_z] = [a_{x'} \quad a_{y'} \quad a_{z'}] \times M \quad (2)$$

Here  $a_x$ ,  $a_y$  and  $a_z$  are accelerometer sensor readings on tri-axial coordinate system relative to cell phone and  $\theta$ ,  $\phi$  and  $\psi$  are orientation sensor readings from the mobile phone and  $M$  is the matrix defined in equation 1.

### 3.2 Design Principle: Gravity Sensor

Gravity sensor returns only the influence of gravity. Gravity vector under the context of the phone coordinate system is given as:  $\vec{G} = (g_{x'}, g_{y'}, g_{z'})$ , and acceleration in the same axis system is given as:  $\vec{A} = (a_{x'}, a_{y'}, a_{z'})$ .

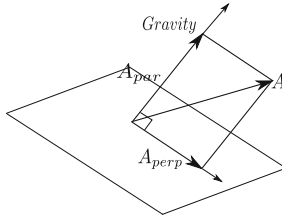


**Fig. 2.** Cellphone Acceleration Along ( $A_{par}$ ) and Perpendicular ( $A_{perp}$ ) to Gravity

From Figure 2, since both vectors are under the same coordinate system, the phone coordinate system by simple vector inner product, the angle between the two can be easily found and thus acceleration component of cellphone parallel to gravity vector is given as below,

$$\overrightarrow{A_{par}} = \vec{a}_z = (\vec{A} \odot \vec{G}) \frac{\vec{G}}{|\vec{G}|^2} \quad (3)$$

Likewise, the perpendicular counterpart is given as below,

$$\overrightarrow{A_{perp}} = \vec{A} - (\vec{A} \odot \vec{G}) \frac{\vec{G}}{|\vec{G}|^2} \quad (4)$$

The absolute value of downward acceleration is given by following equation:

$$|\overrightarrow{A_{par}}| = |a_z| = \frac{a_x' g_{x'} + a_y' g_{y'} + a_z' g_{z'}}{\sqrt{g_{x'}^2 + g_{y'}^2 + g_{z'}^2}} \quad (5)$$

And the absolute acceleration along  $X' - Y'$  plane of cellphone is given as

$$|\overrightarrow{A_{perp}}| = \sqrt{a_{x'}^2 + a_{y'}^2 + a_{z'}^2 - |\overrightarrow{A_{par}}|^2} \quad (6)$$

### 3.3 Orientation Sensor vs. Gravity Sensor

A comparison of vertical downward acceleration component of linear acceleration sensor data using orientation sensor values (Equation 1 and Equation 2) with the same using gravity sensor values is presented in Figure 3. We observe unstable and erroneous values using orientation sensor where as the values using gravity sensor data is stable and accurate. Gyro sensor and Magnetometer sensor suffer through convergence to stabilize values and hence causes a problem which one can see in our experiment. Therefore, it explains why many supposedly promising solutions failed the accuracy test by a huge margin. With this observation, we are motivated to use gravity sensor in our work. To the best of our knowledge, our work is beyond the research already done and includes gravity sensor which is more promising in detecting a real fall than a false fall. The system design using accelerometer and gravity sensor follows next.

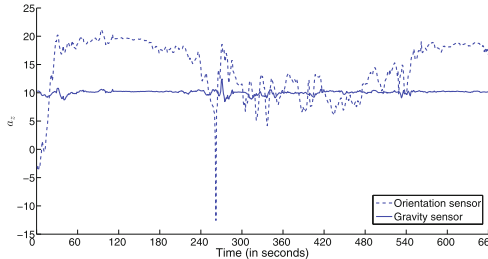


**Fig. 3.** Downward acceleration: Orientation sensor vs. Gravity sensor

## 4 Gradient: System Design

### 4.1 Data Acquisition

The Android application has been developed by considering the importance of each sensor inside the phone. Since application is basically developed to collect data through sensors even when screen is off therefore it is designed to work as a service rather than an activity for collecting data through available sensors in the device. The application is designed to run on any Android platform having at least GingerBread operating system [20]. Application uses both accelerometer and gravity sensors for the data acquisition. Both the sensors are acceleration based sensors and are responsible for measuring acceleration of the device in all three directions. An acceleration sensor measures the acceleration applied to the device, including the force of gravity. The gravity sensor provides a three dimensional vector indicating the direction and magnitude of gravity. Along this configuration, an application uses permissions to write to external storage for saving the data in the form of CSV (Comma-separated values) files. The data is saved in different CSV files based on the type of sensors. *x-axis*, *y-axis*, *z-axis* and timestamp are recorded in the respective files. As the data is acquired, the saved files are used to process and detect fall. Subsection 4.2 describes the our processed methodology.

### 4.2 Algorithm

*Gradient* is based on the observation that when a user falls there is a sudden change in acceleration in vertical downward direction and therefore, downward acceleration component contains enough information to detect fall events. We ran several laboratory experiments to verify this hypothesis. The sensor data is collected on a mobile device using *Gradient* application. Then the differentiation of vertical downward component in time is compared with preset threshold value to identify fall events. It is to be noted that the name *Gradient* is derived from **Gravity-differentiation**, the driving idea behind the proposed solution. The detailed algorithm is presented below:

---

**Algorithm 1.** Fall Detection Algorithm (Using Vectorization)

---

**Data:**  $\vec{A}_d \leftarrow (a_x \ a_y \ a_z);$  //Accelerometer sensor readings  
 $\vec{G}_d \leftarrow (g_x \ g_y \ g_z);$  // Gravity sensor readings  
**Result:** *FallDetected*

$W_s \leftarrow 10;$  //Set window size for moving averages  
 $\vec{A}_v \leftarrow mavg(\vec{A}_d, W_s);$  //Calculate moving averages on accelerometer data  
 $\vec{G}_v \leftarrow mavg(\vec{G}_d, W_s);$  //Calculate moving averages on gravity data  
 $|\vec{A}_{par}| \leftarrow \frac{a_x g_x + a_y g_y + a_z g_z}{\sqrt{g_x^2 + g_y^2 + g_z^2}};$  //Downward acceleration  
 $|\vec{A}_{perp}| \leftarrow \sqrt{a_x^2 + a_y^2 + a_z^2 - |\vec{A}_{par}|^2};$  //Acceleration along X – Y plane  
 $|\vec{A}_{parNew}| \leftarrow \frac{|\vec{A}_{par}|}{dt};$  //Gradient of the downward acceleration  
 $|\vec{A}_{perpNew}| \leftarrow \frac{|\vec{A}_{perp}|}{dt};$  //Gradient along the x-y plane  
 $Th \leftarrow |\vec{A}_{parNew}|;$  //Estimate threshold value as average of  $A_{par}$   
**if**  $|\vec{A}_{parNew}|_i < \theta, \forall i$  **then**  
  └ *FallDetected*  $\leftarrow$  true;

---

## 5 Result and Discussion

In this section, performance of the proposed solution is discussed along with the experiment scenarios. We did not test our system on real fall datasets<sup>1</sup> because gravity sensor values are not available. However, we tried our best to collect fall data in a controlled environment to match the real life natural fall events.

### 5.1 Experiment Set-Up

*Gradient* app distributed among internal members of the research team (4 graduate students and 2 faculty members) to evaluate the user acceptance and feedback of the use of the app and also its accuracy for data acquisition. Data was collected on Samsung Galaxy S4 which has Quad-core 1.6 GHz processor, 2 GB internal RAM and runs on Android OS, v4.2.2 (Jelly Bean). Members of the team carried the smart phone with *Gradient* application during their daily routine of work and activities across different time spans and number of days. Detailed logs of the times when they fall were maintained to check the sustainability of the app post-experimentation and results. Feedbacks were taken from the members to improve the app in every aspect of data acquisition. Two of the experiments performed by the team members are represented in the Figure 4a and 4b respectively. In the first experiment, Figure 4a, there is fall at the end of 6<sup>th</sup> minute of data acquisition. Second fall is clearly visible at end of the 7<sup>th</sup> minute. Similarly in Figure 4b fall can be seen in the mid of 6<sup>th</sup> and 7<sup>th</sup> minute respectively.

---

<sup>1</sup> <http://www.bmi.teicrete.gr/index.php/research/mobifall>

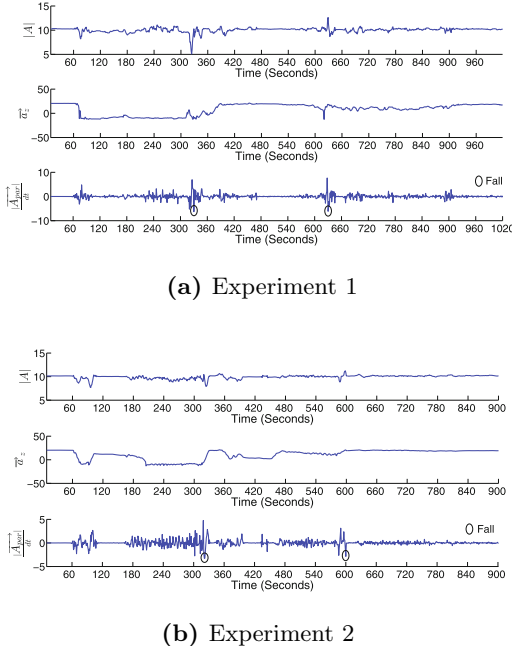


**Fig. 4.** Fall detection experiments

The experiments were conducted by graduate students of the leading author. The students were informed about the procedure and implications of this study. The institute of the leading author also approved this research work. A total of 20 experiments<sup>2</sup> are performed in the closed and safe environment. Total number of actual falls performed by the subjects for the study are 27. It is found that the best threshold value ( $\theta$ ) for the fall detection is -6.15, while applying the *Gradient* approach. The values lesser than  $\theta$  are treated as fall event. The *true positive* falls and *false negative* falls detected by the proposed system are 24 and 3 respectively. On the other hand, *false positive* falls were counted to be 3. On close observation of *false negative* cases, we find that these are the cases where the subject fell from low heights, e.g., from a sofa set. We wish to acknowledge that to distinguish between putting the phone in pocket after receiving a call and falling from a low lying sofa is challenging. These **soft falls** needs further investigation. Also, there is no way to compute the *true negative* cases, so we are not reporting the specificity of the system.

We also attempted to compare our method with a well known Android fall detection application iFall [11]. The iFall detects all 27 fall events but it also raised count of *false negative* to 13, and hence reducing the sensitivity to 67.5% only, see Table 1. We observe that the application is very sensitive to jerks and movements like brisk walking/running. Statistically, our system is more reliable and robust to cope with the real-time activities.

---

<sup>2</sup> All the experiments were performed in controlled and safe environment.

**Table 1.** Comparison between iFall application and Gradient

		Fall		
		Positive	Negative	
<b>Outcome Positive</b>		True positive (TP) = 20	False positive (FP) = 3	<b>Positive predictive value</b> $= \text{TP} / (\text{TP} + \text{FP})$ $= 20 / (20 + 3)$ $= 86.96\%$
<b>Outcome Negative</b>		False negative (FN) = 2	True negative (TN) = 2	<b>Negative predictive value</b> $= \text{TN} / (\text{FN} + \text{TN})$ $= 2 / (2 + 2)$ $= 50.00\%$
		<b>Sensitivity</b> $= \text{TP} / (\text{TP} + \text{FN})$ $= 20 / (20 + 2)$ $= 90.91\%$	<b>Specificity</b> $= \text{TN} / (\text{FP} + \text{TN})$ $= 2 / (3 + 2)$ $= 40.00\%$	<b>Total</b> <b>27</b>

The positive predictive value (86.96%) and sensitivity (90.91%) shows effectiveness of the proposed system in detecting falls.

## 5.2 Gradient in Action

We plotted the time series data in Figure 4. The first subplot is drawn from the magnitude of accelerometer sensor data, which is calculated as:

$$|A| = \sqrt{a_x^2 + a_y^2 + a_z^2}$$

It is to be noted that several researches [11, 13, 15] utilized acceleration data derived by the above Equation for fall detection. However, fall event mainly corresponds to vertical fall therefore, including horizontal components would result into false positives in many activity scenarios where there is a sudden change in horizontal velocity of a person (see next section for further explanation) and clearly, those events are not fall events. For the sake of completeness of this work we have included the absolute value of acceleration in subplot of Figure 4.

The second subplot is derived from value of  $a_z$  from Equation 5. The fall event points are circled in the figure and fall is correctly detected by using the time differential value of  $a_z$ . Although our experimental scenario involves controlled environment, we observe successful detection of all fall events.

## 5.3 Performance Comparison

In this section, we compare our work with one of the most notable work known as iFall [11]. The experiment was performed by running iFall and *Gradient* concurrently along a stop watch to measure the exact time of real falls. The comparison between the iFall and our proposed design is presented in Figure 5. The upper numbered labels 1 through 9 represents falls detected by iFall and the lower numbered labels 1 through 4 represents falls detected by *Gradient*. In Figure 5, we observe although iFall successfully detects fall events, it also

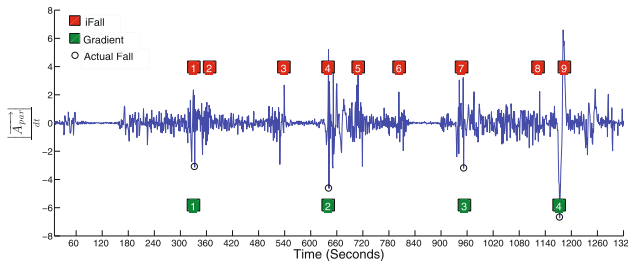


**Fig. 5.** Comparison between iFall (red square) and *Gradient* (blue square)

outputs several false positives in the event of no fall. We observe if the device is on a running motion or on a jerky motion such as shake, iFall records such events as fall events. Clearly, *Gradient* shows better accuracy than iFall.

## 6 Conclusion

Fall is the major health risk among the old-aged people around the world. Fall detection using computational approach has remained a challenging task, that prompted researchers to propose various computational methods to detect the occurrence of fall. But the solution that are user-centric and device-friendly is elusive. In this paper, we proposed a novel approach of fall detection using accelerometer and gravity sensors which are now integral components of smartphones. We designed an Android application to collect experimental data, and applied our algorithm to test the accuracy of the system. Our initial results are very promising and the proposed method has a potential to reduce the false positives which is a common problem with other popular user-centric and device-friendly systems. Furthermore, we believe that this system can help health caretakers, health professionals, and medical practitioners to better manage health hazards due to fall in elder people. In future, we plan to conduct a user study with a healthcare center and test our system on real fall datasets.

## References

1. Haub, C.: World population aging: clocks illustrate growth in population under age 5 and over age 65. Population Reference Bureau, June 18, 2013 (2011)
2. Fulks, J., Fallon, F., King, W., Shields, G., Beaumont, N., Ward-Lonergan, J.: Accidents and falls in later life. Generations Review **12**(3), 2–3 (2002)
3. Duthie Jr, E.: Falls. The Medical clinics of North America **73**(6), 1321–1336 (1989)
4. Graafmans, W., Ooms, M., Hofstee, H., Bezemer, P., Bouter, L., Lips, P.: Falls in the elderly: a prospective study of risk factors and risk profiles. American Journal of Epidemiology **143**(11), 1129–1136 (1996)
5. Tromp, A., Pluijm, S., Smit, J., Deeg, D., Bouter, L., Lips, P.: Fall-risk screening test: a prospective study on predictors for falls in community-dwelling elderly. Journal of Clinical Epidemiology **54**(8), 837–844 (2001)

6. Kleinberger, T., Becker, M., Ras, E., Holzinger, A., Müller, P.: Ambient intelligence in assisted living: enable elderly people to handle future interfaces. In: Stephanidis, C. (ed.) UAHCI 2007 (Part II). LNCS, vol. 4555, pp. 103–112. Springer, Heidelberg (2007)
7. Igual, R., Medrano, C., Plaza, I.: Challenges, issues and trends in fall detection systems. BioMedical Engineering OnLine **12**(1), 1–24 (2013)
8. Phones replacing wrist watches. <http://today.yougov.com/news/2011/05/05/brother-do-you-have-time/> (online accessed April 22, 2014)
9. Ziefle, M., Rocker, C., Holzinger, A.: Medical technology in smart homes: exploring the user's perspective on privacy, intimacy and trust. In: 2011 IEEE 35th Annual Computer Software and Applications Conference Workshops (COMPSACW), pp. 410–415. IEEE (2011)
10. Lindemann, U., Hock, A., Stuber, M., Keck, W., Becker, C.: Evaluation of a fall detector based on accelerometers: A pilot study. Medical and Biological Engineering and Computing **43**(5), 548–551 (2005)
11. Sposaro, F., Tyson, G.: ifall: An android application for fall monitoring and response. In: Annual International Conference of the IEEE Engineering in Medicine and Biology Society, EMBC 2009, pp. 6119–6122. IEEE (2009)
12. Williams, G., Doughty, K., Cameron, K., Bradley, D.: A smart fall and activity monitor for telecare applications. In: Proceedings of the 20th Annual International Conference of the IEEE Engineering in Medicine and Biology Society, 1998, vol. 3, pp. 1151–1154. IEEE (1998)
13. Wibisono, W., Arifin, D.N., Pratomo, B.A., Ahmad, T., Ijthihadie, R.M.: Falls detection and notification system using tri-axial accelerometer and gyroscope sensors of a smartphone. In: 2013 Conference on Technologies and Applications of Artificial Intelligence (TAAI), pp. 382–385. IEEE (2013)
14. Li, Q., Stankovic, J.A., Hanson, M.A., Barth, A.T., Lach, J., Zhou, G.: Accurate, fast fall detection using gyroscopes and accelerometer-derived posture information. In: Sixth International Workshop on Wearable and Implantable Body Sensor Networks, BSN 2009, pp. 138–143. IEEE (2009)
15. Mao, L., Liang, D., Ning, Y., Ma, Y., Gao, X., Zhao, G.: Pre-impact and impact detection of falls using built-in tri-accelerometer of smartphone. In: Zhang, Y., Yao, G., He, J., Wang, L., Smalheiser, N.R., Yin, X. (eds.) HIS 2014. LNCS, vol. 8423, pp. 167–174. Springer, Heidelberg (2014)
16. Brown, G.: An accelerometer based fall detector: development, experimentation, and analysis. University of California, Berkeley (2005)
17. Chen, J., Kwong, K., Chang, D., Luk, J., Bajcsy, R.: Wearable sensors for reliable fall detection. In: 27th Annual International Conference of the Engineering in Medicine and Biology Society, IEEE-EMBS 2005, pp. 3551–3554. IEEE (2006)
18. Lee, Y., Kim, J., Son, M., Lee, J.H.: Implementation of accelerometer sensor module and fall detection monitoring system based on wireless sensor network. In: 29th Annual International Conference of the IEEE Engineering in Medicine and Biology Society, EMBS 2007, pp. 2315–2318. IEEE (2007)
19. Nyan, M., Tay, F.E., Murugasu, E.: A wearable system for pre-impact fall detection. Journal of Biomechanics **41**(16), 3475–3481 (2008)
20. Inc., G.: Android Gingerbread OS (2013). <http://developer.android.com/about/versions/android-2.3-highlights.html> (online accessed April 04, 2014)

# Towards Diet Management with Automatic Reasoning and Persuasive Natural Language Generation

Luca Anselma<sup>(✉)</sup> and Alessandro Mazzei

Dipartimento di Informatica, Università di Torino, Turin, Italy  
[{anselma,mazzei}@di.unito.it](mailto:{anselma,mazzei}@di.unito.it)

**Abstract.** We devise a scenario where the interaction between man and food is mediated by an intelligent system that, on the basis of various factors, encourages or discourages the user to eat a specific dish. The main factors that the system need to account for are (1) the diet that the user intends to follow, (2) the food that s/he has eaten in the last days, and (3) the nutritional values of the dishes and their specific recipes. Automatic reasoning and Natural Language Generation (NLG) play a fundamental role in this project: the compatibility of a food with a diet is formalized as a Simple Temporal Problem (STP), while the NLG tries to motivate the user. In this paper we describe these two facilities and their interface.

**Keywords:** Diet management · Automatic reasoning · Natural language generation

## 1 Introduction

The daily diet is one of the most important factors influencing diseases, in particular for obesity. As highlighted by the World Health Organization, this factor is primarily due to the recent changes in the lifestyle [26]. The necessity to encourage the world's population toward a healthy diet has been sponsored by the FAO [20]. In addition, many states specialized these guidelines by adopting strategies related to their *food history* (for instance, for USA <http://www.choosemyplate.gov>). In Italy, the Italian Society for Human Nutrition has recently produced a prototypical study with recommendations for the use of specialized operators [1].

This scenario suggests the possibility to integrate the directives on nutrition in the daily diet of people by using multimedia tools on mobile devices. The smartphone can be considered as an super-sense that creates new modalities of interaction with food. In recent years there has been a growing interest in using multimedia applications on mobile devices as *persuasive* technologies [13].

Often a user is not able to carefully follow a diet for a number of reasons. When a deviation occurs, it is useful to support the user in devising the consequences of such deviation and to dynamically adapt the rest of the diet in the upcoming meals so that the global Dietary Reference Values (henceforth DRVs)

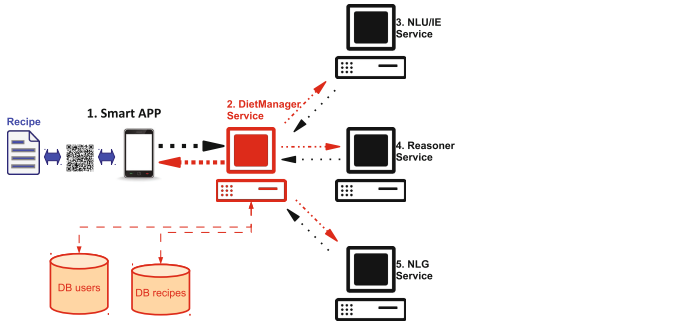


**Fig. 1.** The architecture of the diet management system.

could nevertheless be reached. In particular in this paper we describe a system which is useful for (i) evaluating the compatibility of a dish with a diet allowing small and occasional episodes of diet disobedience, (ii) determining what are the consequences of eating a specific dish on the rest of the diet, (iii) showing such consequences to the user thus empowering her/him and, moreover, (iv) motivating the user in following the diet by persuading her/him to minimize the acts of disobedience. Using automatic reasoning to evaluate the compatibility of a dish with a diet could enhance a smartphone application with a sort of *virtual dietitian*. Artificial intelligence should make the system *tolerant* to diet disobedience, but also *persuasive* to minimize these acts of disobedience. Thus, a critical issue directly related to automatic reasoning is the final presentation to the user of the results. Several studies have addressed the problem of generating natural language sentences that explain the results of automatic reasoning [4, 17].

In our hypothetical scenario the interaction between man and food is mediated by an intelligent system that, on the basis of various factors, encourages or discourages the user to eat a specific dish. The main factors that the system needs to account for are (1) the diet that the user has to follow, (2) the food that s/he has been eating in the last days or that s/he intends to eat in the next days, and (3) the nutritional values of the ingredients of the dish and its specific recipe. In Fig. 1 we report the architecture of our system. It is composed by five modules/services: a smartphone application (APP), a central module that manages the information flow (DietMANager), an information extraction module (NLU/IE), a reasoning module (Reasoner) and a natural language generation module (NLGenerator). In this paper we focus on the description of the Reasoner and NLGenerator modules; some details on the other modules and on the system can be found on the webpage of the project (<http://di.unito.it/madiman>).

We think that this system could be commercially attractive at least in two contexts. The first context is the medical one, where users (e.g. patients affected by essential obesity) are strongly motivated to strictly follow a diet and need tools that help them. The second context is the one involving, e.g., healthy

fast food or restaurant chains, where the effort of deploying the system can be rewarded by an increase in customer retention.

This paper is organized as follows: in Section 2 we describe the automatic reasoning facilities, in Section 3 we describe the design of the persuasive NLG based on different theories of persuasion and, finally, in Section 4 we draw some conclusions.

## 2 Automatic Reasoning for Diet Management

Since our approach to automatic reasoning for diet management is based on the STP framework, first we introduce STP, then we describe how we exploit STP to reason on a diet and how we interpret the results from STP.

### 2.1 Preliminaries: STP

We base our treatment of nutrition constraints on the framework of “Simple Temporal Problem” (STP) [8]. An STP constraint consists in a bound on differences of the form  $c \leq x - y \leq d$ , where  $x$  and  $y$  are temporal points and  $c$  and  $d$  are numbers (their domain can be either discrete or real). An STP constraint can be interpreted in the following way: the temporal distance between the time points  $x$  and  $y$  is between  $c$  – the lower bound of the distance – and  $d$  – the upper bound of the distance. It is also possible to impose strict inequalities (i.e.,  $<$ ) and  $-\infty$  and  $+\infty$  can be used to denote the fact that there is no lower or upper bound, respectively. An STP is a conjunction of STP constraints.

An interesting feature of STP is that the problem of determining the consistency of an STP is tractable and that the algorithm employed, i.e., an all-pairs shortest paths algorithm such as Floyd-Warshall’s one, also obtains the minimal network, that is the minimum and maximum distance between each pair of points. STP can be represented with a graph whose nodes correspond to the temporal points of the STP and whose arcs are labeled with the temporal distance between the points.

**Property.** Floyd-Warshall’s algorithm is correct and complete on STP, i.e. it performs all and only the correct inferences while propagating the STP constraints [8], and obtains a minimal network. Its temporal computational cost is cubic in the number of time points.

### 2.2 Towards Automatically Reasoning on a Diet

**Reasoning on DRVs.** In a diet it is necessary to consider parameters such as the total energy requirements and the specific required amount of nutrients and macronutrients such as proteins, carbohydrates and lipids. In particular in the literature it is possible to find systems of DRVs that are recommended to be followed for significant amounts of time. In the running example, without loss of generality we refer to the Italian values [1]. Such values have to be customized for the specific patients according to their characteristics. In particular, from

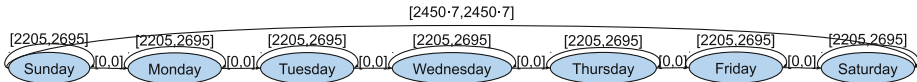


**Fig. 2.** Example of DRVs for a week represented as STP (for space constraints the constraints for the meals are not represented).

weight, gender and age, using Schofield equation [24], it is possible to estimate the basal metabolic rate; for example a 40-year-old male who is 1.80 m tall and weighs 71.3 kg has an estimated basal metabolic rate of 1690 kcal/day. Such value is then adjusted [1] by taking into account the energy expenditure related to the physical activity of the individual; for example a sedentary lifestyle corresponds to a physical activity level of 1.45, thus, in the example, since the physical activity level is a multiplicative factor, the person has a total energy requirement of 2450 kcal/day. Moreover, it is recommended [1] that such energy is provided by the appropriate amount of the different macronutrients, e.g., 260 kcal/day of proteins, 735 kcal/day of lipids and 1455 kcal/day of carbohydrates. In this section we focus on the total energy requirement; the macronutrients can be dealt with separately in the same way.

We represent the DRVs as STPs; more precisely, we use an STP constraint to represent – instead of temporal distance between temporal points – the admissible DRVs. Thus, e.g., a recommendation to eat a lunch of minimum 500 kcal and maximum 600 kcal is represented by the STP constraint  $500 \leq \text{lunch}_E - \text{lunch}_S \leq 600$ , where  $\text{lunch}_E$  and  $\text{lunch}_S$  represent the end and the start of the lunch, respectively.

Furthermore, we exploit the STP framework to allow a user to make small deviations with regard to the “ideal” diet and to know in advance what are the consequences of such deviations on the rest of the diet. Thus, we impose less strict constraints over the shortest periods (i.e., days or meals) and stricter constraints over the longest periods (i.e., months, weeks). For example the recommended energy requirement of 2450 kcal/day, considered over a week, results in a constraint such as  $2450 \cdot 7 \leq \text{week}_E - \text{week}_S \leq 2450 \cdot 7$  and for the single days we allow the user to set, e.g., a deviation of 10%, thus resulting in the constraints  $2450 - 10\% \leq \text{Sunday}_E - \text{Sunday}_S \leq 2450 + 10\%$ , ...,  $2450 - 10\% \leq \text{Saturday}_E - \text{Saturday}_S \leq 2450 + 10\%$  (see Fig. 2). For single meals we can further relax the constraints: for example the user can decide to split the energy assumption for the day among the meals (e.g., 20% for breakfast and 40% for lunch and dinner) and to further relax the constraints (e.g., of 30%), thus resulting in a constraint, e.g.,  $2450 \cdot 20\% - 30\% \leq \text{Sunday\_breakfast}_E - \text{Sunday\_breakfast}_S \leq 2450 \cdot 20\% + 30\%$ .

**Representing and Reasoning on the Diet and the Food.** Along these lines, it is possible to represent the dietary recommendations for a specific user. However, we wish to support such a user into taking advantage of the information regarding the actual meals s/he consumes. In this way, the user can learn what



**Fig. 3.** Example of DRVs represented as STP.

are the consequences on his/her diet of eating a specific dish and s/he could use such information in order to make informed decisions about the current or future meals. Therefore it is necessary to “integrate” the information about the eaten dishes with the dietary recommendations. We devise a system where the user inputs the data about the food s/he is eating using a mobile app where the input is possibly supported by reading a QR code and s/he can also specify the amount of food s/he has eaten. Thus, we allow some imprecision due to possible differences in the portions (in fact, the actual amount of food in a portion is not always the same and, furthermore, a user may not eat a whole portion) or in the composition of the dish [6]. We support such feature by using STP constraints also for representing the nutritional values of the eaten food.

The dietary recommendations can be considered constraints on *classes*, which can be instantiated several times when the user assumes his/her meals. Thus, the problem of checking whether a meal satisfies the constraints of the dietary recommendations corresponds to checking whether the constraints of the instances satisfy the constraints of the classes. This problem has been dealt with in [25] and [2]. In these works the authors have considered the problem of “inheriting” the temporal constraints from classes of events to instances of events in the context of the STP framework, also taking into account problems deriving from correlation between events and from observability. In our setting we have a simpler setting, where correlation is known and observability is complete (even if possibly imprecise). Thus, we generate a new, provisional, STP where we add the new STP constraints deriving from the meals that the user has consumed: the added constraints possibly restrict the values allowed by the constraints in the STP. Then we propagate the constraints in such a new STP and we determine whether the new constraints are consistent and we obtain the new minimal network with the implied relations. For example, let us suppose that the user on Sunday, Monday and Tuesday had an actual intake of 2690 kcal for each day. This corresponds to adding to the STP the new constraints  $2690 \leq Sunday_E - Sundays \leq 2690$ , ...,  $2690 \leq Tuesday_E - Tuesdays \leq 2690$ . Then, propagating the constraints of the new STP (see Fig. 3), we discover that (i) the STP is consistent and thus the intake is compatible with the diet and (ii) on each remaining day of the week the user has to assume a minimum of 2205 kcal and a maximum of 2465 kcal.

### 2.3 Interpretation of STP

Although the information deriving from the STP is complete (and correct), in order to show to the user a meaningful feedback and to make it possible to interface the automatic reasoning module with the NLG module, it is useful

to interpret the results of the STP. In particular we wish to provide the user with a user-friendly information not limited to a harsh “consistent/inconsistent” answer regarding the adequacy of a dish with regard to her/his diet. Therefore we consider the case where the user proposes to our system a dish, we obtain its nutritional values, we translate them, along with the user’s diet and past meals, into STP and, by propagating the constraints, we obtain the minimal network. By taking into account a single macronutrient (carbohydrates, lipids or proteins), the resulting STP allows us to classify the macronutrient in the proposed dish in one of the following five cases: *permanently inconsistent* (I.1), *occasionally inconsistent* (I.2), *consistent and not balanced* (C.1), *consistent and well-balanced* (C.2) and *consistent and perfectly balanced* (C.3).

In the cases I.1 and I.2 the value of the macronutrient is inconsistent. In case I.1 the value for the nutrient is inconsistent with the DRVs as represented in the user’s diet. The dish cannot be accepted even independently of the other food s/he may possibly eat. This case is detected by considering whether the macronutrient violates a constraint on classes. In case I.2 the dish per se does not violate the DRVs, but – considering the past meals s/he has eaten – it would preclude to be consistent with the diet. Thus, it is inconsistent now, but it could become possible to choose it in the future, e.g., next week or month. This case is detected by determining whether the macronutrient, despite it satisfies the constraints on the classes, is inconsistent with the propagated inherited STP.

In the cases C.1, C.2 and C.3 the value of the macronutrient is consistent with the diet, also taking into account the other dishes that the user has already eaten. It is possible to detect that the dish is consistent by exploiting the minimal network of the STP: if the value of the macronutrient is included between the lower and upper bounds of the relative constraint, then we are guaranteed that the STP is consistent and that the dish is consistent with the diet. This can be proven by using the property that in a minimal network every tuple in a constraint can be extended to a solution [19]. A consistent but not balanced choice of a dish will have consequences on the rest of the user’s diet because the user will have to “recover” from it. Thus we distinguish three cases depending on the level of the adequacy of the value of the macronutrient to the diet. In order to discriminate between the cases C.1, C.2 and C.3, we consider how the value of the macronutrient stacks upon the allowed range represented in the related STP constraint. We assume that the mean value is the “ideal” value according to the DRVs and we consider two parametric user-adjustable thresholds relative to the mean: according to the deviation with respect to the mean we classify the macronutrient as not balanced (C.1), well balanced (C.2) or perfectly balanced (C.3) (see Fig. 4). In particular, we distinguish between lack or excess of a specific macronutrient for a dish: if a macronutrient is lacking (in excess) with regard to the ideal value, we tag the dish with the keyword *IPO* (*IPER*). This information will be exploited in the generation of the messages.

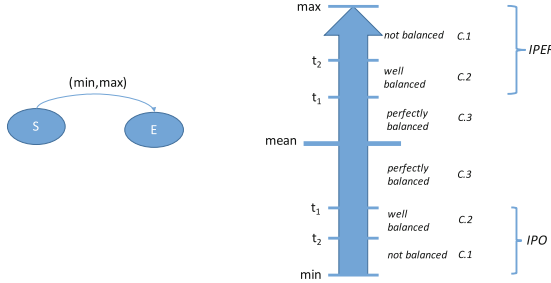


**Fig. 4.** Classification of a consistent value of a macronutrient given the minimum and maximum value of an STP constraint in a minimal network.

### 3 Persuasive NLG for Diet

A number of works considered the problem of NLG for presenting the results of automated reasoning to a user, especially in the case of expert systems for reasoning, e.g., [4, 17]. In order to convert the five possible kinds of output of the STP reasoner (see Section 2.3) in messages, we adopted a simple template-based generator that produces five kinds of messages designed for persuasion. We first describe the generator (Section 3.1) and later we describe the theories that motivated the design of our messages (Section 3.2).

#### 3.1 A Simple Template-Based Generation Architecture

The standard architecture for NLG models generation is a pipeline composed by three distinct modules/processes: the document planning, the micro-planning, and the surface realization [22]. Each one of these modules addresses distinct issues, in particular: (1) In the document planning one decides what to say, that is which information contents will be communicated; (2) In the micro-planning, the focus is on the design of a number of features that are related to the information contents as well as to the specific language, as the choice of the words; (3) In the surface realization, sentences are finally generated on the base of the decision taken by the previous modules and by considering the constraints related to the language specific word order and inflections.

For our system, the contents of information that have to be communicated, i.e. the document planning, are produced by the reasoner. Moreover, with the aim to easily implement in the messages the prescriptions of the persuasion theories, we adopted the simplest architecture for NLG. We treat sentence planning and surface realization in one single module by adopting a *template-based* approach. We use five templates to communicate the five cases of output of the reasoner: in Table 1 we report the cases obtained by the interpretation of the output of the reasoner (column **C**), the direction of the deviation (column **D**), the Italian templates and their rough English translation.

Indeed, the final message is obtained by modifying the templates on the basis of the specific values for the motivation of inconsistency that can be extracted by

**Table 1.** The persuasive message templates: the underline denotes the variable parts of the template. The column **C** contains the classification produced by the STP reasoner, while the column **D** contains the direction of the deviation: *IPO* (*IPER*) stands for the information that the dish is poor (rich) in the value of the macronutrient.

C	D	Message Template	Translation
I.1	IPO	Questo piatto non va affatto bene, contiene <u>davvero</u> pochissime proteine!	This dish is not good at all, it's too poor in proteins!
I.2	IPO	Ora non puoi mangiare questo piatto perché è <u>poco</u> proteico. Ma se domenica mangi un bel piatto di fagioli allora lunedì potrai mangiarlo.	You cannot have this dish now because it doesn't provide enough proteins, but if you eat <u>a nice dish of beans</u> on Sunday, you can have it on Monday.
C.1	IPO	Va bene mangiare <u>le patatine</u> ma nei prossimi giorni dovrai mangiare <u>più</u> proteine.	It's OK to eat chips but in the next days you'll have to eat <u>more</u> proteins.
C.2	IPO	Questo piatto va bene, è solo un po' scarso di <u>proteine</u> . Nei prossimi giorni anche fagioli però! :)	This dish is OK, but it's <u>a bit poor</u> in proteins. In the next days you'll need beans too! :)
C.3	-	Ottima scelta! Questo piatto è perfetto per la tua dieta :)	Great choice! This dish is perfect for your diet :)

interpreting the output of the reasoner (cf. Section 2.3) and possible suggestions that can guide the choices of the user in the next days. The suggestions can be obtained by a simple table that couples the excess (deficiency) of a macronutrient with a dish that could compensate this excess (deficiency). In particular, for the reasoner's outputs I.1, I.2, C.1 and C.2, we need to distinguish the case of a dish poor in a macronutrient (*IPO* in Table 1) with respect to the case of a dish rich in a macronutrient (*IPER*). If the dish is classified as IPO (IPER), we insert into the message a suggestion to consume in the next days a dish that contains a big (small) quantity of that specific macronutrient.

For sake of simplicity we do not describe the algorithm used in the generation module to combine the three distinct outputs of the reasoner on the three distinct macronutrients (i.e. proteins, lipids and carbohydrates). In short, the messages corresponding to each macronutrient need to be *aggregated* into a single message. A number of constraints related to coordination and relative clauses need to be accounted for [22]. In the next Section we describe the three theories of persuasion that influenced and motivated the design of the messages.

### 3.2 Designing Persuasive Messages in the Diet Domain

A number of theories on the design of persuasive textual and multimedial messages have been proposed in the last years [7, 10–12, 14, 16, 21, 23]. Most of these theories can be split in two narrow categories. The first category includes the theories that approach the persuasion from a practical and empirical point of view, by using strategies and methods typical of the psychology and of the interaction design. The second category includes the theories that approach the persuasion from a theoretical point of view, by using strategies and methods typical of strong artificial intelligence and cognitive science. We discuss the three theories that mostly influenced the design of the messages in relation to our project.

CAPTology (Computers As Persuasive Technologies) is the study of computers as persuasive technologies, i.e. “[...] the design, research, and analysis of interactive computing products (computers, mobile phones, websites, wireless technologies, mobile applications, video games, etc.) created for the purpose of changing peoples attitudes or behaviors” [10]. The starting point of Fogg’s theory is that the computer is perceived by users in three coexisting forms, Tool-Media-SocialActor, and each one of these three forms can exercise some forms of persuasion. As a tool, the computer can enhance the capabilities of a user: our system calculates the nutritional contents of the food, and so it enhances the ability to correctly judge the compatibility of a dish with a diet. As a media the computer “provides experience”: in our system, the human memory is enhanced by the reasoner, which indirectly reminds her/him what s/he ate in the last days. As a social actor the computer creates an empathic relationship with the user reminding her/him the “social rules”: in our system the messages guide the user towards the choice of a balanced meal, convincing her/him to follow the diet that her/himself decided. Fogg recently defined a number of rules to design effectively persuasive systems [11], and some of these rules have modeled our messages. For example, the rule: *Learn what is Preventing the target behavior*, proposes to classify an “uncorrect” behavior along three major lines: (1) lack of motivation, (2) lack of ability, (3) lack of a well-timed trigger to perform the behavior. In our system all the three components play a role. Indeed, a user follows a bad diet because (i) s/he is not enough motivated, (ii) because s/he does not know that the dish is in contrast to her/his diet (iii) because s/he does not have the right stimulus at the time of choosing a dish. The reasoning and the generated messages are working on the last two components: the reasoner enhances the user’s abilities allowing her/him to have the relevant information at the right time, the generation system creates a stimulus (the message) when it is really necessary, *kairos* in the Fogg’s terminology, i.e. when the user has to decide what to eat.

Another approach to computational persuasion is strongly related to the concept of *tailoring*, i.e. the adaptation of the output of the computation to a specific user. A pioneering work for tailoring in the field of NLG is described in [21]: the authors have designed an NLG system, called *STOP*, to build a letter that induces a specific reader to quit smoking. The key component of *STOP* is the individuation of a *user type* by using the answers given to a questionnaire. In this way, one can build a specific user profile. By using this profile the system generates a tailored letter on the basis of a template. This simple approach to persuasion unfortunately did not yield the desired results. The experimental protocol has shown, through the use of a control group, that the enhancement given by customization was negligible. At this stage, we do not adopt in our system the ability to create custom messages for a specific user, but, as evidenced by similar experiences, customization of the feedback could improve the performances of the system. A system for tailoring that we partially adopt in our messages is described in [16], where a series of messages are sent via SMS to reduce the consumption of snacks. In this case, the messages adopt six

patterns/templates for persuasion derived from the general theory of persuasion of Cialdini [7]. The six patterns are: (1) Reciprocity: *people feel obligated to return a favor*, (2) Scarcity: *people will value scarce products*, (3) Authority: *people value the opinion of experts*, (4) Consistency: *people do as they said they would*, (5) Consensus: *people do as other people do*, (6) Liking: *we say yes to people we like*. Compared to this classification, all the messages of our generator belong to the patterns of authority and consistency.

One approach to persuasion strictly related to strong artificial intelligence and cognitive science is based on the concept of the computer as an intelligent agent [12, 14, 23]. The system behaves as a real autonomous entity and it is often modeled as a BDI (Beliefs, Desires, Intentions) agent, whose main purpose is to persuade the user to behave in a specific way. This approach has been adopted essentially for research purposes rather than for commercial applications. In contrast to the design of our NL generator, where there is a single module based on templates, such agent-based approach allows a great modularity in the design of a persuasive system. We describe some issues of these systems in order to understand the deficiencies of our simple approach. Hovy defines a number of heuristic rules that constrain the “argument” defined in the process of sentence planning. For example: *Adverbial stress words can only be used to enhance or mitigate expressions that carry some affect already* [14]. In a similar way, De Rosis and Grasso define a number of heuristic rules on the argument structure, to lexically enhance or mitigate a message [23]. The use of certain adverbs, as little bit (*poco*), very (*molto*), really (*davvero*), are used to enhance some specific argument structures. Indeed, we adopt this strategy by using this kind of adverbs in the messages I.1, I.2, C.1 and C.2. Guerini et al. define a detailed taxonomy of persuasion strategies that a system can adopt and relate the strategies to the theory of argumentation [12]. Moreover, they define an architecture for persuasion that follows the standard modularization of NLG systems. This allows for a very rich persuasive action, which begins from the planning of a rhetorical structure in the content planning. Compared to the taxonomy of the proposed strategies, we can see that our messages belong to one single category, called *action\_inducement/goal\_balance/positive\_consequence*. This strategy induces an action (to choose a dish), by using the user’s goal (a balanced diet) and by using the benefits deriving from this goal.

Finally, note that in the messages C.2 and C.3 we used emoticons. Indeed, some studies showed that the use of emoticons in written texts can increase the communicative strength of a message. For example Dirke shows that the use of emoticons sets a tone of friendship to the message type and can increase the positive value of the message [9].

## 4 Conclusions and Related Works

There are a number of academic studies that are related to our project, among them [3, 15], and there is also a great number of smartphone applications related to nutrition, e.g. *DailyBurn*, *Lose It!*, *MyNetDiary*, *A low GI Diet*, *Weight-Watchers*. However, our dietary system presents two elements of novelty: (1) the

use of automatic reasoning as a tool for verifying the compatibility of a specific recipe with a specific diet and for determining the consequences of the choice of a specific dish and (2) the use of NLG techniques to produce the answer.

Some authors have applied Operational Research techniques to tackle the problem of planning a diet (see the survey in [18] or the more recent paper [5]). These techniques are based on the simplex method for solving linear programming problems. However these approaches are meant to plan an entire diet and they do not support the user in choosing a dish and in investigating the consequences of her/his choice. In [6] the authors have tackled the problem of assessing the compatibility of a single meal to a norm and of suggesting to the user some actions to balance the meal (e.g. removing/adding food); they employed fuzzy arithmetic to represent imprecision/uncertainty in quantity and composition of food and heuristic search for determining the actions to be suggested. They did not consider the problem of globally balancing the meals.

In the next future, we intend to improve the NLG module for tailoring. In particular, we want 1) to build a corpus of sentences that a professional dietitian would use to persuade users towards correct dish choices, 2) to separate microplanning from realization, 3) to classify the users in types in order to personalize the messages on the basis, for instance, of the age. Finally, we plan to experiment the system in two settings. First we intend to design a simulation that includes 1) a database of real recipes, 2) a user model that allows to test the persuasion efficacy and 3) a baseline built rigidly sticking to DRVs. Second, we intend to test the system with a focus group in a clinical setting, in particular with patients affected by essential obesity. In this setting we imagine that the system could be used also by human dieticians for the supervision of their patients.

## References

1. LARN - Livelli di Assunzione di Riferimento di Nutrienti ed energia per la popolazione italiana - IV Revisione. SICS Editore, Milan (2014)
2. Anselma, L., Terenziani, P., Montani, S., Bottrighi, A.: Towards a comprehensive treatment of repetitions, periodicity and temporal constraints in clinical guidelines. *Artificial Intelligence in Medicine* **38**(2), 171–195 (2006)
3. Balintfy, J.L.: Menu planning by computer. *Commun. ACM* **7**(4), 255–259 (1964)
4. Barzilay, R., McCullough, D., Rambow, O., Dechristofaro, J., Korelsky, T., Lavoie, B. Inc, C.: A new approach to expert system explanations. In: 9th International Workshop on Natural Language Generation, pp. 78–87 (1998)
5. Bas, E.: A robust optimization approach to diet problem with overall glycemic load as objective function. *Applied Mathematical Modelling* **38**(19–20), 4926–4940 (2014)
6. Buisson, J.C.: Nutri-educ, a nutrition software application for balancing meals, using fuzzy arithmetic and heuristic search algorithms. *Artif. Intell. Med.* **42**(3), 213–227 (2008)
7. Cialdini, R.B.: Influence: science and practice. Pearson Education, Boston (2009)
8. Dechter, R., Meiri, I., Pearl, J.: Temporal constraint networks. *Artif. Intell.* **49**(1–3), 61–95 (1991)

9. Derkx, D., Bos, A.E.R., von Grumbkow, J.: Emoticons in computer-mediated communication: Social motives and social context. *Cyberpsy., Behavior, and Soc. Networking* **11**(1), 99–101 (2008)
10. Fogg, B.: Persuasive Technology: Using computers to change what we think and do. Morgan Kaufmann Publishers, Elsevier, San Francisco (2002)
11. Fogg, B.: The new rules of persuasion (2009). <http://captology.stanford.edu/resources/article-new-rules-of-persuasion.html>
12. Guerini, M., Stock, O., Zancanaro, M.: A taxonomy of strategies for multimodal persuasive message generation. *Applied Artificial Intelligence* **21**(2), 99–136 (2007)
13. Holzinger, A., Dorner, S., Födinger, M., Valdez, A.C., Ziefle, M.: Chances of increasing youth health awareness through mobile wellness applications. In: Leitner, G., Hitz, M., Holzinger, A. (eds.) USAB 2010. LNCS, vol. 6389, pp. 71–81. Springer, Heidelberg (2010)
14. Hovy, E.H.: Generating Natural Language Under Pragmatic Constraints. Lawrence Erlbaum, Hillsdale (1988)
15. Iizuka, K., Okawada, T., Matsuyama, K., Kurihashi, S., Iizuka, Y.: Food menu selection support system: considering constraint conditions for safe dietary life. In: Proceedings of the ACM Multimedia 2012 Workshop on Multimedia for Cooking and Eating Activities, CEA 2012, pp. 53–58. ACM, New York (2012)
16. Kaptein, M., de Ruyter, B.E.R., Markopoulos, P., Aarts, E.H.L.: Adaptive persuasive systems: A study of tailored persuasive text messages to reduce snacking. *TiiS* **2**(2), 10 (2012)
17. Lacave, C., Diez, F.J.: A review of explanation methods for heuristic expert systems. *Knowl. Eng. Rev.* **19**(2), 133–146 (2004)
18. Lancaster, L.M.: The history of the application of mathematical programming to menu planning. *European Journal of Operational Research* **57**(3), 339–347 (1992)
19. Montanari, U.: Networks of constraints: Fundamental properties and applications to picture processing. *Information Sciences* **7**, 95–132 (1974)
20. Nishida, C., Uauy, R., Kumanyika, S., Shetty, P.: The joint WHO/FAO expert consultation on diet, nutrition and the prevention of chronic diseases: process, product and policy implications. *Public Health Nutrition* **7**, 245–250 (2004)
21. Reiter, E., Robertson, R., Osman, L.: Lessons from a Failure: Generating Tailored Smoking Cessation Letters. *Artificial Intelligence* **144**, 41–58 (2003)
22. Reiter, E., Dale, R.: Building Natural Language Generation Systems. Cambridge University Press, New York (2000)
23. de Rosis, F., Grasso, F.: Affective natural language generation. In: Paiva, A. (ed.) *Affective Interactions*. LNCS, vol. 1814, pp. 204–218. Springer, Heidelberg (2000)
24. Schofield, W.N.: Predicting basal metabolic rate, new standards and review of previous work. *Human Nutrition: Clinical Nutrition* **39C**, 5–41 (1985)
25. Terenziani, P., Anselma, L.: A knowledge server for reasoning about temporal constraints between classes and instances of events. *International Journal of Intelligent Systems* **19**(10), 919–947 (2004)
26. World Health Organization: Global strategy on diet, physical activity and health (WHA57.17). In: 75th World Health Assembly (2004)

# Predicting Within-24h Visualisation of Hospital Clinical Reports Using Bayesian Networks

Pedro Pereira Rodrigues<sup>1,2,3(✉)</sup>, Cristiano Inácio Lemes<sup>4</sup>,  
Cláudia Camila Dias<sup>1,2</sup>, and Ricardo Cruz-Correia<sup>1,2</sup>

<sup>1</sup> CINTESIS - Centre for Health Technology and Services Research,  
Rua Dr. Plácido Costa, s/n, 4200-450 Porto, Portugal  
[{pprodrigues,camila,rccorreia}@med.up.pt](mailto:{pprodrigues,camila,rccorreia}@med.up.pt)

<sup>2</sup> CIDES-FMUP, Faculty of Medicine of the University of Porto,  
Alameda Prof. Hernâni Monteiro, 4200-319 Porto, Portugal

<sup>3</sup> LIAAD - INESC TEC, Artificial Intelligence and Decision Support Laboratory,  
Rua Dr. Roberto Frias, 4200-465 Porto, Portugal

<sup>4</sup> ICMC, Institute of Mathematical and Computer Sciences, University of São Paulo,  
Avenida Trabalhador São-carlense, 400, São Carlos 13566-590, Brazil  
[cristiano.inacio.lemes@gmail.com](mailto:cristiano.inacio.lemes@gmail.com)

**Abstract.** Clinical record integration and visualisation is one of the most important abilities of modern health information systems (HIS). Its use on clinical encounters plays a relevant role in the efficacy and efficiency of health care. One solution is to consider a virtual patient record (VPR), created by integrating all clinical records, which must collect documents from distributed departmental HIS. However, the amount of data currently being produced, stored and used in these settings is stressing information technology infrastructure: integrated VPR of central hospitals may gather millions of clinical documents, so accessing data becomes an issue. Our vision is that, making clinical reports to be stored either in primary (fast) or secondary (slower) storage devices according to their likelihood of visualisation can help manage the workload of these systems. The aim of this work was to develop a model that predicts the probability of visualisation, within 24h after production, of each clinical report in the VPR, so that reports less likely to be visualised in the following 24 hours can be stored in secondary devices. We studied log data from an existing virtual patient record ( $n=4975$  reports) with information on report creation and report first-time visualisation dates, along with contextual information. Bayesian network classifiers were built and compared with logistic regression, revealing high discriminating power (AUC around 90%) and accuracy in predicting whether a report is going to be accessed in the 24 hours after creation.

**Keywords:** Bayesian networks · Health services · Virtual patient records

## 1 Introduction

Evidence-based medicine relies on three information sources: patient records, published evidence and the patient itself [25]. Even though great improvements

and developments have been made over the years, on-demand access to clinical information is still inadequate in many settings, leading to less efficiency as a result of a duplication of effort, excess costs and adverse events [10]. Furthermore, a lot of distinct technological solutions coexist to integrate patient data, using different standards and data architectures which may lead to difficulties in further interoperability [7]. Nonetheless, a lot of patient information is now accessible to health-care professionals at the point of care. But, in some cases, the amount of information is becoming too large to be readily handled by humans or to be efficiently managed by traditional storage algorithms. As more and more patient information is stored, it is very important to efficiently select which one is more likely to be useful [8].

The identification of clinically relevant information should enable an improvement both in user interface design and in data management. However, it is difficult to identify what information is important in daily clinical care, and what is used only occasionally. The main problem addressed here is how to estimate the relevance of health care information in order to anticipate its usefulness at a specific point of care. In particular, we want to estimate the probability of a piece of information being accessed during a certain time interval (e.g. first 24 hours after creation), taking into account the type of data and the context where it was generated and to use this probability to prioritise the information (e.g. assigning clinical reports for secondary storage archiving or primary storage access).

Next section presents background knowledge on electronic access to clinical data (2.1), assessment of clinical data relevance (2.2) and machine learning in health care research (2.3), setting the aim of this work (2.4). Then, section 3 presents our methodology to data processing, model learning, and prediction of within-24h visualisation of clinical data, which results are exposed in section 4. Finally, section 5 finalises the exposition with discussion and future directions.

## 2 Background

The practice of medicine has been described as being dominated by how well information is collected, processed, retrieved, and communicated [2].

### 2.1 Electronic Access to Clinical Data

Currently in most hospitals there are great quantities of stored digital data regarding patients, in administrative, clinical, lab or imaging systems. Although it is widely accepted that full access to integrated electronic health records (EHR) and instant access to up-to-date medical knowledge significantly reduces faulty decision making resulting from lack of information [9], there is still very little evidence that life-long EHR improve patient care [4]. Furthermore, there use is often disregarded. For example, studies have indicated that data generated before an emergency visit are accessed often, but by no means in a majority of

times (5% to 20% of the encounters), even when the user was notified of the availability of such data [12].

One usual solution for data integration in hospitals is to consider a virtual patient record (VPR), created by integrating all clinical records, which must collect documents from distributed departmental HIS [3]. Integrated VPR of central hospitals may gather millions of clinical documents, so accessing data becomes an issue. A paradigmatic example of this burden to HIS is the amount of digital data produced in the medical imaging departments, which has increased rapidly in recent years due mainly to a greater use of additional diagnostic procedures, and an increase in the quality of the examinations. The management of information in these systems is usually implemented using Hierarchical Storage Management (HSM) solutions. This type of solution enables the implementation of various layers which use different technologies with different speeds of access, corresponding to different associated costs. However, the solutions which are currently implemented use simple rules for information management, based on variables such as the time elapsed since the last access or the date of creation of information, not taking into account the likely relevance of information in the clinical environment [6].

In a quest to prioritise the data that should be readily available in HIS, several pilot studies have been endured to analyse for how long clinical documents are useful for health professionals in a hospital environment, bearing in mind document content and the context of the information request. Globally, the results show that some clinical reports are still used one year after creation, regardless of the context in which they were created, although significant differences existed in reports created during distinct encounter types [8]. Other results show that half of all visualisations might be of reports more than 2 years-old [20], although this visualisation distribution also varies across clinical department and time of production [21]. Thus, usage of patients past information (data from previous hospital encounters), varied significantly according to the setting of health care and content, and is, therefore, not easy to prioritise.

## 2.2 Assessment of Clinical Data Relevance

As previously noted, and especially in critical and acute care settings, the age of data is one of the factors often used to assess data relevance, making new information more relevant to the current search. However, studies have shown that some clinical reports are still used after one year regardless of the context in which they were created, although significant differences exist in reports created in distinct encounter types and document content, which contradicts the definition of *old data* used in previous studies. Hence the need to define better rules for recommending documents in encounters.

Classifying the relevance of information based only on the time elapsed since the date of acquisition is clearly inefficient. It is expected that the need to consult an examination at a given time will be dependent on several factors beyond the date of the examination, such as type of examination and the patient's pathology. Thus, a system that uses more factors to identify the relevance of information at

a given time would be more efficient in managing the information that is stored in fast memory and slow memory. A recent study from the same group addressed other possibly relevant factors besides document age, including type of encounter (i.e. emergency room, inpatient care, or outpatient consult), department where the report was generated (e.g. gynaecology or internal medicine) and even type of report in each department, but the possibility of modelling visualisations with survival analysis proved to be extremely difficult [21].

Nonetheless, if we could, for instance, discriminate solely between documents that will be needed in the next 24 hours from the remaining, we could efficiently decide which ones to store in a faster-accessible memory device. Furthermore, we could then rank documents according to their probability of visualisation in order to adjust the graphical user interface of the VPR, to improve system's usability. By applying regression methods or other modelling techniques it is possible to identify which factors are associated with the usage or relevance of patient data items. These factors and associations can then be used to estimate data relevance in a specific future time interval.

### 2.3 Machine Learning in Healthcare Research

The definition of clinical decision support systems (most of the times based on expert systems) is currently a major topic since it may help the diagnosis, treatment selection, prognosis of rate of mortality, prognosis of quality of life, etc. They can even be used to administrative tasks like the one addressed by this work. However, the complicated nature of real-world biomedical data has made it necessary to look beyond traditional biostatistics [14] without loosing the necessary formality. For example, naive Bayesian approaches are closely related to logistic regression [22]. Hence, such systems could be implemented applying methods of machine learning [16], since new computational techniques are better at detecting patterns hidden in biomedical data, and can better represent and manipulate uncertainties [22]. In fact, the application of data mining and machine learning techniques to medical knowledge discovery tasks is now a growing research area. These techniques vary widely and are based on data-driven conceptualisations, model-based definitions or on a combination of data-based knowledge with human-expert knowledge [14].

Bayesian approaches have an extreme importance in these problems as they provide a quantitative perspective and have been successfully applied in health care domains [15]. One of their strengths is that Bayesian statistical methods allow taking into account prior knowledge when analysing data, turning the data analysis into a process of updating that prior knowledge with biomedical and health-care evidence [14]. However, only after the 90's we may find evidence of a large interest on these methods, namely on Bayesian networks, which offer a general and versatile approach to capturing and reasoning with uncertainty in medicine and health care [15]. They describe the distribution of probabilities of one set of variables, making possible a two-fold analysis: a qualitative model and a quantitative model, presenting two types of information for each variable.

On a general basis, a Bayesian network represents a joint distribution of one set of variables, specifying the assumption of independence between them, with the inter-dependence between variables being represented by a directed acyclic graph. Each variable is represented by a node in the graph, and is dependent of the set of variables represented by its ascendant nodes; a node X is a ascendant of another node Y if exists a direct arc from X to Y [16]. To give more representational power to the relations represented by the arcs of the graph, it is necessary to associate values to it. The matrix of conditional probability is given for each variable, describing the distribution of probabilities of each variable given its ascendant variables.

After the qualitative and quantitative models are constructed, the next step, and one of the most important, is how to calculate the new probabilities when new evidence is introduced in the network. This process is called inference and works as follows. Each variable has a finite number of categories greater than or equal to two. A node is observed when there is knowledge about the state of that variable. The observed variables have a huge importance because with conditional probabilities they define the prior probabilities of the non observed variables. With the joint probabilities we can calculate the marginal probabilities of each unobserved variable, adding for all categories the probabilities that the variable is in the desired state [15].

## 2.4 Aim

The aim of this work is the development of a decision support model for discriminating between reports that are going to be useful in the next 24 hours and reports which can be otherwise stored in slower storage devices, since they will not be accessed in the next 24 hours, thus improving performance of the entire virtual patient record system.

## 3 Data and Methods

Between May 2003 and May 2004, a virtual patient record (VPR) was designed and implemented at Hospital S. João, a university hospital with over 1350 beds. An agent-based platform, Multi-Agent System for Integration of Data (MAID), ensures the communication among various hospital information systems (see [24] for a description of the system). Clinical documents are retrieved from clinical department information systems (DIS) and stored into a central repository in a browser friendly format. This is done by regularly scanning 14 DIS using different types of agents [17]:

- For each department, a List Agent regularly retrieves report lists from the DIS, with report file references and meta-data, and stores them in the VPR repository.
- The Balancer Agent of that department retrieves the report file references and distributes them to the departmental File Agents.
- File Agents retrieve the actual report files.

As the amount of information available to the agents increases throughout time, there is also an increase in the difficulty of managing that information by humans. Not rarely, a request for a report arrives (after the List Agent has published the existence of that report) before the File Agent was able to retrieve the document. In this cases, an Express Agent is called to retrieve the file, which stresses the entire system's workload, otherwise balanced.

To enable a quantitative analysis (e.g. the likelihood of document access), all actions by users of the VPR are recorded in the log file. Intentionally and originally created and kept for audit purposes, these logs can provide very interesting insights into the information needs of health-care professionals in some particular situations, although most of the times the quality of these logs is not delivering [5].

### 3.1 Studied Variables and Outcomes

Data was collected from the virtual patient record (VPR) with information on report creation and report first-time visualisation dates, along with contextual information. This study focuses on a sample of 5000 reports (2.7% of the entire data for the studied year) and corresponding visualisations, stored in the VPR in 2010. The data used in this study was collected using Oracle SQL Developer from the VPR patient database, containing patient's identification and references to the clinical records. We developed models with seven explanatory variables, including patient data (age and sex), context data (department and type of encounter) and creation time data (hour, day-of-week, daily period), defined as follows. The main outcome of this study was within-24h visualisation of reports.

**AgeCat** (cat) discretised in decades;

**Sex** (binary);

**Department** (cat);

**EncType** (cat) one of outpatient consult, inpatient care, emergency or other;

**Hour** (cat) truncated from creation time;

**DoW** (cat) one of Sun, Mon, Tue, Wed, Thu, Fri or Sat;

**Period** (cat) one of morning (Hour=7-12), afternoon (13-18), night (19-24) or dawn (1-6);

**Visual24h** (binary) target outcome, whether the report has been visualised in the first 24 hours after creation or not.

### 3.2 Model Building and Evaluation

In order to correctly fit the models, only complete cases were considered in the analysis. Logistic regression was applied to all studied variables to predict visualisation. Additionally, two Bayesian network classifiers were built - Naive Bayes (NB) and Tree Augmented Naive Bayes (TAN) - which differ on the number of conditional dependencies (besides the outcome) allowed among variables (NB: zero dependencies; TAN: one dependence), in order to choose the structure which could better represent the problem. Receiver Operating Characteristic (ROC) curve analysis was performed to determine in-sample area under

the curve (AUC). Furthermore, to assess the general structure and accuracy of learned models, stratified 10-fold cross-validation was repeated 10 times, estimating accuracy, sensitivity, specificity, precision (positive and negative predictive values) and the area under the ROC curve, for all compared models.

### 3.3 Software

Logistic regression was done with R package *stats* [18], Bayesian network structure was learned with R package *bnlearn* [23], Bayesian network parameters were fitted with R package *gRain* [11], ROC curves were computed with R package *pROC* [19], and odds ratios (OR) were computed with R package *epitools* [1].

## 4 Results

A total of 4975 reports were included in the analysis. The main characteristics of the reports are shown in Table 1, which were generated from patients with a mean (std dev) age of 55.5 (20.5). Less than 23% of the reports were visualised in the 24 hours following their creation, which were nonetheless more from female patients (almost 55%) with a 24h-visualisation OR=1.51 (95%CI [1.32,1.72]) for female-patient reports. Also significant was the context of report creation, with more reports being created in inpatient care (44.4%) and outpatient consults (41.4%), although compared with the latter context, 24-hour visualisations are more likely for reports generated in inpatient care (OR=8.60 [7.04,10.59]) or in the emergency room (OR=14.50 [11.22,18.83]). Regarding creation time, morning (OR=1.22 [1.05,1.41]), night (OR=1.82 [1.46,2.28]) and dawn (OR=2.88 [2.03,4.07]) have all higher 24-hour visualisation likelihood than the afternoon period.

### 4.1 Qualitative Analysis of the Bayesian Network Model

Figure 1 presents the qualitative model for the Tree-Augmented Naive Bayes network, where interesting connections can be extracted from the resulting model. First, patient's data features are associated. Then, creation time data and context data are also strongly related. However, the most interesting feature is probably the department that created the report, since this was chosen by the algorithm as ancestor of patient's age, time of report creation and type of encounter.

### 4.2 In-Sample Quantitative Analysis

For a quantitative analysis, Figure 2 presents the in-sample ROC curves for logistic regression (left), Naive Bayes (centre) and TAN (right). As expected, increasing model complexity enhances the in-sample AUC (LR 88.6%, NB 86.9% and TAN 90.7) but, globally, all models presented good discriminating power towards the outcome.

**Table 1.** Basic characteristics of included reports: patient's data (sex and age), report creation context (department, encounter) and time (day of week, daily period) data.

	Visualised in 24 hours		
	No	Yes	Total
<b>Outcome, n (%)</b>	3846 (77.3)	1129 (22.7)	4975 (100)
<b>Female, n (%)</b>	1716 (44.6)	619 (54.8)	2335 (46.9)
<b>Age, <math>\mu(\sigma)</math></b>	54.6 (19.8)	58.5 (22.4)	55.5 (20.5)
<b>AgeCat, n (%)</b>			
[0,10[	97 (2.5)	59 (5.2)	156 (3.1)
[10,20[	58 (1.5)	23 (2.0)	81 (1.6)
[20,30[	215 (5.6)	40 (3.5)	255 (5.1)
[30,40[	583 (15.2)	115 (10.2)	698 (14.0)
[40,50[	597 (15.5)	122 (10.8)	719 (14.5)
[50,60[	601 (15.6)	150 (13.3)	751 (15.1)
[60,70[	710 (18.5)	199 (17.6)	909 (18.2)
[70,80[	554 (14.4)	207 (18.3)	761 (15.3)
[80,90[	372 (9.67)	181 (16.0)	553 (11.1)
[90,100[	55 (1.4)	31 (2.8)	86 (1.7)
$\geq 100$	4 (0.1)	2 (0.2)	6 (0.1)
<b>Encounter Type, n (%)</b>			
Outpatient consult	1940 (50.4)	120 (10.6)	2060 (41.4)
Inpatient care	1442 (37.5)	768 (68.0)	2210 (44.4)
Emergency room	217 (5.6)	19 (1.7)	236 (4.7)
Other	247 (6.4)	222 (19.7)	469 (9.4)
<b>Department, n (%)</b>			
1	76 (2.0)	11 (1.0)	87 (1.8)
2	1626 (42.3)	55 (4.9)	1681 (33.8)
3	646 (16.8)	469 (41.5)	1115 (22.4)
5	1057 (27.5)	529 (46.9)	1586 (31.9)
6	154 (4.0)	23 (2.0)	177 (3.6)
7	89 (2.3)	22 (2.0)	111 (2.2)
9	11 (0.3)	7 (0.6)	18 (0.4)
10	10 (0.3)	1 (0.1)	11 (0.2)
12	139 (3.6)	11 (1.0)	150 (3.0)
13	23 (0.6)	0 (0)	23 (0.3)
16	5 (0.1)	0 (0)	5 (0.1)
21	10 (0.3)	1 (0.1)	11 (0.2)
<b>Day-of-Week, n (%)</b>			
Mon	728 (18.9)	303 (26.8)	1031 (20.7)
Tue	671 (17.5)	291 (25.8)	962 (19.3)
Wed	743 (19.3)	208 (18.4)	951 (19.1)
Thu	804 (20.9)	35 (3.1)	839 (16.9)
Fri	673 (17.5)	92 (8.2)	765 (15.4)
Sat	122 (3.2)	99 (8.7)	221 (4.4)
Sun	105 (2.7)	101 (9.0)	206 (4.1)
<b>Daily Period, n (%)</b>			
Morning	1768 (46.0)	521 (46.2)	2289 (46.0)
Afternoon	1661 (43.2)	402 (35.6)	2063 (41.5)
Night	331 (8.6)	146 (13.0)	477 (9.6)
Dawn	86 (2.2)	60 (5.3)	146 (2.9)

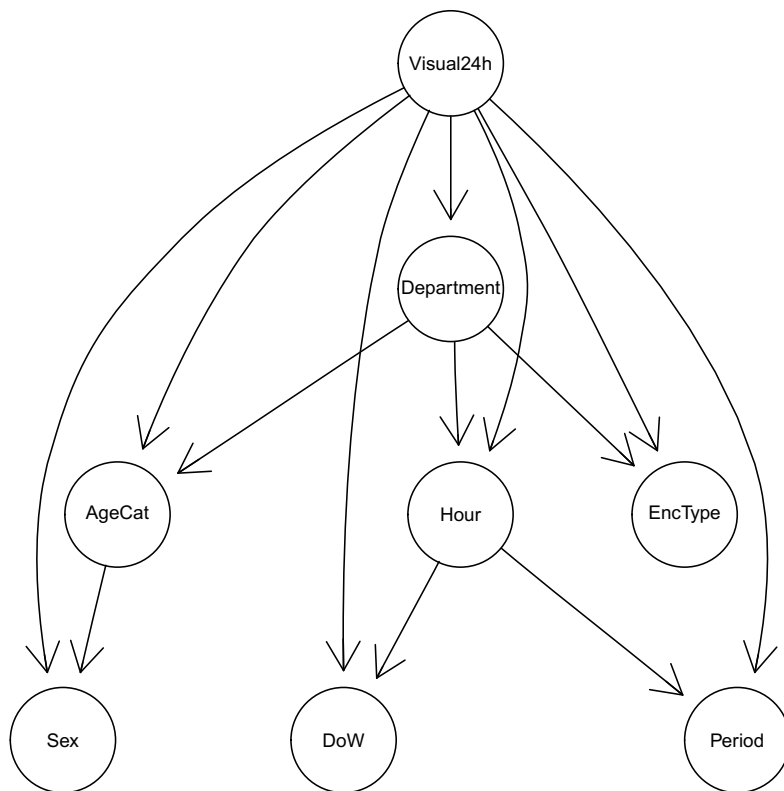


**Fig. 1.** Tree-Augmented Naive Bayes for predicting within 24h visualisation of clinical reports in the virtual patient record.

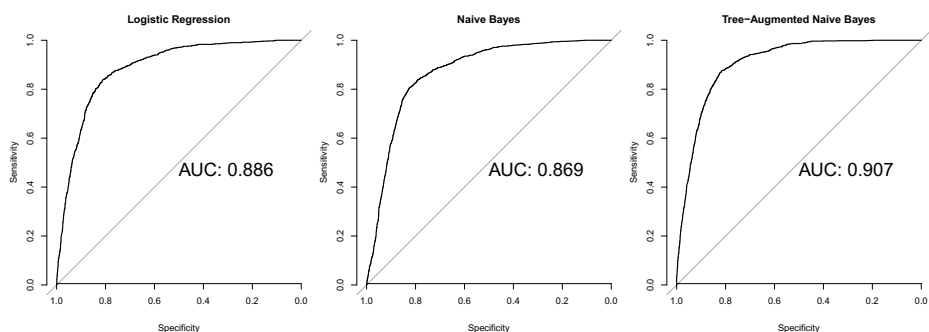


**Fig. 2.** In-sample ROC curves for logistic regression (left), naive Bayes (centre) and Tree-Augmented Naive Bayes (right).

**Table 2.** Validity assessment averaged from 10 times stratified 10-fold cross-validation for logistic regression (LR), naive Bayes (NB) and Tree-Augmented Naive Bayes (TAN).

Measure, % [95%CI]	LR	NB	TAN
Accuracy	82.30 [82.08,82.52]	82.43 [82.14,82.72]	82.80 [82.51,83.09]
Sensitivity	41.33 [40.50,42.16]	60.68 [59.81,61.55]	64.12 [63.36,64.89]
Specificity	94.33 [94.07,94.58]	88.81 [88.50,89.12]	88.28 [87.96,88.61]
Precision (PPV)	68.40 [67.45,69.35]	61.53 [60.80,62.25]	61.75 [61.04,62.47]
Precision (NPV)	84.57 [84.39,84.76]	88.51 [88.29,88.74]	89.35 [89.15,89.56]
AUC	87.58 [87.27,87.89]	86.37 [86.04,86.70]	85.50 [85.13,85.88]

### 4.3 Bayesian Network Generalisable Cross-Validation

In order to assess the ability of the models to generalise beyond the derivation cohort, cross-validation was endured. Table 2 presents the result of the 10-times-repeated stratified 10-fold cross-validation. Although the more complicated model loses in terms of AUC (85% vs 87%), it brings advantages to the precise problem of identifying reports that should be stored in secondary memory as they are less likely to be visualised in the next 24 hours, since it reveals a negative precision of 89% vs 88% (NB) and 84% (LR). Along with this result, it is much better at identifying reports that are going to be needed, as sensitivity rises from 41% (LR) to 64%. Future work should consider different threshold values for the decision boundary (here, 50%) in order to better suit the model to the sensitivity-specificity goals of the problem at hand.

## 5 Concluding Remarks and Future Work

The main contribution of this work is the preliminary study for the development of a decision support model for discriminating between reports that are going to be useful in the next 24 hours and reports which can be safely stored in secondary memory, since they will not be accessed in the next 24 hours.

An initial sample of clinical reports was used to derive Bayesian network models which were then compared with a logistic regression model in terms of in-sample discriminating power and generalisable validity with cross-validation. The studied data was in accordance with previous works in terms of the relevance that some factors may have on the likelihood of visualisation of clinical reports, e.g. department and type of encounter that produced the report [21]. Additionally, patient data and time of report creation were also found relevant for the global model of predicting within 24-hour visualisations.

Given that the main objective of this project is to enable a clear decision on whether a report can safely be stored in secondary memory or not, focus should be given to negative precision, since it represents the probability that a report marked by the system to be stored away is, in fact, irrelevant for the present day. The Bayesian network models achieved negative precision of around 89%, while keeping specificity high (also around 88%).

Future work will be concentrated in a) exploring other variables that might influence the likelihood of visualisation of clinical reports (e.g. actual data from the report, patient's diagnosis, etc.); b) exploiting the maximum amount of data from the log file of the virtual patient record (e.g. 2010 comprises of more than 184K reports); and c) inspecting the usefulness of temporal Bayesian network models [13] for the precise problem of relevance estimation.

Overall, this study presents Bayesian network models as useful techniques to integrate in a virtual patient record that needs to prioritise the accessible documents, both in terms of user-interface optimisation and data management procedures.

**Acknowledgments.** The authors acknowledge the help of José Hilário Almeida during the data gathering process.

## References

1. Aragon, T.J.: epitools: Epidemiology Tools (2012)
2. Barnett, O.: Computers in medicine. JAMA: the Journal of the American Medical Association **263**(19), 2631 (1990)
3. Bloice, M.D., Simonic, K.M., Holzinger, A.: On the usage of health records for the design of virtual patients: a systematic review. BMC Medical Informatics and Decision Making **13**(1), 103 (2013)
4. Clamp, S., Keen, J.: Electronic health records: Is the evidence base any use? Medical Informatics and the Internet in Medicine **32**(1), 5–10 (2007)
5. Cruz-Correia, R., Boldt, I., Lapão, L., Santos-Pereira, C., Rodrigues, P.P., Ferreira, A.M., Freitas, A.: Analysis of the quality of hospital information systems audit trails. BMC Medical Informatics and Decision Making **13**(1), 84 (2013)
6. Cruz-Correia, R., Rodrigues, P.P., Freitas, A., Almeida, F., Chen, R., Costa-Pereira, A.: Data quality and integration issues in electronic health records. In: Hristidis, V. (ed.) Information Discovery on Electronic Health Records, chap. 4. Data Mining and Knowledge Discovery Series, pp. 55–95. CRC Press (2009)
7. Cruz-Correia, R.J., Vieira-Marques, P.M., Ferreira, A.M., Almeida, F.C., Wyatt, J.C., Costa-Pereira, A.M.: Reviewing the integration of patient data: how systems are evolving in practice to meet patient needs. BMC Medical Informatics and Decision Making **7**, 14 (2007)
8. Cruz-Correia, R.J., Wyatt, J.C., Dinis-Ribeiro, M., Costa-Pereira, A.: Determinants of frequency and longevity of hospital encounters' data use. BMC Medical Informatics and Decision Making **10**, 15 (2010)
9. Dick, R., Steen, E.: The Computer-based Patient Record: An Essential Technology for HealthCare. National Academy Press (1997)
10. Feied, C.F., Handler, J.A., Smith, M.S., Gillam, M., Kanhouwa, M., Rothenhaus, T., Conover, K., Shannon, T.: Clinical information systems: instant ubiquitous clinical data for error reduction and improved clinical outcomes. Academic emergency medicine **11**(11), 1162–1169 (2004)
11. Höjsgaard, S.: Graphical independence networks with the gRain package for R. Journal of Statistical Software **46**(10) (2012)
12. Hripcsak, G., Sengupta, S., Wilcox, A., Green, R.: Emergency department access to a longitudinal medical record. Journal of the American Medical Informatics Association **14**(2), 235–238 (2007)

13. Lappenschaar, M., Hommersom, A., Lucas, P.J.F., Lagro, J., Visscher, S., Korevaar, J.C., Schellevis, F.G.: Multilevel temporal Bayesian networks can model longitudinal change in multimorbidity. *Journal of Clinical Epidemiology* **66**, 1405–1416 (2013)
14. Lucas, P.: Bayesian analysis, pattern analysis, and data mining in health care. *Current Opinion in Critical Care* **10**(5), 399–403 (2004)
15. Lucas, P.J.F., van der Gaag, L.C., Abu-Hanna, A.: Bayesian networks in biomedicine and health-care. *Artificial Intelligence in Medicine* **30**(3), 201–214 (2004)
16. Mitchell, T.M.: Machine Learning. McGraw-Hill (1997)
17. Patriarca-Almeida, J.H., Santos, B., Cruz-Correia, R.: Using a clinical document importance estimator to optimize an agent-based clinical report retrieval system. In: Proceedings of the 26th IEEE International Symposium on Computer-Based Medical Systems, pp. 469–472 (2013)
18. R Core Team: R: A Language and Environment for Statistical Computing (2013)
19. Robin, X., Turck, N., Hainard, A., Tiberti, N., Lisacek, F., Sanchez, J.C., Müller, M.: pROC: an open-source package for R and S+ to analyze and compare ROC curves. *BMC Bioinformatics* **12**, 77 (2011)
20. Rodrigues, P.P., Dias, C.C., Cruz-Correia, R.: Improving clinical record visualization recommendations with bayesian stream learning. In: Learning from Medical Data Streams, vol. 765, p. paper4. CEUR-WS.org (2011)
21. Rodrigues, P.P., Dias, C.C., Rocha, D., Boldt, I., Teixeira-Pinto, A., Cruz-Correia, R.: Predicting visualization of hospital clinical reports using survival analysis of access logs from a virtual patient record. In: Proceedings of the 26th IEEE International Symposium on Computer-Based Medical Systems, Porto, Portugal, pp. 461–464 (2013)
22. Schurink, C.A.M., Lucas, P.J.F., Hoepelman, I.M., Bonten, M.J.M.: Computer-assisted decision support for the diagnosis and treatment of infectious diseases in intensive care units. *The Lancet infectious diseases* **5**(5), 305–312 (2005)
23. Scutari, M.: Learning Bayesian Networks with the bnlearn R Package. *Journal of Statistical Software* **35**, 22 (2010)
24. Vieira-Marques, P.M., Cruz-Correia, R.J., Robles, S., Cucurull, J., Navarro, G., Marti, R.: Secure integration of distributed medical data using mobile agents. *Intelligent Systems* **21**(6), 47–54 (2006)
25. Wyatt, J.C., Wright, P.: Design should help use of patients' data. *Lancet* **352**(9137), 1375–1378 (1998)

# On the Efficient Allocation of Diagnostic Activities in Modern Imaging Departments

Roberto Gatta<sup>1(✉)</sup>, Mauro Vallati<sup>2</sup>, Nicola Mazzini<sup>1,2,3</sup>, Diane Kitchin<sup>2</sup>, Andrea Bonisoli<sup>3</sup>, Alfonso E. Gerevini<sup>3</sup>, and Vincenzo Valentini<sup>1</sup>

<sup>1</sup> Radiotherapy Department, Università Cattolica Del Sacro Cuore, Milan, Italy  
[roberto.gatta.bs@gmail.com](mailto:roberto.gatta.bs@gmail.com)

<sup>2</sup> School of Computing and Engineering, University of Huddersfield, Huddersfield, UK  
<sup>3</sup> Dipartimento d'Ingegneria dell'Informazione,  
Università degli Studi di Brescia, Brescia, Italy

**Abstract.** In a modern Diagnostic Imaging Department, managing the schedule of exams is a complex task. Surprisingly, it is still done mostly manually, without a clear, explicit and formally defined objective or target function to achieve.

In this work we propose an efficient approach for optimising the exploitation of available resources. In particular, we provide an objective function, that considers the aspects that have to be optimised, and introduce a two-steps approach for scheduling diagnostic activities. Our experimental analysis shows that the proposed technique can easily scale on large and complex Imaging Departments, and generated allocation plans have been positively evaluated by human experts.

## 1 Introduction

In a modern Diagnostic Imaging Department the allocation and re-allocation of exams is a complex task, that is time-consuming and is still done manually. On the one hand, it is fundamental to keep the waiting lists as short as possible, in order to meet the established waiting time; on the other hand, it is of critical importance to minimise expenses for the Department. Moreover, patient scheduling has to be balanced, in order to plan the best possible allocation according to the staff organisation/skills on different modalities, i.e. computed tomography (CT), Radiography (RX), magnetic resonance (MR) and ultrasound (US) equipment. In order to plan the best possible allocation a lot of available resources must be taken into account: staff (radiologists, nurses, etc.), equipment (US, CT, MR, etc.), examinations performed (tagged by imaging modalities, reimbursement rate, clustered by regions and/or pathologies) and staff characteristics (part-time, full-time, etc.).

The literature on medical appointment scheduling is extensive, but approaches –either automated or in the form of formal guidelines– to deal with diagnostic activities in radiology Departments are rare. Nevertheless, the importance of scheduling activities in hospital services is well-known [8]. Even though a few techniques have been proposed for dealing with part of the allocation problem (see, e.g., [1,4–6]), a complete approach able to manage all the aspects of the

allocation problem of a Radiological Department is still missing. Improvements in that area can lead to a significant reduction of costs and human time.

In this work we propose a formalisation of the activities allocation problem. The formalisation is composed by a set of definitions, constraints and a target function. The model is then exploited by an efficient scheduling approach, based on enforced hill climbing, that aims at optimising the use of available resources. This work encompasses a previous preliminary study by Mazzini et al. [7]. According to our experimental analysis, and to the feedback we received from medical experts, the proposed approach is efficiently able to produce good quality scheduling, following the metric it is required to optimise, which considers at the same time temporal and economic indexes.

## 2 The Diagnostic Activities Allocation Problem

In this section we define the relevant entities involved in the allocation problem, and describe the function used for evaluating the quality of allocation plans.

### Entities

We define a set of entities that can easily fit into most of the Radiology Information Systems (RIS) currently used in diagnostic Imaging Departments [2]. Specifically, the proposed elements can directly fit with Paris, provided by ATS-Teinos, and PRORAM from METRIKA. With some minor changes it can be also fit with Estensa, of Esaote. We are confident it can also be easily adopted in other situations. The most important entities are the following:

**Exam** represents the diagnostic examination that can be performed, e.g., “CT brain”.

**Exam Group** (or cluster) is a group of exams. In many cases it is useful, due to some team specialisation, to group exams for the area of the body (e.g., “head and neck” or “abdominal”) or to group them in order to reflect which Department the patient comes from (e.g., “CT from GPs”). The grouping is done according to the habits of the Imaging Department, team and work-flow: hybrid models can also be implemented.

**Modality** this entity represents a medical device, like an ultrasound, a CT scan, etc. In our model, a modality corresponds to an actual room. This is reasonable since the machinery used for exams is usually not moved between rooms. Such modelisation leads to having an independent agenda per modality. In principle, it is possible to have the machines required for different sorts of exams in the same room. This case, which is extremely rare since it leads to underused resources, is not modelled.

**Personnel** represents the human resources (staff members) available. Each member of staff has at least one role. Each Exam Group has a set of roles assigned, this indicates the specific needs of that group of exams in terms of human resources.

For instance, some exam groups require several nurses to be present in the room, while other exams require technicians to be available.

**Time Slot** we adopted an atomic time slot of 5 minutes in a weekly calendar. The granularity of 5 minutes has been chosen since it is not extremely long, thus limiting the waste time; also, it is not too short, therefore short delays do not affect the overall daily scheduling.

**Temporal horizon** catches the requirements in terms of queue governance. This can represent constraints like “the queue for ‘Brain MRI’ must be lower than 3 months for, at least, the next 12 months”. It should be noted that this is the usual way in which queue governance requirements are expressed.

### Objective Function and Constraints

The optimisation of the scheduling of exams has to deal with two main components. On the one hand, it is important to maximise income for the Department. This should result in the prioritisation of exams that are both frequently requested and expensive. On the other hand, the Department is also providing an important service to the community. Therefore, keeping all the queue lists as short as possible is fundamental. In public hospitals there are strict upper bounds for queues.

For considering both the aforementioned aspects, we designed an objective function (to minimize) that combines the two perspectives. The adopted function is depicted in Equation 1. In particular,  $n$  indicates the number of exams.  $r_i$  is the cost of the  $i$ -th exam.  $q_i$  is the amount of exams of group  $i$  that should be performed.  $\Delta_j$  represents the difference between waiting queue and desired queue length for the  $j$ -th exam group.  $W_j$  is the importance of the queue for the  $j$ -th exam. Finally,  $\alpha$  and  $\beta$  indicate, respectively, the importance that is given to the economic side and to the respect of the limits on the queues’ length. Intuitively, the function synthesises the point of view of the hospital administration (first addend) –focused on the economic side– and of the doctor (second addend) –focused on the quality of the service.

$$f = \alpha \sum_1^n (r_i * q_i) + \beta \sum_1^n (\Delta_j * W_j) \quad (1)$$

In order to guarantee the feasibility of identified allocation plans, a number of constraints have to be satisfied. In particular for each exam group the queue length must not be higher than the provided upper bound for respecting the governance rules on waiting time. Also there is a set of constraints that regulate the correct allocation of exams to suitable modalities and time slots and correct assignment of medical personnel to exam rooms respecting specific limits and maximum consecutive working hours that are in place in hospitals for all the staff. Our implemented prototype takes into account all such constraints.

### 3 The Proposed Two-Steps Algorithm

For the automatic allocation of diagnostic activities, we designed an approach that is composed of two main steps: *generation* and *improvement*. In both steps, groups of exams are considered. In a modern Radiology Department the number of possible exams is usually high (300 – 400), but they can be easily organised in groups, both for administrative issues and similarity of requirements. For example: all the “RX bones” exams are very similar in terms of required roles, funding, used time slots and required modality. Therefore, considering a group instead of a single exam provides a good abstraction: it reduces the number of variables to deal with, thus improving the computability, but does not lead to loss of information. Also, RIS systems normally manage their agenda following the same approach: instead of declaring all the exams which can be assigned to a modality in a period of time, they allow the definition of clusters of exams that can be linked to the modality. As a matter of fact, the medical personnel are trained for performing a specific cluster of exams rather than a single type of examination.

#### **Generation**

This step aims at quickly identifying an allocation of activities and personnel that satisfies all the constraints, regardless of the overall quality. This task is probably the most difficult, because it has to search the huge allocation space and identify a solution that satisfies all the allocation constraints. In particular, the generation step is based on the following tasks, which are executed by considering one week at a time:

1. the available personnel is fully assigned to the rooms. Most of the staff are assigned to morning slots, since it is the period of the day where most exams take place. Some heuristics are followed for reducing the spread of exams of the same group in different rooms, or in very different time slots.
2. A random number of time slots is assigned to each cluster of examinations, according to the hard constraints related to human-resources.
3. After the allocation, free time slots or free human resources are analysed in order to be exploited. For reducing the fragmentation, the preferred solution is to extend the time slot of exams allocated before/after the free slot. Fragmentation leads to waste time due to switching exam equipment between modalities and personnel moving between rooms.

In parallel with *generation*, a waiting lists estimation is performed. This allows assessment of whether the requirements on exam queue lengths will be satisfied, since the proposed approach provides a week-by-week allocation plan.

#### **Improvement**

The first allocation plan is then improved through an enforced hill climbing. At each iteration, a neighbour of the current plan is generated by de-allocating a cluster of exams from a modality, and substituting it with a different cluster. The substitution is a complex step; it is not guaranteed it can be applied for

all the pairs of clusters. This is due to, for example, different requirements in terms of personnel, equipment or time. The choice of the group of exam to be substituted is done by ordering clusters according to the requested resources and number of requests per week. Clusters that require many resources and are rarely performed are suitable to be substituted. The selected cluster is substituted with another that can fit in the released time-slots.

If the new allocation plan has a better target function than the current plan, the former is saved; otherwise the algorithm restarts by considering a different suitable cluster to substitute. The search stops when a specified number of rescheduling attempts, or the time limit, is reached. It should be noted that the designed algorithm is able to provide several solutions of increasing quality.

## 4 Experimental Analysis

We implemented a prototype of the proposed algorithm in C++; as input it requires an XML description of available resources and exams to be performed. We tested the proposed approach in various scenarios. We considered 3 different possible Departments, several values of  $\alpha$  and  $\beta$ , and different settings up to at most 25 exam groups, 90 exams, 10 modalities and 24 staff members, distributed among radiologists, radiographers and nurses. This reflects a medium-sized Department. We observed that a first solution is usually found in about 15 seconds. Incremental improvements, generally from 60 to 250 increasing quality allocation plans, are usually found in less than 10 minutes.

Given the fact that in real-world Departments no quantitative functions are used for evaluating the quality of allocation plans, it is incorrect to compare the allocation plans generated by our approach with existing scheduling.

In order to have a first validation of the generated plans we showed some of them to human experts; namely, to two radiologists, one radiographer technician and one IT specialist employed in a Diagnostic Imaging Department. They considered the plans to be realistic and feasible. Considering the context and the environment of a modern hospital, this is a reasonable way for validating the generated schedules. Moreover, from experts feedback we synthesised a number of useful insights, that are described in the following.

The *generation* step is computationally hard, but it is crucial in order to obtain good final solutions. We observed that a low quality initial solution usually leads to small increments in the subsequently improved allocations. On the other hand, this generation step is not fundamental in real-world applications, since Radiology Departments already have a feasible scheduling in place. Moreover, their current scheduling usually includes thousands of reservations, therefore cannot be suddenly changed without dramatic effects.

Fragmentation should be included in the objective function. In the current model it is not considered, since we believed that dealing with exam groups instead of single exams would have been enough. On the contrary, we observed that exam groups allocated to a modality change frequently; this also causes a frequent change in the staff, which affects the quality of the allocation plan. In

large hospitals, where examination rooms are far from each other, frequent staff movement results in a significant waste of time.

Data entry is time-expensive: changes in personnel, exams, instrumentation or policies are quite frequent in a medium-big Radiology Department, and require updating of the data and re-planning. The best way to efficiently support an operator would be by exporting, from existent RIS, data regarding staff, modalities and dates, in order to save time. Currently, HL7 [3] would probably be the best standard for such integration.

The proposed algorithm can provide useful information about the available resources. In particular, it can be used for identifying the most limiting resource (personnel, modalities, etc.) and evaluating the impact of new resources. Head of Departments highlighted that it is currently a very complex problem to estimate the impact of a new modality, or of increased personnel. By using the proposed algorithm, the impact of new resources can be easily assessed by comparing the quality of plans with and without them, in different scenarios.

New modalities or new staff require an initial “training” period. In the case of new modalities, the staff will initially require more time for performing exams. Newly introduced staff usually need to be trained. The current approach is not able to catch such situations. A possible way for dealing with this is considering a “penalty” for some instrumentation or personnel; a time slot is “longer” –by a given penalty factor– when they are assigned to it. Penalties can be reduced over time.

The current approach does not have a year overview. Some exams are more likely to be required in some periods, thus they should have different priorities with regards to their waiting lists’ requirements. Also, it is common practice that in summer hospital’s personnel is reduced. A good integration with medical and administrative databases will be useful for further refinements of the allocation abilities.

## 5 Conclusion

In many Diagnostic Imaging Departments the allocation of exams is currently done manually. As a result, it is time consuming, it is hard to assess its overall quality, and no information about limiting resources are identified.

In this paper, we addressed the aforementioned issues by introducing: (i) a formal model of the diagnostic activities allocation problem, and (ii) an efficient algorithm for the automated scheduling of diagnostic activities. The proposed model is general, and can therefore fit with any existing Imaging Department. Moreover, a quantitative function for assessing the quality of allocation plans is provided. The two-steps algorithm allows the generation and/or improvement of allocation plans. An experimental analysis showed that the approach is efficiently able to provide useful and valid scheduling for examinations. Feedback received from experts confirms its usefulness, also for evaluating the impact of new instrumentation or staff members.

This work can be seen as a pilot study, which can potentially lead to the exploitation of more complex and sophisticated Artificial Intelligence techniques

for handling the Radiological resource allocation problem. Further investigations are needed both on the reasoning and on the knowledge representation sides. Moreover, larger experimental analysis and stronger validation approaches are envisaged. Future work includes also an extended experimental analysis with data gathered from existing Departments, and the investigation of techniques for reducing fragmentation.

## References

1. Barbati, M., Bruno, G., Genovese, A.: Applications of agent-based models for optimization problems: A literature review. *Expert Systems with Applications* **39**(5), 6020–6028 (2012)
2. Boochever, S.S.: HIS/RIS/PACS integration: getting to the gold standard. *Radiol Manage* **26**(3), 16–24 (2004)
3. Dolin, R.H., Alschuler, L., Boyer, S., Beebe, C., Behlen, F.M., Biron, P.V., Shvo, A.S.: HL7 clinical document architecture, release 2. *Journal of the American Medical Informatics Association* **13**(1), 30–39 (2006)
4. Eagen, B., Caron, R., Abdul-Kader, W.: An agent-based modelling tool (abmt) for scheduling diagnostic imaging machines. *Technology and Health Care* **18**(6), 409–415 (2010)
5. Falsini, D., Perugia, A., Schiraldi, M.: An operations management approach for radiology services. In: Sustainable Development: Industrial Practice, Education and Research (2010)
6. Macal, C.M., North, M.J.: Agent-based modeling and simulation. In: Winter Simulation Conference, pp. 86–98 (2009)
7. Mazzini, N., Bonisoli, A., Ciccolella, M., Gatta, R., Cozzaglio, C., Castellano, M., Gerevini, A., Maroldi, R.: An innovative software agent to support efficient planning and optimization of diagnostic activities in radiology departments. *International Journal of Computer Assisted Radiology and Surgery* **7**(1), 320–321 (2012)
8. Welch, J.D.: N.B.T.: Appointment systems in hospital outpatient departments. *The Lancet* **259**(6718), 1105–1108 (1952)

# Ontology-Based Information Gathering System for Patients with Chronic Diseases: Lifestyle Questionnaire Design

Lamine Benmimoune<sup>1,3(✉)</sup>, Amir Hajjam<sup>1</sup>, Parisa Ghodous<sup>2</sup>, Emmanuel Andres<sup>4</sup>, Samy Talha<sup>4</sup>, and Mohamed Hajjam<sup>3</sup>

<sup>1</sup> IRTES-SET, Université de Technologie Belfort-Montbéliard, 90000 Belfort, France  
[amine.benmimoune@utbm.fr](mailto:amine.benmimoune@utbm.fr)

<sup>2</sup> LIRIS, Université Claude Bernard Lyon 1, 69100 Villeurbanne, France  
<sup>3</sup> Newel, 68100 Mulhouse, France

<sup>4</sup> Hôpital Civil de Strasbourg, 67000 Strasbourg, France

**Abstract.** The aim of this paper is to describe an original approach which consists of designing an Information Gathering System (IGS). This system gathers the most relevant information related to the patient. Our IGS is based on using questionnaire ontology and adaptive engine which collects relevant information by prompting the whole significant questions in connection with the patient's medical background. The formerly collected answers are also taken into consideration in the questions selection process. Our approach improves the classical approach by customizing the interview to each patient. This ensures the selection of all of the most relevant questions. The proposed IGS is integrated within E-care monitoring platform for gathering lifestyle-related patient data.

**Keywords:** Information gathering system · Questionnaire · Health-care · Clinical decision support system · Ontology · Monitoring

## 1 Introduction

Computer-based questionnaires are a new form of data collection, which are designed to offer more advantages compared to pen and paper questionnaires or oral interviewing [13]. They are less time-consuming and more efficient by offering more structure and more details compared to the classical methods [2].

The Information Gathering Systems (IGSs) have had measurable benefits in reducing omissions and errors arising as a result of medical interviews [14]. The medical and health care domain is one of the most active domain in using IGS for gathering patients data [13].

Recently, various research works were conducted to design and to use the IGS as part of clinical decision support system (CDSS). Among them. Bouamrane *et al.* [2], [3] proposed a generic model for context-sensitive self-adaptation of IGS based on questionnaire ontology. The proposed model is implemented as an data collector module in [4] to collect patient medical history for preoperative

risk assessment. Sherimon *et al.* [5], [6], [15] proposed an questionnaire ontology based on [2]. This ontology is used to gather patient medical history, which is then integrated within CDSS to predict the Risk of hypertension. Farooq *et al.* [7] proposed an ontology-based CDSS for chest pain risk assessment, based on [2] the proposed CDSS integrates a data collector to collect patient medical history. Alipour [13] proposed an approach to design an IGS based on the use of ontology-driven generic questionnaire and Pellet inference engine for questions selection process.

Although the presented IGS in the literature permit gathering patient data using ontologies, the created questionnaires are hard coded for specific domains and they are defined under the domain ontologies. These, make them less flexible, more difficult to maintain and even hard to share and to reuse.

Unlike previous approaches, our approach offers more flexibility by separating the ontologies and by integrating a domain ontology to drive the creation of questionnaire. This allows to give meaning to the created questions, and configuring different models of questionnaires without coding and regardless of the content of the domains. Therefore, many CDDSSs can easily integrate and use the proposed IGS for their specific needs.

Furthermore, the proposed approach permits to collect relevant information by prompting the whole significant questions in connection with the patient profile. The formerly collected answers are also taken into consideration in the questions selection process. This improves the classical approach by customizing the interview to each patient.

The proposed IGS is integrated within E-care home health monitoring platform [1], [8] for gathering lifestyle-related patient data.

## 2 Information Gathering System within E-Care Platform

E-care is a home health monitoring platform for patients with chronic diseases such as diabetes, heart failure, high blood pressure, etc. [1] [8]. The aim is early detection of any anomalies or dangerous situations by collecting relevant data from the patient such as physiological data (heart rate, blood pressure, pulse, temperature, weight, etc.) and lifestyle data (tobacco-use, eating habits, physical activity, sleep, stress, etc.).

To improve the accuracy in anomalies detection, the platform needs relevant information that describes as precisely as possible the patient's health status and his lifestyle changes (tobacco-use, lack of physical activity, poor eating habits, etc.). That is why the patient is invited daily to collect his physiological data using medical sensors (Blood Pressure Monitor, Weighing Scale, Pulse Oximeter, etc.) and to answer on lifestyle questionnaires. These questionnaires are automatically generated by the IGS which permits gathering relevant information about the patient lifestyle.

All collected data (physiological data and lifestyle data) is stored in the patient profile ontology which models the health status of patient and then analysed by the inference engine for anomalies detection.

### 3 Information Gathering System Architecture

The proposed architecture consists of four main components: Questionnaire Ontology, Survey History Ontology, Adaptive Engine and User Interfaces.

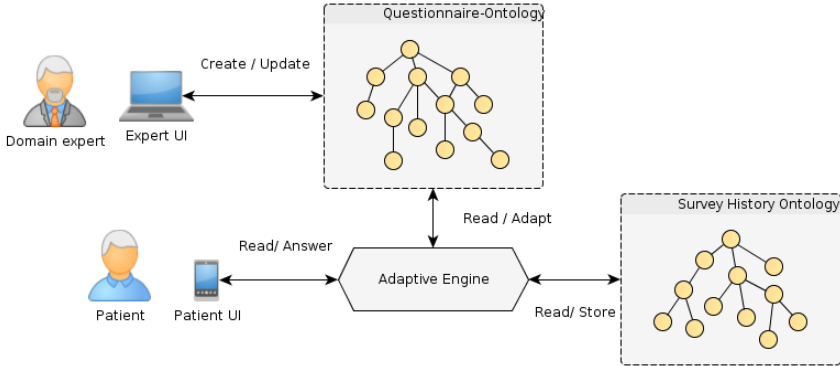


**Fig. 1.** Information Gathering System architecture

**Questionnaire Ontology (QO):** models the concepts representing the common components of a questionnaire. The QO is created based on Bouamrane *et al.*'s research works [2]. It is designed as generic, structured and flexible to accept most of the questionnaire models. The main classes are: *Questionnaire*, *SubQuestionnaire*, *Question* and *PotentialAnswer*. The *Questionnaire* class is composed of *Sub-questionnaires*, which represent a group of thematically related question classes. The question classes could be inter-related by structural properties such as *hasParent*, *hasChild*, *hasSibling*, etc. Each question is characterised by a type and related to one or more potential answers using Adaptive properties such as *ifAnswerToThisQuestionEqualsTo*, *thenGoToQuestion*, etc.

**Survey History Ontology (SHO):** stores all the patient surveys. It includes all the asked questions and the given answers by the patient. It is used in the questions selection process.

**The Adaptive Engine (AE):** it interprets the properties asserted in the questionnaire ontology and prompts the corresponding questions in connection with the patient profile and the formerly collected answers. The AE initially loads all questions except the children questions. It prompts the first question and checks if the question is appropriate to the patient profile (e.g. AE doesn't ask questions about the smoking habits, if the patient is a non-smoker). If it is, the AE asks the question and gets the answer from the UI. If it is not, the AE just prompts the next question.

If however the current question happens to be adaptive (i.e. it has at least a child question), the given answer is then checked against the answers that are expected to lead to children questions. If a match is found, the AE loads the children questions. If no match is found, the next question is prompted. The interaction loop is repeated until there are no more questions to be asked.

**The User Interfaces (UI):** consist of two parts of UI namely: expert UI and Patient UI.

- **Expert UI:** permits the domain experts (clinicians) to configure the IGS by defining questionnaires and to consult the surveys history.
- **Patient UI:** permits to start/stop the survey. It is designed in such a way that the patient can respond to the questionnaire from anywhere using his mobile device (tablet or smart phone).

## 4 Domain Ontology Driven Questionnaire

The domain ontology aims to drive the creation of questionnaires by offering a common and controlled vocabulary. To achieve this goal, we have developed a domain ontology for lifestyle concepts based on recommendations provided by Haute Autorité de Santé (HAS)<sup>1</sup>. The ontology is structured as an hierarchy of concepts and relations between concepts. It is composed of three main entities:

- ***LifeStyleEntities*:** hierarchical concepts that model lifestyle entities such as eating habits, physical activity, smoking habits, etc.
- ***DimensionsEntities*:** hierarchical concepts that model temporal dimensions and physical dimensions (quantity). Each dimension includes a hierarchy of concepts (e.g. *TimesOfDay*, *TimeFrequency* and *TimeUnit* are grouped under the *timeDimension* concept).
- ***CataloguesEntities*:** includes concepts used to give more semantic for the *LifeStyleEntities* concepts. Each catalogue entity includes a hierarchy of concepts that model the types of *LifeStyleEntities* concepts (e.g. *Cigarette*, *E-cigarette* and *Drug* are types of *Tobacco* concept for the *SmokingHabits* concept).

The concepts are related amongst them through properties as follows.

- ***DimensionProperties*:** used to relate the *LifeStyleEntities* to the *DimensionsEntities*, they include a set of properties such as *hasQuantity*, *hasFrequency*, *hasTimesOfDay*, etc.
- ***CatalogueProperties*:** used to relate the *LifeStyleEntities* to the *CataloguesEntities*, they include a set of properties such as *hasExercise*, *hasTobacco*, *hasFood*, etc.

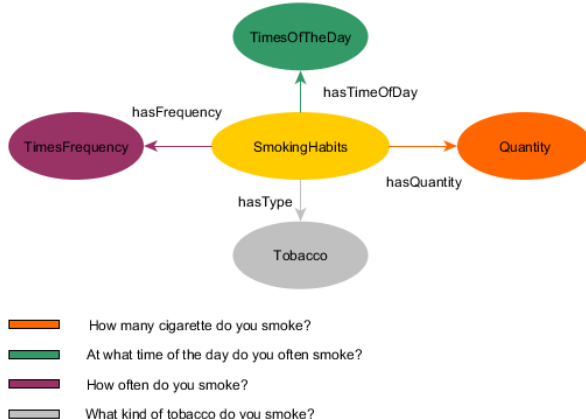


**Fig. 2.** Related questions for the “smoking habits” concept

The example illustrated by figure 2 shows how the domain concepts can be related amongst them and how they are used to design lifestyle questionnaires.

Given the smoking habit that is characterized by a type of tobacco (e.g. cigarette, electronic cigarette, drugs, etc.), time frequency (daily, monthly, weekly, etc.), smoking quantity, etc. Several questions can be created based on *SmokingHabits* concept, with each smoking-related question should be related to the *SmokingHabits* through the domain properties, while the potential answers are related either to the *DimensionsEntities* or to the *CatalogueProperties*. (see figure 2).

## 5 Conclusion and Future Work

In this paper, we presented a novel approach, which aims to design an Ontology-Based Information Gathering System. This system permits gathering the most relevant information by providing personalised questionnaires related to the patient profile. Our IGS consists of a questionnaire ontology which is driven by domain ontology. We have seen how the domain ontology is used to control vocabulary and to give a meaning to the asked questions. Furthermore, the use of a domain ontology can improve the gathering of data and the design of questionnaires can be made easier and faster compared to the hard coding of questionnaires. On the other hand, we have highlighted the interest of using the proposed IGS within E-care health monitoring platform, since it permits gathering relevant information about patients’ lifestyle.

In the near future, we will experiment the proposed IGS in the real life with chronic patients.

<sup>1</sup> <http://www.has-sante.fr>

## References

1. Benyahia, A.A., Hajjam, A., Hilaire, V., Hajjam, M.: E-care ontological architecture for telemonitoring and alerts detection. In: 5th IEEE International Symposium on Monitoring & Surveillance Research (ISMSR): Healthcare-Safety-Security (2012)
2. Bouamrane, M.-M., Rector, A.L., Hurrell, M.: Ontology-driven adaptive medical information collection system. In: An, A., Matwin, S., Raś, Z.W., Ślęzak, D. (eds.) Foundations of Intelligent Systems. LNCS (LNAI), vol. 4994, pp. 574–584. Springer, Heidelberg (2008)
3. Bouamrane, M.M., Rector, A., Hurrell, M.: Gathering precise patient medical history with an ontology-driven adaptive questionnaire. In: 21st IEEE International Symposium on Computer-Based Medical Systems, CBMS 2008, June 17–19, 2008
4. Bouamrane, M.-M., Rector, A., Hurrell, M.: Using ontologies for an intelligent patient modelling, adaptation and management system. In: Meersman, R., Tari, Z. (eds.) OTM 2008, Part II. LNCS, vol. 5332, pp. 1458–1470. Springer, Heidelberg (2008)
5. Sherimon, P.C., Vinu, P.V., Krishnan, R., Takroni, Y.: Ontology Based System Architecture to Predict the Risk of Hypertension in Related Diseases. IJIPM: International Journal of Information Processing and Management **4**(4), 44–50 (2013)
6. Sherimon, P.C., Vinu, P.V., Krishnan, R., Takroni, Y., AlKaabi, Y., AlFars, Y.: Adaptive questionnaire ontology in gathering patient medical history in diabetes domain. In: Herawan, T., Deris, M.M., Abawajy, J. (eds.) DaEng-2013. LNEE, vol. 285, pp. 453–460. Springer, Singapore (2014)
7. Farooq, K., Hussain, A., Leslie, S., Eckl, C., Slack, W.: Ontology driven cardiovascular decision support system. In: 2011 5th International Conference on Pervasive Computing Technologies for Healthcare (PervasiveHealth), May 23–26, 2011
8. Benyahia, A.A., Hajjam, A., Hilaire, V., Hajjam, M., Andres, E.: E-care telemonitoring system: extend the platform. In: 2013 Fourth International Conference on Information, Intelligence, Systems and Applications (IISA), July 10–12, 2013
9. Saripalle, R.K.: Current status of ontologies in Biomedical and clinical Informatics. University of Connecticut. <http://www.engr.uconn.edu/steve/Cse300/saripalle.pdf> (retrieved January 16, 2014)
10. Gruber, T.R.: Toward principles for the design of ontologies used for knowledge sharing? International Journal Human-Computer Studies **43**(5–6), 907–928 (1995)
11. Guarino, N.: Formal Ontology and information systems. Formal ontology in information systems. In: Proceedings of FOIS 1998, Trento, Italy, June 6–8, 1998
12. Noy, N.F., McGuinness, D.L.: Ontology Development 101: A Guide to Creating Your First Ontology. Stanford University (2005)
13. Alipour-Aghdam, M.: Ontology-Driven Generic Questionnaire Design. Thesis for the degree of Master of Science in Computer Science. Presented to The University of Guelph, August 2014
14. Bachman, J.W.: The patient-computer interview: a neglected tool that can aid the clinician. Mayo Clinic Proceedings **78**, 67–78 (2003)
15. Sherimon, P.C., Vinu, P.V., Krishnan, R., Saad, Y.: Ontology driven analysis and prediction of patient risk in diabetes. Canadian Journal of Pure and Applied Sciences **8**(3), 3043–3050 (2014). SENRA Academic Publishers, British Columbia

# Predicting Preterm Birth in Maternity Care by Means of Data Mining

Sónia Pereira, Filipe Portela<sup>(✉)</sup>, Manuel F. Santos, José Machado,  
and António Abelha

Algoritmi Centre, University of Minho, Braga, Portugal  
b7004@dps.uminho.pt, {cfp,mfs}@dsi.uminho.pt,  
{jmac,abelha}@di.uminho.pt

**Abstract.** Worldwide, around 9% of the children are born with less than 37 weeks of labour, causing risk to the premature child, whom it is not prepared to develop a number of basic functions that begin soon after the birth. In order to ensure that those risk pregnancies are being properly monitored by the obstetricians in time to avoid those problems, Data Mining (DM) models were induced in this study to predict preterm births in a real environment using data from 3376 patients (women) admitted in the maternal and perinatal care unit of Centro Hospitalar of Oporto. A sensitive metric to predict preterm deliveries was developed, assisting physicians in the decision-making process regarding the patients' observation. It was possible to obtain promising results, achieving sensitivity and specificity values of 96% and 98%, respectively.

**Keywords:** Data mining · Preterm birth · Real data · Obstetrics care · Maternity care

## 1 Introduction

Preterm birth portrays a major challenge for maternal and perinatal care and it is a leading cause of neonatal morbidity. The medical, education, psychological and social costs associated with preterm birth indicate the urgent need of developing preventive strategies and diagnostic measures to improve the access to effective obstetric and neonatal care [1]. This may be achieved by exploring the information provided from the information systems and technologies increasingly used in healthcare services.

In Centro Hospitalar of Oporto (CHP), a Support Nursing Practice System focused on nursing practices (SAPE) is implemented, producing clinical information. In addition, patient data plus their admission form are recorded through EHR (Electronic Health Record) presented in Archive and Diffusion of Medical Information (AIDA) platform. Both SAPE and EHR are also used by the CHP maternal and perinatal care unit, Centro Materno Infantil do Norte (CMIN). CMIN is prepared to provide medical care / services for women and child. Therefore, using obstetrics and prenatal information recorded from SAPE and EHR, it is possible to extract new knowledge in the context of preterm birth. This knowledge is achieved by means of Data Mining (DM) techniques, enabling predictive models based on evidence. This study accomplished

DM models with sensitivity and specificity values of approximately 96% and 98%, which are going to support the making of preventive strategies and diagnostic measures to handle preterm birth.

Besides the introduction, this article includes a presentation of the concepts and related work in Section 2, followed by the data mining process, described in Section 3. Furthermore, the results are discussed and a set of considerations are made in Section 4. Section 5 presents the conclusions and directions of future work.

## 2 Background and Related Work

### 2.1 Preterm Birth

Preterm birth refers to a delivery prior to 37 completed weeks (259 days) of labour. Symptoms of preterm labour include uterine contractions occurring more often than every ten minutes, or the leaking of fluids. Preterm birth is the leading cause of long-term disability in children, since many organs, including the brain; lungs and liver are still developing in the final weeks of pregnancy [2]. Preterm Birth has not decreased in the last 30 years, due to the failure identifying the high-risk group during routine prenatal care [3]. Many studies were conducted to identify a way to predict preterm deliveries, focusing on physiologic measures, ultrasonography, obstetrics history and socioeconomic status [4]. For instance, in 2011 a model was developed for predicting spontaneous delivery before 34 weeks based on maternal factors, placental perfusion and function at 11-13 weeks' gestation, through screening maternal characteristics and regression analysis. They detected 38.2% of the preterm deliveries in women with previous pregnancies beyond 16 weeks and 18.4% in those without [3]. Most of the efforts to predict preterm birth face limited provision of population based data, since registration of births is incomplete and information is lacking on gestational age [6].

### 2.2 Interoperability Systems and Data Mining in Healthcare

As mentioned in the previous section, this study is based on real data acquired from CMIN. The knowledge extraction depends substantially on the interoperability between SAPE and EHR systems assured through AIDA. This multi-agent platform enables the standardization of clinical systems and overcomes the medical and administrative complexity of the different sources of information from the hospital [5].

In healthcare systems, there is a wealth of data available, although there is a lack of effective analysis tools to extract useful information. Thus, data mining have found numerous applications in scientific and clinical domain [8]. Successful mining applications have been implemented in the healthcare. In obstetrics and maternal care, some of these studies were employed to predict the risk pregnancy in women performing voluntary interruption of pregnancy (VIP) [9] and manage VIP by predicting the most suitable drug administration [7].

### 3 Study Description

This study was conducted by following the Knowledge Discovery in Database (KDD), allowing the extraction of implicit and potentially useful information, through algorithms, taking account the magnitudes of data increasing [10].

The DM methodology employed was the Cross Industry Standard Process for Data Mining (CRIP-DM), a non-rigid sequence of six phases, carried out in this section, which allow the implementation of DM models to be used in real environments [11]. To induce the DM models, four different algorithms were implemented: Decision Trees (DT), Generalized Linear Models (GLM), Support Vector Machine (SVM) and Naïve Bayes (NB). This study used data collected from 3376 patients (women) admitted in the maternal and perinatal care unit (CMIN) of CHP comprising a period between 2012-07-01 and 2015-01-31, in a total of 1120 days.

#### 3.1 Business Understanding

The Business aim of this project is to identify the risk group of preterm delivery, to ensure the proper monitoring and to avoid its associated problems. The DM goal is to develop accurate models able to support the decision-making process by predicting whether or not a woman will be subjected to a preterm delivery, based on data from clinic cases.

#### 3.2 Data Understanding

The initial dataset extracted from SAPE and EHR admission records was analysed and processed in order to be used in the DM process. A set of 13 variables were selected: age (corresponds to the age of the pregnant patient), programmed (indicates whether or not a delivery is programmed), gestation (singular or multiple pregnancies), PG1 and PG2 (first echography measures), motive (reason of intervention - normal delivery or unexpected events), patients' weight and height, BMI (body mass index), blood type, cardiotocography (CTG) (biophysics exam that evaluates the fetal wellbeing), streptococcus (presence of the bacterium streptococcus in the pregnant system) and finally, marital status of the pregnant patient. The target variable *Group Risk* denotes the preterm birth risk and it is presented in Table 1.

**Table 1.** Representation of the target variable *Group Risk*.

Description	Value	Target	Distribu-	Percentage
$\geq 37$ weeks of gestation (Term)	0		3137	92.92%
< 37 weeks of gestation (Preterm)	1		239	7.08%

In Table 2 are shown statistics measures related to the numerical variables age, gestation, PG1, PG2 and BMI, while in Table 3 it is represented the percentage of occurrences for some used variables.

**Table 2.** Statistics measures of age, PG1, PG2, weight, height, BMI variables.

	<b>Minimum</b>	<b>Maximum</b>	<b>Average</b>	<b>Standard Deviation</b>
<i>Age</i>	14	46	29.88	5.81
<i>PG1</i>	5	40	12.81	2.96
<i>PG2</i>	0	8	3.09	1.96
<i>BMI</i>	14.33	54.36	29.40	4.57

**Table 3.** Percentage of occurrences of some variables.

<b>Variable</b>	<b>Class</b>	<b>Cases</b>
<i>Programmed</i>	True	12.53%
<i>Gestation</i>	Singular	89.90%
<i>Motive</i>	Normal	81.33%
<i>Streptococcus</i>	Positive	13.27%
<i>Cardiotocography</i>	Suspect	2.19%

### 3.3 Data Preparation

After understanding the data collected, the variables were prepared to be used by the DM models. The data pre-processing phase started with the identification of null and noise values. These values were eliminated from the dataset. To ensure the data normalization, all the values, such as weight and height, were transformed to International System measures, using the point to separate decimal values.

As shown in Table 1, there is a disparity in the distribution of values of the target variable Risk Group (low percentage of preterm birth cases). In order to balance the target, the oversampling technique was implemented by replicating the preterm birth cases until it reached approximately 50% of the dataset, obtaining 6244 entries.

### 3.4 Modelling

A set of Data Mining models (DMM) were induced using the four DM techniques (DMT) mentioned in Section 3: GLM, SVM, DT and NB. The developed models used two sampling methods Holdout sampling (30% of data for testing) and Cross Validation (all data for testing). Additionally there were implemented two different approaches, one using the raw dataset (3376 entries) and another with oversampling. Different combinations of variables were used, obtaining 5 different scenarios:

**S1:** {Age (A), Gestation (G), Programmed (P), PG1, PG2, Motive (M), Height (H), Weight (W), BMI, Blood Type (B), Marital Status (MS), CTG, Streptococcus (S)}

**S2:** {A, H, W, BMI, B, MS, CTG, S}

**S3:** {G, P, PG1, PG2, M, CTG, S}

**S4:** {A, G, PG1, PG2, M, H, W, BMI, B, CTG, S}

**S5:** {A, G, P, M, H, W, BMI, B}

Therefore, a total of 80 Data Mining models (DMM) were induced:

$$\text{DMM} = \{5 \text{ Scenarios}, 4 \text{ Techniques}, 2 \text{ Sampling Methods}, 2 \text{ Approaches}\}$$

All the models were induced using the Oracle Data Miner with its default configurations. For instance, GLM was induced with automatic preparation, with a confidence level of 0.95 and a reference value of 1.

### 3.5 Evaluation

The study used the confusion matrix (CMX) to assess the induced DM models. Using the CMX, the study estimated some statistical metrics: sensitivity, specificity and accuracy. Table 4 presents the best results achieved by each technique, sampling method and approach. The best accuracy (93.00%) was accomplished with scenario 3 by both DT and NB techniques using oversampling and 30% of data for testing. The best sensitivity (95.71%) was achieved by scenario 4 with oversampling using SVM technique and all the data for testing. Regarding specificity, scenario 2 reached 97.52% using SVM with oversampling and all the data for testing.

**Table 4.** Sensitivity, specificity and accuracy values for the best scenarios for each DMT, approach and sampling method. Below, the best metric values highlighted for each DMT.

DMT	Oversampling	Sampling	Scenario	Sensitivity	Specificity	Accuracy
<b>DT</b>	No	30%	3	<b>0.8889</b>	0.9303	<b>0.9300</b>
	No	All	1	0.2896	<b>0.9723</b>	0.8599
<b>GML</b>	No	All	4	0.2896	<b>0.9723</b>	<b>0.8599</b>
	Yes	All	4	<b>0.8674</b>	0.7126	0.7687
<b>NB</b>	No	30%	3	<b>0.8889</b>	0.9303	<b>0.9300</b>
	No	All	1	0.4868	<b>0.9646</b>	0.9271
<b>SVM</b>	No	All	2	0.1023	<b>0.9752</b>	0.4570
	Yes	All	4	<b>0.9571</b>	0.6647	<b>0.7410</b>

In order to choose the best models a threshold was established, considering sensitivity, accuracy and sensitivity values upper than to 85%. Table 5 shows the models that fulfil the threshold.

**Table 5.** Best model achieving the established threshold.

Scenario	Model	Oversampling	Sampling	Sensitivity	Specificity	Accuracy
3	NB,DT	No	30%	0.8889	0.9303	0.9300

## 4 Discussion

Should be noted that the best sensitivity (95.71%) and specificity (97.52%) are reached by models that did not achieve the threshold defined, showing low values in the remaining statistical measures used to evaluate the models. It can be settled that scenario 3 meets the defined threshold, presenting good results in terms of specificity and sensitivity, as seen in Table 5. Thus, it appears that the most relevant factors that affect the term of birth are: pregnancy variables, Gestation and physical conditions of the pregnant woman. In a clinic perspective, the achieved results will enable the prediction of preterm birth, with low uncertainty, allowing those responsible better monitoring and resource management. In a real time environment, physicians can rely on the model to send a warning informing that a specific patient has a risk pregnancy and it is in danger of preterm delivery. Consequently, the physician can be observant and alert to these cases and can put the patients on special watch, saving resources and time to the healthcare institution.

## 5 Conclusions and Future Work

At the end of this work it is possible to assess the viability of using these variables and classification DM models to predict Preterm Birth. The study was conducted using real data. Promising results were achieved by inducing DT and NB, with oversampling and 30% of the data for testing, in scenario 3, achieving approximately 89% of sensitivity and 93% of specificity, suited to predict preterm births. The developed model support the decision-making process in maternity care by identifying the pregnant patients in danger of preterm delivery, alerting to their monitoring and close observation, preventing possible complications, and ultimately, avoiding preterm birth.

In the future new variables will be incorporated in the predictive models and other types of data mining techniques will be applied. For instance, inducing Clustering techniques would create clusters with the most influential variables to preterm birth.

**Acknowledgments.** This work has been supported by FCT - Fundação para a Ciência e Tecnologia within the Project Scope UID/CEC/00319/2013.

## References

1. Berghella, V. (ed.): Preterm birth: prevention and management. John Wiley & Sons (2010)
2. Spong, C.Y.: Defining “term” pregnancy: recommendations from the Defining “Term” Pregnancy Workgroup. *Jama* **309**(23), 2445–2446 (2013)
3. Beta, J., Akolekar, R., Ventura, W., Syngelaki, A., Nicolaides, K.H.: Prediction of spontaneous preterm delivery from maternal factors, obstetric history and placental perfusion and function at 11–13 weeks. *Prenatal diagnosis* **31**(1), 75–83 (2011)
4. Andersen, H.F., Nugent, C.E., Wanty, S.D., Hayashi, R.H.: Prediction of risk for preterm delivery by ultrasonographic measurement of cervical length. *AJOG* **163**(3), 859–867 (1990)
5. Abelho, A., Analide, C., Machado, J., Neves, J., Santos, M., Novais, P.: Ambient intelligence and simulation in health care virtual scenarios. In: Camarinha-Matos, L.M., Afsarmanesh, H., Novais, P., Analide, C. (eds.) Establishing the Foundation of Collaborative Networks. IFIP — The International Federation for Information Processing, vol. 243, pp. 461–468. Springer, US (2007)
6. McGuire, W., Fowlie, P.W. (eds.): ABC of preterm birth, vol. 95. John Wiley & Sons (2009)
7. Brandão, A., Pereira, E., Portela, F., Santos, M.F., Abelho, A., Machado, J.: Managing voluntary interruption of pregnancy using data mining. *Procedia Technology* **16**, 1297–1306 (2014)
8. Kaur, H., Wasan, S.K.: Empirical study on applications of data mining techniques in healthcare. *Journal of Computer Science* **2**(2), 194 (2006)
9. Brandão, A., Pereira, E., Portela, F., Santos, M.F., Abelho, A., Machado, J.: Predicting the risk associated to pregnancy using data mining. In: ICAART 2015 Portugal. SciTePress (2015)
10. Maimon, O., Rokach, L.: Introduction to knowledge discovery in databases. *Data Mining and Knowledge Discovery Handbook*, pp. 1–17. Springer, US (2005)
11. Chapman, P., Clinton, J., Kerber, R., Khabaza, T., Reinartz, T., Shearer, C., Wirth, R.: CRISP-DM 1.0 Step-by-step data mining guide (2000)

# Clustering Barotrauma Patients in ICU—A Data Mining Based Approach Using Ventilator Variables

Sérgio Oliveira, Filipe Portela<sup>(✉)</sup>, Manuel F. Santos, José Machado,  
António Abelha, Álvaro Silva, and Fernando Rua

Algoritmi Centre, University of Minho, Braga, Portugal  
*sergiomdcoliveira@gmail.com, {cfp,mfs}@dsi.uminho.pt,*  
*{jmac,abelha}@di.uminho.pt, moreirasilva@me.com,*  
*fernandoruа.sci@chporto.min-saude.pt*

**Abstract.** Predicting barotrauma occurrence in intensive care patients is a difficult task. Data Mining modelling can contribute significantly to the identification of patients who will suffer barotrauma. This can be achieved by grouping patient data, considering a set of variables collected from ventilators directly related with barotrauma, and identifying similarities among them. For clustering have been considered k-means and k-medoids algortihms (Partitioning Around Medoids). The best model induced presented a Davies-Bouldin Index of 0.64. This model identifies the variables that have more similarity among the variables monitored by the ventilators and the occurrence of barotrauma.

**Keywords:** Barotrauma · Plateau pressure · Intensive medicine · Data mining · Clustering · Similarity · Correlation

## 1 Introduction

Data Minng (DM) process provides not only the methodology but also the technology to transform the data collected into useful knowledge for the decision-making process [1]. In critical areas of medicine some studies reveal that one of the respiratory diseases with higher incidence in the patients is Barotrauma [2]. Health professionals have identified high levels of Plateau pressure as having a significantly contribute to the Barotrauma occurrence [3]. This study is part of the major project INTCare. In this work a clustering process was addressed in order to characterize patients with barotrauma and analyze the similarity among ventilator variables. The best models achieved a Davies-Bouldin Index of 0.64. The work was tested using data provided by the Intensive Care Unit (ICU) of the Centro Hospitalar do Porto (CHP).

This paper consists of four sections. The first section corresponds to the introduction of the problem and related work. Aspects directly related to this study and supporting technologies for knowledge discovering from databases are then addressed in the second section. The third section formalizes the problem and presents the results in terms of DM models following the methodology Cross Industry Standard Process for Data Mining (CRISP-DM). In the fourth section some relevant conclusions are taken.

## 2 Background

### 2.1 Plateau Pressure, Acute Respiratory Distress Syndrome and Barotrauma

The occurrence of barotrauma happens when a patient has complications in mechanical ventilation. Patients with Acute Respiratory Distress Syndrome (ARDS) have shown that the incidence of pneumothorax and barotrauma varies between 0% and 76% [4]. The occurrence of barotrauma is one of the most dreaded complications when a patient is mechanically ventilated. This occurrence is associated with an increased morbidity and mortality. Several researchers argue that the Positive end-expiratory pressure (PEEP) is related to the occurrence of barotrauma, however there are other researchers not supporting this relationship and enforcing that there was not identified any relationship between PEEP and barotrauma [2]. The Plateau Pressure (PPR) values shall be continuously monitored providing important information for patient diagnosis. It is important to maintain the value of PPR  $\leq 30 \text{ cmH}_2\text{O}$  in order to protect the patient's lungs. An increased in PPR is associated to an increasing elasticity of the respiratory system and decreased compliance of the respiratory system [3].

### 2.2 Related Work

Predicting barotrauma occurrence is important for the patient wellbeing. So it is fundamental to explore the prediction accuracy of the variables and their correlation with barotrauma – PPR values  $\geq 30 \text{ cmH}_2\text{O}$ . In a first stage of this project it was predicted the probability of occurring barotrauma considering only the data provided by the ventilator. This study [5] shown that it is possible to predict PPR class  $<30 \text{ cmH}_2\text{O}$  and  $\geq 30 \text{ cmH}_2\text{O}$ , with an accuracy between 95.52% and 98.71%. The best model was achieved using Support Vector Machines and all the variables considered in the study. However, another good model was obtained (95.52% of accuracy) using only three variables. This model showed a strong correlation among: Compliance Dynamic (CDYN), Means Airway Pressure and Pressure Peak.

### 2.3 INTCare

This work was carried out under the research project INTCare. INTCare is an Intelligent Decision Support System (IDSS) [6] for Intensive Care which is in constantly developing and testing. This intelligent system was deployed in the Intensive Care Unit (ICU) of Centro Hospitalar do Porto (CHP). INTCare allows a continuous patient condition monitoring and a prediction of clinical events using DM. One of the most recent goals addressed is the identification of patients who may have barotrauma.

### 2.4 Data Mining

DM corresponds to the process of using technical features of artificial intelligence, statistical calculations and mathematical metrics able to extract information and

useful knowledge. The knowledge discovery may represent various forms, business rules, similarities, patterns or correlations [7].

This work is mainly focused on the development and analysis of clusters. This is a grouping process based on observing the similarity or interconnection density. This process aims to discover data groups according to the distributions of the attributes that make up the dataset [8]. To develop and assess the application of clustering algorithms in the barotrauma dataset, the statistical system R was chosen.

### **3 Knowledge Discovering Process**

#### **3.1 Business Understanding**

The main goal is to use ventilation data in order to identify groups of objects that belong to the same class, i.e. group sets of similar objects in a single set and dissimilar in different sets. The data used to conduct this study were collected in the ICU of CHP. The clusters were supported only for data monitored by ventilators; the values used were numeric and were from discrete quantitative type.

#### **3.2 Data Understanding**

The initial data sample contained several records without patient identification (PID). This happens because sometimes the patients are admitted for a few hours in the ICU but are not assigned to an Electronic Health Record (EHR). These records were discarded for this study. The sample used was collected from the ventilators and comprises a period between 01.09.2014 and 10.12.2014 and a total of 33023 records. Each record contains fourteen fields: CDYN – (F\_1); CSTAT – (F\_2); FIO2 – (F\_3); Flow – (F\_4); RR – (F\_5); PEEP – (F\_6); PMVA – (F\_7);

Plauteau pressure – (F\_8); Peak pressure – (F\_9); RDYN – (F\_10); RSTAT – (F\_11); Volume EXP – (F\_12); Volume INS – (F\_13); Volume Minute – (F\_14).

The coefficient of variation shows that the distributions are heterogeneous for all the attributes since the results obtained are higher than 20%. This measure corresponds to the dispersion ratio between the standard deviation and the average.

#### **3.3 Data Preparation**

Data transformations were necessary to perform data segmentation using clustering techniques based in resource partition methods. Because these techniques do not handle null values and qualitative data, two operations have been performed:

- Firstly, records having at least one null value were eliminated;
- Then, the records containing qualitative values were eliminated.

#### **3.4 Modelling**

The algorithms k-means and k-medoids were used to create the cluster. The choice is justified by the principle of partition method and the difference in their sensitivity to find outliers.

K-means algorithm is sensitive to outliers, because the objects are far from the majority, which can significantly influence the average value of the cluster. This effect is particularly exacerbated by the use of the squared error function [9].

On the other hand, K-medoids instead of using the value of a cluster object as a referencing point takes on real objects and represents the clusters, creates an object for each cluster. The partitioning method is then performed based on the principle of adding the differences between each  $p$  (intra-clusters distance). It is representing an object (dataset partition) [9] where the  $p$  is always  $\geq 0$ . The K-medoids algorithm is similar to K-means, except that the centroids must belong to a set of grouped data [10]. Some configurations were attempted for each one of the algorithms. In the k-means algorithm the value  $K$  (cluster number) varies between 2 and 10. In order to obtain the appropriate number of  $K$  it was used the sum of squared error (SSE). Each dataset was executed 10 times.

The model  $M_n$  belongs to an approach  $A$  and it is composed by the fields  $F$ , a type of variable  $TV$  and an Algorithm  $AG$ :

$$\begin{aligned} A_f &= \{\text{Description (Clustering)}_1\} \\ F_i &= \{F_{-1_1}, F_{-2_2}, F_{-3_3}, F_{-4_4}, F_{-5_5}, F_{-6_6}, V_{-7_7}, F_{-8_8}, F_{-9_9}, F_{-10_{10}}, F_{-11_{11}} \\ &\quad, F_{-12_{12}}, F_{-13_{13}}, F_{-14_{14}}\} \\ TV_x &= \{\text{Qualitative variables ordinal}_1\} \\ AG_y &= \{K - \text{means}_1, K - \text{medoids}(PAM)_2\} \end{aligned}$$

Being this study related with Barotrauma and Plateau Pressure, all the models included the variable  $F_{\{8\}}$ . Some of the clusters induced are composed by the group of variables defined in the first approach.

### 3.5 Evaluation

This is the last phase of the study. It focuses mainly on the analysis of the results presented through the implementation of clustering algorithms (K-means and PAM). The evaluation of the induced models was made by using the Davies-Bouldin Index. The models which presented most satisfactory results were those obtained by means of the K-means algorithm. In general, some models presented good results, however the models did not achieve optimal results (index near 0). Table 2 presents the best models and the correspondent results.

**Table 1.** Models for clustering

Model	Fields	Number of Clusters	Algorithm	Davies-Boldin Index
$M_1$	$F_{\{1,2,7,8,10\}}$	2	$AG_1$	0.82
$M_2$	$F_{\{1,2,7,8,10\}}$	5	$AG_2$	0.86
$M_3$	$F_{\{1,7,8,10\}}$	2	$AG_1$	0.64
$M_4$	$F_{\{1,7,8,10\}}$	6	$AG_2$	1.17

The  $M_3$  model shown to be the most capable in designing clusters with better distances. Davies-Bouldin Index tends to  $+\infty$  however  $M_3$  model has an index of 0.64. This is not the optimal value, but it is the most satisfactory because it is closest to 0. Figure 1 presents  $M_3$  results.

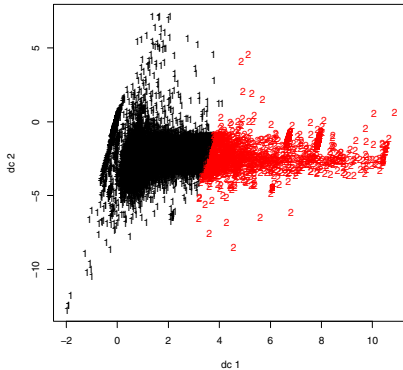


**Fig. 1.** Clusters of model  $M_3$

Table 3 presents the minimum, maximum, average, standard deviation and coefficient of variation of each variable used to host the clusters in  $M_3$ .

**Table 2.** Distributions for each cluster

Clusters	Fields	Min	Max	Average	StDev	CoeVariation
Cluster 1 (30017 rows)	$F_{\{1\}}$	0	73	31.45	16.55	52.63%
	$F_{\{7\}}$	0	38	11.94	2.71	22.73%
	$F_{\{10\}}$	0	100	14.18	7.26	51.2%
	$F_{\{8\}}$	0	99	22.04	6.57	29.82%
Cluster 2 (3006 rows)	$F_{\{1\}}$	73	200	114.72	32.62	28.43%
	$F_{\{7\}}$	3.9	22	11.00	1.68	15.3%
	$F_{\{10\}}$	1.4	46	13.22	5.27	39.88%
	$F_{\{8\}}$	0.2	84	17.88	6.24	34.87%

## 4 Conclusion

This study identified a set of variables that have a great similarity. These variables are related with Plateau Pressure - variable with greater influence in the occurrence of barotrauma. The better result was achieved with the model  $M_3$  obtaining a Davies-Bouldin Index of 0.64, a value near to the optimum value (0).

It should be noted that most of the variables used presented some dispersion however in one of the clusters the higher dispersion value is quite acceptable: 19.42. This result was obtained with the implementation of the K-means algorithm. The CDYN is one of the variables that most influences the clustering, demonstrating a strong

relationship with the PPR and Barotrauma. From the results shown in Table 3 it can be noted that the best corresponding field is CDYN, presenting only a few intersecting values (minimum and maximum). This means that Cluster 1 has CDYN values ranging between [0; 73] and Cluster 2 has CDYN values between [73;200]. The remaining fields used have only few interceptions. Finally, this study demonstrated the feasibility of creating clusters using only data monitored by ventilators and analyzing similar populations. These results motivate further studies in order to induce more adjusted models reliable for classification and clustering at the same time.

**Acknowledgements.** This work has been supported by FCT - Fundação para a Ciência e Tecnologia within the Project Scope UID/CEC/00319/2013 and the contract PTDC/EEI-SII/1302/2012 (INTCare II).

## References

1. Koh, H., Tan, G.: Data mining applications in healthcare. *J. Healthc. Inf. Manag.* **19**(2), 64–72 (2005)
2. Anzueto, A., Frutos-Vivar, F., Esteban, A., Alía, I., Brochard, L., Stewart, T., Benito, S., Tobin, M.J., Elizalde, J., Palizas, F., David, C.M., Pimentel, J., González, M., Soto, L., D'Empaire, G., Pelosi, P.: Incidence, risk factors and outcome of barotrauma in mechanically ventilated patients. *Intensive Care Med.* **30**(4), 612–619 (2004)
3. Al-Rawas, N., Banner, M.J., Euliano, N.R., Tams, C.G., Brown, J., Martin, A.D., Gabrielli, A.: Expiratory time constant for determinations of plateau pressure, respiratory system compliance, and total resistance. *Crit Care* **17**(1), R23 (2013)
4. Boussarsar, M., Thierry, G., Jaber, S., Roudot-Thoraval, F., Lemaire, F., Brochard, L.: Relationship between ventilatory settings and barotrauma in the acute respiratory distress syndrome. *Intensive Care Med.* **28**(4), 406–413 (2002)
5. Oliveira, S., Portela, F., Santos, M.F., Machado, J., Abelha, A., Silva, A., Rua, F.: Predicting plateau pressure in intensive medicine for ventilated patients. In: Rocha, A., Correia, A.M., Costanzo, S., Reis, L.P. (eds.) *New Contributions in Information Systems and Technologies, Advances in Intelligent Systems and Computing* 354. AISC, vol. 354, pp. 179–188. Springer, Heidelberg (2015)
6. Portela, F., Santos, M.F., Machado, J., Abelha, A., Silva, A., Rua, F.: Pervasive and intelligent decision support in intensive medicine – the complete picture. In: Bursa, M., Khuri, S., Renda, M. (eds.) *ITBAM 2014. LNCS*, vol. 8649, pp. 87–102. Springer, Heidelberg (2014)
7. Turban, E., Sharda, R., Delen, D.: *Decision Support and Business Intelligence Systems*. 9a Edição. Prentice Hall (2011)
8. Anderson, R.K.: *Visual Data Mining: The VisMiner Approach*, Chichester, West Sussex, U.K., 1st edn. Wiley, Hoboken (2012)
9. Han, J., Kamber, M., Pei, J.: *Data Mining Concepts and Techniques*. 3a Edição. Morgan Kaufmann (2012)
10. Xindong, W., Vipin, K.: *The Top Ten Algorithms in Data Mining*. CRC Press–Taylor & Francis Group (2009)

# Clinical Decision Support for Active and Healthy Ageing: An Intelligent Monitoring Approach of Daily Living Activities

Antonis S. Billis<sup>1</sup>, Nikos Katzouris<sup>2,3</sup>, Alexander Artikis<sup>2</sup>,  
and Panagiotis D. Bamidis<sup>1(✉)</sup>

<sup>1</sup> Medical Physics Laboratory, Medical School, Faculty of Health Sciences,  
Aristotle University of Thessaloniki, Thessaloniki, Greece

{ampillis, bamidis}@med.auth.gr

<sup>2</sup> Institute of Informatics and Telecommunications, National Center for Scientific Research  
‘Demokritos’, Aghia Paraskevi, Greece

{nkatz, a.artikis}@iit.demokritos.gr

<sup>3</sup> Department of Informatics and Telecommunications,  
National Kapodistrian University of Athens, Athens, Greece

**Abstract.** Decision support concepts such as context awareness and trend analysis are employed in a sensor-enabled environment for monitoring Activities of Daily Living and mobility patterns. Probabilistic Event Calculus is employed for the former; statistical process control techniques are applied for the latter case. The system is tested with real senior users within a lab as well as their home settings. Accumulated results show that the implementation of the two separate components, i.e. Sensor Data Fusion and Decision Support System, works adequately well. Future work suggests ways to combine both components so that more accurate inference results are achieved.

**Keywords:** Decision support · Unobtrusiveness · Sensors · Context awareness · Trend analysis · Statistical process control · Event calculus

## 1 Introduction

Europe’s ageing population is drastically increasing in numbers [1], thereby bearing serious health warnings such as dementias or mental health disorders such as depression [2]. Hence, the immediate need for early and accurate diagnoses becomes apparent. Ambient-Assisted Living (AAL) technologies can provide support to this end [3]. However, most of these research efforts fail to either become easily acceptable by end-users or be useful at a practice level; the obtrusive nature of the utilized technologies invading the daily life of elder adults is probably the one to be blamed [4]. To this end, the approach followed in this paper, which is also aligned with the major objective of the USEFIL project [5], is to apply remote monitoring techniques within an unobtrusive sensor-enabled intelligent monitoring system. The first part of the intelligent monitoring system is an event-based sensor data fusion (SDF) module,

while the second part consists of two major components, i) the trend analysis component and ii) a higher level formal representation model based on Fuzzy Cognitive Maps (FCMs) [5]. The aim of this paper is to present a feasibility study of SDF and Trend Analysis components in real life settings and evaluate their capability of intelligent health monitoring.

## 2 Materials and Methods

### 2.1 The USEFIL Platform

The USEFIL intelligent monitoring system (cf. Fig. 1) comprises of three different layers of processing. Low cost sensors provide unobtrusive low level information, e.g. activity, mood and physiological signs. Event fusion module is the intermediary layer, which combines multimodal low level events and translates them into contextual information. A server-side Decision Support System consumes time stamped contextual information and projects them in the long run, producing alerts, upon recognition of data abnormalities or health deteriorating trends. This information is channeled to seniors or their carers via user-friendly interfaces.

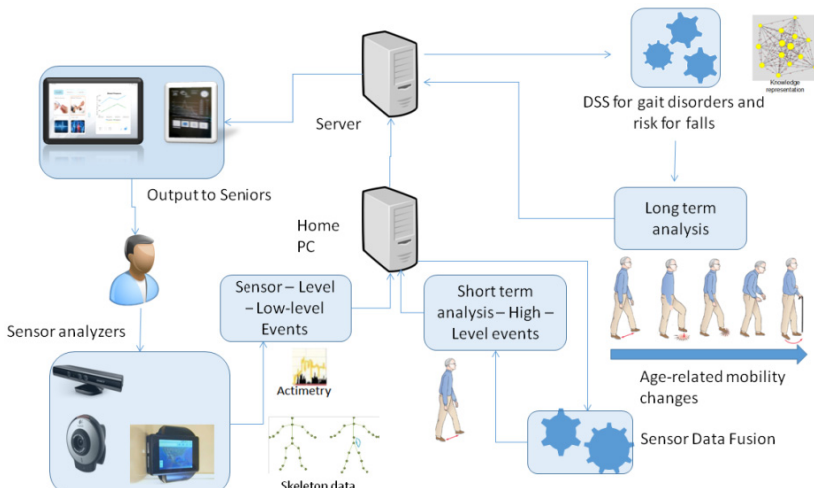


**Fig. 1.** Intelligent Monitoring components

### 2.2 Sensor Data Fusion

The role of the data fusion component in USEFIL is to interpret sensor data into a semantic representation of the user's status. Its tasks range from contextualization of sensor measurements to characterization of functional ability. We employ a Complex Event Recognition methodology [7], which allows to combine heterogeneous data sources by means of event hierarchies. In our setting, input consists of a stream of *low-level events (LLEs)* – such as time-stamped sensor data, and output consists of

recognized complex, or *high-level events* (*HLEs*), that is, spatio-temporal combinations of simpler events and domain knowledge. Our approach is based on the Event Calculus [8], a first-order formalism for reasoning about events and their effects. To address uncertainty, we ported the Event Calculus in the ProbLog language [10], as in [9]. ProbLog is an extention of Prolog, where inference has a robust probabilistic semantics.

Constructing patterns (rules) for the detection of an HLE, amounts to specifying its dependencies with LLEs and other HLEs. As an example, we use the case study of *Barthel-scoring* of Activities of Daily Living (ADL), adapted from [12]. ADL refers to fundamental self-care activities, while the Barthel Index [11] is considered as the “golden standard” for assessing functional ability in ADL. The *Transfer* ADL refers to the ability of a person to sit down or get up from a bed or chair. The corresponding scores in the Barthel Index are evaluations of the performance in this task, based on the ability to perform and the amount of help needed.

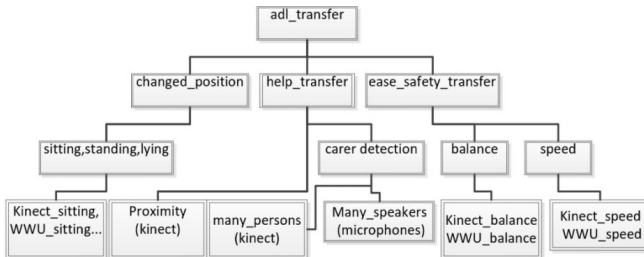


**Fig. 2.** An event hierarchy for the *Transfer* ADL

Fig. 2 presents an event hierarchy for the *transfer* ADL, developed in USEFIL. The leaves in the tree structure represent LLEs, obtained from sensor measurements, while each node represents an HLE. According to this representation, to Barthel-score the *transfer* ADL (root node), one should determine whether the user changed position, while receiving help for this task, taking into account the ease and safety with which the user performs. Each of these indicators (position change, help offered, ease-safety) is represented by an HLE, defined in terms of LLEs and other HLEs in lower levels of the hierarchy. The reader is referred to [12] for a detailed account of the implementation of such a hierarchy in the probabilistic Event Calculus.

### 2.3 Decision Support Module

Health trends identification is based on statistical process control principles. Each parameter may be modeled as a random process with a time-varying mean value and standard deviation. In this work we have followed two steps, namely the baseline extraction and the identification of acute events.

A personalized baseline profile is computed through time-series analysis and statistical process control concepts. More specifically, each variable under investigation (e.g. walking speed) is modeled as a time-series, random process with a time-varying mean value and standard deviation. The computations involved are the following:

Time-series observations are divided into n overlapping windows. The mean ( $\bar{x}$ ) and the standard deviation ( $\bar{r}$ ) of each time window are computed. Then, the mean value and the standard deviation of the entire process are averaged based on the individual runs:

$$\hat{x} = \text{mean}\{\bar{x}\} \quad \hat{r} = \text{mean}\{\bar{r}\} \quad (1)$$

The baseline profile is also consisted of a confidence interval for both the process mean value and the standard deviation. These intervals are defined by the following limits:

$$\text{lim}_{low} = \hat{x} - \frac{3\hat{r}}{\sqrt{n}} \quad \text{lim}_{upper} = \hat{x} + \frac{3\hat{r}}{\sqrt{n}} \quad (2)$$

Ongoing monitoring of the process under consideration is facilitated through the characterization of a further follow-up period based on comparison against the control limits of the baseline process. Single runs that are out of the control limits are considered as acute events.

### 3 Data Collection

In the process of system integration and pilot setup, an e-home like environment was established serving as an Active & Healthy Aging (AHA) Living Lab (see Fig. 3). A total of five (5) senior women aged 65+ (mean  $74.6 \pm 3.85$  years) were recruited. All users provided voluntary participation forms to denote that they chose to participate to this trial voluntarily after being informed of the requirements of their participation. The ability of independent living was assessed by the Barthel index. The real testing and use of the environment took place for several days. Seniors executed several activities of everyday life in a free-form manner, meaning that they were left to perform activities without strict execution orders.



**Fig. 3.** Performance of directed activities, interaction with the system

Apart from the lab environment, the system was also installed in home of lone-living seniors for several days lasting from one to three months. Four (4) elderly women aged  $75.3 \pm 4.1$  years provided their informed consent for their participation in the home study. Recordings over several days in these senior apartments measured, among others, gait patterns, emotional fluctuations and clinical parameters.

## 4 Results

### 4.1 Short-Term Monitoring – Scoring of ADLs

In order to evaluate the SDF module, the Transfer ADL was extracted for each senior. Carers examined seniors and assessed all of them as totally independent, with a

Barthel score equal to "3", which is the ground truth for all cases. Therefore, an overall confusion matrix for all five seniors is built in Table 1. As shown, SDF several times scores seniors as needing help with the Transfer Activity (scores "1" and "2"), although they are totally independent. This paradox can be attributed to the presence of a facilitator during the monitoring sessions.

## 4.2 Long-Term Monitoring – Gait Trends

Data from an initial period of two to four weeks were used so as to calculate the baseline for each elderly participant. The rest of the period was used as a "follow up period", where the actual monitoring was examined. Walking speed as measured by the Kinect sensor was used as the gait parameter to monitor in the long run. Fig. 4 illustrates the baseline process formation of a senior suffering from mobility problems due to osteoporosis. During the monitoring period there are significant deviations from the baseline process (42.4% of days were out of control). This means that older woman's walking speed decreases with respect to her baseline period. Walking speed levels decrease might correlate to early health risk signs, such as falls.

**Table 1.** Confusion matrix of ADL Transfer scoring for all 5 participants

		Predicted class		
		ADL TransferScore1	ADL TransferScore2	ADL TransferScore3
Actual Class	ADL TransferScore3	11	7095	6358

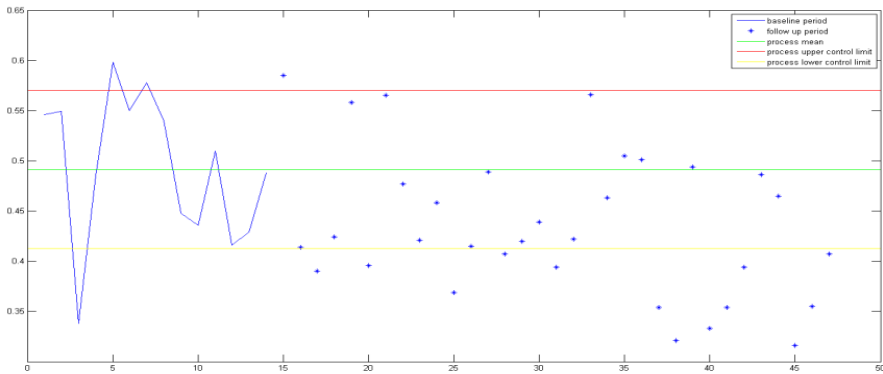


**Fig. 4.** Walking speed control chart. Yellow line: lower control limit, Red line: upper control limit, Blue continuous line: baseline period, Dots: follow up days.

## 5 Discussion

In this paper, mechanisms towards a truly intelligent and unobtrusive monitoring system for active and healthy aging were demonstrated together with a sample of the first series of results. Short-term context awareness was tested with the ADL scenario,

while long-term trend analysis with the gait patterns scenario. In the first case, there were many false positives, due to the challenging, unconstrained nature of the experiment. Personalized thresholds would help SDF algorithm to avoid scoring Barthel equal to “1”. Trend analysis’ baseline extraction and process control limits would possibly refine latter inference results. On the other hand, long term analysis, may benefit by the SDF output, since outliers found to be out of control, could possibly be annotated as logical “noise” through context awareness. This way pathological values may be interpreted as normal based on a-priori knowledge of the context.

This whole notion is remarkably appealing, as it could lead to potential applications where the synergy between the short-term component of the SDF and the long-term Trend analysis component may prove pivotal. Further data collection from home environments, will prove pivotal upon integrating successfully the two components.

**Acknowledgements.** This research was partially funded by the European Union's Seventh Framework Programme (FP7/2007-2013) under grant agreement no 288532. ([www.usefil.eu](http://www.usefil.eu)). The final part of this work was supported by the business exploitation scheme of LLM, namely, LLM Care which is a self-funded initiative at the Aristotle University of Thessaloniki ([www.llmcare.gr](http://www.llmcare.gr)). A.S. Billis also holds a scholarship from Fanourakis Foundation (<http://www.fanourakisfoundation.org/>).

## References

1. Lutz, W., O'Neill, B.C., Scherbov, S.: Europe's population at a turning point. *Science* **28**(299), 1991–1992 (2003)
2. Murrell, S.A., Himmelfarb, S., Wright, K.: Prevalence of depression and its correlates in older adults. *Am. J. Epidemiology* **117**(2), 173–185 (1983)
3. Kleinberger, T., Becker, M., Ras, E., Holzinger, A., Müller, P.: Ambient intelligence in assisted living: enable elderly people to handle future interfaces. In: Stephanidis, C. (ed.) UAHCI 2007 (Part II). LNCS, vol. 4555, pp. 103–112. Springer, Heidelberg (2007)
4. Wild, K., Boise, L., Lundell, J., Foucek, A.: Unobtrusive in-home monitoring of cognitive and physical health: Reactions and perceptions of Older Adults. *Applied Gerontology* **27**(2), 181–200 (2008)
5. <https://www.usefil.eu/>. Retrieved from web at 29/05/2015
6. Billis, A.S., Papageorgiou, E.I., Frantzidis, C.A., Tsatali, M.S., Tsolaki, A.C., Bamidis, P.D.: A Decision-Support Framework for Promoting Independent Living and Ageing Well. *IEEE J. Biomed. Heal. Informatics*, **19**, 199–209 (2015)
7. Opher Etzion and Peter Niblett. Event processing in action. Manning Publications Co. (2010)
8. Kowalski, R., Sergot, M.: A logic-based calculus of events. In: Foundations of Knowledge Base Management, pp. 23–55. Springer (1989)
9. Skarlatidis, A., Artikis, A., Filippou, J., Palioras, G.: A probabilistic logic programming event calculus. *Journal of Theory and Practice of Logic Programming (TPLP)* (2014)
10. Kimmig, A., Demoen, B., De Raedt, L., Santos Costa, V., Rocha, R.: On the implementation of the probabilistic logic programming language ProbLog. In: de la Banda, M.G., Pontelli, E. (eds.) *Theory and Practice of Logic Programming*, vol. 11, pp. 235–262 (2011)
11. Collin, C., Wade, D.T., Davies, S., Horne, V.: The barthel ADL index: a reliability study. *Disability & Rehabilitation* **10**(2), 61–63 (1988)
12. Katzouris, N., Artikis, A., Palioras, G.: Event recognition for unobtrusive assisted living. In: Likas, A., Blekas, K., Kalles, D. (eds.) SETN 2014. LNCS, vol. 8445, pp. 475–488. Springer, Heidelberg (2014)

# Discovering Interesting Trends in Real Medical Data: A Study in Diabetic Retinopathy

Vassiliki Somaraki<sup>1,2(✉)</sup>, Mauro Vallati<sup>1</sup>, and Thomas Leo McCluskey<sup>1</sup>

<sup>1</sup> School of Computing and Engineering, University of Huddersfield, Huddersfield, UK  
`{v.somaraki,m.vallati,t.l.mccluskey}@hud.ac.uk`

<sup>2</sup> St. Paul's Eye Unit, Royal Liverpool University Hospital, Liverpool L7 8XP, UK

**Abstract.** In this work we present SOMA: a Trend Mining framework, based on longitudinal data analysis, that is able to measure the interestingness of the produced trends in large noisy medical databases. Medical longitudinal data typically plots the progress of some medical condition, thus implicitly contains a large number of trends. The approach has been evaluated on a large collection of medical records, forming part of the diabetic retinopathy screening programme at the Royal Liverpool University Hospital, UK.

## 1 Introduction

*Knowledge discovery* is the process of automatically analysing large amount volumes of data searching for patterns that can be considered as knowledge about the data [2]. In large real-world datasets, it is possible to discover a large number of rules and relations, but it may be difficult for the end user to identify the interesting ones. *Trend mining* deals with the process of discovering hidden, but noteworthy, trends in a large collection of temporal patterns. The number of trends that may occur –especially in large medical databases– is huge. Therefore, a methodology to distinguish interesting trends is imperative.

In this paper we report on a framework (SOMA) that is capable of performing trend mining in large databases and evaluating the interestingness of the produced trends. It uses a three-step approach that: (i) exploits logic rules for cleaning noisy data; (ii) mines the data and recognises trends, and (iii) evaluates their interestingness. This work encompasses a previous preliminary study of Somaraki et al. [10]. The temporal patterns of interest, in the context of this work, are frequent patterns that feature some prescribed change in their frequency between two or more “time stamps”. A time stamp is the sequential patient consultation event number, i.e., the date in which some medical features of the patient have been checked and registered. We tested SOMA on the diabetic retinopathy screening data collected by The Royal Liverpool University Hospital, UK, which is a major referral centre for patients with Diabetic Retinopathy (DR). DR is a critical complication of diabetes, and it is one of the most common cause of blindness in working age people in the United Kingdom.<sup>1</sup> It is a chronic

<sup>1</sup> <http://diabeticeye.screening.nhs.uk/diabetic-retinopathy>

disease affecting patients with Diabetes Mellitus, and causes significant damage to the retina.

The contribution of this paper is twofold. First, we provide an automatic approach for evaluating the interestingness of temporal trends. Second, we test the ability of the SOMA framework in automatically extracting interesting temporal trends from a large and complex medical database. The extracted interesting trends have been checked by clinicians, who confirmed their interestingness and potential utility for the early diagnosis of diabetic retinopathy.

## 2 Background

Association Rule Mining (ARM) is a popular, and well researched, category of data mining for discovering interesting relations between variables in large databases. In (ARM) [1], an observation or transaction (e.g. the record of a clinical consultation) is represented as a set of items where an item is an attribute - value pair. Given a set of transactions, we can informally define an *Association rule* (AR) as a rule in the form of  $X \implies Y$ . The *support* of an AR is defined as the percentage of transactions that contain both  $X$  and  $Y$ . It can also be defined as the probability  $P(X \cap Y)$ . Finally, the *confidence* of an AR is defined as the ratio between the number of transactions that contain  $X \cup Y$  and the number of transactions that contain  $X$ .

ARM procedures contain two stages: (i) frequent item set identification, and (ii) AR generation. Piatetsky-Shapiro [8] defined ARM as a method for the description, analysis and presentation of ARs, discovered in databases using different measures of interestingness. ARM is concerned with the discovery, in tabular databases, of rules that satisfy defined threshold requirements. Of these requirements, the most fundamental one is concerned with the support (frequency) of the item sets used to make up the ARs: a rule is applicable only if the relationship it describes occurs sufficiently often in the data.

The topic of mining interesting trends has recently grown due to the availability of large and complex databases. Liu et al. [6] introduced the concept of general impressions. General impressions are if-then clauses that describe the relation between a condition variable and a class value, and reflect the users knowledge of the domain. Based on the users knowledge, the rules can be classified as: unexpected (previously unknown), confirming (confirms previous knowledge) or actionable (can be fruitfully exploited).

Geng and Hamilton [3] used the term “interesting measures” to facilitate a general approach to automatically identifying interesting patterns. They used this term in three ways, or roles, to use their terminology. First, the measures can be used to prune uninteresting patterns during the mining process. Second, measures can be used to rank the patterns according to their interestingness, and finally they are used during post-processing to select interesting patterns.

### 3 The SOMA Framework

The SOMA framework receives raw data from a range of repositories. Firstly, data are pre-processed: data cleansing, creation of data timestamps, selection of subsets for analysis and the application of logic rules take place. Then, by analysing pre-processed information, frequent patterns are generated and trend mining is performed in order to identify interesting trends.

#### Pre-processing

Medical data values are usually from continuous domains. The presence of continuous domains makes it difficult to apply the frequent item set techniques. For this reason, in SOMA pre-processing discretisation is applied. Discretisation allocates continuous values into a limited number of intervals, called bands [5, 7]. Bands can be either defined by domain experts –in our analysis, physicians– or automatically identified.

Real data, particularly from medical repositories, are usually variegated (text, discrete and continuous values) and noisy. In order to deal with missing data, we adopted logic rules, based on expert knowledge. Logic rules are a sequence of if-then-else cases that consider the values of various related fields for identifying missing ones. Given the considered context, clinicians considered logic rules as the most appropriate method to fill in the data.

Finally, pre-processing performs the task of creating time stamped datasets. Data from different sources are usually not collected with the same frequency, thus it is complex to automatically define a clear association between data and time stamps. In fact, this process is domain-specific, and must be addressed by designing domain-specific solutions crafted by domain experts.

#### Processing

The main step of the SOMA framework consists of two processes: (i) association rule mining (ARM), and (ii) trend generation and categorisation.

The ARM process is repeated for every time stamp, and performs the following tasks: (i) identify rules; (ii) evaluate interestingness of rules, and (iii) filter rules accordingly to their evaluation. Rules are created in the usual AR form:  $X \implies Y$ . On frequent item sets, characteristics that measure interestingness are computed. Finally, rules are filtered; only those which are both frequent and interesting are kept. The corresponding threshold are determined by users, according to the amount of knowledge they want to extract.

In applications involving large medical datasets, efficient processing is a fundamental factor. Since the ARM process is repeated for every time step, the technique must be capable of efficiently identifying rules. Given that, we decided to exploit matrix algorithm principles [11] to efficiently identify frequent rules with acceptable confidence, which only requires one pass through the whole dataset.

The subsequent mining of trends is implemented by considering relations on the vectors of support count, in order to show how the support count for each rule changes over time. We considered the following well-known relations: Increasing,

decreasing, constant, jumping and disappearing. For further information, the interested reader is referred to [9].

### Measuring Interestingness

Strong rules based on support and confidence of association rules are not always interesting. The pitfall of confidence can be traced to the fact that its definition ignores the support of the right-hand ( $Y$ ) part of the rule. To determine which trend is interesting or not, we exploited measures introduced by Han et al. [4]. They propose the *lift* correlation and a set of pattern evaluation measures, in order to mathematically determine interestingness. Lift is calculated as :  $Lift(X, Y) = P(X \cup Y)/P(X) \cdot P(Y)$ . Where  $Lift = 1$ , it indicates that  $X$  and  $Y$  are independent; a value greater than 1 indicates a positive correlation, a *Lift* value smaller than 1 refers to negative correlation. The pattern evaluation measures proposed in [4] are: all.confidence, max.confidence, Kulczynski and cosine. Each of them has the following property: its values is only influenced by the supports of  $X$ , and  $Y$ , but not by the total number of transactions. Their values range from 0 to 1 and the higher their value the closer the relationship between  $X$  and  $Y$ . We selected them since they analyse different aspects of data.

The values of those measures are calculated during the trend mining process from SOMA. For each trend, a matrix with dimension  $5 \times T$ , where  $T$  is the number of time stamps is built. There is one line for each measure and in the first column the values for the first time are stored, in the second column the values for the second time stamp and so on. The values are in binary form following that if the value of the measure is equal or greater to its threshold then the value at the matrix is 1 and 0 otherwise. The maximum score for each trend is  $5 \times T$  which is the sum of the elements of the matrix if a trend has values equal or greater than the threshold for all measures for all time stamps. The final score is transformed to a percentage. Thus, according to the threshold provided by the users through a process of empirical validation, rules are deemed to be interesting. Further details can be found in [9].

## 4 Experimental Analysis

In this work we considered the data of the Saint Paul's Eye Clinic of the Royal Liverpool University Hospital, UK. The data (anonymised in order to guarantee patients' privacy) was collected from a warehouse with 22,000 patients, 150,000 visits to the hospital, with attributes including demographic details, visual acuity data, photographic grading results, data from biomicroscopy of the retina and results from biochemistry investigations. Stored information had been collected between 1991 and 2009. Data are noisy and longitudinal; they are repeatedly sampled and collected over a period of time with respect to some set of subjects. Typically, values for the same set of attributes are collected at each sample points. The sample points are not necessarily evenly spaced. Similarly, the data collection process for each subject need not necessarily be commenced at the same time.

In our experimental analysis we considered all the 1420 patients who had readings over 6 time stamps, 887 patients over 7 time stamps, and 546 patients on 8 time stamps. The number of patients decreases when time windows are larger. This is due to the fact that not all the patients are followed by the Clinic for the same amount of time. For instance, a significant amount of patients from the database had 2 visits only; clearly, this does not allow us to derive any meaningful information about general trends. The percentage of missing values is 9.67% for the test with 6 time stamps, 13.16% for the test with 7 time stamps and 18.26% for the test with 8 time stamps.

The medical experts working with us required that the experiments focused on 7 medical features that they believed to be important: age at exam, treatment of the patient, diabetes type, diabetes duration, age at diagnosis, presence of cataract and presence of DR. Features that represent time are continuous, and have been discretised in bands. In particular, age at exam and at diagnosis have been discretised in bands of approximately 10 years; duration features are discretised in 5-year bands. This was done following advice from medical experts. These medical features have some known relationships with regards to the diagnosis of diabetic retinopathy. Therefore, selecting the aforementioned features, and following medical experts' indications, allow us *to validate the SOMA framework* in the following way: if the known interesting trends are identified by SOMA, it increases our confidence that the process is finding valid and interesting knowledge. The interested reader can find more information about the validation process in [9].

For each time stamp we used as support threshold 15% and for confidence 80%. The threshold for lift is 1.5 and for the other measures is set to 0.75. The overall score threshold is set to 80% or where 24 out of the total 30 entries must be 1. Such thresholds have been identified by discussing with medical experts, and by performing some preliminary analysis on small subsets of the available data. It should be noted that different thresholds can significantly affect the set of identified interesting rules. Lower thresholds lead to larger numbers of potentially less interesting rules output, while higher thresholds results in a very small –but highly interesting– set of rules. A major influence on setting parameter values was to guarantee that the configuration would produce *already known associations and trends*, following the aforementioned validation approach.

## Results

SOMA was implemented and executed in a MATLAB environment. On the considered data, six interesting medical clauses regarding DR were discovered:

1. If a diabetic patient has not developed cataract it is not likely to develop diabetic retinopathy.
2. The younger a patient is diagnosed with diabetes the more likely it is that this patient will develop diabetic retinopathy.
3. If a patient has suffered from diabetes type 2 for more than 20 years it is very likely that this patient will develop diabetic retinopathy.

**Table 1.** Scores, with regards to considered metrics, of the six medical clauses at different time stamps (1–6). All Conf stands for the All\_confidence criteria. Max Conf indicates the Max\_confidence criteria.

	Clause 1						Clause 2						Clause 3						Clause 4						Clause 5						Clause 6					
	1	2	3	4	5	6	1	2	3	4	5	6	1	2	3	4	5	6	1	2	3	4	5	6	1	2	3	4	5	6						
Lift	1	1	1	1	1	1	1	1	1	1	1	1	1	1	1	1	1	1	1	1	1	1	1	1	1	1	1	1	1	1						
All Conf	1	1	1	0	0	0	1	0	0	1	0	1	1	0	0	0	1	1	0	0	0	1	1	0	0	1	0	1	1	0	0					
Max Conf	1	1	1	1	1	1	1	0	1	1	1	1	1	1	1	1	1	1	1	0	0	1	1	1	0	0	1	1	1	1						
Kulc	1	1	1	1	1	0	1	0	0	1	0	0	1	1	0	1	1	1	1	1	0	0	0	1	1	1	0	1	0	1						
Cosine	1	1	1	1	0	0	1	0	0	1	0	0	1	1	0	0	1	1	1	0	0	1	1	1	0	0	1	0	1	0						

4. If a patient suffers from diabetes type 1 it is very likely that this patient will develop diabetic retinopathy.
5. If a patient suffers from diabetes type 2 and is on insulin treatment, this patient is likely to suffer from diabetic retinopathy.
6. If a patient suffers from diabetes type 2 and the duration of diabetes is longer than 20 years, this patient is likely to develop diabetic retinopathy.

Table 1 shows the value of the clauses, with regards to the considered criteria, per time stamp. Given a row, it is possible to assess if the corresponding criterion changed its value over time. The maximum score that a clause can get by considering 6 time stamps and 5 criteria is 30; therefore, given the threshold of 80%, at least 24 values should be 1. According to Table 1, only the first medical clause achieves an overall score which is above the threshold. Therefore, clause 1 is deemed to be the most interesting. When using 7 or 8 time stamps, the overall interestingness reduced respectively to 73% and 64%. This is possibly due to the smaller number of considered patients, and to the different impact of missing values on the different datasets. Interestingly, for every considered clause, the lift value is well above the threshold; this means that in rules in the form of  $X \Rightarrow Y$ , X and Y of the medical clauses are positively correlated, and there is associations between X and Y for all medical clauses. It should also be noted that the confidence of the reverse rules is below the threshold: that explains why Kulczynski and cosine and All.conf could not exceed the threshold, and indicates that there is not a strong relevance in the reverse rule. On the contrary, SOMA revealed a very good confidence also for the inverse rule of clause 1. Ophthalmologists of the Saint Paul’s Eye Unit confirm that this result is very interesting, and it highlights a cause-and-effect relationship between cataract of diabetic patients and diabetic retinopathy.

It is well known that diabetes has many factors that affect its progress, and not all of them will necessarily appear in databases. However, in general, according to the clinicians of Saint Paul’s Eye Unit, the first two clauses appear to provide new evidence of previously unknown relations, and are thus worth investigating further. The other 4 clauses fit with accepted thinking, and so while not being actionable knowledge, provide validation to the approach described in this work.

## 5 Conclusion

In this paper we described SOMA, a framework that is able to identify interesting trends in large medical databases. Our approach has been empirically evaluated on the the data of the Saint Paul's Eye Clinic of the Royal Liverpool University Hospital. SOMA is highly configurable. In order to meaningfully set available values, we involved medical experts in the process. In particular, we set parameters in order to allow SOMA to find previously known interesting trends. We used this as a heuristic to indicate that the previously unknown interesting trends identified by SOMA within the same configuration may be valuable. As clinicians confirmed, SOMA was able to identify suspected relations, and to identify previously unknown causal relations, by evaluating the interestingness of corresponding trends in the data.

Future work includes applying SOMA to other medical databases, and the investigation of techniques for visualising trends and results.

**Acknowledgments.** The authors would like to thank Professor Simon Harding and Professor Deborah Broadbent at St. Paul's Eye Unit of Royal Liverpool University Hospital for providing information and support.

## References

1. Agrawal, R., Srikant, R., et al.: Fast algorithms for mining association rules. In: Proc. 20th Int. Conf. Very Large Data Bases, VLDB, vol. 1215, pp. 487–499 (1994)
2. Frawley, W.J., Piatetsky-Shapiro, G., Matheus, C.J.: Knowledge discovery in databases: An overview. *AI Magazine* **13**(3), 57 (1992)
3. Geng, L., Hamilton, H.J.: Interestingness measures for data mining: A survey. *ACM Computing Surveys (CSUR)* **38**(3), 9 (2006)
4. Han, J., Kamber, M., Pei, J.: Data mining: Concepts and techniques, (the morgan kaufmann series in data management systems) (2006)
5. Kotsiantis, S., Kanellopoulos, D.: Discretization techniques: A recent survey. *GESTS International Transactions on Computer Science and Engineering* **32**(1), 47–58 (2006)
6. Liu, B., Hsu, W., Chen, S.: Using general impressions to analyze discovered classification rules. In: KDD, pp. 31–36 (1997)
7. Liu, H., Hussain, F., Tan, C.L., Dash, M.: Discretization: An enabling technique. *Data Mining and Knowledge Discovery* **6**(4), 393–423 (2002)
8. Piatetsky-Shapiro, G.: Discovery, analysis and presentation of strong rules. In: *Knowledge Discovery in Databases*, pp. 229–238 (1991)
9. Somaraki, V.: A framework for trend mining with application to medical data. Ph.D. Thesis, University of Huddersfield (2013)
10. Somaraki, V., Broadbent, D., Coenen, F., Harding, S.: Finding temporal patterns in noisy longitudinal data: a study in diabetic retinopathy. In: Perner, P. (ed.) ICDM 2010. LNCS, vol. 6171, pp. 418–431. Springer, Heidelberg (2010)
11. Yuan, Y.B., Huang, T.Z.: A matrix algorithm for mining association rules. In: Huang, D.-S., Zhang, X.-P., Huang, G.-B. (eds.) ICIC 2005. LNCS, vol. 3644, pp. 370–379. Springer, Heidelberg (2005)

# **Artificial Intelligence in Transportation Systems**

# A Column Generation Based Heuristic for a Bus Driver Rostering Problem

Vítor Barbosa<sup>1()</sup>, Ana Respício<sup>2</sup>, and Filipe Alvelos<sup>3</sup>

<sup>1</sup> Escola Superior de Ciências Empresariais do Instituto Politécnico de Setúbal,  
Setúbal, Portugal

vitor.barbosa@esce.ips.pt

<sup>2</sup> Centro de Matemática, Aplicações Fundamentais e Investigação Operacional,  
Faculdade de Ciências da Universidade de Lisboa, Lisbon, Portugal

alrespicio@fc.ul.pt

<sup>3</sup> Departamento de Produção e Sistemas da Universidade do Minho, Braga, Portugal  
falvelos@dps.uminho.pt

**Abstract.** The Bus Driver Rostering Problem (BDRP) aims at determining optimal work-schedules for the drivers of a bus company, covering all work duties, respecting the Labor Law and the regulation, while minimizing company costs. A new decomposition model for the BDRP was recently proposed and the problem was addressed by a metaheuristic combining column generation and an evolutionary algorithm. This paper proposes a new heuristic, which is integrated in the column generation, allowing for the generation of complete or partial rosters at each iteration, instead of generating single individual work-schedules. The new heuristic uses the dual solution of the restricted master problem to guide the order by which duties are assigned to drivers. The knowledge about the problem was used to propose a variation procedure which changes the order by which a new driver is selected for the assignment of a new duty. Sequential and random selection methods are proposed. The inclusion of the rotation process results in the generation of rosters with better distribution of work among drivers and also affects the column generation performance. Computational tests assess the proposed heuristic ability to generate good quality rosters and the impact of the distinct variation procedures is discussed.

**Keywords:** Rostering · Column generation · Heuristic

## 1 Introduction

Personnel scheduling or rostering [1] consists in defining a work-schedule for each of the workers in a company during a given period. A roster is a plan including the schedules for all workers. An individual work-schedule defines, for each day, if the worker is assigned to work or has a day-off and, in the first case, which daily duty/shift has to be performed. The rostering problem arises because the company usually has diverse duties to assign on each day, sometimes needing particular skills and, on the other hand, the Labour Law and company rules (days-off, rest time, etc.)

restrict the blind assignment of duties to workers. Rostering is addressed in many types of business as recently surveyed in [2] and also some years ago in [3].

The Bus Drivers Rostering problem (BDRP) and most rostering problems are NP-Hard combinatorial optimization problems [4, 5], being computationally challenging to obtain optimal solutions. Many authors address rostering problems with heuristic methods which are usually faster in the achievement of good solutions comparatively to exact methods [4, 6, 7].

The BDRP occurs in the last phase of the transportation planning system, which also includes timetabling, vehicle scheduling and crew scheduling in order to know the drivers demand in each day [8]. It is concerned with the assignment of duties (set of consecutive trips and rest times defining a day of work, previously generated) to drivers, respecting the labour/contractual rules and pursuing the bus company interests in optimizing the drivers use.

Considering the BDRP model proposed in [4], a new decomposition model was proposed for the problem in [9], as well as a new metaheuristic based in the Search-Col framework [10]. In the proposed metaheuristic, column generation and an evolutionary algorithm are used to obtain valid solutions for the problem. The column generation is used to build a pool of schedules for the drivers, resulting from the subproblems' optimization (individual work-schedules), and also to get information about the quality of those schedules (considering their contribution in the optimal linear solution of the column generation).

This paper proposes the integration of a new heuristic in the column generation exact method [11]. The combination of exact and heuristic methods is not new. According to the classification proposed in [12], our combination can be included in the “integrative combinations”, since the heuristic is incorporated in the normal cycle of the column generation, but it can also be classified as a sequential “collaborative combination” since the column generation helps the heuristic, and the heuristic returns new solutions to the column generation.

The new heuristic solves all the subproblems together, avoiding the multiple assignments of the duties to more than one driver, as happens when the subproblems are solved independently. The main contribution of this new heuristic is that it is capable to obtain integer and good quality solutions for the complete problem while performing column generation, without harming its performance. A secondary contribution is that the search-space composed by the solutions obtained with this heuristic is richer in complementary solutions that can be further explored with SearchCol algorithms [10].

The way the heuristic builds rosters or schedules is simple. The novelty is in using the dual solution of the restricted master problem to guide the heuristic. The dual solution is used to set the order by which the duties are selected to be assigned, as well as it is used to define the order by which the drivers are picked to test the assignment of the duty on their schedule. Some variations on the heuristic behaviour are tested where knowledge about the problem is used to obtain rosters with the overtime distributed more evenly between the drivers.

Computational tests show the impact on the column generation performance and on the integer solutions obtained by three configurations of the proposed heuristic.

In the next section the decomposition model for the BDRP is introduced. Section 3 introduces the column generation method, the improvements made by using an heuristic to solve the subproblems and the global heuristic used to solve all the subproblems together. Section 4 presents the computational tests run in a set of BDRP instances, using three configurations of the global heuristic. Section 5 provides some conclusions.

## 2 BDRP Model for Column Generation

The adopted model for the BDRP is an integer programming formulation adapted from the one proposed in [4]. The complete adapted compact model and the decomposition model were presented in [9]. The model is only concerned with the rostering stage, assuming that the construction of duties was previously done by joining trips and rest times to obtain complete daily duties ready to assign to drivers.

In the decomposition model, for each driver, the model considers a set of feasible schedules, represented by the columns built with subproblems' solutions. The set of all the possible valid columns can be so large, making impossible its enumeration. Therefore, only a restricted subset of valid columns are considered, leading to the formulation of a restricted master problem (RMP) of the BDRP decomposition model.

### RMP Formulation:

$$\text{Min } \sum_{v \in V} \sum_{j \in J^v} p_j^v \lambda_j^v \quad (1)$$

Subject to:

$$\sum_{v \in V} \sum_{j \in J^v} a_{ih}^{jv} \lambda_j^v \geq 1, \quad i \in T_h^w, \quad h = 1, \dots, 28, \quad (2)$$

$$\sum_{j \in J^v} \lambda_j^v = 1, \quad v \in V, \quad (3)$$

$$\lambda_j^v \in \{0,1\}, \quad j \in J^v, \quad v \in V. \quad (4)$$

Where:

$\lambda_j^v$  – Binary variable associated to the schedule  $j$  of driver  $v$ , from set of drivers  $V$ ;

$J^v$  – Set of valid schedules for driver  $v$  (generated by subproblem  $v$ );

$p_j^v$  – Cost of the schedule  $j$  obtained from the subproblem of driver  $v$ ;

$a_{ih}^{jv}$  – Assumes value 1 if duty  $i$  of day  $h$  is assigned in the schedule  $j$  of driver  $v$ ;

In this model, the valid subproblem solutions are represented as columns, with cost  $p_j^v$  for the solution with index  $j$  of the subproblem  $v$ , with the assignment of duty  $i$  on day  $h$ , if  $a_{ih}^{jv}=1$ ;

$T_h^w$  is the set of work duties available on day  $h$ .

The objective function is to minimize the total cost of the selected schedules, the first set of constraints, the linking constraints (2), assure that all duties, in each day, are assigned to someone and the last set of constraints, the convexity constraints (3), assure that a work-schedule is selected for each driver/subproblem.

To give some context about the subproblem constraints for the next sections, we describe below the constraints included in its formulation. To see the complete model with the description of the variables and data, we recommend the reading of [9]. The constraints are the following:

- A group of constraints assures that, for each day of the rostering problem, a duty is assigned to the driver (the day-off is also represented as a duty);
- A group of constraints avoids the assignment of incompatible duties in consecutive days (if a driver works in a late duty on day  $h$ , the minimum rest time prevents the assignment of an early duty on day  $h+1$ ). A subset of these constraints considers information from last duty assigned on the previous roster to be considered on the first day assignment;
- A group of constraints avoids the assignment of sequences of work duties that do not respect the maximum number of days without a day-off. A subset of these constraints also considers information from the last roster to force the assignment of the first day-off considering the working days on the end of the previous rostering period;
- A group of constraints forces a minimum number of days-off in each week of the rostering period and also a minimum number of days-off in a Sunday during the rostering period;
- Another group of constraints sets limits on the sum of the working time units each driver can do in each week and in all the rostering period;
- A constraint is used to apply a fixed cost whenever a driver is used (at least one work duty is assigned in the driver' schedule).

### 3 Column Generation Heuristic

In this section an overview of the column generation method is presented to explain how the decomposition model described in the previous section can be solved. After, some improvements to the implementation of the algorithm are detailed. Those improvements intent to reduce the computational time observed when using the standard implementation. The last subsection presents a new heuristic which is combined with the column generation to solve all the subproblems simultaneously, that obtains complete or partial rosters.

Column Generation (CG) is a well-known exact solution method used to obtain solutions to problems where the number of variables is huge compared to the number of constraints. An overview of the origins and evolution of column generation can be found in [13]. For a comprehensive description we propose the reading of [11].

Usually the CG is used to solve problems modeled by a decomposition model where an original model is decomposed in a master problem and some subproblems. Dantzig-Wolfe decomposition [14] is commonly used to obtain the new model.

In the master problem of the decomposition model, new variables represent all the possible solutions of all the subproblems. To avoid the enumeration of all those variables, a restricted master problem is considered. The CG is used to obtain the subproblems solutions that may have a contribution to the improvement of the global solution.

Generally, the CG consists in iteratively optimize the restricted master problem (RMP) to obtain an optimal linear solution (using a simplex algorithm from a solver or similar algorithm). The dual solution of the linking and convexity constraints of the RMP is used to update the objective function of the subproblems. The subproblems are solved with the new objective function values and the subproblems' solutions with negative reduced cost are added as new columns (variables) in the RMP, starting the next iteration. When no new column with negative reduced cost is found, the optimal solution is reached and the algorithm ends.

### 3.1 Improving Column Generation

When using the general CG a *tailing-off effect* is commonly observed. It consists in a slow approximation to the optimal solution [11]. If a high number of iterations are expected, one approach to reduce the global computational time is by reducing the time in each iteration. One option is a deviation of the normal cycle, by changing the number of subproblems solved in each iteration or deciding if all columns are added to the RMP or only the best ones. In the framework presented in [10] these configurations are allowed when running the CG algorithm.

Besides changing the normal path of the CG, a usual approach is to use efficient combinatorial algorithm or heuristics to solve the subproblems, if available, reducing considerably the optimization time. Multiple examples are found in the literature where dynamic programming [15], constraint programming [16] and heuristics [17] are used to obtain subproblem' solutions.

Considering the computational time of the CG in the optimization of the decomposition model for the BDRP presented in [9] and since multiple configurations of the CG algorithm path are already available in the framework where the algorithm is being implemented, we started using an heuristic to obtain valid solutions for the subproblems.

The heuristic used to solve the subproblems of the BDRP decomposition model is based in the decoder algorithm proposed in [4]. The objective of the heuristic is to build schedules with the highest contribution to improve the global solution.

The heuristic described in Figure 1 builds a schedule for a driver trying to assign the duties with the most negative costs (after the update of the objective function with the dual solution of the RMP) following a greedy behavior.

A duty  $i$  cannot be included in the schedule if:

- The day of duty  $i$  has already a duty assigned;
- Duty  $i$  is incompatible with the assigned duty on (day of duty  $i$ )+1 or (day of duty  $i$ )-1 considering the minimum rest time between duties;
- Assignment of duty  $i$  makes a sequence of working days (without a day-off) longer than the maximum allowed;
- Assignment of duty  $i$  exceeds the maximum of working hours allowed by week or for all the rostering period;
- Assignment of duty  $i$  makes it impossible to have the minimum number of days-off in each week of the rostering period or the minimum number of days-off on Sundays in all the rostering period.

---

**Get dual solution from RMP optimization ( $\pi$ );**  
**Update objective function** of the subproblem;  
**Order updated costs** ( $costs[]$ ) in increasing order, keeping information from original position of duty  $i$  ( $origDuty[i]$ );  
**Build empty schedule** for the rostering period size;  
**Initialize driver data:** working time (total and week);  
**FOR**  $i=0$  to size of  $costs[]$   
  **IF**  $costs[i] > 0$  **THEN**  
    **Next**  $i$ ;  
    **Assign**=*TestAssignment*( $origDuty[i]$ );  
    **IF**  $Assign=true$  **THEN**  
      **set** driver as full in the day of  $origDuty[i]$ ;  
      **Update schedule:** add original cost of  $origDuty[i]$  to schedule;  
      **Update driver data:** add  $origDuty[i]$  time length to total working time and corresponding week working time;  
**FOR**  $d=0$  to *number of days of the rostering period*;  
  **IF** no duty was assigned to driver on day  $d$  **THEN**  
    **Assign a day-off** to driver on day  $d$ ;  
**IF** *number assigned duties*  $> 0$  **THEN**  
  **Update schedule:** add fixed cost of driver use;  
**Return** schedule;

---

**Fig. 1.** Driver Schedule Builder Heuristic Algorithm

The function *TestAssignment* used in the heuristic algorithm tests all the conditions previously enumerated, which represent the constraints of the subproblems formulation. If any of the conditions fails, the function returns *false* and only if all the conditions are verified the function returns *true*, allowing the assignment of the duty to the schedule of the driver represented by the subproblem.

Having an heuristic to obtain solutions to the subproblems, the column generation algorithm is changed to use the heuristic, since it does not replace the exact optimization solver, because the solutions of the heuristic are not optimal, only valid. The resulting algorithm is presented in Figure 2 and details the column generation using the heuristic.

---

**DO**  
  **Optimize RMP;**  
  **Update subproblems objective function** with current dual solution of the RMP;  
  **FOR EACH** subproblem  
    **Solve** using heuristic;  
    **Add new columns** into the RMP with subproblems attractive solutions;  
  **IF** no new columns added **THEN**  
    **FOR EACH** subproblem  
      **Solve** using exact optimization solver;  
      **Add new columns** into the RMP with subproblems attractive solutions;  
**WHILE** new columns added  $> 0$

---

**Fig. 2.** Column Generation with Subproblem Heuristic Algorithm

In the new configuration of the column generation cycle, the heuristic is used until no new columns are added from the obtained solutions. At that point, the exact optimization solver is used to obtain the optimal solutions of the subproblems and eventually add new attractive columns. In the next iteration the heuristic is tested again.

In the SearchCol++ framework, the algorithm presented in Figure 2 can have other configurations. It is possible to solve only a single subproblem in each iteration, optimize the RMP again and, in the following iteration solve the next subproblem, iterating by all the subproblems. This strategy results in less columns added to the RMP when the subproblems are returning similar solutions, allowing a faster optimization of the RMP, due to a reduced number of variables.

### 3.2 New Rosters Using Column Generation

Although the improvements to the column generation presented in the previous section, the objective pursued in [9] was to use subproblems' solutions to build good quality rosters by searching the best combination of schedules covering all the duties.

When the BDRP decomposition model was implemented in [9], the standard column generation spent the time set as limit for the column generation and not even the optimization of the RMP using the branch-and-bound method from a commercial solver considering the new column as binary variables was able to achieve low cost rosters.

The use of the heuristic to solve the subproblems was introduced in [18] and an improved version of an evolutionary algorithm was tested to search for valid rosters in the space of solutions resulting from the column generation using the heuristic to solve the subproblems in both configurations: solving all the subproblems in each iteration or solving only one. The improved algorithm behaved better in the search space obtained from the configuration where all the subproblems are solved in each iteration. The search space from that configuration is larger, but similar solutions are repeated for more than one driver/subproblem, allowing finding the best combination of good schedules more easily.

The results obtained in [9, 18] suggest that it is hard to find a combination of schedules that fit together covering all the duties and avoiding over-assignment (a duty assigned to more than one driver) without some additional information in the column generation.

To assure the existence of complementary schedules between each other, we now present a new heuristic that, in the column generation cycle, assigns the duties considering all the subproblems together, as a single one. The cycle does not change, however, instead of generating individual schedules one by one, a new heuristic is called to generate a feasible combination of schedules as well as the schedules *per se*. The primary purpose of solving the subproblems in an aggregated way was to assure the existence of complete or partial rosters without the over-assignment of duties whenever the column generation was stopped. If the solutions included in the initial population of the evolutionary algorithm are already valid rosters, the expected result of the evolution is a better roster.

The heuristic presented in Figure 3 is able to build rosters by testing the assignment of each of the available duties in the schedules of free drivers. Since in each iteration of the column generation a new dual solution is used to update the costs of the duties in the subproblems, the order in which the duties are assigned may vary from iteration to iteration. The objective is that the dual solution of the RMP can guide the generation of distinct, and valid, rosters through the iterations.

When using the aggregated heuristic in the column generation algorithm in Figure 2, the cycle solving the subproblems is replaced by a single call to the new heuristic, which returns schedules for all subproblems/drivers. The exact solver continues to be used when no new attractive columns are built from the heuristic solutions.

---

**Get dual solution** from RMP optimization ( $\pi$ );  
**Order duties** ( $duties[]$ ) in ascending order of the dual solution value of the linking constraints, keeping information from original position of duty  $i$  ( $origDuty[i]$ );  
**Order drivers** ( $drivers[]$ ) in ascending order of the dual solution value of the convexity constraints;  
**Build an empty schedule** for the rostering period size to each of the available drivers (subproblems);  
**Initialize drivers data:** working time (total and week);  
**FOR**  $i=0$  to size of  $duties[]$   
  **FOR**  $v=0$  to *number of drivers*  
    **Select schedule** of  $driver[v]$   
    Assign=**TestAssignment**( $origDuty[i]$ ,  $schedule[driver[v]]$ );  
    **IF** Assign **THEN**  
      Set driver  $v$  as full in the day of  $origDuty[i]$ ;  
      **Update schedule:** add original cost of  $origDuty[i]$  to  $driver[v]$ ' schedule;  
      **Update driver  $v$  data:** add  $origDuty[i]$  time length to total working time and corresponding week ;  
    **EXIT FOR**  
  **FOR**  $v=0$  to *number of drivers*  
    **FOR**  $d=0$  to *number of days of the rostering period*;  
      **IF** no duty was assigned to driver  $v$  on day  $d$  **THEN**  
        **Assign a day-off** to driver  $v$  on day  $d$ ;  
      **IF** number assigned duties to driver  $v > 0$  **THEN**  
        **Update driver  $v$  schedule:** add fixed cost of driver use;  
  **Return**  $schedule[]$ ;

---

**Fig. 3.** Roster Builder Heuristic Algorithm

The BDRP model defines a cost to each unit of time of overtime which may be different to all drivers. However, in our test instances, the drivers are split in a limited number of categories. All the drivers in the same category have the same cost for the overtime labor. This means that we still want to assign first the duties with bigger overtime to the drivers from the category with lower cost of overtime, if possible. However, we want to distribute them among all, avoiding the schedules with extra days-off because of a large concentration of duties with overtime.

Although the ability of the Roster Builder Heuristic to generate valid and distinct rosters, preliminary tests showed that the schedules of the first drivers were filled with the duties with higher overtime. Even if we want to assign the duties with higher overtime to drivers with lower salary, which are the first group in the set of all drivers, if the assignment starts always from the same driver, his/her schedule will be filled with the duties with larger overtime, resulting in an unbalanced work distribution.

Given the existence of different drivers' categories, concerning the value paid by overtime labor, drivers of the same category are grouped and the dual solution values of the convexity constraints are used to order them inside each group.

To assure that when the dual values of the convexity constraints do not lead to the desired diversity in the order of the driver inside each group, we added an additional

---

**Get dual solution** from RMP optimization ( $\pi$ );  
**Order duties** ( $duties[]$ ) in ascending order of the dual solution value of the linking constraints, keeping information from original position of duty  $i$  ( $origDuty[i]$ );  
**Split drivers in groups** with the same category of salary;  
**Order drivers** inside each group according to the dual solution value of the corresponding convexity constraint;  
**Build an empty schedule** for each of the available drivers (subproblems);  
**Initialize drivers data:** working time (total and week);  
**FOR**  $i=0$  to size of  $duties []$   
  **FOR**  $g=0$  to size of *groups of drivers*  
    **Select starting driver** position according to configuration  $r=$  (0 or 1 or random);  
    **FOR**  $j=0$  to  $r$   
      Rotate drivers inside group (remove from the begin and add to the end);  
    **FOR**  $v=0$  to *number of drivers in group g*  
      **Select schedule** of driver  $v$   
      Assign=**TestAssignment**( $origDuty[i]$ ,  $schedule[v]$ );  
      **IF** Assign **THEN**  
        Set driver  $v$  as full in the day of  $origDuty[i]$ ;  
        **Update schedule:** add original cost of  $origDuty[i]$  to  $driver[v]$ ' schedule;  
        **Update driver**  $v$  data: add  $origDuty[i]$  time length to total working time and corresponding week;  
      **EXIT FOR**  
      **IF** Assign **THEN EXIT FOR**  
    **FOR**  $v=0$  to *number of drivers*  
      **FOR**  $d=0$  to *number of days of the rostering period*;  
      **IF** no duty was assigned to driver  $v$  on day  $d$  **THEN**  
        **Assign a day-off** to driver  $v$  on day  $d$ ;  
      **IF** *number assigned duties to driver v >0* **THEN**  
        **Update driver**  $v$  schedule: add fixed cost of driver use;  
**Return**  $schedule[]$ ;

---

**Fig. 4.** Roster Builder Heuristic with drivers' rotation Algorithm

procedure to select the first driver inside each ordered group. We started considering each group of drivers as a circular array. After that, two configuration were prepared to define how a driver is selected when a new duty needs to be assigned.

By default, when a new duty is selected for assignment, the driver to select is the one in the position 0 of the first group. We developed two configurations of the Roster Builder Heuristic with drivers' rotation, namely the sequential and the random configurations. In both, after the assignment of a duty, we rotate the drivers inside the group, the first is removed and inserted at the end. In the sequential configuration, the rotation is of a single position, and in the random configuration, the number of positions rotated is randomly selected between one and the number of drivers in the group minus one, to avoid a complete rotation to the same position.

The inclusion of the rotation leads to a better distribution of the duties with overtime among the group drivers. Figure 4 presents the algorithm of the roster builder heuristic with drivers' rotation. The changes are: the inclusion of the groups of drivers, the selection of the configuration: 'normal' – without rotations; 'sequential' – to rotate one position, picking the drivers sequentially; 'random' - using the stochastic selection by rotating the driver inside the group using a random number of positions.

If a new roster built by the heuristic is better than the best found in previous iterations of the metaheuristic, the best is updated accordingly. The schedules composing the roster are saved in the poll of solutions whenever considered attractive by column generation.

In the next section the computational tests and the results obtained using this new heuristic (column generation with heuristic solving subproblems aggregated) are presented.

## 4 Computational Tests

The decomposition model for the adopted BDRP was implemented in the computational framework SearchCol++ [10]. The BDRP test instances are the ones designated as P80 in [4]. All the instances have 36 drivers available, distributed by four salary categories in groups of equal size (9 drivers). All the tests ran on a computer with Intel Pentium CPU G640, 2,80GHz, 8 Gb of RAM, Windows 7 Professional 64 bits operating system and IBM ILOG 12.5.1 64 bits installed. In all the test configurations, only the column generation stage with the use of the new heuristic was run. It allows to retrieve the lower bounds of the optimal solution (linear), the time consumed to obtain that solution and the integer solution found by the global heuristic (solve all the subproblems aggregated).

In both heuristic configurations where the rotation of the drivers is used, we set that the rotation is not applied in 20% of the iterations (nearly the double of the probability of a driver to be selected randomly inside each group). In practice, for these iterations the assignment starts by the first driver of the ordered group keeping the order defined by the dual values.

Table 1 presents the results obtained from running the three configurations of the Roster Builder Heuristic in each instance, namely, the computational time used by the column generation to achieve the optimal solution (Time) and the value (Value) of the integer solution found. The lower bound (LB) provided by the CG (ceiling of the optimal solution value) is included in the table (the value is the same for all

configurations, only the normal configuration was unable to obtain an optimal solution for the instance P80\_6 in the time limit of two hours). For the random configuration, each instance was solved 20 times. In addition to the best value and its computational time, the table also display the average (Avg) and standard deviation ( $\sigma$ ) of the values and times of the runs.

**Table 1.** Results from the three configurations of the heuristic

Instance	LB	Random						Sequential		Normal	
		Time (s)			Value			Time (s)	Value	Time (s)	Value
		Best	Avg	$\sigma$	Best	Avg	$\sigma$				
P80_1	3512	419.0	534.6	158.5	<b>3601</b>	3679.8	34.7	<b>337.9</b>	3695	917.2	3716
P80_2	2703	150.4	145.0	5.7	<b>2819</b>	2823.2	2.8	143.2	2821	<b>128.2</b>	2830
P80_3	4573	271.1	275.3	45.0	<b>4694</b>	4701.2	5.5	<b>260.3</b>	<b>4694</b>	451.2	4697
P80_4	3566	971.3	827.6	225.6	3759	3761.6	3.1	<b>433.1</b>	<b>3755</b>	860.8	3776
P80_5	3465	<b>535.5</b>	768.6	387.2	<b>3608</b>	3612.2	1.7	766.3	<b>3608</b>	988.0	3617
P80_6	3576	<b>1403.0</b>	1249.6	237.8	<b>3650</b>	3655.2	2.8	2929.4	3666	7315.8	3679
P80_7	3703	765.6	761.9	120.5	<b>3840</b>	3886.5	13.8	768.6	3889	<b>741.4</b>	3895
P80_8	4555	2871.7	2901.5	512.4	<b>4809</b>	4813.5	2.7	4387.0	4813	<b>1696.3</b>	4812
P80_9	3501	<b>323.7</b>	356.7	29.4	<b>3594</b>	3603.2	8.8	383.0	3599	495.7	3611
P80_10	4005	1390.7	1398.3	64.5	<b>4183</b>	4305.0	52.2	1224.7	4269	<b>1218.9</b>	4268
Average		<b>910.2</b>	921.9					1163.4		1481.4	

Under the Time columns, the average time is presented. The “normal” configuration is penalized by instance P80\_6 where the time limit of two hours was reached before obtaining the optimal solution. The best values (time and value) are displayed in bold. Generally the computational times of the rotation heuristics are better, however for the P80\_8 the time is considerably higher when comparing both with the “normal” one. The configurations with rotation were able to reach the best solutions for all instances, particularly the random configuration, which also reduces the average computational time by 39% relatively to normal configuration.

The heuristic solutions were compared with the solution value of the optimization of the compact model using the CPLEX solver with the time limit of 24 hours. Table 2 presents the gaps between the best heuristic solutions with the best known solutions. Only for the instances where the gaps are marked with bold the optimal solution was found by the CPLEX solver before the time limit. The gap of the solutions found by our heuristic is in average 3.2%.

**Table 2.** Gap of the best heuristic integer solution to the best known solution

Instance	Solution	Gap
P80_1	3601	2.0%
P80_2	2819	3.9%
P80_3	4694	2.6%
P80_4	3755	5.2%
P80_5	3608	3.0%
P80_6	3650	1.4%
P80_7	3840	<b>3.7%</b>
P80_8	4809	4.9%
P80_9	3594	<b>1.9%</b>
P80_10	4183	<b>3.5%</b>

The previous results show that all the configurations are able to obtain good quality rosters for the BDRP instances in test and that the separation of the drivers by category groups with the inclusion of the rotation procedure has a significant impact in the column generation optimization time. Besides that, Table 3 shows the impact on the roster when changing the configuration used. For all the configurations, the table presents the average (Avg) units of overtime assigned to a member of the first group (lower cost), the second column ( $\Delta$ ) presents the maximum difference of overtime assigned between the drivers and the last column (days-off) presents the number of extra days-off counted in the schedules of the 9 members of the group.

With the rotation procedures more days-off are counted. However, it is observed that, in average, additional units of overtime were assigned to the drivers, reaching one additional unit, when comparing the sequential and the normal heuristics. The most important change is observed in the uniformity of the distribution of the overtime, where the random configuration reduces the difference for the normal configuration by 5.6 units of time, and the sequential which reduces that value to less than half.

**Table 3.** Comparison of driver' schedules from first group

Instance	Random			Sequential			Normal		
	Avg	$\Delta$	days-off	Avg	$\Delta$	days-off	Avg	$\Delta$	days-off
P80_1	90.6	28	12	91.2	17	9	88.9	40	10
P80_2	85.4	52	9	85.2	26	8	84.2	61	7
P80_3	91.1	6	9	90.9	9	9	90.6	11	9
P80_4	90.3	41	10	90.8	22	9	88.4	44	8
P80_5	93.3	24	9	93.3	13	9	92.3	29	9
P80_6	99.3	36	11	97.6	22	11	96.1	36	9
P80_7	78.4	21	9	81.7	8	9	81.2	11	9
P80_8	84.6	22	9	84.8	10	9	84.9	34	8
P80_9	80.7	54	9	80.8	27	7	79.4	59	4
P80_10	64.1	24	4	65.4	11	1	65.6	39	4
Average	85.8	30.8	9.1	86.2	16.5	8.1	85.2	36.4	7.7

## 5 Conclusions

In this paper, we presented a new heuristic capable of building good quality rosters to the BDRP. The heuristic is integrated with the column generation exact optimization method, using the information from the dual solutions.

In the BDRP, the objective is to define the schedules for all the drivers in the rostering period considered, assuring the assignment of all the duties and optimizing each driver use, reducing bus company costs.

In the proposed method, a decomposition model is implemented in a framework and column generation is used to optimize it. The standard optimization of the subproblems in the column generation iterations is replaced by a global heuristic which solves all the subproblems together. The heuristic is guided by the information from the RMP solution, as it sets the order by which duties are assigned, and also by which order the drivers are selected when assigning a new duty. Three configurations of this heuristic are presented: the normal configuration makes use of the dual

information to guide the assignment of all the duties; the sequential and the random configurations group the drivers by category, and implement a rotation of drivers inside the groups (by 1 and a random number, respectively). The last two configurations intend to obtain rosters with a better distribution of work among drivers and more diversity of schedules.

Computational tests were made in a set of BDRP instances and the results presented. In the results it is observed that the different configurations of the heuristics have impact in the performance of the column generation and also that good quality rosters are obtained by all configurations. The quality of the obtained rosters is evaluated by comparison with the best known integer solutions, where the average gap is 3.2%. An evaluation of the schedules of the first group of drivers shows that the rotation procedure has impact in the distribution of overtime among drivers, particularly when the sequential configuration is used. Besides the better distribution of overtime, the rotation configuration was able to obtain better solutions by augmenting the average overtime units assigned to the drivers of the first group (with lower cost), even with the additional days-off counted. The additional overtime assigned to drivers of the first group compensates the extra days-off assigned.

Our heuristic with the variation configurations seems to work well in the BDRP in most of the instances tested, however it is not guaranteed that the rotation is able to improve the performance of the CG or obtain better solution, as in the instance P80\_8 where the computational time increased greatly when comparing with the normal configuration. If the solutions obtained by the heuristic do not include attractive solutions to the column generation, the computational time can increase.

The proposed heuristic can be used with other problems, provided that there is an heuristic to solve the subproblems and that it is possible to use it in an aggregated way. The variation strategies used need to be tailored using knowledge about each problem.

Future work will focus on tuning this heuristic to improve the column generation performance and, if possible, obtain better integer solutions for the rostering problem. We also intend to generate a search-space composed of solutions provided by this heuristic, so that the concept of the SearchCol can be followed and other metaheuristics can explore the recombination of the obtained rosters (complete or partial) to get closer to the optimal solutions. Application of the current approach to other rostering problems is being considered as future work, since minor changes are needed for adaptation of the general metaheuristic, as well as for the roster generation heuristic here proposed.

**Acknowledgments.** This work is supported by National Funding from FCT - Fundação para a Ciência e a Tecnologia, under the project: UID/MAT/04561/2013.

## References

1. Ernst, A.T., Jiang, H., Krishnamoorthy, M., Sier, D.: Staff scheduling and rostering: A review of applications, methods and models. European Journal of Operational Research **153**, 3–27 (2004)

2. Van den Bergh, J., Beliën, J., De Bruecker, P., Demeulemeester, E., De Boeck, L.: Personnel scheduling: A literature review. *European Journal of Operational Research* **226**, 367–385 (2013)
3. Ernst, A.T., Jiang, H., Krishnamoorthy, M., Owens, B., Sier, D.: An Annotated Bibliography of Personnel Scheduling and Rostering. *Annals of Operations Research* **127**, 21–144 (2004)
4. Moz, M., Respício, A., Pato, M.: Bi-objective evolutionary heuristics for bus driver rostering. *Public Transport* **1**, 189–210 (2009)
5. Dorne, R.: Personnel shift scheduling and rostering. In: Voudouris, C., Lesaint, D., Owusu, G. (eds.) *Service Chain Management*, pp. 125–138. Springer, Heidelberg (2008)
6. Burke, E.K., Kendall, G., Soubeiga, E.: A Tabu-Search Hyperheuristic for Timetabling and Rostering. *Journal of Heuristics* **9**, 451–470 (2003)
7. Respício, A., Moz, M., Vaz Pato, M.: Enhanced genetic algorithms for a bi-objective bus driver rostering problem: a computational study. *International Transactions in Operational Research* **20**, 443–470 (2013)
8. Leone, R., Festa, P., Marchitto, E.: A Bus Driver Scheduling Problem: a new mathematical model and a GRASP approximate solution. *Journal of Heuristics* **17**, 441–466 (2011)
9. Barbosa, V., Respício, A., Alvelos, F.: A Hybrid Metaheuristic for the Bus Driver Rostering Problem. In: Vitoriano, B., Valente, F. (eds.) *ICORES 2013–2nd International Conference on Operations Research and Enterprise Systems*, pp. 32–42. SCITEPRESS, Barcelona (2013)
10. Alvelos, F., de Sousa, A., Santos, D.: Combining column generation and metaheuristics. In: Talbi, E.-G. (ed.) *Hybrid Metaheuristics*, vol. 434, pp. 285–334. Springer, Heidelberg (2013)
11. Lübbecke, M.E., Desrosiers, J.: Selected Topics in Column Generation. *Oper. Res.* **53**, 1007–1023 (2005)
12. Puchinger, J., Raidl, G.R.: Combining metaheuristics and exact algorithms in combinatorial optimization: a survey and classification. In: Mira, J., Álvarez, J.R. (eds.) *First International Work-Conference on the Interplay Between Natural and Artificial Computation*. Springer, Las Palmas (2005)
13. Nemhauser, G.L.: Column generation for linear and integer programming. *Documenta Mathematica Extra Volume: Optimization Stories*, 65–73 (2012)
14. Dantzig, G.B., Wolfe, P.: Decomposition Principle for Linear Programs. *Operations Research* **8**, 101–111 (1960)
15. Cintra, G., Wakabayashi, Y.: Dynamic programming and column generation based approaches for two-dimensional guillotine cutting problems. In: Ribeiro, C.C., Martins, S.L. (eds.) *WEA 2004. LNCS*, vol. 3059, pp. 175–190. Springer, Heidelberg (2004)
16. Yunes, T.H., Moura, A.V., de Souza, C.C.: Hybrid Column Generation Approaches for Urban Transit Crew Management Problems. *Transportation Science* **39**, 273–288 (2005)
17. dos Santos, A.G., Mateus, G.R.: General hybrid column generation algorithm for crew scheduling problems using genetic algorithm. In: *IEEE Congress on Evolutionary Computation. CEC 2009*, pp. 1799–1806 (2009)
18. Barbosa, V., Respício, A., Alvelos, F.: Genetic Algorithms for the SearchCol++ framework: application to drivers' rostering. In: Oliveira, J.F., Vaz, C.B., Pereira, A.I. (eds.) *IO2013 - XVI Congresso da Associação Portuguesa de Investigação Operacional*, pp. 38–47. Instituto Politécnico de Bragança, Bragança (2013)

# A Conceptual MAS Model for Real-Time Traffic Control

Cristina Vilarinho<sup>1</sup>(✉), José Pedro Tavares<sup>1</sup>, and Rosaldo J.F. Rossetti<sup>2</sup>

<sup>1</sup> CITTA, Departamento de Engenharia Civil,  
Faculdade de Engenharia da Universidade do Porto, Porto, Portugal  
[{cvilarinho,ptavares}@fe.up.pt](mailto:{cvilarinho,ptavares}@fe.up.pt)

<sup>2</sup> LIACC, Departamento de Engenharia Informática,  
Faculdade de Engenharia da Universidade do Porto, Porto, Portugal  
[rossetti@fe.up.pt](mailto:rossetti@fe.up.pt)

**Abstract.** This paper presents the description of the various steps to analyze and design a multi-agent system for the real-time traffic control at isolated intersections. The control strategies for traffic signals are a high-importance topic due to impacts on economy, environment and society, affecting people and freight transport that have been studied by many researches during the last decades. The research target is to develop an approach for controlling traffic signals that rely on flexibility and maximal level of freedom in control where the system is updated frequently to meet current traffic demand taking into account different traffic users. The proposed model was designed on the basis of the Gaia methodology, introducing a new perspective in the approach where each isolated intersection is a multi-agent system on its own right.

**Keywords:** Multi-agent system · Traffic signal control · Isolated intersections

## 1 Introduction

Traffic signal control is considered a competitive traffic management strategy for improving mobility and addressing environmental issues in urban areas [1]. Nevertheless, inefficient operation of traffic lights is a common problem that is certainly experienced by all drivers, passengers and pedestrians. This problem annoys road users and negatively affects the local economy.

The research community has been focused on the optimization of traffic signal plans. A traffic signal plan regulates traffic flow through an intersection. Permission for one or more traffic streams to move through the intersection is granted during green-light time intervals. Although there have been relatively successful efforts in optimizing traffic control, these plans often exhibit some shortcomings during operation. This is mainly because traffic control systems are often blind to the surrounding environment, missing the current traffic state, different traffic users and their needs.

In general, the traffic signal controls developed are characterized by lack of flexibility in their control systems, constraining the definition of new green-interval values or new design structures. Their rigidity is responsible for constraining the effectiveness of these strategies. So, this work focuses on isolated intersections to have

more flexibility in operation because coordinated intersections have the drawback of having a common cycle time set to meet the needs of the largest and most complex intersection in a series, which signals at smaller intersections in the series are required to follow. In case traffic flow pattern changes as well, the common cycle time update has to be done more slowly.

The main outcome of this research is the development of an approach for controlling traffic signals that relies on flexibility and a maximal level of control freedom in which the system is updated frequently to match current traffic demand and maintain awareness of the various different traffic users. The use of a multi-agent system (MAS) approach seems to be a step forward to create a system more autonomous and cooperative in real-time control without sacrificing the safety of road users or compromising operation with a significant computational effort.

Researchers attempting to optimize traffic signal control have investigated a wide range of approaches, but several operational challenges have not received sufficient attention from the community. The main problems and challenges at an intersection with which a traffic signal control should be prepared to cope with so as to have an effective control strategy are the following: traffic congestion effect, traffic demand fluctuation, hardware failure, incidents and the mix of different types of road users.

As described, this theme is a very complex system. One way to address the aforementioned issues is to make the traffic control system more intelligent and flexible.

## 2 Literature Review

MASs have been suggested for many transportation problems such as traffic signal control. Zheng, et al. [2] describe their autonomy, their collaboration, and their reactivity as the most appealing characteristics for MAS application in traffic management. The application of MASs to the traffic signal control problem is characterized by decomposition of the system into multiple agents. Each agent tries to optimize its own behavior and may be able to communicate with other agents. The communication can also be seen as a negotiation in which agents, while optimizing their own goals, can also take into account the goals of other agents. The final decision is usually a trade-off between the agent's own preferences against those of others. MAS control is decentralized, meaning that there is not necessarily any central level of control and that each agent operates individually and locally. The communication and negotiation with other agents is usually limited to the neighborhood of the agent, increasing robustness [3]. Although there are many actors in a traffic network that can be considered autonomous agents [4] such as drivers, pedestrians, traffic experts, traffic lights, traffic signal controllers, the most common approach is that in which each agent represents an intersection control [3]. A MAS might have additional attributes that enable it to solve problems by itself, to understand information, to learn and to evaluate alternatives. This section reviews a number of broad approaches in previous research that have been used to create intelligent traffic signal controllers using MASs. In some work [5-8] it was argued that the communication capabilities of MAS can be used to accomplish traffic signal coordination. However, there is no consensus

on the best configuration for a traffic-managing MAS and its protocol [7]. To solve conflicts between agents, in addition to communication approaches, work has been done on i) hierarchical structure, so that conflicts are resolved at an upper level, ii) agents learning how to control, iii) agents being self-organized.

Many authors make use of a hierarchical structure in which higher-level agents are able to monitor lower level agents and intervene whenever necessary. In some approaches [6, 8, 9] there is no communication between agents at the same level. The higher-level agents have the task of resolving conflicts between lower-level agents which they cannot resolve by themselves. In approaches (ii) and (iii), agents need time to learn or self-organize, which may be incompatible with the dynamics of the environment. Agents learning to control (ii) is a popular approach related to controlling traffic signals. One or more agents learn a policy for mapping states to actions by observing the environment and selecting actions; the reinforcement learning technique is the most popular method used [4, 10, 11]. The approach of self-organizing agents (iii) is a progressive system in which agents interact to communicate information and make decisions. Agent behavior is not imposed by hierarchical elements but is achieved dynamically during agent interactions creating feedback to the system [12].

Dresner and Stone [13] view cars as an enormous MAS involving millions of heterogeneous agents. The driver agents approaching the intersection request the intersection manager for a reservation of “green time interval.” The intersection manager decides whether to accept or reject requested reservations according to an intersection control policy. Vasirani and Ossowski [14, 15] extended Dresner’s and Stone’s approach to network intersections. The approach is called market-based in which driver agents, i.e., buyers, trade with the infrastructure agents, i.e., sellers in a virtual marketplace, purchasing reservations to cross intersections. The drivers have an incentive to choose an alternative to the shortest paths.

In summary, since the beginning of this century, interest in application of MAS to traffic control has been increasing. Further, the promising results already achieved by several authors have helped to establish that agent-based approaches are suitable to traffic management control. Most reviewed MASs have focused their attention on network controllers, with or without coordination, rather than on isolated intersections. Another issue is that traffic control approaches focus on private vehicle as the major component of traffic, and may be missing important aspects of urban traffic such as public transport and soft modes (pedestrian, bicycles).

### 3 Methodological Approach

The development of a MAS conceptual model for real-time traffic control at an isolated intersection followed a methodology for agent-oriented analysis and design. In this section an increasingly detailed model is constructed using Gaia [16, 17] as the main methodology, complemented by concepts introduced by Passos, et al. [18].

The first step is an overview of the scenario description and system requirements. The Gaia process starts with an analysis phase whose goal is to collect and establish the organization specifications. The output of this phase is the basis for the second phase, namely the architectural design, and the third phase, which is a detailed design phase.

### 3.1 Scenario Description

The problem addressed is the control of a traffic signal at an isolated intersection at which, depending on the intersection topology and the detected amounts of traffic of various types of road users, the lights regulating traffic streams are to change color to achieve a more efficient traffic management strategy.

The scenario of the proposed traffic signal control is as follows:

- At time X (e.g., each 5 min) or event Y (e.g., traffic conditions, new topology, system failure), a request for a new traffic signal plan is created;
- All information about current topology and traffic conditions is updated to generate new traffic data predictions for the movements of each traffic component. In this way a new traffic signal plan is defined to meet the new intersection characteristics;
- During processing of the new traffic signal plan, if topology has changed, the stage design is developed following the new topology;
- The traffic signal plan is selected based on criteria such as the minimum delay, the system saves the traffic plan information (design, times) and implements it;
- During monitoring, current traffic data are compared with traffic predictions, the topology is verified and data are analyzed by the auditor, which computes the actual level of service and informs the advisor of the results. Depending on the results, the auditor decides if it should make a suggestion for the traffic streams such as to terminate or to extend the current stage or if a new plan should be requested;
- Depending on the information received, traffic streams can continue with the traffic signal plan or negotiate adjustments to it;

The system is responsible for defining and implementing a traffic signal plan as well as deciding when to suspend it, in which case it initiates negotiation between traffic streams to adjust the plan according to traffic flow fluctuations and characteristics (e.g., traffic modes, priority vehicles), or even decides to design a new plan.

As input, the Gaia methodology uses a collection of requirements. The requirements can be collected through analyzing and understanding the scenario in which the organizations are identified, as well as the basic interactions between them to achieve their goals. For early requirements collection, it uses the Tropos methodology [19], in which relevant roles, their goals and intentions, as well as their inter-dependencies are identified and modeled as social actors with dependencies.

### 3.2 Analysis Phase

The goal of the analysis phase is to develop an overview of the system and capture its structure. The division into sub-organizations helps finding system entities with specific goals that interact with other entities of the system and require competencies that are not needed in other parts of the system. From the diagram of the early requirements (Fig.1), 7 actors were found whose goals, soft goals and dependencies are described below.

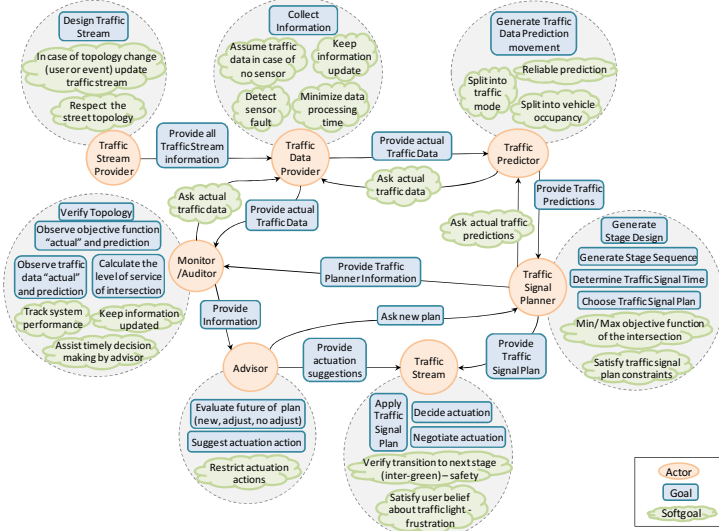


**Fig. 1.** Actors and goal diagram for traffic signal control

The TrafficStreamProvider has the goal to *design a traffic stream*. Each traffic stream is described by movements and by lanes assigned to each movement, including information about traffic sensor locations. To achieve its goal, two soft goals were defined: to respect the intersection topology and to keep the topology information updated in case of topology changes (e.g. road works, accidents). The actor should “provide all traffic stream information” to TrafficDataProvider.

The TrafficDataProvider has the main objective to *collect information* about traffic data from sensors installed at a signalized intersection and aggregate data according to the traffic stream information received. The goal is built upon four sub-goals: to keep traffic data information updated, to minimize data processing time when dependent actors are waiting for the information, assume traffic data if no sensor is installed or if a sensor seems to act strangely. TrafficPredictor requests recent traffic data from this actor and makes its own traffic predictions. Monitor/Advisor also requests traffic data from this actor and uses them for early detection of possible problems and improvements at the intersection control.

The TrafficPredictor has the main goal to *generate a traffic data prediction* for each movement; this is to optimize signal control for imminent demand rather than being reactive to current flow. The strategy may include traffic measurements from a past time period and the current time and uses them to estimate the near future. The generated traffic prediction should be: reliable for future traffic and comprehensive, with total values and splits into traffic modes. The actor requests recent traffic data from TrafficDataProvider and makes its own traffic predictions. TrafficSignalPlanner requests this actor for recent traffic predictions and uses them to optimize the traffic plan.

The TrafficSignalPlanner has the following objectives. *Generate stage design*: search possible signal group sets that can run concurrently respecting a set of safety

constraints; *generate stage sequence*: once possible stage designs are defined, this step compiles strategic groupings of stages to have signal plans designed; *determine traffic signal times*: for each traffic signal plan, the green-interval durations, inter-green and cycle lengths are calculated; and *choose traffic signal plan*, based on a criterion or a weighted combination. Two soft goals were defined for the objective: traffic signal plan selection is based on the best objective function and plan design and timing should be conducted respecting some operational constraints, such as maximum and minimum cycle lengths. The actor requests TrafficPredictor for recent traffic predictions and uses these to optimize its traffic signal plan. It provides the selected plan to TrafficStream to be applied. Advisor asks for a new plan search if the current plan is not adequate to remain active. Finally, Monitor/Auditor receives traffic planner information such as traffic predictions and the objective function so it can monitor independently.

The TrafficStream has three main goals. *Apply a traffic signal plan*, each traffic stream assumes a signal state: red, yellow or green according to the plan or the current actuation action, if it has been defined; *negotiate actuation*, traffic streams cooperate to find possible actuation actions following the advisor's suggestions; and *decide actuation*, traffic stream actors together decide an actuation action to implement. To accomplish its goal, the actor intends: to verify transition to next stage and to satisfy user beliefs about the traffic light to prevent frustration. The actor receives the selected traffic signal plan from TrafficSignalPlanner to apply it and actuation suggestions from Advisor to guide the negotiation phase. If negotiations are needed, Traffic Stream actors discuss these among themselves.

The Advisor's two main objectives are: to *evaluate the future of plan*, choose a possible action depending on information received from Monitor/Auditor: find a new plan, adjust the current plan or continue the implementation; and to *suggest actuation action*, if it is decided to adjust the plan through actuation, the actor prepares a recommendation to guide the actuation process. The *suggest actuation action* has a soft goal defined: formulate a recommendation that will restrict the solution space of actuation negotiation. The actor provides actuation suggestions to TrafficStream. It requests a new plan search from TrafficSignalPlanner if the current plan is not adequate to remain active. Monitor/Auditor sends monitor information to this actor.

The Monitor/Auditor's four main objectives are: verify topology, check if any topology change occurred, and report it to Advisor if so; observe traffic data, "actual" and prediction; observe objective function; and calculate the level of service of the intersection. The data acquired through monitoring are used to evaluate if Advisor should be asked for any plan change. The objectives are complemented with three sub-goals: data collection to keep information updated, track system performance and assist timely decision-making by Advisor to exploit every opportunity to improve the intersection system. The actor requests recent traffic data from TrafficDataProvider and receives them for early detection of possible problems and improvements at the intersection control. It receives traffic planner information such as traffic predictions and the objective function from TrafficSignalPlanner. It sends monitor information to Advisor.

Modeling the environment is one of the agent-oriented methodologies' major activities. The environment model can be viewed in its simplest form as a list of resources that the MAS can exploit, control or consume when working towards the accomplishment of its goal. The resources can be information (e.g., a database) or physical entity

(e.g., a sensor). Six resources were defined for the proposed traffic signal control: topology, traffic detector, traffic database, traffic prediction, traffic signal plan and traffic light. The resources are identified by name and characterized by their types of actions.

A partial list of those resources is:

- Topology has the action to read and change when new topology is detected. The resource contains information regarding intersection topology such as number of traffic arms, their direction, number of approach lanes in each traffic arm, movements assigned in each lane and traffic detector position;
- Traffic Detector is essential for the system because it contains all traffic data (read) and also needs to be frequently updated (change) so it can correspond to the real traffic demand. This makes it possible to know information in each detector about: current traffic data in lane, number of users type, vehicle occupancy, traffic flow distribution by movement, lanes without sensor or equipment failure;

Complex scenarios such as this are very dynamic, so the approach presented by Pasos, Rossetti and Gabriel [18] extends Gaia methodology to include Business Process Management Notation (BPMN) to capture the model dynamics. Business Process (BP) collects related and structured activities that can be executed to satisfy a goal.

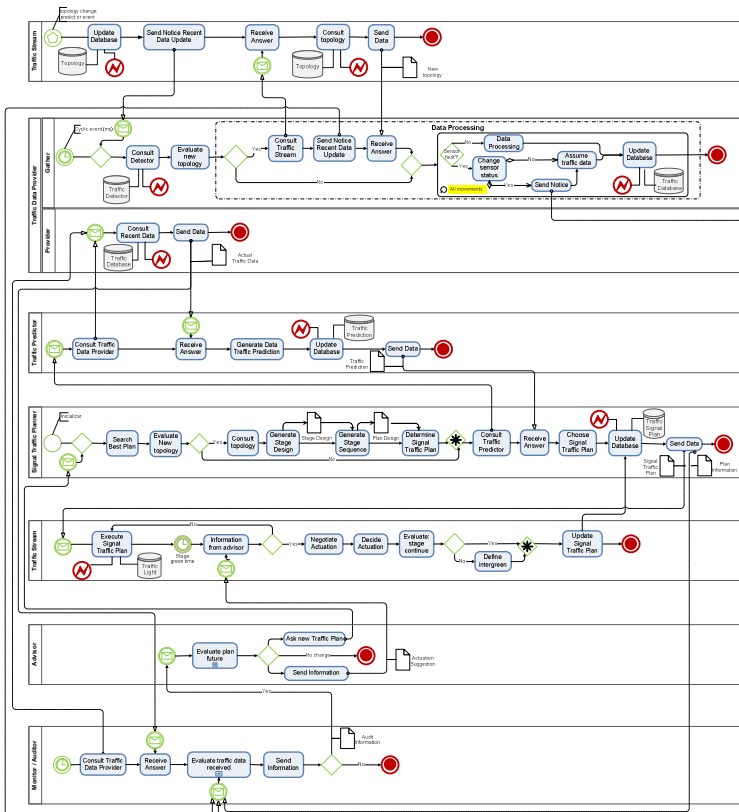


**Fig. 2.** Collaboration diagram of traffic signal control intersection

The diagram in Fig. 2 shows the interactions between the seven participants (actors of Fig. 1) with message exchanges and includes tasks within participants, providing a detailed visualization of the scenario. Their interactions with resources are also present in the diagram.

The actors and goals in diagrams in Fig.1 and Fig.2 help to identify the roles that will build up the final MAS organization. The preliminary roles model defined first, as the name implies, is not a complete configuration at this stage, but it is appropriate to identify system characteristics that are likely to remain. It identifies the basic skills, functionalities and competences required by the organization to achieve its goals. For traffic signal control 13 preliminary roles were defined. A partial list of those roles is:

- RequestTrafficSignalPlan role associated with creating all possible traffic signal plans in order to select one (ChooseTrafficPlan) to be implemented.
  - ChooseTrafficPlan role involves deciding on the best plan to choose based on some criteria.
  - The goal of the preliminary interaction protocol is to describe the interactions between the various roles in the MAS organization. Moreover, the interaction model describes the characteristics and dynamics of each protocol (when, how, and by whom a protocol is to be executed).

### 3.3 Design Phase

The goal of the analysis phase is to define the main characteristics and understand what the MAS will have to be. In the design phase, the preliminary models must be completed. The design phase usually detects missing or incomplete specifications or conflicting requirements demanding a regression back to previous stages of the development process.

From the analysis phase, the organization structure is presented in Fig.3. It is a crucial phase and affects the following steps in MAS development. To represent the organizational structure, we have adopted a graphical representation proposed by Castro and Oliveira [20] that uses the Gaia concept in UML 2.0 representation.

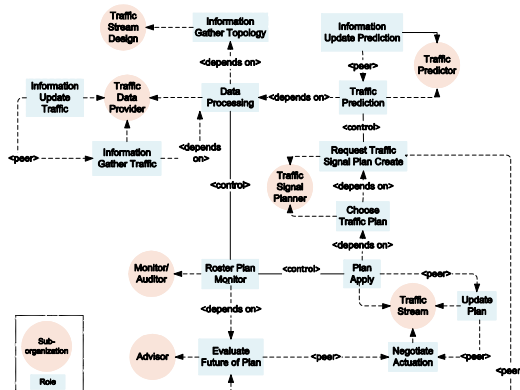


**Fig. 3.** Organizational structure for all system

There are three types of relationships: “depends on”, “controls” and “peer”. “Depends on” is a dependency relationship that means one role relies on resources or knowledge from the other. “Controls” is an association relationship usually meaning that one role has an authoritative relationship with the other role, controlling its actions. “Peer” is a dependency relationship also and usually means that both roles are at the same level and collaborate to solve problems.

After achieving the structural organization, the roles and interactions of the preliminary model can be fulfilled. To complete the role model, it is necessary to include all protocols, the liveness and safety responsibilities. In Table 1, one of 13 roles is described according to the role schema. For complete definition of interaction protocols, they should be revised to respect the organizational structure. Table 2 shows the definition of the “InformPlanEvents” protocol using Gaia notation.

**Table 1.** Role Model example

Id	Properties
RosterPlanMonitor	<p><i>Description:</i> role involves monitoring the traffic condition and traffic signal plan for events related to: Substantial difference: between objective function acceptable value versus current value, or traffic flow (total and by traffic) prediction versus current; Reach some limit of measure of effective (such as maximum queue length); Number maximum of plan repetition; Sensor system fault. After detecting one of these events the RosterPlanMonitor role will request to evaluate what should be done for EvaluateFutureOfPlan role.</p> <ul style="list-style-type: none"> <li>- <i>Protocols and activities:</i> <u>CheckForNewPlanEvents</u>, <u>UpdatePlanEventStatus</u></li> <li><i>Send:</i> reportEventStatus, requestPlanEvaluation; <i>Receive:</i> informPlanEvent, sendEvaluationPlanRequest</li> <li>- Permissions: Read <i>Traffic Detector</i> // to obtain information about sensor system</li> <li>Read <i>Traffic Database</i> // to obtain traffic information about current condition</li> <li>Read <i>Traffic Signal Plan</i> // read and compare plan prediction and current</li> <li>- Responsibilities:</li> <li>Liveness: RosterPlanMonitor = (CheckForNewPlanEvents<sup>w</sup>. informsPlanEvent)<sup>w</sup>    (reportPlanEventStatus<sup>w</sup>. UpdatePlanEventStatus)<sup>w</sup>, w is indefinitely</li> <li>Safety: successful_connection_with_TrafficDetector = true</li> <li>successful_connection_with_TrafficDatabase = true</li> <li>successful_connection_with_TrafficSignalPlan = true</li> </ul>

**Table 2.** Protocol model example

<i>Protocol schema:</i> InformPlanEvents		
<i>Initiator Role:</i> PlanApply	<i>Partner Role:</i> RosterPlanMonitor	<i>Input:</i> Open position information
<i>Description:</i> After an event has been detected it is necessary to analyses the plan adequacy. For that it is necessary to send details about position so plan with his current position can be generated.	<i>Output:</i> The plan is analyzed taking into account the current traffic information.	
<u>CheckForNewPlanEvents</u> , <u>UpdatePlanEventStatus</u> <u>ReceiveMonitorInformation</u> , <u>SendRequest</u>		

To better clarify the organization with its roles and interactions, a final diagram is presented in Fig.4 with the full model, including all protocols and required services that will be the bases for the roles agents choose.

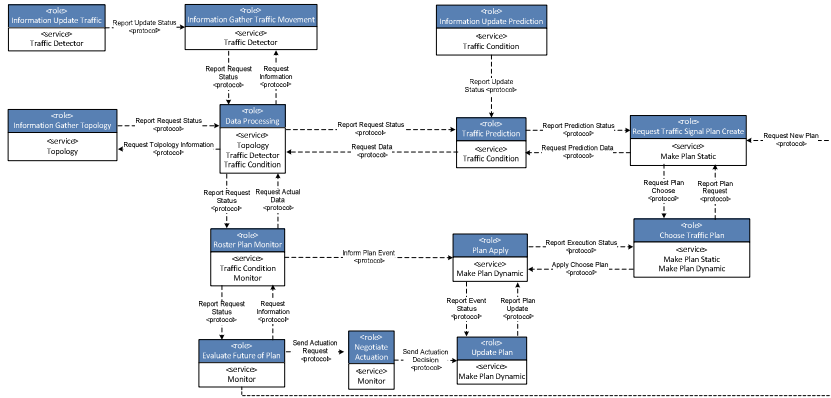


Fig. 4. Final diagram: roles, interactions and services

### 3.4 Detailed Design

The detailed design phase is the last step, and it is responsible for the most important output: the full agent model definition for helping the actual implementation of agents. The agent model identifies the agents from role-interaction analysis. Moreover, it includes a service model. The model design should try to reduce the model complexity without compromising the organization rules. To present the agent model, the dependency relations between agents, roles and services are presented in Fig. 5.

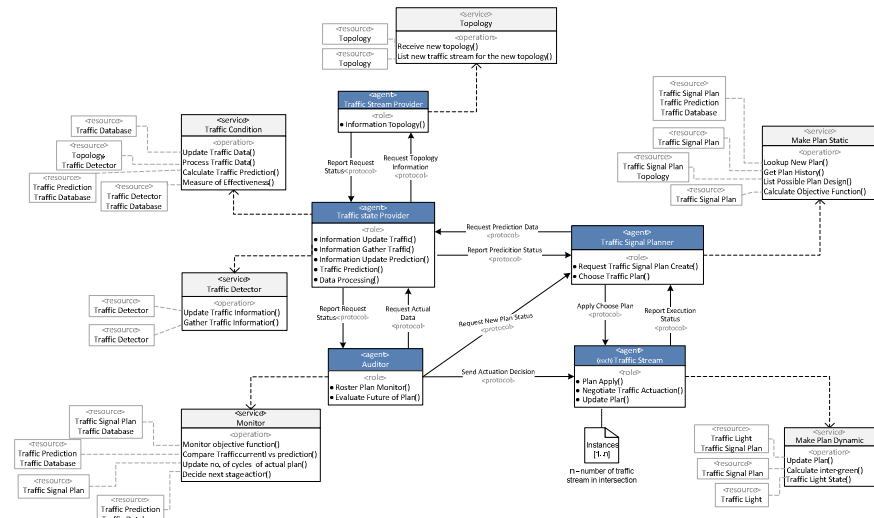


Fig. 5. Full Agent Model

The diagram above should be read as “Traffic Signal Planner agent is responsible to perform the service `Make Plan Static`.” Five types of agents were defined. “Traffic Stream” has  $n$  agents, one for each traffic stream of the intersection, so it depends on

intersection topology. It means that the agent class “Traffic Stream” is defined to play the roles PlanApply, NegotiateTrafficActuation and UpdatePlan, and there are between one and  $n$  instances of this class in MAS. After the completion of the design process, the agent classes defined are ready to be implemented, according to previous models.

## 4 Conclusions

This paper presents the design of a conceptual model of a multi-agent architecture for real-time signal control at isolated traffic intersections using Gaia as the main methodology. The main idea is to make rational decisions about traffic stream lights such that the control is autonomous and efficient under different conditions (e.g., topology, traffic demand, traffic priority, and system failure). The traffic control of an isolated intersection has the advantage that each intersection may have an independent control not limited by neighbors’ control. This allows a control algorithm to be simpler than one for coordinated intersections and more flexible to define plan design and times.

Comparing the proposed strategy with traditional approaches using MAS, it is possible to find several differences. Traditional traffic control methods rely on each agent controlling an intersection within the traffic network. The system usually has a traffic signal plan defined a priori and the system controls how to perform small adjustments such as decreasing, increasing or advancing the green time interval of a traffic stage. Research is being conducted on using MAS to coordinate several neighboring agent controllers, in either a centralized or distributed system. Another feature shared by traditional approaches is the agent decision (action selections) based on learning. From the result of each decision, the learning rule gives the probability with which every action should be performed in the future.

As introduced before, the present approach is distinct from other works to the extent that each traffic stream is an agent and each signalized intersection builds upon independent MASs. Thus, the multitude of agents designed for isolated intersections create, manage and evolve their own traffic signal plans. Therefore this proposed multi-agent control brings the benefit of staged designs and sequences being formed as needed instead of being established a priori. The system structure is flexible, and it has the ability to adapt traffic control decisions to predictions and react to unexpected traffic events.

The validation of this traffic control strategy will be performed using a state-of-the-art microscopic traffic simulator such as, for instance, AIMSUN. The proposed model was developed from scratch rather than by enhancing an existing model.

Finally, it is not our goal to present the process of designing and implementing a MAS or promoting the use of Gaia; there is existing research that is much more adequate for that. However, the methodology applied is well-suited to the problem.

**Acknowledgment.** This project has been partially supported by FCT, under grant SFRH/BD/51977/2012.

## References

1. Park, B., Schneeberger, J.D.: Evaluation of traffic signal timing optimization methods using a stochastic and microscopic simulation program. Virginia Transportation Research Council (2003)
2. Zheng, H., Son, Y., Chiu, Y., Head, L., Feng, Y., Xi, H., Kim, S., Hickman, M.: A Primer for Agent-Based Simulation and Modeling in Transportation Applications. FHWA (2013)
3. McKenney, D., White, T.: Distributed and adaptive traffic signal control within a realistic traffic simulation. *Engineering Applications of Artificial Intelligence* **26**, 574–583 (2013)
4. Bazzan, A.L.C.: Opportunities for multiagent systems and multiagent reinforcement learning in traffic control. *Auton. Agent. Multi-Agent Syst.* **18**, 342–375 (2009)
5. Katwijk, R., Schutter, B., Hellendoorn, H.: Look-ahead traffic adaptive control of a single intersection – A taxonomy and a new hybrid algorithm (2006)
6. Choy, M., Cheu, R., Srinivasan, D., Logi, F.: Real-Time Coordinated Signal Control Through Use of Agents with Online Reinforcement Learning. *Transportation Research Record: Journal of the Transportation Research Board* **1836**, 64–75 (2003)
7. Bazzan, A.L.C., Klügl, F.: A review on agent-based technology for traffic and transportation. *The Knowledge Engineering Review* **29**, 375–403 (2013)
8. Hernández, J., Cuena, J., Molina, M.: Real-time traffic management through knowledge-based models: The TRYTS approach. ERUDIT Tutorial on Intelligent Traffic Management Models, Helsinki, Finland (1999)
9. Rozemond, D.A., Rogier, J.L.: Agent controlled traffic lights. In: ESIT 2000, European Symposium on Intelligent Techniques. Citeseer (2000)
10. Bazzan, A.L.C., Oliveira, D., Silva, B.C.: Learning in groups of traffic signals. *Engineering Applications of Artificial Intelligence* **23**, 560–568 (2010)
11. Wiering, M., Veenen, J., Vreeken, J., Koopman, A.: Intelligent Traffic Light Control (2004)
12. Oliveira, D., Bazzan, A.L.C.: Traffic lights control with adaptive group formation based on swarm intelligence. In: Dorigo, M., Gambardella, L.M., Birattari, M., Martinoli, A., Poli, R., Stützle, T. (eds.) ANTS 2006. LNCS, vol. 4150, pp. 520–521. Springer, Heidelberg (2006)
13. Dresner, K., Stone, P.: A Multiagent Approach to Autonomous Intersection Management. *J. Artif. Intell. Res. (JAIR)* **31**, 591–656 (2008)
14. Vasirani, M., Ossowski, S.: A market-inspired approach to reservation-based urban road traffic management. In: Proceedings of 8th International Conference on AAMAS, pp. 617–624. International Foundation for AAMS (2009)
15. Vasirani, M., Ossowski, S.: A computational market for distributed control of urban road traffic systems. *IEEE Transactions on Intelligent Transportation Systems* **12**, 313–321 (2011)
16. Zambonelli, F., Jennings, N.R., Wooldridge, M.: Developing multiagent systems: The Gaia methodology. *ACM T. Softw. Eng. Meth.* **12**, 317–370 (2003)
17. Wooldridge, M., Jennings, N.R., Kinny, D.: The Gaia methodology for agent-oriented analysis and design. *Auton. Agent. Multi-Agent Syst.* **3**, 285–312 (2000)
18. Passos, L.S., Rossetti, R.J.F., Gabriel, J.: An agent methodology for processes, the environment, and services. In: IEEE Int. C. Intell. Tr., pp. 2124–2129. IEEE (2011)
19. Bresciani, P., Perini, A., Giorgini, P., Giunchiglia, F., Mylopoulos, J.: Tropos: An agent-oriented software development methodology. *Auton. Agent. Multi-Agent Syst.* **8**, 203–236 (2004)
20. Castro, A., Oliveira, E.: The rationale behind the development of an airline operations control centre using Gaia-based methodology. *International Journal of Agent-Oriented Software Engineering* **2**, 350–377 (2008)

# Prediction of Journey Destination in Urban Public Transport

Vera Costa<sup>1()</sup>, Tânia Fontes<sup>1</sup>, Pedro Maurício Costa<sup>1</sup>, and Teresa Galvão Dias<sup>1,2</sup>

<sup>1</sup> Department of Industrial Management, Faculty of Engineering,  
University of Porto, Porto, Portugal

[veracosta@fe.up.pt](mailto:veracosta@fe.up.pt)

<sup>2</sup> INESC-TEC, Porto, Portugal

**Abstract.** In the last decade, public transportation providers have focused on improving infrastructure efficiency as well as providing travellers with relevant information. Ubiquitous environments have enabled traveller information systems to collect detailed transport data and provide information. In this context, journey prediction becomes a pivotal component to anticipate and deliver relevant information to travellers. Thus, in this work, to achieve this goal, three steps were defined: (i) firstly, data from smart cards were collected from the public transport network in Porto, Portugal; (ii) secondly, four different traveller groups were defined, considering their travel patterns; (iii) finally, decision trees (J48), Naïve Bayes (NB), and the Top-K algorithm (Top-K) were applied. The results show that the methods perform similarly overall, but are better suited for certain scenarios. Journey prediction varies according to several factors, including the level of past data, day of the week and mobility spatiotemporal patterns.

**Keywords:** Prediction · Journey destination · Urban public transports

## 1 Introduction

In the last decade, Urban Public Transport (UPT) systems have turned to Information and Communication Technologies (ICT) for improving the efficiency of existing transportation networks, rather than expanding their infrastructures [3, 7]. Public transport providers make use of a wide range of ICT tools to adjust and optimise their service, and plan for future development.

The adoption of smart cards, in particular, has not only enabled providers to access detailed information about usage, mobility patterns and demand, but also contributed significantly towards service improvement for travellers [21, 25]. For instance, inferring journey transfers and destination based on historical smart card data has allowed transportation providers to significantly improve their estimates of service usage – otherwise based on surveys and other less reliable methods [8]. As a result, UPT providers are able to adjust their service accordingly while reducing costs [2]. Furthermore, the combination of UPT and ICT has enabled the development of Traveller Information Systems (TIS), with the goal of providing users with relevant

on-time information. Previous work has shown that TIS have a positive impact on travellers. For instance, providing on-time information at bus stops can significantly increase perception, loyalty and satisfaction [5].

The latest developments in ICT have paved the way for the emergence of ubiquitous environments and ambient intelligence in UPT, largely supported by miniaturised computer devices and pervasive communication networks. Such environments simplify the collection and distribution of detailed real-time data that allow for richer information and support the development of next-generation TIS [6, 20].

In this context, as transportation data is generated and demand for real-time information increases, the need for contextual services arises for assisting travellers, identifying possible disruptions and anticipating potential alternatives [20, 26].

A number of methods have been used for inferring journeys offline (e.g. [1,8,23]). After the journeys are completed, the application of these methods can support different analysis, such as patterns of behaviour (e.g. [13,14]) and traveller segmentation (e.g. [11,12]). In contrast, little research has focused on real-time journey prediction (e.g. [16]). Contextual services, however, require on-time prediction and, unless explicitly stated by the user, the destination of a journey may not be known until alighting.

The prediction of journeys based on past data and mobility patterns is a pivotal component of the next generation of TIS for providing relevant on-time contextual information. Simultaneously, UPT providers benefit from up-to-date travelling information, allowing them to monitor their infrastructures closely and take action.

An investigation of journey prediction is presented, based on a group of bus travellers in Porto, Portugal. Specifically this research focuses on the following questions:

- Is it possible to predict a journey destination of UPT based on past usage? How do past journeys impact the quality of these predictions?
- What is the variation in journey prediction for groups of travellers with different mobility characteristics? Why is so important define such groups?
- Are there variations between groups of travellers over time, specifically for different days of the week?

In order to answer to these questions, this paper is structured as follows: Section 2 describes the data collection and the algorithms used in the work presented; Section 3 presents and discusses the results and the main findings obtained; final conclusions and considerations are presented in Section 4.

## 2 Material and Methods

In order to predict the journey destinations for an individual traveller, three steps were defined: (i) firstly, data from smart cards were collected and pre-processed from the public transport network in Porto, Portugal (see section 2.1); (ii) secondly, four different groups of users were defined, considering their travel patterns (see section 2.2); (iii) finally, three different intelligent algorithms were assessed considering different performance measures (see section 2.3). Figure 1 presents an overview of the overall methodology applied to perform the simulations. While at this stage the analysis is

based on a set of simulations and historical data, the goal is to apply the method for a timely prediction of destinations and which will be implemented in the scope of the Seamless project [4]. Thus, the simulations presented in the present paper enable the evaluation of the importance of groups of travellers, and the best algorithm to use for predicting journey destinations in a real-world environment.

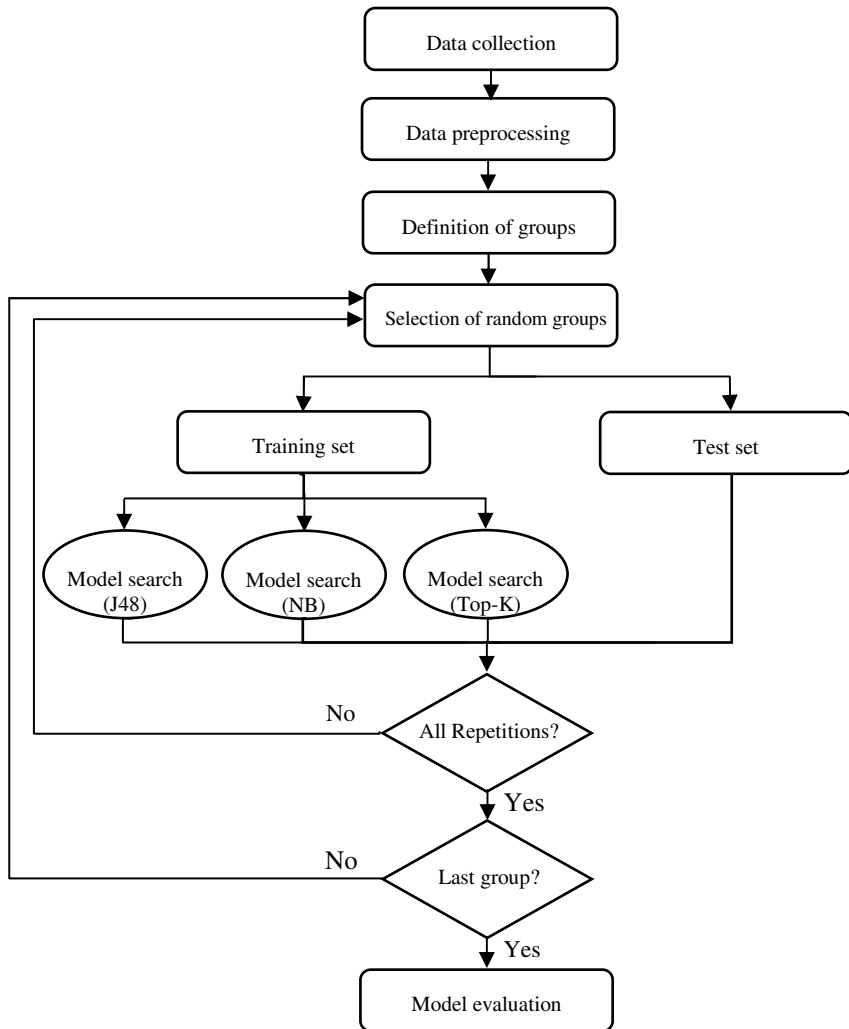


**Fig. 1.** Methodology overview.

## 2.1 Data

The public transport network of the Metropolitan Area of Porto covers an area of 1,575 km<sup>2</sup> and serves 1.75 million of inhabitants [10]. The network is composed of 126 buses lines (urban and regional), 6 metro lines, 1 cable line, 3 tram lines, and 3 train lines [24]. This system is operated by 11 transport providers, of which Metro do Porto and STCP are the largest.

The Porto network is based on an intermodal and flexible ticket system: the Andante. Andante is an open zonal system, based on smart cards, that requires validation only when boarding. A validated occasional ticket allows for unlimited travel within a specified area and time period: 1 hour for the minimum 2-zone ticket, and longer as the number of zones increases. Andante holders can use different lines and transport modes in a single ticket.

In this work, to perform the simulations two months of data were used, April and May of 2010 to perform the simulations. Table 1 shows an example of the data collected for an individual traveller for one week of April 2010. Journey ID is a unique identifier for each trip, sorted in ascending order by the transaction time. For each traveller (i.e. for each Andante smart card), the information related with the boarding time (first boarding on the route), the line (or lines for each trip) and the stop (or stops for each trip) is available. Each trip could have one or more stages. The first line of the table shows a trip with two stages. First the traveller uses stop 1716 and line 303 at 11h34 followed the stop 3175 and line 302. Based on these data the route sequence can be rebuilt.

**Table 1.** Extracted trip chain information for an individual travellers during a week of April, 2010.

Journey ID	Date	First boarding time of the route	Route sequence (Line ID)	Stop sequence (Stop ID)
1036866	10/04/2010	11:24	303 → 302	1716 → 3175
1036867	10/04/2010	16:27	203	1622
1036868	10/04/2010	23:14	200	1035
1036869	12/04/2010	09:05	402	1632
1036870	12/04/2010	12:42	203	1695
1036871	12/04/2010	13:44	203	1632
1036872	12/04/2010	19:45	303	1338
1036873	12/04/2010	22:29	400 → 400	1675 → 1689
1036874	13/04/2010	09:09	402	1632
1036875	13/04/2010	19:11	206	1338
1036876	14/04/2010	08:45	302	1632
1036877	14/04/2010	12:30	402	1338
1036878	14/04/2010	13:43	203	1632
1036879	14/04/2010	19:11	303	1338
1036880	15/04/2010	09:08	402	1632
1036881	15/04/2010	12:57	203	1695
1036882	15/04/2010	14:04	302 → 501	1632 → 1810
1036883	15/04/2010	20:52	303	1338

In order to make a prepossessing of data, an inference algorithm was used [18] to identify the journey destination. Since the Oporto system is based on the validation at the entrance only, this pre-processing is required. In this method, the travel origin of a traveller is the destination of the previous travel of that traveller. However, due to the

absence of information, the results obtained with the application of this algorithm were partially restricted, since data from only one transport provider, the STCP company, were available. Thus, in order to minimize the error, only data from users with at least 80% of destinations inferred with success and, on average, two or more validations per day was used. As a result, the sample consists of 615,647 trips corresponding to 6865 different Andante cards.

The data set consists of a set of descriptive attribute of which three of them were used. The first attribute represents the code of the origin bus stop. The second attribute identifies the date, which represents the day of the week for each validation. The third represents the bus stop as an inferred destination.

## 2.2 Definition of Groups

Sets of travellers were selected from the main dataset for predicting the destination of a journey. Four different groups of travellers were defined with different mobility characteristics. The first three groups (1, 2 and 3) are characterized by patterns of mobility with different usage characteristics. The last group (4) is composed of travellers without a seemingly travel pattern. The spatiotemporal mobility patterns are based on two characteristics: primary journeys and journey schedule. The primary journeys describe spatial regularity, identifying the most frequent journeys in a given route. The journey schedule assesses temporal regularity, based on the departure times. Thus, we have:

- Group 1 (G1): includes individual travellers with a regular spatiotemporal pattern. In this group, individuals with two primary journeys were selected (e.g. home/work/home or home/school/home). These primary journeys represent, in average, 74% of the total journeys. Furthermore, to ensure the temporal travelling regularity, a maximum departure time deviation of one hour was considered. These restrictions resulted in a group of travellers who have a tendency for a rigid journey schedule (e.g. professionals);
- Group 2 (G2): includes travellers with a regular spatial pattern but without temporal regularity. Similar to group one, travellers with two primary journeys (e.g. home/work/home or home/school/home) were selected. These primary journeys represent about 72% of the total journeys. In addition, to exclude temporal regularity of the primary journeys, a departure time deviation greater than one hour was considered. As a result, this group of travellers have a tendency towards a flexible journey schedule (e.g. students);
- Group 3 (G3): includes travellers with a broader spatial regularity. In this group, individuals with four primary journeys were considered (e.g. home/work/home and work/gymnasium/home). These primary journeys represent about 79% of the total journeys. In contrast to the previous two groups, temporal regularity was not taken into account;
- Group 4 (G4): is characterized by a non-regular spatial mobility pattern. In this group, the number of different routes is higher than 50% of the total number of journeys (e.g. occasional travellers).

Table 2 shows the main characteristics of those groups.

**Table 2.** Characteristics of individual journeys considering different groups of travellers.

	Number of travellers (N)	Number of total journeys (X±SD)	Number of different routes (X±SD)	Frequency of primary journeys (%)		Deviation of journey schedule (X±SD)	Representativity of each group in the population
				Top 2 journeys	Top 4 journeys		
<b>G1</b>	200	75.9±12.4	15.8±8.4	73.6%	81.1%	00:17±00:15 <sup>a</sup>	4.6%
<b>G2</b>	200	91.5±30.9	19.1±12.2	72.1%	79.3%	03:08±01:36 <sup>a</sup>	9.6%
<b>G3</b>	200	100.8±26.7	19.2±8.5	48.7%	79.1%	02:04±01:49 <sup>b</sup>	10.5%
<b>G4</b>	200	83.2±35.1	60.0±25.3	0.3%	0.5%	-	12.6%

<sup>a</sup> for the top 2 trips; <sup>b</sup> for the top 4 trips.

## 2.3 Methods

In order to estimate the destination of each traveller, three different algorithms were analysed: (i) the decision trees (J48); (ii) the Naïve Bayes (NB); and (iii) the Top- K algorithm (Top-K).

Decision trees represent a supervised approach to classification. These algorithms are a tree-based knowledge representation methodology, which are used to represent classification rules in a simple structure where non-terminal nodes represent tests on one or more attributes and terminal nodes reflect decision outcomes. The decision tree approach is usually the most useful in classification problems [17]. With this technique, a tree is built to model the classification process. J48 is an implementation of a decision tree algorithm in the WEKA system, used to generate a decision tree model to classify the destination based on the attribute values of the available training data. In R software, the RWeka package was used.

The Naïve Bayes algorithm is a simple probabilistic classifier that calculates a set of probabilities by counting the frequency and combinations of values in a given data set [19]. The probability of a specific feature in the data appears as a member in the set of probabilities and is calculated by the frequency of each feature value within a class of a training data set. The training dataset is a subset, used to train a classifier algorithm by using known values to predict future, unknown values. The algorithm is based on the Bayes theorem and assumes all attributes to be independent given the value of the class variable. In this work the e1071 R package was used.

The Top-K algorithm enables finding the most frequent elements or item sets based on an increment counter [15]. The method is generally divided into counter-based and sketch-based techniques. Counter-based techniques keep an individual counter for a subset of the elements in the dataset, guaranteeing their frequency. Sketch-based techniques, on the other hand, provide an estimation of all elements, with a less stringent guarantee of frequency. Metwally proposed the Space-Saving algorithm, a counter-based version of the Top-K algorithm that targets performance and efficiency for large-scale datasets. This version of the algorithm maintains partial information of interest, with accurate estimates of significant elements supported by a lightweight data structure, resulting in memory saving and efficient processing. It focuses on the influential nodes and discards less connected ones [22]. The main idea

behind this method is to have a set of counters that keep the frequency of individual elements. Invoking a parallelism with social network analysis, the algorithm proposed by Sarmento et al. [22] was changed; a journey is considered to be an edge i.e. a connection between any node (stop) A and B. The algorithm starts to count occurrences of journeys. For each traveller, if the new journey is monitored, the counter is updated. Otherwise, the algorithm adds a new journey in your Top-K list. If the number of unique journeys exceeds  $10^*K$  monitored journeys the algorithm follows the space saving application.

For each algorithm and group of travellers defined previously (see Section 2.2), 15 repetitions were performed. For each repetition, 30 travellers were randomly selected from each group. Figure 2 shows the average number of journeys for the groups. In each simulation, the test size is always one and corresponds to the day under evaluation,  $i$  ( $n_{test} = 1$  day), while the train continuously grows with  $i$  ( $n_{train} = i-1$  day(s)). Table 3 illustrates this procedure.

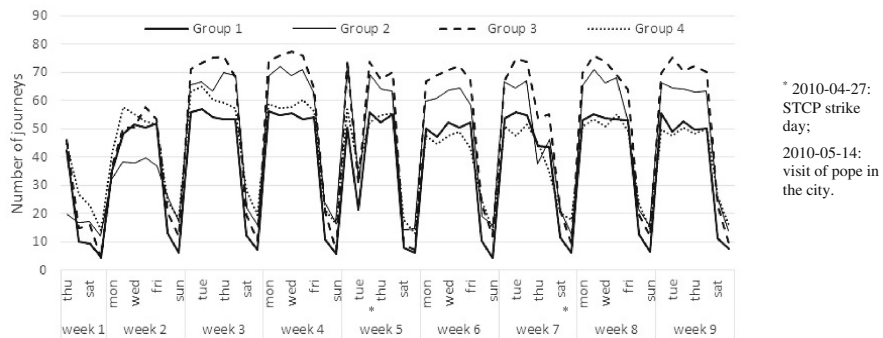


**Fig. 2.** Average number of journeys by each group of travellers.

**Table 3.** Data sets used to train (t) and test (T).

	Days												
	1	2	3	4	5	6	7	8	9	10	(...)	n-1	n
i=1	T												
i=2	t		T										
i=3	t	t		T									
(...)													
i=n	t	t	t	t	t	t	t	t	t	t	(...)	t	T

NOTES: t: days of training set; T: days of the test set.

To evaluate the performance of the different algorithms the Accuracy measure (1), which represents the proportion of correctly identified results, was used. The basis for this approach is the confusion matrix, a two-way table that summarizes the performance of the classifier. Considering one of the classes as the positive (P) class, and other the negative (N) class, four quantities may be defined: the true positives (TP), the true negatives (TN), the false positives (FP) and the false negatives (FN), we have:

$$\text{Accuracy} = \frac{TP + TN}{TP + TN + FP + FN} \quad (1)$$

Nonetheless, due to the sparse usage of the transportation network by travellers, in this work we have an imbalanced sample. In this case, the Accuracy measure by itself is not the most appropriate to analyse the presence of imbalanced data [9]. Therefore, the F-score (2), which combines Precision and Recall measures as a weighted average, was also used. Precision gives an insight on how the classifier behaves in relation to the positive class, giving a measure of how many positive predicted instances are in fact positive, while the Recall gives an insight of the classifier's performance on the positive class, measuring how well the whole positive class is recognized. F-score is given by:

$$F = 2 * \frac{\text{precision} * \text{recall}}{\text{precision} + \text{recall}} \quad (2)$$

### 3 Results and Discussion

Table 4 show the average *Accuracy* and *F-score* obtained for journey destination prediction respectively, by algorithm, group of travellers and day of the week (weekday vs weekend). The analysis of results shows several similarities and differences between the different groups of travellers analysed.

Regarding the comparison of the journey destination prediction between weekdays and weekends, the results shows small differences of performance for the individuals of Group 4. In this case the *Accuracy* and *F-score* for weekdays is around 2% higher than on weekends. Nevertheless, for the remaining groups (G1, G2 and G3), a clear difference is observed for these two periods. As example, while during weekdays for Group 1, the *Accuracy* is, on average, 77-79% (with exception of disruptive events in the city, namely on 2010-04-27, a STCP strike day, and on 2010-05-14, a pope visit to the city, which were removed), during the weekends the values fall down to 47-49%. The same trend is observed to *F-score* (an average value of 80-83% and 51-53% respectively). Therefore, high deviations are observed during the weekends, which suggest uncertainty in predicting for these days, associated with the lack of travelling routines for these groups (G1, G2 and G3). This discrepancy between weekdays and weekends dissipates, as mobility pattern characteristics are less strict. Simultaneously, as weekdays and weekends become indiscernible, so does the average prediction performance, with an average decrease which varies between 6 and 40%.

Regarding the algorithms applied, similar results were found between them. For this comparison, the first four weeks were disregarded to exclude the initial learning period. Thus, the last five weeks represent a more stable account of journey prediction. On average low differences of performance were found during the weekdays (*Accuracy*: G1=2%, G2=3%, G3=2%, and G4=4%; *F-score*: G1=2%, G2=3%, G3=3%, and G4=3%). During the weekends, these differences are generally higher (*Accuracy*: G1=7%, G2=4%, G3=4%, and G4=4%; *F-score*: G1=6%, G2=4%, G3=5%, and G4=4%).

**Table 4.** Accuracy and F-score (%) average (X) and standard deviation (SD), obtained to the prediction of the journey destination, by algorithm (J48, NB and Top-K), day (weekdays and weekends), and group of individual travellers (G1, G2, G3 and G4).

		J48		NB		Top-K	
		X±SD	min-max	X±SD	min-max	X±SD	min-max
Accuracy (%)	Weekday	G1 $78.3 \pm 5.6$	27.0 - 89.8	$77.2 \pm 6.0$	39.8 - 88.7	$79.6 \pm 6.0$	38.8 - 89.4
	Weekend	G2 $74.3 \pm 6.9$	21.0 - 85.7	$72.5 \pm 7.4$	28.7 - 83.7	$75.2 \pm 7.1$	25.5 - 85.0
	Weekday	G3 $63.5 \pm 5.2$	17.5 - 74.2	$63.1 \pm 5.5$	24.3 - 72.3	$62.9 \pm 5.7$	24.2 - 74.1
	Weekend	G4 $21.1 \pm 5.0$	6.9 - 29.4	$18.8 \pm 5.0$	8.4 - 27.0	$19.2 \pm 5.0$	4.9 - 29.0
	Weekday	G1 $49.7 \pm 21.9$	30.2 - 62.6	$47.3 \pm 21.6$	31.2 - 65.7	$47.8 \pm 22.4$	34.2 - 63.8
	Weekend	G2 $65.0 \pm 12.9$	30.3 - 82.6	$63.3 \pm 13.2$	40.2 - 76.7	$65.3 \pm 12.8$	40.2 - 83.4
	Weekday	G3 $56.9 \pm 15.1$	27.8 - 73.9	$59.0 \pm 14.9$	40.3 - 77.1	$58.5 \pm 15.6$	39.1 - 72.5
	Weekend	G4 $19.5 \pm 9.4$	9.0 - 26.8	$17.2 \pm 8.8$	10.8 - 25.9	$15.8 \pm 9.0$	5.8 - 24.0
F-score (%)	Weekday	G1 $81.8 \pm 5.2$	33.9 - 90.9	$80.8 \pm 5.3$	55.9 - 90.3	$83.3 \pm 5.3$	55.8 - 90.3
	Weekend	G2 $77.6 \pm 6.7$	28.2 - 87.7	$75.4 \pm 7.2$	43.6 - 86.0	$78.3 \pm 7.0$	38.8 - 88.1
	Weekday	G3 $66.3 \pm 5.5$	18.4 - 76.4	$65.9 \pm 5.7$	33.1 - 74.9	$66.0 \pm 5.9$	33.0 - 76.2
	Weekend	G4 $22.2 \pm 5.8$	7.7 - 31.2	$20.8 \pm 5.8$	10.6 - 27.5	$20.9 \pm 5.7$	7.3 - 30.9
	Weekday	G1 $52.9 \pm 22.1$	36.0 - 66.4	$51.5 \pm 21.9$	32.6 - 70.0	$52.4 \pm 22.4$	40.9 - 68.1
	Weekend	G2 $66.7 \pm 12.9$	37.2 - 81.5	$65.4 \pm 12.8$	50.6 - 76.6	$67.6 \pm 12.6$	50.9 - 81.7
	Weekday	G3 $58.4 \pm 14.7$	30.0 - 73.4	$60.7 \pm 14.5$	38.9 - 76.7	$60.2 \pm 15.0$	37.8 - 72.3
	Weekend	G4 $20.6 \pm 10.2$	8.8 - 30.3	$18.9 \pm 9.9$	10.5 - 27.1	$17.1 \pm 9.3$	5.5 - 26.2

Shadow area: >75% 75-50% <50%

Removed days: 2010-04-27, STCP strike day; 2010-05-14, visit of pope in the city.

A detailed analysis of *Accuracy* revealed that the three methods have different performance levels related to the spatiotemporal characteristics of the groups. For Group 1 while Top-K shows better performance in the first five weeks, the J48 method performs better for the last four weeks. The NB was better than the other two in only 17% of the days. In Group 2, the Top-K method performs better in 46% of the days, followed by the J48 with 41% and NB with 13%. In contrast to the previous two groups, in Group 3 the NB method performs better in the first three weeks of predictions and in 34% of the days overall, with the J48 method performing better in 46% and the Top-K in 20%. Interestingly, the first three weeks are very similar in terms of performance between the NB and Top-K, with J48 and NB in the remaining ones. Similarly, in Group 4 the NB method performs best in the first two weeks, down to 17% overall. Top-K performs better in only 7% of the days, and J48 in 76% of them.

With the exception of the last Group 4, both *Accuracy* and *F-score* measures show similar results. However, in Group 4, the *F-score* measure reveals that both NB and Top-K perform better in 20% of the days, and J48 in 60%. In addition, the F-score performance tends to show better performance for Top-K for Groups 2, 3 and 4 in detriment of J48. With the exception of the mentioned differences, the similarity between *Accuracy* and *F-score* measures indicates robustness in the results obtained.

Figure 3 shows the average *F-score* for one algorithm, Top-K. Whereas in the first 1-2 weeks of prediction, the F-score values increase steeply, and almost duplicate for Groups 1 and 2, after this period it increases very slowly until 5-6 weeks. The exception is Group 4, with a slow grow tendency for the entire period of 2 months.

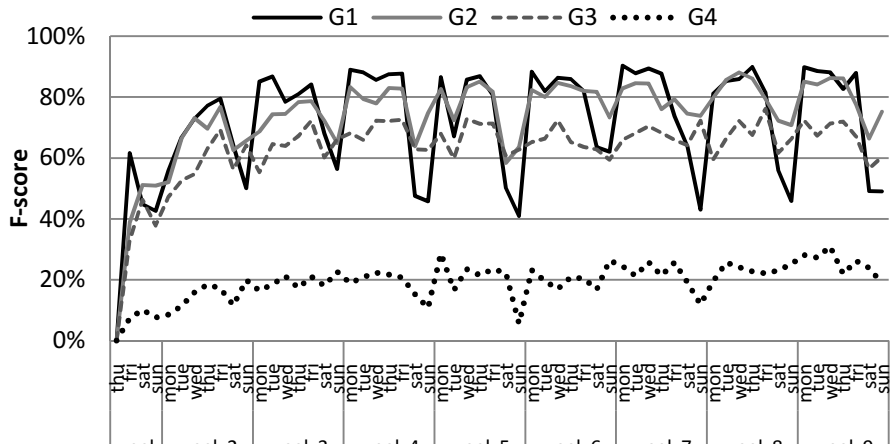


**Fig. 3.** F-score average for the prediction of the journey destination, by group of individual travellers obtained with the application of the Top-K algorithm.

## 4 Conclusions

In this work, an investigation into journey prediction was performed, based on past data and mobility patterns. Three different methods were used to predict journey destination for four different groups of travellers and spatiotemporal characteristics. The main findings obtained are described in the previous Section provide answers to the questions originally formulated as follows:

- The results show that it is indeed possible to predict journey destination in UPT based on past usage, with varying degrees of success depending on the mobility patterns. In addition, the accuracy of journey predictions tends to stabilize after two or more weeks of data (historical journeys), with considerable differences between the groups;
- After the initial two weeks of prediction, the average *Accuracy* and *F-score* has values around 70% for Groups 1 and 2, 60% for Group 3 and 20% for Group 4. The performance of journey predictions seems to be directly related to the mobility patterns, with stricter characteristics scoring higher prediction performance;
- Weekend's present low mean and high standard deviation values of *Accuracy* and *F-score* (between 6% and 40% lower than weekdays). This difference increases in groups with more frequent journeys. Group 1 and 2 have low *Accuracy* and *F-score* in the weekends but higher values in weekdays. The difference is negligible for Group 3 and non-existing in Group 4.

Even though the three methods present similar results overall, the analysis shows that certain scenarios allow them to perform differently. The performance differences are mainly related to the level of historic data, day of the week and travelling patterns. Thus, journey prediction is impacted by a number of factors that inform the design and implementation of TIS.

Future work will enable a comparison between used classifiers regarding processing time and memory efficiency. We did not approach these metrics in this work, due to space restrictions. Further research is also demanded on the characterization of groups of travellers, regarding further analysis to enable the discovery of additional groups of typical traveller's profile. We will hopefully be able to find and study these new profiles with a vaster dataset of users.

**Acknowledgements.** This work was performed under the project "Seamless Mobility" (FCOMP-01-0202-FEDER-038957), financed by European Regional Development Fund (ERDF), through the Operational Programme for Competitiveness Factors (POFC) in the National Strategic Reference Framework (NSRF), within the Incentive System for Technology Research and Development. The authors would also like to acknowledge the bus transport provider of Porto, STCP, which provided travel data for the project.

## References

1. Bagchi, M., White, P.R.: The potential of public transport smart card data. *Transport Policy* **12**(5), 464–474 (2005)
2. Bera, S., Rao, K.V.: Estimation of origin-destination matrix from traffic counts: the state of the art. *European Transport/Trasporti Europei*, ISTIEE, Institute for the Study of Transport within the European Economic Integration, vol. 49, pp. 2–23 (2011)
3. Caragliu, A., Bo, C.D., Nijkamp, P.: Smart Cities in Europe. *J. of Urban Technology* **18**(2), 65–82 (2011)
4. Costa, P.M., Fontes, T., Nunes, A.N., Ferreira, M.C., Costa, V., Dias, T.G., Falcão e Cunha, J.: Seamless Mobility: a disruptive solution for public urban transport. In: 22nd ITS World Congress, 5-9/10, Bordeaux (2015)
5. Dziekan, K., Kottenhoff, K.: Dynamic at-stop real-time information displays for public transport: effects on customers. *Transp. Research Part A* **41**(6), 489–501 (2007)
6. Foth, M., Schroeter, R., Ti, J.: Opportunities of public transport experience enhancements with mobile services and urban screens. *Int. J. of Ambient Computing and Intelligence (IJACI)* **5**(1), 1–18 (2013)
7. Giannopoulos, G.A.: The application of information and communication technologies in transport. *European J. of Operational Research* **152**(2), 302–320 (2004)
8. Gordon, J.B., Koutsopoulos, H.N., Wilson, N.H.M., Attanucci, J.P.: Automated Inference of Linked Transit Journeys in London Using Fare-Transaction and Vehicle Location Data. *Transp. Res. Record: J. of the Transportation Research Board* **2343**, 17–24 (2013)
9. He, H., Garcia, E.: Learning from imbalanced data. *IEEE Transactions on Knowledge and Data Engineering* **21**(9), 1263–1284 (2009)
10. INE (2013). <https://www.ine.pt/>. Instituto Nacional de Estatística I.P., Portugal
11. Kieu, L.M., Bhaskar, A., Chung, E.: Transit passenger segmentation using travel regularity mined from Smart Card transactions data. In: Transportation Research Board 93rd Annual Meeting. Washington, D.C., January 12–16, 2014
12. Krizek, J.J., El-Geneidy, A.: Segmenting preferences and habits of transit users and non-users. *Journal of Public Transportation* **10**(3), 71–94 (2007)
13. Kusakabe, T., Asakura, Y.: Behavioural data mining of transit smart card data: A data fusion approach. *Transp. Research Part C* **46**, 179–191 (2014)

14. Ma, X., Wu, Y.-J., Wang, Y., Chen, F., Liu, J.: Mining smart card data for transit riders' travel patterns. *Transp. Research Part C* **36**, 1–12 (2013)
15. Metwally, A., Agrawal, D.P., El Abbadi, A.: Efficient computation of frequent and top-k elements in data streams. In: Eiter, T., Libkin, L. (eds.) ICDT 2005. LNCS, vol. 3363, pp. 398–412. Springer, Heidelberg (2005)
16. Miklušák, T., Gregor, M., Janota, A.: Using neural networks for route and destination prediction in intelligent transport systems. In: Mikulski, J. (ed.) TST 2012. CCIS, vol. 329, pp. 380–387. Springer, Heidelberg (2012)
17. Nor Haizan, W., Mohamed, W., Salleh, M.N.M., Omar, A.H.: A Comparative Study of Reduced Error Pruning Method in Decision Tree Algorithms. In: International Conference on Control System, Computing and Engineering (IEEE). Penang, Malaysia, November 25, 2012
18. Nunes, A., Dias, T.G., Cunha, J.F.: Passenger Journey Destination Estimation from Automated Fare Collection System Data Using Spatial Validation. *IEEE Transactions on Intelligent Transportation Systems*. Forthcoming
19. Patil, T., Sherekar, S.: Performance Analysis of Naive Bayes and J48 Classification Algorithm for Data Classification. *Int. J. of Comp. Science and Applic.* **5**(2), 256–261 (2013)
20. Patterson, D.J., Liao, L., Gajos, K., Collier, M., Livic, N., Olson, K., Wang, S., Fox, D., Kautz, H.: Opportunity knocks: a system to provide cognitive assistance with transportation services. In: Mynatt, E.D., Siio, I. (eds.) UbiComp 2004. LNCS, vol. 3205, pp. 433–450. Springer, Heidelberg (2004)
21. Pelletier, M.P., Trépanier, M., Morency, C.: Smart card data use in public transit: A literature review. *Transp Research Part C* **19**(4), 557–568 (2011)
22. Sarmento, R., Cordeiro, M., Gama, J.: Streaming network sampling using top-k neworks. In: Proceedings of the 17th International Conference on Enterprise Information Systems (ICEIS 2015), p. to appear. INSTICC (2015)
23. Seaborn, C., Attanucci, J., Wilson, H.M.: Analyzing multimodal public transport journeys in London with smart card fare payment data. *Transp. Research Record: J. of the Transp. Research Board* **2121**(1) (2009)
24. TIP (2015). <http://www.linhandante.com/>. Transportes Intermodais do Porto
25. Utsunomiya, M., Attanucci, J., Wilson, N.H.: Potential Uses of Transit Smart Card Registration and Transaction Data to Improve Transit Planning. *Transp. Research Record: J. of the Transp. Research Board* 119–126 (2006)
26. Zito, P., Amato, G., Amoroso, S., Berrittella, M.: The effect of Advanced Traveller Information Systems on public transport demand and its uncertainty. *Transportmetrica* **7**(1), 31–43 (2011)

# Demand Modelling for Responsive Transport Systems Using Digital Footprints

Paulo Silva, Francisco Antunes<sup>(✉)</sup>, Rui Gomes, and Carlos Bento

Faculdade de Ciências e Tecnologia da Universidade de Coimbra Pólo II,  
Rua Sílvio Lima, 3030-790 Coimbra, Portugal  
[pacsilva@student.dei.uc.pt](mailto:pacsilva@student.dei.uc.pt), [{fnibau,ruig,bento}@dei.uc.pt](mailto:{fnibau,ruig,bento}@dei.uc.pt)

**Abstract.** Traditionally, travel demand modelling focused on long-term multiple socio-economic scenarios and land-use configurations to estimate the required transport supply. However, the limited number of transportation requests in demand-responsive flexible transport systems require a higher resolution zoning. This work analyses users short-term destination choice patterns, with a careful analysis of the available data coming from various different sources, such as GPS traces and social networks. We use a Multinomial Logit Model, with a social component for utility and characteristics, both derived from Social Network Analyses. The results from the model show meaningful relationships between distance and attractiveness for all the different alternatives, with the variable distance being the most significant.

**Keywords:** Innovative transport modes · Public transport operations · Transport demand and behaviour · Urban mobility and accessibility

## 1 Introduction

Transportation systems are a key factor for economic sustainability and social welfare, but providing quality public transportation may be extremely expensive when demand is low, variable and unpredictable, as it is on some periods of the day in urban areas. Demand Responsive Transportation (DRT) services try to address this problem with routes and frequencies that may vary according to the actual observed demand. However, in terms of financial sustainability and quality level, the design of this type of services may be complicated.

Anticipating demand by studying users short-term destination choice can improve the overall efficiency and sustainability of the transport services. Traditionally, demand modelling focused on long-term socio-economic scenarios and land-use to estimate the required level of supply. However, the limited number of transportation requests in DRT systems does not allow the application of traditional models. Also, DRTs require a higher resolution zoning, otherwise it can lead to unacceptable inaccuracies. Information coming from various sources should be used effectively in order to model demand for DRTs trips.

The approach followed in this work analyses users short-term destination choice patterns, with a careful analysis of the available data coming from various different sources, such as, GPS traces and social networks. The theory of

utility maximization, usually through discrete choice modelling, is often used to study individual decision-making. We use the Multinomial Logit Model (MNL) with a social component for utility and characteristics, both derived from Social Network Analyses (SNA), where a network is constructed linking the nodes (decision makers) that have social influence over one another (friendship), and the strength of that influence. To measure different ties strength, mutuality, propinquity, mutual friends and multiplexity factors were used.

We review the state of the art in the next section. The methodology is presented in Section 3 and the results in Section 4. The document ends with the conclusions and possible future lines of work.

## 2 State of the Art

Urban movements profiling has usually relied on traditional survey methods that are expensive and time consuming, giving planners only a picture of what has happened. In contrast, the wide deployment of pervasive computing devices (cell phone, GPS devices and digital cameras) provide unprecedented digital footprints, telling where and when people are. An emerging field of research uses mobile phones for “urban sensing” [1]. Moreover, the past few years have witnessed a huge increase in the adoption of social media and transportation researchers have also realized the potential of SNA for demand modelling [2].

A growing research topic is understanding how trips, trip modes and trip purposes can be derived from GPS data. For instance, [3] propose an approach to predict both the intended destination and route of a person by exploiting personal movement data collected by GPS. GPS data, however, have some limitations, such as (1) GPS signals are usually blocked indoor, (2) GPS devices may get interferences near tall buildings, and (3) continuously collecting GPS data may consume devices energy quickly.

Social networks and human interactions are crucial not only for understanding social activities, but also for travel patterns [2]. [4] connects travel with social networks, arguing that daily life revolves around family, colleagues, friends and shopping. [5] refers to the conformation to social norms, implying that decision-makers are more likely to choose a particular alternative if more peers have already chosen the same alternative. The emergence of geolocated social media seems a good opportunity to address SNA’s lack of geographic consideration. For instance, [6] presents a technique to analyse large-scale geo-location data from social media to infer individual activity patterns.

Previously, for travel demand modelling aggregate approaches were used, such as gravity or entropy models. These approaches were gradually replaced by disaggregated models [7]. In discrete choice modelling, the effect of social dimensions was first formalized for the binomial and the multinomial cases in [8] and [9], respectively. Generically, the agents’ utility is formed by both private and social components. The private component corresponds to the decision-makers characteristics. The social component represents the strength of social utility and the percentage of others in the neighbourhood selecting the same alternative in the choice set [10].

### 3 Methodology

#### 3.1 Data Gathering

We use GPS data traces provided by TU Delft from 80 individuals over the course of four days, and also data collect from social networks, namely Twitter, Instagram and Foursquare. The data obtained is cleared of personal values as to ensure privacy. To get the geo-located points of interest, we use the FourSquare API, extracting the 50 most popular venues, within a radius of 30 meters for each given point, resulting in a total of 37506 venues, in 489 categories, with their identification, geo-location and total number of check-ins made. The subscription zone for Instagram had a radius of 5 kilometers from the city center. For Twitter, we covered a bigger area in order to get Delft surroundings.

#### 3.2 Social Network Analysis

**Friendship.** To get the friendship, we have to use the user unique identification from the post, and request the users that the user followed and that follow him back. The only significant friendships considered are the ones between users that posted around Delft. The total number of friendships used is 35457. Discrete choice model also had to take into account the strength between users. To get and measure the ties strength, tie mutuality, propinquity, mutual friends and multiplexity factors are used.

**Detecting Important Locations.** To build the MNL we also need to know the user home and work location, since we are only interested in the user movement patterns before and after work hours. Home and work are the starting points for which the distance to the points of interest are measured. To get these locations, we use a clustering algorithm, namely *DBScan* [11].

#### 3.3 Data Preparation

In the data set with the posts and associated venues, i.e., the choice set (CS), there is a large amount of data with no use for us, as it does not provide useful information (for instance, useless categories) or represent work or residential places, for which the demand patterns are well established and can be met by traditional transportation services. The data containing those specific categories was erased from the choice set. Since the number of alternatives is quite big, we grouped those venues in 6 main categories: Appointment (17%), Food (17%), Bar (5%), Shop (24%), Entertainment (27%) and Travel (10%).

If we used these categories as our number of different alternatives for the MNL model, we would only get results concerning each of those 6 alternatives, which are quite generic. However, we want to use the model to predict probabilities of destination choices with a higher resolution, so we generated data for all the venues and then use those categories only to filter unnecessary data.

### 3.4 Multinomial Logit Model

Our data corresponds to the observed choices of individuals - revealed preferences data. For each dataset we have the number of alternatives selected in each hour, which is our finite set of alternatives for each individual. The number of alternatives and observations vary significantly along the hours. The variables used for the data-frame are:

- distance : the venue distance to the user central point,
- check-ins : the total number of check-ins in each alternative for each user,
- friendship : the sum of the individual friendship for each alternative,
- choice : the alternative selection.

Since we cannot directly extract user personal information (e.g. age, gender), our data does not contain individual specific variables, and so the alternative specific variables have a generic coefficient, i.e., we consider that the number of check-ins, distance and friendship have the same value for all alternatives. Choice takes values of yes and no, if the alternative was chosen or not by the user. To estimate the MNL we have used the R statistics system with the mlogit package. The following formula was used for our work,

$$\text{Mlogit}(\text{choice} \sim \text{distance} + \text{friendship} + \text{attractiveness}, \text{CS})$$

where choice is the variable that indicates the choice made for each individual among the alternatives and the distance, friendship and attractiveness being the alternative specific variables with generic coefficients from the choice set CS.

## 4 Results

We present the results and estimation parameter for one choice set, namely the one representing the choices made at hour 21, which has 24 alternatives and 91 observations.

The model predictions are reasonable good when tested against the user observed choices. Table 1 presents the average probabilities returned by the model against the observed frequency. The results from the MNL model show meaningful relationships between distance and attractiveness for all the different alternatives, being distance the most significant variable, i.e., longer distances almost always reduce the attractiveness of a destination, all else being equal.

The same can be said for the attractiveness variable, but the friendship variable does not have the same impact to the individual when choosing an alternative. Table 2 illustrates these findings. To show the usefulness of the analyses made, we feed the probabilities predicted by our model to a DRT simulator developed in [12]. Figure 1 shows that most origins and destinations found for the time period and travel objective considered lie outside the service area of the different public transport modes (dotted lines) and DRT could satisfy this demand (solid lines).

**Table 1.** Average probabilities returned by the model

Venue	Freq.	Avg. Prob.
Stadion Feijenoord	0.032967	0.04490835
EkoPlaza	0.065934	0.03791752
Station Den Haag HS	0.054945	0.05494505
La Mer	0.032967	0.03303908
Diner Company	0.032967	0.03777430
LantarenVenster	0.032967	0.04320755
Station Rotterdam Centraal	0.153846	0.12336128
BIRD	0.043956	0.03794951
Maassilo	0.043956	0.03530117
Emma	0.021978	0.02478593
Station Den Haag Centraal	0.054945	0.05070866
Lucent Danstheater	0.032967	0.02519137
Zaal 3	0.032967	0.03212339
De Banier	0.054945	0.09073518
RandstadRail jalavalaan	0.032967	0.02411359
Kot Treinpersoneel	0.032967	0.02666024
Spuimarkt	0.032967	0.02543518
Doerak	0.032967	0.04017886
Paard van Troje	0.032967	0.03294463
Ahoy Rotterdam	0.043956	0.03654922
Restaurant Meram	0.043956	0.03907711
Live Tv Show	0.021978	0.04634078
Stadskwekerij den haag	0.010989	0.03433138
Oudedijk 166 A2	0.032967	0.04312563

**Table 2.** Relationships between variables

Variables	Estimate	Std.error	t-value	p-value
distance	-0.107414	0.022597	-4.7534	2.000e-06
friendship	0.094441	0.081570	1.1578	0.2469
attractiveness	0.342170	0.061907	5.5272	3.254e-08

**Fig. 1.** Simulation results

## 5 Conclusions

Traditionally, travel demand modelling focused on long-term socio-economic scenarios and land-use to estimate the required transport supply. However, the limited number of transportation requests in demand-responsive flexible transport systems require a higher resolution zoning. We analysed users short-term destination choice patterns, with a careful analysis of the available data coming from GPS traces and social networks. We defined a Multinomial Logit Model (MNL), with a social component for utility and characteristics, both derived from Social

Network Analyses. The low frequency of posts with identified locations for each user made it difficult to generate a clear pattern for each user. Nevertheless, the results from the model show meaningful relationships between distance and attractiveness for all the different alternatives, with the variable distance being the most significant.

Since the analyses of the social network done in this work does not produce individual characteristics, like age, gender and socio-economic, it would be interesting for future work to include data mining algorithms to extract some of those values from tweets, and add features specific to each venue, to better understand the motivation behind the choice made.

## References

1. Cuff, D., Hansen, M., Kang, J.: Urban sensing: Out of the woods. *Communications of the ACM* **51**(3), 24–33 (2008)
2. Carrasco, J., Hogan, B., Wellman, B., Miller, E.: Collecting social network data to study social activity-travel behaviour: an egocentric approach. *Environment and Planning B: Planning and Design* **35**, 961–980 (2008)
3. Chen, L., Mingqi, L., Chen, G.: A system for destination and future route prediction based on trajectory mining. *Pervasive and Mobile Computing* **6**(6), 657–676 (2010)
4. Axhausen, K.: Social networks, mobility biographies, and travel: survey challenges. *Environment and Planning B: Planning and Design* **35**, 981–996 (2008)
5. Paáez, A., Scott, D.: Social influence on travel behavior: a simulation example of the decision to telecommute. *Environment and Planning A* **39**(3), 647–665 (2007)
6. Hasan, S., Ukkusuri, S.: Urban activity pattern classification using topic models from online geo-location data. *Transportation Research Part C: Emerging Technologies* **44**, 363–381 (2014)
7. Ben-Akiva, M., Lerman, S.: *Discrete Choice Analysis: Theory and Application to Travel Demand* (1985)
8. Brock, W., Durlauf, S.: Discrete Choice with Social Interactions. *Review of Economic Studies* **68**(2), 235–260 (2001)
9. Brock, W., Durlauf, S.: A multinomial choice model with neighborhood effects. *American Economic Review* **92**, 298–303 (2002)
10. Zanni, A.M., Ryley, T.J.: Exploring the possibility of combining discrete choice modelling and social networks analysis: an application to the analysis of weather-related uncertainty in long-distance travel behaviour. In: International Choice Modelling Conference, Leeds, pp. 1–22 (2011)
11. Ester, M., Kriegel, H., Sander, J., Xu, X.: A density-based algorithm for discovering clusters in large spatial databases with noise. In: Proceedings of 2nd International Conference on Knowledge Discovery and Data Mining, pp. 226–231. AAAI Press (1996)
12. Gomes, R., Sousa, J.P., Galvao, T.: An integrated approach for the design of Demand Responsive Transportation services. In: de Sousa, J.F., Rossi, R. (eds.) *Computer-based Modelling and Optimization in Transportation*. AISC, vol. 232, pp. 223–235. Springer, Heidelberg (2014)

# **Artificial Life and Evolutionary Algorithms**

# A Case Study on the Scalability of Online Evolution of Robotic Controllers

Fernando Silva<sup>1,2,4</sup>(✉), Luís Correia<sup>4</sup>, and Anders Lyhne Christensen<sup>1,2,3</sup>

<sup>1</sup> BioMachines Lab, Lisboa, Portugal

[fsilva@di.fc.ul.pt](mailto:fsilva@di.fc.ul.pt), [anders.christensen@iscte.pt](mailto:anders.christensen@iscte.pt)

<sup>2</sup> Instituto de Telecomunicações, Lisboa, Portugal

<sup>3</sup> Instituto Universitário de Lisboa (ISCTE-IUL), Lisboa, Portugal

<sup>4</sup> BioISI, Faculdade de Ciências, Universidade de Lisboa, Lisboa, Portugal

[luis.correia@ciencias.ulisboa.pt](mailto:luis.correia@ciencias.ulisboa.pt)

**Abstract.** Online evolution of controllers on real robots typically requires a prohibitively long evolution time. One potential solution is to distribute the evolutionary algorithm across a group of robots and evolve controllers in parallel. No systematic study on the scalability properties and dynamics of such algorithms with respect to the group size has, however, been conducted to date. In this paper, we present a case study on the scalability of online evolution. The algorithm used is odNEAT, which evolves artificial neural network controllers. We assess the scalability properties of odNEAT in four tasks with varying numbers of simulated e-puck-like robots. We show how online evolution algorithms can enable groups of different size to leverage their multiplicity, and how larger groups can: (i) achieve superior task performance, and (ii) enable a significant reduction in the evolution time and in the number of evaluations required to evolve controllers that solve the task.

**Keywords:** Evolutionary robotics · Artificial neural network · Evolutionary algorithm · Online evolution · Robot control · Scalability

## 1 Introduction

Evolutionary computation has been widely studied and applied to synthesise controllers for autonomous robots in the field of evolutionary robotics (ER). In *online* ER approaches, an evolutionary algorithm (EA) is executed onboard robots during task execution to continuously optimise behavioural control. The main components of the EA (evaluation, selection, and reproduction) are performed by the robots without any external supervision. Online evolution thus enables addressing tasks that require online learning or online adaptation. For instance, robots can evolve new controllers and modify their behaviour to respond to unforeseen circumstances, such as changes in the task or in the environment.

Research in online evolution started out with a study by Floreano and蒙达 [1], who conducted experiments on a real mobile robot. The authors successfully evolved navigation and obstacle avoidance behaviours for a Khepera robot. The study was a significant breakthrough as it demonstrated the potential of online evolution of controllers. Researchers then focused on how to mitigate the issues posed by evolving controllers directly on real robots, especially the prohibitively long time required [2]. Watson *et al.* [3] introduced an approach called *embodied evolution* in which an online EA is distributed across a group of robots. The main motivation behind the use of multirobot systems was to leverage the potential speed-up of evolution due to robots that evolve controllers in parallel and that exchange candidate solutions to the task.

Over the past decade, numerous approaches to online evolution in multirobot systems have been developed. Examples include Bianco and Nolfi's open-ended approach for self-assembling robots [4], mEDEA by Bredeche *et al.* [5], and odNEAT by Silva *et al.* [6]. When the online EA is decentralised and distributed across a group of robots, one common assumption is that online evolution inherently scales with the number of robots [3]. Generally, the idea is that the more robots are available, the more evaluations can be performed in parallel, and the faster the evolutionary process [3]. The dynamics of the online EA itself, and common issues that arise in EAs from population sizing such as convergence rates and diversity [7] have, however, not been considered. Furthermore, besides ad-hoc experiments with large groups of robots, see [5] for examples, there has been no systematic study on the scalability properties of online EAs across different tasks. Given the strikingly long time that online evolution requires to synthesise solutions to any but the simplest of tasks, the approach remains infeasible on real robots [8].

In this paper, we study the scalability properties of online evolution of robotic controllers. The online EA used in this case study is odNEAT [9], which optimises artificial neural network (ANN) controllers. One of the main advantages of odNEAT is that it evolves both the weights and the topology of ANNs, thereby bypassing the inherent limitations of fixed-topology algorithms [9]. odNEAT is used here as a representative efficient algorithm that has been successfully used in a number of simulation-based studies related to adaptation and learning in robot systems, see [6, 8–11] for examples. We assess the scalability properties and performance of odNEAT in four tasks involving groups of up to 25 simulated e-puck-like robots [12]: (i) an aggregation task, (ii) a dynamic phototaxis task, and (iii, iv) two foraging tasks with differing complexity. Overall, our study shows how online EAs can enable groups of different size to leverage their multiplicity for higher performance, and for faster evolution in terms of evolution time and number of evaluations required to evolve effective controllers.

## 2 Online Evolution with odNEAT

This section provides an overview of odNEAT; for a comprehensive introduction see [9]. odNEAT is an efficient online neuroevolution algorithm designed

for multirobot systems. The algorithm starts with minimal networks with no hidden neurons, and with each input neuron connected to every output neuron. Throughout evolution, topologies are gradually complexified by adding new neurons and new connections through mutation. In this way, odNEAT is able find an appropriate degree of complexity for the current task, and a suitable ANN topology is the result of a continuous evolutionary process [9].

odNEAT is distributed across multiple robots that exchange candidate solutions to the task. The online evolutionary process is implemented according to a physically distributed island model. Each robot optimises an internal population of genomes (directly encoded ANNs) through intra-island variation, and genetic information between two or more robots is exchanged through inter-island migration. In this way, each robot is potentially self-sufficient and the evolutionary process opportunistically capitalises on the exchange of genetic information between multiple robots for collective problem solving [9].

During task execution, each robot is controlled by an ANN that represents a candidate solution to a given task. Controllers maintain a virtual energy level reflecting their individual performance. The fitness value is defined as the mean energy level. When the virtual energy level of a robot reaches a minimum threshold, the current controller is considered unfit for the task. A new controller is then created via selection of two parents from the internal population, crossover of the parents' genomes, and mutation of the offspring. Mutation is both structural and parametric, as it adds new neurons and new connections, and optimises parameters such as connection weights and neuron bias values.

odNEAT has been successfully used in a number of simulation-based studies related to long-term self-adaptation in robot systems. Previous studies have shown: (i) that odNEAT effectively evolves controllers for robots that operate in dynamic environments with changing task parameters [11], (ii) that the controllers evolved are robust and can often adapt to changes in environmental conditions without further evolution [9], (iii) that robots executing odNEAT can display a high degree of fault tolerance as they are able to adapt and learn new behaviours in the presence of faults in the sensors [9], (iv) how to extend the algorithm to incorporate learning processes [11], and (v) how to evolve behavioural building blocks prespecified by the human experimenter [8, 10]. Given previous results, odNEAT is therefore used in our study as a representative online EA. The key research question of our study is if and how online EAs can enable robots to leverage their multiplicity. That is, besides performance and robustness criteria, we are interested in studying scalability with respect to the group size, an important aspect when large groups of robots are considered.

### 3 Methods

In this section, we define our experimental methodology, including the simulation platform and robot model, and we describe the four tasks used in the study: aggregation, phototaxis, and two foraging tasks with differing complexity.

### 3.1 Experimental Setup

We use JBotEvolver [13] to conduct our simulation-based experiments. JBotEvolver is an open-source, multirobot simulation platform and neuroevolution framework. In our experiments, the simulated robots are modelled after the e-puck [12], a 7.5 cm in diameter, differential drive robot capable of moving at speeds up to 13 cm/s. Each robot is equipped with infrared sensors that multiplex obstacle sensing and communication between robots at a range of up to 25 cm.<sup>1</sup> The sensor and actuator configurations for the tasks are listed in Table 1. Each sensor and each actuator are subject to noise, which is simulated by adding a random Gaussian component within  $\pm 5\%$  of the sensor saturation value or of the current actuation value.

The robot controllers are discrete-time ANNs with connection weights in the range [-10,10]. odNEAT starts with simple networks with no hidden neurons, and with each input neuron connected to every output neuron. The ANN inputs are the readings from the sensors, normalised to the interval [0,1]. The output layer has two neurons whose values are linearly scaled from [0,1] to [-1,1] to set the signed speed of each wheel. In the two foraging tasks, a third output neuron sets the state of a gripper. The gripper is activated if the output value of the neuron is higher than 0.5, otherwise it is deactivated. If the gripper is activated, the robot collects the closest resource within a range of 2 cm, if there is any. Depending on the foraging task (see below), the robot may need to actively select which type of resources to collect and to avoid other types.

**Aggregation Task.** In an aggregation task, dispersed robots must move close to one another to form a single cluster. Aggregation combines several aspects of multirobot tasks, including distributed individual search, coordinated movement, and cooperation. Furthermore, aggregation plays an important role in robotics because it is a precursor of other collective behaviours such as group transport of heavy objects [14]. In our aggregation task, robots are evaluated based on criteria that include the presence of robots nearby, and the ability to explore the arena and move fast, see [9] for details. The initial virtual energy level  $E$  of each controller is set to 1000 and limited to the range [0, 2000] units. At each control cycle, the update of the virtual energy level,  $E$ , is given by:

$$\frac{\Delta E}{\Delta t} = \alpha(t) + \gamma(t) \quad (1)$$

where  $t$  is the current control cycle,  $\alpha(t)$  is a reward proportional to the number  $n$  of different genomes received in the last  $P = 10$  control cycles. Because robots executing odNEAT exchange candidate solutions, the number of different

---

<sup>1</sup> The original e-puck infrared range is 2-3 cm [12]. In real e-pucks, the *liblrcm* library, see <http://www.e-puck.org>, extends the range up to 25 cm and multiplexes infrared communication with proximity sensing.

**Table 1.** Controller details. Light sensors have a range of 50 cm (phototaxis task). Other sensors have a range of 25 cm.

<i>Aggregation task – controller details</i>	
<b>Input neurons:</b>	18
	8 for IR robot detection
	8 for IR wall detection
	1 for energy level reading
	1 for reading the number of different genomes received
<b>Output neurons:</b>	2 Left and right motor speeds
<i>Phototaxis task – controller details</i>	
<b>Input neurons:</b>	25
	8 for IR robot detection
	8 for IR wall detection
	8 for light source detection
	1 for energy level reading
<b>Output neurons:</b>	2 Left and right motor speeds
<i>Foraging tasks – controller details</i>	
<b>Input neurons:</b>	25
	4 for IR robot detection
	4 for IR wall detection
	1 for energy level reading
	8 for resource A detection
	8 for resource B detection
<b>Output neurons:</b>	3
	2 for left and right motor speeds
	1 for controlling the gripper

genomes received is used to estimate the number of robots nearby.  $\gamma(t)$  is a factor related to the quality of movement computed as:

$$\gamma(t) = \begin{cases} -1 & \text{if } v_l(t) \cdot v_r(t) < 0 \\ \Omega_s(t) \cdot \omega_s(t) & \text{otherwise} \end{cases} \quad (2)$$

where  $v_l(t)$  and  $v_r(t)$  are the left and right wheel speeds,  $\Omega_s(t)$  is the ratio between the average and maximum speed, and  $\omega_s(t) = \sqrt{v_l(t) \cdot v_r(t)}$  rewards controllers that move fast and straight at each control cycle.

**Phototaxis Task.** In a phototaxis task, robots have to search and move towards a light source. Following [9], we use a dynamic version of the phototaxis task in which the light source is periodically moved to a new random location. As a result, robots have to continuously search for and reach the light source, which eliminates controllers that find the light source by chance. The virtual energy

level  $E \in [0, 100]$  units, and controllers are assigned an initial value of 50 units. At each control cycle,  $E$  is updated as follows:

$$\frac{\Delta E}{\Delta t} = \begin{cases} S_r & \text{if } S_r > 0.5 \\ 0 & \text{if } 0 < S_r \leq 0.5 \\ -0.01 & \text{if } S_r = 0 \end{cases} \quad (3)$$

where  $S_r$  is the maximum value of the readings from light sensors, between 0 (no light) and 1 (brightest light). Light sensors have a range of 50 cm and robots are therefore only rewarded if they are close to the light source. Remaining sensors have a range of 25 cm.

**Foraging Tasks.** In a foraging task, robots have to search for and pick up objects scattered in the environment. Foraging is a canonical testbed in cooperative robotics domains, and is evocative of tasks such as toxic waste clean-up, harvesting, and search and rescue [15].

We setup a foraging task with different types of resources that have to be collected. Robots spend virtual energy at a constant rate and must learn to find and collect resources. When a resource is collected by a robot, a new resource of the same type is placed randomly in the environment so as to keep the number of resource constant throughout the experiments. We experiment with two variants of a foraging task: (i) one in which there are only type A resources, henceforth called *standard foraging task*, and (ii) one in which there are both type A and type B resources, henceforth called *concurrent foraging task*. In the concurrent foraging task, resources A and B have to be consumed sequentially. That is, besides learning the foraging aspects of the task, robots also have to learn to collect resources in the correct order. The energy level of each controller is initially set to 100 units, and limited to the range [0,1000]. At each control cycle,  $E$  is updated as follows:

$$\frac{\Delta E}{\Delta t} = \begin{cases} reward & \text{if right type of resource is collected} \\ penalty & \text{if wrong type of resource is collected} \\ -0.02 & \text{if no resource is consumed} \end{cases} \quad (4)$$

where  $reward = 10$  and  $penalty = -10$ . The constant decrement of 0.02 means that each controller will execute for a period of 500 seconds if no resource is collected since it started operating. Note that the *penalty* component applies only to the concurrent foraging task. To enable a meaningful comparison of performance when groups of different size are considered, the number of resources of each type is set to the number of robots multiplied by 10.

### 3.2 Experimental Parameters and Treatments

We analyse the impact of the group size on the performance of odNEAT by conducting experiments with groups of 5, 10, 15, 20, and 25 robots. For each

experimental configuration, we conduct 30 independent evolutionary runs. Each run lasts 100 hours of simulated time. odNEAT parameters are set as in previous studies [9], including a population size of 40 genomes per robot and a control cycle frequency of 100 ms. Robots operate in a square arena surrounded by walls. In the aggregation and phototaxis tasks, the area of the arena is increased proportionally to the number of robots (5 robots: 9 m<sup>2</sup>, 10 robots: 18 m<sup>2</sup>, ..., 25 robots: 45 m<sup>2</sup>). Notice that if we maintained the same size of the environment, comparisons would not be meaningful. For instance, in the aggregation task, with the increasing density of robots in the environment, the task becomes easier to solve simply because robots encounter each other more frequently. In the phototaxis task, the number of light sources in the environment is also increased proportionally to the number of robots.

## 4 Experimental Results and Discussion

In this section, we present our experimental results. We analyse: (i) the task performance of controllers in terms of their individual fitness score, (ii) the number of evaluations, that is, the number of controllers tested by each robot before a solution to the task is found, and (iii) the corresponding evolution time. We use the two-tailed Mann-Whitney U test to compute statistical significance of differences between results because it is a non-parametric test, and therefore no strong assumptions need to be made about the underlying distributions.

### 4.1 Quality of the Solutions and Population-Mixing

We first compare the individual fitness scores of the final controllers. In the aggregation task and in the phototaxis tasks, groups of 5 robots are typically

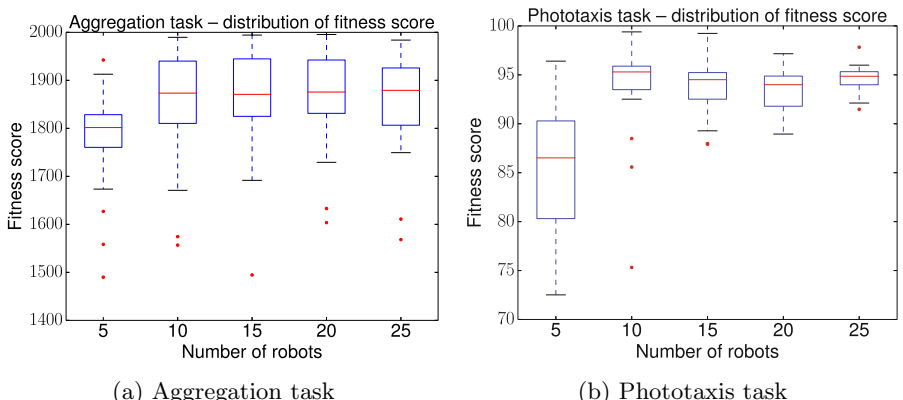


**Fig. 1.** Distribution of the fitness score of the final controllers in: (a) aggregation task, and (b) phototaxis task.

**Table 2.** Summary of the individual fitness score of final solutions in the two foraging tasks.

Task	Robots	Mean	Std. dev.	Minimum	Maximum
Standard foraging	5	96.03	45.62	41.88	268.02
	10	105.31	62.31	29.57	396.47
	15	107.98	119.79	33.64	981.34
	20	112.06	109.29	36.69	968.27
	25	136.37	158.39	39.03	994.47
Concurrent foraging	5	104.02	73.11	32.62	459.83
	10	112.02	115.61	39.67	949.35
	15	144.54	153.29	38.85	975.81
	20	165.39	165.82	38.77	971.42
	25	179.29	196.58	38.08	978.56

outperformed by larger groups ( $\rho < 0.001$ , see Fig. 1). In the phototaxis task, groups of 25 robots also perform significantly better than groups with 20 robots ( $\rho < 0.01$ ). Specifically, results suggest that a minimum of 10 robots are necessary for high-performing controllers to be evolved in a consistent manner.

A summary of the results obtained in the two foraging tasks is shown in Table 2. Given the dynamic nature of task, especially as the number of robots increases, the fitness score of the final controllers displays a high variance. The results, however, further show that larger groups typically yield better performance both in terms of the mean and of the maximum fitness scores, and is an indication that decentralised online approaches such as odNEAT can indeed capitalise on larger groups to evolve more effective solutions to the current task.

To quantify to what extent is a robot dependent on the candidate solutions it receives from other robots, we analyse the origin of the information stored in the population of each robot. In the phototaxis task, when capable solutions have been evolved approximately 86.85% (5 robots) to 93.95% (25 robots) of genomes maintained in each internal population originated from other robots, whereas the remaining genomes stored were produced by the robots themselves (analysis of the results obtained in the other tasks revealed a similar trend). The final solutions executed by each robot to solve the task have on average from 87.26% to 89.10% matching genes. Moreover, 39.73% (5 robots) to 47.70% (25 robots) of these solutions have more than 90% of their genes in common. The average weight difference between matching connection genes varies from 2.48 to 4.37, with each weight in [-10, 10], which indicates that solutions were refined by the EA on the receiving robot. Local exchange of candidate controllers therefore appears to be a crucial part in the evolutionary dynamics of decentralised online EAs because it serves as a substrate for collective problem solving. In the following section, we analyse how the exchange of such information enables online EAs to capitalise on increasingly larger groups of robots for faster evolution of solutions to the task.

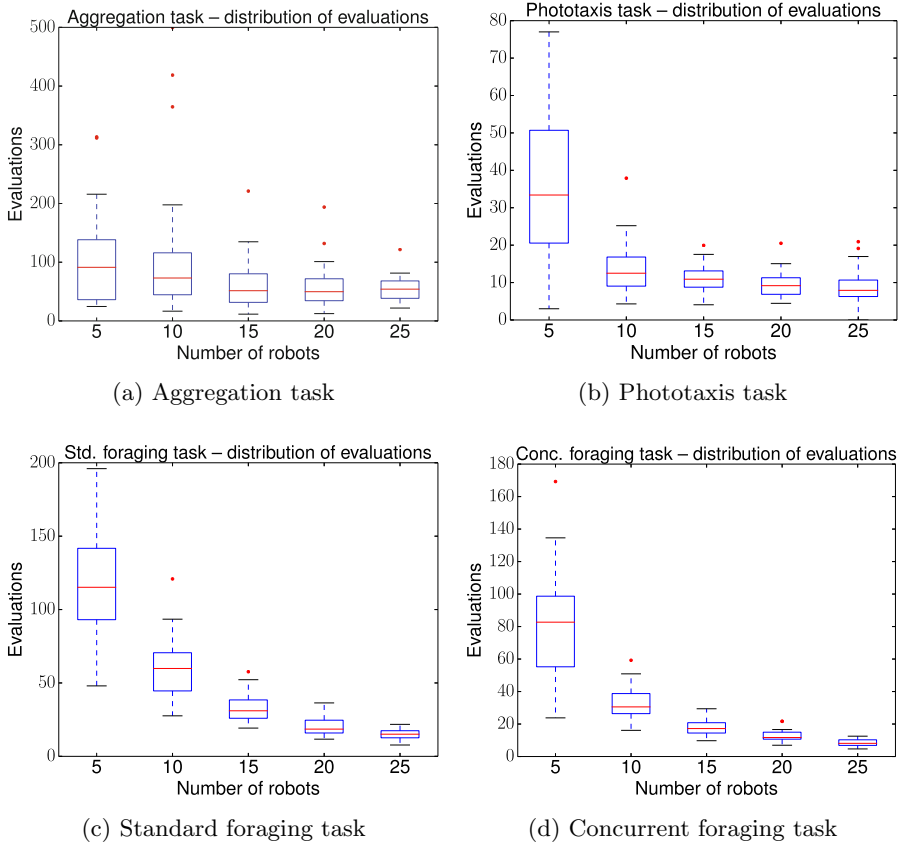


**Fig. 2.** Distribution of evaluations in: (a) aggregation task, (b) phototaxis task, (c) standard foraging task, and (d) concurrent foraging task.

## 4.2 Evaluations and Time Analysis

The distribution of evaluations with respect to the group size is shown in Fig. 2. In the aggregation task, the number of evaluations required to evolve solutions to the task decreases as the group size is increased, and becomes significantly lower when the group size is increased from 10 to 15 robots ( $\rho < 0.001$ ). On average, the number of evaluations decreases from 104 for groups of 5 robots to 55 for groups of 25 robots. The mean evolution time is of 6.22 hours for groups of 5 robots, 2.34 hours for 10 robots, 1.80 hours for 15 robots, 1.48 hours for 20 robots, and 1.12 hours for 25 robots. Hence, adding more robots also enables a significant reduction of the evolution time ( $\rho < 0.01$  for every group increment). With the increase in the size of the environment, there is a larger area to search for other robots and to explore. Task conditions become more challenging because, in relative terms, each robot senses a smaller portion of the environment. Robots are, however, still able to evolve successful controllers in fewer evaluations and less evolution time.

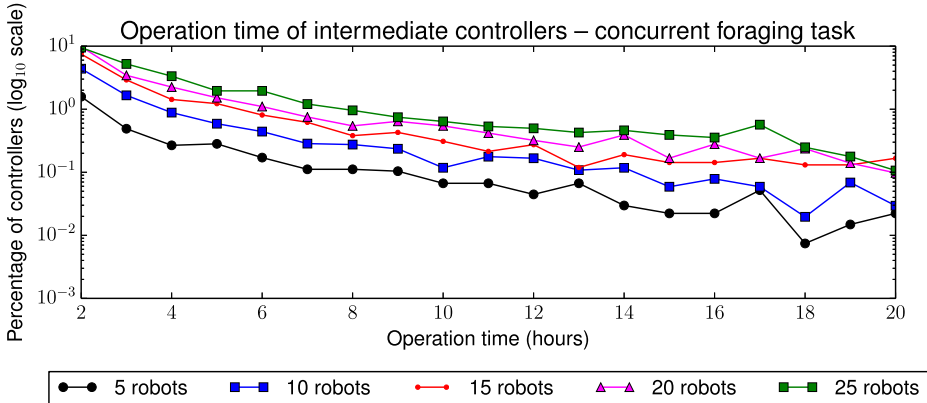


**Fig. 3.** Operation time of intermediate controllers in the concurrent foraging task. 67% to 96% of intermediate controllers operate for few minutes before they fail (not shown for better plot readability).

The speed up of evolution with the increase of group size also occurs in the phototaxis task. The number of evaluations is significantly reduced ( $\rho < 0.001$ ) with the increase of the group size from 5 to 10 robots (mean number of evaluations of 39 and 14, respectively). The mean evolution time is of 39.16 hours for groups of 5 robots, 9.51 hours for 10 robots, 7.20 hours for 15 robots, 6.30 hours for 20 robots, and 5.27 hours for 25 robots. Similarly to the number of evaluations, the evolution time yields on average a 4-fold-decrease when the group is enlarged from 5 to 10 robots ( $\rho < 0.001$ ). Larger groups enable further improvements ( $\rho < 0.001$  for increases up to 20 robots,  $\rho < 0.01$  when group size is changed from 20 to 25 robots), but at comparatively smaller rates. Chiefly, the results of the aggregation task and of the phototaxis task show quantitatively distinct speed-ups of evolution when groups are enlarged.

With respect to the two foraging tasks, the distribution of the number of evaluations shown in Fig. 2 is inversely proportional, with a gentle slope, to the number of robots in the group. For both tasks, differences in the number of evaluations are significant across all comparisons ( $\rho < 0.001$ ). In effect, the number of evaluations is reduced on average: (i) from 115 evaluations (5 robots) to 15 evaluations (25 robots) in the standard foraging task, which corresponds to a 7.67-fold decrease in terms of evaluations, and (ii) from 82 evaluations (5 robots) to 8 evaluations in the concurrent foraging task, which amounts to a 10.25-fold decrease. These results show that decentralised online evolution can scale well in terms of evaluations, even when task complexity is increased.

Regarding the evolution time, results show a similar trend for both foraging tasks. On average, the evolution time varies from approximately 35 and 36 hours for groups of 5 robots to 21 and 23 hours for groups of 25 robots. That is, despite significant improvements in terms of the number of evaluations, the evolution time required to evolve the final controllers to the task is still prohibitively long. This result is due to the controller evaluation policy. Online evolution approaches

typically employ a policy in which robots substitute controllers at regular time intervals, see [5] for an example. This approach has been shown to lead to incongruous group behaviour and to poor performance in collective tasks that explicitly require continuous collective coordination and cooperation [9]. odNEAT, on the other hand, adopts a different approach by allowing a controller to remain active as long as it is able to solve the task. A new controller is thus only synthesised if the current one fails. As shown in Fig. 3 for the concurrent foraging task, the evaluation policy results in intermediate controllers that operate for a significant amount of time (the standard foraging task displays a similar trend). While 67% to 96% of intermediate controllers only operate for a few minutes (data not shown for better plot readability), there are a few intermediate controllers that operate up to 20 hours of consecutive time before they fail. Although such controllers yield high fitness scores comparable to those of the final solutions, typically 1% to 4% less, they delay the synthesis of more effective solutions.

## 5 Concluding Discussion and Future Work

In this paper, we presented a case study on the scalability properties and performance of online evolutionary algorithms. We used odNEAT, a decentralised online evolution algorithm in which robots optimise controllers in parallel and exchange candidate solutions to the task. We conducted experiments with groups of up to 25 e-puck-like-robots [12] in four tasks: (i) aggregation, (ii) dynamic phototaxis, and (iii, iv) two foraging tasks with differing complexity.

We showed that larger groups of robots typically enable: (i) superior task performance in terms of the fitness score, and (ii) significant improvements both in terms of the number of evaluations required to evolve solutions to the task and of the corresponding evolution time. There are, however, specific conditions in which intermediate controllers are able to operate up to 20 hours of consecutive time. These controllers yield high performance levels as their fitness score is typically 1% to 4% less than the fitness score of the final solutions. In addition, while additional robots may further speed up evolution, there are specific group sizes after which speed-ups are comparatively smaller. One key research question regarding scalability is therefore how to best leverage *all* robots so that they can learn appropriate behaviours, constitute differentiated groups, and perform cooperative or competitive actions reflecting the structure of the task.

The immediate follow-up work includes studying novel evaluation policies for online evolution of robotic controllers. Regarding odNEAT, the algorithm typically enables a significant reduction in the number of evaluations as the group increases. Hence, if intermediate controllers that operate for long periods of time can be detected and discarded via, for instance, established methods such as early stopping algorithms or racing techniques, there is the potential to enable timely and efficient online evolution in real robots.

**Acknowledgments.** This work was partly supported by FCT under grants UID/EEA/50008/2013, SFRH/BD/89573/2012, UID/Multi/04046/2013, and EXPL/EEI-AUT/0329/2013.

## References

1. Floreano, D., Mondada, F.: Automatic creation of an autonomous agent: Genetic evolution of a neural-network driven robot. In: 3rd International Conference on Simulation of Adaptive Behavior, pp. 421–430. MIT Press, Cambridge (1994)
2. Matarić, M., Cliff, D.: Challenges in evolving controllers for physical robots. *Robotics and Autonomous Systems* **19**(1), 67–83 (1996)
3. Watson, R.A., Ficici, S.G., Pollack, J.B.: Embodied evolution: Distributing an evolutionary algorithm in a population of robots. *Robotics and Autonomous Systems* **39**(1), 1–18 (2002)
4. Bianco, R., Nolfi, S.: Toward open-ended evolutionary robotics: evolving elementary robotic units able to self-assemble and self-reproduce. *Connection Science* **16**(4), 227–248 (2004)
5. Bredeche, N., Montanier, J., Liu, W., Winfield, A.: Environment-driven distributed evolutionary adaptation in a population of autonomous robotic agents. *Mathematical and Computer Modelling of Dynamical Systems* **18**(1), 101–129 (2012)
6. Silva, F., Urbano, P., Oliveira, S., Christensen, A.L.: odNEAT: An algorithm for distributed online, onboard evolution of robot behaviours. In: 13th International Conference on the Simulation and Synthesis of Living Systems, pp. 251–258. MIT Press, Cambridge (2012)
7. De Jong, K.A.: Evolutionary computation: a unified approach. MIT Press, Cambridge (2006)
8. Silva, F., Duarte, M., Oliveira, S.M., Correia, L., Christensen, A.L.: The case for engineering the evolution of robot controllers. In: 14th International Conference on the Synthesis and Simulation of Living Systems, pp. 703–710. MIT Press, Cambridge (2014)
9. Silva, F., Urbano, P., Correia, L., Christensen, A.L.: odNEAT: An algorithm for decentralised online evolution of robotic controllers. *Evolutionary Computation* (2015) (in press). [http://www.mitpressjournals.org/doi/pdf/10.1162/EVCO\\_a.00141](http://www.mitpressjournals.org/doi/pdf/10.1162/EVCO_a.00141)
10. Silva, F., Correia, L., Christensen, A.L.: Speeding Up online evolution of robotic controllers with macro-neurons. In: Esparcia-Alcázar, A.I., Mora, A.M. (eds.) *EvoApplications 2014*. LNCS, vol. 8602, pp. 765–776. Springer, Heidelberg (2014)
11. Silva, F., Urbano, P., Christensen, A.L.: Online evolution of adaptive robot behaviour. *International Journal of Natural Computing Research* **4**(2), 59–77 (2014)
12. Mondada, F., Bonani, M., Raemy, X., Pugh, J., Cianci, C., Klaptocz, A., Magnenat, S., Zufferey, J., Floreano, D., Martinoli, A.: The e-puck, a robot designed for education in engineering. In: 9th Conference on Autonomous Robot Systems and Competitions, pp. 59–65. IPCB, Castelo Branco (2009)
13. Duarte, M., Silva, F., Rodrigues, T., Oliveira, S.M., Christensen, A.L.: JBot-Evolver: A versatile simulation platform for evolutionary robotics. In: 14th International Conference on the Synthesis and Simulation of Living Systems, pp. 210–211. MIT Press, Cambridge (2014)
14. Groß, R., Dorigo, M.: Towards group transport by swarms of robots. *International Journal of Bio-Inspired Computation* **1**(1–2), 1–13 (2009)
15. Cao, Y., Fukunaga, A., Kahng, A.: Cooperative mobile robotics: Antecedents and directions. *Autonomous Robots* **4**(1), 1–23 (1997)

# Spatial Complexity Measure for Characterising Cellular Automata Generated 2D Patterns

Mohammad Ali Javaheri Javid<sup>(✉)</sup>, Tim Blackwell, Robert Zimmer,  
and Mohammad Majid Al-Rifaie

Department of Computing Goldsmiths, University of London,  
London SE14 6NW, UK  
[{m.javaheri,t.blackwell,r.zimmer,m.majid}@gold.ac.uk](mailto:{m.javaheri,t.blackwell,r.zimmer,m.majid}@gold.ac.uk)

**Abstract.** Cellular automata (CA) are known for their capacity to generate complex patterns through the local interaction of rules. Often the generated patterns, especially with multi-state two-dimensional CA, can exhibit interesting emergent behaviour. This paper addresses quantitative evaluation of spatial characteristics of CA generated patterns. It is suggested that the structural characteristics of two-dimensional (2D) CA patterns can be measured using mean information gain. This information-theoretic quantity, also known as conditional entropy, takes into account conditional and joint probabilities of cell states in a 2D plane. The effectiveness of the measure is shown in a series of experiments for multi-state 2D patterns generated by CA. The results of the experiments show that the measure is capable of distinguishing the structural characteristics including symmetry and randomness of 2D CA patterns.

**Keywords:** Cellular automata · Spatial complexity · 2D patterns

## 1 Introduction

Cellular automata (CA) are one of the early bio-inspired systems invented by von Neumann and Ulam in the late 1940s to study the logic of self-reproduction in a material-independent framework. CA are known to exhibit complex behaviour from the iterative application of simple rules. The popularity of the Game of Life drew the attention of a wider community of researchers to the unexplored potential of CA applications and especially in their capacity to generate complex behaviour. The formation of complex patterns from simple rules sometimes with high aesthetic qualities has been contributed to the creation of many digital art works since the 1960s. The most notable works are “*Pixillation*”, one of the early computer generated animations [11], the digital art works of Struycken [10], Brown [3] and evolutionary architecture of Frazer [5]. Furthermore, CA have been used for music composition, for example, Xenakis [17] and Miranda [9].

Although classical one-dimensional CA with binary states can exhibit complex behaviours, experiments with multi-state two-dimensional (2D) CA reveal a very rich spectrum of symmetric and asymmetric patterns [6, 7].

There are numerous studies on the quantitative [8] and qualitative behaviour [14–16] of CA but they are mostly concerned with categorising the rule space and the computational properties of CA. In this paper, we investigate information gain as a spatial complexity measure of multi-state 2D CA patterns. Although the Shannon entropy is commonly used to measure complexity, it fails to discriminate accurately structurally different patterns in two-dimensions. The main aim of this paper is to demonstrate the effectiveness of information gain as a measure of 2D structural complexity.

This paper is organised as follows. Section 2 provides formal definitions and establishes notation. Section 3 demonstrates that Shannon entropy is an inadequate measure of 2D cellular patterns. In the framework of the objectives of this study a spatial complexity spectrum is formulated and the potential of information gain as a structural complexity measure is discussed. Section 4 gives details of experiments that test the effectiveness of information gain. The paper closes with a discussion and summary of findings.

## 2 Cellular Automata

This section serves to specify the cellular automata considered in this paper, and to define notation.

A cellular automaton  $\mathcal{A}$  is specified by a quadruple  $\langle L, S, N, f \rangle$  where:

- $L$  is a finite square lattice of cells  $(i, j)$ .
- $S = \{1, 2, \dots, k\}$  is set of states. Each cell  $(i, j)$  in  $L$  has a state  $s \in S$ .
- $\mathcal{N}$  is neighbourhood, as specified by a set of lattice vectors  $\{e_a\}$ ,  $a = 1, 2, \dots, N$ . The neighbourhood of cell  $r = (i, j)$  is  $\{r + e_1, r + e_2, \dots, r + e_N\}$ . A cell is considered to be in its own neighbourhood so that one of  $\{e_a\}$  is the zero vector  $(0, 0)$ . With an economy of notation, the cells in the neighbourhood of  $(i, j)$  can be numbered from 1 to  $N$ ; the neighbourhood states of  $(i, j)$  can therefore be denoted  $(s_1, s_2, \dots, s_N)$ . Two common neighbourhoods are the five-cell von Neumann neighbourhood  $\{(0, 0), (\pm 1, 0), (0, \pm 1)\}$  and the nine-cell Moore neighbourhood  $\{(0, 0), (\pm 1, 0), (0, \pm 1), (\pm 1, \pm 1)\}$ . Periodic boundary conditions are applied at the edges of the lattice so that complete neighbourhoods exist for every cell in  $L$ .
- $f$  is the update rule.  $f$  computes the state  $s_1(t+1)$  of a given cell from the states  $(s_1, s_2, \dots, s_N)$  of cells in its neighbourhood:  $s_1(t+1) = f(s_1, s_2, \dots, s_N)$ . A quiescent state  $s_q$  satisfies  $f(s_q, s_q, \dots, s_q) = s_q$ .

The collection of states for all cells in  $L$  is known as a configuration  $c$ . The global rule  $F$  maps the whole automaton forward in time; it is the synchronous application of  $f$  to each cell. The behaviour of a particular  $\mathcal{A}$  is the sequence  $c^0, c^1, c^2, \dots, c^{t-1}$ , where  $c^0$  is the initial configuration (IC) at  $t = 0$ .

CA behaviour is sensitive to the IC and to  $L, S, N$  and  $f$ . The behaviour is generally nonlinear and sometimes very complex; no single mathematical analysis can describe, or even estimate, the behaviour of an arbitrary automaton. The vast size of the rule space, and the fact that this rule space is unstructured,

mean that knowledge of the behaviour of a particular cellular automaton, or even of a set of automata, gives no insight into the behaviour of any other CA. In the lack of any practical model to predict the behaviour of a CA, the only feasible method is to run simulations. Fig. 1 illustrates some experimental configurations generated by the authors to demonstrate the capabilities of CA in exhibiting complex behaviour with visually pleasing qualities.

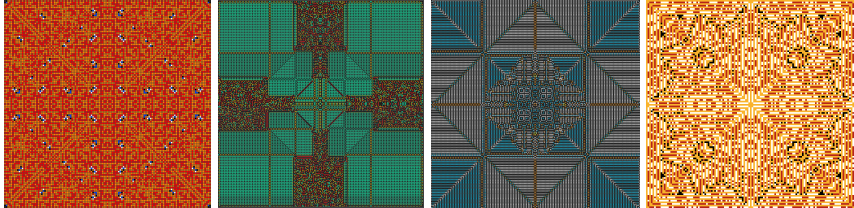


**Fig. 1.** Samples of multi-state 2D CA patterns

### 3 Spatial Complexity Measure of 2D Patterns

The introduction of information theory by Shannon provided a mathematical model to measure the order and complexity of systems. Shannon's information theory was an attempt to address communication over an unreliable channel [12]. Entropy is the core of this theory [4]. Let  $\mathcal{X}$  be discrete alphabet,  $X$  a discrete random variable,  $x \in \mathcal{X}$  a particular value of  $X$  and  $P(x)$  the probability of  $x$ . Then the entropy,  $H(X)$ , is:

$$H(X) = - \sum_{x \in \mathcal{X}} P(x) \log_2 P(x) \quad (1)$$

The quantity  $H$  is the average uncertainty in bits,  $\log_2(\frac{1}{p})$  associated with  $X$ . Entropy can also be interpreted as the average amount of information needed to describe  $X$ . The value of entropy is always non-negative and reaches its maximum for the uniform distribution,  $\log_2(|\mathcal{X}|)$ :

$$0 \leq H \leq \log_2(|\mathcal{X}|) \quad (2)$$

The lower bound of relation (2) corresponds to a deterministic variable (no uncertainty) and the upper bound corresponds to a maximum uncertainty associated with a random variable. Another interpretation of entropy is as a measure of *order* and *complexity*. A low entropy implies low uncertainty so the message is highly predictable, ordered and less complex. And high entropy implies a high uncertainty, less predictability, highly disordered and complex. Despite the dominance of Shannon entropy as a measure of complexity, it fails to reflect on structural characteristics of 2D patterns. The main reason for this drawback is that it only reflects on the distribution of the symbols, and not on their ordering. This is illustrated in Fig. 2 where, following [1], the entropy of 2D patterns

with various structural characteristics is evaluated. Fig. 2a-b are patterns with ordered structures and Fig. 2c is a pattern with repeated three element structure over the plane. Fig. 2d is a fairly structureless pattern.

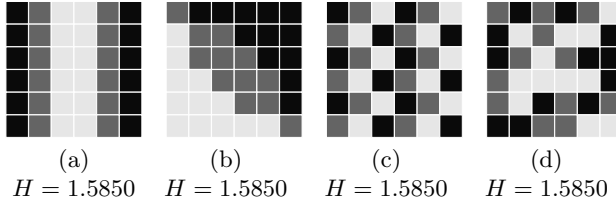


**Fig. 2.** Measure of  $H$  for structurally different patterns with uniform distribution of elements

Fig. 2 clearly demonstrates the failure of entropy to discriminate structurally different 2D patterns. In other words, entropy is invariant to spatial rearrangement of composing elements. This is in contrast to our intuitive perception of the complexity of patterns and is problematic for the purpose of measuring the complexity of multi-state 2D CA behaviour.

Taking into account our intuitive perception of complexity and structural characteristics of 2D patterns, a complexity measure must be bounded by two extreme points of complete order and disorder. It is reasonable to assume that *regular structures*, *irregular structures* and *structureless* patterns lie along between these extremes, as illustrated in Fig. 3.

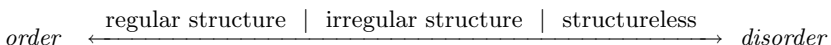


**Fig. 3.** The spectrum of spatial complexity.

A complete regular structure is a pattern of high symmetry, an irregular structure is a pattern with some sort of structure but not as regular as a fully symmetrical pattern and finally a structureless pattern is a random arrangement of elements.

A measure introduced in [1, 2, 13] and known as information gain, has been suggested as a means of characterising the complexity of dynamical systems and of images. It measures the amount of information gained in bits when specifying the value,  $x$ , of a random variable  $X$  given knowledge of the value,  $y$ , of another random variable  $Y$ ,

$$G_{x,y} = -\log_2 P(x|y). \quad (3)$$

$P(x|y)$  is the conditional probability of a state  $x$  conditioned on the state  $y$ . Then the *mean information gain*,  $\bar{G}_{X,Y}$ , is the average amount of information

gain from the description of the all possible states of  $Y$ :

$$\overline{G}_{X,Y} = \sum_{x,y} P(x,y) G_{x,y} = - \sum_{x,y} P(x,y) \log_2 P(x|y) \quad (4)$$

where  $P(x,y)$  is the joint probability,  $\text{prob}(X = x, Y = y)$ .  $\overline{G}$  is also known as the conditional entropy,  $H(X|Y)$  [4]. Conditional entropy is the reduction in uncertainty of the joint distribution of  $X$  and  $Y$  given knowledge of  $Y$ ,  $H(X|Y) = H(X, Y) - H(Y)$ . The lower and upper bounds of  $\overline{G}_{X,Y}$  are

$$0 \leq \overline{G}_{X,Y} \leq \log_2 |\mathcal{X}|. \quad (5)$$

where  $y \in \mathcal{Y}$ .

In principle,  $\overline{G}$  can be calculated for a 2D pattern by considering the distribution of cell states over pairs of cells  $r, s$ ,

$$\overline{G}_{r,s} = - \sum_{s_r, s_s} P(s_r, s_s) \log_2 P(s_r, s_s) \quad (6)$$

where  $s_r, s_s$  are the states at  $r$  and  $s$ . Since  $|\mathcal{S}| = N$ ,  $\overline{G}_{r,s}$  is a value in  $[0, N]$ .

In particular, horizontal and vertical near neighbour pairs provide four MIGs,  $\overline{G}_{(i,j),(i+1,j)}$ ,  $\overline{G}_{(i,j),(i-1,j)}$ ,  $\overline{G}_{(i,j),(i,j+1)}$  and  $\overline{G}_{(i,j),(i,j-1)}$ . In the interests of notational economy, we write  $\overline{G}_s$  in place of  $\overline{G}_{r,s}$ , and omit parentheses, so that, for example,  $G_{i+1,j} \equiv G_{(i,j),(i+1,j)}$ . The relative positions for non-edge cells are given by matrix  $M$ :

$$M = \begin{bmatrix} & & (i,j+1) \\ & (i-1,j) & (i,j) & (i+1,j) \\ & & (i,j-1) \end{bmatrix}. \quad (7)$$

Correlations between cells on opposing lattice edges are not considered. Fig. 4 provides an example. The depicted pattern is composed of four different symbols  $S = \{\text{light-grey}, \text{grey}, \text{white}, \text{black}\}$ . The *light-grey* cell correlates with two neighbouring *white* cells ( $i + 1, j$ ) and ( $i, j - 1$ ). On the other hand, The *grey* cell has four neighbouring cells of which three are *white* and one is *black*. The result of this edge condition is that  $G_{i+1,j}$  is not necessarily equal to  $\overline{G}_{i-1,j}$ . Differences between the horizontal (vertical) mean information rates reveal left/right (up/down) orientation.



**Fig. 4.** A sample 2D pattern

The mean information gains of the sample patterns in Fig. 2 are presented in Fig. 5. The merits of  $\overline{G}$  in discriminating structurally different patterns ranging from the structured and symmetrical (Fig. 5a-b), to the partially structured

(Fig. 5c) and the structureless and random (Fig. 5d), are clearly evident. The cells in the columns of pattern (a) are completely correlated. However knowledge of cell state does not provide complete predictability in the horizontal direction and, as a consequence, the horizontal  $\bar{G}$  is finite. Pattern (b) has non-zero, and identical  $\bar{G}$ 's indicating a symmetry between horizontal and vertical directions, and a lack of complete predictability. Analysis of pattern (c) is similar to (a) except the roles of horizontal and vertical directions are interchanged. The four  $\bar{G}$ s in the final pattern are all different, indicating a lack of vertical and horizontal symmetry; the higher values show the increased randomness. Details of calculations for a sample pattern are provided in the appendix.

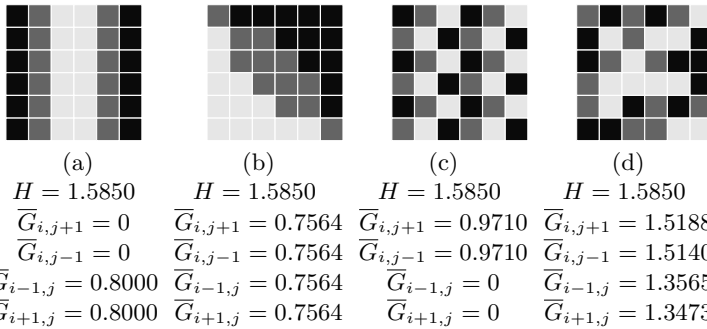


**Fig. 5.** The comparison of  $H$  with measures of  $\bar{G}_{i,j}$  for structurally different patterns.

## 4 Experiments and Results

A set of experiments was designed to examine the effectiveness of  $\bar{G}$  in discriminating the particular patterns that are generated by a multi-state 2D cellular automaton. The (outer-totalistic) CA is specified in Table 1. The chosen experimental rule maps three states, represented by *green*, *red* and *white*; the quiescent state is *white*.

**Table 1.** Specifications of experimental cellular automaton

$$L = 129 \times 129 \text{ (16641 cells).}$$

$$S = \{0, 1, 2\} \equiv \{\text{white, red, green}\}$$

$\mathcal{N}$ : von Neumann neighbourhood

$$f : S^9 \mapsto S$$

$$f(s_{i,j})(t) = s_{i,j}(t+1) = \begin{cases} 1 & \text{if } s_{(i,j)}(t) = 1, 2 \text{ and } \sigma = 0 - 2 \\ 2 & \text{if } s_{(i,j)}(t) = 2, 3 \text{ and } \sigma = 1 \\ 2 & \text{if } s_{(i,j)}(t) = 2 \quad \text{and } \sigma = 2 \\ 0 & \text{otherwise} \end{cases}$$

where  $\sigma$  is the sum total of the neighbourhood states.

The experiments are conducted with two different ICs: (1) all white cells except for a single *red* cell and (2) a random configuration with 50% *white* quiescent states (8320 cells), 25% *red* and 25% *green*. The experimental rule has been iterated synchronously for 150 successive time steps. Fig. 6 and Fig. 7 illustrate the space-time diagrams for a sample of time steps starting from single and random ICs.

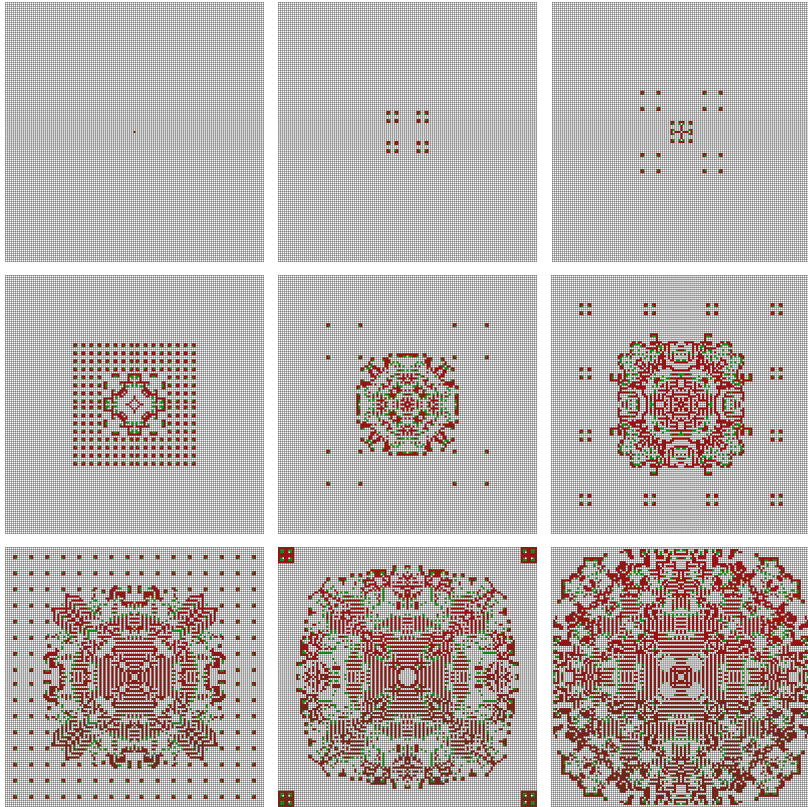


**Fig. 6.** Space-time diagram of the experimental cellular automaton for sample time steps starting from the single cell IC.

The behaviour of cellular automaton from the single cell IC is a sequence of symmetrical patterns (Fig. 6). The directional measurements of  $\bar{G}_{i,j}$  for the single cell IC start with  $\bar{G}_{i,j+1} = \bar{G}_{i,j-1} = \bar{G}_{i-1,j} = \bar{G}_{i+1,j} = 0.00094$  and  $H = 0.00093$ , and they attain  $\bar{G}_{i,j+1} = \bar{G}_{i,j-1} = \bar{G}_{i-1,j} = \bar{G}_{i+1,j} = 1.13110$  and  $H = 1.13714$  (and Figs 8, 11) at the end of the runs.

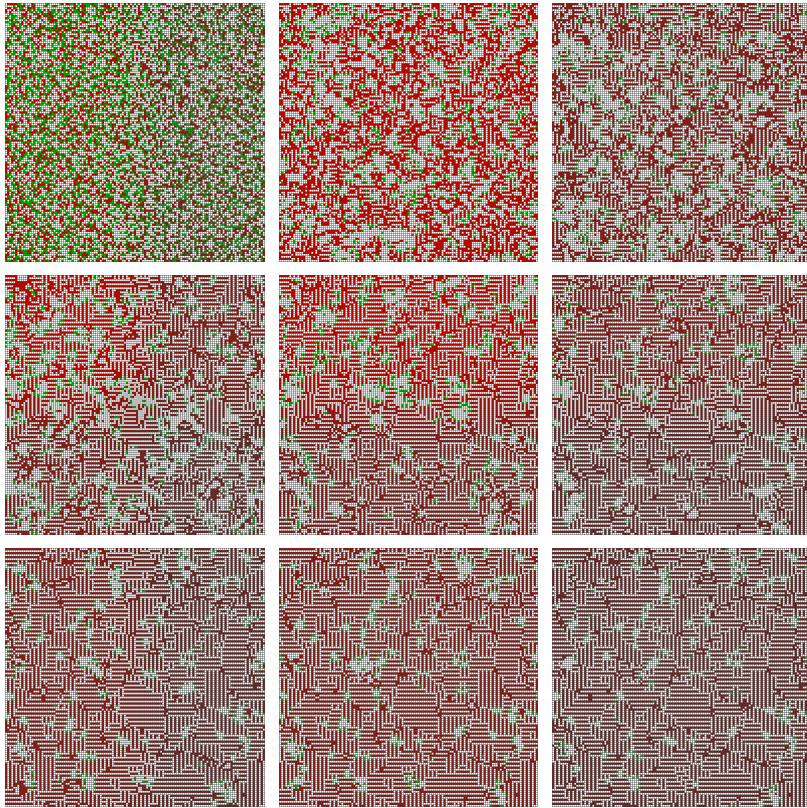


**Fig. 7.** Space-time diagram of the experimental cellular automaton for sample time steps starting from the random IC.

The sequence of states can be analysed by considering the differences between the up/down and left/right mean information gains, as defined by

$$\Delta \bar{G}_{i,j\pm 1} = |\bar{G}_{i,j+1} - \bar{G}_{i,j-1}| \quad (8)$$

$$\Delta \bar{G}_{i\pm 1,j} = |\bar{G}_{i+1,j} - \bar{G}_{i-1,j}|. \quad (9)$$

For the single cell IC,  $\Delta \bar{G}_{i,j\pm 1}$  and  $\Delta \bar{G}_{i\pm 1,j}$  are constant for the 150 time steps ( $\Delta \bar{G}_{i,j\pm 1} = \Delta \bar{G}_{i\pm 1,j} = 0$ ). This indicates the development of the symmetrical patterns along the up/down and left/right directions.

The behaviour of cellular automaton from the random IC is a sequence of irregular structures (Fig. 7). The formation of patterns with local structures has reduced the values of  $\bar{G}_{i,j}$  until a stable oscillating pattern is attained (Figs 7, 9). This is an indicator of the development of irregular structures. However the patterns are not random patterns since  $\bar{G}_{i,j} \approx 1.1$  is less than the maximum three-state value  $\log_2(3) = 1.5850$  (see Eq. 5). Mean information rate differences

$\Delta\bar{G}_{i,j\pm 1}$  and  $\Delta\bar{G}_{i\pm 1,j}$  for both ICs are plotted in Fig. 10. The structured but asymmetrical patterns emerging from the random start are clearly distinguished from the symmetrical patterns of the single cell IC.

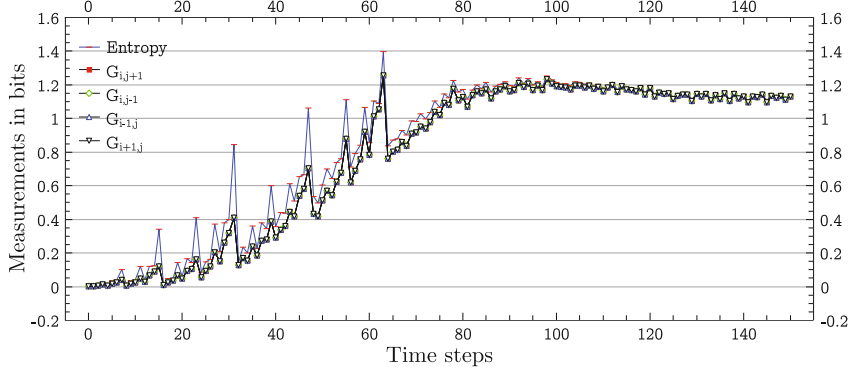


**Fig. 8.** Measurements of  $H$ ,  $\bar{G}_{i,j+1}$ ,  $\bar{G}_{i,j-1}$ ,  $\bar{G}_{i+1,j}$ ,  $\bar{G}_{i-1,j}$  for 150 time steps starting from the single cell IC.

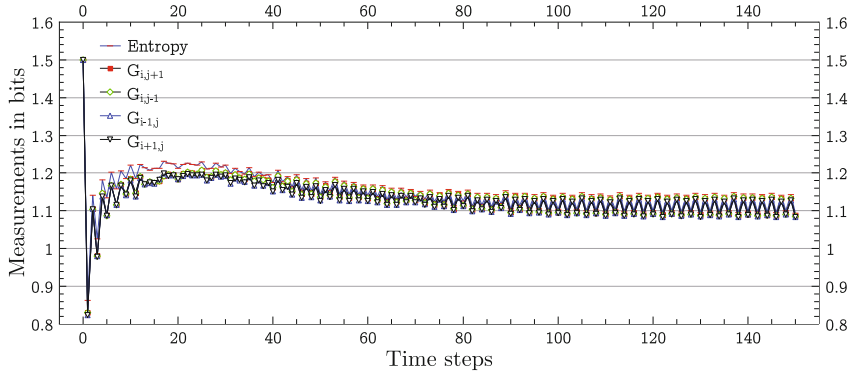


**Fig. 9.** Measurements of  $H$ ,  $\bar{G}_{i,j+1}$ ,  $\bar{G}_{i,j-1}$ ,  $\bar{G}_{i+1,j}$ ,  $\bar{G}_{i-1,j}$  for 150 time steps starting from the random IC.

These experiments demonstrate that a cellular automaton rule seeded with different ICs leads to the formation of patterns with structurally different characteristics. The gradient of the mean information rate along lattice axes is able to detect the structural characteristics of patterns generated by this particular multi-state 2D CA. From the comparison of  $H$  with  $\Delta\bar{G}_{i,j\pm 1}$  and  $\Delta\bar{G}_{i\pm 1,j}$  in the set of experiments, it is clear that entropy fails to discriminate between the diversity of patterns that can be generated by various CA.

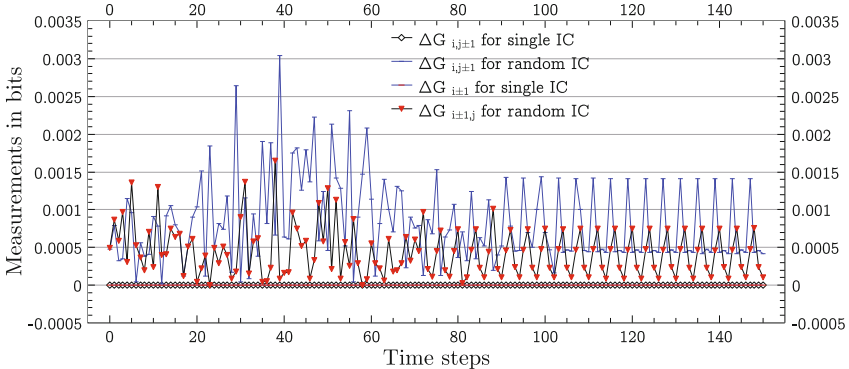


**Fig. 10.** Plots of  $\Delta\bar{G}_{i,j\pm 1}$  and  $\Delta\bar{G}_{i\pm 1,j}$  for two different ICs

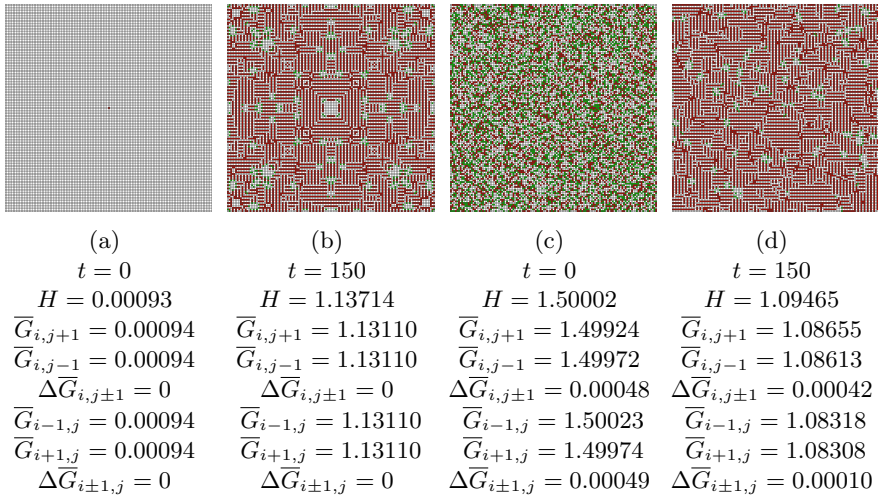


**Fig. 11.** Comparison of the cellular automaton's  $H$  with four directional measure of  $\bar{G}_{i,j}$ ,  $\Delta\bar{G}_{i,j\pm 1}$  and  $\Delta\bar{G}_{i\pm 1,j}$  starting from single (a, b) and random ICs (c, d).

## 5 Conclusion

Cellular automata (CA) are one of the early bio-inspired models of self-replicating systems and, in 2D, are powerful tools for the pattern generation. Indeed, multi-state 2D CA can generate many interesting and complex patterns with various structural characteristics. This paper considers an information-theoretic classification of these patterns.

Entropy, which is a statistical measure of the distribution of cell states, is not in general able to distinguish these patterns. However mean information gain, as proposed in [1, 2, 13], takes into account conditional and joint probabilities

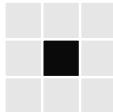
between pairs of cells and, since it is based on correlations between cells, holds promise for pattern classification.

This paper reports on a pair of experiments for two different initial conditions of an outer-totalistic CA. The potential of mean information gain for distinguishing multi-state 2D CA patterns is demonstrated. Indeed, the measure appears to be particular good at distinguishing symmetry from non-random non-asymmetric patterns.

Since CA are one of the generative tools in computer art, means of evaluating the aesthetic qualities of CA generated patterns could have a substantial contribution towards further automation of CA art. This is the subject of on-going research.

## Appendix

In this example the pattern is composed of two different cells  $S = \{\text{white}, \text{black}\}$  where the set of permutations with repetition is  $\{ww, wb, bb, bw\}$ . Considering the mean information gain (Eq. 4) and given the positional matrix  $M$  (Eq. 7), the calculations can be performed as follows:



*white – white*

$$P(w, s_{(i,j+1)}) = \frac{5}{6}$$

$$P(w|w_{(i,j+1)}) = \frac{4}{5}$$

$$P(w, w_{(i,j+1)}) = \frac{5}{6} \times \frac{4}{5} = \frac{2}{3}$$

$$G(w, w_{(i,j+1)}) = \frac{2}{3} \log_2 P(\frac{1}{5})$$

$$G(w, w_{(i,j+1)}) = 0.2146 \text{ bits}$$

*white – black*

$$P(w, s_{(i,j+1)}) = \frac{5}{6}$$

$$P(w|b_{(i,j+1)}) = \frac{1}{5}$$

$$P(w, b_{(i,j+1)}) = \frac{5}{6} \times \frac{1}{5} = \frac{1}{6}$$

$$\overline{G}(w, b_{(i,j+1)}) = \frac{1}{6} \log_2 P(\frac{1}{5})$$

$$\overline{G}(w, b_{(i,j+1)}) = 0.3869 \text{ bits}$$

$$\overline{G} = G(w, w_{(i,j+1)}) + G(w, b_{(i,j+1)}) + G(b, b_{(i,j+1)}) + G(b, w_{(i,j+1)})$$

$$\overline{G} = 0.6016 \text{ bits}$$

*black – black*

$$P(b, s_{(i,j+1)}) = \frac{1}{6}$$

$$P(b|b_{(i,j+1)}) = \frac{1}{1}$$

$$P(b, b_{(i,j+1)}) = \frac{1}{6} \times \frac{1}{1} = \frac{1}{6}$$

$$G(b, b_{(i,j+1)}) = \frac{1}{6} \log_2 P(1)$$

$$G(b, b_{(i,j+1)}) = 0 \text{ bits}$$

*black – white*

$$P(b, s_{(i,j+1)}) = \frac{1}{6}$$

$$P(b|w_{(i,j+1)}) = \frac{0}{1}$$

$$P(b, w_{(i,j+1)}) = \frac{1}{6} \times 0$$

$$G(b, w_{(i,j+1)}) = 0 \text{ bits}$$

In *white – white* case  $G$  measures the uniformity and spatial property where  $P(w, s_{(i,j+1)})$  is the joint probability that a cell is white and it has a neighbouring cell at its  $(i, j + 1)$  position,  $P(w|w_{(i,j+1)})$  is the conditional probability of a cell is white given that it has white neighbouring cell at its  $(i, j + 1)$  position,  $P(w, w_{(i,j+1)})$  is the joint probability that a cell is white and it has neighbouring cell at its  $(i, j + 1)$  position,  $G(w, w_{(i,j+1)})$  is information gain in *bits* from specifying a white cell where it has a white neighbouring cell at its  $(i, j + 1)$  position. The same calculations are performed for the rest of cases; *black-black*, *white-black* and *black-white*.

## References

1. Andrienko, Y.A., Brilliantov, N.V., Kurths, J.: Complexity of two-dimensional patterns. *Eur. Phys. J. B* **15**(3), 539–546 (2000)
2. Bates, J.E., Shepard, H.K.: Measuring complexity using information fluctuation. *Physics Letters A* **172**(6), 416–425 (1993)
3. Brown, P.: Stepping stones in the mist. In: *Creative Evolutionary Systems*, pp. 387–407. Morgan Kaufmann Publishers Inc. (2001)
4. Cover, T.M., Thomas, J.A.: *Elements of Information Theory* (Wiley Series in Telecommunications and Signal Processing). Wiley-Interscience (2006)
5. Frazer, J.: An evolutionary architecture. Architectural Association Publications, Themes VII (1995)
6. Javaheri Javid, M.A., Al-Rifaie, M.M., Zimmer, R.: Detecting symmetry in cellular automata generated patterns using swarm intelligence. In: Dediu, A.-H., Lozano, M., Martín-Vide, C. (eds.) *TPNC 2014. LNCS*, vol. 8890, pp. 83–94. Springer, Heidelberg (2014)
7. Javaheri Javid, M.A., te Boekhorst, R.: Cell dormancy in cellular automata. In: Alexandrov, V.N., van Albada, G.D., Sloot, P.M.A., Dongarra, J. (eds.) *ICCS 2006. LNCS*, vol. 3993, pp. 367–374. Springer, Heidelberg (2006)
8. Langton, C.G.: Studying artificial life with cellular automata. *Physica D: Nonlinear Phenomena* **22**(1), 120–149 (1986)
9. Miranda, E.: *Composing Music with Computers*. No. 1 in *Composing Music with Computers*. Focal Press (2001)
10. Scha, I.R.: *Kunstmatige Kunst. De Commectie* **2**(1), 4–7 (2006)
11. Schwartz, L., Schwartz, L.: *The Computer Artist's Handbook: Concepts, Techniques, and Applications*. W W Norton & Company Incorporated (1992)
12. Shannon, C.: A mathematical theory of communication. *The Bell System Technical Journal* **27**, 379–423, 623–656 (1948)
13. Wackerbauer, R., Witt, A., Atmanspacher, H., Kurths, J., Scheingraber, H.: A comparative classification of complexity measures. *Chaos, Solitons & Fractals* **4**(1), 133–173 (1994)
14. Wolfram, S.: Statistical mechanics of cellular automata. *Reviews of Modern Physics* **55**(3), 601–644 (1983)
15. Wolfram, S.: Universality and complexity in cellular automata. *Physica D: Nonlinear Phenomena* **10**(1), 1–35 (1984)
16. Wolfram, S.: *A New Kind of Science*. Wolfram Media Inc. (2002)
17. Xenakis, I.: *Formalized music: thought and mathematics in composition*. Pendragon Press (1992)

# Electricity Demand Modelling with Genetic Programming

Mauro Castelli<sup>1</sup>, Matteo De Felice<sup>2</sup>, Luca Manzoni<sup>3(✉)</sup>,  
and Leonardo Vanneschi<sup>1</sup>

<sup>1</sup> NOVA IMS, Universidade Nova de Lisboa, 1070-312 Lisboa, Portugal  
[{mcastelli,lvanneschi}@novaims.unl.pt](mailto:{mcastelli,lvanneschi}@novaims.unl.pt)

<sup>2</sup> Energy and Environment Modeling Technical Unit (UTMEA), ENEA,  
Casaccia Research Center, 00123 Roma, Italy  
[matteo.defelice@enea.it](mailto:matteo.defelice@enea.it)

<sup>3</sup> Dipartimento di Informatica, Sistemistica E Comunicazione,  
Università Degli Studi di Milano Bicocca, 20126 Milano, Italy  
[luca.manzoni@disco.unimib.it](mailto:luca.manzoni@disco.unimib.it)

**Abstract.** Load forecasting is a critical task for all the operations of power systems. Especially during hot seasons, the influence of weather on energy demand may be strong, principally due to the use of air conditioning and refrigeration. This paper investigates the application of Genetic Programming on day-ahead load forecasting, comparing it with Neural Networks, Neural Networks Ensembles and Model Trees. All the experimentations have been performed on real data collected from the Italian electric grid during the summer period. Results show the suitability of Genetic Programming in providing good solutions to this problem. The advantage of using Genetic Programming, with respect to the other methods, is its ability to produce solutions that explain data in an intuitively meaningful way and that could be easily interpreted by a human being. This fact allows the practitioner to gain a better understanding of the problem under exam and to analyze the interactions between the features that characterize it.

## 1 Introduction

Load forecasting is the task of predicting the electricity demand on different time scales, such as minutes (very short-term), hours/days (short-term), and months and years (long-term). This information has to be used to plan and schedule operations on power systems (dispatch, unit commitment, network analysis) in a way to control the flow of electricity in an optimal way, with respect to various aspects (quality of service, reliability, costs, etc). An accurate load forecasting has great benefits for electric utilities and both negative or positive errors lead to increased operating costs [10]. Overestimate the load leads to an unnecessary energy production or purchase and, on the contrary, underestimation causes unmet demand with a higher probability of failures and costly operations. Several factors influence electricity demand: day of the week and holidays (the so-called

“calendar effects”), special or unusual events, and weather conditions. In warm countries, the last factor is particularly critical during summer, when the use of refrigeration, irrigation and air conditioning becomes more common than in the rest of the year.

Most of the used methods for Load forecasting are time-series approaches, like Box-Jenkins models, or artificial intelligence methods, like Neural Networks (NN). There is a large literature about the use of computer science for load forecasting, in Section 2 a review of this literature is proposed. In the last decades, techniques based on Computational Intelligence (CI) methods have been proposed to overcome the most common problems of traditional methods, especially in most difficult scenarios. These techniques have demonstrated their effectiveness in several cases, often becoming a valid alternative to conventional methods.

A CI method is Genetic Programming [11,21] (GP). GP has several advantages over others machine learning methods, including the ones that have been considered in this work, that are Neural Networks and Model Trees. In particular, one interesting feature is the ability of GP to produce human-readable solutions. This property may allow an in depth analysis of the features that characterize a specific problem. It is important to underline that GP trees are usually very large and have significant redundancy (introns) even with parsimony measures. Thus, they can be very difficult to interpret. However, these trees can be usually simplified, producing a compact and readable model. In this work, the term human-readable is related to the fact that GP produces a model that represents interactions between variables, and that can be used for a better understanding of the problem under examination, a property that is particularly useful in real-life problems. This property is not true when, for instance, Neural Networks are considered. In fact NNs produce numerical matrices of weights, which does not facilitate the practitioner’s task of obtaining a better understanding of the relations between the features that characterize a specific problem. In this work we use GP for the load forecast problem during summer period, and we provide a comparison between GP and three different machine learning techniques on this problem.

The paper is organized as follows: Section 2 introduces the load forecasting problem and gives an overview of the state of the art approaches to deal with this problem. Section 3 briefly presents the techniques considered in this paper: neural networks, neural networks ensemble, model trees and GP. Section 4 describes the experimental phase, reporting the experimental settings and discussing the results. Section 5 concludes the paper and summarizes the results of this work.

## 2 Short-Term Load Forecasting

Load forecasting is commonly defined “short-term” when the prediction horizon is from one hour to one week. For this kind of problem various factors might be considered, such as weather data or, more in general, all the factors influencing the load pattern (e.g. day of the week). Load data normally exhibit seasonality: the load at time  $t$  tends to be similar to the load at time  $t - k$  with  $k$  usually

representing a day, a week or a month, depending on the dataset. In this paper, we are focusing on daily average load and we can observe that the load at the day  $t$  is usually similar to the one at the same day of the previous week (i.e., weekly seasonality), with the exception of holidays and weekends, when the load pattern is usually more unpredictable.

## 2.1 Forecasting Methods: State of the Art

Different methods have been used to cope with load forecasting, mainly classical statistical methods and machine learning techniques. The first approach, time series analysis, consists of the determination of the relationship between process input and output with a linear model. To do that, observations that are assumed equispaced discrete-time samples are used. There is a wide variety of models to deal with this problem, the most popular in engineering applications are probably autoregression (AR) and moving-average (MA) models with their combinations (ARMA, ARIMA, etc) and a common methodology is the iterative one proposed by Box & Jenkins [4]. Since Park's paper in 1991 [20], Neural Networks have been widely applied to the Load forecasting problem. The main advantage of NNs is their implicit nonlinearity which can potentially allow modeling complex dynamics. On the other hand, NNs present numerous parameters that are usually tuned with empirical approaches. Furthermore, NNs computational needs become expensive with high-dimensional problems and large datasets. Some reviews on the application of NNs can be found in [1, 7, 9]. Model trees, which we will introduce in the next section, have been used less frequently and, to the best of our knowledge, there are only few works using them for forecasting [19, 24, 25].

While GP has been used [3, 16] to face the load forecasting problem, it is not a widely applied technique like other CI approaches. This is probably due to the fact that GP is computationally expensive, in particular the evaluation of candidate solutions requires more time with respect to other machine learning techniques. On the other hand, differently from other machine learning techniques like Neural Networks, GP is able to produce solutions that are easier to read and interpret by humans [11], a feature that can be particularly useful in some applications. Moreover, like other Evolutionary Algorithms, the practitioner may design a specific fitness function in order to make the algorithm focusing on a specific problem feature [14]. While this makes the whole task "technically" more difficult, on the other hand the algorithm becomes more versatile: depending on how the fitness function is defined (or functions if multi-objective optimization is considered), it is possible to direct GP towards different parts of the solution space. In other words, it is possible to steer GP to particular behaviors, that are much more difficult to obtain with other machine learning techniques. Hence, it could be not only used for producing a forecasting model, but also to have some hints on the role of the variables that influence the forecasting model itself. As reported in [12], GP has been used to produce many instances of results that are competitive with human-produced results. These human-competitive results come from a wide variety of fields, including quantum computing circuits [2],

analog electrical circuits [14], antennas [18], mechanical systems [17], photonic systems [22], optical lens systems [13] and sorting networks [15].

### 3 Considered Techniques for the Load Forecasting Problem

This section briefly introduces the techniques used in this paper: neural networks, model trees, and genetic programming.

#### 3.1 Neural Networks

Neural Networks are a non-linear statistical modeling tool. In this work we use feed-forward neural networks trained with Levenberg-Marquardt back-propagation training algorithm, implemented in MATLAB. In addition to single neural networks, we use an ensemble of 100 neural networks with their outputs combined using an arithmetic mean. Neural networks ensemble have been introduced in [8] and this approach has already been used for load forecasting in [5].

#### 3.2 Model Trees

Model trees (M5 system) can be considered an extension of regression trees introduced by Quinlan in 1992 [23]. A regression tree is a type of prediction tree where in each leaf (terminal node) there is a zero-order model (i.e., constant value) predicting the target variable. On the other hand, trees built with the M5 algorithm [23] have at their leaves a multivariate linear model (i.e., first-order model). This linear model is the one that best fits those training points that satisfy the conditions represented in the internal nodes that are on the path from the root to the linear model itself. In these binary trees each internal node represents a “rule” that defines which sub-branch of the tree we have to use to make a prediction on a particular case. Model trees are basically a combination between conventional regression trees and linear regression models. They are particularly useful in the cases where a single global model is hard to obtain. Their ability in partitioning the sample space allows finding the part of the data space where a linear model best fits. The advantages of this technique are several: easiness of implementation, possibility to cope with not-smooth regression surfaces and existence of fast and reliable learning algorithms. In this work, we used a MATLAB implementation of the M5 algorithm<sup>1</sup>. For a description of the algorithm we refer to the Quinlan original paper [23] and to the improvement made by Wang [26].

---

<sup>1</sup> M5PrimeLab is an open source toolbox for MATLAB/Octave available at <http://www.cs.rtu.lv/jekabsons/regression.html>

### 3.3 Genetic Programming

GP is a machine learning technique inspired by Darwin's theory of evolution. In GP terminology [11] each candidate solution is called individual and the quality of the solution is called fitness. Fitness is a function that associates a real number to each possible individual. In minimization (respectively maximization) problems the objective is to find the solution with the minimal (respectively maximal) fitness (or a good-enough approximation of it). The GP algorithm is an iterative process (every iteration is called generation) that explores the search space to find good individuals (solutions) by evolving a population (set of possible solutions). In doing this exploration GP uses several genetic operators to mimic the natural evolution process: selection, mutation, and crossover. In GP individuals are traditionally represented as LISP-like trees. The selection operator selects individuals in function of their fitness with better solutions having higher probability of being selected. The selection operator is the only GP operator that works on fitness. The two operators that can change the structure of GP individuals are mutation and crossover. Mutation can be defined as random manipulation that operates on only one individual. The aim of the mutation is to avoid local optima and to move the search to new areas of the search space [11]. This operator selects a point in the GP tree randomly and replaces the existing sub-tree at that point with a new randomly generated sub-tree. The crossover operator combines the genetic material of two parents by swapping a sub-tree of one parent with a part of the other. The crossover operator is used to combine the pairs of selected individuals (parents) to create new individuals that potentially have a higher fitness than either of their parents. For a complete description of GP and ability to solve real-world problems, the reader is referred to [11, 21].

In GP every internal node is a function whose arguments are its children (that can also be other functions). Leaf nodes are constants or variables. Thus, a GP individual is a mathematical function and the sequence of composition of "basic functions" needed to produce it. Thus, it is important to underline that, differently from the aforementioned model trees, GP produces a solution that represents an algorithm to solve a particular problem and not a method to partition the sample space. In this work we used our C++ implementation of GP.

## 4 Experiments

In this work we compare the performances of different machine learning techniques on the electric load forecasting problem using Italian national grid data provided by TERNA<sup>2</sup>. We collected the daily average load  $y$  during the working days in June and July for the years 2003-2009, for a final data set of 300 samples.

---

<sup>2</sup> TERNA is the owner of the Italian transmission grid and the responsible for energy transmission and dispatching. Real-time data about electricity demand are available on their homepage [www.terna.it](http://www.terna.it)

The aim of this forecasting task is the load at time  $t$  ( $y_t$ ) providing information until day  $t - 1$  (one-day ahead forecasting) using the past samples of the load and the information provided by temperature. We built a data set with 9 input variables:  $x_0, x_1, \dots, x_6$  representing the daily load for each past day. The variable  $x_0$  refers to the load at time  $t - 7$  while  $x_6$  to the load at time  $t - 1$ . The value  $x_7$  is the daily average temperature (Celsius degrees) at day  $t - 1$  while  $x_8$  is the daily average temperature the same day of the forecast.

Temperature data have been obtained with an average of all the data available in Italy provided by the ECMWF (European Centre for Medium-Range Weather Forecasts) ERA-Interim reanalysis [6]. For the variable  $x_8$ , we assume to have a perfect forecast for the day  $t$  and hence we use the observed data.

#### 4.1 Experimental Settings

As explained before, the techniques we have considered are the standard GP algorithm, back propagation Neural Networks, and M5 Model Trees.

Training and test sets have been obtained by randomly splitting the dataset described in the previous section. In particular 50 different partitions of the original dataset with its same size, have been considered. In each partition 70% of the data have been randomly selected (without replacement) with uniform probability and inserted into the training set, while the remaining 30% form the test set (i.e., they are not used during the training phase). For each partition a total of 50 runs were performed with each technique (2500 runs in total). This setup has been implemented in order to perform a fair comparison between different techniques. In fact, unlike M5 algorithm, GP and NNs are stochastic methods and thus their performances can be influenced by initial conditions.

**Neural Networks.** Feed-forward neural networks with 9 inputs, 3 hidden neurons (with hyperbolic tangent transfer function) and 1 output have been used. The number of hidden neurons has been chosen after a set of preliminary tests. For each dataset we created 100 neural networks with different initial weights and, after the training phase, their output has been combined using an arithmetic mean and hence evaluated on the test set. For investigation purposes, in this paper we present both the results for the ensemble and for the best-training NN, i.e., the NN with the lower error during the training phase.

**M5 Model Trees.** In this case we performed a single execution for each dataset, in fact the M5 algorithm is not stochastic and so there is no need to perform multiple runs. We set as 10 the minimum number of training data cases represented by each leaf, this value has been selected after a set of exploratory tests.

**Genetic Programming.** Regarding the experimental settings related to standard GP, all the runs used populations of 100 individuals allowed to evolve for 100 generations. Tree initialization was performed with the Ramped Half-and-Half method [21] with a maximum initial depth of 6. The function set contained

the four binary operators  $+$ ,  $-$ ,  $*$ , and  $/$  protected as in [21]. The terminal set contained 9 variables and 100 random constants randomly generated in the range  $[0, 40000]$ . This range has been chosen considering the magnitude of the values at stake in the considered application. Because the cardinalities of the function and terminal sets were so different, we have explicitly imposed functions and terminals to have the same probability of being chosen when a random node is needed. The reproduction (replication) rate was 0.1, meaning that each selected parent has a 10% chance of being copied to the next generation instead of being engaged in breeding. Standard tree mutation and standard crossover (with uniform selection of crossover and mutation points) were used with probabilities of 0.1 and 0.9, respectively. Recall that the use crossover and mutation are applied only on individuals not selected for the replication. The new random branch created for mutation has maximum depth 6. Selection for survival was elitist, with the best individual preserved in the next generation. The selection method used was tournament selection with size 6. The maximum tree depth is 17. This depth value is considered the standard value for this parameter [11]. Despite the higher number of parameters, parameter tuning in GP was not particularly problematic with respect to the other methods since there are some general rules (e.g., low mutation and high crossover rate) that provide a good starting point for setting the parameters.

## 4.2 Results

We outline here the results obtained after the performed experimentation on the 50 different partitions of the dataset.

The objective of the learning process is to minimize the root mean squared error (RMSE) between outputs and targets. For each partition of the dataset, we collected the RMSE on test set of the best individual produced at the end of the training process. Thus, we have 50 values for each partition and we considered the median of these 50 values. The median was preferred over the arithmetic mean due to its robustness to outliers. Repeating this process with all the considered 50 partitions results in a set of 50 values. Each value is the median of the error on test set at the end of the learning process, for a specific partition of the dataset.

Table 1 reports median and standard deviation of all the median errors achieved considering all the 50 partitions of the dataset for the considered techniques. The same results are shown with a boxplot in Fig. 1(a). Denoting by  $IQR$  the interquartile range, the ends of the whiskers represent the lowest datum still within  $1.5 \cdot IQR$  of the lower quartile, and the highest datum still within  $1.5 \cdot IQR$  of the upper quartile. Errors for each dataset are shown in Fig. 1(b) where it is particularly visible that GP and M5 have similar performances.

GP is the best performer, considering both the median and the standard deviation. To analyze the statistical significance of these results, a set of statistical tests has been performed on the resulting median errors. The Kolmogorov-Smirnov test shows that the data are not normally distributed hence a rank-based statistic has been used. The Mann Whitney rank-sum test for pairwise data comparison is used under the alternative hypothesis that the samples do

**Table 1.** Median and standard deviation of median test errors of the dataset's partitions for the considered techniques.

Technique	Median [kW]	Standard deviation ( $\sigma$ )
Neural Networks (best)	27.599	6.731
Ensemble	24.887	7.467
Genetic Programming	22.993	4.622
M5 Model Trees	23.122	4.730

not have equal medians. The p-values obtained are  $3.9697 \cdot 10^{-7}$  when GP is compared to Neural Networks, 0.0129 when it is compared to a Neural Network ensemble and 0.9862 when GP is compared to M5 trees. Therefore, when using a significance level  $\alpha = 0.05$  with a Bonferroni correction for the value  $\alpha$ , we obtain that in the first two cases GP produces fitness values that are significantly lower (i.e., better) than the other methods, but the same conclusion cannot be reached when comparing to M5 (the p-value is equal to 0.9862). Results of Mann Whitney test are summarized in Table 2.

For a better understanding of the dynamic of the evolutionary process for this particular real-world problem, in Fig. 2 the median of the test fitness generation by generation is reported.

**Table 2.** p-values of Mann Whitney rank-sum test. In **bold** values that can not reject the null hypothesis with 5% significance value, meaning that errors difference is not significative.

p-value	NNs	NN Ens.	GP	M5
NNs	-	0.0074	$3.9697 \cdot 10^{-7}$	$1.0069 \cdot 10^{-7}$
NN Ens.	0.0074	-	0.0129	0.0182
GP	$3.9697 \cdot 10^{-7}$	0.0129	-	<b>0.9862</b>
M5	$1.0069 \cdot 10^{-7}$	0.0182	<b>0.9862</b>	-

### 4.3 Analysis of Results

We applied four different techniques to face the load forecasting problem and the solutions achieved have different forms. As stated before, GP and M5 produce, differently from NNs, solutions that could be easily interpreted. Hence, in this section we want to analyze the structure of the best solution returned by both these techniques.

We achieved 50 model trees with the M5 algorithm, one for each testing dataset. We analyzed all the linear models present in the tree leaves with the aim of understanding which variables are most used. We found that the variable  $x_8$  is used 55 times. Moreover variables from  $x_7$  to  $x_4$  are used respectively 45, 55, 3 and 3 times. The variable  $x_0$  is used 9 times and  $x_2$  only once. Then, as expected, the most common used variables are temperatures and day-before

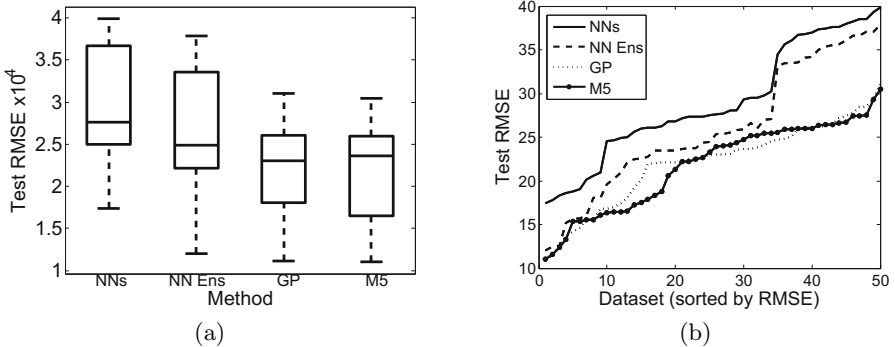


**Fig. 1.** Summary of test errors.

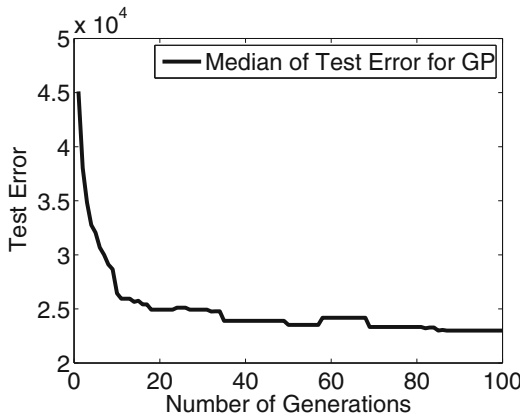
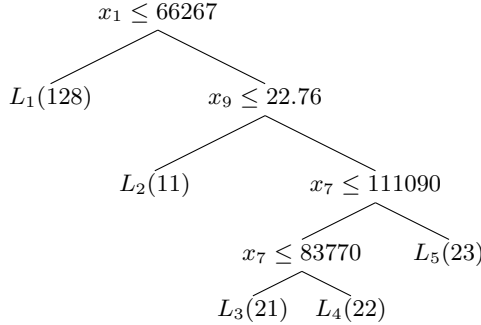


**Fig. 2.** Median of test fitness generation by generation. 50 independent runs have been considered.

load. In particular  $x_8$  is the temperature at the day of the forecasting,  $x_7$  is the temperature at the day before the forecasting and  $x_6$  is the energy consumption the day before the forecasting. Median values for the coefficients of  $x_6$ ,  $x_7$  and  $x_8$  are respectively 0.9164, -9435 and 10057 (relative standard deviations 17.6%, 20.7% and 25.5%). In Figure 3 a sample model tree is shown, it consists of five linear models of which three are constants. Considering the best individuals obtained by GP in all the considered partitions of the dataset, we can observe that all of them show a common structure. In particular, best individuals have this structure:

$$x_6 + f(x_7, x_8)$$

where  $x_6$  is the energy consumption at time  $t - 1$  and  $f$  is a polynomial (that we call “correction”) that only considers the temperatures at time  $t - 1$  and  $t$ . Below we report two (simplified) individuals returned by GP:



- $L_1 : y = -69185 + 0.718 x_7 + 3642 x_9$
- $L_2 : y = 36364$
- $L_3 : y = 81604$
- $L_4 : y = 101605$
- $L_5 : y = -205637 + 13344 x_9$

**Fig. 3.** A sample model tree. In brackets the number of data samples represented by the specific linear model is given.

$$\begin{aligned} I_1 &: x_6 + x_7 - x_8 + 4x_7 \cdot (2x_7 + (-x_7 + x_8) \cdot (x_7 + 6x_8)) - 3,968.452198 \\ I_2 &: x_6 + x_7 - x_8 + (x_7 - x_8) \cdot x_8 + x_7^2 x_8 \cdot (-x_7 + x_8) + 1,507.852134 \end{aligned}$$

As it is possible to see, GP returns solutions that could be understood and interpreted more easily than Neural Networks and M5 Model Trees. In fact, with respect to the latter, GP does not provide a tree with decision nodes and a linear model in every leaf. Instead, it provides a more compact non-linear model and it also performs an automatic feature selection; in fact, the final model contains only three variables. Furthermore, the form of the model ( $x_6 + f(x_7, x_8)$ ) is preserved in all the solutions produced during the performed runs. We want also to point out that while many standard techniques used for prediction are either limited in the form of the solution presented or in the legibility of the solutions, GP has neither problems. In fact, the expressiveness of GP is limited only by the choice of functional and terminal symbols and by the size of the trees.

Figure 4 reports the polynomial  $P$  obtained considering the average correction of the 50 best individuals:

$$P(x_7, x_8) = \frac{1}{50} \sum_{i=1}^{50} f_i(x_7, x_8) \quad (1)$$

The bigger is the difference between  $x_7$  and  $x_8$ , the bigger is the “correction”. This result matches our intuition regarding energy demand pattern: if in a particular day  $D$ , with a temperature equal to  $T$ , the energy consumption is  $E$ , we expect that the day  $D+1$  the energy consumption will be greater than  $E$ .

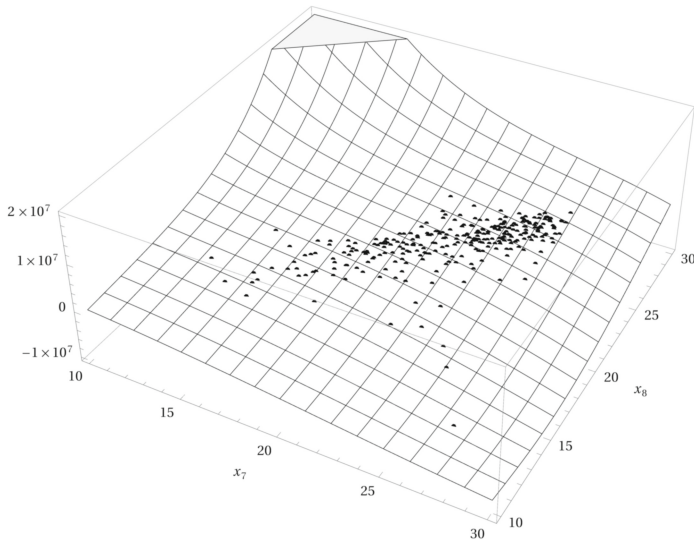


**Fig. 4.** Average correction considering the best individuals of all the considered datasets.  $x_7$  is the temperature at time  $t - 1$  while  $x_8$  is the temperature at time  $t$ . The black points represent the pairs of temperatures present in the dataset.

if the temperature is higher than  $T$  while we expect to have a lower energy consumption otherwise. As we stated before, the electricity demand in Italy during summer is strongly affected by the use of the air conditioning systems.

Having a model that is easily understandable and that respects our intuition of the problem (we could informally say a model that “makes sense”) allows a manual validation by the end user. It is a crucial issue in convincing practitioners to really use it for their applications. In our opinion, the GP models are the only ones (among the studied techniques) that have this characteristic of intuitivity and practical consistence with our interpretation of the problem. Basically, GP is saying to us that the energy consumption in a given day is the same as the one of previous day plus (or minus) a given quantity that directly depends on the temperature increase (or decrease) between that day and the previous one. Any practitioner would understand and trust such a model as a reliable explanation of the data. In fact, GP performs an effective (and intuitively meaningful) automatic feature selection that results in the preservation of only three variables. Differently, NNs always use all the provided variables in their solutions unless an appropriate feature selection algorithm is used in a preprocessing phase. M5 Model trees also use a different subset of variables in each of the linear models that are present in their leaves while GP always uses the same 3 features, consistently in all the best individuals found in all the runs.

## 5 Conclusions

Energy load forecasting can provide important information regarding future energy consumption. In this work, a genetic programming based forecasting method has been presented and a comparison with other machine learning techniques has been performed. Experimental results show that GP and M5 perform quite similar, with a difference that is not statistically significant. Neural networks and the ensemble method have returned results of poorer quality. GP, differently from the other methods, produces solutions that explain data in a simple and intuitively meaningful way and could be easily interpreted. Hence, GP has been used in this work not only to build a model, but also to evaluate the effect of the parameters of the model. In fact, for the considered problem GP highlighted the relationship between the energy consumption and the external temperature. Moreover, GP demonstrates the ability to perform feature selection in an automatic and effective way, using a more compact set of variables than the other techniques and using always the same limited set of variables in all the returned solutions. When other machine learning techniques are considered, the analysis of the solutions is much more difficult and less intuitive. Possible future works may consider longer forecasting periods, also with the use of data provided by temperatures forecasts.

## References

1. Adya, M., Collopy, F.: How effective are neural networks at forecasting and prediction? A review and evaluation. *Journal of Forecasting* **17**, 481–495 (1998)
2. Barnum, H., Bernstein, H.J., Spector, L.: Quantum circuits for OR and AND of ORs. *Journal of Physics A: Mathematical and General* **33**, 8047–8057 (2000)
3. Bhattacharya, M., Abraham, A., Nath, B.: A linear genetic programming approach for modelling electricity demand prediction in victoria. In: *Hybrid Information Systems*, pp. 379–393. Springer (2002)
4. Box, G., Jenkins, G.M., Reinsel, G.: *Time Series Analysis: Forecasting & Control*, 3rd edn. Prentice Hall, February 1994
5. De Felice, M., Yao, X.: Neural networks ensembles for short-term load forecasting. In: *IEEE Symposium Series in Computational Intelligence (SSCI)* (2011)
6. Dee, D., Uppala, S., Simmons, A., Berrisford, P., Poli, P., Kobayashi, S., Andrae, U., Balmaseda, M., Balsamo, G., Bauer, P., et al.: The ERA-Interim reanalysis: configuration and performance of the data assimilation system. *Quarterly Journal of the Royal Meteorological Society* **137**(656), 553–597 (2011)
7. Feinberg, E.A., Genethliou, D.: Load forecasting. In: Chow, J., Wu, F., Momoh, J. (eds.) *Applied Mathematics for Restructured Electric Power Systems: Optimization, Control and Computational Intelligence*, pp. 269–285. Springer (2005)
8. Hansen, J., Nelson, R.: Neural networks and traditional time series methods: a synergistic combination in state economic forecasts. *IEEE Transactions on Neural Networks* **8**(4), 863–873 (1997)
9. Hippert, H., Pedreira, C., Souza, R.: Neural networks for short-term load forecasting: a review and evaluation. *IEEE Transactions on Power Systems* **16**(1), 44–55 (2001)

10. Hobbs, B., Jitprapaikulsarn, S., Konda, S., Chankong, V., Loparo, K., Maratukulam, D.: Analysis of the value for unit commitment of improved load forecasts. *IEEE Transactions on Power Systems* **14**(4), 1342–1348 (1999)
11. Koza, J.R.: *Genetic programming: on the programming of computers by natural selection*. MIT Press, Cambridge (1992)
12. Koza, J.R.: Human-competitive results produced by genetic programming. *Genetic Programming and Evolvable Machines* **11**, 251–284 (2010)
13. Koza, J.R., Al-Sakran, S.H., Jones, L.W.: Automated ab initio synthesis of complete designs of four patented optical lens systems by means of genetic programming. *Artif. Intell. Eng. Des. Anal. Manuf.* **22**(3), 249–273 (2008)
14. Koza, J.R., Andre, D., Bennett, F.H., Keane, M.A.: *Genetic Programming III: Darwinian Invention & Problem Solving*, 1st edn. Morgan Kaufmann Publishers Inc., San Francisco (1999)
15. Koza, J.R., Bade, S.L., Bennett, F.H.: Evolving sorting networks using genetic programming and rapidly reconfigurable field-programmable gate arrays. In: *Workshop on Evolvable Systems. International Joint Conference on Artificial Intelligence*, pp. 27–32. IEEE Press (1997)
16. Lee, D.G., Lee, B.W., Chang, S.H.: Genetic programming model for long-term forecasting of electric power demand. *Electric Power Systems Research* **40**(1), 17–22 (1997)
17. Lipson, H.: Evolutionary synthesis of kinematic mechanisms. *Artif. Intell. Eng. Des. Anal. Manuf.* **22**(3), 195–205 (2008)
18. Lohn, J.D., Hornby, G.S., Linden, D.S.: Human-competitive evolved antennas. *Artif. Intell. Eng. Des. Anal. Manuf.* **22**(3), 235–247 (2008)
19. Troncoso Lora, A., Riquelme, J.C., Martínez Ramos, J.L., Riquelme Santos, J.M., Gómez Expósito, A.: Influence of kNN-based load forecasting errors on optimal energy production. In: Pires, F.M., Abreu, S.P. (eds.) *EPIA 2003. LNCS (LNAI)*, vol. 2902, pp. 189–203. Springer, Heidelberg (2003)
20. Park, D., El-Sharkawi, M., Marks, R., Atlas, L., Damborg, M.: Electric load forecasting using an artificial neural network. *IEEE Transactions on Power Systems* **6**, 442–449 (1991)
21. Poli, R., Langdon, W.B., McPhee, N.F.: A field guide to genetic programming, published via Lulu.com (2008). <http://www.gp-field-guide.org.uk/>
22. Preble, S., Lipson, M., Lipson, H.: Two-dimensional photonic crystals designed by evolutionary algorithms. *Applied Physics Letters* **86**(6) (2005)
23. Quinlan, R.J.: Learning with continuous classes. In: *5th Australian Joint Conference on Artificial Intelligence*, pp. 343–348. World Scientific, Singapore (1992)
24. Solomatine, D., Xue, Y.: M5 model trees and neural networks: application to flood forecasting in the upper reach of the Huai River in China. *Journal of Hydrologic Engineering* **9**(6), 491–501 (2004)
25. Štravas, L., Brilly, M.: Development of a low-flow forecasting model using the M5 machine learning method. *Hydrological Sciences Journal* **52**(3), 466–477 (2007)
26. Wang, Y., Witten, I.: Inducing model trees for continuous classes. In: *Proceedings of the Ninth European Conference on Machine Learning*, pp. 128–137 (1997)

# The Optimization Ability of Evolved Strategies

Nuno Lourenço<sup>1</sup>(✉), Francisco B. Pereira<sup>1,2</sup>, and Ernesto Costa<sup>1</sup>

<sup>1</sup> CISUC, Department of Informatics Engineering, University of Coimbra,  
Polo II - Pinhal de Marrocos, 3030 Coimbra, Portugal

{naml,xico,ernesto}@dei.uc.pt

<sup>2</sup> Instituto Politécnico de Coimbra, ISEC, DEIS, Rua Pedro Nunes,  
Quinta da Nora, 3030-199 Coimbra, Portugal

**Abstract.** Hyper-Heuristics (HH) is a field of research that aims to automatically discover effective and robust algorithmic strategies by combining low-level components of existing methods and by defining the appropriate settings. Standard HH frameworks usually comprise two sequential stages: Learning is where promising strategies are discovered; and Validation is the subsequent phase that consists in the application of the best learned strategies to unseen optimization scenarios, thus assessing its generalization ability.

Evolutionary Algorithms are commonly employed by the HH learning step to evolve a set of candidate strategies. In this stage, the algorithm relies on simple fitness criteria to estimate the optimization ability of the evolved strategies. However, the adoption of such basic conditions might compromise the accuracy of the evaluation and it raises the question whether the HH framework is able to accurately identify the most promising strategies learned by the evolutionary algorithm. We present a detailed study to gain insight into the correlation between the optimization behavior exhibited in the learning phase and the corresponding performance in the validation step. In concrete, we investigate if the most promising strategies identified during learning keep the good performance when generalizing to unseen optimization scenarios. The analysis of the results reveals that simple fitness criteria are accurate predictors of the optimization ability of evolved strategies.

## 1 Introduction

Hyper-Heuristics (HH) is a field of research that aims to automatically discover effective and robust optimization algorithms [1]. HH frameworks can generate metaheuristics for a given computational problem either by selecting/ combining low level heuristics or by designing a new method based on components of existing ones. In [1], Burke *et al.* have presented a detailed discussion of these HH categories, complemented with several representative examples. HH are commonly divided in two sequential stages: *Learning* is where the strategies are automatically created, whilst, in *Validation*, the most promising learned solutions are applied to unseen and more challenging scenarios.

Evolutionary Algorithms (EAs) are regularly applied as HH search engines to learn effective algorithmic strategies for a given problem or class of related

problems. Each strategy created by the EA needs to be evaluated to estimate its optimization ability. In concrete, every individual from the population is applied to an instance of the problem under consideration and the quality of the solutions found is used as an estimator of its optimization ability. To keep the computational effort at a reasonable level, the evaluation step of the EA search engine relies on small instances and simplified fitness criteria. However, it is known that the training conditions impact the properties of the algorithms being evolved [5–7, 12] and it is not clear if the limited evaluation conditions adopted by HH frameworks compromise the accurate identification of the best optimization strategies. In this paper we address this question by investigating if the fitness criteria used in learning provide enough information to identify the most effective and robust strategies.

The study is performed with a well-known Grammatical Evolution (GE) [9] HH framework, originally proposed in 2012 [14]. This computational model is able to automatically generate complete Ant Colony Optimization (ACO) [2] algorithms that can effectively solve different traveling salesperson problem (TSP) instances. It allows for a flexible definition of the components and settings to be used by the algorithm, as well as its general structure. Results presented in the aforementioned reference confirm that this HH framework is able to evolve novel ACO architectures, competitive with state-of-the-art human designed variants.

The analysis presented in this paper reveals that the most promising strategies discovered in the learning phase tend to maintain the good performance in the validation step. This outcome supports the adoption of simple and somehow inaccurate fitness criteria in the learning phase, as this does not compromise the ability of the HH framework to identify the most effective and robust optimization strategies. Additionally, we investigate the existence of overfitting in the learning phase, i.e., the over interpretation of relationships that only occur in the learning data. Preliminary results suggest that learning is able to avoid the overfitting of the data.

The paper is structured as follows: Section 2 describes the general properties of the HH framework adopted in this work, whereas section 3 reviews the main features of the ACO HH model used in the experiments. Section 4 contains the experimental setup and presents an empirical study to assess the optimization ability of the learned strategies. Finally, Section 5 gathers the main conclusions and suggests some ideas for future work.

## 2 Hyper-Heuristics

HH is a recent area of research that addresses the construction of specific, high-level, heuristic problem solvers, by searching the space of possible low-level heuristics for the particular problem one wants to solve. HH can be divided in two major groups [1]: the selection group comprises the search for the best sequence of low-level heuristics, selected from a set of predefined methods usually applied to a specific problem; the other group includes methods that promote the creation of new heuristics. In the later case, the HH iteratively learns a novel

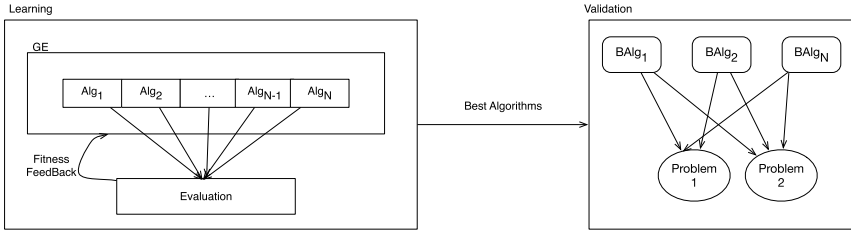


**Fig. 1.** Hyper-Heuristic Framework Architecture

algorithm which is then applied to solve the problem at hand. During this process, the HH are usually guided by feedback obtained through the execution of each candidate solution in simple instances of the problem under consideration. Genetic Programming (GP), a branch of EAs, has been increasingly adopted as the HH search engine to learn effective algorithmic strategies [10]. In the recent years, Grammatical Evolution (GE) [9], a linear form of GP, has received increasing attention from the HH community since it allows for a straightforward enforcement of semantic and syntactic restrictions, by means of a grammar.

## 2.1 Framework

In this work a two phase architecture is adopted (see Fig. 1). In the first phase, *Learning*, a GE-based HH will construct algorithmic strategies. GE is a GP branch that decouples the genotype from the phenotype by encoding solutions as a linear string of integers. The evaluation of an individual requires the application of a genotype-phenotype mapping that decodes the linear string into a syntactically legal algorithmic strategy, by means of a grammar. GE grammars are composed by a set of production rules written in the Backus-Naur format, defining the general structure of the programs being evolved and also the components that can be selected to build a given strategy (consult [9] for details concerning GE algorithms).

The quality of a strategy generated by the GE should reflect its ability to solve a given problem. During evolution, each GE solution is applied to a pre-determined problem instance and its fitness corresponds to the quality of the best solution found. Given this modus operandi, the GE evaluation step is a computationally intensive task. To prevent the learning process from taking an excessive amount of time, some simple evaluation conditions are usually defined: i) one single and small problem instance is used to assign fitness; ii) only one run is performed; iii) the number of iterations is kept low. Clearly, the adoption of such simple conditions might compromise the results by hindering differences between competing strategies, leading to an inaccurate assessment of the real optimization ability of evolved solutions. The experiments described in section 4 aim to gain insight into this situation.

The second phase of the HH framework is *Validation*. The most promising strategies ( $BAlg$ ) identified in the previous step, *i.e.*, those that obtained better fitness in the learning task, are applied to unseen scenarios to confirm their effectiveness and robustness.

## 2.2 Related Work

Recent works have shown that the conditions used in the learning phase influence the structure of algorithmic strategies that are being evolved. In [13], Smit *et al.* shows that using different performance measures like mean best fitness or success rate may yield very different algorithmic strategies. Lourenço *et al.* [5] presented a study on how a GE-based HH to evolve full-fledged EAs is affected by the learning conditions used to evaluate the quality of the algorithm. More precisely, they investigated how different population sizes and/or number of generations influenced the components that were selected by the HH to build the EA. Later, in [6] they presented a HH to learn selection strategies to EAs, and showed that the levels of selective pressure would depend on the EA where the strategy was inserted. In [7] Martin *et al.* evolved Black-Box Search Algorithms (BBSAs) and showed that using multiple instances of the problem affect the algorithmic structure of the strategies.

In [3], Eiben *et al.* present a discussion on how evolved algorithms should be selected, and present robustness as being a key factor to determine the quality of algorithms. Robustness is related to performance and its variance across some dimension. One of these dimensions is the range of problems (or problem instances) that the algorithm can tackle. Based on this, they define two properties: *fallibility* which indicates that the algorithms can clearly fail on some specific problems; *applicability* which indicates the range of problems that the algorithm can successfully tackle. Note that the applicability depends on a certain performance threshold  $T$ . An algorithm is robust if it performs well across several problems (high applicability), and if it has small performance variances.

## 3 Design of Ant Algorithms with Grammatical Evolution

The HH framework, originally proposed by Tavares *et al.* [14] to evolve full-fledged ACO algorithms, will be used as the testbed for our experiments. Ant Colony Optimization (ACO) algorithms are a set of population-based methods, loosely inspired by the behaviour of ant foraging [2]. Following the original Ant System (AS) algorithm proposed by Marco Dorigo in 1992, many other variants and extensions have been described in the literature. To help researchers and practitioners to select and tailor the most appropriate variant to a given problem, several automatic ACO design frameworks have been proposed in the last few years [4, 11, 14]. The production set of the above mentioned framework defines the general architecture of an ACO-like algorithm, comprising an initialisation step followed by an optimization cycle. The first stage initialises the pheromone matrix and other settings of the algorithm. The main loop consists

of the building of the solutions, pheromone trail update and daemon actions. Each component contains several alternatives to implement a specific task. As an example, the decision policy adopted by the ants to build a trail can be either the random proportional rule used by AS methods or the q-selection pseudorandom proportional rule introduced by the Ant Colony System (ACS) variant. If the last option is selected, the GE engine also defines a specific value for the q-value parameter. The grammar allows the replication of all main ACO algorithms, such as AS, ACS, Elitist Ant System (EAS), Rank-based Ant System (RAS), and Max-Min Ant System (MMAS). Additionally, it can generate novel combinations of blocks and settings that define alternative ACO algorithms. Results presented in [14] show that the GE-HH framework is able to learn original ACO architectures, different from standard strategies. Moreover, results obtained in validation instances reveal that the evolved strategies generalize well and are competitive with human-designed variants (consult the aforementioned reference for a detailed analysis of the results).

## 4 Experimental Analysis

Experiments described in this section aim to gain insight into the capacity of the GE-based HH to identify the most promising solutions during the learning step. In concrete, we determine the relation between the quality of strategies as estimated by the GE and their optimization ability when applied to unseen and harder scenarios. Such study will provide valuable information about the capacity of the GE to build and identify strategies that are robust, i.e., highly applicable and with small fallibility.

In practical terms, we take all strategies belonging to the last generation of the GE and rank them by the fitness obtained in the learning evaluation instance. Since the GE relies on a steady-state replacement method, the last generation contains the best optimization strategies identified during the learning phase. Then, these strategies are applied to unseen instances and ranked again based on the new results achieved. The comparison of the ranks obtained in different phases will provide relevant information in what concerns the generalization ability of the evolved strategies.

**Table 1.** GE Learning Parameters: adapted from [14]

Runs	30
Population Size	64
Generations	40
Individual Size	25
Wrapping	No
Crossover Operator	One-Point with a 0.7 rate
Mutation Operator	Integer-Flip with a 0.05 rate
Selection	Tournament with size 3
Replacement	Steady State
Learning Instances	pr76, ts225

The GE settings used in the experiments are depicted in Table 1. The population size is set to 64 individuals, each one composed by 25 integer codons, which is an upper bound on the number of production rules needed to generate an ACO strategy using the grammar from [14]. As this grammar does not contain recursive production rules, it is possible to determine the maximum number of values needed to create a complete phenotype. Also, wrapping is not necessary since the mapping process never goes beyond the end of the integer string.

We selected several TSP instances from the TSPLIB<sup>1</sup> for the experimental analysis. Two different instances were selected to learn the ACO strategies: pr76 and ts225 (the numerical values represent how many cities the instance has). Each ACO algorithm encoded in a GE solution is executed once during 100 iterations. The fitness assigned to this strategy corresponds to the best solution found. The strategies encode all the required settings to run the ACO algorithm, with the exception of the colony size, which is set to 10% of the number of cities (truncated the closest integer).

In what concerns the validation step, the best ACO strategies are applied to four different TSP instances: lin105, pr136, pr226, lin318. In this phase, all ACO algorithms are run for 30 times and the number of iterations is increased to 5000. The size of the colony is the same (10% of the size of the instance being optimised). Table 2 summarises the parameters used. In both phases, the results are expressed as a normalised distance to the optimum.

**Table 2.** ACO Validation Parameters

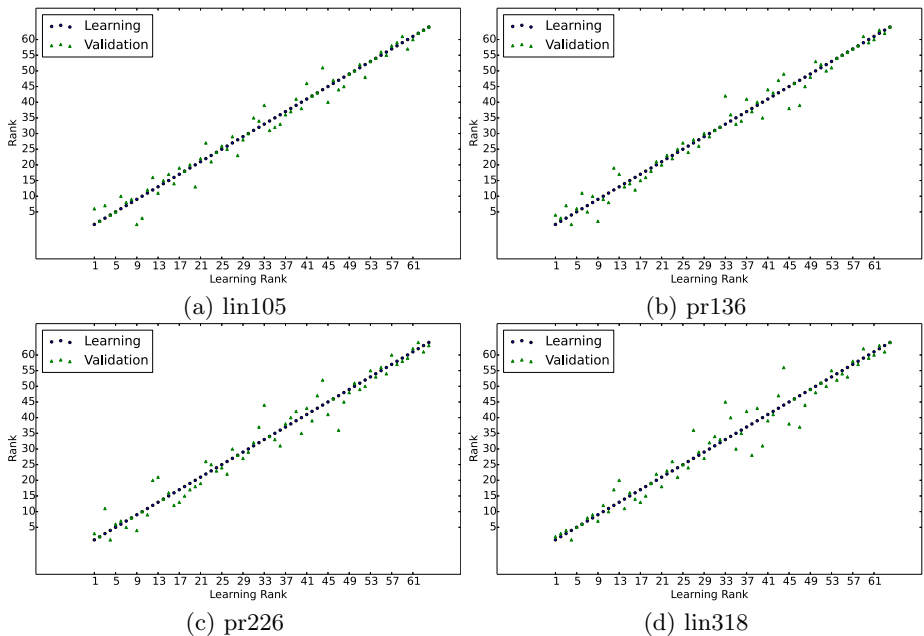
Runs	30
Iterations	5000
Colony Size	10% of the Instance Size
Instances	lin105, pr136, pr226, lin318

Fig. 2 displays the ranking distributions of the best ACO strategies learned with the pr76 instance. The 4 panels correspond to the 4 different validation instances. Each solution from the last GE generation is identified using an integer from 1 to 64, displayed in the horizontal axis. These solutions are ranked by the fitness obtained in training (solution 1 is the best strategy from the last generation, whilst solution 64 is the worst). The vertical axis corresponds to the position in the rank. Small circles highlight the learning rank and, given the ordering of the solutions from the GE last generation, we see a perfect diagonal in all panels. The small triangles identify the ranking of the solutions achieved in the 4 validation tasks (one on each panel). Ideally, these rankings should be identical to the ones obtained in training, i.e., the most promising solutions identified by the GE would be those that generalize better to unseen instances.

An inspection of the results reveals an evident correlation between the behavior of the strategies in both phases. An almost perfect line of triangles is visible in

---

<sup>1</sup> <http://comopt.ifii.uni-heidelberg.de/software/TSPLIB95/>



**Fig. 2.** Ranking distribution of the best ACO strategies discovered with the pr76 learning instance.

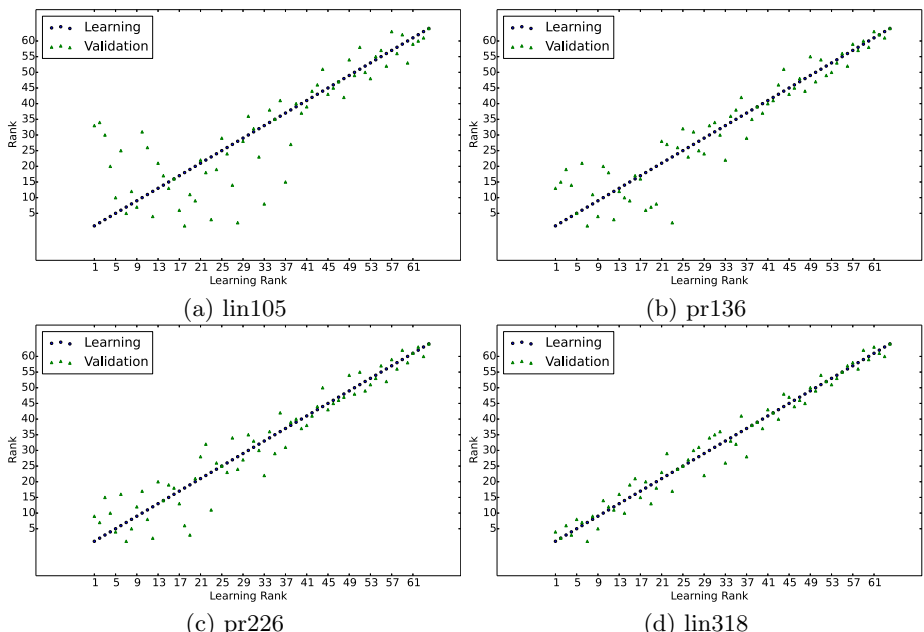


**Fig. 3.** Ranking distribution of the best ACO strategies discovered with the ts225 learning instance.

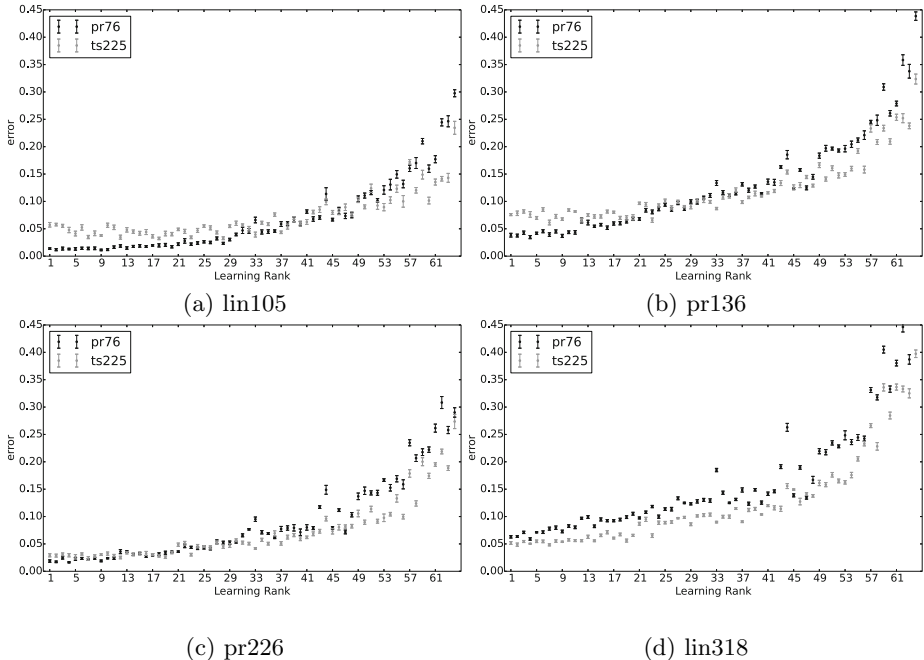
the 4 panels, confirming that the best strategies from training keep the good performance in validation. This trend is visible across all the validation instances and shows that, with the pr76 instance, training is accurately identifying the more robust and effective ACO strategies.

Fig. 3 displays the ranking distributions of the best ACO strategies learned with the ts225 instance. Although the general trend is maintained, a close inspection of the results reveals some interesting disagreements. The best ACO strategies learned with ts225 tend to have a modest performance when applied to small validation instances, such as lin105 and pr136. On the contrary, they behave well on larger instances (see, e.g., the results obtained with the validation instance from panel d)). This outcome confirms that the training conditions impact the structure of the evolved algorithmic strategies, which is in agreement with other findings reported in the literature [5, 13]. The ts225 instance is considered a hard TSP instance [8] and, given the results displayed in Fig. 3, it promotes the evolution of ACO strategies particularly suited for TSP problems with a higher number of cities. In the remainder of this section we present some additional results that help gain insight into these findings.

To authenticate the correlation between learning and validation we computed the Pearson correlation coefficient between the rankings obtained in each phase. This coefficient ranges between -1 and 1, where -1 identifies a completely negative correlation and 1 highlights a total correlation (the best strategies in learning are the best in validation). The results obtained are presented in Table 3. Columns contain instances used in learning, whilst rows correspond to validation instances. The values from the table confirm that there is always a clearly positive correlation between the two phases, i.e., the quality obtained by a solution in learning is an accurate estimator of its optimization ability. The lowest values of the Pearson coefficient are obtained by strategies learned with the ts225 instance and validated in small TSP problems, confirming the visual inspection of Fig. 3. In this correlation analysis we adopted a significance level of  $\alpha = 0.05$ . All the  $p$ -values obtained were smaller than  $\alpha$ , thus confirming the statistical significance of the study.

To complement the analysis, we present in Fig. 4 the absolute performance of the best learned ACO strategies in the 4 selected validation instances. Each panel comprises one of the validation scenarios and contains a comparison between the optimization performance of strategies evolved with different learning instances (black mean and error bars are from ACO strategies trained with the pr76 instances, whilst the grey are from algorithms evolved with the ts225 instance). In general, for all panels and for strategies evolved with the two training instances, the deviation from the optimum increases with the training ranking, confirming that the best algorithms from phase 1 are those that exhibit a better optimization ability. However, the results reveal an interesting pattern in what concerns the absolute behavior of the algorithms. For the smaller validation instances (lin 105 and pr136 in panels a) and b)), the ACO strategies evolved by the smaller learning instances achieve a better performance. On the contrary, ACO algorithms learned with the ts225 instance are better equipped to

handle the largest validation problem (lin318 in panel d)). This is another piece of evidence that confirms the impact of the training conditions on the structure of the evolved solutions. A detailed analysis of the algorithmic structure reveals that the pr76 training instance promotes the appearance of extremely greedy ACO algorithms (e.g., they tend to have very low evaporation levels), particularly suited for the quick optimization of simple instances. On the contrary, strategies evolved with the ts225 training instance strongly rely on full evaporation, thus promoting the appearance of methods with increased exploration ability, particularly suited for larger and harder TSP problems.



**Fig. 4.** MBF of the best evolved ACO strategies in the 4 validation instances. Black symbols identify results from strategies learned with the pr76 instance and grey symbols correspond to results from strategies obtained with the ts225 instance.

#### 4.1 Measuring Overfitting

To complete our analysis we investigate the evolution of overfitting while learning ACO strategies. To estimate the occurrence of overfitting we selected one additional instance for each training scenario, with the same size of the instance used in training (eil76 and tsp225, respectively). In each GE generation, the current best ACO strategy is applied to this new test instance and the quality of the obtained solution is recorded (this value is never used for training).

Fig. 5 and 6 present the evolution of the *Mean Best Fitness* (MBF) during the learning phase, respectively for the pr76 and ts225 instances. Both figures contain two panels: panel a) exhibits the evolution of the MBF measured by the learning instance, which corresponds to the value used to guide the GE exploration; panel b) displays the MBF obtained with the testing instance and it is only used to detect overfitting.

The results depicted in panels 5a and panel 6a show that the HH framework gradually learns better strategies. A brief perusal of the MBF evolution reveals a rapid decrease in the first generations, followed by a slower convergence. This is explained by the fact that in the beginning of the evolutionary process the GE combines different components provided by the grammar to build a robust strategy, whilst at the end it tries to fine-tune the numeric parameters. The search for a meaningful combination of components has a stronger impact on fitness than modifying numeric values.

Overfitting occurs when the fitness of the learning strategies keeps improving, whilst it deteriorates in testing. Panels 5b and 6b show the MBF for the testing step. An inspection of the results shows that it tends to decrease throughout the evolutionary run. This shows that the strategies being evolved are not becoming overspecialized, i.e., they maintain the ability to solve instances different from the ones used in training.

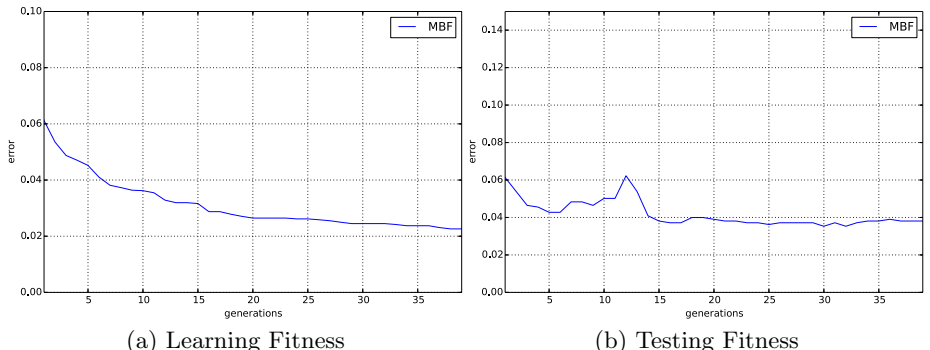


**Fig. 5.** Evolution of the MBF for the pr76 learning instance and the corresponding eil76 testing instance.

**Table 3.** Pearson correlation coefficients

	pr76	ts225
lin105	0.98	0.81
pr136	0.90	0.90
pr226	0.97	0.95
lin318	0.95	0.98

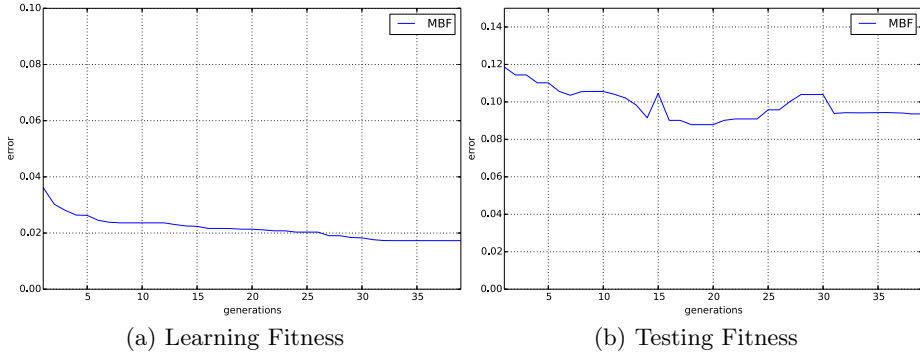


**Fig. 6.** Evolution of the MBF for the ts225 learning instance and the corresponding tsp225 testing instance.

## 5 Conclusions

HH is an area of research that aims to automate the design of algorithmic strategies by combining low-level components of existing methods. Most of the HH frameworks are divided two phases. The first phase, Learning, is where the strategies are built and evaluated. Afterwards, the robustness of the best solutions is validated in unseen scenarios. Usually, researchers select the best learned strategies based only simple and somehow inaccurate criteria. Given this situation, there is the risk of failing the identification of the most effective learned algorithmic strategies.

In this work we studied the correlation between the quality exhibited by strategies during learning and their effective optimization ability when applied to unseen scenarios. We relied on an existing GE-based HH to evolve full-fledged ACO algorithms to perform the analysis. Results revealed a clear correlation between the quality exhibited by the strategies in both phases. As a rule, the most promising algorithms identified in learning generalize better to unseen validation instances. This study provides valuable guidelines for HH practitioners, as it suggests that the limited training conditions do not seriously compromise the identification of the algorithmic strategies with the best optimization ability. The outcomes also confirmed the impact of the training conditions on the structure of the evolved solutions. Training with small instances promotes the appearance of greedy optimization strategies particularly suited for simple problems, whereas larger (and harder) training cases favor algorithmic solutions that excel in more complicated scenarios. Finally, a preliminary investigation revealed that training seems to be overfitting free, *i.e.*, the strategies being learned are not becoming overspecialized to the specific instance used in the evaluation.

There are several possible extension to this work. In the near future we aim to validate the correlation study in alternative training evaluations conditions. Also, a complete understanding of overfitting is still in progress and we will extend this analysis to a wider range of scenarios (e.g., the size, structure and

the number of the instances used for testing might influence the results). Finally, we will investigate if the main results hold for different HH frameworks.

**Acknowledgments.** This work was partially supported by Fundação para a Ciência e Tecnologia (FCT), Portugal, under the grant SFRH/BD/79649/2011.

## References

1. Burke, E.K., Gendreau, M., Hyde, M., Kendall, G., Ochoa, G., Özcan, E., Qu, R.: Hyper-heuristics: A survey of the state of the art. *Journal of the Operational Research Society* **64**(12), 1695–1724 (2013)
2. Dorigo, M., Stützle, T.: *Ant Colony Optimization*. Bradford Company, Scituate (2004)
3. Eiben, A., Smit, S.: Parameter tuning for configuring and analyzing evolutionary algorithms. *Swarm and Evolutionary Computation* **1**(1), 19–31 (2011)
4. López-Ibáñez, M., Stützle, T.: Automatic configuration of multi-objective ACO algorithms. In: Dorigo, M., Birattari, M., Di Caro, G.A., Doursat, R., Engelbrecht, A.P., Floreano, D., Gambardella, L.M., Groß, R., Şahin, E., Sayama, H., Stützle, T. (eds.) *ANTS 2010. LNCS*, vol. 6234, pp. 95–106. Springer, Heidelberg (2010)
5. Lourenço, N., Pereira, F.B., Costa, E.: The importance of the learning conditions in hyper-heuristics. In: *Proceedings of the 15th Annual Conference on Genetic and Evolutionary Computation, GECCO 2013*, pp. 1525–1532 (2013)
6. Lourenço, N., Pereira, F., Costa, E.: Learning selection strategies for evolutionary algorithms. In: Legrand, P., Corsini, M.-M., Hao, J.-K., Monmarché, N., Lutton, E., Schoenauer, M. (eds.) *EA 2013. LNCS*, vol. 8752, pp. 197–208. Springer, Heidelberg (2014)
7. Martin, M.A., Tauritz, D.R.: A problem configuration study of the robustness of a black-box search algorithm hyper-heuristic. In: *Proceedings of the 2014 Conference Companion on Genetic and Evolutionary Computation Companion, GECCO Comp. 2014*, pp. 1389–1396 (2014)
8. Merz, P., Freisleben, B.: Memetic algorithms for the traveling salesman problem. *Complex Systems* **13**(4), 297–346 (2001)
9. O'Neill, M., Ryan, C.: Grammatical evolution: evolutionary automatic programming in an arbitrary language, vol. 4. Springer Science (2003)
10. Pappa, G.L., Freitas, A.: *Automating the Design of Data Mining Algorithms: An Evolutionary Computation Approach*, 1st edn. Springer Publishing Company, Incorporated (2009)
11. Runka, A.: Evolving an edge selection formula for ant colony optimization. In: *Proceedings of the GECCO 2009*, pp. 1075–1082 (2009)
12. de Sá, A.G.C., Pappa, G.L.: Towards a method for automatically evolving bayesian network classifiers. In: *Proceedings of the 15th Annual Conference Companion on Genetic and Evolutionary Computation*, pp. 1505–1512. ACM (2013)
13. Smit, S.K., Eiben, A.E.: Beating the world champion evolutionary algorithm via revac tuning. In: *IEEE Congress on Evolutionary Computation (CEC) 2010*, pp. 1–8. IEEE (2010)
14. Tavares, J., Pereira, F.B.: Automatic design of ant algorithms with grammatical evolution. In: Moraglio, A., Silva, S., Krawiec, K., Machado, P., Cotta, C. (eds.) *EuroGP 2012. LNCS*, vol. 7244, pp. 206–217. Springer, Heidelberg (2012)

# Evolution of a Metaheuristic for Aggregating Wisdom from Artificial Crowds

Christopher J. Lowrance<sup>(✉)</sup>, Omar Abdelwahab, and Roman V. Yampolskiy

Department of Computer Engineering and Computer Science,  
University of Louisville, Louisville, KY 40292, USA

{chris.lowrance,omar.abdelwahab,roman.yampolskiy}@louisville.edu  
<https://louisville.edu/speed/computer>

**Abstract.** Approximation algorithms are often employed on hard optimization problems due to the vastness of the search spaces. Many approximation methods, such as evolutionary search, are often indeterminate and tend to converge to solutions that vary with each search attempt. If multiple search instances are executed, then the wisdom among the crowd of stochastic outcomes can be exploited by aggregating them to form a new solution that surpasses any individual result. Wisdom of artificial crowds (WoAC), which is inspired by the wisdom of crowds phenomenon, is a post-processing metaheuristic that performs this function. The aggregation method of WoAC is instrumental in producing results that consistently outperform the best individual. This paper extends the contributions of existing work on WoAC by investigating the performance of several aggregation methods. Specifically, existing and newly proposed WoAC aggregation methods are used to synthesize parallel genetic algorithm (GA) searches on a series of traveling salesman problems (TSPs), and the performance of each approach is compared. Our proposed method of weighting the input of crowd members and incrementally increasing the crowd size is shown to improve the chances of finding a solution that is superior to the best individual solution by 51% when compared to previous methods.

**Keywords:** Wisdom of crowds · Evolutionary combinatorial optimization · Aggregation metaheuristic · Parallel search aggregation

## 1 Introduction

Computing the optimal solution using an exhaustive search becomes intractable as the size of the problem grows for computationally hard (NP-hard) problems [1]. Consequently, heuristics and stochastic search algorithms are commonly used in an effort to find reasonable approximations to difficult problems in a polynomial time [1, 2]. These approximation algorithms are often incomplete and can produce indeterminate results that vary when repeated on larger search spaces [3, 4]. The variance produced by these types of searches, assuming several search attempts have been made, can be exploited in a collaborative effort to form better

approximations to difficult problems. The post-processing metaheuristic known as the Wisdom of Artificial Crowds (WoAC) is based on this concept [1,5]. In essence, the WoAC algorithm operates on a group of indeterminate search outcomes from the same problem space, and then aggregates them with the goal of forming a solution that is superior to any individual outcome within the group. It is inspired by a more widely known sociological phenomenon referred to as the Wisdom of Crowds (WoC) [6], and likewise, seeks to perform reasoning and aggregation based on commonality observed within a group of converged and best-fit search outcomes.

WoAC operates on a pool of converged search results that can be obtained via any indeterminate search method. Evolutionary algorithms, such as the genetic algorithm (GA) used in this paper, are well-suited for WoAC because they are easily parallelizable [3]. Multiple search instances can be conducted in parallel, which can speed up the process of generating a pool of best-fit candidate approximations.

The means of aggregating the group of best-fit solutions is the essence of WoAC, and this process is critical to the goal of producing a solution that is paramount to any individual contributor within the crowd of possible solutions. As a result, this paper focuses on the evaluating several means of WoAC aggregation. The primary contribution of this paper includes the introduction and evaluation of new methods for performing WoAC aggregation. We show that our proposed aggregation algorithm improves the consistency of forming a superior solution when compared to existing methods. Our findings also highlight some key factors that were previously unreported and that heavily influence the performance of WoAC. These factors include the importance of weighting the crowd members based on fitness and iteratively attempting aggregation after each new member has been added to the crowd.

This paper utilizes the well-known TSP as the combinatorial optimization problem for evaluating the aggregation components of the WoAC algorithm. As our search method, we employ a GA for generating pools of possible TSP solutions. We selected these options because of their familiarity among the research community, and as a result, abstract details about the fundamentals of the TSP and the GA. Instead, we focus our attention on the WoAC algorithm and note that the metaheuristic is applicable to a wide range of optimization problems and indeterminate search techniques other than the TSP and GA, respectively.

The remainder of this paper is organized as follows. Section 2 reviews the related research involving aggregation methods for WoC and WoAC. Subsequently, in Section 3, we review the existing WoAC algorithm, and also, provide the details on the newly proposed means of aggregation. Afterwards, we evaluate the experimental results in Section 4, and finally, we provide our conclusions and future work in Section 5.

## 2 Related Work

The concept of applying WoC to the TSP has shown promising results in several works. Yi and Dry aggregated human-generated TSP responses and demonstrated

that it is possible to generate an aggregate response that is superior to any individual [7]. This concept was extended to computer-generated TSP approximations by Yampolskiy and El-Barkouky [1] and was coined WoAC. In that study, 90% of the 20 contributors must agree on a TSP connection before it is kept as part of the aggregate. In another study [5], Yampolskiy, Ashby, and Hassan remove the 90% agreement stipulation and have the group of 10 GA outcomes vote with equal weights similar to [7].

Others researchers applied the concept of WoC with varying levels of success to other applications [8–12], but none of these studies compared different methods of aggregation, nor weighted the input of crowd members. Velic, Grzinic, and Padavic applied the WoC concept in a stock market prediction algorithm [12]. The algorithm at times produced results reflective of the group-think phenomenon, where less knowledgeable contributors negate the influence of highly experienced experts and negatively impact the outcome. In another study, Moore and Clayton tested the effect of WoC in detecting phishing websites and found that inexperienced users, who frequently made mistakes, often voted similarly [11]. Kittur and Kraut leveraged WoC in managing Wikipedia content and showed that coordination between writers on Wikipedia is vital for content quality, especially as the crowd size grows [10]. Yu et al. proposed a WoC-based algorithm for traffic route planning and used a non-Markovian aggregation tree for fusing the results from route planning agents [9]. In [8], Hoshen, Ben-Artzi, and Peleg proposed a means to combine multiple video streams into an improved video using the WoC concept. Lastly, WoAC has also been applied to a number of computer games [13–16].

Based on research using human groups, Wagner and Suh concluded that the size of the crowd influences the performance of WoC, and they found that improvement saturates as the crowd size grows beyond a certain size [17]. We suspect that crowd size also affects the performance of artificial crowds. Hence, this dynamic is investigated by our work, unlike the aforementioned studies.

Another dynamic that affects WoAC performance is the weight given to individual contributors. The related works of this section generally used an aggregation method that provided equal weight to each crowd member. When the worth of a contribution from an agent cannot be evaluated, then providing equal weight might be the only prudent option. However, in most combinatorial optimization problems, search results can be evaluated according to their performance with respect to other potential solutions. Giving more weight to better-performed members may be an important aspect to avoiding common mistakes (i.e. suboptimal choices) taken by several members of the crowd. In other words, problems, similar to the groupthink phenomenon observed in [12] and the common mistakes observed in [11], could be mitigated by favoring better performers and suppressing less fit contributors. The concept of merging multiple hypotheses using weight assignments has also been explored in ensemble learning. For instance, Puuronen et al. assigned different weights to the outputs of component classifiers based on their predicted classification error, and used a stacked (i.e. second-level) classifier to determine the final output based on the weighted votes received from

the component classifiers [17]. However, the weighting techniques explored in this paper are generated differently than in ensemble learning, and we apply the concept in the application domain of optimization, not supervised learning.

A final factor that likely impacts the performance of WoC, but was not investigated in the previous works, is the level of difficulty involved in the problem. As noted in a study using a group of human responses to various questions [18], the performance of WoC suffers as the task difficulty increases. We posit that the same holds true for artificial crowds and investigate this issue more closely in Section 4 and show how weighting opinions can mitigate this issue.

### 3 WoAC Algorithm Description

The original WoAC algorithm proposed in [5, 7] constructs new approximations to optimization problems based on the trends and commonality observed among the pool of candidate solutions. The identification of popular search selections (i.e. edge connections) is accomplished through a histogram matrix, which reflects the frequency of every edge option. In graph-based problems, the algorithm consists of scanning each individual graph, and then, recording its specific edge selections by updating the frequency counts stored in the matrix.

Similarly, we use an  $n \times n$  matrix that serves as a histogram for recording the frequency of TSP edge occurrences witnessed while examining each contributing proposal within the crowd; the variable,  $n$ , corresponds to the number of nodes in the TSP. Each position in the matrix (i.e. row and column combination) corresponds to a possible edge connection between nodes. The initial step of the WoAC algorithm is to review every search result within the crowd pool and update the histogram accordingly based on the observed edge connections of each solution. Once every search result is reviewed and the histogram matrix is fully constructed, the positions with higher values correspond to the more common selections made by the crowd members; hence, based on the WoC principle, such node connections tend to be wise choices that should be a part of the new route.

After the histogram is constructed, the WoAC algorithm then proceeds to build the new solution. For the TSP, this is accomplished by choosing a starting node and then searching the histogram's entire row or column corresponding to this particular node. The matrix position that has the highest value is selected as the adjacent node. This process is repeated for every adjacent node until the Hamiltonian cycle is complete. If a node is already in the newly constructed path, then the next highest occurrence is selected and so on. The objective function (i.e. spatial information) is only referenced if all options in the histogram have been exhausted, meaning that the crowd's preferred choices have already been selected as part of the newly constructed graph. In this case, a greedy heuristic is used to find the nearest node as the next destination based on the objective function. Finally, every node is attempted as the starting node and the route yielding the lowest cost is chosen as the WoAC solution.

### 3.1 Modifications to the WoAC Algorithm

We propose extending the aforementioned WoAC algorithm and incorporating two primary modifications. The first modification deals with weighting the suggestions from contributors based on the range of fitness observed in the crowd pool, instead of treating them equally as previously described. The new weighting process can easily be accomplished with minimal processing because the fitness scores of the candidates are already known from the convergence of each preliminary search. We propose two new types of weighted aggregation methods and later compare them to the equal weight distribution method of [5, 7]. In order to support these new means of weighting contributions, we modify the WoAC algorithm to maintain three separate histograms: one for each method of weighting.

The other alteration we propose to WoAC is to vary the crowd size by incrementally building and evaluating the weighted histograms. In other words, the modified WoAC algorithm would review the edge selections of an individual solution, then update each weighted histogram based on its fitness score with respect to the group, and afterwards, iterate through the WoAC aggregation process. This process is repeated for every member in the crowd pool. In contrast, the previous version of WoAC selects some arbitrary crowd size *a priori*, and then, complies their selection choices in a single histogram matrix before running the final aggregation process only once. Instead, we effectively vary the crowd size and build a new WoAC aggregate after every individual member is added to each histogram matrices. Once all crowd members have been considered, the lowest cost solution from all WoAC aggregation attempts would be propagated as the algorithm output.

**Percentage Weight.** The first considered aggregation alternative to the equal weight method used in [5, 7] is a simple percentage weight. The new method assigns a weight to each edge selection of a contributor based on its objective function ranking among its peers in the crowd pool. Assuming that minimal cost is desirable, we can represent the fitness of each candidate using

$$\underline{c} = \{c_1, c_2, \dots, c_n\} \quad (1)$$

where  $\underline{c}$  is the cost vector (i.e. array) that contains the fitness associated with each individual crowd member and  $n$  represents the total number of crowd members. Given the range of costs associated with the candidates, we can formulate a cost-distance using

$$d_i = \frac{c_i - \min(\underline{c})}{\max(\underline{c}) - \min(\underline{c})} \quad (2)$$

where  $d_i$  is the cost-distance ratio for the  $i^{th}$  member of the crowd. This calculation provides a ratio or a percentage of how far away a candidate's solution is from the best agent in the crowd with respect to the worst. This metric varies from 0-1, and as individual fitness scores approach the best, the metric

approaches zero. Finally, this ratio is transformed into a weight that is with respect to the candidate's proximity to the best agent by

$$w_{p_i} = 1 - d_i \quad (3)$$

where  $w_{p_i}$  is the percentage weight assigned to the  $i^{th}$  candidate's edge contributions, which are stored in the histogram dedicated for percentage weight. Using this approach, the best GA candidate solution among the crowd is given the full weight of one, while the worst candidate is ignored by assigning it zero.

**Exponential Weight.** In order to provide more weight to better-performed candidates and more rapidly diminish the contributions of those less favorable solutions, an exponential weighting algorithm for WoAC was also investigated. Specifically, the weight of individual contributions was based on the exponential function

$$w_{e_i} = e^{-x_i} \quad (4)$$

where  $w_{e_i}$  is the exponential weight of the  $i^{th}$  candidate in the crowd of suggested solutions and  $x_i$  is a constant that is associated with  $d_i$  above, which is a measure of the candidate's distance from the best option in the crowd. Specifically, the constant  $x_i$  is obtained by multiplying  $d_i$  by another constant,  $m$ , which facilitates the mapping of  $d_i$  to a range of values suitable for generating a weighting range from 0-1 using the exponential function. In the following equation,

$$x_i = d_i * m \quad (5)$$

$m$  is the constant that maps the ratio,  $d_i$ , to a range of values between 0 to  $m$ . Based on (5), the best option within the crowd would be assigned 0 because  $d_i$  would be 0, and the worst-fit candidate would be assigned  $m$  because  $d_i$  would be 1. Therefore, the weight assigned to an individual solution's contribution to the WoAC aggregate, as described in (4), would be a maximum of 1, while options with a higher cost (i.e. less fit) are assigned a weight less than 1. In this paper, we let  $m = 5$ , as  $e^{-5}$  is approximately zero, yielding a weighting factor that ranges from 1-0, with exponential decay as the candidate solution moves away from the top candidate.

### Pseudocode for the Modified WoAC

```

BEGIN
1 C1,C2,...,Cn = gather_crowd(n) //Perform n independent searches
2 best_performer = MAX(C1,C2,...,Cn) //Most-fit crowd member
3 worst_performer = MIN(C1,C2,...,Cn) //Least-fit crowd member
4 FOR i = 1 to n // Iterate through all crowd members
5     d = calc_dist_ratio(C(i)), best_performer,worst_performer)
        // see eqn. (2)
    
```

```

6      p(i) = calc_percent_weight(d)    // see eqn. (3)
7      e(i) = calc_exp_weight(d)      // see eqns. (4) & (5)
8      FOR j = 1 to edge_count    // Iterate through entire graph
9          row,column = identify_connected_vertices(C(i),j)
10         // given the current edge in cycle i,
11         // return the connected vertices
12         update_equal_histogram(row,column)
13         // update matrix position corresponding to
14         // connected vertices with: cnt = cnt + 1
15         update_percent_histogram(row,column,p(i))
16         // update matrix position corresponding to
17         // connected vertices with: cnt = cnt + p(i)
18         update_exp_histogram(row,column,e(i))
19         // update matrix position corresponding to
20         // connected vertices with: cnt = cnt + e(i)
21     ENDFOR
22     equal_graph = build_graph(equal_histogram)
23     percent_graph = build_graph(percent_histogram)
24     exp_graph = build_graph(exp_histogram)
25     current_best = MIN(equal_graph,percent_graph,exp_graph)
26     // find the least expense cycle from the 3 options
27     IF (current_best < overall_best) then
28         overall_best = current_best
29         // if new WoAC cycle is better than all previous,
30         // then store it
31     ENDIF
32 ENDFOR
END

```

## 4 Experimental Evaluation

### 4.1 Evaluation Overview

The modified WoAC algorithm was repetitively tested to evaluate its performance. Every trial run of the algorithm consisted of the following two-step process. First, a crowd (i.e. pool) of approximations were generated to a specific TSP by instantiating 30 GA searches. After the searches converged, the post-processing metaheuristic was executed according to the procedure outlined in Section 3. The best aggregate solutions of each method, as well as their respective crowd sizes, were logged for statistical purposes.

Before reviewing the evaluation statistics, we will provide some preliminary information about the testing environment. The evaluation process was repeated on four different TSP datasets, and a total of 100 trials were executed on each. The TSP datasets were randomly generated using Concorde [19], and the sizes and optimal (i.e. best-known) costs of each are displayed in Table 1. The optimal costs were obtained using the TSP solver in Concorde.

**Table 1.** Sizes and Optimal Costs of the TSP Datasets

Num. of Nodes	Best-known Cost
44	549
77	707
97	794
122	868

The parameters of the GA used on the TSP datasets are outlined in Table 2. A total of 30 parallel instances of the GA were allowed to search and converge before executing the WoAC algorithm. The GA generally produced crowd members (i.e. candidate approximations) that were near, but slightly suboptimal to the costs generated by Concorde. Therefore, there was opportunity for the WoAC algorithm to improve upon the pool of candidate solutions and aggregate them to form a new solution closer to the best-known optimum.

**Table 2.** Parameters of the Genetic Algorithm

GA Parameter	Setting
Population Size	20
Parent Selection	Fitness Tournament (uniformly random among top 5)
Crossover Operator	Single-point (uniformly random)
Mutation Operator	Combination of Two Mutation Steps: 1. Uniformly random 1% mutation 2. Greedy custom - adjacent node swap until improved

As an illustrative example of the evaluation procedure, Fig. 1 shows the evolutionary development of a crowd of GAs that worked on the 44 node TSP. After the convergence of all 30 search instances, the WoAC algorithm was initiated. The percentage and exponential weights assigned to the crowd members as part of the modified WoAC are also shown in Fig. 1. Together the plots indicate that the crowd had some diversity in opinions (i.e. edge selections), which is an important aspect in attempting to recombine these opinions into a unique aggregate. Some level of diversity is important, but the original WoAC algorithm is fundamentally based on making decisions using group consensus. However, the newly proposed weighting concept skews this fundamental bias towards group decision making, and instead, gives greater consideration to those contributors known to be wiser. The goal of the evaluation was to distinguish between these different approaches and to identify the most effective means of aggregating the crowd members to form superior solutions.

## 4.2 Evaluation Analysis

First, we will focus on the impact that weighting crowd members had on improving the chances of surpassing the best GA. The success rates of the different

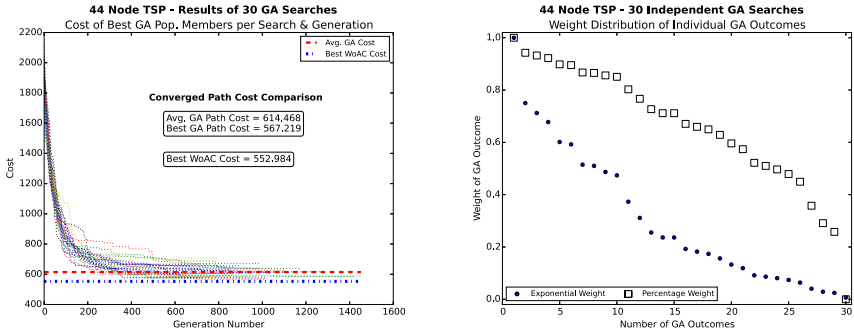


**Fig. 1.** The plot on the left shows the convergence of 30 independent instances of the same GA searching for the optimum tour on a TSP. The plot on the right corresponds to the exponential (*dotted*) and percentage (*square*) weights assigned to the 30 converged GA outcomes as part of the modified WoAC algorithm.

**Table 3.** Success Rate of the Modified WoAC Aggregation Methods

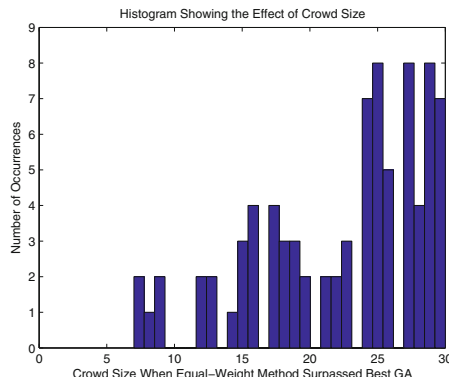
Dataset	Percent Success in Surpassing Best GA			
	Equal	Percentage	Exponential	Combined
TSP 44	22%	36%	36%	51%
TSP 77	52%	60%	48%	77%
TSP 97	4%	9%	32%	42%
TSP 122	5%	7%	33%	41%
All (Mean)	20.8%	28%	37.3%	52.8%

weighting techniques are summarized in Table 3. The percentages are based on the number of times the aggregation methods surpassed the best GA search, given that 100 evaluations were performed on each TSP dataset. From the table, it is evident that the exponential weighting method outperformed the other methods more consistently. On the other hand, the reliability of the equal- and percentage-weight techniques are shown to decrease as the TSPs became larger (i.e. more challenging). By comparing Tables 1 and 4, the GA crowd pool for the larger datasets are farther away from the global optimum and the pools are more spread apart (i.e. diverse). Therefore, the crowd was generally noisier (i.e. possessed less consensus) in these cases, which appeared to cause problems for the equal- and percentage-weighting schemes. These methods do not appear to provide a strong enough distinction between the candidates' performances in these noisy environments. In contrast, the exponential technique favors the wiser contributors more than the others, while also diminishing the opinions of the more inferior candidates. Overall, the results show that biasing the input of stronger contributors is critical to improving the success rate of the WoAC algorithm.

**Table 4.** Mean Costs ( $\mu$ ) and Standard Deviations ( $\sigma$ ) of Crowd Members and WoAC Aggregates

Dataset	Crowd of GAs		Best GA		Equal		Percentage		Exponential	
	$\mu$	$\sigma$	$\mu$	$\sigma$	$\mu$	$\sigma$	$\mu$	$\sigma$	$\mu$	$\sigma$
TSP 44	613.3	26.5	566.4	7.3	576.3	12.6	570.8	10.9	565.1	9.1
TSP 77	827.2	37.2	761.6	12.5	760.3	19.5	755.5	18.3	757.8	16.4
TSP 97	944.0	41.0	868.6	14.8	915.0	28.7	895.8	23.9	873.9	22.0
TSP 122	1044.9	45.5	963.2	13.7	1007.8	30.2	994.3	24.0	969.5	21.8

The other dynamic investigated during the evaluation of the modified WoAC algorithm was the concept of varying the crowd size and incrementally adding new opinions (i.e. approximations) to the crowd one-at-a-time. In the original WoAC algorithm [1,5], a fixed crowd size was determined *a priori* and all opinions were aggregated only once after considering the votes from all contributors. The success rate for the equal-weight technique in Table 3 was based on varying the crowd size; however, if the crowd size was not varied and fixed at 30, then the mean success rate of the equal-weight technique would drop to 1.8%, given the results from all the TSP trials (i.e. 400 experiments). To better visualize the impact of crowd size, Fig. 2 shows a histogram of the number of members in the crowd when the equal-weight technique successfully surpassed the best GA during the 400 trials. It indicates that the number of opinions needed to outperform the best GA is unpredictable and should not be fixed *a priori*; therefore, varying the crowd size is effective at mitigating this challenge and improving the success rate of the metaheuristic.

**Fig. 2.** The crowd size at the time when the equal-weight technique surpassed the best GA. This statistic, which is based on 400 trials from all TSP datasets, is plotted as a histogram.

In summary, the experimental results show that weighting the opinions of crowd members and varying the crowd size are vital to the success of WoAC. For instance, if we consider that the original configuration of the algorithm (i.e. fixed crowd size and equal-weight) succeeded 1.8% of the time, and that the combined success rate of the modified WoAC (i.e. all weighting techniques and variable crowd size) was 52.8% (see Table 3), then the new approach improved the algorithm's success rate by 51%.

### 4.3 Conclusion and Future Work

This paper investigated ways of improving the WoAC metaheuristic, which aggregates collective searches in an attempt to form superior approximations to computationally-hard problems. Specifically, we explored the heuristic's means of aggregation and discovered the critical factors that influence its performance. As a result, we proposed two beneficial modifications to the algorithm, which significantly improved its performance in surpassing the best candidate within the crowd. These modifications include iteratively adjusting the crowd size and intelligently weighting the input of the crowd members based on their fitness within the pool.

The crowds (i.e. converged searches) generated in this paper were collected using several parallel instances of the same genetic algorithm (GA). In the future, we are interested in using non-uniform GAs as part of the crowd gathering process. Such an approach could introduce more diversified opinions within the crowd and provide the potential for increased performance. However, with increased diversity, we suspect that assigning weights to the better-performed outcomes would become even more important in order to dampen the noise in the crowd caused by less efficient contributors. We are also interested in applying WoAC to other computationally hard problems and comparing its performance to other metaheuristics.

## References

- Yampolskiy, R.V., El-Barkouky, A.: Wisdom of artificial crowds algorithm for solving NP-hard problems. *International Journal of Bio-Inspired Computation* **3**(6), 358–369 (2011)
- Collet, P., Rennard, J.-P.: Stochastic optimization algorithms (2007). arXiv preprint [arXiv:0704.3780](https://arxiv.org/abs/0704.3780)
- Hoos, H.H., Sttzle, T.: Stochastic search algorithms, vol. 156. Springer (2007)
- Kautz, H.A., Sabharwal, A., Selman, B.: Incomplete Algorithms. *Handbook of Satisfiability* **185**, 185–204 (2009)
- Yampolskiy, R.V., Ashby, L., Hassan, L.: Wisdom of Artificial Crowds - A Meta-heuristic Algorithm for Optimization. *Journal of Intelligent Learning Systems and Applications* **4**, 98 (2012)
- Surowiecki, J.: The wisdom of crowds. Random House LLC (2005)
- Yi, S.K.M., Steyvers, M., Lee, M.D., Dry, M.: Wisdom of the Crowds in Traveling Salesman Problems. *Memory and Cognition* **39**, 914–992 (2011)

8. Hoshen, Y., Ben-Artzi, G., Peleg, S.: Wisdom of the crowd in egocentric video curation. In: 2014 IEEE Conference on Computer Vision and Pattern Recognition Workshops (CVPRW), pp. 587–593, June 23–28, 2014
9. Jiangbo, Y., Kian Hsiang, L., Oran, A., Jaillet, P.: Hierarchical Bayesian nonparametric approach to modeling and learning the wisdom of crowds of urban traffic route planning agents. In: 2012 IEEE/WIC/ACM International Conferences on Web Intelligence and Intelligent Agent Technology (WI-IAT), pp. 478–485, December 4–7, 2012
10. Kittur, A., Kraut, R.E.: Harnessing the wisdom of crowds in wikipedia: quality through coordination. Paper presented at the Proceedings of the 2008 ACM conference on Computer supported cooperative work, San Diego, CA, USA
11. Moore, T., Clayton, R.C.: Evaluating the wisdom of crowds in assessing phishing websites. In: Tsudik, G. (ed.) FC 2008. LNCS, vol. 5143, pp. 16–30. Springer, Heidelberg (2008)
12. Velic, M., Grzinic, T., Padavic, I.: Wisdom of crowds algorithm for stock market predictions. In: Proceedings of the International Conference on Information Technology Interfaces, ITI, pp. 137–144 (2013)
13. Ashby, L.H., Yampolskiy, R.V.: Genetic algorithm and wisdom of artificial crowds algorithm applied to light up. In: 2011 16th International Conference on Computer Games (CGAMES), pp. 27–32, July 27–30, 2011
14. Hughes, R., Yampolskiy, R.V.: Solving Sudoku Puzzles with Wisdom of Artificial Crowds. International Journal of Intelligent Games and Simulation **7**(1), 6 (2013)
15. Khalifa, A.B., Yampolskiy, R.V.: GA with Wisdom of Artificial Crowds for Solving Mastermind Satisfiability Problem. International Journal of Intelligent Games and Simulation **6**(2), 6 (2011)
16. Port, A.C., Yampolskiy, R.V.: Using a GA and wisdom of artificial crowds to solve solitaire battleship puzzles. In: 2012 17th International Conference on Computer Games (CGAMES), pp. 25–29, July 30, 2012–August 1, 2012
17. Puuronen, S., Terziyan, V., Tsymbal, A.: A dynamic integration algorithm for an ensemble of classifiers. In: Ra, Z., Skowron, A. (eds.) Foundations of Intelligent Systems. Lecture Notes in Computer Science, vol. 1609, pp. 592–600. Springer, Berlin Heidelberg (1999)
18. Wagner, C., Ayoung, S.: The wisdom of crowds: impact of collective size and expertise transfer on collective performance. In: 2014 47th Hawaii International Conference on System Sciences (HICSS), pp. 594–603, January 6–9, 2014
19. Concorde TSP Solver. <http://www.math.uwaterloo.ca/tsp/concorde/index.html>

# The Influence of Topology in Coordinating Collective Decision-Making in Bio-hybrid Societies

Rob Mills<sup>(✉)</sup> and Luís Correia

BioISI – Biosystems and Integrative Sciences Institute,  
Faculty of Sciences, University of Lisbon, Lisbon, Portugal  
[rob.mills@fc.ul.pt](mailto:rob.mills@fc.ul.pt)

**Abstract.** Collective behaviours are widespread across the animal kingdom, many of which result from self-organised processes, making it difficult to understand the individual behaviours that give rise to such results. One method to improve our understanding is to develop bio-hybrid societies, in which robots and animals interact, combining elements whose behaviours are under our control (robots) with elements that are not (animals). Recent work has shown that a bio-hybrid society comprising simulated robots and honeybees is able to reach collective decisions that are the product of self-organisation among the robots and the bees, and that these decisions can be coordinated across multiple groups that reside in distinct habitats via robot–robot communication. Here we examine how sensitive the collective decision-making is to the specific topologies of information sharing in such bio-hybrid societies, using agent-based simulation modelling. We find that collective decision-making across multiple groups occupying distinct habitats is possible for a range of inter-habitat interaction topologies, where the rate of coordinated outcomes has a positive relationship with the number of inter-habitat links. This indicates that system-wide coordination states are relatively robust and do not require as strong inter-habitat coupling as had previously been used.

**Keywords:** Collective behaviour · Mixed animal-robot societies

## 1 Introduction

Social living is integral to organisms across many magnitudes of scale and complexity, from bacterial biofilms [1] to primates [2], and such societies frequently exhibit behaviours at the level of the collective, such as moving together by following a leader [3] or self-organised aggregation [4]. Many social animals and behaviours have a substantial impact on humanity, both beneficial (*e.g.*, pollination) and detrimental (*e.g.*, spread of disease). Since collective behaviours can emerge from a combination of self-organised interactions, it can be problematic to understand what triggers, modulates, or suppresses their emergence. One emerging methodology used to examine collective behaviours is to develop

bio-hybrid societies, in which robots are integrated into the animal society [5, 6]. In so doing, such an approach allows direct testing of hypotheses regarding individual behaviours and how they are modulated by the group context (for example, confirming a hypothesised behaviour by showing that a collective behaviour is not changed when some animals are substituted by robots [6]). Alternatively, it becomes possible to use robot behaviours that can manipulate the overall collective behaviours [5].

Our research aims to develop bio-hybrid societies, ultimately comprising multiple species that interact with robots, which thus form an interface between animals that need not naturally share a habitat. Interfacing in this manner has the added advantage that we can monitor precisely what information is exchanged between animal groups (and permits experiments that attenuate or amplify specific information types). To move towards addressing this overarching aim, here we use a simplified system that comprises multiple populations of the same species, and we examine this using individual-based simulation modelling.

In recent work, it has been shown that juvenile honeybees interacting with robots can reach collective decisions jointly with those robots, and moreover, that such collective decisions can be coordinated across multiple populations of animals that reside in distinct habitats [7]. This work showed that robots using cross-inhibition and local excitation led to high levels of collective decision-making. However, it only compared ‘all-or-nothing’ coupling between the two habitats. In this paper, we examine the sensitivity of decision-making and coordination of those decisions across arenas, with respect to the inter-robot communication topology. We find that even relatively sparse numbers of links between habitats can be sufficient to coordinate outcomes across those habitats. These findings improve our understanding about the interactions that are sufficient to coordinate behaviours among separated groups of animals, and the limits that can be tolerated.

## 1.1 Related Work

Individual-based modelling and embodiment of behaviour in robots are becoming increasingly used as tools for studying animal behaviour, at both the individual level [8] and the collective level [9, 10]. Moreover, rather than merely attempt to replicate (or to abstract) a behaviour under study with robots, using robots to interact with animals can enable investigation of social behaviours in a more direct way [6]. For instance, [3] present a programmable fish that is used to investigate leadership among fish movement. [5] present robot cockroaches that are accepted by the insects, and together exhibit group dynamics equivalent to wholly animal societies. This work also showed that by changing the behaviour of the robots they could modulate the overall collective decisions reached.

Honeybees are another social insect that aggregate in environmental regions that they favour: [11] studies thermal conditions (rather than the light level preferences in cockroaches). Individual animals do not systematically select these preferred regions however: it is a collective decision that depends on being part of a group of a sufficient size [12].

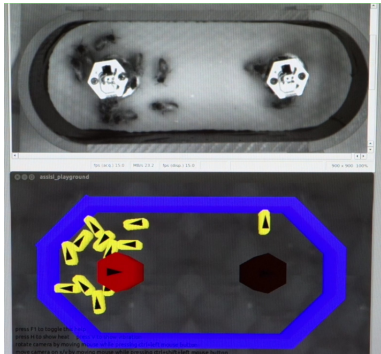


**Fig. 1.** A preliminary experiment with a hybrid society comprising robots, real bees, virtual bees and simulated robots, yielding collective decisions among virtual and real bees.

Our recent work [7] has examined how collective decisions can be reached by hybrid animal–robot societies, with individual-based simulation following preliminary work that coupled real bees to simulated bees via physical and simulated robots (see Fig. 1). This work uses robots that are able to manipulate key environmental variables for honeybees, including the temperature, light, and vibration in the vicinity of the robot [13], as well as being able to detect the presence of bees nearby. Using two robots, when we introduced a positive feedback loop between the heat each robot emits and the presence of bees nearby, the animals make a collective decision by aggregating around one of the robots. There was nothing to discriminate between the robots to start with, but the action of the bee population breaks symmetry – initially by chance, but reinforced by one or other robot. Moreover, we also showed that collective decisions made in two separate arenas, each with a population of bees and two robots, can be coordinated when the robots share task-specific information with another robot in the other arena. The current paper builds on these results, examining the influence of the inter-robot links used to couple two arenas of simulated honeybees.

## 2 Methods

We use a real-time platform for 2D robot simulation<sup>1</sup> to simulate the interaction of bees and robots. We model both bees and robots as agents in this world, making use of a basic motile robot for the bees, and use a fixed robot with a customised model that corresponds to the bespoke robots designed in our laboratory-based work [13]. While simulation modelling cannot fully replace reality, it does allow us to explore relationships between key micro-level mechanisms and how these can give rise to observed macro-level dynamics. The simulator design enables execution of the exact same robot controllers in simulation

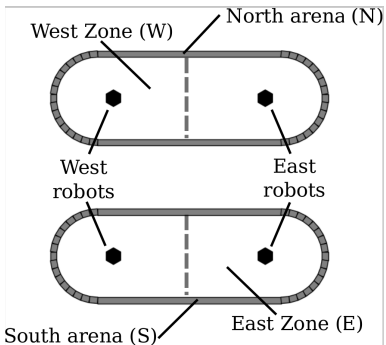


**Fig. 2.** How we split and name the arenas into zones during the analysis.

<sup>1</sup> Enki – an open source fast 2D robot simulator <http://home.gna.org/enki/>

and the physical robots, adding substantial value to the resolution of models employed, within the larger cycle of modelling and empirical work.

We model juvenile honeybee behaviour using Beeclust [14]. This is a social model that results in aggregations in zones of highly favoured stimulus. This model was developed based on observations of honeybees: specifically, that they exhibit a preference to aggregate in regions with temperatures in the range 34°C–38°C; that groups of bees are able to identify optimal temperature zones, but individual bees do not do so; and that specific inter-animal chemical cues (*e.g.*, pheromones) have not been shown to be important in this collective aggregation [14]. It has previously been used to illustrate light-seeking behaviour in a swarm of robots [9]. Here we simulate the bees in a thermal environment.

The robot and bee models used in this work are the same as those in [7] and for completeness we describe them fully in the remainder of this section.

## 2.1 Bee Model

There are two main phases in the bee behaviour: (i) random exploration; and (ii) pausing; in addition to obstacle avoidance (this interrupts (i)). When a bee encounters or collides with another bee, it enters the pausing state, and remains paused for a duration proportional to the local temperature (warmer regions yield longer pauses). There is a positive feedback loop between pause duration and the chance of further exploring bees encountering a bee in a given location, and thus an aggregation in a warm zone can undergo amplification.

We model bees that can discriminate between conspecifics and inanimate obstacles at close proximity, using infra-red (IR) sensors that provide a distance  $d$  and object type  $y$ . The bees have three sensors  $l, f, r$  that are oriented at  $-45^\circ$ ,  $0^\circ$ ,  $+45^\circ$  relative to the bee's bearing. The behaviour is defined as follows.

loop:

1. **delay(dt)**
2.  $((y_l, y_f, y_r), (d_l, d_f, d_r)) \leftarrow \text{read\_sensors}(l, f, r)$
3. if  $\exists i, (d_i < 0.5 \wedge y_i = \text{bee})$ , for  $i \in [l, f, r]$ ,
  - (a) **stop()**
  - (b)  $T \leftarrow \text{measure temperature}$
  - (c)  $t_{\text{wait}} \leftarrow \text{compute\_wait}(T)$
  - (d) **sleep( $t_{\text{wait}}$ )**
  - (e) **random\\_turn()**
4. else if  $\exists i, (d_i < 0.5 \wedge y_i = \text{obstacle})$ , for  $i \in [l, f, r]$ ,
**random\\_turn()**
5. else:
**forwards()**

end loop

We use data observed in juvenile honeybees (collected and analysed by Univ. Graz, fitted with a hill function) to define the **compute\_wait( $T$ )** mapping:

$$t_{\text{wait}} = \left( \frac{(a + b \cdot T)^c}{(a + b \cdot T)^c + d^c} \right) \cdot e + f, \quad (1)$$

where  $a = 3.09$ ,  $b = -0.0403$ ,  $c = -28.5$ ,  $d = 1.79$ ,  $e = 22.5$ , and  $f = 0.645$ . It is similar to a sigmoid, with low waiting times ( $\sim 1$  s) for  $T < 25^\circ\text{C}$  and high waiting times ( $\sim 25$  s) for  $T = 38^\circ\text{C}$ .

## 2.2 Robot Controller

In our research we employ custom-designed robotic devices which are able to generate stimuli of several modalities that the animals are sensitive to, including heat and light; and the robots can also sense various environmental factors (*e.g.*, temperature, IR) [13]. The robots occupy fixed positions within the experimental arenas to interact with the animals. In this paper we use the robots' thermal actuators and 6 IR proximity sensors. The robots can also communicate with specific neighbours (the topologies are described below). The following program defines how the robots determine their temperatures through time.

At initialisation: set vector  $m$  of length  $m_{max}$  to zero for  $m[0]..m[m_{max} - 1]$ . For each timestep,  $t$ :

1.  $d_{raw} \leftarrow$  count IR sensors above their threshold
2.  $m[\text{mod}(t, m_{max})] \leftarrow \text{saturate}(d_{raw})$
3.  $\text{send}(\hat{m}, \text{neighbours})$
4. if  $\text{mod}(t, t_{update}) = 0$ :
  - (a)  $\mathbf{d}_x \leftarrow$  receive message(s) from  $\text{neighbour(s)}$
  - (b)  $T_{new} \leftarrow \text{density\_to\_heat}(\hat{m}, \mathbf{d}_x)$

where  $d_{raw}$  is a raw estimate of local bee density in a given timestep,  $\hat{m}$  is a time-averaged estimate computed as the mean value of the memory vector  $m$ ,  $\mathbf{d}_x$  is a vector of density estimates received from other robots in the interaction neighbourhood. In this paper, robots have zero, one, or two neighbours depending on the specific topology under test.

We use  $\text{saturate}(s) = \min(4, s)$  in this study. The density to heat function maps the time-averaged detection count to an output temperature via a linear transformation, and is parameterised to allow for different topologies examined. Each involved robot  $x$  makes a contribution  $c_x = \frac{\hat{d}_x}{4}(T_{max} - T_{min})$  that depends on a robot's temperature. These are combined as a weighted sum:

$$T_{new} = T_{min} + \sum_{x \in \{l, r, c\}} c_x w_x, \quad (2)$$

where the relative weights of each robot's contribution depends on the specific setup. Each robot can be influenced by the local environment  $c_l$ , cross-inhibitory signals from a competitor  $c_c$ , and collaborative signals from a specific remote robot  $c_r$ . In this paper we use cross-inhibition  $w_c = -0.5$  throughout. When a robot has an incoming collaborative link then we set  $w_l = w_r = 0.5$ , and otherwise set  $w_l = 1$  and  $w_r = 0$ . The topologies tested are shown below.

### 2.3 Measuring Collective Decisions

Characterising behaviours at the group level is not as clear cut as for decisions at the individual level. However, by using binary choice assays where individuals can exhibit a clear choice, we can use statistical tests to formally quantify when the frequency of choices differs significantly from an accidental outcome. We follow the methodology of [5] and [12] that uses the binomial test to formally quantify when a collective decision is reached. Extending the setup to include multiple binary choices affords these benefits of quantifiable behaviours at the level of collective while also admitting more complex environments.

Specifically, at the end of each experiment, we divide the location of the bees into two different zones within each arena, such that one of the two robots has ‘won’ the competition for that bee (see Fig. 2). We define the null hypothesis to be that the bees made their choice at random and without bias. When the outcome differs significantly from this, we consider it a collective decision (CD).

Since here we concentrate on the ability to coordinate the collective decisions (CCD) reached in two arenas, we also consider a test that lumps together all bees from both populations, as if they were in a single group. We use the binomial test to quantify when such outcomes are significant within a single experiment. We also apply  $\chi^2$  tests and binomial tests across a set of repeats and between different conditions, to verify when outcomes are significantly different.

### 2.4 Parameters and Setup

With our choices, we aim to reflect key conditions used in our animal-based experiments, such as the arena and robot setup, and the temperatures used are in a range that is relevant for the animals without harming them.

In the experiments below,  $T_{min} = 28^\circ\text{C}$  and  $T_{max} = 38^\circ\text{C}$ ; the ambient temperature is  $27^\circ\text{C}$ . The modelled bees measure  $13.5 \text{ mm} \times 5 \text{ mm}$  (based on our measurements), and detection range is 5 mm. Memory length  $m_{max} = 18$ ,  $t_{update} = 3 \text{ s}$ ,  $t_{resample} = 0.5 \text{ s}$ . Since other methods did not provide more accurate estimates in preliminary testing we use a simple time average across the whole memory  $m$ . To facilitate the observation of binary choices, the arenas used are rectangular with rounded ends (see Fig. 1). They have dimensions  $210 \times 65 \text{ mm}$  (internal). The two robots are positioned 60 mm either side of the centre, on the midline. Bees are initialised with random position and orientation.

## 3 Simulation Experiments

This paper aims to examine the sensitivity of coordinating collective decision-making between arenas as a function of inter-arena communication links. To address this aim, we examine a range of different topologies within the limits examined in prior work, employing a basic setup that uses two identical arenas, each comprising a population of bees and two robots. We vary the inter-arena links, keeping the link weights positive where present. We use six different topologies that vary in the number and direction of coupling that they provide between

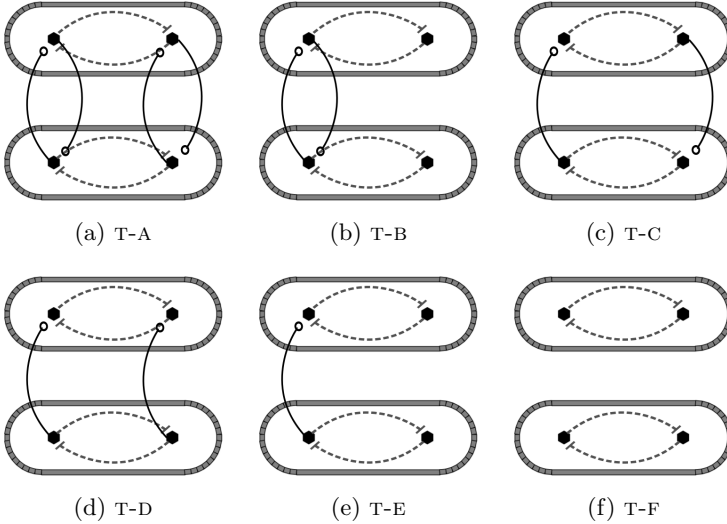


**Fig. 3.** Topologies tested in the multi-arena experiments. Solid lines indicate positive contributions and dashed lines indicate negative contributions, with respect to the receiving robot. From top-left to bottom-right, the two arenas become more loosely coupled.

the two arenas. Fig. 3 shows these topologies. Moving from top-left to bottom-right, T-A has the strongest coupling; T-B and T-C have some reciprocal paths; T-D and T-E have links in one direction only. T-F is the other extreme without any between-arena links, which we use to establish a baseline for the other outcomes. These motifs give broad coverage of the space and while other topologies are possible with more links or more classes of link, our motivation to understand sparser networks is better served by these networks with fewer rather than more inter-arena links.

Our prior work showed strong coordination under (a) and confirmed that the absence of links (f) does not lead to coordination [7]. Intuitively, we expect a weaker ability to coordinate as the links become sparser; however, we do not know what the limits are or how gracefully the system will degrade.

We run 50 independent repeats for each of the six topologies, each experiment lasting for 15 mins. Fig. 5 shows the frequency of statistically collective decisions made, for each of the topologies. Fig. 4 provides a slightly different view of the experiments by showing the mean percentage of bees that were present in the east Zone during the last 120 s. All 50 repeats in each topology have a point plotted in this graph, and while it is not always the case that the points in the extremes correspond to a significant collective decision at the time of measurement, the two views are strongly linked.

Considering the distributions shown in Fig. 5, we perform the following statistical tests to identify the collective decision-making and coordination that arises

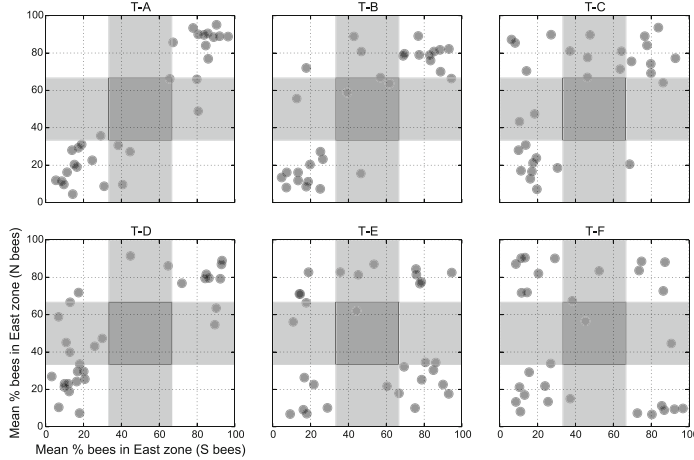


**Fig. 4.** Final states of each of the topologies, with one point shown per experiment. When the system has coordinated the decisions made in each arena, the points only appear in two of the four corners (indicating that the decisions are mutually constrained).

under each topology. Using a  $\chi^2$  test with a null model of equal likelihood for each of the four possible decision pairings, topologies T-E and T-F do not deviate significantly from the null model ( $\rho > 0.05$ ). The other four topologies all deviate significantly, *i.e.*, they exhibit coordination between the two arenas. We also compare the overall rate of collective decision-making across different topologies. The three cases that use two links (T-B, T-C, T-D) have similar ability to induce coordinated collective decisions as T-A (binomial test,  $\rho > 0.05$ ). Comparing the rate of collective decision within the two arenas separately (*i.e.*, any of the four outcomes), T-B, T-C, T-E have significantly lower rates than T-A (binomial test,  $\rho < 0.05$ ); however, although the T-D rate is lower, it is not significantly lower ( $\rho > 0.05$ ). None of the topologies exhibit a bias towards either coordinated outcome (binomial test,  $\rho > 0.05$ ), with the exception of T-D ( $\rho < 0.05$ ).

Overall, these results show that: (i) All topologies with two or more links coupling the two arenas are able to coordinate the decision-making. T-E, the sparsest topology, is not able to reliably coordinate the decision-making (nor is the unlinked case T-F but of course this is to be expected). (ii) Most of the sparser topologies are less frequently able to induce collective decision-making than the most tightly linked case T-A. T-D is a marginal exception in this regard. (iii) T-D exhibits some anomalies regarding a bias towards the WW outcome over the EE outcome. Given the absence of bias in the model or the topology, this is somewhat surprising and requires further investigation to identify the source of this bias.

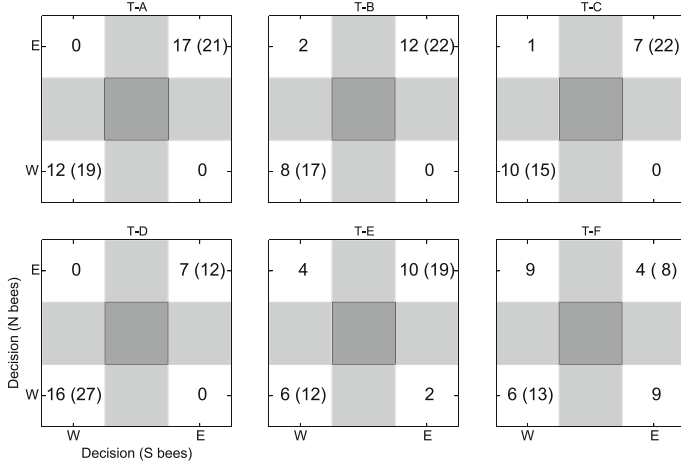


**Fig. 5.** Frequency of runs with significant collective decisions, from 50 repeats. Values in brackets indicate the frequency of coordinated collective decisions made, i.e., lumping together both populations. Other values indicate assessment of the two populations separately.

To obtain a better understanding of the differences between the different conditions, we inspect some example trajectories (Fig. 6), which illustrate some of the issues faced by different topologies. (The runs are characteristic of several seen in each case, but frame (c) was selected to highlight a difficulty rather than be the most frequent trajectory type). These figures divide the bee locations into two zones per arena, one for each robot (see Fig. 2). We compute the average percentage of bees in the East zone during each period (here, 30 s), and additionally, apply a binomial test to quantify whether a significant collective decision is reached at the end of each period (for  $\rho < 0.05$ ). In frame (a), we see that the strong coupling of T-A results in tight changes in bee location in each arena. In frame (b), the two populations initially move towards opposite ends, but as the decision in the South arena solidifies, it is able to coordinate this decision with the North arena. The progression of the two populations is not typically as tightly in lock-step as for T-A, with reciprocal feedback, but the topology does result in coordination with a high frequency. In frame (c) there is only one link (T-E), and it is far slower for the South arena to exert a coordinating influence over the North arena. In this case it was able to coordinate within 15 mins, but in other cases different decisions are reached in each arena and the single link is not always able to overturn the result.

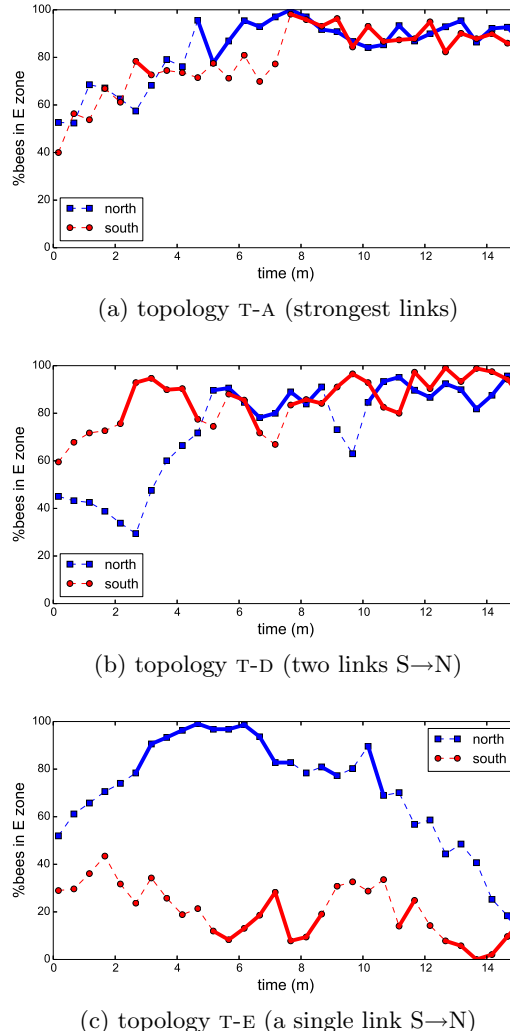


**Fig. 6.** Example trajectories showing a fraction of bees in East half of each arena, and annotated for where the collective decisions are made with thick, solid lines.

## 4 Discussion and Future Work

The different topologies vary in strength of coupling between the two arenas, and this also results in varying abilities to coordinate the collective decisions reached within those arenas. With four links in two reciprocal pairs (T-A), the activity in the two arenas is tightly coupled and reliably results in coordination across both bee populations. With two links forming a reciprocal network (T-B, T-C), the two arenas still coordinate frequently, although to a lesser extent than for T-A. Using two links in the same direction (T-D) is able to couple the decisions made at a slightly higher rate than the other two-link topologies, although clearly the

single direction of information-sharing may not always be appropriate. Using only a single link (T-E) is not sufficient coupling to significantly coordinate the decisions made across the two arenas.

In summary, we find that the topology influences the ability of multiple populations to coordinate their activities, but also that relatively few links are still sufficient to result in some coordination. This is welcome news, since it suggests that such distributed collective systems will exhibit favourable tolerance to failures in links (provided some ability to detect those failures – for instance, monitoring an absence of messages received over a given link could be used to adapt the robot’s behaviour). Moreover, as we begin to consider larger systems, sparse networks of localised interactions are generally preferable.

The scenarios modelled above all have static background environments. We are also interested in how dynamic environments (*e.g.*, exogenous shocks) affect coordination ability. This introduces the question: can the overall system restore a coordinated state following disruption? which may more strongly discriminate between different topologies. Perturbations could be due to an exogenous heat source, or another stimulus modality that modulates the bee behaviour (for example, it is thought that vibrations can act as stop signals). Interestingly, when considering a multi-species bio-hybrid system, the source of variability could also be endogenous, and the role of the robots in enabling coordination would be even greater. In any of these more dynamic scenarios, it would become important to measure the speed of coordinated decision-making, as well as the longevity (see *e.g.*, [15]). A further open question relates to the advantages and tradeoffs within an extended system comprising more sub-groups of animals (each of which offers some distributed ‘memory’ of a coordinated decision): more smaller groups may be better able to retain a decision; but dividing into groups that are too small will likely degrade the ability of each group to form a decision in the first place. In more complex scenarios such as these we aim to investigate how further adaptive mechanisms within the robot network can improve efficiency.

In this paper we have investigated how inter-robot interaction topology influences the ability of system-level coordinated decisions. We have shown that the rate of coordination does depend on topology, but also that the basin of attraction for coordinated states is relatively robust. In general, better understanding the limits and affordances of interactions in such systems will enable the development of more capable mixed animal–robot societies.

**Acknowledgments.** This work is supported by: EU-ICU project “ASSISI|bf” no. 601074, and by centre grant (to BioISI, ref: UID/MULTI/04046/2013), from FCT/MCTES/ PIDDAC, Portugal.

## References

1. Nadell, C.D., Xavier, J.B., Foster, K.R.: The sociobiology of biofilms. *FEMS Microbiol. Rev.* **33**(1), 206–224 (2009)
2. King, A.J., Cowlishaw, G.: Leaders, followers, and group decision-making. *Commun. Integr. Biol.* **2**(2), 147–150 (2009)

3. Faria, J.J., Dyer, J.R., Clément, R.O., Couzin, I.D., Holt, N., Ward, A.J., Waters, D., Krause, J.: A novel method for investigating the collective behaviour of fish: introducing ‘robofish’. *Behav. Ecol. Sociobiol.* **64**(8), 1211–1218 (2010)
4. Parrish, J.K., Edelstein-Keshet, L.: Complexity, pattern, and evolutionary trade-offs in animal aggregation. *Science* **284**(5411), 99–101 (1999)
5. Halloy, J., Sempo, G., Caprari, G., Rivault, C., Asadpour, M., Tâche, F., Said, I., Durier, V., Canonge, S., Amé, J.M., et al.: Social integration of robots into groups of cockroaches to control self-organized choices. *Science* **318**(5853), 1155–1158 (2007)
6. De Schutter, G., Theraulaz, G., Deneubourg, J.L.: Animal-robots collective intelligence. *Ann. Math. Artif. Intel.* **31**(1–4), 223–238 (2001)
7. Mills, R., Zahadat, P., Silva, F., Miklic, D., Mariano, P., Schmickl, T., Correia, L.: Coordination of collective behaviours in spatially separated agents. In: *Proc. ECAL* (2015)
8. Webb, B.: Can robots make good models of biological behaviour? *Behav. Brain. Sci.* **24**(06), 1033–1050 (2001)
9. Kernbach, S., Thenius, R., Kernbach, O., Schmickl, T.: Re-embodiment of honeybee aggregation behavior in an artificial micro-robotic system. *Adapt. Behav.* **17**(3), 237–259 (2009)
10. Campo, A., Garnier, S., Dédriche, O., Zekkri, M., Dorigo, M.: Self-organized discrimination of resources. *PLoS ONE* **6**(5), e19888 (2011)
11. Grodzicki, P., Caputa, M.: Social versus individual behaviour: a comparative approach to thermal behaviour of the honeybee (*Apis mellifera* L.) and the american cockroach (*Periplaneta americana* L.). *J. Insect. Physiol.* **51**(3), 315–322 (2005)
12. Szopek, M., Schmickl, T., Thenius, R., Radspieler, G., Crailsheim, K.: Dynamics of collective decision making of honeybees in complex temperature fields. *PLoS ONE* **8**(10), e76250 (2013)
13. Griparic, K., Haus, T., Bogdan, S., Miklic, D.: Combined actuator sensor unit for interaction with honeybees. In: *Sensor Applications Symposium* (2015)
14. Schmickl, T., Thenius, R., Moeslinger, C., Radspieler, G., Kernbach, S., Szymanski, M., Crailsheim, K.: Get in touch: cooperative decision making based on robot-to-robot collisions. *Auton. Agent. Multi. Agent. Syst.* **18**(1), 133–155 (2009)
15. Gautrais, J., Michelena, P., Sibbald, A., Bon, R., Deneubourg, J.L.: Allelomimetic synchronization in merino sheep. *Anim. Behav.* **74**(5), 1443–1454 (2007)

# A Differential Evolution Algorithm for Optimization Including Linear Equality Constraints

Helio J.C. Barbosa<sup>1,2(✉)</sup>, Rodrigo L. Araujo<sup>2</sup>, and Heder S. Bernardino<sup>2</sup>

<sup>1</sup> Laboratório Nacional de Computação Científica, Petrópolis, RJ, Brazil  
[hcbm@lncc.br](mailto:hcbm@lncc.br)

<http://www.lncc.br/~hcbm>

<sup>2</sup> Universidade Federal de Juiz de Fora, Juiz de Fora, MG, Brazil  
[rdgleppaus@gmail.com](mailto:rdgleppaus@gmail.com), [heder@ice.ufjf.br](mailto:heder@ice.ufjf.br)  
<http://www.lncc.br/~hedersb>

**Abstract.** In this paper a differential evolution technique is proposed in order to tackle continuous optimization problems subject to a set of linear equality constraints, in addition to general non-linear equality and inequality constraints. The idea is to exactly satisfy the linear equality constraints, while the remaining constraints can be dealt with via standard constraint handling techniques for metaheuristics. A procedure is proposed in order to generate a random initial population which is feasible with respect to the linear equality constraints. Then a mutation scheme that maintains such feasibility is defined. The procedure is applied to test-problems from the literature and its performance is also compared with the case where the constraints are handled via a selection scheme or an adaptive penalty technique.

## 1 Introduction

Constrained optimization problems are common in many areas, and due to the growing complexity of the applications tackled, nature-inspired metaheuristics in general, and evolutionary algorithms in particular, are becoming increasingly popular. That is due to the fact that they can be readily applied to situations where the objective function(s) and/or constraints are not known as explicit functions of the decision variables, and when potentially expensive computer models must be run in order to compute the objective function and/or check the constraints every time a candidate solution needs to be evaluated.

As move operators are usually blind to the constraints (i.e. when operating upon feasible individuals they do not necessarily generate feasible offspring) standard metaheuristics must be equipped with a constraint handling technique. In simpler situations, repair techniques [18], special move operators [19], or special decoders [9] can be designed to ensure that all candidate solutions are feasible. We will not attempt to survey the current literature on constraint handling here, and the reader is referred to [4], [13], and [5].

Here we will focus on obtaining solutions automatically satisfying all linear equality constraints (in the form  $Ex = c$ ). Any remaining constraints present in the problem can be dealt with using constraint handling techniques available in the literature.

The first approach to this problem seems to be the GENOCOP system approach [14] where the linear equalities are used to eliminate some of the variables, which are now written as a function of the remaining ones, thus reducing the number of variables. As a result, any linear inequality constraint present in the problem has to be adequately modified. Another idea is that of the use of a homomorphous mapping [10] that transforms a space constrained by  $Ex = c$  into a space that is not only fully unconstrained, but also of lower dimensionality [15]. In [16] two modifications of the particle swarm optimization (PSO) technique were proposed to tackle linear equality constraints: LPSO and CLPSO. LPSO starts from a feasible initial population and then maintains feasibility by modifying the standard PSO formulas for particle velocity. CLPSO tries to improve on some observed shortcomings of LPSO and changes the equation for the best particle in the swarm so that it explores the feasible domain using a random velocity vector in the null space of  $E$ , that is, this velocity vector keeps the best particle feasible with respect to the linear equality constraints.

In this paper a simple modification of the differential evolution technique (denoted here by DELEqC) is proposed in order to exactly treat the linear equality constraints present in continuous optimization problems that may also include additional non-linear equality and inequality constraints, which can be dealt with via existing constraint handling techniques. Starting from a population which is feasible with respect to the linear equality constraints, feasibility is maintained by avoiding the standard DE crossover and using an adequate mutation scheme along the search process.

## 2 The Problem

The problem considered here is to find  $x \in \mathbb{R}^n$  that minimizes the objective function  $f(x)$  subject to  $m < n$  linear equality constraints, written as  $Ex = c$ , in addition to  $p$  general inequality constraints  $g_i(x) \leq 0$  and  $q$  general equality constraints  $h_j(x) = 0$ .

When using metaheuristics, general equality constraints are usually relaxed to  $|h_j(x)| \leq \epsilon$  where the parameter  $\epsilon > 0$  must be conveniently set by the user. As a result, candidate solutions strictly feasible with respect to all equality constraints are very hard to be obtained. Whenever  $x$  violates the  $j$ -th constraint one defines the corresponding constraint violation as  $v_j(x) = |h_j(x)| - \epsilon$  and aggregates for the individual  $x$  as  $v(x) = \sum_j v_j(x)$ .

Being able to exactly satisfy all linear equalities is a valuable improvement in a general constrained optimization setting, and should thus be pursued.

It is assumed here that the constraints are linearly independent so that  $E$  has full rank ( $\text{rank}(E) = m$ ). A candidate solution  $x_1 \in \mathbb{R}^n$  is said to be feasible if  $x_1 \in \mathcal{E}$  where  $\mathcal{E}$  denotes the feasible set:

$$\mathcal{E} = \{x \in \mathbb{R}^n : Ex = c\}$$

A vector  $d \in \mathbb{R}^n$  is said to be a feasible direction at the point  $x \in \mathcal{E}$  if  $x + d$  is feasible:  $E(x + d) = c$ . It follows that the feasible direction  $d$  must satisfy  $Ed = 0$  or, alternatively, that any feasible direction belongs to the null space of the matrix  $E$

$$\mathcal{N}(E) = \{x \in \mathbb{R}^n : Ex = 0\}$$

Now, given two feasible vectors  $x_1$  and  $x_2$  it is easy to see that  $d = x_1 - x_2$  is a feasible direction, as  $E(x_1 - x_2) = 0$ . As a result, one can see that the standard mutation formulae adopted within DE (see Section 3) would always generate a feasible vector whenever the vectors involved in the differences are themselves feasible. If crossover is avoided, one could start from a feasible random initial population and proceed, always generating feasible individuals.

### 3 Differential Evolution

Differential evolution (DE) [20] is a simple and effective algorithm for global optimization, specially for continuous variables. The basic operation performed is the addition to each design variable in a given candidate solution of a term which is the scaled difference between the values of such variable in other candidate solutions in the population. The number of differences applied, the way in which the individuals are selected, and the type of recombination performed define the DE variant (also called DE strategy). Although many DE variants can be found in the literature [17], the simplest one (DE/rand/1/bin) is adopted here:

$$u_{i,j,G+1} = x_{r_1,j,G} + F \cdot (x_{r_2,j,G} - x_{r_3,j,G})$$

where  $r_1, r_2$  and  $r_3$  correspond to distinct randomly picked indexes, and  $G$  denotes the iteration counter of the search technique.

In addition, in the general case, a crossover operation is performed, according to the parameter CR. However, in order to maintain feasibility, crossover is not performed in the proposed DE variant. Here,  $u_{i,j,G+1}$  replaces  $x_{i,j,G}$  when  $u$  is better than  $x$  for each  $i$ .

#### 3.1 A Selection Scheme

In order to handle the constraints, a popular technique is Deb's selection scheme [6] (denoted here by DSS) which enforces the following criteria: (i) any feasible solution is preferred to any infeasible solution, (ii) between two feasible solutions, the one having better objective function value is preferred, and (iii) between two infeasible solutions, the one having smaller constraint violation ( $v(x)$ ) is preferred.

### 3.2 An Adaptive Penalty Technique

A parameterless adaptive penalty method (APM) was developed in [2, 3, 11] which does not require the knowledge of the explicit form of the constraints as a function of the design variables, and is free of parameters to be set by the user. An adaptive scheme automatically sizes the penalty parameter corresponding to each constraint along the evolutionary process. The fitness function proposed is written as:

$$F(x) = \begin{cases} f(x), & \text{if } x \text{ is feasible,} \\ \bar{f}(x) + \sum_{j=1}^m k_j v_j(x), & \text{otherwise} \end{cases}$$

$$\bar{f}(x) = \begin{cases} f(x), & \text{if } f(x) > \langle f(x) \rangle, \\ \langle f(x) \rangle & \text{otherwise} \end{cases} \quad k_j = |\langle f(x) \rangle| \frac{\langle v_j(x) \rangle}{\sum_{l=1}^m |\langle v_l(x) \rangle|^2}$$

where  $\langle f(x) \rangle$  is the average of the objective function values in the current population and  $\langle v_l(x) \rangle$  is the violation of the  $l$ -th constraint averaged over the current population. The idea is that the values of the penalty coefficients should be distributed in a way that those constraints which are more difficult to be satisfied should have a relatively higher penalty coefficient.

## 4 The Proposal

Differently from penalty or selection schemes, and from special decoders, the proposed DE algorithm that satisfies linear equality constraints is classified as a feasibility preserving approach.

In order to generate a feasible initial population of size  $NP$  one could think of starting from a feasible vector  $x_0$  and proceed by moving from  $x_0$  along random feasible directions  $d_i$ :  $x_i = x_0 + d_i, i = 1, 2, \dots, NP$ . A random feasible direction can be obtained by projecting a random vector onto the null space of  $E$ . The projection matrix is given by [12]

$$P_{N(E)} = I - E^T (E E^T)^{-1} E \quad (1)$$

where the superscript  $T$  denotes transposition. Random feasible candidate solutions can then be generated as

$$x_i = x_0 + P_{N(E)} v_i, \quad i = 1, 2, \dots, NP$$

where  $v_i \in \mathbb{R}^n$  is randomly generated and  $x_0$  is computed as  $x_0 = E^T (E E^T)^{-1} c$ . It is clear that  $x_0$  is a feasible vector, as  $E x_0 = E E^T (E E^T)^{-1} c = c$ .

It should be mentioned that the matrix inversion in eq. 1 is not actually performed and, then,  $P_{N(E)}$  is never computed (see Algorithm 1).

The Differential Evolution for Linear Equality Constraints (DELEqC) algorithm is defined as DE/rand/1/bin, equipped with the feasible initial population generation procedure in Algorithm 1, and running without crossover.

Notice that any additional non-linear equality or inequality constraint can be dealt with via existing constraint handling techniques, such as those in sections 3.1 and 3.2.

**Algorithm 1.** Algorithm CreateInitialPopulation.

---

```

input : NP (population size)
1  $M = EE^T$  ;
2 Perform LU Decomposition:  $M = LU$  ;
3 Solve  $My = c$  ( $Lw = c$  and  $Uy = w$ ) ;
4  $x_0 = E^T y$  ;
5 for  $i \leftarrow 1$  to NP do
6    $d \in \mathbb{R}^n$  is randomly generated;
7    $z = Ed$ ;
8   Solve  $Mu = z$  ( $Lw = z$  and  $Uu = w$ ) ;
9    $v = E^T u$  ;
10   $x_i = x_0 + d - v$ ;
```

---

## 5 Computational Experiments

In order to test the proposal (DELEqC) and assess its performance, a set of test problems with linear equality constraints was taken from the literature (their descriptions are available in Appendix A). The results produced are then compared with those from alternative procedures available in the metaheuristics literature [15, 16], as well as running them with established constraint handling techniques (Deb's selection scheme and an adaptive penalty method) to enforce the linear equality constraints. One hundred independent runs were executed in all experiments.

Initially, computational experiments were performed aiming at selecting the values for population size (NP) and F. The tested values here are  $NP \in \{5, 10, 20, 30, \dots, 90, 100\}$  and  $F \in \{0.1, 0.2, \dots, 0.9, 1\}$ . Due the large number of combinations, performance profiles [7] were used to identify the parameters which generate the best results. We adopted the maximum budget allowed in [15, 16] as a stop criterion and the final objective function value as the quality metric. The area under the performance profiles curves [1] indicates that the best performing parameters according to these rules are  $NP = 50$  and  $F = 0.7$ , and these values were then used for all DEs in the computational experiments.

### 5.1 Results

First, we analyze how fast the proposed technique is in order to find the best known solution of each test-problem when compared with a DE using (i) Deb's selection scheme (DE+DSS) or (ii) an adaptive penalty method (DE+APM). The objective in this test case is to verify if DELEqC is able to obtain the best known solutions using a similar number of objective function evaluations. We used  $CR = 0.9$ ,  $NP = 50$ , and  $F = 0.7$  for both DE+DSS and DE+APM. Statistical information (best, median, mean, standard deviation, worst), obtained from 100 independent runs, The number of successful runs (sr) is also shown. A successful run is one in which the best known solution is found (absolute error less or

**Table 1.** Statistical comparisons. Number of objective function evaluations required to obtain the best known solution with a absolute error less or equal to  $10^{-4}$ . The bounds  $[-1000; 1000]$  were adopted for all test-problems. For DE+APM and DE+DSS, the tolerance for equality constraints is  $\epsilon = 0.0001$ .

	TP	technique	best	median	mean	st. dev.	worst	sr
		DELEqC	<b>2800</b>	<b>3475</b>	<b>3458.00</b>	$2.51e + 02$	<b>4050</b>	100
1	DE+APM	14750	16400	16456.50	$6.68e + 02$	18200	100	
		DE+DSS	16300	18350	18336.00	$7.54e + 02$	20250	100
		DELEqC	<b>2750</b>	<b>3300</b>	<b>3249.50</b>	$1.93e + 02$	<b>3600</b>	100
2	DE+APM	13050	15375	15385.00	$7.79e + 02$	17350	100	
		DE+DSS	16300	18100	18121.50	$6.92e + 02$	20150	100
		DELEqC	<b>1500</b>	<b>2050</b>	<b>2029.00</b>	$1.74e + 02$	<b>2400</b>	100
3	DE+APM	12950	14250	14256.50	$5.49e + 02$	15800	100	
		DE+DSS	18300	20225	20158.50	$7.68e + 02$	22000	100
		DELEqC	<b>1250</b>	<b>1900</b>	<b>1906.00</b>	$1.61e + 02$	<b>2250</b>	100
4	DE+APM	12250	14350	14280.00	$7.30e + 02$	15650	100	
		DE+DSS	17200	19000	19060.50	$7.60e + 02$	20800	100
		DELEqC	<b>1700</b>	<b>2050</b>	<b>2055.00</b>	$1.46e + 02$	<b>2350</b>	100
5	DE+APM	13950	15300	15382.83	$6.17e + 02$	16650	99	
		DE+DSS	17550	19150	19157.50	$6.93e + 02$	21400	100
		DELEqC	<b>1450</b>	<b>1950</b>	<b>1932.50</b>	$1.56e + 02$	<b>2250</b>	100
6	DE+APM	13850	15600	15582.00	$6.32e + 02$	17150	100	
		DE+DSS	16850	18850	18916.50	$7.45e + 02$	20750	100
		DELEqC	<b>6550</b>	<b>7300</b>	<b>7326.00</b>	$3.24e + 02$	<b>8150</b>	100
7	DE+APM	77050	83750	83938.00	$3.55e + 03$	95750	100	
		DE+DSS	104050	118550	118711.50	$7.01e + 03$	134100	100
		DELEqC	<b>6700</b>	<b>8050</b>	<b>8018.00</b>	$4.05e + 02$	<b>8950</b>	100
8	DE+APM	80850	88675	88901.00	$3.71e + 03$	98600	100	
		DE+DSS	108250	122000	122199.50	$7.26e + 03$	139000	100
		DELEqC	<b>18150</b>	<b>26100</b>	<b>30482.76</b>	$1.59e + 04$	<b>91400</b>	58
9	DE+APM	117150	140950	148259.78	$2.19e + 04$	208900	46	
		DE+DSS	145950	175875	182394.57	$2.63e + 04$	256150	46
		DELEqC	<b>6900</b>	<b>7900</b>	<b>7959.00</b>	$4.65e + 02$	<b>9200</b>	100
10	DE+APM	68200	77000	77211.50	$3.46e + 03$	86150	100	
		DE+DSS	98000	119175	119015.00	$7.54e + 03$	138350	100
		DELEqC	<b>12150</b>	<b>25975</b>	<b>31196.50</b>	$1.51e + 04$	<b>73150</b>	100
11	DE+APM	101850	109600	121478.57	$2.76e + 04$	210700	14	
		DE+DSS	131450	141350	143682.14	$9.04e + 03$	165550	14

**Table 2.** Results for the test-problems 7, 8, 9, 10, and 11 using the reference budget ( $rb$ ) and  $2 \times rb$ .

TP	nofe	technique	best	median	mean	st. dev.	worst
Results using the reference budget ( $rb$ )							
7	1,250	DELEqC	39.5143	<b>115.8354</b>	122.5069	5.03e + 01	260.6652
		Genocop II [16]	38.322	-	739.438	8.40e + 02	1.63e + 3
		LPSO [16]	37.420	-	7.03e + 03	8.01e + 03	4.63e + 4
		CLPSO [16]	<b>32.138</b>	-	<b>35.197</b>	2.21e + 01	<b>252.826</b>
8	5,000	DELEqC	35.3784	<b>35.3961</b>	<b>35.4051</b>	2.78e - 02	<b>35.5360</b>
		Genocop II	37.939	-	104.192	5.99e + 01	262.656
		LPSO	240.101	-	8.46e + 3	1.05e + 04	7.79e + 4
		CLPSO	<b>35.377</b>	-	82.077	6.10e + 01	197.389
9	5,000	DELEqC	40.5363	<b>58.7789</b>	58.1392	8.04e + 00	77.4060
		Genocop II	49.581	-	<b>56.694</b>	8.93e + 00	<b>75.906</b>
		LPSO	36.981	-	77.398	2.35e + 01	149.429
		CLPSO	<b>36.975</b>	-	72.451	2.57e + 01	167.644
10	10,000	DELEqC	<b>21485.2614</b>	<b>21485.2983</b>	<b>21485.2962</b>	5.87e - 03	<b>21485.3000</b>
		Genocop II	22334.971	-	58249.328	6.25e + 04	2.00e + 5
		LPSO	1.95e + 5	-	1.38e + 9	4.48e + 09	3.55e + 10
		CLPSO	21485.306	-	6.52e + 8	2.39e + 09	2.23e + 10
11	5,000	DELEqC	<b>0.3091</b>	<b>0.5910</b>	<b>0.5821</b>	9.56e - 02	<b>0.8099</b>
		Genocop II	0.713	-	1.009	1.30e - 01	1.131
		LPSO	0.529	-	6.853	6.20e + 00	36.861
		CLPSO	0.632	-	7.470	7.27e + 00	44.071
Results using twice the reference budget ( $2 \times rb$ )							
7	2,500	DELEqC	32.5550	<b>34.2880</b>	34.7973	1.97e + 00	41.1522
		Genocop II	37.612	-	304.884	3.88e + 02	1.17e + 3
		LPSO	<b>32.137</b>	-	445.316	8.03e + 02	4.51e + 3
		CLPSO	<b>32.137</b>	-	32.139	6.69e - 03	32.183
		Constricted PSO [15]	<b>32.137</b>	-	<b>32.137</b>	2.00e - 10	<b>32.137</b>
		BareBones PSO [15]	<b>32.137</b>	-	<b>32.137</b>	1.00e - 14	<b>32.137</b>
		PSOGauss [15]	<b>32.137</b>	-	<b>32.137</b>	1.00e - 14	<b>32.137</b>
8	10,000	DELEqC	<b>35.3769</b>	<b>35.3770</b>	<b>35.3770</b>	2.57e - 05	<b>35.3770</b>
		Genocop II	35.393	-	49.945	1.10e + 01	82.221
		LPSO	35.400	-	758.525	1.50e + 03	1.12e + 4
		CLPSO	<b>35.377</b>	-	68.570	5.39e + 01	196.067
		Constricted PSO	<b>35.377</b>	-	36.165	3.12e + 00	55.538
		BareBones PSO	<b>35.377</b>	-	40.019	9.61e + 00	75.147
		PSOGauss	<b>35.377</b>	-	38.998	8.59e + 00	72.482
9	10,000	DELEqC	<b>36.9755</b>	<b>44.9910</b>	<b>46.7872</b>	8.30e + 00	<b>67.1005</b>
		Genocop II	37.116	-	52.379	7.50e + 00	67.564
		LPSO	<b>36.975</b>	-	76.487	3.07e + 01	232.979
		CLPSO	<b>36.975</b>	-	69.039	2.16e + 01	154.379
		Constricted PSO	<b>36.975</b>	-	50.431	1.23e + 01	85.728
		BareBones PSO	<b>36.975</b>	-	55.921	1.61e + 01	119.556
		PSOGauss	<b>36.975</b>	-	55.622	1.48e + 01	119.094
10	20,000	DELEqC	<b>21485.2614</b>	<b>21485.2983</b>	<b>21485.2962</b>	5.87e - 03	<b>21485.3000</b>
		Genocop II	21490.840	-	21630.020	1.54e + 02	22030.988
		LPSO	21554.158	-	4.44e + 6	2.28e + 07	2.18e + 8
		CLPSO	21485.305	-	7.45e + 5	7.12e + 06	7.11e + 7
		Constricted PSO	<b>21485.3</b>	-	<b>21485.3</b>	6.00e - 11	<b>21485.3</b>
		BareBones PSO	<b>21485.3</b>	-	<b>21485.3</b>	6.00e - 11	<b>21485.3</b>
		PSOGauss	<b>21485.3</b>	-	<b>21485.3</b>	6.00e - 11	<b>21485.3</b>
11	10,000	DELEqC	<b>0.1509</b>	<b>0.4299</b>	<b>0.4163</b>	1.07e - 01	<b>0.6677</b>
		Genocop II	0.417	-	0.702	1.87e - 01	0.971
		LPSO	0.387	-	2.997	2.94e + 00	15.805
		CLPSO	0.236	-	3.049	3.10e + 00	16.427
		Constricted PSO	<b>0.151</b>	-	0.488	1.68e - 01	0.83
		BareBones PSO	0.203	-	0.523	1.81e - 01	0.912
		PSOGauss	<b>0.151</b>	-	0.53	1.68e - 01	0.958

**Table 3.** Results for the test-problems 7, 8, 9, 10, and 11 using  $3 \times rb$  and  $4 \times rb$ .

TP	nofe	technique	best	median	mean	st. dev.	worst
Results using three times the reference budget ( $3 \times rb$ )							
7	3,750	DELEqC	32.1447	<b>32.1881</b>	32.2008	5.53e - 02	32.5202
		Genocop II	33.837	-	69.154	2.67e + 01	124.820
		LPSO	<b>32.137</b>	-	35.071	2.15e + 01	244.077
		CLPSO	<b>32.137</b>	-	<b>32.137</b>	1.83e - 04	<b>32.138</b>
8	15,000	DELEqC	<b>35.3769</b>	<b>35.3770</b>	<b>35.3770</b>	2.57e - 05	<b>35.3770</b>
		Genocop II	35.772	-	42.393	6.86e + 00	60.110
		LPSO	<b>35.377</b>	-	125.727	2.31e + 02	1.72e + 3
		CLPSO	<b>35.377</b>	-	59.001	5.00e + 01	196.065
9	15,000	DELEqC	<b>36.9751</b>	<b>37.1959</b>	<b>39.6822</b>	4.52e + 00	<b>54.5931</b>
		Genocop II	37.326	-	47.643	8.45e + 00	67.128
		LPSO	<b>36.975</b>	-	74.338	2.83e + 01	234.968
		CLPSO	37.970	-	77.409	3.09e + 01	224.024
10	30,000	DELEqC	<b>21485.2614</b>	<b>21485.2983</b>	<b>21485.2962</b>	5.87e - 03	<b>21485.3000</b>
		Genocop II	21487.098	-	21546.332	8.53e + 01	21836.797
		LPSO	21483.373	-	3.71e + 5	2.41e + 06	2.05e + 7
		CLPSO	21485.305	-	21485.305	9.83e - 08	21485.305
11	15,000	DELEqC	<b>0.1508</b>	<b>0.2361</b>	<b>0.2605</b>	8.79e - 02	<b>0.5190</b>
		Genocop II	0.351	-	0.702	1.72e - 01	0.962
		LPSO	0.250	-	2.653	2.72e + 00	14.405
		CLPSO	0.250	-	2.146	2.21e + 00	11.983
Results using four times the reference budget ( $4 \times rb$ )							
7	5,000	DELEqC	<b>32.1371</b>	<b>32.1381</b>	32.1386	1.41e - 03	32.1436
		Genocop II	32.544	-	54.846	1.69e - 01	107.584
		LPSO	<b>32.137</b>	-	<b>32.137</b>	7.18e - 12	<b>32.137</b>
		CLPSO	<b>32.137</b>	-	<b>32.137</b>	3.02e - 06	<b>32.137</b>
		Constricted PSO	<b>32.137</b>	-	<b>32.137</b>	1.00e - 14	<b>32.137</b>
		BareBones PSO	<b>32.137</b>	-	<b>32.137</b>	1.00e - 14	<b>32.137</b>
		PSOGauss	<b>32.137</b>	-	<b>32.137</b>	1.00e - 14	<b>32.137</b>
8	20,000	DELEqC	<b>35.3769</b>	<b>35.3770</b>	<b>35.3770</b>	2.57e - 05	<b>35.3770</b>
		Genocop II	35.410	-	39.500	6.78e + 00	56.613
		LPSO	<b>35.377</b>	-	59.762	3.98e + 01	246.905
		CLPSO	<b>35.377</b>	-	39.832	1.09e + 01	71.380
		Constricted PSO	<b>35.377</b>	-	35.783	2.39e + 00	55.538
		BareBones PSO	<b>35.377</b>	-	37.079	5.33e + 00	55.538
		PSOGauss	<b>35.377</b>	-	35.589	5.28e - 01	36.892
9	20,000	DELEqC	<b>36.9748</b>	<b>36.9755</b>	<b>38.5722</b>	3.27e + 00	<b>51.4201</b>
		Genocop II	37.011	-	43.059	6.14e + 00	59.959
		LPSO	38.965	-	75.011	2.77e + 01	184.226
		CLPSO	<b>36.975</b>	-	76.896	2.73e + 01	151.394
		Constricted PSO	<b>36.975</b>	-	46.199	7.48e + 00	76.736
		BareBones PSO	<b>36.975</b>	-	49.238	1.02e + 01	76.774
		PSOGauss	<b>36.975</b>	-	47.11	8.14e + 00	68.802
10	40,000	DELEqC	<b>21485.2614</b>	<b>21485.2983</b>	<b>21485.2962</b>	5.87e - 03	<b>21485.3000</b>
		Genocop II	21485.363	-	21485.714	4.00e - 01	21486.646
		LPSO	21485.925	-	1.260e + 05	1.04e + 06	1.04e + 07
		CLPSO	21485.305	-	21485.305	9.40e - 08	21485.305
		Constricted PSO	<b>21485.3</b>	-	<b>21485.3</b>	6.00e - 11	<b>21485.3</b>
		BareBones PSO	<b>21485.3</b>	-	<b>21485.3</b>	6.00e - 11	<b>21485.3</b>
		PSOGauss	<b>21485.3</b>	-	<b>21485.3</b>	6.00e - 11	<b>21485.3</b>
11	20,000	DELEqC	<b>0.1482</b>	<b>0.2019</b>	<b>0.2241</b>	6.11e - 02	<b>0.3849</b>
		Genocop II	0.201	-	0.584	1.31e - 01	0.843
		LPSO	0.338	-	1.695	1.92e + 00	14.401
		CLPSO	0.236	-	1.900	2.38e + 00	17.259
		Constricted PSO	0.151	-	0.413	1.45e - 01	0.792
		BareBones PSO	0.151	-	0.444	1.58e - 01	0.83
		PSOGauss	0.151	-	0.454	1.74e - 01	0.83

equal to  $10^{-4}$ ) using up to the maximum allowed number of objective function evaluations (5,000,000). The best results are highlighted in boldface. It is easy to see that DELEqC requires much less objective function evaluations to find the best known solutions of the test-problems when compared to DE+DSS and DE+APM. Also, notice that DELEqC obtained more successful runs than both DE+DSS and DE+APM. Finally, it is important to highlight that the results obtained by the proposed technique are statistically different:  $p$ -values < 0.05, with respect to (i) pairwise comparisons using Wilcoxon rank-sum test, and (ii)  $p$ -values adjusted by Bonferroni correction.

We also investigated if the proposed technique produces results better or similar to those available in the literature using the same number of objective function evaluations. To do so, test-problems 7-11 were considered as in [15, 16]. Each test-problem has its allowed number of objective function evaluations (nofe) grouped in 4 different computational budgets: a reference budget ( $rb$ ),  $2 \times rb$ ,  $3 \times rb$ , and  $4 \times rb$ . Statistical information of the results is presented in Tables 2 and 3, where the best results are highlighted in boldface.

Analyzing the results in Tables 2 and 3, it is important to highlight that DELEqC obtains the best mean values in 15 of the 20 cases considered here (5 test-problems and 4 different budgets). Also, the best results with respect to the best value found were attained in 15 situations. Notice that CLPSO, the best performing technique in [16], obtained the best mean values in only 6 cases, and the best results, concerning the best value found, in 14 cases.

When compared to Constricted PSO –the best performing technique in [15] and which has results available for 10 of the 20 cases considered here– one can notice that DELEqC obtained the best mean values in 8 cases, and the best results, concerning the best value found, in 9 of the 10 cases, while Constricted PSO found the best mean values in only 3 cases, and the best results, concerning the best value found, in 9 of the 10 cases.

It should be noted that sometimes more than one algorithm reached the best result. In general, for test-problems 7-11, one can notice that despite the use of the simplest DE variant in DELEqC: (i) it performed similarly to the techniques from the literature with respect to best results, concerning the best value found; (ii) it obtained the best mean values in more test-cases; and (iii) it performed well independently of the number of objective function evaluations tested here.

## 6 Concluding Remarks

Existing metaheuristics usually only approximately satisfy equality constraints (according to a user specified tolerance value), even when they are linear. Here, a modified DE algorithm (DELEqC) is proposed to exactly satisfy linear equality constraints while allowing any available constraint handling technique to be applied to the remaining constraints of the optimization problem. A procedure for the generation of a random feasible initial population is proposed. By avoiding the standard DE crossover and using mutation operator formulae containing only differences of feasible candidate solutions, a DE algorithm is proposed

which maintains feasibility with respect to the linear equality constraints along the search process. Results from the computational experiments indicate that DELEqC outperforms the few alternatives that could be found in the literature and is a useful additional tool for the practitioner.

Further ongoing work concerns the extension of DELEqC so that linear inequality constraints are also exactly satisfied, as well as the introduction of a crossover operator that maintains feasibility with respect to the linear equality constraints.

**Acknowledgments.** The authors would like to thank the reviewers for their comments, which helped improve the paper, and the support provided by CNPq (grant 310778/2013-1), CAPES, and Pós-Graduação em Modelagem Computacional da Universidade Federal de Juiz de Fora (PGMC/UFJF).

## References

1. Barbosa, H.J.C., Bernardino, H.S., Barreto, A.M.S.: Using performance profiles to analyze the results of the 2006 CEC constrained optimization competition. In: IEEE Congress on Evolutionary Computation, pp. 1–8 (2010)
2. Barbosa, H.J.C., Lemonge, A.C.C.: An adaptive penalty scheme in genetic algorithms for constrained optimization problems. In: Langdon, W.B., et al. (ed.) Proc. of the Genetic and Evolutionary Computation Conference. USA (2002)
3. Barbosa, H.J.C., Lemonge, A.C.C.: A new adaptive penalty scheme for genetic algorithms. *Information Sciences* **156**, 215–251 (2003)
4. Coello, C.A.C.: Theoretical and numerical constraint-handling techniques used with evolutionary algorithms: a survey of the state of the art. *Computer Methods in Applied Mechanics and Engineering* **191**(11–12), 1245–1287 (2002)
5. Datta, R., Deb, K. (eds.): Evolutionary Constrained Optimization. Infosys Science Foundation Series. Springer, India (2015)
6. Deb, K.: An efficient constraint handling method for genetic algorithms. *Comput. Methods Appl. Mech. Engrg* **186**, 311–338 (2000)
7. Dolan, E., Moré, J.J.: Benchmarking optimization software with performance profiles. *Math. Programming* **91**(2), 201–213 (2002)
8. Hock, W., Schittkowski, K.: Test Examples for Nonlinear Programming Codes. Springer-Verlag New York Inc., Secaucus (1981)
9. Koziel, S., Michalewicz, Z.: A decoder-based evolutionary algorithm for constrained parameter optimization problems. In: Eiben, A.E., Bäck, T., Schoenauer, M., Schwefel, H.-P. (eds.) PPSN 1998. LNCS, vol. 1498, pp. 231–240. Springer, Heidelberg (1998)
10. Koziel, S., Michalewicz, Z.: Evolutionary algorithms, homomorphous mappings, and constrained parameter optimization. *Evol. Comput.* **7**(1), 19–44 (1999)
11. Lemonge, A.C.C., Barbosa, H.J.C.: An adaptive penalty scheme for genetic algorithms in structural optimization. *Intl. Journal for Numerical Methods in Engineering* **59**(5), 703–736 (2004)
12. Luenberger, D.G., Ye, Y.: Linear and Nonlinear Programming. Springer-Verlag (2008)
13. Mezura-Montes, E., Coello, C.A.C.: Constraint-handling in nature-inspired numerical optimization: Past, present and future. *Swarm and Evolutionary Computation* **1**(4), 173–194 (2011)

14. Michalewicz, Z., Janikow, C.Z.: Genocop: A genetic algorithm for numerical optimization problems with linear constraints. *Commun. ACM* **39**(12es), 175–201 (1996)
15. Monson, C.K., Seppi, K.D.: Linear equality constraints and homomorphous mappings in PSO. *IEEE Congress on Evolutionary Computation* **1**, 73–80 (2005)
16. Paquet, U., Engelbrecht, A.P.: Particle swarms for linearly constrained optimisation. *Fundamenta Informaticae* **76**(1), 147–170 (2007)
17. Price, K.V.: An introduction to differential evolution. *New Ideas in Optimization*, pp. 79–108 (1999)
18. Salcedo-Sanz, S.: A survey of repair methods used as constraint handling techniques in evolutionary algorithms. *Computer Science Review* **3**(3), 175–192 (2009)
19. Schoenauer, M., Michalewicz, Z.: Evolutionary computation at the edge of feasibility. In: Ebeling, W., Rechenberg, I., Voigt, H.-M., Schwefel, H.-P. (eds.) *PPSN 1996. LNCS*, vol. 1141, pp. 245–254. Springer, Heidelberg (1996)
20. Storn, R., Price, K.V.: Differential evolution - a simple and efficient heuristic for global optimization over continuous spaces. *Journal of Global Optimization* **11**, 341–359 (1997)

## Appendix A. Test-Problems

Test-problems 1 to 6 and 7 to 11 were taken from [8] and [15], respectively. Also note that problems 7 to 11 are subject to the same set of linear constraints (2).

**Problem 1** - The solution is  $x^* = (1, 1, 1, 1, 1)^T$  with  $f(x^*) = 0$ .

$$\begin{aligned} \min & (x_1 - 1)^2 + (x_2 - x_3)^2 + (x_4 - x_5)^2 \\ \text{s.t. } & x_1 + x_2 + x_3 + x_4 + x_5 = 5 \\ & x_3 - 2x_4 - 2x_5 = -3 \end{aligned}$$

**Problem 2** - The solution is  $x^* = (1, 1, 1, 1, 1)^T$  with  $f(x^*) = 0$ .

$$\begin{aligned} \min & (x_1 - x_2)^2 + (x_3 - 1)^2 + (x_4 - 1)^4 + (x_5 - 1)^6 \\ \text{s.t. } & x_1 + x_2 + x_3 + 4x_4 = 7 \\ & x_3 + 5x_5 = 6 \end{aligned}$$

**Problem 3** - The solution is  $x^* = (1, 1, 1, 1, 1)^T$  with  $f(x^*) = 0$ .

$$\begin{aligned} \min & (x_1 - x_2)^2 + (x_2 - x_3)^2 + (x_3 - x_4)^4 + (x_4 - x_5)^2 \\ \text{s.t. } & x_1 + 2x_2 + 3x_3 = 6 \\ & x_2 + 2x_3 + 3x_4 = 6 \\ & x_3 + 2x_4 + 3x_5 = 6 \end{aligned}$$

**Problem 4** - The solution is  $x^* = (1, 1, 1, 1, 1)^T$  with  $f(x^*) = 0$ .

$$\begin{aligned} \min & (x_1 - x_2)^2 + (x_2 + x_3 - 2)^2 + (x_4 - 1)^2 + (x_4 - 1)^2 + (x_5 - 1)^2 \\ \text{s.t. } & x_1 + 3x_2 = 4 \\ & x_3 + x_4 - 2x_5 = 0 \\ & x_2 - x_5 = 0 \end{aligned}$$

**Problem 5** - The solution is  $x^* = (-33/349, 11/349, 180/349, -158/349, 1/349)^T$  with  $f(x^*) = 5.326647564$ .

$$\begin{aligned} & \min (4x_1 - x_2)^2 + (x_2 + x_3 - 2)^2 + (x_4 - 1)^2 + (x_5 - 1)^2 \\ \text{s.t. } & x_1 + 3x_2 = 0 \\ & x_3 + x_4 - 2x_5 = 0 \\ & x_2 - x_5 = 0 \end{aligned}$$

**Problem 6** - The solution is  $x^* = (-33/43, 11/43, 27/43, -5/43, 11/43)^T$  with  $f(x^*) = 4.093023256$ .

$$\begin{aligned} & \min (x_1 - x_2)^2 + (x_2 + x_3 - 2)^2 + (x_4 - 1)^2 + (x_5 - 1)^2 \\ \text{s.t. } & x_1 + 3x_2 = 0 \\ & x_3 + x_4 - 2x_5 = 0 \\ & x_2 - x_5 = 0 \end{aligned}$$

**Problem 7 (Sphere)** -  $f(x^*) = 32.137$

$$\min_{x \in \mathcal{E}} \sum_{i=1}^{10} x_i^2$$

The feasible set  $\mathcal{E}$  is given by the linear equality constraints:

$$\left\{ \begin{array}{l} -3x_2 - x_3 + 2x_6 - 6x_7 - 4x_9 - 2x_{10} = 3 \\ -x_1 - 3x_2 - x_3 - 5x_7 - x_8 - 7x_9 - 2x_{10} = 0 \\ x_3 + x_6 + 3x_7 - 2x_9 + 2x_{10} = 9 \\ 2x_1 + 6x_2 + 2x_3 + 2x_4 + 4x_7 + 6x_8 + 16x_9 + 4x_{10} = -16 \\ -x_1 - 6x_2 - x_3 - 2x_4 - 2x_5 + 3x_6 - 6x_7 - 5x_8 - 13x_9 - 4x_{10} = 30 \end{array} \right. \quad (2)$$

**Problem 8 (Quadratic)** -  $f(x^*) = 35.377$

$$\min_{x \in \mathcal{E}} \sum_{i=1}^{10} \sum_{j=1}^{10} e^{-(x_i - x_j)^2} x_i x_j + \sum_{i=1}^{10} x_i$$

**Problem 9 (Rastrigin)** -  $f(x^*) = 36.975$

$$\min_{x \in \mathcal{E}} \sum_{i=1}^{10} x_i^2 + 10 - 10 \cos(2\pi x_i)$$

**Problem 10 (Rosenbrock)** -  $f(x^*) = 21485.3$

$$\min_{x \in \mathcal{E}} \sum_{i=1}^9 100(x_{i+1} - x_i^2)^2 + (x_i - 1)^2$$

**Problem 11 (Griewank)** -  $f(x^*) = 0.151$

$$\min_{x \in \mathcal{E}} \frac{1}{4000} \sum_{i=1}^{10} x_i^2 - \prod_{i=10}^{10} \cos\left(\frac{x_i}{\sqrt{i}}\right) + 1$$

# Multiobjective Firefly Algorithm for Variable Selection in Multivariate Calibration

Lauro Cássio Martins de Paula<sup>(✉)</sup> and Anderson da Silva Soares

Institute of Informatics, Federal University of Goiás, Goiânia, Goiás, Brazil

{laurocassio, anderson}@inf.ufg.br

<http://www.inf.ufg.br>

**Abstract.** Firefly Algorithm is a newly proposed method with potential application on several real world problems, such as variable selection problem. This paper presents a Multiobjective Firefly Algorithm (MOFA) for variable selection in multivariate calibration models. The main objective is to propose an optimization to reduce the error value prediction of the property of interest, as well as reducing the number of variables selected. Based on the results obtained, it is possible to demonstrate that our proposal may be a viable alternative in order to deal with conflicting objective-functions. Additionally, we compare MOFA with traditional algorithms for variable selection and show that it is a more relevant contribution for the variable selection problem.

**Keywords:** Firefly algorithm · Multiobjective optimization · Variable selection · Multivariate calibration

## 1 Introduction

Multivariate calibration may be considered as a procedure for constructing a mathematical model that establishes the relationship between the properties measured by an instrument and the concentration of a sample to be determined [3]. However, the building of a model from a subset of explanatory variables usually involves some conflicting objectives, such as extracting information from a measured data with many possible independent variables. Thus, a technique called variable selection may be used [3]. In this sense, the development of efficient algorithms for variable selection becomes important in order to deal with large and complex data. Furthermore, the application of Multiobjective Optimization (MOO) may significantly contribute to efficiently construct an accurate model [8].

Previous works about multivariate calibration have demonstrated that while monoobjective formulation uses a bigger number of variables, multiobjective algorithms can use fewer variables with a lower prediction error [2][1]. On the one hand, such works have used only genetic algorithms for exploiting MOO. On the other hand, the application of MOO in bioinspired metaheuristics such as Firefly Algorithm may be a better alternative in order to obtain a model with

a more appropriate prediction capacity [8]. In this sense, some works have used FA to solve many types of problems. Regarding multiobjective characteristic, Yang [8] was the first one to present a multiobjective FA (MOFA) to solve optimization problems and showed that MOFA has advantages in dealing with multiobjective optimization.

As far as we know, the application of MOO-based Firefly Algorithm is not still widely used. There is no work in the literature that uses a multiobjective FA to select variables in multivariate calibration. Therefore, this paper presents an implementation of a MOFA for variable selection in multivariate calibration models. Additionally, estimates from the proposed MOFA are compared with predictions from the following traditional algorithms: Successive Projections Algorithm (SPA-MLR) [6], Genetic Algorithm (GA-MLR) [1] and Partial Least Squares (PLS). Based on the results obtained, we concluded that our proposed algorithm may be a more viable tool for variable selection in multivariate calibration models.

Section 2 describes multivariate calibration and the original FA. The proposed MOFA is presented in Section 3. Section 4 describes the material and methods used in the experiments. Results are described in Section 5. Finally, Section 6 shows the conclusions of the paper.

## 2 Background

### 2.1 Multivariate Calibration

The multivariate calibration model provides the value of a quantity  $y$  based on values measured from a set of explanatory variables  $\{x_1, x_2, \dots, x_k\}^T$  [3]. The model can be defined as:

$$y = \beta_0 + \beta_1 x_1 + \dots + \beta_k x_k + \varepsilon, \quad (1)$$

where  $\beta_0, \beta_1, \dots, \beta_k$ ,  $i = 1, 2, \dots, k$ , are the coefficients to be determined, and  $\varepsilon$  is a portion of random error. Equation (2) shows how the regression coefficients may be calculated using the Moore-Penrose pseudoinverse [4]:

$$\beta = (\mathbf{X}^T \mathbf{X})^{-1} \mathbf{X}^T \mathbf{y}, \quad (2)$$

where  $\mathbf{X}$  is the matrix of samples and independent variables,  $\mathbf{y}$  is the vector of dependent variables, and  $\beta$  is the vector of regression coefficients.

As shown in Equations (3) and (4), the predictive ability of MLR models comparing predictions with reference values for a test set from the squared deviations can be calculated by RMSEP or MAPE [3][5]:

$$\text{RMSEP} = \sqrt{\frac{\sum_{i=1}^N (\mathbf{y}_i - \hat{\mathbf{y}}_i)^2}{N}}, \quad (3)$$

where  $\mathbf{y}$  is the reference value of the property of interest,  $N$  is the number of observations, and  $\hat{\mathbf{y}} = \{\hat{y}_1, \hat{y}_2, \dots, \hat{y}_k\}^T$  is the estimated value.

$$MAPE = \frac{\sum |\frac{\mathbf{y}_i - \hat{\mathbf{y}}_i}{\mathbf{y}_i}|}{N} (100) = \frac{\sum |\frac{e_i}{\mathbf{y}_i}|}{N} (100), \quad (4)$$

where  $\mathbf{y}_i$  is the actual data at variable  $i$ ,  $\hat{\mathbf{y}}_i$  is the forecast at variable  $i$ ,  $e_i$  is the forecast error at variable  $i$ , and  $N$  is the number of samples.

## 2.2 Firefly Algorithm

Nature-inspired metaheuristics have been a powerful tool in solving various types of problems [8]. FA is a recently developed optimization algorithm proposed by Yang [8]. It is based on the behaviour of the flashing characteristics of fireflies. A pseudocode for the original FA can be obtained in the work of Yang [8]. In the original algorithm, there are two important issues to be treated: i) the variation of light intensity; and ii) the attractiveness formulation. The attractiveness of a firefly is determined by its brightness or light intensity, which is associated with the encoded objective function [8].

As a firefly's attractiveness is proportional to the light intensity seen by adjacent fireflies, one can define the attractiveness  $\omega$  of a firefly by:

$$\omega = \omega_o e^{-\gamma r^2}, \quad (5)$$

where  $\omega_o$  is the attractiveness at  $r = 0$ .

According to Yang [8], a firefly  $i$  is attracted to a brighter firefly  $j$  and its movement is determined by:

$$x_i = x_j + \omega_0 e^{-\gamma r_{i,j}^2} (x_j - x_i) + \alpha(\text{rand} - \frac{1}{2}), \quad (6)$$

where  $\text{rand}$  is a random number generated in  $[0, 1]$ .

## 3 Proposal

Previous works have showed that multiobjective algorithms can use fewer variables and obtain lower prediction error [2]. Thus, this paper presents a Multiobjective Firefly Algorithm (MOFA) for variable selection in multivariate calibration. In the multiobjective formulation of FA, the choice of current best solution is based on two conditions: *i*) error of prediction; and *ii*) number of variables selected. Among non-dominated solutions, it is applied a multiobjective decision maker method called *Wilcoxon Signed-Rank*<sup>1</sup> to choose the final best one [2]. Algorithm 1 shows a pseudocode for the proposed MOFA. In line 9 of Algorithm 1, a firefly  $i$  dominates another firefly  $j$  when its RMSEP/MAPE and number of variables selected are lower.

---

<sup>1</sup> *Wilcoxon Signed-Rank* is a nonparametric hypotheses test used when comparing two related samples to evaluate if the rank of the population means are different [7].

---

**Algorithm 1.** Proposed Multiobjective Firefly Algorithm.

---

1. **Parameters:**  $\mathbf{X}_{n \times m}$ ,  $\mathbf{y}_{n \times 1}$
  2.  $s \leftarrow$  number of fireflies
  3. **for**  $n = 1 : MaxGeneration$
  4.   Generate randomly a population  $Pop_{s \times m}$  of fireflies
  5.   Compute Equations (2), (3), and the number of variables selected for each firefly
  6.   **for**  $i = 1 : s$
  7.     **for**  $j = 1 : s$
  8.       if firefly  $i$ -th dominates firefly  $j$ -th
  9.         Move firefly  $j$  towards firefly  $i$  using Equation (6)
  10.      **end if**
  11.     **end for**  $j$
  12.   **end for**  $i$
  13. **end for**  $n$
  14. Calculate RMSEP and variables selected for all fireflies
  15. Select the best firefly by a decision maker based in [2]
- 

## 4 Experimental Results

The proposed MOFA was implemented using  $\alpha = 0.2$ ,  $\gamma = 1$  and  $\omega_0 = 0.97$ . The number of fireflies and the number of generations were 200 and 100, respectively. We have used for RMSEP comparison three traditional methods for variable selection: SPA-MLR [6], GA-MLR [1] and the PLS. The number of iterations was the same for all algorithms and the multiobjective approach was not applied in this three traditional methods.

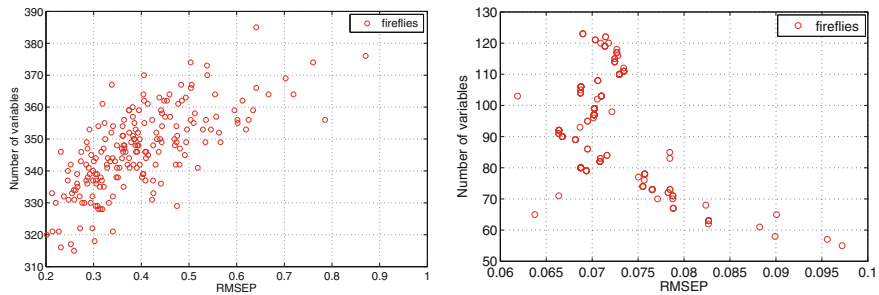
The dataset employed in this work consists of 775 NIR spectra of whole-kernel wheat, which were used as shoot-out data in the 2008 International Diffuse Reflectance Conference (<http://www.idrc-chambersburg.org/shootout.html>). Protein content (%) was used as the y-property in the regression calculations.

All calculations were carried out by using a desktop computer with an Intel Core i7 2600 (3.40 GHz), 8 GB of RAM memory and Windows 7 Professional. The Matlab 8.1.0.604 (R2013a) software platform was employed throughout. Regarding the outcomes, it is important to note that all of them were obtained by averaging fifty executions.

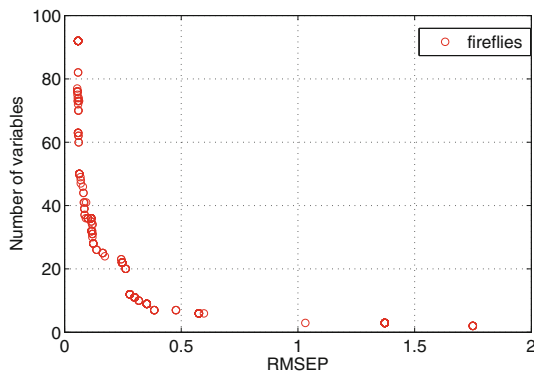
## 5 Results and Discussion

Figure 1(a) shows the first population of fireflies generated. Figure 1(b) illustrates the behaviour of fireflies when a monoojective formulation is employed. In the chart, the only goal was to reduce RMSEP.

The application of multiobjective optimization is presented in Figure 2. The fireflies create a relatively perfect Pareto Front tending to a minimum error value as well as a minimum number of variables selected. It is possible to note that the



**Fig. 1.** Behaviour of fireflies with: (a) randomly generated fireflies.; (b) monoobjective formulation.



**Fig. 2.** Behaviour of fireflies with multiobjective optimization.

**Table 1.** Results for the FA, MOFA, SPA-MLR, GA-MLR and PLS.

	Number of variables	RMSEP	MAPE
GA-MLR	146	0.21	1.50%
FA	103	0.07	0.81%
MOFA	37	0.05	0.72%
PLS	15	0.21	1.50%
SPA-MLR	13	0.20	1.43%

application of multiobjective formulation can move fireflies to more appropriate solutions using the non-dominance characteristic.

A comparison between MOFA and traditional algorithms is showed in Table 1. Despite SPA-MLR was able to yield the lowest number of variables

selected, MOFA presented the lowest RMSEP and MAPE<sup>2</sup>. A comparison of computational time between these algorithms can be obtained in [4].

## 6 Conclusion

This paper proposed a Multiobjective Firefly Algorithm (MOFA) for variable selection in multivariate calibration models. The objective was to present an optimization to reduce the error value prediction of the property of interest as well as reducing the number of variables selected. In terms of error reduction, MOFA presented the lowest values when compared with traditional algorithms. Therefore, through the results obtained we were able to demonstrate that MOFA may be a better solution for obtaining a model with an adequate prediction capacity.

**Acknowledgments.** Authors thank the research agencies CAPES and FAPEG for the support provided to this work.

## References

1. Soares, A.S., de Lima, T.W., Soares, F.A.A.M.N., Coelho, C.J., Federson, F.M., Delbem, A.C.B., Van Baalen, J.: Mutation-based compact genetic algorithm for spectroscopy variable selection in determining protein concentration in wheat grain. *Electronics Letters* **50**, 932–934 (2014)
2. Lucena, D.V., Soares, A.S., Soares, T.W., Coelho, C.J.: Multi-Objective Evolutionary Algorithm NSGA-II for Variables Selection in Multivariate Calibration Problems. *International Journal of Natural Computing Research* **3**, 43–58 (2012)
3. Martens, H.: *Multivariate Calibration*. John Wiley & Sons (1991)
4. Paula, L.C.M., Soares, A.S., Soares, T.W., Delbem, A.C.B., Coelho, C.J., Filho, A.R.G.: Parallelization of a Modified Firefly Algorithm using GPU for Variable Selection in a Multivariate Calibration Problem. *International Journal of Natural Computing Research* **4**, 31–42 (2014)
5. Hibon, M., Makridakis, S.: Evaluating Accuracy (or Error) Measures. INSEAD (1995)
6. Arajo, M.C.U., Saldanha, T.C., Galvo, R.K., Yoneyama, T.: The successive projections algorithm for variable selection in spectroscopic multicomponent analysis. *Chemometrics and Intelligent Laboratory Systems* **57**, 65–73 (2001)
7. Ramsey, P.H.: Significance probabilities of the wilcoxon signed-rank test. *Journal of Nonparametric Statistics* **2**, 133–153 (1993)
8. Yang, X.S.: Multiobjective firefly algorithm for continuous optimization. *Engineering with Computers* **29**, 175–184 (2013)

---

<sup>2</sup> It is worth noting that the Successive Projections Algorithm is composed of three phases, and its main objective is to select a subset of variables with low collinearity [6].

# Semantic Learning Machine: A Feedforward Neural Network Construction Algorithm Inspired by Geometric Semantic Genetic Programming

Ivo Gonçalves<sup>1,2(✉)</sup>, Sara Silva<sup>1,2,3</sup>, and Carlos M. Fonseca<sup>1</sup>

<sup>1</sup> CISUC, Department of Informatics Engineering,  
University of Coimbra, 3030-290 Coimbra, Portugal

[icpg@dei.uc.pt](mailto:icpg@dei.uc.pt)

<sup>2</sup> BioISI - Biosystems & Integrative Sciences Institute, Faculty of Sciences,  
University of Lisbon, 1749-016 Campo Grande, Lisbon, Portugal

[sara@fc.ul.pt](mailto:sara@fc.ul.pt)

<sup>3</sup> NOVA IMS, Universidade Nova de Lisboa, 1070-312 Lisbon, Portugal  
[cmfonsec@dei.uc.pt](mailto:cmfonsec@dei.uc.pt)

**Abstract.** Geometric Semantic Genetic Programming (GSGP) is a recently proposed form of Genetic Programming in which the fitness landscape seen by its variation operators is unimodal with a linear slope by construction and, consequently, easy to search. This is valid across all supervised learning problems. In this paper we propose a feedforward Neural Network construction algorithm derived from GSGP. This algorithm shares the same fitness landscape as GSGP, which allows an efficient search to be performed on the space of feedforward Neural Networks, without the need to use backpropagation. Experiments are conducted on real-life multidimensional symbolic regression datasets and results show that the proposed algorithm is able to surpass GSGP, with statistical significance, in terms of learning the training data. In terms of generalization, results are similar to GSGP.

## 1 Introduction

Moraglio et al. [6] recently proposed a new Genetic Programming formulation called Geometric Semantic Genetic Programming (GSGP). GSGP derives its name from the fact that it is formulated under a geometric framework [5] and from the fact that it operates directly in the space of the underlying semantics of the individuals. In this context, semantics is defined as the outputs of an individual over a set of data instances. The most interesting property of GSGP is that the fitness landscape seen by its variation operators is always unimodal with a linear slope (cone landscape) by construction. This implies that there are no local optima, and consequently, that this type of landscape is easy to search. When applied to multidimensional real-life datasets, GSGP has shown competitive results in learning and generalization [3, 7]. In this paper, we adapt

the geometric semantic mutation to the realm of feedforward Neural Networks by proposing the Semantic Learning Machine (SLM). Section 2 defines the SLM. Section 3 describes the experimental setup. Section 4 presents and discusses the results of the SLM and GSGP, and Section 5 concludes.

## 2 Semantic Learning Machine

Given that the geometric semantic operators are defined over the semantic space (outputs), they can be extended for different representations. The Semantic Learning Machine (SLM) proposed in this section is based on a derivation of the GSGP mutation operator for real-value semantics. This implies that the SLM shares the same semantic landscape properties as GSGP. Particularly, the fitness landscape induced by its operator is always unimodal with a linear slope (cone landscape) by construction, and consequently easy to search. This is valid across all supervised learning problems.

### 2.1 A Geometric Semantic Mutation Operator for Feedforward Neural Networks

The GSGP mutation for real-value semantics [6] is defined as follows:

**Definition 1. (GSGP Mutation).** *Given a parent function  $T : \mathbb{R}^n \rightarrow \mathbb{R}$ , the geometric semantic mutation with mutation step  $ms$  returns the real function  $T_M = T + ms \cdot (T_{R1} - T_{R2})$ , where  $T_{R1}$  and  $T_{R2}$  are random real functions.*

This mutation essentially performs a linear combination of two individuals: the parent and a randomly generated tree (which results from subtracting the two subtrees  $T_{R1}$  and  $T_{R2}$ ). The degree of semantic change is controlled by the mutation step.

An equivalent geometric semantic mutation operator can be derived for feed-forward Neural Networks (NN). The only three small restrictions for this NN mutation operator are: the NN must have at least one hidden layer; the output layer must have only one neuron; and the output neuron must have a linear activation function. Each application of the operator adds a new neuron to the last hidden layer. The weight from the new neuron to the output neuron is defined by the learning step (SLM parameter). This learning step is the equivalent of the mutation step in the GSGP mutation. It defines the amount of semantic change for each application of the operator. The weights from the last hidden layer to the previous layer are randomly generated. This is the equivalent of generating the two random subtrees in the GSGP mutation. In this work these weights are generated with uniform probability between -1.0 and 1.0. If more than one hidden layer is used, all other weights remain constant once initialized. In this work all experiments are conducted with a single hidden layer. The activation function for the neurons in the last hidden layer can be freely chosen. However, it has been recently shown, in the context of GSGP, that applying a structural bound to the randomly generated tree (which results from subtracting

the two subtrees  $T_{R1}$  and  $T_{R2}$ ) results in significant improvements in terms of generalization ability [3]. In fact, if an unbounded mutation (equivalent to using a linear activation function) is used, there is a tendency for GSGP to greatly overfit the training data [3]. For this reason, it is recommended that the activation function for the neurons in the last hidden layer to be a function with a relatively small codomain. In this work a modified logistic function (transforming the logistic function output to range in the interval  $[-1, 1]$ ) is used for this purpose. In terms of generalization ability, it is also essential to use a small learning/mutation step [3]. If more than one hidden layer is used, the activation functions for the remaining neurons may be freely chosen.

## 2.2 Algorithm

The SLM algorithm is essentially a geometric semantic hill climber for feedforward neural networks. The idea is to perform a semantic sampling with a given size (SLM parameter) by applying the mutation operator defined in the previous subsection. As is common in hill climbers, only one solution (in this case a neural network) is kept along the run. At each iteration, the mentioned semantic sampling is performed to produce  $N$  neighbors. At the end of the iteration, the best individual from the previous best and the newly generated individuals is kept. The process is repeated until a given number of iterations (SLM parameter) has been reached. As mentioned in the previous subsection, the mutation operator always adds a new neuron to the last hidden layer, so the number of neurons in the last hidden layer is at most the same as the number of iterations. This number of neurons can be smaller than the number of iterations if in some iterations it was not possible to generate an individual superior to the current best.

## 3 Experimental Setup

The experimental setup is based on the setup of Vanneschi et al. [7] and Gonçalves et al. [3], since these works recently provided results for GSGP. Experiments are run for 500 iterations/generations because that is where the statistical comparisons were made in the mentioned works. 30 runs are conducted. Population/sample size is 100. Training and testing set division is 70% - 30%. Fitness is computed as the root mean squared error. The initial tree initialization is performed with the ramped half-and-half method, with a maximum depth of 6. Besides GSGP, the Semantic Stochastic Hill Climber (SSHC) [6] is also used as baseline for comparison. The variation operators used are the variants defined for real-value semantics [6]: SGXM crossover for GSGP, and SGMR mutation for GSGP and SSHC. For GSGP a probability of 0.5 is used for both operators. The function set contains the four binary arithmetic operators: +, -, \*, and / (protected). No constants are used in the terminal set. Parent selection in GSGP is based on tournaments of size 4. Also for GSGP, survivor selection is elitist as the best individual always survives to the next generation. All claims

of statistical significance are based on Mann-Whitney U tests, with Bonferroni correction, and considering a significance level of  $\alpha = 0.05$ . For each dataset 30 different random partitions are used. Each method uses the same 30 partitions. Experiments are conducted on three multidimensional symbolic regression real-life datasets. These datasets are the Bioavailability (hereafter Bio), the Plasma Protein Binding (hereafter PPB), and the Toxicity (hereafter LD50). The first two were also used by Vanneschi et al. [7] and Gonçalves et al. [3]. These datasets have, respectively: 359 instances and 241 features; 131 instances and 626 features; and 234 instances and 626 features. For a detailed description of these datasets the reader is referred to Archetti et al. [1]. These datasets have also been used in other Genetic Programming studies, e.g., [2, 4].

## 4 Experimental Study

Figure 1 presents the training and testing error evolution plots for SLM, GSGP and SSHC. These evolution plots are constructed by taking the median over 30 runs of the training and testing error of the best individuals in the training data. The mutation/learning step used was 1 for the the Bio and PPB datasets (as in Vanneschi et al. [7] and Gonçalves et al. [3]), and 10 for the LD50 as it was found, in preliminary testing, to be a suitable value (other values tested were: 0.1, 1, and 100). A consideration for the different initial values (at iteration/generation 0) is in order. The SLM presents much higher errors than GSGP/SSHC after the random initialization. This is explained by the fact that the weights for the SLM are generated with uniform probability between -1.0 and 1.0, and consequently, the amount of data fitting is clearly bounded. On the other hand, GSGP and SSHC have no explicit bound on the random trees and therefore can provide a superior initial explanation of the data. It is interesting to note that, despite this initial disadvantage, the SLM compensates with a much higher learning rate. This higher learning efficiency is confirmed by the statistically significant superiority found in terms of training error across all datasets, against GSGP (p-values: Bio  $2.872 \times 10^{-11}$ , PPB  $2.872 \times 10^{-11}$  and LD50  $7.733 \times 10^{-10}$ ), and against SSHC (p-values: Bio  $2.872 \times 10^{-11}$ , PPB  $2.872 \times 10^{-11}$  and LD50  $3.261 \times 10^{-5}$ ).

This learning superiority is particularly interesting when considering that the SLM and the SSHC use the exact same geometric semantic mutation operator. This raise the question: how can two methods with the same variation operator, the same induced semantic landscape, and the same parametrizations achieve such different outcomes? The answer lies in the different semantic distributions that result from the random initializations. Different representations have different natural ways of being randomly initialized. This translates into different semantic distributions and, consequently, to different offspring distributions. From the results it is clear that the distribution induced by the random initialization of a list of weights (used in SLM), is more well-behaved than the initialization of a random tree (used in SSHC). In the original GSGP proposal, Moraglio et al. [6] provided a discussion on whether syntax (representation) matters in terms of search. They argued that, in abstract, the offspring distributions may be affected by the different syntax initializations. In our work, we

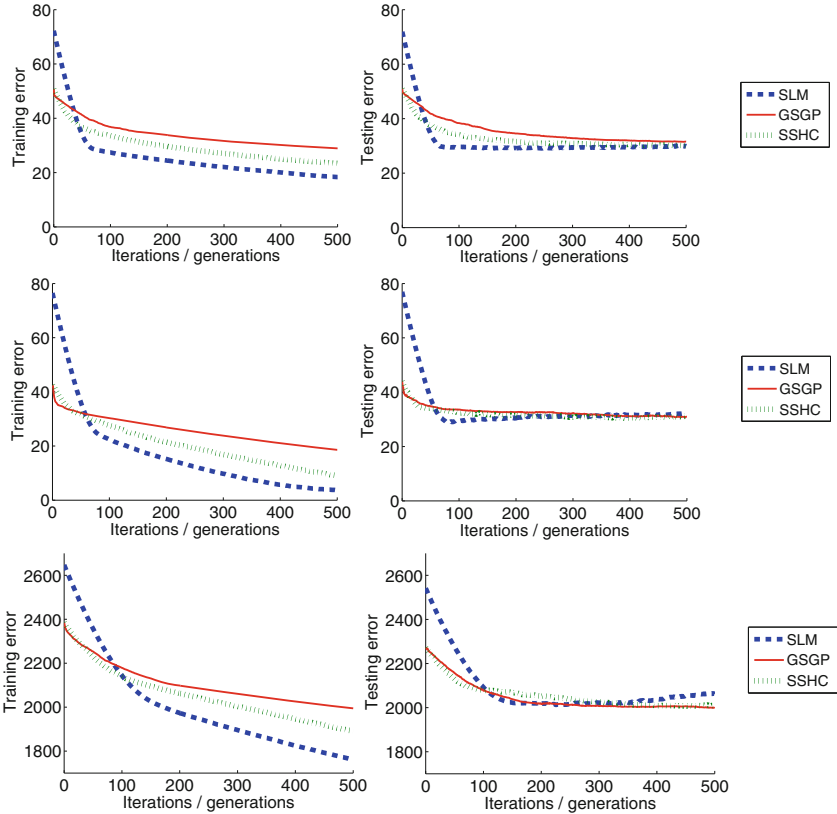


**Fig. 1.** Bio (top), PPB (center) and LD50 (bottom) training and testing error evolution plots

can empirically see how different representations induce different offspring distributions and consequently reach considerably different outcomes. A possible research venue lies in analyzing the semantic distributions induced by different tree initialization methods, and to possibly propose new tree initializations that are more well-behaved.

In terms of generalization, results show that all methods achieve similar results. The only statistically significant difference shows that the SLM is superior to GSGP in the Bio dataset ( $p$ -value:  $1.948 \times 10^{-4}$ ). However, it seems that in this case, GSGP is still evolving and that in a few more generations may reach a generalization similar to the SLM. On a final note, the evolution plots also show that SSHC consistently learns the training data faster and better than GSGP. This should be expected as the semantic space has no local optima and consequently the search can be focused around the best individual in the population. These differences are confirmed as statistically significant ( $p$ -values: Bio  $2.872 \times 10^{-11}$ , PPB  $2.872 \times 10^{-11}$  and LD50  $1.732 \times 10^{-4}$ ). There are no statistically significant differences in terms of generalization.

## 5 Conclusions

This work presented a novel feedforward Neural Network (NN) construction algorithm, derived from Geometric Semantic Genetic Programming (GSGP). The proposed algorithm shares the same fitness landscape as GSGP, which enables an efficient search for any supervised learning problem. Results in regression datasets show that the proposed NN construction algorithm is able to surpass GSGP, with statistical significance, in terms of learning the training data. Generalization results are similar to those of GSGP. Future work involves extending the experimental analysis to other regression datasets and to provide results for classification tasks. Comparisons with other NN algorithms and other commonly used supervised learning algorithms (e.g. Support Vector Machines) are also in order.

**Acknowledgments.** This work was partially supported by national funds through FCT under contract UID/Multi/04046/2013 and projects PTDC/EEI-CTP/2975/2012 (MaSSGP), PTDC/DTP-FTO/1747/2012 (InteleGen) and EXPL/EMS-SIS/1954/2013 (CancerSys). The first author work is supported by FCT, Portugal, under the grant SFRH/BD/79964/2011.

## References

1. Archetti, F., Lanzeni, S., Messina, E., Vanneschi, L.: Genetic programming for computational pharmacokinetics in drug discovery and development. *Genetic Programming and Evolvable Machines* **8**(4), 413–432 (2007)
2. Gonçalves, I., Silva, S.: Balancing learning and overfitting in genetic programming with interleaved sampling of training data. In: Krawiec, K., Moraglio, A., Hu, T., Etaner-Uyar, A.S., Hu, B. (eds.) *EuroGP 2013. LNCS*, vol. 7831, pp. 73–84. Springer, Heidelberg (2013)
3. Gonçalves, I., Silva, S., Fonseca, C.M.: On the generalization ability of geometric semantic genetic programming. In: Machado, P., Heywood, M.I., McDermott, J., Castelli, M., García-Sánchez, P., Burelli, P., Risi, S., Sim, K. (eds.) *Genetic Programming. LNCS*, vol. 9025, pp. 41–52. Springer, Heidelberg (2015)
4. Gonçalves, I., Silva, S., Melo, J.B., Carreiras, J.M.B.: Random sampling technique for overfitting control in genetic programming. In: Moraglio, A., Silva, S., Krawiec, K., Machado, P., Cotta, C. (eds.) *EuroGP 2012. LNCS*, vol. 7244, pp. 218–229. Springer, Heidelberg (2012)
5. Moraglio, A.: Towards a Geometric Unification of Evolutionary Algorithms. Ph.D. thesis, Department of Computer Science, University of Essex, UK, November 2007
6. Moraglio, A., Krawiec, K., Johnson, C.G.: Geometric semantic genetic programming. In: Coello, C.A.C., Cutello, V., Deb, K., Forrest, S., Nicosia, G., Pavone, M. (eds.) *PPSN 2012, Part I. LNCS*, vol. 7491, pp. 21–31. Springer, Heidelberg (2012)
7. Vanneschi, L., Castelli, M., Manzoni, L., Silva, S.: A new implementation of geometric semantic GP and its application to problems in pharmacokinetics. In: Krawiec, K., Moraglio, A., Hu, T., Etaner-Uyar, A.S., Hu, B. (eds.) *EuroGP 2013. LNCS*, vol. 7831, pp. 205–216. Springer, Heidelberg (2013)

# Eager Random Search for Differential Evolution in Continuous Optimization

Miguel Leon<sup>(✉)</sup> and Ning Xiong

Mälardalen University, Västerås, Sweden  
[{miguel.leonortiz,ning.xiong}@mdh.se](mailto:{miguel.leonortiz,ning.xiong}@mdh.se)

**Abstract.** This paper proposes a memetic computing algorithm by incorporating Eager Random Search (ERS) into differential evolution (DE) to enhance its search ability. ERS is a local search method that is eager to move to a position that is identified as better than the current one without considering other opportunities. Forsaking optimality of moves in ERS is advantageous to increase the randomness and diversity of search for avoiding premature convergence. Three concrete local search strategies within ERS are introduced and discussed, leading to variants of the proposed memetic DE algorithm. The results of evaluations on a set of benchmark problems have demonstrated that the integration of DE with Eager Random Search can improve the performance of pure DE algorithms while not incurring extra computing expenses.

**Keywords:** Evolutionary algorithm · Differential evolution · Eager Random Search · Memetic algorithm · Optimization

## 1 Introduction

Differential evolution [1] presents a class of metaheuristics [2] to solve real parameter optimization tasks with nonlinear and multimodal objective functions. DE has been used as very competitive alternative in many practical applications due to its simple and compact structure, easy use with fewer control parameters, as well as high convergence in large problem spaces. However, the performance of DE is not always excellent to ensure fast convergence to the global optimum. It can easily get stagnation resulting in low precision of acquired results or even failure.

Hybridization of EAs with local search (LS) techniques can greatly improve the efficiency of the search. EAs that are augmented with LS for self-refinement are called Memetic Algorithms (MAs) [3]. Memetic computing has been used with DE to refine individuals in their neighborhood. Norman and Iba [4] proposed a crossover-based adaptive method to generate offspring in the vicinity of parents. Many other works apply local search mechanisms to certain individuals of every generation to obtain possibly even better solutions, see examples in ([5], [6], [7]). Other Researchers investigate adaptation of control parameters of DE to improve the performance ([8], [9]).

This paper proposes a new memetic DE algorithm by incorporating Eager Random Search (ERS) to enhance the performance of a conventional DE algorithm. ERS is a local search method that is eager to move to a position that is identified as better than the current one without considering other opportunities in the neighborhood. This is different from common local search methods such as gradient descent or hill climbing which seek local optimal actions during the search. Forsaking optimality of moves in ERS is advantageous to increase randomness and diversity of search for avoiding premature convergence. Three concrete local search strategies within ERS are introduced and discussed, leading to variants of the proposed memetic DE algorithm. In addition, only a small subset of randomly selected variables is used in every step of the local search for randomly deciding the next trial point. The results of tests on a set of benchmark problems have demonstrated that the hybridization of DE with Eager Random Search can bring improvement of performance compared to pure DE algorithms while not incurring extra computing expenses.

## 2 Basic DE

DE is a stochastic and population based algorithm with  $N_p$  individuals in the population. Every individual in the population stands for a possible solution to the problem. One of the  $N_p$  individuals is represented by  $X_{i,g}$  with  $i = 1, 2, \dots, N_p$  and  $g$  is the index of the generation. DE has three consecutive steps in every iteration: mutation, recombination and selection. The explanation of these steps is given below:

**MUTATION.**  $N_p$  mutated individuals are generated using some individuals of the population. The vector for the mutated solution is called mutant vector and it is represented by  $V_{i,g}$ . There are some ways to mutate the current population, but the most common one is called random mutation strategy. This mutation strategy will be explained below. The other mutation strategies and their performance are given in [10].

$$V_{i,g} = X_{r_1,g} + F \times (X_{r_2,g} - X_{r_3,g}) \quad (1)$$

where  $V_{i,g}$  represents the mutant vector,  $i$  stands for the index of the vector,  $g$  stands for the generation,  $r_1, r_2, r_3 \in \{1, 2, \dots, N_p\}$  are random integers and  $F$  is the scaling factor in the interval  $[0, 2]$ .

**CROSSOVER.** In step two we recombine the set of mutated solutions created in step 1 (mutation) with the original population members to produce trial solutions. A new trial vector is denoted by  $T_{i,g}$  where  $i$  is the index and  $g$  is the generation. Every parameter in the trial vector is calculated with equation 2.

$$T_{i,g}[j] = \begin{cases} V_{i,g}[j] & \text{if } \text{rand}[0, 1] < CR \text{ or } j = j_{rand} \\ X_{i,g}[j] & \text{otherwise} \end{cases} \quad (2)$$

where  $j$  stands for the index of every parameter in a vector, CR is the probability of the recombination and  $j_{rand}$  is a randomly selected integer in  $[1, N_p]$  to ensure that at least one parameter from the mutant vector is selected.

**SELECTION.** In this last step we compare the fitness of a trial vector with the fitness of its parent in the population with the same index  $i$ , selecting the individual with the better fitness to enter the next generation. So we compare

### 3 DE Integrated with ERS

This section is devoted to the proposal of the memetic DE algorithm with integrated ERS for local search. We will first introduce ERS as a general local search method together with its three concrete (search) strategies, and then we shall outline how ERS can be incorporated into DE to enable self-refinement of individuals inside a DE process.

#### 3.1 Eager Random Local Search (ERS)

The main idea of ERS is to immediately move to a randomly created new position in the neighborhood without considering other opportunities as long as this new position receives a better fitness score than the current position. This is different from some other conventional local search methods such as Hill Climbing in which the next move is always to the best position in the surroundings. For-saking optimality of moves in ERS is beneficial to achieve more randomness and diversity of search for avoiding local optima. Further, in exploiting the neighborhood, only a small subset of randomly selected variables undergoes changes to randomly create a trial solution. If this trial solution is better, it simply replaces the current one. Otherwise a new trial solution is generated with other randomly selected variables. This procedure is terminated when a given number of trial solutions have been created without finding improved ones.

The next more detailed issue with ERS is how to change a selected variable in making a trial solution in the neighborhood. Our idea is to solve this issue using a suitable probability function. We consider three probability distributions (uniform, normal, and Cauchy) as alternatives for usage when generating a new value for a selected parameter/variable. The use of different probability distributions lead to different local search strategies within the ERS family, which will be explained in the sequel.

**Random Local Search (RLS).** In Random Local Search (RLS), we simply use a uniform probability distribution when new trial solutions are created given a current solution. To be more specific, when dimension  $k$  is selected for change, the trial solution  $X'$  will get the following value on this dimension regardless of its initial value in the current solution:

$$X'[k] = \text{rand}(a_i, b_i) \quad (3)$$

where  $\text{rand}(a_i, b_i)$  is a uniform random number between  $a_i$  and  $b_i$ , and  $a_i$  and  $b_i$  are the minimum and maximum values respectively on dimension  $k$ .

**Normal Local Search (NLS).** In Normal Local Search (NLS), we create a new trial solution by disturbing the current solution in terms of a normal probability distribution. This means that, if dimension  $k$  is selected for change, the value on this dimension for trial solution  $X'$  will be given by

$$X'[k] = X[k] + N(0, \delta) \quad (4)$$

where  $N(0, \delta)$  represents a random number generated according to a normal density function with its mean being zero.

**Cauchy Local Search (CLS).** In this third local search strategy, we apply the Cauchy density function in creating trial solutions in the neighborhood. It is called Cauchy Local search (CLS). A nice property of the Cauchy function is that it is centered around its mean value whereas exhibiting a wider distribution than the normal probability function. The value of trial solution  $X'$  will be generated as follows:

$$X'[k] = X[k] + t \times \tan(\pi \times (\text{rand}(0, 1) - 0.5)) \quad (5)$$

where  $\text{rand}(0, 1)$  is a random uniform number between 0 and 1.

### 3.2 The Proposed Memetic DE Algorithm

Here with we propose a new memetic DE algorithm by combining basic DE with Eager Random Search (ERS). ERS is applied in each generation after completing the mutation, crossover and selection operators. The best individual in the population is used as the starting point when ERS is executed. If ERS terminates with a better solution, it is inserted into the population and the current best member in the population is discarded.

We use DERLS, DENLS, and DECLS to refer to the variants of the proposed memetic DE algorithm that adopt RLS, NLS, and CLS respectively as local search strategies.

## 4 Experiments and Results

To examine the merit our proposed memetic DE algorithm compared to basic DE, we tested the algorithms in thirteen benchmark functions [10]. Functions 1 to 7 are unimodal and functions 8 to 13 are multimodal functions that contain many local optima.

### 4.1 Experimental Settings

DE has three main control parameters: population size ( $N_p$ ), crossover rate ( $CR$ ) and the scaling factor ( $F$ ) for mutation. The following specification of these parameters was used in the experiments:  $N_p = 60$ ,  $CR = 0.85$  and  $F = 0.9$ . All

the algorithms were applied to the benchmark problems with the aim to find the best solution for each of them. Every algorithm was executed 30 times on every function to acquire a fair result for the comparison. The condition to finish the execution of DE programs is that the error of the best result found is below 10e-8 with respect to the true minimum or the number of evaluations has exceeded 300,000. In DECLS,  $t = 0.2$ .

## 4.2 Performance of the Memetic DE with Random Mutation Strategy

First, random mutation strategy (DE/rand/1) was used in all DE approaches to study the effect of the ERS local search strategies in the memetic DE algorithm. The results can be observed in Table 1 and the values in boldface represent the lowest average error found by the approaches.

**Table 1.** Average error of the found solutions on the test problems with random mutation strategy

F.	DE	DERLS	DENLS	DECLS
f1	<b>0,00E+00</b> (4,56E-14)	<b>0,00E+00</b> (6,80E-13)	<b>0,00E+00</b> (1,21E-13)	<b>0,00E+00</b> (1,33E-14)
f2	1,82E-08 (1,13E-08)	5,30E-08 (2,39E-08)	2,26E-08 (1,32E-08)	<b>1,42E-08</b> (1,07E-08)
f3	6,55E+01 (3,92E+01)	8,01E+01 (4,88E+01)	1,11E+00 (1,10E+00)	<b>6,54E-01</b> (1,47E+01)
f4	6,22E+00 (5,07E+00)	2,37E+00 (1,87E+00)	1,80E-02 (7,28E-01)	<b>5,66E-01</b> (3,68E-01)
f5	2,31E+01 (2,00E+01)	2,27E+01 (1,81E+01)	2,65E+01 (2,41E+01)	<b>2,03E+01</b> (2,62E+01)
f6	<b>0,00E+00</b> (0,00E+00)	<b>0,00E+00</b> (0,00E+00)	<b>0,00E+00</b> (0,00E+00)	<b>0,00E+00</b> (0,00E+00)
f7	1,20E-01 (3,79E-03)	1,15E-02 (3,16E-03)	1,23E-02 (3,29E-03)	<b>1,05E-02</b> (3,61E-03)
f8	2,72E+03 (8,15E+02)	<b>2,31E+02</b> (1,50E+02)	1,86E+03 (5,46E+02)	1,58E+03 (5,16E+02)
f9	1,30E+01 (3,70E+00)	1,28E+01 (3,72E+00)	<b>6,17E+00</b> (2,06E+00)	7,72E+00 (2,43E+00)
f10	1,88E+01 (4,28E+00)	<b>1,87E+00</b> (4,76E+00)	4,94E+00 (8,11E+00)	5,50E+00 (7,53E+00)
f11	<b>8,22E-04</b> (2,49E-03)	<b>8,22E-04</b> (2,49E-03)	1,49E-02 (2,44E-02)	1,44E-02 (2,70E-02)
f12	3,46E-03 (1,86E-02)	3,46E-03 (1,86E-02)	1,04E-02 (3,11E-02)	<b>0,00E+00</b> (8,49E-15)
f13	3,66E-04 (1,97E-03)	<b>0,00E+00</b> (2,14E-13)	<b>0,00E+00</b> (1,31E-14)	<b>0,00E+00</b> (3,37E-15)

We can see in Table 1 that DECLS is the best in all the unimodal functions except on Function 4 that is the second best. In multimodal functions, DERLS is the best on Functions 8, 10 and 11. DECLS found the exact optimum all the times in Functions 12 and 13. The basic, DE performed the worst in multimodal functions. According to the above analysis, we can say that DECLS improve a lot the performance of basic DE with random mutation strategy and also we found out that DERLS is really good in multimodal functions particularly on Function 8, which is the most difficult function. Considering all the functions, the best algorithm is DECLS and the weakest one is the basic DE.

## 5 Conclusions

In this paper we propose a memetic DE algorithm by incorporating Eager Random Search (ERS) as a local search method to enhance the search ability of a pure DE algorithm. Three concrete local search strategies (RLS, NLS, and CLS)

are introduced and explained as instances of the general ERS method. The use of different local search strategies from the ERS family leads to variants of the proposed memetic DE algorithm, which are abbreviated as DERLS, DENLS and DECLS respectively. The results of the experiments have demonstrated that the overall ranking of DECLS is superior to the ranking of basic DE and other memetic DE variants considering all the test functions. In addition, we found out that DERLS is much better than the other counterparts in very difficult multimodal functions.

**Acknowledgment.** The work is funded by the Swedish Knowledge Foundation (KKS) grant (project no 16317). The authors are also grateful to ABB FACTS, Prevas and VOITH for their co-financing of the project.

## References

1. Storn, R., Price, K.: Differential evolution - a simple and efficient heuristic for global optimization over continuous spaces. *Journal of Global Optimization* **11**(4), 341–359 (1997)
2. Xiong, N., Molina, D., Leon, M., Herrera, F.: A walk into metaheuristics for engineering optimization: Principles, methods, and recent trends. *International Journal of Computational Intelligence Systems* **8**(4), 606–636 (2015)
3. Krasnogor, N., Smith, J.: A tutorial for competent memetic algorithms: Model, taxonomy, and design issue. *IEEE Transactions on Evolutionary Computation* **9**(5), 474–488 (2005)
4. Norman, N., Ibai, H.: Accelerating differential evolution using an adaptative local search. *IEEE Transactions on Evolutionary Computation* **12**, 107–125 (2008)
5. Ali, M., Pant, M., Nagar, A.: Two local search strategies for differential evolution. In: Proc. 2010 IEEE Fifth International Conference on Bio-Inspired Computing: Theories and Applications (BIC-TA), Changsha, China, pp. 1429–1435 (2010)
6. Dai, Z., Zhou, A.: A differential ecolution with an orthogonal local search. In: Proc. 2013 IEEE Congress on Evolutionary Computation (CEC), Cancun, Mexico, pp. 2329–2336 (2013)
7. Leon, M., Xiong, N.: Using random local search helps in avoiding local optimum in diefferential evolution. In: Proc. Artificial Intelligence and Applications, AIA2014, Innsbruck, Austria, pp. 413–420 (2014)
8. Qin, A., Suganthan, P.: Self-adaptive differential evolution algorithm for numerical optimization. In: The 2005 IEEE Congress on Evolutionary Computation, vol. 2, pp. 1785–1791 (2005)
9. Leon, M., Xiong, N.: Greedy adaptation of control parameters in differential evolution for global optimization problems. In: IEEE Conference on Evolutionary Computation, CEC2015, Japan, pp. 385–392 (2015)
10. Leon, M., Xiong, N.: Investigation of mutation strategies in differential evolution for solving global optimization problems. In: Rutkowski, L., Korytkowski, M., Scherer, R., Tadeusiewicz, R., Zadeh, L.A., Zurada, J.M. (eds.) ICAISC 2014, Part I. LNCS, vol. 8467, pp. 372–383. Springer, Heidelberg (2014)

# Learning from Play: Facilitating Character Design Through Genetic Programming and Human Mimicry

Swen E. Gaudl<sup>1</sup>(✉), Joseph Carter Osborn<sup>2</sup>, and Joanna J. Bryson<sup>1</sup>

<sup>1</sup> Department of Computer Science, University of Bath, Bath, UK  
swen.gaudl@gmail.com, jjb@bath.ac.uk

<sup>2</sup> Baskin School of Engineering, University of California SC, Santa Cruz, USA  
jcosborn@soe.ucsc.edu

**Abstract.** Mimicry and play are fundamental learning processes by which individuals can acquire behaviours, skills and norms. In this paper we utilise these two processes to create new game characters by mimicking and learning from actual human players. We present our approach towards aiding the design process of game characters through the use of genetic programming. The current state of the art in game character design relies heavily on human designers to manually create and edit scripts and rules for game characters. Computational creativity approaches this issue with fully autonomous character generators, replacing most of the design process using black box solutions such as neural networks. Our GP approach to this problem not only mimics actual human play but creates character controllers which can be further authored and developed by a designer. This keeps the designer in the loop while reducing repetitive labour. Our system also provides insights into how players express themselves in games and into deriving appropriate models for representing those insights. We present our framework and preliminary results supporting our claim.

**Keywords:** Agent design · Machine learning · Genetic programming · Games

## 1 Introduction

Designing intelligence is a sufficiently complex task that it can itself be aided by the proper application of AI techniques. Here we present a system that mines human behaviour to create better Game AI. We utilise genetic programming (GP) to generalise from and improve upon human game play. More importantly, the resulting representations are amenable to further authoring and development. We introduce a GP system for evolving game characters by utilising recorded human play. The system uses the platformerAI toolkit, detailed in section 3, and the JAVA genetic algorithm and genetic programming package (JGAP) [6]. JGAP provides a system to evolve agents when given a set of command genes, a fitness function, a genetic selector and an interface to the target

application. Thereafter, our system generates players by creating and evolving JAVA program code which is fed into the PLATFORMERAI toolkit and evaluated using our player-based fitness function.

The rest of this paper is organised as follows. In section 2 we describe how our system derives from and improves upon the start of the art. Section 3 describes our system and its core components, including details of our fitness function. We conclude our work by describing our initial results and possible future work.

## 2 Background and Related Work

In practice, making a good game is achieved by a good concept and long iterative cycles in refining mechanics and visuals, a process which is resource consuming. It requires a large number of human testers to evaluate the qualities of a game. Thus, analysing tester feedback and incrementally adapting games to achieve better play experience is tedious and time consuming. This is where our approach comes into play by trying to minimise development, manual adaptation and testing time, yet allow the developer to remain in full control.

*Agent Design* initially no more than creating 2D shapes on the screen, e.g. the aliens in SPACEINVADERS. Due to early hardware limitations, more complex approaches were not feasible. With more powerful computers it became feasible to integrate more complex approaches from science. In 2002 Isla introduced the BEHAVIOURTREE (BT) for the game Halo, later elaborated by Champandard [2]. BT has become the dominant approach in the industry. BTs are a combination of a decision tree (DT) with a pre-defined set of node types. A related academic predecessor of the BT were the POSH dynamic plans of BOD [1,3].

*Generative Approaches* [4,7] build models to create better and more appealing agents. In turn, a generative agent uses machine learning techniques to increase its capabilities. Using data derived from human interaction with a game—referred to as human play traces—can allow the game to act on or *react* to input created by the player. By training on such data it is possible to derive models able to mimic certain characteristics of players. One obvious disadvantage of this approach is that the generated model only learns from the behaviour exhibited in the data provided to it. Thus, interesting behaviours are not accessible because they were never exhibited by a player.

In contrast to other generative agent approaches [7,9,15] our system combines features which allow the generation and development of truly novel agents. The first is the use of un-authored recorded player input as direct input into our fitness function. This allows the specification of agents only by playing. The second feature is that our agents are actual programs in the form of java code which can be altered and modified after evolving into a desired state, creating a white box solution. While Stanley and Miikkulainen[13] use neural networks (NN) to create better agents and enhance games using Neuroevolution, we utilise genetic programming [10] for the creation and evolution of artificial players in human readable and modifiable form. The most comparable approach is that of Perez et al.[9] which uses grammar based evolution to derive BTs given an

initial set and structure of subtrees. In contrast, we start with a clean slate to evolve novel agents as directly executable programs.

### 3 Setting and Environment

Evolutionary algorithms have the potential to solve problems in vast search spaces, especially if the problems require multi-parameter optimisation [11, p.2]. For those problems humans are generally outperformed by programs [12]. Our GP approach uses a pool of program chromosomes  $P$  and evolves those in the form of decision trees (DTs) exploring the possible solution space. For our experiments the PLATFORMERAI toolkit (<http://www.platformersai.com>) was used. It consists of a 2D platformer game, similar to existing commercial products and contains modules for recording a player, controlling agents and modifying the environment and rules of the game.

The *Problem Space* is defined by all actions an agent can perform. Within the game, agent  $A$  has to solve the complex task of selecting the appropriate action each given frame. The game consists of  $A$  traversing a level which is not fully observable. A level is 256 spatial units long and  $A$  should traverse it left to right. Each level contains objects which act in a deterministic way. Some of those objects can alter the player's score, e.g. coins. Those bonus objects present a secondary objective. The goal of the game, move from start to finish, is augmented with the objective of gaining points.  $A$  can get points by collecting objects or jumping onto enemies. To make it comparable to the experience of similar commercial products we use a realistic time frame in which a human would need to solve a level, 200 time units. The level observability is limited to a  $6 \times 6$  grid centred around the player, cf. Perez et al.[9].

*Agent Control* is handled through a 6-bit vector  $C$ : *left*, *right*, *up*, *down*, *jump* and *shoot|run*. The vector is required each frame, simulating an input device. However, some actions span more than one frame. This is a simple task for a human but quite complex to learn for an agent. One such example, the high jump, requires the player to press the jump button for multiple frames. Our system has a gene for each element of  $C$  plus 14 additional genes formed of five gene types: sensory information about the level or agent, executable actions, logical operators, numbers and structural genes. All those are combined on creation time into a chromosome represented as a DT using the grammar underlying the JAVA language. Structural genes allow the execution of  $n$  genes in a fixed sequence, reducing the combinatorial freedom provided by JAVA.

*Evaluation of Fitness* in our system is done using the Gamalyzer-based play trace metric which determines the fitness of individual chromosomes based on human traces as an evaluation criterion. For finding optimal solutions to a problem statistical fitness functions offer near-optimal results when optimality can be defined. We are interested in understanding and modelling human-like or human-believable behaviour in games. There is no known algorithm for measuring how human-like behaviour is; identifying this may even be computationally intractable. A near-best solution for the problem space of finding the optimal

way through a level was given by Baumgarten [14] using the  $A^*$  algorithm. This approach produces agents which are extremely good at winning the level within a minimum amount of time but at the same time are clearly distinguishable from actual human players. For games and game designers a less distinguishable approach is normally more appealing—based on our initial assumptions.

## 4 Fitness Function

Based on the biological concept of selection, all evolutionary systems require some form of judgement about the quality of a specific individual—the fitness value of the entity. Our *Player Based Fitness* (PBF) uses multiple traces of human,  $t_h$ , and agent,  $t_a$ , players to derive a fitness value by judging their similarity. For that purpose we integrate the Gamalyzer Metric—a game independent measurement of the difference between two play traces. It is based on the syntactic edit distance  $d_{dis}$  between pairs of sequences of player inputs [8]. It takes pairs of sequences of events gathered during a game play along with designer-provided rules for comparing individual events and yields a numerical value in  $[0, 1]$ . Identical traces have distance  $d_{dis} = 0$  and incomparably different traces  $d_{dis} = 1$ . Gamalyzer finds the least expensive way to turn one play trace into another by repeatedly deleting an event from the first trace, inserting an event of the second trace into the first trace, or changing an event of the first trace into an event of the second trace. The game designer or analyst must also provide a comparison function which describes the difficulty of changing one event into another. The other important feature of Gamalyzer, warp window  $\omega$ , is a constraint that prevents early parts of the first trace from comparing against late parts of the second. This is important for correctness (a running leap at the beginning of the level has a very different connotation from a running leap at the pole at the end of each stage). For our purpose, only the input commands players use to control the agent are encoded—the six commands introduced earlier. This allows us to compare against direct controller input for future studies and to help designers sitting in front of the controls analysing the resulting character program. The PBF currently offers two parameters: the chunk size,  $cpf$ , and the warp window size,  $\omega$ . The main advantage over a pure statistical fitness function is that a designer can feed our system specific play traces of human players without having to modify implicit values of a fitness score.

To make a stronger emphasis on playing the game well, we create a multi-objective problem using an aggregation function  $g$  to take  $\Delta d$ —the moved distance—and the fitness  $f(a)$  for an agent using the playerbased metric PBF into account, see formula (1). Using  $g$  we were able to put equal focus on the trace metric,  $f_{ptm} \in [0 \dots 1] \subset \mathbb{R}$ , and the advancement along the game,  $\Delta d \in [0 \dots 256] \subset \mathbb{N}$ .

$$f(a) = g(f_{ptm}(t_a, t_h), \Delta d) \quad (1)$$

## 5 Preliminary Results and Future Work

Using our experimental configuration and the PBF fitness function we are now able to execute, evaluate and compare platformerAI agents against human traces. We are using the settings supplied in table 1. As a selection mechanism, the weighted roulette wheel is used and we additionally preserve the fittest individual of a generation. We use single point tree branch crossover on two selected parent chromosomes and expose the resulting child to a single point mutation before it is put into the new generation. Figure 1 illustrates the convergence of the program pool against the global optimum. Good solutions are on average reached after 700 generations, when an agent finishes the given level. Our first experiments show that our approach is able to train on and converge against raw human play traces without stopping at local optima, visible in the two dents of the averaged fitness (black) diverging from the fittest individual (red). A next step would be to investigate the generated modifiable programs further and analyse their benefit in understanding players better. However, our current solution already offers a way to design agents for a game by simply playing it and creating learning agents from those traces. Other possible directions could be expansion of the model underlying Gamalyzer to model specific events within the game rather than pure input actions. This should provide interesting feedback and offer a better matching of expressed player behaviour and model generation. Our current agent model consists of an unweighted tree representation containing program genes. Currently subtrees are not taken into consideration when calculating the fitness of an individual. By including those weights it would be possible to narrow down the search space of good solutions for game characters dramatically, also potentially reducing the bloat of the DT. So, to enhance the quality of our

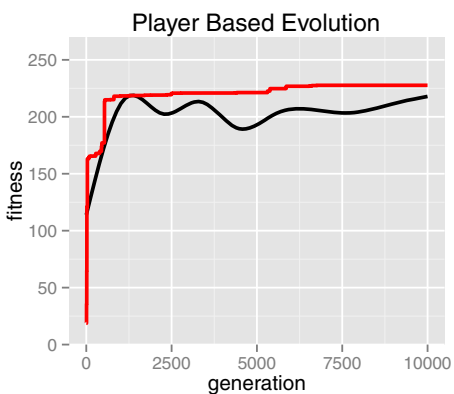


**Fig. 1.** The evolved agents' fitness using PBF (10000 generations), in red the fittest individuals, in black the averaged fitness of all agents per generation.

**Table 1.** GP parameters used in our system.

Parameter	Value
Initial Population Size	100
Selection	Weighted Roulette Wheel
Genetic Operators	Branch Typing CrossOver and Single Point Mutation
Initial Operator probabilities	0.6 crossover, 0.2 new chromosomes, 0.01 mutation, fixed
Survival	Elitism
Function Set	<i>ifelse</i> , <i>not</i> , <i>&amp;&amp;</i> , <i>  </i> , <i>sub</i> , <i>IsCoinAt</i> , <i>IsEnemyAt</i> , <i>IsBreakAbleAt</i> , ...
Terminal Set	Integers [-6,6], $\leftarrow$ , $\rightarrow$ , $\downarrow$ , <i>IsTall</i> , <i>Jump</i> , <i>Shoot</i> , <i>Run</i> <i>Wait</i> , <i>CanJump</i> , <i>CanShoot</i> , ...

reproduction component we believe it might be interesting to investigate the applicability of behavior-programming for GP (BPGP) [5] into our system.

## References

1. Bryson, J.J., Stein, L.A.: Modularity and design in reactive intelligence. In: Proceedings of the 17th International Joint Conference on Artificial Intelligence, pp. 1115–1120. Morgan Kaufmann, Seattle, August 2001
2. Champandard, A.J.: AI Game Development. New Riders Publishing (2003)
3. Gaudl, S.E., Davies, S., Bryson, J.J.: Behaviour oriented design for real-time-strategy games - an approach on iterative development for starcraft ai. In: Proceedings of the Foundations of Digital Games, pp. 198–205. Society for the Advancement of Science of Digital Games (2013)
4. Holmgard, C., Liapis, A., Togelius, J., Yannakakis, G.: Evolving personas for player decision modeling. In: 2014 IEEE Conference on Computational Intelligence and Games (CIG), pp. 1–8, August 2014
5. Krawiec, K., O'Reilly, U.M.: Behavioral programming: a broader and more detailed take on semantic gp. In: Proceedings of the 2014 Conference on Genetic and Evolutionary Computation, pp. 935–942. ACM (2014)
6. Meffert, K., Rotstan, N., Knowles, C., Sangiorgi, U.: Jgap-java genetic algorithms and genetic programming package, September 2000. <http://jgap.sf.net> (last viewed: January 2015)
7. Ortega, J., Shaker, N., Togelius, J., Yannakakis, G.N.: Imitating human playing styles in super mario bros. Entertainment Computing 4(2), 93–104 (2013)
8. Osborn, J.C., Mateas, M.: A game-independent play trace dissimilarity metric. In: Proceedings of the Foundations of Digital Games. Society for the Advancement of Science of Digital Games (2014)
9. Perez, D., Nicolau, M., O'Neill, M., Brabazon, A.: Evolving behaviour trees for the mario ai competition using grammatical evolution. In: Di Chio, C., et al. (eds.) EvoApplications 2011, Part I. LNCS, vol. 6624, pp. 123–132. Springer, Heidelberg (2011)
10. Poli, R., Langdon, W.B., McPhee, N.F., Koza, J.R.: A field guide to genetic programming. Lulu. com (2008)
11. Schwefel, H.P.P.: Evolution and optimum seeking: the sixth generation. John Wiley & Sons, Inc. (1993)
12. Smit, S.K., Eiben, A.E.: Comparing parameter tuning methods for evolutionary algorithms. In: IEEE Congress on Evolutionary Computation, CEC 2009, pp. 399–406. IEEE (2009)
13. Stanley, K.O., Miikkulainen, R.: Evolving neural networks through augmenting topologies. Evolutionary Computation 10, 99–127 (2002)
14. Togelius, J., Karakovskiy, S., Baumgarten, R.: The 2009 mario ai competition. In: 2010 IEEE Congress on Evolutionary Computation (CEC), pp. 1–8. IEEE (2010)
15. Togelius, J., Yannakakis, G., Karakovskiy, S., Shaker, N.: Assessing believability. In: Hingston, P. (ed.) Believable Bots, pp. 215–230. Springer, Heidelberg (2012)

# Memetic Algorithm for Solving the 0-1 Multidimensional Knapsack Problem

Abdellah Rezoug<sup>1</sup>(✉), Dalila Boughaci<sup>2</sup>, and Mohamed Badr-El-Den<sup>3</sup>

<sup>1</sup> Department of Computer Science, University Mhamed Bougarra of Boumerdes, Boumerdes, Algeria  
[abdellah.rezoug@gmail.com](mailto:abdellah.rezoug@gmail.com)

<sup>2</sup> FEI, Department of Computer Science Beb-Ezzouar, USTHB, Algiers, Algeria  
[dboughaci@usthb.dz](mailto:dboughaci@usthb.dz), [dalila.info@yahoo.fr](mailto:dalila.info@yahoo.fr)

<sup>3</sup> School of Computing, Faculty of Technology, University of Portsmouth, Portsmouth, UK  
[mohamed.bader@port.ac.uk](mailto:mohamed.bader@port.ac.uk)

**Abstract.** In this paper, we propose a memetic algorithm for the Multidimensional Knapsack Problem (MKP). First, we propose to combine a genetic algorithm with a stochastic local search (GA-SLS), then with a simulated annealing (GA-SA). The two proposed versions of our approach (GA-SLS and GA-SA) are implemented and evaluated on benchmarks to measure their performance. The experiments show that both GA-SLS and GA-SA are able to find competitive results compared to other well-known hybrid GA based approaches.

**Keywords:** Multidimensional knapsack problem · Stochastic local search · Genetic algorithm · Simulated annealing · Local search · Memetic algorithm

## 1 Introduction

The Multidimensional Knapsack Problem (MKP) is a strong NP-hard combinatorial optimization problem [14]. The MKP has been extensively considered because of its theoretical importance and wide range of applications. Many practical engineering design problems can be formulated as MKP such as: the capital budgeting problem [17], the project selection [2] and so on.

The solutions for MKP can be classified into exact, approximate and hybrid. The exact solutions are used for problems of small size. Branch and bound, branch and cut, linear, dynamic and quadratic programming, etc. are the principal exact methods used for solving MKP [13, 21]. The approximate solutions are used when the data size is high but it is not sure to obtain the optimal results. They are mainly based on heuristics such as: simulated annealing, tabu search, genetic algorithm, ant colony particle swarm, harmony search, etc [5, 6, 20]. The hybrid solutions combine two or more exact or/and approximate solutions. These solutions are the most used in the field of optimization and especially for MKP such as [4, 8–12, 18] and so on.

In this paper, we propose a memetic algorithm for MKP. We developed two versions of our method for MKP. The first denoted GA-SLS is a GA combined with the stochastic local search (SLS) [3]. The second denoted GA-SA is a combination of GA with the simulated annealing (SA) [16]. The two versions are implemented and evaluated on some well-known benchmarks for MKP where the sizes of benchmarks arrange from small to large. A comparative study is done with a pure GA and some algorithms for MKP. The objective is to show the impact of the local search in the performance of the memetic approach.

The rest of the paper is organized as follows. Section 2 gives the MKP model. The proposed Memetic approaches are detailed in Section 3. Section 4 describes the experiments. Finally, Section 5 concludes the paper.

## 2 The Multidimensional Knapsack Problem

The MKP is composed of  $N$  items and a knapsack with  $m$  different capacities  $b_i$  where  $i \in \{1, \dots, m\}$ . Each item  $j$  where  $j \in \{1, \dots, n\}$  has a profit  $c_j$  and can take  $a_{ij}$  of the capacity  $i$  of the knapsack. The goal is to pack the items in the knapsack so as to maximize the profits of items without exceeding the capacities of the knapsack. The MKP is modeled as the following integer program:

$$\text{Maximize} \sum_{j=1}^n c_j x_j \quad (1)$$

$$\text{Subject to : } \sum_{j=1}^n a_{ij} x_j \leq b_i \quad i \in \{1 \dots m\} \quad (2)$$

$$x_j \in \{0, 1\} \quad j \in \{1 \dots n\}$$

## 3 The Proposed Approaches for MKP

Two versions of memetic approach have been studied. The first one is the Genetic Algorithm-Stochastic Local Search (GA-SLS) where GA is combined with SLS. The second one is the Genetic Algorithm-Simulated Annealing (GA-SA) which is GA combined with SA. The structures of both approaches are similar in the GA part. The difference is in the local search. The GA-SLS applies SLS while GA-SA applies SA. Their process consists in: Create the initial population  $P$  using the Random Key method (RK)[1] and initialize  $Q = \{\}$ ,  $NI$  and  $T = T_0$  ( $T$  for GA-SA only). Select two parents  $X_1$  and  $X_2$  that are the two best individuals in  $P$  and  $X_1, X_2 \notin Q$ . Exchange  $NCB$  items between the parents  $X_1$  and  $X_2$  to produce two new infeasible offspring  $X'_1$  and  $X'_2$ , then if conflict exists in  $X'_1$  or  $X'_2$ , repeatedly remove either the worst items or an item chosen randomly according to a probability  $rp$ . Push the two parents  $X_1$  and  $X_2$  in  $Q$ . Apply the local search (SLS for GA-SLS or SA for GA-SA) on offspring  $X'_1$ ,  $X'_2$ . Find the best individuals  $X_{best}$  in  $P$  and replace randomly a number of items in  $X'_1$  and  $X'_2$  by items in  $X_{best}$ . If the quality of  $X'_1$  and  $X'_2$  is better than the two

**Algorithm 1.** GA-SLS Algorithm.

---

**Require:** An MKP instance,  $NI$  and  $Q = \emptyset$ .  
**Ensure:** An best solution found  $X^*$ .

- 1: Create the initial population  $P$  by the *RK* method.
- 2: **for** ( $Cpt = 1$  to  $NI$ ) **do**
- 3:   Selection of the two best individuals  $X_1, X_2$  in  $P$  and  $X_1, X_2 \notin Q$ .
- 4:   Crossover  $X_1, X_2$  to produce offsprings  $X'_1, X'_2$
- 5:   Repair offsprings  $X'_1, X'_2$
- 6:   Apply the local search method on  $X'_1, X'_2$
- 7:   Mutation on  $X'_1, X'_2$  with  $X_{best}$  of  $P$
- 8:    $X_{worst} \leftarrow$  the worst individual in  $P$
- 9:   **if** ( $f(X'_1) > f(X_{worst})$ ) **then**
- 10:      $P = P - \{X_{worst}\}$
- 11:      $P = P \cup \{X'_1\}$
- 12:   **end if**
- 13:    $X_{worst} \leftarrow$  the worst individual in  $P$
- 14:   **if** ( $f(X'_2) > f(X_{worst})$ ) **then**
- 15:      $P = P - \{X_{worst}\}$
- 16:      $P = P \cup \{X'_2\}$
- 17:   **end if**
- 18:    $Q = Q \cup \{X_1, X_2\}$
- 19: **end for**
- 20: Return the best individual found.

---

worst individuals in  $P$ , then they replace them. If the number of iterations  $NI$  is not attend then go to *STEP 2..* Otherwise return the best individual in  $P$ . The GA-SLS and GA-SA can be expressed by Algorithm 1.

## 4 The Experiments

GA, GA-SA and GA-SLS were implemented in C++ on 2 GHz Intel Core 2 Duo processor and 2 GB RAM. They were tested on the OR-Library [22] 54 benchmarks, with  $m = 2$  to 30 and  $n = 6$  to  $n = 105$  and on the OR-Library GK [22] with  $m = 15$  to  $m = 50$  and  $n = 100$  to  $n = 1500$ . In all experiments the parameters are chosen empirically such as: the number of iteration  $NI = 30000$ , the population size  $PS = 100$ , the waiting time  $WT = 50$ , the number of crossing bites  $NCB = 1/10$ . the initial temperature  $T_0 = 50$ , the walk probability  $wp = 0.93$ , the number of local iteration  $N = 100$  and the number of runs is 30.

**Results for the SAC-94 Standard Instances.** The average fitness (*Result*), the average gap (*GAP*), the best (*Best*) and the worst fitness (*Worst*), the number of success runs (*NSR*), the number of success instance (*NSI*) and the rate of success runs (*RSR*) have been recorded by analyzing the recorded obtained fitness. Also, the average CPU runtime (*Time*) has been calculated. All the results and statistics computed by the GA, GA-SA and GA-SLS are reported in Tables 1-2. From results, GA resolved to optimality one instance of 54 with average gap of 4,454 %, GA-SA 35 instances with a global gap of 0,093 % and GA-SLS 39 instances with a global gap of 0,0221 %. GA-SLS reached the optimum at least once in 50 instances followed by GA-SA in 49 instances then GA in 18 instances. The *RSR* show that GA-SLS totally solved instances of groups *hp*, *pb*

**Table 1.** Comparison of GA, GA-SA and GA-SLS on SAC-94 datasets.

Dataset	GA			GA-SA			GA-SLS	
	Opt	Result	GAP	Result	GAP	Result	GAP	
hp	3418	3381,07	1,080	3418	0	3418	0	
	3186	3120,63	2,052	3186	0	3186	0	
	<b>Average</b>	3302	3250,85	1,566	<b>3302</b>	<b>0</b>	<b>3302</b>	<b>0</b>
	3090	3060,27	0,962	3090	0	3090	0	
	3186	3139,13	1,471	3186	0	3186	0	
	<b>Average</b>	95168	93093,5	2,180	95168	0	95168	0
pb	2139	2079,93	2,762	2139	0	2139	0	
	776	583,767	24,772	776	0	776	0	
	1035	1018,13	1,630	1035	0	1035	0	
	<b>Average</b>	17565,666	17162,454	5,629	<b>17565,666</b>	<b>0</b>	<b>17565,666</b>	<b>0</b>
	87061	86760,1	0,346	87061	0	87061	0	
pet	4015	4015	0	4015	0	4015	0	
	6120	6091	0,474	6120	0	6120	0	
	12400	12380,3	0,159	12400	0	12400	0	
	10618	10560,9	0,538	10609,1	0,084	10608,6	0,089	
	16537	16373,9	0,986	16528,1	0,054	16528,3	0,053	
	<b>Average</b>	22791,833	22696,866	0,417	<b>22788,866</b>	<b>0,023</b>	22788,816	0,024
sento	7772	7606,03	2,135	7772	0	7772	0	
	8722	8569,7	1,746	8721,2	0,009	8722	0	
	<b>Average</b>	8247	8087,865	1,941	8246,6	0,005	<b>8247</b>	<b>0</b>
weing	141278	141263	0,011	141278	0	141278	0	
	130883	130857	0,020	130883	0	130883	0	
	95677	94496,2	1,234	95677	0	95677	0	
	119337	118752	0,490	119337	0	119337	0	
	98796	97525,3	1,286	98796	0	98796	0	
	130623	130590	0,025	130623	0	130623	0	
	1095445	1086484,2	0,818	1094579,6	0,079	1095432,7	0,0011	
	624319	581683	6,829	623727	0,095	624319	0	
	<b>Average</b>	304545,375	297707,062	1,339	304362,625	0,022	<b>304543,22</b>	<b>0,0001</b>
	4554	4530,03	0,526	4554	0	4554	0	
weish	4536	4506,77	0,644	4536	0	4536	0	
	4115	4009,37	2,567	4115	0	4115	0	
	4561	4131,07	9,426	4561	0	4561	0	
	4514	4159,73	7,848	4514	0	4514	0	
	5557	5491,73	1,175	5557	0	5557	0	
	5567	5428,37	2,490	5567	0	5567	0	
	5605	5509,43	1,705	5605	0	5605	0	
	5246	5104,5	2,697	5246	0	5246	0	
	6339	6014,23	5,123	6339	0	6339	0	
	5643	5234,33	7,242	5643	0	5643	0	
	6339	5916	6,673	6339	0	6339	0	
	6159	5769,5	6,324	6159	0	6159	0	
	6954	6495,6	6,592	6954	0	6954	0	
	7486	6684,6	10,705	7486	0	7486	0	
	7289	6878,4	5,633	7289	0	7289	0	
	8633	8314,73	3,687	8629,5	0,041	8633	0	
	9580	9146,5	4,525	9559,63	0,213	9568,63	0,119	
	7698	7223,17	6,168	7698	0	7698	0	
	9450	8632,1	8,655	9448,63	0,014	9449,37	0,007	
	9074	8114,4	10,575	9073,23	0,008	9073,33	0,007	
	8947	8321,17	6,995	8926,73	0,227	8938,83	0,091	
	8344	7603,77	8,871	8321,97	0,264	8318,93	0,3	
	10220	9685,77	5,227	10152,9	0,657	10164,2	0,546	
	9939	9077,9	8,664	9900,07	0,392	9910,73	0,284	
	9584	8728,87	8,922	9539,4	0,465	9560,53	0,245	
	9819	8873,7	9,627	9777,9	0,419	9802,03	0,173	
	9492	8653,57	8,833	9423,87	0,718	9442,17	0,525	
	9410	8466,67	10,025	9359,5	0,537	9369,5	0,430	
	11191	10250,1	8,408	11106,3	0,757	11128,7	0,557	
<b>Average</b>	7394,833	6898,536	6,218	7379,386	0,157	<b>7386,772</b>	<b>0,109</b>	

**Table 2.** Results of NSR, RSR and Time parameters obtained by GA, GA-SA and GA-SLS.

	GA			GA-SA			GA-SLS		
	NSR	RSR	Time	NSR	RSR	Time	NSR	RSR	Time
hp	1	1,67	1,798	<b>2</b>	<b>100</b>	6,077	<b>2</b>	<b>100</b>	7,101
pb	4	3,33	1,811	<b>6</b>	<b>100</b>	3,443	<b>6</b>	<b>100</b>	4,681
pet	4	32,78	1,395	<b>6</b>	<b>81,67</b>	11,296	<b>6</b>	80,55	12,179
sento	0	0,00	2,616	<b>2</b>	66,67	46,584	<b>2</b>	<b>100</b>	24,277
weing	6	39,58	1,669	<b>8</b>	76,25	10,259	<b>8</b>	<b>99,58</b>	10,586
weish	3	4,55	1,620	25	66,89	17,352	<b>26</b>	<b>76,88</b>	17,146
Average	18	13,65	1,818	49	81,91	15,835	<b>50</b>	<b>92,83</b>	<b>12,662</b>

**Table 3.** Results of the approaches test on the GK dataset.

Dataset	GA		GA-SA		GA-SLS			
	Instance	Optimal	Result	Gap	Result	Gap	Result	Gap
1	3766	3673,5	2,456	3,456	3704,3	1,638	3704,2	1,641
2	3958	3860,7	2,458	3,458	3894,8	1,596	3897,7	1,523
3	5656	5511,5	2,554	3,554	5538,8	2,072	5535,7	2,127
4	5767	5630,6	2,365	3,365	5655,2	1,938	5655,4	1,935
5	7560	7351,3	2,76	3,76	7395,1	2,181	7391,3	2,231
6	7677	7505,7	2,231	3,231	7528,4	1,935	7528,1	1,939
7	19220	18612,1	3,162	4,162	18691	2,752	18692,4	2,745
8	18806	18330,2	2,53	3,53	18393	2,196	18392,4	2,199
9	58091	56198,5	3,257	4,257	56371,1	2,96	56381,4	2,943
10	57295	55837,9	2,543	3,543	55959,3	2,331	55961,9	2,326
Average	18779,6	18251,2	2,632	3,632	18313,1	2,484	<b>18314,05</b>	<b>2,479</b>

and *sento* followed by GA-SA. GA-SLS obtained a total *RSR* better than GA-SA (92,83% and 81,91%, respectively). At the same time, GA-SA and GA-SLS widely surpass GA (13,65%). *RSR* shows that hybridization of GA with SA has improved the success rate of 79,18% and its hybridization with SLS of 68,49%. From Table 2, GA is the fastest with an global average CPU time of 1.818 sec.

**Results for the Ten Large Instances.** From results on the GK shown in Table 3 GA-SA has the best value of *Result* and *GAP* for 1, 3, 5, 6 and 8 instances. GA-SLS has the best value of *Result* and *GAP* for instances 2, 4, 7, 9 and 10. Global, GA-SLS has the best performance for all instances with an total average *GAP* of 2.479 %. GA-SA has almost the same performance with average *GAP* of 2.484 %. Also, GA is not very far from GA-SA and GA-SLS with an total average *GAP* of 2.632 %.

**Comparison with Other GA Approaches.** We compared results of the proposed GA-SA and GA-SLS to other approaches. The results of the KHBA [15], COTRO [7], TEVO [19], CHEBE [6] and HGA [10] were obtained from [10]. From Table 4 GA-SA and GA-SLS gave improved results compared to KHBA, COTRO and TEVO, for almost all instances. GA-SA and GA-SLS were able to find the optimal solutions to 6, and 3 of 7 problems respectively. Furthermore, GA-SA performs results quite similar to CHEBE and HGA.

**Table 4.** Comparison of GA-SA and GA-SLS with some GA-based approaches.

	KHBA	COTRO	TEVO	CHBE	HGA	GA-SA	GA-SLS
problem	Optimum	Sol A.	Sol A.	Sol A.	Sol A.	Sol A.	Sol A.
sento1	7772	7626	7767,9	7754,2	<b>7772</b>	<b>7772</b>	<b>7772</b>
sento2	8722	8685	8716,3	8719,5	<b>8722</b>	<b>8722</b>	8721,2
weing7	1095445	1093897	1095296,1	1095398,1	<b>1095445</b>	<b>1095445</b>	1094579,6
weing8	624319	613383	622048,1	622021,3	<b>624319</b>	<b>624319</b>	<b>624319</b>
weish23	8344	8165,1	8245,8	8286,7	<b>8344</b>	<b>8344</b>	8344
hp1	3418	3385,1	3394,3	3401,6	<b>3418</b>	<b>3418</b>	<b>3418</b>
pb2	3186	3091	3131,2	3112,5	<b>3186</b>	<b>3186</b>	<b>3186</b>

## 5 Conclusion

In this paper we addressed the multidimensional knapsack problem (MKP). We proposed, compared and tested two combinations: GA-SLS and GA-SA. GA-SLS combines the genetic algorithm and the stochastic local search (SLS) while GA-SA uses the simulated annealing (SA) instead of SLS. The experiments have shown the performance of our methods for MKP. Also, the hybridization of GA with local search methods allows to greatly improving its performance. As perspectives, we plan to study the impact of local search method when used with other evolutionary approaches such as: harmony search and particle swarm.

## References

1. Bean, J.C.: Genetics and random keys for sequencing and optimization. *ORSA Journal of Computing* **6**(2), 154–160 (1994)
2. Beaujon, G.J., Martin, S.P., McDonald, C.C.: Balancing and optimizing a portfolio of R&D projects. *Naval Research Logistics* **48**, 18–40 (2001)
3. Boughaci, D., Benhamou, B., Drias, H.: Local Search Methods for the Optimal Winner Determination Problem in Combinatorial Auctions. *Math. Model. Algor.* **9**(1), 165–180 (2010)
4. Chih, M., Lin, C.J., Chern, M.S., Ou, T.Y.: Particle swarm optimization with time-varying acceleration coefficients for the multidimensional knapsack problem. *Applied Mathematical Modelling* **38**, 1338–1350 (2014)
5. Cho, J.H., Kim, Y.D.: A simulated annealing algorithm for resource-constrained project scheduling problems. *Operational Research Society* **48**, 736–744 (1997)
6. Chu, P., Beasley, J.: A Genetic Algorithm for the Multidimensional Knapsack Problem. *Heuristics* **4**, 63–86 (1998)
7. Cotta, C., Troya, J.: A Hybrid Genetic Algorithm for the 0–1 Multiple Knapsack problem. *Artificial Neural Nets and Genetic Algorithm* **3**, 250–254 (1994)
8. Deane, J., Agarwal, A.: Neural, Genetic, And Neurogenetic Approaches For Solving The 0–1 Multidimensional Knapsack Problem. *Management & Information Systems - First Quarter 2013* **17**(1) (2013)
9. Della Croce, F., Grosso, A.: Improved core problem based heuristics for the 0–1 multidimensional knapsack problem. *Comp. & Oper. Res.* **39**, 27–31 (2012)
10. Djannaty, F., Doostdar, S.: A Hybrid Genetic Algorithm for the Multidimensional Knapsack Problem. *Contemp. Math. Sciences* **3**(9), 443–456 (2008)
11. Feng, L., Ke, Z., Ren, Z., Wei, X.: An ant colony optimization approach for the multidimensional knapsack problem. *Heuristics* **16**, 65–83 (2010)

12. Feng, Y., Jia, K., He, Y.: An Improved Hybrid Encoding Cuckoo Search Algorithm for 0–1 Knapsack Problems. Computational Intelligence and Neuroscience, ID 970456 (2014)
13. Fukunaga, A.S.: A branch-and-bound algorithm for hard multiple knapsack problems. Annals of Operations Research **184**, 97–119 (2011)
14. Garey, M.R., Johnson, D.S.: Computers and intractability: A guide to the theory of NP-completeness. W. H. Freeman & Co, New York (1979)
15. Khuri, S., Bäck, T., Heitkötter, J.: The zero-one multiple knapsack problem and genetic algorithms. In: Proceedings of the ACM Symposium on Applied Computing, pp. 188–193 (1994)
16. Kirkpatrick, S., Gelatt, C.D., Vecchi, P.M.: Optimization By Simulated Annealing. Science **220**, 671–680 (1983)
17. Meier, H., Christofides, N., Salkin, G.: Capital budgeting under uncertainty—an integrated approach using contingent claims analysis and integer programming. Operations Research **49**, 196–206 (2001)
18. Tuo, S., Yong, L., Deng, F.: A Novel Harmony Search Algorithm Based on Teaching-Learning Strategies for 0–1 Knapsack Problems. The Scientific World Journal Article ID 637412, 19 pages (2014)
19. Thiel, J., Voss, S.: Some Experiences on Solving Multiconstraint Zero-One Knapsack Problems with Genetic Algorithms. INFOR **32**, 226–242 (1994)
20. Vasquez, M., Vimont, Y.: Improved results on the 0–1 multidimensional knapsack problem. Eur. J. Oper. Res. **165**, 70–81 (2005)
21. Yoon, Y., Kim, Y.H.: A Memetic Lagrangian Heuristic for the 0–1 Multidimensional Knapsack Problem. Discrete Dynamics in Nature and Society, Article ID 474852, 10 pages (2013)
22. <http://people.brunel.ac.uk/~mastjjb/jeb/orlib/mknapsackinfo.html>

# Synthesis of In-Place Iterative Sorting Algorithms Using GP: A Comparison Between STGP, SFGP, G3P and GE

David Pinheiro<sup>(✉)</sup>, Alberto Cano, and Sebastián Ventura

Department of Computer Science and Numerical Analysis, University of Córdoba,  
Córdoba, Spain  
`{dpinheiro,acano,sventura}@uco.es`

**Abstract.** This work addresses the automatic synthesis of in-place, iterative sorting algorithms of quadratic complexity. Four approaches (Strongly Typed Genetic Programming, Strongly Formed Genetic Programming, Grammar Guided Genetic Programming and Grammatical Evolution) are analyzed and compared considering their performance and scalability with relation to the size of the primitive set, and consequently, of the search space. Performance gains, provided by protecting composite data structure accesses and by another layer of knowledge into strong typing, are presented. Constraints on index assignments to grammar productions are shown to have a great performance impact.

**Keywords:** Automatic algorithm synthesis · Genetic programming · Sorting

## 1 Introduction

This work compares four approaches, namely Strongly Typed Genetic Programming (STGP), Strongly Formed Genetic Programming (SFGP), Grammar Guided Genetic Programming (G3P) and Grammatical Evolution (GE), at evolving sorting algorithms. Special emphasis is given on their ability to scale well in spite of bigger primitive sets.

We restrict ourselves to iterative (non-recursive), in-place, comparison based sorting algorithms, expecting quadratic running times ( $\mathcal{O}(n^2)$ ) and constant ( $\mathcal{O}(1)$ ) additional memory. We make no assumptions about stability and adaptability of the evolved algorithms. Bloat analysis and solution will be left for future work.

## 2 Implementation and Experimental Context

The experiments were done on top of the EpochX [1] GP java library and were designed to be as fair as possible. However our goal is to get a grasp of the

**Table 1.** GP parameters used in the experiments

	<b>STGP</b>	<b>SFGP</b>	<b>G3P</b>	<b>GE</b>		
Population size	500					
Initialization	Grow initializer					
Selection	Tournament selection with a small size of 2 to prevent a lack of population diversity and to have a small selection pressure					
Crossover operator	Subtree Crossover	Whigham Crossover	One point Crossover			
Crossover probability	90%					
Mutation operator	Subtree Mutation	Whigham Mutation	Point Mutation			
Mutation probability	10%					
Elitism	Only one individual, to keep the best genome seen so far but with minimal impact on genetic diversity					
Reproduction	No reproduction. 90% of individuals are obtained by crossover and the remaining 10% by mutation					
Max Initial Depth*	10	24				
Max Depth*	10	32				
Number of generations	50					
Number of Runs	500					
Fitness Function	Levenshtein Distance					

\* As there is no easy direct relation between tree sizes in strongly typed and grammar guided GP (since the first uses expression trees in which all nodes contribute to the computation and the second uses parse trees in which only leafs contribute) several maximum tree depths were tested and the ones that showed the best results, for the bigger primitive sets, were chosen.

scalability related to the primitive set size, therefore we will not delve into fine tuning the choices made for operators and values (shown in Table 1).

The nonterminals used are shown in Table 2. In the first three columns a number is attributed to every syntactic element to help understand the results, followed by the name and a description. The node data type and the needed child data types, used by STGP and SFGP, and the node type and child node types, used by SFGP, fulfill the last four columns. The approaches based on grammars do not need to define data or node types, for the very grammar contains the specification of the requirements and restrictions on the types of data and syntactic form of the solutions. The strongly typed approaches were designed to achieve side effects, to change global variables, for that reason the Statement nonterminals return data type Void. SFGP nonterminal nodes belong to only three supertypes, namely CodeBlock, Statement and Expression. The implementation uses polymorphism then whenever it is required to use an Expression, for example, any Expression subtype can be used. Only two terminals were used, the minimum for quadratic algorithms, which in practice work as indexes to array elements (next section tests the use of more terminals). Using insight from human-made algorithms, the loops were restricted to a small set of widely used variants, like looping from a specified position of the array, ascending or descending. To prevent infinite loops, a limit of 100 cycles in each loop was set.

**Table 2.** Non-terminal syntactic elements

#	Name	Description	Data type	Child data types	Node super-type	Child node types
1	Swap	Swap two given array elements	Void	Array, Int, Int	Statement	Variable, Expression, Expression
2	For Each	Loop for each element of the array	Void	Array, Int, Void	Statement	Variable, Variable, CodeBlock
3	If Then	Conditional statement	Void	Bool, Void	Statement	Expression, CodeBlock
4	Less Than	Relational less than operator, <	Bool	Int, Int	Expression	Expression, Expression
5	For Each From	Loop for each array element, starting from a given position	Void	Array, Int, Int, Void	Statement	Variable, Variable, Variable, CodeBlock
6	Swap Next	Swap with the next element	Void	Array, Int	Statement	Variable, Expression
7	And	Logical AND operator	Bool	Bool, Bool	Expression	Expression, Expression
8	Decreasing For Each From	Decreasing loop, for each array element starting from a given position	Void	Array, Int, Int, Void	Statement	Variable, Variable, Variable, CodeBlock
9	Swap Previous	Swap with the previous element	Void	Array, Int	Statement	Variable, Expression
10	If Then Else	Conditional statement with the 'else' clause	Void	Bool, Void, Void	Statement	Expression, CodeBlock, CodeBlock
11	Greater Than	Relational greater than operator, >	Bool	Int, Int	Expression	Expression, Expression
12	Lesser Than or Equal	Relational less than or equal operator, <=	Bool	Int, Int	Expression	Expression, Expression
13	Greater Than or Equal	Relational greater than or equal operator, >=	Bool	Int, Int	Expression	Expression, Expression
14	Equal	Relational equality, ==	Bool	Int, Int	Expression	Expression, Expression
15	Unequal	Relational inequality, !=	Bool	Int, Int	Expression	Expression, Expression
16	Not	Logical NOT operator	Bool	Bool	Expression	Expression
17	Or	Logical OR operator	Bool	Bool, Bool	Expression	Expression, Expression
18	Decreasing For Each	Decreasing loop, for each array element from the last to the first	Void	Array, Int, Void	Statement	Variable, Variable, CodeBlock

The experiments use sets of 4, 5, 7, 10 and 18 nonterminal primitives. They were chosen in order to give a perspective of the asymptotic behavior. Set sizes correspond to the numbers on the first column of Table 2. For example the set of size 7 uses the nonterminals numbered 1 to 7, inclusive. Starting from the set of size 4 it is possible to obtain a simple Selection Sort algorithm and thereafter Bubble Sort and Insertion Sort.

The fitness function is defined by the Levenshtein Distance (an error measure that needs to be minimized). Every evolved program runs against the five arrays presented in [2]. If the program correctly sorts all of them, it runs against 30 arrays of random sizes between 10 and 20, filled with random integers between 0 and 100.

### 3 Experiments, Results and Analysis

To analyze the experiments we used the minimal computational effort required to find a solution with 99% confidence, presented in [3], but without the ceiling operator, as suggested in [4]. Confidence intervals at 95% (shown between parentheses in Table 3) were calculated using the Wilson score method [5].

*Performance and scalability.* The performance and scalability of the approaches with growing primitive set sizes are shown in Figure 1 and compiled in the lines titled UAA (Unprotected Array Accesses) in Table 3. In our setup, SFGP and G3P provided the best performance. Both G3P and GE reveal

the particularity that the set of size 18 presents more useful constructs to evolve sorting algorithms than the set of size 10.

*Protection against out of bounds array accesses.* A recurrent situation that happens when using indexed data types, for example arrays, is that the indexes can get out of bounds of the data type when used inside some of the loops, causing run-time exceptions. In this experiment we protected against out of bounds array accesses, using the % (mod) operator against the size of the array, to ensure that the index is always in the correct bounds, and obtained the results presented in Figure 2 and Table 3. The important positive impact that this tweak had on the performance and scalability of the approaches can be ascertained by comparing lines named PAA (Protected Array Accesses) and UAA.

*Influence of grammar context insensitivity.* Context-free Grammars (CFG), used in G3P and GE, show a lack of expressiveness to describe semantic constraints<sup>1</sup> [6]. Their context insensitivity can have an appreciable negative impact on the size of the search space, especially in the presence of loops and swaps that repeatedly require the same index. As our system doesn't allow us to specify that certain terminal (index) assignments should be repeated in a given nonterminal, we obtained the same result changing the grammar so that the rules which require more than one index are split into two, one specifically for the index i, another specifically for the index j<sup>2</sup>. This acts as a kind of context sensitivity, forcing these constructs to always correctly match the indexes. The results, presented in Figure 3 and lines PAACS (Protected Array Accesses with Context Sensitivity) of Table 3, attest that this has a huge positive impact on the performance of grammar guided approaches, even to the point that almost all runs produce a correct individual.

*Performance and scalability with bigger terminal sets.* The last experiment tests the performance and scalability of SFGP in the presence of bigger terminal sets, the same number of terminals as nonterminals, between 4 and 18 of each. The terminals consist of integers of node type Variable. From Figure 4 and line PAANT (Protected Array Accesses with N Terminals) of Table 3 one can see that the number of terminals has an important negative impact in the performance but nevertheless SFGP remains scalable, showing almost the same performance for sets of size 10 and 18. This gives us confidence in the introduction of more data types in the evolutionary process, such as trees, graphs, stacks, etc., with the important goal of evolving not-in-place algorithms.

---

<sup>1</sup> For example, to define a loop, the grammar can state

```
<for> ::= for(<index> = 0; <index> < array.length; <index>++);  
<index> ::= i | j | k;
```

which can be evaluated as

```
for(i = 0; j < array.length; k++){};
```

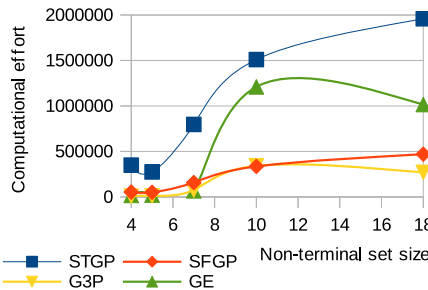
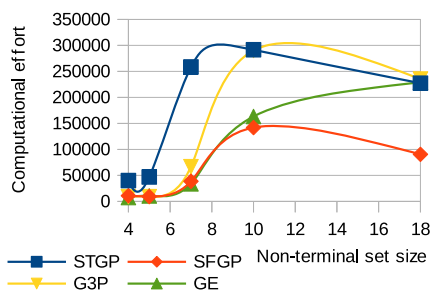
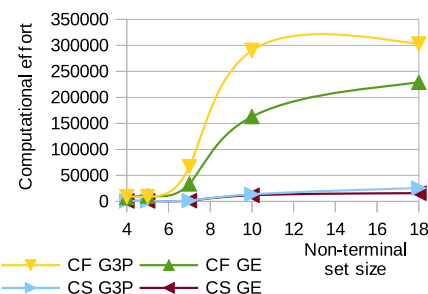
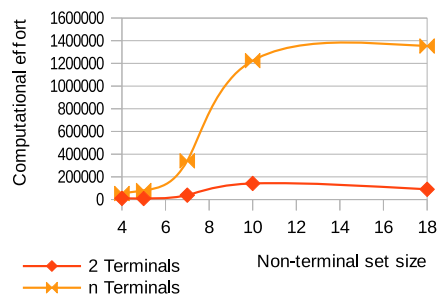
or any other combination of indexes that give an infinite loop. This situation could be overcome by the evolutionary system, indicating that the second and third indexes should be the same as the first.

<sup>2</sup> For example, the for loop was subdivided into one loop for each index:

```
<loop_i> ::= for(i = 0; i < array.length; i++){}  
<loop_j> ::= for(j = 0; j < array.length; j++){};
```

**Table 3.** Non-terminal syntactic elements

		Nonterminal Set Size				
		4	5	7	10	18
SFGP	UAA	53,506 (47874-60134)	51,172 (33872-77608)	157,263 (139132-178635)	334,924 (284776-395599)	469,402 (387056-571624)
	PAA	10,800 (8862-13218)	9,364 (7777-11322)	38,537 (26893-55438)	142,002 (122458-165396)	90,467 (80221-102535)
	PAANT	52,907 (54206-67532)	79,542 (70970-89627)	340,904 (288677-404302)	1,224,842 (914425-1647128)	1,353,136 (995924-1845724)
STGP	UAA	349,348 (296183-413822)	274,308 (235619-320754)	797,004 (627793-1015894)	1,509,921 (1093099-2093891)	1,957,807 (1357643-2834324)
	PAA	39,955 (27707-57843)	46,810 (31529-69768)	258,519 (217208-308988)	291,612 (239267-356876)	227,370 (191936-270492)
	PAACS	8,109 (7170-9304)	11,380 (10212-12801)	75,596 (45923-124924)	342,219 (258684-454526)	270,186 (210357-348421)
G3P	UAA	9,079 (7560-10950)	8,988 (10212-12801)	66,565 (45923-124924)	290,221 (220009-384361)	235,359 (184705-301109)
	PAA	741 (579-1026)	741 (579-1026)	1,642 (1477-1837)	13,576 (10901-16978)	25,606 (19052-34550)
	PAACS	16,265 (12812-20733)	20,147 (15475-26335)	66,565 (41660-106773)	1,209,531 (734764-1998785)	1,015,323 (731689-1414445)
GE	UAA	7,317 (6192-8682)	10,436 (8588-12733)	33,723 (24067-47439)	163,316 (79315-337577)	229,105 (98122-537000)
	PAA	741 (579-1026)	741 (579-1026)	1,308 (1177-1464)	11,747 (9565-14486)	15,751 (12451-20007)
	PAACS					

**Fig. 1.** Unprotected Array Accesses**Fig. 2.** Protected Array Accesses**Fig. 3.** Context Free vs Context Sensitive index assignment**Fig. 4.** Use of  $n$  terminals in SFGP with Protected Array Accesses

## 4 Conclusions and Future Work

In general all the approaches showed good promise for Automatic Algorithm Synthesis, always converging in their scalability, and responding positively in terms of performance to the techniques introduced to reduce the search space.

SFGP revealed effective consistent performance and scalability improvements over STGP in all experiments. We argue that the introduction of types of nodes, in addition to data types, functions as another layer of restrictions on the search space, and causes a substantial and structural reduction of its size.

Protected accesses to the array, in order to prevent index out of bounds exceptions, revealed overall performance gains. The use of constraints on index assignment in the grammar rules of Context Free Grammars had a great positive impact on the performance and scalability of G3P and GE. The introduction of the same number of terminals as nonterminals revealed that, although the performance worsens, SFGP maintains its scalability. This result requires further analysis, but increases our confidence in the possibility of introducing high level abstract data structures to support the synthesis of not-in-place algorithms.

Future work will include: Implement the divide and conquer paradigm (recursion), along with a technique to assess algorithm performance, in order to enable and encourage the evolution of faster ( $\mathcal{O}(n \log n)$ ) sorting algorithms; Introduce composite data structures as terminals, to enable the evolution of not-in-place algorithms; Add nonterminals obtained from algorithms developed by humans, to allow the application of GP to other areas beyond sorting; Analyze and reduce bloat, applying strategies to obtain compact unbloated algorithms.

**Acknowledgments.** This research was supported by the Spanish Ministry of Science and Technology, project TIN2014-55252-P, and by FEDER funds. This research was also supported by the Spanish Ministry of Education under FPU grant AP2010-0042.

We thank Tom Castle for kindly giving access to his SFGP code.

## References

1. Otero, F., Castle, T., Johnson, C.: Epochx: genetic programming in java with statistics and event monitoring. In: Proceedings of the 14th Annual Conference Companion on Genetic and Evolutionary Computation, pp. 93–100 (2012)
2. O'Neill, M., Nicolau, M., Agapitos, A.: Experiments in program synthesis with grammatical evolution: a focus on Integer Sorting. In: IEEE Congress on Evolutionary Computation (CEC), pp. 1504–1511 (2014)
3. Koza, J.R.: Genetic programming: on the programming of computers by means of natural selection, vol. 1. MIT press (1992)
4. Christensen, S., Oppacher, F.: An analysis of koza's computational effort statistic for genetic programming. In: Foster, J.A., Lutton, E., Miller, J., Ryan, C., Tettamanzi, A.G.B. (eds.) EuroGP 2002. LNCS, vol. 2278, pp. 182–191. Springer, Heidelberg (2002)
5. Walker, M., Edwards, H., Messom, C.H.: Confidence intervals for computational effort comparisons. In: Ebner, M., O'Neill, M., Ekárt, A., Vanneschi, L., Esparcia-Alcázar, A.I. (eds.) EuroGP 2007. LNCS, vol. 4445, pp. 23–32. Springer, Heidelberg (2007)
6. Orlov, M., Sipper, M.: FINCH: a system for evolving Java (bytecode). In: Genetic Programming Theory and Practice VIII, Springer, pp. 1–16 (2011)

# **Computational Methods in Bioinformatics and Systems Biology**

# Variable Elimination Approaches for Data-Noise Reduction in 3D QSAR Calculations

Rafael Dolezal<sup>1,2(✉)</sup>, Agata Bodnarova<sup>3</sup>, Richard Cimler<sup>3</sup>, Martina Husakova<sup>3</sup>, Lukas Najman<sup>1</sup>, Veronika Racakova<sup>1</sup>, Jiri Krenek<sup>1</sup>, Jan Korabecny<sup>1,2</sup>, Kamil Kuca<sup>1,2</sup>, and Ondrej Krejcar<sup>1</sup>

<sup>1</sup> Center for Basic and Applied Research, Faculty of Informatics and Management, University of Hradec Kralove, Rokitanskeho 62, 50003 Hradec Kralove, Czech Republic  
{rafael.dolezal,lukas.najman,veronika.racakova,jiri.krenek,  
jan.korabecny,kamil.kuca,ondrej.krejcar}@uhk.cz

<sup>2</sup> Biomedical Research Center, University Hospital Hradec Kralove, Hradec Kralove, Czech Republic

<sup>3</sup> Department of Information Technologies, Faculty of Informatics and Management, University of Hradec Kralove, Hradec Kralove, Czech Republic  
{agata.bodnarova,richard.cimler,martina.husakova.2}@uhk.cz

**Abstract.** In the last several decades, the drug research has moved to involve various IT technologies in order to rationalize the design of novel bioactive chemical compounds. An important role among these computer-aided drug design (CADD) methods is played by a technique known as quantitative structure-activity relationship (QSAR). The approach is utilized to find a statistically significant model correlating the biological activity with more or less extent data derived from the chemical structures. The present article deals with approaches for discriminating unimportant information in the data input within the three dimensional variant of QSAR – 3D QSAR. Special attention is turned to uninformative and iterative variable elimination (UVE/IVE) methods applicable in connection with partial least square regression (PLS). Herein, we briefly introduce 3D QSAR approach by analyzing 30 antituberculosis. The analysis is examined by four UVE/IVE-PLS based data-noise reduction methods.

**Keywords:** UVE/IVE · Data-noise reduction · 3D QSAR · PLS · CADD

## 1 Introduction

The principle behind quantitative structure-activity relationships (QSAR) has been known for more than 150 years. It was a logical inference resulting from discovering the molecular structure of the matter. A first mathematical formalization of QSAR being often highlighted in historical reviews on rational drug design methods is the equation introduced by Crum-Brown and Fraser (Eq. 1).

$$\varphi = (C) \quad (1)$$

Here,  $\phi$  means the biological effect of a substance which is characterized by a set of structural features  $C$  [1]. The equation (Eq. 1) was published in 1869 as a proposition of a correlation between the biological activity of different atropine derivatives and their molecular structure. Although the validity of the Crum Brown-Fraser equation was confirmed after a 25 years' lag, it has undoubtedly become a corner stone of rational approaches in drug design and discovery.

In simplest terms, QSAR refers to a strategy aimed at building a statistically significant correlation model between the biological activity and various molecular descriptors by chemometric tools. The biological activity can be expressed as minimal inhibition concentration (MIC), concentration causing 50% enzyme inhibition ( $IC_{50}$ ), binding affinity ( $K_i$ ), lethal dose ( $LD_{50}$ ), etc. Regarding the description of the molecular structure, a great progress has been achieved since the genesis of classical models by Hansch or Free-Wilson in the sixties of the twentieth century [2, 3]. So far, thousands of various molecular descriptors have been developed for utilization in QSAR analyses. In order to build a statistically significant QSAR model from known biological activities and molecular descriptors, linear (e.g. multiple linear regression MLR, partial least squares PLS, principal component regression PCR) or non-linear (e.g. artificial neural networks ANN, k-nearest neighbors kNN, Bayesian nets) data-mining methods are commonly employed in QSAR analyses.

In the present paper, three dimensional version of QSAR (3D QSAR) methodology is particularly studied. It is a method based on statistical processing of molecular interaction fields (MIFs). The MIF matrix is regularly data-mined by PLS to build a linear predictive 3D QSAR model. Unfortunately, PLS itself is not a sufficient tool for finding a stable model utilizing the original MIFs since it considerably suffers from abundant and noisy information in the input. The objective of our study is to evaluate several statistical methods applicable in building robust 3D QSAR models. Chapter 2 introduces in simple terms what the principles of 3D QSAR analysis are. Data-processing and noise reduction approaches based on uninformative/iterative variable elimination (UVE/IVE) are depicted in Chapter 3. Finally, the merits of these methods are demonstrated by 3D QSAR analysis of 30 antituberculotics in Chapter 4.

## 2 3D QSAR – Principles and Methodology

The core of 3D QSAR method, originally named comparative molecular field analysis (CoMFA), was designed by Cramer et al. in 1988 as a four-step procedure: 1) superimposition of ligand molecules on a selected template structure, 2) representation of ligand molecules by molecular interaction fields (MIFs), 3) data analysis of MIFs and biological activities by PLS, utilizing cross-validation to select the most robust 3D QSAR model, 4) graphical explanation of the results through three-dimensional pseudo  $\beta^{PLS}$  coefficients contour plots.

Within the 3D QSAR analysis, a starting set of molecular models can be prepared with any chemical software capable of creating and geometrically optimizing chemical structures (e.g. HyperChem, Spartan, ChemBio3D Ultra, etc.). Usually, a molecular dynamics method (e.g. simulated annealing, quenched molecular dynamics,

Langevin dynamics, Monte Carlo) is employed to obtain the most thermodynamically representative conformers. Having the chemical structures in a suitable geometry, preferably the most biologically active one is chosen as a template and the others denoted as candidate ligands. In the alignment step, all candidates are superimposed on the template structure using a distance-based scoring function implemented in an optimizing algorithm to find “the tightest” molecular alignment set. Once an optimum molecular alignment set is gained, molecular interaction fields (MIFs) may be calculated for all candidates as well as the template compound. The MIFs calculations may be adumbrated as calculating the steric and electrostatic potential in a gridbox surrounding the ligand molecule (Fig. 1).

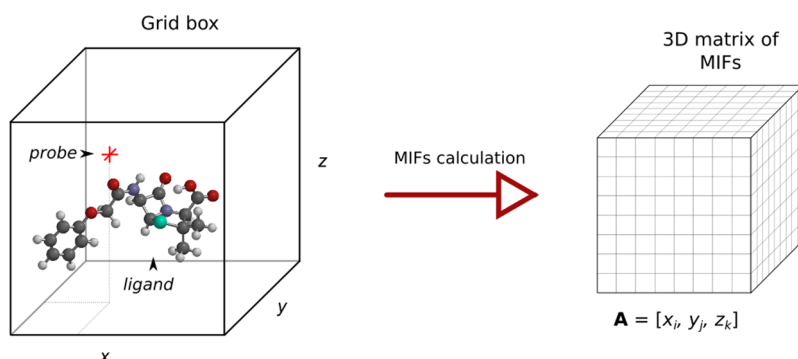


**Fig. 1.** Calculation of MIFs.

The potential energies (e.g. Lennard-Jones, van der Waals (VDW) and Coulomb electrostatic potential energies (ESP)) experienced by unit charge or atom probe at various points ( $x_i, y_j, z_k$ ) around the studied molecules are usually regressed by PLS on the biological activities to reveal significant correlations. Generally, any supervised learning method is applicable in 3D QSAR analysis instead of PLS, provided it is able to process many thousands of “independent” x variables within a reasonable time [4]. A common MIF related to a 1.0 Å spaced gridbox of the size 30.0 x 30.0 x 30.0 Å represents a chemical compound by 27 000 real numbers. Because not all points in MIFs are typically related with the observed biological activity, the redundant information in the data input may bring about overlearning which mostly causes unreliable prediction for compounds outside the training and test sets. As a rule, the raw input data for 3D QSAR analysis must be pre-processed by data-noise reduction methods prior to building the final model by PLS. The data-noise reduction techniques like fractional factor design (FFD), uninformative variable elimination (UVE) or iterative variable elimination (IVE) frequently utilize cross-validated coefficient of determination ( $Q^2$ ) as a cost-function for selecting the most robust 3D QSAR model [5]. The final step in deciding whether the derived 3D QSAR model is trustworthy is statistical validation. Such methods as progressive Y-scrambling, randomization, leave-two-out (LTO) or multiple leave-many-out cross-validation (LMO), and, above all, external validation are employed for these ends [6].

Besides quantitative predictions of unknown biological activities, 3D QSAR analysis enables to disclose influential features in the studied chemical structures through the spatial visualization of pseudo  $\beta^{PLS}$ -coefficients. Usually, pseudo  $\beta^{PLS}$ -coefficients are additionally multiplied by standard deviation of MIFs column vectors (noted as SD) to underline more varied regions in the chemicals structures. Since the pseudo  $\beta^{PLS}$ -coefficients quantitatively indicate how much each point of MIFs contributes to the biological activity, the pharmacophore within the studied compound set may be revealed. An example of 3D contour maps outlining pseudo  $\beta^{PLS} \times$  SD coefficients is given in Fig. 2. Data for the illustration were taken from the literature [5].

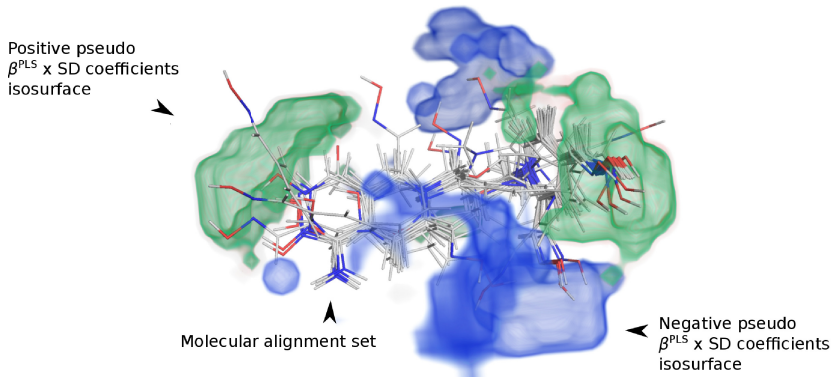


**Fig. 2.** 3D contour map of pseudo  $\beta^{PLS} \times$  SD coefficients.

By 3D contour maps of pseudo  $\beta^{PLS} \times$  SD coefficients one can disclose which molecular features are crucial for the biological activity observed. Accordingly, medicinal chemists can utilize the information to design novel drugs through their chemical intuition or they can employ the found 3D QSAR model in ligand-based virtual screening of convenient drug databases (e.g. [zinc.docking.org](http://zinc.docking.org)).

### 3 Variable Elimination as Data-Noise Reduction Method for 3D QSAR Analysis

Currently, 3D QSAR analysis has been involved in a variety of drug research branches. Examples of such successful projects are discovery of biphenyl-based cytostatics, design of mitochondrial cytochrome P450 enzyme inhibitors, investigation of sirtuin 2 inhibitors as potential therapeutics for neurodegenerative diseases or development of improved acetylcholinesterase reactivators [5, 7]. However, many of recent 3D QSAR studies are justified only by internal coefficient of determination  $R^2 > 0.8$  and by its leave-one-out (LOO) cross-validated counterpart  $Q^2_{LOO} > 0.6$ . In scarcer cases, external validation of the 3D QSAR models is reported. On the other hand, it is very well known among QSAR experts that mostly unstable 3D QSAR

models result *via* PLS regression when a proper selection of independent variables from the original MIFs is neglected. This drawback, which challenges not only 3D QSAR models, manifests especially in external prediction or exhaustive LMO cross-validation. Lately, several variable selection algorithms have been developed to address the overlearning in PLS based models. In the present study, a special attention is turned to variable elimination methods applicable in 3D QSAR analysis.

### 3.1 PLS Regression Analysis of Molecular Interaction Fields

The MIFs obtained by consecutive probing the molecules in 3D lattice box by different probes are regularly reordered into long row vectors and stored as **X** descriptor matrix. Each row represents individual chemical compound and each column contains the values of interaction energy at a given lattice intersection. Since the **X** matrix usually consists of thousands of columns and tens of rows, common MLR is useless for data-mining these data due to singularities arising during the inversion of ( $\mathbf{X}^T \mathbf{X}$ ) matrix. A method of choice for processing MIFs in 3D QSAR analysis has become the partial least square regression (PLS). It is a supervised learning method which combines principal component analysis (PCA) and MLR. By extracting orthogonal factors (i.e. latent variables - LVs) from the original **X** matrix PLS aims to predict one or more dependent variables ( $\hat{\mathbf{y}}$  column vector or  $\hat{\mathbf{Y}}$  matrix).

PLS is a convenient method for deriving a linear regression model correlating a set of dependent variables (i.e. biological activities) with an extent set of predictors (i.e. MIFs or molecular descriptors). A significant strength of PLS is the possibility to process multidimensional data with high degree of intercorrelation. Although PLS was originally developed in social sciences, it has become one the most favorite chemometric tool utilized in 3D QSAR. The benefits of PLS are appreciated especially when the number of **X** rows is decreased after splitting the input data into training, test and external sets. The nature of PLS may be briefly characterized as simultaneous decomposition of **X** and **Y** matrices. Formally, PLS works with several coupled matrices (Eq. 2):

$$\hat{\mathbf{Y}} = \mathbf{X}\boldsymbol{\beta}^{PLS} = \mathbf{T}\mathbf{P}^T\boldsymbol{\beta}^{PLS} = \mathbf{T}\mathbf{B}\mathbf{C}^T; \quad \mathbf{T} = \mathbf{X}\mathbf{W}; \quad \mathbf{U} = \mathbf{Y}\mathbf{C}; \quad \mathbf{B} = \mathbf{T}^T\mathbf{U} \quad (2)$$

where  $\boldsymbol{\beta}^{PLS}$  means the pseudo  $\beta^{PLS}$  regression coefficients; **W** and **C** denote the weight matrices; **P** means the loading matrix; **T** and **U** are the score matrices. The columns of **T** are orthogonal and called the latent variables ( $\mathbf{T}^T \mathbf{T} = \mathbf{I}$ ). The crucial operation within PLS analysis consists in simplifying the complexity of the system by selecting only few LVs to build the model. The number of involved LVs is often determined by cross-validation. When  $Q^2_{LOO}$  starts dropping or the standard error of prediction (SDEP) increases, the optimum number of latent variables has been exceeded (Fig. 3). Considerably more robust algorithms for latent variable selection implement leave-many-out cross-validated  $Q^2_{LMO}$  or coefficient of determination for external prediction  $R^2_{ext}$  as a control function.

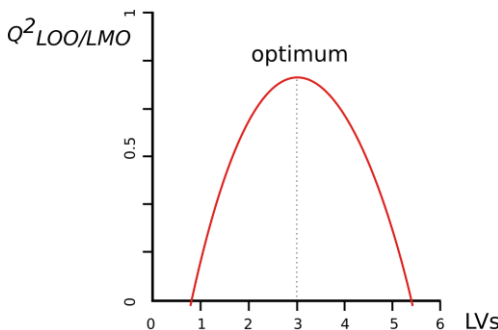


**Fig. 3.** Determining the optimal number of LVs through cross-validation.

Since PLS is a PCA based method, it is highly sensitive to the variance of the values included in the input data. This problematic feature of PLS can lead to masking significant information by data assuming greater values. For instance, the information on weak hydrophobic interactions is suppressed by Coulombic interactions and hydrogen bonding that are stronger. However, it has become evident that hydrophobic interactions play such an important role in drug binding to receptors that they cannot be neglected in 3D QSAR calculations. To prevent discriminating variables with relatively low values, the MIFs as well as the biological activities have to be column centered and normalized prior to PLS. In 3D QSAR analysis, different MIFs may be also scaled as separated blocks by block unscaled weighting (BUW) to give each probe the same significance in PLS [8]. PLS regression can be performed by a number of subtle differing algorithms (e.g. NIPALS, SIMPLS, Lanczos bidiagonalization) [9]. In case  $\mathbf{Y}$  consists only of one column, then NIPALS algorithm may be simply illustrated as follows:

```
[X,Y] = autoscale(X, Y); % Centering and normalization
T=[]; P=[]; W=[]; Q=[]; B=[]; % initialization
for a=1:LV % Calculate the entered number of LVs
    w=(Y'*X)'; % Calculate weighting vector
    w=w/sqrt(w'*w); % Normalization to unit length
    t=X*w; % Calculate X scores
    if a>1 t=t - T*(inv(T'*T)*(t'*T)'); end;
    u=t/(t'*t);
    p=(u'*X)'; % Calculate X loadings
    X=X - t*p'; % Calculate X residuals
    T=[T t]; % Calculate X scores
    P=[P p]; % Calculate X loadings
    W=[W w]; % Calculate X weights
    Q=[Q;y'*u]; % Calculate Y loadings
    B=[B W*inv(P'*W)*Q]; % Calculate PLS coefficients
end
Y_pred=X*B; % Internal prediction
```

The above PLS algorithm derives the entered number of LVs and utilizes them in the internal prediction of the autoscaled dependent variable  $\mathbf{Y}$ . The robustness of the resulting PLS model can be easily controlled by incorporating a cross-validation into the algorithm. Nonetheless, the prediction instability of the 3D QSAR models has to be solved mainly through preselecting the input data.

### 3.2 Unsupervised Preselection in the MIFs before PLS Analysis

Calculation of the physically based interactions between the probe and the molecules placed into a gridbox necessarily leads to dramatic increase of the energy when the probe gets closer to atom nuclei. Conversely, the energy calculated in gridpoints relatively far from a molecule may assume negligible magnitude from the QSAR's point of view. These MIF properties enable to perform, to certain extension, a preliminary input data clearance. It is a common practice in 3D QSAR analysis to remove from the MIFs such points (i.e. whole columns in  $\mathbf{X}$  matrix) where the maximum energy exceeds a chosen threshold (e.g. > 50 kcal/mol for steric van der Waals MIF, > 30 kcal/mol for electrostatic MIF). Other possible unsupervised techniques to eliminate unimportant data in the MIFs are: zeroing all gridpoints having absolute value below 0.05 kcal/mol, removing all MIFs vectors of the standard deviation lower than 0.1 kcal/mol, removing all MIFs vectors assuming only several levels with skewed distribution. By such type preselection it is possible to remove from 1% to 80% uninformative MIFs vectors depending on the cutoff levels used. Commonly, several hundreds or thousands MIFs columns are left after unsupervised preselection to other variable reduction approaches.

### 3.3 Uninformative Variable Elimination

The main goal of 3D QSAR analysis is to develop a stable mathematical model which can be used for prediction of unseen biological activities. From this somewhat narrowed point of view, any model that is not able to prove itself in external prediction must be rejected from further consideration. However, such refusal does not provide any suggestion why different models are successful or fail in predictions and how to boost the predictive ability.

The method introduced by Centner and Massart focuses on what is noisy and/or irrelevant information and how to discriminate it [10]. Comparing to other variable selection techniques like forward selection, stepwise selection, genetic and evolutionary algorithms, uninformative variable elimination (UVE) does not attempt to find the best subset of variables to build a statistically significant model but to remove such variables that contain no useful information. Centner and Massart took their inspiration from previously published studies which tried to eliminate those variables having small loadings or pseudo  $\beta^{PLS}$  coefficient in a model derived by PLS.

UVE-PLS method resembles stepwise variable selection used in MLR. The  $j$ -th variable (i.e. a MIF vector) is eliminated from the original vector pool if its  $c_j$  value is lower than a certain cutoff level (Eq. 3)

$$c_j = \frac{\bar{\beta}_j^{PLS}}{sd(\bar{\beta}_j^{PLS})} \quad (3)$$

In order to obtain the mean ( $\bar{\beta}_j^{PLS}$ ) and the standard deviation ( $sd(\bar{\beta}_j^{PLS})$ ) of pseudo  $\beta_j^{PLS}$  coefficient for each variable, a cross-validation is necessary to carry out. A critical point in this method is how to determine the cutoff level for the elimination. For this purposes, Centner and Massart proposed to add several artificial random variables into the original  $\mathbf{X}$  matrix and to calculate their  $c_j^{random}$  values. The original variables that exhibit lower  $c_j$  than the maximum in  $c_j^{random}$ 's determined for the artificial variables are removed. Although the UVE method is capable to discriminate uninformative variables, the artificial variables used have to be of low magnitude comparing to the original variables so as they do not disturb significantly the model. The artificial random matrix  $\mathbf{R}$  is proposed to be of the same dimension as the  $\mathbf{X}$  matrix.

According to Centner and Massart, the UVE-PLS procedure can be summarized in the following steps: 1) determination of the optimum number of LVs as the minimum of the root-mean-square error prediction function RMSEP (Eq. 4); 2) generation of the random matrix  $\mathbf{R}$  and its scaling by a small factor (e.g.  $10^{-10}$ ); 3) PLS regression of the conjugate  $\mathbf{RX}$  matrix and leave-one-out cross-validation; 4) calculation of  $c_j$  values for all variables; 5) determination of  $\max(\text{abs}(c_j^{random}))$ ; 6) elimination of all original variables for which  $\text{abs}(c_j) < \max(\text{abs}(c_j^{random}))$ ; 7) evaluating of the new model by leave-one-out cross-validation.

$$\text{RMSEP} = \sqrt{\sum_{i=1}^n \frac{(\hat{y}_i - y_i)^2}{n}} \quad (4)$$

Here,  $y_i$  is the observed biological activity for i-th compound,  $\hat{y}_i$  stands for the predicted biological activity of i-th compound, n is the number of compounds in the set. The above-mentioned UVE algorithm can be transformed to a more robust variant by expressing the  $c_j$  as median ( $\bar{\beta}_j^{PLS}$ )/interquartile range ( $\bar{\beta}_j^{PLS}$ ). The criterion for variable elimination may be substituted for a 90-95 quantile of  $\text{abs}(c_j^{random})$ .

### 3.4 Iterative Variable Elimination

Uninformative variable elimination was designed to improve the predictive power and the interpretability of 3D QSAR models *via* removing those MIFs parts which do not contain fecund information in comparison to random noise introduced to the input data. The UVE method is based on calculation of  $c_j$  values indicating the ratio of the size and standard deviation of pseudo  $\beta_j^{PLS}$  coefficient related to j-th vector of MIFs. All MIF vectors with  $c_j$  smaller then a cutoff derived from  $c$  values of the random variables are removed from the  $\mathbf{X}$  matrix in a single step procedure.

A modification of the UVE algorithm suggested by Polanski and Gieleciak revises the very one-step elimination of MIF vectors with low  $c_j$  values [11, 12]. Their improved algorithm named iterative variable elimination (IVE) does not remove the selected vectors in a single step but in a sequential manner. In the first version of IVE, the MIF vector having the lowest pseudo  $\beta_j^{PLS}$  coefficient is eliminated and the

remaining  $\mathbf{X}_{(-i)}$  matrix is regressed by PLS to evaluate the benefit. The iterative IVE procedure can be described by the following protocol: 1) carry out PLS analysis with a fixed number of LVs and estimate the performance by leave-one-out cross-validation; 2) eliminate the  $\mathbf{X}$  matrix column with the lowest absolute value of pseudo  $\beta^{PLS}$  coefficient; 3) carry out PLS analysis of the reduced  $\mathbf{X}_{(-i)}$  matrix and estimate the performance by leave-one-out cross-validation; 4) go to step 1 and repeat until the maximal leave-one-out cross-validated coefficient of determination  $Q^2_{LOO}$  is reached (Eq. 5).

$$Q^2_{LOO} = 1 - \frac{\sum_i^n (\hat{y}_{i(-1)} - y_i)^2}{\sum_i^n (y_i - \bar{y})^2} \quad (5)$$

Here,  $y_i$  means the observed biological activity for  $i$ -th compound,  $\hat{y}_{i(-1)}$  denotes the biological activity of  $i$ -th compound predicted by the model derived without the  $i$ -th compound,  $n$  is the number of compounds in the set. In the first version, the IVE procedure was based on iterative elimination of MIF vectors with the lowest absolute values of pseudo  $\beta^{PLS}$  coefficients. In the next IVE variants, the criterion for MIF vector elimination was substituted by  $c_j$  values obtained by leave-one-out cross-validation. The most robust form of IVE was proposed to involve optimization of the LV number and  $c_j$  values defined as median ( $\beta_j^{PLS}$ )/interquartile range ( $\beta_j^{PLS}$ ). It was proved by Polanski and Gieleciak that the robust IVE form surpassed the other variants and gave the most reliable 3D QSAR models in terms of the highest  $Q^2_{LOO}$  and sufficient resolution of pseudo  $\beta^{PLS}$  coefficient contour maps.

### 3.5 Hybrid Variable Elimination

The issue concerning the selection or elimination of the right variables in 3D QSAR studies can be addressed in several ways [13]. A logical candidate to be implemented in improving the ability of 3D QSAR models seems to be genetic algorithm (GA) that enables evaluating different sets of MIF vectors. However, thanks to many variables in MIFs there is no guarantee that GA-PLS procedure can straightforwardly converge to achieve the best solution. Other promising alternatives of variable selection/elimination techniques relevant in 3D QSAR are sub-window permutation analysis coupled with PLS (SwPA-PLS), iterative predictor weighting PLS (IPW-PLS), regularized elimination procedure (REP-PLS), interactive variable selection (IVS-PLS), soft-thresholding PLS (ST-PLS) or powered PLS (PPLS) (see [13]).

Noteworthy, the MIFs generated for chemical compounds are not independent variables but spatially inter-correlated. In the original 3D MIF matrix, the energy values are ordered according to a molecular structure probed in a gridbox. This internal information is neglected and stays hidden when transforming the 3D MIF matrices into row vectors of the  $\mathbf{X}$  matrix. Application of UVE and IVE methods on such unfolded data therefore does not reflect the chemical information born by MIFs but treats it as different molecular descriptors. To utilize also the spatial contiguity of the original 3D MIFs, a methodology named smart region definition (SRD) has found its important

position in 3D QSAR analysis. SRD procedure aims to rearrange the unfolded MIFs into group variables related to the same chemical regions (e.g. points around the same atoms). These groups of neighboring variables are explicitly associated with chemical structures and when treated as logical units, the resulting 3D QSAR models are less prone to chance correlations and easier to interpret [14]. Since the SRD procedure clusters similar MIF vectors into groups, the time consumed by UVE or IVE analyses is shorter than in the standard processing of all individual MIF vectors. The SRD algorithm involves three major operations: 1) selecting the most important MIF vectors (seeds) having the highest PLS weights; 2) building 3D Voronoi polyhedra around the seeds; 3) collapsing Voronoi polyhedral into larger regions.

The starting point of the SRD procedure is PLS analysis of the whole  $\mathbf{X}$  matrix which reveals through the magnitude of weights significant MIF vectors. Depending on the user's setting, a selection of important MIF vectors is denoted as seeds. In next step, the remaining MIF vectors are assigned to the nearest seed according to preset Euclidian distance. In case a MIF vector is too far from each seed, it is assigned to "zero" region and eliminated from the  $\mathbf{X}$  matrix. After distributing the MIF vectors into Voronoi polyhedra, further variable absorption is performed. Neighboring Voronoi polyhedra are statistically analysed and if found significantly correlated, they are merged into one larger Voronoi polyhedra. The cutoff distances for initial building the Voronoi polyhedra as well as for subsequent collapsing are critical points which decide on the merit of SRD and, thus, have to be cautiously optimized.

## 4 Performance Comparison of UVE and IVE Based Methods

In order to practically evaluate the performance of the UVE and IVE based noise-reduction methods, a 3D QSAR analysis has been carried out. We selected a group of 30 compounds, which are currently considered as potential antituberculotics [15, 16], and analyzed them in Open3DAAlign and Open3DQSAR programs [17, 18]. Since we cannot provide a detailed description of all undertaken steps of the analysis in this article, we will confine the present study only to the performance of the UVE and IVE algorithms and their SRD hybridized variants. In the 3D QSAR analyses, the most common or default setting was used.

First, the set of 30 compounds published in the literature was modeled in Hyper-Chem 7.0 to prepare the initial molecular models. Then, the molecular ensemble was submitted to quenched molecular dynamics and the resulting conformers were processed by an aligning algorithm in Open3DAAlign program to determine the optimal molecular superimposition. In Open3DQSAR program two MIFs were generated (i.e. van der Waals MIF and Coulombic MIF) and processed by four 3D QSAR methods: 1) UVE-PLS, 2) IVE-PLS, 3) UVE-SRD-PLS and 4) IVE-SRD-PLS (Fig. 4). As a dependent variable, we used the published logMICs against *Mycobacterium tuberculosis*. To evaluate the 3D QSAR model, the original set of compounds was randomly divided into training and test sets in ratio 25 : 5.

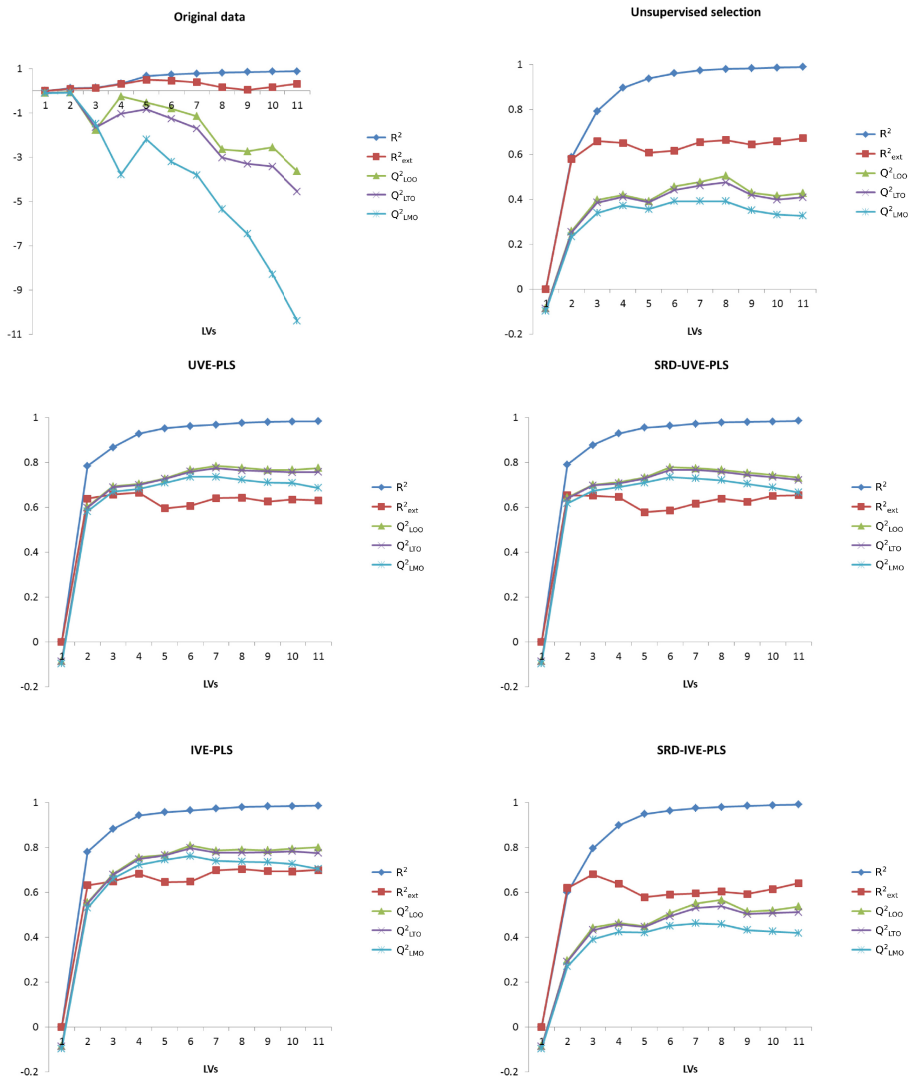


**Fig. 4.** Comparison of statistical performance of PLS 3D QSAR models after application of various data-noise reduction methods. The results are related to 30 antituberculosis. The vertical y-axes in all graphs represent  $R^2$ ,  $R^2_{ext}$ ,  $Q^2_{LOO}$ ,  $Q^2_{LTO}$  and  $Q^2_{LMO}$  values.

From the above plots follows that an efficient data noise reduction is crucial to achieve a stable PLS model in cross-validation. The original dataset provided all  $Q^2_{LOO/LTO/LMO}$  with negative values, which indicate an overtrained PLS model. Significant improvement was reached even by unsupervised preselection of the  $\mathbf{X}$  matrix. UVE and SRD-UVE PLS models showed considerable better performance and exhibited nearly the same robustness in cross-validation. Top scoring model resulted when applying SRD/UVE-PLS with 6-7 LVs ( $Q^2_{LMO} = 0.7352 - 0.7361$ ). The best 3D QSAR

model was obtained by IVE-PLS (5 LVs;  $Q^2_{LMO} = 0.7652$ ). It is interesting that application of SRD-IVE-PLS caused significant deterioration of the IVE-PLS model stability in cross-validation ( $\max(Q^2_{LMO}) = 0.4617$ ; 6 LVs). It is likely a consequence of stepwise elimination of larger groups of MIF vectors grouped by SRD. Without SRD, the IVE algorithm iteratively investigates all MIF vectors and is better able to find the critical portion of eliminated information from the input data. Numbers of eliminated MIF vectors by the used data-noise reduction methods are given in Table 1.

**Table 1.** Remaining MIF vectors after data-noise reductions.

MIF	Number of MIF vectors remaining after data-noise reduction					
	Original dataset	Unsupervised preselection	UVE	SRD-UVE	IVE	SRD-IVE
VDW	11500	1261	237	128	344	536
ESP	11500	11479	4752	275	6026	576

## 5 Conclusion

In medicinal chemistry and bioinformatics various computerized technologies are increasingly utilized to facilitate drug discovery. One of them is 3D QSAR analysis of molecular interaction fields. By prediction of unseen biological activities, the time and costs needed to develop a novel drug can be substantially decreased. However, the benefit of such computational methods depends on reliability of the derived models. We demonstrated in this work that a data-noise reduction algorithm to select only significant MIF vectors from the original  $\mathbf{X}$  matrix is essential to build a stable 3D QSAR model. A promising method for elimination of useless information in 3D QSAR analysis seems to be iterative variable elimination (IVE) coupled with PLS. It was shown that IVE-PLS method surpassed other techniques for data-noise reduction and provided the most statistically significant 3D QSAR model for 30 selected antituberculotics.

**Acknowledgements.** The paper is supported by the project of specific science “Application of Artificial Intelligence in Bioinformatics” at the Faculty of Informatics and Management, University of Hradec Kralove, Czech Republic and by the long term development plan FNHK.

## References

1. Brown, A.C., Fraser, T.R.: XX.—On the Connection between Chemical Constitution and Physiological Action. Part II.—On the Physiological Action of the Ammonium Bases derived from Atropia and Conia. *Trans. Roy. Soc. Edinburgh* **25**, 693–739 (1869)
2. Hansch, C., Fujita, T.:  $\rho$ - $\sigma$ - $\pi$  Analysis. A method for the correlation of biological activity and chemical structure. *J. Am. Chem. Soc.* **86**, 1616–1626 (1964)
3. Free, S.M., Wilson, J.W.: A mathematical contribution to structure-activity studies. *J. Med. Chem.* **7**, 395–399 (1964)
4. Cramer III, R.D.: Partial least squares (PLS): its strengths and limitations. *Perspect. Drug. Discov.* **1**, 269–278 (1993)

5. Dolezal, R., Korabecny, J., Malinak, D., Honegr, J., Musilek, K., Kuca, K.: Ligand-based 3D QSAR analysis of reactivation potency of mono- and bis-pyridinium aldoximes toward VX-inhibited rat acetylcholinesterase. *J. Mol. Graph. Model.* **56c**, 113–129 (2014)
6. Tropsha, A., Gramatica, P., Gombar, V.K.: The importance of being earnest: validation is the absolute essential for successful application and interpretation of QSPR models. *QSAR Comb. Sci.* **22**, 69–77 (2003)
7. Chuang, Y.C., Chang, C.H., Lin, J.T., Yang, C.N.: Molecular modelling studies of sirtuin 2 inhibitors using three-dimensional structure-activity relationship analysis and molecular dynamics simulations. *Mol. Biosyst.* **11**, 723–733 (2015)
8. Kastenholz, M.A., Pastor, M., Cruciani, G., Haaksma, E.E., Fox, T.: GRID/CPCA: a new computational tool to design selective ligands. *J. Med. Chem.* **43**, 3033–3044 (2000)
9. Bro, R., Elden, L.: PLS works. *J. Chemometr.* **23**, 69–71 (2009)
10. Centner, V., Massart, D.L., de Noord, O.E., de Jong, S., Vandeginste, B.M., Sterna, C.: Elimination of uninformative variables for multivariate calibration. *Anal. Chem.* **68**, 3851–3858 (1996)
11. Polanski, J., Gielegiak, R.: The comparative molecular surface analysis (CoMSA) with modified uninformative variable elimination-PLS (UVE-PLS) method: application to the steroids binding the aromatase enzyme. *J. Chem. Inf. Comp. Sci.* **43**, 656–666 (2003)
12. Gielegiak, R., Polanski, J.: Modeling robust QSAR. 2. iterative variable elimination schemes for CoMSA: application for modeling benzoic acid pKa values. *J. Chem. Inf. Model.* **47**, 547–556 (2007)
13. Mehmood, T., Liland, K.H., Snipen, L., Sæbø, S.: A review of variable selection methods in partial least squares regression. *Chemometr. Intel. Lab.* **118**, 62–69 (2012)
14. Pastor, M., Cruciani, G., Clementi, S.: Smart region definition: a new way to improve the predictive ability and interpretability of three-dimensional quantitative structure-activity relationships. *J. Med. Chem.* **40**, 1455–1464 (1997)
15. Dolezal, R., Waisser, K., Petrlikova, E., Kunes, J., Kubicova, L., Machacek, M., Kaustova, J., Dahse, H.M.: N-Benzylsalicylthioamides: Highly Active Potential Antituberculosis. *Arch. Pharm.* **342**, 113–119 (2009)
16. Waisser, K., Matyk, J., Kunes, J., Dolezal, R., Kaustova, J., Dahse, H.M.: Highly Active Potential Antituberculosis: 3-(4-Alkylphenyl)-4-thioxo-2H-1,3-benzoxazine-2(3H)-ones and 3-(4-Alkylphenyl)-2H-1,3-benzoxazine-2,4(3H)-dihiones Substituted in Ring-B by Halogen. *Archiv Der Pharmazie* **341**, 800–803 (2008)
17. Tosco, P., Balle, T., Shiri, F.: Open3DALIGN: an open-source software aimed at unsupervised ligand alignment. *J. Comput. Aid. Mol. Des.* **25**, 777–783 (2011)
18. Tosco, P., Balle, T.: Open3DQSAR: a new open-source software aimed at high-throughput chemometric analysis of molecular interaction fields. *J. Mol. Model.* **17**, 201–208 (2011)

# Pattern-Based Biclustering with Constraints for Gene Expression Data Analysis

Rui Henriques<sup>(✉)</sup> and Sara C. Madeira

Inesc-ID, Instituto Superior Técnico, Universidade de Lisboa, Lisboa, Portugal  
`{rmch,sara.madeira}@tecnico.ulisboa.pt`

**Abstract.** Biclustering has been largely applied for gene expression data analysis. In recent years, a clearer understanding of the synergies between pattern mining and biclustering gave rise to a new class of biclustering algorithms, referred as pattern-based biclustering. These algorithms are able to discover exhaustive structures of biclusters with flexible coherency and quality. Background knowledge has also been increasingly applied for biological data analysis to guarantee relevant results. In this context, despite numerous contributions from domain-driven pattern mining, there is not yet a solid view on whether and how background knowledge can be applied to guide pattern-based biclustering tasks.

In this work, we extend pattern-based biclustering algorithms to effectively seize efficiency gains in the presence of constraints. Furthermore, we illustrate how constraints with succinct, (anti-)monotone and convertible properties can be derived from knowledge repositories and user expectations. Experimental results show the importance of incorporating background knowledge within pattern-based biclustering to foster efficiency and guarantee non-trivial yet biologically relevant solutions.

## 1 Introduction

Biclustering, the task of finding subsets of rows with a coherent pattern across subsets of columns in real-valued matrices, has been largely used for expression data analysis [9, 11]. Biclustering algorithms based on pattern mining methods [9, 11, 12, 18, 22, 25], referred in this work as pattern-based biclustering, are able to perform flexible and exhaustive searches. Initial attempts to use background knowledge for biclustering based on user expectations [5, 7, 15] and knowledge-based repositories [18, 20, 26] show its key role to guide the task and guarantee relevant solutions. In this context, two valuable synergies can be identified based on these observations. First, the optimality and flexibility of pattern-based biclustering provide an adequate basis upon which knowledge-driven constraints can be incorporated. Contrasting with pattern-based biclustering, alternative biclustering algorithms place restrictions on the structure (number, size and positioning), coherency and quality of biclusters, which may prevent the incorporation of certain constraints [11, 16]. Second, the effective use of background knowledge to guide pattern mining searches has been largely researched in the context of domain-driven pattern mining [4, 23].

Despite these synergies, there is a lack of literature on the feasibility and impact of integrating domain-driven pattern mining and biclustering. In particular, there is a lack of research on how to map the commonly available background knowledge in the form of parameters or constraints to guide the biclustering task. Additionally, the majority of existing pattern-based biclustering algorithms rely on searches dependent on bitset vectors [18, 22, 25], which may turn their performance impracticable for large and dense biological datasets. Although new searches became recently available for biclustering large and dense data [13], there are not yet contributions on how these searches can be adapted to seize the benefits from the available background knowledge.

In this work, we address these problems. First, we list an extensive set of key constraints with biological relevance and show how they can be specified for pattern-based biclustering. Second, we extend F2G [13], a recent pattern-growth search that tackles the efficiency bottlenecks of peer searches, to be able to effectively use constraints with succinct, (anti-)monotone and convertible properties.

To achieve these goals, we propose BiC2PAM (**Bi**Clustering with **C**onstraints using **P**Attern **M**ining), an algorithm that integrates recent breakthroughs on pattern-based biclustering [9, 11, 12] and extends them to effectively incorporate constraints. Experimental results confirm the role of BiC2PAM to foster the biological relevance of pattern-based biclustering solutions and to seize large efficiency gains by adequately pruning the search space.

The paper is structured as follows. *Section 2* provides background on pattern-based biclustering and domain-driven pattern mining. *Section 3* surveys key contributions and limitations from related work. *Section 4* lists biologically meaningful constraints and proposes BiC2PAM for their effective incorporation. *Section 5* provides initial empirical evidence of BiC2PAM’s efficiency and ability to unravel non-trivial yet biologically significant biclusters from gene expression data. Finally, concluding remarks are synthesized.

## 2 Background

**Definition 1.** Given a matrix,  $A=(X, Y)$ , with a set of rows  $X=\{x_1, \dots, x_n\}$ , a set of columns  $Y=\{y_1, \dots, y_m\}$ , and elements  $a_{ij} \in \mathbb{R}$  relating row  $i$  and column  $j$ : the **biclustering task** aims to identify a set of biclusters  $\mathcal{B}=\{B_1, \dots, B_m\}$ , where each bicluster  $B_k = (I_k, J_k)$  is a submatrix of  $A$  ( $I_k \subseteq X$  and  $J_k \subseteq Y$ ) satisfying specific criteria of *homogeneity* and *significance* [11].

A real-valued matrix can thus be described by a (multivariate) distribution of background values and a *structure* of biclusters, where each bicluster satisfies specific criteria of *homogeneity* and *significance*. The *structure* is defined by the number, size and positioning of biclusters. Flexible structures are characterized by an arbitrary-high set of (possibly overlapping) biclusters. The *coherency* (homogeneity) of a bicluster is defined by the observed correlation of values (see Definition 2). The *quality* of a bicluster is defined by the type and amount of accommodated noise. The statistical *significance* of a bicluster determines the deviation of its probability of occurrence from expectations.

**Definition 2.** Let the elements in a bicluster  $a_{ij} \in (I, J)$  have coherency across rows given by  $a_{ij} = k_j + \gamma_i + \eta_{ij}$ , where  $k_j$  is the expected value for column  $j$ ,  $\gamma_i$  is the adjustment for row  $i$ , and  $\eta_{ij}$  is the noise factor [16]. For a given real-valued matrix  $A$  and coherency strength  $\delta$ :  $a_{ij} = k_j + \gamma_i + \eta_{ij}$  where  $\eta_{ij} \in [-\delta/2, \delta/2]$ .

As motivated, the discovery of exhaustive and flexible structures of biclusters satisfying certain homogeneity criteria (Definition 2) is a desirable condition to effectively incorporate knowledge-driven constraints. However, due to the complexity of such biclustering task, most of the existing algorithms are either based on greedy or stochastic approaches, producing sub-optimal solutions and placing restrictions (e.g. fixed number of biclusters, non-overlapping structures, and simplistic coherencies) that prevent the flexibility of the biclustering task [16]. Pattern-based biclustering appeared in recent years as one of various attempts to address these limitations. As follows, we provide background on this class of biclustering algorithms, as well as on constraint-based searches.

**Pattern-Based Biclustering.** Patterns are itemsets, rules, sequences or other structures that appear in symbolic datasets with frequency above a specified threshold. Patterns can be mapped as a bicluster with constant values across rows ( $a_{ij} = c_j$ ), and specific coherency strength determined by the number of symbols in the dataset,  $\delta = 1/|\mathcal{L}|$  where  $\mathcal{L}$  is the alphabet of symbols. The relevance of a pattern is primarily defined by its support (number of rows) and length (number of columns). To allow this mapping, the pattern mining task needs to output not only the patterns but also their supporting transactions (*full-patterns*). Definitions 3 and 4 illustrate the paradigmatic mapping between full-pattern mining and biclustering.

**Definition 3.** Let  $\mathcal{L}$  be a finite set of items, and  $P$  an itemset  $P \subseteq \mathcal{L}$ . A symbolic matrix  $D$  is a finite set of transactions in  $\mathcal{L}$ ,  $\{P_1, \dots, P_n\}$ . Let the coverage  $\Phi_P$  of an itemset  $P$  be the set of transactions in  $D$  in which  $P$  occurs,  $\{P_i \in D \mid P \subseteq P_i\}$ , and its support  $\text{supp}_P$  be the coverage size,  $|\Phi_P|$ .

A full-pattern is a pair  $(P, \Phi_P)$ , where  $P$  is an itemset and  $\Phi_P$  the set of all transactions that contain  $P$ . A closed full-pattern  $(P, \Phi_P)$  is a full-pattern where  $P$  is not subset of another itemset with the same support,  $\forall_{P' \supset P} |P'| < |P|$ .

Given  $D$  and a minimum support threshold  $\theta$ , the **full-pattern mining** task [13] consists of computing:  $\{(P, \Phi_P) \mid P \subseteq \mathcal{L}, \text{supp}_P \geq \theta, \forall_{P' \supset P} |P'| < |P|\}$ .

Given an illustrative symbolic matrix  $D = \{(t_1, \{a, c, e\}), (t_2, \{a, b, d\}), (t_3, \{a, c, e\})\}$ , we have  $\Phi_{\{a, c\}} = \{t_1, t_3\}$ ,  $\text{supp}_{\{a, c\}} = 2$ . For a minimum support  $\theta = 2$ , the full-pattern mining task over  $D$  returns the set of closed full-patterns,  $\{\{\{a\}, \{t_1, t_2, t_3\}\}, (\{a, c, e\}, \{t_1, t_3\})\}$  (note that  $|\Phi_{\{a, c\}}| \leq |\Phi_{\{a, c, e\}}|$ ). Fig. 1 illustrates how full-pattern mining can be used to derive constant biclusters<sup>1</sup>.

**Definition 4.** Given a symbolic matrix  $D$  in  $\mathcal{L}$ , let a matrix  $A$  be the concatenation of  $D$  elements with their column indexes. Let  $\Psi_P$  be the column indexes

<sup>1</sup> Association rule mining, sequential pattern mining and graph mining can be also used to respectively mine biclusters with noisy, order-preserving and differential coherencies [9, 12].

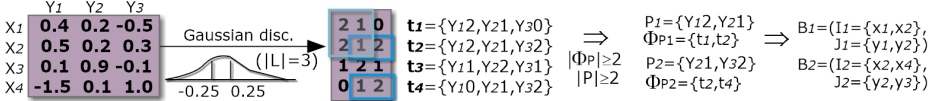


**Fig. 1.** Discovery of biclusters with constant coherency on rows from full-patterns.

of an itemset  $P$ , and  $\Upsilon_P$  be the original items of  $P$  in  $\mathcal{L}$ . The set of **maximal biclusters**  $\cup_k B_k = (I_k, J_k)$  can be derived from the set of closed full-patterns  $\cup_k P_k$  from  $A$ , by mapping  $I_k = \Phi_{P_k}$  and  $J_k = \Psi_{P_k}$ , to compose constant biclusters with coherency across rows with pattern  $\Upsilon_P$  [11].

The inherent simplicity, efficiency and flexibility of pattern-based bioclustering explains the increasing attention [11, 12, 18, 22, 25]. The major contributions of pattern-based approaches for bioclustering include: 1) efficient analysis of large matrices due to the monotone search principles (and the support for distributed/partitioned data settings and approximate patterns [8]). 2) biclusters with parameterizable coherency strength (beyond differential assumption) and type (possibility to accommodate additive, multiplicative, order-preserving and plaid models) [9, 11, 12]; 3) flexible structures of biclusters (arbitrary positioning of biclusters) and searches (no need to fix the number of biclusters apriori) [22, 25]; and 4) robustness to noise, missings and discretization problems [11].

**Constraint-Based Pattern Mining.** A *constraint* is a predicate on the powerset of items  $C : 2^{\mathcal{L}} \rightarrow \{\text{true}, \text{false}\}$ . A full-pattern  $(P, \Phi_P)$  satisfies  $C$  if  $C(P)$  is true. Minimum support is the default constraint in full-pattern mining,  $C_{freq}(P) = |\Phi_P| \geq \theta$ . Typical constraints with interesting properties include: regular expressions on the items in the pattern, and inequalities based on aggregate functions, such as length, maximum, minimum, range, sum, average and variance [24].

**Definition 5.** Let each item have a correspondence with a real value,  $\mathcal{L} \rightarrow \mathbb{R}$ , when numeric operators are considered.  $C$  is **monotone** if for any  $P$  satisfying  $C$ ,  $P$  supersets satisfy  $C$  (e.g.  $\text{range}(P) \geq v$ ).  $C$  is **anti-monotone** if for any  $P$  not satisfying  $C$ ,  $P$  supersets do not satisfy  $C$  (e.g.  $\text{max}(P) \leq v$ ). Let  $P_1$  satisfy  $C$ ,  $C$  is **succint** if for any  $P_2$  satisfying  $C$ ,  $P_1 \subseteq P_2$  (e.g.  $\min(P_2) \leq v$ ).  $C$  is **convertible** w.r.t. an ordering of items  $R_{\Sigma}$  if for any  $P$  satisfying  $C$ ,  $P$  suffixes satisfy  $C$  or/and itemsets with  $P$  as suffix satisfy  $C$  (e.g.  $\text{avg}(P) \geq v$ ).

To illustrate these constraints, consider  $\{(t_1, \{a, b, c\}), (t_2, \{a, b, c, d\}), (t_3, \{a, d\})\}$ ,  $\theta=1$  and  $\{a:0,b:1,c:2,d:3\}$  value correspondence. The set of closed full-patterns under the monotone  $\text{range}(P) \geq 2$  is  $\{\{\{a, b\}, \{t_1, t_2\}\}, \{\{a, d\}, \{t_1, t_3\}\}\}$ ; the anti-monotone  $\text{sum}(P) \leq 1$  is  $\{\{\{a, b\}, \{t_1, t_2\}\}\}$ ; the succinct  $P \supseteq \{c, d\}$  is  $\{\{\{a, b, c, d\}, \{t_2\}\}\}$ ; and the convertible  $\text{avg}(P) \geq 2$  is  $\{\{\{b, c, d\}, \{t_2\}\}\}$ .

### 3 Related Work

**Knowledge-Driven Bioclustering.** The use of background knowledge to guide bioclustering has been increasingly motivated since solutions with good homo-

geneity and statistical significance may not necessarily be biologically relevant. However, only few biclustering algorithms are able to incorporate background knowledge. AI-ISA [26], GenMiner [18] and scatter biclustering [20] are able to annotate data with functional terms retrieved from repositories with ontologies, and use these annotations to guide the search. COBIC [19] is able to adjust its behavior (maximum-flow/minimum-cut parameters) in the presence of background knowledge. Similarly, the priors and architectures of generative biclustering algorithms can also incorporate background knowledge [10]. However, COBIC and generative peers are not able to deliver flexible biclustering solutions and only consider simplistic constraints. Fang et al. [5] propose a constraint-based algorithm that turns possible the discovery of dense biclusters associated with high-order combinations of single-nucleotide polymorphisms (SNPs). Data-Peeler [7], as well as algorithms from formal concept analysis [15] and bi-sets mining [1], are able to efficiently discover dense biclusters in binary matrices in the presence of (anti-)monotone constraints. However, these last sets of algorithms impose a very restrictive form of homogeneity in the delivered biclusters.

**Full-Pattern Mining for Biclustering.** The majority of existing full-pattern miners rely on frequent itemset mining with implementations based on bitset vectors to represent transaction-sets. There are two major classes of searches with this behavior. First, Apriori-based searches [8], generally suffering from costs of candidate generation for low support thresholds (commonly required for biological tasks [22]). Efficient implementations include LCM and CLOSE, used respectively by BiModule [22] and GenMiner [18] biclustering algorithms. Second, vertical-based searches, such as Eclat and Carpenter [8]. These searches rely on intersection operations over transaction-sets to generate candidates, requiring structures such as bitset vectors or diffsets. However, for datasets with a high number of transactions the bitset cardinality becomes large, these structures consume a significant amount of memory and operations become costly. MAFIA is an implementation used by DeBi [25]. Only in recent years, a third class of searches without the bottlenecks associated with bitset vectors were made available by extending pattern-growth searches for the discovery of full-patterns using frequent-pattern trees (FP-Trees) annotated with transactions. F2G [13] used by default in BicPAM [11] implements this third type of searches.

**Constraint-Based Pattern Mining.** A large number of studies explore how constraints can be used with pattern mining. Two major paradigms are available: constraint-programming (CP) and dedicated searches. First, CP allows the pattern mining task to be declaratively defined according to sets of constraints [4, 14]. These declarative models are expressive as they can allow mathematical expressions over itemsets and transaction-sets. Nevertheless, due to the poor scalability of CP methods, they have been only used in highly constrained settings, small-to-medium data, or to mine approximative patterns [4, 14].

Second, pattern mining methods have been adapted to optimally seize efficiency gains from different types of constraints. Such efforts replace naïve solutions: post-filtering patterns that satisfy constraints. Instead, the constraints

are pushed as deeply as possible within the mining step for an optimal pruning of the search space. The nice properties exhibited by constraints, such as anti-monotone and succinct properties, have been initially seized by Apriori methods [21] to affect the generation of candidates. Convertible constraints, can hardly be pushed in Apriori but can be handled by FP-Growth approaches [23]. FICA, FICM, and more recently MCFPTree, are FP-Growth extensions to seize the properties of anti-monotone, succinct and convertible constraints [23]. The inclusion of monotone constraints is more complex. Filtering methods, such as ExAnte, are able to combine anti-monotone and monotone pruning based on reduction procedures [2]. Reductions are optimally handled in FP-Trees [3].

## 4 Pattern-Based Biclustering with Constraints

BicPAM [11], BicSPAM [12] and BiP [9] are the state-of-the-art algorithms for pattern-based biclustering. They integrate the dispersed contributions of previous pattern-based algorithms and extend them to discover non-constant coherencies and to guarantee their robustness to discretization (by assigning multi-items to a single element [11]), noise and missings. In this section, we propose BiC2PAM (**B**iClustering with **C**onstraints using **P**Attern **M**ining) to integrate their contributions and adapt them to effectively incorporate constraints. BiC2PAM is a composition of three major steps: 1) *preprocessing* to itemize real-valued data; 2) *mining* step, corresponding to the application of full-pattern miners; and 3) *postprocessing* to merge, reduce, extend and filter similar biclusters. As follows, *Section 4.1* lists native constraints supported by parameterizations along these steps. *Section 4.2* lists biologically meaningful constraints with properties of interest. Finally, we extend a pattern-growth search to seize efficiency gains from succinct, (anti-)monotone and convertible constraints (*Section 4.3*).

### 4.1 Native Constraints

Below we list a set of structural constraints that can be incorporated by adapting the parameters that control the behavior of pattern-based biclustering algorithms along their three major steps.

Relevant constraints provided in the pre-processing step:

- combined inclusion of annotations (such as functional terms) with succinct constraints. A functional term is associated with an interrelated group of genes, and thus it can be appended as a new dedicated symbol to the respective transactions/genes, possibly leading to a set of transactions with varying length. Illustrating, consider  $T_1$  and  $T_2$  terms to be respectively associated with genes  $\{g_1, g_3, g_4\}$  and  $\{g_3, g_5\}$ , an illustrative dataset for this scenario would be  $\{(g_1, \{a_{11}, \dots, a_{1m}, T_1\}), (g_2, \{a_{21}, \dots, a_{2m}\}), (g_3 \{a_{31}, \dots, a_{3m}, T_1, T_2\}), \dots\}$ . Pattern mining can then be applied on top of these annotated transactions with succinct constraints to guarantee the inclusion of certain terms (such as  $P \cap \{T_1, T_2\} \neq \emptyset$ ). This is useful to discover, for instance, biclusters with genes participating in specific functions of interest.

- ranges of values (or symbols) to ignore from the input matrix,  $\text{remove}(S)$  where  $S \subseteq \mathbb{R}^+$  (or  $S \subseteq \mathcal{L}$ ). In gene expression, elements with default/non-differential expression are generally less relevant and thus can be removed. This is achieved by removing these elements from the transactions. Despite the simplicity of this constraint, this option is not easily supported by peer biclustering algorithms [16].
- minimum coherency strength (or number of symbols) of the target biclusters:  $\delta=1/|\mathcal{L}|$ . Decreasing the coherency strength (increasing the number of symbols) reduces the noise-tolerance of the resulting set of biclusters and it is often associated with solutions composed by a larger number of biclusters with smaller areas.
- level of relaxation to handle noise by increasing the  $\eta_{ij}$  noise range (Definition 2). This constraint is used to adjust the behavior of BiC2PAM in the presence of noise or discretization problems (values near a boundary of discretization). By default, one symbol is associated with an element. Yet, this constraint gives the possibility to assign an additional symbol to an element when its value is near a boundary of discretization, or even a parameterizable number of symbols per element for a high tolerance to noise (proof in [11]).

Relevant constraints provided in the mining step:

- minimum pattern length (minimum number of columns in the bicluster).
- stopping criteria: either the anti-monotone minimum support length (minimum number of rows in the bicluster), or iteratively decreasing support until minimum number of biclusters is discovered or minimum area of the input matrix is coverage by the discovered biclusters.
- type of coherency and orientation. Currently, BiC2PAM supports the selection of constant, additive, multiplicative, symmetric, order-preserving and plaid models with coherency on rows or columns (according to [9, 11]).
- pattern representation: simple (all coherent biclusters), closed (all maximal biclusters), and maximal (solutions with a compact number of biclusters with a preference towards a high number of columns).

Understandably, constraints addressed at the postprocessing stage are not desirable since they are not able to seize major efficiency gains. Nevertheless, BiC2PAM supports two key types of constraints that could imply additional computational costs, but are addressed with heightened efficiency: 1) maximum percentage of noisy and missing elements per bicluster (based on merging procedures [11]), and 2) minimum homogeneity of the target biclusters (using extension and reduction procedures with a parameterizable merit function [11]).

## 4.2 Biologically Meaningful Constraints

Different types of constraints were introduced in Definition 5. In order to illustrate how such constraints can be specified and instantiated, a symbolic gene expression matrix (and associated “price table”) is provided in Fig. 2, where the rows correspond to different genes and the values correspond to observed levels of expressions for a specific condition (column). The  $\{-3, -2\}$ ,  $\{-1, 0, 1\}$  and  $\{2, 3\}$  sets of symbols are respectively associated with repressed (down-regulated), default (preserved) and activated (up-regulated) levels of expression.

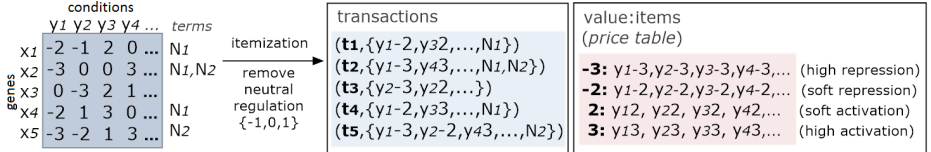


**Fig. 2.** Illustrative symbolic dataset and “price table” for expression data analysis.

First, **succinct** constraints in gene expression analysis allow the discovery of genes with specific constrained levels of expression across a subset of conditions. Illustrating,  $\min(P) = -3$  implies an interest in biclusters (biological processes) where genes are at least highly repressed in one condition. Alternatively, succinct constraints can be used to discover non-trivial biclusters by focusing on non-highly differential expression (e.g. patterns with symbols {-2,2}). Such option contrasts with the large focus on dense biclusters [16]. Finally, succinct constraints can also be used to guarantee that a specific condition of interest appears in the resulting set (e.g.  $P \cap \{y_2-3, y_2-2, y_22, y_23\} \neq \emptyset$  to include  $y_2$ ), or a specific annotation ( $P \cap \{N_1, N_2\} \neq \emptyset$ ).

Second, **(anti-)monotone** constraints are key to capture background knowledge and guide bioclustering. Illustrating, the non-succinct monotonic constraint  $\text{countVal}(P) \geq 2$  implies that at least two different levels of expression must be present within a bicluster (biological process). In gene expression analysis, biclusters should be able to accommodate genes with different degrees of up-regulation and/or down-regulation. Yet, the majority of existing bioclustering approaches are only able to model constant values across conditions [11, 16]. When constraints, such as the value-counting inequality, are available, the pruning of the search space allows an efficient handling of very low support thresholds for these non-trivial biclusters to be discovered.

Finally, **convertible** constraints also play an important role in biological settings to guarantee, for instance, that the observed patterns have an average of values within a specific range. Illustrating, the anti-monotonic convertible constraint  $\text{avg}(P) \leq 0$  indicates a preference for patterns with repression mechanisms without a strict exclusion of activation mechanisms. These constraints are useful to focus the discovery on specific expression levels, while still allowing for noise deviations. Understandably, they are a robust alternative to the use of strict bounds from succinct constraints with maximum-minimum inequalities.

### 4.3 Effective Use of Constraints in Pattern-based Bioclustering

Although native constraints are supported through adequate parameterizations of pattern-based bioclustering algorithms, the previous (non-native) constraints are not directly supported. Nevertheless, as surveyed, pattern mining searches have been extended to seize efficiency gains when succinct, (anti-)monotone or convertible constraints are considered. Although there is large consensus that pattern-growth searches are better positioned to seize efficiency gains from constraints than peer methods based on bitset vectors, there is not yet proof whether

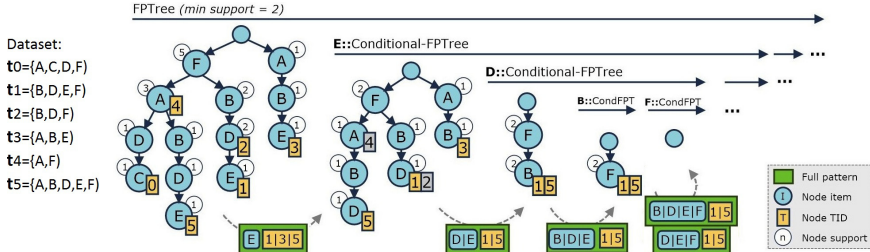


**Fig. 3.** Illustrative behavior of F2G [13].

this observation remains valid in the context of full-pattern mining. As such, we extend the recently proposed F2G algorithm to guarantee an optimal pruning of the search space in the presence of constraints and integrate F2G in BiC2PAM. F2G implements a pattern-growth search that does not suffer from efficiency bottlenecks since it relies on tree structures where transaction-IDs are stored without duplicates<sup>2</sup>. F2G behavior is illustrated in Fig.3. In this section, we first show the compliance of F2G with principles to handle succinct and convertible constraints [23]. Second, we show the compliance of F2G with principles to handle difficult combinations of monotone and anti-monotone constraints [3].

**Compliance with Different Types of Constraints.** Unlike candidate generation methods, pattern growth methods (such as FP-Growth) provide further pruning opportunities. Pruning principles can be standardly applied on both the original database (full FP-Tree) and on each projected database (conditional FP-Tree). CFG extensions to FP-Growth [23] seize the properties of such constraints under three simple principles. First, supersets of itemsets violating anti-monotone constraints are removed for each (conditional) FP-Tree (e.g. for  $y_{12}$  conditional database, remove conflicting items  $\cup_{i=1}^m \{y_{i2}, y_{i3}\}$  as their sum violates  $\text{sum}(P) \leq 3$ ). For an effective pruning, it is recommended to order the symbols in the header table according to their value and support [23, 24]. F2G is compliant with these removals, since it allows the rising of transaction-IDs in the FP-Tree according to the order of candidate items for removal in the header table (property explained in [13]).

For the particular case of an anti-monotone convertible constraint, itemsets that satisfy the constraint are efficiently generated under a pattern-growth search [24] (e.g.  $\{y_{1-3}, y_{22}, y_{42}\}$  itemset is not included in the generated pattern set respecting  $\text{avg}(P) \leq 0$ ), and provide a simple criterion to either stop FP-tree projections or prune items in a (conditional) FP-Tree.

Finally, the removal of conflicting transactions (e.g.  $t_1$  and  $t_4$  does not satisfy the illustrated succinct constraint) and of individual items (e.g.  $\cup_{i=1}^m \{y_i\}$

<sup>2</sup> The FP-tree is recursively mined to enumerate all full-patterns. Unlike peer pattern-growth searches, transaction-IDs are not lost at the first scan. Full-patterns are generated by concatenating the pattern suffixes with the full-patterns discovered from conditional FP-trees where suffixes are removed. F2G is applicable on top of FP-Close trees to mine closed full-patterns [13].

$1, y_{i0}, y_{i1}\})$  do not cause changes in the FP-Tree construction methods. Additionally, constraint checks can be avoided for subsets of itemsets satisfying a monotone constraint (e.g. no further checks of  $\text{countVal}(P) \geq 2$  constraint when the range of values in the suffix is  $\geq 2$  under the  $\{y_{i0}, y_{i1}\}$ -conditional FP-Tree).

**Combination of Constraints.** The previous extensions of pattern-growth searches are not able to effectively comply with monotone constraints when anti-monotone constraints (such as minimum support) are also considered. In FP-Bonsai [3], principles to further explore the monotone properties for pruning the search space are considered without reducing anti-monotone pruning opportunities. This method is based on the ExAnte synergy of two data-reduction operations that seize the properties of monotone constraints:  $\mu$ -reduction, which deletes transactions not satisfying  $C$ ; and  $\alpha$ -reduction, which deletes from transactions single items not satisfying  $C$ . Thanks to the recursive projecting approach of FP-growth, the ExAnte data-reduction methods can be applied on each conditional FP-tree to obtain a compact number of smaller FP-Trees (FP-Bonsais). The FP-Bonsai method can be combined with the previously introduced principles, which are particularly prone to handle succinct and convertible anti-monotone constraints. Since F2G can be extended to support the pruning of FP-Trees, it complies with the FP-Bonsai extension.

## 5 Results and Discussion

In this section, we assess the performance of BiC2PAM on synthetic and real datasets with different types of constraints and three distinct full-pattern miners: AprioriTID<sup>3</sup>, Eclat<sup>3</sup> and F2G. BiC2PAM is implemented in Java (JVM v1.6.0-24). The experiments were computed using an IC i5 2.30GHz with 6GB of RAM.

**Results on Synthetic Data.** The generated data settings are described in Table 1. Biclusters with different shapes and coherency strength ( $|\mathcal{L}| \in \{4, 7, 10\}$ ) were planted by varying the number of rows and columns using Uniform distributions with ranges in Table 1. For each setting we instantiated 20 matrices with background values generated with Uniform and Gaussian distributions.

**Table 1.** Properties of the generated dataset settings.

Matrix size (#rows $\times$ #columns)	500 $\times$ 50	1000 $\times$ 100	2000 $\times$ 200	4000 $\times$ 400
Nr. of hidden patterns	5	10	15	25
Nr. transactions for the hidden patterns	[10, 14]	[14, 30]	[30, 50]	[50, 100]
Nr. items for the hidden patterns	[5, 7]	[6, 8]	[7, 9]	[8, 10]

BiC2PAM was applied with a default merging option (70% of overlapping) and a decreasing support until a minimum number of 50 (maximal) biclusters was found. Fig.4 provides the results of parameterizing BiC2PAM with different pattern miners and two simple constraints defining the target coherency strength

<sup>3</sup> <http://www.philippe-fournier-viger.com/spmf/>

and symbols to remove. We observe that the proposed F2G miner is the most efficient option for denser data settings (looser coherency). Also, in contrast with existing biclustering algorithms, BiC2PAM seizes large efficiency gains from neglecting specific ranges of values (symbols) from the input matrix.

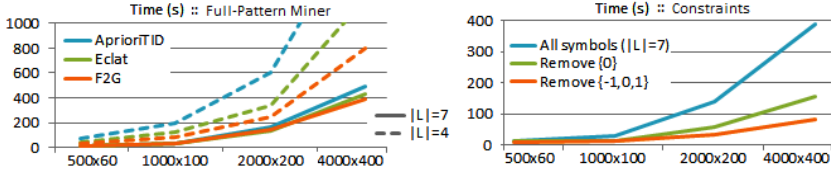


**Fig. 4.** BiC2PAM performance in the presence of simplistic native constraints.

In order to test the ability of BiC2PAM to seize further efficiency gains in the presence of non-trivial constraints, we fixed the  $2000 \times 200$  setting with 6 symbols/values  $\{-3,-2,-1,1,2,3\}$ . In the baseline performance, constraints were satisfied using post-filtering procedures. Fig.5 illustrates this analysis. As observed, the use of constraints can significantly reduce the search complexity when they are properly incorporated within the full-pattern mining method. In particular, CFG principles [23] are used to seize efficiency gains from convertible constraints and FP-Bonsai [3] to seize efficiency gains from monotonic constraints.

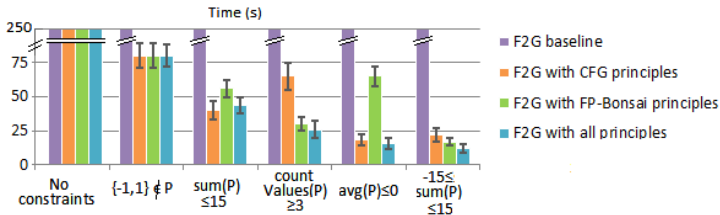


**Fig. 5.** Efficiency gains of considering constraints in F2G using different principles.

**Results on Real Data.** Fig.6 shows the (time and memory) efficiency of applying BiC2PAM in the yeast<sup>4</sup> expression dataset with different pattern miners and varying support thresholds for a desirable coherency strength of 10% ( $|\mathcal{L}|=10$ ). The proposed F2G is the most efficient option in terms of time and, along with Apriori, a competitive choice for efficient memory usage.

Finally, Figs.7 and 8 show the impact of biologically meaningful constraints in the efficiency and effectiveness of BiC2PAM. For this purpose, we used the complete gasch dataset ( $6152 \times 176$ ) [6] with six levels of expression ( $|\mathcal{L}|=6$ ). The effect of constraints in the efficiency is shown in Fig.7. This analysis supports their key role of providing opportunities to solve hard biomedical tasks.

<sup>4</sup> <http://www.upo.es/eps/bigs/datasets.html>

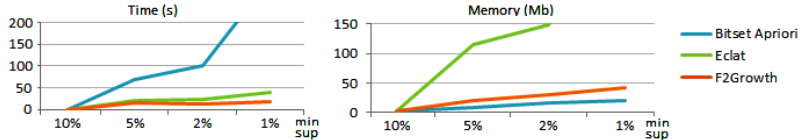


Fig. 6. Computational time and memory of full-pattern miners for yeast ( $2884 \times 17$ ).

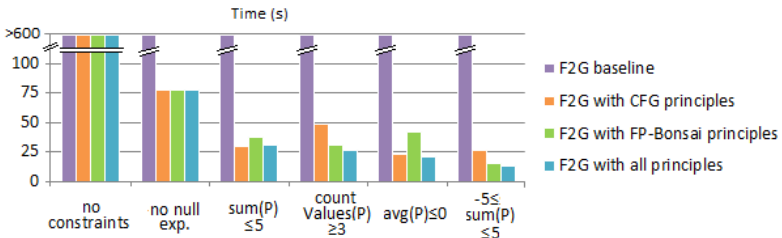


Fig. 7. Efficiency gains from using biological constraints for gasch ( $6152 \times 176$ ).

The impact of these constraints in the relevance of pattern-based bioclustering solutions is illustrated in Fig. 8. The biological relevance of each bicluster was derived from the functionally enriched terms using an hypergeometric test of Gene Ontology (GO) annotations [17]. As a measure of significance, we counted the number of terms with Bonferroni corrected p-values below 0.01 [17]. Two major observations can be retrieved. First, when focusing on properties of interest (e.g. differential expression), the average significance of biclusters increases as their genes have higher propensity to be functionally co-regulated. This trend is observed despite the smaller size of the constrained biclusters. Second, when focusing on rare expression profiles ( $\geq 3$  distinct levels of expression), the average relevance of biclusters slightly decreases as their co-regulation is less obvious. Yet, such non-trivial biclusters hold unique properties with potential interest.

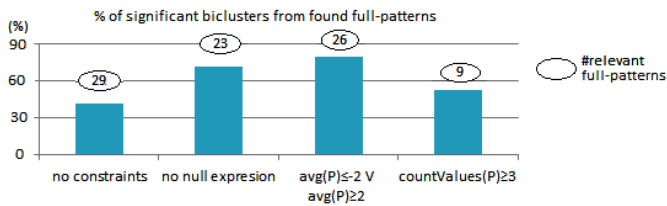


Fig. 8. Biological relevance of F2G for multiple constraint-based profiles of expression.

## 6 Conclusions

This work motivates the task of bioclustering biological data in the presence of constraints. To answer this task, we explore the synergies between pattern-based

biclustering and domain-driven pattern mining. As a result, BiC2PAM algorithm is proposed to effectively incorporate constraints derived from user expectations and available background knowledge.

Two major sets of constraints were proposed for the discovery of biclusters with specific interestingness criteria. First, native constraints to guarantee the discovery of biclusters with parameterizable coherency, noise-tolerance and shape, and to consider annotations from knowledge-based repositories. Second, constraints with succinct, monotone, anti-monotone and convertible properties to focus the search space on non-trivial yet biologically meaningful patterns.

In this context, we extended a recent pattern-growth search to optimally explore efficiency gains in the presence of different types of constraints.

Results from synthetic and real data show that biclustering benefits from large efficiency gains in the presence of constraints derived from background knowledge. We further provide evidence of the relevance of the supported types of constraints to discover non-trivial yet meaningful biclusters in expression data.

**Acknowledgments.** This work was supported by *FCT* under the project UID/CEC/50021/2013 and the PhD grant SFRH/BD/75924/2011 to RH.

## References

1. Besson, J., Robardet, C., De Raedt, L., Boulicaut, J.-F.: Mining Bi-sets in numerical data. In: Džeroski, S., Struyf, J. (eds.) KDID 2006. LNCS, vol. 4747, pp. 11–23. Springer, Heidelberg (2007)
2. Bonchi, F., Giannotti, F., Mazzanti, A., Pedreschi, D.: Exante: a preprocessing method for frequent-pattern mining. *IEEE Intel. Systems* **20**(3), 25–31 (2005)
3. Bonchi, F., Goethals, B.: FP-Bonsai: the art of growing and pruning small FP-trees. In: Dai, H., Srikant, R., Zhang, C. (eds.) PAKDD 2004. LNCS (LNAI), vol. 3056, pp. 155–160. Springer, Heidelberg (2004)
4. Bonchi, F., Lucchese, C.: Extending the state-of-the-art of constraint-based pattern discovery. *Data Knowl. Eng.* **60**(2), 377–399 (2007)
5. Fang, G., Haznadar, M., Wang, W., Yu, H., Steinbach, M., Church, T.R., Oetting, W.S., Van Ness, B., Kumar, V.: High-Order SNP Combinations Associated with Complex Diseases: Efficient Discovery, Statistical Power and Functional Interactions. *Plos One* **7** (2012)
6. Gasch, A.P., Werner-Washburne, M.: The genomics of yeast responses to environmental stress and starvation. *Functional & integrative genomics* **2**(4–5), 181–192 (2002)
7. Guerra, I., Cerf, L., Foscarini, J., Boaventura, M., Meira, W.: Constraint-based search of straddling biclusters and discriminative patterns. *JIDM* **4**(2), 114–123 (2013)
8. Han, J., Cheng, H., Xin, D., Yan, X.: Frequent pattern mining: current status and future directions. *Data Min. Knowl. Discov.* **15**(1), 55–86 (2007)
9. Henriques, R., Madeira, S.: Biclustering with flexible plaid models to unravel interactions between biological processes. *IEEE/ACM Trans. Computational Biology and Bioinfo* (2015). doi:[10.1109/TCBB.2014.2388206](https://doi.org/10.1109/TCBB.2014.2388206)
10. Henriques, R., Antunes, C., Madeira, S.C.: Generative modeling of repositories of health records for predictive tasks. *Data Mining and Knowledge Discovery*, pp. 1–34 (2014)

11. Henriques, R., Madeira, S.: Bicpam: Pattern-based bioclustering for biomedical data analysis. *Algorithms for Molecular Biology* **9**(1), 27 (2014)
12. Henriques, R., Madeira, S.: Bicspam: Flexible bioclustering using sequential patterns. *BMC Bioinformatics* **15**, 130 (2014)
13. Henriques, R., Madeira, S.C., Antunes, C.: F2g: Efficient discovery of full-patterns. In: ECML /PKDD IW on New Frontiers to Mine Complex Patterns. Springer-Verlag, Prague, CR (2013)
14. Khiari, M., Boizumault, P., Crémilleux, B.: Constraint programming for mining n-ary patterns. In: Cohen, D. (ed.) CP 2010. LNCS, vol. 6308, pp. 552–567. Springer, Heidelberg (2010)
15. Kuznetsov, S.O., Poelmans, J.: Knowledge representation and processing with formal concept analysis. *Wiley Interdisc. Reviews: Data Mining and Knowledge Discovery* **3**(3), 200–215 (2013)
16. Madeira, S.C., Oliveira, A.L.: Bioclustering algorithms for biological data analysis: A survey. *IEEE/ACM Trans. Comput. Biol. Bioinformatics* **1**(1), 24–45 (2004)
17. Martin, D., Brun, C., Remy, E., Mouren, P., Thieffry, D., Jacq, B.: Gotoobox: functional analysis of gene datasets based on gene ontology. *Genome Biology* (12), 101 (2004)
18. Martinez, R., Pasquier, C., Pasquier, N.: Genminer: Mining informative association rules from genomic data. In: BIBM, pp. 15–22. IEEE CS (2007)
19. Mouhoubi, K., Létocart, L., Rouveiro, C.: A knowledge-driven bi-clustering method for mining noisy datasets. In: Huang, T., Zeng, Z., Li, C., Leung, C.S. (eds.) ICONIP 2012, Part III. LNCS, vol. 7665, pp. 585–593. Springer, Heidelberg (2012)
20. Nepomuceno, J.A., Troncoso, A., Nepomuceno-Chamorro, I.A., Aguilar-Ruiz, J.S.: Integrating biological knowledge based on functional annotations for bioclustering of gene expression data. *Computer Methods and Programs in Biomedicine* (2015)
21. Ng, R.T., Lakshmanan, L.V.S., Han, J., Pang, A.: Exploratory mining and pruning optimizations of constrained associations rules. *SIGMOD R.* **27**(2), 13–24 (1998)
22. Okada, Y., Fujibuchi, W., Horton, P.: A bioclustering method for gene expression module discovery using closed itemset enumeration algorithm. *IPSJ T. on Bioinfo.* **48**(SIG5), 39–48 (2007)
23. Pei, J., Han, J.: Can we push more constraints into frequent pattern mining? In: KDD. pp. 350–354. ACM, New York (2000)
24. Pei, J., Han, J.: Constrained frequent pattern mining: a pattern-growth view. *SIGKDD Explor. Newsl.* **4**(1), 31–39 (2002)
25. Serin, A., Vingron, M.: Debi: Discovering differentially expressed biclusters using a frequent itemset approach. *Algorithms for Molecular Biology* **6**, 1–12 (2011)
26. Visconti, A., Cordero, F., Pensa, R.G.: Leveraging additional knowledge to support coherent biocluster discovery in gene expression data. *Intell. Data Anal.* **18**(5), 837–855 (2014)

# A Critical Evaluation of Methods for the Reconstruction of Tissue-Specific Models

Sara Correia and Miguel Rocha<sup>(✉)</sup>

Centre of Biological Engineering, University of Minho, Braga, Portugal  
mrocha@di.uminho.pt

**Abstract.** Under the framework of constraint based modeling, genome-scale metabolic models (GSMMs) have been used for several tasks, such as metabolic engineering and phenotype prediction. More recently, their application in health related research has spanned drug discovery, biomarker identification and host-pathogen interactions, targeting diseases such as cancer, Alzheimer, obesity or diabetes. In the last years, the development of novel techniques for genome sequencing and other high-throughput methods, together with advances in Bioinformatics, allowed the reconstruction of GSMMs for human cells. Considering the diversity of cell types and tissues present in the human body, it is imperative to develop tissue-specific metabolic models. Methods to automatically generate these models, based on generic human metabolic models and a plethora of omics data, have been proposed. However, their results have not yet been adequately and critically evaluated and compared.

This work presents a survey of the most important tissue or cell type specific metabolic model reconstruction methods, which use literature, transcriptomics, proteomics and metabolomics data, together with a global template model. As a case study, we analyzed the consistency between several omics data sources and reconstructed distinct metabolic models of hepatocytes using different methods and data sources as inputs. The results show that omics data sources have a poor overlapping and, in some cases, are even contradictory. Additionally, the hepatocyte metabolic models generated are in many cases not able to perform metabolic functions known to be present in the liver tissue. We conclude that reliable methods for *a priori* omics data integration are required to support the reconstruction of complex models of human cells.

## 1 Introduction

Over the last years, genome-scale metabolic models (GSMMs) for several organisms have been developed, mainly for microbes with an interest in Biotechnology [6, 20]. These models have been used to predict cellular metabolism and promote biological discovery [17], under constraint-based approaches such as Flux Balance Analysis (FBA) [18]. FBA finds a flux distribution that maximizes biomass production, considering the knowledge of stoichiometry and reversibility of reactions, and taking some simplifying assumptions, namely assuming quasi steady-state conditions.

Recently, efforts on model reconstruction have also addressed more complex multicellular organisms, including humans [5, 9, 25]. In biomedical research, they have been used, for instance, to elucidate the role of proliferative adaptation causing the Warburg effect in cancer [23], to predict metabolic markers for inborn errors of metabolism [24] and to identify drug targets for specific diseases [11].

However, the human organism is quite complex, with a large number of cell types/tissues and huge diversity in their metabolic functions. This led to the need of developing tissue/cell type specific metabolic models, which could allow studying in more depth specific cell phenotypes. Towards this end, it was imperative to better characterize specific cell types, gathering relevant data. Indeed, an important set of technological advances in the last decades greatly increased available biological data through high-throughput studies that allow the identification and quantification of cell components (gene expression, proteins and metabolites). These are collectively known as ‘omics’ data and have generated new fields of study, such as transcriptomics, proteomics and metabolomics.

The most widely available omics data are transcriptomics, the quantification of gene expression levels in a cell, using DNA microarrays or sequencing (e.g. RNA-seq). The most significant databases for gene expression data are the Gene Expression Omnibus (GEO) [3] and the ArrayExpress [19]. Other resources use those databases as references to synthesize their information, such as the Gene Expression Barcode [16], which provides absolute measures of expression for the most annotated genes, organized by tissue, cell-types and diseases.

In the cells, mRNA is not always translated into protein, and the amounts of protein depend on gene expression but also on other factors. Thus, knowledge about the amounts of proteins in the cell, provided by proteomics data, is of foremost relevance. These data can confirm the presence of proteins and provide measurements of their quantities for each protein within a cell. For human cells, a database is available with millions of high-resolution images showing the spatial distribution of protein expression profiles in normal tissues, cancer and cell lines - the Human Protein Atlas (HPA) portal [26].

Another source of information is provided by metabolomics data that involve the quantification of the small molecules present in cells, tissues, organs and biological fluids using techniques such as Nuclear Magnetic Resonance spectroscopy or Gas Chromatography combined with Mass Spectrometry [13]. The Human Metabolome Database (HMDB) [28] contains spectroscopic, quantitative, analytic and molecular-scale information about human metabolites, associated enzymes or transporters, their abundance and disease-related properties.

Resources for omics data, together with generic human metabolic models, have been used to generate context-specific models. This has been achieved through the development of methods, such as the Model Building Algorithm (MBA) [12], the Metabolic Context-specificity Assessed by Deterministic Reaction Evaluation (mCADRE)[27] and the Task-driven Integrative Network Inference for Tissues (tINIT)[2].

The reconstructed models have allowed, for instance, to find metabolic targets to inhibit the proliferation of cancer cells [29], to study the interaction

between distinct brain cells [14], and to find potential therapeutic targets for the treatment of non-alcoholic steatohepatitis [15].

However, the aforementioned methods have not yet been critically and systematically evaluated on standardized case studies. Indeed, each of the methods is proposed and validated with distinct cases and taking distinct omics data sources as inputs. Thus, the impact of using different omics datasets on the final results of those algorithms is a question that remains to be answered. Here, we present a critical evaluation of the most important methods for the reconstruction of tissue-specific metabolic models published until now.

We have developed a framework where we implemented different methods for the reconstruction of tissue-specific metabolic models. In this scenario, the algorithms use sets of metabolites and/or maps of scores for each reaction as input. So, in our framework the algorithms are independent from the omics data source, and the separation of these two layers allows to use different data sources in each algorithm for the generation of tissue-specific metabolic models. As a case study, to compare the three different approaches implemented, metabolic models were reconstructed for hepatocytes, using the same set of data sources as inputs for each algorithm. Moreover, distinct combinations of data sources are evaluated to check their influence on the final results.

## 2 Materials and Methods

### 2.1 Human Metabolic Models

Modeling metabolic systems requires the analysis and prediction of metabolic flux distributions under diverse physiological and genetic conditions. The human organism is one of the most complex organisms to build a metabolic model since the number of genes, types of cells and their diversity are huge. In the last years, a few human metabolic models were proposed [5,9,15,25]. In this work, we will use the Recon 2 human metabolic model that accounts for 7440 reactions, 5063 metabolites and 1789 enzyme-encoding genes. This model is a community-driven expansion of the previous human reconstruction, Recon 1 [5], with additional information from different resources: EHMN [9], Hepatonet1[8], Ac-FAO module[21] and the small intestinal enterocyte reconstruction [22].

### 2.2 Algorithms for Tissue-Specific Metabolic Models Reconstruction

Although there are several applications of the human GSMMs, the specificity of cell types requires the reconstruction of tissue-specific metabolic models. Some approaches have been proposed based on existing generic human models. Here, we present three of the most well-known approaches for this task that will be used in the remaining of this work.

**MBA.** The Model-Building Algorithm (MBA) [12] reconstructs a tissue-specific metabolic model from a generic model and two sets of reactions, denoted as core reactions ( $C_H$ ) and reactions with a moderate probability to be carried out in the specific tissue ( $C_M$ ). These sets were previously built according to evidence levels based on omics data, literature and experimental knowledge. In general, the  $C_H$  set includes human-curated tissue-specific reactions and the  $C_M$  set includes reactions certified by omics data. The algorithm iteratively removes one reaction from the generic model, in a random order, and validates if the model remains consistent. The process ends when the removal of all reactions, except the ones in  $C_H$ , is tried. As a result, this algorithm reconstructs a model containing all the  $C_H$  reactions, as many as possible  $C_M$  reactions, and a minimal set of other reactions that are required for obtaining overall model consistency (for each reaction there is a flux distribution in which it is active).

Since reactions are scanned in a random order, the authors recommend to run the algorithm a large number of times to generate intermediate models. After this step, a score per each reaction is calculated, according to the number of times it appears in these models. The final model is built starting from  $C_H$  and iteratively adding reactions ordered by their scores, until a final consistent model is achieved.

**INIT/ tINIT.** The Integrative Network Inference for Tissues (INIT) [1] uses the Human Protein Atlas (HPA) as its main source of evidence. Expression data can be used when proteomic evidence is missing. It also allows the integration of metabolomics data by imposing a positive net production of metabolites for which there is experimental support, for instance in HMDB. The algorithm is formulated using mixed integer-linear programming (MILP), so that the final model contains reactions with high scores from HPA data. This algorithm does not impose strict steady-state conditions for all internal metabolites, allowing a small net accumulation rate. A couple of years later, a new version of this algorithm was proposed, the Task-driven Integrative Network Inference for Tissues (tINIT) [2], which reconstructs tissue-specific metabolic models based on protein evidence from HPA and a set of metabolic tasks that the final context-specific model must perform. These tasks are used to test the production or uptake of external metabolites, but also the activation of pathways that occur in a specific tissue. Another improvement from the previous version is the addition of constraints to guarantee that irreversible reactions operate in one direction only.

**mCADRE.** The Metabolic Context specificity Assessed by Deterministic Reaction Evaluation (mCADRE) [27] method is able to infer a tissue-specific network based on gene expression data, network topology and reaction confidence levels. Based on the expression score, the reactions of the global model, used as template, are ranked and separated in two sets - core and non-core. All reactions with expression-based scores higher than a threshold value are included in the core set, while the remaining reactions make the non-core set. In this method, the expression score does not represent the level of expression, but

rather the frequency of expressed states over several transcript profiles. So, it is necessary to previously binarize the expression data. Thus, it is possible to use data retrieved from the Gene Expression Barcode project that already contains binary information on which genes are present or not in a specific tissue/cell type. Reactions from the non-core set are ranked according to the expression scores, connectivity-based scores and confidence level-based scores. Then, sequentially, each reaction is removed and the consistency of the model is tested. The elimination only occurs if the reaction does not prevent the production of a key-metabolite and the core consistency is preserved. Comparing with the MBA algorithm, mCADRE presents two improvements: it allows the definition of key metabolites, i.e. metabolites that have evidence to be produced in the context-specific model reconstruction, and relaxes the condition of including all core reactions in the final model.

Table 1 shows the mathematical formulation and pseudocode for all algorithms described above.

**Table 1.** Formulation and description of algorithms of MBA, tINIT and mCADRE. In the table  $R_G$  represents the list of reaction from the global model,  $R_C$  the set of core reaction on mCADRE algorithm,  $C_H$  and  $C_M$  the core and moderate probability sets used in MBA algorithm,  $r$  a reaction and the  $for(i)$  and the  $rev(i)$  represent the  $i$ -th reaction direction (forward and reverse).

MBA	tINIT	mCADRE
<i>generateModel(<math>R_G, C_H, C_M</math>)</i>	$\min \sum_{i \in R} w_i * y_i$ s.t. $Sv = b$ $ v_i  \leq v_{max}$ $0 < v_i + (v_{max} * y_i) \leq v_{max}$ $b_j \geq \delta j \in Metabolomics$ $b_j = 0 j \notin Metabolomics$ $y_{for(i)} + y_{rev(i)} \leq 1$ $v_i \geq \delta, i \in RequiredReac$ $y_i \in 0, 1$ $w_i, score \text{ for } i \in R$	<i>generateModel(<math>R_G, threshold</math>)</i> $R_P \leftarrow R_G$ $R_C \leftarrow score(R_P) > threshold$ $coreActiveG \leftarrow flux(r)! = 0, r \in R_C$ $R_{NC} \leftarrow R_P \setminus R_C$ <i>for</i> ( $r \in order(R_{NC})$ ) <i>inactiveR</i> $\leftarrow CheckModel(R_P, r)$ $s1 =  inactiveR \cap R_C $ $s2 =  inactiveR \cap R_{NC} $ <i>if</i> ( $r \notin withExpressionValues AND$ $s1 \setminus s2 \leq RACIO AND$ <i>checkModelFunction</i> ( $R_p \setminus inactiveR$ )) $R_P \leftarrow R_P \setminus inactiveR$ <i>elseif</i> ( $ s1  == 0 AND$ <i>checkModelFunction</i> ( $R_p \setminus inactiveR$ )) $R_P \leftarrow R_P \setminus inactiveR$ <i>endif</i> <i>return</i> $R_P$ <i>endfunction</i>
$R_P \leftarrow R_G$		
$R_S \leftarrow R_P \setminus (C_H \cup C_M)$		
$P \leftarrow randomPermutation(R_S)$		
<i>for</i> ( $r \in P$ )		
<i>inactiveR</i> $\leftarrow CheckModel(R_P, r)$		
$e_H \leftarrow inactiveR \cap C_H$		
$e_M \leftarrow inactiveR \cap C_M$		
$e_X \leftarrow inactiveR \setminus (C_H \cup C_M)$		
<i>if</i> ( $ e_H  == 0 AND  e_M  < \delta *  e_X $ )		
$R_P \leftarrow R_P \setminus (e_M \cup e_X)$		
<i>endif</i>		
<i>endfor</i>		
<i>return</i> $R_P$		
<i>endfunction</i>		

### 2.3 Omics Data

Proteomics data used in this work were retrieved from the Human Protein Atlas (HPA) [26], which contains the profiles of human proteins in all major human healthy and cancer cells. We collected information for the liver tissue (hepatocytes) from HPA version 12 and Ensembl [7] version 73.37. After a conversion from Ensembl gene identifiers to gene symbols, duplicated genes with different evidence levels were removed (Table S1 from supplementary data)<sup>1</sup>.

<sup>1</sup> All supplementary files are provided in <http://darwin.di.uminho.pt/epia2015>

Transcriptomics data were collected from Gene Expression Barcode (GEB) [16] (HG U133plus2 (Human) cells v3). The conversion to gene expression levels was done considering the average level of probes for each gene. The mapping between probes and gene symbols was performed using the library “hgu133plus2.db” [4] from Bioconductor. The gene expression is classified as *High*, *Moderate* and *Low* if the gene expression evidence on that tissue is greater than 0.9, between 0.5 and 0.9, and between 0.1 and 0.5, respectively. The genes with expression evidence below 0.1 were considered not expressed in hepatocytes.

The reaction scores were obtained through the Gene-Protein-Rules present in the Recon2 model, based on the scores associated with each gene in the data. The reaction scores were calculated by taking the maximum (minimum) value of expression scores for genes connected by an “OR” (“AND”). If one of the gene scores is unknown, the other gene score is assumed in the conversion rule.

### 3 Results

To compare the metabolic models generated by the different algorithms and the effects of distinct omics data sources, we chose the reconstruction of hepatocytes metabolic models as our case study. Hepatocytes are the principal site of the metabolic conversions underlying the diverse physiological functions of the liver [10]. The hepatocytes metabolic models were generated using Recon2 as a template model and the GEB, HPA and the sets  $C_H$  and  $C_M$  from [12] as input data, for the three methods described in the previous section.

In the experiments, we seek to answer two main questions: Are omics data consistent across different data sources? What is the overlap of the resulting metabolic models obtained using different methods and different data sources? In 2010, a manually curated genome-scale metabolic network of human hepatocytes was presented, the HepatoNet1 [8], used as a reference in the validation process.

#### 3.1 Omics Data Consistency

The HPA has evidence information related with 16324 genes in hepatocytes. The reliability of the data is also scored as “supportive” or “uncertain”, depending on similarity in immunostaining patterns and consistency with protein/gene characterization data. On the other hand, the GEB transcriptome has information for 20149 genes, of which 5772 have evidence of being expressed in hepatocytes.

Together, these two data sources have information for 21921 genes, but only 14552 are present in both (Figure 1A). Moreover, the number of genes with evidence of being expressed in the tissue in both sources is only of 3549, around 24% of all shared genes (Figure 1B). These numbers decrease significantly if using only HPA information marked as “supportive”. In this scenario, only 3868 genes are present also in GEB and only 1294 of them have expression evidence.

Next, evidence levels frequencies (*High*, *Moderate*, *Low*) were calculated across the GEB and HPA, as shown in Figure 2. Only a small number of genes have similar evidence levels in both data sources. Furthermore, a significant

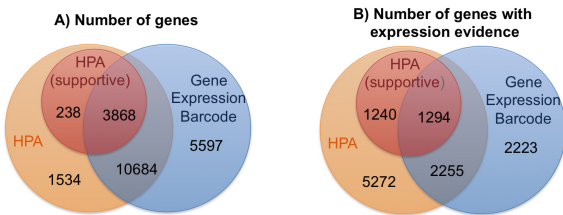


**Fig. 1.** A) Number of genes present in Gene Expression Barcode and Human Protein Atlas. In HPA, the number of genes with reliability “supportive” and “uncertain” are shown. B) Number of genes with evidence level “Low”, “Moderate” or “High” in HPA and gene expression evidence higher than 0 in Gene Expression Barcode.

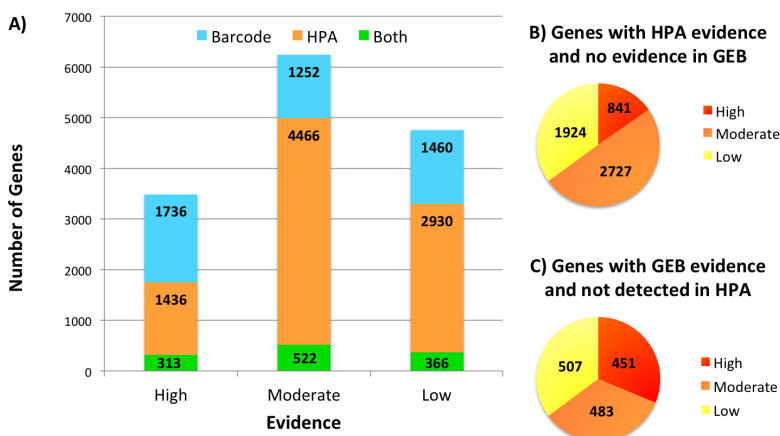


**Fig. 2.** A) Distribution of genes from Gene Expression Barcode project and Human Protein Atlas across the evidence levels - “High”, “Moderate” and “Low”. The ranges [0.9, 1], [0.5, 0.9[ and [0.1, 0.5[ were used to classify the data into “Low”, “Moderate” and “High” levels. B) Genes with no evidence to be present in hepatocytes from GEB, but with evidence in the HPA. C) Genes with no evidence to be present in hepatocytes from HPA, but with evidence in GEB.

number of genes have contradictory levels of evidence - genes with expression evidence in one data source and not expressed in the other. If we focus only in the genes present in the model Recon2 with information in GEB and HPA (supportive), there are 15% of genes with “High” or “Moderate” evidence in one of the sources and not expressed in the other. This number increases to 22% if we also consider “Low” evidence level (Supplementary Figure S1).

The methods to reconstruct tissue-specific metabolic models use reaction scores calculated based on omics data to determine their inclusion in the final models. So, we analyzed the impact of these omics discrepancies in the values of reaction scores and compared those with the manually curated set  $C_H$  from Jerby et al. [12]. In Figure 3A, the poor overlap of the reaction scores calculated based

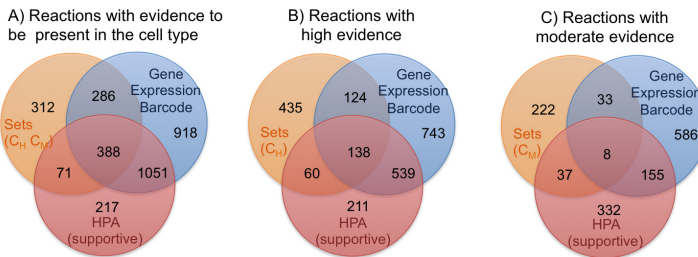


**Fig. 3.** A) Reactions with evidence that support their inclusion in the hepatocytes metabolic model. B) Number of reactions that have a high level of evidence of expression for each data source. C) Number of reactions that have a moderate evidence of expression for each data source

on different sources can be observed. Considering all data sources, 3243 reactions show some evidence that support their inclusion in the hepatocytes metabolic model, but only 388 are supported by all sources. The numbers are further dramatically reduced if we consider only moderate or high levels of evidence (Figure 3 B-C).

### 3.2 Metabolic Models

We applied each of the three algorithms to each omics data source, resulting in nine metabolic models for hepatocytes. In the application of mCADRE, we consider the list of key metabolites as published in the original article and a threshold of 0.5 to calculate the core set. A set of core metabolic tasks, that should occur in all cell types, was retrieved from [2] and used in the tINIT algorithm. The final MBA models were constructed based on 50 intermediate metabolic models. According to [12], a larger number would be desirable, but the time needed to generate each model prevented larger numbers of replicates. The detailed list of reactions that compose each metabolic model are available in supplementary material.

In Figure 4 A-C, we observe the consistency of the intermediate models generated by MBA, as well as the number of occurrences of reactions present in the final model. Moreover, Figure 4D shows the relations between the nine metabolic models generated through hierarchical clustering. The models obtained using the  $C_H$  and  $C_M$  sets as input data group together. Regarding the remaining, the mCADRE and MBA resulting models group according to their data (HPA and GEB), while the models created by tINIT cluster together. Overall, the data used as input seems to be the most relevant factor in the final result.

A more detailed comparison between the models reconstructed using the same algorithm or the same data source is available in Figure 5, A and B respectively. Considering the models generated by the same algorithm, it is observed that mCADRE has a smaller overlap (only 812 reactions) compared to the other methods. This could be explained by the possibility of removing core reactions during the mCADRE reconstruction process. Note that both reactions with

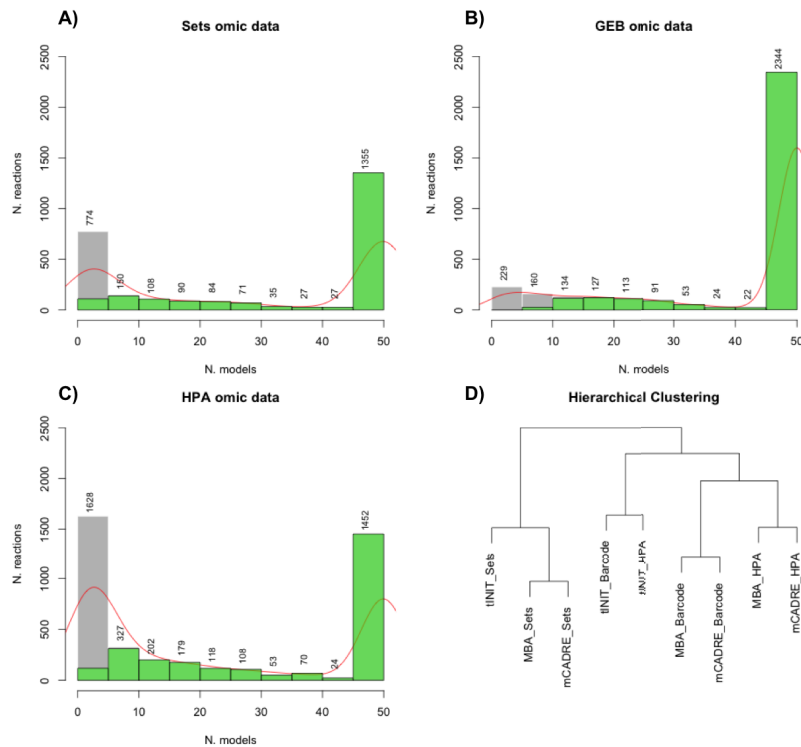


**Fig. 4.** A-C) Distribution of reactions across the 50 models for each data type. Grey bars show an histogram with the number of reactions present in a certain number of models. Green bars show the reactions that are present in the final model. D) Results from hierarchical clustering of the resulting nine models.

“High” and “Moderate” evidence levels, and from  $C_H$  and  $C_M$  sets, are all considered as belonging to the core. Furthermore, the mean of reactions that belong to all models of the same algorithm is around 45%. When the comparison is made by grouping models with the same input data, the variance between models is lower than grouping by algorithm. Here, the mean of reactions common to all models with the same data source is around 67% (Supplementary Table S3). Again, the variability of the final results seems to be dominated by the data source factor.

The quality of the metabolic models was further validated using the metabolic functions that are known to occur in hepatocytes [8]. The generic Recon2 human metabolic model, used as template in the reconstruction process, is able to satisfy 337 of the 408 metabolic functions available. Metabolic functions related with disease or involving metabolites not present in Recon2 were removed from the original list.

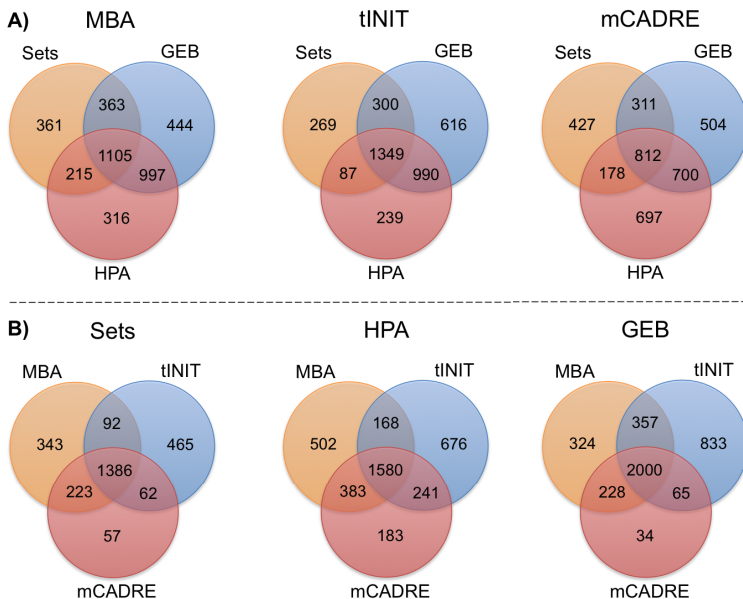


**Fig. 5.** Metabolic models reaction intersection considering: (A) the same algorithm; (B) the same omics data source.

**Table 2.** Number of reactions and the percentage of liver metabolic functions that each metabolic model performs when compared with the template model - Recon 2.

Method	Sets		HPA		GEB	
	N. Reac.	Tasks	N. Reac	Tasks	N. Reac.	Tasks
MBA	2044	18%	2633	24%	2909	6%
mCADRE	1728	2%	2387	3%	2327	4%
tINIT	2005	4%	2665	5%	3255	6%

The results of this functional validation, showing also the number of reactions in each metabolic model, are given on Table 2. These show that the number of satisfied metabolic tasks is very low compared with the manual curated metabolic model HepatoNet1. The metabolic model which performs the higher number of metabolic tasks was obtained using the MBA algorithm with the HPA evidence. Nevertheless, the success percentage is less than 25% when comparing with the performance by the template metabolic model - Recon2.

## 4 Conclusions

In this work, we present a survey of the most important methods for the reconstruction of tissue-specific metabolic models. Each method was proposed to use

different data sources as input. Here, we analyze the consistency of information across important omics data sources used in this context and verify the impact of such differences in the final metabolic models generated by the methods.

The results show that metabolic models obtained depend more on the data sources used as inputs, than on the algorithm used for the reconstruction. To validate the accuracy of the obtained metabolic models, a set of metabolic functions that should be performed in hepatocytes was tested for each metabolic model. We found that the number of satisfied liver metabolic functions was surprisingly low. This shows that methods for the reconstruction of tissue-specific metabolic models based on a single omics data source are not enough to generate high quality metabolic models. Methods to combine several omics data sources to rank the reactions for the reconstruction process could be a solution to improve the results of these methods. Indeed, this study emphasizes the need for the development of reliable methods for omics data integration, which seem to be required to support the reconstruction of complex models of human cells, but also reinforce the need to be able to incorporate known phenotypical data available from literature or human experts.

**Acknowledgments.** S.C. thanks the FCT for the Ph.D. Grant SFRH/BD/80925/2011. The authors thank the FCT Strategic Project of UID/BIO/04469/2013 unit, the project RECI/BBB-EBI/0179/2012 (FCOMP-01-0124-FEDER-027462) and the project “BioInd - Biotechnology and Bioengineering for improved Industrial and Agro-Food processes”, REF. NORTE-07-0124-FEDER-000028 Co-funded by the Programa Operacional Regional do Norte (ON.2 - O Novo Norte), QREN, FEDER.

## References

- Agren, R., Bordel, S., Mardinoglu, A., Pornputtapong, N., Nookaew, I., Nielsen, J.: Reconstruction of Genome-Scale Active Metabolic Networks for 69 Human Cell Types and 16 Cancer Types Using INIT. *PLoS Computational Biology* **8**(5), e1002518 (2012)
- Agren, R., Mardinoglu, A., Asplund, A., Kampf, C., Uhlen, M., Nielsen, J.: Identification of anticancer drugs for hepatocellular carcinoma through personalized genome-scale metabolic modeling. *Molecular Systems Biology* **10**, 721 (2014)
- Barrett, T., Troup, D.B., Wilhite, S.E., Ledoux, P., et al.: NCBI GEO: archive for functional genomics data sets - 10 years on. *Nucleic Acids Research* **39**(suppl 1), D1005–D1010 (2011)
- Carlson, M.: hgu133plus2.db: Affymetrix Human Genome U133 Plus 2.0 Array annotation data (chip hgu133plus2) (2014). r package version 3.0.0
- Duarte, N.C., Becker, S.A., Jamshidi, N., Thiele, I., Mo, M.L., Vo, T.D., Srivas, R., Palsson, B.O.: Global reconstruction of the human metabolic network based on genomic and bibliomic data. *Proceedings of the National Academy of Sciences of the United States of America* **104**(6), 1777–1782 (2007)
- Duarte, N.C., Herrgård, M.J., Palsson, B.O.: Reconstruction and validation of *Saccharomyces cerevisiae* iND750, a fully compartmentalized genome-scale metabolic model. *Genome Research* **14**(7), 1298–1309 (2004)

7. Flicek, P., Amode, M.R., Barrell, D., et al.: Ensembl 2014. *Nucleic Acids Research* **42**(D1), D749–D755 (2014)
8. Gille, C., Bölling, C., Hoppe, A., et al.: HepatoNet1: a comprehensive metabolic reconstruction of the human hepatocyte for the analysis of liver physiology. *Molecular Systems Biology* **6**(411), 411 (2010)
9. Hao, T., Ma, H.W., Zhao, X.M., Goryanin, I.: Compartmentalization of the Edinburgh Human Metabolic Network. *BMC Bioinformatics* **11**, 393 (2010)
10. Ishibashi, H., Nakamura, M., Komori, A., Migita, K., Shimoda, S.: Liver architecture, cell function, and disease. *Seminars in Immunopathology* **31**(3) (2009)
11. Jerby, L., Ruppin, E.: Predicting Drug Targets and Biomarkers of Cancer via Genome-Scale Metabolic Modeling. *Clinical Cancer Research : An Official Journal of the American Association for Cancer Research* **18**(20), 5572–5584 (2012)
12. Jerby, L., Shlomi, T., Ruppin, E.: Computational reconstruction of tissue-specific metabolic models: application to human liver metabolism. *Molecular Systems Biology* **6**(401), 401 (2010)
13. Kaddurah-Daouk, R., Kristal, B., Weinshilboum, R.: Metabolomics: a global biochemical approach to drug response and disease. *Annu. Rev. Pharmacol. Toxicol.* **48**, 653–683 (2008)
14. Lewis, N.E., Schramm, G., Bordbar, A., Schellenberger, J., Andersen, M.P., Cheng, J.K., Patel, N., Yee, A., Lewis, R.A., Eils, R., König, R., Palsson, B.O.: Large-scale in silico modeling of metabolic interactions between cell types in the human brain. *Nature Biotechnology* **28**(12), 1279–1285 (2010)
15. Mardinoglu, A., Agren, R., Kampf, C., Asplund, A., Uhlen, M., Nielsen, J.: Genome-scale metabolic modelling of hepatocytes reveals serine deficiency in patients with non-alcoholic fatty liver disease. *Nature Communications* **5**, Jan 2014
16. McCall, M.N., Jaffee, H.A., Zelisko, S.J., Sinha, N., et al.: The Gene Expression Barcode 3.0: improved data processing and mining tools. *Nucleic Acids Research* **42**(D1), D938–D943 (2014)
17. Oberhardt, M.A., Palsson, B.O., Papin, J.A.: Applications of genome-scale metabolic reconstructions. *Molecular Systems Biology* **5**(320), 320 (2009)
18. Orth, J.D., Thiele, I., Palsson, B.O.: What is flux balance analysis? *Nature Biotechnology* **28**(3), 245–248 (2010)
19. Parkinson, H., Sarkans, U., Shojatalab, M., Abeygunawardena, N., et al.: ArrayExpress-a public repository for microarray gene expression data at the EBI. *Nucleic Acids Research* **33**(Database issue), Jan 2005
20. Reed, J.L., Vo, T.D., Schilling, C.H., Palsson, B.O.: An expanded genome-scale model of Escherichia coli K-12 ( i JR904 GSM / GPR ) **4**(9), 1–12 (2003)
21. Sahoo, S., Franzson, L., Jonsson, J.J., Thiele, I.: A compendium of inborn errors of metabolism mapped onto the human metabolic network. *Mol. BioSyst.* **8**(10), 2545–2558 (2012)
22. Sahoo, S., Thiele, I.: Predicting the impact of diet and enzymopathies on human small intestinal epithelial cells. *Human Molecular Genetics* **22**(13), 2705–2722 (2013)
23. Shlomi, T., Benyamin, T., Gottlieb, E., Sharan, R., Ruppin, E.: Genome-scale metabolic modeling elucidates the role of proliferative adaptation in causing the Warburg effect. *PLoS Computational Biology* **7**(3), e1002018 (2011)
24. Shlomi, T., Cabili, M.N., Ruppin, E.: Predicting metabolic biomarkers of human inborn errors of metabolism. *Molecular Systems Biology* **5**(263), 263 (2009)
25. Thiele, I., Swainston, N., Fleming, R.M.T., et al.: A community-driven global reconstruction of human metabolism. *Nature Biotechnology* **31**(5), May 2013

26. Uhlen, M., Oksvold, P., Fagerberg, L., Lundberg, E., et al.: Towards a knowledge-based Human Protein Atlas. *Nat Biotech* **28**(12), 1248–1250 (2010)
27. Wang, Y., Eddy, J.A., Price, N.D.: Reconstruction of genome-scale metabolic models for 126 human tissues using mCADRE. *BMC Systems Biology* **6**(1), 153 (2012)
28. Wishart, D.S., Knox, C., Guo, A.C., Eisner, R., et al.: HMDB: a knowledgebase for the human metabolome. *Nucleic Acids Research* **37**(suppl 1), Jan 2009
29. Yizhak, K., Le Dévédec, S.E., Rogkoti, V.M.M., et al.: A computational study of the Warburg effect identifies metabolic targets inhibiting cancer migration. *Molecular Systems Biology* **10**(8) (2014)

# Fuzzy Clustering for Incomplete Short Time Series Data

Lúcia P. Cruz, Susana M. Vieira, and Susana Vinga<sup>(✉)</sup>

IDMEC, Instituto Superior Técnico, Universidade de Lisboa, Lisboa, Portugal  
[{lucia.cruz,susana.vieira,susanavinga}](mailto:{lucia.cruz,susana.vieira,susanavinga}@tecnico.ulisboa.pt)@tecnico.ulisboa.pt

**Abstract.** The analysis of clinical time series is currently a key topic in biostatistics and machine learning applications to medical research. The extraction of relevant features from longitudinal patients data brings several problems for which novel algorithms are warranted. It is usually impossible to measure many data points due to practical and also ethical restrictions, which leads to short time series (STS) data. The sampling might also be at unequally spaced time-points and many of the predicted measurements are often missing. These problems constitute the rationale of the present work, where we present two methods to deal with missing data in STS using fuzzy clustering analysis. The methods are tested and compared using data with equal and varying time sampling interval lengths, with and without missing data. The results illustrate the potential of these methods in clinical studies for patient classification and feature selection using biomarker time series data.

**Keywords:** Short time series · Missing data · Fuzzy c-means (FCM) clustering

## 1 Introduction

In medical care, the efficient acquisition of information is subject to many obstacles related with ethical and experimental restrictions, which usually leads to longitudinal data with unequal and long sampling periods. Furthermore, these time series are usually sparse and incomplete, which further hampers their analysis. Along with this, the high costs associated with medical analysis lead to the necessity of performing less frequent tests. For Intensive Care Unit (ICU) cases, for example, this issues have been studied. In [1] the issue of missing data, in medical datasets, was addressed. In oncological studies, survival analysis is usually applied to identify probability distributions. Regression methods, such as Cox proportional hazards models, are further used to identify the statistically significant features associated with survival [2,3]. In this type of clinical studies it is common to have biomarkers time series, which may be used to diagnose and predict the outcome of the disease.

The main motivation of this work is to developed and test clustering algorithms for biomarkers time series, a problem arising for example in the analysis of

bone metastatic patients. Due to the problems referred before, these biomarkers measurements are commonly short time series with missing data. Many methods are not able to deal, at the same time, with missing data and short time series, let alone, with unevenly sampled time series. The proposed clustering algorithm is able to take into account both missing data and short time series, evenly or unevenly sampled. The approaches are unsupervised, since the marker study objective is to relate the outcome of the unsupervised clustering with outcomes of the patient's health.

## 2 Methods for Short Incomplete Time Series Data

In this section we present the definitions and clustering algorithms to deal with a collection of  $n$  short time series with missing data. All the presented approaches are based on fuzzy c-means (FCM) algorithm [4].

A time series  $k$  of length  $s$  can be represented as  $\mathbf{x}_k = (x_{k1}, \dots, x_{kj}, \dots, x_{ks})$  with  $x_{kj} \equiv x_k(t_j)$ , with  $1 \leq j \leq s$  and  $1 \leq k \leq n$ .

Furthermore, with the creation of cluster prototypes,  $v_{ij}$ , for FCM algorithm,  $i$  represents cluster numbers, subject to  $1 \leq i \leq c$ , where  $c$  is the selected cluster number.

### 2.1 Incomplete Data

In this section several approaches to deal with missing data are presented. These might include some sort of imputation and deletion [1], further compared for pattern recognition problems in [5] and explored in a fuzzy clustering setting [4]. The two methods here presented are the *Partial Distance Strategy* (PDS) [4] and *Optimal Completion Strategy* (OCS) [4], both applied to fuzzy clustering. Both use the Euclidean distance, but any other metric can also be used.

The PDS method computes the distance between two vectors, scaling it to the proportion of non missing values to complete vectors size. For the entries with missing values, the distance is simply updated with zero, as expressed in Eq. 1:

$$D_{ik} = \frac{s}{I_k} \sum_{j=1}^s (x_{kj} - v_{ij})^2 I_{kj}, \quad (1)$$

where  $I_k = \sum_{j=1}^s I_{kj}$  and  $I_{kj} = \begin{cases} 0, & \text{if } x_{kj} \in X_M \\ 1, & \text{if } x_{kj} \in X_P \end{cases}$ , for  $1 \leq j \leq s$ ,  $1 \leq k \leq n$ .

The OCS approach is an imputation method where the entries with missing data,  $x_{kj}$ , are substituted with a given value. For fuzzy clustering these values are initialized at random, and their update results from the computation of Eq. 2, using the partition matrix  $U_{ik}$  and cluster prototypes  $v_{ij}$ . This equation derives from the calculation of the cluster prototypes [4].

$$x_{kj} = \frac{\sum_{i=1}^c (U_{ik})^m v_{ij}}{\sum_{i=1}^c (U_{ik})^m} \quad (2)$$

## 2.2 Short Time Series

This section presents the Short Time Series (STS) approach, where both even and uneven sampled time series can be dealt with.

In survey [6] the only method capable of handling short time series is presented in [7], which also deals with unevenly sampled time series. The STS distance proposed  $d_{STS}(x, v) = \sum_{j=0}^s \left( \frac{v_{(j+1)} - v_j}{t_{(j+1)} - t_j} - \frac{x_{(j+1)} - x_j}{t_{(j+1)} - t_j} \right)^2$  is computed between the cluster prototypes,  $v_j$ , and the time series data points,  $x_j$ , including the corresponding times,  $t_j$ . Based in the STS approach, two new methods to deal with STS were developed.

*1st order derivative calculation with normalization (Slopes):* It uses the approximate derivatives between each consecutive data point as input. First the  $z$ -score normalization of the series is calculated [7],  $z_k = \frac{x_k - \bar{x}}{s_x}$ , where  $\bar{x}$  is the mean value of  $x_k$  and  $s_x$  is the standard deviation of  $x_k$ . The derivatives of each consecutive points are then computed,  $dv_{kj} = \frac{z_{(j+1)} - z_j}{t_{(j+1)} - t_j}$ .

*Combination of 1st order derivatives of time points (Slopes Comb):* This method's objective is to generate a combination of time series data points derivatives yet with different, increasing lags. A vector is created with the derivatives of consecutive data points (or intervals of one point). It is then incremented with the derivatives of data points separated by two sample points, and so on and so forth, until no more points separation is possible (maximum lag possible is attained with  $x_s$  and  $x_1$ ).

As an example lets consider the time series  $S = (x_1, x_2, x_3, x_4)$  and equivalent time points  $T = (t_1, t_2, t_3, t_4)$ . The vector creation,  $V = (V_1, V_2, V_3)$ , would be  $V_1 = \left( \frac{x_2 - x_1}{t_2 - t_1}, \frac{x_3 - x_2}{t_3 - t_2}, \frac{x_4 - x_3}{t_4 - t_3} \right)$ ,  $V_2 = \left( \frac{x_3 - x_1}{t_3 - t_1}, \frac{x_4 - x_2}{t_4 - t_2} \right)$  and  $V_3 = \left( \frac{x_4 - x_1}{t_4 - t_1} \right)$ , where  $V_1$  is the derivative of data points with interval of one point,  $V_2$  is the derivative of data points with interval of two points and  $V_3$  is the derivative of data points with interval of three points. The vector  $V$  will be the input used in this method.

## 2.3 Short Incomplete Time Series Fuzzy Clustering Algorithms

The algorithm construction is described as follows, making use of FCM [4]. For the FCM algorithm the objective function for any of the methods is to minimize  $J(x, v, U) = \sum_{i=1}^c \sum_{k=1}^n U_{i,k}^m d^2(x_k, v_i)$ .

Having the methods to deal with missing data (PDS and OCS) and the method to deal with short time series (STS), we propose 5 combinations: *PDS-Slopes*, *OCS-Slopes*, *PDS-Slopes Comb*, *OCS-Slopes Comb* and *STS-OCS*. For the combinations with *Slopes* and *Slopes Comb*, the FCM algorithm is the same as in [4]. The alterations occur prior to the algorithm calculations, where to generate the new dataset to be used it is applied either *Slopes* or *Slopes Comb*.

The *STS - OCS* case uses mainly the algorithm described in [7], with the STS distance, yet the dataset to be used needs to be initialized with the missing values imputation. This imputation is done after the normalization part in the algorithm [7], and is based on Eq. 2, however the cluster prototypes calculation follows the procedure described in [7].

### 3 Results and Discussion

These methods were tested on 4 datasets generated according to [7]. Each original dataset contains 20 time series classified into four classes (five time series per class) but with different characteristics, depending on the number of time points  $t$  and if they are equally or unequally spaced. In Fig. 1 these datasets are represented, where each cluster is defined with the same line type.

Every method was tested with the complete information (0% missing values) and with an increasing percentage of missing entries. These were generated randomly, equally distributed through all the dataset. The restrictions imposed were that no line (time series samples) nor column (time points) could be entirely composed of missing data. The results presented were obtained for 500 runs with 500 different random seeds. The 500 seeds are kept the same for every method tested to guarantee comparison exactness. In Fig. 2 the results for the 4 datasets tested are presented in terms of accuracy of the final clustering obtained. We compared the *Mean number of misclassifications* with the *Percentage of missing data (%)*, given that these results are the mean values of the 500 runs results. The percentages of missing data tested were 0% (complete dataset), 10%, 20%, 30% and 40%. Since all datasets contain 20 time series samples, for e.g. a *mean number of misclassification* of 10 time series corresponds to 50% of misclassifications. By observing Fig. 2 it is clear that the more missing values the dataset has, the more misclassifications will be obtained. PDS and OCS roughly maintain their performance throughout increasing percentages of missings. *STS-OCS* is the method which deteriorated the fastest, most likely due to the bias caused by the imputation and the inadequate missing values update. When comparing *Slopes* with *Slopes* and *Slopes Comb* with *Slopes Comb*, it is noteworthy that the

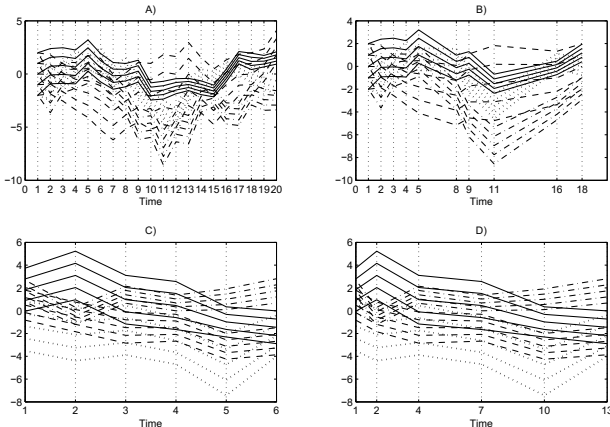


**Fig. 1.** Time Series classification. For each dataset the 20 time series are divided by the 4 clusters, specified by the different contours.

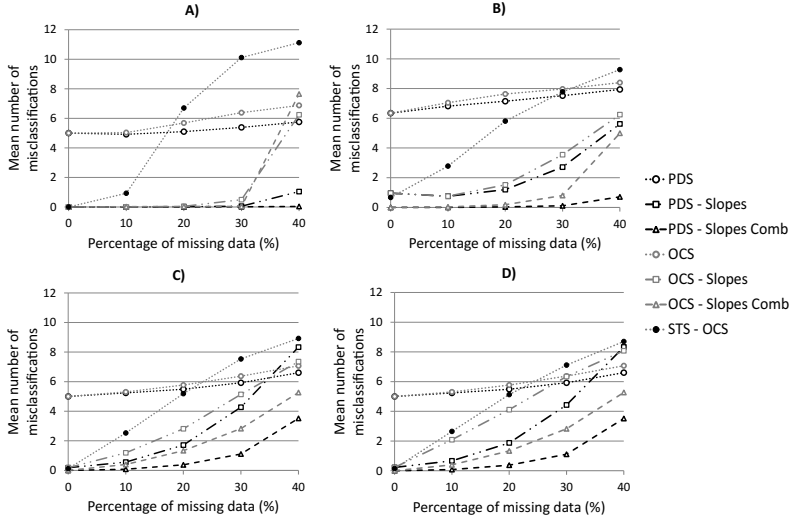


**Fig. 2.** Misclassifications of clustering methods. Average number of misclassifications for 500 runs of time series with 20 samples, four classes, using different sampling time points  $T$  and intervals.

**Table 1.** Results of FCM variations for 40% missing data.

Datasets	Methods	Iteration Count	Misclassifications	Objective Function Error	NID
$T = 20$ equal	PDS	70.52 (22.69)	5.75 (1.51)	5.26E-03 (6.06E-02)	0
	PDS - Slopes	25.57 (13.85)	1.04 (1.67)	9.13E-05 (1.38E-03)	22
	PDS - Slopes Comb	16.32 (4.98)	<b>0.03 (0.42)</b>	5.95E-06 (2.25E-06)	0
	OCS	88.21 (16.00)	6.88 (1.61)	5.97E-03 (3.49E-02)	0
	OCS - Slopes	52.10 (31.12)	6.24 (3.82)	4.92E-03 (3.50E-02)	0
	OCS - Slopes Comb	51.67 (24.58)	7.64 (3.93)	6.19E-03 (5.66E-02)	6
$T = 10$ unequal	STS - OCS	49.45 (30.62)	11.12 (1.56)	8.27E-04 (4.93E-03)	0
	PDS	63.62 (23.89)	7.94 (1.48)	1.47E-03 (1.51E-02)	0
	PDS - Slopes	34.89 (18.52)	5.62 (2.34)	1.39E-05 (7.45E-05)	358
	PDS - Slopes Comb	24.69 (12.77)	<b>0.71 (1.31)</b>	9.87E-06 (5.61E-05)	11
	OCS	75.65 (21.06)	8.40 (1.54)	1.24E-03 (1.41E-02)	0
	OCS - Slopes	89.17 (18.78)	6.24 (2.02)	9.65E-04 (5.49E-03)	0
$T = 6$ equal	OCS - Slopes Comb	71.19 (28.97)	4.99 (3.55)	1.36E-02 (9.08E-02)	1
	STS - OCS	80.67 (20.11)	9.27 (1.78)	2.14E-04 (9.26E-04)	0
	PDS	54.80 (22.06)	6.60 (1.44)	1.64E-03 (2.39E-02)	0
	PDS - Slopes	27.67 (5.51)	8.33 (3.21)	7.10E-06 (2.52E-06)	497
	PDS - Slopes Comb	28.13 (15.10)	<b>3.52 (2.30)</b>	2.22E-04 (3.14E-03)	285
	OCS	63.84 (24.28)	7.07 (1.50)	1.03E-03 (2.15E-02)	0
$T = 6$ unequal	OCS - Slopes	85.38 (19.71)	7.36 (1.81)	7.49E-04 (4.69E-03)	0
	OCS - Slopes Comb	87.09 (19.73)	5.26 (2.06)	4.23E-03 (2.90E-02)	1
	STS - OCS	70.46 (23.40)	8.92 (1.72)	1.83E-04 (1.53E-03)	0
	PDS	54.80 (22.06)	6.60 (1.44)	1.64E-03 (2.39E-02)	0
	PDS - Slopes	15.67 (5.13)	8.33 (2.31)	4.22E-06 (3.96E-06)	497
	PDS - Slopes Comb	28.13 (15.10)	<b>3.52 (2.30)</b>	2.22E-04 (3.14E-03)	285
	OCS	63.84 (24.28)	7.07 (1.50)	1.03E-03 (2.15E-02)	0
	OCS - Slopes	74.89 (23.76)	8.08 (1.78)	3.72E-04 (3.10E-03)	0
	OCS - Slopes Comb	87.09 (19.73)	5.27 (2.05)	4.23E-03 (2.90E-02)	1
	STS - OCS	45.31 (20.40)	8.70 (1.69)	1.36E-05 (7.26E-05)	0

PDS performs better than the OCS, probably due to the bias arising from the imputation. In all datasets, the *PDS-Slopes Comb* method performed the best.

In Table 1 the results for 40% of missing data are summarised. For each dataset every method was computed with 500 runs, and the mean and standard

deviation of *Iteration Count*, *Misclassifications*, *Objective Function Error* and *Number of Ignored Datasets* (NID) is shown. Highlighted in each table are the best results for each dataset. The NID has values different from zero only for *Slopes* and *Slopes Comb*. This occurs whenever a time series sample has only one non missing value. It is noteworthy that the OCS approach avoids this problem through imputation while the PDS cannot overcome it.

## 4 Conclusions

This work describes and compares several algorithms for the clustering of short and incomplete time series data. As expected, all methods perform very well with complete data and the performance decreases when the percentage of missing data increases. Nevertheless it is possible to maintain a reasonable accuracy in the final classification even for values as large as 40%. When the original time series have some sort of underlying patterns or evident trends, the methods using the combination of different slopes (*Slopes comb*) with all possible lags is preferable. Overall, PDS with combined slopes achieves an excellent performance in the datasets tested, with average values of zero misclassified series when 10% of the values are missing. Interestingly, even for higher percentage of missing values, the performance of this method with combined derivatives or slopes is very high, with average misclassification much lower than what would be expected.

These algorithms can be applied directly in several areas of clinical studies, namely in oncology. One possible future application is the stratification of patients based on biomarker evolution, which is expected to have a direct impact on feature selection methods and survival analysis of oncological patients.

**Acknowledgments.** This work was supported by FCT, through IDMEC, under LAETA, project UID/EMS/50022/2013, CancerSys (EXPL/EMS-SIS/1954/2013) and Program Investigador FCT (IF/00653/2012 and IF/00833/2014), co-funded by the European Social Fund (ESF) through the Operational Program Human Potential (POPH).

## References

1. Cismundi, F., et al.: Missing data in medical databases: Impute, delete or classify? *Artificial Intelligence in Medicine* **58**(1), 63–72 (2013)
2. Westhoff, P.G., et al.: An Easy Tool to Predict Survival in Patients Receiving Radiation Therapy for Painful Bone Metastases. *International Journal of Radiation Oncology\*Biology\*Physics* **90**(4), 739–747 (2014)
3. Harries, M., et al.: Incidence of bone metastases and survival after a diagnosis of bone metastases in breast cancer patients. *Cancer Epidemiology* **38**(4), 427–434 (2014)
4. Hathaway, R.J., Bezdek, J.C.: Fuzzy c-means clustering of incomplete data. *IEEE Transactions on Systems, Man, and Cybernetics. Part B, Cybernetics : a Publication of the IEEE Systems, Man, and Cybernetics Society* **31**(5), 735–744 (2001)

5. Dixon, J.K.: Pattern recognition with partly missing data. *IEEE Transactions on Systems, Man and Cybernetics* **9**(10), 617–621 (1979)
6. Warren Liao, T.: Clustering of time series data - A survey. *Pattern Recognition* **38**(11), 1857–1874 (2005)
7. Möller-Levet, C.S., Klawonn, F., Cho, K.-H., Wolkenhauer, O.: Fuzzy clustering of short time-series and unevenly distributed sampling points. In: Berthold, M., Lenz, H.-J., Bradley, E., Kruse, R., Borgelt, C. (eds.) IDA 2003. LNCS, vol. 2810, pp. 330–340. Springer, Heidelberg (2003)

# **General Artificial Intelligence**

# Allowing Cyclic Dependencies in Modular Logic Programming

João Moura<sup>(✉)</sup> and Carlos Viegas Damásio

CENTRIA / NOVA Laboratory for Computer Science and Informatics

(NOVA-LINCS), Universidade NOVA de Lisboa, Lisbon, Portugal

[joaomoura@yahoo.com](mailto:joaomoura@yahoo.com), [cd@fct.unl.pt](mailto:cd@fct.unl.pt)

**Abstract.** Even though modularity has been studied extensively in conventional logic programming, there are few approaches on how to incorporate modularity into Answer Set Programming, a prominent rule-based declarative programming paradigm. A major approach is Oikarinen and Janhunen's Gaifman-Shapiro-style architecture of program modules, which provides the composition of program modules. Their module theorem properly strengthens Lifschitz and Turner's splitting set theorem for normal logic programs. However, this approach is limited by module conditions that are imposed in order to ensure the compatibility of their module system with the stable model semantics, namely forcing output signatures of composing modules to be disjoint and disallowing positive cyclic dependencies between different modules. These conditions turn out to be too restrictive in practice and after recently discussing alternative ways of lifting the first restriction [17], we now show how one can allow positive cyclic dependencies between modules, thus widening the applicability of this framework and the scope of the module theorem.

## 1 Introduction

Over the last few years, answer set programming (ASP) [2, 6, 12, 15, 18] emerged as one of the most important methods for declarative knowledge representation and reasoning. Despite its declarative nature, developing ASP programs resembles conventional programming: one often writes a series of gradually improving programs for solving a particular problem, e.g., optimizing execution time and space. Until recently, ASP programs were considered as integral entities, which becomes problematic as programs become more complex, and their instances grow. Even though modularity is extensively studied in logic programming, there are only a few approaches on how to incorporate it into ASP [1, 5, 8, 19] or other module-based constraint modeling frameworks [11, 22]. The research on modular systems of logic program has followed two main-streams [3], one is programming in-the-large where compositional operators are defined in order to combine different modules [8, 14, 20]. These operators allow combining programs algebraically, which does not require an extension of the theory of logic programs. The other direction is programming-in-the-small [10, 16], aiming at enhancing logic programming with scoping and abstraction mechanisms available in other

programming paradigms. This approach requires the introduction of new logical connectives in an extended logical language. The two mainstreams are thus quite divergent.

The approach of [19] defines modules as structures specified by a program (knowledge rules) and by an interface defined by input and output atoms which for a single module are, naturally, disjoint. The authors also provide a module theorem capturing the compositionality of their module composition operator. However, two conditions are imposed: there cannot be positive cyclic dependencies between modules and there cannot be common output atoms in the modules being combined. Both introduce serious limitations, particularly in applications requiring integration of knowledge from different sources. The techniques used in [5] for handling positive cycles among modules are shown not to be adaptable for the setting of [19].

In this paper we discuss two alternative solutions to the cyclic dependencies problem, generalizing the module theorem by allowing positive loops between atoms in the interfaces of the modules being composed. A use case for this requirement can be found in the following example.

*Example 1.* Alice wants to buy a safe and inexpensive car; she preselected 3 cars, namely  $c_1$ ,  $c_2$  and  $c_3$ . Her friend Bob says that car  $c_2$  is expensive and Charlie says that car  $c_3$  is expensive. Meanwhile, she consulted two car magazines reviewing all three cars. The first considered  $c_1$  safe and the second considered  $c_1$  to be safe while saying that  $c_3$  may be safe if it has an optional airbag. Furthermore, if a friend declares that a car is expensive, then she will consider it safe. Alice is very picky regarding safety, and so she seeks some kind of agreement between the reviews.

The described situation can be captured with five modules, one for Alice, other three for her friends, and another for each magazine. Alice should conclude that  $c_1$  is safe since both magazines agree on this. Therefore, one would expect Alice to opt for car  $c_1$  since it is not expensive, and it is safe. ■

In summary, the fundamental results of [19] require a syntactic operation to combine modules – basically corresponding to the union of programs –, and a compositional semantic operation joining the models of the modules. The module theorem states that the models of the combined modules can be obtained by applying the semantics of the natural join operation to the original models of the modules – which is compositional.

This paper proceeds in Section 2 with an overview of the modular logic programming paradigm, identifying some of its shortcomings. In Section 3 we discuss alternative methods for lifting the restriction that disallows positive cyclic dependencies. We finish with conclusions and a general discussion.

## 2 Modularity in Answer Set Programming

Modular aspects of ASP have been clarified in recent years, with authors describing how and when two program parts (modules) can be composed [5, 11, 19] under

the stable model semantics. In this paper, we will make use of Oikarinen and Janhunen's logic program modules defined in analogy to [8] which we review after presenting the syntax of ASP.

*Answer Set Programming* Logic programs in the ASP paradigm are formed by finite sets of rules  $r$  having the following syntax:

$$L_1 \leftarrow L_2, \dots, L_m, \text{not } L_{m+1}, \dots, \text{not } L_n. \quad (n \geq m \geq 0) \quad (1)$$

where each  $L_i$  is a logical atom without the occurrence of function symbols – arguments are either variables or constants of the logical alphabet.

Considering a rule of the form (1), let  $\text{Head}_P(r) = L_1$  be the literal in the head,  $\text{Body}_P^+(r) = \{L_2, \dots, L_m\}$  be the set with all positive literals in the body,  $\text{Body}_P^-(r) = \{L_{m+1}, \dots, L_n\}$  be the set containing all negative literals in the body, and  $\text{Body}_P(r) = \{L_2, \dots, L_n\}$  be the set containing all literals in the body. If a program is positive we will omit the superscript in  $\text{Body}_P^+(r)$ . Also, if the context is clear we will omit the subscript mentioning the program and write simply  $\text{Head}(r)$  and  $\text{Body}(r)$  as well as the argument mentioning the rule. The semantics of stable models is defined via the reduct operation [9]. Given an interpretation  $M$  (a set of ground atoms), the reduct  $P^M$  of a program  $P$  with respect to  $M$  is program  $P^M = \{\text{Head}(r) \leftarrow \text{Body}^+(r) \mid r \in P, \text{Body}^-(r) \cap M = \emptyset\}$ . An interpretation  $M$  is a stable model (SM) of  $P$  iff  $M = LM(P^M)$ , where  $LM(P^M)$  is the least model of program  $P^M$ .

The syntax of logic programs has been extended with other constructs, namely weighted and choice rules [18]. In particular, choice rules have the following form:

$$\{A_1, \dots, A_n\} \leftarrow B_1, \dots, B_k, \text{not } C_1, \dots, \text{not } C_m. \quad (n \geq 1) \quad (2)$$

As observed by [19], the heads of choice rules possessing multiple atoms can be freely split without affecting their semantics. When splitting such rules into  $n$  different rules

$$\{a_i\} \leftarrow B_1, \dots, B_k, \text{not } C_1, \dots, \text{not } C_m \text{ where } 1 \leq i \leq n,$$

the only concern is the creation of  $n$  copies of the rule body

$$B_1, \dots, B_k, \text{not } C_1, \dots, \text{not } C_m.$$

However, new atoms can be introduced to circumvent this. There is a translation of these choice rules to normal logic programs [7], which we assume is performed throughout this paper but that is omitted for readability. We deal only with ground programs and use variables as syntactic place-holders.

## 2.1 Modular Logic Programming (MLP)

Modules in the sense of [19] are essentially sets of rules with Input/Output interfaces:

**Definition 1 (Program Module).** A logic program module  $\mathcal{P}$  is a tuple  $\langle R, I, O, H \rangle$  where:

1.  $R$  is a finite set of rules;
2.  $I$ ,  $O$ , and  $H$  are pairwise disjoint sets of input, output, and hidden atoms;
3.  $At(R) \subseteq At(\mathcal{P})$  defined by  $At(\mathcal{P}) = I \cup O \cup H$ ; and
4.  $Head(R) \cap I = \emptyset$ .

The set of atoms in  $At_v(\mathcal{P}) = I \cup O$  are considered to be *visible* and hence accessible to other modules composed with  $\mathcal{P}$  either to produce input for  $\mathcal{P}$  or to make use of the output of  $\mathcal{P}$ . We use  $At_i(\mathcal{P}) = I$  and  $At_o(\mathcal{P}) = O$  to represent the input and output signatures of  $\mathcal{P}$ , respectively. The hidden atoms in  $At_h(\mathcal{P}) = At(\mathcal{P}) \setminus At_v(\mathcal{P}) = H$  are used to formalize some auxiliary concepts of  $\mathcal{P}$  which may not be sensible for other modules but may save space substantially. The condition  $head(R) \notin I$  ensures that a module may not interfere with its own input by defining input atoms of  $I$  in terms of its rules. Thus, input atoms are only allowed to appear as conditions in rule bodies.

*Example 2.* The use case in Example 1 is encoded into the five modules shown here:

$$\begin{aligned} \mathcal{P}_A = & < \{ buy(X) \leftarrow car(X), safe(X), \text{not } exp(X). \\ & \quad car(c_1). \quad car(c_2). \quad car(c_3). \}, \\ & \{ safe(c_1), safe(c_2), safe(c_3), exp(c_1), exp(c_2), exp(c_3) \}, \\ & \{ buy(c_1), buy(c_2), buy(c_3) \}, \\ & \{ car(c_1), car(c_2), car(c_3) \} > \\ \mathcal{P}_B = & < \{ exp(c_2). \}, \{ \}, \{ exp(c_2), exp(c_3) \}, \{ \} > \\ \mathcal{P}_C = & < \{ exp(c_3). \}, \{ \}, \{ exp(c_1), exp(c_2), exp(c_3) \}, \{ \} > \\ \mathcal{P}_{mg_1} = & < \{ \leftarrow \text{not } safe(c_1). \quad airbag(C) \leftarrow safe(C). \}, \\ & \{ safe(C) \}, \\ & \{ airbag(C) \}, \\ & \{ \} > \\ \mathcal{P}_{mg_2} = & < \{ safe(X) \leftarrow car(X), airbag(X). \\ & \quad car(c_1). \quad car(c_2). \quad car(c_3). \leftarrow \text{not } airbag(c_1). \{ \leftarrow \text{not } airbag(c_3) \}. \}, \\ & \{ airbag(C) \}, \\ & \{ safe(c_1), safe(c_2), safe(c_3) \}, \\ & \{ airbag(c_1), airbag(c_2), airbag(c_3), car(c_1), car(c_2), car(c_3) \} > \blacksquare \end{aligned}$$

In Example 2, module  $\mathcal{P}_A$  encodes the rule used by Alice to decide if a car should be bought. The safe and expensive atoms are its inputs, and the buy atoms its outputs; it uses hidden atoms  $car/1$  to represent the domain of variables. Modules  $\mathcal{P}_B$ ,  $\mathcal{P}_C$  and  $\mathcal{P}_{mg_1}$  captures the factual information in Example 1 and depends on input literal  $safe$  to determine if its output states that a car has an *airbag* or not. They have no input and no hidden atoms, but *Bob* has only analyzed the price of cars  $c_2$  and  $c_3$ . The ASP program module for the second magazine is more interesting<sup>1</sup>, and expresses the rule used to determine if a car

<sup>1</sup> *car* belongs to both hidden signatures of  $\mathcal{P}_A$  and  $\mathcal{P}_{mg_2}$  which is not allowed when composing these modules, but for clarity we omit a renaming of the *car*/1 predicate.

is safe, namely that a car is safe if it has an airbag; it is known that car  $c_1$  has an airbag,  $c_2$  does not, and the choice rule states that car  $c_3$  may or may not have an airbag.

Next, the SM semantics is generalized to cover modules by introducing a generalization of the Gelfond-Lifschitz's fixpoint definition. In addition to weakly negated literals (i.e., *not* ), also literals involving input atoms are used in the stability condition. In [19], the SMs of a module are defined as follows:

**Definition 2 (Stable Models of Modules).** An interpretation  $M \subseteq At(\mathcal{P})$  is a SM of an ASP program module  $\mathcal{P} = \langle R, I, O, H \rangle$ , iff  $M = LM(R^M \cup \{a. | a \in M \cap I\})$ . The SMs of  $\mathcal{P}$  are denoted by  $AS(\mathcal{P})$ .

Intuitively, the SMs of a module are obtained from the SMs of the rules part, for each possible combination of the input atoms.

*Example 3.* Program modules  $\mathcal{P}_B$ ,  $\mathcal{P}_C$ , and  $\mathcal{P}_{mg_1}$  have each a single answer set:

$AS(\mathcal{P}_B) = \{\{exp(c_2)\}\}$ ,  $AS(\mathcal{P}_C) = \{\{exp(c_3)\}\}$ , and  $AS(\mathcal{P}_{mg_1}) = \{\{safe(c_1), airbag(c_1)\}\}$ .

Module  $\mathcal{P}_{mg_2}$  has two SMs, namely:

$\{safe(c_1), car(c_1), car(c_2), car(c_3), airbag(c_1)\}$ , and  
 $\{safe(c_1), safe(c_3), car(c_1), car(c_2), car(c_3), airbag(c_1), airbag(c_3)\}$ .

Alice's ASP program module has  $2^6 = 64$  models corresponding each to an input combination of safe and expensive atoms. Some of these models are:

$$\begin{aligned} &\{buy(c_1), car(c_1), car(c_2), car(c_3), safe(c_1)\} \\ &\{buy(c_1), buy(c_3), car(c_1), car(c_2), car(c_3), safe(c_1), safe(c_3)\} \\ &\{buy(c_1), car(c_1), car(c_2), car(c_3), exp(c_3), safe(c_1), safe(c_3)\} \blacksquare \end{aligned}$$

## 2.2 Composing Programs from Models

The composition of models is obtained from the union of program rules and by constructing the composed output set as the union of modules' output sets, thus removing from the input all the specified output atoms. [19] define their first composition operator as follows: Given two modules  $\mathcal{P}_1 = \langle R_1, I_1, O_1, H_1 \rangle$  and  $\mathcal{P}_2 = \langle R_2, I_2, O_2, H_2 \rangle$ , their composition  $\mathcal{P}_1 \oplus \mathcal{P}_2$  is defined when their output signatures are disjoint, that is,  $O_1 \cap O_2 = \emptyset$ , and they respect each others hidden atoms, i.e.,  $H_1 \cap At(\mathcal{P}_2) = \emptyset$  and  $H_2 \cap At(\mathcal{P}_1) = \emptyset$ . Then their composition is

$$\mathcal{P}_1 \oplus \mathcal{P}_2 = \langle R_1 \cup R_2, (I_1 \setminus O_2) \cup (I_2 \setminus O_1), O_1 \cup O_2, H_1 \cup H_2 \rangle$$

However, the conditions given for  $\oplus$  are not enough to guarantee compositionality in the case of answer sets and as such they define a restricted form:

**Definition 3 (Module Union Operator  $\sqcup$ ).** Given modules  $\mathcal{P}_1, \mathcal{P}_2$ , their union is  $\mathcal{P}_1 \sqcup \mathcal{P}_2 = \mathcal{P}_1 \oplus \mathcal{P}_2$  whenever (i)  $\mathcal{P}_1 \oplus \mathcal{P}_2$  is defined and (ii)  $\mathcal{P}_1$  and  $\mathcal{P}_2$  are mutually independent meaning that there are no positive cyclic dependencies among rules in different modules, defined as loops through input and output signatures.

Natural join ( $\bowtie$ ) on visible atoms is used in [19] to combine the stable models of modules as follows:

**Definition 4 (Join).** Given modules  $\mathcal{P}_1$  and  $\mathcal{P}_2$  and sets of interpretations  $A_1 \subseteq 2^{At(\mathcal{P}_1)}$  and  $A_2 \subseteq 2^{At(\mathcal{P}_2)}$ , the natural join of  $A_1$  and  $A_2$  is:

$$A_1 \bowtie A_2 = \{ M_1 \cup M_2 \mid M_1 \in A_1, M_2 \in A_2 \text{ and } M_1 \cap At_v(\mathcal{P}_2) = M_2 \cap At_v(\mathcal{P}_1) \}$$

This leads to their main result, stating that:

**Theorem 1 (Module Theorem).** If  $\mathcal{P}_1, \mathcal{P}_2$  are modules such that  $\mathcal{P}_1 \sqcup \mathcal{P}_2$  is defined, then:

$$AS(\mathcal{P}_1 \sqcup \mathcal{P}_2) = AS(\mathcal{P}_1) \bowtie AS(\mathcal{P}_2)$$

Still according to [19], their module theorem also straightforwardly generalizes for a collection of modules because the module union operator  $\sqcup$  is commutative, associative, and has the identity element  $< \emptyset, \emptyset, \emptyset, \emptyset >$ .

*Example 4.* Consider the composition  $\mathcal{Q} = (\mathcal{P}_A \sqcup \mathcal{P}_{mg_1}) \sqcup \mathcal{P}_B$ . First, we have

$$\mathcal{P}_A \sqcup \mathcal{P}_{mg_1} = \left\langle \begin{array}{l} \{buy(X) \leftarrow car(X), safe(X), not\ exp(X)\}, \\ \{car(c_1). car(c_2). car(c_3). safe(c_1).\}, \\ \{\exp(c_1), \exp(c_2), \exp(c_3)\}, \\ \{buy(c_1), buy(c_2), buy(c_3), safe(c_1), safe(c_2), safe(c_3)\}, \\ \{car(c_1), car(c_2), car(c_3)\} \end{array} \right\rangle$$

It is immediate to see that the module theorem holds in this case. The visible atoms of  $\mathcal{P}_A$  are  $safe/1$ ,  $exp/1$  and  $buy/1$ , and the visible atoms for  $\mathcal{P}_{mg_1}$  are  $\{safe(c_1), safe(c_2)\}$ . The only model for  $\mathcal{P}_{mg_1} = \{safe(c_1)\}$  when naturally joined with the models of  $\mathcal{P}_A$ , results in eight possible models where  $safe(c_1)$ ,  $not\ safe(c_2)$ , and  $not\ safe(c_3)$  hold, and  $exp/1$  vary. The final ASP program module  $\mathcal{Q}$  is

$$\left\langle \begin{array}{l} \{buy(X) \leftarrow car(X), safe(X), not\ exp(X)\}, \\ \{car(c_1). car(c_2). car(c_3). \exp(c_2). safe(c_1).\}, \\ \{\exp(c_1)\}, \\ \{buy(c_1), buy(c_2), buy(c_3), \exp(c_2), safe(c_1), safe(c_2), safe(c_3)\}, \\ \{car(c_1), car(c_2), car(c_3)\} \end{array} \right\rangle$$

The SMs of  $\mathcal{Q}$  are thus:

$$\{safe(c_1), \exp(c_1), \exp(c_2), car(c_1), car(c_2), car(c_3)\} \text{ and} \\ \{buy(c_1), safe(c_1), \exp(c_2), car(c_1), car(c_2), car(c_3)\}$$

## 2.3 Shortcomings

The conditions imposed in these definitions bring about some shortcomings such as the fact that the output signatures of two modules must be disjoint which disallows many practical applications e.g., we are not able to combine the results of program module  $\mathcal{Q}$  with any of  $\mathcal{P}_C$  or  $\mathcal{P}_{mg_2}$ , and thus it is impossible to obtain

the combination of the five modules. Also because of this, the module union operator  $\sqcup$  is not reflexive. By trivially waiving this condition, we immediately get problems with conflicting modules. The compatibility criterion for the operator  $\bowtie$  also rules out the compositionality of mutually dependent modules, but allows positive loops inside modules or negative loops in general. We illustrate this in Example 5, which has been solved recently in [17] and the issue with positive loops between modules in Example 6.

*Example 5 (Common Outputs).* Given  $\mathcal{P}_B$  and  $\mathcal{P}_C$ , which respectively have:

$AS(\mathcal{P}_B) = \{\{exp(c_2)\}\}$  and  $AS(\mathcal{P}_C) = \{\{exp(c_3)\}\}$ ,  
the single SM of their union  $AS(\mathcal{P}_B \sqcup \mathcal{P}_C)$  is:  $\{exp(c_2), exp(c_3)\}$ . However, the join of their SMs is  $AS(\mathcal{P}_B) \bowtie AS(\mathcal{P}_C) = \emptyset$ , invalidating the module theorem. ■

*Example 6 (Cyclic Dependencies).* Take the following two program modules (a simplification of the magazine modules in Example 2):

$$\begin{aligned} \mathcal{P}_1 &= \langle \{airbag \leftarrow safe.\}, \{safe\}, \{airbag\}, \emptyset \rangle \\ \mathcal{P}_2 &= \langle \{safe \leftarrow airbag.\}, \{airbag\}, \{safe\}, \emptyset \rangle \end{aligned}$$

Their SMs are:  $AS(\mathcal{P}_1) = AS(\mathcal{P}_2) = \{\{\}, \{airbag, safe\}\}$  while the single SM of the union  $AS(\mathcal{P}_1 \sqcup \mathcal{P}_2)$  is the empty model  $\{\}$ . Therefore  $AS(\mathcal{P}_1 \sqcup \mathcal{P}_2) \neq AS(\mathcal{P}_1) \bowtie AS(\mathcal{P}_2) = \{\{\}, \{airbag, safe\}\}$ , also invalidating the module theorem. ■

### 3 Positive Cyclic Dependencies Between Modules

To attain a generalized form of compositionality we need to be able to deal with both restrictions identified previously and in particular cyclic dependencies between modules. In the literature, [5] presents a solution based on a model minimality property. It forces one to check for minimality on every comparable models of all program modules being composed. It is not applicable to our setting though, which can be seen in Example 7 where logical constant  $\perp$  represents value *false*. Example 7 shows that [5] is not compositional in the sense of Oikarinen and Janhunen.

*Example 7.* Given modules  $\mathcal{P}_1 = \langle \{a \leftarrow b. \perp \leftarrow not b.\}, \{b\}, \{a\}, \{\} \rangle$  with one SM  $\{a, b\}$ , and  $\mathcal{P}_2 = \langle \{b \leftarrow a.\}, \{a\}, \{b\}, \{\} \rangle$  with SMs  $\{\}$  and  $\{a, b\}$ , their composition has no inputs and no intended SMs while their minimal join contains  $\{a, b\}$ . ■

Another possible solution requires the introduction of extra information in the models to allow detecting mutual positive dependencies. This route has been identified before [21] and is left for future work.

### 3.1 Model Minimization

We present a model join operation that requires one to look at every model of both modules being composed in order to check for minimality on models comparable on account of their inputs. However, this operation is able to distinguish between atoms that are self supported through positive loops and atoms with proper support, allowing one to lift the condition in Definition 3 disallowing positive dependencies between modules.

**Definition 5 (Minimal Join).** *Given modules  $\mathcal{P}_1$  and  $\mathcal{P}_2$ , let their composition be  $\mathcal{P}_C = \mathcal{P}_1 \oplus \mathcal{P}_2$ . Define  $AS(\mathcal{P}_1) \bowtie^{min} AS(\mathcal{P}_2) = \{M \mid M \in AS(\mathcal{P}_1) \bowtie AS(\mathcal{P}_2)$  such that  $\nexists_{M' \in AS(\mathcal{P}_1) \bowtie AS(\mathcal{P}_2)} : M' \subset M \text{ and } M \cap At_i(\mathcal{P}_C) = M' \cap At_i(\mathcal{P}_C)\}$*

*Example 8 (Minimal Join).* A car is safe if it has an airbag and it has an airbag if it is safe and the airbag is an available option. This is captured by two modules, namely:  $\mathcal{P}_1 = \langle \{\text{airbag} \leftarrow \text{safe}, \text{available\_option}.\}, \{\text{safe}, \text{available\_option}\}, \{\text{airbag}\}, \emptyset \rangle$  and  $\mathcal{P}_2 = \langle \{\text{safe} \leftarrow \text{airbag}.\}, \{\text{airbag}\}, \{\text{safe}\}, \emptyset \rangle$  which respectively have  $AS(\mathcal{P}_1) = \{\{\}, \{\text{safe}\}, \{\text{available\_option}\}, \{\text{airbag}, \text{safe}, \text{available\_option}\}\}$  and  $AS(\mathcal{P}_2) = \{\{\}, \{\text{airbag}, \text{safe}\}\}$ . The composition has as its input signature  $\{\text{available\_option}\}$  and therefore its answer set  $\{\text{airbag}, \text{safe}, \text{available\_option}\}$  is not minimal regarding the input signature of the composition because  $\{\text{available\_option}\}$  is also a SM (and the only intended model among these two). Thus  $AS(\mathcal{P}_1 \oplus \mathcal{P}_2) = AS(\mathcal{P}_1) \bowtie^{min} AS(\mathcal{P}_2) = \{\{\}, \{\text{available\_option}\}\}$ . ■

This join operator allows us to lift the prohibition of composing mutually dependent modules under certain situations. Integrity constraints containing only input atoms in their body are still a problem with this approach as these would exclude models that would otherwise be minimal in the presence of unsupported loops.

**Theorem 2 (Minimal Module Theorem).** *If  $\mathcal{P}_1, \mathcal{P}_2$  are modules such that  $\mathcal{P}_1 \oplus \mathcal{P}_2$  is defined (allowing cyclic dependencies between modules), and that only normal rules are used in modules, then:*

$$AS(\mathcal{P}_1 \oplus \mathcal{P}_2) = AS(\mathcal{P}_1) \bowtie^{min} AS(\mathcal{P}_2)$$

### 3.2 Annotated Models for Composing Mutualy Dependent Modules

Because the former operator is not general and it forces us to compare one model with every other model for minimality, thus it is not local, we present next an alternative that requires adding annotations to models. We start by looking at positive cyclic dependencies (loops) that are formed by composition. It is known from the literature (e.g. [21]) that in order to do without looking at the rules of the program modules being composed, which in the setting of MLP we assume not having access to, we need to have extra information incorporated into the models.

**Definition 6 (Dependency Transformation).** Let  $\mathcal{P}$  be an MLP. Its dependency transformation is defined as the set of rules  $(R_{\mathcal{P}})^A$  obtained from  $R_{\mathcal{P}}$  by replacing each clause  $L_1 \leftarrow L_2, \dots, L_m, \text{not } L_{m+1}, \dots, \text{not } L_n. (n \neq m)$  in  $R_{\mathcal{P}}$  with the following clause, where  $n \neq m$  and  $D = D_2 \cup \dots \cup D_m$  is a set of dependency sets:

$$(1) \quad L_1 : D \leftarrow L_2 : D_2, \dots, L_m : D_m, \text{not } L_{m+1} : D_{m+1}, \dots, \text{not } L_n : D_n.$$

**Definition 7 (Annotated Model).** Given a module  $\mathcal{P} = \langle R^A, I, O, H \rangle$ , its set of annotated models is constructed as before: An interpretation  $M \subseteq At^A(\mathcal{P})$  is an annotated answer set of an ASP program module  $\mathcal{P} = \langle R, I, O, H \rangle$ , if and only if:

$$M = LM \left( (R^A)^M \cup \{a : \{\{a\}\} \mid a : D \in M \cap I\} \right),$$

where  $(R^A)_I^M$  is the version of the Gelfond-Lifschitz reduct allowing weighted and choice rules, of the dependency transformation of  $R$ , and  $LM$  is the operator returning the least model of the positive program argument. The set of annotated stable models of  $\mathcal{P}$  is denoted by  $AS^A(\mathcal{P})$ .

**Semantic of Annotated Programs.** An annotated interpretation maps every atom into a set of subsets of input atoms, tracking the dependencies of the atom in combinations of input atoms. The semantics of annotated programs is obtained by iterating an immediate consequences monotonic operator applied to a definite program, defined as follows:

$$T_P(I)(L_1) = \bigcup \{ T_P(I)(L_2) \cup \dots \cup T_P(I)(L_m) \mid L_1 \leftarrow L_2, \dots, L_m \in R^A \}$$

starting from the interpretation mapping every atom into the empty set. In order to consider input atoms in modules we set  $I(a) = \{\{a\}\}$  for every  $a \in M \cap I$ , and  $\{\}$  otherwise.

**Collapsed Annotated Models.** Previous Definition 7 generates equivalent models for each alternative rule where atoms from the model belong to the head of the rule. We need to merge them into a collapsed annotated model where the alternatives are listed as sets of annotations, in order to retain a one to one correspondence between these and the SMs of the original program. As we are only interested in this collapsed form, we will henceforth take collapsed annotated models as annotated models.

**Definition 8 (Collapsed Annotated Model).** Let  $M'$  and  $M''$  be two annotated models such that for every atom  $a \in M'$ , it is also the case that  $a \in M''$  and vice-versa. A collapsed annotated model  $M$  of  $M'$  and  $M''$  is constructed as follows:

$$M = \{a : \{D', D''\} \mid a : D' \in M' \text{ and } a : D'' \in M''\}$$

Given a module  $\mathcal{P}$ , a program  $P(M)$  can conversely be constructed from one of the module's annotated models  $M$  simply by adding rules of the form  $a \leftarrow D_1, \dots, D_m$ , for each annotated atom  $a_{\{D_1, \dots, D_m\}} \in M$ . Such constructed program  $P(M)$  will be equivalent (but not strongly equivalent [13]) to taking the original program and adding facts that belong to the annotated model  $M$ , intersected with the input signature of  $\mathcal{P}$ , correspondingly.

*Example 9 (Annotated Model).* Let  $\mathcal{P} = \langle \{a \leftarrow b, c. \ b \leftarrow d, \text{not } e, \text{not } f.\}, \{d, f\}, \{a, b\}, \emptyset \rangle$  be a module.  $\mathcal{P}$  has one annotated model as per Definition 7:  $\{b_{\{d\}}, d\}$ . ■

In the previous example, the first rule  $a \leftarrow b, c.$  can never be activated because  $c$  is not an input atom ( $c \notin I$ ) and it is not satisfied by the rules of the module ( $R_{\mathcal{P}} \not\models c$ ). Thus, the only potential positive loop is identified by  $\{b_{\{d\}}, d\}$ . If we compose  $\mathcal{P}$  with a module containing e.g., rule  $d \leftarrow b.$  and thus with an annotated model  $\{d_{\{b\}}, b\}$ , then it is easy to identify this as being a loop and if any atoms in the loop are satisfied by the module composition then there will be a stable model reflecting that. Also notice that since  $e$  is not a visible atom, it does not interfere with other modules, as long as it is respected, and thus it does not need to be in the annotation.

**Cyclic Compatibility.** We define next the compatibility of mutually dependent models. We assume that the outputs are disjoint as per the original definitions. The compatibility is defined as a two step criterion. The first is similar to the original compatibility criterion, only adapted to dealing with annotated models by disregarding the annotations. This first step makes annotations of negative dependencies unnecessary. The second step takes models that are compatible according to the first step and, after reconstructing two possible programs from the compatible annotated models, implies computing the minimal model of the union of these reconstructed programs and see if the union of the compatible models is a model of the union of the reconstructed programs.

**Definition 9 (Basic Model Compatibility).** Let  $\mathcal{P}_1$  and  $\mathcal{P}_2$  be two modules. Let  $AS^A(\mathcal{P}_1)$ , respectively  $AS^A(\mathcal{P}_2)$  be their annotated models. Let now  $M_1 \in AS^A(\mathcal{P}_1)$  and  $M_2 \in AS^A(\mathcal{P}_2)$  be two models of the modules, they will be compatible if:

$$M_1 \cap At_v(\mathcal{P}_2) = M_2 \cap At_v(\mathcal{P}_1)$$

Now, for the second step of the cyclic compatibility criterion one takes models that passed the basic compatibility criterion and reconstruct their respective possible programs as defined previously. Then one computes the minimal model of the union of these reconstructed programs and see if the union of the originating models is a model of the union of their reconstructed programs.

**Definition 10 (Annotation Compatibility).** Let  $\mathcal{P}_1$  and  $\mathcal{P}_2$  be two modules. Let  $AS^A(\mathcal{P}_1)$ , respectively  $AS^A(\mathcal{P}_2)$  be their annotated models. Let now  $M_1 \in AS^A(\mathcal{P}_1)$  and  $M_2 \in AS^A(\mathcal{P}_2)$  be two compatible models according to Definition 9. They will be compatible annotated models if  $AS^A(\mathcal{P}_1 \cup \mathcal{P}_2) = M_1 \cup M_2$ .

### 3.3 Attaining Cyclic Compositionality

After setting the way by which one can deal with positive loops by using annotations in models, the join operator needs to be redefined. The original composition operators are applicable to annotated modules after applying Definition 6. This way, their atoms positive dependencies are added to their respective models.

**Definition 11 (Modified Join).** *Given two compatible annotated (in the sense of Definition 10) modules  $\mathcal{P}_1, \mathcal{P}_2$ , their composition is  $\mathcal{P}_1 \otimes \mathcal{P}_2 = \mathcal{P}_1 \oplus \mathcal{P}_2$  provided that (i)  $\mathcal{P}_1 \oplus \mathcal{P}_2$  is defined. This way, given modules  $\mathcal{P}_1$  and  $\mathcal{P}_2$  and sets of annotated interpretations  $A_1^A \subseteq 2^{A_t(\mathcal{P}_1)}$  and  $A_2^A \subseteq 2^{A_t(\mathcal{P}_2)}$ , the natural join of  $A_1^A$  and  $A_2^A$ , denoted by  $A_1^A \bowtie_A A_2^A$ , is defined as follows for intersecting output atoms:*

$$\{M_1 \cup M_2 \mid M_1 \in A_1, M_2 \in A_2, \text{s.t. } M_1 \text{ and } M_2 \text{ are compatible.}\}$$

**Theorem 3 (Cyclic Module Theorem).** *If  $\mathcal{P}_1, \mathcal{P}_2$  are modules with annotated models such that  $\mathcal{P}_1 \sqcup \mathcal{P}_2$  is defined, then:*

$$AS^A(\mathcal{P}_1 \sqcup \mathcal{P}_2) = AS^A(\mathcal{P}_1) \bowtie_A AS^A(\mathcal{P}_2)$$

### 3.4 Shortcomings Revisited

By adding the facts contained in stable models of one composing module to the other composing module, through a program transformation, one is able to counter the fact that the inputs of the composed module are removed if they are met by the outputs of either composing modules [17]. As for positive loops, going back to Example 6, the new composition operator also produces desired results:

*Example 10 (Cyclic Dependencies Revisited).* Take again the two program modules in Example 6:

$$\begin{aligned} \mathcal{P}_1 &= \langle \{airbag \leftarrow safe.\}, \{safe\}, \{airbag\}, \emptyset \rangle \\ \mathcal{P}_2 &= \langle \{safe \leftarrow airbag.\}, \{airbag\}, \{safe\}, \emptyset \rangle \end{aligned}$$

which respectively have annotated models  $AS^A(\mathcal{P}_1) = \{\{\}, \{airbag_{\{safe\}}\}, safe\}$  and  $AS^A(\mathcal{P}_2) = \{\{\}, \{airbag\}, safe_{\{airbag\}}\}$  while  $AS^A(\mathcal{P}_1 \otimes \mathcal{P}_2) = \{\{\}, \{airbag_{\{safe\}}\}, safe_{\{airbag\}}\}$ . Because of this,  $AS^A(\mathcal{P}_1 \otimes \mathcal{P}_2) = AS^A(\mathcal{P}_1) \bowtie_A AS^A(\mathcal{P}_2)$ . Now, take  $\mathcal{P}_3 = \langle \{airbag.\}, \{\}, \{airbag\}, \emptyset \rangle$  and compose it with  $\mathcal{P}_1 \otimes \mathcal{P}_2$ . We get  $AS^A(\mathcal{P}_1 \otimes \mathcal{P}_2 \otimes \mathcal{P}_3) = \{\{airbag, safe\}\}$ . ■

## 4 Conclusions and Future Work

We lift the restriction that disallows composing modules with cyclic dependencies in the framework of Modular Logic Programming [19]. We present a model join operation that requires one to look at every model of two modules being

composed in order to check for minimality of models that are comparable on account of their inputs. This operation is able to distinguish between atoms that are self supported through positive loops and atoms with proper support, allowing one to lift the condition disallowing positive dependencies between modules. However, this approach is not local as it requires comparing every models and, as it is not general because it does not allow combining modules with integrity constraints, it is of limited applicability.

Because of this lack of generality of the former approach, we present an alternative solution requiring the introduction of extra information in the models for one to be able to detect dependencies. We use models annotated with the way they depend on the atoms in their module's input signature. We then define their semantics in terms of a fixed point operator. After setting the way by which one deals with positive loops by using annotations in models, the join operator needs to be redefined. The original composition operators are applicable to annotated modules after applying Definition 7. This way, their positive dependencies are added to their respective models. This approach turns out to be local, in the sense that we need only look at two models being joined and unlike the first alternative we presented, it works well with integrity constraints.

As future work we can straightforwardly extend these results to probabilistic reasoning with ASP by applying the new module theorem to [4], as well as to DLP functions and general stable models. An implementation of the framework is also foreseen in order to assess the overhead when compared with the original benchmarks in [19].

**Acknowledgments.** The work of João Moura was supported by grant SFRH/BD/69006/2010 from Fundação para a Ciéncia e Tecnologia (FCT) from the Portuguese Ministério do Ensino e da Ciéncia.

## References

1. Babb, J., Lee, J.: Module theorem for the general theory of stable models. *TPLP* **12**(4–5), 719–735 (2012)
2. Baral, C.: Knowledge Representation, Reasoning, and Declarative Problem Solving. Cambridge University Press (2003)
3. Bugliesi, M., Lamma, E., Mello, P.: Modularity in logic programming. *J. Log. Program.* **19**(20), 443–502 (1994)
4. Viegas Damásio, C., Moura, J.: Modularity of P-log programs. In: Delgrande, J.P., Faber, W. (eds.) LPNMR 2011. LNCS, vol. 6645, pp. 13–25. Springer, Heidelberg (2011)
5. Dao-Tran, M., Eiter, T., Fink, M., Krennwallner, T.: Modular nonmonotonic logic programming revisited. In: Hill, P.M., Warren, D.S. (eds.) ICLP 2009. LNCS, vol. 5649, pp. 145–159. Springer, Heidelberg (2009)
6. Eiter, T., Faber, W., Leone, N., Pfeifer, G.: Computing preferred and weakly preferred answer sets bymeta-interpretation in answer set programming. In: Proceedings AAAI 2001 Spring Symposium on Answer Set Programming, pp. 45–52. AAAI Press (2001)

7. Ferraris, P., Lifschitz, V.: Weight constraints as nested expressions. *TPLP* **5**(1–2), 45–74 (2005)
8. Gaifman, H., Shapiro, E.: Fully abstract compositional semantics for logic programs. In: *Symposium on Principles of Programming Languages*, POPL, pp. 134–142. ACM, New York (1989)
9. Gelfond, M., Lifschitz, V.: The stable model semantics for logic programming. In: *Proceedings of the 5th International Conference on Logic Program*. MIT Press (1988)
10. Giordano, L., Martelli, A.: Structuring logic programs: a modal approach. *The Journal of Logic Programming* **21**(2), 59–94 (1994)
11. Järvisalo, M., Oikarinen, E., Janhunen, T., Niemelä, I.: A module-based framework for multi-language constraint modeling. In: Erdem, E., Lin, F., Schaub, T. (eds.) *LPNMR 2009. LNCS*, vol. 5753, pp. 155–168. Springer, Heidelberg (2009)
12. Lifschitz, V.: Answer set programming and plan generation. *Artificial Intelligence* **138**(1–2), 39–54 (2002)
13. Lifschitz, V., Pearce, D., Valverde, A.: Strongly equivalent logic programs. *ACM Transactions on Computational Logic* **2**, 2001 (2000)
14. Mancarella, P., Pedreschi, D.: An algebra of logic programs. In: *ICLP/SLP*, pp. 1006–1023 (1988)
15. Marek, V.W., Truszcynski, M.: Stable models and an alternative logic programming paradigm. In: *The Logic Programming Paradigm: A 25-Year Perspective* (1999)
16. Miller, D.: A theory of modules for logic programming. In: *In Symp. Logic Programming*, pp. 106–114 (1986)
17. Moura, J., Damásio, C.V.: Generalising modular logic programs. In: *15th International Workshop on Non-Monotonic Reasoning (NMR 2014)* (2014)
18. Niemelä, I.: Logic programs with stable model semantics as a constraint programming paradigm. *Annals of Mathematics and Artificial Intelligence* **25**, 72–79 (1998)
19. Oikarinen, E., Janhunen, T.: Achieving compositionality of the stable model semantics for smodels programs. *Theory Pract. Log. Program.* **8**(5–6), 717–761 (2008)
20. O’Keefe, R.A.: Towards an algebra for constructing logic programs. In: *SLP*, pp. 152–160 (1985)
21. Slota, M., Leite, J.: Robust equivalence models for semantic updates of answer-set programs. In: Brewka, G., Eiter, T., McIlraith, S.A. (eds.) *Proc. of KR 2012*. AAAI Press (2012)
22. Tasharrofi, S., Ternovska, E.: A semantic account for modularity in multi-language modelling of search problems. In: Tinelli, C., Sofronie-Stokkermans, V. (eds.) *FroCoS 2011. LNCS*, vol. 6989, pp. 259–274. Springer, Heidelberg (2011)

# Probabilistic Constraint Programming for Parameters Optimisation of Generative Models

Massimiliano Zanin<sup>(✉)</sup>, Marco Correia, Pedro A.C. Sousa, and Jorge Cruz

NOVA Laboratory for Computer Science and Informatics,

FCT/UNL, Caparica, Portugal

[m.zanin@campus.fct.unl.pt](mailto:m.zanin@campus.fct.unl.pt), [{mvc,pas,jcrc}@fct.unl.pt](mailto:{mvc,pas,jcrc}@fct.unl.pt)

**Abstract.** Complex networks theory has commonly been used for modelling and understanding the interactions taking place between the elements composing complex systems. More recently, the use of generative models has gained momentum, as they allow identifying which forces and mechanisms are responsible for the appearance of given structural properties. In spite of this interest, several problems remain open, one of the most important being the design of robust mechanisms for finding the optimal parameters of a generative model, given a set of real networks. In this contribution, we address this problem by means of Probabilistic Constraint Programming. By using as an example the reconstruction of networks representing brain dynamics, we show how this approach is superior to other solutions, in that it allows a better characterisation of the parameters space, while requiring a significantly lower computational cost.

**Keywords:** Probabilistic Constraint Programming · Complex networks · Generative models · Brain dynamics

## 1 Introduction

The last decades have witnessed a revolution in science, thanks to the appearance of the concept of *complex systems*: systems that are composed of a large number of interacting elements, and whose interactions are as important as the elements themselves [1]. In order to study the structures created by such relationships, several tools have been developed, among which *complex networks theory* [2,3], a statistical mechanics understanding of graph theory, stands out.

Complex networks have been used to characterise a large number of different systems, from social [4] to transportation ones [5]. They have also been valuable in the study of brain dynamics, as one of the greatest challenges in modern science is the characterisation of how the brain organises its activity to carry out complex computations and tasks. Constructing a complete picture of the computation performed by the brain requires specific mathematical, statistical and computational techniques. As brain activity is usually complex, with different regions coordinating and creating temporally multi-scale, spatially extended

networks, complex networks theory appears as the natural framework for its characterisation.

When complex networks are applied to brain dynamics, nodes are associated to sensors (*e.g.* measuring the electric and magnetic activity of neurons), thus to specific brain locations, and links to some specific conditions. For instance, brain functional networks are constructed such that pairs of nodes are connected if some kind of synchronisation, or correlated activity, is detected in those nodes - the rationale being that a coordinated dynamics is the result of some kind of information sharing [6]. Once these networks are reconstructed, graph theory allows endowing them with a great number of quantitative properties, thus vastly enriching the set of objective descriptors of brain structure and function at neuroscientists' disposal. This has especially been fruitful in the characterisation of the differences between healthy (control) subjects and patients suffering from neurologic pathologies [7].

Once the topology (or structure) of a network has been described, a further question may be posed: can such topology be explained by a set of simple generative rules, like a higher connectivity of neighbouring regions, or the influence of nodes physical position? When a set of rules (a *generative model*) has been defined, it has to be optimised and validated: one ought to obtain the best set of parameters, such that the networks yielded by the model are topologically equivalent to the real ones. This usually requires maximising a function of the *p*-values representing the differences between the characteristics of the synthetic and real networks. In spite of being accepted as a standard strategy, this method presents several drawbacks. First, its high computational complexity: large sets of networks have to be created and analysed for every possible combination of parameters; and second, its unfitness for assessing the presence of multiple local minima.

In this contribution, we propose the use of *probabilistic constraint programming* (PCP) for characterising the space created by the parameters of a generative model, *i.e.* a space representing the distance between the topological characteristics of real and synthetic networks. We show how this approach allows recovering a larger quantity of information about the relationship between model parameters and network topology, with a fraction of the computational cost required by other methods. Additionally, PCP can be applied to single subjects (networks), thus avoiding the constraints associated with working with a large and homogeneous population. We further validate the PCP approach by studying a simple generative model, and by applying it to a data set of brain activity of healthy people.

The remainder of the text is organised as follows. Besides this introduction, Sections 2 and 2.1 respectively review the state of the art in constraint programming and its probabilistic version. Afterwards, the application of PCP is presented in Section 3 for a data set of brain magneto-encephalographic recordings, and the advantages of PCP are discussed in Section 4. Finally, some conclusions are drawn in Section 5.

## 2 Constraint Programming

A constraint satisfaction problem [8] is a classical artificial intelligence paradigm characterised by a set of variables and a set of constraints, the latter specifying relations among subsets of these variables. Solutions are assignments of values to all variables that satisfy all the constraints.

Constraint programming is a form of declarative programming, in the sense that instead of specifying a sequence of steps to be executed, it relies on properties of the solutions to be found that are explicitly defined by the constraints. A constraint programming framework must provide a set of constraint reasoning algorithms that take advantage of constraints to reduce the search space, avoiding regions inconsistent with the constraints. These algorithms are supported by specialised techniques that explore the specificity of the constraint model, such as the domain of its variables and the structure of its constraints.

Continuous constraint programming [9, 10] has been widely used to model safe reasoning in applications where uncertainty on the values of the variables is modelled by intervals including all their possibilities. A Continuous Constraint Satisfaction Problem (CCSP) is a triple  $\langle X, D, C \rangle$ , where  $X$  is a tuple of  $n$  real variables  $\langle x_1, \dots, x_n \rangle$ ,  $D$  is a Cartesian product of intervals  $D(x_1) \times \dots \times D(x_n)$  (a box), each  $D(x_i)$  being the domain of variable  $x_i$ , and  $C$  is a set of numerical constraints (equations or inequalities) on subsets of the variables in  $X$ . A solution of the CCSP is a value assignment to all variables satisfying all the constraints in  $C$ . The feasible space  $F$  is the set of all CCSP solutions within  $D$ .

Continuous constraint reasoning relies on branch-and-prune algorithms [11] to obtain sets of boxes that cover exact solutions for the constraints (the feasible space  $F$ ). These algorithms begin with an initial crude cover of the feasible space (the initial search space,  $D$ ) which is recursively refined by interleaving pruning and branching steps until a stopping criterion is satisfied. The branching step splits a box from the covering into sub-boxes (usually two). The pruning step either eliminates a box from the covering or reduces it into a smaller (or equal) box maintaining all the exact solutions. Pruning is achieved through an algorithm [12] that combines constraint propagation and consistency techniques [13]: each box is reduced through the consecutive application of narrowing operators associated with the constraints, until a fixed-point is attained. These operators must be correct (do not eliminate solutions) and contracting (the obtained box is contained in the original). To guarantee such properties, interval analysis methods are used.

Interval analysis [14] is an extension of real analysis that allows computations with intervals of reals instead of reals, where arithmetic operations and unary functions are extended for interval operands. For instance,  $[1, 3] + [3, 7]$  results in the interval  $[4, 10]$ , which encloses all the results from a point-wise evaluation of the real arithmetic operator on all the values of the operands. In practice these extensions simply consider the bounds of the operands to compute the bounds of the result, since the involved operations are monotonic. As such, the narrowing operator  $Z \leftarrow Z \cap (X + Y)$  may be associated with constraint  $x + y = z$  to prune the domain of variable  $z$  based on the domains of variables  $x$  and  $y$ .

Similarly, in solving the equation with respect to  $x$  and  $y$ , two additional narrowing operators can be associated with the constraint, to safely narrow the domains of these variables. With this technique, based on interval arithmetic, the obtained narrowing operators are able to reduce a box  $X \times Y \times Z = [1, 3] \times [3, 7] \times [0, 5]$  into  $[1, 2] \times [3, 4] \times [4, 5]$ , with the guarantee that no possible solution is lost.

## 2.1 Probabilistic Constraint Programming

In classical CCSPs, uncertainty is modelled by intervals that represent the domains of the variables. Constraint reasoning reduces uncertainty, providing a safe method for computing a set of boxes enclosing the feasible space. Nevertheless this paradigm cannot distinguish between different scenarios, and all combination of values within such enclosure are considered equally plausible. In this work we use probabilistic constraint programming [15], which extends the continuous constraint framework with probabilistic reasoning, allowing to further characterise uncertainty with probability distributions over the domains of the variables.

In the continuous case, the usual method for specifying a probabilistic model [16] assumes, either explicitly or implicitly, a joint probability density function (p.d.f.) over the considered random variables, which assigns a probability measure to each point of the sample space  $\Omega$ . The probability of an event  $\mathcal{H}$ , given a p.d.f.  $f$ , is its multidimensional integral on the region defined by the event:

$$P(\mathcal{H}) = \int_{\mathcal{H}} f(\mathbf{x}) d\mathbf{x} \quad (1)$$

The idea of probabilistic constraint programming is to associate a probabilistic space to the classical CCSP by defining an appropriate density function. A probabilistic constraint space is a pair  $\langle \langle X, D, C \rangle, f \rangle$ , where  $\langle X, D, C \rangle$  is a CCSP and  $f$  is a p.d.f. defined in  $\Omega \supseteq D$  such that:  $\int_{\Omega} f(\mathbf{x}) d\mathbf{x} = 1$ .

A constraint (or a conjunction of constraints) can be viewed as an event  $\mathcal{H}$  whose probability can be computed by integrating the density function  $f$  over its feasible space as in equation (1). The probabilistic constraint framework relies on continuous constraint reasoning to get a tight box cover of the region of integration  $\mathcal{H}$ , and computes the overall integral by summing up the contributions of each box in the cover. Generic quadrature methods may be used to evaluate the integral at each box.

In this work, Monte Carlo methods [17] are used to estimate the value of the integrals at each box. The integral can be estimated by randomly selecting  $N$  points in the multidimensional space and averaging the function values at these points. This method displays  $\frac{1}{\sqrt{N}}$  convergence, *i.e.* by quadrupling the number of sampled points the error is halved, regardless of the number of dimensions.

The advantages obtainable from this close collaboration between constraint pruning and random sampling were previously illustrated in ocean colour remote sensing studies [18], where this approach achieved quite accurate results even with small sampling rates. The success of this technique relies on the reduction

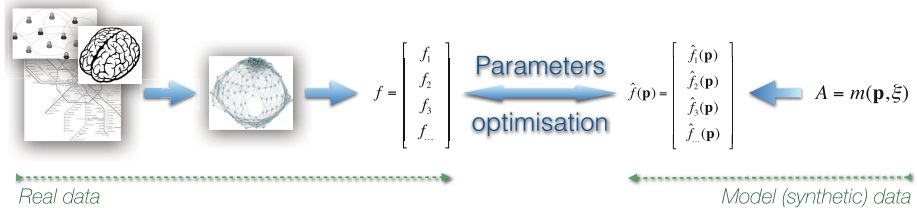


**Fig. 1.** Schematic representation of the use of generative models for analysing functional networks.  $f$  and  $\hat{f}$  respectively represent real and synthetic topological features, as the ones described in Sec. 3.2. Refer to Sec. 3 for a description of all steps of the analysis.

of the sampling space, where a pure non-naïve Monte Carlo (adaptive) method is not only hard to tune, but also impractical in small error settings.

### 3 From Brain Activity to Network Models

In order to validate the use of PCP for analysing the parameters space of a generative models, here we consider a set of magneto-encephalographic (MEG) recordings. A series of preliminary steps are required, as shown in Fig. 1. First, starting from the left, real brain data (or data representing any other real complex system) have to be recorded and encoded in networks, then transformed into a set of topological (structural) features. In parallel, as depicted in the right part, a generative model has to be defined: this allows to generate networks as a function of the model parameters, and extract their topological features. Finally, both features should be matched, *i.e.* the model parameters should be optimised to minimise the distance between the vectors of topological features of the synthetic and real networks.

#### 3.1 MEG Data Recording

Magneto-encephalographic (MEG) scans were obtained for 19 right handed elderly and healthy participants, recruited from the Geriatric Unit of the Hospital Universitario San Carlos Madrid and the Centro de Prevención del Deterioro Cognitivo, Ayuntamiento de Madrid, Spain. Before the task execution, all participants or legal representatives gave informed consent to participate in the study. The study was approved by the local ethics committee.

Brain activity scans correspond to a modified version of the Sternberg's letter-probe task [19], a standard task used to evaluate elders memory proficiency. MEG signals were recorded with a 254 Hz sampling rate, using 148-channel whole head magnetometer, confined in a magnetically shielded room (MSR). 35 artefact-free epochs were randomly chosen from those corresponding to correct answers for each of participant.

### 3.2 Networks Reconstruction and Evaluation

Following the diagram of Fig. 1, MEG recordings are converted in functional networks. Nodes, corresponding to MEG sensors and therefore to different brain regions, are pairwise connected when some kind of common dynamics is detected between the corresponding time series. Such relationship is assessed through Synchronization Likelihood (SL) [20], a metric able to detect *generalised synchronisation*, *i.e.* situations in which two time series react to a given input in different, yet consistent ways [21]. It thus goes beyond simple linear correlations, as it is able to detect non-linear and potentially chaotic relations. Applying SL yields a correlation matrix  $C\{w_{ij}\}$  of size  $148 \times 148$  (the number of sensors in the MEG machine) for each epoch available. In order to filter any kind of transient or noise specific to one epoch, the 35 matrices corresponding to each subjects have been averaged: the final result is then a single weight matrix  $\tilde{C}\{w_{ij}\}$  for each subject.

While a correlation matrix can readily be interpreted as a weighted fully-connected network, few metrics are available to describe the structure of such objects. It is then customary to apply a threshold, *i.e.* discard all links whose weight is not significant, and thus obtain an unweighted network. This presents several advantages. First of all, brain networks are expected to be naturally sparse, as increasing the connectivity implies a higher physiological cost. Furthermore, low synchronisation values may be the result of statistical fluctuations, *e.g.* of correlated noise; in such cases, deleting spurious links can only improve the understanding of the system. Lastly, a pruning can also help deleting indirect, second order correlations, which do not represent direct dynamical relationships.

The final step involves the calculation of the topological metrics associated to each pruned network, *i.e.* the  $fs$  of Fig. 1. Two have here been considered, representing two complementary aspects of brain information processing; their selection has been motivated by the generative model used afterwards (see Section 3.3):

**Clustering Coefficient.** The *clustering coefficient*, also known as *transitivity*, measures the presence of triangles in the network [22]. Mathematically, it is defined as the relationship between the number of triangles and the number of connected triples in the network:  $C = 3N_\Delta/N_3$ . Here, a triangle is a set of three nodes with links between each pair of them, while a connected triple is a set of three nodes where each one can be reached from each other (directly or indirectly). From a biological point of view, the clustering coefficient represents how brain regions are locally connected, creating dense communities computing some information in a collaborative way.

**Efficiency.** It is defined as the inverse of the harmonic mean of the length of the shortest paths connecting pairs of nodes [23]:

$$E = \frac{1}{N(N-1)} \sum_{i \neq j} \frac{1}{d_{ij}}, \quad (2)$$

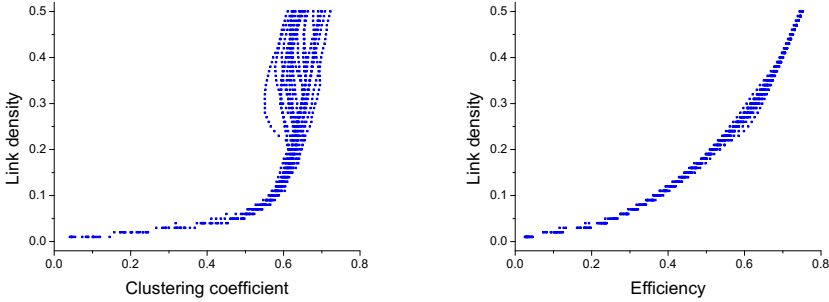


**Fig. 2.** Evolution of clustering coefficient (Left) and efficiency (Right) as a function of the link density for the 19 functional brain networks reconstructed in Sec. 3.2.

$d_{ij}$  being the distance between nodes  $i$  and  $j$ , i.e. the number of jumps required to travel between them. A low value of  $E$  implies that all brain regions are connected by short paths.

It has to be noticed how these two measures are complementary, the clustering coefficient and efficiency respectively representing the *segregation* and *integration* of information [24, 25]. Additionally, both  $C$  and  $E$  are here defined as a function of the threshold  $\tau$  applied to prune the networks - their evolution is represented in Fig. 2.

### 3.3 Generative Model Definition

Jumping to the right side of Fig. 1, it is now necessary to define a generative model. As an example, we have here implemented a *Economical Clustering Model* model as defined in [26, 27]. Given two nodes  $i$  and  $j$ , the probability of creating a connection between them is given by:

$$P_{i,j} \propto k_{i,j}^\gamma d_{i,j}^{-\eta}. \quad (3)$$

$k_{i,j}$  is the number of neighbours common to  $i$  and  $j$ , and  $d_{i,j}$  is the physical distance between the two nodes. This model thus includes two different forces that compete to create links. On one side,  $\gamma$  controls the appearance of triangles in the network, by positive biasing the connectivity between nodes having nearest neighbours in common; it thus defines the clustering coefficient and the appearance of computational communities. On the other side,  $\eta$  accounts for the distance in the connection, such that long-range connections, which are biologically costly, are penalised.

### 3.4 Parameters Estimation Through P-values

The problem is now identifying the best values of  $\gamma$  and  $\eta$  that permit recovering the topological properties obtained in Sec. 3.2 for the experimental brain networks.

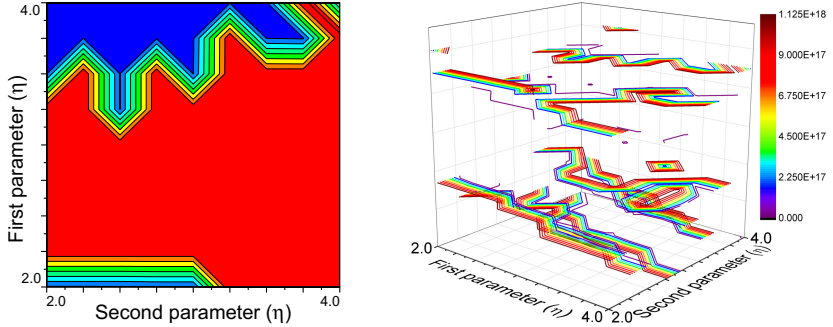


**Fig. 3.** (Left) Contour plot of the energy  $E$  (see Eq. 4) in the parameters space, for a link density of 0.3. (Right) Energy contour plots for ten link densities, from 0.05 (bottom) to 0.5 (top); for the sake of clarity, only region outlines are visible.

As an example of a standard  $p$ -value based mechanism, we here use a simplified version of the energy function proposed in Refs. [26, 27]:

$$E = 1 / \prod_i P_i. \quad (4)$$

$P_i$  represents the  $p$ -value of the Kolmogorov-Smirnov (K-S) test between the distributions estimated from the model and experimental networks, and  $i$  runs over all topological metrics. As just two topological properties are here studied, the previous formula simplifies to:  $E = 1 / (P_E \cdot P_C)$ .

For each considered value of  $\gamma$  and  $\eta$ , a set of networks have been generated according to the model of Eq. 3; their topological features extracted; and the resulting probability distribution compared with the distribution corresponding to the real networks, through a K-S test.

Fig. 3 presents the result of plotting the energy evolution in the parameters space. Specifically, Fig. 3 Left reports the evolution of the energy for a link density of 0.3. It can be noticed that a large portion of the space, constructed around the values of  $\gamma$  and  $\eta$  suggested in [26], maximises the energy. Fig. 3 Right represents the same information for ten different link densities, from 0.05 (bottom part) to 0.5 (upper part).

### 3.5 Parameters Estimation Through Probabilistic Constraint Programming

As an alternative solution, the previously described PCP method is here used to recover the shape of the parameters space. Two preliminary steps have to be completed: first, reconstruct a set of synthetic networks using the generative model of Eq. 3, for different  $\gamma$  and  $\eta$  values, and extract their topological characteristics; and second, obtain approximated functions describing the evolution of the topological metrics as a function of the model parameters, *i.e.*  $C = \tilde{f}_C(\gamma, \eta)$

and  $E = \tilde{f}_E(\gamma, \eta)$ . Afterwards, each observed feature  $o_i$  is modelled as a function  $f_i$  of the model parameters plus an associated error term  $\epsilon_i \sim \mathcal{N}(\mu = 0, \sigma^2)$ :

$$o_i = f_i(\gamma, \eta) + \epsilon_i$$

For  $n$  observations, a probabilistic constraint space is considered with random variables  $\gamma$  and  $\eta$ , a set of constraints  $C$ ,

$$C = \{-3\sigma \leq o_i - f_i(\gamma, \eta) \leq 3\sigma | 1 \leq i \leq n\}$$

$3\sigma$  being chosen to keep the error within reasonable bounds, and the joint p.d.f.  $f$ ,

$$f(\gamma, \eta) = \prod_{i=1}^n g(o_i - f_i(\gamma, \eta)) \quad (5)$$

where  $g$  is the normal distribution with 0 mean and standard deviation  $\sigma$ .

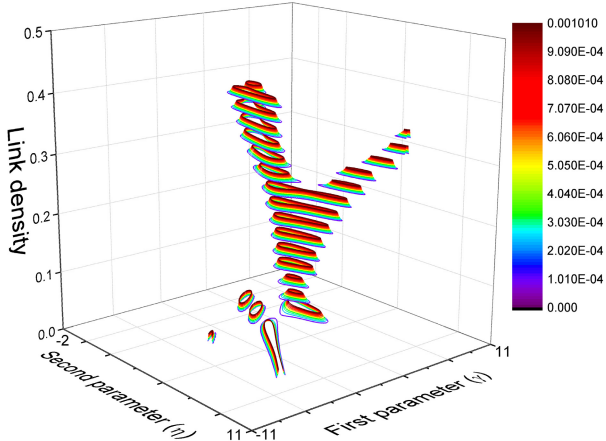
To compute the probability distribution of the random variables  $\gamma$  and  $\eta$ , a grid is constructed over their domains and a branch-and-prune algorithm is initially used to obtain a grid box cover of the feasible space (where each box belongs to a single grid cell). Then, for each box in the cover, a Monte Carlo method is used to compute its contribution to equation (1) with the p.d.f. defined in equation (5). The probability of the respective cell is updated accordingly and normalised in end of the process.

Fig. 4 reports the results obtained, *i.e.* the probability of obtaining networks with the generative model which are compatible with the real ones, as a function of the two parameters  $\gamma$  and  $\eta$ , and as a function of the link density. In the next Section, both approaches and their results are compared.

## 4 Comparing P-value and Probabilistic Constraint Programming

Results presented in Sec. 3.4 and 3.5 allow comparing the  $p$ -value and PCP methods, and highlight the advantages that the latter presents over the former.

The extremely high computational cost of analysing the parameters space by means of K-S tests seldom allows a full characterisation of such space. This is due to the fact that, for any set of parameters, a large number of networks have to be created and characterised. Increasing the resolution of the analysis, or enlarging the region of the space considered, increases the computational cost in a linear way. This problem is far from being trivial, as, for instance, the networks required to create Fig. 3 represents approximatively 3 GB of information and several days of computation in a standard computer. Such computational cost implies that it is easy to miss some important information. Let us consider, for instance, the result presented in Fig. 3 Left. The shape of the iso-lines suggests that the maximum is included in the region under analysis, and that no further explorations are required - while Figs. 4 and 5 prove otherwise.



**Fig. 4.** Contour plot of the parameters space, as obtained by the PCP method, for the whole population of subjects and as a function of the link density. The colour of each point represents the normalised probability of generating topologically equivalent networks.

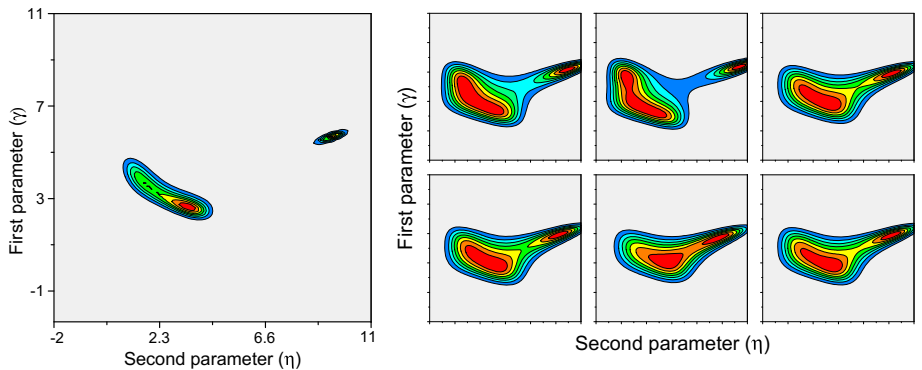


**Fig. 5.** (Left) Parameters space, as obtained with the PCP method, for a link density of 0.3 and for the whole studied population. (Right) Parameters space for six subjects. The scale of the right graphs is the same as the left one; the colour scale is the same of the one of Fig. 4.

On the other hand, estimating the functions  $\tilde{f}_C$  and  $\tilde{f}_E$  requires the creation and analysis of a constant number of networks, independently on the size of the parameters space. The total computational cost drops below the hour in a standard computer, implying a 3 orders of magnitude reduction. This has important consequences on the kind of information one can obtain. Fig. 5 Left presents the same information as Fig. 3 Left, but calculated by means of PCP

over a larger region. It is then clear that the maximum identified in Fig. 3 is just one of the two maxima presents in the system.

The second important advantage is that, while the PCP can yield results for just one network or subject, a *p*-value analysis requires a probability distribution. It is therefore not possible to characterise the parameters space for just one subject, but only for a large population. Fig. 5 Right explores this issue, by showing the probability evolution in the parameters space for six different subjects. It is interesting to notice how subjects are characterised by different shapes in the space. This allows a better description of subjects, aimed for instance at detecting differences among them.

## 5 Conclusions

In this contribution, we have presented the use of Probabilistic Constraint Programming for optimising the parameters of a generative model, aimed at describing the mechanisms responsible for the appearance of some given topological structures in real complex networks. As a validation case, we have here presented the results corresponding to functional networks of brain activity, as obtained through MEG recordings of healthy people.

The advantages of this method against other customary solutions, *e.g.* the use of *p*-values obtained from Kolmogorov-Smirnoff tests, have been discussed. First, the lower computational cost, and especially its independence on the size of the parameters space and on the resolution of the analysis. This allows a better characterisation of such space, reducing the risk of missing relevant results when multiple local minima are present. Second, the possibility of characterising the parameters space for single subjects, thus avoiding the need of having data for a full population. This will in turn open new doors for understanding the differences between individuals: as, for instance, for the identification of characteristics associated to specific diseases in diagnosis and prognosis tasks.

## References

1. Anderson, P.W.: More is different. *Science* **177**, 393–396 (1972)
2. Albert, R., Barabási, A.L.: Statistical mechanics of complex networks. *Reviews of Modern Physics* **74**, 47 (2002)
3. Newman, M.E.: The structure and function of complex networks. *SIAM Review* **45**, 167–256 (2003)
4. Costa, L.D.F., Oliveira Jr, O.N., Travieso, G., Rodrigues, F.A., Villas Boas, P.R., Antiqueira, L., Viana, M.P., Correa Rocha, L.E.: Analyzing and modeling real-world phenomena with complex networks: a survey of applications. *Advances in Physics* **60**, 329–412 (2011)
5. Zanin, M., Lillo, F.: Modelling the air transport with complex networks: A short review. *The European Physical Journal Special Topics* **215**, 5–21 (2013)
6. Bullmore, E., Sporns, O.: Complex brain networks: graph theoretical analysis of structural and functional systems. *Nature Reviews Neuroscience* **10**, 186–198 (2009)

7. Papo, D., Zanin, M., Pineda-Pardo, J.A., Boccaletti, S., Buldú, J.M.: Functional brain networks: great expectations, hard times and the big leap forward. *Philosophical Transactions of the Royal Society of London B: Biological Sciences* **369**, 20130525 (2014)
8. Mackworth, A.K.: Consistency in networks of relations. *Artificial Intelligence* **8**, 99–118 (1977)
9. Lhomme, O.: Consistency techniques for numeric CSPs. In: Proc. of the 13th IJCAI, pp. 232–238 (1993)
10. Benhamou, F., McAllester, D., van Hentenryck, P.: CLP(intervals) revisited. In: ISLP, pp. 124–138 (1994)
11. Van Hentenryck, P., McAllester, D., Kapur, D.: Solving polynomial systems using a branch and prune approach. *SIAM Journal on Numerical Analysis* **34**, 797–827 (1997)
12. Granvilliers, L., Benhamou, F.: Algorithm 852: realpaver: an interval solver using constraint satisfaction techniques. *ACM Transactions on Mathematical Software* **32**, 138–156 (2006)
13. Benhamou, F., Goualard, F., Granvilliers, L., Puget, J.-F.: Revising hull and box consistency. In: Procs. of ICLP, pp. 230–244 (1999)
14. Moore, R.: Interval analysis. Prentice-Hall, Englewood Cliffs (1966)
15. Carvalho, E.: Probabilistic constraint reasoning. PhD Thesis (2012)
16. Halpern, J.Y.: Reasoning about uncertainty. MIT, Cambridge (2003)
17. Hammersley, J.M., Handscomb, D.C.: Monte Carlo methods. Methuen, London (1964)
18. Carvalho, E., Cruz, J., Barahona, P.: Probabilistic constraints for nonlinear inverse problems. *Constraints* **18**, 344–376 (2013)
19. Maestú, F., Fernández, A., Simos, P.G., Gil-Gregorio, P., Amo, C., Rodriguez, R., Arrazola, J., Ortiz, T.: Spatio-temporal patterns of brain magnetic activity during a memory task in Alzheimer’s disease. *Neuroreport* **12**, 3917–3922 (2001)
20. Stam, C.J., Van Dijk, B.W.: Synchronization likelihood: an unbiased measure of generalized synchronization in multivariate data sets. *Physica D: Nonlinear Phenomena* **163**, 236–251 (2002)
21. Yang, S., Duan, C.: Generalized synchronization in chaotic systems. *Chaos, Solitons & Fractals* **9**, 1703–1707 (1998)
22. Newman, M.E.: Scientific collaboration networks. I. Network construction and fundamental results. *Physical Review E* **64**, 016131 (2001)
23. Latora, V., Marchiori, M.: Efficient behavior of small-world networks. *Physical Review Letters* **87**, 198–701 (2001)
24. Tononi, G., Sporns, O., Edelman, G.M.: A measure for brain complexity: relating functional segregation and integration in the nervous system. *Proceedings of the National Academy of Sciences* **91**, 5033–5037 (1994)
25. Rad, A.A., Sendiña-Nadal, I., Papo, D., Zanin, M., Buldu, J.M., del Pozo, F., Boccaletti, S.: Topological measure locating the effective crossover between segregation and integration in a modular network. *Physical Review Letters* **108**, 228701 (2012)
26. Vértes, P.E., Alexander-Bloch, A.F., Gogtay, N., Giedd, J.N., Rapoport, J.L., Bullmore, E.T.: Simple models of human brain functional networks. *Proceedings of the National Academy of Sciences* **109**, 5868–5873 (2012)
27. Vértes, P.E., Alexander-Bloch, A., Bullmore, E.T.: Generative models of rich clubs in Hebbian neuronal networks and large-scale human brain networks. *Philosophical Transactions of the Royal Society B: Biological Sciences* **369**, 20130531 (2014)

# Reasoning over Ontologies and Non-monotonic Rules

Vadim Ivanov, Matthias Knorr<sup>(✉)</sup>, and João Leite

NOVA LINCS, Departamento de Informática, Faculdade Ciências e Tecnologia,

Universidade Nova de Lisboa, Caparica, Portugal

[mkn@fct.unl.pt](mailto:mkn@fct.unl.pt)

**Abstract.** Ontology languages and non-monotonic rule languages are both well-known formalisms in knowledge representation and reasoning, each with its own distinct benefits and features which are quite orthogonal to each other. Both appear in the Semantic Web stack in distinct standards – OWL and RIF – and over the last decade a considerable research effort has been put into trying to provide a framework that combines the two. Yet, the considerable number of theoretical approaches resulted, so far, in very few practical reasoners, while realistic use-cases are scarce. In fact, there is little evidence that developing applications with combinations of ontologies and rules is actually viable. In this paper, we present a tool called NoHR that allows one to reason over ontologies and non-monotonic rules, illustrate its use in a realistic application, and provide tests of scalability of the tool, thereby showing that this research effort can be turned into practice.

## 1 Introduction

Ontology languages in the form of Description Logics (DLs) [4] and non-monotonic rule languages as known from Logic Programming (LP) [6] are both well-known formalisms in knowledge representation and reasoning (KRR) each with its own distinct benefits and features. This is also witnessed by the emergence of the Web Ontology Language (OWL) [18] and the Rule Interchange Format (RIF) [7] in the ongoing standardization of the Semantic Web driven by the W3C<sup>1</sup>.

On the one hand, ontology languages have become widely used to represent and reason over taxonomic knowledge and, since DLs are (usually) decidable fragments of first-order logic, are monotonic by nature which means that once drawn conclusions persist when adopting new additional information. They also allow reasoning on abstract information, such as relations between classes of objects even without knowing any concrete instances and a main theme inherited from DLs is the balance between expressiveness and complexity of reasoning. In fact, the very expressive general language OWL 2 with its high worst-case complexity includes three tractable (polynomial) profiles [27] each with a different application purpose in mind.

---

<sup>1</sup> <http://www.w3.org>

On the other hand, non-monotonic rules are focused on reasoning over instances and commonly apply the Closed World Assumption (CWA), i.e., the absence of a piece of information suffices to derive it being false, until new information to the contrary is provided, hence the term non-monotonic. This permits to declaratively model defaults and exceptions, in the sense that the absence of an exceptional feature can be used to derive that the (more) common case applies, and also integrity constraints, which can be used to ensure that the considered data is conform with desired specifications.

Combining both formalisms has been frequently requested by applications [1]. For example, in clinical health care, large ontologies such as SNOMED CT<sup>2</sup>, that are captured by the OWL 2 profile OWL 2 EL and its underlying description logic (DL)  $\mathcal{EL}^{++}$  [5], are used for electronic health record systems, clinical decision support systems, or remote intensive care monitoring, to name only a few. Yet, expressing conditions such as dextrocardia, i.e., that the heart is exceptionally on the right side of the body, is not possible and requires non-monotonic rules.

Finding such a combination is a non-trivial problem due to the considerable differences as to how decidability is ensured in each of the two formalisms and a naive combination is easily undecidable. In recent years, there has been a considerable amount of effort devoted to combining DLs with non-monotonic rules as known from Logic Programming – see, e.g., related work in [12, 28]) – but this has not been accompanied by similar variety of reasoners and applications. In fact, only very few reasoners for combining ontologies and non-monotonic rules exist and realistic use-cases are scarce. In other words, there is little evidence so far that developing applications in combinations of ontologies and rules is actually viable.

In this paper, we want to contribute to showing that this paradigm is viable by describing a tool called NoHR and show how it can be used to handle a real use-case efficiently as well as its scalability. NoHR is theoretically founded in the formalism of Hybrid MKNF under the well-founded semantics [22] which comes with two main arguments in its favor. First, the overall approach, which was introduced in [28] and is based on the logic of minimal knowledge and negation as failure (MKNF) [26], provides a very general and flexible framework for combining DL ontologies and non-monotonic rules (see [28]). Second, [22], which is a variant of [28] based on the well-founded semantics [13] for logic programs, has a lower data complexity than the former – it is polynomial for polynomial DLs – and is amenable for applying top-down query procedures, such as **SLG(O)** [2], to answer queries based only on the information relevant for the query, and without computing the entire model – no doubt a crucial feature when dealing with large ontologies and huge amounts of data.

NoHR is realized as a plug-in for the ontology editor Protégé 4.X<sup>3</sup>, that allows the user to query combinations of  $\mathcal{EL}_\perp^+$  ontologies and non-monotonic rules in a top-down manner. To the best of our knowledge, it is the first Protégé plug-in to integrate non-monotonic rules and top-down queries. We describe its

---

<sup>2</sup> <http://www.ihtsdo.org/snomed-ct/>

<sup>3</sup> <http://protege.stanford.edu>

**Table 1.** Syntax and semantics of  $\mathcal{EL}_\perp^+$ .

	Syntax	Semantics
atomic concept	$A \in \mathbf{N}_C$	$A^\mathcal{I} \subseteq \Delta^\mathcal{I}$
atomic role	$R \in \mathbf{N}_R$	$R^\mathcal{I} \subseteq \Delta^\mathcal{I} \times \Delta^\mathcal{I}$
individual	$a \in \mathbf{N}_I$	$a^\mathcal{I} \in \Delta^\mathcal{I}$
top	$\top$	$\Delta^\mathcal{I}$
bottom	$\perp$	$\emptyset$
conjunction	$C \sqcap D$	$C^\mathcal{I} \cap D^\mathcal{I}$
existential restriction	$\exists R.C$	$\{x \in \Delta^\mathcal{I} \mid \exists y \in \Delta^\mathcal{I} : (x, y) \in R^\mathcal{I} \wedge y \in C^\mathcal{I}\}$
concept inclusion	$C \sqsubseteq D$	$C^\mathcal{I} \subseteq D^\mathcal{I}$
role inclusion	$R \sqsubseteq S$	$R^\mathcal{I} \subseteq S^\mathcal{I}$
role composition	$R_1 \circ \dots \circ R_k \sqsubseteq S$	$(x_1, x_2) \in R_1^\mathcal{I} \wedge \dots \wedge (x_k, y) \in R_k^\mathcal{I} \rightarrow (x_1, y) \in S^\mathcal{I}$
concept assertion	$C(a)$	$a^\mathcal{I} \in C^\mathcal{I}$
role assertion	$R(a, b)$	$(a^\mathcal{I}, b^\mathcal{I}) \in R^\mathcal{I}$

features including the possibility to load and edit rule bases, and define predicates with arbitrary arity; guaranteed termination of query answering, with a choice between one/many answers; robustness w.r.t. inconsistencies between the ontology and the rule part and demonstrate its effective usage on the application use-case combining  $\mathcal{EL}_\perp^+$  ontologies and non-monotonic rules outlined in the following and adapted from [29], as well as an evaluation for real ontology SNOMED CT with over 300,000 concepts.

*Example 1.* The customs service for any developed country assesses imported cargo for a variety of risk factors including terrorism, narcotics, food and consumer safety, pest infestation, tariff violations, and intellectual property rights. Assessing this risk, even at a preliminary level, involves extensive knowledge about commodities, business entities, trade patterns, government policies and trade agreements. Parts of this knowledge is ontological information and taxonomic, such as the classification of commodities, while other parts require the CWA and thus non-monotonic rules, such as the policies involving, e.g., already known suspects. The overall task then is to access all the information and assess whether some shipment should be inspected in full detail, under certain conditions randomly, or not at all.

The remainder of the paper is structured as follows. In Sect. 2, we briefly recall the DL  $\mathcal{EL}_\perp^+$  and MKNF knowledge bases as a tight combination of the former DL and non-monotonic rules. Then, in Sect. 3, we present the Protégé plug-in NoHR, and, in Sect. 4, we discuss the cargo shipment use case and its realization using NoHR. We present some evaluation data in Sect. 5, before we conclude in Sect. 6<sup>4</sup>.

<sup>4</sup> Details on the translation of  $\mathcal{EL}$  ontologies into rules used in NoHR can be found in [19].

## 2 Preliminaries

### 2.1 Description Logic $\mathcal{EL}_\perp^+$

We start by recalling the syntax and semantics of  $\mathcal{EL}_\perp^+$ , a large fragment of  $\mathcal{EL}^{++}$  [5], the DL underlying the tractable profile OWL 2 EL [27], following the presentation in [21]. For a more general and thorough introduction to DLs we refer to [4].

The language of  $\mathcal{EL}_\perp^+$  is defined over countably infinite sets of *concept names*  $N_C$ , *role names*  $N_R$ , and *individual names*  $N_I$  as shown in the upper part of Table 1. Building on these, *complex concepts* are introduced in the middle part of Table 1, which, together with atomic concepts, form the set of *concepts*. We conveniently denote individuals by  $a$  and  $b$ , (atomic) roles by  $R$  and  $S$ , atomic concepts by  $A$  and  $B$ , and concepts by  $C$  and  $D$ . All expressions in the lower part of Table 1 are *axioms*. A *concept equivalence*  $C \equiv D$  is an abbreviation for  $C \sqsubseteq D$  and  $D \sqsubseteq C$ . Concept and role assertions are *ABox axioms* and all other axioms *TBox axioms*, and an *ontology* is a finite set of axioms.

The semantics of  $\mathcal{EL}_\perp^+$  is defined in terms of an *interpretation*  $\mathcal{I} = (\Delta^\mathcal{I}, \cdot^\mathcal{I})$  consisting of a non-empty domain  $\Delta^\mathcal{I}$  and an *interpretation function*  $\cdot^\mathcal{I}$ . The latter is defined for (arbitrary) concepts, roles, and individuals as in Table 1. Moreover, an interpretation  $\mathcal{I}$  *satisfies* an axiom  $\alpha$ , written  $\mathcal{I} \models \alpha$ , if the corresponding condition in Table 1 holds. If  $\mathcal{I}$  satisfies all axioms occurring in an ontology  $\mathcal{O}$ , then  $\mathcal{I}$  is a *model* of  $\mathcal{O}$ , written  $\mathcal{I} \models \mathcal{O}$ . If  $\mathcal{O}$  has at least one model, then it is called *consistent*, otherwise *inconsistent*. Also,  $\mathcal{O}$  *entails* axiom  $\alpha$ , written  $\mathcal{O} \models \alpha$ , if every model of  $\mathcal{O}$  satisfies  $\alpha$ . *Classification* requires to compute all concept inclusions between atomic concepts entailed by  $\mathcal{O}$ .

### 2.2 MKNF Knowledge Bases

MKNF knowledge bases (KBs) build on the logic of minimal knowledge and negation as failure (MKNF) [26]. Two main different semantics have been defined [22, 28], and we focus on the well-founded version [22], due to its lower computational complexity and amenability to top-down querying without computing the entire model. Here, we only point out important notions, and refer to [22] and [2] for the details.

We start by recalling MKNF knowledge bases as presented in [2] to combine an  $(\mathcal{EL}_\perp^+)$  ontology and a set of non-monotonic rules (similar to a normal logic program).

**Definition 2.** Let  $\mathcal{O}$  be an ontology. A function-free first-order atom  $P(t_1, \dots, t_n)$  s.t.  $P$  occurs in  $\mathcal{O}$  is called *DL-atom*; otherwise *non-DL-atom*. A rule  $r$  is of the form

$$H \leftarrow A_1, \dots, A_n, \mathbf{not} B_1, \dots, \mathbf{not} B_m \quad (1)$$

where the head of  $r$ ,  $H$ , and all  $A_i$  with  $1 \leq i \leq n$  and  $B_j$  with  $1 \leq j \leq m$  in the body of  $r$  are atoms. A program  $\mathcal{P}$  is a finite set of rules, and an MKNF

knowledge base  $\mathcal{K}$  is a pair  $(\mathcal{O}, \mathcal{P})$ . A rule  $r$  is DL-safe if all its variables occur in at least one non-DL-atom  $A_i$  with  $1 \leq i \leq n$ , and  $\mathcal{K}$  is DL-safe if all its rules are DL-safe. The ground instantiation of  $\mathcal{K}$  is the KB  $\mathcal{K}_G = (\mathcal{O}, \mathcal{P}_G)$  where  $\mathcal{P}_G$  is obtained from  $\mathcal{P}$  by replacing each rule  $r$  of  $\mathcal{P}$  with a set of rules substituting each variable in  $r$  with constants from  $\mathcal{K}$  in all possible ways.

DL-safety ensures decidability of reasoning with MKNF knowledge bases and can be achieved by introducing a new predicate  $o$ , adding  $o(i)$  to  $\mathcal{P}$  for all constants  $i$  appearing in  $\mathcal{K}$  and, for each rule  $r \in \mathcal{P}$ , adding  $o(X)$  for each variable  $X$  appearing in  $r$  to the body of  $r$ . Therefore, we only consider DL-safe MKNF knowledge bases.

The semantics of  $\mathcal{K}$  is based on a transformation of  $\mathcal{K}$  into an MKNF formula to which the MKNF semantics can be applied (see [22, 26, 28] for details). Instead of spelling out the technical details of the original MKNF semantics [28] or its three-valued counterpart [22], we focus on a compact representation of models for which the computation of the well-founded MKNF model is defined<sup>5</sup>. This representation is based on a set of **K**-atoms and  $\pi(\mathcal{O})$ , the translation of  $\mathcal{O}$  into first-order logic.

**Definition 3.** Let  $\mathcal{K}_G = (\mathcal{O}, \mathcal{P}_G)$  be a ground hybrid MKNF knowledge base. The set of **K**-atoms of  $\mathcal{K}_G$ , written  $\text{KA}(\mathcal{K}_G)$ , is the smallest set that contains (i) all ground atoms occurring in  $\mathcal{P}_G$ , and (ii) an atom  $\xi$  for each ground **not**-atom **not** $\xi$  occurring in  $\mathcal{P}_G$ . For a subset  $S$  of  $\text{KA}(\mathcal{K}_G)$ , the objective knowledge of  $S$  w.r.t.  $\mathcal{K}_G$  is the set of first-order formulas  $\text{OB}_{\mathcal{O}, S} = \{\pi(\mathcal{O})\} \cup S$ .

The set  $\text{KA}(\mathcal{K}_G)$  contains all atoms occurring in  $\mathcal{K}_G$ , only with **not**-atoms substituted by corresponding atoms, while  $\text{OB}_{\mathcal{O}, S}$  provides a first-order representation of  $\mathcal{O}$  together with a set of known/derived facts. In the three-valued MKNF semantics, this set of **K**-atoms can be divided into true, undefined and false atoms. Next, we recall operators from [22] that derive consequences based on  $\mathcal{K}_G$  and a set of **K**-atoms that is considered to hold.

**Definition 4.** Let  $\mathcal{K}_G = (\mathcal{O}, \mathcal{P}_G)$  be a positive, ground hybrid MKNF knowledge base. The operators  $R_{\mathcal{K}_G}$ ,  $D_{\mathcal{K}_G}$ , and  $T_{\mathcal{K}_G}$  are defined on subsets of  $\text{KA}(\mathcal{K}_G)$ :

$$\begin{aligned} R_{\mathcal{K}_G}(S) &= \{H \mid \mathcal{P}_G \text{ contains a rule of the form } H \leftarrow A_1, \dots, A_n \\ &\quad \text{such that, for all } i, 1 \leq i \leq n, A_i \in S\} \\ D_{\mathcal{K}_G}(S) &= \{\xi \mid \xi \in \text{KA}(\mathcal{K}_G) \text{ and } \text{OB}_{\mathcal{O}, S} \models \xi\} \\ T_{\mathcal{K}_G}(S) &= R_{\mathcal{K}_G}(S) \cup D_{\mathcal{K}_G}(S) \end{aligned}$$

The operator  $T_{\mathcal{K}_G}$  is monotonic, and thus has a least fixpoint  $T_{\mathcal{K}_G} \uparrow \omega$ . Transformations can be defined that turn an arbitrary hybrid MKNF KB  $\mathcal{K}_G$  into a positive one (respecting the given set  $S$ ) to which  $T_{\mathcal{K}_G}$  can be applied. To ensure coherence, i.e., that classical negation in the DL enforces default negation in the rules, two slightly different transformations are defined (see [22] for details).

---

<sup>5</sup> Strictly speaking, this computation yields the so-called well-founded partition from which the well-founded MKNF model is defined (see [22] for details).

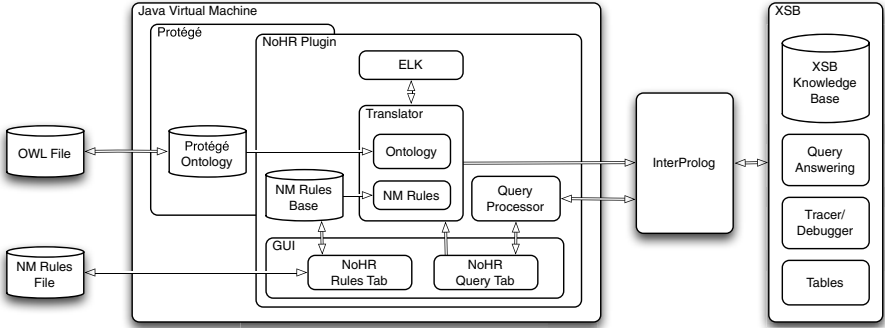


Fig. 1. System Architecture of NoHR

**Definition 5.** Let  $\mathcal{K}_G = (\mathcal{O}, \mathcal{P}_G)$  be a ground hybrid MKNF knowledge base and  $S \subseteq \text{KA}(\mathcal{K}_G)$ . The MKNF transform  $\mathcal{K}_G/S$  is defined as  $\mathcal{K}_G/S = (\mathcal{O}, \mathcal{P}_G/S)$ , where  $\mathcal{P}_G/S$  contains all rules  $H \leftarrow A_1, \dots, A_n$  for which there exists a rule of the form (1) in  $\mathcal{P}_G$  with  $B_j \notin S$  for all  $1 \leq j \leq m$ . The MKNF-coherent transform  $\mathcal{K}_G//S$  is defined as  $\mathcal{K}_G//S = (\mathcal{O}, \mathcal{P}_G//S)$ , where  $\mathcal{P}_G//S$  contains all rules  $H \leftarrow A_1, \dots, A_n$  for which there exists a rule of the form (1) with  $B_j \notin S$  for all  $1 \leq j \leq m$  and  $\text{OB}_{\mathcal{O}, S} \not\models \neg H$ . We define  $\Gamma_{\mathcal{K}_G}(S) = T_{\mathcal{K}_G/S} \uparrow \omega$  and  $\Gamma'_{\mathcal{K}_G}(S) = T_{\mathcal{K}_G//S} \uparrow \omega$ .

Based on these two antitonic operators [22], two sequences  $\mathbf{P}_i$  and  $\mathbf{N}_i$  are defined, which correspond to the true and non-false derivations.

$$\begin{array}{ll} \mathbf{P}_0 = \emptyset & \mathbf{N}_0 = \text{KA}(\mathcal{K}_G) \\ \mathbf{P}_{n+1} = \Gamma_{\mathcal{K}_G}(\mathbf{N}_n) & \mathbf{N}_{n+1} = \Gamma'_{\mathcal{K}_G}(\mathbf{P}_n) \\ \mathbf{P}_\omega = \bigcup \mathbf{P}_i & \mathbf{N}_\omega = \bigcap \mathbf{N}_i \end{array}$$

The fixpoints yield the well-founded MKNF model [22] (in polynomial time).

**Definition 6.** The well-founded MKNF model of an MKNF-consistent ground hybrid MKNF knowledge base  $\mathcal{K}_G = (\mathcal{O}, \mathcal{P}_G)$  is defined as  $(\mathbf{P}_\omega, \text{KA}(\mathcal{K}_G) \setminus \mathbf{N}_\omega)$ .

If  $\mathcal{K}$  is MKNF-consistent, then this partition does correspond to the unique model of  $\mathcal{K}$  [22], and, like in [2], we call the partition the *well-founded MKNF model*  $M_{wf}(\mathcal{K})$ . Here,  $\mathcal{K}$  may indeed not be MKNF-consistent if the  $\mathcal{EL}^+$  ontology alone is inconsistent, which is possible if  $\perp$  occurs, or by the combination of appropriate axioms in  $\mathcal{O}$  and  $\mathcal{P}$ , e.g.,  $A \sqsubseteq \perp$  and  $A(a) \leftarrow$ . In the former case, we argue that the ontology alone should be consistent and be repaired if necessary before combining it with non-monotonic rules. Thus, we assume in the following that  $\mathcal{O}$  occurring in  $\mathcal{K}$  is consistent.

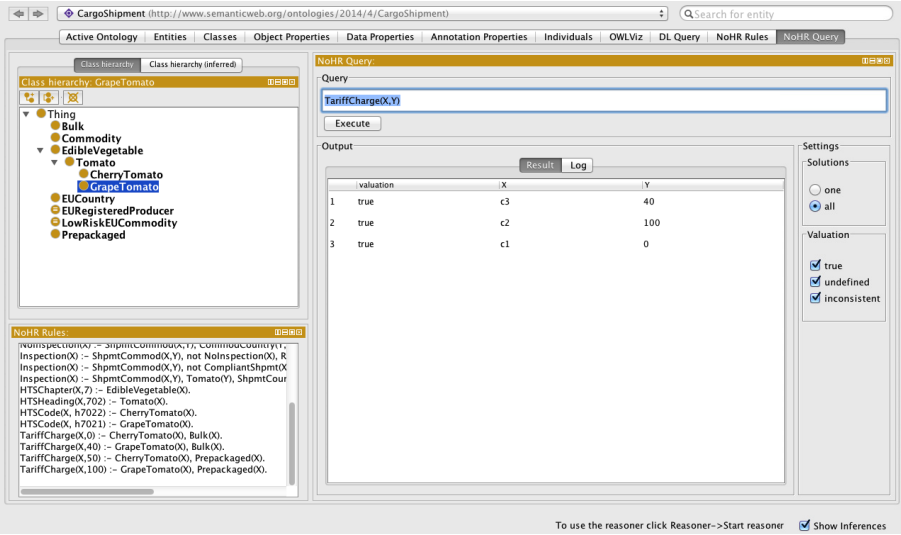


**Fig. 2.** NoHR Query tab with a query for  $\text{TariffCharge}(x,y)$  (see Sect. 4)

### 3 System Description

In this section, we briefly describe the architecture of the plug-in for Protégé as shown in Fig. 1 and discuss some features of the implementation and how querying is realized.

The input for the plug-in consists of an OWL file in the DL  $\mathcal{EL}^+$  as described in Sect. 2.1, which can be manipulated as usual in Protégé, and a rule file. For the latter, we provide a tab called NoHR Rules that allows us to load, save and edit rule files in a text panel following standard Prolog conventions.

The NoHR Query tab (see Fig. 2) also allows for the visualization of the rules, but its main purpose is to provide an interface for querying the combined KB. Whenever the first query is posed by pushing “Execute”, a translator is started, initiating the ontology reasoner ELK [21] tailored for  $\mathcal{EL}^+$  and considerably faster than other reasoners when comparing classification time [21]. ELK is used to classify the ontology  $\mathcal{O}$  and then return the inferred axioms to the translator. It is also verified whether *DisjointWith* axioms appear in  $\mathcal{O}$ , i.e., in  $\mathcal{EL}^+$  notation, axioms of the form  $C \sqcap D \sqsubseteq \perp$  for arbitrary classes  $C$  and  $D$ , which determines whether inconsistencies may occur in the combined hybrid knowledge base. Then the result of the classification is translated into rules and joined with the already given non-monotonic rules in  $\mathcal{P}$ , and the result is conditionally further transformed if inconsistency detection is required.

The result is used as input for the top-down query engine XSB Prolog<sup>6</sup> which realizes the well-founded semantics for logic programs [13]. To guarantee

<sup>6</sup> <http://xsb.sourceforge.net>

full compatibility with XSB Prolog's more restrictive admitted input syntax, the joint resulting rule set is further transformed such that all predicates and constants are encoded using MD5. The result is transferred to XSB via InterProlog [9]<sup>7</sup>, which is an open-source Java front-end allowing the communication between Java and a Prolog engine.

Next, the query is sent via InterProlog to XSB, and answers are returned to the query processor, which collects them and sets up a table showing for which variable substitutions we obtain true, undefined, or inconsistent valuations (or just shows the truth value for a ground query). The table itself is shown in the Result tab (see Fig. 2) of the Output panel, while the Log tab shows measured times of pre-processing the knowledge base and answering the query. XSB itself not only answers queries very efficiently in a top-down manner, with tabling, it also avoids infinite loops.

Once the query has been answered, the user may pose other queries, and the system will simply send them directly without any repeated preprocessing. If the user changes data in the ontology or in the rules, then the system offers the option to recompile, but always restricted to the part that actually changed.

## 4 Cargo Shipment Use Case

The customs service for any developed country assesses imported cargo for a variety of risk factors including terrorism, narcotics, food and consumer safety, pest infestation, tariff violations, and intellectual property rights<sup>8</sup>. Assessing this risk, even at a preliminary level, involves extensive knowledge about commodities, business entities, trade patterns, government policies and trade agreements. Some of this knowledge may be external to a given customs agency: for instance the broad classification of commodities according to the international Harmonized Tariff System (HTS), or international trade agreements. Other knowledge may be internal to a customs agency, such as lists of suspected violators or of importers who have a history of good compliance with regulations.

Figure 3 shows a simplified fragment  $\mathcal{K} = (\mathcal{O}, \mathcal{P})$  of such a knowledge base. In this fragment, a shipment has several attributes: the country of its origination, the commodity it contains, its importer and producer. The ontology contains a geographic classification, along with information about producers who are located in various countries. It also contains (partial) information about three shipments:  $s_1$ ,  $s_2$  and  $s_3$ . There is also a set of rules indicating information about importers, and about whether to inspect a shipment either to check for compliance of tariff information or for food safety issues. For that purpose, the set of rules also includes a classification of commodities based on their harmonized tariff information (HTS chapters, headings and codes, cf. <http://www.usitc.gov/tata/hts>), and tariff information, based on the classification of commodities as given by the ontology.

---

<sup>7</sup> <http://www.declarativa.com/interprolog/>

<sup>8</sup> The system described here is not intended to reflect the policies of any country or agency.

---

\* \* \*  $\mathcal{O}$  \* \* \*

$\text{Commodity} \equiv (\exists \text{HTSCode}. \top)$	$\text{Tomato} \sqsubseteq \text{EdibleVegetable}$
$\text{CherryTomato} \sqsubseteq \text{Tomato}$	$\text{GrapeTomato} \sqsubseteq \text{Tomato}$
$\text{CherryTomato} \sqcap \text{GrapeTomato} \sqsubseteq \perp$	$\text{Bulk} \sqcap \text{Prepackaged} \sqsubseteq \perp$
$\text{EURegisteredProducer} \equiv (\exists \text{RegisteredProducer}. \text{EUCountry})$	
$\text{LowRiskEUCommodity} \equiv (\exists \text{ExpeditableImporter}. \top) \sqcap (\exists \text{CommodCountry}. \text{EUCountry})$	
$\text{ShpmtCommod}(s_1, c_1)$	$\text{ShpmtDeclHTSCode}(s_1, \text{h7022})$
$\text{ShpmtImporter}(s_1, i_1)$	$\text{CherryTomato}(c_1) \quad \text{Bulk}(c_1)$
$\text{ShpmtCommod}(s_2, c_2)$	$\text{ShpmtDeclHTSCode}(s_2, \text{h7022})$
$\text{ShpmtImporter}(s_2, i_2)$	$\text{GrapeTomato}(c_2) \quad \text{Prepackaged}(c_2)$
$\text{ShpmtCountry}(s_2, \text{portugal})$	
$\text{ShpmtCommod}(s_3, c_3)$	$\text{ShpmtDeclHTSCode}(s_3, \text{h7021})$
$\text{ShpmtImporter}(s_3, i_3)$	$\text{GrapeTomato}(c_3) \quad \text{Bulk}(c_3)$
$\text{ShpmtCountry}(s_3, \text{portugal})$	$\text{ShpmtProducer}(s_3, p_1)$
$\text{RegisteredProducer}(p_1, \text{portugal})$	$\text{EUCountry}(\text{portugal})$
$\text{RegisteredProducer}(p_2, \text{slovakia})$	$\text{EUCountry}(\text{slovakia})$

\* \* \*  $\mathcal{P}$  \* \* \*

$\text{AdmissibleImporter}(\mathbf{x}) \leftarrow \text{ShpmtImporter}(\mathbf{y}, \mathbf{x}), \text{notSuspectedBadGuy}(\mathbf{x}).$
$\text{SuspectedBadGuy}(i_1).$
$\text{ApprovedImporterOf}(i_2, \mathbf{x}) \leftarrow \text{EdibleVegetable}(\mathbf{x}).$
$\text{ApprovedImporterOf}(i_3, \mathbf{x}) \leftarrow \text{GrapeTomato}(\mathbf{x}).$
$\text{CommodCountry}(\mathbf{x}, \mathbf{y}) \leftarrow \text{ShpmtCommod}(\mathbf{z}, \mathbf{x}), \text{ShpmtCountry}(\mathbf{z}, \mathbf{y}).$
$\text{ExpeditableImporter}(\mathbf{x}, \mathbf{y}) \leftarrow \text{ShpmtCommod}(\mathbf{z}, \mathbf{x}), \text{ShpmtImporter}(\mathbf{z}, \mathbf{y}),$
$\text{AdmissibleImporter}(\mathbf{y}), \text{ApprovedImporterOf}(\mathbf{y}, \mathbf{x}).$
$\text{CompliantShpmt}(\mathbf{x}) \leftarrow \text{ShpmtCommod}(\mathbf{x}, \mathbf{y}), \text{HTSCode}(\mathbf{y}, \mathbf{z}), \text{ShpmtDeclHTSCode}(\mathbf{x}, \mathbf{z}).$
$\text{Random}(\mathbf{x}) \leftarrow \text{ShpmtCommod}(\mathbf{x}, \mathbf{y}), \text{notRandom}(\mathbf{x}).$
$\text{NoInspection}(\mathbf{x}) \leftarrow \text{ShpmtCommod}(\mathbf{x}, \mathbf{y}), \text{CommodCountry}(\mathbf{y}, \mathbf{z}), \text{EUCountry}(\mathbf{z}).$
$\text{Inspection}(\mathbf{x}) \leftarrow \text{ShpmtCommod}(\mathbf{x}, \mathbf{y}), \text{notNoInspection}(\mathbf{x}), \text{Random}(\mathbf{x}).$
$\text{Inspection}(\mathbf{x}) \leftarrow \text{ShpmtCommod}(\mathbf{x}, \mathbf{y}), \text{notCompliantShpmt}(\mathbf{x}).$
$\text{Inspection}(\mathbf{x}) \leftarrow \text{ShpmtCommod}(\mathbf{x}, \mathbf{y}), \text{Tomato}(\mathbf{y}), \text{ShpmtCountry}(\mathbf{x}, \text{slovakia}).$
$\text{HTSChapter}(\mathbf{x}, 7) \leftarrow \text{EdibleVegetable}(\mathbf{x}).$
$\text{HTSHeading}(\mathbf{x}, 702) \leftarrow \text{Tomato}(\mathbf{x}).$
$\text{HTSCode}(\mathbf{x}, \text{h7022}) \leftarrow \text{CherryTomato}(\mathbf{x}).$
$\text{HTSCode}(\mathbf{x}, \text{h7021}) \leftarrow \text{GrapeTomato}(\mathbf{x}).$
$\text{TariffCharge}(\mathbf{x}, 0) \leftarrow \text{CherryTomato}(\mathbf{x}), \text{Bulk}(\mathbf{x}).$
$\text{TariffCharge}(\mathbf{x}, 40) \leftarrow \text{GrapeTomato}(\mathbf{x}), \text{Bulk}(\mathbf{x}).$
$\text{TariffCharge}(\mathbf{x}, 50) \leftarrow \text{CherryTomato}(\mathbf{x}), \text{Prepackaged}(\mathbf{x}).$
$\text{TariffCharge}(\mathbf{x}, 100) \leftarrow \text{GrapeTomato}(\mathbf{x}), \text{Prepackaged}(\mathbf{x}).$

---

**Fig. 3.** MKNF knowledge base for Cargo Imports

The overall task then is to access all the information and assess whether some shipment should be inspected in full detail, under certain conditions randomly, or not at all. In fact, an inspection is considered if either a random inspection is indicated, or some shipment is not compliant, i.e., there is a mismatch between the filed cargo codes and the actually carried commodities, or some suspicious cargo is observed, in this case tomatoes from slovakia. In the first case, a potential random inspection is indicated whenever certain exclusion conditions do not hold. To ensure that one can distinguish between strictly required and random inspections, a random inspection is assigned the truth value undefined based on the rule  $\text{Random}(x) \leftarrow \text{ShpmtCommod}(x, y), \text{notRandom}(x)$ .

The result of querying this knowledge base for  $\text{Inspection}(x)$  reveals that of the three shipments,  $s_2$  requires an inspection (due to mislabeling) while  $s_1$  may be subject to a random inspection as it does not knowingly originate from the EU. It can also be verified using the tool that preprocessing the knowledge base can be handled within 300ms and the query only takes 12ms, which certainly suffices as interactive response. Please also note that the example indeed utilizes the features of rules and ontologies: for example exceptions to the potential random inspections can be expressed, but at the same time, taxonomic and non-closed knowledge is used, e.g., some shipment may in fact originate from the EU, this information is just not available.

## 5 Evaluation

In this section, we present some tests showing that a) the huge  $\mathcal{EL}^+$  ontology SNOMED CT can be preprocessed for querying in a short period of time, b) adding rules increases the time of the translation only linearly, and c) querying time is in comparison to a) and b) in general completely neglectable. We performed the tests on a Mac book air 13 under Mac OS X 10.8.4 with a 1.8 GHz Intel Core i5 processor and 8 GB 1600 MHz DDR3 of memory. We ran all tests in a terminal version and Java with the “-XX:+AggressiveHeap” option, and test results are averages over 5 runs.

We considered SNOMED CT, freely available for research and evaluation<sup>9</sup>, and added a varying number of non-monotonic rules. These rules were generated arbitrarily, using predicates from the ontology and additional new predicates (up to arity three), producing rules with a random number of body atoms varying from 1 to 10 and facts (rules without body atoms) with a ratio of 1:10. Note that, due to the translation of the DL part into rules, all atoms literally become non-DL-atoms. So ensuring that each variable appearing in the rule is contained in at least one non-negated body atom suffices to guarantee DL-safety for these rules.

The results are shown in Fig. 4 (containing also a constant line for classification of ELK alone and starting with the values for the case without additional rules), and clearly show that a) preprocessing an ontology with over 300,000 concepts takes less than 70 sec. (time for translator+loading in XSB), b) the

---

<sup>9</sup> <http://www.ihtsdo.org/licensing/>

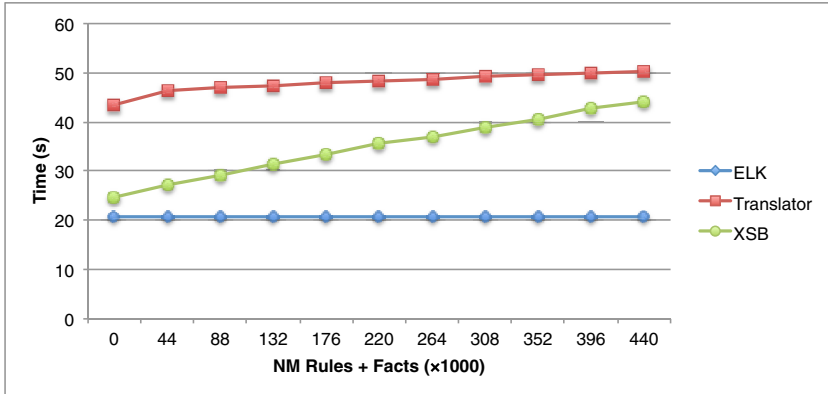


**Fig. 4.** Preprocessing time for SNOMED with a varying number of Rules

time of translator and loading the file in XSB only grows linearly on the number of rules with a small degree, in particular in the case of translator, and c) even with up to 500,000 added rules the time for translating does not surpass ELK classification, which itself is really fast [21], by more than a factor 2.5. All this data indicates that even on with a very large ontology, preprocessing can be handled very efficiently.

Finally, we also tested the querying time. To this purpose, we randomly generated and handcrafted several queries of different sizes and shapes using SNOMED with a varying number of non-monotonic rules as described before. In all cases, we observed that the query response time is interactive, observing longer reply times only if the number of replies is very high because either the queried class contains many subclasses in the hierarchy or if the arbitrarily generated rules create too many meaningless links, thus in the worst case requiring to compute the entire model. Requesting only one solution avoids this problem. Still, the question of realistic randomly generated rule bodies for testing querying time remain an issue of future work.

## 6 Conclusions

We have presented NoHR, the first plug-in for the ontology editor Protégé that integrates non-monotonic rules and top-down queries with ontologies in the OWL 2 profile OWL 2 EL. We have discussed how this procedure is implemented as a tool and shown how it can be used to implement a real use case on cargo shipment inspections. We have also presented an evaluation which shows that the tool is applicable to really huge ontologies, here SNOMED CT.

There are several relevant approaches discussed in the literature. Most closely related are probably [15, 23], because both build on the well-founded MKNF semantics [22]. In fact, [15] is maybe closest in spirit to the original idea of

**SLG( $\mathcal{O}$ )** oracles represented in [2] on which the implementation of NoHR is theoretically founded. It utilizes the CDF framework already integrated in XSB, but its non-standard language is a drawback if we want to achieve compatibility with standard OWL tools based on the OWL API. On the other hand, [23], presents an OWL 2 QL oracle based on common rewritings in the underlying DL DL-Lite [3]. Less closely related is the work pursued in [8, 14] that investigates direct non-monotonic extensions of  $\mathcal{EL}$ , so that the main reasoning task focuses on finding default subset inclusions, unlike this query-centered approach.

Two other related tools are DReW [30] and HD Rules [10], but both are based on different underlying formalisms to combine ontologies and non-monotonic rules. The former builds on dl-programs [12] and focuses on datalog-rewritable DLs [17], and the latter builds on Hybrid Rules [11]. While a more detailed comparison is surely of interest, the main problem is that both underlying formalisms differ from MKNF knowledge bases in the way information can flow between its two components and how flexible the language is [12, 28].

We conclude with pointing out that given the successful application of the tool to the use-case as well as its evaluation, an obvious next step will be to try applying it to other use-case domains. This will allow gathering data, which may then be used for a) further dissemination in particular of query processing, which would b) stimulate application-driven optimizations and enhancements of the tool NoHR. Other future directions are extensions to paraconsistency [20] or more general formalisms [16, 24, 25].

**Acknowledgments.** We would like to thank the referees for their comments. We acknowledge partial support by FCT under project ERRO (PTDC/EIA-CCO/121823/2010) and under strategic project NOVA LINCS (PEst/UID/CEC/04516/2013). V. Ivanov was partially supported by a MULTIC – Erasmus Mundus Action 2 grant and M. Knorr was also partially supported by FCT grant SFRH/BPD/86970/2012.

## References

- Alberti, M., Knorr, M., Gomes, A.S., Leite, J., Gonçalves, R., Slota, M.: Normative systems require hybrid knowledge bases. In: Procs. of AAMAS, IFAAMAS, pp. 1425–1426 (2012)
- Alferes, J.J., Knorr, M., Swift, T.: Query-driven procedures for hybrid MKNF knowledge bases. ACM Trans. Comput. Log. **14**(2), 1–43 (2013)
- Artale, A., Calvanese, D., Kontchakov, R., Zakharyaschev, M.: The *DL-Lite* family and relations. J. Artif. Intell. Res. (JAIR) **36**, 1–69 (2009)
- Baader, F., Calvanese, D., McGuinness, D.L., Nardi, D., Patel-Schneider, P.F. (eds.): The Description Logic Handbook: Theory, Implementation, and Applications, 3rd edn. Cambridge University Press (2010)
- Baader, F., Brandt, S., Lutz, C.: Pushing the  $\mathcal{EL}$  envelope. In: Procs. of IJCAI (2005)
- Baral, C., Gelfond, M.: Logic programming and knowledge representation. J. Log. Program. **19**(20), 73–148 (1994)
- Boley, H., Kifer, M. (eds.): RIF Overview. W3C Recommendation, February 5, 2013 (2013). <http://www.w3.org/TR/rif-overview/>

8. Bonatti, P.A., Faella, M., Sauro, L.:  $\mathcal{EL}$  with default attributes and overriding. In: Patel-Schneider, P.F., Pan, Y., Hitzler, P., Mika, P., Zhang, L., Pan, J.Z., Horrocks, I., Glimm, B. (eds.) ISWC 2010, Part I. LNCS, vol. 6496, pp. 64–79. Springer, Heidelberg (2010)
9. Calejo, M.: InterProlog: towards a declarative embedding of logic programming in java. In: Alferes, J.J., Leite, J. (eds.) JELIA 2004. LNCS (LNAI), vol. 3229, pp. 714–717. Springer, Heidelberg (2004)
10. Drabent, W., Henriksson, J., Maluszynski, J.: Hd-rules: a hybrid system interfacing prolog with dl-reasoners. In: Procs. of ALPSWS, vol. 287 (2007)
11. Drabent, W., Maluszynski, J.: Hybrid rules with well-founded semantics. *Knowl. Inf. Syst.* **25**(1), 137–168 (2010)
12. Eiter, T., Ianni, G., Lukasiewicz, T., Schindlauer, R., Tompits, H.: Combining answer set programming with description logics for the semantic web. *Artif. Intell.* **172**(12–13), 1495–1539 (2008)
13. Gelder, A.V., Ross, K.A., Schlipf, J.S.: The well-founded semantics for general logic programs. *J. ACM* **38**(3), 620–650 (1991)
14. Giordano, L., Gliozzi, V., Olivetti, N., Pozzato, G.L.: Reasoning about typicality in low complexity dls: the logics  $\mathcal{EL}^\perp\text{T}_{min}$  and  $DL\text{-Lite}_c\text{T}_{min}$ . In: Procs. of IJCAI (2011)
15. Gomes, A.S., Alferes, J.J., Swift, T.: Implementing query answering for hybrid MKNF knowledge bases. In: Carro, M., Peña, R. (eds.) PADL 2010. LNCS, vol. 5937, pp. 25–39. Springer, Heidelberg (2010)
16. Gonçalves, R., Alferes, J.J.: Parametrized logic programming. In: Janhunen, T., Niemelä, I. (eds.) JELIA 2010. LNCS, vol. 6341, pp. 182–194. Springer, Heidelberg (2010)
17. Heymans, S., Eiter, T., Xiao, G.: Tractable reasoning with dl-programs over datalog-rewritable description logics. In: Procs of ECAI, pp. 35–40. IOS Press (2010)
18. Hitzler, P., Krötzsch, M., Parsia, B., Patel-Schneider, P.F., Rudolph, S. (eds.): OWL 2 Web Ontology Language: Primer (Second Edition). W3C Recommendation, December 11, 2012 (2012). <http://www.w3.org/TR/owl2-primer/>
19. Ivanov, V., Knorr, M., Leite, J.: A query tool for  $EL$  with non-monotonic rules. In: Alani, H., Kagal, L., Fokoue, A., Groth, P., Biemann, C., Parreira, J.X., Aroyo, L., Noy, N., Welty, C., Janowicz, K. (eds.) ISWC 2013, Part I. LNCS, vol. 8218, pp. 216–231. Springer, Heidelberg (2013)
20. Kaminski, T., Knorr, M., Leite, J.: Efficient paraconsistent reasoning with ontologies and rules. In: Procs. of IJCAI. IJCAI/AAAI (2015)
21. Kazakov, Y., Krötzsch, M., Simančík, F.: The incredible ELK: From polynomial procedures to efficient reasoning with  $\mathcal{EL}$  ontologies. *Journal of Automated Reasoning* **53**, 1–61 (2013)
22. Knorr, M., Alferes, J.J., Hitzler, P.: Local closed world reasoning with description logics under the well-founded semantics. *Artif. Intell.* **175**(9–10), 1528–1554 (2011)
23. Knorr, M., Alferes, J.J.: Querying OWL 2 QL and non-monotonic rules. In: Aroyo, L., Welty, C., Alani, H., Taylor, J., Bernstein, A., Kagal, L., Noy, N., Blomqvist, E. (eds.) ISWC 2011, Part I. LNCS, vol. 7031, pp. 338–353. Springer, Heidelberg (2011)
24. Knorr, M., Hitzler, P., Maier, F.: Reconciling OWL and non-monotonic rules for the semantic web. In: Procs. of ECAI, pp. 474–479. IOS Press (2012)
25. Knorr, M., Slota, M., Leite, J., Homola, M.: What if no hybrid reasoner is available? Hybrid MKNF in multi-context systems. *J. Log. Comput.* **24**(6), 1279–1311 (2014)

26. Lifschitz, V.: Nonmonotonic databases and epistemic queries. In: Procs. of IJCAI (1991)
27. Motik, B., Cuenca Grau, B., Horrocks, I., Wu, Z., Fokoue, A., Lutz, C. (eds.): OWL 2 Web Ontology Language: Profiles. W3C Recommendation, February 5, 2013. <http://www.w3.org/TR/owl2-profiles/>
28. Motik, B., Rosati, R.: Reconciling description logics and rules. J. ACM **57**(5) (2010)
29. Slota, M., Leite, J., Swift, T.: Splitting and updating hybrid knowledge bases. TPLP **11**(4–5), 801–819 (2011)
30. Xiao, G., Eiter, T., Heymans, S.: The DReW system for nonmonotonic dl-programs. In: Procs. of SWWS 2012. Springer Proceedings in Complexity. Springer (2013)

# On the Cognitive Surprise in Risk Management: An Analysis of the Value-at-Risk (VaR) Historical

Davi Baccan<sup>1(✉)</sup>, Elton Sbruzzi<sup>2</sup>, and Luis Macedo<sup>1</sup>

<sup>1</sup> CISUC, Department of Informatics Engineering, University of Coimbra,  
Coimbra, Portugal

{baccan,macedo}@dei.uc.pt

<sup>2</sup> CCFEA, University of Essex, Colchester, UK  
efsbru@essex.ac.uk

**Abstract.** Financial markets are environments in which a variety of products are negotiated by heterogeneous agents. In such environments, agents need to cope with uncertainty and with different kinds of risks. In trying to assess the risks they face, agents use a myriad of different approaches to somewhat quantify the occurrence of risks and events that may have a significant impact. In this paper we address the problem of risk management from the cognitive science perspective. We compute the cognitive surprise “felt” by an agent relying on a popular risk management tool known as Value-at-Risk (VaR) historical. We applied this approach to the S&P500 index from 26-11-1990 to 01-07-2009, and divided the series into two subperiods, a calm period and a crash period. We carried out an experiment with twelve different treatments and for each treatment we compare the intensity of surprise “felt” by the agent under these two different regimes. This interdisciplinary work contributes toward the truly understanding and improvement of complex economical and financial systems, specifically in providing insights on the behaviour of cognitive agents in those contexts.

**Keywords:** Agent-based computational economics · Artificial agents · Cognitive architectures · Cognitive modelling · Social simulation and modelling

## 1 Introduction

Financial markets such as stock markets are complex and dynamic environments in which a variety of products are negotiated by a very large number of heterogeneous agents ([1], [2]). Agents, either human, artificial or hybrid, are heterogeneous in the sense that they have, for instance, different preferences, beliefs, goals, and trading strategies (e.g., [3], [4]). Additionally, in such environments agents need to cope with uncertainty and with different kinds of risks [5].

Generally speaking, in economical and financial systems, agents usually try to assess in an objective or subjective way the risks they face. Ideally they would

be able to come up with probabilities, either mathematical or not (e.g., subjective belief), to the occurrence of events that may have a positive or negative impact (e.g., [6], [7]) given his/her preferences and considering his/her goals [8]. Furthermore, agents tend to typically trade based on the risk-return trade-off, i.e., lower (higher) levels of risk are generally associated with lower (higher) levels of potential returns [9].

There are several different theories and hypotheses that try to explain how agents behave and how a stock market works (e.g., [3]). In short, there are two different and opposite perspectives. On the one hand, traditional economic theories (e.g., Efficient Market Hypothesis (EMH) [1]) rely, for instance, on the assumption that, when confronted with decisions that involve risk, agents are able to correctly form their probabilistic assessments according to the laws of probability [10], calculating which of the alternative courses of action maximize their expected utility. On the other hand, behavioral economics (e.g., [11]), i.e., the combination of psychology and economics that aims to understand human decision-making under risk as well as how this behaviour matters in economic contexts, have documented that there are deviations, known as behavioral biases, from the so-called rational behaviour. These behavioral biases are believed to be ubiquitous to humans, and several of them are clearly counterproductive from the economics perspective. Although the discussion regarding these different perspectives is of importance and fascinating for us, it is out of the scope of this work.

Nevertheless, we claim that, given the nature and complexity of financial markets together with the sophisticated and complex human decision-making mechanism (which is influenced by a myriad of intertwined factors), that the task of risk management is quite complex and falls on the category of those who requires the application of different and novel approaches in order to be improved ([12], [13], [14]). For instance, there are extensive empirical evidence (e.g., [5]) suggesting that the financial crisis of 2007/2008 was significantly aggravated by inappropriate risk management systems and tools.

However, perhaps more important for agents than having a good risk management system or tool is to rely on a system or tool that is in line with his/her behavioral and emotional profile. For instance, the underestimation of the occurrence of a given event may lead a particular agent to make a risky decision (e.g., excessive leverage) that may eventually elicit the surprise emotion in the agent with a high level of intensity as well as may probably result in substantial financial losses [15].

In this paper we address the problem of risk management from the cognitive science perspective by computing the cognitive surprise “felt” by an agent relying on a popular and widespread used risk management tool known as Value-at-Risk (VaR) historical. To this end, we model the VaR historical based on the principles of cognitive emotion theories and compute the cognitive surprise based on an artificial surprise model. We applied this approach to the S&P500 index and divide the series into two subperiods, a calm period and a crash period. We carried out an experiment with twelve different treatments, and for each treatment we compare the intensity of surprise “felt” by the agent under these two different regimes.

## 2 Value-at-Risk (VaR)

The Value-at-Risk (VaR) tool is one of the most popular financial risk measures, used by financial institutions all over the world [16]. The objective of the VaR is to measure the probability for significant loss in a portfolio of financial assets [17]. Generally speaking, we can assume that for a given time horizon  $t$  and a confidence level  $p$ , VaR is the loss in market value over the time horizon  $t$  that is exceeded with probability  $1 - p$  [18]. For example, suppose a period of one-day ( $t = 1$ ) and a confidence level  $p$  of 95%, the VaR would be 0.05 or 5% the critical value. There are several different methods for calculating VaR. For instance, let us briefly present the following two methods to calculate VaR, the statistical and historical approach [19].

The VaR statistical assumes that the historical returns respect the EMH. The EMH in turn assumes that the series of historical financial returns are Gaussian, with the average value  $\mu$  of zero and constant variance of  $\sigma^2$ , i.e., returns  $\sim \mathcal{N}(0, \sigma^2)$ . Based on the EMH assumptions and on the Gaussian characteristics, we could compute that VaR statistical for a confidence level  $p$  of 99% and 95% are  $-2\sigma$  and  $-3\sigma$ , respectively. For example, if a series of returns show a standard deviation of 5%, the VaR statistical for a confidence level of 99% and 95% are -10% and -15%, respectively.

Unlike the VaR statistical method, an alternative way to calculate VaR is to rank the historical simulation from the smallest to the highest, which is named VaR historical. Suppose that the series of  $T$  returns are  $r_1, \dots, r_t$ , we define that this series of returns are ranked if  $r_1 \leq r_2 \leq \dots \leq r_T$ . In this case, the VaR historical is the return on the position integer  $((1 - p) T)$ . For example, suppose a confidence level  $p$  of 99% and  $T$  of 250, the VaR historical would be  $r_3$ . In the case of  $p$  of 95%, the VaR historical would be  $r_5$ .

We consider the VaR historical as the most appropriate method for this work for several reasons. First, because the VaR historical method is widely used by practitioners ([20], [21], [22]). Second, because it is an easy to understand measure that computes the estimation based on historical data and a confidence level (we will later explain in Section 3.2 the particular importance of confidence). Last but not least, because unlike the VaR statistical, VaR historical is free of the assumption about the distribution of the series of returns [19].

## 3 Surprise in Cognitive Science

From the perspective of cognitive emotions theories (e.g., [23], [24]), surprise can be thought of as a belief-disconfirmation signal or a mismatch generated as a result of the comparison between a newly acquired belief and a pre-existing belief. Formally speaking, surprise is a neutral valence emotion, defined as a peculiar state of mind, usually of brief duration, caused by unexpected events, or proximally the detection of a contradiction or conflict between a newly acquired and pre-existing belief ([25], [26]).

Surprise serves us in many functions and can be considered as a key element for survival in a complex and rapidly changing environment. It is closely related

to how beliefs are stored in memory. Our semantic memory, i.e., our general knowledge and concepts about the world, is assumed to be represented in memory through knowledge structures known as schemas (e.g., [27]). A schema is a well-integrated chunk of knowledge or sets of beliefs, which main source of information available comes from abstraction from repeated personally experienced events or generalizations, that are our episodic memory.

### 3.1 The Surprise Process

Meyer and colleagues [25] proposed a cognitive-psychoevolutionary model of surprise. They claim surprise-eliciting events elicit a four-step sequence of processes. The first step is the appraisal of an event as unexpected or schema-discrepant.

Then in the second step, if the degree of unexpectedness or schema-discrepancy exceeds a certain threshold, surprise is experienced, ongoing mental process are interrupted and resources such as attention are reallocated towards the unexpected event.

The third step is the analysis and evaluation of the unexpected event. It generally includes a set of subprocesses namely the verification of the schema discrepancy, the analysis of the causes of the unexpected event, the evaluation of the unexpected event's significance for well-being, and the assessment of the event's relevance for ongoing action. It is assumed that some aspects of the analysis concerning the unexpected event are stored as part of the schema for this event so that in the future analysis of similar events can be significantly reduced both in terms of time and cognitive effort.

The fourth step is the schema update. It involves producing the immediate reactions to the unexpected event, and/or operations such as the update, extension, or revision of the schema or sets of beliefs that gave rise to the discrepancy. The schema change ideally enables one to some extent to predict and control future occurrences of the schema-discrepant event and, if possible, to avoid the event if it is negative and uncontrollable, or to ignore the event if it is irrelevant for action.

### 3.2 Artificial Surprise

Two models of artificial surprise for artificial agents can be stressed, namely the model proposed by Macedo and Cardoso [28] and the model proposed by Lorini and Castelfranchi [29]. Both models were mainly inspired by the cognitive-psychoevolutionary model of surprise proposed by Meyer and colleagues [25] and have influence of the analysis of the cognitive causes of surprise from a cognitive science perspective proposed by Ortony and Partridge [30]. The comparative study of these two models is out of the scope of this work. To a detailed description of the similarities and differences of the models please see [26]. The empirical tests we performed provide evidence in favor of using the model proposed by Macedo and Cardoso in our work.

Macedo and colleagues carried out an empirical study [28] with the goal of investigating how to compute the intensity of surprise in an artificial agent.

This study suggests that the intensity of surprise about an event  $E_g$ , from a set of mutually exclusive events  $E_1, E_2, \dots, E_m$ , is a nonlinear function of the difference, or contrast, between its probability/belief and the probability/belief of the highest expected event ( $E_h$ ) in the set of mutually exclusive events  $E_1, E_2, \dots, E_m$ .

Formally, let  $(\Omega, A, P)$  be a probability space where  $\Omega$  is the sample space (i.e., the set of possible outcomes of the event),  $A = A_1, A_2, \dots, A_n$ , is a  $\sigma$ -field of subsets of  $\Omega$  (also called the event space, i.e., all the possible events), and  $P$  is a probability measure which assigns a real number  $P(F)$  to every member  $F$  of the  $\sigma$ -field  $A$ . Let  $E = E_1, E_2, \dots, E_m$ ,  $E_i \in A$ , be a set of mutually exclusive events in that probability space with probabilities  $P(E_i) \geq 0$ , such that  $\sum_{i=1}^m P(E_i) = 1$ .

Let  $E_h$  be the highest expected event from  $E$ . The intensity of surprise about an event  $E_g$ , defined as  $S(E_g)$ , is calculated as  $S(E_g) = \log_2(1 + P(E_h) - P(E_g))$  (Equation 1). In each set of mutually exclusive events, there is always at least one event whose occurrence is unsurprising, namely  $E_h$ .

## 4 Experiments and Results

The goal of our experiment is to compute the cognitive surprise “felt” by an agent relying on a popular risk management tool known as Value-at-Risk (VaR) historical under different financial settings and regimes.

First, we selected the S&P500, i.e., an index based on market capitalization that includes 500 companies in leading industries in the U.S. economy, from 26-11-1990 to 01-07-2009, in a total of 4688 days. The S&P500 index is recognized as one of the most important stock market indexes (perhaps the most important). First, we applied a method similar to the work of Halbleib and Pohlmeier [20] to divide the selected S&P500 period into two parts, a calm period from 26-11-1990 to 31-08-2008 (total of 4478 days), and a crash period from 01-09-2008 to 01-07-2009 (total of 210 days). The data was obtained free of charge from Yahoo Finance. Figure 1 presents the daily close, daily return, and the histogram of daily returns of the S&P500 from 26-11-1990 to 01-07-2009. Figure 2 presents the daily close and the histogram of daily returns of the S&P500 of calm and crash periods.

We employed two different approaches in our experiment. The first approach consists in specifying a rolling window size and a confidence level, which combination is used by the VaR historical to compute the estimation by considering the most recent returns. The windows size set contains the 50, 125, 250, and 500 values. The confidence level set contains the 0.95 and 0.99 values. The combination of the window size values with the confidence level values result in 8 different treatments.

The second approach consists in specifying a decay function so that recent daily returns gain more weight as opposed to old returns. Decay functions are generally used with the objective of emulating to a certain extent the human memory process of “forgetting” as well as to contemplate some findings from

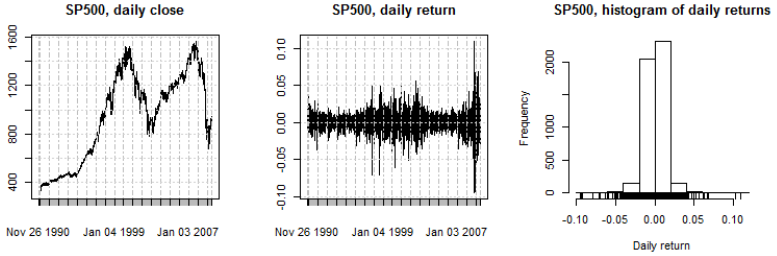


**Fig. 1.** SP500, daily close (left), daily return (center), and histogram of daily return (right).

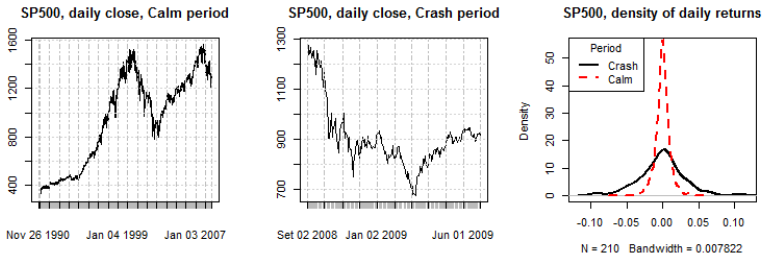


**Fig. 2.** SP500, daily close of calm period (left), daily close of crash period (center), and histogram of daily return of calm period and crash period (right)

how humans use past experience in decision-making (e.g., [31]) which indicate that in revising their beliefs, people tend to overweight recent information and underweight prior information. The alpha set contains the 0.995, 0.99, 0.97, 0.94 values. A higher (lower) alpha implies a smaller (higher) level of forgetfulness. Unlike the first approach, we opted to use just a confidence level of 0.99. The reason is that we observed in our initial experiments that the combination of a confidence level of 0.95 with the previous alpha values caused the agent to “forget” too many returns, generating in the end a quite low and poor VaR historical estimation. Therefore, in the second approach we have four treatments. We conducted an experiment with these twelve different treatments.

The algorithm we used in our experiment works as follows. We first perform initial adjustments to ensure that all iterations are actually carried out within a specified period. For each simulation (1) for a window size value,  $window_k \in \{50, 125, 250, 500\}$ , (2) according to a uniform distribution function, we select a begin day  $d_i$  within the period (for the calm period we fixed the  $d_i = 01-09-2008$ ), (3) we compute the VaR historical estimations  $\text{VaR}_{95}$  and  $\text{VaR}_{99}$  based on  $window_k$  daily returns preceding the  $d_i$  as well as the confidence levels  $p \in \{0.95, 0.99\}$ , respectively, (4) for each day  $d_k$  beginning in the day after  $d_i$ , from  $k = i + 1$  to  $k = 210$  (for the next 210 days), we check if daily return of  $d_k \leq \text{VaR}_{95}$  and if daily return of  $d_k \leq \text{VaR}_{99}$ , (5) we advance the rolling window one day, i.e.,

$i = i + 1$ , and (6) we back to step (3). For the alpha approach the algorithm is similar, except for some minor adjustments, specifically in step (1) since the algorithm runs for each alpha value  $\in \{0.995, 0.99, 0, 97, 0.94\}$ , and in step (3) since we modify the preceding daily returns by applying the current alpha value and compute the VaR historical estimation with a confidence level  $p$  of 0.99. All other steps are exactly the same.

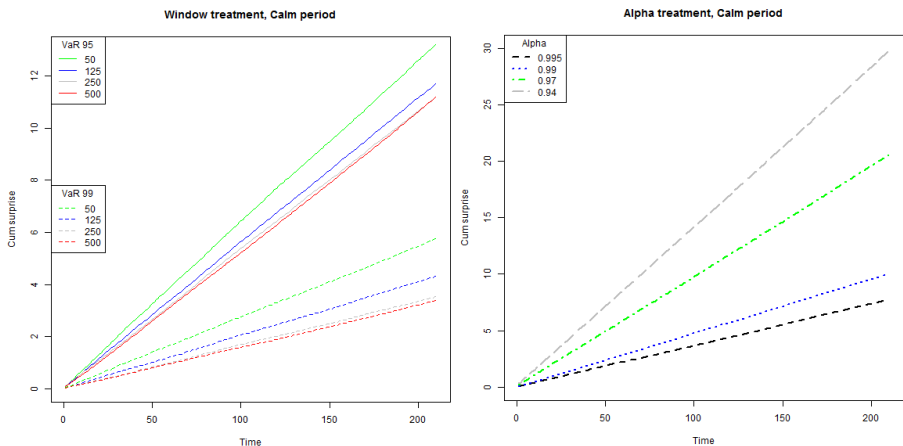
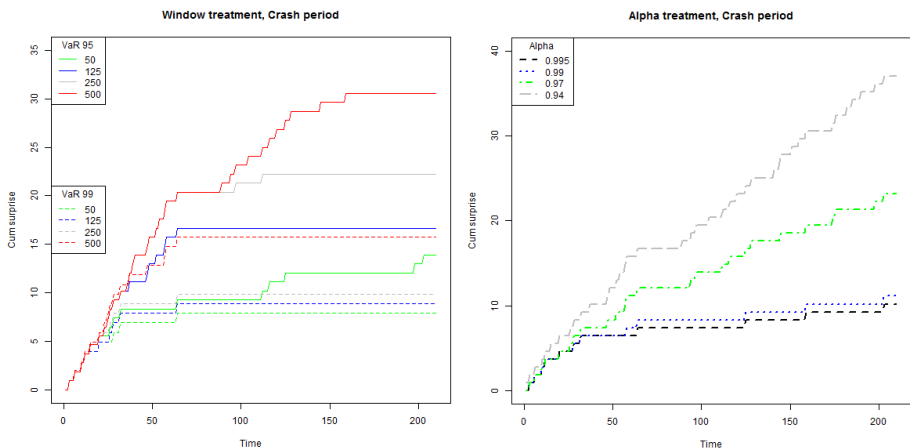
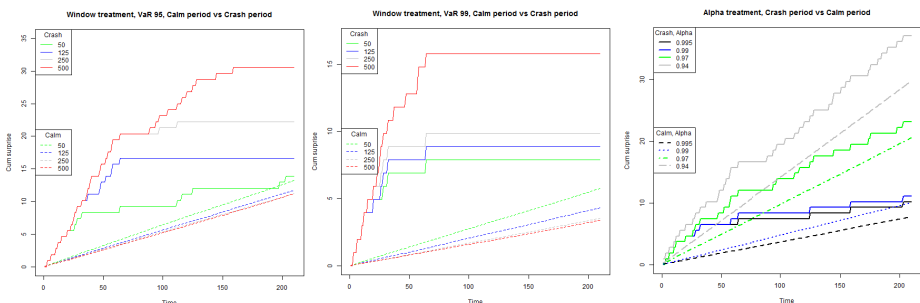
Let us now describe how we address this problem in the context of the artificial surprise, presented in Section 3. We essentially applied the concepts, ideas, and method presented by Baccan and Macedo [32]. This work can be thought of as a continuation and expansion of their initial work to other contexts. We assume, for the sake of the experiment and simplicity, the confidence levels  $p$  (0.99, and 0.95) as the subjective belief of the agent in the accurateness of the VaR historical estimation. By making this assumption and considering a higher subjective belief, we are empowering the agent with a “firmly believe” in the accurateness of the VaR historical estimation. So, suppose an event  $E_g$  as VaR historical estimation that can assume two mutually exclusive events, meaning that it can be either correct ( $E_1$ ), i.e., daily return is not lower than estimation, or incorrect ( $E_2$ ), i.e., daily return is lower than estimation.

The agent will either “feels” no surprise (a higher intensity of surprise) as what he/she considered as more (less) likely, i.e., correct ( $E_1$ ) (incorrect ( $E_2$ )), happened. More precisely, for the confidence level of 0.99 the surprise about event  $E_2$  would be 0.9855004, i.e.,  $S(E_g) = \log_2(1 + 0.99 - 0.01)$ . Similarly, for the confidence level of 0.95 the surprise about event  $E_2$  would be 0.9259994, i.e.,  $S(E_g) = \log_2(1 + 0.95 - 0.05)$ . For each day  $d_k$  in which the VaR historical estimation is tested in step (4) of the algorithm described above, if the daily return of  $d_k \leq \text{VaR}_p$ , then we compute the cognitive surprise,  $surprise_k$ .

In the end we have a sequence  $\{surprise_1, \dots, surprise_{210}\}$ . Afterwards, for each simulation, we compute the cumulative sum of the surprise. It means that we generate a sequence of 210 elements as a result of the partial sums  $surprise_1$ ,  $surprise_1 + surprise_2$ ,  $surprise_1 + surprise_2 + surprise_3$ , and so forth. In the case of the calm period, we added the cumulative sum of the surprise of each treatment and then average it by the number of simulations. The cumulative sum and the average assumption make it easier both the observation of surprise over time as well as the comparison of surprise between the calm and crash period. The average cumulative sum of the surprise for a given treatment is presented in the next figures for the calm period.

We ran  $10^4$  independent simulations for each treatment for the calm period and one simulation for each treatment for the crash period (since the begin day  $d_i = 01-09-2008$  is fixed).

Figures 3 and 4 present the behaviour of all treatments for the calm period and crash period, respectively. Figures 5 present a comparison between different rolling window treatments and alpha treatments, respectively, for both periods.

**Fig. 3.** All treatments for the calm period.**Fig. 4.** All treatments for the crash period.**Fig. 5.** Comparing different treatments for different periods.

## 5 Discussion

First of all, it is important to bear in mind that financial markets are by their very nature complex and dynamic systems. Such complexity significantly increases if we take into account the sophisticated and complex human decision-making mechanism. As a result, we believe that the task of risk management in finance and economics is indeed quite difficult. Therefore, we do not have in this work the goal of providing evidence neither in favor of nor against to a particular risk management tool or system. Instead, our goal is to compute, in a systematic and clear method, the cognitive surprise “felt” by an agent relying on the VaR historical during different periods, a calm period and a crash period.

Let us then begin by analyzing some characteristics of the calm period in comparison with the crash period. We can see in Figure 1 that daily returns seem, as expected and in line with the existing literature, to reproduce some statistical regularities that are often found in a large set of different assets and markets known as stylized facts [33]. Specifically we can observe that returns do not follow a Gaussian distribution (are not normally distributed), seem to exhibit what is known as fat-tails, as well as to reproduce the volatility clustering fact, i.e., high-volatility events tend to cluster in time. Volatility clustering resembles the concept of entropy used in a variety of areas such as information and communication theory. We can see in Figure 2 that the comparison between the daily returns of the calm period with the daily returns of the crash period allows us to claim that the daily returns for the crash period seem to exhibit fat tail distributions. We can also see that during the crash period the SP&500 depreciated almost 50% in value in a short period of time.

We now turn our attention to the analysis of the cognitive surprise. For the calm period, we can observe in Figure 3 that the cumulative surprise for alpha treatment (right) is higher when compared to all window treatments (left). Additionally, the lower the alpha, the higher the cumulative surprise and, similarly, the larger the window size, the lower the surprise. The cumulative surprise of the window treatments with a confidence level  $p$  of 0.95,  $\text{VaR}_{95}$  is, in turn, higher when compared to the cumulative surprise with a confidence level  $p$  of 0.99,  $\text{VaR}_{99}$ . Interestingly, if we assume that alpha somewhat emulates the human memory process of “forgetting” and considering that a lower alpha implies a higher level of forgetfulness, we may argue that an agent should be careful in forgetting the past, at least in the context of a stock market, since the cognitive surprise “felt” by an agent under this treatment is significantly higher than the window treatment.

For the crash period, we first observe in Figure 4 that, once again, the lower the alpha, the higher the cumulative surprise (right). However, quite contrary to the calm period, the lower the window size, the lower the surprise (left). The cognitive surprise “felt” is higher for agents that rely on a larger window size. It may be explained by the fact that the crash period is indeed a period in which the volatility is high. Therefore, a VaR historical based on a larger window size takes more time to adapt to this new and changing environment, in comparison with a VaR historical based on a smaller window size.

When comparing in Figure 5 how treatments behave during the calm period and the crash period, we can observe that, as expected, the cognitive surprise is higher during the crash period.

Generally speaking, each day the agent “felt” surprise represents a failed VaR historical estimation. Therefore, the higher the surprise, the wrong a given VaR historical treatment is. The analysis of the results indicate that it may be quite difficult for an agent not to “feel” surprise when relying on VaR historical. Indeed, there are several issues with models, like VaR historical, that take into account historical data for their estimation. These models somewhat assume the past is a good indicator of what may happen in the future, i.e., history repeats itself. However, this inductive reasoning often underestimate the probability of extreme returns and, consequently, underestimates the level of risk. Additionally, an essential flaw of this kind of rationale is not to truly acknowledge that “absence of evidence is not evidence of absence” and the existence of “unknown unknowns” [34].

Consider, for instance, the turkey paradox ([35]). There is a butcher and a turkey. Every day for let us say 100 days the butcher feeds the turkey. As time goes by the turkey increases its belief that in the next day it will receive food from the butcher. However, at a given day, for the “shock” and “surprise” of the turkey, instead of being feed by the butcher, the butcher kills the turkey. The same analogy may be applied to the black swan scenario [6] as well as to other complex and risky financial operations that provide small but regular gains, until the day they blow all the gains, resulting in huge losses [15].

The main contribution of our work resides in the fact that we have applied in a systematic, clear and easy to reproduce way the ideas, concepts and methods described by Baccan and Macedo [32] to the context of risk, uncertainty, and therefore risk management. Our interdisciplinary work is in line with those who claim that there is a need for novel approaches so that complex and financial systems may be improved (e.g., [12], [13], [14]). It is, as far as we know, one of the first attempts to apply a cognitive science perspective to risk management.

## 6 Conclusion and Future Work

In this paper we addressed the problem of risk management from the cognitive science perspective<sup>1</sup>. We computed the cognitive surprise “felt” by an agent relying on a popular risk management tool known as Value-at-Risk (VaR) historical. We applied this approach to the S&P500 stock market index from 26-11-1990 to 01-07-2009, and divide the series into two subperiods, a calm period and a crash period. We carried out an experiment with twelve different treatments and for each treatment we compare the intensity of surprise “felt” by the agent under these two different regimes. This interdisciplinary work is in line with a broader movement and contributes toward the truly understanding and improvement of

---

<sup>1</sup> This work was supported by FCT, Portugal, SFRH/BD/60700/2009, and by TribeCA project, funded by FEDER through POCentro, Portugal.

complex economical and financial systems, specifically in providing insights on the behaviour of cognitive agents in those risky and uncertain contexts.

The use of cognitive modeling approaches to the study of complex and dynamic systems is in its early stages. We consider that the use of relatively simple but powerful tools in conjunction with cognitive models, like those discussed in this work, offers a rich and novel set of possibilities. For instance, the use of cognitive agents would allow us to carry out a variety of different agent and multi-agent-based simulations of significant economical and financial events, so that we would be able to compute individual cognitive surprise and, in the end, the global surprise of agents regarding some event. It may provide contributions toward the understanding of the behaviour of agents individually as well as of the system as a whole. Last but not least, it would be interesting to compare the global surprise with other market sentiment indexes (e.g., VIX, the “fear” indicator).

## References

1. Fama, E.F.: Efficient capital markets: A review of theory and empirical work. *The Journal of Finance* **25**(2), 383–417 (1970)
2. Fama, E.F.: Two pillars of asset pricing. *American Economic Review* **104**(6), 1467–1485 (2014)
3. Lo, A.W.: Reconciling efficient markets with behavioral finance: The adaptive markets hypothesis. *Journal of Investment Consulting* **7**, 21–44 (2005)
4. Treleaven, P., Galas, M., Lachand, V.: Algorithmic trading review. *Commun. ACM* **56**(11), 76–85 (2013)
5. Lo, A., Mueller, M.: WARNING: physics envy may be hazardous to your wealth!. *Journal of Investment Management* **8**, 13–63 (2010)
6. Taleb, N.N.: *The Black Swan: The Impact of the Highly Improbable*, 1st edn. Random House, April 2007
7. Meder, B., Lec, F.L., Osman, M.: Decision making in uncertain times: what can cognitive and decision sciences say about or learn from economic crises? *Trends in Cognitive Sciences* **17**(6), 257–260 (2013)
8. Markowitz, H.: Portfolio selection. *Journal of Finance* **7**, 77–91 (1952)
9. Kahneman, D.: The myth of risk attitudes. *The Journal of Portfolio Management* **36**(1), 1 (2009)
10. Chiodo, A., Guidolin, M., Owyang, M.T., Shimoji, M.: Subjective probabilities: psychological evidence and economic applications. Technical report, Federal Reserve Bank of St. Louis (2003)
11. Kahneman, D., Tversky, A.: Prospect theory: An analysis of decision under risk. *Econometrica* **47**(2), 263–291 (1979)
12. Farmer, J.D., Foley, D.: The economy needs agent-based modelling. *Nature* **460**(7256), 685–686 (2009)
13. Bouchaud, J.: Economics needs a scientific revolution. *Nature* **455**(7217), 1181 (2008)
14. Gatti, D., Gaffeo, E., Gallegati, M.: Complex agent-based macroeconomics: a manifesto for a new paradigm. *Journal of Economic Interaction and Coordination* **5**(2), 111–135 (2010)

15. Taleb, N.N.: *Antifragile: Things That Gain from Disorder*. Reprint edition edn. Random House Trade Paperbacks, New York (2014)
16. Kawata, R., Kijima, M.: Value-at-risk in a market subject to regime switching. *Quantitative Finance* **7**(6), 609–619 (2007)
17. Alexander, C., Sarabia, J.M.: Quantile Uncertainty and Value-at-Risk Model Risk. *Risk Analysis* **32**(8), 1293–1308 (2012)
18. Duffie, D., Pan, J.: An Overview of Value at Risk. *The Journal of Derivatives* **4**(3), 7–49 (1997)
19. Jorion, P.: *Value at Risk: The New Benchmark for Managing Financial Risk*, 3rd edn. McGraw-Hill (2006)
20. Halbleib, R., Pohlmeier, W.: Improving the value at risk forecasts: Theory and evidence from the financial crisis. *Journal of Economic Dynamics and Control* **36**(8), 1212–1228 (2012)
21. David Cabedo, J., Moya, I.: Estimating oil price Value at Risk using the historical simulation approach. *Energy Economics* **25**(3), 239–253 (2003)
22. Hendricks, D.: Evaluation of value-at-risk models using historical data. *Economic Policy Review*, 39–69, April 1996
23. Reisenzein, R., Hudlicka, E., Dastani, M., Gratch, J., Hindriks, K., Lorini, E., Meyer, J.J.: Computational modeling of emotion: Towards improving the inter- and intradisciplinary exchange. *IEEE Transactions on Affective Computing* **99**(1), 1 (2013)
24. Reisenzein, R.: Emotions as metarepresentational states of mind: Naturalizing the belief-desire theory of emotion. *Cognitive Systems Research* **10**(1), 6–20 (2009)
25. Meyer, W.U., Reisenzein, R., Schutzwohl, A.: Toward a process analysis of emotions: The case of surprise. *Motivation and Emotion* **21**, 251–274 (1997)
26. Macedo, L., Cardoso, A., Reisenzein, R., Lorini, E., Castelfranchi, C.: Artificial surprise. In: *Handbook of Research on Synthetic Emotions and Sociable Robotics: New Applications in Affective Computing and Artificial Intelligence*, pp. 267–291 (2009)
27. Baddeley, A., Eysenck, M., Anderson, M.C.: *Memory*, 1 edn. Psychology Press, February 2009
28. Macedo, L., Reisenzein, R., Cardoso, A.: Modeling forms of surprise in artificial agents: empirical and theoretical study of surprise functions. In: *26th Annual Conference of the Cognitive Science Society*, pp. 588–593 (2004)
29. Lorini, E., Castelfranchi, C.: The cognitive structure of surprise: looking for basic principles. *Topoi: An International Review of Philosophy* **26**, 133–149 (2007)
30. Ortony, A., Partridge, D.: Surprisingness and expectation failure: what's the difference? In: *Proceedings of the 10th International Joint Conference on Artificial Intelligence*, vol. 1, pp. 106–108. Morgan Kaufmann Publishers Inc., Milan (1987)
31. Griffin, D., Tversky, A.: The weighing of evidence and the determinants of confidence. *Cognitive Psychology* **24**(3), 411–435 (1992)
32. Baccan, D., Macedo, L., Sbruzzi, E.: Towards modeling surprise in economics and finance: a cognitive science perspective. In: *STAIRS 2014. Frontiers in Artificial Intelligence and Applications*, vol. 264, Prague, Czech Republic, pp. 31–40 (2014)
33. Cont, R.: Empirical properties of asset returns: stylized facts and statistical issues. *Quantitative Finance* **1**(2), 223 (2001)
34. Rumsfeld, D.: DoD News Briefing (2002)
35. Taleb, N.N.: *Fooled by Randomness: The Hidden Role of Chance in Life and in the Markets*, 2 edn. Random House, October 2008

# Logic Programming Applied to Machine Ethics

Ari Saptawijaya<sup>1,2(✉)</sup> and Luís Moniz Pereira<sup>1</sup>

<sup>1</sup> NOVA Laboratory for Computer Science and Informatics (NOVA LINCS), Departamento de Informática, Faculdade de Ciências e Tecnologia, Universidade Nova de Lisboa, Lisboa, Portugal  
`ar.saptawijaya@campus.fct.unl.pt, lmp@fct.unl.pt`

<sup>2</sup> Faculty of Computer Science, Universitas Indonesia, Depok, Indonesia

**Abstract.** This paper summarizes our investigation on the application of LP-based reasoning to machine ethics, a field that emerges from the need of imbuing autonomous agents with the capacity for moral decision-making. We identify morality viewpoints (concerning moral permissibility and the dual-process model) as studied in moral philosophy and psychology, which are amenable to computational modeling. Subsequently, various LP-based reasoning features are applied to model these identified morality viewpoints, via classic moral examples taken off-the-shelf from the literature.

## 1 Introduction

The need for systems or agents that can function in an ethically responsible manner is becoming a pressing concern, as they become ever more autonomous and act in groups, amidst populations of other agents, including humans. Its importance has been emphasized as a research priority in AI with funding support [26]. Its field of enquiry, named *machine ethics*, is interdisciplinary, and is not just important for equipping agents with some capacity for moral decision-making, but also to help better understand morality, via the creation and testing of computational models of ethical theories.

Several logic-based formalisms have been employed to model moral theories or particular morality aspects, e.g., deontic logic in [2], non-monotonic reasoning in [6], and the use of Inductive Logic Programming (ILP) in [1]; some of them only abstractly, whereas others also provide implementations (e.g., using ILP-based systems [1], an interactive theorem prover [2], and answer set programming (ASP) [6]). Despite the aforementioned logic-based formalisms, Logic Programming (LP) itself is rather limitedly explored. The potential and suitability of LP, and of computational logic in general, for machine ethics, is identified and discussed at length in [11], on the heels of our work. LP permits declarative knowledge representation of moral cases with sufficiently level of detail to distinguish one moral case from other similar cases. It provides a logic-based programming paradigm with a number of practical Prolog systems, thus allowing not only addressing morality issues in an abstract logical formalism, but also via a Prolog implementation as proof of concept and a testing ground for experimentation. Furthermore, LP are also equipped with various reasoning features,

as identified in the paragraph below, whose applications to machine ethics are promising, but still unexplored. This paper summarizes our integrative investigation on the appropriateness of various LP-based reasoning to machine ethics, not just abstractly, but also furnishing a proof of concept implementation for the morality issues in hand.

We identify conceptual morality viewpoints, which are covered in two morality themes: (1) *moral permissibility*, taking into account viewpoints such as the Doctrines of Double Effect (DDE) [15], Triple Effect (DTE) [10], and Scanlon's contractualist moral theory [23]; and (2) *the dual-process model* [3,14], which stresses the interaction between deliberative and reactive behaviors in moral judgment. The mapping of all these considered viewpoints into LP-based reasoning benefits from its features and their integration, such as abduction with integrity constraints (ICs) [22], preferences over abductive scenarios [4], probabilistic reasoning [7], updating [21], counterfactuals [20], and from LP tabling technique [25].

We show, in Section 2, how these various LP-based reasoning features are employed to model the aforementioned morality viewpoints, including: (1) The use of a priori ICs and a posteriori preferences over abductive scenarios to capture deontological and utilitarian judgments; (2) Probabilistic moral reasoning, to reason about actions, under uncertainty, that might have occurred, and thence provide judgment adhering to moral principles within some prescribed uncertainty level. This permits to capture a form of argumentation (wrt. Scanlon's contractualism [23]) in courts, through presenting different evidences as a consideration whether an exception can justify a verdict of guilty (beyond reasonable doubt) or non-guilty; (3) The use of QUALM, which combines LP abduction, updating, and counterfactuals, supported by LP tabling mechanisms (based on [20–22]) to examine moral permissibility wrt. DDE and DTE, via counterfactual queries. Finally, QUALM is also employed to experiment with the issue of moral updating, allowing for other (possibly overriding) moral rules (themselves possibly subsequently overridden) to be adopted by an agent, on top of those it currently follows.

## 2 Modeling Morality with Logic Programming

### 2.1 Moral Permissibility with Abduction, a Priori ICs and a Posteriori Preferences

In [17], moral permissibility is modeled through several cases of the classic trolley problem [5], by emphasizing the use of ICs in abduction and preferences over abductive scenarios. The cases, which include moral principles, are modeled in order to deliver appropriate moral decisions that conform with those the majority of people make, on the basis of empirical results in [9]. DDE [15] is utilized in [9] to explain the consistency of judgments, shared by subjects from demographically diverse populations, on a series of trolley dilemmas. In addition to DDE, we also consider DTE [10].

Each case of the trolley problem is modeled individually; their details being referred to [17]. The key points of their modeling are as follows. The DDE and DTE are modeled via a priori ICs and a posteriori preferences. Possible decisions are modeled as abducibles, encoded in ACORDA by even loops over default negation. Moral decisions are therefore accomplished by satisfying a priori ICs, computing abductive stable models from all possible abductive solutions, and then appropriately preferring amongst them (by means of rules), a posteriori, just some models, on the basis of their abductive solutions and consequences. Such preferred models turn out to conform with the results reported in the literature.

*Capturing Deontological Judgment via a Priori ICs.* In this application, ICs are used for two purposes. First, they are utilized to force the goal in each case (like in [9]), by observing the desired end goal resulting from each possible decision. Such an IC thus enforces all available decisions to be abduced, together with their consequences, from all possible observable hypothetical end goals. The second purpose of ICs is for ruling out impermissible actions, viz., actions that involve intentional killing in the process of reaching the goal, enforced by the IC:  $false \leftarrow \text{intentional\_killing}$ . The definition of *intentional\_killing* depends on rules in each case considered and whether DDE or DTE is to be upheld. Since this IC serves as the first filter of abductive stable models, by ruling out impermissible actions, it affords us with just those abductive stable models that contain only permissible actions.

*Capturing Utilitarian Judgment via a Posteriori Preferences.* Additionally, one can further prefer amongst permissible actions those resulting in greater good. That is, whereas a priori ICs can be viewed as providing an agent's reactive behaviors, generating intuitively intended responses that comply with deontological judgment (enacted by ruling out the use of intentional harm), a posteriori preferences amongst permissible actions provides instead a more involved reasoning about action-generated models, capturing utilitarian judgment that favors welfare-maximizing behaviors (in line with the dual-process model [3]).

In this application, a preference predicate (e.g., based on a utility function concerning the number of people died) is defined to select those abductive stable models [4] containing decisions with greater good of overall consequences. The reader is referred to [17] for the results of various trolley problem cases.

## 2.2 Probabilistic Moral Reasoning

In [8], probabilistic moral reasoning is explored, where an example is contrived to reason about actions, under uncertainty, and thence provide judgment adhering to moral rules within some prescribed uncertainty level. The example takes a variant of the Footbridge case within the context of a jury trials in court, in order to proffer verdicts beyond reasonable doubt: *Suppose a board of jurors in a court is faced with the case where the actual action of an agent shoving the man onto the track was not observed. Instead, they are just presented with the*

*fact that the man on the bridge died on the side track and the agent was seen on the bridge at the occasion. Is the agent guilty (beyond reasonable doubt), in the sense of violating DDE, of shoving the man onto the track intentionally?*

To answer it, abduction is enacted to reason about the verdict, given the available evidence. Considering the active goal *judge*, to judge the case, two abducibles are available: *verdict(guilty\_brd)* and *verdict(not\_guilty)*, where *guilty\_brd* stands for ‘guilty beyond reasonable doubt’. Depending on how probable each verdict (the value of which is determined by the probability *pr\_int\_shove(P)* of intentional shoving), a preferred *verdict(guilty\_brd)* or *verdict(not\_guilty)* is abduced as a solution.

The probability with which shoving is performed intentionally is causally influenced by evidences and their attending truth values. Two evidences are considered, viz., (1) Whether the agent was running on the bridge in a hurry; and (2) Whether the bridge was slippery at the time. The probability *pr\_int\_shove(P)* of intentional shoving is therefore determined by the existence of evidence, expressed as dynamic predicates *evd\_run/1* and *evd\_slip/1*, whose sole argument is *true* or *false*, standing for the evidences that the agent was running in a hurry and that the bridge was slippery, resp.

Based on this representation, different judgments can be delivered, subject to available (observed) evidences and their attending truth value. By considering the standard probability of proof beyond reasonable doubt –here the value of 0.95 is adopted [16]– as a common ground for the probability of guilty verdicts to be qualified as ‘beyond reasonable doubt’, a form of argumentation (à la Scanlon contractualism [23]) may take place through presenting different evidence (via updating of observed evidence atoms, e.g., *evd\_run(true)*, *evd\_slip(false)*, etc.) as a consideration to justify an exception. Whether the newly available evidence is accepted as a justification to an exception –defeating the judgment based on the priorly presented evidence– depends on its influence on the probability *pr\_int\_shove(P)* of intentional shoving, and thus eventually influences the final verdict. That is, it depends on whether this probability is still within the agreed standard of proof beyond reasonable doubt. The reader is referred to [8], which details a scenario capturing this moral jurisprudence viewpoint.

### 2.3 Modeling Morality with QUALM

Distinct from the two previous applications, QUALM emphasizes the interplay between LP abduction, updating and counterfactuals, supported furthermore by their joint tabling techniques.

*Counterfactuals in Morality.* We revisit moral permissibility wrt. DDE and DTE, but now applying counterfactuals. Counterfactuals may provide a general way to examine DDE in dilemmas, like the classic trolley problem, by distinguishing between a *cause* and a *side-effect* as a result of performing an action to achieve a goal. This distinction between causes and side-effects may explain the permissibility of an action in accordance with DDE. That is, *if some morally wrong effect E happens to be a cause for a goal G that one wants to achieve by performing*

*an action A, and E is not a mere side-effect of A, then performing A is impermissible.* This is expressed by the counterfactual form below, in a setting where action A is performed to achieve goal G: “*If not E had been true, then not G would have been true.*”

The evaluation of this counterfactual form identifies permissibility of action A from its effect E, by identifying whether the latter is a necessary cause for goal G or a mere side-effect of action A: if the counterfactual proves valid, then E is instrumental as a cause of G, and not a mere side-effect of action A. Since E is morally wrong, achieving G that way, by means of A, is impermissible; otherwise, not. Note, the evaluation of counterfactuals in this application is considered from the perspective of agents who perform the action, rather than from that of observers. Moreover, the emphasis on causation in this application focuses on agents’ deliberate actions, rather than on causation and counterfactuals in general.

We demonstrate in [18] the application of this counterfactual form in machine ethics. First, we use counterfactual queries to distinguish moral permissibility between two off-the-shelf military cases from [24], viz., terror bombing vs. tactical bombing, according to DDE. In the second application, we show that counterfactuals may as well be suitable to justify permissibility, via a process of argumentation (wrt. Scanlon contractualism [23]), using a scenario built from cases of the trolley problem that involve both DDE and DTE. Alternatively, we show that moral justification can also be addressed via ‘compound counterfactuals’ – *Had I known what I know today, then if I were to have done otherwise, something preferred would have followed* – for justifying with hindsight a moral judgment that was passed under lack of current knowledge.

*Moral Updating.* Moral updating (and evolution) concerns the adoption of new (possibly overriding) moral rules on top of those an agent currently follows. Such adoption often happens in the light of situations freshly faced by the agent, e.g., when an authority contextually imposes other moral rules, or due to some cultural difference. In [12], moral updating is illustrated in an interactive storytelling (using ACORDA), where the robot must save the princess imprisoned in a castle, by defeating either of two guards (a giant spider or a human ninja), while it should also attempt to follow (possibly conflicting) moral rules that may change dynamically as imposed by the princess (for the visual demo, see [13]).

The storytelling is reconstructed in this paper using QUALM, to particularly demonstrate: (1) The direct use of LP updating so as to place a moral rule into effect; and (2) The relevance of contextual abduction to rule out tabled but incompatible abductive solutions, in case a goal is invoked by a non-empty initial abductive context (the content of this context may be obtained already from another agent, e.g., imposed by the princess). A simplified program modeling the knowledge of the princess-savior robot in QUALM is shown below, where *fight/1* is an abducible predicate:

```

guard(spider).      guard(ninja).      human(ninja).
survive_from(G) ← utilVal(G, V), V > 0.6.    utilVal(spider, 0.4).    utilVal(ninja, 0.7).
intend_savePrincess ← guard(G), fight(G), survive_from(G).
intend_savePrincess ← guard(G), fight(G).

```

The first rule of *intend\_savePrincess* corresponds to a utilitarian moral rule (wrt. the robot's survival), whereas the second one to a 'knight' moral, viz., to intend the goal of saving the princess at any cost (irrespective of the robot's survival chance). Since each rule in *QUALM* is assigned a unique name in its transform (based on rule name fluent in [21]), the name of each rule for *intend\_savePrincess* may serve as a unique moral rule identifier for updating by toggling the rule's name, say via rule name fluents `#rule(utilitarian)` and `#rule(knight)`, resp. In the subsequent plots, query `?- intend_savePrincess` is referred, representing the robot's intent on saving the princess.

In the first plot, when both rule name fluents are retracted, the robot does not adopt any moral rule to save the princess, i.e., the robot has no intent to save the princess, and thus the princess is not saved. In the second (restart) plot, in order to maximize its survival chance in saving the princess, the robot updates itself with the utilitarian moral: the program is updated with `#rule(utilitarian)`. The robot thus abduces *fight(ninja)* so as to successfully defeat the ninja instead of confronting the humongous spider.

The use of tabling in contextual abduction is demonstrated in the third (start again) plot. Assuming that the truth of *survive\_from(G)* implies the robot's success in defeating (killing) guard *G*, the princess argues that the robot should not kill the *human* ninja, as it violates the moral rule she follows, say a 'Gandhi' moral, expressed by the following rule in her knowledge (the first three facts in the robot's knowledge are shared with the princess): *follow\_gandhi*  $\leftarrow$  *guard(G)*, *human(G)*, *not fight(G)*. That is, the princess abduces *not fight(ninja)* and imposes this abductive solution as the initial (input) abductive context of the robot's goal (viz., *intend\_savePrincess*). This input context is inconsistent with the tabled abductive solution *fight(ninja)*, and as a result, the query fails: the robot may argue that the imposed 'Gandhi' moral conflicts with its utilitarian rule (in the visual demo [13], the robot reacts by aborting its mission). In the final plot, as the princess is not saved yet, she further argues that she definitely has to be saved, by now additionally imposing on the robot the 'knight' moral. This amounts to updating the rule name fluent `#rule(knight)` so as to switch on the corresponding rule. As the goal *intend\_savePrincess* is still invoked with the input abductive context *not fight(ninja)*, the robot now abduces *fight(spider)* in the presence of the newly adopted 'knight' moral. Unfortunately, it fails to survive, as confirmed by the failing of the query `?- survive_from(spider)`.

The plots in this story reflect a form of deliberative employment of moral judgments within Scanlon's contractualism. For instance, in the second plot, the robot may justify its action to fight (and kill) the ninja due to the utilitarian moral it adopts. This justification is counter-argued by the princess in the subsequent plot, making an exception in saving her, by imposing the 'Gandhi' moral, disallowing the robot to kill a human guard. In this application, rather than employing updating, this exception is expressed via contextual abduction with tabling. The robot may justify its failing to save the princess (as the robot leaving the scene) by arguing that the two moral rules it follows (viz., utilitarian

and ‘Gandhi’) are conflicting wrt. the situation it has to face. The argumentation proceeds, whereby the princess orders the robot to save her whatever risk it takes, i.e., the robot should follow the ‘knight’ moral.

### 3 Conclusion and Future Work

The paper summarizes our investigation on the application of LP-based reasoning to the *terra incognita* of machine ethics, a field that is now becoming a pressing concern and receiving wide attention. Our research shows a number of original inroads, exhibiting a proof of possibility to model morality viewpoints systematically using a combination of various LP-based reasoning features (such as LP abduction, updating, preferences, probabilistic LP and counterfactuals) afforded by the-state-of-the-art tabling mechanisms, through moral examples taken off-the-shelf from the literature. Given the broad dimension of the topic, our contributions touch solely on a dearth of morality issues. Nevertheless, it prepares and opens the way for additional research towards employing various features in LP-based reasoning to machine ethics. Several topics can be further explored in the future, as summarized below.

So far, our application of counterfactuals in machine ethics is based on the evaluation of counterfactuals in order to determine their validity. It is interesting to explore in future other aspects of counterfactual reasoning relevant for moral reasoning. First, we can consider *assertive counterfactuals*: rather than evaluating the truth validity of counterfactuals, they are asserted (known) as being a valid statement. The causality expressed by such a valid counterfactual may be useful for refining moral rules, which can be achieved through incremental rule updating. Second, we may extend the antecedent of a counterfactual with a rule, instead of just literals, allowing to express exception in moral rules, such as “If killing the giant spider had been done by a noble knight, then it would not have been wrong”. Third, we can imagine the situation where the counterfactual’s antecedent is not given, though its conclusion is, the issue being that the conclusion is some moral wrong. In this case, we want to abduce the antecedent in the form of interventions that would prevent some wrong: “What could I have done to prevent a wrong?”.

This paper contemplates the individual realm of machine ethics: it stresses individual moral cognition, deliberation, and behavior. A complementary realm stresses collective morals, and emphasizes instead the emergence, in a population, of evolutionarily stable moral norms, of fair and just cooperation, to the advantage of the whole evolved population. The latter realm is commonly studied via Evolutionary Game Theory by resorting to simulation techniques, typically with pre-determined conditions, parameters, and game strategies (see [19] for references). The bridging of the gap between the two realms [19] would appear to be promising for future work. Namely, how the study of individual cognition of morally interacting multi-agent (in the context of this paper, by using LP-based reasoning features) is applicable to the evolution of populations of such agents, and vice versa.

**Acknowledgments.** Both authors acknowledge the support from FCT/MEC NOVA LINCS PEst UID/CEC/ 04516/2013. Ari Saptawijaya acknowledges the support from FCT/MEC grant SFRH/BD/72795/2010.

## References

1. Anderson, M., Anderson, S.L.: EthEl: Toward a principled ethical eldercare robot. In: Procs. AAAI Fall 2008 Symposium on AI in Eldercare (2008)
2. Bringsjord, S., Arkoudas, K., Bello, P.: Toward a general logicist methodology for engineering ethically correct robots. *IEEE Intelligent Systems* **21**(4), 38–44 (2006)
3. Cushman, F., Young, L., Greene, J.D.: Multi-system moral psychology. In: Doris, J.M. (ed.) *The Moral Psychology Handbook*. Oxford University Press (2010)
4. Dell'Acqua, P., Pereira, L.M.: Preferential theory revision. *Journal of Applied Logic* **5**(4), 586–601 (2007)
5. Foot, P.: The problem of abortion and the doctrine of double effect. *Oxford Review* **5**, 5–15 (1967)
6. Ganascia, J.-G.: Modelling ethical rules of lying with answer set programming. *Ethics and Information Technology* **9**(1), 39–47 (2007)
7. Anh, H.T., Kencana Ramli, C.D.P., Damásio, C.V.: An implementation of extended P-Log using XASP. In: Garcia de la Banda, M., Pontelli, E. (eds.) ICLP 2008. LNCS, vol. 5366, pp. 739–743. Springer, Heidelberg (2008)
8. Han, T.A., Saptawijaya, A., Pereira, L.M.: Moral reasoning under uncertainty. In: Bjørner, N., Voronkov, A. (eds.) LPAR-18 2012. LNCS, vol. 7180, pp. 212–227. Springer, Heidelberg (2012)
9. Hauser, M., Cushman, F., Young, L., Jin, R.K., Mikhail, J.: A dissociation between moral judgments and justifications. *Mind and Language* **22**(1), 1–21 (2007)
10. Kamm, F.M.: *Intricate Ethics: Rights, Responsibilities, and Permissible Harm*. Oxford U. P (2006)
11. Kowalski, R.: *Computational Logic and Human Thinking: How to be Artificially Intelligent*. Cambridge U. P (2011)
12. Lopes, G., Pereira, L.M.: Prospective storytelling agents. In: Carro, M., Peña, R. (eds.) PADL 2010. LNCS, vol. 5937, pp. 294–296. Springer, Heidelberg (2010)
13. Lopes, G., Pereira, L.M.: Visual demo of “Princess-saviour Robot” (2010). [http://centria.di.fct.unl.pt/~lmp/publications/slides/padl10/quick\\_moral\\_robot.avi](http://centria.di.fct.unl.pt/~lmp/publications/slides/padl10/quick_moral_robot.avi)
14. Mallon, R., Nichols, S.: Rules. In: Doris, J.M. (ed.) *The Moral Psychology Handbook*. Oxford University Press (2010)
15. McIntyre, A.: Doctrine of double effect. In: Zalta, E.N. (ed.) *The Stanford Encyclopedia of Philosophy*. Center for the Study of Language and Information, Stanford University, Fall 2011 edition (2004). <http://plato.stanford.edu/archives/fall2011/entries/double-effect/>
16. Newman, J.O.: Quantifying the standard of proof beyond a reasonable doubt: a comment on three comments. *Law, Probability and Risk* **5**(3–4), 267–269 (2006)
17. Pereira, L.M., Saptawijaya, A.: Modelling morality with prospective logic. In: Anderson, M., Anderson, S.L. (eds.) *Machine Ethics*, pp. 398–421. Cambridge U. P (2011)
18. Pereira, L.M., Saptawijaya, A.: Abduction and beyond in logic programming with application to morality. Accepted in “Frontiers of Abduction”, Special Issue in IfCoLog Journal of Logics and their Applications (2015). <http://goo.gl/yhmZzy>

19. Pereira, L.M., Saptawijaya, A.: Bridging two realms of machine ethics. In: White, J.B., Searle, R. (eds.) *Rethinking Machine Ethics in the Age of Ubiquitous Technology*. IGI Global (2015)
20. Pereira, L.M., Saptawijaya, A.: Counterfactuals in Logic Programming with Applications to Agent Morality. Accepted at a special volume of *Logic, Argumentation & Reasoning* (2015). <http://goo.gl/6ERgGG> (preprint)
21. Saptawijaya, A., Pereira, L.M.: Incremental tabling for query-driven propagation of logic program updates. In: McMillan, K., Middeldorp, A., Voronkov, A. (eds.) *LPAR-19 2013. LNCS*, vol. 8312, pp. 694–709. Springer, Heidelberg (2013)
22. Saptawijaya, A., Pereira, L.M.: TABDUAL: a Tabled Abduction System for Logic Programs. *IfCoLog Journal of Logics and their Applications* **2**(1), 69–123 (2015)
23. Scanlon, T.M.: *What We Owe to Each Other*. Harvard University Press (1998)
24. Scanlon, T.M.: *Moral Dimensions: Permissibility, Meaning, Blame*. Harvard University Press (2008)
25. Swift, T.: Tabling for non-monotonic programming. *Annals of Mathematics and Artificial Intelligence* **25**(3–4), 201–240 (1999)
26. The Future of Life Institute. Research Priorities for Robust and Beneficial Artificial Intelligence (2015). [http://futureoflife.org/static/data/documents/research\\_priorities.pdf](http://futureoflife.org/static/data/documents/research_priorities.pdf)

# **Intelligent Information Systems**

# Are Collaborative Filtering Methods Suitable for Student Performance Prediction?

Hana Bydžovská<sup>(✉)</sup>

CSU and KD Lab Faculty of Informatics, Masaryk University, Brno, Czech Republic  
bydzovska@fi.muni.cz

**Abstract.** Researchers have been focusing on prediction of students' behavior for many years. Different systems take advantages of such revealed information and try to attract, motivate, and help students to improve their knowledge. Our goal is to predict student performance in particular courses at the beginning of the semester based on the student's history. Our approach is based on the idea of representing students' knowledge as a set of grades of their passed courses and finding the most similar students. Collaborative filtering methods were utilized for this task and the results were verified on the historical data originated from the Information System of Masaryk University. The results show that this approach is similarly effective as the commonly used machine learning methods like Support Vector Machines.

**Keywords:** Student performance · Prediction · Collaborative filtering methods · Recommender system

## 1 Introduction

Students have to accomplish all the study requirements defined by their university. The most important is to pass all mandatory courses and to select elective and voluntary courses that they are able to pass. Masaryk University offers a vast amount of courses to its students. Therefore, it is very difficult for students to make a good decision. It is important for us to understand students' behavior to be able to guide them through their studies to graduate. Our goal is to design an intelligent module integrated into the Information System of Masaryk University that will help students with selecting suitable courses and warn them against too difficult ones. Necessarily, we need to be able to predict whether a student will succeed or fail in an investigated course in order to realize the module. We need the information at the beginning of a term when we have no information about students' knowledge, skills or enthusiasm for any particular course. We also do not want to obtain the information directly from students using questionnaires. Since the questionnaires tend to have a lower response rate, we use only verifiable data from the university information system.

We have drawn inspiration from techniques utilized in recommender systems. Nowadays, usage of *collaborative filtering (CF) methods* [5] spreads over many areas including the educational environment. Walker et al. [9] designed a system called

Altered Vista that was specifically aimed at teachers and students who reviewed web resources targeted at education. The system implemented CF methods in order to recommend web resources to its users. Many researchers aimed at e-learning, e.g. Loll et al. [6] designed a system that enables students to solve their exercises and to criticize their schoolmates' solutions. The system based on students' answers could reveal difficult tasks and recommend good solutions to enhance students' knowledge.

In this paper, we report on the possibility to estimate student performance in particular courses based only on knowledge of students' previously passed courses. We utilize different CF to estimate the final prediction. The preliminary work can be seen in [1]. Now we explore the most suitable settings of the approach in detail and compare the results with our previous approach using classification algorithms [2].

## 2 Our Previous Approach

Many researchers successfully used machine learning approach to predict students' performance [7]. In order to characterize students, we collected many different data about students that are stored in the Information System of Masaryk University [2]. The study-related data contained attributes such as gender, year of birth, year of admission, number of credits gained from passed courses. The social data described students' behavior and co-operation with other students, e.g. weighted average grades of their friends, importance in the sociogram computed for example from the communication statistics, students' publication co-authoring, and comments among students.

We also utilized algorithms implemented in Weka [10] with different data sets in order to obtain the best possible results. We utilized algorithms for regression and classification, and we also computed the mean absolute error from confusion matrix. In order to lower the number of attributes, we employed feature selection (FS) algorithms. Support Vectors Machines (SMO) and Random Forests were the most suitable methods in combination with FS algorithms. The comparison of this approach with the results obtained by CF methods on the same data set can be seen in Section 4.

## 3 Experiment

Our hypothesis is that students' knowledge can be characterized by the grades of courses that students enrolled during their studies. Based on this information we can select students with similar interests and knowledge and subsequently predict whether a particular student has sufficient skills needed for a particular course.

For our purposes, each student can be represented with a vector of grades of courses passed in one of the student's studies. In order to confirm our hypothesis, we selected 62 courses with different success rates that were offered to students in the years 2010 – 2013 at Masaryk University. The students for whom we were not able to give any prediction – students without any history in the system and without any passed course – were omitted from the experiment. The extracted data set comprised of 3,423 students enrolled at least in one of the 62 courses and their 42,635 grades.

Our aim was to predict the grades of students enrolled in the investigated courses in the year 2012 based on the results of similar students enrolled in the same courses in the years 2010 and 2011. Then we could verify the predictions with the real grades and evaluate the methods and the settings. Then we selected the most suitable method and verified it on data about students enrolled in the same courses in the year 2013.

**Similarity of Students.** For each student, we constructed four vectors of grades characterizing the knowledge. The values were computed with respect to the number of repetition of each course. We consider only the last grade (NEWEST), a grade of each attempt at the last year (YEAR), only the last grades of each repetition (LAST), and all grades (ALL). For example, a student failed a course in the first year using three attempts and got the grades 444. The student had to repeat the course next year. Supposing he or she got the grades 442, the student's values for this particular course were the following: NEWEST: 2, YEAR: 4+4+2, LAST: 4+2, ALL: 4+4+4+4+4+2.

Vectors of grades were compared by five methods. *Mean absolute difference (MAD)* and *Root mean squared difference (RMSD)* measure the mean difference of the investigated student's grades and the grades of students' in their shared courses. The lower the value, the better the result is. The other methods return values near 1 for the best results. *Cosine similarity (COS)* and *Pearson's correlation coefficient (PC)* define the similarity of grades of shared courses. *Jaccard's coefficient (JC)* defines the ratio of shared and different courses. Supposing that students' knowledge can be represented with passed courses, it was very important to calculate the overlap of students' courses.

**Neighborhood Selection.** We selected several methods to compute a suitable neighborhood:

- Top  $x$ , where  $x \in [1; 50]$  with step 1; (the analysis [4] indicates that the neighborhood of 20 - 50 neighbors is usually optimal).
- More similar than the threshold  $y$ , where  $y \in [0; 1]$  with step 0.1.
- We also utilized the idea of baseline user [8]. We selected only these students to the neighborhood that were more similar to the investigated one than the investigated one to the baseline user. We decided to calculate two types of baseline user:
  - Average student – we characterized an average student by the average grades of courses in which the investigated students were enrolled in.
  - Uniform student – we characterized a uniform student by grades with values 2.5 (the average grade through all courses) of all courses in which the investigated student was enrolled in.

**Grade Prediction.** As the neighborhood was defined, we could make a prediction. We used different approaches to estimate grades from grades of students in the neighborhood: mean, median, and the majority class. We also utilized the significance weighting [3], also its extension using average grades of compared students (sig. weighting +), and lowering the importance of students with only few co-ratings [4].

## 4 Results

Mean absolute error (MAE) represents the size of the prediction error. The exact grade prediction is very difficult and even less powerful prediction can be sufficient. Therefore, we also predicted the grades as good (1) / bad (2) / failure (4) or just success or failure. The results of the CF methods were compared with our previous work described in Section 2 where the predictions were obtained using classification algorithms (CA). We used a confusion matrix for calculating MAE. We mined study-related data and data about social behavior of students.

The comparison of both approaches can be seen in Table 1. Although both the approaches used different data from the information system and utilized different processing, the results showed that their performance was almost similar. The only one significant difference can be seen in grade prediction when CF methods were slightly better. We consider the accuracy of 78.5% for student success or failure prediction reliable enough considering that we did not know students' skills or enthusiasm for courses. MAE of good / bad / failure prediction was around 0.6. We consider MAE less than one degree in the modified grade scale to be very satisfactory. Even in the grade (1, 1.5, 2, 2.5, 3, and 4) prediction, MAE was around 0.7 which means only slightly more than one degree in the grade scale. In general, these results were positive but the grade prediction was still not trustworthy.

**Table 1.** Comparison of approaches

<b>Approach</b>	<b>Selection</b>	<b>Grade</b>	<b>Good/bad/failure</b>	<b>Success/failure</b>
		<b>MAE</b>		<b>Accuracy</b>
<b>CA</b>	2012	0.67	0.58	81.04%
	2013	0.84	0.61	78.72%
<b>CF</b>	2012	0.64	0.57	80.44%
	2013	0.68	0.64	78.58%

The advantage of the CF approach is that all information systems store the data about students' grades. Therefore, this approach can be used in all systems. Our previous approach was based on mining data obtained from the information system. But not all systems store the data about social behavior of students. We proved that this data improve the accuracy of the results significantly [2].

## 5 Discussion

The settings of the CF approach that reached the best average results can be seen in Table 2. As the results show, PC worked properly in combination with the uniform student for selecting a proper neighborhood and significance weighting with an extension using average grades of compared students for the final prediction. On the other hand, for MAD, a Top  $x$  function was the best option for selecting the neighborhood and median for the final prediction. Both the approaches reached very similar results

in all tasks and we consider them to be trustworthy. We also investigated the most suitable  $x$  for these tasks. We searched for the minimal  $x$  with the best possible results. We derived  $x = 25$  to be the best choice generally for all methods and settings. The most suitable classification algorithms were SMO and Random Forests (Table 3).

**Table 2.** The settings of the CF approach that reached the best average results

	<b>Sim. function</b>	<b>Neighborhood</b>	<b>Estimation approach</b>
<b>Grade</b>	PC	Uniform student	Sig. weighting +
<b>Good/bad/failure</b>	PC	Uniform student	Sig. weighting +
<b>Success/failure</b>	MAD	Top 25	Median

**Table 3.** The settings of the classification algorithms that reached the best average results

	<b>Classification algorithm</b>	<b>Feature selection algorithm</b>
<b>Grade</b>	SMO	InfoGainAttributeEval
<b>Good/bad/failure</b>	SMO	OneRAttributeEval
<b>Success/failure</b>	Random Forests	5 attributes selected by each FS algorithm for each course

We also investigated the influence of different details of grades described in Section 3. The conclusion was that only the NEWEST grade was expressive enough for a satisfactory prediction. More detailed information about the grades did not improve the results significantly.

## 6 Conclusion

In this paper, we used CF methods for student modeling. Our experiment provides evidence that CF approach is also suitable for student performance prediction. The data set comprised of 62 courses taught in 4 years with almost 3,423 students and their 42,635 grades. We confirmed our hypothesis, that students' knowledge can be sufficiently characterized only by their previously passed courses that should cover their knowledge of the field of study. We processed data about students' grades stored in the Information System of Masaryk University to be able to estimate students' interests, enthusiasm and prerequisites for passing enrolled courses at the beginning of each term. For each investigated student, we searched for students enrolled in the same courses in the last years who were the most similar ones to the investigated student. Based on their study results, we predicted the students' performance.

We compared the results with the results obtained by classification algorithms that researchers usually utilize for student performance prediction. The results were almost the same. The main advantage of CF approach is that all university information systems store the data about students' grades needed for the prediction. On the other hand, this approach is not suitable if we have no information about the history of the particular students. Now, we are able to predict the student success or failure with the accuracy of 78.5%, whether the grade will be good, bad, or failure with the MAE of

0.6 and the exact grade with the MAE of 0.7. We consider the results to be very satisfactory and CF approach can be considered as expressive as the commonly used classification algorithms.

Based on this approach we can recommend suitable voluntary courses for each student with respect to his or her interests and skills. We hope that this information will also encourage students to study hard when they have to enroll in a mandatory course that seems to be too difficult for them. Moreover, teachers can utilize this information to identify potentially weak students and help them before they will be at risk to fail the course. This approach can be also beneficially used in an intelligent tutoring system as the basic estimation of students' potentials before they start to operate with the system in the investigated course.

**Acknowledgement.** We thank Michal Brandejs, Lubomír Popelínský, and all colleagues of Knowledge Discovery Lab, and also IS MU development team for their assistance. This work has been partially supported by Faculty of Informatics, Masaryk University.

## References

1. Bydžovská, H.: Student performance prediction using collaborative filtering methods. In: Conati, C., Heffernan, N., Mitrovic, A., Verdejo, M. (eds.) AIED 2015. LNCS, vol. 9112, pp. 550–553. Springer, Heidelberg (2015)
2. Bydžovská, H., Popelínský, L.: The Influence of social data on student success prediction. In: Proceedings of the 18th International Database Engineering & Applications Symposium, pp. 374–375 (2014)
3. Herlocker, J.L., Konstan, J.A., Borchers, A., Riedl, J.: An algorithmic framework for performing collaborative filtering. In: Proceedings of the 22nd Annual International ACM SIGIR Conference, pp. 230–237 (1999)
4. Herlocker, J.L., Konstan, J.A., Riedl, J.: Explaining collaborative filtering recommendations. In: Proceedings of the ACM Conference on Computer Supported Cooperative Work, pp. 241–250 (2000)
5. Jannach, D., Zanker, M., Felfernig, A., Friedrich, G.: Recommender Systems: An Introduction. Cambridge University Press (2010)
6. Loll, F., Pinkwart N.: Using collaborative filtering algorithms as elearning tools. In: Proceedings of the 42nd Hawaii International Conference on System Sciences (2009)
7. Marquez-Vera, C., Romero, C., Ventura, S.: Predicting school failure using data mining. In: Pechenizkiy, M., et al. (eds.) EDM, pp. 271–276 (2011)
8. Matuszyk, P., Spiliopoulou, M.: Hoeffding-CF: neighbourhood-based recommendations on reliably similar users. In: Dimitrova, V., Kuflík, T., Chin, D., Ricci, F., Dolog, P., Houben, G.-J. (eds.) UMAP 2014. LNCS, vol. 8538, pp. 146–157. Springer, Heidelberg (2014)
9. Walker, A., Recker, M.M., Lawless, K., Wiley, D.: Collaborative Information Filtering: A Review and an Educational Application. International Journal of Artificial Intelligence in Education **14**(1), 3–28 (2004)
10. Witten, I., Frank, E., Hall, M.: Data Mining: Practical Machine Learning Tools and Techniques, 3rd edn. Morgan Kaufmann Publishers (2011)

# **Intelligent Robotics**

# A New Approach for Dynamic Strategic Positioning in RoboCup Middle-Size League

António J.R. Neves<sup>(✉)</sup>, Filipe Amaral, Ricardo Dias, João Silva,  
and Nuno Lau

Intelligent Robotics and Intelligent Systems Lab,  
IEETA/DETI – University of Aveiro, Aveiro, Portugal  
[an@ua.pt](mailto:an@ua.pt)

**Abstract.** Coordination in multi-robot or multi-agent systems has been receiving special attention in the last years and has a prominent role in the field of robotics. In the robotic soccer domain, the way that each team coordinates its robots, individually and together, in order to perform cooperative tasks is the base of its strategy and in large part dictates the success of the team in the game. In this paper we propose the use of Utility Maps to improve the strategic positioning of a robotic soccer team. Utility Maps are designed for different set pieces situations, making them more dynamic and easily adaptable to the different strategies used by the opponent teams. Our approach has been tested and successfully integrated in normal game situations to perform passes in free-play, allowing the robots to choose, in real-time, the best position to receive and pass the ball. The experimental results obtained, as well as the analysis of the team performance during the last RoboCup competition show that the use of Utility Maps increases the efficiency of the team strategy.

## 1 Introduction

RoboCup (“Robot Soccer World Cup”) is a scientific initiative with an annual international meeting and competition that started in 1997. The aim is to worldwide promote developments in Artificial Intelligence, Robotics and Multi-agent systems. Robot soccer represents one of the attractive domains promoted by RoboCup for the development and testing of multi-agent collaboration techniques, computer vision algorithms and artificial intelligence approaches, only to name a few.

In the RoboCup Middle Size League (MSL), autonomous mobile soccer robots must coordinate and collaborate for playing and winning a game of soccer, similar to the human soccer games. They have to assume dynamic roles in the field, to share information about visible objects of interest or obstacles and to position themselves in the field so that they can score goals and prevent the opponent team from scoring. Decisions such as game strategies, positioning and team coordination play a major role in the MSL soccer games.

This paper introduces Utility Maps as a tool for the dynamic positioning of soccer robots on the field and for opportunistic passing between robots, under

different situations that will be presented throughout the paper. As far as the authors know, no previous work has been presented about the use of Utility Maps in the Middle Size League of RoboCup.

The paper is structured into 8 sections, first of them being this Introduction. In Section 2 we present a summary of the work already done on strategic positioning. Section 3 introduces the use of Utility Maps in the software structure of the CAMBADA MSL team. In Section 4 we describe the construction of Utility Maps. Section 5 describes the use of Utility Maps for the positioning of the robots in defensive set pieces. In Section 6 we present the use of Utility Maps in offensive set pieces, while Section 7 presents their use in Free Play. Finally, Section 8 introduces some measures of the impact of the Utility Maps on the performance of the team and discusses a series of results that prove the efficiency of the team strategy, based on Utility Maps.

## 2 Related Work

Strategic positioning is a topic with broad interest within the RoboCup community. As teams participating in the RoboCup Soccer competitions gradually managed to solve the most basic tasks involved in a soccer game, such as locomotion, ball detection and ball handling, the need of having smarter and more efficient robotic soccer players arose. Team coordination and strategic positioning are nowadays the key factors when it comes to winning a robotic soccer game.

The first efforts for achieving coordination in multi-agent soccer teams has been presented in [2] [3]. Strategic Positioning with Attraction and Repulsion (SPAR) takes into account the positions of other agents as well as that of the ball. The following forces are evaluated when taking a decision regarding the positioning of an agent: repulsion from opponents and team members, attraction to the active team member and ball and attraction to the opponents' goal.

In the RoboCup Soccer Simulation domain, Situation Based Strategic Position (SBSP) [4] is a well known technique used for the positioning of the software agents. The positioning of an agent only takes into consideration the ball position, as focal point, and does not consider other agents. However, if all agents are assumed to always devote their attention to the ball position, then cooperative behavior can be achieved indirectly. An agent defines its base strategic position based on the analysis of the tactic and team formation. Its position is adjusted accordingly to ball pose and game situation. This approach has been adapted to the Middle Size League constraints and has been presented in [5].

In [6] a method for Dynamic Positioning based on Voronoi Cells(DPVC) was introduced. The robotic agents are placed based on attraction vectors. These vectors represent the attraction of the players towards objects, depending on the current state of the game and roles.

The Delaunay Triangulation formations (DT) [7] divide the soccer pitch into several triangles based on given training data. Each training datum affects only the divided region to which it belongs. A map is built from a focal point, such as ball position, to the positioning of the agents.

For more than 20 years, grid-based representations have been used in robotics in order to show different kinds of spacial information, allowing a more accurately and simplified world perception and modelling [8] [9]. Usually, this type of representations are oriented to a specific goal. Utility functions have been presented before [10] [11] as a tool for role choosing within multi-agents systems.

Taking into account the successful use of this approach, a similar idea was applied to the CAMBADA agents, but with different functionalities and purpose. The aim of the proposed approach was to improve the collective behavior in some specific game situations. Utility Maps have been developed as support tools for the positioning of soccer robots in defensive and offensive set pieces, as well as in freeplay passes situations.

### 3 Utility Maps of CAMBADA MSL Team

The general architecture of the CAMBADA robots has been described in [1]. The decision about the strategic positioning of the robots is taken by the high level agent. This is a process that, at each cycle, is responsible for the high-level control of the robots, which is divided in several stages. The first stage is the sensor fusion, executed by an integrator module, with the objective of gathering the noisy information from the sensors and from its team mates and updating the state of the world. This world state will be used by the high-level decision and coordination modules.

In the second stage of the high-level control of the robots, the agent has to decide how to act given the state of the world that he built. At the higher level it assumes a Role and operates on the field with a given attitude, for example, as role **Striker**. A detailed description about the Roles used in CAMBADA team can be found in [13]. The actions it can take are defined by lower level Behaviors, which define the orders to be send to the actuators in order to fulfill a task, for example, a **Move** behavior, to reach a given point on the field.

During a MSL game, there are three possible game situations: **defensive set pieces** when for some reason (a fault, ball outside the field or a valid goal) the game stops and the ball belongs to the opponent team; **offensive set pieces** when for some reason the game stops and the ball belongs to our team and **free play** when the ball is moving on the field after a game stop.

In **defensive set pieces** only one role is involved, role **Barrier**. The robot will stay in this role until the ball is considered to be in game. The ball is in game when it moves more than 20cm or if 10 seconds passed since the start signal has been given by the referee. After this point, the game enters in free play mode and new roles will be assigned to the robots, as described next.

In **offensive set pieces** two roles are involved, role **Replacer** and role **Receiver**. The robot closest to the ball will assume the role **Replacer** and all the others, except for the goal keeper, will assume the role **Receivers**. After the ball has been passed, the robot that will receive the ball becomes **Striker** and all the other robots are **Midfielders**. After a successful pass or when our robots detect that the ball has been gathered by the opponent team, the game state changes to free play.

When the game is in **free play**, a robot can assume one of two roles: **Striker** or **Midfielder**, depending on the relative robot position regarding the ball.

## 4 Building the Utility Maps

In this paper we propose an approach for dynamic strategy positioning in MSL based on Utility Maps. The position of each robot that takes part in a specific game situation is dynamically obtained based on the information about the environment around the robot, namely its position on the field, the position of obstacles and the ball position.

The CAMBADA robots use a catadioptric vision system, often named omnidirectional vision system. The algorithms for detecting the objects of interest are presented in [14]. The information acquired by the vision system is merged with other information of the robot to build the worldstate information, namely its position on the field and a list of valid balls and a list of valid obstacles. A detailed description of the algorithms used to build the worldstate is presented in [15].

The information about the obstacles in the current version of the CAMBADA robot worldstate is a list of objects containing their absolute positions on the field and their classification of being team mates or opponents. The algorithm for obstacles detection and identification is described in [15].

The Utility Map is constructed merging the relevant information about the environment, namely the team mates positions, obstacles and ball positions, using the information of the robot and the information shared by the colleagues [12].

The first step to obtain the Utility Map is to build an occupancy map that gives the robot a global idea about the state of the world around it. Then, depending on the game situation and the role in which the Utility Map will be used, a Field of Vision (FOV) is calculated on top of the occupancy map. FOV represents the area that is considered visible from the point in which it was calculated. For example, it is possible to calculate a FOV from the ball, from the robot itself, from the goal, etc. An example of a FOV calculated from robot number 3 is shown on Fig. 1.

Finally, the Utility Map is created taking into consideration the occupancy map, the FOVs and some conditions, restrictions and metrics for decisions depending on the game situation. Taking as example the offensive set pieces, there are some restrictions included in the process of building the Utility Map. The two main restrictions are that the robots cannot be inside the goal areas and they have to receive the ball from at least 2 meters from the ball. Moreover, it is possible to combine three metrics to build the Utility Maps in order to decide the best positions to receive the ball. One is the free space between the pass line and the closest obstacle. The second one is the weighted average between the distance to the ball, the distance to the opponent goal, the rotation angle for a shot on target and the distance from the point on the map to the position of the robot. Finally, the third metric is the angle of each map position to the opponent goal.

The use of these Utility Maps allow the robots to easily take decisions regarding their positioning simply choosing the local maximum on the maps. The Utility Maps are calculated locally on the robots and are part of their worldstate so that they are easily accessible by any behavior or role. In terms of implementation, the TCOD<sup>1</sup> library has been used. The library provides built-in toolkits for management of height maps, which in the context of this work are used as Utility Maps, and field of view calculations. It takes, on average, 4ms to update the necessary maps in each cycle of the agent software execution. The robots are currently working with a cycle of 20 ms, controlled by the vision process that works at 50 frames per second [14].

The identified opponent robots lead to hills in the map on their position, with some persistence to improve the stability of the decisions based on the maps. It takes 5 agent cycles (100 milliseconds) for a new obstacle to reach the maximum cost level. In the end, the map is normalized, thus always holding values between 0.0 and 1.0.

## 5 Positioning in Defensive Set Pieces

In defensive set pieces the main objective is to prevent the opponent team to perform a pass and to gain ball possession. In order to prevent the opponent players to pass the ball, our robots must be positioned between the ball and the possible receivers from the opponent team and to follow them while they move.

To calculate the base position for the **Barriers**, the role assumed by the robots during the opponent set pieces, we use a Delaunay Triangulation (DT) [7] to interpolate all possible robots positions on the field, depending on the ball position on the field. On top of that, the rules restrictions are applied. These restrictions are: minimum 3m distance to the ball, except in a drop ball situation, when the required distance is only 1m and only one player inside our penalty area. This player does not need to respect the previous rule as long it is inside the penalty area.

Figure 1 shows the tool used to configure the DT positions. Here, the ball position is used as triangle vertex and each vertex represents the given training data. Each vertex produces output values for the position of the robots for that triangle. When the ball is inside a triangle, the position of the agent is calculated using the interpolation algorithm described in [7].

It is possible to configure each one of the **Barriers** to dynamically cover the opponent robots or to simply stay in the base positions given by the DT configuration. When there are no obstacles on the field, the robots only use this position. In the presence of obstacles, the position of the cover robots are obtained from an Utility Map, following the approach proposed in this paper.

In order to avoid any possible error in the identification of obstacles, it is necessary to filter the information received from different agents. Obstacles close to each other are merged using a clustering algorithm, and obstacles too close to

---

<sup>1</sup> <http://roguecentral.org/doryen/libtcod/>

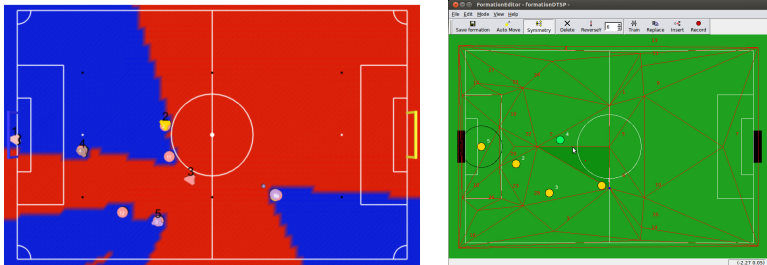


**Fig. 1.** On the left, the FOV calculated from robot number 3. The ball is represented by a small circle and the robots as larger circles. The circles with numbers are considered team mates. The red areas are considered visible from the point of view of the robot. On the right, the configuration tool used for the positioning of our robots in opponent set pieces and during free play (DT).

a team mate are ignored, unless that team mate sees it. The filtered information is then used to build the map.

From each cluster of obstacles, a valley is carved in direction to the ball. After that, the calculated map is added with a predefined height map that defines the priorities of the positions (see Figure 2). This map takes into consideration that it is more important to cover the opponent robots in the direction of our goal, rather than in the direction of their goal. Finally, all the restrictions (minimum distance to the ball, positions inside the field and avoidance of penalty areas) are added.

In Fig. 2 we can see a game situation where robots number 3, 4 and 5 are configured to cover the opponent robots. The best position given by the Utility Map for each robot is represented in red. As intended, these positions are between the ball and the opponent robots. Robot 2 is in its base position provided by the DT configuration.

The distance between our team robot and the opponent robot that it is trying to cover can be configured (in the configuration file of the robot). The human coach can specify, in the same configuration file, what are the robots allowed to perform covering.

## 6 Positioning in Offensive Set Pieces

To configure our set pieces we use a graphical tool (Figure 3) that implements an SBSP algorithm. The field is divided into 10 zones. Each zone defines a set of positions for the **Replacer** (the role of the robot closer to the ball and responsible for putting the ball in play) and **Receivers** (the role of the other robots, except the **Goalie**). The position to kick by default in a situation where there is no **Receiver** available can also be configured. The position of the **Receivers** can be absolute or relative to the ball. We can also define if the **Receiver** needs to have a clear line between its position and the ball and an option to force the

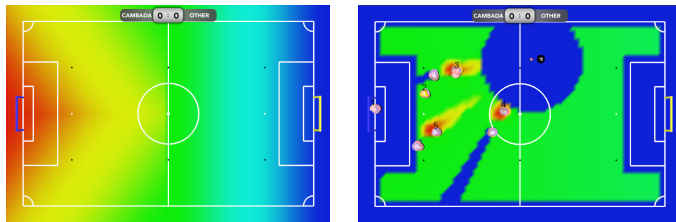


**Fig. 2.** On the left, cover priorities height map used to define the priority of the cover positions in the field. Red is the more prioritary and blue is the least prioritary. On the right, example of a cover Utility Map. As we can see, the best position for the robots number 3, 4 and 5 are between the ball and the robots of the opponent team (red color).

**Receiver** to be aligned with the goal. The priority for each receiver is indicated as well, in the case that for a specific region will be more than one configured and available. The one with more priority will be tested first for receiving a pass. The action to be performed by the **Replacer** to that specific **Receiver** is also configurable. This action can be a pass, a cross or none. In the last case, the **Receiver** will never be considered as an option. It is possible to configure differently each one of the possible set pieces (corner, free kick, drop ball, throw in and kick off) for each one of the regions.

When the set pieces using the referred tool are configured, the opponent team is not taken into account. After the opponent team has positioned itself, our configured positions can be positions where the receiver is not able to receive a pass. To deal with these situations, there is the need to have an alternative reception position that has to be calculated dynamically, taking into account the opponent team. An Utility Map is used to calculate the alternative position for the **Receiver**.

All the constraints imposed by the rules, namely minimum distance to the ball (2m) and no entering in the goal areas are taken into account for the construction of the **Receiver** Utility Map. The field is divided into two zones for the application of different metrics to calculate the utility value for each position. On our side of the field, only one metric is used. This metric is the distance to the halfway line. Three metrics are used on the opponent side of the field. One is the free space between the pass line and the closest obstacle. The second one is the weighted average between the distance to the ball, the distance to the opponent goal, the rotation angle for a shot on target and the distance from the point on the map to the position of the robot. Finally, the third metric is the angle of each map position to the opponent goal. The weights for the second metric are easily configurable in the configuration file of the robot. These metrics are only applied within a circle whose radius is also defined in the configuration file. This circle is centered on the position of the ball in the set piece, and only the positions that have FOV from the ball (positions where the ball can be passed) are considered.

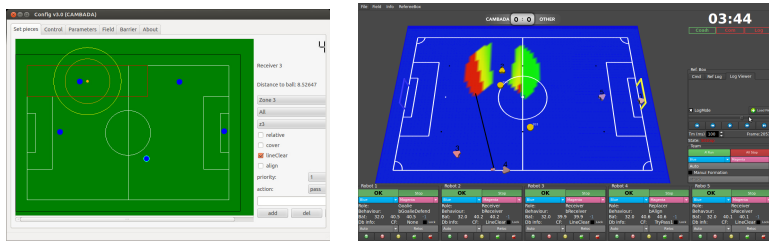


**Fig. 3.** On the left, the configuration tool used for our set pieces. On the right, an example of a Utility Map for a **Receiver**. Example of an alternative positioning map for **Receiver** calculated for Robot number 2. CAMBADA is attacking towards the blue goal. The black line goes from the ball to the alternative position indicated by Robot number 2 to receive the ball.

The robots move to the best position extracted from the Utility Map only after the referee gives the start signal to prevent the opponent robots to follow them. In Fig. 3 all the receivers are sharing that they have line clear to receive the ball (`lineClear` is information associated to each robot). Robot number 4 is the **Replacer** already chosen to pass the ball to robot number 2. The pass line it is trying to make is represented by the black line. Robot number 2 will move to that position to receive the ball.

## 7 Positioning in Freeplay

Free-play passes are a true challenge in terms of coordination among robots, being thus much more complex to achieve. This is mainly due to the complete freedom that the opponent team has to approach our **Striker** or cover a **Midfielder**. Since the robot that wants to make the pass has the ball in its possession, its movement is very limited. Taking this into consideration, the development of an Utility Map to estimate the best position of the **Midfielders** on the field is more than necessary in order to improve the capability of performing passes in free play.

A Delaunay Triangulation (DT) as in their set pieces is used to calculate the base position for the **Midfielders** we use. On top of that, the restrictions from the rules are applied, namely the avoidance of the goal areas.

The algorithm to calculate the Utility Map for the **Midfielders** is similar to the one described in our set pieces. An example of an Utility Map in a free play game situation is presented in Fig. 4. The best positions on the field to receive the ball are in red. Only positions inside the field are considered, as well as only positions outside both penalty areas. Positions near the opponent corners (dead angles) are also avoided. A minimum distance of 2 meters to the **Striker** is required and a preference is given to positions near the last chosen position, near the strategic position returned by DT and also near the actual **Receiver**. A FOV for the ball is also required. With these constraints, the free-play receiver

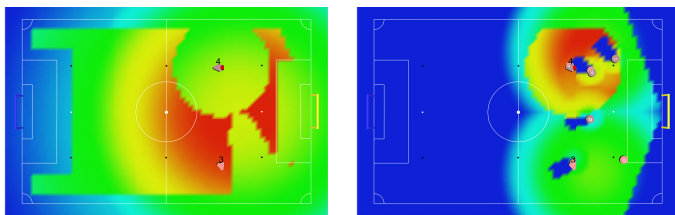


**Fig. 4.** On the left, the Free-play utility map calculated by the **Midfielders**. The best positions on the field to receive the ball are in red. On the right, the Free-play Utility Map to be used by the **Striker** to choose the best position to perform a pass or a kick to the goal, when dribbling the ball. The robot will dribble to the positions on red.

robot will be constantly adapting to the changes of the opponent formation and the ball position.

The **Striker**, the robot holding the ball or closer to it, also uses an Utility Map for selecting the best position to perform a pass or to kick towards the goal. The calculated map (Figure 4) deals with the constraints regarding a generic dribble behavior, complying with the current MSL rules, that do not allow a robot to dribble for more than 3 meters. Some areas of the field have less utility, namely both penalty areas, areas outside the field and outside a 3 meter radius circle centered on the point where the ball was grabbed. More priority is given to the areas close the limits of the field since it is more advantageous to kick to the goal from there.

## 8 Results and Discussions

CAMBADA won third place in the last RoboCup MSL competition. After a thorough analysis of the log files and game videos, it is safe to say that the approach we present in this paper for a dynamic strategic positioning of the robots, has had a major contribution to the success of the team. We present in this section the analysis of the presented approach and we discuss its impact on the performance of the team. While a clear distinction between the performance of the team prior to the use of Utility Maps and its current performance cannot be pursued due to the continuously evolving dynamism of the MSL soccer games and the improvements of each of the participating teams each year, the following results prove that the use of Utility Maps had a major contribution for bringing the robotic soccer game as close to the human soccer games as possible.

Looking to the examples of the Utility Maps presented above regarding the three game situations, we can confirm that the maps were correctly built since the position of the robots in a specific game situation are the intended positions, in order to maximize the success of the game.

The video that we submitted together with this paper represents, to our view, the best experimental results to show the effectiveness of the proposed approach for dynamic strategic positioning. Moreover, we analysed the videos and log files

**Table 1.** Defensive set pieces cover efficiency during the last two games of RoboCup2014. According to the rules, the defending team has to be at least 3 meters from the ball. In these situations it is impossible to intercept the ball.

Game	Opponent	<3m	Intercepted		% Sucess
			Yes	No	
Semi-final	Tech United	11	10	3	77
3rd place	MRL	14	4	3	57
Total		25	14	6	70

**Table 2.** Attacking set pieces efficiency during the last two games of RoboCup2014. We are considering the success of the ball reception after a pass.

Game	Opponent	Pass	% Sucess	
			Yes	No
Semi-final	Tech United	10	8	56
3rd place	MRL	15	6	71
Total		25	14	64

from the RoboCup games. This analysis reveals that the team reached a 70% success rate in the interception of the ball in defensive set pieces (see Table 1), performed 64% successful passes in offensive set pieces (see Table 2) and a high percentage of successful passes in free play, being these last situations hard to analyze due to the high dynamism of the games.

Looking at Table 1, considering that most of the times when the attacking team made a short pass means that was forced into it by not having other pass option, we have a success rate of 70% in defensive set pieces situations.

Looking further into the unsuccessful situations, the problem was clearly identified and it is not related to the cover position obtained from the Utility Maps. The problem was rather the transition from the **Barrier** role into the **Midfielder** or **Striker** role, situations where the cover position are not used. This is still an open issue to be addressed in the near future.

In the last two games of RoboCup 2014, the final and semi-final - which were probably the most dynamic games, there was a total of 45 defensive set pieces situations. An average of 22 defensive set pieces per game, in a game of 30 minutes, which means a defensive set piece situation every 1 minute and 20 seconds.

In Fig. 5 we can see two game situations were the CAMBADA robots are in strategic positions. By being in those positions, the CAMBADA robots do not allow the attacking team to perform a pass in a proper way.

In the same last two games of RoboCup 2014, the final and semi-final, there was a total of 39 offensive set pieces situation. An average of 20 offensive set pieces per game, in a game of 30 minutes, which means an offensive set piece situation every 1 minute and 30 seconds. In 64% of the situations the robots were able to properly receive the ball. Looking further into the unsuccessful situations, there were cases were the ball was passed to a position far from the **Receiver**



**Fig. 5.** Defensive game situations during RoboCup 2014. CAMBADA team has blue markers and it is the defending team.

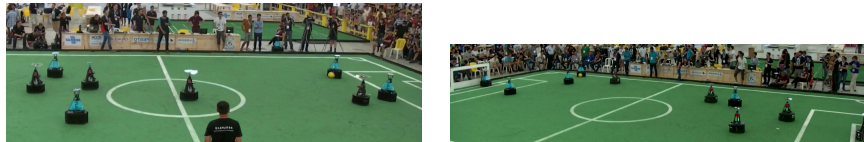


**Fig. 6.** Offensive game situations during RoboCup 2014. CAMBADA team is with blue markers and is the attacking team.

and it was lost and some other cases where the reception was not properly done mainly due to misalignment of the **Receiver**. These situations were not due to a wrong positioning given by the Utility Map. We just counted a total of 3 interceptions by the opponent team of the ball for long passes.

In Fig. 6 we can see two game situations where the CAMBADA robots are in strategic positions, which allows them to receive the ball with success.

Based upon this study, we are convinced that the use of Utility Maps is an advantageous approach in extremely dynamic environments, such as the one of robotic soccer. Without great complexity being added to the structure of the agents, as it was described in the previous sections, it was possible to introduce the desired dynamism that led to the increase of the team competitiveness and improved its overall performance.

## References

1. Neves, A., Azevedo, J., Lau, N., Cunha, B., Silva, J., Santos, F., Corrente, G., Martins, D.A., Figueiredo, N., Pereira, A., Almeida, L., Lopes, L.S., Pedreiras, P.: CAMBADA soccer team: from robot architecture to multiagent coordination, chapter 2, pp. 19–45. I-Tech Education and Publishing, Vienna, January 2010
2. Veloso, M., Bowling, M., Achim, S., Han, K., Stone, P.: The cmunited-98 champion small robot team (accessed February 27, 2014)
3. Stone, P.: Layered Learning in Multiagent Systems: A Winning Approach to Robotic Soccer. MIT Press (2000)
4. Reis, L.P., Lau, N., Oliveira, E.C.: Situation based strategic positioning for coordinating a team of homogeneous agents. In: Hannebauer, M., Wendler, J., Pagello, E. (eds.) ECAI-WS 2000. LNCS (LNAI), vol. 2103, pp. 175–197. Springer, Heidelberg (2001)

5. Lau, N., Lopes, L.S., Corrente, G.: CAMBADA: information sharing and team coordination. In: Proc. of the 8th Conference on Autonomous Robot Systems and Competitions, Portuguese Robotics Open - ROBOTICA 2008, pp. 27–32, Aveiro, Portugal, April 2008
6. Dashti, H.A.T., Aghaeepour, N., Asadi, S., Bastani, M., Delafkar, Z., Disfani, F.M., Ghaderi, S.M., Kamali, S.: Dynamic positioning based on voronoi cells (DPVC). In: Bredenfeld, A., Jacoff, A., Noda, I., Takahashi, Y. (eds.) RoboCup 2005. LNCS (LNAI), vol. 4020, pp. 219–229. Springer, Heidelberg (2006)
7. Akiyama, H., Noda, I.: Multi-agent positioning mechanism in the dynamic environment. In: Visser, U., Ribeiro, F., Ohashi, T., Dellaert, F. (eds.) RoboCup 2007: Robot Soccer World Cup XI. LNCS (LNAI), vol. 5001, pp. 377–384. Springer, Heidelberg (2008)
8. Elfes, A.: Using occupancy grids for mobile robot perception and navigation. Computer **22**(6), 46–57 (1989)
9. Rosenblatt, J.K.: Utility fusion: map-based planning in a behavior-based system. In: Zelinsky, A. (ed.) Field and Service Robotics, pp. 411–418. Springer, London (1998)
10. Chaimowicz, L., Kumar, V.: Mario Fernando Montenegro Campos. A paradigm for dynamic coordination of multiple robots. Auton. Robots **17**(1), 7–21 (2004)
11. Spaan, M.T.J., Groen, F.C.A.: Team coordination among robotic soccer players. In: Kaminka, G.A., Lima, P.U., Rojas, R. (eds.) RoboCup 2002. LNCS (LNAI), vol. 2752, pp. 409–416. Springer, Heidelberg (2003)
12. Santos, F., Almeida, L., Lopes, L.S., Azevedo, J.L., Cunha, M.B.: Communicating among robots in the robocup middle-size league. In: Baltes, J., Lagoudakis, M.G., Naruse, T., Ghidary, S.S. (eds.) RoboCup 2009. LNCS, vol. 5949, pp. 320–331. Springer, Heidelberg (2010)
13. Lau, N., Lopes, L.S., Corrente, G., Filipe, N., Sequeira, R.: Robot team coordination using dynamic role and positioning assignment and role based setplays. Mechatronics **21**(2), 445–454 (2011)
14. Trifan, A., Neves, A.J.R., Cunha, B., Azevedo, J.L.: UAVision: a modular time-constrained vision library for soccer robots. In: Bianchi, R.A.C., Akin, H.L., Ramamoorthy, S., Sugiura, K. (eds.) RoboCup 2014. LNCS, vol. 8992, pp. 490–501. Springer, Heidelberg (2015)
15. Silva, J., Lau, N., António, J.R., Neves, A.J., Azevedo, J.L.: World modeling on an MSL robotic soccer team. Mechatronics **21**(2), 411–422 (2011)

# Intelligent Wheelchair Driving: Bridging the Gap Between Virtual and Real Intelligent Wheelchairs

Brígida Mónica Faria<sup>1,2,3(✉)</sup>, Luís Paulo Reis<sup>2,4</sup>, Nuno Lau<sup>3,5</sup>,  
António Paulo Moreira<sup>6,7</sup>, Marcelo Petry<sup>2,7,8</sup>, and Luís Miguel Ferreira<sup>3</sup>

<sup>1</sup> ESTSP/IPP - Escola Sup. Tecnologia de Saúde do Porto,  
Inst Politécnico do Porto, Vila Nova de Gaia, Portugal

btf@estsp.ipp.pt

<sup>2</sup> LIACC – Lab. Inteligência Artificial e Ciência de Computadores, Porto, Portugal  
lpreis@dsi.uminho.pt, marcelo.petry@ufsc.br

<sup>3</sup> IEETA - Inst. Engenharia Electrónica e Telemática de Aveiro, Aveiro, Portugal  
{nunolau, luismferreira}@ua.pt

<sup>4</sup> Dep. de Sistemas de Informação, EEUM - Escola de Engenharia da Universidade do Minho,  
Guimarães, Portugal

<sup>5</sup> DETI/UA – Dep de Electrónica, Telecomunicações e Informática da Univ. Aveiro,  
Aveiro, Portugal

<sup>6</sup> FEUP - Faculdade de Engenharia, Universidade do Porto, Porto, Portugal  
amoreira@fe.up.pt

<sup>7</sup> INESC TEC - INESC Tecnologia e Ciência, Porto, Portugal

<sup>8</sup> UFSC - Universidade Federal de Santa Catarina, Blumenau, Brazil

**Abstract.** Wheelchairs are important locomotion devices for handicapped and senior people. With the increase in the number of senior citizens and the increment of people bearing physical deficiencies, there is a growing demand for safer and more comfortable wheelchairs. So the new Intelligent Wheelchair (IW) concept was introduced. Like many other robotic systems, the main capabilities of an intelligent wheelchair should be: autonomous navigation with safety, flexibility and capability of avoiding obstacles; intelligent interface with the user; communication with other devices. In order to achieve these capabilities a good testbed is needed on which trials and users' training may be safely conducted. This paper presents an extensible virtual environment simulator of an intelligent wheelchair to fulfill that purpose. The simulator combines the main features of robotic simulators with those built for training and evaluation of prospective wheelchair users. Experiments with the real prototype allowed having results and information to model the virtual intelligent wheelchair. Several experiments with real users of electric wheelchairs (suffering from cerebral palsy) and potential users of an intelligent wheelchair were performed. The System Usability Score allowed having the perception of the users in terms of the usability of the IW in the virtual environment. The mean score was 72 indicating a satisfactory level of the usability. It was possible to conclude with the experiments that the virtual intelligent wheelchair and environment are usable instruments to test and train potential users.

**Keywords:** Intelligent wheelchair · Intelligent robotics · Intelligent simulation · Virtual reality · Multimodal interface

## 1 Introduction

Recently, virtual reality has attracted much interest in the field of motor rehabilitation engineering [1]. Virtual reality has been applied to provide safe and interesting training scenarios with near-realistic environments for subjects to interact with it [2]. The performance of elements within these virtual environments proved to be representative of the elements' abilities in the real world and their real-world skills showed significant improvements following the virtual reality training [3-5]. Until now, electric powered wheelchairs simulators were mainly developed to either facilitate patient training and skill assessment [6] [7] or assist in testing and development of semi-autonomous intelligent wheelchairs [8]. While in the training simulators the focus is on user interaction and immersion, the main objective of the robotics simulators is the accurate simulation of sensors and physical behaviour. The simulator presented here addresses the need to combine these approaches. It is a simple design that provides the user training ability while supporting a number of sensors and ensuring physically feasible simulation for intelligent wheelchairs' development. The simulator is a part of a larger project where the IntellWheels prototype will include all typical IW capabilities, like facial expression recognition based command, voice command, sensor base command, advanced sensorial capabilities, the use of computer vision as an aid for navigation, obstacle avoidance, intelligent planning of high-level actions and communication with other devices.

The experiments with real wheelchair users allowed to access information about the usability of the virtual intelligent wheelchair and virtual environment. These users besides using a wheelchair to move around are also potential users of an intelligent wheelchair. In fact, they suffer from cerebral palsy which is a group of permanent disorders in the development of movement and posture.

This paper is organized with five sections; the first one is composed with this introduction. Section two presents an overview of the methodologies for wheelchair simulation and the criteria to select the platform to simulate the IW and the environment. A special attention is given to the USARSim which was the chosen platform to produce the simulation. In section three a brief description of the IntellWheels project is presented. Section four presents the experiments and results and finally the last section refers the conclusions and future work.

## 2 Methodologies for Wheelchair Simulation

Assistive technologies are defined as any product, instrument, equipment or adapted technology specially designed to improve the functional levels of the disabled person. Resorting to these products can help reduce the limitations in mobility [9] [10] [11] [12]. The electronic wheelchair wheels are an enabling technology, used by people, due to a wide range of diseases including cerebral palsy [13]. Simulators allow users to test and train several of these assistive technologies [14]. This section contains an overview of the methodologies available for developing a wheelchair simulator.

The methodologies that typically are concerned with rendering 2D and 3D are known as graphics engine. Usually they are aggregate inside games engine using specific libraries for rendering. Examples of graphics engines are OpenSceneGraph [15], Object- Oriented Graphics Rendering Engine (OGRE) [16], jMonkey Engine [17] and Crystal Space [18]. The physics engines are software applications with the objective of simulate the physics reality of objects and world. Bullet [19], Havok [20], Open Dynamics Engine (ODE) [21] and PhysX [22] are examples of physics engines. These engines also contribute for robotics simulation for more realistic motion generation of the robot. The game engines are software framework that developers use to create games. The game engines normally include a graphic engine and a physics engine. The collision detection/ response, sound, scripting, animation, artificial intelligence, networking, streaming, memory management, localization support and scene graph are also functionalities included in this kind of engine. Examples of game engine are Unreal Engine 3 [23], Blender Game Engine [24], HPL Engine [25] and Irrlicht Engine [26]. The robotics simulator is a platform to develop software for robots modulation and behaviour simulation in a virtual environment. In several cases it is possible to transfer the application develops in the simulation to the real robots without any extra modification. In the literature there are several commercial examples of robotics simulators: AnyKode Marilou (for mobile robots, humanoids and articulated arms) [27]; Webots (for educational purposes it has a large choice of simulated sensors and actuators is available to prepare each robot) [28]; Microsoft Robotics Developer Studio (HRDS) (allows an easy access to simulated sensors and actuators) [29]; Workspace 5 (environment based on Windows and allows the creation, manipulation and modification of images in 3DCad and several ways of communication) [30]. The non-commercial robotics simulators are also available: SubSim [31]; SimRobot [32]; Gazebo [33]; USARSim [34]; Simbad [35] and SimTwo [36]. A comparison of the most used 3D robotics simulator according several criteria was presented by Petry et al. [37]. Petry et al. [37] also presented the requirements and characteristics for simulation of intelligent wheelchairs and in particularly to the IntellWheels prototype.

The USARSim, acronym of Unified System for Automation and Robot Simulation, is a high-fidelity simulation of robots and environments, based on the Unreal Tournament game engine [34]. Initially was created as a research tool designated as a simulation of Urban Search And Rescue (USAR) robots and environments for the study of human-robot interaction (HRI) and multi-robot coordination [37]. USARSim is the basis for the RoboCup rescue virtual robot competition (RoboCup) as well as the IEEE Virtual Manufacturing Automation Competition (VMAC) [34].

Nowadays, the simulator uses the Unreal Engine UDK and the NVIDIA's PhysX physics engine. The version used to develop the IntellSim was the Unreal Engine 2.5 and the Karma physics engine (which are integrated into the Unreal Tournament 2004 game) which maintain and render the virtual environment and model the physical behaviour of its elements respectively.

### 3 IntellWheels Project

IntellWheels project aims at providing a low cost platform to electric wheelchairs in order to transform them into intelligent wheelchairs. The simulated environment allows to test and train potential users of the intelligent wheelchair. And select the appropriate interface, among the available possibilities, for a specific user. After the first set of experiments [38] it was necessary to improve the realism of the simulated environment and behaviour of the IW. For that reason and trying to maintain the principle of producing the IntellWheels' project as the lowest cost possible the USARSim was the choice for the new simulator. There were other reasons to decide by the USARSim such as, having an advance support on robots with wheels, allowing it the independent configuration; allowing the importation of object and robots modelled in different platforms in order to facilitate for instance the wheelchair modulation; being possible to program robots and control them in the network which can be implemented in the mixed reality [39].

One of the main objectives of the project is also the creation of a development platform for intelligent wheelchairs [40], entitled IntellWheels Platform (IWP). The project main focus is the research and design of a multi-agent platform, enabling easy integration of different sensors, actuators, devices for extended interaction with the user [41], navigation methods and planning techniques and methodologies for intelligent cooperation to solve problems associated with intelligent wheelchairs [42].

The IntellWheels platform allows the system to work in real mode (the IW has a real body), simulated (the body of the wheelchair is virtual) or mixed reality (real IW with perception of real and virtual objects). In real mode it is necessary to connect the system (software) to the IW hardware. In the simulated mode, the software is connected to the IWP simulator. In the mixed reality mode, the system is connected to both (hardware and simulator). Several types of input devices were used in this project to allow people with different disabilities to be able to drive the IW. The intention is to offer the patient the freedom to choose the device they find most comfortable and safe to drive the wheelchair. These devices range from traditional joysticks, accelerometers, to commands expressed by speech, facial expressions or a combination of some of them. Moreover, these multiple inputs for interaction with the IW can be integrated with a control system responsible for the decision of enabling or disabling any kind of input, in case of any observed conflict or dangerous situation. To compose the necessary set of hardware to provide the wheelchair's ability to avoid obstacles, follow walls, map the environment and see the holes and unevenness in the ground, two side bars were designed, constructed and place on the wheelchair. In these bars were incorporated 16 sonars and a laser range finder. Two encoders were also included, and coupled to the wheels to allow the odometry.

#### 3.1 IntellWheels Simulator

The system module, named IntellWheels Simulator [43] or more recent IntellSim, allows the creation of a virtual world where one can simulate the environment of a building (e.g. a floor of a hospital), as well as wheelchairs and generic objects (tables, doors and other objects). The purpose of this simulator is essentially to support the testing of algorithms, analyse and test the modules of the platform and safely train users of the IW in a simulated environment.

The virtual intelligent wheelchair was modelled using the program 3DStudioMax [44]. The visualizing part, which appears on the screen, was imported to the UnrealEditor as separated static meshes (\*.usx) file. The model was then added to USARSim by writing appropriate UnrealScript classes and modifying the USARSim configuration file. The physics property of the model was described in Unreal Script language, using a file for each robot's part. The model has fully autonomous caster wheels and two differential steering wheels. In the simulation it is equipped with: camera; front sonar ring; odometry sensor and encoders. Fig. 1 shows different perspectives of the real and virtual wheelchair.



**Fig. 1.** The real and virtual prototype of the IW

An important factor affecting the simulation of any model in UT2004 is its mass distribution and associated inertial properties. These were calculated using estimated masses of the different parts of the real chair (70 kg) with batteries and literature values for average human body parameters (60 kg). The values obtained for the center of mass and tensor of inertia were used to calculate the required torque for the two simulated motors using the manufacturer's product specification as a guideline. The sensors used in the simulated wheelchair are the same as those used in the real IW. As in the real prototype 16 sonars and a laser range finder were placed in two side bars. Two encoders were also included, and coupled to the wheels to allow odometry. These sensors provide the wheelchair's ability to avoid obstacles, follow walls, map the environment and see the holes and unevenness in the ground. Using the simulator it was also possible to model rooms with low illumination and noisy environments and test the performance of users while driving the wheelchair. The map created was done using the Unreal Editor 3 and it is similar to the local where the patients are used to move around. Several components in the map were modelled using 3DStudioMax. In order to increase the realism of the virtual environment it was implemented several animations using sequence scripts. The simulator runs on a dual-core PC with a gaming standard dual-view graphics card. And other supported input devices include keyboard, mouse, mouse replacement devices and gaming joysticks.

## 4 Experiments and Results

The initial experiments were conducted to have more information about the real prototype and with the objective of being able to model and simulate the behaviour of

the real wheelchair more precisely in virtual environment. The final experiments involved real wheelchair users and potential users of the intelligent wheelchair. Therefore the experiments were divided into two components: wheelchair technical information and users' feeling about the simulated wheelchair and the virtual environment modelled.

#### 4.1 Real Intelligent Wheelchair Characteristics

The technical information was obtained using the manual of the electric wheelchair which the platform was applied, measurements taken and experiments with the real intelligent wheelchair prototype (Table 1 resumes that information).

**Table 1.** Real intelligent wheelchair prototype characteristics

Real Intelligent Wheelchair Prototype Characteristics			
<b>Weight (with batteries)</b>	70 kg	<b>Motor</b>	180w 24 volt, 2.5A max, 3800 RPM (32:1)
<b>Big wheel diameter</b>	0.315 m	<b>Brakes</b>	electromagnetic automatic brakes
<b>Small wheel diameter</b>	0.185 m	<b>Maximum speed</b>	7km/h
<b>Distance between rear wheels</b>	0.535 m	<b>Time for a total rotation</b>	7''
<b>Distance between axes</b>	0.48 m	<b>Sensors</b>	16 sonares, 1 laser range finder (URG-04LX Hokuyo), 2 encoders (rear wheels)



**Fig. 2.** Real intelligent wheelchair experiments

Fig. 2 shows some of the experiments done with real intelligent wheelchair prototype. It was analyzed the velocity and time for the total rotation with the new adaptations applied to the real prototype. The results obtained, using the real prototype, were considered in order to develop the virtual intelligent wheelchair.

## 4.2 IntellSim Experiments

The *IntellSim* experiments were performed by patients suffering from cerebral palsy, all of them wheelchairs users. Using *IntellSim* several experiments were performed changing the conditions of the environment, using the joystick and the manual control. A map was created integrating paths with degrees of difficulty. The overall circuit (Fig. 3) passes through two floors and the link between floors is a ramp. The map was divided into three parts. The first part is characterized by having simple and large corridors without any kind of obstacles except pillars. The second part has narrow corridors, ramps and obstacles. The last part involved a circuit entering in three rooms with different kind of illumination and noise.

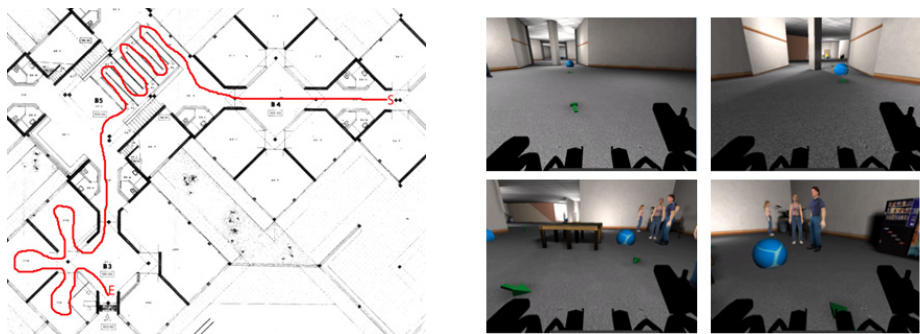


**Fig. 3.** Overall circuit and snapshots of the first person view during the game

After the experiments the users respond to the System Usability Scale [45] which is a simple ten-item *Likert* scale giving a global view of individual assessments of usability (with a score between 0 and 100) and some more questions about safety and control managing the IW, if it was easy to drive the IW in tight places and the attention needed to drive the IW.

### 4.2.1 Sample Characterization

To better understand the next results the sample characterization will be presented. It is important to reinforce that cerebral palsy is defined as a group of permanent disorders in the development of movement and posture. It causes limitations at the level of daily activities because of a non-progressive disturbance which occurs in the brain during the fetal and infant development [46]. The motor disorders in cerebral palsy are associated with deficits of perception, cognition, communication and behaviour. In general, there are also episodes of epilepsy and secondary musculoskeletal problems [46]. The individuals included in this study suffer from cerebral palsy and were classified in the levels IV (26%) and V (74%) of Gross Motor Function Measure (GMF). These are the highest levels in the cerebral palsy severity degree. The sample size was composed of the 19 individuals and all require the use of a wheelchair. The mean of age was 29 years old with 79% males and 21% females. In terms of school level 15% did not answer, 10% are

illiterate, 16% just have the elementary school, 16% have the middle school, 37% have the high school and only 5% have a BSc. The dominant hand was divided as: 12 for left, 6 for right hand and 1 did not answer. Another question was the frequency of use of information and communication technologies: 27% did not answer; 42% answered rarely; 21% sometimes; 5% lots of times and 5% always. The aspects related to experience of using manual and electric wheelchair were also questioned. Table 2 shows the distribution of answers about autonomy and independency using the wheelchair and constraints presented by these individuals.

**Table 2.** Experience using wheelchair, autonomy, independence and constraints of the cerebral palsy users

<b>Experience, Autonomy, Independence and Constraints</b>					
<b>Variables</b>	<b>n</b>	<b>Variables</b>		<b>n</b>	
Use manual wheelchair		Cognitive constraints		no	8
				yes	11
Use electric wheelchair		Motor constraints		no	0
				yes	19
Autonomy using wheelchair		Visual constraints		no	11
				yes	8
Independence using wheelchair		Auditive constraints		no	19
				yes	0

#### 4.2.2 *IntellSim* Results

The results obtained reveal a satisfactory usability in terms of the experiments using the *IntellSim*. In fact all of them could easily identify that the virtual environment was a replica of the cerebral palsy institution where they are used to be.

**Table 3.** Results of the experiments in *IntellSim*

<b>IntellSim experiments with patients suffering from cerebral palsy</b>					
	<b>Mean</b>	<b>Median</b>	<b>Std</b>	<b>Min</b>	<b>Max</b>
<b>Usability and Safety</b>					
Score SUS	72.0	70.0	11.7	57.5	95
Safety managing IW	--	Agree	--	Ind	S Agree
Control of the IW	--	Agree	--	Ind	S Agree
Easy to drive the IW in tight places	--	Agree	--	Dis	S Agree
The IW do not need to much attention	--	Dis	--	S Dis	Agree
<b>Satisfaction</b>	--	VSatis	--	Ind	V Satis
<b>Performance</b>					
Time	12.6	9.5	8.6	5.6	42.4
Number of objects collected	12.7	14	3.6	4	15

Legend: S Dis – strongly disagree; Dis – disagree; Ind – indifferent; S Agree – strongly agree; V Diss – very dissatisfied; Diss – dissatisfied; Satis – satisfied; VSatis – very satisfied

The SUS mean score was satisfactory and all the users considered the usability positive (higher than 57.5). Overall, the users were very satisfied with the experience. The users made the circuit with a median of 9.5 minutes. The best time was made by a user in 5.6 minutes and the worst time 42.4 minutes was made by a user with severe difficulties and without autonomy or independence in driving a wheelchair. The data from the logs allows plotting the circuits after the experiment. It is a way of analysing the behaviour of the users (Fig. 4).

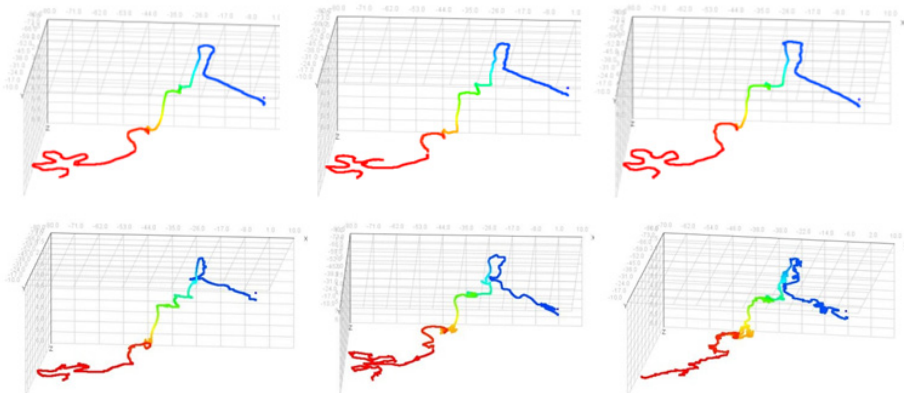


**Fig. 4.** Circuits performed by patients suffering from cerebral palsy with joystick

It is interesting to notice that the path is smooth using the joystick in manual mode and using the *IntellSim*. These three individuals are autonomous and independent in driving their own electric wheelchairs with joystick (Level IV of the GMF). The next three circuits' examples (second line in the Fig. 4) were executed by the users that took the longest times. In the left example the user took 17.7 minutes to collect 14 objects and to finish the circuit. In the middle the user took 22.35 to collect 12 objects and on the right side there is the circuit performed by the user that took the longest time of 42.4 minutes to collect only 9 objects. Although these three examples are the worst in terms of performance it is necessary to enhance that they are classified in the most severe degree of the GMF and do not have the autonomy and independence to drive a conventional wheelchair. However, the *IntellSim* can be used to train these users and with appropriate methodologies, such as shared or automatic controls, it is possible to drive the IW in efficient and effective manner.

## 5 Conclusions and Future Work

The attention given to the autonomy and independence of the individual is nowadays an actual subject. The scientific community is concerned in develop and present many prototypes, such as intelligent wheelchairs, however most of them only execute experimental work in the labs and without real potential users. The virtual reality wheelchair

simulator presented here addresses an important gap in wheelchair simulation in that it can be used for both patient training or evaluation and design and development of semi-autonomous intelligent wheelchairs. Because of its flexibility and the long (and expanding) list of sensors inherited from the USARSim project, the current system provides a perfect test bed for development and testing of intelligent wheelchair systems. Experimental work with the real IW prototype enable having information about weight, wheels diameters, distance between axes and wheels, motor characteristics, maximum speed, time for total rotation and localization and sensors characteristics in order to realistic model the virtual wheelchair. The experiments with real patients suffering from cerebral palsy allow having a confirmation about the usability of the IW in the *IntellSim*. The performance results also present evidences that it is possible to use the *IntellSim* as a training and test tool.

After this exploratory work for bridging the gap between the real and virtual IW and for future work the full capabilities of the IW are going to be tested with real patients. The possibility of driving the IW using a multimodal interface and a shared control that allows the correction of the trajectory of the user with severe constraints are some of the issues that are going to be tested.

**Acknowledgments.** This work is financed by LIACC (PEst-OE/EEI/UI0027/2014) and ERDF – European Regional Development Fund through the COMPETE Programme (operational programme for competitiveness) and by National Funds through the FCT – Fundação para a Ciência e a Tecnologia (Portuguese Foundation for Science and Technology) within project «FCOMP-01-0124-FEDER-037281».

## References

- Holden, M.K.: Virtual environments for motor rehabilitation: review. *J. Cyberpsychol Behav.* **8**(3), 187–211 (2005)
- Boian, R.F., Burdea, G.C., Deutsch, J.E., Windter, S.H.: Street crossing using a virtual environment mobility simulator. In: Proceedings of IWVR, Lausanne, Switzerland (2004)
- Inman, D.P., Loge, K., Leavens, J.: VR education and rehabilitation. *Commun. ACM* **40**(8), 53–58 (1997)
- Harrison, A., Derwent, G., Enticknap, A., Rose, F.D., Attree, E.A.: The role of virtual reality technology in the assessment and training of inexperienced powered wheelchair users. *Disabil Rehabil* **24**(8), 599–606 (2002)
- Adelola, I.A., Cox, S.L., Rahman, A.: VEMS - training wheelchair drivers, Assistive Technology, vol. 16, pp. 757–761. IOS Press (2005)
- Desbonnet, M., Cox, S.L., Rahman, A.: Development and evaluation of a virtual reality based training system for disabled children. In: Sharkey, P., Sharkeand, R., Lindström, J.-I. (eds.) The Second European Conference on Disability, Virtual Reality and Associated Technologies, Mount Billingen, Skvde, Sweden, pp. 177–182 (1998)
- Niniss, H., Inoue, T.: Electric wheelchair simulator for rehabilitation of persons with motor disability, Symp Virtual Reality VIII, Belém (PA). Brazilian Comp. Society (BSC) (2006)
- Röfer, T.: Strategies for using a simulation in the development of the Bremen autonomous wheelchair. In: 12th European Simulation Multi Conference 1998 Simulation: Past, Present and Future, ESM 1998, Manchester, UK, pp. 460–464 (1998)

9. Tefft, D., Guerette, P., Furumasu, J.: Cognitive predictors of young children's readiness for powered mobility. *Dev. Medicine and Child Neurology* **41**(10), 665–670 (1999)
10. Faria, B.M., Silva, A., Faias, J., Reis, L.P., Lau, N.: Intelligent wheelchair driving: a comparative study of cerebral palsy adults with distinct boccia experience. In: Rocha, Á., Correia, A.M., Tan, F., Stroetmann, K. (eds.) *New Perspectives in Information Systems and Technologies*, Volume 2. AISC, vol. 276, pp. 329–340. Springer, Heidelberg (2014)
11. Palisano, R.J., Tieman, B.L., Walter, S.D., Bartlett, D.J., Rosenbaum, P.L., Russell, D., et al.: Effect of environmental setting on mobility methods of children with cerebral palsy. *Developmental Medicine & Child Neurology* **45**(2), 113–120 (2003)
12. Wiart, L., Darrah, J.: Changing philosophical perspectives on the management of children with physical disabilities-their effect on the use of powered mobility. *Disability & Rehabilitation* **24**(9), 492–498 (2002)
13. Edlich, R.F., Nelson, K.P., Foley, M.L., Buschbacher, R.M., Long, W.B., Ma, E.K.: Technological advances in powered wheelchairs. *Journal Of Long-Term Effects of Medical Implants* **14**(2), 107–130 (2004)
14. Faria, B.M., Teixeira, S.C., Faias, J., Reis, L.P., Lau, N.: Intelligent wheelchair simulator for users' training: cerebral palsy children's case study. In: 8th Iberian Conf. on Information Systems and Technologies, vol. I, pp. 510–515 (2013)
15. Wang, R., Qian, X.: *OpenSceneGraph 3 Cookbook*. Packt Pub. Ltd., Birmingham (2012)
16. Koranne, S.: *Handbook of Open Source Tools*, West Linn. Springer, Oregon (2010)
17. jMonkeyEngine (2012). <http://jmonkeyengine.com/> (current May 2014)
18. Space, C.: Crystal Space user manual, Copyright Crystal Space Team. [http://www.crystarspace3d.org/main/Documentation#Stable\\_Release\\_1.4.0](http://www.crystarspace3d.org/main/Documentation#Stable_Release_1.4.0) (current May 2014)
19. Gu, J., Duh, H.B.L.: *Handbook of Augmented Reality*. Springer, Florida (2011)
20. Havok, Havok (2012). <http://havok.com/> (current May 2014)
21. Smith, R.: *Open Dynamics Engine* (2007). <http://www.ode.org/> (current May 2014)
22. Rhodes, G.: *Real-Time Game Physics*, in *Introduction to Game Development*, Boston, Course Technology, pp. 387–420 (2010)
23. Busby, J., Parrish, Z., Wilson, J.: *Mastering Unreal Technology*. Sams Publishing, Indianapolis (2010)
24. Flavell, L.: *Beginning Blender - Open Source 3D Modeling, Animation and Game Design*. Springer, New York (2010)
25. Games, F.: *Frictional Games* (2010). <http://www.frictionalgames.com/site/about> (current May 2014)
26. Kyaw, A.S.: *Irrlicht 1.7 Realtime 3D Engine – Beginner's Guide*. Packt Publishing Ltd., Birmingham (2011)
27. Marilou, April 2012. <http://doc.anykode.com/frames.html?frmname=topic&frmfile=index.html> (current May 2014)
28. Cyberbotics, Webots Reference Manual, April 2012. <http://www.cyberbotics.com/reference.pdf> (current May 2014)
29. Johns, K., Taylor, T.: *Microsoft Robotics Developer Studio*. Wrox, Indiana (2008)
30. Workspace, Workspace Robot Simulation, WAT Solutions (2012). <http://www.workspaceelt.com/> (current May 2014)
31. Boeing, A., Braunl, T.: SubSim: an autonomous underwater vehicle simulation package. In: 3rd Int. Symposium on A. Minirobots for Research and Edut, Fukui, Japan
32. Laue, T., Röfer, T.: SimRobot - development and applications. In: Proceedings of the International Conference on Simulation, Modeling and Programming for Autonomous Robots, Venice, Italy (2008)
33. Gazebo, Gazebo. <http://gazebosim.org/> (current May 2014)

34. Carpin, S., Lewis, M., Wang, J., Balakirsky, S., Scrapper, C.: USARSim: a robot simulator for research and education. In: Proceedings of the IEEE International Conference on Robotics and Automation, Roma, Italy (2007)
35. Hugues, L., Bredeche, N.: Simbad Project Home, May 2011. <http://simbad.sourceforge.net/> (current May 2014)
36. Costa, P.: SimTwo - A Realistic Simulator for Robotics, March 2012. <http://paginas.fe.up.pt/~paco/pmwiki/index.php?n=SimTwo.SimTwo> (current May 2014)
37. Petry, M., Moreira, A.P., Reis, L.P., Rossetti, R.: Intelligent wheelchair simulation: requirements and architectural issues. In: 11th International Conference on Mobile Robotics and Competitions, Lisbon, pp. 102–107 (2011)
38. Faria, B.M., Vasconcelos, S., Reis, L.P., Lau, N.: Evaluation of Distinct Input Methods of an Intelligent Wheelchair in Simulated and Real Environments: A Performance. The Official Journal of RESNA (Rehabilitation Engineering and Assistive Technology Society of North America) **25**(2), 88–98 (2013). USA
39. Namee, B.M., Beaney, D., Dong, Q.: Motion in Augmented Reality Games: An engine for creating plausible physical interactions in augmented reality games. International Journal of Computer Games Technology (2010)
40. Braga, R., Petry, M., Moreira, A., Reis, L.P.: A development platform for intelligent wheelchairs for disabled people. In: 5th Int. Conf Informatics in Control, Automation and Robotics, vol. 1, pp. 115–121 (2008)
41. Reis, L.P., Braga, R.A., Sousa, M., Moreira, A.P.: IntellWheels MMI: a flexible interface for an intelligent wheelchair. In: Baltes, J., Lagoudakis, M.G., Naruse, T., Ghidary, S.S. (eds.) RoboCup 2009. LNCS, vol. 5949, pp. 296–307. Springer, Heidelberg (2010)
42. Braga, R., Petry, M., Moreira, A., Reis, L.P.: Platform for intelligent wheelchairs using multi-level control and probabilistic motion model. In: 8th Portuguese Conf. Automatic Control, pp. 833–838 (2008)
43. Braga, R.A., Malheiro, P., Reis, L.P.: Development of a realistic simulator for robotic intelligent wheelchairs in a hospital environment. In: Baltes, J., Lagoudakis, Michail G., Naruse, Tadashi, Ghidary, Saeed Shiry (eds.) RoboCup 2009. LNCS, vol. 5949, pp. 23–34. Springer, Heidelberg (2010)
44. Murdock, K.L.: 3ds Max 2011 Bible. John Wiley & Sons, Indianapolis (2011)
45. Brooke, J.: SUS: A quick and dirty usability scale, in Usability evaluation in industry, pp. 189–194. Taylor and Francis, London (1996)
46. Rosenbaum, P., Paneth, N., Leviton, A., Goldstein, M., Bax, M., Damiano, D., Dan, B., Jacobsson, B.: A report: the definition and classification of cerebral palsy April 2006. Developmental Medicine & Child Neurology - Supplement **49**(6), 8–14 (2007)

# A Skill-Based Architecture for Pick and Place Manipulation Tasks

Eurico Pedrosa<sup>(✉)</sup>, Nuno Lau, Artur Pereira, and Bernardo Cunha

Department of Electronics, Telecommunications and Informatics, IEETA, IRIS,  
University of Aveiro, Aveiro, Portugal  
`{efp,nunolau,artur}@ua.pt, mbc@det.ua.pt`

**Abstract.** Robots can play a significant role in product customization but they should leave a repetitive, low intelligence paradigm and be able to operate in unstructured environments and take decisions during the execution of the task. The EuRoC research project addresses this issue by posing as a competition to motivate researchers to present their solution to the problem. The first stage is a simulation competition where Pick & Place type of tasks are the goal and planning, perception and manipulation are the problems. This paper presents a skill-based architecture that enables a simulated moving manipulator to solve these tasks. The heuristics that were used to solve specific tasks are also presented. Using computer vision methods and the definition of a set of manipulation skills, an intelligent agent is able to solve them autonomously. The work developed in this project was used in the simulation competition of EuRoC project by team IRIS and enabled them to reach the 5<sup>th</sup> rank.

## 1 Introduction

The trend in industry is clearly for higher levels of customization of products, which must be enabled by fast customization and adaptability of the production lines to different requirements. Robots can play a significant role in this customization but they should leave a repetitive, low intelligence paradigm and be able to operate in unstructured environments and take decisions during the execution of the task. The European Robotics Challenges (EuRoC) is a research project based on a robotics competition that aims to present solutions to the European manufacturing industry. Exploring our healthy competitive nature, we try to build and developed a robot, or robots, to accomplish a task better than the competition. Usually, the final outcome is a push in the boundary of our knowledge. Take for example the DARPA Grand Challenge from which self-driving cars are a reality, e.g. [12].

The EuRoC project is divided in three challenges, each with different motivations and objectives. Our focus is the *Shop Floor Logistics and Manipulation* challenge, or Challenge 2 (C2), a challenge that presents tasks to be solved by a mobile robot with manipulation capabilities in a industrial shop floor. The first stage of the challenge, was a simulation contest where the contesting teams had

to solve several tasks in a *Simulation Environment* in order to score (Sect. 2). In the end, the best fifteen teams became candidates for entering a second stage.

The *Simulation Environment* of EuRoC C2 exposes an interface with the simulation using the Robotic Operating System (ROS) communications middleware. To address this requirement we propose a *System Architecture* that is mapped into ROS without the loss of generality (Sect. 3). The analysis of the properties of the environment allowed us to design a generic agent that can be used to solve any task (Sect. 4). On top of this architecture and agent design, the logistics and manipulation tasks are solved using computer vision methods and a set of manipulation skills ruled by several heuristics (Sect. 5). Some related work is presented in Sect. 6 and final conclusion in Sect. 7.

## 2 Shop Floor Logistics and Manipulation

The motivation of this challenge is to bring a mobile robot onto the shop floor for dexterous manipulations and logistics carries. Enabling an autonomous robot to operate in an unstructured environment and establishing a safe and effective human-robot interaction are two of the main research issues to be addressed.

The first stage consists of a sequence of tasks to be performed in a simulated environment, with increasing difficulties in the problem to be solved. The *Simulation Environment* consist of a Light-Weight-Robot (LWR), with a two-jaw-gripper, mounted on a moving XY axis on a table top, and a fixed mast with a Pan & Tilt (PT) actuator. Additionally, a vision system made by a pair of RGB and Depth cameras is installed on the PT and another on the Tool Center Point (TCP). The objects to be manipulated assume a basic shape, i.e. cylinder or box, or a compound of basic shapes. An overview is depicted in Fig. 1.

All tasks include a Pick & Place (P&P) scenario where objects (e.g. Fig. 2) have to be picked from unknown locations and placed on target locations. Required actions to accomplish a task includes: perception, to locate the objects; manipulation, to pick and place them; and planning, to move the arm to the target locations. For demonstrating these problems four different tasks are considered.

**P&P.** The goal is to pick all objects in the working space and place them in the proper location without any particular order. The task contains three objects of different shape and color on the table (e.g. Figures 2c, 2b 2d). The pose of the objects in the environment are unknown but their properties (color and shape composition) and corresponding place zone are given. The LWR base cannot move. Scoring is achieved by picking an object and place it in the correct zone.

**P&P with Significant Errors and Noise.** This is the same task as P&P but with the difference that there are significant errors in the robot precision and also significant noise in all sensors. This implies an operation of the LWR in an imprecise and uncalibrated environment.

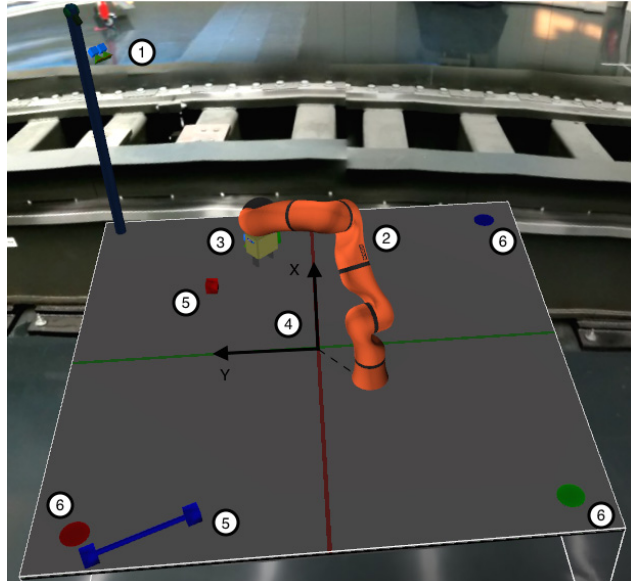


**Fig. 1.** Overview of the simulation environment. 1) Mast with a PT, 2) LWR, 3) Gripper, 4) XY Axis, 5) Object to pick, 6) Place zone.

**Mobile P&P with Typical Errors and Noise.** This is based on the P&P task, but with typical calibration errors and sensor noise. The LWR can now use the *XY* axis to move. This task introduces the concept of mobility, meaning that pick and place positions may not be in range of the LWR, not considering the additional axis.

**Loose Assembly of a Puzzle.** In this tasks, a puzzle made up of pieces like the ones depicted in Fig. 2a and Fig. 2e, initially scattered across the table in unknown locations has to be loosely done. Each puzzle part is composed of basic blocks and has to be placed into a puzzle of size 4x4. To allow parts to be pushed, the puzzle fixture has two fixed sides. Scoring is achieved by covering the puzzle with the correct blocks.

### 3 System Architecture Overview

The tasks to be accomplished were different. However, while studying the problems to be solved, common subtasks were identified. In order to take advantage of this fact, a system architecture to solve all tasks was developed. This architecture, shown in Fig. 3, is divided into three components: *Simulation Environment*, *Interface Node*, and *Agent*.

The *Interface Node*, supplied by the EuRoC partners to all teams, provides an abstraction of the *Simulation Environment*. The purpose of this abstraction

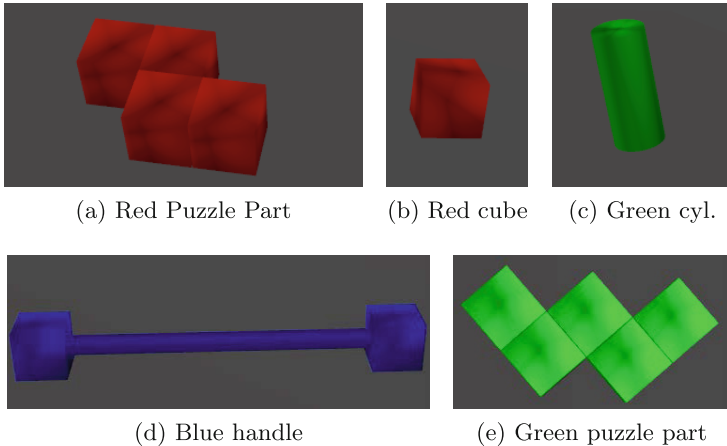


**Fig. 2.** Examples of objects that appear in the simulated environment. The puzzle parts are only examples of the set of valid shapes. Objects may vary on scale and color.

is to allow a future replacement of the *Simulation Environment* with a *Real Environment*, where a real robot in a real shop floor would be used instead with minimum modifications of the *Agent*.

The proposed *Agent* is composed of a *Solver*, multiple *Skills* and a *Sensory Data Adapter*. The *Solver* is responsible for making decisions on how to solve the current task based on the current sensory data and available *Skills*. A *Skill* is the capacity of doing a particular task like, for instance, picking an object or moving the end-effector of the manipulator to a desired pose. The role of the *Sensory Data Adapter* is to convert the sensor data format transmitted by the *Interface Node* to the format used inside the *Agent*.

The provided interface with the *Simulation Environment* is implemented using ROS [6]. This communications middleware is a publish-subscribe infrastructure where a **topic** is a communication channel that forwards **messages** from the publisher to the subscriber. A **node**, which is a system process, can subscribe or advertise  $n$  **topics**, with  $n \geq 0$ . In addition, it provides a request-response infrastructure through **services**.

The *Interface Node*, as the bridge between the *Simulation Environment* and the *Agent*, is a **node** that provides a continuous stream of sensory data and a set of functions to interact with the simulation effectors. The sensory data stream includes the images from the cameras and effectors feedback (i.e. telemetry), and is sent through **topics**. The provided functions include: inverse and forward kinematics calculation, joint motion planning and execution, and operation mode control. All functions are available as **services**.

The *Sensory Data Adapter* is a ROS **node** that converts the joints state information to a transformation tree using ROS **tf** package. This allows the user to keep track the multiple coordinate frames over time. The telemetry information is only provided upon request, i.e. by service call. The reason for this choice

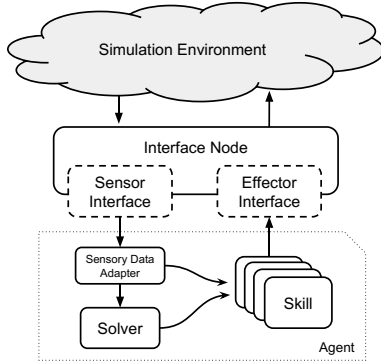


**Fig. 3.** Diagram of the system architecture.

is based on the fact that the telemetry information is published at a rate of 1 kHz that would introduce a computation overhead to all **nodes** that require this information. This way only the *Sensory Data Adaptor* suffers from a computation overhead, other nodes needing this information may request it at a desired rate.

Each *Skill* is implemented as a ROS **node** that exposes itself as a **service**. Only a *Skill* knows how to interact with the simulation effectors, doing it by using the appropriate functions of the *Interface Node*.

The *Solver* is the decision-making module implemented in a single **node**. Based on the task to be solved and on an initially analysis of the environment, it defines a plan to solve the task and executes it using the available skills.

## 4 Agent Design

The EuRoC project exposes a set of tasks with perception and manipulation problems to be completed. To solve these tasks we need a proper *agent* capable of perceiving the environment through sensors and act upon that environment using actuators [8]. To design such *agent* we have to analyze the properties of the environment, which in this case is a well defined *Simulated Environment*, to develop a generic as possible solution capable of handling all tasks. Our proposal is summarized in algorithm form in Fig. 4.

The set  $\mathcal{O}$  of objects to be manipulated in each task, including their properties and place zones, is known in advance. The algorithm starts by determining the order by which the objects have to be manipulated. The order is restricted by a direct acyclic graph (dag), which represents a dependency graph between objects in terms of order of manipulation. Leafs represent objects that need to be handled first. A dummy object  $\lambda$  is added to represent the graph root.

Once an object is manipulated, it is removed from the graph. Thus, at any moment in the task execution, leafs represent objects that can be manipulated. When the dummy object is the only one in the graph, the task is completed.

```

1:  $\mathcal{G} \leftarrow \text{BUILDORDERGRAPH}(\mathcal{O})$ ,  $\mathcal{S} \leftarrow \text{buildSearchSpace}(\mathcal{G})$ 
2: while leafs( $\mathcal{G}$ )  $\neq \lambda$  do  $\triangleright \lambda$  is the empty root
3:    $\mathcal{L} \leftarrow \text{leafs}(\mathcal{G})$ 
4:    $obj \leftarrow \text{detectObject}(\mathcal{L})$ 
5:   while  $obj$  is not found do
6:      $s \leftarrow \text{next}(\mathcal{S})$ 
7:     move( $s$ )
8:      $obj \leftarrow \text{detectObject}(\mathcal{L})$ 
9:   end while
10:  focusObject( $obj$ )
11:  plan =  $\text{MAKEPLAN}(obj)$ 
12:  success = execute(plan)
13:  if success then
14:    removeLeaf( $\mathcal{G}, obj$ )
15:  end if
16: end while

```

**Fig. 4.** Generic algorithm to solve a task.

If the TCP is over an object, its vision system is in a privileged position to help in its location and pick up operation. However it has to move to there first. In the other side, and despite of being in a high position, it can be not possible, even using its pan and tilt capabilities, to cover all the objects in the table with the vision system placed in the mast. For instance, an object could be occluded by the LWR. Thus, both vision systems are used.

To ensure that all object are eventually detected, a set of search poses  $\mathcal{S}$  is calculated by the procedure *buildSearchSpace*, insuring that the entire workspace is covered. To improve the search, the vision system on the PT is used to detect objects in the environment and the obtained poses are put in the head of  $\mathcal{S}$  in the order defined by  $\mathcal{G}$ . It may not detect any object, but if it does, the system can gain in overall execution time due to good initial search poses. Thus, each pose in  $\mathcal{S}$  represents a region containing one or more objects or a region that should be locally explored using the TCP vision system. The set  $\mathcal{S}$  is encoded as a circular list so that search poses never ends. The algorithm then executes two nested loops that, making the TCP move around the searchable poses, finishes when all objects are placed in their target positions. Each searchable pose is explored to see if a leaf object is there. If so, a sequence of steps is performed to put the object in its target position.

First, the TCP is moved in such a way that the focus axis of the RGB camera intercepts the geometry center of the object, giving preference to positions in which the gripper is perpendicular to the object's plane. This way the object appears in the center of the image, which results in two benefits: the distortion of the object in the image is reduced; and it copes better with noise in sensors and effectors by restricting the problem to a bounded local space.

In order to properly transfer the object to its target position a plan is computed. A plan is a sequence of actions that allows to properly pick the object,

move the TCP and place the object properly in the target position. Those actions depend on a priori calculation of the pick and place pose. The way the plan is calculated depends on the task being solved and on the disposition of the object and its target position. For instance, the target position could be non-reachable from the top, then the object has to be picked from a different direction. If the execution of the plan succeed, the leaf corresponding to the processed object is removed from the graph and the algorithm goes to the next iteration.

From this design only two procedures are task dependent, `BUILDORDERGRAPH` and `MAKEPLAN`. This fosters the re-utilization of software code and facilitates the task solving job, since the developer only has to focus on the creation of a plan. To aid the definition of a plan, a set of skills was defined and implemented.

#### 4.1 Object Detection Pipeline

The objective of the object detection module is, as the name implies, to detect an object in the environment. It creates information about an object by processing the fed sensory data. The input data is the RGB and depth images created by one of the two available vision systems. The data is processed by several submodules managed by a pipeline (Fig. 5).

**Depth and RGB Integration.** Before any processing takes place it is necessary to match every depth value to the corresponding RGB value [3]. The depth and the RGB images come from different cameras separated by an offset, thus they do not overlap correctly. To solve this issue, for each depth value in the depth image, the corresponding 3D space position is calculated and then re-projected into the image plane of the RGB camera. The registered depth is then transformed into an organized point cloud in the coordinates frame of the LWR.

**Height Filter.** The purpose of the *Height Filter* is to reduce the search space for objects of interest using the fact that they are on top of a table (e.g. Fig. 6a). A filter is applied to the pointcloud where positions with  $z$  value below a threshold are set to not-a-number (NaN), identifying a non searchable position. The output of this block is a mask defined by the filtered pointcloud that identifies the searchable areas in the RGB image (Fig. 6b).

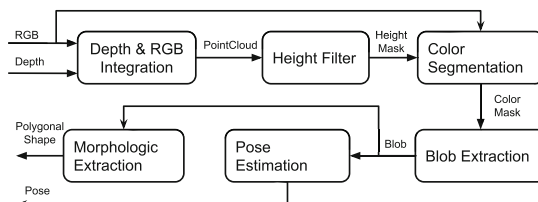


**Fig. 5.** Object detection pipeline.

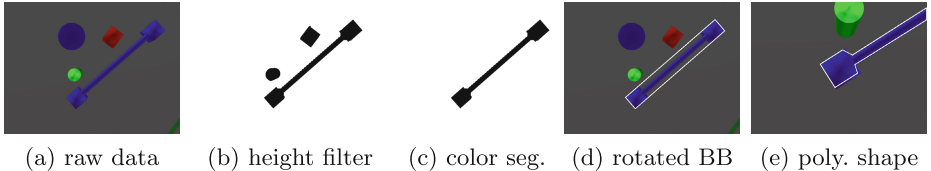


**Fig. 6.** View of several stages in the object detection pipeline.

**Color Segmentation.** The color of the object is a known attribute, it is homogeneous but subject to different light conditions (e.g. shadows). Using color segmentation we can further identify the object of interest. The segmentation is applied on HSV color space to reduce the influence of different light conditions [10]. The output of this block is a mask defined by the segmentation (Fig. 6c).

**Blob Extraction.** At this stage, it is expected that the input mask defines one or more undefined shape areas. More than one blob can happen if two, or more, objects share the same color. However, we are only interested in one object, thus only the blob with the biggest area is considered. This is a safe action because different objects have different shapes and can be disambiguated by matching the shape from the blob contours with the correct object. To extract a blob, the contours of the segmented areas are calculated by contour detection function [11]. The output mask is a set of points that delimits the area of the blob.

**Pose Estimation.** After the identification of the object blob in the image we calculate its position ( $x, y, z$ ) and orientation  $\theta$ . We start by calculating the rotated bounding box that best fits the select blob (e.g. Fig. 6d). The center of the rectangle in the image provide us enough information to extract its position because we have a registered point cloud where  $(u, v)$  coordinate from the RGB image has a corresponding  $(x, y, z)$ . Furthermore, from the rotation of the rectangle we can now extract the orientation of the object relative to the LWR.

**Morphologic Extraction.** The goal is to extract a useful shape from the blob (e.g. Fig. 6e). All objects are treated as polygons, even the cylinder that is a circle when looked from above – a circle can be approximated by a polygon. The shape is obtained by a function that approximates the blob to a polygon [2]. The polygon shape can then be used to disambiguate an object detection.

## 4.2 Agent Skills

A *Skill* is the capability to perform a specialized action with a semantic meaning. Performing an action will always imply a physical motion by one or more actuators. In the *Simulated Environment* we have several actuators, already described, that are controlled by joints, either rotational or linear. All joints can be actuated on to provoke motion at the same time, meaning that a skill is not necessarily

bound to one actuator. For example, moving the LWR and the *XY* axis at the same time can be considered a single skill.

To solve any task we need a set of skills that are enough for the tasks ahead, but at the same time keep their number low as possible. The idea is to create skills that can be used as atoms from more complex skills. To solve a task we need the capability to move the LWR so that its TCP is in the desired position, e.g. a search pose to perceive the environment. Objects needs to be picked and place, so this actions are also necessary. It may not always be possible to position an object with a place action, for example, the Gripper may hit a wall when placing right next to it. This can be solved by pushing the object to its rightfull place.

**Simple Move.** This skill uses only the LWR actuator. Its objective is to put the LWR's TCP on the requested pose. This action requires at first the calculation of the inverse-kinematics, and then the control of the joints to the desired position.

**Move XY Axis.** The reach of the LWR can be increased by using the *XY* axis to move it. This skill only requires *x, y* positions to move. The values are directly applied to the joints.

**Pick Object.** The LWR and Gripper are used together to provide this skill. It expects as input a pick pose that must correspond to the tip of the Gripper end-effector. The skill will do the necessary calculation to transform the input pose to the corresponding TCP pose to move the LWR. Then it takes the proper actions to safely grab the object.

**Place Object.** This skill uses the LWR and Gripper to place the object in the requested pose. The input pose is adjusted to the TCP and then a safe position is calculated to ensure that the object will hover the floor before the actual place. Then it will lower the object with a lower velocity to prevent any undesirable collisions due to higher accelerations.

**Push Object.** When it is not possible to place an object without a harmful collision a push strategy can be applied. Assuming that the object is near its final position, we can use the Gripper to push the object until it reaches the final destination. This is achieved by defining a path between two points to be covered by the end-effector of the Gripper. If an object is in the path, as a product of the LWR motion the object will be pushed. The skill is sensible enough to ask for a motion with force limits. If the limit is not reached it means the object could be pushed to its final position.

## 5 Experiments with Solving Tasks

To evaluate the proposed architecture for logistics and manipulation tasks we set to solve the already described tasks: all P&P tasks and Loose Assembly of a Puzzle. As stated, to solve a task we have to concentrate our efforts on the objects order and planning. Most planning involve finding the correct pick and place positions and then make use of the available skills to accomplish that.

### 5.1 Pick and Place Tasks

In these tasks, the order by which the objects are picked and placed is not relevant and so graph  $\mathcal{G}$  does not contain any order dependency. Thus, once an object is detected it can be picked and placed in its target location.

The agent assumes all objects are pickable. This implies that there is a part of the object the gripper is able to grab. Since the shapes of the objects are known in advance, the grab pose, defined in the object's frame of reference, can be pre-determined. The gripper's grabbing pose can be obtained by merging this information with the rotated bounding box (RBB) that encloses the object, estimated by the object detection module. For basic shape objects, the grab pose coincides with the center of the RBB. For compound objects, the grab pose can be obtained from the center of the RBB, adding half of its width and subtracting half of its height. This approach worked well even in the presence of significant noise.

The preferable way to pick an object is applying a top-down trajectory to the gripper (Fig. 7a). However, this may not be possible due to constraints in the freedom of motion of the LWR. In such cases, an angular adjustment is applied to make the pick operation possible (Fig. 7c). This drawback can be mitigated when the LWR's movement along the  $XY$  axes is available, since the LWR can be moved to a better position to pick the object of interest.

After an object is picked it must be placed in its target location. The most efficient move is to place it keeping the gripper orientation. But, again, it may not be possible. When this happens, a fake placement is done instead: an appropriated location is chosen, the object is placed there, and a failure signal is returned so that the object is picked again. Similarly as before, the availability of robot movement along the  $XY$  axes can avoid this drawback.

### 5.2 Loose Assembly of a Puzzle

The assembly of the puzzle can not be done by putting the parts from above. The margin of error for the positioning is very thin, making it difficult to use an approach where the parts are put from the top. Then, using the puzzle fixture boundary and the already in place parts, a pushing approach can be used. To

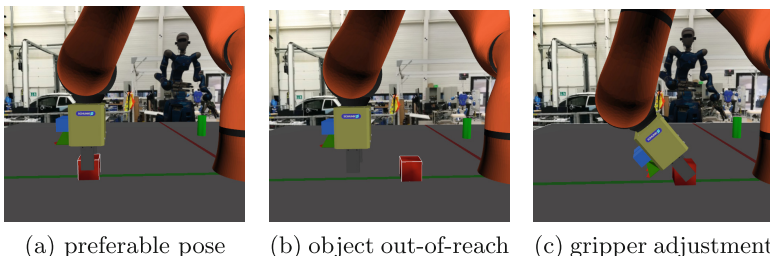


**Fig. 7.** Example of an out-of-reach situation for the preferable pick pose.

find the right order we search all permutations for ordering the objects in their insertion in the puzzle. The valid solutions must comply with the following rule: the pushing of the object, horizontally or vertically, is not prevented by any other object. After a solution is found the graph  $\mathcal{G}$  is built.

The pick position is selected from one of the convex terminations of the part that has a width smaller than the Gripper maximum width. The parts of the puzzle are always assembled from cubes with a width smaller than the gripper maximum width, hence the pick position must consider a convex termination with the width of a cube. To calculate the pick position the vertices of the polygon shape are used. The vertices  $v$  are properly ordered and ring accessible by  $v_i$ . The main idea is to search for an edge  $\mathbf{e}_i = (v_i, v_{i+1})$  that is part of the frame of reference. An edge  $\mathbf{e}_i$  is a candidate when:

$$\|\mathbf{e}_i\| \approx \ell \quad \wedge \quad \angle(\mathbf{e}_{i-1}, \mathbf{e}_i) \approx \angle(\mathbf{e}_i, \mathbf{e}_{i+1}) \approx \frac{\pi}{2}$$

where  $\ell$  is the length of a cube edge. Approximate values are considered to handle errors. Afterward, all candidates go through a final validation. To recognize the object frame of reference, which is needed to correctly place the object, we assume that the vertices  $v_i$  is the origin, then, the number of blocks at the left, right, top and bottom are compared with the original object shape definition. Once an edge is selected the pick position is given by sum of the normalized edges  $\mathbf{e}_i$  and  $\mathbf{e}_{i+1}$ , and the orientation is given by the normal direction of  $\mathbf{e}_i$ . The  $XY$  is available for this task, thus any object can be picked in the preferable way.

The next step is to define the set of actions to position the puzzle part in its rightful place. An offset is added to the final position  $p$  of the puzzle part in the puzzle fixture  $p_o = p + \text{offset}$  to prevent an overlap of parts. The offset takes into account how the parts are connected. After it is placed at  $p_o$ , it has to be pushed towards  $p$ . The first push is towards the closest fixed axis and the next it against the supporting piece – or axis. Doing a single pushing sequence may not be enough. For some reason the piece may get stuck, therefore, the sequence must be repeated. Detecting a stuck piece is simple, since the TCP reports the applied force and when a force above a threshold is detected a termination is triggered.

## 6 Related Work

ROS has become the robot middleware of choice for researcher and the industry. For example, MoveIt! [1] is a mobile manipulation software suitable for research and the industry. In addition to manipulation, the creation of behaviors is also a topic of interest, e.g. ROSCo [5]. Task level programming of robots is an important exercise for industrial applications. The authors of SkiROS [7] propose a paradigm based on a hierarchy movement primitives, skills and planning. For P&P tasks, the authors of [9] propose a manipulation planner under continuous grasps and placements, while a decomposition of the tasks is proposed by [4].

## 7 Conclusion

The tasks to be accomplished were different. However, while studying the problems to be solved, we identified common subtasks. In order to take advantage of that fact, a general system architecture to solve all tasks was developed. Additionally, the architecture works seamlessly in the ROS infrastructure. This solution allowed our team to achieve the 5<sup>th</sup> rank.

**Acknowledgments.** This research is supported by the European Union's FP7 under EuRoC grant agreement CP-IP 608849; and by the Foundation for Science and Technology in the context of UID/CEC/00127/2013 and Incentivo/EEI/UI0127/2014.

## References

1. Chitta, S., Sucan, I., Cousins, S.: Moveit! [ros topics]. *IEEE Robotics Automation Magazine* **19**(1), 18–19 (2012)
2. Douglas, D.H., Peucker, T.K.: Algorithms for the reduction of the number of points required to represent a digitized line or its caricature. *Cartographica: The International Journal for Geographic Information and Geovisualization* (1973)
3. Henry, P., Krainin, M., Herbst, E., Ren, X., Fox, D.: RGB-D mapping: Using Kinect-style depth cameras for dense 3D modeling of indoor environments. *I. J. Robotic Res.* **31**(5), 647–663 (2012)
4. Lozano-Pérez, T., Jones, J.L., Mazer, E., O'Donnell, P.A.: Task-level planning of pick-and-place robot motions. *IEEE Computer* **22**(3), 21–29 (1989)
5. Nguyen, H., Ciocarlie, M., Hsiao, K., Kemp, C.: Ros commander (rosco): Behavior creation for home robots. In: ICRA, pp. 467–474 (May 2013)
6. Quigley, M., Gerkey, M., Conley, K., Faust, J., Foote, T., Leibs, J., Berger, E., Wheeler, R., Ng, A.: ROS: An open-source robot operating system. In: ICRA Workshop on Open Source Software, Kobe, Japan (May 2009)
7. Rovida, F., Chrysostomou, D., Schou, C., Bøgh, S., Madsen, O., Krüger, V., Andersen, R.S., Pedersen, M.R., Grossmann, B., Damgaard, J.S.: Skiros: A four tiered architecture for task-level programming of industrial mobile manipulators. In: 13th International Conference on Intelligent Autonomous System, Padova (July 2013)
8. Russell, S., Norvig, P.: *Artificial Intelligence: A Modern Approach*, 3rd edn., Prentice Hall (2010)
9. Simeon, T., Cortes, J., Sahbani, A., Laumond, J.P.: A manipulation planner for pick and place operations under continuous grasps and placements. In: Proceedings of the Robotics and Automation, ICRA 2002, vol. 2, pp. 2022–2027 (2002)
10. Sural, S., Qian, G., Pramanik, S.: Segmentation and histogram generation using the hsv color space for image retrieval. In: Proceedings of the 2002 International Conference on Image Processing 2002, vol. 2, pp. II-589–II-592 (2002)
11. Suzuki, S., Abe, K.: Topological structural analysis of digitized binary images by border following. *Computer Vision, Graphics and Image Processing* **30**(1), 32–46 (1985)
12. Urmson, C., Baker, C.R., Dolan, J.M., Rybski, P.E., Salesky, B., Whittaker, W., Ferguson, D., Darms, M.: Autonomous Driving in Traffic: Boss and the Urban Challenge. *AI Magazine* **30**(2), 17–28 (2009)

# Adaptive Behavior of a Biped Robot Using Dynamic Movement Primitives

José Rosado<sup>1(✉)</sup>, Filipe Silva<sup>2</sup>, and Vítor Santos<sup>3</sup>

<sup>1</sup> Department of Computer Science and Systems Engineering, Coimbra Institute of Engineering, IPC, 3030-199 Coimbra, Portugal  
jfr@isec.pt

<sup>2</sup> Department of Electronics, Telecommunications and Informatics, Institute of Electronics and Telematics Engineering of Aveiro, University of Aveiro, 3810-193 Aveiro, Portugal  
fmsilva@ua.pt

<sup>3</sup> Department of Mechanical Engineering, Institute of Electronics and Telematics Engineering of Aveiro, University of Aveiro, 3810-193 Aveiro, Portugal  
vitor@ua.pt

**Abstract.** Over the past few years, several studies have suggested that adaptive behavior of humanoid robots can arise based on phase resetting embedded in pattern generators. In this paper, we propose a movement control approach that provides adaptive behavior by combining the modulation of dynamic movement primitives (DMP) and interlimb coordination with coupled phase oscillators. Dynamic movement primitives (DMP) represent a powerful tool for motion planning based on demonstration examples. This approach is currently used as a compact policy representation well-suited for robot learning. The main goal is to demonstrate and evaluate the role of phase resetting based on foot-contact information in order to increase the tolerance to external perturbations. In particular, we study the problem of optimal phase shift in a control system influenced by delays in both sensory information and motor actions. The study is performed using the V-REP simulator, including the adaptation of the humanoid robot's gait pattern to irregularities on the ground surface.

**Keywords:** Biped locomotion · Adaptive behavior · Movement primitives · Interlimb coordination · Phase resetting

## 1 Introduction

The coordination within or between legs is an important element for legged systems independently of their size, morphology and number of legs. Evidences from neurophysiology indicate that pattern generators in the spinal cord contribute to rhythmic movement behaviors and sensory feedback modulates proper coordination dynamics [1], [2]. In this context, several authors studied the role of phase shift and rhythm resetting. Phase resetting is a common strategy known to have several advantages in legged locomotion, namely by endowing the system with the capability to switch among different gait patterns or to restore coordinated patterns in the face of

disturbances. In human biped walking the maintenance of reciprocal out-of-phase motions of the legs is critical for stable and efficient gait patterns [3], [4].

In the same line of thought, coordination dynamics is important for humanoid robots operating in real world environments. Further, this dynamics often needs to be adapted to account for variations in the environment conditions and external perturbations. Over the past few years different approaches to coordination has been applied to biped locomotion robots in which the emergence and change of coordination patterns are governed by dynamical equations [5], [6]. These authors have explored the role of phase resetting for adaptive walking based on foot-contact information using theoretical models and physical robots. Adaptation of the interlimb parameters largely restores symmetry of the gait cycle with inherent advantages for stability. In other words, the adjustment of the phase between legs helps to substantially increase the range of parameters (*e.g.*, average speed) and the tolerance to disturbances for which stable walking is possible.

In this paper, we propose a movement control approach that provides adaptive behavior by combining the modulation of dynamic movement primitives (DMP) and interlimb coordination with coupled phase oscillators. DMP appeared as a powerful tool for motion planning based on demonstration examples. This approach is currently used as a compact policy representation well-suited for robot learning. Here, rhythmic DMP are employed as trajectory representations learned in task-space from a single demonstration. Once learned, new movements are generated by simply modifying the parameters of the DMP. Adaptive biped locomotion based on phase resetting, which is the main focus of this paper, is studied and evaluated using the ASTI robot model in the V-REP simulation software [10]. The main goal is to demonstrate and evaluate the role of phase resetting based on foot-contact information in order to increase the tolerance to external perturbations. In particular, we study the problem of optimal phase shift in a control system influenced by delays in both sensory information and motor actions.

The remainder of the paper is organized as follows: Section 2 describes the proposed approach for trajectory formation based on rhythmic movement primitives learned in the task space and their modulation capabilities. Section 3 presents the interlimb coordination strategy based on coupled phase oscillators and phase resetting embedded with the movement control. In Section 4 the applicability of these concepts is demonstrated by numerical simulations. Section 5 concludes the paper and discusses future work.

## 2 Rhythmic Movement Primitives

### 2.1 Trajectory Formation

Dynamical system movement primitives have become a robust policy representation, for both discrete and periodic movements, that facilitates the process of learning and improving the desired behavior [7]. The basic idea behind DMP is to use an analytically well-understood dynamical system with convenient stability properties and modulate it with nonlinear terms such that it achieves a desired point or limit cycle

attractor. The approach was originally proposed by Ijspeert et al. [8] and, since then, other mathematical variants have been proposed [9].

In the case of rhythmic movement, the dynamical system is defined in the form of a linear second order differential equation that defines the convergence to the goal  $g$  (baseline, offset or center of oscillation) with an added nonlinear forcing term  $f$  that defines the actual shape of the encoded trajectory. This model can be written in first-order notation as follows:

$$\begin{aligned}\ddot{z} &= \alpha_z [\beta_z(g - y) - z] + f \\ \dot{y} &= z\end{aligned}, \quad (1)$$

where  $\tau$  is a time constant the parameters  $\alpha_z, \beta_z > 0$  are selected and kept fixed, such as the system converge to the oscillations given by  $f$  around the goal  $g$  in a critically damped manner. The forcing function  $f$  (nonlinear term) can be defined as a normalized combination of fixed basis functions:

$$\begin{aligned}f(\phi) &= \frac{\sum_{i=1}^N \psi_i \omega_i}{\sum_{i=1}^N \psi_i} r \\ \psi_i(\phi) &= \exp(-h_i(\cos(\phi - c_i) - 1)),\end{aligned} \quad (2)$$

where  $\omega$  are adjustable weights,  $r$  characterizes the amplitude of the oscillator,  $\psi_i$  are von Mises basis functions,  $N$  is the number of periodic kernel functions,  $h_i > 0$  are the widths of the kernels and  $c_i$  equally spaced values from 0 to  $2\pi$  in  $N$  steps ( $N, h_i$  and  $c_i$  are chosen a priori and kept fixed). The phase variable  $\phi$  bypasses explicit dependency on time by introducing periodicity in a rhythmic canonical system. This is a simple dynamical system that, in our case, is defined by a phase oscillator:

$$\tau \dot{\phi} = \Omega, \quad (3)$$

where  $\Omega$  is the frequency of the canonical system. In short, there are two main components in this approach: one providing the shape of the trajectory patterns (the transformation system) and the other providing the synchronized timing signals (the canonical system). In order to encode a desired demonstration trajectory  $y_{demo}$  as a DMP, the weight vector has to be learned with, for example, statistical learning techniques such as locally weighted regression (LWR) given their suitability for online robot learning.

## 2.2 Extension to Multiple Degrees-of-Freedom

The extension of the previous concepts to multiple degrees-of-freedom (DOF) is commonly performed by sharing one canonical system among all DOFs, while maintaining a set of transformation systems and forcing terms for each DOF. In brief, the canonical system provides the temporal coupling among DOFs, the transformation

system achieves the desired attractor dynamics for each individual DOF and the respective forcing terms modulate the shape of the produced trajectories.

The adaptation of learned motion primitives to new situations becomes difficult when the demonstrated trajectories are available in the joint space. The problem occurs because, in general, a change in the primitive's parameters does not correspond to a meaningful effect on the given task. Having this in mind, the proposed solution is to learn the DMP in task space and relate their parameters to task variables. To concretely formulate the dynamical model, a task coordinate system is fixed to the hip section that serves as a reference frame where tasks are presented. The  $y$ -axis is aligned with the direction of movement, the  $z$ -axis is oriented downwards and the  $x$ -axis points towards the lateral side to form a direct system.

In line with this, a total of six DMP are learned to match the Cartesian trajectories of the lower extremities of both feet (end-effectors), using a single demonstration. It is worth note that a DMP contains one independent dynamical system per dimension of the space in which it is learned. At the end, the outputs of these DMP are converted, through an inverse kinematic algorithm, to the desired joint trajectories used as reference input to a low-level feedback controller. Fig. 1 shows the close match between the reference signals (solid lines) and the learned ones (dashed lines) as defined in the reference frame. The gray shaded regions show the phases of double-support.

Once the complete desired movement  $\{y, \dot{y}, \ddot{y}\}$  is learned (*i.e.*, encoded as a DMP), new trajectories with similar characteristics can be easily generated. In this work, the DMP parameters resulting from the previous formulation (*i.e.*, amplitude, frequency and offset) are directly related to task variables, such as step length, hip height, foot clearance and forward velocity. For example, the frequency is used for speed up or slow down the motion, the amplitudes of the DMP associated with the  $y$ - and  $z$ -coordinates are used to modify the step length and the hip height (or foot clearance) of the support leg (or swing leg), respectively.

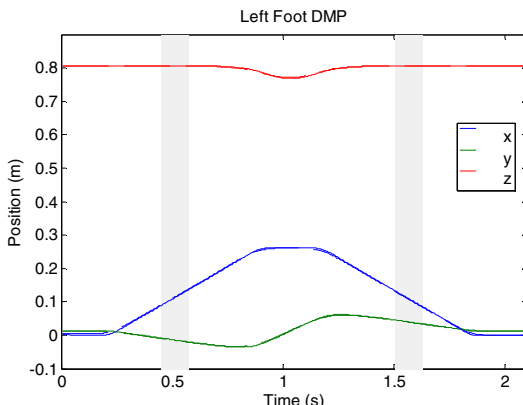


**Fig. 1.** Result of learning the single-demonstration: the task is specified by the  $x$ ,  $y$  and  $z$ -coordinates of the robot's foot in the reference frame. Reference signal (solid line) and trained signal (dashed line) are superimposed. Gray shaded regions show double-support phases.

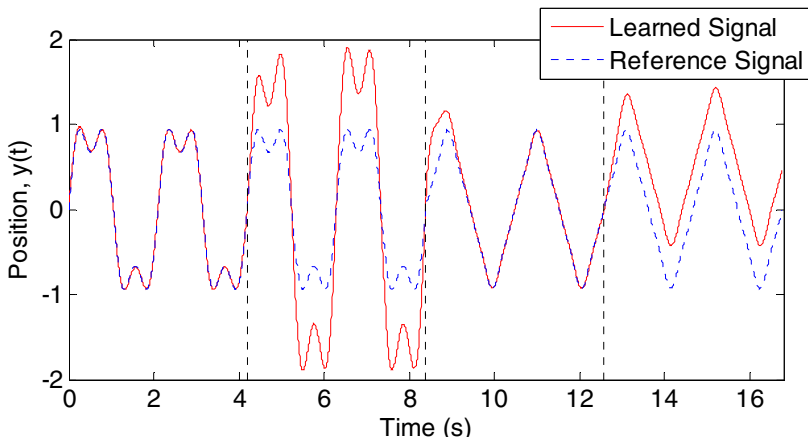
### 3 Adaptive Biped Locomotion

#### 3.1 Modulation of the DMP Parameters

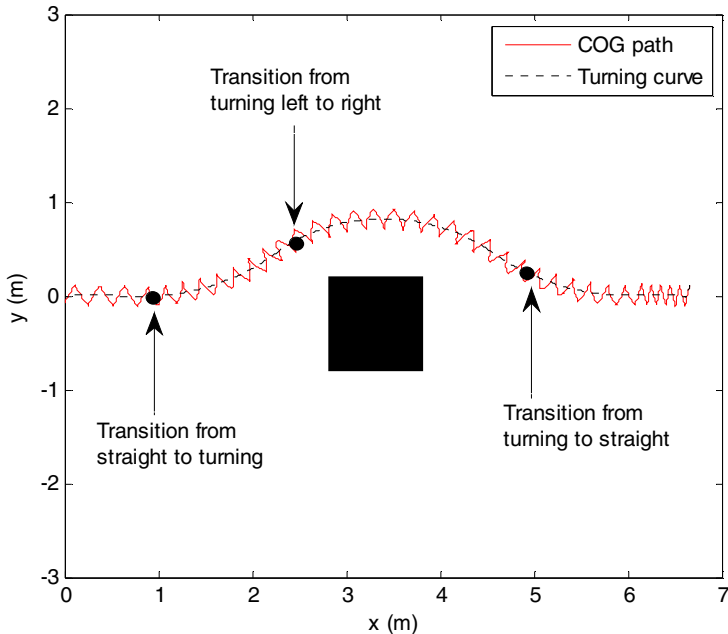
The formulation of DMP includes a few parameters which allow changing the learned behavior. This subsection provides examples of how new movements can be generated by simply modifying the parameters of a rhythmic DMP. These parameters can potentially be used to adapt the learned movement to new situations in order, for example, to adapt the final goal position, the movement amplitude or the duration of the movement. Therefore, the amplitude, frequency and offset parameters will be modified by scaling the corresponding parameters  $r$ ,  $\Omega$  and  $g$ , respectively.

Fig. 2 shows the time evolution of the rhythmic motion associated to a canonical system with frequency  $\Omega = 2\text{Hz}$  and whose weights  $\omega$  are learned to fit two different trajectories: the first is the sum of the first two harmonics of a rectangular wave defined in the interval between  $t = 0$  and  $t = 8\text{s}$ ; the second trajectory is the sum of the first three harmonics of a triangular wave defined in the interval between  $t = 8\text{s}$  and  $t = 16\text{s}$ . The reference input signal is superimposed and vertical dashed lines marks events where the parameters are changed: the instant in which the learned signal doubles the amplitude  $r$  (at  $t = 4\text{s}$ ), change the reference signal (at  $t = 8\text{s}$ ) and modulates the baseline  $g$  (at  $t = 12.5\text{s}$ ). The main observation is that the changes of parameters result in smooth variations of the trajectory  $y(t)$  to be reproduced by the robot.

An example of the use of DMP modulation to biped locomotion is shown in Fig 3. The original signal that was used to train the DMP was modified in order to change the relative step length of each leg and the corresponding foot clearances. This strategy allows the robot to turn with a smooth curve around an obstacle placed on its path (a video is available at <http://www.youtube.com/watch?v=Y3Y-6WNhxHE>).



**Fig. 2.** Time courses of the rhythmic dynamical system with continuous learning (solid line) and the input reference signal (dashed-line). The vertical dashed-lines in the plot indicate, from left to right, the instant in which the learned signal doubles the amplitude  $r$  (at  $t = 4\text{s}$ ), change the reference signal (at  $t = 8\text{s}$ ) and modulates the baseline  $g$  (at  $t = 12.5\text{s}$ ).



**Fig. 3.** View of the movement path of the robot’s COG projected on the ground and the corresponding turning curve. The black box represents an obstacle placed on the path.

### 3.2 Interlimb Coordination

DMP exhibit a desirable property in the context of robot learning from demonstration: the system does not depend on an explicit time variable, giving them the ability to handle spatial or temporal perturbations. This property makes them attractive in order to create smooth kinematics control policies that can robustly replicate and adapt demonstrations. However, adaptation of inter-limb parameters is essential to restore the symmetry of the gait cycle in order to reduce the likelihood of becoming unstable. For example, whenever a leg is constrained, for example, by external perturbations, compensatory reactions in the other leg are expected such as to restore the out-of-phase relationship between legs.

In this study, one canonical system per leg and multiple transformation systems associated with the  $x$ -,  $y$ - and  $z$ -coordinates of the robot’s end-effectors are adopted. Intra-limb coordination results from planning trajectories in the Cartesian space, constraining the leg to act as one unit. Phase coordination between legs is provided by two separate canonical oscillators coupled such that the left and the right limbs move 180 degrees out-of-phase. At the same time, phase resetting of the oscillator phase is based on foot-contact information (a kinematic event) that depends on force sensors placed on the feet.

As a result, the dynamics of the phase oscillators in (3), for the left and the right leg, are modified according to:

$$\begin{aligned}\tau\dot{\phi}_{left} &= \Omega - K_\phi \sin(\phi_{left} - \phi_{right} - \pi) - (\phi_{left} - \phi^{contact})\delta(t - t_{left}^{contact} - \Delta t), \\ \tau\dot{\phi}_{right} &= \Omega - K_\phi \sin(\phi_{right} - \phi_{left} - \pi) - (\phi_{right} - \phi^{contact})\delta(t - t_{right}^{contact} - \Delta t)\end{aligned}\quad (4)$$

where  $K_\phi$  is the coupling strength parameter ( $K_\phi > 0$ ),  $\phi^{contact}$  is the phase value to be reset when the foot touch the ground,  $\delta(\cdot)$  is the Dirac's delta function,  $t_i^{contact}$  ( $i = \text{left, right}$ ) is the time when the foot touch the ground and  $\Delta t$  is a factor used to study the influence of delays in both sensory information an motor control.

## 4 Numerical Simulations

The applicability of these concepts is demonstrated by numerical simulations performed in V-REP, Virtual Robot Experimentation Platform [17], using the ASTI robot model available in their libraries. Two specific experiments are conducted demonstrate the important role of phase resetting to achieve adaptive locomotion subject to perturbations.

### 4.1 Robustness Against Disturbing Forces

In the first experiment, an external force is applied to the trunk section of the humanoid robot in two situations: a horizontal force is applied on the direction of the movement or, instead, on the backward direction. Specifically, after the robot has achieved a steady-state stable walking, a horizontal force is applied for 0.1 s at its center-of-gravity (COG). The instant in which this external force is applied varies, from the moment the left foot leaves the ground to the instant when the same foot touches the ground, in intervals of 50ms. In both cases, the maximum force tolerated by robot without falling was measured, with and without phase resetting. Fig. 4 shows the increase on the tolerated forces with phase reset for the backward and the forward force application, respectively. It is worth noting that the tolerance to disturbing forces is greatly affected by the phase value to be reset requiring its optimization.

The result of applying a force to the robot, with and without phase resetting is observed on the variation of the COG velocity on the direction of movement (see Fig. 5). Here a force was applied around the 11.6s and we can see that without phase resetting the robot lost the stability with a high increase on the COG velocity leaving to the fall a few seconds after (blue curve). With phase resetting, the impact produces a moderate increase on the COG velocity, but after a few seconds the normal cyclic pattern is recovered. Also, the coupling between the phase oscillators recovers the phase offset of 180° between each leg. In fact, as we can see on the black curve, the phase resetting produces an increase on the phase offset to around 205° degrees at the moment of the force application and the coupling returns this offset to the 180° after a few seconds.

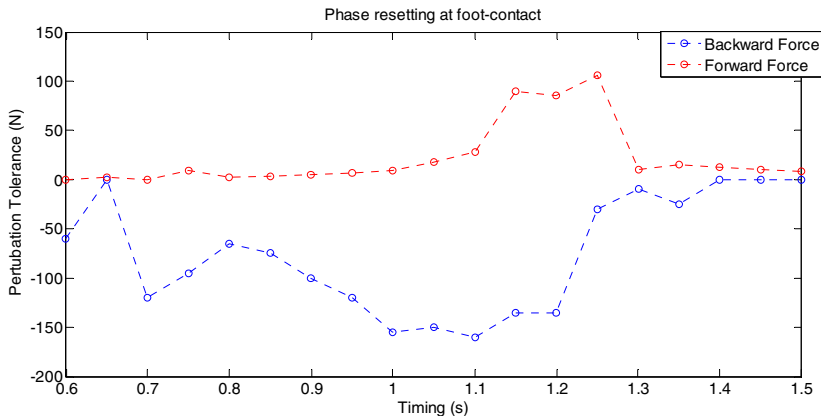


**Fig. 4.** Additional tolerance to perturbation forces applied at different instants of the movement cycle when using phase resetting.

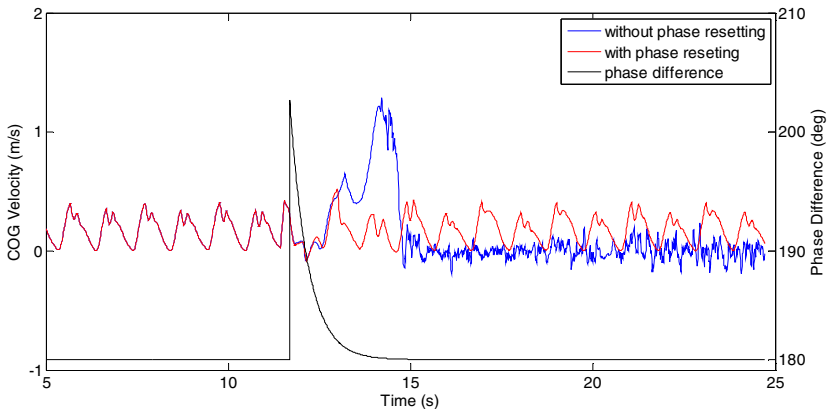


**Fig. 5.** Velocity of the COG in the direction of the motion with a perturbation force applied at 11.5s without and with the use of phase resetting; the time course of the phase difference between the oscillators is represented in a different vertical axis.

#### 4.2 Adaptation to Irregular Terrains

Biped walking in irregular terrains depends on prediction about when the swing foot touches the ground. In the first experiment, the humanoid robot walks over a level surface when it finds a small step of 2 cm high used to approximate irregularities of the environments. The learned DMP phase is reset online to properly incorporate the sensory information from the force sensors mounted on the robot feet. More concretely, the dynamic event corresponds to foot-contact information at the instant of impact of the swing foot with the ground. Fig. 6 illustrates snapshots of the robot walking response without and with phase reset. It was found that using the locomotion pattern as defined by the learned DMP, without any modulation, the robot tolerates step

irregularities up to 0.5 cm height. Here, the proposed strategy is to change the phase of the canonical system to a value corresponding to the point of ground contact on the normal signal generation (when there's no early contact with the ground).

In the second experiment, it is examined how the phase reset of the canonical oscillator provides changes on the DMP that allows the robot to overcome a set of irregularities that assemble like a set of steps of a small staircase. These consist of two consecutive steps up followed by two steps down, each one with 2cm high. Beside this the robot system is also supposed to receive visual information regarding the stairs location and height in order to modify the basic gait pattern (foot clearance and step size). Fig. 7 shows the path the robot has to go through and the sequence of captured images of the robot stepping on the first step, followed by the second step and after a few steps on this, the first down step followed by the final down step takes the robot to the ground level. As in the previous example, a phase reset is applied as soon the robot senses the foot as hit the ground sooner than expected.

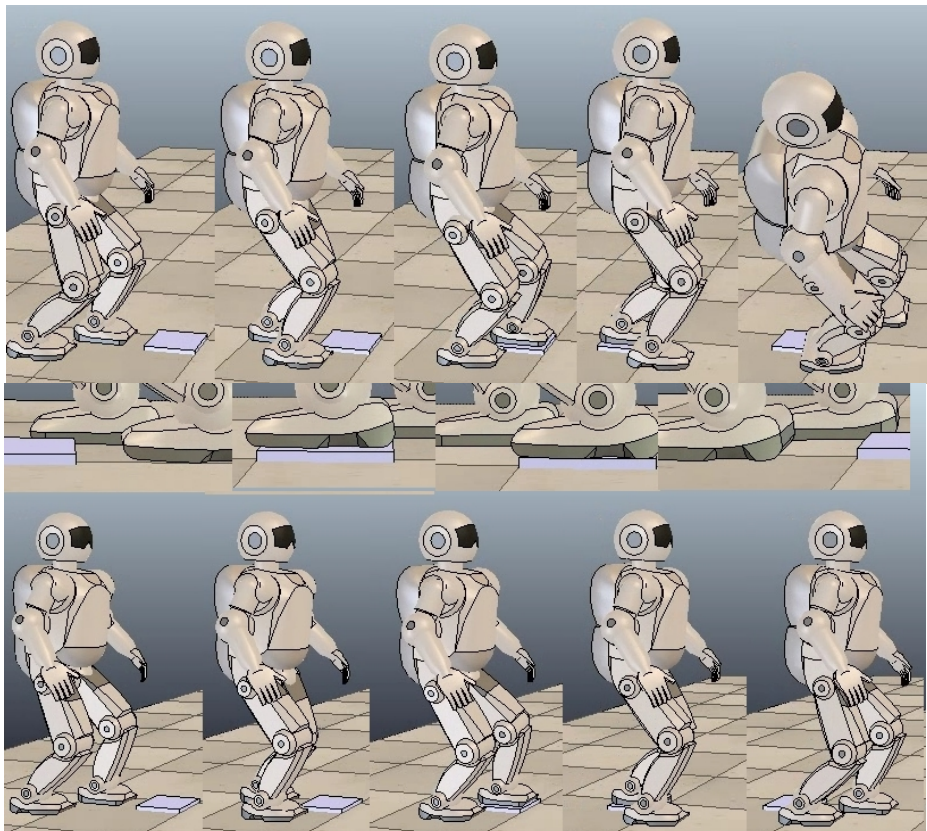


**Fig. 6.** Snapshots of the robot walking on a level surface when it finds a small step 2 cm high that disturbs its balance (top: without phase resetting; bottom: with phase resetting). Numerical simulations performed in V-REP [10].

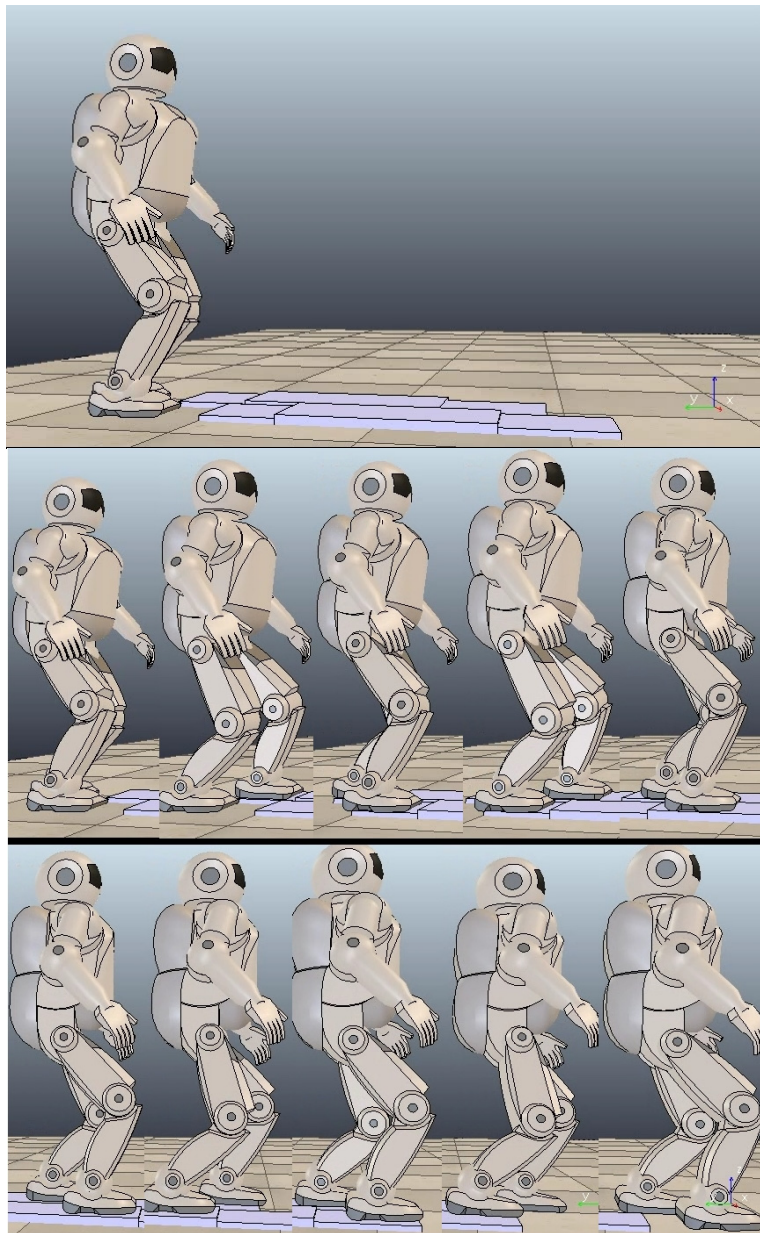


**Fig. 7.** Top: full view of the path the robot has to go through; center and bottom: sequence of the robot walking through the path. Numerical simulations performed in V-REP [10] (a video of this experiment is available at: <http://www.youtube.com/watch?v=WjBq27hAJE>).

## 5 Conclusions

This paper presents a study in which online modulation of the DMP parameters and interlimb coordination through phase coupling providing adaptation of biped locomotion with improvement to external perturbations. By using the DMP in the task space, new tasks are easily accomplished by modifying simple DMP parameters that directly relate to the task, such as step length, velocity, foot clearance. By introducing coupling between members and using phase reset we have shown that adaption to irregularities on the terrain are successful. The phase resetting methodology also allowed increasing the tolerance to external perturbations, such as forces that push or pull the robot on the direction of the movement. Future work will address problems like the role of phase resetting and DMP parameters change in sudden changes on the trunk mass, stepping up stairs, climbing up and down on ramps. Demonstrations from human data behavior will be collected using a VICON system and used to train the DMP in new tasks.

**Acknowledgements.** This work is partially funded by FEDER through the Operational Program Competitiveness Factors - COMPETE and by National Funds through FCT - Foundation for Science and Technology in the context of the project FCOMP-01-0124-FEDER-022682 (FCT reference Pest-C/EEI/UI0127/ 2011).

## References

1. Hultborn, H., Nielsen, J.: Spinal control of locomotion – from cat to man. *Acta Physiologica* **189**(2), 111–121 (2007)
2. Grillner, S.: Locomotion in vertebrates: central mechanisms and reflex interaction. *Physiological Reviews* **55**(2), 247–304
3. Aoi, S., Ogiwara, N., Funato, T., Sugimoto, Y., Tsuchiya, K.: Evaluating the functional roles of phase resetting in generation of adaptive human biped walking with a physiologically based model of the spinal pattern generator. *Biological Cybernetic* **102**, 373–387 (2010)
4. Yamasaki, T., Nomura, T., Sato, S.: Possible functional roles of phase resetting during walking. *Biological Cybernetic* **88**, 468–496 (2013)
5. Aoi, S., Tsuchiya, K.: Locomotion control of a biped robot using nonlinear oscillators. *Autonomous Robots* **19**(3), 219–232 (2005)
6. Nakanishi, J., Morimoto, J., Endo, G., Cheng, G., Schaal, S., Kawato, M.: A framework for learning biped locomotion with dynamical movement primitives. *International Journal of Humanoid Robots* (2004)
7. Argall, B., Chernova, S., Veloso, M., Browning, B.: A survey of robot learning from demonstration. *Robotics and Autonomous Systems* **57**(5), 469–483 (2009)
8. Ijspeert, A., Nakanishi, J., Schaal, S.: Movement imitation with nonlinear dynamical systems in humanoid robots. In: Proceedings of the 2002 IEEE International Conference on Robotics and Automation, pp. 1398–1403 (2002)
9. Ijspeert, A., Nakanishi, J., Hoffmann, H., Pastor, P., Schaal, S.: Dynamical movement primitives: learning attractor models for motor behaviors. *Neural Computation* **25**, 328–373 (2013)
10. Rohmer, E., Singh, S., Freese, M.: V-REP: A versatile and scalable robot simulation framework. In: IEEE/RSJ International Conference on Intelligent Robots and Systems, pp. 1321–1326 (2013)

# Probabilistic Constraints for Robot Localization

Marco Correia, Olga Meshcheryakova, Pedro Sousa, and Jorge Cruz<sup>(✉)</sup>

NOVA Laboratory for Computer Science and Informatics,  
DI/FCT/UNL, Caparica, Portugal  
[{mvc,jcrc}@fct.unl.pt](mailto:{mvc,jcrc}@fct.unl.pt)

**Abstract.** In robot localization problems, uncertainty arises from many factors and must be considered together with the model constraints. Probabilistic robotics is the classical approach for dealing with hard robotic problems that relies on probability theory. This work describes the application of probabilistic constraint techniques in the context of probabilistic robotics to solve robot localization problems. Instead of providing the most probable position of the robot, the approach characterizes all positions consistent with the model and their probabilities (in accordance with the underlying uncertainty). It relies on constraint programming to get a tight covering of the consistent regions combined with Monte Carlo integration techniques that benefit from such reduction of the sampling space.

**Keywords:** Probabilistic robotic · Constraint programming · Robot localization

## 1 Introduction

Uncertainty plays a major role in modeling most real-world continuous systems and, in particular, robotic systems. A reliable framework for decision support must provide an expressive mathematical model for a sound integration of the system and uncertainty.

Stochastic approaches associate a probabilistic model to the problem and reason on approximations of the most likely scenarios. In highly nonlinear problems such approximations may miss relevant satisfactory scenarios leading to erroneous decisions. In contrast, constraint programming (CP) approaches reason on safe enclosures of all consistent scenarios. Model-based reasoning and what-if scenarios are supported through safe constraint techniques, which only eliminate scenarios that do not satisfy model constraints. However, safe reasoning based exclusively on consistency may be inappropriate to sufficiently reduce the space of possibilities on large uncertainty settings.

This paper shows how probabilistic constraints can be used for solving global localization problems providing a probabilistic characterization of the robot positions (consistent with the environment) given the uncertainty on the sensor measurements.

## 2 Probabilistic Robotics

Probabilistic robotics [1] is a generic approach for dealing with hard robotic problems that relies on probability theory to reason with uncertainty in robot perception and action. The idea is to model uncertainty explicitly, representing information by probability distributions over all space of possible hypotheses instead of relying on best estimates.

Probabilistic approaches are typically more robust in the face of sensor limitations and noise, and often scale much better to unstructured environments. However, the required algorithms are usually less efficient when compared with nonprobabilistic algorithms, since entire probability densities are considered instead of best estimates. Moreover, the computation of probability densities require working exclusively with parametric distributions or discretizing the probability space representation.

In global localization problems, a robot is placed somewhere in the environment and has to localize itself from local sensor data. The probabilistic paradigm maintains over time, the robot's location estimate which is represented by a probability density function over the space of all locations. Such estimate is updated whenever new information is gathered from sensors, taking into account its underlying uncertainty.

A generic algorithm known as Bayes filter [2] is used for probability estimation. The Bayes filter is a recursive algorithm that computes a probability distribution at a given moment from the distribution at the previous moment accordingly to the new information gathered. Two major strategies are usually adopted for the implementation of Bayes filters in continuous domains: Gaussian filters and nonparametric filters.

Gaussian techniques share the idea that probabilities are represented by multivariate normal distributions. Among this techniques the most popular are (Extended) Kalman Filters [3,4] which are computationally efficient but inadequate for problems where distributions are multimodal and subject to highly nonlinear constraints.

Nonparametric techniques [5,6] approximate continuous probabilities by a finite number of values. Representatives of these techniques for robot localization problems are Grid and Monte Carlo Localization algorithms [7,8]. Both techniques do not make any assumptions on the shape of the probability distribution and have the property that the approximation error converges uniformly to zero as the the number of values used to represent the probabilistic space goes to infinity. The computational cost is determined by the granularity of the approximation (the number of values considered) which is not easy to tune depending both on the model constraints and on the underlying uncertainty.

## 3 Constraint Programming

Continuous constraint programming [9,10] has been widely used to model safe reasoning in applications where uncertainty on the values of the variables is modeled by intervals including all their possibilities. A Continuous Constraint

Satisfaction Problem (CCSP) is a triple  $\langle X, D, C \rangle$  where  $X$  is a tuple of  $n$  real variables  $\langle x_1, \dots, x_n \rangle$ ,  $D$  is a Cartesian product of intervals  $X_i \times \dots \times X_n$  (a box), where each  $X_i$  is the domain of  $x_i$  and  $C$  is a set of numerical constraints (equations or inequalities) on subsets of the variables in  $X$ . A solution of the CCSP is a value assignment to all variables satisfying all the constraints in  $C$ . The feasible space  $F$  is the set of all CCSP solutions within  $D$ .

Continuous constraint reasoning relies on branch-and-prune algorithms [11] to obtain sets of boxes that cover the feasible space  $F$ . These algorithms begin with an initial crude cover of the feasible space ( $D$ ) which is recursively refined by interleaving pruning and branching steps until a stopping criterion is satisfied. The branching step splits a box from the cover into sub-boxes (usually two). The pruning step either eliminates a box from the covering or reduces it into a smaller (or equal) box maintaining all the exact solutions. Pruning is achieved by performing constraint propagation [12] based on interval analysis methods [13].

---

**Algorithm 1.**  $probDist(D, C, G)$ 


---

```

1  $S \leftarrow Branch\&Prune(D, C);$ 
2  $\forall_{1 \leq i_1 \leq g_1 \dots 1 \leq i_n \leq g_n} M_{i_1, \dots, i_n} \leftarrow 0;$ 
3  $P \leftarrow 0;$ 
4 foreach  $B \in S$  do
5    $\langle i_1, \dots, i_n \rangle \leftarrow getIndex(B);$ 
6    $M_{i_1, \dots, i_n} \leftarrow MCIntegrate(B);$ 
7    $P \leftarrow P + M_{i_1, \dots, i_n};$ 
8 if  $P = \emptyset$  then return  $M;;$ 
9  $\forall_{1 \leq i_1 \leq g_1 \dots 1 \leq i_n \leq g_n} M_{i_1, \dots, i_n} \leftarrow$ 
   $M_{i_1, \dots, i_n} / P;$ 
10 return  $M;$ 

```

---

CCSP by defining an appropriate density function. A probabilistic constraint space is a pair  $\langle \langle X, D, C \rangle, f \rangle$ , where  $\langle X, D, C \rangle$  is a CCSP and  $f$  a p.d.f. defined in  $\Omega \supseteq D$  such that:  $\int_{\Omega} f(\mathbf{x}) d\mathbf{x} = 1$ . The constraints  $C$  specify an event  $\mathcal{H}$  whose probability can be computed by integrating  $f$  over its feasible space,  $P(\mathcal{H}) = \int_{\mathcal{H}} f(\mathbf{x}) d\mathbf{x}$ . The probabilistic constraint framework performs constraint propagation to get a box cover of the region of integration  $\mathcal{H}$  and compute the overall integral by summing up the contributions of each box in the cover. In this work, classical Monte Carlo methods [15] are used to estimate the value of the integrals at each box, by randomly selecting  $N$  points in the multidimensional space and averaging the function values at these points. The success of this technique relies on the reduction of the sampling space where a pure Monte Carlo method is not only hard to tune but also impractical in small error settings.

Probability distributions are computed by algorithm 1 which assumes a grid over the feasible region and computes a conditional probability distribution of the random vector  $X$  given the event  $\mathcal{H}$  that satisfies all constraints in  $C$ . The grid is specified by the input  $G = \langle g_1, \dots, g_n \rangle$  which is an array that defines the number or partitions considered at each dimension. The output matrix  $M$  is the conditional probability at each grid cell. The algorithm first computes a grid

**Probabilistic Constraint Programming.** In classical CCSPs, uncertainty is modeled by intervals that represent the domains of the variables. Nevertheless this paradigm cannot distinguish between different scenarios and all combination of values within such enclosure are considered equally plausible. In this work an extension of the classical CP paradigm is used to support probabilistic reasoning. Probabilistic constraint programming [14] associates a probabilistic space to the classical

box cover  $S$  for the feasible space of the model constraints  $C$  (line 1). Function *Branch&Prune* (see [14] for details) is used with a grid oriented parametrization, i.e., it splits the boxes in the grid and choose to process only those boxes that are not yet inside a grid cell, stopping when there are no more eligible boxes. Matrix  $M$  is initialized to zero (line 2) as well as the normalization factor  $P$  that will contain, in the end, the overall sum of all non normalized parcels (line 3). For each box  $B$  in the cover  $S$  (lines 4-7), its corresponding index of the matrix cell is identified (line 5) and its probability is computed by function *MCIntegrate* (that implements the Monte Carlo method to compute the contribution of  $B$ ) and assigned to the value in that cell (line 6). The normalization factor is updated (line 7) and used in the end to normalize the computed probabilities (line 9).

## 4 Probabilistic Constraints for Robot Localization

The location of the robot is confined to a box that characterises the environment's coordinate system on which prior knowledge is represented as a set of segments (walls). A robot pose is a triplet  $\langle x, y, \alpha \rangle$  where  $(x, y)$  defines its location and  $\alpha \in [0, 2\pi]$  characterises its heading direction. This work focus on the information gathered by a ladar which provides a panoramic view of the environment gathering distance measurements within a given maximum range  $\delta_{max}$  (for a given direction it provides the distance to the closest wall in that direction). We consider  $n$  ladar measurements, each represented as a pair: the angle relative to the robot heading direction and the recorded distance.

Figure 1(above) illustrates 3 environments confined to the box  $[0,1000] \times [0,1000]$  and their respective robot poses. The robot is pictured as a small circle centered at its location coordinates (with radius 30) and its heading direction is shown by the inner tick. The straight dotted lines illustrate the distance measurements that would be captured by a ladar from the robot pose. It considers 7 measurements with direction angles covering the ladar panoramic range and a maximum distance range  $\delta_{max} = 300$  (dotted circle).

In general, the information provided by the robot sensors is subject to different sources of noise. We assume that all ladar measurement errors are independent and normally distributed with 0 mean and  $\sigma$  standard deviation. For  $n$  ladar measurements, their joint error probability density is the Gaussian function  $(\sigma\sqrt{2\pi})^{-n} e^{-\frac{1}{2\sigma^2}\sum_i \epsilon_i^2}$  where  $\epsilon_i$  is the error committed in the  $i$ th measurement. Without loss of generality, other pdf could be used to model the uncertainty on other sensor measurements.

Figure 1(below) illustrates the results (projected in the  $xy$  plan). It shows the grid over the initial coordinates box and the  $xy$  cells consistent with the measurements with grey levels that reflect the computed probability.

The Gaussian pdf for the current pose  $\langle x, y, \alpha \rangle$  of the robot given  $n$  ladar measurements (used by the function *MCIntegrate*) is computed as follows. For each ladar measurement  $i$ , the direction of the observation  $\alpha_i$  is given by the robot angle  $\alpha$  plus the relative angle of the measurement. The predicted value for the distance is computed as the distance from the robot pose to the closest

object in the direction  $\alpha_i$  (or is  $\delta_{max}$  if such distance exceeds the maximum ladar range). The difference between the predicted and the distance recorded by the ladar is the measurement error and its square is accumulated for all measurements and used to compute the pdf.

The specialized function that narrows a domains box accordingly to the ladar measurements maintains a set of numerical constraints that can be enforced over the variables of the problem and then calls the generic interval arithmetic narrowing procedure [16]. The numerical constraints may result from each ladar measurement. Firstly a geometric function is used to determine which of the walls in the map can eventually be seen by a robot positioned in the box with an angle of vision within the range of the robot pose angle plus the relative angle of the ladar measurement. If no wall can be seen, the predicted distance is the maximum ladar range  $\delta_{max}$  and a constraint is added to enforce the error between the predicted and the ladar measurement not to exceed a predefined threshold  $\epsilon_{max}$ . If it is only possible to see a single wall, an adequate numerical constraint is enforced to restrain the error between the ladar measurement and the predicted distance for a pose  $(x, y, \alpha)$ . Notice that whenever there is the possibility of seeing more than one wall it cannot be decided which constraint to enforce, and the algorithm proceeds without associating any constraint to the ladar measurement.

## 5 Experimental Results

The probabilistic constraint framework was applied on a set of global localization problems covering different simulated environments and robot poses and are illustrative of the potential and limitations of the proposed approach. The algorithms were implemented in C++ over the RealPaver constraint solver [16] and the experiments were carried out on an Intel Core i7 CPU at 2.4 GHz. Our grid approach adopted as reference a grid granularity commonly used in indoor environments [1]: 15 cm for the  $xy$  dimensions (10 units represents 1.5 cm), and 4 degrees for the rotational dimension. Based on previous experience on the hybridization of Monte Carlo techniques with constraint propagation we adopted a small sampling size of  $N = 100$ .

In all our experiments increasing the sampling size did not improve the quality of the results. Similarly the reference value of 4 degrees for the grid size of the rotational dimension was fixed since coarser grids prevented constraint pruning and finer grids increased the computation time without providing better results. In the following problems, to illustrate the effect of the resolution of the  $xy$  grid we consider, apart from the reference grid size, a 4 times coarser grid (60 cm) and a 4 times finer grid (3.75 cm).

Fig. 1(left) illustrates a problem where, from the given input, the robot location can be circumscribed to a unique compact region. The results obtained with the coarse grid clearly identify a single cell enclosing the simulated robot location. The obtained enclosure for the heading direction is guaranteed to be between 40 and 48 degrees (not shown). With the reference and the fine-grained grids the results were similar. The CPU time was 5s, 10s and 30s for increasing grid resolutions.

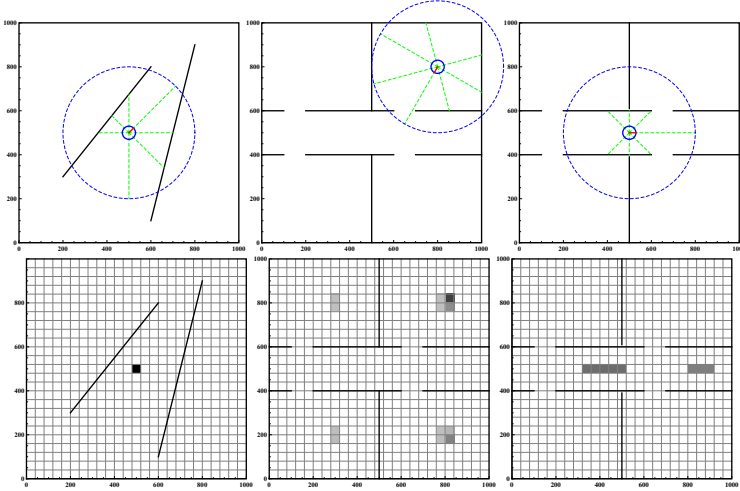


**Fig. 1.** (above) environment and robot poses with the distance measurements captured by the robot sensors; (below) computed solutions given the environment and the measurements.

Fig. 1(center) illustrates a problem where local symmetry of the environment (with 4 similar rooms) makes it impossible to localize the robot into a unique compact region, coexisting several possible alternatives. In this case, all the consistent locations were identified despite the adopted grid resolution. The predicted heading directions point towards the respective room entrance. The CPU time was 5s, 8s and 13s for increasing grid resolutions.

Fig. 1(right), illustrates a problem where there is a continuum of indistinguishable locations for the robot (along the corridor). Again, despite the adopted grid resolution, all the consistent locations were successfully identified. Notice that the possible locations are represented as two sets of adjacent cells and the probability of the cells in the left is larger because here the robot may be faced towards two opposite directions (left or right) whereas within the right cells the robot must be heading left. This example reflects the limitations of grid approaches to represent a continuum of possibilities - the CPU time severely degrades for increasing grid resolutions: about 4s, 16s and 117s.

## 6 Conclusions

In this paper we propose the application of probabilistic constraint programming to probabilistic robotics. We show how the approach can be used to support sound reasoning in global localization problems integrating prior knowledge on the environment with the uncertainty information gathered by the robot sensors. Preliminary experiments on a set of simulated problems highlighted the potential and limitations of the approach.

In the future the authors aim to extend the approach to address kinematic constraints and their underlying uncertainty. Probabilistic constraint reasoning

has the potential to combine all sources of uncertainty information providing a valuable probabilistic characterization of the set of robot poses consistent with the kinematic constraints.

## References

1. Thrun, S., Burgard, W., Fox, D.: Probabilistic Robotics. The MIT Press (2006)
2. Särkkä, S.: Bayesian filtering and smoothing. Cambridge University Press (2013)
3. Kalman, R.E.: A new approach to linear filtering and prediction problems. ASME Journal of Basic Engineering (1960)
4. Julier, S.J., Jeffrey, Uhlmann, K.: Unscented filtering and nonlinear estimation. Proceedings of the IEEE, 401–422 (2004)
5. Kaplow, R., Atrash, A., Pineau, J.: Variable resolution decomposition for robotic navigation under a pomdp framework. In: IEEE Robotics and Automation, pp. 369–376 (2010)
6. Arulampalam, M., Maskell, S., Gordon, N.: A tutorial on particle filters for online nonlinear/non-gaussian bayesian tracking. IEEE Trans. Signal Proc. **50**, 174–188 (2002)
7. Wang, Y., Wu, D., Seifzadeh, S., Chen, J.: A moving grid cell based mcl algorithm for mobile robot localization. In: IEEE Robotics and Biomimetics, pp. 2445–2450 (2009)
8. Dellaert, F., Fox, D., Burgard, W., Thrun, S.: Monte carlo localization for mobile robots. In: IEEE Robotics and Automation, pp. 1322–1328 (1999)
9. Lhomme, O.: Consistency techniques for numeric CSPs. In: Proc. of the 13th IJCAI (1993)
10. Benhamou, F., McAllester, D., van Hentenryck, P.: CLP(intervals) revisited. In: ISLP, pp. 124–138. MIT Press (1994)
11. Hentenryck, P.V., Mcallester, D., Kapur, D.: Solving polynomial systems using a branch and prune approach. SIAM Journal Numerical Analysis **34**, 797–827 (1997)
12. Benhamou, F., Goualard, F., Granvilliers, L., Puget, J.F.: Revising hull and box consistency. In: Procs. of ICLP, pp. 230–244. MIT (1999)
13. Moore, R.: Interval Analysis. Prentice-Hall, Englewood Cliffs (1966)
14. Carvalho, E.: Probabilistic Constraint Reasoning. PhD thesis, FCT/UNL (2012)
15. Hammersley, J., Handscomb, D.: Monte Carlo Methods. Methuen, London (1964)
16. Granvilliers, L., Benhamou, F.: Algorithm 852: Realpaver an interval solver using constraint satisfaction techniques. ACM Trans. Mathematical Software **32**(1), 138–156 (2006)

# Detecting Motion Patterns in Dense Flow Fields: Euclidean Versus Polar Space

Andry Pinto<sup>(✉)</sup>, Paulo Costa, and Antonio Paulo Moreira

Robotics and Intelligent Systems - INESC TEC and Faculty of Engineering,  
University of Porto, Porto, Portugal  
`{andry.pinto,paco,amoreira}@fe.up.pt`

**Abstract.** This research studies motion segmentation based on dense optical flow fields for mobile robotic applications. The optical flow is usually represented in the Euclidean space however, finding the most suitable motion space is a relevant problem because techniques for motion analysis have distinct performances. Factors like the processing-time and the quality of the segmentation provide a quantitative evaluation of the clustering process. Therefore, this paper defines a methodology that evaluates and compares the advantage of clustering dense flow fields using different feature spaces, for instance, Euclidean and Polar space. The methodology resorts to conventional clustering techniques, Expectation-Maximization and K-means, as baseline methods. The experiments conducted during this paper proved that the K-means clustering is suitable for analyzing dense flow fields.

**Keywords:** Visual perception · Optical flow · Motion segmentation

## 1 Introduction

The work presented by this research studies and compares techniques for motion analysis and segmentation using dense optical flow fields. Motion segmentation is the process of dividing an image into different regions using motion information in a way that each region presents homogeneous characteristics. Two techniques are considered during this research, the Expectation-Maximization (EM) and K-means. The performance and the behavior of these techniques is well-known in the scientific community since they have been applied in countless applications of machine learning; however, this paper presents their performance for clustering dense motion fields obtained by a realistic robotic application [5]. The optical flow technique [7] is used this paper because it estimates dense flow fields in short time and makes it suitable for robotic applications without specialized computer devices however, the quality of the flow fields that are obtained is lower when compared to the most recent methods.

Four different feature spaces are considered in this research: the motion vector is represented in Cartesian space or Polar space, and the feature can have the positional information of the image location. Mathematically, this is represented

by the following features:  $f_l^c = (\bar{x}, \bar{y}, \bar{u}, \bar{v})$ ,  $f_l^p = (\bar{x}, \bar{y}, \bar{m}, \bar{\phi})$ ,  $f^c = (u, v)$  and  $f^p = (m, \phi)$ , where  $(x, y)$  is the image location,  $(u, v)$  is the flow vector in Cartesian space and the  $(m, \phi)$  is the flow vector in Polar space (magnitude and angle). In most cases, a normalization is performed [3] due to different physical meanings of the feature's components:  $\bar{v} = \frac{mean(v)}{\sigma_v}$ , where  $\sigma_v$  is the standard deviation of the component  $v$ . As can be noticed, the influence of this normalization on the segmentation procedure is also analyzed.

Therefore, contributions of this articles include: study about motion analysis in dense optical flow fields and for a practical use in a mobile robot. The goal is to segment different objects according to their motion coherence; comparison about the most suitable feature space for clustering dense flow fields; extensive qualitative and quantitative evaluations considering several baseline and pixel-wise clustering techniques, namely the K-means and the Expectation-Maximization.

## 2 Related work

The work [3] evaluates the performance of several clustering methods namely, K-means, self-tuning spectral clustering and nonlinear dimension reduction. Authors defend that one most important factor for clustering dense flow fields is the proper choice of the distance measure. They considered the feature space to be formed by the pixel coordinates and motion vectors, whose values are normalized by taking into consideration the mean and standard deviation of each feature. Results show the difficulty of segmenting dense flow fields because no technique was outperformed and, thereby, the choice of the most suitable clustering technique and distance metric must be investigated for a specific context and environment. An accurate segmentation technique that resorts to dense flow fields and uses long term point trajectories is presented in [1]. By clustering trajectories over time, it is possible to use a metric that measures the distance between these trajectories. The work in [4] proposes a sparse approach for detecting salient regions in the sequences. Feature points are tracked over time in order to pursue saliency detection as violation of co-visibility. The evaluation of the method shows that it cannot achieve a real-time computational performance since it took 32.6 seconds to process a single sequence. The [2] addresses the problem of motion detection and segmentation in dynamic scenes with small camera movements and resorting to a set of moving points. They use the Lukas-Kanade optical flow to compute the sparse flow field (features obtained by the Harris corner). Afterwards, these points are clustered using a variable bandwidth mean-shift technique and, finally, the cluster segmentation is conducted using graph cuts.

## 3 Practical Results

An extensive set of experiments was conducted as part of this research. They aimed to analyze and understand the behavior of two parametric techniques for

motion analysis in a robotic and surveillance context [7]. The EM and the K-means are used in this research as baselines for segmenting dense optical flow fields and they were implemented as standard functions. In the first experiment, the assessment was performed using an objective (quantitative) and subjective (qualitative) evaluation. The objective metric F-score [6] provides quantitative quality evaluations of the clustering results since it weights the average of precision and recall and reaches the best value at 1. The baseline methods provide a pixel-wise segmentation and factors such as the computational effort and the quality of the visual clustering are considered. Experiments were performed <sup>1</sup> considering four feature spaces:  $f_l^c$ ,  $f_l^p$ ,  $f^c$  and  $f^p$ .

The results start by demonstrating the segmentation performed by the EM and K-means in several testing sequences that capture a real surveillance scenario (indoor). Figures 1(a), 1(b) and 1(c) depict only three dense flow fields that were obtained from these sequences. Using the EM and the K-means for clustering the flow field represented in  $f^p$  have resulted in figures 2(d) to 2(f) and 3(d) to 3(f), respectively. Figures 2(a) to 2(c) and 3(a) to 3(c) depict results for the Cartesian space.

As can be noticed, the segmentation conducted by the EM in  $f^c$  do not originate a suitable segmentation because the clusters of people appear larger and they have spatially isolated regions that are meaningless (hereafter, called clustering noise). This issue is more depicted in figure 2(c) however, the same flow field segmented in Polar space originated a result that represents more faithfully the person's movement since it is less affected by meaningless and isolated regions, see figure 2(f). On the other hand, the visual illustration of the motion segmentation conducted by the K-means in  $f^p$  is similar to  $f^c$ . The qualitative analysis of these results is not possible however; and independently of the feature space that is considered ( $f^p$  or  $f^c$ ), the result of the K-means is better than the EM since the person's movements are more faithfully depicted. In addition, the clustering noise of the K-means is lower than the EM for these two feature spaces. The K-means is simpler than the EM however, it is a powerful technique to cluster the input dataset.

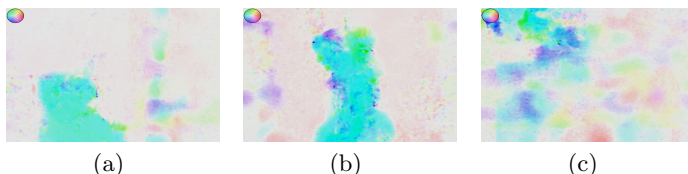


**Fig. 1.** Figures of the first row depict dense flow fields that were obtained from the technique proposed in [7]. The HSV color space is used to represent the direction (color) and magnitude (saturation) of the flow.

<sup>1</sup> The results in this section were obtained using an I3-M350 2.2GHz and manually annotated images.

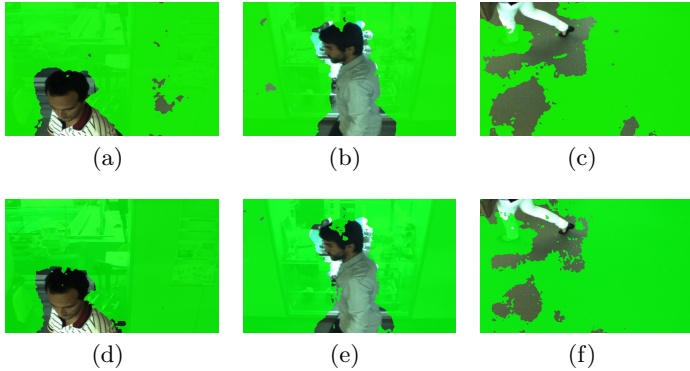


**Fig. 2.** Comparison between the EM in  $f^c$  (first row) and EM in  $f^p$  (second row). Motion segmentation for the flow fields represented in figures 1(a), 1(b) and 1(c).

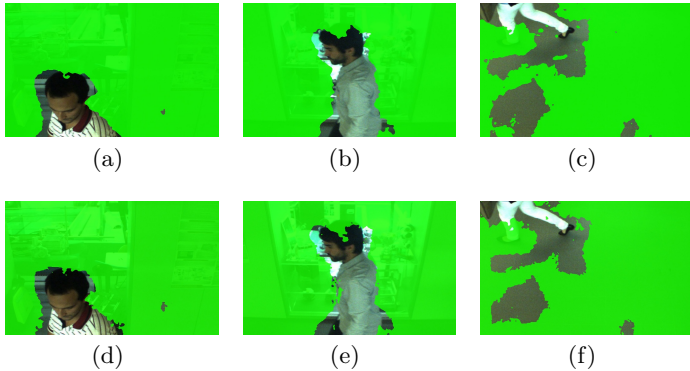


**Fig. 3.** Comparison between the K-means in  $f^c$  (first row) and K-means in  $f^p$  (second row). Motion segmentation for the flow fields represented in figures 1(a), 1(b) and 1(c).

The visual illustration of the motion segmentation based K-means produced inconclusive results in terms of the best feature space. Therefore, quantitative evaluations were conducted based on manually annotated images that represent the ground truth of the segmentation. Table 1 presents the results evaluated using the objective metric F-score, for the spaces  $f^c$  and  $f^p$ . The superscripts “ $c$ ” and “ $p$ ” represent the segmentation result in Cartesian and Polar space. The motion segmentation conducted by the K-means<sup>c</sup> was close to the K-means<sup>p</sup>, although with a lower amount of noise. This table confirms the visual illustration of the previous results since, the EM<sup>p</sup> had a F-score that is in average 0.178 higher than EM<sup>c</sup>, while the K-means<sup>c</sup> produced clusters with a F-score that is 0.040 higher than K-means<sup>p</sup>. This means, the F-score of the EM<sup>c</sup> and

$\text{EM}^p$  was 0.630 and 0.809; the  $\text{K-means}^c$  and  $\text{K-means}^p$  was 0.893 and 0.852 (in average). Therefore, the Polar feature space is a clear advantage for the EM technique while the quality of the segmentation produced by the K-means is not so affected by the feature space. Both clustering techniques were able to characterize the two motion models present in each trial although, EM technique produces clusters affected by a higher level of noise. This may be caused due to a process that is more complex in nature since it is an iterative scheme that computes the posterior probabilities and the log-likelihood. Therefore, it is less robust to noisy data relatively to the K-means that is a more simpler technique. In addition, table 1 proves that the quality of the segmentation obtained by the EM was substantially better when compared to the experiments with  $f^c$ . In detail, the performance of the EM increased by 43.3% however, the average performance of the K-mean was similar to the result obtained in  $f^c$ . Generally, the  $f_l^c$  makes possible for the EM and K-means to achieve a better segmentation quality (despising the first sequence). These trials depict that the EM and K-mean are not suitable for the Polar feature space with information about the image location,  $f_l^p$ , since results are inconclusive (only some trials reported an improved quality).

**Table 1.** F-score - Performance comparison between the EM and K-means in  $f^c$ ,  $f^p$ ,  $f_l^c$  and  $f_l^p$ . Parameters such the precision (“Prec.”) and the recall (“Rec.”) are presented. Experiences 1, 2 and 3 represent the results for the flow fields 1(a), 1(b) and 1(c), respectively.

Sequence	EM <sup>c</sup>			K-means <sup>c</sup>			EM <sup>p</sup>			K-means <sup>p</sup>		
	Pre.	Rec.	F-score	Pre.	Rec.	F-score	Pre.	Rec.	F-score	Pre.	Rec.	F-score
1	0.404	1.000	0.575	0.981	0.944	0.962	0.797	0.936	0.861	0.881	0.928	0.904
2	0.631	0.999	0.774	1.000	0.853	0.921	0.875	0.917	0.896	0.924	0.837	0.879
3	0.455	0.994	0.624	0.543	0.926	0.685	0.496	0.894	0.638	0.535	0.885	0.667
4	0.638	0.996	0.778	0.987	0.866	0.922	0.805	0.939	0.867	0.923	0.934	0.929
5	0.367	0.998	0.537	0.999	0.852	0.919	0.715	0.905	0.799	0.852	0.846	0.849
6	0.330	0.999	0.496	0.998	0.899	0.946	0.668	0.974	0.792	0.828	0.947	0.884

Sequence	EM <sub><i>l</i></sub> <sup><i>c</i></sup>			K-means <sub><i>l</i></sub> <sup><i>c</i></sup>			EM <sub><i>l</i></sub> <sup><i>p</i></sup>			K-means <sub><i>l</i></sub> <sup><i>p</i></sup>		
1	0.912	0.927	0.919	0.578	0.916	0.708	0.717	0.936	0.812	0.303	0.976	0.463
2	0.934	0.897	0.915	0.999	0.853	0.920	0.589	0.969	0.733	0.906	0.836	0.870
3	0.882	0.968	0.923	0.979	0.948	0.963	0.418	0.975	0.585	0.874	0.937	0.904
4	0.879	0.998	0.935	0.977	0.920	0.947	0.922	0.900	0.911	0.910	0.901	0.906
5	0.697	0.972	0.812	0.998	0.858	0.923	0.923	0.726	0.813	0.843	0.871	0.857
6	0.885	0.951	0.917	0.998	0.901	0.947	0.909	0.866	0.887	0.822	0.942	0.878

Finally, the computational performance was evaluated for the EM and K-means in both  $f^c$  and  $f^p$ . The computation of the techniques took in average, 7.127 seconds ( $\text{EM}^c$ ), 3.787 seconds ( $\text{EM}^p$ ), 0.142 seconds ( $\text{K-means}^c$ ) and 0.122 seconds ( $\text{K-means}^p$ ). As can be seen, the Polar feature space accelerates the

convergence of the clustering in both techniques since the processing time is substantially reduced, especially for the EM case whose processing time is reduced by 46.9% while the processing time of the K-means is reduced by 14.1%.

## 4 Conclusion

Therefore, the paper presented an important research topic for motion perception and analysis because the segmentation produces poor results when the features space is not properly adjusted. This compromises the ability of the mobile robot to understand its surrounding environment. An extensive set of experiments were conducted as part of this work and several factors were considered and studied such as, space (Cartesian and Polar) and dimensionality of the feature vector. Results prove that choosing a good feature space for the detection of motion patters is not a trivial problem since it influences the performance of the Expectation-Maximization and K-means. This last technique in Cartesian space revealed the best performance for motion segmentation of flow fields (with a resolution of  $640 \times 480$ ). It originates a good visual segmentation (evaluated using the F-score metric) in a reduced period of time since it took 0.122 seconds to compute.

This work was funded by the project FCOMP - 01-0124-FEDER-022701.

## References

1. Brox, T., Malik, J.: Object segmentation by long term analysis of point trajectories. In: Daniilidis, K., Maragos, P., Paragios, N. (eds.) *ECCV 2010, Part V*. LNCS, vol. 6315, pp. 282–295. Springer, Heidelberg (2010)
2. Bugeau, A., Prez, P.: Detection and segmentation of moving objects in complex scenes. *Computer Vision and Image Understanding* **113**(4), 459–476 (2009)
3. Eibl, G., Brandle, N.: Evaluation of clustering methods for finding dominant optical flow fields in crowded scenes. In: International Conference on Pattern Recognition, pp. 1–4 (December 2008)
4. Georgiadis, G., Ayvaci, A., Soatto, S.: Actionable saliency detection: Independent motion detection without independent motion estimation. In: IEEE Conference on Computer Vision and Pattern Recognition (CVPR), pp. 646–653 (2012)
5. Pinto, A.M., Costa, P.G., Correia, M.V., Paulo Moreira, A.: Enhancing dynamic videos for surveillance and robotic applications: The robust bilateral and temporal filter. *Signal Processing: Image Communication* **29**(1), 80–95 (2014)
6. Dan Melamed, I., Green, R., Turian, J.P.: Precision and recall of machine translation. In: Proceedings of the 2003 Conference of the North American Chapter of the Association for Computational Linguistics on Human Language Technology: Companion Volume of the Proceedings of HLT-NAACL, NAACL-Short 2003, pp. 61–63. Association for Computational Linguistics, Stroudsburg (2003)
7. Pinto, A.M., Paulo Moreira, A., Correia, M.V., Costa, P.G.: A flow-based motion perception technique for an autonomous robot system. *Journal of Intelligent and Robotic Systems*, 1–25 (2013) (in press)

# Swarm Robotics Obstacle Avoidance: A Progressive Minimal Criteria Novelty Search-Based Approach

Nesma M. Rezk<sup>(✉)</sup>, Yousra Alkabani, Hassan Bedour, and Sherif Hammad

Computer and Systems Department Faculty of Engineering,  
Ain Shams University, Cairo, Egypt

{nesma.rezk,yousra.alkabani,hassan\_bedour,shef.hammad}@eng.asu.edu.eg

**Abstract.** Swarm robots are required to explore and search large areas. In order to cover largest possible area while keeping communications, robots try to maintain hexagonal formation while moving. Obstacle avoidance is an extremely important task for swarm robotics as it saves robots from hitting objects and being damaged.

This paper introduces novelty search evolutionary algorithm to swarm robots multi-objective obstacle avoidance problem in order to overcome deception and reach better solutions.

This work could teach robots how to move in different environments with 2.5% obstacles coverage while keeping their connectivity more than 82%. Percentage of robots reached the goal was more than 97% in 70% of the environments and more than 90% in the rest of the environments.

**Keywords:** Maintaining formation · Novelty search · Obstacle avoidance

## 1 Introduction

Our main interest in this work, is to teach swarm robots by using novelty search evolutionary algorithm how to reach a certain goal while maintaining formation and avoiding obstacles.

## 2 Related Work

### 2.1 Novelty Search

Lehman and Stanley proposed a new change in genetic algorithms [1]. Instead of calculating a fitness function and selecting individuals with the best fitness values, individuals who have more novel behaviour than other individuals are selected to be added to the new generation.

Novelty search can be easily implemented on top of most evolutionary algorithms. Basically, the fitness value would be replaced with what is called a novelty metric. The novelty metric (sparseness of an individual) is calculated as the

average distance between behavior vectors of the individual and its  $k_{th}$  nearest neighbors, and an archive.

Pure novelty search for large search spaces is not enough to reach solutions as the algorithm will spend a lot of time searching behaviors that are not meeting the goal. So, novelty search can overcome deception but cannot work alone without the guidance of the fitness value.

In MCNS (Minimal Criteria Novelty Search) only individuals who have a fitness value greater than a minimal criteria would be assigned their novelty score [2]. Otherwise their novelty score would be zero. Zero novelty value individuals would only be used for reproduction if no other individuals meet the minimal criteria. It is clear that MCNS acts as random search until individuals that meet the minimal criteria are reproduced. So, MCNS should be seeded with initial population that meets the minimal criteria.

Progressive minimal criteria novelty search was proposed by Gomes *et al.* to overcome the need of seeding the MCNS algorithm with initial population [3]. The minimal criteria is a dynamic fitness threshold initially set to zero. The fitness threshold progressively increases among generations to avoid the search from exploring irrelevant solutions. In each generation, the new criteria is found by determining the value of the P-th percentile of the fitness scores in the current population. This means that P percent of the fitness values would fall under the minimal criteria.

## 2.2 Evolutionary Obstacle Avoidance

Hettiarachchi and Spears proposed an evolutionary algorithm for swarm robots offline learning [4]. The genetic algorithm is to teach robots how to reach their goal while preserving their hexagonal formation and avoiding obstacles at the same time. To get optimum coverage with least number of robots and efficient multi-hop communications network hexagonal formation is the best formation as discussed in [5].

Lennard Jones force law is used to control the robot. The robot moves according to the net force calculated from the forces that are exerted upon it by other robots and environment. As the robot moves in the environment it interacts with three types of objects: robots, obstacles and a goal. It is required to set the parameters for three copies of the force law one for each object in order to keep the robot at distance R from neighbor robots which will lead to the hexagonal formation, keep away from obstacles, and reach goal.

An evolutionary algorithm is used to optimize the parameters for the three copies of the force law. The penalty function (1) is a minimizing multi-objective fitness function. The function consists of three components: penalty for not reaching the goal, penalty for collisions, and penalty for lack of cohesion.

$$\text{Penalty} = P_{\text{collisions}} + P_{\text{connectivity}} + P_{\text{notreachingthegoal}} \quad (1)$$

### 3 Applying PMCNS

To apply PMCNS, we have several issues to handle. The penalty function of our problem is a minimizing function. It needs to minimize the penalty for not reaching the goal, penalty for non-cohesion and penalty for collisions. The PMCNS algorithm equations assumes that the fitness function is a maximizing function. It allows individuals that have fitness values higher than the minimal criteria to be selected for the next generation. We have two options to apply. The first option is to change all of the equations of the algorithm to be a maximal criteria algorithm not a minimal criteria.

The second option (which was adopted in this work) is to inverse all the penalty values to change the problem from a minimizing to a maximizing problem. The minimum value would be the maximum value and the maximum value would be the minimum value . Equation (2) shows how the penalty value would be inverted.

$$\text{inversed\_penalty}(i) = \text{max\_penalty} - \text{penalty}(i) \quad (2)$$

where  $\text{max\_penalty}$  is the maximum penalty of the current generation.  $\text{penalty}(i)$  is subtracted from current generation maximum penalty so the inverted penalty values will have the same range of penalty values.

We need to decide how to capture the behavior vector, and how to apply PMCNS to a multi-objective problem. To fill the behaviour vector, we need to make the vector express how the controller behave through simulation. For two reasons, we chose the genomes of the individual to express the behaviour vector. The first reason is that the genomes are the parameters of the three versions of the force law. Those parameters decide how the robot will behave with robots, obstacles, and the goal, so they express the behaviour of the controller. The second reason is that Cuccu and Gomez stated that the simplest way to fill the behavior vector is to fill it with the individual genomes [6].

## 4 Experiments and Results

### 4.1 PMCNS Experiment

This experiment was held to compare objective-based search to progressive minimal criteria novelty search. The environments generated for the evaluation module contains 40 robots and 90 obstacles like the experiment held by Hettiarachchi and Spears [4]. The evolution was run for 80 generations. Each individual was evaluated 20 times. The evaluation module of the genetic algorithm was distributed over 30 computers to gain speedup [7].

There are differences in the way the two algorithms act. The objective-based search would start faster than PMCNS but PMCNS could reach less penalty values than objective-based search. Fig. 1 shows the minimum penalty found in all generations during evolution for both objective-based and PMCNS with percentile = 50%.

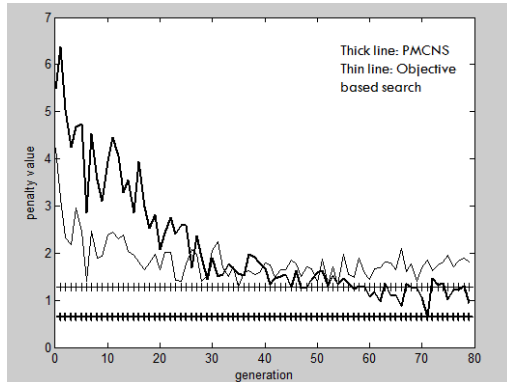


**Fig. 1.** Minimum penalty of each generation for both objective-based and novelty search evolutionary algorithms.

## 4.2 Evaluation Module Experiments

The next experiments were held to examine the changes can be done in the evaluation module to reach better solutions. Since the previous experiment showed that PMCNS can perform better than objective-based search, we used PMCNS in the rest of experiments. In these experiments PMCNS evolutionary algorithm with percentile= 50% was used.

The target of these experiments is to train robots to move in environments with obstacle coverage less than or equal 2.5%. So, the environments for training contained 40 robots and 50 obstacles. The diameter of the obstacle is 0.2 units, while the diameter of the robot is 0.02 units. The arena dimensions are 9 x 7 units, so the obstacles coverage is 2.5% of the environment. Robots are initially placed at the bottom left of the arena and the goal is located at the top right of the arena. Obstacles are randomly placed in the arena. There is an area around the nest where no obstacles are placed to prevent proximity collisions.

Robot can sense goal at any distance. A penalty is added at the end of simulation (1500 time step) if less than 80% of the robots did not reach the goal area. The goal area is 4R from the center of the goal. Each individual was evaluated 20 times. Most of those settings are like Hettiarachchi and Spears experimental settings in their work [4]. For each experiment the best penalty value individual performance was tested over 20, 40, 60, 80, and 100 robots moving in environments that contain 10, 20, 30, 40, and 50 obstacles corresponding to obstacle coverages equal 0.5, 1, 1.5, 2 and 2.5% of the environment. So, the total number of performance experiments=25. Each experiment is evaluated 50 times.

### 1. First Penalty Function (Penalty Experiment 1)

In this experiment, robot can sense neighbor robots at distance 1.5R where R is the desired separation between robots. Robot attracts its neighbors if neighbors are 1.5R distance away, and repulses its neighbors if the neighbors

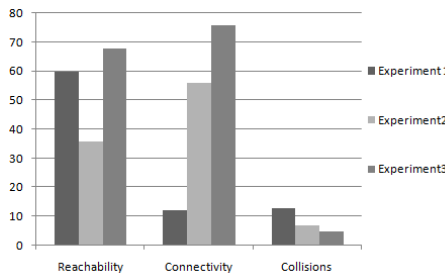


**Fig. 2.** Summary of the penalty evaluation experiments results.

are closer than  $1.5R$  distance. A penalty for non cohesion is added if less than or more than 6 robots are found at distance  $R$  from the robot.

Obstacles are sensed at distance equals double the obstacle diameter from the center of the robot to the center of the obstacle. Robot starts to interact with the obstacle at distance equals double the obstacle diameter from the center of the robot to the center of the obstacle. A penalty is added for collision if the distance between center of robot and center of obstacle is less than robot diameter.

2. Second Penalty Function (Penalty Experiment 2) In this experiment, we changed the distances of doing action and adding penalty for cohesion (robot to robot interaction). Robot can sense neighbor robots at distance  $1.5R$ , where  $R$  is the desired separation between robots. Robot attracts its neighbors if the neighbors are  $R$  distance away and repulses its neighbors if the neighbors are closer than  $R$  distance. A penalty for non cohesion is added if less than or more than 6 robots are found at distance  $R$  from the robot
3. Applying Harder Problem on Third Penalty Function (Penalty Experiment 3) In the last two experiments, we noticed that results are the worst at 50 obstacle environments, so we decided to hold a new experiment with same settings of penalty experiment 2, but the training environments contain 60 obstacles instead of 50 obstacles to see if the training environments were harder would the robots behave better for easier environments.

**Penalty Experiments Results.** Experiment 1 is the best in the percentage of robots reached the goal but the worst in the minimum percentage of robots remained connected and the number of collisions. Experiment 2 is much better than experiment 1 in the minimum percentage of robots remained connected but less number of robots reached the goal. Experiment 3 is the same like experiment 2 but only the training environments were harder. Experiment 3 showed the best results for all objectives.

Fig. 2 shows graphically the results of the experiments. Reachability tells us how many times in the reachability performance experiments the percentage of robots reached the goal was over 97%. Connectivity tells us how many times in the connectivity performance experiments the minimum percentage of robots

remained connected was over 90%. The number of collisions shows the total number of collisions found in each experiment.

## 5 Conclusion and Future Work

This work shows that progressive minimal criteria novelty search can perform in a different way than objective-based search. It can reach better solutions than objective-based search for a multi-objective task for swarm robots. However we believe that as the task is deceptive we can have better solutions and better evolutionary behavior using novelty search algorithms than the behavior reached in this work.

The purpose of the upcoming experiments is to find the part of the fitness function that was decepted by the multi-objective problem to describe it in the behavior vector and apply novelty search. Otherwise, we shall prove that the way used in this work for calculating the fitness value using the multi-objective function was able to overcome the deception of the problem and novelty search will not be of a big value.

This work examined different changes in the evaluation module of the multi-objective genetic algorithm settings. These changes can enhance one objective, but another objective may get worse. This work proved that using harder problem for learning during the evolutionary algorithm will give us better solutions for easier problems.

## References

- Lehman, J., Stanley, K.: Improving evolvability through novelty search and self-adaptation. In: Proceedings of the 2011 IEEE Congress on Evolutionary Computation (CEC), Piscataway, NJ, US (2011)
- Lehman, J., Stanley, K.: Revising the evolutionary computation abstraction: minimal criteria novelty search. In: Proceedings of the Genetic and Evolutionary Computation Conference (GECCO), New York, US (2010)
- Gomes, J., Urbano, P., Christensen, A.L.: Progressive minimal criteria novelty search. In: Pavón, J., Duque-Méndez, N.D., Fuentes-Fernández, R. (eds.) IBERAMIA 2012. LNCS, vol. 7637, pp. 281–290. Springer, Heidelberg (2012)
- Hettiarachchi, S., Spears, W., Spears, D.: Physicomimetics, chapter 14, pp. 441–473. Springer, Heidelberg (2011)
- Prabhu, S., Li, W., McLurkin, J.: Hexagonal lattice formation in multi-robot systems. In: 11th International Conference on Autonomous Agents and Multiagent Systems (AAMAS) (2012)
- Cuccu, G., Gomez, F.: When novelty is not enough. In: Di Chio, C., Cagnoni, S., Cotta, C., Ebner, M., Ekárt, A., Esparcia-Alcázar, A.I., Merelo, J.J., Neri, F., Preuss, M., Richter, H., Togelius, J., Yannakakis, G.N. (eds.) EvoApplications 2011, Part I. LNCS, vol. 6624, pp. 234–243. Springer, Heidelberg (2011)
- Rezk, N., Alkabani, Y., Bedour, H., Hammad, S.: A distributed genetic algorithm for swarm robots obstacle avoidance. In: IEEE 9th International Conference on Computer Engineering and Systems (ICCES), Cairo, Egypt (2014)

# **Knowledge Discovery and Business Intelligence**

# An Experimental Study on Predictive Models Using Hierarchical Time Series

Ana M. Silva<sup>1,2</sup>, Rita P. Ribeiro<sup>1,3(✉)</sup>, and João Gama<sup>1,2</sup>

<sup>1</sup> LIAAD-INESC TEC, University of Porto, Porto, Portugal

{201001541, jgama}@fep.up.pt, rpribeiro@dcc.fc.up.pt

<sup>2</sup> Faculty of Economics, University Porto, Porto, Portugal

<sup>3</sup> Faculty of Sciences, University Porto, Porto, Portugal

**Abstract.** Planning strategies play an important role in companies' management. In the decision-making process, one of the main important goals is sales forecasting. They are important for stocks planning, shop space maintenance, promotions, etc. Sales forecasting uses historical data to make reliable projections for the future. In the retail sector, data has a hierarchical structure. Products are organized in hierarchical groups that reflect the business structure. In this work we present a case study, using real data, from a Portuguese leader retail company. We experimentally evaluate standard approaches for sales forecasting and compare against models that explore the hierarchical structure of the products. Moreover, we evaluate different methods to combine predictions for the different hierarchical levels. The results show that exploiting the hierarchical structure present in the data systematically reduces the error of the forecasts.

**Keywords:** Data mining · Hierarchical time-series · Forecasting in retail

## 1 Introduction

Nowadays, with the increasing competitiveness, it is important for companies to adopt management strategies that allow them to value up against the competition. In the retail sector, in particular, there is an evident relationship among different time series. The problem presented here is related to a Portuguese leader company in the retail sector, in the electronics area. As we see in Figure 1, the total sales of the company can be divided into five business units: Home Appliances (U51), Entertainment (U52), Wifi (U53), Image (U54) and Mobile (U55), each one can be divided in 137 different stores.

In this paper, we propose a predictive model that estimates the monthly sales revenue for all stores of this company. We then compare this flat model that ignores the hierarchy present in the time series, with three other ways, existing in the literature, to combine the obtained forecasts, by exploring its hierarchical structure (e.g. [1,2,3,4]): *bottom-up*, *top-down* and *combination* of predictions made at different levels of the hierarchy. The experimental results

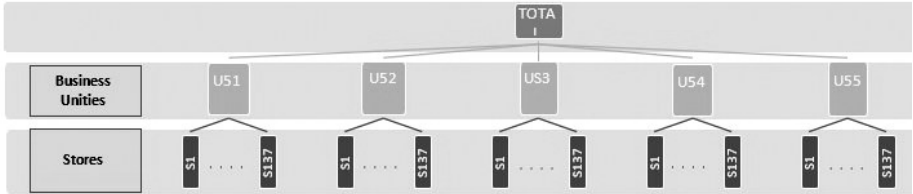


**Fig. 1.** Hierarchical structure of our time series data

obtained with our case study comprove that taking advantage of the hierarchical structure present in the data leads to an improvement of the models performance as it reduces the error of the forecasts.

This paper is organized as follows: in Section 2 the related work is presented; furthermore, in Section 3, is described how the forecast model was built and how we do the comparison between the different hierarchical models; and finally, in Section 4 are exposed the conclusions of the work and future work.

## 2 Related Work

Increasingly, the data mining techniques have been applied in time series analysis [5]. In the retail sector, where the time series display well defined components of trend and seasonality, the usage of learning algorithms such as Artificial Neural Networks (ANN) proves to be more efficient than the application of traditional methods, once that this one can capture the non-linear dynamics associated to these components and their interactions [6]. However, to apply these algorithms we must study the best way to present the data. Some studies show that, as standard, the ANNs are most efficient when applied to time series with trend and seasonality correction [7]. In addition, in the retail sector, normally, there are several variables that can somehow justify fluctuations in sales. In [8], ANNs are applied in daily sales forecasting of a company in the shoe's industry, using as explanatory variables: month of the year, day of the week, holidays, promotions or special events, sales period, weeks pre/post Christmas and Easter, the average temperature, the turnover index in retail sale of textiles, clothing, footwear and leather articles and the daily sales of previous seven days with correction of trend and seasonality.

In [9] the predictive power of ANNs is compared with the Support Vector Regression Machines [10] (SVRs) - this second algorithm also compares the use of the *linear kernel* function with the *Gaussian kernel* function. In that work, these learning algorithms are applied to five different artificial time series: stationary, with additive seasonality, with linear trend, with linear trend and additive seasonality and linear trend and multiplicative seasonality. The results showed that the SVRs with *Gaussian kernel* function is the most efficient algorithm in the forecasting of time series without trend. However, in series with trend, the predictions shown are disastrous, while the ANNs and SVRs with *linear kernel*

function produce robust predictions, even without performing pre-processing of the data.

In hierarchical databases, it is frequently useful to explore the relationship of dependency between different time series, thus ensuring consistency in time series forecasting belonging to different levels. In [1] is presented a methodology that explores the different levels of aggregation hierarchies and the predictions for different time periods. In this case, forecasting the next elements of the time series are obtained by aggregating the predictions of descendants series in the hierarchy associated with this dimension.

Normally, when climbing into the hierarchy the forecast error decreases, since at these levels some of the deviations and fluctuations are neutralized. The two most commonly used strategies are *bottom-up* and *top-down*. While with the first method the forecasts are calculated on the lower level of the hierarchy and then aggregated to provide the higher dimension series predictions; in the second, the forecasts are calculated at the top level and then disaggregated to the lower levels [2]. When using this second case, there is no universal form of breakdown, but there are several methodologies that can be adopted [3]. Although the algorithm *top-down* is easy to build and produce reliable predictions of aggregated levels, when we go down in the hierarchy, it can lead to loss of information related to the dynamics of the series in descending hierarchies and the distribution of predictions by lower levels is not always easy to accomplish. Furthermore, with the algorithm *bottom-up*, the loss of information is not so big, but there are many series to predict and the noise presented in the data below hierarchies is often high. However, there is no consensus on the best approach.

More recently, it was proposed a method which produces better results when compared to the application of algorithms *bottom-up* and *top-down*. This method consists in the calculation of independent projections in all levels of the hierarchy, applying then a regression model to optimize the combination of these predictions [4]. The main advantage of this approach is the fact that the predictions obtained for all time series of all levels can come from the application of any learning algorithm, which allows you to use all available data, as well as inherent time series dynamics. After that, the forecasts will be revised and transformed by applying a weighted average, which will use all other forecasts.

To better explain how this method works, let us consider the time series hierarchy illustrated in Figure 2.

The authors [4] start by proposing the translation of the time series hierarchy to a matrix notation where:

- each line  $i$  represents a node in the hierarchy in breadth traversal order;
- each column  $j$  represents a node of the bottom level;
- each position  $(i, j)$  of the matrix is 1 if the time series contained in the bottom level node  $j$  contributes to the time series in node  $i$ ; otherwise, it should be 0.

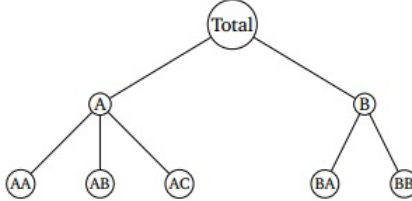


**Fig. 2.** Example of a hierarchical relationship with two levels

Thus, the hierarchy shown in Figure 2 is represented by the following matrix  $S$  (cf. Equation 1).

$$S = \begin{pmatrix} 1 & 1 & 1 & 1 & 1 \\ 1 & 1 & 1 & 0 & 0 \\ 0 & 0 & 0 & 1 & 1 \\ 1 & 0 & 0 & 0 & 0 \\ 0 & 1 & 0 & 0 & 0 \\ 0 & 0 & 1 & 0 & 0 \\ 0 & 0 & 0 & 1 & 0 \\ 0 & 0 & 0 & 0 & 1 \end{pmatrix} \quad (1)$$

The authors [4] also showed that, assuming that the forecasting errors of the hierarchy take the same distribution of the aggregated data, it is possible to obtain reasonable forecasts by solving the expression shown in Equation 2,

$$\tilde{Y}_t(h) = S(S^t S)^{-1} S^t \times \hat{Y}_t(h) \quad (2)$$

where  $\tilde{Y}_t(h)$  represents the recalculated prediction for series  $h$  at time  $t$ ,  $\hat{Y}_t(h)$  represents the prediction obtained independently for the time series  $h$  at time  $t$  and  $S$  is the matrix that represents the hierarchy of the time series.

The calculation of  $S(S^t S)^{-1} S^t$  gives us the weights we need to do the forecast adjustment. Considering the matrix  $S$  (cf. Equation 1), we obtain the weights matrix (cf. Equation 3) corresponding to all series of the different hierarchy nodes.

$$S(S^t S)^{-1} S^t = \begin{pmatrix} 0.58 & 0.30 & 0.28 & 0.10 & 0.10 & 0.10 & 0.14 & 0.14 \\ 0.31 & 0.51 & -0.20 & 0.17 & 0.17 & 0.17 & -0.10 & -0.10 \\ 0.27 & -0.21 & 0.48 & -0.07 & -0.07 & 0.07 & 0.24 & 0.24 \\ 0.10 & 0.18 & -0.08 & 0.72 & -0.27 & -0.27 & -0.04 & -0.04 \\ 0.10 & 0.18 & -0.08 & -0.27 & 0.72 & -0.27 & -0.04 & -0.04 \\ 0.10 & 0.18 & -0.08 & -0.27 & -0.27 & 0.72 & -0.04 & -0.04 \\ 0.15 & -0.09 & 0.24 & -0.03 & -0.03 & -0.03 & 0.62 & -0.38 \\ 0.15 & -0.09 & 0.24 & -0.03 & -0.03 & -0.03 & -0.38 & 0.62 \end{pmatrix} \quad (3)$$

For example, the forecast value for the times series  $AA$  would be obtained by using the weights of the fourth line of this weights matrix, as shown in Equation 4.

$$\begin{aligned}\tilde{Y}_{AA} = & 0.10 \times \hat{Y}_{Total} + 0.18 \times \hat{Y}_A - 0.08 \times \hat{Y}_B + 0.72 \times \hat{Y}_{AA} \\ & - 0.27 \times \hat{Y}_{AB} - 0.27 \times \hat{Y}_{AC} - 0.04 \times \hat{Y}_{BA} - 0.04 \times \hat{Y}_{BB}\end{aligned}\quad (4)$$

We should note that the negative weights are associated to the time series which are not directly influencing the considered time series. This coefficient is negative, instead of null, since we want to extract the effect of this series in the series on the top levels.

The same authors made available in R [11], the package `hts` [12] which has the implementation of an algorithm that automatically returns predictions for all hierarchical levels based on the idea described previously. However, it only allows the use of a linear model to predict each set.

### 3 The Case Study

#### 3.1 Data Description

The challenge lies in building a model to forecast the sales revenue of the company, per month. Additionally, this forecast should be made by store - there are 137 stores across the country - and by business unit - i.e., is not intended a forecast for the whole store, but for a particular set products. In this particular business, there are five business units: Home Appliances (U51), Entertainment (U52), Wifi (U53), Image (U54) and Mobile (U55). The goal is at the 15th day of each month, foreseen the sales revenue of the following month.

This problem is as a regression problem - since it is the forecast of a continuous variable - and the available data will be used to train the algorithms, i.e., we will have a supervised learning process.

We have monthly aggregated data since January 2011 until December 2014. We keep the last six months of 2014 to evaluate our models, using the remaining data for training. Due to the reduced number of instances, we decided to use a growing window with a time horizon of two months. This means that to predict the sales of July 2014, we use as training window all the data until May 2014. Then, the training window grows by incorporating the data of June 2014, to predict the sales of August 2014, and so on.

#### 3.2 Non-hierarchical Model

From a first analysis of our data, we have noticed that the sales evolution regarding each business unit in each store exhibits very different behaviours. In these conditions, it is unfeasible to obtain a single model that would have a good performance for every store and business unit. Thus, in order to avoid very large errors, we have started by applying the k-means algorithm [13] to our stores, setting the number of clusters to three. Our aim was to cluster the stores by the three main areas of the country: north, center and south. The stores that constituted the centroid of each cluster, were used to tune the learning methods parameters for the time series corresponding to the total and the business unit of each store.

To the tuning process, we used the function `experimentalComparison` from the package `DMwR` [14], which chooses the best parameters that minimize the mean squared error (MSE).

In a first modelling approach, we have applied the *Autoregressive integrated moving average* (`arima`) - from R package `forecast` [15] - to obtain the sales forecast for each business unit in each store and each store total. Still, no good results were obtained.

In this context, and since we have a huge variety of time series with different features, we decided to apply different learning algorithms to each time series and use a simple ensemble to combine the models predictions. The final prediction was obtained by summing up the prediction made by the best model, i.e. the model that achieved the lowest MSE estimation, weighted by 0.75, with the prediction made by the second best model, weighted by 0.25. The used learning algorithms in our ensemble were: *Artificial Neural Networks* - from R packages `nnet` [16] and `caret` [17] -, *Support Vector Machines* - from R packages `e1071` [18] and `kernlab` [19] - and Random Forests - from R package `randomForest` [20]. These non-linear learning algorithms have shown better results in comparison to the linear model `arima` and the ensemble has shown better results when compared with each simple learning algorithm alone.

Using this modelling strategy, and based on [8], we also conducted a study to see if the addition/change of variables to the original time series would justify the sales' fluctuations and, thus, positively influence the results of the sales forecast. After some tests, the following changes to the original time series lead to overall better results. The sales values were normalized to the  $[0, 1]$  interval. New variables were added with information on the month of year, the number of Saturdays/Sundays in the month, indication of the Easter month, and promotional campaigns and their time intervals of impact on the sales. It was also verified that the results became worse when the sales of earlier periods were used - either in the original format and in the data corrected of trend and/or seasonality, thus it was not used. It was also found that there was no significant correlation between considered variables.

There were some recent stores for which we did not had the information from the beginning of 2011. For these stores, we found the oldest store with the most similar behaviour and used it to predict the new one.

### 3.3 Hierarchical Models

Our flat modelling approach, described in previous section, of predicting sales for each store, each business unit, and total of the company shown some drawbacks. The sum of the forecasts of the series of lower levels, does not correspond exactly to the value of the upper level. In this context, we found that would be useful to explore the hierarchies present in the database, which will also help to build a more consistent model in time series forecasts from different hierarchical levels. Therefore, based on the forecasts obtained with our base model, we considered the following four different modelling approaches.

**Non-hierarchical Model (**NonHierarch**):** model that predicts the sales for each store, each business unit, and total of the company, ignoring the hierarchical relationship.

**Bottom-up Model (**BottomUp**):** model obtained using a *bottom-up* approach, which means that the predictions made for the lower level of the hierarchy are used to forecast levels above; for each level the prediction is given by the sum of the predictions made in the level below.

**Top-Down Model (**TopDown**):** model obtained using a *top-down* approach, which means that the forecasts made for the total of the company are used predict the sales of lower hierarchical levels; the prediction uses an a priori measure of the weight of each business unit in the total of sales total, based on the history of the considered month.

**Hierarchical Combination Model (**HierarchComb**):** model that uses all the predictions obtained independently for each hierarchical level, and applies them the regression model suggested by [21] to optimize the combination of the obtained predictions.

### 3.4 Experimental Results

The comparative results of the Mean Absolute Percentage Error (MAPE) obtained for the total sales of the company and for each business unit are shown in Table 1. This error metric was used in order to compare the results obtained with the error rates previously set by the company.

From the analysis of Table 1, we verify that for the series corresponding to the total sales of the company, the months of July, October and November (i.e. 50% of the test set) are better predicted by **HierarchComb**, while the remaining months are better predicted by the model **BottomUp** - 17% - and **NonHierarch** and **TopDown** - 33%. These two last models are, in fact, the same because **TopDown** uses the forecast obtained for the total of sales. Regarding the business units level, the models **BottomUp** and **HierarchComb** are the best in the same number of forecasts - 33% each - followed by models **NonHierarch** and **TopDown**, in 17% of the forecasts, each.

The results for each store, by business unit, are illustrated in Figure 3. We have also the results for the total of each store, obtained accordingly with each model.

In fact, looking at Figure 3, there is mainly a reduction of the highest error rates when using the model **HierarchComb** in comparison with model **NonHierarch**. Moreover, except for some small rounding errors, the predictions obtained by models **NonHierarch** and **BottomUp** are equal, since the model **BottomUp** uses all independent forecasts of the bottom level. On the other hand, the error rate obtained by the model **TopDown** is higher than the others, which can be justified by the noise introduced in the disaggregation process.

In order to verify if the results obtained by the different models were statistically significant in the bottom level, we applied an hypothesis test. Since we have a high sample size, the *Central Limit Theorem* allow us to consider that the sample follows a distribution approximately *Normal*. So, visually, we observe

**Table 1.** MAPE of sales forecast per business unit and total sales of the company by four modelling approaches to combine predictions of the different hierarchical levels.

Business Unit	Modelling Approach	Forecast Month					
		Jul	Aug	Sept	Oct	Nov	Dec
U51	NonHierarch	2.62%	13.31%	6.08%	0.91%	<b>2.89%</b>	1.96%
	BottomUp	2.71%	<b>3.81%</b>	<b>3.81%</b>	3.82%	6.54%	1.34%
	TopDown	2.46%	6.32%	4.21%	2.71%	5.42%	2.10%
	HierarchComb	<b>1.93%</b>	9.42%	5.82%	<b>0.46%</b>	3.15%	<b>1.04%</b>
U52	NonHierarch	12.42%	5.10%	<b>2.31%</b>	2.37%	16.36%	15.22%
	BottomUp	6.24%	12.68%	2.67%	3.28%	<b>7.02%</b>	13.42%
	TopDown	<b>4.12%</b>	6.76%	2.52%	4.02%	9.51%	14.22%
	HierarchComb	9.22%	<b>4.97%</b>	2.39%	<b>2.36%</b>	15.21%	<b>13.11%</b>
U53	NonHierarch	4.91%	23.94%	6.3%	2.21%	9.63%	<b>5.89%</b>
	BottomUp	<b>2.98%</b>	<b>8.10%</b>	6.56%	3.06%	6.78%	15.60%
	TopDown	5.02%	8.43%	<b>5.78%</b>	<b>1.98%</b>	<b>5.59%</b>	7.20%
	HierarchComb	4.76%	22.71%	7.21%	2.15%	8.52%	6.26%
U54	NonHierarch	9.30%	1.41%	3.51%	1.52%	3.25%	4.02%
	BottomUp	<b>1.47%</b>	1.70%	<b>2.70%</b>	2.89%	<b>2.87%</b>	4.30%
	TopDown	3.56%	2.87%	3.87%	2.81%	4.56%	<b>3.89%</b>
	HierarchComb	8.67%	<b>1.37%</b>	3.70%	<b>1.40%</b>	4.02%	4.07%
U55	NonHierarch	1.87%	14.48%	<b>2.07%</b>	<b>0.03%</b>	6.76%	11.89%
	BottomUp	13.22%	<b>9.86%</b>	4.05%	1.91%	<b>4.49%</b>	12.15%
	TopDown	4.20%	11.21%	3.42%	1.32%	5.02%	12.67%
	HierarchComb	<b>2.04%</b>	10.17%	4.12%	0.12%	6.05%	<b>11.65%</b>
Total	NonHierarch	1.51%	9.18%	<b>0.56%</b>	0.16%	1.85%	<b>4.42%</b>
	BottomUp	1.58%	<b>2.24%</b>	0.93%	0.45%	2.42%	5.02%
	TopDown	1.51%	9.18%	<b>0.56%</b>	0.16%	1.85%	<b>4.42%</b>
	HierarchComb	<b>1.46%</b>	5.76%	0.68%	<b>0.14%</b>	<b>1.23%</b>	6.33%

that **TopDown** has higher error rates and we also know that for this hierarchical level, the models **NonHierarch** and **BottomUp** are equal. Therefore, and since parametric tests are more powerful than non-parametric tests, we used the *t-test* for paired samples, considering the difference between the pairs of error rates observations, and the null hypothesis tests whether the mean of these differences is null, instead of the alternative hypothesis, which tests if the mean value of the differences is higher than zero, which means the errors obtained by the model **HierarchComb** are lower than that obtained by the model **BottomUp**. We got a *p-value* less than 1% so, for this level of significance, we reject the null hypothesis. We conclude that the model **HierarchComb** produces better forecasts than the model **BottomUp**, and the differences are statistically significant. In fact, graphically, the model **HierarchComb** particularly reduces larger errors, which have great impact on the average.

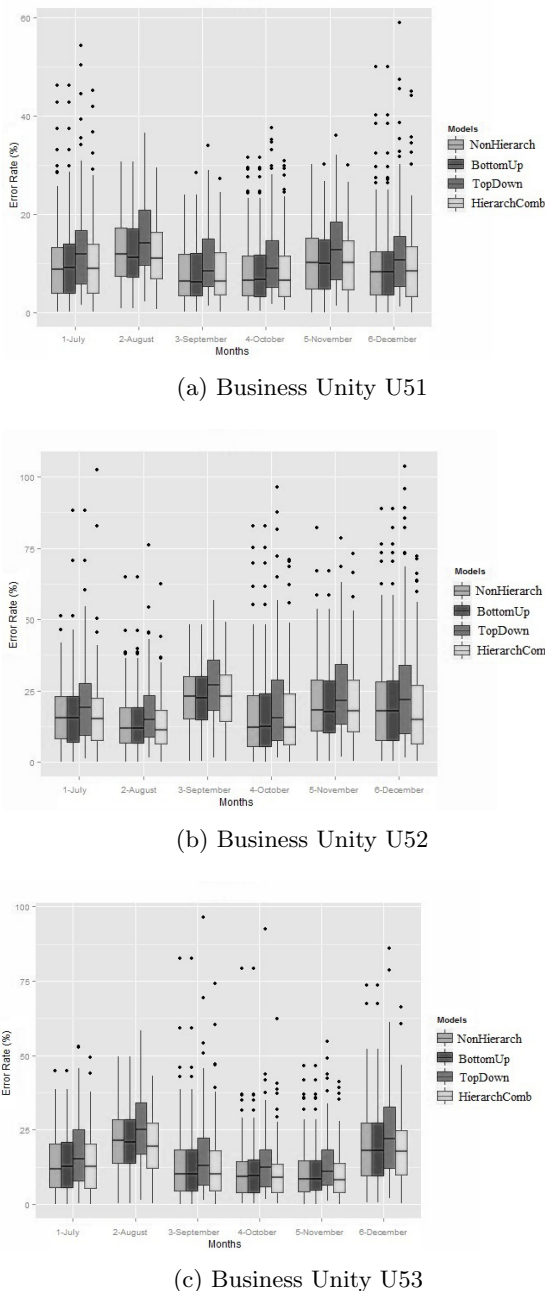
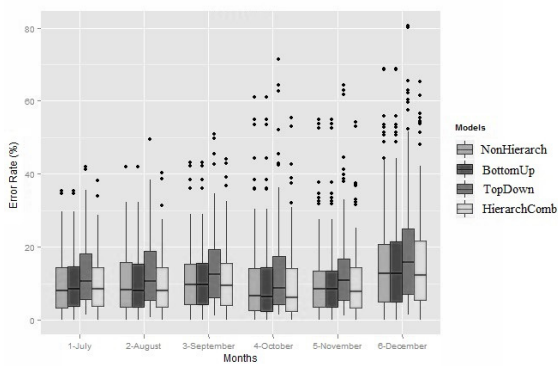
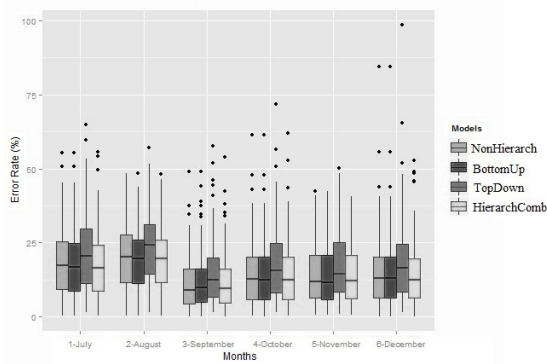


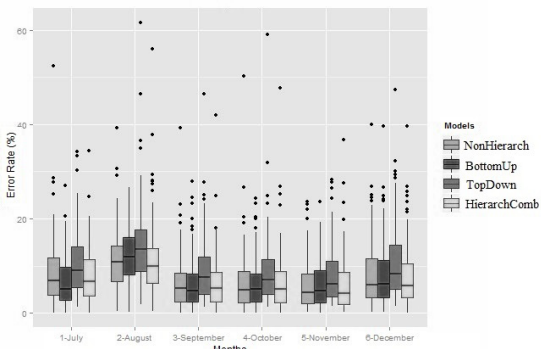
**Fig. 3.** Distribution of MAPE of sales forecast for all the stores in business units U51, U52 and U53 by four modelling approaches: NonHierarch, BottomUp, TopDown and HierarchComb



(d) Business Unity U54



(e) Business Unity U55



(f) total by store

**Fig. 3.** (*Continued*)

## 4 Conclusions and Future Work

The main goal of this paper is sales forecasting. We present a case study using real data from a Portuguese company leader of non-food retail sector. We study predictive models to obtain predictions for monthly sales revenue, by business unity, for all stores of the company. In our study we compare the standard flat approach, that ignores the hierarchical structure, and 3 different models that exploit the hierarchical structure. Our results show that when we descend in the hierarchy, the error rates tend to increase, given that, at higher levels we have a more uniform history. Our results confirmed that exploiting the hierarchical structure of the time series leads to more accurate forecasts. Namely, the approach proposed by [21] that combines the predictions made at each hierarchy level produced globally better results, for all hierarchical levels. This type of model tends to reduce the higher error rates and it can be seen as a valuable alternative when compared with the flat approach, and the bottom-up and top-down approaches. As future work, we plan to study how the forecasting variance depends on the inherent interactions between the time series in the same level. Moreover, as there are many real world problems where data presents an hierarchical structure, we intent to explore the application of this methodology to other real problems.

**Acknowledgments.** This work was supported by the European Commission through the project MAESTRA (Grant number ICT-2013-612944).

## References

1. Ferreira, N., Gama, J.: Análise exploratória de hierarquias em base de dados multidimensionais. *Revista de Ciências da Computação* **7**, 24–42 (2012)
2. Fliedner, G.: Hierarchical forecasting: issues and use guidelines. *Industrial Management and Data Systems* **101**, 5–12 (2001)
3. Gross, C.W., Sohl, J.E.: Disaggregation methods to expedite product line forecasting. *Journal of Forecasting* **9**(3) (1990)
4. Hyndman, R.J., Ahmed, R.A., Athanasopoulos, G., Shang, H.L.: Optimal combination forecasts for hierarchical time series. *Computational Statistics & Data Analysis* **55**, 2579–2589 (2011)
5. Azevedo, J.M., Almeida, R., Almeida, P.: Using data mining with time series data in short-term stocks prediction: A literature review. *International Journal of Intelligence Science* **2**, 176 (2012)
6. Alon, I., Qi, M., Sadowski, R.J.: Forecasting aggregate retail sales: A comparison of artificial neural networks and traditional methods. *Journal of Retailing and Consumer Services*, 147–156 (2001)
7. Zhang, G.P.: Neural networks for retail sales forecasting. In: *Encyclopedia of Information Science and Technology* (IV), pp. 2100–2104. Idea Group (2005)
8. Sousa, J.: Aplicação de redes neurais na previsão de vendas para retalho. Master's thesis, Faculdade de Engenharia da Universidade do Porto (2011)
9. Crone, S.F., Guajardo, J., Weber, R.: A study on the ability of support vector regression and neural networks to forecast basic time series patterns. In: Bramer, M. (ed.) *Artificial Intelligence in Theory and Practice*. LNCS, vol. 217, pp. 149–158. Springer, Boston (2006)

10. Drucker, H., Burges, C.J.C., Kaufman, L., Smola, A.J., Vapnik, V.: Support vector regression machines. In: Advances in Neural Information Processing Systems 9, December 2–5, NIPS, Denver, CO, USA, pp. 155–161 (1996)
11. R Core Team: R: A Language and Environment for Statistical Computing. R Foundation for Statistical Computing, Vienna, Austria (2014)
12. Hyndman, R.J., Wang, E., with contributions from Roman, A., Ahmed, A.L., to earlier versions of the package, H.L.S.: hts: Hierarchical and grouped time series. R package version 4.4 (2014)
13. Hartigan, J.A., Wong, M.A.: A k-means clustering algorithm. JSTOR: Applied Statistics **28**(1), 100–108 (1979)
14. Torgo, L.: Data Mining with R, learning with case studies. Chapman and Hall/CRC (2010)
15. With contributions from George Athanasopoulos, R.J.H., Razbash, S., Schmidt, D., Zhou, Z., Khan, Y., Bergmeir, C., Wang, E.: forecast: Forecasting functions for time series and linear models. R package version 5.6 (2014)
16. Ripley, B.: nnet: Feed-forward Neural Networks and Multinomial Log-Linear Models R package version 7.3-8 (2014)
17. Kuhn, M.: caret: Classification and Regression Training. R package version 6.0-35 (2014)
18. Meyer, D., Dimitriadou, E., Hornik, K., Weingessel, A., Leisch, F.: e1071: Misc Functions of the Department of Statistics (e1071), TU Wien. R package version 1.6-4 (2014)
19. Karatzoglou, A., Smola, A., Hornik, K., Zeileis, A.: kernlab - an S4 package for kernel methods in R. Journal of Statistical Software **11**(9), 1–20 (2004)
20. Breiman, L., Cutler, A., Liaw, A., Wiener, M.: Random forests for classification and regression. R package version 4.6-10 (2014)
21. Hyndman, R.J., Athanasopoulos, G.: Optimally reconciling forecasts in a hierarchy. Foresight: The International Journal of Applied Forecasting (35), 42–48 (2014)

# Crime Prediction Using Regression and Resources Optimization

Bruno Cavadas<sup>1,2</sup>, Paula Branco<sup>3,4(✉)</sup>, and Sérgio Pereira<sup>5</sup>

<sup>1</sup> Instituto de Investigação e Inovação em Saúde,  
Universidade do Porto, Porto, Portugal  
[brunomcavadas@gmail.com](mailto:brunomcavadas@gmail.com)

<sup>2</sup> Instituto de Patologia e Imunologia Molecular da,  
Universidade do Porto, Porto, Portugal

<sup>3</sup> LIAAD - INESC TEC, Porto, Portugal  
[pao@branco@gmail.com](mailto:pao@branco@gmail.com)

<sup>4</sup> DCC - Faculdade de Ciências, Universidade do Porto, Porto, Portugal

<sup>5</sup> ALGORITMI Centre, University of Minho, Braga, Portugal  
[pereirasrm@gmail.com](mailto:pereirasrm@gmail.com)

**Abstract.** Violent crime is a well known social problem affecting both the quality of life and the economical development of a society. Its prediction is therefore an important asset for law enforcement agencies, since due to budget constraints, the optimization of resources is of extreme importance. In this work, we tackle both aspects: prediction and optimization.

We propose to predict violent crime using regression and optimize the distribution of police officers through an Integer Linear Programming formulation, taking into account the previous predictions. Although some of the optimization data are synthetic, we propose it as a possible approach for the problem. Experiments showed that Random Forest performs better among the other evaluated learners, after applying the SmoteR algorithm to cope with the rare extreme values. The most severe violent crime rates were predicted for southern states, in accordance with state reports. Accordingly, these were the states with more police officers assigned during optimization.

**Keywords:** Violent crime · Prediction · SmoteR · Regression · Optimization

## 1 Introduction

Violent crime is a severe problem in society. Its prediction can be useful for the law enforcement agents to identify problematic regions to patrol. Additionally, it can be a valuable information to optimize available resources ahead of time.

In the United States of America (USA), according to the Uniform Crime Reports (UCR) published by the Federal Bureau of Investigation (FBI) [1], violent crimes imply the use of force or threat of using force, such as rape, murder,

robbery, aggravated assault, and non-negligent manslaughter. In 2013, it was reported 1,163,146 violent crimes, with an average of 367.9 per 100k inhabitants. This was equivalent to one violent crime every 27.1 seconds. In 2012, according to the United States Department of Labor [2], there were 780,000 police officers and detectives in the USA, with a median salary of \$56,980 per year. Therefore, the optimization of police officers can be useful to optimize costs, while guaranteeing the safety of the population.

In this paper, the contributions are twofold. Firstly, we propose to predict the violent crime per 100k population using regression. To the best of our knowledge, this is the first time that such problem is tackled in this way. Moreover, we pre-process the data using smoteR algorithm to improve predictions on the most critical values: the extreme high. Having the predictions, we also propose an Integer Linear Programming formulation for the optimization of police officers distribution across states. This distribution takes into account the crime severity, population, density and budget of the states.

The remaining of the paper is organized as follows. In Section 2 a brief survey on related work is presented. Materials and methods are exposed in Section 3, including the description of the data set, the prediction-related procedures and the optimization scheme. Then, in Section 4, results are presented and discussed, while in Section 5 the main conclusions are pointed out.

## 2 Related Work

Crime prediction has been extensively studied throughout the literature due to its relevance to society. These studies employ diverse machine learning techniques to tackle the crime forecasting problem.

Nath [3] combined K-means clustering and a weighting algorithm, considering a geographical approach, for the clustering of crimes according to their types. Liu et al. [4] proposed a search engine for extracting, indexing, querying and visualizing crime information using spatial, temporal, and textual information and a scoring system to rank the data. Shah et al. [5] went a step further and proposed CROWDSAFE for real-time and location-based crime incident searching and reporting, taking into account Internet crowd sourcing and portable smart devices. Automatic crime prediction events based on the extraction of Twitter posts has also been reported [6].

Regarding the UCI data set used in this work, Iqbal et al. [7] compared Naive Bayesian and decision trees methods by dividing the data set into three classes based on the risk level (Low, medium and high). In this study, decision trees outperformed Naive Bayesian algorithms, but the pre-processing procedures were rudimentary. Somayeh Shojaee et al. [8], applied a more rigorous data processing methodology for a binary class and applied the usage of two different feature selection methods to a wider range of learning algorithms (Naive Bayesian, decision trees, support vector machine, neural networks and K-Nearest neighbors). In these studies no class balancing methodologies were employed. Other approaches such as the fuzzy association rule mining [9] and case-based editing [10] have also been performed.

After prediction, optimization of resources can be achieved by several strategies. Donovan et al. [11] used integer linear programming for the optimization of fire-fighting resources, solving one of the most commonly constrains faced by fire managers. The same strategy was used by Caulkins et al. [12] in the optimization of software system security measures given a fixed budget.

Regarding the problem of police officer optimization, Mitchell [13] used a P-median model to determine the patrol areas in California, while Daskin [14] applied a Backup Coverage Model to maximize the number of areas covered. More recently, Li et al. [15] relied on the concept of “crime hot-spots” to create a cross entropy approach to produce randomized optimal patrol routes.

### 3 Materials and Methods

#### 3.1 Data Set Description

The *Communities and Crime Unnormalized Data Set*<sup>1</sup> provides information on several crimes in the USA, combining socio-economical and law enforcement data from 90' Census, 1990 Law Enforcement Management and Admin Stats survey and the 1995 FBI UCR. It includes 2215 examples, 124 numeric and 1 nominal attribute. It also contains 4 non-predictive attributes with information about the community name, county, code and fold. Among the several possible target variables we chose the number of violent crimes per 100k population.

#### 3.2 Prediction

We started by pre-processing the data set. The violent crime is our target variable, thus we removed all the other 17 possible target variables contained in the data set. We also eliminated all the examples that had a missing value on our target variable and removed all the attributes that had more than 80% of missing values. The data set contained four non-predictive attributes, which we have also eliminated. Finally, we have removed one more example that still had a missing value, and have normalized all the remaining attributes.

Although this problem was previously tackled as a classification task, we opted for addressing it as a regression task. This is an innovative aspect of our proposal and this choice is also based on the fact that we will use the numeric results obtained with the predictions for solving an optimization problem. Therefore, it makes sense to use a continuous variable throughout the work, instead of discretizing the target variable and latter recovering a numeric value.

Another challenge involving this data set is the high number of attributes. To address this problem we have applied the same feature selection scheme with two different percentages. The scheme applies a hierarchical clustering analysis, using the Pearson Correlation Coefficient. This step removes a percentage of the features less correlated with the target variable. Then, a Random Forest (RF)

---

<sup>1</sup> Available at UCI repository in

<https://archive.ics.uci.edu/ml/datasets/Communities+and+Crime+Unnormalized>.

learner is applied to compute the remaining features importance based on the impact in the Mean Squared Error. A percentage of the most important features provided is selected. Two different sets of features were selected by applying different percentages in the previous scheme. In one of the pre-processed data we aimed at obtaining 50% of the original features and in the other the goal was to select only 30% of the original features. This way we obtained two data sets with 52 and 32 features corresponding to 50% and 30% percentages.

In our regression problem we are interested in predicting the number of violent crimes per 100k inhabitants. However, we are more concerned with the errors made in the higher values of the target variable, i.e., the consequences of missing a high value of violent crimes by predicting it as low are worst than the reverse type of error. The extreme high values of the violent crime variable are the most important and yet the less represented in the data set. When addressed as a classification problem, this is clearly a problem with imbalanced classes, where the most important class has few examples. SmoteR algorithm is a proposal to address this type of problems within regression which was presented in [16, 17]. This proposal uses the notion of utility-based Regression [18] and relies on the definition of a relevance function. The relevance function expresses the user preferences regarding the importance assigned to the target variable range. Ribeiro [18] proposes automatic methods for estimating the relevance function of the target variable. We have used those methods because they correspond to our specific concerns: the extreme rare values are the most important. The essential idea of SmoteR algorithm is to balance the data set by under-sampling the most frequent cases and over-sampling the rare extreme examples. The over-sampling strategy generates new synthetic examples by interpolating existing rare cases. More details can be obtained in [16, 17]. The motivation for applying this procedure is to force the learning systems to focus on the rare extreme cases which would be difficult to achieve in the original imbalanced data. Our experiences included several variants of smoteR which were applied to the two pre-processed data sets. The smoteR variants used in the experiences included all combinations of the following parameters: under-sampling percentage 50% and 100%; over-sampling percentage 200% and 400%; number of neighbours 5.

For the prediction task we have used three learning algorithms: Support Vector Machines (SVM), RF and Multivariate Adaptive Regression Splines (MARS). More details on the experimented parameters and the evaluation are described in Section 4.1.

### 3.3 Optimization Through Integer Linear Programming

Given the predicted violent crime per 100k population, we propose to optimize the distribution of available police officers by state. We present our proposal as a proof of concept, since more detailed data and insight into the problem would be needed to implement a more realistic solution. Given that the number of officers by state is an integer quantity, it is used Integer Linear Programming. To solve the optimization problem it was applied the Branch-and-bound algorithm.

**Problem Formulation.** We considered as resources a certain amount of police officers to freely distribute by the states of the USA. The optimization takes into account the predictions on violent crime per 100k population to assign more officers by the states with more violent criminality. This assignment is constrained by an ideal number of officers that each state would like to receive and the available budget. However, every state should receive a minimum amount of officers to guarantee the security of its citizens.

In the data set, the instances are defined by communities, with several of them belonging to the same state. Since we wanted to distribute officers by state, it was calculated the mean violent crime predictions by state.

The optimization problem was defined as,

$$\begin{aligned} & \text{maximize} \sum_{i=1}^m s_i x_i \\ & \text{subject to} \sum_{i=1}^m x_i = N; \quad x_i \leq H_i; \\ & \quad x_i \geq f_i H_i; \quad c_i x_i \leq B_i; \\ & \quad x_i \in \mathbb{N} \end{aligned}$$

where  $i \in \{1, \dots, m\}$  indexes each of the  $m$  states, with  $m = 46$ ,  $x_i$  is the number of officers to distribute by state,  $s_i$  is the violent crime predictions by state,  $H_i$  is the ideal number of officers by state,  $f_i$  is a fraction on the ideal number of officers that each state accepts as the minimum,  $c_i$  is the cost that each state should pay for each officer, and  $B_i$  is the available budget for each state.

The ideal number of officers was defined in function of the violent crime prediction of the state and the population (number of citizens), since bigger populations, with more violent crime, have higher demands regarding police officers. To this end, the violent crime predictions were scaled ( $s_{s_i}$ ) to the interval  $[v_l, v_h]$ . This way, it acts as a proportion on the population. However, since some populations have millions of citizens, this value was divided by 100 to get more realistic estimates for the ideal number of officers. So,

$$H_i = \frac{s_{s_i} p_i}{100} \quad (1)$$

where  $p_i$  is the real population of the state  $i$ .

It was defined that the minimum number of officers should be a fraction on the ideal number, taking into account the crime predictions. Defining a lower ( $l_b$ ) and an upper ( $u_b$ ) bound for the fraction, the previously scaled violent crime predictions are linearly mapped to the interval  $[l_b, u_b]$ . Knowing that it is in the interval  $[v_l, v_h]$ , the fraction on the ideal number of officers is calculated as,

$$f_i = \frac{s_i - v_l}{v_h - v_l} (u_b - l_b) + l_b \quad (2)$$

Budget was defined in function of the population and its density. Such definition is based on the intuition that a small and less dense population needs less budget and officers than a highly dense and big population. However, the

population numbers are several orders of magnitude higher than density, which would make the effect of density negligible. So, we have rescaled both population and density to the range [0, 100] ( $p_{s_i}$  and  $d_{s_i}$ ). Moreover, the budget for each state is a part of the total national budget ( $B_T$ ). So,  $B_i$  was calculated as

$$B_i = \frac{(d_{s_i} + a \cdot p_{s_i}) B_T}{\sum_{i=1}^m d_{s_i} + a \cdot p_{s_i}} \quad (3)$$

where  $a > 0$  is a parameter to tune the weight of the density and population over the budget calculation.

## 4 Experimental Analysis

We have divided our problem, and analysis, into two sub-problems: prediction and optimization. In this section, we describe the tools, metrics, and evaluation methodology for each sub-problem. Then we focus in each sub-problem results.

### 4.1 Experimental Setup

**Prediction.** The main goal of our experiments is to select one of the two pre-processed data sets, a smoteR variant (in case it has a positive impact) and a model (among SVM, RF and MARS) to apply in the optimization task.

The experiments were conducted with R software. Table 1 summarizes the learning algorithms that were used and the respective parameter variants. All combinations of parameters were tried for the learning algorithms, which led to 4 SVM variants, 6 RF variants and 8 MARS variants.

We started by splitting each data set in train and test sets, approximately corresponding to 80% and 20% of the data. The test set was held apart to be used in the optimization, after predicting its crime severities. This set was randomly built with stratification and with the condition of including at least one example for each possible state of the USA.

In imbalanced domains, it is necessary to use adequate metrics since traditional measures are not suitable for assessing the performance. Most of these specific metrics, such as precision and recall, exist for classification problems. The notions of precision and recall were adapted to regression problems with non-uniform relevance of the target values by Torgo and Ribeiro [19] and Ribeiro [18]. We will use the framework proposed by these authors to evaluate and compare our results. More details on this formulation can be obtained in[18].

All the described alternatives were evaluated according to the F-measure with  $\beta = 1$ , which means that the same importance was given to both precision and recall scores. The values of  $F_1$  were estimated by means of 3 repetitions of a 10-fold Cross Validation process and the statistical significance of the observed paired differences was measured using the non-parametric pairwise Wilcoxon signed-rank test.

**Table 1.** Regression algorithms, parameter variants, and respective R packages.

Learner	Parameter Variants	R package
MARS	$nk = \{10, 17\}$ , $degree = \{1, 2\}$ , $thresh = \{0.01, 0.001\}$	<b>earth</b> [20]
SVM	$cost = \{10, 150\}$ , $gamma = \{0.01, 0.001\}$	<b>e1071</b> [21]
Random Forest	$mtry = \{5, 7\}$ , $ntree = \{500, 750, 1500\}$	<b>randomForest</b> [22]

**Optimization.** In the optimization sub-problem the objective was to assign to each state a certain amount of police officers, given the total budget, the total number of available officers, and the violent criminality predictions. The optimization was carried out in R software, with the package “lpSolve”.

The values for the population and the density are real values, obtained from the estimates for 2014 [23]. However, the total budget, the number of available police officers, and the individual cost of the officers by state were defined by us. Although they are not real values, they serve as proof of concept. The cost of each officer by state was chosen randomly, and uniformly, from the interval [5, 15] once, then the same values were used in all experiments. Additionally, the values for  $u_b$  and  $l_b$  were set to 0.12 and 0.08, while  $v_l$  and  $v_h$  were set to 0.125 and 0.7, respectively.

## 4.2 Results and Discussion

**Prediction.** We started by examining the results obtained with all the parameters selected for the two pre-processed data sets, the three types of learners and the smoteR variants. All combinations of parameters were tested by means of 3 repetitions of a 10-fold cross validation process. Figure 1 shows these results.

We have also analysed the statistical significance of the differences observed in the results. Table 2 contains the several p-values obtained when comparing the SmoteR variants and the different learners, using the non-parametric pairwise Wilcoxon signed rank test with Bonferroni correction for multiple testing.

The p-value for the differences between the two data sets (with 30% and 50% of the features) was 0.17. Therefore we chose the data set with less features to continue to the optimization problem. This was mainly because of: i) the non statistical significant differences and ii) the smaller size of the data (less features can explain well the target variable, so we chose the most efficient alternative).

**Table 2.** Pairwise Wilcoxon signed rank test with Bonferroni correction for the SmoteR strategies (left) and the learning systems (right).

Strategies	none	S.o2.u0.5	S.o2.u1	S.o4.u0.5	Learners	svm	rf
S.o2.u0.5	1.3e-14	-	-	-	rf	<2e-16	-
S.o2.u1	< 2e-16	1	-	-	mars	0.077	<2e-16
S.o4.u0.5	2.3e-16	1	1	-			
S.o4.u1	< 2e-16	0.18	1	1			

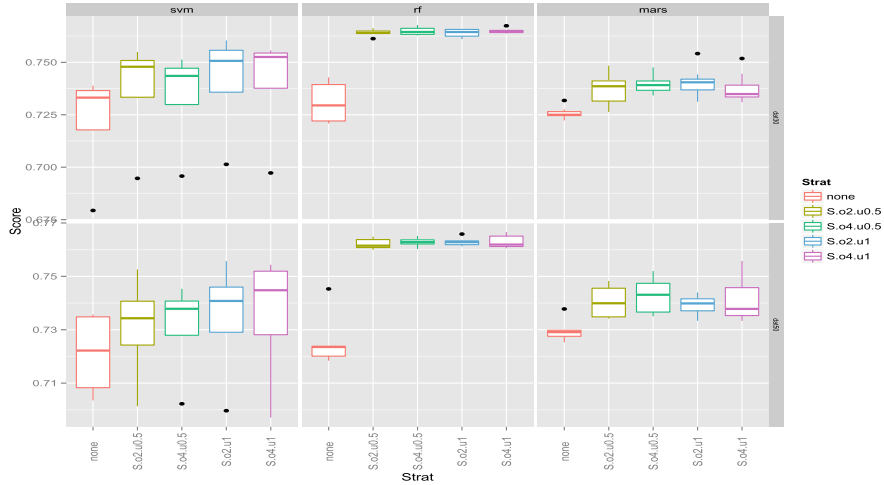


**Fig. 1.** Results from  $3 \times 10$ -fold CV by learning system and SmoteR variant. (none-original data; S-smoteR;  $ox-x \times 100\%$  over-sampling;  $uy-y \times 100\%$  under-sampling)

Regarding the SmoteR strategy, Figure 1 and Table 2 provide clear evidence of the advantages of this procedure. Moreover, we also observed that the differences between the several variants of this procedure are not statistically significant. Therefore, we have opted for the variant which leads to a smaller data set and consequently a lower run time. For the optimization sub-problem we chose to use the smoteR variant with 200% of over-sampling percentage and 100% of under-sampling percentage. The learning system that provides a better performance is clearly the RF. With this learner, there is almost no differences among the several experimented variants.

Considering these results, we chose the following setting to generate a model for the optimization sub-problem:

- Pre-processing to remove missing values and select 30% of the most relevant features;
- Apply the smoteR strategy with parameters  $k=5$ ; over-sampling percentage=200; under-sampling percentage=100;
- RF model with parameters:  $mtry=7$ ;  $ntree=750$ .

After generating the model we obtained the predictions for the test set which was held apart to use in the optimization sub-problem. These predictions were used as input of the optimization task.

**Optimization.** Several parameters were experimented. It was verified that with high budget and number of available officers, states with more criminality are assigned more officers. When the weight of the population increases, the most populated states, such as California, receive more police officers. When

this weight is decreased, those states lost officers, while, for instance, Vermont obtained the ideal number, although the population is one of the lowest

Table 3 shows the results of distributing 500,000 police officers, with a budget of 8,000,000, and  $a = 1$ . Figure 2 shows the same results in a map of the USA, where brighter red is associated with higher criminality, and the radius of the circles is proportional to the amount of officers assigned to the state. The color of the circle indicates which restriction limited the number of officers. Therefore, green means that the state received the ideal number, the minimum is represented in blue, yellow means that the budget of the state did not allow more

**Table 3.** Distribution of 500,000 police officers by state, subjected to a total budget of 8,000,000.

State	Crime Prediction	Budget	Min. Off.	Ideal Off.	Dist. Off.	Cost
NJ	676.8	320390.4	1597	18614	18614	182659.9
PA	276.1	323802.5	1279	15991	1279	11413.7
OR	638.3	87076.7	678	7951	7951	59607.0
NY	893.1	504835.7	4445	49991	41007	504830.6
MO	381.3	12559.3	123	1503	123	1280.8
MA	408.1	233862.6	842	10283	842	5457.7
IN	726.6	164404.1	1247	14420	14420	162921.4
TX	821.1	648307.0	5643	64214	64214	477378.9
CA	850.2	948629.7	8369	94781	68083	948620.3
KY	655.6	104572.9	769	8996	8996	66277.2
AR	928.2	64349.2	691	7726	5885	64346.6
CT	355.4	146317.7	413	5090	413	6109.4
OH	542.8	90044.9	587	6997	587	8778.9
NH	312.6	33606.1	142	1760	142	2027.5
FL	1313.2	503583.7	6432	67716	52441	503581.4
WA	557.3	168051.3	1089	12954	12954	120927.3
LA	1721.0	109854.6	1994	19765	11893	109847.5
WY	528.1	1846.3	87	1036	87	778.2
NC	1315.6	247220.2	3221	33900	27118	247214.5
MS	1089.4	65686.5	808	8801	7149	65677.9
VA	851.7	208745.0	1798	20363	14106	208734.1
SC	1171.5	119505.3	1397	15028	10543	119498.9
WI	325.7	136544.5	629	7793	629	5271.4
TN	712.7	160819.6	1219	14128	10940	160817.3
UT	794.8	61723.4	599	6850	4253	61723.1
OK	488.6	86322.2	545	6560	545	5960.0
ND	342.0	6056.3	83	1026	83	618.2
AZ	500.5	155514.1	962	11554	962	11214.4
CO	791.7	121546.9	1087	12432	12432	84710.8
WV	551.2	39327.5	283	3371	283	3485.0
RI	440.9	110983.5	138	1680	138	1327.7
AL	1452.9	113590.5	1738	17915	7786	113576.2
GA	1254.6	248026.3	3120	33144	26054	248017.1
ID	444.8	28553.6	216	2616	216	2020.0
ME	275.9	23475.0	133	1663	133	1942.2
KS	1286.4	60751.9	920	9724	9724	52508.6
SD	568.5	8853.4	133	1585	1403	8851.3
NV	920.6	58244.7	656	7350	7350	56186.7
IA	556.7	67617.0	479	5696	2243	15039.1
MD	1271.9	191051.4	1872	19832	13217	191045.6
MN	862.1	125640.6	1191	13465	13465	96440.4
NM	835.6	39199.9	443	5031	3950	39199.7
DE	1161.9	48882.5	268	2891	2891	16497.7
VT	517.2	8881.3	92	1097	92	548.1
AK	932.3	64349.2	694	7752	7752	45227.2
DC	3044.8	926793.2	553	4612	4612	67407.4

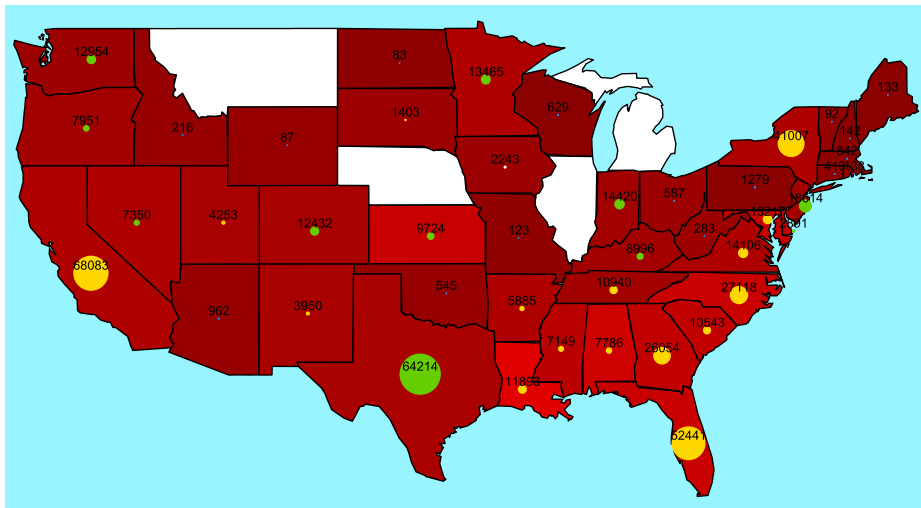


**Fig. 2.** Map of the USA representing the level of violent criminality by state, the amount of police officers assigned, and the restriction that imposed that number. White states are not represented in the data set.

officers, and white means that the state received a middle value of officers, which is less than the ideal or the maximum allowed by the budget, but higher than the minimum. It is possible to observe that ten states received the ideal number of officers. Some of them were associated with low or moderate levels of criminality, but the density or the population was high, such as New Jersey or Texas. Others are less populated, such as Oregon, but the ideal number of officers was also lower than other states constraint by the budget. The violent crime rate was particularly important in Kansas, since with a lower density and population, its budget allowed the state to receive the ideal number of officers. It is, also, possible to observe that the states with more violent criminality reached the number of officers allowed by their budget, such as Alabama or South Carolina. Accordingly, many states with less criminality received the minimum number of officers that they would allow (North Dakota), or values between the minimum and the ideal, without being constrained by the budget (Iowa). This behaviour may be desirable, since having too many officers in states with less criminality may be a waste of resources. The influence of the crime severity may be perceived when comparing Arizona with Nevada. The former has more population, higher density and budget than the latter, but received less officers because of the lower criminality rating.

According to the FBI [1], the region with more violent crime incidents is the South, followed by the West, Midwest and Northeast. It is interesting to notice that, in Figure 2, it was predicted more severe criminality for the southern states. These were the states that receive more police officers.

## 5 Conclusions

In this paper, we proposed a pipeline for predicting violent crime and a resources optimization scheme. Prediction encompasses feature selection through correlation and feature importance analysis, over-sampling of the rare extreme values of the target variable and regression. Among the evaluated learning systems, RF presented the best performance. This pipeline itself is one of the contributions of this work, given that, to the best of our knowledge, this problem in this data set was never approached as regression. Having the predictions, we propose a decision support scheme through the optimization of police officers across states, while taking into account the violent crime predictions, population, density and budget of the states. This contribution is presented as a proof of concept, since some of the parameters were synthesized and may not correspond to the real scenario. Nevertheless, our results show an higher crime burden in states located in the southern part of the USA compared with the states in the north. For this reason, southern states tend to have an higher assignment of police officers. These predictions are in accordance with some national reports, and although some parameters of the optimization are not completely realistic, it seems to work as expected.

This work, although limited to the United States, can be easily applied to various other countries. So, as future work we consider that it would be interesting to apply the proposed framework in other countries or regions.

**Acknowledgments.** This work is financed by the FCT – Fundação para a Ciência e a Tecnologia (Portuguese Foundation for Science and Technology) within project UID/EEA/50014/2013. Sérgio Pereira and Paula Branco were supported by scholarships from the Fundação para a Ciência e Tecnologia (FCT), Portugal (scholarships number PD/BD/105803/2014 and PD/BD/105788/2014). We would like to thank the useful comments of Manuel Filipe Santos, Paulo Cortez, Rui Camacho and Luis Torgo.

## References

1. FBI, Crime in the United States 2013 (2014). <http://www.fbi.gov/about-us/cjis/ucr/crime-in-the-u.s./2013/crime-in-the-u.s.-2013> (accessed: January 21, 2015)
2. Labor-Statistics, B.: United States Department of Labor - Bureau of Labor Statistics: Police and detectives (2012). <http://www.bls.gov/ooh/protective-service/police-and-detectives.htm#tab-1> (accessed: January 21, 2015)
3. Nath, S.V.: Crime pattern detection using data mining. In: 2006 IEEE/WIC/ACM International Conference on Web Intelligence and Intelligent Agent Technology Workshops, WI-IAT 2006 Workshops, pp. 41–44. IEEE (2006)
4. Liu, X., Jian, C., Lu, C.-T.: A spatio-temporal-textual crime search engine. In: Proceedings of the 18th SIGSPATIAL International Conference on Advances in Geographic Information Systems, pp. 528–529. ACM (2010)
5. Shah, S., Bao, F., Lu, C.-T., Chen, I.-R.: CrowdSafe: crowd sourcing of crime incidents and safe routing on mobile devices. In: Proceedings of the 19th ACM SIGSPATIAL International Conference on Advances in Geographic Information Systems, pp. 521–524. ACM (2011)

6. Wang, X., Gerber, M.S., Brown, D.E.: Automatic crime prediction using events extracted from twitter posts. In: Yang, S.J., Greenberg, A.M., Endsley, M. (eds.) SBP 2012. LNCS, vol. 7227, pp. 231–238. Springer, Heidelberg (2012)
7. Iqbal, R., Murad, M.A.A., Mustapha, A., Panahy, P.H.S., Khanahmadliravi, N.: An experimental study of classification algorithms for crime prediction. Indian Journal of Science and Technology **6**(3), 4219–4225 (2013)
8. Shojaee, S., Mustapha, A., Sidi, F., Jabar, M.A.: A study on classification learning algorithms to predict crime status. International Journal of Digital Content Technology and its Applications **7**(9), 361–369 (2013)
9. Buczak, A.L., Gifford, C.M.: Fuzzy association rule mining for community crime pattern discovery. In: ACM SIGKDD Workshop on Intelligence and Security Informatics, p. 2. ACM (2010)
10. Redmond, M.A., Highley, T.: Empirical analysis of case-editing approaches for numeric prediction. In: Innovations in Computing Sciences and Software Engineering, pp. 79–84. Springer (2010)
11. Donovan, G., Rideout, D.: An integer programming model to optimize resource allocation for wildfire containment. Forest Science **49**(2), 331–335 (2003)
12. Caulkins, J., Hough, E., Mead, N., Osman, H.: Optimizing investments in security countermeasures: a practical tool for fixed budgets. IEEE Security & Privacy **5**(5), 57–60 (2007)
13. Mitchell, P.S.: Optimal selection of police patrol beats. The Journal of Criminal Law, Criminology, and Police Science, 577–584 (1972)
14. Daskin, M.: A maximum expected covering location model: formulation, properties and heuristic solution. Transportation Science **17**(1), 48–70 (1983)
15. Li, L., Jiang, Z., Duan, N., Dong, W., Hu, K., Sun, W.: Police patrol service optimization based on the spatial pattern of hotspots. 2011 IEEE International Conference on in Service Operations, Logistics, and Informatics, pp. 45–50. IEEE (2011)
16. Torgo, L., Ribeiro, R.P., Pfahringer, B., Branco, P.: SMOTE for regression. In: Reis, L.P., Correia, L., Cascalho, J. (eds.) EPIA 2013. LNCS, vol. 8154, pp. 378–389. Springer, Heidelberg (2013)
17. Torgo, L., Branco, P., Ribeiro, R.P., Pfahringer, B.: Resampling strategies for regression. Expert Systems (2014)
18. Ribeiro, R.P.: Utility-based Regression. PhD thesis, Dep. Computer Science, Faculty of Sciences - University of Porto (2011)
19. Torgo, L., Ribeiro, R.: Precision and recall for regression. In: Gama, J., Costa, V.S., Jorge, A.M., Brazdil, P.B. (eds.) DS 2009. LNCS, vol. 5808, pp. 332–346. Springer, Heidelberg (2009)
20. Milborrow, S.: earth: Multivariate Adaptive Regression Spline Models. Derived from mda:mars by Trevor Hastie and Rob Tibshirani (2012)
21. Dimitriadou, E., Hornik, K., Leisch, F., Meyer, D., Weingessel, A.: e1071: Misc Functions of the Department of Statistics (e1071), TU Wien (2011)
22. Liaw, A., Wiener, M.: Classification and regression by randomforest. R News **2**(3), 18–22 (2002)
23. U.S.C. Bureau, Population Estimates (2012). <http://www.census.gov/popest/data/index.html> (accessed: January 23, 2015)

# Distance-Based Decision Tree Algorithms for Label Ranking

Cláudio Rebelo de Sá<sup>1,3(✉)</sup>, Carla Rebelo<sup>3</sup>, Carlos Soares<sup>2,3</sup>,  
and Arno Knobbe<sup>1</sup>

<sup>1</sup> LIACS Universiteit Leiden, Leiden, The Netherlands  
[{c.f.de.sa,a.j.knobbe}@liacs.leidenuniv.nl](mailto:{c.f.de.sa,a.j.knobbe}@liacs.leidenuniv.nl)

<sup>2</sup> Faculdade de Engenharia, Universidade do Porto, Porto, Portugal  
[csoares@fe.up.pt](mailto:csoares@fe.up.pt)

<sup>3</sup> INESC TEC Porto, Porto, Portugal

**Abstract.** The problem of Label Ranking is receiving increasing attention from several research communities. The algorithms that have developed/adapted to treat rankings as the target object follow two different approaches: distribution-based (e.g., using Mallows model) or correlation-based (e.g., using Spearman’s rank correlation coefficient). Decision trees have been adapted for label ranking following both approaches. In this paper we evaluate an existing correlation-based approach and propose a new one, Entropy-based Ranking trees. We then compare and discuss the results with a distribution-based approach. The results clearly indicate that both approaches are competitive.

## 1 Introduction

Label Ranking (LR) is an increasingly popular topic in the machine learning literature [7,8,18,19,24]. LR studies a problem of learning a mapping from instances to rankings over a finite number of predefined labels. It can be considered as a natural generalization of the conventional classification problem, where only a single label is requested instead of a ranking of all labels [6]. In contrast to a classification setting, where the objective is to assign examples to a specific class, in LR we are interested in assigning a complete preference order of the labels to every example.

There are two main approaches to the problem of LR: methods that transform the ranking problem into multiple binary problems and methods that were developed or adapted to treat the rankings as target objects, without any transformation. An example of the former is the ranking by pairwise comparison of [11]. Examples of algorithms that were adapted to deal with rankings as the target objects include decision trees [6,23], naive Bayes [1] and  $k$ -Nearest Neighbor [3,6].

Some of the latter adaptations are based on statistical distribution of rankings (e.g., [5]) while others are based on rank correlation measures (e.g., [19,23]). In this paper we carry out an empirical evaluation of decision tree approaches for LR based on correlation measures and compare it to distribution-based approaches.

We implemented and analyzed the algorithm previously presented in [17]. We also propose a new decision tree approach for LR, based on the previous one, which uses information gain as splitting criterion. The results clearly indicate that both are viable LR methods and are competitive with state of the art methods.

## 2 Label Ranking

The Label Ranking (LR) task is similar to classification. In classification, given an instance  $x$  from the instance space  $\mathbb{X}$ , the goal is to predict the label (or class)  $\lambda$  to which  $x$  belongs, from a pre-defined set  $\mathcal{L} = \{\lambda_1, \dots, \lambda_k\}$ . In LR, the goal is to predict the ranking of the labels in  $\mathcal{L}$  that are associated with  $x$  [11]. A ranking can be represented as a total order over  $\mathcal{L}$  defined on the permutation space  $\Omega$ . In other words, a total order can be seen as a permutation  $\pi$  of the set  $\{1, \dots, k\}$ , such that  $\pi(a)$  is the position of  $\lambda_a$  in  $\pi$ .

As in classification, we do not assume the existence of a deterministic  $\mathbb{X} \rightarrow \Omega$  mapping. Instead, every instance is associated with a *probability distribution* over  $\Omega$  [6]. This means that, for each  $x \in \mathbb{X}$ , there exists a probability distribution  $\mathcal{P}(\cdot|x)$  such that, for every  $\pi \in \Omega$ ,  $\mathcal{P}(\pi|x)$  is the probability that  $\pi$  is the ranking associated with  $x$ . The goal in LR is to learn the mapping  $\mathbb{X} \rightarrow \Omega$ . The training data is a set of instances  $D = \{\langle x_i, \pi_i \rangle\}, i = 1, \dots, n$ , where  $x_i$  is a vector containing the values  $x_i^j, j = 1, \dots, m$  of  $m$  independent variables describing instance  $i$  and  $\pi_i$  is the corresponding target ranking.

Given an instance  $x_i$  with label ranking  $\pi_i$ , and the ranking  $\hat{\pi}_i$  predicted by an LR model, we evaluate the accuracy of the prediction with a loss function on  $\Omega$ . One such function is the number of discordant label pairs,

$$\mathcal{D}(\pi, \hat{\pi}) = \#\{(a, b) | \pi(a) > \pi(b) \wedge \hat{\pi}(a) < \hat{\pi}(b)\}$$

If normalized to the interval  $[-1, 1]$ , this function is equivalent to Kendall's  $\tau$  coefficient [12], which is a correlation measure where  $\mathcal{D}(\pi, \pi) = 1$  and  $\mathcal{D}(\pi, \pi^{-1}) = -1$  ( $\pi^{-1}$  denotes the inverse order of  $\pi$ ).

The accuracy of a model can be estimated by averaging this function over a set of examples. This measure has been used for evaluation in recent LR studies [6, 21] and, thus, we will use it here as well. However, other correlation measures, like Spearman's rank correlation coefficient [22], can also be used.

### 2.1 Ranking Trees

One of the advantages of tree-based models is how they can clearly express information about the problem because their structure is relatively easy to interpret even for people without a background on learning algorithms. It is also possible to obtain information about the importance of the various attributes for the prediction depending on how close to the root they are used. The Top-Down Induction of Decision Trees (TDIDT) algorithm is commonly used for induction

of decision trees [13]. It is a recursive partitioning algorithm that iteratively splits data into smaller subsets which are increasingly more homogeneous in terms of the target variable (Algorithm 1).

It starts by determining the split that optimizes a given splitting criterion. A split is a test on one of the attributes that divides the dataset into two disjoint subsets. For instance, given a numerical attribute  $x^2$ , a split could be  $x^2 \geq 5$ . Without a stopping criterion, the TDIDT algorithm only stops when the nodes are pure, i.e., when the value of the target attribute is the same for all examples in the node. This usually leads the algorithm to overfit, i.e., to generate models that fit not only to the patterns in the data but also to the noise. One approach to address this problem is to introduce a stopping criterion in the algorithm that tests whether the best split is significantly improving the quality of the model. If not, the algorithm stops and returns a leaf node. This node is represented by the prediction that will be made for new examples that fall into that node. This prediction is generated by a rule that solves potential conflicts in the set of training examples that are in the node. In classification, the prediction rule is usually the most frequent class among the training examples. If the stopping criterion is not verified, then the algorithm is executed recursively for the subsets of the data obtained based on the best split.

---

**Algorithm 1.** TDIDT algorithm

---

```

BestSplit = Test of the attributes that optimizes the SPLITTING CRITERION
if STOPPING CRITERION == TRUE then
    Determine the leaf prediction based on the target values of the examples in D
    Return a leaf node with the corresponding LEAF PREDICTION
else
    LeftSubtree = TDIDT( $D_{\neg BestSplit}$ )
    RightSubtree = TDIDT( $D_{BestSplit}$ )
end if

```

---

An adaptation of the TDIDT algorithm for the problem of learning rankings has been proposed [23], called Ranking Trees (RT) which is based on the clustering trees algorithm [2]. Adaptation of this algorithm for label ranking involves an appropriate choice of the splitting criterion, stopping criterion and the prediction rule.

*Splitting Criterion.* The splitting criterion is a measure that quantifies the quality of a given partition of the data. It is usually applied to all the possible splits of the data that can be made based on individual tests of the attributes.

In RT the goal is to obtain leaf nodes that contain examples with target rankings as similar between themselves as possible. To assess the similarity between the rankings of a set of training examples, we compute the mean correlation between them, using Spearman's correlation coefficient. The quality of the split is given by the weighted mean correlation of the values obtained for the subsets, where the weight is given by the number of examples in each subset.

**Table 1.** Illustration of the splitting criterion

Attribute	Condition values	Condition rank corr.	Negated condition values rank corr.	
			rank corr.	rank corr.
$x^1$	a	0.3	b, c	-0.2
	b	0.2	a, c	0.1
	c	0.5	a, b	0.2
$x^2$	< 5	-0.1	$\geq 5$	0.1

The splitting criterion of ranking trees is illustrated both for nominal and numerical attributes in Table 1. The nominal attribute  $x^1$  has three values ( $a$ ,  $b$  and  $c$ ). Therefore, three binary splits are possible. For the numerical attribute  $x^2$ , a split can be made in between every pair of consecutive values. In this case, the best split is  $x^1 = c$ , with a mean correlation of 0.5 for the training examples that verify the test and a mean correlation of 0.2 for the remaining, i.e., the training examples for which  $x^1 = a$  or  $x^1 = b$ .

*Stopping Criterion.* The stopping criterion is used to determine if it is worthwhile to make a split to avoid overfitting [13]. A split should only be made if the similarity between examples in the subsets increases substantially. Let  $S_{parent}$  be the similarity between the examples in the parent node and  $S_{split}$  the weighted mean similarity in the subsets obtained with the best split. The stopping criterion is defined in [17] as follows:

$$(1 + S_{parent}) \geq \gamma(1 + S_{split}) \quad (1)$$

Note that the significance of the increase in similarity is controlled by the  $\gamma$  parameter.

*Prediction Rule.* The prediction rule is a method to generate a prediction from the (possibly conflicting) target values of the training examples in a leaf node. In RT, the method that is used to aggregate the  $q$  rankings that are in the leaves is based on the mean ranks of the items in the training examples that fall into the corresponding leaf. The average rank for each setting is  $\bar{\pi}(j) = \sum_i \pi_i(j) / n$ . The predicted ranking  $\hat{\pi}$  will be the average ranking  $\bar{\pi}$  after assigning ranks to  $\pi(j)$ . Table 2 illustrates the prediction rule used in this work.

**Table 2.** Illustration of the prediction rule.

	$\lambda_1$	$\lambda_2$	$\lambda_3$	$\lambda_4$
$\pi_1$	1	3	2	4
$\pi_2$	2	1	4	3
$\bar{\pi}$	1.5	2	3	3.5
$\hat{\pi}$	1	2	3	4

## 2.2 Entropy Ranking Trees

Decision trees, like ID3 [15], use Information Gain (IG) as a splitting criterion to look for the best split points.

**Information Gain.** IG is a statistical property that measures the difference in entropy, between the prior and actual state relatively to a target variable [13]. In other words, considering a set  $S$  of size  $n_S$ , as entropy -  $H$  - is a measure of disorder, IG is basically how much uncertainty in  $S$  is reduced after splitting on attribute A:

$$IG(A, T; S) = H(S) - \frac{|S_1|}{n_S}H(S_1) - \frac{|S_2|}{n_S}H(S_2)$$

where  $|S_1|$  and  $|S_2|$  are the number of instances on the left side ( $S_1$ ) and the number of instances on the right side ( $S_2$ ), respectively, of the cut point  $T$  in attribute A.

Using the same tree generation algorithm, the TDIDT (Section 2.1), we propose an alternative approach of decision trees for ranking data, the Entropy-based Ranking Trees (ERT). The difference is on the splitting and stopping criteria. ERT use  $IG$  to assess the splitting points and  $MDLPC$  [10] as stopping criterion. Using the measure of entropy for rankings [20], the splitting and stopping criteria come in a natural way.

The entropy for rankings [20] is defined as:

$$H_{ranking}(S) = \sum_{i=1}^K P(\pi_i, S) \log(P(\pi_i, S)) \log(\overline{kt}(S)) \quad (2)$$

where  $K$  is the number of distinct rankings in  $S$  and  $\overline{kt}(S)$  is the average normalized Kendall  $\tau$  distance in the subset  $S$ :

$$\overline{kt}(S) = \frac{\sum_{i=1}^K \sum_{j=1}^n \frac{\tau(\pi_i, \pi_j) + 1}{2}}{K \times n_S}$$

where  $K$  is the number of distinct target values in  $S$ .

As in Section 2.1 the leafs of the tree should not be forced to have pure leafs. Instead, they should have a stop criterion to avoid overfitting and be robust to noise in rankings. As shown in [20], the *MDLPC Criterion* can be used as a splitting criterion with the adapted version of entropy  $H_{ranking}$ . This entropy measure also works with partial orders, however, in this work, we only use total orders.

One other ranking tree approach based in Gini Impurity, which will not be presented in detail in this work, was proposed in [25].

## 3 Experimental Setup

The data sets in this work were taken from KEBI Data Repository in the Philipps University of Marburg [6] (Table 3). Two different transformation methods were

used to generate these datasets: (A) the target ranking is a permutation of the classes of the original target attribute, derived from the probabilities generated by a naive Bayes classifier; (B) the target ranking is derived for each example from the order of the values of a set of numerical variables, which are no longer used as independent variables. Although these are somewhat artificial datasets, they are quite useful as benchmarks for LR algorithms.

The statistics of the datasets used in our experiments is presented in Table 3.  $U_\pi$  is the proportion of distinct target rankings for a given dataset.

**Table 3.** Summary of the datasets

Datasets	type	#examples	#labels	#attributes	$U_\pi$
autorship	A	841	4	70	2%
bodyfat	B	252	7	7	94%
calhousing	B	20,640	4	4	0.1%
cpu-small	B	8,192	5	6	1%
elevators	B	16,599	9	9	1%
fried	B	40,769	5	9	0.3%
glass	A	214	6	9	14%
housing	B	506	6	6	22%
iris	A	150	3	4	3%
pendigits	A	10,992	10	16	19%
segment	A	2310	7	18	6%
stock	B	950	5	5	5%
vehicle	A	846	4	18	2%
vowel	A	528	11	10	56%
wine	A	178	3	13	3%
wisconsin	B	194	16	16	100%

The code for all the examples in this paper has been written in R ([16]).

The performance of the LR methods was estimated using a methodology that has been used previously for this purpose [11]. It is based on the ten-fold cross validation performance estimation method. The evaluation measure is Kendall's  $\tau$  and the performance of the methods was estimated using ten-fold cross-validation.

## 4 Results

RT uses a parameter,  $\gamma$ , that can affect the accuracy of the model. A  $\gamma \geq 1$  does not increase the purity of nodes. On the other hand, small  $\gamma$  values will rarely generate any nodes. We vary  $\gamma$  from 0.50 to 0.99 and measure the accuracy on several KEBI datasets.

To show in what extent  $\gamma$  affects the accuracy of RT we show in Figure 1 the results obtained for some of the datasets in Table 3. From Figure 1 it is clear

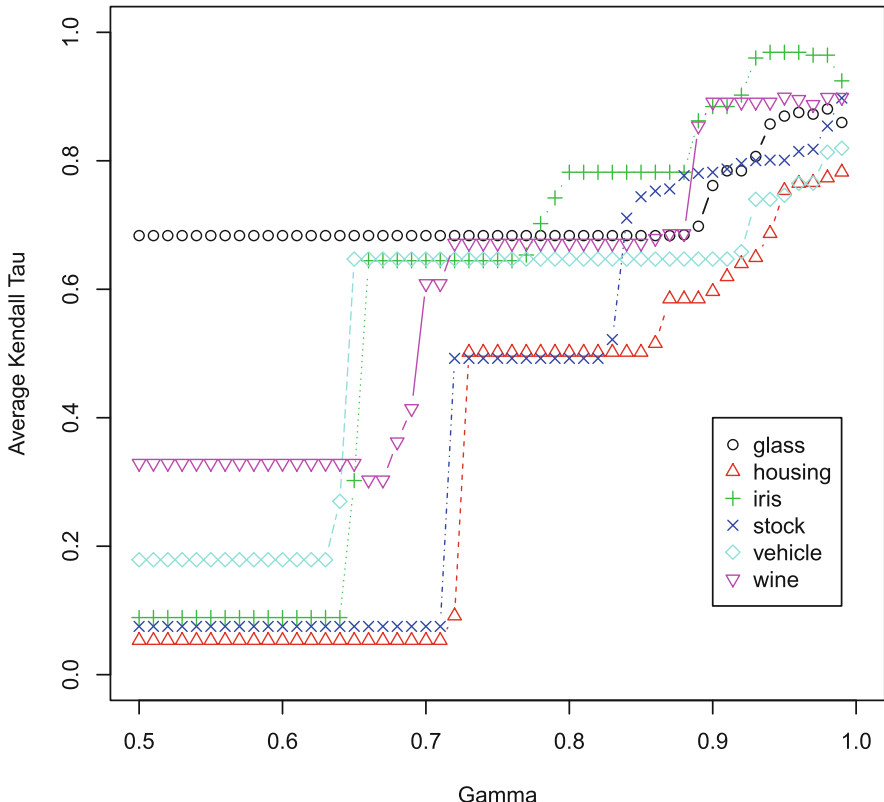


**Fig. 1.** Comparison of the accuracy obtained on some datasets by RT as  $\gamma$  varies from 0.5 to 0.99.

that  $\gamma$  plays an important role in the accuracy of RT. It seems that the best values lie between 0.95 and 0.98. We will use  $\gamma = 0.98$  for the Ranking Trees (RT).

Table 4 presents the results obtained by the two methods presented in comparison to the results for Label Ranking Trees (LRT) obtained in [6]. Even though LRT perform better in the cases presented, given the closer values to it, both RT and ERT give interesting results.

To compare different ranking methods we use a method proposed in [4] which is a combination of Friedmans test and Dunns Multiple Comparison Procedure [14]. First we run the Friedman's test to check whether the results are different or not, with the following hypotheses:

**Table 4.** Results obtained for Ranking Trees on KEBI datasets. (The mean accuracy is represented in terms of Kendall's tau,  $\tau$ )

	RT	ERT	LRT
authorship	.879	.890	.882
bodyfat	.104	.183	.117
calhousing	.181	.292	.324
cpu-small	.461	.437	.447
elevators	.710	.758	.760
fried	.796	.773	.890
glass	.881	.854	.883
housing	.773	.704	.797
iris	.964	.853	.947
pendigits	.055	.042	.935
segment	.895	.902	.949
stock	.854	.859	.895
vehicle	.813	.786	.827
vowel	.085	.054	.794
wine	.899	.907	.882
wisconsin	-.039	-.035	.343

**Table 5.** P-values obtained for the comparison of the 3 methods

	RT	ERT	LRT
RT		1.0000	0.2619
ERTt	1.0000		0.1529
LRT	0.2619	0.1529	

- $H_0$ . There is no difference in the mean average correlation coefficients for the 3 methods
- $H_1$ . There are some differences in the mean average correlation coefficients for the three methods

Using the *friedman.test* function from the *stats* package [16] we got a p-value < 1%, which shows strong evidence against  $H_0$ .

Now that we know that there are some differences between the 3 methods we will test which are different from one another with the Dunns Multiple Comparison Procedure [14]. Using the R package *dunn.test* [9] with a Bonferroni adjustment, as in [4], we tested the following hypotheses for each pair of methods  $a$  and  $b$ :

- $H_0$ . There is no difference in the mean average correlation coefficients between  $a$  and  $b$
- $H_1$ . There is some difference in the mean average correlation coefficients between  $a$  and  $b$

The p-values obtained are presented in Table 5. Table 5 indicates that there is no strong statistically evidence that the methods are different. One other conclusion

is that both RT and ERT are very equivalent approaches. While RT and ERT does not seem to outperform LRT in most of the cases studied, from the statitical tests we can say that both approaches are competitive.

## 5 Conclusions

In this work we implemented a decision tree method for Label Ranking, *Ranking Trees* (RT) and proposed an alternative approach *Entropy-based Ranking Trees* (ERT). We also present an empirical evaluation on several datasets of correlation-based methods, RT and ERT, and compare with the state of the art distribution-based *Label Ranking Trees* (LRT). The results indicate that both RT and ERT are reliable LR methods.

Our implementation of Ranking Trees (RT) shows that the method is a competitive approach in the LR field. We showed that the input parameter,  $\gamma$ , can have a great impact on the accuracy of the method. The tests performed on KEBI datasets indicate that the best results are obtained when  $0.95 < \gamma < 1$ .

The method proposed in this paper, ERT, which uses IG as a splitting criterion achieved very similar results to the RT presented in [17]. Statistical tests indicated that there is no strong evidence that the methods (RT, ERT and LRT) are significantly different. This means that both RT and ERT are valid approaches, and, since they are correlation-based methods, we can also say that this kind of approaches is also worth pursuing.

## References

1. Aiguzhinov, A., Soares, C., Serra, A.P.: A similarity-based adaptation of naive bayes for label ranking: application to the metalearning problem of algorithm recommendation. In: Pfahringer, B., Holmes, G., Hoffmann, A. (eds.) DS 2010. LNCS, vol. 6332, pp. 16–26. Springer, Heidelberg (2010)
2. Blockeel, H., Raedt, L.D., Ramon, J.: Top-down induction of clustering trees. CoRR cs.LG/0011032 (2000). <http://arxiv.org/abs/cs.LG/0011032>
3. Brazdil, P., Soares, C., Costa, J.: Ranking Learning Algorithms: Using IBL and Meta-Learning on Accuracy and Time Results. Machine Learning **50**(3), 251–277 (2003)
4. Brazdil, P., Soares, C., da Costa, J.P.: Ranking learning algorithms: Using IBL and meta-learning on accuracy and time results. Machine Learning **50**(3), 251–277 (2003). <http://dx.doi.org/10.1023/A:1021713901879>
5. Cheng, W., Dembczynski, K., Hüllermeier, E.: Label ranking methods based on the plackett-luce model. In: ICML, pp. 215–222 (2010)
6. Cheng, W., Huhn, J.C., Hüllermeier, E.: Decision tree and instance-based learning for label ranking. In: Proceedings of the 26th Annual International Conference on Machine Learning, ICML 2009, June 14–18, Montreal, Quebec, Canada, pp. 161–168 (2009)
7. Cheng, W., Hüllermeier, E.: Label ranking with abstention: Predicting partial orders by thresholding probability distributions (extended abstract). Computing Research Repository, CoRR abs/1112.0508 (2011). <http://arxiv.org/abs/1112.0508>

8. Cheng, W., Hüllermeier, E., Waegeman, W., Welker, V.: Label ranking with partial abstention based on thresholded probabilistic models. In: Advances in Neural Information Processing Systems 25: 26th Annual Conference on Neural Information Processing Systems 2012. Proceedings of a meeting held December 3–6, Lake Tahoe, Nevada, United States, pp. 2510–2518 (2012). [http://books.nips.cc/papers/files/nips25/NIPS2012\\_1200.pdf](http://books.nips.cc/papers/files/nips25/NIPS2012_1200.pdf)
9. Dinno, A.: dunn.test: Dunn's Test of Multiple Comparisons Using Rank Sums, r package version 1.2.3 (2015). <http://CRAN.R-project.org/package=dunn.test>
10. Fayyad, U.M., Irani, K.B.: Multi-interval discretization of continuous-valued attributes for classification learning. In: Proceedings of the 13th International Joint Conference on Artificial Intelligence, August 28–September 3, Chambéry, France, pp. 1022–1029 (1993)
11. Hüllermeier, E., Fürnkranz, J., Cheng, W., Brinker, K.: Label ranking by learning pairwise preferences. *Artificial Intelligence* **172**(16–17), 1897–1916 (2008)
12. Kendall, M., Gibbons, J.: Rank correlation methods. Griffin London (1970)
13. Mitchell, T.: Machine Learning. McGraw-Hill (1997)
14. Neave, H., Worthington, P.: Distribution-free Tests. Routledge (1992). <http://books.google.nl/books?id=1Y1QcgAACAAJ>
15. Quinlan, J.R.: Induction of decision trees. *Machine Learning* **1**(1), 81–106 (1986). <http://dx.doi.org/10.1023/A:1022643204877>
16. R Development Core Team: R: A Language and Environment for Statistical Computing. R Foundation for Statistical Computing, Vienna, Austria (2010). <http://www.R-project.org> ISBN 3-900051-07-0
17. Rebelo, C., Soares, C., Costa, J.: Empirical evaluation of ranking trees on some metalearning problems. In: Chomicki, J., Conitzer, V., Junker, U., Perny, P. (eds.) Proceedings 4th AAAI Multidisciplinary Workshop on Advances in Preference Handling (2008)
18. Ribeiro, G., Duivesteijn, W., Soares, C., Knobbe, A.: Multilayer perceptron for label ranking. In: Villa, A.E.P., Duch, W., Érdi, P., Masulli, F., Palm, G. (eds.) ICANN 2012, Part II. LNCS, vol. 7553, pp. 25–32. Springer, Heidelberg (2012)
19. de Sá, C.R., Soares, C., Jorge, A.M., Azevedo, P., Costa, J.: Mining association rules for label ranking. In: Huang, J.Z., Cao, L., Srivastava, J. (eds.) PAKDD 2011, Part II. LNCS, vol. 6635, pp. 432–443. Springer, Heidelberg (2011)
20. de Sá, C.R., Soares, C., Knobbe, A.: Entropy-based discretization methods for ranking data. *Information Sciences* in Press (2015) (in press)
21. de Sá, C.R., Soares, C., Knobbe, A., Azevedo, P., Jorge, A.M.: Multi-interval discretization of continuous attributes for label ranking. In: Fürnkranz, J., Hüllermeier, E., Higuchi, T. (eds.) DS 2013. LNCS, vol. 8140, pp. 155–169. Springer, Heidelberg (2013)
22. Spearman, C.: The proof and measurement of association between two things. *American Journal of Psychology* **15**, 72–101 (1904)
23. Todorovski, L., Blockeel, H., Džeroski, S.: Ranking with predictive clustering trees. In: Elomaa, T., Mannila, H., Toivonen, H. (eds.) ECML 2002. LNCS (LNAI), vol. 2430, pp. 444–455. Springer, Heidelberg (2002)
24. Vembu, S., Gärtner, T.: Label ranking algorithms: A survey. In: Fürnkranz, J., Hüllermeier, E. (eds.) Preference Learning, pp. 45–64. Springer, Heidelberg (2010)
25. Xia, F., Zhang, W., Li, F., Yang, Y.: Ranking with decision tree. *Knowl. Inf. Syst.* **17**(3), 381–395 (2008). <http://dx.doi.org/10.1007/s10115-007-0118-y>

# A Proactive Intelligent Decision Support System for Predicting the Popularity of Online News

Kelwin Fernandes<sup>1(✉)</sup>, Pedro Vinagre<sup>2</sup>, and Paulo Cortez<sup>2</sup>

<sup>1</sup> INESC TEC Porto/Universidade Do Porto, Porto, Portugal

<sup>2</sup> ALGORITMI Research Centre, Universidade Do Minho, Braga, Portugal

[kelwinfc@gmail.com](mailto:kelwinfc@gmail.com)

**Abstract.** Due to the Web expansion, the prediction of online news popularity is becoming a trendy research topic. In this paper, we propose a novel and proactive Intelligent Decision Support System (IDSS) that analyzes articles prior to their publication. Using a broad set of extracted features (e.g., keywords, digital media content, earlier popularity of news referenced in the article) the IDSS first predicts if an article will become popular. Then, it optimizes a subset of the articles features that can more easily be changed by authors, searching for an enhancement of the predicted popularity probability. Using a large and recently collected dataset, with 39,000 articles from the Mashable website, we performed a robust rolling windows evaluation of five state of the art models. The best result was provided by a Random Forest with a discrimination power of 73%. Moreover, several stochastic hill climbing local searches were explored. When optimizing 1000 articles, the best optimization method obtained a mean gain improvement of 15 percentage points in terms of the estimated popularity probability. These results attest the proposed IDSS as a valuable tool for online news authors.

**Keywords:** Popularity prediction · Online news · Text mining · Classification · Stochastic local search

## 1 Introduction

Decision Support Systems (DSS) were proposed in the mid-1960s and involve the use of Information Technology to support decision-making. Due to advances in this field (e.g., Data Mining, Metaheuristics), there has been a growing interest in the development of Intelligent DSS (IDSS), which adopt Artificial Intelligence techniques to decision support [1]. The concept of Adaptive Business Intelligence (ABI) is a particular IDSS that was proposed in 2006 [2]. ABI systems combine prediction and optimization, which are often treated separately by IDSS, in order to support decisions more efficiently. The goal is to first use data-driven models for predicting what is more likely to happen in the future, and then use modern optimization methods to search for the best possible solution given what can be currently known and predicted.

Within the expansion of the Internet and Web 2.0, there has also been a growing interest in online news, which allow an easy and fast spread of information around the globe. Thus, predicting the popularity of online news is becoming a recent research trend (e.g., [3,4,5,6,7]). Popularity is often measured by considering the number of interactions in the Web and social networks (e.g., number of shares, likes and comments). Predicting such popularity is valuable for authors, content providers, advertisers and even activists/politicians (e.g., to understand or influence public opinion) [4]. According to Tatar et al. [8], there are two main popularity prediction approaches: those that use features only known after publication and those that do not use such features. The first approach is more common (e.g., [3,5,9,6,7]). Since the prediction task is easier, higher prediction accuracies are often achieved. The latter approach is more scarce and, while a lower prediction performance might be expected, the predictions are more useful, allowing (as performed in this work) to improve content prior to publication.

Using the second approach, Petrovic et al. [10] predicted the number of retweets using features related with the tweet content (e.g., number of hashtags, mentions, URLs, length, words) and social features related to the author (e.g., number of followers, friends, is the user verified). A total of 21 million tweets were retrieved during October 2010. Using a binary task to discriminate retweeted from not retweeted posts, a top F-1 score of 47% was achieved when both tweet content and social features were used. Similarly, Bandari et al. [4] focused on four types of features (news source, category of the article, subjectivity language used and names mentioned in the article) to predict the number of tweets that mention an article. The dataset was retrieved from Feedzilla and related with one week of data. Four classification methods were tested to predict three popularity classes (1 to 20 tweets, 20 to 100 tweets, more than 100; articles with no tweets were discarded) and results ranged from 77% to 84% accuracy, for Naïve Bayes and Bagging, respectively. Finally, Hensinger et al. [11] tested two prediction binary classification tasks: popular/unpopular and appealing/non appealing, when compared with other articles published in the same day. The data was related with ten English news outlets related with one year. Using text features (e.g., bag of words of the title and description, keywords) and other characteristics (e.g., date of publishing), combined with a Support Vector Machine (SVM), the authors obtained better results for the appealing task when compared with popular/unpopular task, achieving results ranging from 62% to 86% of accuracy for the former, and 51% to 62% for the latter.

In this paper, we propose a novel proactive IDSS that analyzes online news *prior* to their publication. Assuming an ABI approach, the popularity of a candidate article is first estimated using a prediction module and then an optimization module suggests changes in the article content and structure, in order to maximize its expected popularity. Within our knowledge, there are no previous works that have addressed such proactive ABI approach, combining prediction and optimization for improving the news content. The prediction module uses a large list of inputs that includes purely new features (when compared with the literature [4,11,10]): digital media content (e.g., images, video); earlier popular-

ity of news referenced in the article; average number of shares of keywords prior to publication; and natural language features (e.g., title polarity, Latent Dirichlet Allocation topics). We adopt the common binary (popular/unpopular) task and test five state of the art methods (e.g., Random Forest, Adaptive Boosting, SVM), under a realistic rolling windows. Moreover, we use the trendy Mashable ([mashable.com/](http://mashable.com/)) news content, which was not previously studied when predicting popularity, and collect a recent and large dataset related with the last two years (a much larger time period when compared with the literature). Furthermore, we also optimize news content using a local search method (stochastic hill climbing) that searches for enhancements in a partial set of features that can be more easily changed by the user.

## 2 Materials and Methods

### 2.1 Data Acquisition and Preparation

We retrieved the content of all the articles published in the last two years from Mashable, which is one of the largest news websites. All data collection and processing procedures described in this work (including the prediction and optimization modules) were implemented in Python by the authors. The data was collected during a two year period, from January 7 2013 to January 7 2015. We discarded a small portion of special occasion articles that did not follow the general HTML structure, since processing each occasion type would require a specific parser. We also discarded very recent articles (less than 3 weeks), since the number of Mashable shares did not reach convergence for some of these articles (e.g., with less than 4 days) and we also wanted to keep a constant number of articles per test set in our rolling windows assessment strategy (see Section 2.3). After such preprocessing, we ended with a total of 39,000 articles, as shown in Table 1. The collected data was donated to the UCI Machine Learning repository (<http://archive.ics.uci.edu/ml/>).

**Table 1.** Statistical measures of the Mashable dataset.

Articles per day					
Number of articles	Total days	Average	Standard Deviation	Min	Max
39,000	709	55.00	22.65	12	105

We extracted an extensive set (total of 47) features from the HTML code in order to turn this data suitable for learning models, as shown in Table 2. In the table, the attribute types were classified into: number – integer value; ratio – within  $[0, 1]$ ; bool –  $\in \{0, 1\}$ ; and nominal. Column **Type** shows within brackets (#) the number of variables related with the attribute. Similarly to what is executed in [6,7], we performed a logarithmic transformation to scale the unbounded numeric features (e.g., number of words in article), while the nominal attributes were transformed with the common *1-of-C* encoding.

We selected a large list of characteristics that describe different aspects of the article and that were considered possibly relevant to influence the number of shares. Some of the features are dependent of particularities of the Mashable service: articles often reference other articles published in the same service; and articles have meta-data, such as keywords, data channel type and total number of shares (when considering Facebook, Twitter, Google+, LinkedIn, StumbleUpon and Pinterest). Thus, we extracted the minimum, average and maximum number of shares (known before publication) of all Mashable links cited in the article. Similarly, we rank all article keyword average shares (known before publication), in order to get the worst, average and best keywords. For each of these keywords, we extract the minimum, average and maximum number of shares. The data channel categories are: “lifestyle”, “bus”, “entertainment”, “socmed”, “tech”, “viral” and “world”.

We also extracted several natural language processing features. The Latent Dirichlet Allocation (LDA) [12] algorithm was applied to all Mashable texts (known before publication) in order to first identify the five top relevant topics and then measure the closeness of current article to such topics. To compute the subjectivity and polarity sentiment analysis, we adopted the Pattern web mining module (<http://www.clips.ua.ac.be/pattern>) [13], allowing the computation of sentiment polarity and subjectivity scores.

**Table 2.** List of attributes by category.

Feature	Type (#)	Feature	Type (#)
<b>Words</b>		<b>Keywords</b>	
Number of words in the title	number (1)	Number of keywords	number (1)
Number of words in the article	number (1)	Worst keyword (min./avg./max. shares)	number (3)
Average word length	number (1)	Average keyword (min./avg./max. shares)	number (3)
Rate of non-stop words	ratio (1)	Best keyword (min./avg./max. shares)	number (3)
Rate of unique words	ratio (1)	Article category (Mashable data channel)	nominal (1)
Rate of unique non-stop words	ratio (1)	<b>Natural Language Processing</b>	
<b>Links</b>		Closeness to top 5 LDA topics	ratio (5)
Number of links	number (1)	Title subjectivity	ratio (1)
Number of Mashable article links	number (1)	Article text subjectivity score and its absolute difference to 0.5	ratio (2)
Minimum, average and maximum number of shares of Mashable links	number (3)	Title sentiment polarity	ratio (1)
<b>Digital Media</b>		Rate of positive and negative words	ratio (2)
Number of images	number (1)	Pos. words rate among non-neutral words	ratio (1)
Number of videos	number (1)	Neg. words rate among non-neutral words	ratio (1)
<b>Time</b>		Polarity of positive words (min./avg./max.)	ratio (3)
Day of the week	nominal (1)	Polarity of negative words (min./avg./max.)	ratio (3)
Published on a weekend?	bool (1)	Article text polarity score and its absolute difference to 0.5	ratio (2)
<b>Target</b>			
Number of article Mashable shares		number (1)	

## 2.2 Intelligent Decision Support System

Following the ABI concept, the proposed IDSS contains three main modules (Figure 1): data extraction and processing, prediction and optimization. The first module executes the steps described in Section 2.1 and it is responsible

for collecting the online articles and computing their respective features. The prediction module first receives the processed data and splits it into training, validation and test sets (data separation). Then, it tunes and fits the classification models (model training and selection). Next, the best classification model is stored and used to provide article success predictions (popularity estimation). Finally, the optimization module searches for better combinations of a subset of the current article content characteristics. During this search, there is an heavy use of the classification model (the oracle). Also, some of the new searched feature combinations may require a recomputing of the respective features (e.g., average keyword minimum number of shares). In the figure, such dependency is represented by the arrow between the feature extraction and optimization. Once the optimization is finished, a list of article change suggestions is provided to the user, allowing her/him to make a decision.

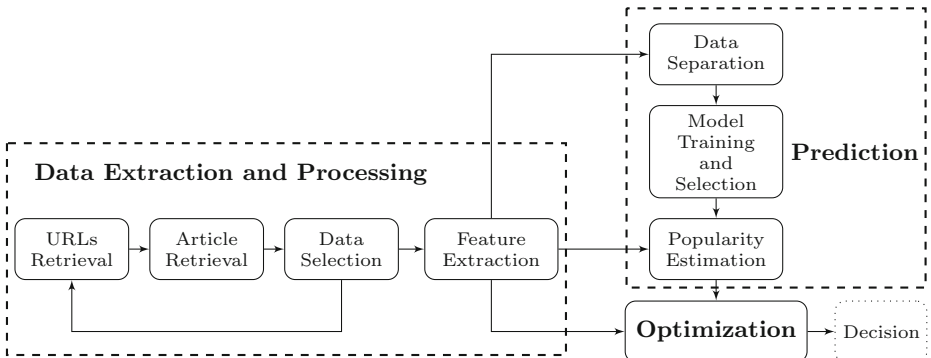


**Fig. 1.** Flow diagram describing the IDSS behavior.

### 2.3 Prediction Module

We adopted the Scikit learn [14] library for fitting the prediction models. Similarly to what is executed in [10,4,11], we assume a binary classification task, where an article is considered “popular” if the number of shares is higher than a fixed decision threshold ( $D_1$ ), else it is considered “unpopular”.

In this paper, we tested five classification models: Random Forest (RF); Adaptive Boosting (AdaBoost); SVM with a Radial Basis Function (RBF) kernel; K-Nearest Neighbors (KNN) and Naïve Bayes (NB). A grid search was used to search for the best hyperparameters of: RF and AdaBoost (number of trees); SVM ( $C$  trade-off parameter); and KNN (number of neighbors). During this grid search, the training data was internally split into training (70%) and validation sets (30%) by using a random holdout split. Once the best hyperparameter is selected, then the model is fit to all training data.

The receiver operating characteristic (ROC) curve shows the performance of a two class classifier across the range of possible threshold ( $D_2 \in [0, 1]$ ) values, plotting one minus the specificity ( $x$ -axis) versus the sensitivity ( $y$ -axis) [15]. In this work, the classification methods assume a probabilistic modeling, where a class is considered positive if its predicted probability is  $p > D_2$ . We computed several classification metrics: Accuracy, Precision, Recall, F1 score (all using a fixed  $D_2 = 0.5$ ); and the Area Under the ROC (AUC, which considers all  $D_2$  values). The AUC metric is the most relevant metric, since it measures the classifier's discrimination power and it is independent of the selected  $D_2$  value [15]. The ideal method should present an AUC of 1.0, while an AUC of 0.5 denotes a random classifier. For achieving a robust evaluation, we adopt a rolling windows analysis [16]. Under this evaluation, a training window of  $W$  consecutive samples is used to fit the model and then  $L$  predictions are performed. Next, the training window is updated by replacing the  $L$  oldest samples with  $L$  more recent ones, in order to fit a new model and perform a new set of  $L$  predictions, and so on.

## 2.4 Optimization

Local search optimizes a goal by searching within the neighborhood of an initial solution. This type of search suits our IDSS optimization module, since it receives an article (the initial solution) and then tries to increase its predicted popularity probability by searching for possible article changes (within the neighborhood of the initial solution). An example of a simple local search method is the hill climbing, which iteratively searches within the neighborhood of the current solution and updates such solution when a better one is found, until a local optimum is reached or the method is stopped. In this paper, we used a stochastic hill climbing [2], which works as the pure hill climbing except that worst solutions can be selected with a probability of  $P$ . We tested several values of  $P$ , ranging from  $P = 0$  (hill climbing) to  $P = 1$  (Monte-Carlo random search).

For evaluating the quality of the solutions, the local search maximizes the probability for the “popular” class, as provided by the best classification model. Moreover, the search is only performed over a subset of features that are more suitable to be changed by the author (adaptation of content or change in day of publication), as detailed in Table 3. In each iteration, the neighborhood search space assumes small perturbations (increase or decrease) in the feature original values. For instance, if the current number of words in the title is  $n = 5$ , then a search is executed for a shorter ( $n' = 4$ ) or longer ( $n' = 6$ ) title. Since the day of the week was represented as a nominal variable, a random selection for a different day is assumed in the perturbation. Similarly, given that the set of keywords ( $K$ ) is not numeric, a different perturbation strategy is proposed. For a particular article, we compute a list of suggested keywords  $K'$  that includes words that appear more than once in the text and that were used as keywords in previous articles. To keep the problem computationally tractable, we only considered the best five keywords in terms of their previous average shares. Then, we generate perturbations by adding one of the suggested keywords or by removing one

of the original keywords. The average performance when optimizing  $N$  articles (i.e.,  $N$  local searches), is evaluated using the Mean Gain (MG) and Conversion Rate (CR):

$$MG = \frac{1}{N} \sum_{i=1}^N (Q'_i - Q_i) \quad (1)$$

$$CR = \overline{U'}/U$$

where  $Q_i$  denotes the quality (estimated popularity probability) for the original article ( $i$ ),  $Q'_i$  is the quality obtained using the local search,  $U$  is the number of unpopular articles (estimated probability  $\leq D_2$ , for all  $N$  original articles) and  $\overline{U'}$  is the number of converted articles (original estimated probability was  $\leq D_2$  but after optimization changed to  $> D_2$ ).

**Table 3.** Optimizable Features.

Feature	Perturbations
Number of words in the title ( $n$ )	$n' \in \{n - 1, n + 1\}, n \geq 0 \wedge n' \neq n$
Number of words in the content ( $n$ )	$n' \in \{n - 1, n + 1\}, n \geq 0 \wedge n' \neq n$
Number of images ( $n$ )	$n' \in \{n - 1, n + 1\}, n \geq 0 \wedge n' \neq n$
Number of videos ( $n$ )	$n' \in \{n - 1, n + 1\}, n \geq 0 \wedge n' \neq n$
Day of week ( $w$ )	$w' \in [0..7], w' \neq w$
Keywords ( $K$ )	$k' \in \{K \cup i\} \cup \{K - j\}, i \in K' \wedge j \in K$

### 3 Experiments and Results

#### 3.1 Prediction

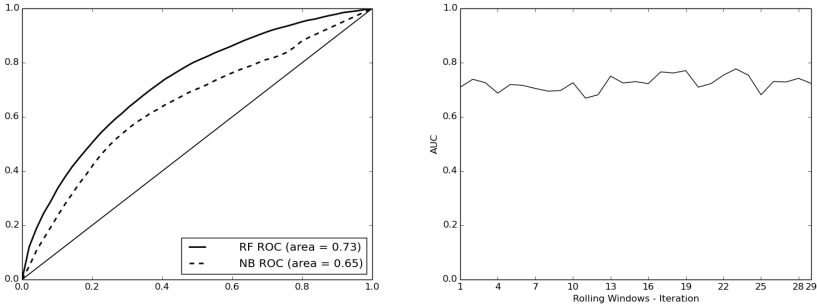
For the prediction experiments, we adopted the rolling windows scheme with a training window size of  $W = 10,000$  and performing  $L = 1,000$  predictions at each iteration. Under this setup, each classification model is trained 29 times (iterations), producing 29 prediction sets (each of size  $L$ ). For defining a popular class, we used a fixed value of  $D_1 = 1,400$  shares, which resulted in a balanced “popular”/“unpopular” class distribution in the first training set (first 10,000 articles). The selected grid search ranges for the hyperparameters were: RF and AdaBoost – number of trees  $\in \{10, 20, 50, 100, 200, 400\}$ ; SVM –  $C \in \{2^0, 2^1, \dots, 2^6\}$ ; and KNN – number of neighbors  $\in \{1, 3, 5, 10, 20\}$ .

Table 4 shows the obtained classification metrics, as computed over the union of all 29 test sets. In the table, the models were ranked according to their performance in terms of the AUC metric. The left of Figure 2 plots the ROC curves of the best (RF), worst (NB) and baseline (diagonal line, corresponds to random predictions) models. The plot confirms the RF superiority over the NB model for all  $D_2$  thresholds, including more sensitive ( $x$ -axis values near zero,  $D_2 >> 0.5$ ) or specific ( $x$ -axis near one,  $D_2 << 0.5$ ) trade-offs. For the best model (RF), the right panel of Figure 2 shows the evolution of the AUC metric

over the rolling windows iterations, revealing an interesting steady predictive performance over time. The best obtained result ( $AUC=0.73$ ) is 23 percentage points higher than the random classifier. While not perfect, an interesting discrimination level, higher than 70%, was achieved.

**Table 4.** Comparison of models for the rolling window evaluation (best values in **bold**).

Model	Accuracy	Precision	Recall	F1	AUC
Random Forest (RF)	<b>0.67</b>	0.67	<b>0.71</b>	<b>0.69</b>	<b>0.73</b>
Adaptive Boosting (AdaBoost)	0.66	0.68	0.67	0.67	0.72
Support Vector Machine (SVM)	0.66	0.67	0.68	0.68	0.71
K-Nearest Neighbors (KNN)	0.62	0.66	0.55	0.60	0.67
Naïve Bayes (NB)	0.62	<b>0.68</b>	0.49	0.57	0.65



**Fig. 2.** ROC curves (left) and AUC metric distribution over time for RF (right).

Table 5 shows the relative importance (column **Rank** shows ratio values, # denotes the ranking of the feature), as measured by the RF algorithm when trained with all data (39,000 articles). Due to space limitations, the table shows the best 15 features and also the features that are used by the optimization module. The keyword related features have a stronger importance, followed by LDA based features and shares of Mashable links. In particular, the features that are optimized in the next section (**with keywords** subset) have a strong importance (33%) in the RF model.

### 3.2 Optimization

For the optimization experiments, we used the best classification model (RF), as trained during the last iteration of the rolling windows scheme. Then, we selected all articles from the last test set ( $N = 1,000$ ) to evaluate the local search methods. We tested six stochastic hill climbing probabilities ( $P \in \{0.0, 0.2, 0.4, 0.6, 0.8, 1.0\}$ ). We also tested two feature optimization subsets

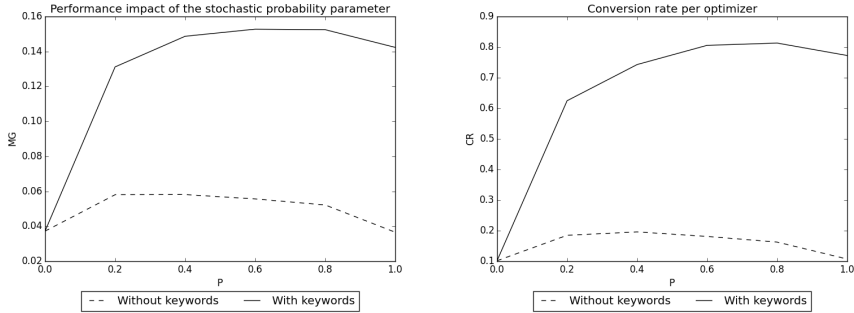
**Table 5.** Ranking of features according to their importance in the RF model.

Feature	Rank (#)	Feature	Rank (#)
Avg. keyword (avg. shares)	0.0456 (1)	Closeness to top 1 LDA topic	0.0287 (11)
Avg. keyword (max. shares)	0.0389 (2)	Rate of unique non-stop words	0.0274 (12)
Closeness to top 3 LDA topic	0.0323 (3)	Article text subjectivity	0.0271 (13)
Article category (Mashable data channel)	0.0304 (4)	Rate of unique tokens words	0.0271 (14)
Min. shares of Mashable links	0.0297 (5)	Average token length	0.0271 (15)
Best keyword (avg. shares)	0.0294 (6)	Number of words	0.0263 (16)
Avg. shares of Mashable links	0.0294 (7)	Day of the week	0.0260 (18)
Closeness to top 2 LDA topic	0.0293 (8)	Number of words in the title	0.0161 (31)
Worst keyword (avg. shares)	0.0292 (9)	Number of images	0.0142 (34)
Closeness to top 5 LDA topic	0.0288 (10)	Number of videos	0.0082 (44)

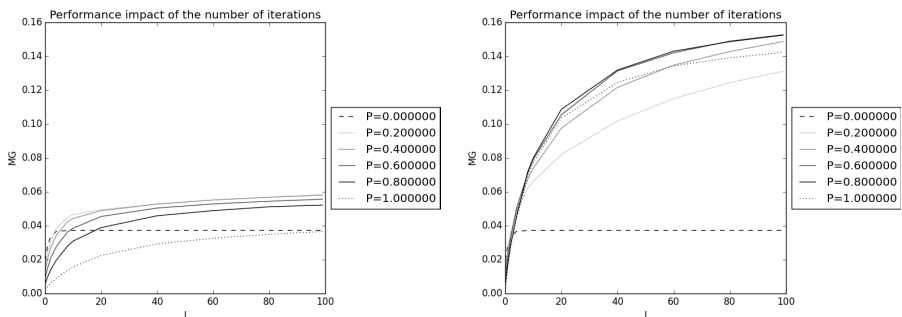
related with Table 3: using all features except the keywords (*without keywords*) and using all features (*with keywords*). Each local search is stopped after 100 iterations. During the search, we store the best results associated with the iterations  $I \in \{0, 1, 2, 4, 8, 10, 20, 40, 60, 80, 100\}$ .

Figure 3 shows the final optimization performance (after 100 iterations) for variations of the stochastic probability parameter  $P$  and when considering the two feature perturbation subsets. The convergence of the local search (for different values of  $P$ ) is also shown in Figure 3. The extreme values of  $P$  (0 – pure hill climbing; 1 – random search) produce lower performances when compared with their neighbor values. In particular, Figure 4 shows that the pure hill climbing is too greedy, performing a fast initial convergence that quickly gets flat. When using the *without keywords* subset, the best value of  $P$  is 0.2 for MG and 0.4 for CR metric. For the *with keywords* subset, the best value of  $P$  is 0.8 for both optimization metrics. Furthermore, the inclusion of keywords-related suggestions produces a substantial impact in the optimization, increasing the performance in both metrics. For instance, the MG metric increases from 0.05 to 0.16 in the best case ( $P = 0.8$ ). Moreover, Figure 3 shows that the *without keywords* subset optimization is an easier task when compared with the *with keywords* search. As argued by Zhang and Dimitroff [17], metadata can play an important role on webpage visibility and this might explain the importance of the keywords in terms of its influence when predicting (Table 5) and when optimizing popularity (Figure 3).

For demonstration purposes, Figure 5 shows an example of the interface of the implemented IDSS prototype. A more recent article (from January 16 2015) was selected for this demonstration. The IDSS, in this case using the *without keywords* subset, estimated an increase in the popularity probability of 13 percentage points if several changes are executed, such as decreasing the number of title words from 11 to 10. In another example (not shown in the figure), using the *with keywords* subset, the IDSS advised a change from the keywords  $K \in \{\text{"television"}, \text{"showtime"}, \text{"uncategorized"}, \text{"entertainment"}, \text{"film"}, \text{"homeland"}, \text{"recaps"}\}$  to the set  $K' \in \{\text{"film"}, \text{"relationship"}, \text{"family"}, \text{"night"}\}$  for an article about the end of the “Homeland” TV show.



**Fig. 3.** Stochastic probability ( $P$ ) impact on the Mean Gain (left) and in the Conversion Rate (right).



**Fig. 4.** Convergence of the local search under the *without keywords* (left) and *with keywords* (right) feature subsets ( $y$ -axis denotes the Mean Gain and  $x$ -axis the number of iterations).

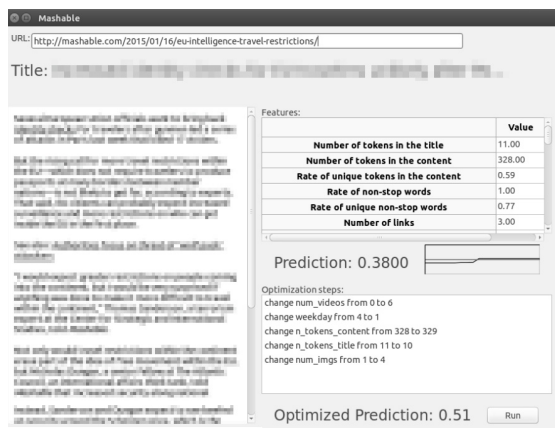


**Fig. 5.** Example of the interface of the IDSS prototype.

## 4 Conclusions

With the expansion of the Web, there is a growing interest in predicting online news popularity. In this work, we propose an Intelligent Decision Support System (IDSS) that first extracts a broad set of features that are known prior to an article publication, in order to predict its future popularity, under a binary classification task. Then, it optimizes a subset of the article features (that are more suitable to be changed by the author), in order to enhance its expected popularity.

Using large and recent dataset, with 39,000 articles collected during a 2 year period from the popular Mashable news service, we performed a rolling windows evaluation, testing five state of the art classification models under distinct metrics. Overall, the best result was achieved by a Random Forest (RF), with an overall area under the Receiver Operating Characteristic (ROC) curve of 73%, which corresponds to an acceptable discrimination. We also analyzed the importance of the RF inputs, revealing the keyword based features as one of the most important, followed by Natural Language Processing features and previous shares of Mashable links. Using the best prediction model as an oracle, we explored several stochastic hill climbing search variants aiming at the increase in the estimated article probability when changing two subsets of the article features (e.g., number of words in title). When optimizing 1,000 articles (from the last rolling windows test set), we achieved 15 percentage points in terms of the mean gain for the best local search setup. Considering the obtained results, we believe that the proposed IDSS is quite valuable for Mashable authors.

In future work, we intend to explore more advanced features related to content, such as trends analysis. Also, we plan to perform tracking of articles over time, allowing the usage of more sophisticated forecasting approaches.

**Acknowledgements.** This work has been supported by FCT - Fundação para a Ciência e Tecnologia within the Project Scope UID/CEC/00319/2013. The authors would like to thank Pedro Sernadela for his contributions in previous work.

## References

1. Arnott, D., Pervan, G.: Eight key issues for the decision support systems discipline. *Decision Support Systems* **44**(3), 657–672 (2008)
2. Michalewicz, Z., Schmidt, M., Michalewicz, M., Chiriac, C.: Adaptive business intelligence. Springer (2006)
3. Ahmed, M., Spagna, S., Huici, F., Niccolini, S.: A peek into the future: predicting the evolution of popularity in user generated content. In: Proceedings of the sixth ACM international conference on Web search and data mining, pp. 607–616. ACM (2013)
4. Bandari, R., Asur, S., Huberman, B.A.: The pulse of news in social media: forecasting popularity. In: ICWSM (2012)
5. Kaltenbrunner, A., Gomez, V., Lopez, V.: Description and prediction of slashdot activity. In: Web Conference, LA-WEB 2007, pp. 57–66. IEEE, Latin American (2007)

6. Szabo, G., Huberman, B.A.: Predicting the popularity of online content. *Communications of the ACM* **53**(8), 80–88 (2010)
7. Tatar, A., Antoniadis, P., De Amorim, M.D., Fdida, S.: From popularity prediction to ranking online news. *Social Network Analysis and Mining* **4**(1), 1–12 (2014)
8. Tatar, A., de Amorim, M.D., Fdida, S., Antoniadis, P.: A survey on predicting the popularity of web content. *Journal of Internet Services and Applications* **5**(1), 1–20 (2014)
9. Lee, J.G., Moon, S., Salamatian, K.: Modeling and predicting the popularity of online contents with cox proportional hazard regression model. *Neurocomputing* **76**(1), 134–145 (2012)
10. Petrovic, S., Osborne, M., Lavrenko, V.: RT to win! predicting message propagation in twitter. In: Fifth International AAAI Conference on Weblogs and Social Media (ICWSM), pp. 586–589 (2011)
11. Hensinger, E., Flaounas, I., Cristianini, N.: Modelling and predicting news popularity. *Pattern Analysis and Applications* **16**(4), 623–635 (2013)
12. Blei, D.M., Ng, A.Y., Jordan, M.I.: Latent dirichlet allocation. *Journal of Machine Learning Research* **3**, 993–1022 (2003)
13. De Smedt, T., Nijs, L., Daelemans, W.: Creative web services with pattern. In: Proceedings of the Fifth International Conference on Computational Creativity (2014)
14. Pedregosa, F., Varoquaux, G., Gramfort, A., Michel, V., Thirion, B., Grisel, O., Blondel, M., Prettenhofer, P., Weiss, R., Dubourg, V., Vanderplas, J., Passos, A., Cournapeau, D., Brucher, M., Perrot, M., Duchesnay, E.: Scikit-learn: Machine learning in Python. *Journal of Machine Learning Research* **12**, 2825–2830 (2011)
15. Fawcett, T.: An introduction to roc analysis. *Pattern Recognition Letters* **27**(8), 861–874 (2006)
16. Tashman, L.J.: Out-of-sample tests of forecasting accuracy: an analysis and review. *International Journal of Forecasting* **16**(4), 437–450 (2000)
17. Zhang, J., Dimitroff, A.: The impact of metadata implementation on webpage visibility in search engine results (part ii). *Information Processing & Management* **41**(3), 691–715 (2005)

# Periodic Episode Discovery Over Event Streams

Julie Soulas<sup>1,2(✉)</sup> and Philippe Lenca<sup>1,2</sup>

<sup>1</sup> UMR 6285 Lab-STICC, Institut Mines-Telecom, Telecom Bretagne,  
Technopôle Brest Iroise CS 83818, 29238 Brest Cedex 3, France

{julie.soulas,philippe.lenca}@telecom-bretagne.eu

<sup>2</sup> Université Européenne de Bretagne, Rennes, France

**Abstract.** Periodic behaviors are an important component of the life of most living species. Daily, weekly, or even yearly patterns are observed in both human and animal behaviors. These behaviors are searched as frequent periodic episodes in event streams. We propose an efficient algorithm for the discovery of frequent and periodic episodes. Update procedures allow us to take into account that behaviors also change with time, or because of external factors. The interest of our approach is illustrated on two real datasets.

## 1 Introduction

The discovery of patterns based on the temporality in their occurrences is of great interest in a wide range of applications, such as social interactions analysis [9], biological sustainability studies [10], elderly people monitoring [15], mobility data analysis [2], etc. The rhythm of the patterns appearances is studied in order to determine whether the patterns occur regularly (the time gaps between the occurrences are bounded [1, 16]), periodically (some occurrences form repeating cycles of time intervals), or mostly in a specific time interval.

Periodicity highlights habits. For example, Li et al. [10] studied the travel behaviors of animals, building rules such as: “*From 6 pm to 6 am, it has 90% probability staying at location A*”. Soulard et al. [15] studied the living habits of elderly people, and discovered periodic episodes as such “*The user has 70% probability having breakfast around 9:22 ± 40 min*”. The discovery of such behaviors enhances understanding of the needs of the living beings, and the factors governing their behavior. It is also useful to detect anomalies in routines due to major events such as environmental change [10] or the onset of disorders [15].

The discovery of periodic behaviors and their evolution involves three sub-problems: (i) the detection of the periods (daily, weekly, etc), (ii) the discovery of periodic behaviors and (iii) the update of the periods and patterns when new data arrives. We here focus on sub-problems (ii) and (iii). Period determination has already been extensively studied [2, 10]. Moreover, the experts in the target applications domains usually have background knowledge on the interesting periods, or require particular periods to be investigated: e.g., the physicians monitoring elderly people express the need to study daily and weekly behaviors.

The main contributions of the paper are: a new frequent parallel episode mining algorithm on data streams; and a heuristic for the online estimation of the periodicity of the episodes. The rest of the paper is organized as follows: section 2 presents some prominent related work. Section 3 details the proposition for frequent periodic pattern mining and updating. Experiments (section 4) on two real datasets illustrate the interest of this approach. Finally, some conclusions are drawn, and ideas for future work are presented.

## 2 Related Work

Frequent episode mining has attracted a lot of attention since its introduction by Mannila et al. [12]. The algorithms (e.g. [11–13, 18]) differ from one another by their target episodes (sequential or parallel), their search strategies (breadth or depth first search), the considered occurrences (contiguous, minimal, overlapping, etc.), and the way they count support. However, most algorithms consider only static data. The formalism used in this paper (see section 3.1) is loosely inspired from the formalism used in [11] and [18].

With the rapidly increasing amount of data recording devices (network traffic monitoring, smart houses, sensor networks,...), stream data mining has gained major attention. This evolution led to paradigm shifts. For an extensive problem statement and review of the current trends, see [6]. In particular, item set [3, 17] and episode [11, 13, 14] mining in streams have been investigated. The application context of [14] is close to the behavior we are searching for: the focus is set on the extraction of human activities from home automation sensor streams. However, periodicity is not taken into account.

Due to their powerful descriptive and predictive capabilities, periodic patterns are studied in several domains. For instance, Kiran and Reddy [8] discover frequent and periodic patterns in transactional databases. Periodicity is also defined and used with event sequences, for example with the study of parallel episodes in home automation sensor data for the monitoring of elderly people [7, 15]. These three periodic pattern mining algorithms process only static data.

To the best of our knowledge, few studies have focused on mining both frequent and periodic episodes over data streams. One can however point out some rather close studies: Li et al. [10] and Baratchi et al. [2] both use geo-spatial data in order to detect areas of interest for an individual (respectively eagles and people) and periodic movement patterns. They both also determine the period of the discovered patterns. However, their periodicity descriptions are based on single events, not episodes.

## 3 Frequent Periodic Pattern Discovery and Update Over Data Streams

### 3.1 Problem Statement

Behavioral patterns are searched in the form of episodes (definition 2) in an event (definition 1) sequence, which is processed using the classical sliding window

framework (length of the window:  $T_W$ ). Indeed, recent behaviors are observable in recent events.

**Definition 1 (Event).** *An event is a  $(e, t)$  pair, where  $e$  is the event label, taking values in a finite alphabet  $\mathcal{A}$ ; and  $t$  is the timestamp.*

**Definition 2 (Episode, episode length).** *An episode  $E$  is a set of  $n$  event labels  $\{e_1, \dots, e_n\}$  taken from the alphabet  $\mathcal{A}$ . The length of episode  $E$  is  $n$ .*

**Definition 3 (Episode occurrence, occurrence duration).** *An episode  $E = \{e_1, \dots, e_n\}$  occurs if there are  $n$  events whose labels match the  $n$  items in  $E$ . Formally, there is an occurrence  $o$  of  $E$  at time  $t_1$  if there exists a permutation  $\sigma$  on  $(1, \dots, n)$  and  $n$  timestamps  $t_1 \leq \dots \leq t_n$ , such that  $o = \langle (e_{\sigma(1)}, t_1), \dots, (e_{\sigma(n)}, t_n) \rangle$  is a subsequence of the event stream. The duration of  $o$  is  $\delta t_o = t_n - t_1$ .*

The label order in the occurrence is not taken into account: it corresponds to the episodes referred to as *parallel* in the problem definition of episode mining [12]. The events making the occurrence may be interleaved with other events.

The events occurring in the vicinity of each other are more likely linked to a same behavior than distant events. A stricter constraint  $T_{ep}$  on the *maximal episode duration* can thus be set ( $T_W$  is used otherwise).  $T_{ep}$  exploits expert or statistical knowledge regarding the expected behavior durations. It also serves as a heuristic for the reduction of the search space (see section 3.2).

**Definition 4 (Minimal occurrence - MO).** *Let  $E = \{e_1, \dots, e_n\}$  be an episode, occurring on  $o = \langle (e_{\sigma(1)}, t_1), \dots, (e_{\sigma(n)}, t_n) \rangle$ .  $o$  is a minimal occurrence if there is no other, shorter occurrence that occurs within the time span of  $o$ . That is to say,  $\neg \exists o' = \langle (e_{\sigma'(1)}, t'_1), \dots, (e_{\sigma'(n)}, t'_n) \rangle$  such that  $t_1 \leq t'_1$ ,  $t'_n \leq t_n$  and  $t'_n - t'_1 < t_n - t_1$ .*

**Definition 5 (Time queue - TQ).** *The time queue of an episode  $E$  (noted  $TQE$ ) is the list containing the distinct pairs of beginning and end timestamps of its minimal occurrences.*

We consider here only the minimal occurrences. The *support* of an episode is the length of its time queue. An episode is *frequent* if its support is greater than a *minimal support* threshold  $S_{min}$ . Minimal occurrences have convenient properties for the mining of frequent episodes, namely:

- An episode  $E$  has at most one time queue entry that starts (respectively finishes) at a given timestamp  $t$  (**observation 1**);
- Let  $E$  be an episode, and  $E'$  a subepisode (subset) of  $E$ . For every entry in the TQ of  $E$ , there is at least one entry in the TQ of  $E'$  (**observation 2**);
- As a consequence, the support of  $E'$  is greater or equal to this of  $E$ : the support verifies the downward closure property (**observation 3**);
- A new event  $(e, t)$  can be part of an occurrence of episode  $E' = \{e\} \cup E$  (where  $e \notin E$ ) if the latest entry in the TQ of  $E$  started less than  $T_{ep}$  (or  $T_W$ ) ago (**observation 4a**). This occurrence is minimal if the beginning of the latest entry in  $TQE$  starts strictly after the latest entry in  $TQE'$  (**observation 4b**). This gives a particular importance to the recently observed episodes.

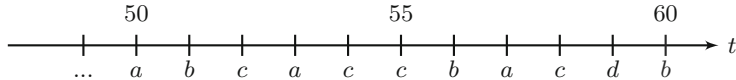


**Fig. 1.** Example: a segment of an event stream

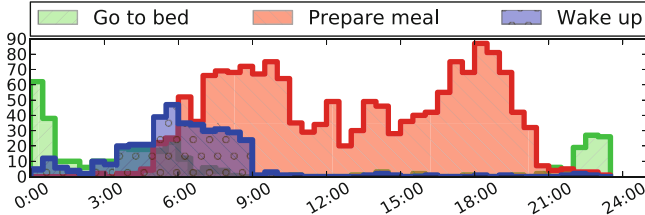


**Fig. 2.** Example of an histogram representing the observed occurrence times for some daily habits of an elderly person living in a smart home

**Example.** Figure 1 presents an example of a event stream segment. The current window contains 11 events  $(a, 50)$ ,  $(b, 51)$ , etc. The last seen event is  $(b, 60)$ , and the labels take values in the alphabet  $\mathcal{A} = \{a, b, c, d\}$ . With  $T_{ep} = 3$ , episode  $\{a, c\}$  occurs on  $\langle(a, 50), (c, 52)\rangle, \langle(c, 52), (a, 53)\rangle, \langle(a, 53), (c, 54)\rangle, \langle(a, 53), (c, 55)\rangle$  etc:  $\langle(a, 53), (c, 54)\rangle$  is minimal, but  $\langle(a, 53), (c, 55)\rangle$  is not. The time queue for episode  $\{a, b, c\}$  is  $[(50, 52), (51, 53), (53, 56), (55, 57), (56, 58), (57, 60)]$ , and its support is 6.  $(54, 57)$  is not in the TQ because it does not correspond to a MO. A one-to-one mapping between a time queue entry and a MO is not guaranteed: the time queue entry  $(53, 56)$  of episode  $\{a, b, c\}$ , corresponds to two MO:  $\langle(a, 53), (c, 54), (b, 56)\rangle$  and  $\langle(a, 53), (c, 55), (b, 56)\rangle$ .

**Periodicity.** Humans and animals tend to follow routines [10, 15]. A typical example of periodic behavior is the daily occurrences of some human activities of daily living. Figure 2 presents the occurrence times of three such activities, recorded in a smart home over a six-month period (CASAS dataset, presented in section 4.1). It highlights some of the characteristics these activities may have:

- The occurrence times vary from one day to the next, and this variability is user- and activity-dependent: here `go to bed` is less variable than `wake up`,
- Activities may have several components. Here, there seems to be two meals at home a day: a breakfast around 8:00 and a dinner around 18:00,
- Each component has its own preferential occurrence time (mean  $\mu$ ) and variability (standard deviation  $\sigma$ ),
- Some occurrences do not follow the periodic patterns.

This leads us to describe the periodicity of an episode as a distribution of its *relative* occurrence times within the period of interest (e.g 1 day, 1 week). This is done thanks to Gaussian Mixture Models (GMM), since they take into account the aforementioned characteristics.

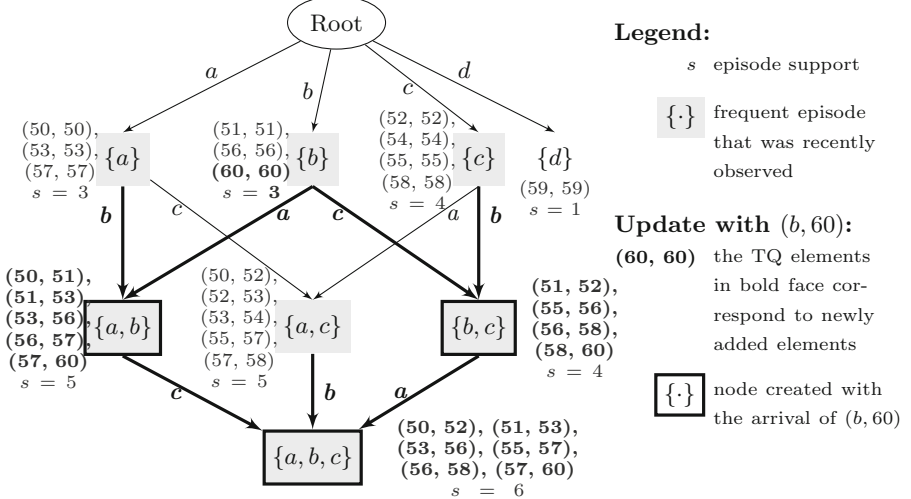


**Fig. 3.** Lattice corresponding to the example stream figure 1, when  $(b, 60)$  is the last seen event. The update when  $(b, 60)$  arrives is highlighted in boldface.

For a periodicity model  $\{\text{period } T, n \text{ components } (\mu_1, \sigma_1), \dots (\mu_n, \sigma_n)\}$ , an occurrence is expected to occur in every time interval  $k \cdot T + \mu_i(\pm \sigma_i)$ , such that  $1 \leq i \leq n$  and for every integer  $k \geq 0$  such that  $k \cdot T + \mu_i$  is in the current window. The quality of a periodicity description is evaluated on its *accuracy*, that is to say the proportion of the expected occurrences that were actually observed.

### 3.2 Frequent Episode Discovery and Updating

In order to be habits, episodes need to be frequent. However, the periodic episodes are not necessarily the most frequent ones, which is why the support threshold should remain rather low. We propose to handle the task of frequent episode mining over an event stream thanks to a frequent episode lattice (FEL).

**Episode Lattice.** The frequent episodes and their time queues are stored in a frequent episode lattice (FEL). The nodes in the FEL correspond either to length-1 episodes, or to frequent episodes. Length-1 episodes are kept even if they are not frequent (yet) in order to build longer episodes when they do. The parents of a node (located at depth  $d$ ) correspond to its sub-episodes of length  $d - 1$ , and its children to its super-episodes of length  $d + 1$ . The edges linking two episodes are indexed on the only event label that is present in the child episode but not in the parent. Each node retains the TQ of the corresponding episode and the GMM description that best fits the episode (see section 3.3). The episode lattice corresponding to the example in figure 1 is given in figure 3. In spite of its possibly big edge count, the lattice structure was chosen over the standard prefix tree because it allows faster episode retrieval and update.

**Algorithm 1.** Computation of  $E = E_1 \cup E_2$ 's TQ from the TQ of  $E_1$  and  $E_2$ 


---

**Input:**  $TQ_1$  (resp.  $TQ_2$  the time queue of  $E_1$  (resp.  $E_2$ ), indexed on  $i$  (resp.  $j$ )

- 1:  $i \leftarrow 0; j \leftarrow 0; TQ \leftarrow []$ ; support  $s \leftarrow 0$
- 2: **while**  $i < |TQ_1|$  and  $j < |TQ_2|$  **do**
- 3:   **if**  $TQ_1[i]$  finishes after  $TQ_2[j]$  **then**
- 4:     Increment  $j$  as long as  $TQ_2[j]$  ends before  $TQ_1[i]$
- 5:   **else**
- 6:     Increment  $i$  as long as  $TQ_1[i]$  ends before  $TQ_2[j]$
- 7:    $start \leftarrow \min(TQ_1[i][0], TQ_2[j][0])$
- 8:    $end \leftarrow \min(TQ_1[i][1], TQ_2[j][1])$
- 9:   **if**  $end - start < T_{ep}$  **then**
- 10:     Add  $(start, end)$  to  $TQ$ ;  $s \leftarrow s + 1$                    /\* New minimal occurrence \*/
- 11:     Increment the index of the TQ whose current element started earlier (both if  $TQ_1[i][0] == TQ_2[j][0]$ )
- 12: **return**  $TQ, s$

---

**Update with a New Event.** We keep track of the recently modified nodes (RMN, the nodes describing an episode that occurred recently, i.e. less than  $T_{ep}$ , or  $T_W$ , ago). Indeed (see observations 4a and 4b), the recent occurrences of these episodes can be extended with new, incoming events to form longer episodes. The RMN are stored in a collection of lists (nodes at depth 1, depth 2, etc). The TQ of a newly frequent length- $n$  episode is computed thanks to the time queues of a length- $(n-1)$  sub-episode and the length-1 episode containing the missing item, using algorithm 1.

When a new event  $(e, t)$  arrives, it can be a new occurrence (and also a MO) of the length-1 episode  $\{e\}$ . It can also form a new MO of an episode  $E' = E \cup \{e\}$ , where  $E$  is a recently observed episode. The lattice update follows these steps:

1. If label  $e$  is new: create a node for episode  $\{e\}$  and link it to the FEL root;
2. Update the time queue of episode  $\{e\}$ ;
3. If  $\{e\}$  is frequent:
  - (a) Add it to the RMN list;
  - (b) For each node  $N_E$  in the RMN list, try to build a new occurrence of  $E \cup \{e\}$ , following algorithm 2, which takes advantage of observations 1–4. If an episode  $E' = E \cup \{e\}$  becomes frequent, a new node  $N_{E'}$  is created, and is linked to its parents in the lattice. The parents are the nodes describing the episodes  $E' \setminus \{e'\}$  for each  $e' \in E$ , and are accessible via  $N_E.parent(e').child(e)$ , where  $N_E$  is the node for the known subset  $E$ . Since the RMN list is layered, and explored by increasing node depth,  $N_E.parent(e').child(e)$  is always created before  $N_{E'}$  tries to access it.

The update process of the FEL is illustrated with the arrival of a new event  $(b, 60)$  in figure 3.  $(b, 60)$  makes  $\{b\}$  a frequent episode. The nodes in the RMN list ( $\{a\}$ ,  $\{c\}$  and  $\{a, c\}$ ) are candidate for the extension with the (frequent) new event. This allows the investigation of episodes  $\{a, b\}$  (extension of  $\{a\}$ ),  $\{b, c\}$  (extension of  $\{c\}$ ), and  $\{a, b, c\}$  (extension of  $\{a, c\}$ ), which indeed become frequent.

**Algorithm 2.** RMN-based update when a new event  $(e, t)$  arrives

---

**Input:** new event  $(e, t)$ ; recently modified node  $N_E$ , characterizing episode  $E$ 

```

1: if  $e \in E$  then
2:   pass           /*  $E$  cannot be extended with label  $e$ :  $E$  already contains it */
3: else
4:   if  $E.lastMO$  starts before  $t - T_{ep}$  then
5:     Remove  $N_E$  from RMN list: the last MO of  $E$  is too old to be extended
6:   else
7:     if  $N_E$  has a child  $N_{E'}$  on label  $e$  then          /*  $E'$  is already frequent */
8:       if  $E.lastMO$  starts strictly after  $E'.lastMO$  then      /* New MO */
9:         Add new entry to  $N_{E'}.TQ$ ; Add  $N_{E'}.TQ$  to the RMN list
10:      else        /* There is already a MO for  $E'$  starting in  $E.lastMO.start$ :
11:        there cannot be another one */
12:        pass
13:      else          /*  $E'$  may become frequent */
14:         $TQ, S \leftarrow \text{ALGORITHM1}(TQE, TQE')$ 
15:        if  $S \geq S_{min}$  then
16:          Create node  $N_{E'}$  for  $E'$ . Link it to its parents.
17:          Add  $N_{E'}$  to the RMN list
17: return          /* The FEL is updated with the information from event  $(e, t)$  */

```

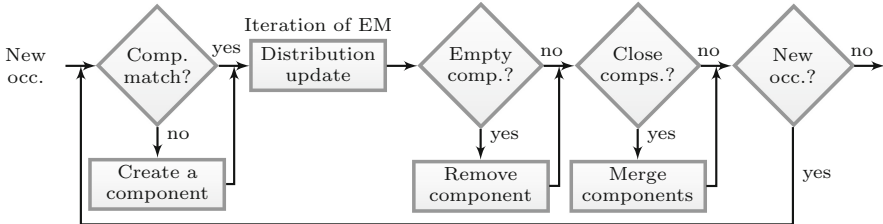
---

**Removal of Outdated Information.** Events older than  $T_W$  are outdated, and their influence in the FEL needs to be removed. The TQ construction makes it so that its entries are ordered by start timestamp: the entries that need to be removed are thus at the beginning of the nodes TQ. Moreover, according to observation 2, for every TQ entry (and thus every outdated entry) there is at least one (outdated) entry in the TQ of one of the parent nodes. The FEL can thus be traversed from the root using a breadth-first search algorithm, where nodes are investigated and updated only if at least one of their parents presents outdated occurrences. Episodes becoming rare are removed from the FEL.

### 3.3 Periodicity Discovery

The periodicity of an episode is described thanks to a GMM. Each node in the FEL is associated with a GMM describing the periodicity of the episode, which is updated when new MO are observed or occurrences removed. Usually, a GMM is trained with the Expectation-Maximization algorithm [5] (EM): for each component of the GMM (the number of components being a user-given parameter), and each data point  $x$ , the probability that  $x$  was generated by the component is computed. The components characteristics (mean, standard deviation) are then tweaked to maximize the likelihood of the data point/component attribution.

But streaming data may be non-stationary, the number of components may evolve, as well as their characteristics. It is not acceptable to ask the user for the number of components, especially since the suitable number depends on the considered episode. We here extend EM with heuristics for the addition, removal and merging of components.

**Algorithm 3.** Overview of the periodicity update (comp=GMM component)

Algorithm 3 presents the general workflow for the periodicity update. When a new MO is detected for the episode, the position of the timestamp in the period  $t_r = \text{timestamp} \bmod \text{period}$  is computed. If  $t_r$  does not match any of the existing components, i.e. for each component  $(\mu, \sigma)$ ,  $|t_r - \mu| > \sigma$ , a new component is added. When outdated data is removed, some components lose their importance. When too rare, they are removed from the GMM. Finally, when two components  $(\mu_1, \sigma_1), (\mu_2, \sigma_2)$  become close to one another, i.e if  $|\mu_1 - \mu_2| < a * (\sigma_1 + \sigma_2)$  (with  $a = 1.5$  in the experiments), the two components are merged. In the general case, GMM updates do not change much the model. Thus, when the number of components does not change, a single EM iteration is necessary to update the characteristics of the components.

The interest of this approach was evaluated on synthetic data, following known mixture of gaussian models evolving with time. The heuristics allow the detection of the main trends in the data: emergence of new components, disparition of old and rare components, shiftings in characteristics of the components.

## 4 Experimentation

A prototype was implemented in Python. It was also instrumented to record the episodes and lattice updates. The instrumentation slows down the experimentations: the execution times given in the next subsections are over-estimated.

### 4.1 Ambient Assisted Living Dataset

The CASAS project [4] uses home automation devices to improve ageing at home. Over the years, they collected and published several datasets. We present here our experimentations on the Aruba dataset<sup>1</sup>. The house of an elderly woman was equipped with motion detectors and temperature sensors. The obtained information was annotated with activities (11 labels, such as *Sleeping*, *Housekeeping*, etc.; 22 when dissociating the begin and end timestamp of each activity). These annotations are our events (12 953 events, from Nov. 2010 to Jun. 2011).

<sup>1</sup> <http://wsucasas.wordpress.com/datasets/>, number 17, consulted on Dec 4<sup>th</sup>, 2014.

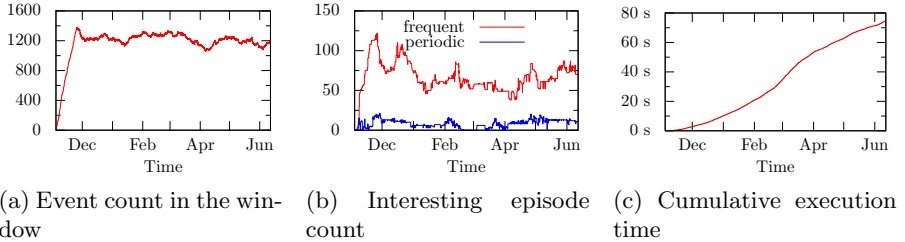


**Fig. 4.** Execution log for the CASAS Aruba annotation dataset

The dataset was processed using a period of one day, a window  $T_W$  of 3 weeks, a minimal support  $S_{min}$  of 15, a maximal episode duration  $T_{ep}$  of 30 minutes, and an accuracy threshold of 70%. The parameter setting was reinforced by a descriptive analysis of the data (e.g., it showed that most activities last less than 30 minutes). The results obtained throughout the course of the execution are given in figure 4. During the first 3 weeks, the sliding window fills with the incoming events, and the first frequent and periodic episodes appear. Then, the number of events in the window remains quite stable, but the behaviors keep evolving. The execution time (figure 4c) shows the scalability of the approach for this kind of application. The contents of the FEL in the last window is investigated, some of periodic episodes with the highest accuracy  $A$  are:

- $\{\text{Sleeping end}\}$ : 50 MO, 1 component,  $\mu = 6:00$ ,  $\sigma = 2$  hours,  $A = 100\%$
- $\{\text{Sleeping end, Meal_Preparation begin, Meal_Preparation end, Relax begin}\}$ : 26 MO, 1 component,  $\mu = 6:00$ ,  $\sigma = 1.45$  hours,  $A = 82\%$
- $\{\text{Enter_Home begin, Enter_Home end}\}$ : 61 MO, 1 component,  $\mu = 14:00$ ,  $\sigma = 3$  hours,  $A = 88\%$

These patterns can be interpreted as habits: the person woke up every morning around 6:00, and also had breakfast in 82% of the mornings. The third episode describes a movement pattern: the inhabitant usually goes out of home at some time (it is another episode), and comes back in the early afternoon.

Figure 5 presents the influence of the minimal support  $S_{min}$ , maximal episode duration  $T_{ep}$ , and window length  $T_W$  on the maximal size of the FEL and the execution time. In particular, it shows that the execution time is reasonable and scalable. The duration of the episodes also has a large impact on the size of the FEL.

## 4.2 Travian Game Dataset

Travian is a web-browser game, where players, organized into alliances, fight for the fulfilling of objectives and the control of territories. The game company releases each day a snapshot of the server status: it contains information on the players (villages, alliance membership). These daily updates were collected for the 2014 fr5 game round, from July 8<sup>th</sup> to November 23<sup>rd</sup>. We focus here on the

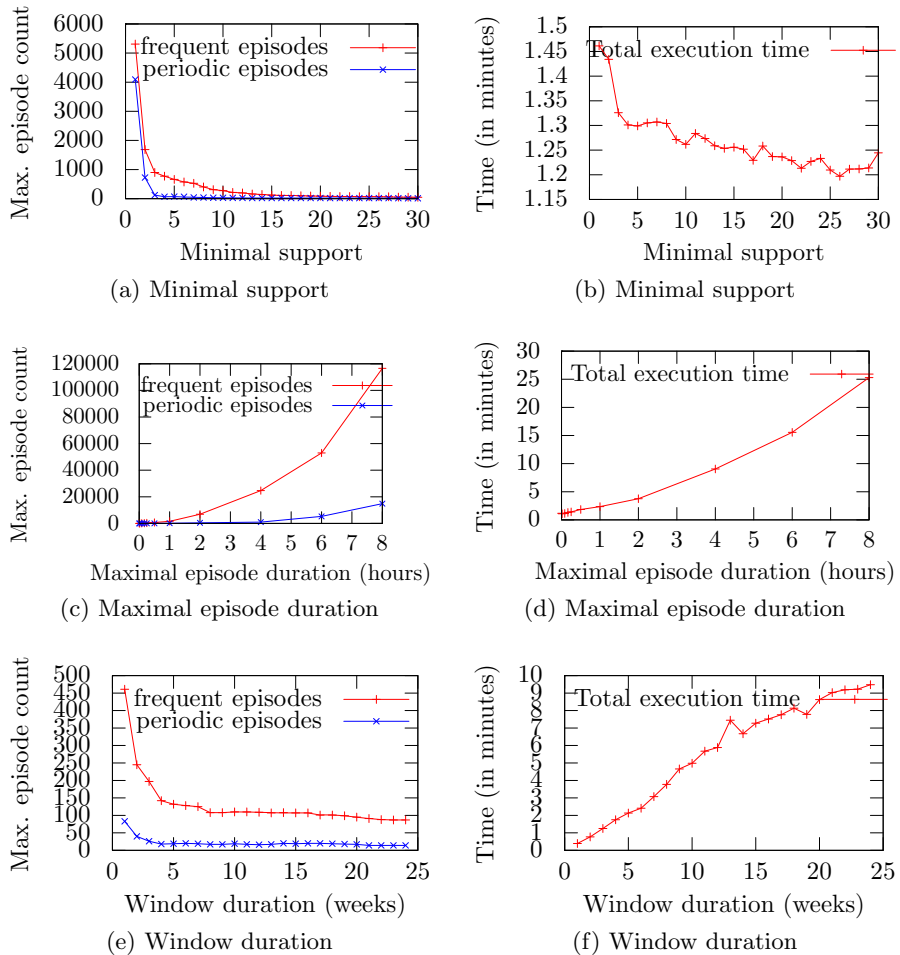


**Fig. 5.** Influence of the algorithm configuration on the frequent and periodic episode counts, and on the execution time for the CASAS Aruba dataset

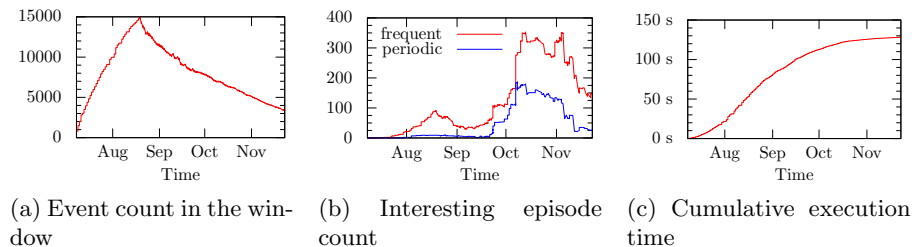


**Fig. 6.** Execution log for the Travian fr5 alliance membership dataset

players alliance shifts: the event labels look like “*Player P [joined|left] alliance A*”. 27674 such events are recorded, but most labels are rare (25985 labels).

The dataset was processed with a period of one week, a window  $T_W =$  six weeks, a minimal support  $S_{min} = 5$  and a maximal episode duration  $T_{ep} = 1$  day. Figure 6 presents the evolution of the window size, episode counts, and execution time during the mining. The results are fairly different from those of the home automation dataset, but were explained by a player (picturing a domain expert). During the first 6 weeks, the window fills rapidly with events: new players register onto the game, and the diplomacy begins. The players join or switch alliances. After the 6 weeks, the event count in the window decreases with time. Several explanations: (i) the opening of a new game round (on August 22<sup>nd</sup>) slowed down the number of new player registrations (players tend to join the most recent game round); (ii) most players have found an alliance they like: they stop changing alliances. Until October, little frequent and periodic patterns are detected, but their number increases rapidly after that. The periodic episodes discovered in the Sep, 18<sup>th</sup> – Oct, 30<sup>th</sup> (maximal count of periodic episodes) contain notably:

- $\{1SixCentDix8 \text{ left } Vtrans, 1SixCentDix8 \text{ joined } iChiefs\}$ : 8 MO, 2 components,  $\mu_1 = \text{Fri. 0:00}$ ,  $\mu_2 = \text{Mon. 0:00}$ ,  $\sigma_1 = \sigma_2 = 0$ ,  $A = 80\%$
- $\{1SixCentDix8 \text{ left } iChiefs, 1SixCentDix8 \text{ joined } Vtrans\}$ : 8 MO, 2 components,  $\mu_1 = \text{Sat. 0:00}$ ,  $\mu_2 = \text{Tue. 0:00}$ ,  $\sigma_1 = \sigma_2 = 0$ ,  $A = 80\%$
- $\{Jill \text{ left } Bakka, Jill \text{ joined } LI\}$ : 10 MO, 2 components,  $\mu_1 = \text{Mon. 18:00}$ ,  $\sigma_1 = 1$  day,  $\mu_2 = \text{Fri. 0:00}$ ,  $\sigma_2 = 0$ ,  $A = 75\%$

Some players periodically change of alliance: *1SixCentDix8* leaves *Vtrans* for *iChiefs* on Mondays and Fridays, and goes back to *Vtrans* one day later. *Jill* goes from *Bakka* to *LI* either on Mondays or Tuesdays, as well as on Fridays. This actually highlights a strategy allied alliances (*iChiefs* and *Vtrans* on one side, and *Bakka* and *LI* on the other side) have developed to share with one another the effects of artifacts owned by players *1SixCentDix8* and *Jill*, respectively.

## 5 Conclusion

Behavior pattern (episode) mining over event sequences is an important data mining problem, with many applications, in particular for ambient assisted living, or wildlife behavior monitoring. Several frequent episode mining algorithms have been proposed for both static data and data streams. But while periodicity can also be an interesting characteristic for the study of behaviors, very few algorithm have addressed frequent and periodic patterns. We propose an efficient algorithm to mine frequent periodic episodes in data streams. We briefly illustrate the interest of this algorithm with two case studies. As a perspective of this work, the experiments can be extensively increased, and applied to other application domains. It also be interesting to include a period-determination algorithm in order to automatically adapt the period to each pattern. Closed episodes and non-overlapping occurrences could also be investigated.

## References

1. Amphawan, K., Lenca, P., Surarerks, A.: Efficient mining top-k regular-frequent itemset using compressed tidsets. In: Cao, L., Huang, J.Z., Bailey, J., Koh, Y.S., Luo, J. (eds.) PAKDD Workshops 2011. LNCS, vol. 7104, pp. 124–135. Springer, Heidelberg (2012)
2. Baratchi, M., Meratnia, N., Havinga, P.J.M.: Recognition of periodic behavioral patterns from streaming mobility data. In: Stojmenovic, I., Cheng, Z., Guo, S. (eds.) MOBIQUITOUS 2013. LNCS, vol. 131, pp. 102–115. Springer, Heidelberg (2014)
3. Calders, T., Dexters, N., Goethals, B.: Mining frequent itemsets in a stream. In: ICDM, pp. 83–92 (2007)
4. Cook, D.J., Crandall, A.S., Thomas, B.L., Krishnan, N.C.: Casas: A smart home in a box. IEEE Computer **46**(7), 62–69 (2013)
5. Dempster, A., Laird, N., Rubin, D.: Maximum likelihood from incomplete data via the EM algorithm. Journal of the Royal Statistical Society. Series B (Methodological), 1–38 (1977)
6. Gama, J.: A survey on learning from data streams: current and future trends. Progress in Artificial Intelligence **1**(1), 45–55 (2012)
7. Heierman, E.O., Youngblood, G.M., Cook, D.J.: Mining temporal sequences to discover interesting patterns. In: KDD Workshop on mining temporal and sequential data (2004)
8. Kiran, R.U., Reddy, P.K.: Mining periodic-frequent patterns with maximum items' support constraints. In: ACM COMPUTE Bangalore Conference, pp. 1–8 (2010)
9. Lahiri, M., Berger-Wolf, T.Y.: Mining periodic behavior in dynamic social networks. In: ICDM, pp. 373–382. IEEE Computer Society (2008)
10. Li, Z., Han, J., Ding, B., Kays, R.: Mining periodic behaviors of object movements for animal and biological sustainability studies. Data Mining and Knowledge Discovery **24**(2), 355–386 (2012)
11. Lin, S., Qiao, J., Wang, Y.: Frequent episode mining within the latest time windows over event streams. Appl. Intell. **40**(1), 13–28 (2014)
12. Mannila, H., Toivonen, H., Verkamo, A.I.: Discovering frequent episodes in sequences. In: Fayyad, U.M., Uthurusamy, R. (eds.) KDD, pp. 210–215. AAAI Press (1995)
13. Patnaik, D., Laxman, S., Chandramouli, B., Ramakrishnan, N.: Efficient episode mining of dynamic event streams. In: ICDM, pp. 605–614 (2012)
14. Rashidi, P., Cook, D.J.: Mining sensor streams for discovering human activity patterns over time. In: Webb, G.I., Liu, B., Zhang, C., Gunopulos, D., Wu, X. (eds.) ICDM 2010, The 10th IEEE International Conference on Data Mining, Sydney, Australia, December 14–17, 2010, pp. 431–440. IEEE Computer Society (2010)
15. Soulàs, J., Lenca, P., Thépaut, A.: Monitoring the habits of elderly people through data mining from home automation devices data. In: Reis, L.P., Correia, L., Cascalho, J. (eds.) EPIA 2013. LNCS, vol. 8154, pp. 343–354. Springer, Heidelberg (2013)

16. Surana, A., Kiran, R.U., Reddy, P.K.: An efficient approach to mine periodic-frequent patterns in transactional databases. In: Cao, L., Huang, J.Z., Bailey, J., Koh, Y.S., Luo, J. (eds.) PAKDD Workshops 2011. LNCS, vol. 7104, pp. 254–266. Springer, Heidelberg (2012)
17. Wong, R.W., Fu, A.C.: Mining top-k frequent itemsets from data streams. Data Mining and Knowledge Discovery **13**(2), 193–217 (2006)
18. Zhu, H., Wang, P., He, X., Li, Y., Wang, W., Shi, B.: Efficient episode mining with minimal and non-overlapping occurrences. In: ICDM, pp. 1211–1216 (2010)

# Forecasting the Correct Trading Actions

Luís Baía<sup>1,2(✉)</sup> and Luís Torgo<sup>1,2</sup>

<sup>1</sup> LIAAD - INESC TEC, Porto, Portugal

[luisbaia\\_1992@hotmail.com](mailto:luisbaia_1992@hotmail.com), [ltorgo@dcc.fc.up.pt](mailto:ltorgo@dcc.fc.up.pt)

<sup>2</sup> DCC - Faculdade de Ciências - Universidade do Porto, Porto, Portugal

**Abstract.** This paper addresses the problem of decision making in the context of financial markets. More specifically, the problem of forecasting the correct trading action for a certain future horizon. We study and compare two different alternative ways of addressing these forecasting tasks: i) using standard numeric prediction models to forecast the variation on the prices of the target asset and on a second stage transform these numeric predictions into a decision according to some pre-defined decision rules; and ii) use models that directly forecast the right decision thus ignoring the intermediate numeric forecasting task. The objective of our study is to determine if both strategies provide identical results or if there is any particular advantage worth being considered that may distinguish each alternative in the context of financial markets.

## 1 Introduction

Many real world applications require decisions to be made based on forecasting some numeric quantity. Sales forecasting may lead to some important decisions concerning the production process. Asset price forecasting may lead investors to buy or sell some financial product. Forecasting the future evolution of some indicator of a patient may lead a medical doctor to some important treatment prescriptions. These are just a few examples of concrete applications that fit this general setting: decisions based on numeric forecasts of some variable. In most cases the decision process is based on a pre-defined protocol that associates intervals of the range of the numeric variable with concrete actions/decisions. This means that once we have a prediction for the numeric variable we will use some deterministic process to reach the action/decision to be taken. This work is focused on this particular type of situations in the context of financial markets. In this domain the goal of investors is to make the correct decision (Sell, Buy or Hold) at any given point in time. These decisions are taken based on the investor's expectations on the future evolution of the asset prices. In this work we approach this decision problem using predictive models. More specifically, we will compare two possible ways of trying to forecast what is the correct trading decision at any point in time.

In our target applications we assume that there are deterministic decision rules that given the estimated evolution of the prices of the asset will indicate the trading action to be taken. For instance, a rule could state that if the forecast

of the variation of prices is a 2.5% increase then the correct decision is to buy the asset as this will allow covering transaction costs and still have some profit. Given the deterministic mapping from forecasted values into decisions we can define the prediction task in two different ways. The first consists on obtaining a numeric prediction model that we can then use to obtain predictions of the future variation of the prices which are then transformed (deterministically) into trading decisions (e.g. [1], [2]). The second alternative consists of directly forecasting the correct trading decisions (e.g. [3], [4], [5]). Which is the best option in terms of the resulting financial results? To the best of our knowledge no comparative study was carried out to answer this question. This is the goal of the current paper: to compare these two approaches and provide experimental evidence of the advantages and disadvantages of each alternative.

## 2 Problem Formalization

The problem of decision making based on forecasts of a numerical (continuous) value can be formalized as follows. We assume there is an unknown function that maps the values of  $p$  predictor variables into the values of a certain numeric variable  $Y$ . Let  $f$  be this unknown function that receives as input a vector  $\mathbf{x}$  with the values of the  $p$  predictors and returns the value of the target numeric variable  $Y$  whose values are supposed to depend on these predictors,

$$\begin{aligned} f: \mathbb{R}^p &\rightarrow \mathbb{R} \\ \mathbf{x} &\mapsto f(\mathbf{x}). \end{aligned}$$

We also assume that based on the values of this variable  $Y$  some decisions need to be made. Let  $g$  be another function that given the values of this target numeric variable transforms them into actions/decisions,

$$\begin{aligned} g: \mathbb{R} &\rightarrow \mathcal{A} = \{a_1, a_2, a_3, \dots\} \\ Y &\mapsto g(Y). \end{aligned}$$

where  $\mathcal{A}$  represents a set of possible actions.

In our target applications, functions  $f$  and  $g$  are very different. Function  $g$  is known and deterministic, in the sense that it is part of the domain background knowledge. Function  $f$  is unknown and uncertain. The only information we have about function  $f$  is an historical record of mappings from  $\mathbf{x}$  into  $Y$ , i.e. a data set that can be used to learn an approximation of the function  $f$ . Given that the variable  $Y$  is numeric this approximation could be obtained using some existing multiple regression tool. This means that given a data set  $D_r = \{\langle \mathbf{x}_i, Y_i \rangle_{i=1}^n\}$  we can use some regression tool to obtain a model  $\hat{r}(\mathbf{x})$  that is an approximation of  $f$ . From an operational perspective this would mean that given a test case  $\mathbf{q}$  for which a decision needs to be made we would proceed by first using  $\hat{r}$  to obtain a prediction for  $Y$  and then apply  $g$  to this predicted value to get the

predicted action/decision, i.e.  $\mathbf{q} \mapsto \hat{r}(\mathbf{q}) \mapsto g(\hat{r}(\mathbf{q}))$ . In the context of financial markets the predictors describe the currently observed dynamics of the prices of some financial asset and the target numeric variable  $Y$  represents the future variation of this price. This means that  $f$  is the unknown function that maps the currently observed price dynamics into a future evolution of the price. On the other hand  $g$  is a deterministic function (typically based on domain knowledge and risk preferences of traders) that maps the prediction of the future evolution of prices into one of three possible decisions: Sell, Hold or Buy.

Given the deterministic nature of  $g$  we can use an alternative process for obtaining decisions. More specifically, we can build an alternative data set  $D_c = \{\langle \mathbf{x}_i, g(Y_i) \rangle_{i=1}^n\}$ , where the target variable is the decision associated with each known  $Y$  value in the historical record of data. This means that we have a nominal target variable, i.e. we are facing a classification task. Once again we can use some standard classification tool to obtain an approximation  $\hat{c}$  of the unknown function that maps the predictors into the correct actions/decisions. Once such model is obtained we can use it given a query case  $\mathbf{q}$  to directly estimate the correct decision by applying the learned model to the case, i.e.  $\mathbf{q} \mapsto \hat{c}(\mathbf{q})$ . This means that given the description of the current dynamics of the price we will use function  $\hat{c}$  to forecast directly the correct trading action for this context.

Independently of the approach followed, the final goal of the applications we are targeting is always to make correct decisions. This means that whatever process we use to reach a decision, it will be evaluated in terms of the “quality” of the decisions it generates. In this context, it seems that the classification approach, by having as target variable the decisions, would be easier to bias towards optimal actions. However, this approach completely ignores the intermediate numeric variable that is supposed to influence decisions, though one may argue that information on the relationship between  $Y$  and the decisions is “encoded” when building the training set  $D_c$  by using as target the values of  $g(Y_i)$ . On the other hand, while the regression approach is focused on obtaining accurate predictions of  $Y$ , it completely ignores questions like eventual different cost/benefits of the different possible decisions that could be easily encoded into the classification tasks. All these potential trade-offs motivate the current study. The main goal of this paper is to compare these two approaches in the context of financial markets.

### 3 Material and Methods

This section describes the main issues involved in the experimental comparison we will carry out with the goal of comparing the two possible approaches described in the previous section.

#### 3.1 The Tasks

The problem addressed in this paper is very common in automatic trading systems where decisions are based on the forecasts of some prediction models.

The decisions to open or close short/long positions are typically the result of a deterministic mapping from the predicted prices variation.

In our experiments, we have used the assets prices of 12 companies. Each data set has a minimum of 7 years of daily data and a maximum of 30 years. In order to simplify the study, we will be working with a one-day horizon, i.e. take a decision based on the forecasts of the assets variation for one day ahead. Moreover, we will be working exclusively with the closing prices of each trading session, i.e. we assume trading decisions are to be made after the markets close.

The decision function for this application receives as input the forecast of the daily variation of the assets closing prices and returns a trading action. We will be using the following function in our experiments:

$$g: \mathbb{R} \rightarrow \mathcal{A} = \{\text{hold}, \text{buy}, \text{sell}\}$$

$$Y \mapsto \begin{cases} \text{buy}, & Y > 0.02 \\ \text{sell}, & Y < -0.02 \\ \text{hold}, & \text{other cases} \end{cases} .$$

This means we are assuming that any variation above 2% will be sufficient to cover the transaction costs and still obtain some profit. Concerning the data that will be used as predictors for the forecasting models (either forecasting the prices variation ( $Y$ ) or directly the trading action ( $A$ )) we have used the price variations on recent days as well as some trading indicators, such as the annual volatility, the Welles Wilder's style moving average [6], the stop and reverse point indicator developed by J. Welles Wilder [6], the usual moving average and others. The goal of this selection of predictors is to provide the forecasting models with useful information on the recent dynamics of the assets prices.

Regarding the performance metrics we will use to compare each approach, we will use two metrics that capture important properties of the economic results of the trading decisions made by the alternative models. More specifically, we will use the Sharpe Ratio as a measure of the risk (volatility) associated with the decisions, and the percentage Total Return as a measure of the overall financial results of these actions. To make our experiments more realistic we will consider a transaction cost of 2% for each Buy or Sell decision a model may take.

At this stage it is important to remark that the prediction tasks we are facing have some characteristics that turn them into particularly challenging tasks. One of the main hurdles results from the fact that interesting events, from a trading perspective, are rare in financial markets. In effect, large movements of prices are not very frequent. This means that the data sets we will provide to the models have clearly imbalanced distributions of the target variables (both the numeric percentage variations and the trading actions). To make this imbalance problem harder the situations that are more interesting from a trading perspective are rare in the data sets which creates difficulties to most modelling techniques. In the next section, we will describe some of the measures we have taken to alleviate this problem.

### 3.2 The Models

In this section we will list all the model variants that will be used in the experimental comparison. The point is to ensure that both approaches have the same conditions for a fair comparison. Several variants for each family of models (SVM, Random Forests, etc) were tested in order to make sure our conclusions were not biased by the choice of models. The Table 1 and Table 2 shows all the model variants used, where nearly 182 model variants were tested.

**Table 1.** Regression models used for the experimental comparisons. SVM stands for Support Vectorial Machines, KNN for K-nearest neighbours, NNET for Neural Networks and MARS for Multivariate Adaptive Regression Spline models

Model	Variants	R Package
SVM	cost={1,5,10}, $\epsilon = \{0.1,0.05,0.01\}$ , tolerance={0.001,0.005},kernel=linear	e1071
SVM	cost={1,10}, $\epsilon = \{0.1,0.05,0.01\}$ , degree={2,3,5},kernel=polynomial	e1071
Random Forest	ntree={500,750,1000,2000,3000},mtry={4,5,6}	randomForest
Trees (pruned)	se={0,0.5,1,1.5,2},cp=0, minsplit=6	DMwR
KNN	k={1,3,5,7,11,15}	DMwR
NNET	size={2,4,6},decay={0.05,0.1,0.15}	nnet
MARS	thresh={0.001,0.0005,0.002}, degree={1,2,3},minspan={0,1}	earth
AdaBoost	dist={gaussian},n.trees={10000,20000}, shrinkage={0.001,0.01},interaction.depth={1,2})	gbm

**Table 2.** Classification models used for the experimental comparisons. SVM stands for Support Vectorial Machines, KNN for K-nearest neighbours, NNET for Neural Networks and MARS for Multivariate Adaptive Regression Spline models

Model	Variants	R Package
SVM	cost={1,3,7,10},kernel=linear tolerance={0.001,0.005,0.0005,0.002}	e1071
SVM	cost={1,10}, $\epsilon = \{0.1,0.05\}$ , degree={2,3,4,5},kernel=polynomial	e1071
Random Forest	ntree={500,750,1000,2000,3000},mtry={3,4,5}	randomForest
Trees (pruned)	se={0,0.5,1,1.5,2},cp=0, minsplit=6	DMwR
KNN	k={1,3,5,7,11,15}	DMwR
NNET	size={2,4,6},decay={0.05,0.1,0.15}	nnet
AdaBoost	coeflearn = c('Breiman','Freund','Zhu'), mfinal=c(500,1000,2000)	boosting

The predictive tasks we are facing have two main difficulties: (i) the fact that the distribution of the target variables is highly imbalanced, with the more relevant values being less frequent; and (ii) the fact that there is an implicit ordering among the decisions. The first problem causes most modelling techniques to

focus on cases (the most frequent) that are not relevant for the application goals. The second problem is specific to classification tasks as these algorithms do not distinguish among the different types of errors, whilst in our target application confusing a Buy decision with a Hold decision is less serious than confusing it with a Sell.

These two problems lead us to consider several alternatives to our base modelling approaches described in Tables 1 and 2. For the first problem of imbalance we have considered the hypothesis of using resampling to balance the distribution of the target variable before obtaining the models. In order to do that, we have used the SMOTE algorithm [7]. This method is well known for classification models, consisting basically of oversampling the minority classes and under-sampling the majority ones. The goal is to modify the data set in order to ensure that each class is similarly represented. Regarding the regression tasks we have used the work by Torgo et. al [8], where a regression version of SMOTE was presented. Essentially, the concept is the same as in classification, using a method to try to balance the continuous distribution of the target variable by oversampling and under-sampling different ranges of its domain.

We have thoroughly tested the hypothesis that using resampling before obtain ghe models would boost the performance of the different models we have considered for our tasks. Our experiments confirmed that resampling lead the models to issue more Buy and Sell signals (the one that are less frequent but more interesting). However, this increased number of signals was accompanied by an increased financial risk that frequently lead to very poor economic results, with very few exceptions.

Regarding the second problem of the order among the classes we have also considered a frequently used approach to this issue. Namely, we have used a cost-benefit matrix that allows us to distinguish between the different types of classification errors. Using this matrix, and given a probabilistic classifier, we can predict for each test case the class that maximises the utility instead of the class that has the highest probability.

We have used the following procedure to obtain the cost-benefit matrices for our tasks. Correctly predicted *buy/sell* signals have a positive benefit estimated as the average return of the *buy/sell* signals in the training set. On the other hand, in the case of incorrectly predicting a true *hold* signal as *buy* (or *sell*), we we assign it minus the average return of the *buy* (or *sell*) signals. Basically, the benefit associated to correctly predicting one rare signal is entirely lost when the model suggests an investment when the correct action would be doing nothing. In the extreme case of confusing the *buy* and *sell* signals, the penalty will be minus the sum of the average return of each signal. Choosing such a high penalty for these cases will eventually change the model to be less likely to make this type of very dangerous mistakes. Considering the case of incorrectly predicting a true *sell* (or *buy*) signal as *hold*, we also charge for it, but in a less severe way. Therefore, the average of the *sell* (or *buy*) signal is considered, but divided by two. This division was our way of “teaching” the model that it is preferable to miss an opportunity to earn money rather than making the investor lose money.

Finally, correctly predicting a *hold* signal gives no penalty nor reward, since no money is either won or lost. Table 3 shows an example of such cost-benefit matrix that was obtained with the data from 1981-01-05 to 2000-10-13 of Apple.

**Table 3.** Example cost-benefit matrix for Apple shares.

		Trues		
		s	h	b
s		0.49	-0.49	-0.82
Pred	h	-0.24	0.00	-0.17
b		-0.82	-0.33	0.33

We have also thoroughly tested the hypothesis that using cost-benefit matrices to implement utility maximisation would improve the performance of the models. Our tests have shown that nearly half the model variants see their performance boosted with this approach.

### 3.3 The Experimental Methodology

In this section we present the experimental methodology used in our comparative experiments. Due to the temporal nature of the used data sets, the usual cross-validation methodology should not be used to estimate the performance of a certain model. Namely, this procedure assumes that the data has no order and by using it we would obtain unreliable estimates. In this context, we have decided to use a Monte Carlo simulation method for obtaining our estimates. This methodology consists of randomly selecting a series of  $N$  points in time within the available data set. For each of these random dates, we use a certain consecutive past window as training set for obtaining the alternative models that are then tested/compared in a sub-sequent and consecutive test window. The Monte Carlo estimates are formed by the average scores obtained on the  $N$  repetitions. In our experiments we have used  $N = 10$ , 50% of the data as the size of the training window, and 25% of the data as size of the test sets.

With respect to testing the statistical significance of the observed differences between the estimated scores we have used the recommendations of the work by Demsar [9]. More specifically, in situations where we are comparing  $k$  alternative models on one specific task we have used the Wilcoxon signed rank test to test the significance of the differences. On the experiments where  $k$  models are compared on  $t$  tasks we use the Friedman test followed by a post-hoc Nemenyi test to check the significance of the difference between the average ranks of the  $k$  models across the  $t$  tasks.

## 4 Experimental Results

This section presents the results of the experimental comparisons between the two general approaches to making trading decisions based on forecasting models.

In our experiments we have considered 76 classification models. For each of these models we have also tried the version with resampling and the version with cost-benefit matrices, totaling  $76 \times 3 = 228$  different classification variants. In terms of regression we have a slightly large set of 97 base models that were then tried with and without resampling, for a total of  $97 \times 2 = 194$  variants. All these variants were compared on the data sets of the 12 companies described in Section 3.1 using the methodology described in Section 3.3.

We have divided our experimental analysis in two main parts. In the first one, for each company and for each metric, we have compared the best regression and classification variant using a Wilcoxon signed rank statistical test with a significance level of 0.05 to check if we can reject the null hypothesis that there is not significant difference between the best classification and regression variants. This leads to 12 statistical tests for each metric (one test for each company), where the models compared for each company are not necessarily the same. The motivation of this first part is to compare the best classification variant against the best regression task for each company and metric. Figure 1 shows the result of this comparison for the Total Return and Sharpe Ratio financial evaluation metrics. The results on these figures are somewhat correlated. In effect, whenever we have found a significant difference in terms of Total Return, the same also happened in terms of Sharpe Ratio. Regarding the left graph (Total Return), we have one significant win for each approach and 6 against for 4 non significant wins for classification and regression, respectively. With respect to the right graph (Sharpe Ration) we can observe a slight advantage of the classification approach, with one more significant win and 8 vs 1 non-significant wins. Paying respect to the second figure, one more significant win for classification is obtained and this approach achieved 8 non significant wins against 1 for the regression one. Overall, we have observed a very slight advantage of the best classification approach against the best regression variant.

From an economical perspective we have observed contradictory results. For instance, there is a very high level of Total Return for the Meg company (above 60% return), but the best Sharpe Ratio was very low. This means that the best model for the first metric was taking enormous amounts of risk and that the high level of return achieved was probably due to pure luck. On the other hand, there are some high values for the Total Return accompanied by high levels of Sharpe Ratio, such as for the Exas company. This strongly suggests that the models could actually provide some profit with low risk, thus indicating that the model actually predicted meaningful signals. Given the high variability of the results across companies, taking conclusions solely based on the analysis of the best variant per model and per metric may lead to wrong results. This establishes the motivation for the second part of our experiments.

In this second part of our experiments, instead of grouping by metric and company, we will just group by metric and study the average rank of each model across all the companies (top 5 of each approach are considered). With the use of the Friedman test followed by the post-hoc Nemenyi test, we check whether there are statistically significant differences among these rankings. This way, if

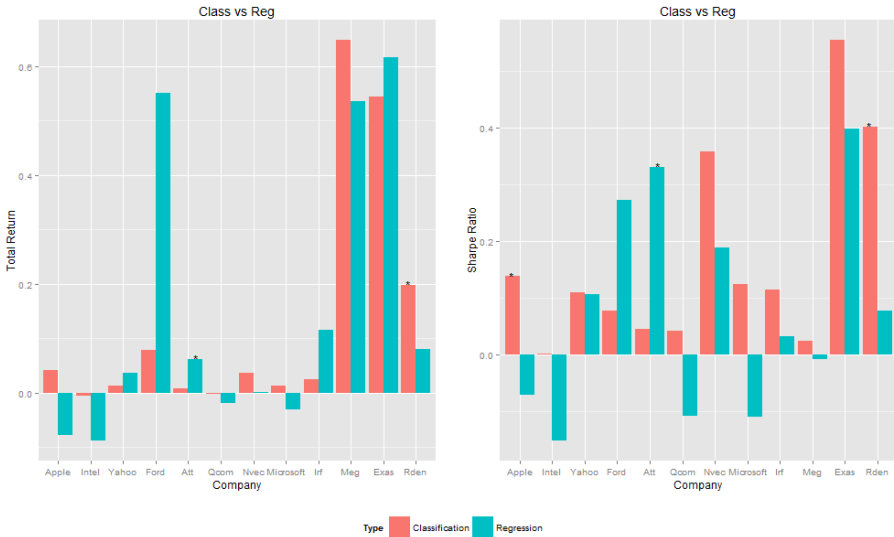


**Fig. 1.** Best classification variant against the best regression one for the Total Return and Sharpe Ratio metrics (asterisks denote that the respective variant is significantly better, according to a Wilcoxon test with  $\alpha = 0.05$ ).

a model obtains a very good result for one company but poor for all the others (meaning that it was lucky in that specific company), its average ranking will be low allowing the top average rankings to be populated by the true top models that perform well across most companies.

Table 4 summarises the results in terms of Total Return. Since we could not reject the Friedman's null hypothesis, the post-hoc Nemenyi's test was not performed. This means that we can not say with 95% confidence that there is some difference in terms of Total return between these modelling approaches. Nevertheless, there are some observations to remark. The model with the best average ranking is a classification model using cost-benefit matrices. All the remaining classification variants are in their original form (without using cost-benefit matrices) and occupying mostly the last positions. Moreover, not a single variant obtained with SMOTE appears in this top 5 for each approach, which means that we confirm that resampling does not seem to pay off for this class of applications due to the economic costs of making more risky decisions. Furthermore, another very interesting remark is that all the top models are using SVMs as the base learning algorithm. Overall we can not say that any of the two approaches (forecasting directly the trading actions using classification models or forecasting the price returns before using regression) is better than the other.

Table 5 shows the results of the same experiment in terms of Sharpe Ratio, i.e. the risk exposure of the alternatives. The conclusions are quite similar to

**Table 4.** The average rank of the top 5 Classification and Regression models in terms of Total Return. The Friedman test returned a  $p$ -value of 0.3113477, meaning that there is no statistical difference between all the 10 variants compared. Note: BC means the model was obtained using a benefit-cost matrix, while (p)/(l) means the SVM model was obtained using a polynomial/linear kernel. The vx labels represent the different parameter settings that were considered within each variant.

Rank Variant	Avg. Rank	Rank Variant	Avg. Rank
1 CLASS SVM(p) BC v3	4.54	6 CLASS SVM(l) v1	5.83
2 REG SVM(l) v1	5.12	7 CLASS SVM(l) v5	5.83
3 REG SVM(l) v11	5.12	8 CLASS SVM(l) v9	5.83
4 REG SVM(l) v2	5.25	9 REG SVM(l) v3	5.83
5 CLASS SVM(l) v6	5.67	10 REG SVM(l) v18	5.96

the Total Return metric. Once again, no significant differences were observed. Still, one should note that the first 5 places are dominated by the classification approaches. The best variant for the Total Return is also the best variant for the Sharpe Ratio, which makes this variant unarguably the best one of our study when considering the 12 different companies. Hence, ultimately we can state that the most solid model belongs to the classification approach using an SVM with cost-benefit matrices, since it obtained the highest returns with lowest associated risk. Finally, unlike the results for Total Return, in this case we observe other learning algorithms appearing in the top 5 best results.

**Table 5.** Top 5 average rankings of the Classification and Regression models for the Sharpe Ratio. The Friedman test returned a  $p$ -value of 0.1037471, implying there is no statistical difference between all the 10 variants tested.

Rank Variant	Avg. Rank	Rank Variant	Avg. Rank
1 CLASS SVM(p) BC v3	4.88	6 CLASS SVM(l) v1	5.58
2 CLASS SVM(l) BC v15	5.38	7 REG TREE v4	5.58
3 REG NNET v1	5.38	8 REG TREE v5	5.58
4 CLASS SVM(l) v14	5.42	9 REG NNET v2	5.67
5 CLASS SVM(l) v6	5.50	10 REG SVM(l) v1	6.04

In conclusion, we can not state that one approach performs definitely better than the other in the context of financial trading decisions. The scientific community typically puts more effort into the regression models, but this study strongly suggests that both have at least the same potential. Actually, the most consistent model we could obtain is a classification approach. Another interesting conclusion is that, of a considerably large set of different types of models, SVMs achieved better results both when considering classification or regression tasks.

## 5 Conclusions

This paper presents a study of two different approaches to financial trading decisions based on forecasting models. The first, and more conventional, approach uses regression tools to forecast the future evolution of prices and then uses some decision rules to choose the “correct” trading decision based on these predictions. The second approach tries to directly forecast the “correct” trading decision. Our study is a specific instance of the more general problem of making decisions based on numerical forecasts. In this paper we have focused on financial trading decisions because this is a specific domain that requires specific trade-offs in terms of economic results. This means that our conclusions from this study in this area should not be generalised to other application domains.

Overall, the main conclusion of this study is that, for this specific application domain, there seems to not be any statistically significant difference between these two approaches to decision making. Given the large set of classification and regression models that were considered, as well as different approaches to the learning task, we claim that this conclusion is supported by significant experimental evidence.

The experiments carried out in this paper have also allowed us to draw some other conclusions in terms of the applicability of resampling and cost-benefit matrices in the context of financial forecasting. Namely, we have observed that the application of resampling, although increasing the number of trading decisions made by the models, would typically bring additional financial risks that would make the models unattractive to traders. On the other hand the use of cost-benefit matrices in an effort to maximise the utility of the predictions of the models, did bring some advantages to a high percentage of modelling variants.

As future work we plan to extend our comparisons of these two forms of addressing decision making based on numeric forecasting, to other application domains, in an effort to provide general guidelines to the community on how to address these relevant real world tasks.

**Acknowledgments.** This work is financed by the FCT Fundação para a Ciência e a Tecnologia (Portuguese Foundation for Science and Technology) within project UID/EEA/50014/2013.

## References

1. Lu, C.J., Lee, T.S., Chiu, C.C.: Financial time series forecasting using independent component analysis and support vector regression. *Decision Support Systems* **47**(2), 115–125 (2009). cited By 112
2. HELLSTRÖM, T.: Data snooping in the stock market. *Theory of Stochastic Processes* **21**, 33–50 (1999) (1999b)
3. Luo, L., Chen, X.: Integrating piecewise linear representation and weighted support vector machine for stock trading signal prediction. *Applied Soft Computing* **13**(2), 806–816 (2013)

4. Ma, G.Z., Song, E., Hung, C.C., Su, L., Huang, D.S.: Multiple costs based decision making with back-propagation neural networks. *Decision Support Systems* **52**(3), 657–663 (2012)
5. Teixeira, L.A., de Oliveira, A.L.I.: A method for automatic stock trading combining technical analysis and nearest neighbor classification. *Expert Systems with Applications* **37**(10), 6885–6890 (2010)
6. Wilder, J.: New Concepts in Technical Trading Systems. Trend Research (1978)
7. Chawla, N.V., Bowyer, K.W., Hall, L.O., Kegelmeyer, W.P.: Smote: synthetic minority over-sampling technique. *Journal of Artificial Intelligence Research* **16**(1), 321–357 (2002)
8. Torgo, L., Branco, P., Ribeiro, R.P., Pfahringer, B.: Resampling strategies for regression. *Expert Systems* (2014)
9. Demšar, J.: Statistical comparisons of classifiers over multiple data sets. *The Journal of Machine Learning Research* **7**, 1–30 (2006)

# CTCHAID: Extending the Application of the Consolidation Methodology

Igor Ibarguren<sup>(✉)</sup>, Jesús María Pérez, and Javier Muguerza

Department of Computer Architecture and Technology, University of the Basque Country UPV/EHU, Manuel Lardizabal 1, 20018 Donostia, Spain  
[{igor.ibarguren,txus.perez,j.muguerza}@ehu.es](mailto:{igor.ibarguren,txus.perez,j.muguerza}@ehu.es)  
<http://www.sc.ehu.es/aldapa/>

**Abstract.** The consolidation process, originally applied to the C4.5 tree induction algorithm, improved its discriminating capacity and stability. Consolidation creates multiple samples and builds a simple (non-multiple) classifier by applying the ensemble process during the model construction times. A benefit of consolidation is that the understandability of the base classifier is kept. The work presented aims to show the consolidation process can improve algorithms other than C4.5 by applying the consolidation process to another algorithm, CHAID\*. The consolidation of CHAID\*, CTCHAID, required solving the handicap of consolidating the value groupings proposed by each CHAID\* tree for discrete attributes. The experimentation is divided in three classification contexts for a total of 96 datasets. Results show that consolidated algorithms perform robustly, ranking competitively in all contexts, never falling into lower positions unlike most of the other 23 rule inducting algorithms considered in the study. When performing a global comparison consolidated algorithms rank first.

## 1 Introduction

In some problems that make use of classification techniques, the reason of why a decision is made is almost as important as the accuracy of the decision, thus the classifier must be comprehensible. Decision trees are considered comprehensible classifiers. The most common way of improving the discriminating capacity of decision trees is to build ensemble classifiers. However with ensembles, the explaining capacity individual trees possess is lost. The consolidation of algorithms is an alternative that resamples the training sample multiple times and applies the ensemble voting process while the classifier is being built, so that the final classifier is a single classifier (with explaining capacity) built using the knowledge of multiple samples. The well-known C4.5 tree induction algorithm [10] has successfully been consolidated in the past [9].

With the aim of studying the benefit of the consolidation process on other algorithms, maintaining the explaining capacity of the classifier, in this work we apply this methodology on a variation of the CHAID [7,8] algorithm (CHAID\* [5]), one of the first tree induction algorithms along with C4.5 and CART. We propose the

consolidation of CHAID\* and using tests for statistical significance [4] we compare its results in three different classification contexts (amounting a total of 96 datasets) against 16 genetics-based and 7 classical algorithms and also the original CTC (Consolidated Tree Construction) algorithm.

The rest of the paper is organized as follows. Section 2 details the related work. Section 3 explains the consolidation version of the CHAID\*, CTCHAID. Section 4 defines the experimental methodology. Section 5 lays out the obtained results. Finally, section 6 gives this work's conclusions.

## 2 Related Work on CHAID\* and Consolidation

The CHAID (Chi-squared Automatic Interaction Detector) [7,8] is a tree induction algorithm that uses the chi-squared ( $\chi^2$ ) as the split function and it only works with discrete variables. CHAID\* [5] is a variation of CHAID that differs in three main aspects:

- Handling of attributes: The original CHAID algorithm lacks the ability to handle continuous variables. Inspired by how C4.5 handles continuous variables, CHAID\* uses the  $\chi^2$  to determine the best cutting point to divide the variable into two sets.
- Missing values on continuous variables: Three options are considered to treat the examples with missing values: grouping them with those examples with a value lower or equal to the cutting point, grouping them with examples whose value is greater than the cutting point or creating a branch just for the examples with a missing value.
- Pruning: CHAID\* uses the same strategy as C4.5 by applying the Reduced-error pruning mechanism.

The consolidation approach aims at improving the discriminating capacity and the stability while reducing the complexity of the classifier [9]. It works by applying the ensemble voting process while building the simple classifier instead of building multiple simple classifiers and performing the ensemble vote only when classifying new examples. Recently the term “Inner Ensembles” has been coined to group methodologies following this approach [1].

The first consolidated algorithm was the well-known C4.5 decision tree induction algorithm, creating the CTC (Consolidated Tree Construction) algorithm. CTC works by first creating multiple samples from the training samples, usually by subsampling. Then, from each sample a C4.5 tree begins to grow. However on each node, execution “stops”. Each tree proposes a new split based on their unique sample. A vote takes place and a common split is agreed. All trees comply with the majority vote and make the split accordingly, even if it is not what they have voted. This continues until the majority decides not to split any more. Because of this process, the structure of the trees grown from all subsamples is the same and the outcome is a single tree model. Then, for each leaf node, the *a posteriori* probabilities for each class are computed by averaging the probabilities on that particular leaf using the same samples used to build the consolidated tree.

### 3 CTCHAID

As explained in section 2 the changes made to CHAID\* make it very similar to the C4.5 algorithm, which makes the implementation of CTCHAID very similar to the implementation of CTC45 (Consolidated C4.5) described in section 2. Aside from the split function, the other main difference between the algorithms is how discrete variables (nominal and ordinal) are handled. By default, when splitting using a discrete variable C4.5 creates a branch for every possible value for the attribute. On the other hand, CHAID\* considers grouping more than one value on each branch. In each node a contingency table is created for each variable. Each of these tables describes the relationship between the values a variable can take and how the examples with this value are distributed among all possible classes. CHAID\* uses Kass' algorithm [7] on all contingency tables to find the most significant variable and value-group to make the split.

When consolidating CHAID\* the behavior is different depending on the type of variable. First the contingency tables are built from each sample and processed with Kass' algorithm to find the most important grouping. From each subsample a variable is proposed and voting takes place as with CTC45. If the voted variable is continuous the median value of the proposed cut-point values will be used. For categorical values, the contingency tables from each tree for the chosen variable are averaged into a single table. This averaged table is processed with Kass' algorithm to find the most significant combination of categories.

### 4 Experimental Methodology

This experiment follows a very similar structure as the works in [3] and [6] as we compare to the results published in those works. The same three classification contexts are analyzed: 30 standard (mostly multi-class) datasets, 33 two-class imbalanced datasets and the same 33 imbalanced datasets preprocessed with SMOTE (Synthetic Minority Over-sampling Technique [2]) until the two classes were balanced by oversampling the minority class. Fernández *et al.* [3] proposed a taxonomy to classify genetics-based machine learning (GBML) algorithms for rule induction. They listed 16 algorithms and classified them in 3 categories and 5 subcategories. They compared the performance of these algorithms with a set of classical algorithms (CART, AQ, CN2, C4.5, C4.5-Rules and Ripper). In our work, for each of the contexts, the winner for each of the 5 GBML categories, 7 classical algorithms (including CHAID\*), CTC45 and CTCHAID are compared. Finally a global ranking is also computed. All algorithms used the same 5-run  $\times$  5-fold cross-validation strategy and the same training/test partitions (found in the KEEL repository<sup>1</sup>). The tables containing all the information have been omitted from this article for space issues and have been moved to the website with the additional material for this paper<sup>2</sup>.

<sup>1</sup> <http://sci2s.ugr.es/keel/datasets.php>

<sup>2</sup> <http://www.aldapa.eus/res/2015/ctchaid/>

For CTC45 and CTCHAID, following the conclusions of the latest work on consolidation [6], the subsamples used in this work are balanced and the number of examples per class is the number of examples the least populous class has in the original training sample. The number of samples for each dataset has been determined using a coverage value of 99% based on the results of [6]. The tables detailing the number of samples for each dataset have been moved to the additional material. The pruning used for C4.5, CHAID\*, CTC45 and CTCHAID was C4.5's reduced-error pruning. However, when pruning resulted in a tree with just the root node, the tree was kept unpruned. This is due to the fact that a root node tree results in zero for most performance measures used in this paper. Thus, the results shown for C4.5 are not those previously published by Fernández *et al.* using the KEEL platform but Quinlan's implementation of the algorithm.

## 5 Results

As described in the Experimental Methodology section, we divide the study into three contexts. For each context we analyze and compare the behavior of 14 algorithms: 5 GBML algorithms (the best for each subcategory proposed by Fernández *et al.*), 7 classical algorithms, CTC45 and CTCHAID. The GBML algorithms change from context to context while the classical stay the same (CART, AQ, CN2, C4.5, C45-Rules, Ripper and CHAID\*).

The significance of the average performance values achieved by the algorithms has been tested using the Friedman Aligned Ranks test, as proposed by [4]. When this test finds statistically significant differences between algorithms Holm's post-hoc test has been used to find which algorithms perform significantly worse than the best ranking algorithm. The average performance values have been moved to the website with the additional material for this article. Figure 1 offers a visual representation of the average ranks achieved by the algorithms on different contexts. In that figure a thick black line covers algorithms without statistically significant differences with the best ranking algorithm. The lower the rank the better the performance is.

Although CTCHAID does not rank first for any of the three contexts. The differences with the best ranking algorithm for each context are never found to be significant by the Holm test.

In a similar fashion to what was done in [6] we perform a global analysis combining the results of the three contexts. The rankings of this global analysis are found in Figure 2. For the standard dataset classification, only the kappa measure is used. In this case CTC45 ranks first followed by CTCHAID. The Friedman Aligned Ranks test computes a  $p$ -value of  $4.8 \times 10^{-12}$ (test statistic 89.51) indicating the clear presence of statistically significant differences between the performance of the algorithms. According to the Holm test DT-GA, SIA, UCS, CART, OCEC, CORE, AQ and CN2 perform significantly worse than CTC45.

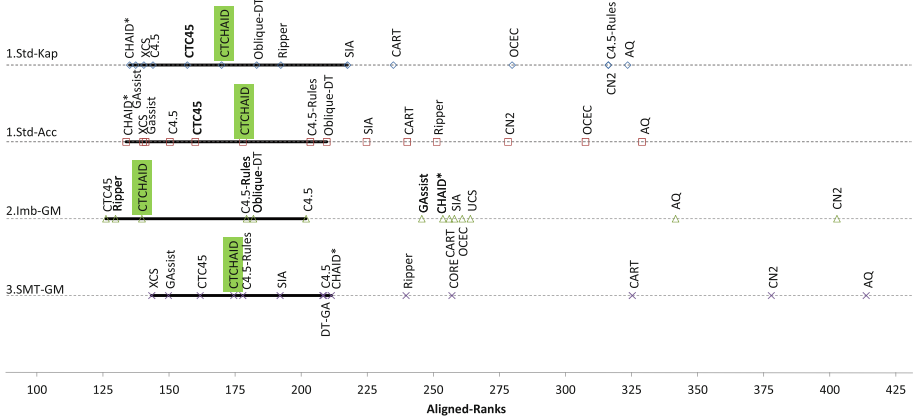


**Fig. 1.** Visual representation of Friedman Aligned Ranks for the three contexts.

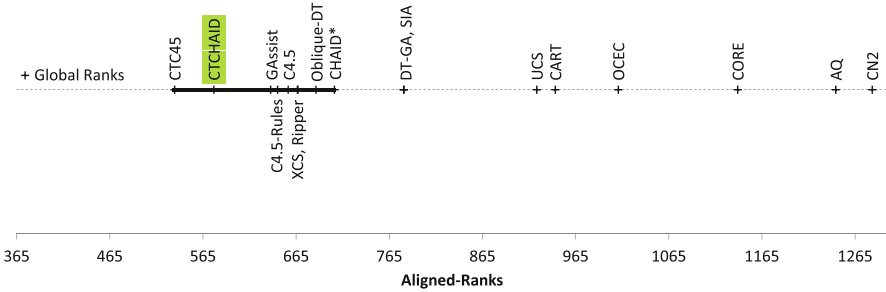


**Fig. 2.** Visual representation of Friedman Aligned Ranks for the global ranking.

## 6 Conclusions and Future Work

Results show that CTCHAID performs competitively. In summary, CTCHAID ranks in the upper half for all three contexts and in the first quartile for two out of three. As most algorithms fall into much lower positions for at least one context, CTCHAID ranks competitively in global terms. This behavior shows the robustness brought by the consolidation process in contrast to the behavior of the base algorithms, C4.5 and CHAID\*, that fall into lower positions in some contexts, ranking worse globally. This shows that the consolidation process can bring improvement to multiple algorithms.

As future work we would like to study the performance of the CTC45 and CTCHAID algorithms under different pruning strategies: standard pruning, the strategy used in this work, disabling pruning, alternatives to pruning, etc. in order to tackle the class imbalance problem. Also in the same spirit, we would like to consolidate other tree and rule-induction algorithms.

**Acknowledgments.** This work was funded by the University of the Basque Country UPV/EHU (BAILab, grant UFI11/45); by the Department of Education, Universities and Research and by the Department of Economic Development and Competitiveness of the Basque Government (grant PRE-2013-1-887; BOPV/2013/128/3067, grant IT-395-10, grant IE14-386); and by the Ministry of Economy and Competitiveness of the Spanish Government (eGovernAbility, grant TIN2014-52665-C2-1-R).

## References

1. Abbasian, H., Drummond, C., Japkowicz, N., Matwin, S.: Inner ensembles: using ensemble methods inside the learning algorithm. In: Blockeel, H., Kersting, K., Nijssen, S., Železný, F. (eds.) ECML PKDD 2013, Part III. LNCS, vol. 8190, pp. 33–48. Springer, Heidelberg (2013)
2. Chawla, N.V., Bowyer, K.W., Hall, L.O., Kegelmeyer, W.P.: SMOTE: Synthetic minority over-sampling technique. Journal of Artificial Intelligence Research **16**(1), 321–357 (2002)
3. Fernández, A., García, S., Luengo, J., Bernadó-Mansilla, E., Herrera, F.: Genetics-based machine learning for rule induction: State of the art, taxonomy, and comparative study. IEEE Transactions on Evolutionary Computation **14**(6), 913–941 (2010)
4. García, S., Fernández, A., Luengo, J., Herrera, F.: Advanced nonparametric tests for multiple comparisons in the design of experiments in computational intelligence and data mining: Experimental analysis of power. Information Sciences **180**(10), 2044–2064 (2010)
5. Ibarguren, I., Lasarguren, A., Pérez, J.M., Muguerza, J., Arbelaitz, O., Gurrutxaga, I.: BFPART: Best-first PART. Submitted to Information Sciences
6. Ibarguren, I., Pérez, J.M., Muguerza, J., Gurrutxaga, I., Arbelaitz, O.: Coverage-based resampling: Building robust consolidated decision trees. Knowledge-Based Systems **79**, 51–67 (2015)
7. Kass, G.V.: Significance testing in automatic interaction detection (a.i.d.). Journal of the Royal Statistical Society. Series C (Applied Statistics) **24**(2), 178–189 (1975)
8. Morgan, J.A., Sonquist, J.N.: Problems in the analysis of survey data, and a proposal. J. Amer. Statistics Ass. **58**, 415–434 (1963)
9. Pérez, J.M., Muguerza, J., Arbelaitz, O., Gurrutxaga, I., Martín, J.I.: Combining multiple class distribution modified subsamples in a single tree. Pattern Recognition Letters **28**(4), 414–422 (2007)
10. Quinlan, J.R.: C4.5: programs for machine learning. Morgan Kaufmann Publishers Inc., San Francisco (1993)

# Towards Interactive Visualization of Time Series Data to Support Knowledge Discovery

Jan Géryk<sup>(✉)</sup>

KD Lab, Faculty of Informatics, Masaryk University, Brno, Czech Republic  
xgeryk@fi.muni.cz

**Abstract.** Higher education institutions have a significant interest in increasing the educational quality and effectiveness. A major challenge in modern education is the large amount of time-dependent data, which requires efficient tools and methods to improve decision making. Methods like motion charts (MC) show changes over time by presenting animations in two-dimensional space and by changing element appearances. In this paper, we present a visual analytics tool which makes use of enhanced animated data visualization methods. The tool is primarily designed for exploratory analysis of academic analytics (AA) and offers several interactive visualization methods that enhance the MC design. An experiment is conducted to evaluate the efficacy of both static and animated data visualization methods. To interpret the experiment results, we utilized one-way repeated measures ANOVA.

**Keywords:** Animation · Motion charts · Visual analytics · Academic analytics · Experiment

## 1 Introduction

A key requirement of Business Intelligence (BI) is to improve the decision making process and to facilitate users to get all the needed information at the right time. There is an increasing distinction made between academic analytics (AA) and traditional BI because of the unique type of information that university executives and administrators require for decision making. In [1], hundreds of higher education executives were surveyed on their analytic needs. Authors resulted that advanced analytics should support better decision-making, studying enrollment trends, and measuring student retention. They also pointed out that management commitment and staff skills are more important in deploying AA than the technology.

Visualizations are common methods used to gain a qualitative understanding of data prior to any computational analysis. By displaying animated presentations of the data and providing analysts with interactive tools for manipulating the data, visualizations allow human pattern recognition skills to contribute to the analytic process. The most commonly used statistical visualization methods generally focus on univariate or bivariate data. The methods are usually used for tasks ranging from the exploration to the confirmation of models, including the presentation of the results. However, fewer

methods are available for visualizing data with more than two dimensions (e.g. motion charts or parallel coordinates), as the logical mapping of the data dimension to the screen dimension cannot be directly applied.

Although a snapshot of the data can be beneficial, presenting changes over time can provide a more sophisticated perspective. Animations allow knowledge discovery in complex data and make it easier to see meaningful characteristics of changes over time. The dynamic nature of Motion Charts (MC) allows a better identification of trends in the longitudinal multivariate data and enables visualization of more element characteristics simultaneously, as presented in [2]. The authors also conducted an experiment whose results concluded that MC excels at data presentation. MC is a dynamic and interactive visualization method that enables analysts to display complex and quantitative data in an intelligible way.

In this paper, we show the assets of animated data visualizations for successful understanding of complex and large data. In the next section, we describe our VA tool that implements visualization methods which make use of enhanced MC design. Further, we conduct an empirical study with 16 participants on their data comprehension to compare the efficacy of various static data visualizations with our enhanced methods. We then discuss the implications of our experiment results. Finally, we draw the conclusion and outline future work.

## 2 The Visual Analytics Tool

Visualization tools represent an effective way to make statistical data understandable to analysts, as showed in [3]. MC methods proved to be useful for data presentation and the approach was verified to be successfully employed to show the story in data [4] or support decision making [5]. Several web-based tools allowing analysts to interactively explore associations, patterns, and trends in data with temporal characteristics are available. In [6], authors presented a visualization of energy statistics using an existing web-based data analysis tools, including IBM's Many Eyes, and Google Motion Charts.

The motivation to develop advanced MC methods was to improve expression capabilities, as well as to facilitate analysts to depict each student or study as a central object of their interest. Moreover, the implementation enhances the number of animations that express the students' behavior during their studies more precisely. We partly validated usefulness of the developed methods with a case study where we successfully utilized the capabilities of the tool for the purpose of confirming hypothesis concerning student retention. Although, we concluded that the methods proved to be useful for analytic purposes, more adjustments were needed.

Two main challenges are addressed by the presented VA tool. It enables visualization of multivariate data and the qualitative exploration of data with temporal characteristics. The technical advantages over other implementations of MC are its flexibility and the ability to manage many animations simultaneously. Technical aspects of the enhanced MC methods are elaborately described in [7].

To create an effective and efficient knowledge discovery process, it is important to support common data manipulation tasks by creating quick, responsive and intuitive interaction methods. The tool offers several beneficial configurable interactive features for a more convenient analytic process. User interface features are highly customizable and allow analysts to arrange a display and variable mapping according to his or her needs. Available features include a mouse-over data display, color and plot size representation, traces, animated time plot, variable animation speed, changing of axis series, changing of axis scaling, distortion, and the support of statistical methods.

### 3 Experiment

Any quantitative research of AA also requires a preliminary exploratory data analysis. Though useful, advanced MC methods involve several drawbacks in comparison with common data visualization methods. Thus, empirical data is needed to evaluate its actual usability and efficacy. In this section, we describe the experiment for the purpose of evaluating the efficacy of the MC methods implemented in our tool. We present the results including a detailed discussion. Sixteen subjects (7 female, 9 male) with an average age of 23.44 ( $SD = 2.12$ ) participated in our experiment. The participants ranged from 21 to 26 years of age. All participants came from professions requiring the use of data visualizations, including college students, analysts, and administrators.

We performed a study to test the benefits of the animated methods over static methods when employed to analyze study related data. The experiment used a 3 (visualization)  $\times$  2 (size) within-subjects design. The visualizations varied between the static and the animated methods. The methods were represented by motion charts (MC), line charts (LC), and scatter plots (SP) which were generated for each semester. The size of datasets varied between small and large ones with the threshold of 500 elements. For the experiment, we utilized study related data about students admitted to bachelor studies of the Faculty of Informatics Masaryk University between the years of 2006 and 2008.

#### 3.1 Hypotheses

We designed the experiment to address the following three hypotheses:

- H1. The MC methods will be more effective than both the static methods for all datasets. That is, the subjects will be (a) faster and (b) make fewer errors when using MC.
- H2. The subjects will be more effective with the small datasets than with the large datasets for all methods. That is, participants will be (a) faster and (b) make fewer errors when working with small datasets.

In each trial, the participants completed 12 tasks, each with 1 to 3 required answers. Each task had identification numbers of students or fields of study as the answer. Several questions have more correct answers than requested. The participants selected

answers by selecting IDs in the legend box located in the upper right from the chart area. In order to complete the task, two buttons could be used—either “OK” button to confirm the participant’s choice or “Skip Question” button to proceed to the next task without saving the answer. There was no time limit during the experiment. For each task, the order of the datasets was fixed with the smaller ones first.

The participants were asked to proceed as quickly and accurately as possible. In order to reduce learning effects, the participants were told to make use of as many practice trials as they needed. It was followed by 12 tasks (6 small dataset tasks and 6 large dataset tasks in this particular order). After that, the subjects completed survey with questions specific for the visualization. Each block lasted about 1.5 hours. The subjects were screened to ensure that they were not color-blind and understood common data visualization methods. To test for significant effects, we conducted repeated measures analysis of variance (RM-ANOVA). Post-hoc analyses were performed by using the Bonferroni technique. Only significant results are reported.

### 3.2 Results

**Accuracy.** Since some of the tasks required multiple answers, accuracy was calculated as a percentage of the correct answers. Thus, when a subject selected only one correct answer from two, we calculated the answer as 50 % accurate rather than an incorrect answer. The analysis revealed several significant accuracy results at the .05 level. The type of visualization had a statistically significant effect on the accuracy for large datasets ( $F(1.413, 21.194) = 20.700, p < 0.001$ ). Pair-wise comparison of the visualizations found significant differences showing that MC was significantly more accurate than the LC ( $p < 0.001$ ). MC was also more accurate than the SP ( $p < 0.001$ ). There was no statistically significant difference between the LC and the SP. For the small datasets, visualizations were not statistically distinguishable. Second, the subjects were more accurate with the small datasets ( $F(1, 15) = 50.668, p < 0.001$ ). This fact supports our hypothesis H2.b.

**Task Completion Time.** An answer was considered to be incorrect if none of the correct answers was provided. In terms of time to task completion, we observed a statistically significant effect ( $F(2, 30) = 107.474, p < 0.001$ ). Post-hoc tests revealed that MC was fastest with the large datasets. The LC was faster than the SP ( $p < 0.017$ ). The mean time for MC was 48.56 seconds compared to 59.39 seconds for the LC—about 22% slower, and 62.88 seconds for the LC—about 29% slower. For the small datasets, static methods were faster than MC. Pair-wise comparison of the visualizations found significant differences between all of them. MC was slower than the LC ( $p < 0.003$ ) and the SP ( $p < 0.001$ ). The LC was slower than the SP ( $p < 0.016$ ). The mean time for MC was 42.19 seconds compared to 35.94 seconds for the LC—about 17% faster, and 31.94 seconds for the SP—about 32% faster. This only partially supports the hypothesis H1.a. MC is faster than both the static methods when used for the large datasets.

**Subjective Preferences.** For each experiment block, the subjects completed a survey where the subjects assessed their preferences regarding analysis. The subjects rated LC, SP, and MC on a five-point Likert scale (1 = strongly disagree, 5 = strongly agree). Using RM-ANOVA, we revealed statistically significant effects ( $F(1.364, 20.453) = 4.672, p = 0.033$ ). Post-hoc analysis found that MC was significantly more helpful than LC ( $p = 0.046$ ).

**Table 1.** The resulted mean values of the preferences.

	SP	LC	MC
The visualization was helpful when solving the tasks.	3.50	3.44	3.94
I found this visualization entertaining and interesting.	2.56	2.31	4.13
I prefer visualization for the small datasets.	3.88	4.00	2.63
I prefer visualization for the large datasets.	2.38	2.69	3.69

The significant differences indicate that MC was judged to be more helpful than the static methods. The subjects preferred the static methods to MC for the small datasets. However, MC was judged to be more beneficial than static methods for the large datasets ( $p < 0.001$ ). The results also showed that MC was more entertaining and interesting than the static methods ( $p < 0.001$ ).

## 4 Discussion

Our first hypothesis (H1) was that MC would outperform both the static methods for all dataset sizes, but the hypothesis was only partially confirmed. Contrary to the hypothesis, the static methods proved to achieve better speed than the animated methods for the small datasets. Moreover, the methods were not statistically distinguishable in terms of accuracy. We also hypothesized that the accuracy would increase for the smaller datasets (H2). Hypothesis H2.a was supported, because the subjects were faster with the small datasets. The mean time for the large datasets was 56.94 seconds and for the small datasets was 36.69 seconds. Hypothesis H2.b was also supported, because the subjects made fewer errors with the small datasets when compared with the large datasets. Accuracy is an issue for static visualizations when the large datasets are employed.

The study supports the intuition that using animations in analysis requires convenient interactive tools to support effective use. The study suggests that MC leads to fewer errors. Also, the subjects found MC method to be more entertaining and exciting. The evidence from the study indicates that the animations were more effective at building the subjects' comprehension of large datasets. However, the simplicity of static methods was more effective for small datasets. These observations are consistent with the verbal reports in which the subjects refused to abandon the static visual methods generally. Results supported the thoughts that MC does not represent a replacement of common statistic data visualizations but a powerful addition. The overall accuracy was quite low in the study with average about 75%. However, only one question was skipped.

## 5 Conclusion and Future Work

In the tool, we enhanced the MC design and expanded it to be more suitable for AA analysis. We also developed an intuitive, yet powerful, interactive user interface that provides analysts with instantaneous control of MC properties and data configuration, along with several customization options to increase the efficacy of the exploration process. We validate the usefulness and general applicability of the tool with the experiment to assess an efficacy of the described methods.

The study suggests that animated methods lead to fewer errors for the large datasets. Also, the subjects find MC to be more entertaining and interesting. The entertainment value probably contributes to the efficacy of the animation, because it serves to hold the subjects' attention. This fact can be useful for the purpose of designing methods in academic settings.

Despite the findings of the study, further investigation is required to evaluate the general applicability of the animated methods. We also plan to combine our animated interactive methods with common DM methods to follow the VA principle more precisely. We already implemented a standalone method utilizing decision tree algorithm providing interactive visual representation. We prefer decision trees because of their clarity and simplicity to comprehend. We will also finish the integration of the tool with our university information system to allow university executives and administrators easy access when analyzing AA and to better support decision making.

## References

1. Goldstein, P.J.: Academic analytics: The uses of management information and technology in higher education. *Educause* (2005)
2. Al-Aziz, J., Christou, N., Dinov, I.D.: SOCR Motion Charts: an efficient, open-source, interactive and dynamic applet for visualizing longitudinal multivariate data. *Journal of Statistics Education* **18**(3), 1–29 (2010)
3. Grossenbacher, A.: The globalisation of statistical content *Statistical Journal of the IAOS. Journal of the International Association for Official Statistics*, 133–144 (2008)
4. Baldwin, J., Damian, D.: Tool usage within a globally distributed software development course and implications for teaching. *Collaborative Teaching of Globally Distributed Software Development*, 15–19 (2013)
5. Sultan, T., Khedr, A., Nasr, M., Abdou, R.: A Proposed Integrated Approach for BI and GIS in Health Sector to Support Decision Makers. *Editorial Preface* (2013)
6. Vermylen, J.: Visualizing Energy Data Using Web-Based Applications. *American Geo-physical Union* (2008)
7. Géryk, J., Popelínský, L.: Visual analytics for increasing efficiency of higher education institutions. In: Abramowicz, W., Kokkinaki, A. (eds.) *BIS 2014 Workshops. LNBP*, vol. 183, pp. 117–127. Springer, Heidelberg (2014)

# Ramex-Forum: Sequential Patterns of Prices in the Petroleum Production Chain

Pedro Tiple<sup>1</sup>, Luís Cavique<sup>2</sup>, and Nuno Cavalheiro Marques<sup>3(✉)</sup>

<sup>1</sup> GoBusiness Finance, Lisbon, Portugal

<sup>2</sup> Universidade Aberta, Lisbon, Portugal

<sup>3</sup> NOVA Laboratory for Computer Science and Informatics, DI-FCT,  
Universidade Nova de Lisboa, Lisbon, Portugal  
[nmm@fct.unl.pt](mailto:nmm@fct.unl.pt)

**Abstract.** We present a sensibility analysis and new visualizations using an improved version of the Ramex-Forum algorithm applied to the study of the petroleum production chain. Different combinations of parameters and new ways to visualize data will be used. Results will highlight the importance of Ramex-Forum and its proper parameterizations for analyzing relevant relations among price variations in petroleum and other similar markets.

**Keywords:** Ramex-forum · Financial data analysis · Petroleum price · Petroleum production chain · Business intelligence

## 1 Introduction

Petroleum is one of the most important resources to the developed world and still is a major variable influencing the Economy and markets. The price of petroleum and its derivatives isn't influenced simply by supply and demand; taxes, speculation, wars, costs in refinement and transportation all contribute in setting prices. Due to its lengthy refinement process, a significant increase in the price of the source material can only reflect in the price of its derivatives after the time it takes to refine (usually within 3-4 weeks [1]). Moreover, due to its high economic importance and cost, the price of crude oil should always reflect on the final price [2].

This work presents a study on a method to quantify how the price of the crude oil (raw material) can influence the price of manufactured products, by using Ramex-Forum. This paper departs from the work of [3], with the original Ramex-forum proposal [4]. It analysis how this proposal can be improved and then tunned for finding sequential patterns using the prices of petroleum and derivatives. Sect. 2 presents the basic method and introduces the main concepts and Sect. 3 presents an evaluation on how the price of derivatives are influenced by the price of the crude oil (the source material). Finally, some conclusions are presented.

## 2 Counting Co-occurrences in Financial Markets

We assume a crossover strategy to buy and sell financial products. Given the product price index in time ‘ $t$ ’, denoted  $I(t)$ , and the moving average of that price index, with length of  $N_{MA}$  days, calculated by:  $MA(t, N_{MA}) = \sum I(t-w)/N_{MA}, \forall w \in \{0 : N_{MA}\}$ , the decision is as follows:

- Buy, if  $I(t) \cdot (1 + \epsilon) \geq MA(t, N_{MA})$
- Sell, if  $I(t) \cdot (1 - \epsilon) \leq MA(t, N_{MA})$

For each moment  $t$ , if there is a decision of either Buy or Sell, respective counters ( $Counter_B$ ,  $Counter_S$ ) will be incremented by one unit. If neither of those decisions is made, both counters are reset. This way, each counter has the number of consecutive moments where the same decision is made. See example in the Fig. 1, the ‘B’ (Buy) an ‘S’ (Sell) char illustrate the crossover strategy for a large enough  $\epsilon$  and  $N_{MA}$ . In this paper (except when explicitly mentioned otherwise), we will use a standard 1% error, i.e.  $\epsilon = 0.01$ . Other parameter is also used when defining an influence: parameter  $\delta$  is the maximum trading period length where a check for relations between two assets is made. Finally we can define  $\#Influence(A, B, \delta)$ : a cumulative influence counter of a given Buy or Sell decision for a market signal  $A$  to a market signal  $B$  (denoted  $A \rightarrow B$ ), counts how many times  $0 < (|Counter_A| - |Counter_B|) \leq \delta \wedge Counter_B \neq 0$ .



**Fig. 1.** Financial product (normalized DJI index in black) and respective moving average (blue) and crossover starting *Buy* (green) and *Sell* (red) decision with  $\epsilon$  confidence.

## 3 Results on the Petroleum Production Chain

Petroleum is refined into a relatively extensive list [5], with each category having hundreds of sub-products. Moreover this division and classification mostly depends on its social usage. This study is based on the repository of publicly

available historical values for a wide range of petroleum related products provided by the U.S. Energy Information Administration<sup>1</sup>. The variations in the prices of these products are also compared with the stock market value of eleven corporations dedicated to extracting, processing, and selling of crude and crude related products. The prices of the 55 products are separated into retail/bulk price and spot price (for some items the price is taken from retail sellers and for other items it is the security price at that day). The data is separated into four categories of known benchmarks [6] for: crude oil (West Texas Intermediate as OklahomaWTI, European Brent, and the OPEC Basket); Refinery price for Gasoline, RBOB Gasoline, Diesel, Kerosene Jet, Propane, and Heating Oil; National, state, and city averages for regular gasoline and diesel; Corporation stock values.

This paper studies the influence and best values for parameters  $\delta$ ,  $\epsilon$  thresholds, and moving average size. Focus will be put on the *Buy* comparison because in the selected data the increase/decrease of prices is very asymmetrical with a strong lean towards increases. Also, for better parameter comparison, an additional measure is used in our results, the average edge weight: a relation between the weight sum of output edges divided by the number of edges in the graph:  $AverageEdgeWeight(V, E) = \sum weight(e)/|E|, \forall e \in E$ .

*Parameter  $\delta$*  was analyzed regarding its effect on the average edge weight changes. The result can be seen in Fig. 2A. The chart shows the average edge weight change for each increment in the value of  $\delta$ . Each line represents the results obtained using different moving average sizes. Several big spikes can be seen every 5 days, this is because gas and diesel prices at the pump are only registered on a weekly basis, so for each 5 day increase in  $\delta$  the algorithm will pick up another change in value. This makes the analysis somewhat harder but it's still useful as now changes in retail prices are clearly identified. The first thing noted is that at the first week there is already a noticeable increase in the average edge weight, however some of it is due to influences between retail prices and not only from refinery to retail prices. Second, after the fourth week the individual increases in  $\delta$  barely produce a meaningful increase in value, still the cumulative increases are significant. The parameter  $\delta$  was fixed at a value of 30 working days (around six weeks: two weeks more than the expected).

*Parameter  $\epsilon$*  was studied by trying to find the best combination of parameters. The algorithm was ran several times and the average edge weight value was recorded for each run. The best values for threshold interval and the moving average size are represented in Fig. 2B. The graph shows the progression of the average edge weight, in relation to increase in threshold size. The parameters that lead to the highest increase in average weight can be clearly identified as the moving average size of 240 days with a threshold of around 26% of the moving average. However things change when the influence event count is also

---

<sup>1</sup> The used data was downloaded from <http://www.eia.gov/> on June 2014 and ranges from January 2006 to June 2014.

considered: increasing the threshold rapidly decreases the number of detected events (a threshold of 26% will reduce the number of events by about 80%). In this case, the starting average is around 130 events and falls to 30, in the 3 years period analyzed: a very low average number of events. For this case study the choice was made to maximize the event count so that a broader spectrum of influences can be detected instead of restricting the analysis to situations where the prices rise or fall sharply (which is what higher threshold values restrict the analysis to). Small increases in the  $\epsilon$  threshold will raise the average weight while only lowering the event count by small amounts. Nevertheless, random fluctuations do not advise going for a threshold of 0%, so this trade-off seems to favor the usage of smaller values for  $\epsilon$ .

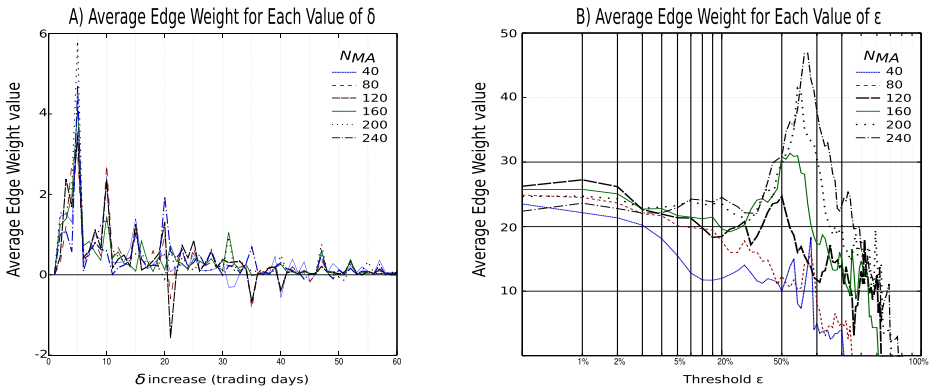


**Fig. 2.** Graphs showing the change in: (A) average edge weight with each increment of  $\delta$  using the *Buy* comparison; (B) average edge weight and number of nodes with each  $\epsilon_{t+1} = \epsilon_t + 1\%$  increment in the threshold interval for  $\delta = 30$  using the *Buy* comparison.

*Moving Average Size,  $N_{MA}$*  The choices for available moving average sizes were based on [4] and the graphs show that maximizing this parameter yields the best results and even raises the question of how further increases in the size would fare. The user still needs to take into account of what it means to increase the moving average size: the bigger it is the moving average, the smoother the curve will be and thus it will behave like a noise filter (ie., by becoming less and less sensitive to small changes in the behavior of the product). The values overlap for small  $\epsilon$  values and it is hard to read the effects of the first increments in a linear scale, so Fig. 2B uses a logarithmic scale for representing  $\epsilon$  values, showing that the 240 and 120 moving average sizes have a very similar behavior. The average weight for a moving average of 120 days has a higher starting value than the 240 days one, this means that for a buy signal best thresholds are:  $\epsilon = 1\% \wedge \delta = 30 \wedge N_{MA} = 120$ . Fig. 3 shows that it is possible to find more than just sequential patterns with this parameters.

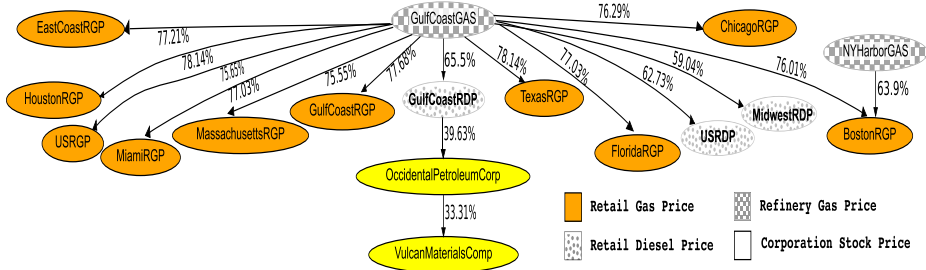


**Fig. 3.** Part of the graph showing the resulting Buy tree after applying Ramex Forum on the data with the selected parameters.

In the complete result graph (available in [3]) colors were added to each node according to their product type. These colors show a clear grouping of product types, with same color nodes mostly close to each other. This was expected for gas to gas and diesel to diesel influences. However even the stock, refinery, and reference benchmark prices tend to group together at least in pairs. Furthermore, refineries are almost exclusively related to the same type of product, gas producing refineries are connected to retail gas prices and diesel producing refineries are connected to diesel retail prices. The Gulf Coast GAS refinery node (Fig. 2) does not exactly meet the previous observation as it is shown influencing some diesel products, even so, this might be a positive thing as it will alert an attentive analyst to the weight behind the Gulf Coast refinery gas prices. After further analysis Gulf Coast GAS is identified as the most influential node as it has at least one detected event for all other products and its average edge weight is the highest by a margin of 5%, probably due to huge oil production in this area it is mostly the start of oil production chain. In [3], it was also observed that specificities of gas usage in the Rocky Mountain retail gas price could trigger third level dependences. Next the most glaring aspect of the graph is how influential specific products are, the tree is not just an assorted web of relations but groups of products aggregating around very influential/influenced products. There are some expected trend setters like the OPECBasket that is used as a benchmark for oil price, the Gulf Coast refineries and then some unexpected like the Minnesota retail gas price. For other tested data and parameters, equal graphs were observed. Indeed, color coding also showed very similar results with strong groupings of colors and some few select products influencing groups of others.

## 4 Conclusions

The presented case study, using real world data and deep analysis, aims to provide an illustrative and useful example of Ramex-Forum: the signal-to-noise ratio on the Petroleum production chain analysis already shows that sequential

patterns of prices can provide a much deeper description of product dependencies based on events. Moreover the  $\delta$  and  $\epsilon$  parameters seem both consistent, intuitive and adaptable alternative for measuring long term dependencies that are not directly possible with more instantaneous methods. So far only the connections themselves have been considered, if the influence weights are also taken into account the analysis becomes more complex. Future work in this area should extend the number of products used and their detail. Some related studies (namely [7]) show that less classical hybrid approaches can be used to complement the crossover event detection approach and are good candidates for future experiments. Of particular interest will be to include a better characterization of algorithm behavior during a global market crisis, namely by quantifying the drives and consequences of the recent crisis in oil prices.

**Acknowledgments.** This research is supported by the GoBusiness Research project (<http://www.gobusinessfinance.ch/en/research>). The authors would like to thank GoBusiness Finance for partial financial support and for data sets and financial knowledge used in present work.

## References

1. Borenstein, S., Shepard, A.: Sticky Prices, Inventories, and Market Power in Wholesale Gasoline Markets. NBER working paper series, vol. 5468. National Bureau of Economic Research (1996)
2. Suviolahti, H.: The influence of volatile raw material prices on inventory valuation and product costing. Master Thesis, Department of Business Technology, Helsinki School of Economics (2009)
3. Tiple, P.: Tool for discovering sequential patterns in financial markets. Master Thesis in Engenharia Informática, Faculdade de Ciências e Tecnologia da Universidade Nova de Lisboa (2014)
4. Marques, N.C., Cavique, L.: Sequential pattern mining of price interactions. In: Advances in Artificial Intelligence – Proceedings of the Workshop Knowledge Discovery and Business Intelligence, EPIA-KDBI, Portuguese Conference on Artificial Intelligence, pp. 314–325 (2013)
5. Gary, J., Handwerk, G.: Petroleum Refining. Institut français du pétrole publications. Taylor & Francis (2001)
6. Hammoudeh, S., Ewing, B.T., Thompson, M.A.: Threshold cointegration analysis of crude oil benchmarks. The Energy Journal **29**(4), 79–96 (2008)
7. Matos, D., Marques, N., Cardoso, M.: Stock market series analysis using self-organizing maps. Revista de Ciências da Computação **9**(9), 79–90 (2014)

# Geocoding Textual Documents Through a Hierarchy of Linear Classifiers

Fernando Melo and Bruno Martins<sup>(✉)</sup>

Instituto Superior Técnico and INESC-ID, Universidade de Lisboa, Lisbon, Portugal  
[{fernando.melo,bruno.g.martins}@ist.utl.pt](mailto:{fernando.melo,bruno.g.martins}@ist.utl.pt)

**Abstract.** In this paper, we empirically evaluate an automated technique, based on a hierarchical representation for the Earth's surface and leveraging linear classifiers, for assigning geospatial coordinates to previously unseen documents, using only the raw text as input evidence. We measured the results obtained with models based on Support Vector Machines, over collections of geo-referenced Wikipedia articles in four different languages, namely English, German, Spanish and Portuguese. The best performing models obtained state-of-the-art results, corresponding to an average prediction error of 83 Kilometers, and a median error of just 9 Kilometers, in the case of the English Wikipedia collection.

**Keywords:** Text mining · Document geocoding · Hierarchical text classification

## 1 Introduction

Geographical Information Retrieval (GIR) has recently captured the attention of many different researchers that work in fields related to language processing and to the retrieval and mining of relevant information from large document collections. For instance, the task of resolving individual place references in textual documents has been addressed in several previous works, with the aim of supporting subsequent GIR processing tasks, such as document retrieval or the production of cartographic visualizations from textual documents [5,6]. However, place reference resolution presents several non-trivial challenges [8,9], due to the inherent ambiguity of natural language discourse. Moreover, there are many vocabulary terms, besides place names, that can frequently appear in the context of documents related to specific geographic areas [1]. Instead of resolving individual references to places, it may be interesting to instead study methods for assigning entire documents to geospatial locations [1,11].

In this paper, we describe a technique for assigning geospatial coordinates of latitude and longitude to previously unseen textual documents, using only the raw text of the documents as evidence, and relying on a hierarchy of linear models built with basis on a discrete hierarchical representation for the Earths surface, known in the literature as the HEALPix approach [4]. The regions at each level of this hierarchical representation, corresponding to equally-distributed curvilinear

and quadrilateral areas of the Earth's surface, are initially associated to textual contents (i.e., we use all the documents from a training set that are known to refer to particular geospatial coordinates, associating each text to the corresponding region). For each level in the hierarchy, we build classification models using the textual data, relying on a vector space model representation, and using the quadrilateral areas as the target classes. New documents are assigned to the most likely quadrilateral area, through the usage of the classifiers inferred from training data. We finally assign documents to their respective coordinates of latitude and longitude, taking the centroid coordinates from the quadrilateral areas.

The proposed document geocoding technique was evaluated with samples of geo-referenced Wikipedia documents in four different languages. We achieved an average prediction error of 83 Kilometers, and a median error of just 9 Kilometers, in the case of documents from the English Wikipedia. These results are slightly better than those reported in previous state-of-the-art studies [11, 12].

## 2 Previous and Related Work

While most work on geographic information retrieval relies on specific keywords such as place names, Adams and Janowicz proposed an approach for geocoding documents that uses only non-geographic expressions, concluding that even ordinary textual terms may be good predictors of geographic locations [1]. The proposed technique used Latent Dirichlet Allocation (LDA) to discover latent topics from general vocabulary terms occurring in a training collection of geo-referenced documents, together with Kernel Density Estimation (KDE) to interpolate a density surface, over each LDA topic. New documents are assigned to the geospatial areas having the highest aggregate density, computed from the per-document topic distributions and from the KDE surfaces.

Wing and Baldridge evaluated approaches for automatically geocoding documents based on their textual contents, specifically leveraging generative language models learned from Wikipedia [11]. The authors applied a regular geodesic grid to divide the Earth's surface into discrete rectangular cells. Each cell can be seen as a virtual document that concatenates all the training documents located within the cell's region. Three different methods were compared in the task of finding the most similar cell, for a new document, namely (i) the Kullback-Leibler divergence, (ii) naïve Bayes, and (iii) a baseline method corresponding to the average cell probability. Method (i) obtained the best results, i.e. a median prediction error of just 11.8 Kilometers, and a mean error of 271 Kilometers, on tests with documents taken from the English Wikipedia. More recently, Dias et al. [2] reported on experiments with an adapted version of the method described by Wing and Baldridge, which used language models based on character  $n$ -grams together with a discrete representation for the surface of the Earth based on an equal-area hierarchical triangular mesh approach [3]. Another improvement over the language modeling method was latter reported by Roller et al. [7], where the authors collapsed nearby training documents through the

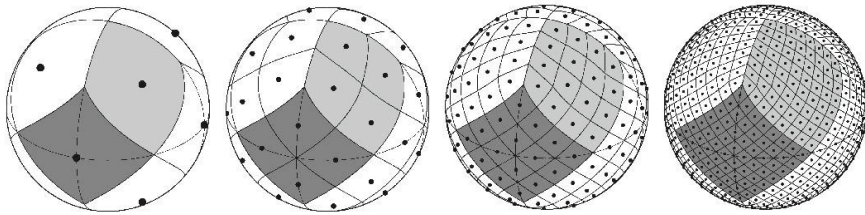


**Fig. 1.** Orthographic views associated to the first four levels of the HEALPix sphere tessellation.

usage of a k-d tree data structure. Moreover, Roller et al. proposed to assign the centroid coordinates of the training documents contained in the most probable cell, instead of just using the center point for the cell. These authors report on a mean error of 181 Kilometers and a median error of 11 Kilometers, when geocoding documents from the English Wikipedia.

More recently, Wing and Baldridge also reported on tests with discriminative classifiers [12]. To overcome the computational limitations of discriminative classifiers, in terms of the maximum number of classes they can handle, the authors proposed to leverage a hierarchical classification procedure that used feature hashing and an efficient implementation of logistic regression. In brief, the authors used an hierarchical approach in which the Earth's surface is divided according to a rectangular grid (i.e., using either a regular grid or a k-d tree), and where an independent classifier is learned for every non-leaf node of the hierarchy. The probability of any node in the hierarchy is the product of the probabilities of that node and all of its ancestors, up to the root. The most probable leaf node is used to infer the final geospatial coordinates. Rather than greedily using the most probable node from each level, or rather than computing the probability of every leaf node, the authors used a stratified beam search. This procedure starts at the root, keeping the  $b$  highest-probability nodes at each level, until reaching the leafs. Wing and Baldridge report on results over English Wikipedia data corresponding to a mean error of 168.7 Kilometers and a median error of 15.3 Kilometers.

### 3 The Proposed Document Geocoding Method

The proposed document geocoding approach is based on discretizing the surface of the Earth into hierarchically organized sets of regions, as given by the HEALPix procedure and where each set corresponds to a different partitioning resolution. Having documents associated to these discrete regions allows us to predict locations with standard discriminative classification approaches (e.g., with linear Support Vector Machines classifiers).

HEALPix is an acronym for Hierarchical Equal Area isoLatitude Pixelization of a sphere, and the procedure results on a multi level recursive subdivision

**Table 1.** Number of regions and approximate area for HEALPix grids of different resolutions.

Resolution	4	64	256	1024
Total number of regions	192	49,152	786,432	12,582,912
Approximate area of each region (Km <sup>2</sup> )	2,656,625	10,377	649	41

for a spherical approximation to the Earth’s surface, according to curvilinear quadrilateral regions, in which each resulting subdivision covers an equal surface area. Figure 3, adapted from an original illustration provided in the HEALPix website<sup>1</sup>, shows from left to right the resolution increase by three steps from the base level with 12 different regions [4].

The HEALPix representation scheme contains a parameter  $N_{side}$  that controls the resolution, i.e. the number of divisions along the side of a base-resolution region that is needed to reach a desired high-resolution partition, and which naturally will also define the area of the curvilinear quadrilaterals. In our experiments, we used a hierarchy of 4 different representations with different resolutions, equaling the  $N_{side}$  parameter to the values of 4, 64, 256 and 1024. Table 1 presents the total number of regions in each of the considered resolution levels (i.e.,  $n = 12 \times N_{side}^2$ ), together with the approximate area, in squared Kilometers, corresponding to each region.

Another important question relates to the choice of how to represent the textual documents. We used a vector space model representation, where each document is seen as a vector of features. The feature weights in the vectors that represent each document are given according to the term frequency times inverse document frequency (TF-IDF) scheme, where the weight for a term  $i$  on a document  $j$  can be computed as:

$$\text{TF-IDF}_{i,j} = \log_2(1 + \text{TF}_{i,j}) \times \log_2 \left( \frac{N}{n_i} \right) \quad (1)$$

In the formula,  $\text{TF}_{i,j}$  is the term frequency for term  $i$  on document  $j$ ,  $N$  is the total number of documents in the collection, and  $n_i$  is the number of documents containing the term  $i$ . The TF-IDF weight is 0 if  $\text{TF}_{i,j} = 0$ .

With the hierarchy of discrete representations given by the HEALPix method, together with the document representations based on TF-IDF, we then used linear classification algorithms to address the document geocoding task. We trained a separate classification model for each node in the hierarchy of discrete representations, taking all documents whose coordinates lay within the region corresponding to each node, as the training data for each classifier. When geocoding a test document, we first apply the root-level classifier to decide the most likely region, and then proceed greedily by applying the classifier for each of the most likely nodes, up to the leafs. After reaching a leaf region from the

---

<sup>1</sup> <http://healpix.jpl.nasa.gov>

hierarchical representation, the geospatial coordinates of latitude and longitude are assigned by taking the centroid coordinates of the leaf region.

Support Vector Machines (SVMs) are one of the most popular approaches for learning classifiers from training data. In our experiments, we used the multi-class linear SVM implementation from scikit-learn<sup>2</sup> with default parameters (e.g., with the default regularization constant), which in turn is a wrapper over the LIBLINEAR<sup>3</sup> package.

## 4 Experimental Validation

In our experiments, we used samples with geocoded articles from the English (i.e., 847,783 articles), German (i.e., 307,859 articles), Spanish (i.e., 180,720 articles) and Portuguese (i.e., 131,085 articles) Wikipedias, taken from database dumps produced in 2014. Separate experiments evaluated the quality of the document geocoders built for each of the four languages, in terms of the distances from the predictions towards the correct geospatial coordinates. We processed the Wikipedia dumps to extract the raw text from the articles, and for extracting the geospatial coordinates of latitude and longitude from the corresponding infoboxes. We used 90% of the geocoded articles of each Wikipedia for model training, and the other 10% for model validation.

In what regards the geospatial distributions of documents, we have that some regions (e.g, North America or Europe) are considerable more dense in terms of document associations than others (e.g, Africa), and that oceans and other large masses of water are scarce in associations to Wikipedia documents. This implies that the number of classes that has to be considered by our model is much smaller than the theoretical number of classes given by the HEALPix procedure. In our English dataset, there are a total of 286,966 regions containing associations to documents at a resolution level of  $N_{side} = 1024$ , and a total of 82,574, 15,065, and 190 regions, respectively at resolutions 256, 64, and 4. These numbers are even smaller in the collections for the other languages.

Table 2 presents the obtained results for the different Wikipedia collections. The prediction errors shown in Table 2 correspond to the distance in Kilometers, computed through Vincenty’s geodetic formulae [10], from the predicted locations to the true locations given in Wikipedia. The accuracy values correspond to the relative number of times that we could assign documents to the correct region (i.e., the HEALPix region where the document’s true geospatial coordinates of latitude and longitude are contained), for each level of hierarchical classification. Table 2 also presents upper and lower bounds for the average and median errors, according to a 95% confidence interval and as measured through a sampling procedure.

The results attest for the effectiveness of the proposed method, as we measured slightly inferior errors than those reported in previous studies [2, 7, 11, 12], which besides different classifiers also used simpler procedures for representing

---

<sup>2</sup> <http://scikit-learn.org/>

<sup>3</sup> <http://www.csie.ntu.edu.tw/~cjlin/liblinear/>

**Table 2.** The results obtained for each different language.

	Classifier accuracy				Errors in terms of distance	
	1st	2nd	3rd	4th	Average	Median
English	0.966	0.785	0.540	0.262	82.501 ( $\pm 4.340$ )	8.874 [5.303 - 15.142]
German	0.972	0.832	0.648	0.396	62.995 ( $\pm 5.753$ )	4.974 [3.615 - 8.199]
Spanish	0.950	0.720	0.436	0.157	165.887 ( $\pm 16.675$ )	13.410 [8.392 - 22.691]
Portuguese	0.951	0.667	0.336	0.104	105.238 ( $\pm 10.059$ )	21.872 [13.611 - 33.264]

textual contents and for representing the geographical space. It should nonetheless be noted that the datasets used in our tests may be slightly different from those used in previous studies (e.g., they were taken from different Wikipedia dumps), despite their similar origin.

## 5 Conclusions and Future Work

Through this work, we empirically evaluated a simple method for geo-referencing textual documents, relying on a hierarchy of linear classifiers for assigning documents to their corresponding geospatial coordinates. We have shown that the automatic identification of the geospatial location of a document, based only on its text, can be performed with high accuracy by using out-of-the-box implementations of well-known supervised classification methods, and leveraging a hierarchical procedure based on HEALPix [4].

Despite the interesting results, there are also many ideas for future work. The geospatial coordinates estimated from our document geocoding procedure can for instance be used as prior evidence (i.e., as document-level priors) to support the resolution of individual place references in text [8]. In terms of future work, we would also like to experiment with other types of classification approaches and with different text representation and feature weighting schemes.

**Acknowledgments.** This work was supported by Fundação para a Ciência e a Tecnologia (FCT), through project grants with references EXCL/EEI-ESS/0257/2012 (DataStorm research line of excellency), EXPL/EEI-ESS/0427/2013 (KD-LBSN), and also UID/CEC/50021/2013 (INESC-ID's associate laboratory multi-annual funding).

## References

1. Adams, B., Janowicz, K.: On the geo-indicativeness of non-georeferenced text. In: Proceedings of the International AAAI Conference on Weblogs and Social Media (2012)
2. Dias, D., Anastácio, I., Martins, B.: A language modeling approach for georeferencing textual documents. Actas del Congreso Español de Recuperación de Información (2012)
3. Dutton, G.: Encoding and handling geospatial data with hierarchical triangular meshes. In: Kraak, M.J., Molenaar, M., (eds.) Advances in GIS Research II. CRC Press (1996)

4. Górski, K.M., Hivon, E., Banday, A.J., Wandelt, B.D., Hansen, F.K., Reinecke, M., Bartelmann, M.: HEALPIX - a framework for high resolution discretization, and fast analysis of data distributed on the sphere. *The Astrophysical Journal* **622**(2) (2005)
5. Lieberman, M.D., Samet, H.: Multifaceted toponym recognition for streaming news. In: Proceedings of the International ACM SIGIR Conference on Research and Development in Information Retrieval (2011)
6. Mehler, A., Bao, Y., Li, X., Wang, Y., Skiena, S.: Spatial analysis of news sources. *IEEE Transactions on Visualization and Computer Graphics* **12**(5) (2006)
7. Roller, S., Speriosu, M., Rallapalli, S., Wing, B., Baldridge, J.: Supervised text-based geolocation using language models on an adaptive grid. In: Proceedings of the Conference on Empirical Methods on Natural Language Processing (2012)
8. Santos, J., Anastácio, I., Martins, B.: Using machine learning methods for disambiguating place references in textual documents. *GeoJournal* **80**(3) (2015)
9. Speriosu, M., Baldridge, J.: Text-driven toponym resolution using indirect supervision. In: Proceedings of the Annual Meeting of the Association for Computational Linguistics (2013)
10. Vincenty, T.: Direct and inverse solutions of geodesics on the ellipsoid with application of nested equations. *Survey Review* **XXIII**(176) (1975)
11. Wing, B., Baldridge, J.: Simple supervised document geolocation with geodesic grids. In: Proceedings of the Annual Meeting of the Association for Computational Linguistics (2011)
12. Wing, B., Baldridge, J.: Hierarchical discriminative classification for text-based geolocation. In: Proceedings of the Conference on Empirical Methods on Natural Language Processing (2014)

# A Domain-Specific Language for ETL Patterns Specification in Data Warehousing Systems

Bruno Oliveira<sup>(✉)</sup> and Orlando Belo

Algoritmi R&D Centre, Department of Informatics, School of Engineering,  
University of Minho, Campus de Gualtar, 4710-057 Braga, Portugal  
[obelo@di.uminho.pt](mailto:obelo@di.uminho.pt)

**Abstract.** During the last few years many research efforts have been done to improve the design of ETL (Extract-Transform-Load) systems. ETL systems are considered very time-consuming, error-prone and complex involving several participants from different knowledge domains. ETL processes are one of the most important components of a data warehousing system that are strongly influenced by the complexity of business requirements, their changing and evolution. These aspects influence not only the structure of a data warehouse but also the structures of the data sources involved with. To minimize the negative impact of such variables, we propose the use of ETL patterns to build specific ETL packages. In this paper, we formalize this approach using BPMN (Business Process Modelling Language) for modelling more conceptual ETL workflows, mapping them to real execution primitives through the use of a domain-specific language that allows for the generation of specific instances that can be executed in an ETL commercial tool.

**Keywords:** Data warehousing systems · ETL conceptual modelling · ETL patterns · BPMN specification models · Domain-Specific languages

## 1 Introduction

Commercial tools that support ETL (Extract, Transform, and Load) processes development and implementation have a crucial impact in the implementation of any data warehousing system populating process. They provide the generation of very detailed models under a specific methodology and notation. Usually, such kind of documentation follows a proprietary format, which is intrinsically related to architectural issues of the development tool. For that reason, ETL teams must have skills and experience on such tools that allow for them to use and explore appropriately the tools. In the case of a migration process of ETL migration to another ETL tool environment, the ETL development team will need to understand all specificities provided by the new tool and start a new project often almost from scratch. We believe that ETL systems development requires a simply and reliable approach. A more abstract view of the processes and data structures is very convenient as well as a more effective mapping to some kind of execution primitives allowing for its execution inside the environments of commercial tools. Using a pallet of specific ETL patterns representing some of the most used ETL tasks in real world applica-

tion scenarios – e.g. *Surrogate Key Pipelining* (SKP), *Slowly Changing Dimensions* (SCD) or *Change Data Capture* (CDC) –, we designed a new ETL development layer on top of a traditional method, making possible to use ETL tools from the very beginning of the project, in order to plan and implement more appropriated ETL processes. To do that we used the *Business Process Modelling Notation* (BPMN) [1] for ETL processes representation, extending its original meta-model for including the ETL pattern specification we designed. The inclusion of these patterns distinguishes clearly two very relevant aspects in ETL design and implementation: process flow coordination and data processing tasks. BPMN is very suitable for this kind of processes, simply because it provides some very convenient features like expressiveness and flexibility on the specification of processes. Thus, after a brief exposure of some related work (section 2), we present and discuss briefly a demonstration scenario using one of the most useful (and crucial) ETL process: a *Data Quality Enhancement* (DQE) (section 3). Next, in section 4, we present a DQE specification skeleton, its internal behaviour and how we can configure using a *Domain-Specific Language* (DSL) to enable its execution. Finally, we discuss the experiments done so far, analysing results and presenting some conclusions and future work (section 5).

## 2 Related Work

With the exception of some low-level methods for ETL development [2], most approaches presented so far use conceptual or logical models as the basis for ETL modelling. Such models reduce complexity, produce detailed documentation and provide the ability to easily communicate with business users. Some of the proposals presented by Vassiliadis and Simitsis cover several aspects of ETL conceptual specification [3], its representation using logical views [4, 5], and its implementation using a specific ETL tool [6]. Later, Trujillo [7] and Muñoz [8] provided an UML extension for ETL conceptual modelling, reducing some of the communication issues that the proposal of Vassiliadis et al. revealed previously. However, the translation to execution primitives they made was not very natural, since UML is essentially used to describe system requirements and not to support its execution. The integration of existing organizational tasks with ETL processes was addressed by Wilkinson et al. [9], which exposed a practical approach for the specification of ETL conceptual models using BPMN. BPMN was firstly introduced by Akkaoui and Zimanyi [10] on ETL systems specification. Subsequently, Akkaoui et al. [11] provided a BPMN-based meta-model for an independent ETL modelling approach. They explored and discussed the bridges to a model-to-text translation, providing its execution in some ETL commercial tools. Still using BPMN notation, Akkaoui et al. [12] provided a BPMN meta-model covering two important architectural layers related to the specification of ETL processes. More recently and following the same guidelines from previous works, Akkaoui et al. [13] disposed a framework that allows for the translation of abstract BPMN models to its concrete execution in a target ETL tool using model-to-text transformations.

### 3 Pattern-Based ETL Modelling

We designed a high-level approach for ETL conceptual modelling using patterns. An ETL pattern is a task class that is characterized using a set of pre-established activities (internal composition) and their correspondent input and output interfaces, i.e. how the pattern interacts within a workflow context. Patterns avoid rewriting some of the most repetitive tasks that are used regularly in an ETL system. The use of ETL patterns produces simpler conceptual models, because finer grain tasks will be omitted from the global ETL schema. The descriptive models provided by BPMN supported all this. Using the ETL terminology, we defined three categories of ETL patterns: (1) Gathers that represent typical data extraction processes; (2) Transformers, which are used for data transformations such as cleaning or conforming tasks, and (3) Loaders, which are used to load data into the data warehouse repository. With these categories we can group all the most frequent ETL patterns and we can identify in a conventional ETL system all its operational stages.

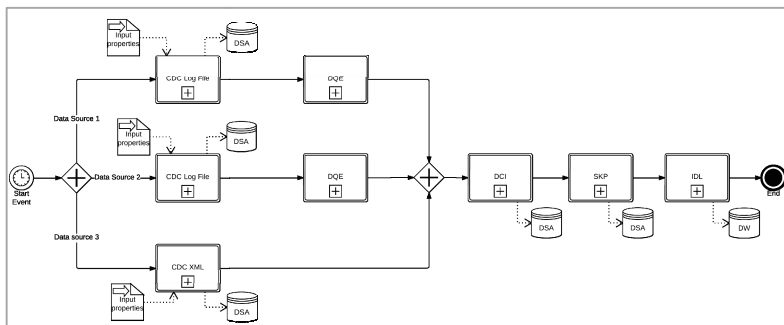


**Fig. 1.** A BPMN pattern specification for an ETL process

To demonstrate the application of ETL patterns in an ETL system solution we selected a simple application case. We represent the whole process with the ETL patterns we proposed using the BPMN notation, both in terms of the data orchestration and the representation of composite tasks. The process begins with a ‘Start Event’ having a ‘Timer’ representing an automatic execution of the process according to a specific time frame. This process starts with a parallel invocation of two data flows using a parallel gateway (Fig. 1). For each data source, a CDC pattern was used for data extraction. For the first and second flow, two other CDC patterns acting over log files were used. In the third flow we selected another CDC pattern for working with XML data structures. These tasks have the ability to identify new, updated, or deleted records, extracting and putting them into a *Data Staging Area* (DSA). We used BPMN ‘Data input’ and ‘Data Store’ objects to represent the input/output interfaces for each pattern. On the first two flows, we used a DQE pattern configured with some specific data cleaning and data conforming procedures. Next, the remaining two flows were synchronized using a parallel gateway, being data integrated using a *data conciliation pattern* (DCI) to identify common records based on a specific set of conciliation rules. Posteriorly, a SKP pattern

assigns the surrogate keys to the data extracted, maintaining the correspondence meta-data stored in specific mapping tables located in the DSA. After the SKP process appears an IDL pattern that loads data into the data warehouse, establishing all the necessary correspondences to the data warehouse schema.

## 4 Specification of a DQE Pattern

Usually, operational data are stored in specific data schemas built to serve particular business needs. Independently from the sources involved (single or multiple), many problems can occur at schema and instance level when executing a loading data process [14]. Several procedures can be applied on transformation and cleaning tasks to eliminate problems like these to avoid schema ambiguities, data inconsistencies, data entry errors, missing information or invalid data. To instantiate patterns a generator should know how they must be created following a specific template. In particular, for ETL processes the description of the structure of a pattern was studied already [15]. We do not intend to describe patterns in a natural language but essentially using some descriptive primitives to support their instantiation. For that, we divide ETL patterns specification in three parts: 1) input meta-data for pattern execution, which is composed by source schema(s), attribute(s) and the procedures that should be applied to the source data; 2) output meta-data, which describes the output schemas in which output data will be stored; and 3) exception handling, which represents the identification of unexpected scenarios and correspondent policies to perform. To receive these configuration aspects, we developed a DSL for configuring the components of ETL patterns. The use of a DSL facilitates pattern configuration and provides the necessary meanings to make it suitable for computer interpretation. One of the most common DQE procedures is the decomposition of a string in its meaningful parts. The decomposition of an attribute typically involves several database attributes such as a name or an address. Usually, these attributes need to be decomposed in  $n$  parts according to a certain condition.

```
Use Decomposition[
  Header:
    [Name: 'DecTask',
     Description: 'Decomposition ...']
  Content:
    [Id: AUTO,
     Input[Schema= 'Sale',
      Attribute= 'FullName']
    Output[Schema= 'SaleT',
      Attributes: [FirstName String;
      LastName String;]]
    Rule[Regex= '\s',
      Limit [FIRST, LAST]]]
Use Decomposition[
  Header: [...],
  Content: [...]
  Exception:
    [Event= EmptyAttribute,
     Action: Compensation:
       Quarantine[Table= 'CustomerQ'],
     Log: [Name= 'CustomerLog',
        Type= RelationalTable,
        Details[DATE AS 'mydate',
        SOURCETABLE AS 'mytable',
        SOURCEATTRIBUTE AS myAttr']]])
    [Event= InvalidDecompositionRule,
     Action: Error= Terminate [...]]]
```

**Fig. 2.** A decomposition procedure (left) and its exception handling description (right)

Fig. 2 shows an example of the DSL proposed for a typical decomposition procedure used as sub-part of a DQE pattern that splits the customer full name in two new attributes: 'FirstName' and 'LastName'. The decomposition rule is performed based on a regular expression: '\s', which means that an original string must be split using a

space as delimiter. The pattern configuration starts with the description of the pattern, using the ‘Name’ and the ‘Description’ keywords inside of a ‘Header’ block. Blocks are identified using square brackets delimiters. Next, a decomposition block is used in order to describe the internal components of a decomposition pattern. This block must have an internal ‘ID’, which can be manually or automatically assigned (‘AUTO’ keyword). Next, three blocks are used: ‘Input’ block for input metadata, ‘Output’ block for output metadata, and ‘Rule’ for a decomposition rule specification. Both input and output blocks use a target data schema name storing the original/resulted data, and a collection of attributes (and data types) used for each block. We distinguished single assignments (a singular value) and composite assignments (composite data structures) using an equal operator for atomic attributions and square brackets for composite attributions. The ‘Rule’ block describes the regular expression that should be applied to the original string using the ‘Regex’ keyword. The ‘Limit’ keyword is used to control the number of times that a pattern is applied affecting the length of the returned result set. Two special identifiers (‘FIRST’ and ‘LAST’) are used to extract the first and last occurrence matching the regular expression. The results of the output rule (‘FirstName’ and ‘LastName’) are mapped to the ‘Output’ attributes. The DSL also includes some compensation and error exception statements associated to each pattern. The compensation events provide an alternative approach to handle a specific exception event, e.g. storing the non-conform records in quarantine tables for later evaluation or applying automatic error. The error events block or end the process execution. Fig. 2 (right) presents an exception block with compensation and error policies associated. The ‘Exception’ block is formed by three mandatory constructs: 1) Event that specifies an exception that may occur, e.g. ‘EmptyAttribute’ or ‘InvalidDecompositionRule’; 2) Action that identifies the action that should be performed, e.g. record that started the exception can be stored to specific quarantine table or can abort the workflow; and 3) Log activity that stores the exception occurrences to a specific log file structure. With these domain-level instructions, it is possible generating dynamically the instances following the language rules. For that, we can implement code generators to translate the DSL to specifics formats supported by ETL commercial tools.

## 5 Conclusions and Future Work

In this paper we showed how a typical ETL process can be represented exclusively using ETL patterns on BPMN models, and how these patterns can be integrated in a single ETL system package. To demonstrate their practical application, we selected and discussed a DQE pattern, describing its internal composition and providing a specific DSL for its configuration. From a conceptual modelling point of view, we consider that ETL models should not include any kind of implementation infrastructure specification or any criteria associated with its execution. All infrastructures that support the implementation of conceptual models are related to specific classes of users involving therefore the application of specific constructors. The BPMN provides this kind of abstraction, focusing essentially on the coordination of ETL patterns, promoting the reusability of patterns across several systems, and making the system more robust to process changes. Additionally, the DSL proposed dispose an effective way to formalize each pattern configuration, allowing for its posterior mapping to a programming language such

as Java. Using a domain-level DSL it is possible to describe more naturally each part of an ETL process without having the need to program each component. In the short term, we intend to have an extended family of ETL patterns that will allow for building a complete ETL system from scratch, covering all coordination and communication aspects as well as the description of all the tasks required to materialize it. Additionally, a generic transformation plug-in for generating ETL physical schemas for data integration tools is also planned.

## References

1. OMG, Documents Associated With Business Process Model And Notation (BPMN) Version 2.0 (2011)
2. Thomsen, C., Pedersen, T.B.: Pygrametl: a powerful programming framework for extract-transform-load programmers. In: Proceeding of the ACM Twelfth International Workshop on Data Warehousing and OLAP, DOLAP 2009, pp. 49–56 (2009)
3. Vassiliadis, P., Simitsis, A., Skiadopoulos, S.: Conceptual modeling for ETL processes. In: Proceedings of the 5th ACM International Workshop on Data Warehousing and OLAP, DOLAP 2002, pp. 14–21 (2002)
4. Vassiliadis, P., Simitsis, A., Skiadopoulos, S.: On the logical modeling of ETL processes. In: Pidduck, A., Mylopoulos, J., Woo, C.C., Ozsu, M. (eds.) CAiSE 2002. LNCS, vol. 2348, pp. 782–786. Springer, Heidelberg (2002)
5. Simitsis, A., Vassiliadis, P.: A method for the mapping of conceptual designs to logical blueprints for ETL processes. *Decis. Support Syst.* **45**, 22–40 (2008)
6. Vassiliadis, P., Vagena, Z., Skiadopoulos, S., Karayannidis, N., Sellis, T.: Arktos: A Tool for Data Cleaning and Transformation in Data Warehouse Environments. *IEEE Data Eng. Bull.* **23**(4), 42–47 (2000)
7. Luján-Mora, S., Trujillo, J., Song, I.-Y.: A UML profile for multidimensional modeling in data warehouses. *Data Knowl. Eng.* **59**, 725–769 (2006)
8. Trujillo, J., Luján-Mora, S.: A UML based approach for modeling ETL processes in data warehouses. *Concept. Model.* **28***13*, 307–320 (2003)
9. Wilkinson, K., Simitsis, A., Castellanos, M., Dayal, U.: Leveraging business process models for ETL design. In: Parsons, J., Saeki, M., Shoval, P., Woo, C., Wand, Y. (eds.) ER 2010. LNCS, vol. 6412, pp. 15–30. Springer, Heidelberg (2010)
10. El Akkaoui, Z., Zimányi, E.: Defining ETL workflows using BPMN and BPEL. In: Proceedings of the ACM Twelfth International Workshop on Data Warehousing and OLAP, DOLAP 2009, pp. 41–48 (2009)
11. El Akkaoui, Z., Zimányi, E., Mazón, J.-N., Trujillo, J.: A model-driven framework for ETL process development. In: Proceedings of the ACM 14th International Workshop on Data Warehousing and OLAP, DOLAP 2011, pp. 45–52 (2011)
12. El Akkaoui, Z., Mazón, J.-N., Vaisman, A., Zimányi, E.: BPMN-based conceptual modeling of ETL processes. In: Cuzzocrea, A., Dayal, U. (eds.) DaWaK 2012. LNCS, vol. 7448, pp. 1–14. Springer, Heidelberg (2012)
13. El Akkaoui, Z., Zimányi, E., Mazon, J.-N., Trujillo, J.: A BPMN-based design and maintenance framework for ETL processes. *Int. J. Data Warehos. Min.* **9**, 46 (2013)
14. Rahm, E., Do, H.: Data cleaning: Problems and current approaches. *IEEE Data Eng. Bull.* **23**, 3–13 (2000)
15. Köppen, V., Brüggemann, B., Berendt, B.: Designing Data Integration: The ETL Pattern Approach. *Eur. J. Informatics Prof.* **XII** (2011)

# Optimized Multi-resolution Indexing and Retrieval Scheme of Time Series

Muhammad Marwan Muhammad Fuad<sup>(✉)</sup>

Forskningsparken 3, Institutt for Kjemi, NorStruct,  
The University of Tromsø – The Arctic University of Norway, 9037 Tromsø, Norway  
[marwan.fuad@uit.no](mailto:marwan.fuad@uit.no)

**Abstract.** Multi-resolution representation has been successfully used for indexing and retrieval of time series. In a previous work we presented Tight-MIR, a multi-resolution representation method which speeds up the similarity search by using distances pre-computed at indexing time. At query time Tight-MIR applies two pruning conditions to filter out non-qualifying time series. Tight-MIR has the disadvantage of storing all the distances corresponding to all resolution levels, even those whose pruning power is low. At query time Tight-MIR also processes all stored resolution levels. In this paper we optimize the Tight-MIR algorithm by enabling it to store and process only the resolution levels with the maximum pruning power. The experiments we conducted on the new optimized version show that it does not only require less storage space, but it is also faster than the original algorithm.

**Keywords:** Multi-resolution indexing and retrieval · Optimization · Tight-MIR · Time series

## 1 Introduction

A time series is a chronological collection of observations. The particular nature of these data makes them more appropriate to be handled as whole entities rather than separate numeric observations. In the last decade a great deal of research was devoted to the development of time series data mining because of its various applications in finance, medicine, engineering, and other domains.

Time series are usually represented by *Dimensionality Reduction Techniques* which map the time series onto low-dimension spaces where the query is processed.

Several dimensionality reduction techniques exist in the literature, of those we mention: *Piecewise Linear Approximation* (PLA) [1], and *Adaptive Piecewise Constant Approximation* (APCA) [2].

Multi-resolution dimensionality reduction techniques map the time series to several spaces instead of one. In a previous work [3] we presented a multi-resolution indexing and retrieval method of time series called Weak-MIR. Weak-MIR uses pre-computed distances and two filters to speed up the similarity search. In [4] we presented another multi-resolution indexing and retrieval method, MIR-X, which associates our multi-resolution approach with another dimensionality reduction technique. In a third work

[5] we introduced Tight-MIR which has the advantages of the two previously mentioned methods. Tight-MIR, however, stores distances corresponding to all resolution levels, even though some of them might have a low pruning power. In this paper we present an optimized version of Tight-MIR which stores and processes only the resolution levels with the maximum pruning power.

The rest of the paper is organized as follows: Section 2 is a background section. The optimized version is presented in Section 3 and tested in Section 4. We conclude this paper with Section 5.

## 2 Background

In [3] we presented *Multi-resolution Indexing and Retrieval Algorithm* (Weak-MIR). The motivation behind this method is that traditional dimensionality reduction techniques use a “one-resolution” approach to indexing and retrieval, where the dimension of the low-dimension space is selected at indexing time, so the performance of the algorithm at query time depends completely on the choice made at indexing time. But in practice, we do not necessarily know a priori the optimal dimension of the low-dimension space.

Weak-MIR uses a multi-resolution representation of time series. During indexing time the algorithm computes and stores distances corresponding to a number of resolution levels, with lower resolution levels having lower dimensions. The algorithm uses these pre-computed distances to speed up the retrieval process. The basis of Weak-MIR is as follows: let  $U$  be the original  $n$ -dimension space and  $R$  be a  $2m$ -dimension space, where  $2m \leq n$ . At indexing time each time series  $u \in U$  is divided into  $m$  segments each of which is approximated by a function (we used a first degree polynomial in [3]) so that the approximation error between each segment and the corresponding polynomial is minimal. The  $n$ -dimension vector whose components are the images of all the points of all the segments of a time series on that approximating function is called the *image vector* and denoted by  $\bar{u}$ . The images of the two end points of the segment are called the *main image* of that segment. The  $2m$  main images of each time series are the *projection vector*  $u^R$ .

Weak-MIR uses two distances, the first is  $d$  which is defined on a  $n$ -dimension space, so it is the distance between two time series in the original space, i.e.  $d(u_i, u_j)$ , or the distance between the original time series and its image vector, i.e.  $d(u_i, \bar{u}_i)$ . The second distance is  $d^R$  which is defined on a  $2m$ -dimension space, so it is the distance between two projection vectors, i.e.  $d^R(u_i^R, u_j^R)$ . We proved in [3] that  $d^R$  is a lower bound of  $d$  when the Minkowski distance is used.

The resolution level  $k$  is an integer related to the dimensionality of the reduced space  $R$ . So the above definitions of the projection vector and the image vector can be extended to further segmentation of the time series using different values  $\leq m_k$ . The image vector and the projection vector at level  $k$  are denoted by  $\bar{u}^{(k)}$  and  $u^{R(k)}$ , respectively.

Given a query  $(q, \varepsilon)$ , let  $\bar{u}, \bar{q}$  be the projection vectors of  $u, q$ , respectively, on their approximating functions, where  $u \in U$ . By applying the triangle inequality we get:

$$|d(u, \bar{u}) - d(q, \bar{q})| > \varepsilon \quad (1)$$

This relation represents a pruning condition which is the first filter of Weak-MIR. By applying the triangle inequality again we get:

$$d^R(u^{R(k)}, q^{R(k)}) > \varepsilon + d(q, \bar{q}^{(k)}) + d(u, \bar{u}^{(k)}) \quad (2)$$

This relation is the second filter of Weak-MIR.

In [4] we introduced MIR-X which combines a representation method with a multi-resolution time series. MIR-X uses one of the two filters that Weak-MIR uses together with the low-dimension distance of a time series dimensionality reduction technique. We showed how MIR-X can boost the performance of Weak-MIR.

In [5] we presented Tight-MIR which has the advantages of both Weak-MIR and MIR-X in that it is a standalone method, like Weak-MIR, yet it has the same competitive performance of MIR-X. In Tight-MIR instead of using the projection vector to construct the second filter, we access the raw data in the original space directly using a number of points that corresponds to the dimensionality of the reduced space at that resolution level. In other words, we use  $2m$  raw points, instead of  $2m$  main images, to compute  $d^R$ . There are several advantages to this modification; the first is that the new  $d^R$  is obviously tighter than  $d^R$  as computed in [4]. The second is that when using a Minkowski distance  $d^R$  is a lower bound of the original distance in the original space. The direct consequence of this is that the two distances  $d(q, \bar{q}^{(k)}), d(u, \bar{u}^{(k)})$  become redundant, so the second filter is overwritten by the usual lower bounding condition  $d^R(u^{R(k)}, q^{R(k)}) > r$ .

At indexing time the distances  $d(u, \bar{u}^{(k)}) \forall u \in U$  are computed and stored. At query time the algorithm starts at the lowest level and applies (1) to the first time series in  $U$ . If the time series is filtered out the algorithm moves to the next time series, if not, the algorithm applies equation (2). If all the time series in the database have been pruned the algorithm terminates, if not, the algorithm moves to a higher level.

Finally, after all levels have been exploited, we get a candidate answer set which we then scan sequentially to filter out all the non-qualifying time series and return the final answer set.

### 3 An Optimized Multi-resolution Indexing and Retrieval Scheme

The disadvantage of the indexing scheme presented in the previous section is that it is “deterministic”, meaning that at indexing time the time series are indexed using a top-down approach, and the algorithm behaves in a like manner at query time. If some resolution levels have low utility in terms of pruning power, the algorithm will still

use the pre-computed distances related to these levels, and at query time these levels will also be examined. Whereas the use of the first filter does not require any query time distance evaluation, applying the second does include calculating distances and thus we might be storing and calculating distances for little pruning benefit.

We propose in this paper an optimized multi-resolution indexing and retrieval scheme. Taking into account that the time series to which we apply equations (1) and (2) are those which have not been filtered out at lower resolution levels, this optimized scheme should determine the optimal combination of resolution levels the algorithm should keep at indexing time and consequently use at query time.

The optimization algorithm we use to solve this problem is the *Genetic Algorithm*. The Genetic Algorithm (GA) is a famous evolutionary algorithm that has been applied to solve a variety of optimization problems. GA is a population-based global optimization algorithm which mimics the rules of Darwinian selection in that weaker individuals have less chance of surviving the evolution process than stronger ones. GA captures this concept by adopting a mechanism that preserves the “good” features during the optimization process.

In GA a population of candidate solutions (*chromosomes*) explores the search space and exploits this by sharing information. These chromosomes evolve using genetic operations (selection, crossover, mutation, and replacement).

GA starts by randomly initializing a population of chromosomes inside the search space. The fitness function of these chromosomes is evaluated. According to the values of the fitness function new offspring chromosomes are generated through the aforementioned genetic operations. The above steps repeat for a number of generations or until a predefined stopping condition terminates the GA.

The new algorithm, which we call *Optimized Multi-Resolution Indexing and Retrieval* – O-MIR, works as follow; we proceed in the same manner described for Tight-MIR to produce  $k$  candidate resolution levels. The next step is handled by the optimizer to select  $op$  resolution levels of the  $k$  resolution levels, where these  $op$  levels provide the maximum pruning power. For the current version of our algorithm the number of resolution levels to be kept,  $op$ , is chosen by the user according to the storage and processing capacity of the system. In other words, our algorithm will decide which are the  $op$  optimal resolution levels to be kept out of the  $k$  resolution levels produced by the indexing step.

Notice that when  $op = 1$  we have one resolution level, which is the case with traditional dimensionality reduction techniques.

The optimization stage of O-MIR starts by randomly initializing a population of chromosomes  $V_j = \langle v_1^j, v_2^j, \dots, v_{op}^j \rangle$  where  $j = 1, \dots, popSize$  and where  $v_1^j < v_2^j < \dots < v_{op}^j$ . Each chromosome represents a possible configuration of the resolution levels to be kept. The fitness function of our optimization problem is the pruning power of this configuration. As in [5], the performance criterion is based on the latency time concept presented in [6]. The latency time is calculated by the number of cycles the processor takes to perform the different arithmetic operations ( $>, + - , *, \text{abs}, \text{sqrt}$ ) which are required to execute the similarity search query. This number for each operation is multiplied by the latency time of that operation to get the total latency time of the similarity search query. The latency time is 5 cycles for ( $>$ ,  $+ -$ ), 1 cycle

for (abs), 24 cycles for (\*), and 209 cycles for (sqrt) [6]. The latency time for each chromosome is the average of the latency time of  $nQ$  random queries.

As with other GAs, our algorithm selects a percentage  $sRate$  of chromosomes for mating and mutates a percentage  $mRate$  of genes. The above steps repeat for  $nGen$  generations.

## 4 Experiments

We compared O-MIR with Tight-MIR on similarity search experiments on different time series datasets from different time series repositories [7], and [18] using different threshold values, and for different values of  $op$ . Since the value of  $op$  is related to the value of  $k$ , which in turn depends on the length of the time series tested, we denote the percentage of the resolution levels kept to the total resolution levels by  $pk = op/k$ .

As for the parameters of the algorithm that we used in the experiments; the population size,  $popSize$ , was 16, the number of generations  $nGen$  was 100, the mutation rate,  $mRate$ , was 0.2, the selection rate,  $sRate$ , was 0.5, and the number of queries,  $nQ$ , was set to 10.

We show in Fig. 1 the results of our experiments. For (CBF), (Wafer), and (GunPoint) we have 5 resolution levels ( $k = 5$ ). For these datasets we chose  $pk = 40\%, 60\%, 80\%$ . (motoCurrent) has 8 resolution levels ( $k = 8$ ), we chose  $pk = 25\%, 50\%, 75\%$ . As we can see, the results are promising in terms of latency time and storage space. For the three first datasets O-MIR is faster than Tight-MIR and in addition, it required less storage space. This is also the case with (motoCurrent) except for  $pk = 20\%$  where the latency time for O-MIR was longer than that of Tight-MIR. However, for this value of  $pk$  the gain of storage space is substantial without much increase in latency time.

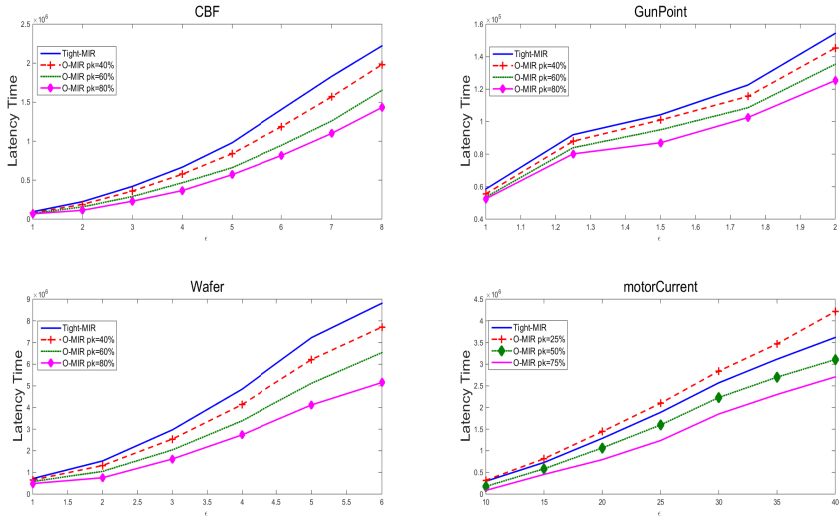


**Fig. 1.** Comparison of the latency time between Tight-MIR and O-MIR on datasets (CBF), (Wafer), (GunPoint), and (motoCurrent) for different values of  $pk$

## 5 Conclusion

In this paper we presented an optimized version of our previous Tight-MIR multi-resolution indexing and retrieval method of time series. Whereas the original method stores and processes all the resolution levels the indexing step produces, the new algorithm, O-MIR, optimizes this process by applying the genetic algorithms to choose the resolution levels with the maximum pruning power. The experiments we conducted show that O-MIR is faster than Tight-MIR, and it also has the advantage of requiring less storage space.

We believe that the main advantage of the new method is that it reduces the storage space requirement of the original method which can be a burden when applying such multi-resolution methods to large datasets.

## References

1. Morinaka, Y., Yoshikawa, M., Amagasa, T., Uemura, S.: The L-index: an indexing structure for efficient subsequence matching in time sequence databases. In: Proc. 5th Pacific Asia Conf. on Knowledge Discovery and Data Mining (2001)
2. Keogh, E., Chakrabarti, K., Pazzani, M., Mehrotra, S.: Locally Adaptive Dimensionality Reduction for Similarity Search in Large Time Series Databases. SIGMOD (2001)
3. Muhammad Fuad, M.M., Marteau P.F.: Multi-resolution approach to time series retrieval. In: Fourteenth International Database Engineering & Applications Symposium– IDEAS 2010, Montreal, QC, Canada (2010)
4. Muhammad Fuad, M.M., Marteau P.F.: Speeding-up the similarity search in time series databases by coupling dimensionality reduction techniques with a fast-and-dirty filter. In: Fourth IEEE International Conference on Semantic Computing– ICSC 2010, Carnegie Mellon University, Pittsburgh, PA, USA (2010)
5. Muhammad Fuad, M.M., Marteau, P.F.: Fast retrieval of time series by combining a multi-resolution filter with a representation technique. In: The International Conference on Advanced Data Mining and Applications–ADMA 2010, ChongQing, China, November 21, 2010
6. Schulte, M.J., Lindberg, M. Laxminarain, A.: Performance evaluation of decimal floating-point arithmetic. In: IBM Austin Center for Advanced Studies Conference, February 2005
7. <http://povinelli.eece.mu.edu/>
8. Keogh, E., Zhu, Q., Hu, B., Hao, Y., Xi, X., Wei, L., Ratanamahatana, C.A.: The UCR Time Series Classification/Clustering (2011). [www.cs.ucr.edu/~eamonn/time\\_series\\_data/](http://www.cs.ucr.edu/~eamonn/time_series_data/)

# **Multi-agent Systems: Theory and Applications**

# Minimal Change in Evolving Multi-Context Systems

Ricardo Gonçalves<sup>(✉)</sup>, Matthias Knorr, and João Leite

NOVA LINCS, Departamento de Informática, Faculdade Ciências e Tecnologia,  
Universidade Nova de Lisboa, Caparica, Portugal  
`rjrg@fct.unl.pt`

**Abstract.** In open environments, agents need to reason with knowledge from various sources, possibly represented in different languages. The framework of *Multi-Context Systems* (MCSs) offers an expressive, yet flexible, solution since it allows for the integration of knowledge from different heterogeneous sources in an effective and modular way. However, MCSs are essentially static as they were not designed for dynamic scenarios. The recently introduced *evolving Multi-Context Systems* (eMCSs) extend MCSs by also allowing the system to both react to, and reason in the presence of dynamic observations, and evolve by incorporating new knowledge, thus making it even more adequate in Multi-Agent Systems characterised by their dynamic and open nature.

In dynamic scenarios which admit several possible alternative evolutions, the notion of *minimal change* has always played a crucial role in determining the most plausible choice. However, different KR formalisms – as combined within eMCSs – may require different notions of minimal change, making their study and their interplay a relevant highly non-trivial problem. In this paper, we study the notion of minimal change in eMCSs, by presenting and discussing alternative minimal change criteria.

## 1 Introduction

Open and dynamic environments create new challenges for knowledge representation languages for agent systems. Instead of having to deal with a single static knowledge base, each agent has to deal with multiple sources of distributed knowledge possibly written in different languages. These sources of knowledge include the large number of available ontologies and rule sets, as well as the norms and policies published by *institutions*, the information communicated by other agents, to name only a few.

The need to incorporate in agent-oriented programming languages the ability to represent and reason with heterogeneous distributed knowledge sources, and the flow of information between them, has been pointed out in [1–4], although a general adequate practical solution is still not available.

Recent literature in knowledge representation and reasoning contains several proposals to combine heterogeneous knowledge bases, one of which – Multi-Context Systems (MCSs) [5–7] – has attracted particular attention because it

provides an elegant solution by considering each source of knowledge as a module and then providing means to model the interaction between these modules. More specifically, an MCS consists of a set of contexts, each of which is a knowledge base in some KR formalism, such that each context can access information from the other contexts using so-called bridge rules. Such non-monotonic bridge rules add their heads to the context's knowledge base provided the queries (to other contexts) in their bodies are successful. Managed Multi-Context Systems (mMCSs) [8] extend MCSs by allowing operations, other than simple addition, to be expressed in the heads of bridge rules, thus allowing mMCSs to properly deal with the problem of consistency management within contexts. MCSs have gained some attention by agent developers [9–11].

Whereas mMCSs are quite general and flexible to address the problem of integration of different KR formalisms, they are essentially static in the sense that the contexts do not evolve to incorporate the changes in dynamic scenarios. In such scenarios, new knowledge and information is dynamically produced, often from several different sources – e.g., a stream of raw data produced by some sensors, new ontological axioms written by some user, newly found exceptions to some general rule, observations, etc.

Evolving Multi-Context Systems (eMCSs) [12] inherit from mMCSs the ability to integrate and manage knowledge represented in heterogeneous KR formalisms, and at the same time are able to react to dynamic observations, and evolve by incorporating knowledge. The semantics of eMCSs is based on the stable model semantics, and allows alternative models for a given evolution, in the same way as answer sets represent alternative solutions to a given ASP program.

One of the main principles of belief revision is minimal change, which in case of eMCSs means that information should be maintained by inertia unless it is required to change. In dynamic scenarios where systems can have alternative evolutions, it is thus desirable to have some minimal change criteria to be able to compare possible alternatives. This problem is particularly interesting and non-trivial in dynamic frameworks based on MCSs, because of the heterogeneity of KR frameworks that may exist in an MCS – each of which may require different notions of minimal change –, and also because the evolution of such systems is based not only on the semantics, but also on the evolution of the knowledge base of each context.

In this paper, we study minimal change in eMCSs, by presenting different minimal change criteria to be applied to the possible evolving equilibria of an eMCS, and by discussing the relation between them.

The remainder of this paper is as follows. We introduce the framework of eMCSs in Sect. 2. Then, we present and study some minimal change criteria in eMCSs in Sect. 3, and conclude with a discussion of related work and possible future directions in Sect. 4.

## 2 Evolving Multi-Context Systems

In this section, we revisit evolving Multi-Context Systems as introduced in [12], which generalize mMCSs [8] to dynamic scenarios in which contexts are enabled to react to external observations and evolve.

An evolving multi-context system (eMCS) consists of a collection of components, each of which contains knowledge represented in some *logic*, defined as a triple  $L = \langle \mathbf{KB}, \mathbf{BS}, \mathbf{ACC} \rangle$  where **KB** is the set of well-formed knowledge bases of  $L$ , **BS** the set of possible belief sets, and  $\mathbf{ACC} : \mathbf{KB} \rightarrow 2^{\mathbf{BS}}$  a function describing the semantics of  $L$  by assigning to each knowledge base a set of acceptable belief sets. We assume that each element of **KB** and **BS** is a set, and define  $F = \{s : s \in kb \wedge kb \in \mathbf{KB}\}$ .

In addition to the knowledge base in each component, *bridge rules* are used to interconnect the components, specifying what operations to perform on its knowledge base given certain beliefs held in the components of the eMCS. For that purpose, each component of an eMCS is associated with a *management base*, which is a set of operations that can be applied to the possible knowledge bases of that component. Given a management base  $OP$  and a logic  $L$ , let  $OF = \{op(s) : op \in OP \wedge s \in F\}$  be the *set of operational formulas* over  $OP$  and  $L$ . Each component of an eMCS gives semantics to operations in its management base using a *management function* over a logic  $L$  and a management base  $OP$ ,  $mng : 2^{OF} \times \mathbf{KB} \rightarrow (2^{\mathbf{KB}} \setminus \{\emptyset\})$ , i.e.,  $mng(op, kb)$  is the (non-empty) set of knowledge bases that result from applying the operations in  $op$  to the knowledge base  $kb$ . We assume that  $mng(\emptyset, kb) = \{kb\}$ .

In an eMCS some contexts are assumed to be *observation contexts* whose knowledge bases will be constantly changing over time according to the observations made, similar, e.g., to streams of data from sensors.<sup>1</sup> The changing observations will then affect the other contexts by means of the bridge rules. As we will see, such effect can either be instantaneous and temporary, i.e., limited to the current time instant, similar to (static) mMCSs, where the body of a bridge rule is evaluated in a state that already includes the effects of the operation in its head, or persistent, but only affecting the next time instant. To achieve the latter, the operational language is extended with a unary meta-operation *next* that can only be applied on top of operations. Given a management base  $OP$  and a logic  $L$ , we define  $eOF$ , the evolving operational language, as  $eOF = OF \cup \{next(op(s)) : op(s) \in OF\}$ .

The idea of observation contexts is that each such context has a language describing the set of possible observations of that context, along with its current observation. The elements of the language of the observation contexts can then be used in the body of bridge rules to allow contexts to access the observations. Formally, an *observation context* is a tuple  $O = \langle \Pi_O, \pi \rangle$  where  $\Pi_O$  is the *observation language* of  $O$  and  $\pi \subseteq \Pi_O$  is its *current observation*.

We can now define *evolving Multi-Context Systems* (eMCS).

---

<sup>1</sup> For simplicity of presentation, we consider discrete steps in time here.

**Definition 1.** An eMCS is a sequence  $M_e = \langle C_1, \dots, C_n, O_1, \dots, O_\ell \rangle$ , such that, for each  $i \in \{1, \dots, \ell\}$ ,  $O_i = \langle \Pi_{O_i}, \pi_i \rangle$  is an observation context, and, for each  $i \in \{1, \dots, n\}$ ,  $C_i$  is an evolving context defined as  $C_i = \langle L_i, kb_i, br_i, OP_i, mng_i \rangle$  where

- $L_i = \langle \mathbf{KB}_i, \mathbf{BS}_i, \mathbf{ACC}_i \rangle$  is a logic
- $kb_i \in \mathbf{KB}_i$
- $br_i$  is a set of bridge rules of the form

$$H(\sigma) \leftarrow a_1, \dots, a_k, \mathbf{not} \ a_{k+1}, \dots, \mathbf{not} \ a_n \quad (1)$$

- such that  $H(\sigma) \in eOF_i$ , and each  $a_i$ ,  $i \in \{1, \dots, n\}$ , is either of the form  $(r:b)$  with  $r \in \{1, \dots, n\}$  and  $b$  a belief formula of  $L_r$ , or of the form  $(r@b)$  with  $r \in \{1, \dots, \ell\}$  and  $b \in \Pi_{O_r}$
- $OP_i$  is a management base
  - $mng_i$  is a management function over  $L_i$  and  $OP_i$ .

Given an eMCS  $M_e = \langle C_1, \dots, C_n, O_1, \dots, O_\ell \rangle$  we denote by  $\mathbf{KB}_{M_e}$  the set of knowledge base configurations for  $M_e$ , i.e.,  $\mathbf{KB}_{M_e} = \{\langle k_1, \dots, k_n \rangle : k_i \in \mathbf{KB}_i$  for each  $1 \leq i \leq n\}$ . A belief state for  $M_e = \langle C_1, \dots, C_n, O_1, \dots, O_\ell \rangle$  is a sequence  $S = \langle S_1, \dots, S_n \rangle$  such that, for each  $1 \leq i \leq n$ , we have  $S_i \in \mathbf{BS}_i$ . We denote by  $\mathbf{BS}_{M_e}$  the set of belief states for  $M_e$ .

An instant observation for  $M_e$  is a sequence  $\mathcal{O} = \langle o_1, \dots, o_\ell \rangle$  such that, for each  $1 \leq i \leq \ell$ , we have that  $o_i \subseteq \Pi_{O_i}$ .

Given a belief state  $S = \langle S_1, \dots, S_n \rangle$  for  $M_e$  and an instant observation  $\mathcal{O} = \langle o_1, \dots, o_\ell \rangle$  for  $M_e$ , we define the satisfaction of bridge literals of the form  $(r:b)$  as  $S, \mathcal{O} \models (r:b)$  if  $b \in S_r$  and  $S, \mathcal{O} \models \mathbf{not} (r:b)$  if  $b \notin S_r$ . The satisfaction of bridge literal of the form  $(r@b)$  depends on the current observations, i.e., we have that  $S, \mathcal{O} \models (r@b)$  if  $b \in o_r$  and  $S \models \mathbf{not} (r@b)$  if  $b \notin o_r$ . For a set  $B$  of bridge literals, we have that  $S, \mathcal{O} \models B$  if  $S, \mathcal{O} \models L$  for every  $L \in B$ .

We say that a bridge rule  $\sigma$  of a context  $C_i$  is *applicable given a belief state  $S$  and an instant observation  $\mathcal{O}$*  if its body is satisfied by  $S$  and  $\mathcal{O}$ , i.e.,  $S, \mathcal{O} \models B(\sigma)$ . We denote by  $app_i(S, \mathcal{O})$  the set of heads of bridges rules of the context  $C_i$  which are applicable given the belief state  $S$  and the instant observation  $\mathcal{O}$ . Recall that the heads of bridge rules in an eMCS may be of two types: those that contain *next* and those that do not. The former are to be applied to the current knowledge base and not persist, whereas the latter are to be applied in the next time instant and persist. Therefore, we distinguish these two subsets.

**Definition 2.** Let  $M_e = \langle C_1, \dots, C_n, O_1, \dots, O_\ell \rangle$  be an eMCS,  $S$  a belief state for  $M_e$ , and  $\mathcal{O}$  an instant observation for  $M_e$ . Then, for each  $1 \leq i \leq n$ , consider the following sets:

- $app_i^{next}(S, \mathcal{O}) = \{op(s) : next(op(s)) \in app_i(S, \mathcal{O})\}$
- $app_i^{now}(S, \mathcal{O}) = \{op(s) : op(s) \in app_i(S, \mathcal{O})\}$

If we want an effect to be instantaneous and persistent, this can be achieved using two bridge rules with identical body, one with and one without *next*.

Similar to equilibria in mMCS, the (static) equilibrium is defined to incorporate instantaneous effects based on  $app_i^{now}(S, \mathcal{O})$  alone.

**Definition 3.** Let  $M_e = \langle C_1, \dots, C_n, O_1, \dots, O_\ell \rangle$  be an eMCS, and  $\mathcal{O}$  an instant observation for  $M_e$ . A belief state  $S = \langle S_1, \dots, S_n \rangle$  for  $M_e$  is an equilibrium of  $M_e$  given  $\mathcal{O}$  iff for each  $1 \leq i \leq n$ ,  $S_i \in \text{ACC}_i(kb)$  for some  $kb \in mng_i(\text{app}^{now}(S, \mathcal{O}), kb_i)$ .

To be able to assign meaning to an eMCS evolving over time, we introduce evolving belief states, which are sequences of belief states, each referring to a subsequent time instant.

**Definition 4.** Let  $M_e = \langle C_1, \dots, C_n, O_1, \dots, O_\ell \rangle$  be an eMCS. An evolving belief state of size  $s$  for  $M_e$  is a sequence  $S_e = \langle S^1, \dots, S^s \rangle$  where each  $S^j$ ,  $1 \leq j \leq s$ , is a belief state for  $M_e$ .

To enable eMCSs to react to incoming observations and evolve, a sequence of observations (defined below) has to be processed. The idea is that the knowledge bases of the observation contexts  $O_i$  change according to that sequence.

**Definition 5.** Let  $M_e = \langle C_1, \dots, C_n, O_1, \dots, O_\ell \rangle$  be an eMCS. A sequence of observations for  $M_e$  is a sequence  $\text{Obs} = \langle \mathcal{O}^1, \dots, \mathcal{O}^m \rangle$ , such that, for each  $1 \leq j \leq m$ ,  $\mathcal{O}^j = \langle o_1^j, \dots, o_\ell^j \rangle$  is an instant observation for  $M_e$ , i.e.,  $o_i^j \subseteq \Pi_{O_i}$  for each  $1 \leq i \leq \ell$ .

To be able to update the knowledge bases and the sets of bridge rules of the evolving contexts, we need the following notation. Given an evolving context  $C_i$ , and a knowledge base  $k \in \mathbf{KB}_i$ , we denote by  $C_i[k]$  the evolving context in which  $kb_i$  is replaced by  $k$ , i.e.,  $C_i[k] = \langle L_i, k, br_i, OP_i, mng_i \rangle$ . For an observation context  $O_i$ , given a set  $\pi \subseteq \Pi_{O_i}$  of observations for  $O_i$ , we denote by  $O_i[\pi]$  the observation context in which its current observation is replaced by  $\pi$ , i.e.,  $O_i[\pi] = \langle \Pi_{O_i}, \pi \rangle$ . Given  $K = \langle k_1, \dots, k_n \rangle \in \mathbf{KB}_{M_e}$  a knowledge base configuration for  $M_e$ , we denote by  $M_e[K]$  the eMCS  $\langle C_1[k_1], \dots, C_n[k_n], O_1, \dots, O_\ell \rangle$ .

We now define when certain evolving belief states are evolving equilibria of an eMCS  $M_e$  given a sequence of observations  $\text{Obs} = \langle \mathcal{O}^1, \dots, \mathcal{O}^m \rangle$  for  $M_e$ . The intuitive idea is that, given an evolving belief state  $S_e = \langle S^1, \dots, S^s \rangle$  for  $M_e$ , in order to check if  $S_e$  is an evolving equilibrium, we need to consider a sequence of eMCSs,  $M^1, \dots, M^s$  (each with  $\ell$  observation contexts), representing a possible evolution of  $M_e$  according to the observations in  $\text{Obs}$ , such that each  $S^j$  is a (static) equilibrium of  $M^j$ . The current observation of each observation context  $O_i$  in  $M^j$  is exactly its corresponding element  $o_i^j$  in  $\mathcal{O}^j$ . For each evolving context  $C_i$ , its knowledge base in  $M^j$  is obtained from the one in  $M^{j-1}$  by applying the operations in  $\text{app}^{next}(S^{j-1}, \mathcal{O}^{j-1})$ .

**Definition 6.** Let  $M_e = \langle C_1, \dots, C_n, O_1, \dots, O_\ell \rangle$  be an eMCS,  $S_e = \langle S^1, \dots, S^s \rangle$  an evolving belief state of size  $s$  for  $M_e$ , and  $\text{Obs} = \langle \mathcal{O}^1, \dots, \mathcal{O}^m \rangle$  an observation sequence for  $M_e$  such that  $m \geq s$ . Then,  $S_e$  is an evolving equilibrium of size  $s$  of  $M_e$  given  $\text{Obs}$  iff, for each  $1 \leq j \leq s$ , the belief state  $S^j$  is an equilibrium of  $M^j = \langle C_1[k_1^j], \dots, C_n[k_n^j], O_1[o_1^j], \dots, O_\ell[o_\ell^j] \rangle$  where, for each  $1 \leq i \leq n$ ,  $k_i^j$  is defined inductively as follows:

- $k_i^1 = kb_i$
- $k_i^{j+1} \in mng_i(\text{app}^{next}(S^j, \mathcal{O}_i^j), k_i^j)$ .

### 3 Minimal Change

In this section, we discuss some alternatives for the notion of minimal change in eMCSs. What makes this problem interesting is that there are different parameters that we may want to minimize in a transition from one time instant to the next one. In the following discussion we focus on two we deem most relevant: the operations that can be applied to the knowledge bases, and the distance between consecutive belief states.

We start by studying minimal change at the level of the operations. In the following discussion we consider fixed an eMCS  $M_e = \langle C_1, \dots, C_n, O_1, \dots, O_\ell \rangle$ .

Recall from the definition of evolving equilibrium that, in the transition between consecutive time instants, the knowledge base of each context  $C_i$  of  $M_e$  changes according to the operations in  $app_i^{next}(S, \mathcal{O})$ , and these depend on the belief state  $S$  and the instant observation  $\mathcal{O}$ . The first idea to compare elements of this set of operations is to, for a fixed instant observation  $\mathcal{O}$ , distinguish those equilibria of  $M_e$  which generate a minimal set of operations to be applied to the current knowledge bases to obtain the knowledge bases of the next time instant. Formally, given a knowledge base configuration  $K \in \mathbf{KB}_{M_e}$  and an instant observation  $\mathcal{O}$  for  $M_e$ , we can define the set:

$$\begin{aligned} MinEq(K, \mathcal{O}) = \{S : S \text{ is an equilibrium of } M_e[K] \text{ given } \mathcal{O} \text{ and there is no} \\ \text{equilibrium } S' \text{ of } M_e[K] \text{ given } \mathcal{O} \text{ such that, for all } 1 \leq i \leq n, \\ app_i^{next}(S', \mathcal{O}) \subset app_i^{next}(S, \mathcal{O})\} \end{aligned}$$

This first idea of comparing equilibria based on inclusion of the sets of operations can, however, be too strict in most cases. Moreover, different operations usually have different costs,<sup>2</sup> and it may well be that, instead of minimizing based on set inclusion, we want to minimize the total cost of the operations to be applied. For that, we need to assume that each context has a cost function over the set of operations, i.e.,  $cost_i : OP_i \rightarrow \mathbb{N}$ , where  $cost_i(op)$  represents the cost of performing operation  $op$ .

Let  $S$  be a belief state for  $M_e$  and  $\mathcal{O}$  an instant observation for  $M_e$ . Then, for each  $1 \leq i \leq n$ , we define the cost of the operations to be applied to obtain the knowledge base of the next time instant as:

$$Cost_i(S, \mathcal{O}) = \sum_{op(s) \in app_i^{next}(S, \mathcal{O})} cost_i(op)$$

Summing for all evolving contexts, we obtain the global cost of  $S$  given  $\mathcal{O}$ :

$$Cost(S, \mathcal{O}) = \sum_{i=1}^n Cost_i(S, \mathcal{O})$$

Now that we have defined a cost function over belief states, we can define a minimization function over possible equilibria of eMCS  $M_e[K]$  for a fixed knowledge base configuration  $K \in \mathbf{KB}_{M_e}$ . Formally, given  $\mathcal{O}$  an instant observation for  $M_e$ , we define the set of equilibria of  $M_e[K]$  given  $\mathcal{O}$  which minimize the global

---

<sup>2</sup> We use the notion of cost in an abstract sense, i.e., depending on the context, it may refer to, e.g., the computational cost of the operation, or its economic cost.

cost of the operations to be applied to obtain the knowledge base configuration of the next time instant as:

$$\begin{aligned} \text{MinCost}(K, \mathcal{O}) = \{S : S \text{ is an equilibrium of } M_e[K] \text{ given } \mathcal{O} \text{ and} \\ \text{there is no equilibrium } S' \text{ of } M_e[K] \text{ given } \mathcal{O} \\ \text{such that } \text{Cost}(S', \mathcal{O}) < \text{Cost}(S, \mathcal{O})\} \end{aligned}$$

Note that, instead of using a global cost, we could have also considered a more fine-grained criterion by comparing costs for each context individually, and define some order based on these comparisons. Also note that the particular case of taking  $\text{cost}_i(op) = 1$  for every  $i \in \{1, \dots, n\}$  and every  $op \in OP_i$ , captures the scenario of minimizing the total number of operations to be applied.

The function  $\text{MinCost}$  allows for the choice of those equilibria that are minimal with respect to the operations to be performed to the current knowledge base configuration in order to obtain the knowledge base configuration of the next time instant. Still, for each choice of an equilibrium  $S$ , we have to deal with the existence of several alternatives in the set  $mng_i(app_i^{next}(S, \mathcal{O}), kb_i)$ . Our aim now is to discuss how we can apply some notion of minimal change that allows us to compare the elements in  $mng_i(app_i^{next}(S, \mathcal{O}), kb_i)$ . The intuitive idea is to compare the distance between the current equilibria and the possible equilibria resulting from the elements in  $mng_i(app_i^{next}(S, \mathcal{O}), kb_i)$ . Of course, given the possible heterogeneity of contexts in an eMCS, we cannot assume a global notion of distance between belief sets. Therefore, we assume that each evolving context has its own distance function between its beliefs sets. Formally, for each  $1 \leq i \leq n$ , we assume the existence of a distance function  $d_i$ , i.e.,  $d_i : \mathbf{BS}_i \times \mathbf{BS}_i \rightarrow \mathbb{R}$  satisfying for all  $S_1, S_2, S_3 \in \mathbf{BS}_i$ :

1.  $d_i(S_1, S_2) \geq 0$
2.  $d_i(S_1, S_2) = 0$  iff  $S_1 = S_2$
3.  $d_i(S_1, S_2) = d_i(S_2, S_1)$
4.  $d_i(S_1, S_3) \leq d_i(S_1, S_2) + d_i(S_2, S_3)$

There are some alternatives to extend the distance function of each context to a distance function between belief states. In the following we present two natural choices. One is to consider the maximal distance between belief sets of each context. The other is to consider the average of distances between belief sets of each context. Formally, given  $S^1$  and  $S^2$  belief states of  $M_e$  we define two functions  $\bar{d}_{\max} : \mathbf{BS}_{M_e} \times \mathbf{BS}_{M_e} \rightarrow \mathbb{R}$  and  $\bar{d}_{\text{avg}} : \mathbf{BS}_{M_e} \times \mathbf{BS}_{M_e} \rightarrow \mathbb{R}$  as follows:

$$\begin{aligned} \bar{d}_{\max}(S^1, S^2) &= \text{Max}\{d_i(S_i^1, S_i^2) \mid 1 \leq i \leq n\} \\ \bar{d}_{\text{avg}}(S^1, S^2) &= \frac{\sum_{i=1}^n d_i(S_i^1, S_i^2)}{n} \end{aligned}$$

We can prove that  $\bar{d}_{\max}$  and  $\bar{d}_{\text{avg}}$  are distance functions between belief states.

**Proposition 1.** *The functions  $\bar{d}_{\max}$  and  $\bar{d}_{\text{avg}}$  defined above are both distance functions, i.e., satisfy the axioms 1) - 4).*

We now study how we can use one of these distance functions between belief states to compare the possible alternatives in the sets  $mng_i(app_i^{next}(S, \mathcal{O}), kb_i)$ , for each  $1 \leq i \leq n$ . Recall that the intuitive idea is to minimize the distance between the current belief state  $S$  and the possible equilibria that each element of  $mng_i(app_i^{next}(S, \mathcal{O}), kb_i)$  can give rise to. We explore here two options, which differ on whether the minimization is global or local. The idea of global minimization is to choose only those knowledge base configurations  $\langle k_1, \dots, k_n \rangle \in \mathbf{KB}_{M_e}$  with  $k_i \in mng_i(app_i^{next}(S, \mathcal{O}), kb_i)$ , which guarantee minimal distance between the original belief state  $S$  and the possible equilibria of the obtained eMCS. The idea of local minimization is to consider all possible tuples  $\langle k_1, \dots, k_n \rangle$  with  $k_i \in mng_i(app_i^{next}(S, \mathcal{O}), kb_i)$ , and only apply minimization for each such choice, i.e., for each such knowledge base configuration we only allow equilibria with minimal distance from the original belief state.

We first consider the case of pruning those tuples  $\langle k_1, \dots, k_n \rangle$  such that  $k_i \in mng_i(app_i^{next}(S, \mathcal{O}), kb_i)$ , which do not guarantee minimal change with respect to the original belief state. We start by defining an auxiliary function. Let  $S$  be a belief state for  $M_e$ ,  $K = \langle k_1, \dots, k_n \rangle \in \mathbf{KB}_{M_e}$  a knowledge base configuration for  $M_e$ , and  $\mathcal{O} = \langle o_1, \dots, o_\ell \rangle$  an instant observation for  $M_e$ . Then we define the set of knowledge base configurations that are obtained from  $K$  given the belief state  $S$  and the instant observation  $\mathcal{O}$  as:

$$\begin{aligned} NextKB(S, \mathcal{O}, \langle k_1, \dots, k_n \rangle) = \{ \langle k'_1, \dots, k'_n \rangle \in \mathbf{KB}_{M_e} : & \text{ for each } 1 \leq i \leq n \\ & \text{we have that } k'_i \in mng_i(app_i^{next}(S, \mathcal{O}), k_i) \} \end{aligned}$$

For each choice  $\bar{d}$  of a distance function between belief states, we define the set of knowledge base configurations that minimize the distance to the original belief state. Let  $S$  be a belief state for  $M_e$ ,  $K = \langle k_1, \dots, k_n \rangle \in \mathbf{KB}_{M_e}$  a knowledge base configuration for  $M_e$ , and  $\mathcal{O}^j$  and  $\mathcal{O}^{j+1}$  instant observations for  $M_e$ .

$$MinNext(S, \mathcal{O}^j, \mathcal{O}^{j+1}, K) = \{ (S', K') : K' \in NextKB(S, \mathcal{O}^j, K) \text{ and}$$

$$\begin{aligned} S' &\in MinCost(M_e[K'], \mathcal{O}^{j+1}) \text{ s.t. there is no} \\ K'' &\in NextKB(S, \mathcal{O}^j, K) \text{ and no} \\ S'' &\in MinCost(M_e[K''], \mathcal{O}^{j+1}) \text{ with} \\ \bar{d}(S, S'') &< \bar{d}(S, S') \}. \end{aligned}$$

Note that  $MinNext$  applies minimization over all possible equilibria resulting from every element of  $NextKB(S, \mathcal{O}^j, K)$ . Using  $MinNext$ , we can now define a minimal change criterion to be applied to evolving equilibria of  $M_e$ .

**Definition 7.** Let  $M_e = \langle C_1, \dots, C_n, O_1, \dots, O_\ell \rangle$  be an eMCS,  $Obs = \langle \mathcal{O}^1, \dots, \mathcal{O}^m \rangle$  an observation sequence for  $M_e$ , and let  $S_e = \langle S^1, \dots, S^s \rangle$  be an evolving equilibrium of  $M_e$  given  $Obs$ . We assume that  $\langle K^1, \dots, K^s \rangle$ , with  $K^j = \langle k_1^j, \dots, k_n^j \rangle$ , is the sequence of knowledge base configurations associated with  $S_e$  as in Definition 6. Then,  $S_e$  satisfies the strong minimal change criterion for  $M_e$  given  $Obs$  if, for each  $1 \leq j \leq s$ , the following conditions are satisfied:

- $S^j \in MinCost(M_e[K^j], \mathcal{O}^j)$
- $(S^{j+1}, K^{j+1}) \in MinNext(S^j, \mathcal{O}^j, \mathcal{O}^{j+1}, K^j)$

We call this minimal change criterion the *strong* minimal change criterion because it applies minimization over all possible equilibria resulting from every possible knowledge base configuration in  $\text{NextKB}(S, \mathcal{O}^j, K)$ .

The following proposition states the desirable property that the existence of an equilibrium guarantees the existence of an equilibrium satisfying the strong minimal change criterion. We should note that this is not a trivial statement since we are combining minimization of two different elements: the cost of the operations and the distance between belief states. This proposition in fact follows from their careful combination in the definition of  $\text{MinNext}$ .

**Proposition 2.** *Let  $\text{Obs} = \langle \mathcal{O}^1, \dots, \mathcal{O}^m \rangle$  be an observation sequence for  $M_e$ . If  $M_e$  has an evolving equilibrium of size  $s$  given  $\text{Obs}$ , then at least one evolving equilibrium of size  $s$  given  $\text{Obs}$  satisfies the strong minimal change criterion.*

Note that in the definition of the strong minimal change criterion, the knowledge base configurations  $K \in \text{NextKB}(S^j, \mathcal{O}^j, K^j)$ , for which the corresponding possible equilibria are not at a minimal distance from  $S^j$ , are not considered. However, there could be situations in which this minimization criterion is too strong. For example, it may well be that all possible knowledge base configurations in  $\text{NextKB}(S^j, \mathcal{O}^j, K^j)$  are important, and we do not want to disregard any of them. In that case, we can relax the minimization condition by applying minimization individually for each knowledge base configuration in  $\text{NextKB}(S^j, \mathcal{O}^j, K^j)$ . The idea is that, for each fixed  $K \in \text{NextKB}(S^j, \mathcal{O}^j, K^j)$  we choose only those equilibria of  $M_e[K]$  which minimize the distance to  $S^j$ .

Formally, let  $S$  be a belief state for  $M_e$ ,  $K \in \mathbf{KB}_{M_e}$  a knowledge base configuration for  $M_e$ , and  $\mathcal{O}$  an instant observation for  $M_e$ . For each distance function  $\bar{d}$  between belief states, we can define the following set:

$$\begin{aligned} \text{MinDist}(S, \mathcal{O}, K) = & \{S' : S' \in \text{MinCost}(M_e[K], \mathcal{O}) \text{ and} \\ & \text{there is no } S'' \in \text{MinCost}(M_e[K], \mathcal{O}) \\ & \text{such that } \bar{d}(S, S'') < \bar{d}(S, S')\} \end{aligned}$$

Using this more relaxed notion of minimization we can define an alternative weaker minimal change criterion to be applied to evolving equilibria of an eMCS.

**Definition 8.** *Let  $M_e = \langle C_1, \dots, C_n, O_1, \dots, O_\ell \rangle$  be an eMCS,  $\text{Obs} = \langle \mathcal{O}^1, \dots, \mathcal{O}^m \rangle$  an observation sequence for  $M_e$ , and  $S_e = \langle S^1, \dots, S^s \rangle$  an evolving equilibrium of  $M_e$  given  $\text{Obs}$ . We assume that  $\langle K^1, \dots, K^s \rangle$ , with  $K^j = \langle k_1^j, \dots, k_n^j \rangle$ , is the sequence of knowledge base configurations associated with  $S_e$  as in Definition 6. Then,  $S_e$  satisfies the weak minimal change criterion of  $M_e$  given  $\text{Obs}$ , if for each  $1 \leq j \leq s$  the following conditions are satisfied:*

- $S^j \in \text{MinCost}(M_e[K^j], \mathcal{O}^j)$
- $S^{j+1} \in \text{MinDist}(S^j, K^{j+1}, \mathcal{O}^{j+1})$

We can now prove that the existence of an evolving equilibrium implies the existence of an equilibrium satisfying the weak minimal change criterion. Again note that the careful combination of the two minimizations – cost and distance – in the definition of  $\text{MinDist}$  is fundamental to obtain the following result.

**Proposition 3.** Let  $\text{Obs} = \langle O^1, \dots, O^m \rangle$  be an observation sequence for  $M_e$ . If  $M_e$  has an evolving equilibrium of size  $s$  given  $\text{Obs}$ , then at least one evolving equilibrium of size  $s$  of  $M_e$  given  $\text{Obs}$  satisfies the weak minimal change criterion.

We can now prove that the strong minimal change criterion is, in fact, stronger than the weak minimal change criterion.

**Proposition 4.** Let  $M_e$  be an eMCS,  $\text{Obs} = \langle O^1, \dots, O^m \rangle$  an observation sequence for  $M_e$ , and  $S_e = \langle S^1, \dots, S^s \rangle$  an evolving equilibrium of  $M_e$  given  $\text{Obs}$ . If  $S_e$  satisfies the strong minimal change criterion of  $M_e$  given  $\text{Obs}$ , then  $S_e$  satisfies the weak minimal change criterion of  $M_e$  given  $\text{Obs}$ .

## 4 Related and Future Work

In this paper we have studied the notion of minimal change in the context of the dynamic framework of eMCSs [12]. We have presented and discussed some alternative definitions of minimal change criteria for evolving equilibria of an eMCS.

Closely related to eMCSs is the framework of reactive Multi-Context Systems (rMCSs) [13–15] inasmuch as both aim at extending mMCSs to cope with dynamic observations. The key difference between them is that the operator *next* of eMCSs allows for a clear separation between persistent and non-persistent effects, and the specification of transitions based on the current state.

Another framework closely related to eMCSs is that of evolving logic programs EVOLP [16] which deals with updates of generalized logic programs, and the two frameworks of reactive ASP, one implemented as a solver *oclingo* [17] and one described in [13]. Whereas EVOLP employs an update predicate that is similar in spirit to the *next* predicate of eMCSs, it does not deal with heterogeneous knowledge, neither do both versions of Reactive ASP. Moreover, no notion of minimal change is studied for these frameworks.

This work raises several interesting paths for future research. Immediate future work includes the study of more global approaches to the minimization of costs of operations, namely by considering the global cost of an evolving equilibrium, instead of minimizing costs at each time instant. A topic worth investigating is how to perform AGM-style belief revision at the (semantic) level of the equilibria, as in Wang et al [18], though necessarily different since knowledge is not incorporated in the contexts. Also interesting is to study a paraconsistent version of eMCSs, grounded on the work in [19] on paraconsistent semantics for hybrid knowledge bases. Another important issue open for future work is a more fine-grained characterization of updating bridge rules (and knowledge bases) as studied in [20] in light of the encountered difficulties when updating rules [21–23] and the combination of updates over various formalisms [22, 24]. Also, as already outlined in [25, 26], we can consider generalized notions of minimal and grounded equilibria [5] for eMCSs to avoid, e.g., self-supporting cycles introduced by bridge rules, or the use of preferences to deal with several evolving equilibria an eMCS can have for the same observation sequence. Also interesting

is to apply the ideas in this paper to study the dynamics of frameworks closely related to MCSs, such as those in [27–30].

Finally, and in line with the very motivation set out in the introduction, we believe that the research in MCSs – including eMCSs with the different notions of minimal change – provides a blue-print on how to represent and reason with heterogeneous dynamic knowledge bases which could (should) be used by developers of practical agent-oriented programming languages, such as JASON [31], 2APL [32], or GOAL [33], in their quest for providing users and programmers with greater expressiveness and flexibility in terms of the knowledge representation and reasoning facilities provided by such languages. To this end, an application scenario that could provide interesting and rich examples would be that of norm-aware multi-agent systems [34–39].

**Acknowledgments.** We would like to thank the referees for their comments, which helped improve this paper. R. Gonçalves, M. Knorr and J. Leite were partially supported by FCT under project ERRO (PTDC/EIA-CCO/121823/2010) and under strategic project NOVA LINCS (PEst/UID/CEC/04516/2013). R. Gonçalves was partially supported by FCT grant SFRH/BPD/100906/2014 and M. Knorr was partially supported by FCT grant SFRH/BPD/86970/2012.

## References

1. Dastani, M., Hindriks, K.V., Novák, P., Tinnemeier, N.A.M.: Combining multiple knowledge representation technologies into agent programming languages. In: Baldoni, M., Son, T.C., van Riemsdijk, M.B., Winikoff, M. (eds.) DALT 2008. LNCS (LNAI), vol. 5397, pp. 60–74. Springer, Heidelberg (2009)
2. Klapiscak, T., Bordini, R.H.: JASDL: A practical programming approach combining agent and semantic web technologies. In: Baldoni, M., Son, T.C., van Riemsdijk, M.B., Winikoff, M. (eds.) DALT 2008. LNCS (LNAI), vol. 5397, pp. 91–110. Springer, Heidelberg (2009)
3. Moreira, Á.F., Vieira, R., Bordini, R.H., Hübner, J.F.: Agent-oriented programming with underlying ontological reasoning. In: Baldoni, M., Endriss, U., Omicini, A., Torroni, P. (eds.) DALT 2005. LNCS (LNAI), vol. 3904, pp. 155–170. Springer, Heidelberg (2006)
4. Alberti, M., Knorr, M., Gomes, A.S., Leite, J., Gonçalves, R., Slota, M.: Normative systems require hybrid knowledge bases. In: van der Hoek, W., Padgham, L., Conitzer, V., Winikoff, M. (eds.) Procs. of AAMAS, pp. 1425–1426. IFAAMAS (2012)
5. Brewka, G., Eiter, T.: Equilibria in heterogeneous nonmonotonic multi-context systems. In: Procs. of AAAI, pp. 385–390. AAAI Press (2007)
6. Giunchiglia, F., Serafini, L.: Multilanguage hierarchical logics or: How we can do without modal logics. Artif. Intell. **65**(1), 29–70 (1994)
7. Roelofsen, F., Serafini, L.: Minimal and absent information in contexts. In: Kaelbling, L., Saffiotti, A. (eds.) Procs. of IJCAI, pp. 558–563. Professional Book Center (2005)
8. Brewka, G., Eiter, T., Fink, M., Weinzierl, A.: Managed multi-context systems. In: Walsh, T. (ed.) Procs. of IJCAI, pp. 786–791. IJCAI/AAAI (2011)
9. Benerecetti, M., Giunchiglia, F., Serafini, L.: Model checking multiagent systems. J. Log. Comput. **8**(3), 401–423 (1998)

10. Dragoni, A., Giorgini, P., Serafini, L.: Mental states recognition from communication. *J. Log. Comput.* **12**(1), 119–136 (2002)
11. Sabater, J., Sierra, C., Parsons, S., Jennings, N.R.: Engineering executable agents using multi-context systems. *J. Log. Comput.* **12**(3), 413–442 (2002)
12. Gonçalves, R., Knorr, M., Leite, J.: Evolving multi-context systems. In: Schaub, T., Friedrich, G., O’Sullivan, B. (eds.) *Procs. of ECAI. Frontiers in Artificial Intelligence and Applications*, vol. 263, pp. 375–380. IOS Press (2014)
13. Brewka, G.: Towards reactive multi-context systems. In: Cabalar, P., Son, T.C. (eds.) *LPNMR 2013. LNCS*, vol. 8148, pp. 1–10. Springer, Heidelberg (2013)
14. Ellmauthaler, S.: Generalizing multi-context systems for reactive stream reasoning applications. In: *Procs. of ICCSW. OASICS*, vol. 35, pp. 19–26. Schloss Dagstuhl - Leibniz-Zentrum fuer Informatik, Germany (2013)
15. Brewka, G., Ellmauthaler, S., Pührer, J.: Multi-context systems for reactive reasoning in dynamic environments. In: Schaub, T., Friedrich, G., O’Sullivan, B., (eds.) *Procs. of ECAI. Frontiers in Artificial Intelligence and Applications*, vol. 263, pp. 159–164. IOS Press (2014)
16. Alferes, J.J., Brogi, A., Leite, J., Moniz Pereira, L.: Evolving logic programs. In: Flesca, S., Greco, S., Leone, N., Ianni, G. (eds.) *JELIA 2002. LNCS (LNAI)*, vol. 2424, p. 50. Springer, Heidelberg (2002)
17. Gebser, M., Grote, T., Kaminski, R., Schaub, T.: Reactive answer set programming. In: Delgrande, J.P., Faber, W. (eds.) *LPNMR 2011. LNCS*, vol. 6645, pp. 54–66. Springer, Heidelberg (2011)
18. Wang, Y., Zhuang, Z., Wang, K.: Belief change in nonmonotonic multi-context systems. In: Cabalar, P., Son, T.C. (eds.) *LPNMR 2013. LNCS*, vol. 8148, pp. 543–555. Springer, Heidelberg (2013)
19. Kaminski, T., Knorr, M., Leite, J.: Efficient paraconsistent reasoning with ontologies and rules. In: *Procs. of IJCAI. IJCAI/AAAI* (2015)
20. Gonçalves, R., Knorr, M., Leite, J.: Evolving bridge rules in evolving multi-context systems. In: Bulling, N., van der Torre, L., Villata, S., Jamroga, W., Vasconcelos, W. (eds.) *CLIMA 2014. LNCS*, vol. 8624, pp. 52–69. Springer, Heidelberg (2014)
21. Slota, M., Leite, J.: On semantic update operators for answer-set programs. In Coelho, H., Studer, R., Wooldridge, M., (eds.) *Procs. of ECAI. Frontiers in Artificial Intelligence and Applications*, vol. 215, pp. 957–962. IOS Press (2010)
22. Slota, M., Leite, J.: Robust equivalence models for semantic updates of answer-set programs. In: Brewka, G., Eiter, T., McIlraith, S.A. (eds.) *Procs. of KR. AAAI* Press (2012)
23. Slota, M., Leite, J.: The rise and fall of semantic rule updates based on se-models. *TPLP* **14**(6), 869–907 (2014)
24. Slota, M., Leite, J.: A unifying perspective on knowledge updates. In: del Cerro, L.F., Herzog, A., Mengin, J. (eds.) *JELIA 2012. LNCS*, vol. 7519, pp. 372–384. Springer, Heidelberg (2012)
25. Gonçalves, R., Knorr, M., Leite, J.: Towards efficient evolving multi-context systems (preliminary report). In: Ellmauthaler, S., Pührer, J. (eds.) *Procs. of React-Know* (2014)
26. Knorr, M., Gonçalves, R., Leite, J.: On efficient evolving multi-context systems. In: Pham, D.-N., Park, S.-B. (eds.) *PRICAI 2014. LNCS*, vol. 8862, pp. 284–296. Springer, Heidelberg (2014)
27. Knorr, M., Slota, M., Leite, J., Homola, M.: What if no hybrid reasoner is available? hybrid MKNF in multi-context systems. *J. Log. Comput.* **24**(6), 1279–1311 (2014)

28. Gonçalves, R., Alferes, J.J.: Parametrized logic programming. In: Janhunen, T., Niemelä, I. (eds.) *JELIA 2010*. LNCS, vol. 6341, pp. 182–194. Springer, Heidelberg (2010)
29. Knorr, M., Alferes, J., Hitzler, P.: Local closed world reasoning with description logics under the well-founded semantics. *Artif. Intell.* **175**(9–10), 1528–1554 (2011)
30. Ivanov, V., Knorr, M., Leite, J.: A query tool for  $\mathcal{EL}$  with non-monotonic rules. In: Alani, H., Kagal, L., Fokoue, A., Groth, P., Biemann, C., Parreira, J.X., Aroyo, L., Noy, N., Welty, C., Janowicz, K. (eds.) *ISWC 2013*, Part I. LNCS, vol. 8218, pp. 216–231. Springer, Heidelberg (2013)
31. Bordini, R.H., Hübler, J.F., Wooldridge, M.: *Programming Multi-Agent Systems in AgentSpeak Using Jason* (Wiley Series in Agent Technology). John Wiley & Sons (2007)
32. Dastani, M.: 2APL: a practical agent programming language. *Journal of Autonomous Agents and Multi-Agent Systems* **16**(3), 214–248 (2008)
33. Hindriks, K.V.: Programming rational agents in GOAL. In: El Fallah Seghrouchni, A., Dix, J., Dastani, M., Bordini, R.H. (eds.) *Multi-Agent Programming*, pp. 119–157. Springer, US (2009)
34. Criado, N., Argente, E., Botti, V.J.: THOMAS: an agent platform for supporting normative multi-agent systems. *J. Log. Comput.* **23**(2), 309–333 (2013)
35. Meneguzzi, F., Rodrigues, O., Oren, N., Vasconcelos, W.W., Luck, M.: BDI reasoning with normative considerations. *Eng. Appl. of AI* **43**, 127–146 (2015)
36. Cardoso, H.L., Oliveira, E.: A context-based institutional normative environment. In: Hübler, J.F., Matson, E., Boissier, O., Dignum, V. (eds.) *COIN 2008*. LNCS, vol. 5428, pp. 140–155. Springer, Heidelberg (2009)
37. Gerard, S.N., Singh, M.P.: Evolving protocols and agents in multiagent systems. In: Gini, M.L., Shehory, O., Ito, T., Jonker, C.M. (eds.) *Procs. of AAMAS*, pp. 997–1004. IFAAMAS (2013)
38. Vasconcelos, W.W., Kollingbaum, M.J., Norman, T.J.: Normative conflict resolution in multi-agent systems. *Autonomous Agents and Multi-Agent Systems* **19**(2), 124–152 (2009)
39. Panagiotidi, S., Alvarez-Napagao, S., Vázquez-Salceda, J.: Towards the norm-aware agent: bridging the gap between deontic specifications and practical mechanisms for norm monitoring and norm-aware planning. In: Balke, T., Dignum, F., van Riemsdijk, M.B., Chopra, A.K. (eds.) *COIN 2013*. LNCS, vol. 8386, pp. 346–363. Springer, Heidelberg (2014)

# Bringing Constitutive Dynamics to Situated Artificial Institutions

Maiquel de Brito<sup>1</sup>(✉), Jomi F. Hübner<sup>1</sup>, and Olivier Boissier<sup>2</sup>

<sup>1</sup> Federal University of Santa Catarina, Florianópolis, SC, Brazil  
[maiquel.b@posgrad.ufsc.br](mailto:maiquel.b@posgrad.ufsc.br), [jomi.hubner@ufsc.br](mailto:jomi.hubner@ufsc.br)

<sup>2</sup> Laboratoire Hubert Curien UMR CNRS 5516, Institut Henri Fayol,  
MINES Saint-Etienne, Saint-Etienne, France  
[Olivier.Boissier@emse.fr](mailto:Olivier.Boissier@emse.fr)

**Abstract.** The Situated Artificial Institution (SAI) model, as proposed in the literature, conceives the regulation of Multi-Agent Systems as based on a constitutive state that is consequence of the institutional interpretation of facts issued by the environment. The different nature of these facts (e.g. past sequence of events, states holding) implies various dynamic behaviours that need to be considered to properly define the life cycle of the constitutive state. This paper aims to bring such a dynamic to SAI. It defines a formal apparatus (i) for the institutional interpretation of environmental facts based on constitutive rules and (ii) for the management of the resulting constitutive state.

## 1 Introduction

Among the different works related to artificial institutions, [1, 2] are concerned with the grounding of norms in the environment where the agents act, keeping a clear separation among regulative, constitutive, and environmental elements involved in the regulation of Multi-Agent Systems (MAS). In this paper we consider and extend the Situated Artificial Institution (SAI) model [2]. The choice of SAI is motivated by its available specification language, that is interesting to specify norms decoupled but still grounded in the environment as shown in [3]. For example, the norm stating that “the winner of the auction is obliged to pay its offer” is specified on top of a constitutive level that defines who, in the environment, is the winner that must pay its offer and what must be done, in the environment, to comply with that expectation. Norms abstracting from the environment are more stable and flexible but must be connected to the environment [1], as the regulation of the system (realised in what we call *institutions*) is, in fact, the regulation of what happens in the environment.

The notion of *constitution* proposed by John Searle [4] has inspired different works addressing the relation between the environment and the regulative elements in MAS. Among them, SAI goes in a particular direction, considering that constitutive rules specify how agents acting, events occurring, and states holding in the environment compose (or *constitute*) the constitutive level of the institution. In the previous example, a constitutive rule could state that the agent that

acts in the environment placing the best bid counts, in the constitutive level, as the winner of the auction (Figure 1).

While the notion of constitution in SAI is well defined, a precise and formal definition of the dynamics of the constitutive level, resulting of the interpretation of constitutive rules, is still lacking. Interpreting the constitutive rules and managing the SAI constitutive state require to consider (*i*) how to tackle with the different natures of the environmental elements that may constitute the relevant elements to the institutional regulation (i.e. agents, events, states) and (*ii*) how to base the dynamic of the constitution both on the occurrences of these elements in the environment and on the production of new constitutive elements in the institution itself. Taking as granted that the institutional regulation depends on the constitutive state, this paper departs from the SAI conceptual model to propose clear defined semantics answering to these two challenges.

The paper begins with a global overview of the SAI model (Section 2), on which we base our contributions, that are presented in the sections 3 and 4. While the Section 3 introduces the necessary representations to support the interpretation of the constitutive rules, the Section 4 is focused on the dynamic aspects of this interpretation. Before concluding and pointing some perspectives for future work, Section 5 discusses the contributions of this paper with respect to related work.

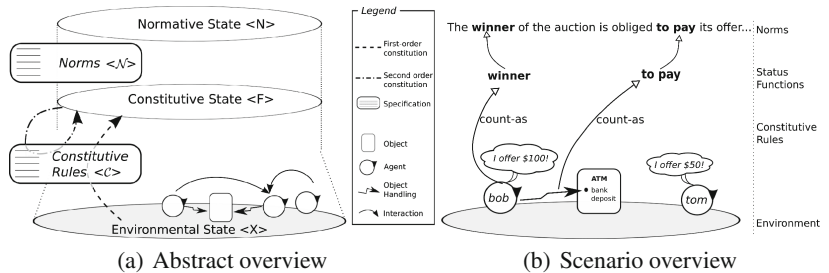


**Fig. 1.** SAI overview

## 2 Background

Before presenting our contributions in the next sections, this section briefly describes the SAI model proposed in [2]. In SAI, norms define the expected behaviour from the agents in an abstract level that is not directly related to the environment. For example, the norm “*the winner of an auction is obliged to pay its offer*” does not specify neither who is the winner that is obliged to fulfil the norm nor what the winner must concretely do to fulfil it. The effectiveness of a norm depends on its connection to the environment as its dynamics (activation, fulfilment, etc) results of facts occurring there. Such a connection

is established when the components of the norms – the *status functions* – are constituted, according to *constitutive rules*, from the *environmental elements* (Figure 1). These elements are described below:

- The environmental elements, represented by  $\mathcal{X} = \mathcal{A}_{\mathcal{X}} \cup \mathcal{E}_{\mathcal{X}} \cup \mathcal{S}_{\mathcal{X}}$ , are organized in the set  $\mathcal{A}_{\mathcal{X}}$  of agents possibly acting in the system, the set  $\mathcal{E}_{\mathcal{X}}$  of events that may happen in the environment, and the set  $\mathcal{S}_{\mathcal{X}}$  of properties used to describe the possible states of the environment.
- The status functions of a SAI, represented by  $\mathcal{F} = \mathcal{A}_{\mathcal{F}} \cup \mathcal{E}_{\mathcal{F}} \cup \mathcal{S}_{\mathcal{F}}$ , are the set  $\mathcal{A}_{\mathcal{F}}$  of agent-status functions (i.e. status functions assignable to agents), the set  $\mathcal{E}_{\mathcal{F}}$  of event-status functions (i.e. status functions assignable to events), and the set  $\mathcal{S}_{\mathcal{F}}$  of state-status functions (i.e. status functions assignable to states). Status functions are functions that the environmental elements (agents, events, and states) perform from the institutional perspective [4]. For example, in an auction, an agent may have the function of *winner*, the utterance “I offer \$100” may have the function of *bid*, and the state of “more than 20 people placed in a room at Friday 10am” may mean the *minimum quorum* for its realization.
- The *constitutive rules* defined in  $\mathcal{C}$  specify the constitution of the status functions of  $\mathcal{F}$  from the environment element of  $\mathcal{X}$ . A constitutive rule  $c \in \mathcal{C}$  is a tuple  $\langle x, y, t, m \rangle$  where  $x \in \mathcal{F} \cup \mathcal{X} \cup \{\varepsilon\}$ ,  $y \in \mathcal{F}$ ,  $t \in \mathcal{E}_{\mathcal{F}} \cup \mathcal{E}_{\mathcal{X}} \cup \top$ ,  $m \in W$ , and  $W = W_{\mathcal{F}} \cup W_{\mathcal{X}}$ .  $W_{\mathcal{F}}$  is the set of status-functions-formulae (sf-formulae) and  $W_{\mathcal{X}}$  is the set of environment-formulae (e-formulae), defined later. A constitutive rule  $\langle x, y, t, m \rangle$  specifies that  $x$  counts as  $y$  when  $t$  has happened while  $m$  holds. If  $x = \varepsilon$ , then there is a *freestanding assignment* of the status function  $y$ , i.e. an assignment where there is not a concrete environmental element carrying  $y$  [2,4]. When  $x$  actually counts as  $y$  (i.e. when the conditions  $t$  and  $m$  declared in the constitutive rule are true), we say that there is a *status function assignment* (SFA) of the status function  $y$  to the element  $x$ . The establishment of a SFA of  $y$  to some  $x$  is the *constitution* of  $y$ . The set of all SFAs of a SAI composes its *constitutive state* (see Def. 4).

The sf-formulae  $w_{\mathcal{F}} \in W_{\mathcal{F}}$  are logical formulae, based on status functions (see the Expression 1 below). The e-formulae  $w_{\mathcal{X}} \in W_{\mathcal{X}}$  are logical formulae, based on environmental elements (see the Expression 2 below). Section 3 defines the proper semantics of these formulae, based on SFA and on the actual environment.

$$w_{\mathcal{F}} ::= e_{\mathcal{F}} | s_{\mathcal{F}} | \neg w_{\mathcal{F}} | w_{\mathcal{F}} \vee w_{\mathcal{F}} | w_{\mathcal{F}} \wedge w_{\mathcal{F}} | x \text{ is } y | \perp | \top \quad (1)$$

$$w_{\mathcal{X}} ::= e_{\mathcal{X}} | s_{\mathcal{X}} | \neg w_{\mathcal{X}} | w_{\mathcal{X}} \vee w_{\mathcal{X}} | w_{\mathcal{X}} \wedge w_{\mathcal{X}} | \perp | \top \quad (2)$$

Considering these definitions of SAI, the challenges stated in the introduction are addressed in the next sections by (i) defining a uniform constitutive dynamics considering the agent, state or event proper life cycles, and (ii) enriching this uniform dynamics with the life cycle of the SFA themselves since constitutions may be stated by already constituted status functions. The first sub-objective requires to consider both instantaneous and fluent<sup>1</sup> dynamics coming from events

---

<sup>1</sup> *Fluent* refers to the possibility of holding along many states and *instantaneous* refers to the holding during a single state.

or states in the environment. Addressing the second sub-objective requires to consider the constitutive state as condition to the constitution (i.e. constitutions may take place under specific constitutive states) but also as the container of elements to whom status function can be assigned.

### 3 Constitutive Dynamics - Preliminaries

The semantics of the constitutive rules requires, as presented in this section, a formal representation of the elements related to the SAI constitutive dynamics.<sup>2</sup>

**Definition 1 (SAI state).** *The SAI state is composed by an environmental state  $X$ , a constitutive state  $F$ , and a normative state  $N$ . It is represented by  $SAI_{Dyn} = \langle X, F, N \rangle$ .*

The formal representation of  $X$  and  $F$  is introduced below. As the normative state dynamics is beyond the scope of this paper,  $N$  is introduced as part of the SAI state but it is not detailed here.

**Definition 2 (SAI history).** *The history of a SAI is the sequence of its  $i \in \mathbb{N}$  states (where  $\mathbb{N}$  is the set of the natural numbers).*

The SAI state at the  $i^{th}$  step of its history is represented by  $SAI_{Dyn}^i = \langle X^i, F^i, N^i \rangle$ . The set of all states between the first step and the  $i^{th}$  step is represented by  $SAI_{Dyn}^{[i]} = \langle X^{[i]}, F^{[i]}, N^{[i]} \rangle$ .

**Definition 3 (Environmental state).** *The environmental state is represented by  $X = \langle A_X, E_X, S_X \rangle$  where (i)  $A_X$  is the set of agents participating in the system, (ii)  $E_X$  is the set of events occurring in the environment and (iii)  $S_X$  is the set of environmental properties describing the environmental state.*

Agents in  $A_X$  are represented by their names. States in  $S_X$  are represented by first order logic atomic formulae. Events in  $E_X$  are represented by pairs  $(e, a)$  where  $e$  is the event, represented by a first order logic atomic formula, triggered by the agent  $a$ . Events can be triggered by actions of the agents (e.g. the utterance of a bid in an auction, the handling of an environmental artifact, etc) but can be also produced by the environment itself (e.g. a clock tick). In this case, events are represented by pairs  $(e, \varepsilon)$ . We use  $X = \langle A_X, E_X, S_X \rangle$  to denote the current state of the environment. When it is necessary to explicitly refer to the state of  $X$  at the step  $i$  of the SAI history, we use  $X^i = \langle A_X^i, E_X^i, S_X^i \rangle$ . The environmental state  $X$  is used to evaluate e-formulae (see Expression 2 for

---

<sup>2</sup> Similarly to the SAI specification, the SAI dynamics can be divided in two parts: (i) *constitutive dynamics*, consisting of the status functions assignments and revocations, and (ii) *normative dynamics*, consisting of the norm activations, fulfilments, violations, etc. The normative dynamic is beyond the scope of this paper.

syntax)<sup>3</sup>:

$$S_X \models w_{\mathcal{X}} \text{ iff } \exists \theta : w_{\mathcal{X}} \in \mathcal{S}_{\mathcal{X}} \wedge w_{\mathcal{X}} \theta \in S_X \quad (3)$$

$$E_X \models w_{\mathcal{X}} \text{ iff } \exists \theta : w_{\mathcal{X}} \in \mathcal{E}_{\mathcal{X}} \wedge w_{\mathcal{X}} \theta \in E_X \quad (4)$$

**Definition 4 (Constitutive state).** *The constitutive state of a SAI is represented by  $F = \langle A_F, E_F, S_F \rangle$  where (i)  $A_F \subseteq A_X \times \mathcal{A}_F$  is the set of agent-status function assignments, (ii)  $E_F \subseteq E_X \times \mathcal{E}_F \times A_X$  is the set of event-status function assignments and (iii)  $S_F \subseteq S_X \times \mathcal{S}_F$  is the set of state-status function assignments.*

As introduced in the previous section, SFA are relations between environmental elements and status functions. Elements of  $A_F$  are pairs  $\langle a_X, a_F \rangle$  meaning that the agent  $a_X \in A_X$  has the status function  $a_F \in \mathcal{A}_F$ . Elements of  $E_F$  are triples  $\langle e_X, e_F, a_X \rangle$  meaning that the event-status function  $e_F \in \mathcal{E}_F$  is assigned to the event  $e_X \in E_X$  produced by the agent  $a_X \in A_X$ . As events are supposed to be considered at the individual agent level in normative systems [6], it is important to record the agent that causes an event-status function assignment. Elements of  $S_F$  are pairs  $\langle s_X, s_F \rangle$  meaning that the state  $s_X \in S_X$  carries the status function  $s_F \in \mathcal{S}_F$ . In the following, we will note  $F = \langle A_F, E_F, S_F \rangle$  to denote the current constitutive state and  $F^i = \langle A_F^i, E_F^i, S_F^i \rangle$  will be used to refer to the constitutive state  $F$  at the step  $i$  of the SAI history.

The constitutive state  $F$  is used to evaluate the sf-formulae (see Expression 1 for syntax). If an agent  $x$  participates in the system (i.e.  $x \in A_X$ ) and carries the status function  $y$  (i.e. if  $\langle x, y \rangle \in A_F$ ), then the formula  $x \mathbf{is} y$  is true in current state  $F$ :

$$A_F \models x \mathbf{is} y \text{ iff } x \in A_X \wedge y \in \mathcal{A}_F \wedge \langle x, y \rangle \in A_F \quad (5)$$

In the same way, event-status function semantics is defined in the Expression 6. In addition, if an event-status function is assigned to some environmental event, then this event-status function follows from the current constitutive state  $F$  (Expression 7):

$$E_F \models x \mathbf{is} y \text{ iff } x \in E_X \wedge x = \langle e, a \rangle \wedge y \in \mathcal{E}_F \wedge \langle e, y, a \rangle \in E_F \quad (6)$$

$$E_F \models w_{\mathcal{F}} \text{ iff } w_{\mathcal{F}} \in \mathcal{E}_F \wedge \exists e_X : e_X \mathbf{is} w_{\mathcal{F}} \quad (7)$$

State-status function semantics is similarly defined in the Expression 8. In addition, if there is some assignment involving a state-status function, then this state-status function follows from the current constitutive state  $F$  (Expression 9):

$$S_F \models x \mathbf{is} y \text{ iff } x \in S_X \wedge y \in \mathcal{S}_F \wedge \langle x, y \rangle \in S_F \quad (8)$$

$$S_F \models w_{\mathcal{F}} \text{ iff } w_{\mathcal{F}} \in \mathcal{S}_F \wedge \exists s_X : s_X \mathbf{is} w_{\mathcal{F}} \quad (9)$$

The *constitutive state* defines how the institution is situated. The next section defines how this constitutive state is deduced from the environmental state and from the constitutive state itself.

<sup>3</sup> In this paper, a *substitution* is always represented by  $\theta$ . A *substitution* is a finite set of pairs  $\{\alpha_1/\beta_1, \dots, \alpha_n/\beta_n\}$  where  $\alpha_i$  is a variable and  $\beta_i$  is a term. If  $\theta$  is a substitution and  $\rho$  is a literal, then  $\rho\theta$  is the literal resulting from the replacement of each  $\alpha_i$  in  $\rho$  by the corresponding  $\beta_i$  [5].

```

status_functions:
  agents: auctioneer, bidder, current_winner, winner.
  events: to_bid(Value), to_pay(Value), to_fine_winner, commercial_transaction.
  states: auction_running, auction_finished, current_value(Value).
norms:
  1:auction.finished: winner obliged to_pay(current.value).
constitutive_rules:
  /* The agent that proposes an auction is the auctioneer */
  1: Agent count-as auctioneer when (propose(auction),Agent) while not auction.finished.
  /* While the auction is running, any agent other than the auctioneer is a bidder */
  2: Agent count-as bidder while not(Agent is auctioneer)& auction.running.
  /* Auctioneer and bidders are auction participants */
  3: auctioneer count-as auction.participant
  4: bidder count-as auction.participant
  /* The agent that performs the best bid is the current.winner */
  5: Agent count-as current.winner when (to_bid(Value),Agent)
      while (not(current.value(=Current)) & Current>Value)& (auction.running|auction.finished).
  /* The current winner is the (final) winner if the auction is finished */
  6: current.winner count-as winner while auction.finished.
  /* An auction is running while there is an agent being the auctioneer */
  7: count-as auction.running while _ is auctioneer.
  /* Auctioneer hitting the hammer means that the auction is finished */
  8: count-as auction.finished when (hit锤, Agent) while Agent is auctioneer.
  /* An offer done by a bidder while the auction is running is a bid */
  9: (offer(Value),Agent) count-as to_bid(Value) while auction.running & Agent is bidder.
  /* An offered value if it is greater than the last one */
  10: count-as current.value(Value) when (to_bid(Value),Agent)
      while Agent is bidder & (not(Current is current.value) & Current>Value)& (auction.running|auction.finished).
  /* A bid is a commercial transaction */
  11: to_bid count-as commercial.transaction.
  /* A bank deposit from the winner to the auctioneer is a payment */
  12: (bank.deposit(Creditor,Value),Agent) count-as to_pay(Value)
      while Creditor is auctioneer & Agent is winner & auction.finished & current.value(Value).

```

**Fig. 2.** SAI Specification

## 4 Constitutive Dynamics

The interpretation of the constitutive rules produces the SFA composing the SAI constitutive state. Constitutive rules can specify two kinds of constitution of status functions: *first-order constitution* (Section 4.1) and *second-order constitution* (Section 4.2). From these two definitions, Section 4.3 defines the constitutive dynamics of SAI. This is all illustrated considering an auction scenario whose regulation is specified in the Figure 2, according to the SAI specification language proposed in [2].

### 4.1 First-Order Constitution

The *first-order constitution*, explained in def. 5 to 7, explicitly assigns a status function to agents, events, and states from the environment stating, for example that the agent *bob* counts as a *bidder*.

**Definition 5 (First-order constitution of agent-status-functions).** *The set of agent-status function assignments due to first-order constitution in the  $i^{th}$  step of the SAI history is given by the function  $f\text{-}const_a$  defined as follows:*

$$\begin{aligned}
 f\text{-}const_a(\mathcal{F}, \mathcal{C}, X^{[i-1]}, F^{[i-1]}) = & \{ \langle x\theta, y \rangle | \exists \theta \ \exists \langle x, y, t, m \rangle \in \mathcal{C} \ \exists s \in \mathbb{N} \ \forall k \in [s, i-1] : \\
 & (y \in \mathcal{A}_F) \wedge (E_X^s \cup E_F^s \models t\theta) \wedge (X^k \cup F^k \models m\theta) \wedge x\theta \in A_X^{i-1} \}
 \end{aligned}$$

Informally, (i) if exists a constitutive rule  $\langle x, y, t, m \rangle$  whose element  $t$ , under a substitution  $\theta$ , represents an event occurred at the step  $s$  and (ii) if along all the steps  $k$  from  $s$  to  $i - 1$  the formula  $m$ , under  $\theta$ , is entailed by the environmental and constitutive states, then the agent identified by the element  $x$  under  $\theta$  carries the agent-status function  $y$  in the step  $i$ . Note that the function defines that an SFA to an agent only holds while the agent participates in the system. If it leaves the system, all its SFAs are dropped. The function also explicits our proposed approach to deal with combined instantaneous events and fluent states as conditions to constitution when it defines that an SFA belongs to the constitutive state if  $m$  holds in all steps  $k$  from the occurrence of  $t$  (at the step  $s$ ) until the step  $i - 1$ . Some points to observe in this definition are: (i) the repetition of the event  $t$  does not affect the SFA and (ii) a SFA is dropped if  $m$  ceases to hold and is not undropped if the  $m$  turns to hold (unless the event  $t$  happens again while  $m$  is again holding).

The rule 1 in the Figure 2 defines a first-order constitution of an agent-status function. If  $(propose(auction), bob) \in E_X^1$ , meaning that the agent  $bob$  has proposed an auction at the step 1, then  $bob$  carries the status function  $auctioneer$  (i.e.  $\langle bob, auctioneer \rangle \in f\text{-}const_a(\mathcal{F}, \mathcal{C}, X^{[i-1]}, F^{[i-1]})$ ) for all steps  $i$ , starting from the 2<sup>nd</sup> one, while the property  $auction\_finished$  does not hold (considering  $\theta = \{Agent/bob\}$ ).

**Definition 6 (First-order constitution of state-status-functions).** *The set of state-status-function assignments due to first-order constitution in the  $i^{th}$  step of the SAI history is given by the function  $f\text{-}const_s$  defined as follows:*

$$\begin{aligned} f\text{-}const_s(\mathcal{F}, \mathcal{C}, X^{[i-1]}, F^{[i-1]}) = & \{ \langle x\theta, y \rangle | \exists \theta \ \exists \langle x, y, t, m \rangle \in \mathcal{C} \exists s \in \mathbb{N} \ \forall k \in [s, i-1] : \\ & (y \in \mathcal{S}_F) \wedge (E_X^s \cup E_F^s \models t\theta) \wedge (X^k \cup F^k \models m\theta) \wedge ((x = \varepsilon) \vee (x\theta \in S_X^{i-1})) \end{aligned}$$

Similar to the constitution of agent-status functions, (i) a SFA to a state  $x \in S_X$  only holds while  $x$  holds in the environment and (ii) the constitution of state-status functions is conditioned to the holding of  $m$  in all steps from the occurrence of the event  $t$ . Besides, the function  $f\text{-}const_s$  explicits our conception that the constitution of state-status functions may result in freestanding assignments.

The rule 8 in the Figure 2 defines a first-order constitution of a state-status function. If  $(hit\_hammer, bob) \in E_X^3$ , meaning that  $bob$  has hitted a hammer at the step 3, then the assignment  $\langle \varepsilon, auction\_finished \rangle$  is active from the step 4 while  $bob$  has the status function of  $auctioneer$  (considering  $\theta = \{Agent/bob\}$ ).

**Definition 7 (First-order constitution of event-status-functions).** *The set of event-status-function assignments due to first-order constitution in the  $i^{th}$  step of the SAI history is given by the function  $f\text{-}const_e$  defined as follows:*

$$\begin{aligned} f\text{-}const_e(\mathcal{F}, \mathcal{C}, X^{[i-1]}, F^{[i-1]}) = & \{ \langle e\theta, y, a\theta \rangle | \exists \theta \ \exists \langle x, y, t, m \rangle \in \mathcal{C} : (y \in \mathcal{E}_F) \wedge \\ & (E_X^{i-1} \cup E_F^{i-1} \models t\theta) \wedge (X^{i-1} \cup F^{i-1} \models m\theta) \wedge x = (e, a) \wedge (e\theta, a\theta) \in E_X^{i-1} \} \end{aligned}$$

Compared to agent- and state-status functions, the constitution of event-status functions is differently related to the SAI history. Event-status function assignments are assumed to hold only in the step after which the conditions  $t$  and  $m$  hold, mimicking, thus, in the constitutive level, the atomic nature of the environmental events [7]. Thus, the holding of  $m$  during many steps of the SAI history does not imply in the holding of an event-status function assignment.

The rule 9 in the Figure 2 defines a first-order constitution of an event-status function. If  $(offer(100), tom) \in E_X^2$  meaning that  $tom$  has uttered an offer of \$100 at the step 2, then the assignment  $\langle offer(100), to\_bid, tom \rangle$  holds in the step 3, i.e.  $\langle offer(100), to\_bid, tom \rangle \in f\text{-}const_e(\mathcal{F}, \mathcal{C}, X^{[2]}, F^{[2]})$  (considering  $\theta = \{Value/100, Agent/tom\}$ ). When  $t \neq \top$ , the event-status-function assignment is assigned to the event  $x$  conditioned to the occurrence of two events at the same step: the event  $x$  itself and the event  $t$ .

## 4.2 Second-Order Constitution

Constitutive rules specifying second-order constitution define that a status function counts as another status function. But even specifying a relation between two status functions, the assignments resulting of the second-order constitution are also relations between status functions and environmental elements. That is to say, whenever status function  $s_1$  counts as a status function  $s_2$  all the elements constituting  $s_1$  constitute also  $s_2$ . For example, even the rule 3 in the Figure 2 states that the *auctioneer* counts as an *auction-participant*, the status function of *auction-participant* is actually assigned to all the concrete agents carrying the status function of *auctioneer*.

Defining the set of SFA due to second order constitution is an iterative process, as each change in the constitutive state may produce new SFA. To deal with this, the functions defined as follows have the index  $n$  (e.g.  $s\text{-}const_a^n$ ), representing the  $n^{th}$  iteration in the evaluation of second-order constitution in a same step of the SAI history. Each iteration  $n$  takes into account the assignments produced in the iteration  $n - 1$ . The whole set of SFA due to second-order constitution in a step  $i$  of the SAI history is found when the SFAs produced in the iterations  $n$  and  $n - 1$  are the same.

**Definition 8 (Second-order constitution of agent-status-functions).** *Given the function  $s\text{-}const_a^n$  ( $n \geq 0$ ) defined below, the set of agent-status function assignments due to second-order constitution in the  $i^{th}$  step of the SAI history is given by  $s\text{-}const_a = s\text{-}const_a^n$  for the lowest  $n$  s.t.  $s\text{-}const_a^n = s\text{-}const_a^{n-1}$ :*

$$\begin{aligned} s\text{-}const_a^n(\mathcal{F}, \mathcal{C}, X^{[i]}, F^{[i]}) &= \{\langle a_X, y \rangle | \exists \theta \ \exists \langle x, y, t, m \rangle \in \mathcal{C} \ \exists s \in \mathbb{N} \ \forall k \in [s, i-1] : \\ &(y \in \mathcal{A}_F) \wedge (E_X^s \cup E_F^s \models t\theta) \wedge (X^k \cup F^k \models m\theta) \wedge (x\theta \in \mathcal{A}_F \wedge \langle a_X, x\theta \rangle \in A)\} \end{aligned}$$

$$\text{where } A = \begin{cases} A_F^{[i]} & \text{if } n = 0 \\ A_F^{[i]} \cup s\text{-}const_a^{n-1}(\mathcal{F}, \mathcal{C}, X^{[i]}, F^{[i]}) & \text{otherwise} \end{cases}$$

Informally, if there is a constitutive rule  $\langle x, y, t, m \rangle$  whose element  $x$ , under a substitution  $\theta$ , corresponds to a status function already assigned to an agent  $a_X$ , then this agent carries also the status function  $y \in \mathcal{A}_F$  (subject to the conditions  $t$  and  $m$ , as in the first-order constitution (Def.5)). When the agent  $a_X$  ceases to carry the status function  $x\theta$ , it also ceases to carry the status function  $y$ .

The rule 3 of the Figure 2 defines a second-order constitution of an agent-status function. Considering  $\theta = \{\text{Agent}/\text{bob}\}$ , if  $\text{bob}$  is *auctionner* at the  $i^{\text{th}}$  step (i.e.  $\langle \text{bob}, \text{auctioneer} \rangle \in A_{\mathcal{F}}^i$ ), then  $\langle \text{bob}, \text{auction\_participant} \rangle \in s\text{-const}_a^n(\mathcal{F}, \mathcal{C}, X^{[i]}, F^{[i]})$ , for  $n \geq 0$ , and, eventually,  $\text{bob} \in A_{\mathcal{F}}^i$ . Informally, the rule states that an agent having the status function of *auctioneer* counts as an *auction\_participant* and, as *bob* has the status function of *auctioneer*, he has also the status function of *auction\_participant*.

#### **Definition 9 (Second-order constitution of state-status-functions).**

Given the function  $s\text{-const}_s^n$  ( $n \geq 0$ ) defined below, the set of state-status function assignments due to second-order constitution in the  $i^{\text{th}}$  step of the SAI history is given by  $s\text{-const}_s = s\text{-const}_s^n$  for the lowest  $n$  s.t.  $s\text{-const}_s^n = s\text{-const}_s^{n-1}$ :

$$s\text{-const}_s^n(\mathcal{F}, \mathcal{C}, X^{[i]}, F^{[i]}) = \{ \langle s_X, y \rangle | \exists \theta \ \exists \langle x, y, t, m \rangle \in \mathcal{C} \ \exists s \in \mathbb{N} \ \forall k \in [s, i-1] : \\ (y \in \mathcal{S}_{\mathcal{F}}) \wedge (E_X^s \cup E_F^s \models t\theta) \wedge (X^k \cup F^k \models m\theta) \wedge (x\theta \in \mathcal{S}_{\mathcal{F}} \wedge \langle s_X, x\theta \rangle \in S) \}$$

$$\text{where } S = \begin{cases} S_F^{[i]} & \text{if } n = 0 \\ S_F^{[i]} \cup s\text{-const}_s^{n-1}(\mathcal{F}, \mathcal{C}, X^{[i]}, F^{[i]}) & \text{otherwise} \end{cases}$$

If there is a constitutive rule  $\langle x, y, t, m \rangle$  whose element  $x$ , under a substitution  $\theta$ , corresponds to a status function already assigned to a state  $s_X$ , then this state carries also the status function  $y \in \mathcal{S}_{\mathcal{F}}$  (subject to the conditions  $t$  and  $m$ , as in the first-order constitution (Def.6)). When  $s_X$  ceases to carry the status function  $x\theta$ , it also ceases to carry the status function  $y$ .

Let's consider the status function *payment\_phase* in an auction scenario and a constitutive rule stating that *auction\_finished* count-as *payment\_phase*. Thus, if  $\langle \varepsilon, \text{auction\_finished} \rangle \in S_F^i$ , then  $\langle \varepsilon, \text{payment\_phase} \rangle \in s\text{-const}_s^n(\mathcal{F}, \mathcal{C}, X^{[i]}, F^{[i]})$ , for  $n \geq 0$  and, eventually,  $\langle \varepsilon, \text{payment\_phase} \rangle \in S_F^i$ .

#### **Definition 10 (Second-order constitution of event-status-functions).**

Given the function  $s\text{-const}_e^n$  ( $n \geq 0$ ) defined below, the set of event-status function assignments due to second-order constitution in the  $i^{\text{th}}$  step of the SAI history is given by  $s\text{-const}_e = s\text{-const}_e^n$  for the lowest  $n$  s.t.  $s\text{-const}_e^n = s\text{-const}_e^{n-1}$ :

$$s\text{-const}_e^n(\mathcal{F}, \mathcal{C}, X^{[i]}, F^{[i]}) = \{ \langle e_X, y, a_X \rangle | \exists \theta \ \exists \langle x, y, t, m \rangle \in \mathcal{C} : (y \in \mathcal{E}_{\mathcal{F}}) \wedge \\ (E_X^{i-1} \cup E_F^{i-1} \models t\theta) \wedge (X^{i-1} \cup F^{i-1} \models m\theta) \wedge x\theta \in \mathcal{E}_{\mathcal{F}} \wedge \langle e_X, x\theta, a_X \rangle \in E \}$$

$$\text{where } E = \begin{cases} E_F^{[i]} & \text{if } n = 0 \\ E_F^{[i]} \cup s\text{-const}_e^{n-1}(\mathcal{F}, \mathcal{C}, X^{[i]}, F^{[i]}) & \text{otherwise} \end{cases}$$

If there is a constitutive rule  $\langle x, y, t, m \rangle$  whose element  $x$ , under a substitution  $\theta$ , corresponds to a status function already assigned to the event  $e_X$ , then  $e_X$

carries also the status function  $y \in \mathcal{E}_F$  (subject to the conditions  $t$  and  $m$ , as in the first-order constitution (Def.7)). The assignment of  $y$  to  $e_X$  holds while the assignment of  $x$  to  $e_X$  holds.

The constitutive rule 11 in the Figure 2 states that bidding in an auction is a commercial transaction. Supposing that the agent *tom* has uttered an offer at the step  $i - 1$ , then by the rule 9,  $\langle \text{offer}(100), \text{to\_bid}, \text{tom} \rangle \in E_F^i$  and, by the rule 12,  $\langle \text{offer}(100), \text{commercial\_transaction}, \text{tom} \rangle \in s\text{-const}_e^n(\mathcal{F}, \mathcal{C}, X^{[i]}, F^{[i]})$ , for  $n \geq 0$ , and eventually  $\langle \text{offer}(100), \text{commercial\_transaction}, \text{tom} \rangle \in E_F^i$  because (i) the term  $x$  of the rule is an event-status-function that (ii) is already assigned to the event *offer*(100).

From the definitions 8 to 10 we can see define how status functions being assigned to status functions allows to ground the institution in the environment while it enables different kinds of manipulations inside the constitutive level, such as the definition of multiple levels of abstraction (defining, for example, that the status functions  $y_1$  counts as  $y_2$ , that, on its turn, counts as  $y_3$ ), as well allowing to define relations inside the constitutive level such as generalization (e.g.  $y_1$  and  $y_2$  count as  $y_3$ ), etc.

### 4.3 SAI Constitutive State

The previously presented functions permit to formally define the constitutive state in the  $i^{th}$  step of the SAI history as  $F^i = \langle A_F^i, E_F^i, S_F^i \rangle$  where:

$$\begin{aligned} A_F^i &= \{f\text{-const}_a(\mathcal{F}, \mathcal{C}, X^{[i-1]}, F^{[i-1]}) \cup s\text{-const}_a(\mathcal{F}, \mathcal{C}, X^{[i]}, F^{[i]})\} \\ E_F^i &= \{f\text{-const}_e(\mathcal{F}, \mathcal{C}, X^{[i-1]}, F^{[i-1]}) \cup s\text{-const}_e(\mathcal{F}, \mathcal{C}, X^{[i]}, F^{[i]})\} \\ S_F^i &= \{f\text{-const}_s(\mathcal{F}, \mathcal{C}, X^{[i-1]}, F^{[i-1]}) \cup s\text{-const}_s(\mathcal{F}, \mathcal{C}, X^{[i]}, F^{[i]})\} \end{aligned}$$

### 4.4 Illustration of the Constitutive Dynamic within SAI

Following the semantics proposed in the previous sections, the interpretation of the constitutive rules produces the assignments and revocations of status functions, i.e. the constitutive dynamics of SAI. Such a constitutive dynamics is illustrated here with a running example related to the auction scenario previously explored.

The Table 1 shows 8 steps of the SAI history focusing on the environmental state  $X$  and on the constitutive one  $F$ . The environmental state evolves as follows: at step 1, the agents *bob* and *tom* act in the system; at the step 2, *bob* utters a proposal for an auction; at the step 5, *tom* utters an offer and the agent *ana* enters in the system; at the step 6, *bob* hits the hammer. The constitutive rules, interpreted as described in Section 4, build the constitutive state  $F$ . The column *C.Rule* shows the constitutive rule from the Figure 2 that has produced each SFA. For example, in the step 4,  $\langle \text{bob}, \text{auctioneer} \rangle$  is produced by constitutive rule 1,  $\langle \text{bob}, \text{auction\_participant} \rangle$  by the rule 3, and  $\langle \varepsilon, \text{auction\_running} \rangle$  by rule 7.

**Table 1.** Running example

Step	Environmental State ( $X$ )	Constitutive State ( $F$ )	C.Rule
1	$X_a = \{bob, tom\}$		
2	$X_a = \{bob, tom\}$ $X_e = \{(propose(auction), bob)\}$		
3	$X_a = \{bob, tom\}$	$A_F = \{\langle bob, auctioneer \rangle, \langle bob, auction\_participant \rangle\}$	1,3
4	$X_a = \{bob, tom\}$	$A_F = A_F^3$ $S_F = \{\langle \varepsilon, auction\_running \rangle\}$	1, 3 7
5	$X_a = \{bob, tom, ana\}$ $X_e = \{(offer(100), tom)\}$	$A_F = A_F^4 \cup \{\langle tom, bidder \rangle, \langle tom, auction\_participant \rangle\}$ $S_F = S_F^4$	1, 3, 2, 4 7
6	$X_a = \{bob, tom, ana\}$ $X_e = \{(hit_hammer, bob)\}$	$A_F = A_F^5 \cup \{\langle ana, bidder \rangle, \langle ana, auction\_participant \rangle\}$ $E_F = \{\langle offer(100), to\_bid, tom \rangle\}$ $S_F = S_F^5$	1, 3, 2, 4, 2, 4 9 7
7	$X_a = \{bob, tom, ana\}$	$A_F = A_F^6 \cup \{\langle tom, current\_winner \rangle\}$ $S_F = S_F^6 \cup \{\langle \varepsilon, current\_value(100) \rangle, \langle \varepsilon, auction\_finished \rangle\}$	1, 3, 2, 4, 2, 4, 5 7, 10, 8
8	$X_a = \{bob, tom, ana\}$	$A_F = \{\langle tom, current\_winner \rangle, \langle tom, winner \rangle\}$ $S_F = \{\langle \varepsilon, current\_value(100) \rangle, \langle \varepsilon, auction\_finished \rangle\}$	5, 6 10, 8

Note that the proposed semantics does not define just the establishment of the SFA but it defines also their revocations. For example, the constitutive rule 1 in the Figure 2 defines that the agent that proposes an auction is the *auctioneer* while the auction is not finished. In the example, this condition ceases to hold in the step 7, leading to a new state (8) where the assignment of the status function *auctioneer* to the agent *bob* is revoked.

## 5 Related Work

Different approaches in the literature investigate how environmental facts affect artificial institutions. Some, contrary to us, do not consider the environment producing some kind of dynamic inside the institution: in [1,8], the environmental elements are related to the concepts appearing in the norm specification but they do not produce facts related to the dynamics of norms (violations, fulfilments, etc); in [9], environmental facts determine properties that should hold in the institution but the institution is in charge to take such information and produce some dynamic where appropriate.

Some approaches, as we do, consider that environmental facts produce some kind of dynamics in the institution: in [10] they affect the dynamics of organisations producing role assignments, goal achievements, etc; they produce institutional events in [11]; they affect the normative dynamics in [12,13] producing norm fulfilments, violations, etc. Compared to these related works, this paper deals with the definition of how the environment determines another fact in the institution, that is namely the *constitution of status functions*, defining (and not just affecting) the *constitutive dynamics* that is the base of the regulation in SAI.

When the constitution of each kind of status functions is considered in isolation, some relations can be made, for example, between the constitution of

state-status functions and the constitution of *states of affairs* proposed in [14], or between the constitution of event-status functions and the generation of *institutional events* proposed in [11]. But we deal with the constitution of agent-, event-, and state-status function as, together, determining the dynamics of the constitutive state of SAI. This constitutive state is not viewed just as a container of constituted status functions but as a system having particular – and well defined by this paper – dynamics taking into account the different nature of their components. We deal with the constitution considering the particular nature of the three different kinds of status function, but we also consider the constitution of the three different status functions affecting each other.

Works such as those in line with [8], are concerned with the ontological aspects of the count-as, i.e. with the constitution defining and providing meaning to the institutional vocabulary. These aspects are also part of SAI conceptual model and, regarding to them, this paper contributes providing clear representations and semantics to actually ground the institutional vocabulary in the environment. In addition, by dealing with the second-order constitution, we clearly define how the manipulation of concepts of the institutional vocabulary – not explicitly related to the environment – is grounded in the environment.

## 6 Discussion and Perspectives

To be compliant with SAI definitions [2], the dynamics of the constitutive state must consider that status functions are assigned to (and only to) agents, events, and states under a uniform definition of constitution. Thus, our first sub-objective was to define a uniform constitutive dynamics considering that SFA may have specific life cycles according to their nature. To achieve it, we first defined the life cycles of the SFAs that even being produced by similar definition of constitutive rules, may be distinguished into: (i) agent-status function assignments holding only while the agent that carries the status function participates to the system, (ii) state-status function assignments holding while the state carrying the status function holds in the environment and (iii) event-status function assignments holding only during a single step of the SAI history. These definitions have been then complemented by the explicitation of the instantaneous and fluent expressions conditioning these constitutions. We captured important properties on this dynamics such as: proper dynamics of status function assignment for event, state or agents, stability of constituted status functions wrt repetition of events, dropping of constituted status function as soon as state condition is no more holding, etc.

The second sub-objective was to enrich the proposed dynamics issued of the environmental elements with the dynamics of the constituted status functions themselves. The approach that we took concerned first the conditions of constitutive rules where constituted status functions may appear (defs. 5 to 10), and definition of second-order constitution dynamics that highlights an important property of SAI conceptual model: production of new constitutive states based on facts that are indirectly related to the environment. This property is

important in the sense that it makes possible to situate the institution in the environment while making possible to consider the definition and dynamics of constitutive abstractions, generalisations, etc.

Future work include investigations about the normative state affecting the SAI constitutive state, normative dynamics on top of the constitutive dynamic, and manipulations inside the constitutive level through second-order constitution.

**Acknowledgments.** The authors thanks the financial support given by CAPES (PDSE 4926-14-5) and CNPq (grants 448462/2014-1 e 306301/2012-1).

## References

1. Aldewereld, H., Álvarez Napagao, S., Dignum, F., Vázquez-Salceda, J.: Making norms concrete. In: van der Hoek, W., Kaminka, G.A., Lespérance, Y., Luck, M., Sen, S. (eds.) AAMAS 2010, pp. 807–814 (2010)
2. de Brito, M., Hübner, J.F., Boissier, O.: A conceptual model for situated artificial institutions. In: Bulling, N., van der Torre, L., Villata, S., Jamroga, W., Vasconcelos, W. (eds.) CLIMA XV 2014. LNCS (LNAI), vol. 8624, pp. 35–51. Springer, Heidelberg (2014)
3. De Brito, M., Thevin, L., Garbay, C., Boissier, O., Hübner, J.F.: Situated artificial institution to support advanced regulation in the field of crisis management. In: Demazeau, Y., Decker, K.S., Bajo Pérez, J., De la Prieta, F. (eds.) PAAMS 2015. LNCS (LNAI), vol. 9086, pp. 66–79. Springer, Heidelberg (2015)
4. Searle, J.: Making the Social World. The Structure of Human Civilization. Oxford University Press (2009)
5. Brachman, R., Levesque, H.: Knowledge Representation and Reasoning. Morgan Kaufmann Publishers Inc., San Francisco (2004)
6. Vos, M.D., Balke, T., Satoh, K.: Combining event-and state-based norms. In: AAMAS 2013, pp. 1157–1158 (2013)
7. Cassandras, C.G., Lafortune, S.: Introduction to Discrete Event Systems. Springer-Verlag New York Inc., Secaucus (2006)
8. Grossi, D., Meyer, J.-J.C., Dignum, F.P.M.: Counts-as: classification or constitution? an answer using modal logic. In: Goble, L., Meyer, J.-J.C. (eds.) DEON 2006. LNCS (LNAI), vol. 4048, pp. 115–130. Springer, Heidelberg (2006)
9. de Brito, M., Hübner, J.F., Bordini, R.H.: Programming institutional facts in multi-agent systems. In: Aldewereld, H., Sichman, J.S. (eds.) COIN 2012. LNCS (LNAI), vol. 7756, pp. 158–173. Springer, Heidelberg (2013)
10. Piunti, M., Boissier, O., Hübner, J.F., Ricci, A.: Embodied organizations: a unifying perspective in programming agents, organizations and environments. In: MALLOW 2010. CEUR, vol. 627 (2010)
11. Cliffe, O., De Vos, M., Padgett, J.: Answer set programming for representing and reasoning about virtual institutions. In: Inoue, K., Satoh, K., Toni, F. (eds.) CLIMA 2006. LNCS (LNAI), vol. 4371, pp. 60–79. Springer, Heidelberg (2007)

12. Dastani, M., Grossi, D., Meyer, J.-J.C., Tinnemeier, N.: Normative multi-agent programs and their logics. In: Meyer, J.-J.C., Broersen, J. (eds.) KRAMAS 2008. LNCS (LNAI), vol. 5605, pp. 16–31. Springer, Heidelberg (2009)
13. Campos, J., López-Sánchez, M., Rodríguez-Aguilar, J.A., Esteva, M.: Formalising situatedness and adaptation in electronic institutions. In: Hübner, J.F., Matson, E., Boissier, O., Dignum, V. (eds.) COIN 2008. LNCS (LNAI), vol. 5428, pp. 126–139. Springer, Heidelberg (2009)
14. Jones, A., Sergot, M.: A formal characterisation of institutionalised power. Logic Journal of IGPL 4(3), 427–443 (1996)

# Checking WECKTLK Properties of Timed Real-Weighted Interpreted Systems via SMT-Based Bounded Model Checking

Agnieszka M. Zbrzezny<sup>(✉)</sup> and Andrzej Zbrzezny

IMCS, Jan Długosz University, Al. Armii Krajowej 13/15,

42-200 Częstochowa, Poland

{agnieszka.zbrzezny,a.zbrzezny}@ajd.czest.pl

**Abstract.** In this paper, we present the SMT-based bounded model checking (BMC) method for Timed Real-Weighted Interpreted Systems and for the existential fragment of the Weighted Epistemic Computation Tree Logic. We performed the BMC algorithm on Timed Weighted Generic Pipeline Paradigm benchmark. We have implemented SMT-BMC method and made preliminary experimental results, which demonstrate the efficiency of the method. To perform the experiments we used the state of the art SMT-solver Z3.

## 1 Introduction

The formalism of *interpreted systems* (ISs) was introduced in [2] to model multi-agent systems (MASs) [7], which are intended for reasoning about the agents' epistemic and temporal properties. *Timed interpreted systems* (TIS) was proposed in [9] to extend interpreted systems in order to make possible reasoning about real-time aspects of MASs. The formalism of weighted interpreted systems (WISs) [10] extends ISs to make the reasoning possible about not only temporal and epistemic properties, but also about agents's quantitative properties.

Multi-agent systems (MASs) are composed of many intelligent agents that interact with each other. The agents can share a common goal or they can pursue their own interests. Also, the agents may have deadline or other timing constraints to achieve intended targets. As it was shown in [2], knowledge is a useful concept for analyzing the information state and the behaviour of agents in multi-agent systems. Another different extensions of temporal logics [1] with doxastic [4], and deontic [5] modalities have been proposed. In this paper, we consider the existential fragment of a weighted epistemic computation tree logic (WECKTLK) interpreted over Timed Real-Weighted Interpreted Systems (TRWISs).

SMT-based bounded model checking (BMC) consists in translating the existential model checking problem for a modal logic and for a model to the satisfiability modulo theory problem (SMT-problem) of a quantifier-free first-order formula.

The original contributions of the paper are as follows. First, we define TRWIS as a model of MASs with the agents that have real-time deadlines to achieve intended goals and each transition holds a weight, which can be any non-negative real value. Second, we introduce the language WECTLK. Third, we propose a SMT-based BMC technique for TRWIS and for WECTLK.

To the best of our knowledge, there is no work that considers SMT-based BMC methods to check multi-agent systems modelled by means of timed real-weighted interpreted systems. Thus, in this paper we offer such a method. In particular, we make the following contributions. Firstly, we define and implement an SMT-based BMC method for WECTLK and for TRWISs. Secondly, we report on the initial experimental evaluation of our SMT-based BMC method. To this aim we use a scalable benchmark: the *timed weighted generic pipeline paradigm* [8, 10].

The structure of the paper is as follows. In Section 2 we shortly introduce the theory of timed real-weighted interpreted systems and the WECTLK language. In Section 3 we present our SMT-based BMC method. In Section 4 we experimentally evaluate the performance of our SMT-based BMC encoding. We conclude the paper in Section 5.

## 2 Preliminaries

In this section we first explain some notations used through the paper, and next we define timed real-weighted interpreted systems, and next we introduce syntax and semantics of WECTLK.

Let  $\mathbb{N}$  be a set of natural numbers,  $\mathbb{N}_+ = \mathbb{N} \setminus \{0\}$ ,  $\mathbb{R}$  be the set of non-negative real numbers, and  $\mathcal{X}$  be a finite set of non-negative natural variables, called *clocks* ranging over a set of non-negative natural numbers. A clock valuation is a function  $v : \mathcal{X} \rightarrow \mathbb{N}$  that assigns to each clock  $x \in \mathcal{X}$  a non-negative natural value  $v(x)$ . A set of all the clock valuations is denoted by  $\mathbb{N}^{|\mathcal{X}|}$ . The valuation  $v' = v[\mathcal{X}' := 0]$ , for  $\mathcal{X}' \subseteq \mathcal{X}$  is defined as:  $\forall_{x \in \mathcal{X}'} v'(x) = 0$  and  $\forall_{x \in \mathcal{X} \setminus \mathcal{X}'} v'(x) = v(x)$ . For  $\delta \in \mathbb{N}$ ,  $v + \delta$  denotes the valuation that assigns the value  $v(x) + \delta$  to each clock  $x$ .

The grammar

$$\varphi := \mathbf{true} \mid x < c \mid x \leq c \mid x = c \mid x \geq c \mid x > c \mid \varphi \wedge \varphi$$

generates the set  $\mathcal{C}(\mathcal{X})$  of clock constraints over  $\mathcal{X}$ , where  $x \in \mathcal{X}$  and  $c \in \mathbb{N}$ . A clock valuation  $v$  satisfies a clock constraint  $\varphi$ , written as  $v, \varphi$ , iff  $\varphi$  evaluates to be true using the clock values given by  $v$ .

Let  $c_{max}$  be a constant and  $v, v' \in \mathbb{N}^{|\mathcal{X}|}$  two clock valuation. We say that  $v \simeq v'$  iff the following condition holds for each  $x \in \mathcal{X}$ :

$$v(x) > c_{max} \text{ and } v'(x) > c_{max} \text{ or } v(x) \leq c_{max} \text{ and } v'(x) \leq c_{max} \text{ and } v(x) = v'(x)$$

The clock valuation  $v'$  such that for each clock  $x \in \mathcal{X}$ ,  $v'(x) = v(x) + 1$  if  $v(x) \leq c_{max}$ , and  $v'(x) = c_{max} + 1$  otherwise, is called a time successor of  $v$  (written  $\text{succ}(v)$ ).

**TRWISs.** Let  $Ag = \{1, \dots, n\}$  denotes a non-empty and finite set of agents, and  $\mathcal{E}$  be a special agent that is used to model the environment in which the agents operate and  $\mathcal{PV} = \bigcup_{\mathbf{c} \in Ag \cup \{\mathcal{E}\}} \mathcal{PV}_{\mathbf{c}}$  be a set of propositional variables, such that  $\mathcal{PV}_{\mathbf{c}_1} \cap \mathcal{PV}_{\mathbf{c}_2} = \emptyset$  for all  $\mathbf{c}_1, \mathbf{c}_2 \in Ag \cup \{\mathcal{E}\}$ . The *timed real-weighted interpreted system* (TRWIS) is a tuple

$$(L_{\mathbf{c}}, Act_{\mathbf{c}}, \mathcal{X}_{\mathbf{c}}, P_{\mathbf{c}}, t_{\mathbf{c}}, \mathcal{V}_{\mathbf{c}}, \mathcal{I}_{\mathbf{c}}, d_{\mathbf{c}})_{\mathbf{c} \in Ag \cup \{\mathcal{E}\}, \iota},$$

where  $L_{\mathbf{c}}$  is a non-empty set of *local states* of the agent  $\mathbf{c}$ ,  $S = L_1 \times \dots \times L_n \times L_{\mathcal{E}}$  is the set of all global states,  $\iota \subseteq S$  is a non-empty set of initial states,  $Act_{\mathbf{c}}$  is a non-empty set of *possible actions* of the agent  $\mathbf{c}$ ,  $Act = Act_1 \times \dots \times Act_n \times Act_{\mathcal{E}}$  is the set of *joint actions*,  $\mathcal{X}_{\mathbf{c}}$  is a non-empty set of *clocks*,  $P_{\mathbf{c}} : L_{\mathbf{c}} \rightarrow 2^{Act_{\mathbf{c}}}$  is a *protocol function*,  $t_{\mathbf{c}} : L_{\mathbf{c}} \times \mathcal{C}(\mathcal{X}_{\mathbf{c}}) \times 2^{\mathcal{X}_{\mathbf{c}}} \times Act \rightarrow L_{\mathbf{c}}$  is a (partial) *evolution function*,  $\mathcal{V}_{\mathbf{c}} : L_{\mathbf{c}} \rightarrow 2^{\mathcal{PV}}$  is a *valuation function* assigning to each local state a set of propositional variables that are assumed to be true at that state,  $\mathcal{I}_{\mathbf{c}} : L_{\mathbf{c}} \rightarrow \mathcal{C}(\mathcal{X}_{\mathbf{c}})$  is an *invariant function*, that specifies an amount of time the agent  $\mathbf{c}$  may spend in a given local state, and  $d_{\mathbf{c}} : Act_{\mathbf{c}} \rightarrow \mathbb{IR}$  is a *weight function*.

For a given TRWIS we define a *timed real-weighted model* (or a *model*) as a tuple  $\mathcal{M} = (Act, S, \iota, T, \mathcal{V}, d)$ , where:

- $Act = Act_1 \times \dots \times Act_n \times Act_{\mathcal{E}}$  is the set of all the joint actions,
- $S = (L_1 \times \mathbb{IN}^{|\mathcal{X}_1|}) \times \dots \times (L_n \times \mathbb{IN}^{|\mathcal{X}_n|}) \times (L_{\mathcal{E}} \times \mathbb{IN}^{|\mathcal{X}_{\mathcal{E}}|})$  is the set of all the *global states*
- $\iota = (\iota_1 \times \{0\}^{|\mathcal{X}_1|}) \times \dots \times (\iota_n \times \{0\}^{|\mathcal{X}_n|}) \times (\iota_{\mathcal{E}} \times (\{0\}^{|\mathcal{X}_{\mathcal{E}}|})$  is the set of all the *initial global states*,
- $\mathcal{V} : S \rightarrow 2^{\mathcal{PV}}$  is the valuation function defined as  $\mathcal{V}(s) = \bigcup_{\mathbf{c} \in Ag \cup \{\mathcal{E}\}} \mathcal{V}_{\mathbf{c}}(l_{\mathbf{c}}(s))$ ,
- $T \subseteq S \times (Act \cup \mathbb{IN}) \times S$  is a transition relation defined by action and time transitions. For  $a \in Act$  and  $\delta \in \mathbb{IN}$ :
  1. action transition:  $(s, a, s') \in T$  (or  $s \xrightarrow{a} s'$ ) iff for all  $\mathbf{c} \in Ag \cup \mathcal{E}$ , there exists a local transition  $t_{\mathbf{c}}(l_{\mathbf{c}}(s), \varphi_{\mathbf{c}}, \mathcal{X}', a) = l_{\mathbf{c}}(s')$  such that  $v_{\mathbf{c}}(s) \models \varphi_{\mathbf{c}} \wedge \mathcal{I}(l_{\mathbf{c}}(s))$  and  $v'_{\mathbf{c}}(s') = v_{\mathbf{c}}(s)[\mathcal{X}' := 0]$  and  $v'_{\mathbf{c}}(s') \models \mathcal{I}(l_{\mathbf{c}}(s'))$ ;
  2. time transition  $(s, \delta, s') \in T$  iff for all  $\mathbf{c} \in Ag \cup \mathcal{E}$ ,  $l_{\mathbf{c}}(s) = l_{\mathbf{c}}(s')$  and  $v'_{\mathbf{c}}(s') = v_{\mathbf{c}}(s) + \delta$  and  $v'_{\mathbf{c}}(s') \models \mathcal{I}(l_{\mathbf{c}}(s'))$ .
- $d : Act \rightarrow \mathbb{IR}$  is the “joint” weight function defined as follows:  $d((a_1, \dots, a_n, a_{\mathcal{E}})) = d_1(a_1) + \dots + d_n(a_n) + d_{\mathcal{E}}(a_{\mathcal{E}})$ .

Given a TRWIS we can define the indistinguishability relation  $\sim_{\mathbf{c}} \subseteq S \times S$  for any agent  $\mathbf{c}$  as follows:  $s \sim_{\mathbf{c}} s'$  iff  $l_{\mathbf{c}}(s') = l_{\mathbf{c}}(s)$  and  $v_{\mathbf{c}}(s') \simeq v_{\mathbf{c}}(s)$ . A run of TRWIS is an infinite sequence  $\rho = s_0 \xrightarrow{\delta_0, a_0} s_1 \xrightarrow{\delta_1, a_1} s_2 \xrightarrow{\delta_2, a_2} \dots$  of global states such that the following conditions hold for all  $i \in \mathbb{IN} : s_i \in S, a_i \in Act, \delta_i \in \mathbb{IN}_+$ , and there exists  $s'_i \in S$  such that  $(s_i, \delta_i, s'_i) \in T$  and  $(s_i, a_i, s_{i+1}) \in T$ . Notice that the definition of a run does not permit two consecutive joint actions to be performed one after the other, i.e., between each two joint actions some time must pass; such a run is called *strongly monotonic*.

**WECKTLK.** WECKTLK has been defined in [8] as the existential fragment of the weighted CTLK with integer cost constraints on *all* temporal modalities. We

extend WECTLK logic by adding non-negative real cost constraints. In the syntax of WECTLK we assume the following:  $p \in \mathcal{PV}$  is an atomic proposition,  $\mathbf{c} \in Ag$ ,  $\Gamma \subseteq Ag$ ,  $I$  is an interval in  $\mathbb{R} = \{0\ldots\}$  of the form:  $[a, \infty)$  and  $[a, b)$ , for  $a, b \in \mathbb{N}$  and  $a \neq b$ . Moreover, hereafter, by  $\text{right}(I)$  we denote the right end of the interval  $I$ . The WECTLK formulae are defined by the following grammar:

$$\varphi ::= \mathbf{true} \mid \mathbf{false} \mid p \mid \neg p \mid \varphi \vee \varphi \mid \varphi \wedge \varphi \mid \mathbf{EX}_I \varphi \mid \mathbf{E}(\varphi \mathbf{U}_I \varphi) \mid \mathbf{EG}_I \varphi \mid \overline{\mathbf{K}}_c \varphi \mid \overline{\mathbf{D}}_\Gamma \varphi \mid \overline{\mathbf{E}}_\Gamma \varphi \mid \overline{\mathbf{C}}_\Gamma \varphi.$$

In the semantics we assume the following definitions of epistemic relations:  $\sim_E^{\Gamma} \stackrel{\text{def}}{=} \bigcup_{\mathbf{c} \in \Gamma} \sim_{\mathbf{c}}$ ,  $\sim_C^{\Gamma} \stackrel{\text{def}}{=} (\sim_E^{\Gamma})^+$  (the transitive closure of  $\sim_E^{\Gamma}$ ),  $\sim_D^{\Gamma} \stackrel{\text{def}}{=} \bigcap_{\mathbf{c} \in \Gamma} \sim_{\mathbf{c}}$ , where  $\Gamma \subseteq Ag$ .

A WECTLK formula  $\varphi$  is *true* in a model  $\mathcal{M}$  (in symbols  $\mathcal{M} \models \varphi$ ) iff  $\mathcal{M}, s^0 \models \varphi$  for some  $s^0 \in \iota$  (i.e.,  $\varphi$  is true at some initial state of the model  $\mathcal{M}$ ). For every  $s \in S$  the relation  $\models$  is defined inductively as follows:

- $-\mathcal{M}, s \models \mathbf{true}$ ,  $\mathcal{M}, s \not\models \mathbf{false}$ ,  $\mathcal{M}, s \models p$  iff  $p \in \mathcal{V}(s)$ ,  $\mathcal{M}, s \models \neg p$  iff  $p \notin \mathcal{V}(s)$ ,
- $-\mathcal{M}, s \models \alpha \wedge \beta$  iff  $\mathcal{M}, s \models \alpha$  and  $\mathcal{M}, s \models \beta$ ,
- $-\mathcal{M}, s \models \alpha \vee \beta$  iff  $\mathcal{M}, s \models \alpha$  or  $\mathcal{M}, s \models \beta$ ,
- $-\mathcal{M}, s \models \mathbf{EX}_I \alpha$  iff  $(\exists \pi \in \Pi(s))(D\pi[0..1] \in I \text{ and } \mathcal{M}, \pi(1) \models \alpha)$ ,
- $-\mathcal{M}, s \models \mathbf{EG}_I \alpha$  iff  $(\exists \pi \in \Pi(s))(\forall i \geq 0)(D\pi[0..i] \in I \text{ implies } \mathcal{M}, \pi(i) \models \alpha)$ ,
- $-\mathcal{M}, s \models \mathbf{E}(\alpha \mathbf{U}_I \beta)$  iff  $(\exists \pi \in \Pi(s))(\exists i \geq 0)(D\pi[0..i] \in I \text{ and } \mathcal{M}, \pi(i) \models \beta \text{ and } (\forall j < i) \mathcal{M}, \pi(j) \models \alpha)$ ,
- $-\mathcal{M}, s \models \overline{\mathbf{K}}_c \alpha$  iff  $(\exists \pi \in \Pi)(\exists i \geq 0)(s \sim_c \pi(i) \text{ and } \mathcal{M}, \pi(i) \models \alpha)$ ,
- $-\mathcal{M}, s \models Y\alpha$  iff  $(\exists \pi \in \Pi)(\exists i \geq 0)(s \sim \pi(i) \text{ and } \mathcal{M}, \pi(i) \models \alpha)$ , where  $Y \in \{\mathbf{D}_\Gamma, \mathbf{E}_\Gamma, \mathbf{C}_\Gamma\}$  and  $\sim \in \{\sim_E^{\Gamma}, \sim_C^{\Gamma}, \sim_D^{\Gamma}\}$ .

**Abstract Model.** Let  $\mathbb{ID}_{\mathbf{c}} = \{0, \dots, c_{\mathbf{c}} + 1\}$  with  $c_{\mathbf{c}}$  be the largest constant appearing in any enabling condition or state invariants of agent  $\mathbf{c}$  and  $\mathbb{ID} = \bigcup_{\mathbf{c} \in Ag \cup \mathcal{E}} \mathbb{ID}_{\mathbf{c}}^{|\mathcal{X}_{\mathbf{c}}|}$ . A tuple  $\mathcal{M} = (Act, S, \iota, T, \mathcal{V}, d)$ , is an *abstract model*, where  $\iota = \prod_{\mathbf{c} \in Ag \cup \mathcal{E}} \iota_{\mathbf{c}} \times \{0\}^{|\mathcal{X}_{\mathbf{c}}|}$  is the set of all initial global states,  $S = \prod_{\mathbf{c} \in Ag \cup \mathcal{E}} L_{\mathbf{c}} \times \mathbb{ID}_{\mathbf{c}}^{|\mathcal{X}_{\mathbf{c}}|}$  is the set of all abstract global states.  $\mathcal{V} : S \rightarrow 2^{\mathcal{PV}}$  is the valuation function such that:  $p \in \mathcal{V}(s)$  iff  $p \in \bigcup_{\mathbf{c} \in Ag \cup \mathcal{E}} \mathcal{V}_{\mathbf{c}}(l_{\mathbf{c}}(s))$  for all  $p \in \mathcal{PV}$ ; and  $T \subseteq S \times (Act \cup \tau) \times S$ . Let  $a \in Act$ . Then,

1. Action transition:  $(s, a, s') \in T$  iff  $\forall_{\mathbf{c} \in Ag} \exists_{\phi_{\mathbf{c}} \in \mathcal{C}(\mathcal{X}_{\mathbf{c}})} \exists_{\mathcal{X}'_{\mathbf{c}} \subseteq \mathcal{X}_{\mathbf{c}}} (t_{\mathbf{c}}(l_{\mathbf{c}}(s), \phi_{\mathbf{c}}, \mathcal{X}'_{\mathbf{c}}, a) = l_{\mathbf{c}}(s') \text{ and } v_{\mathbf{c}} \models \phi_{\mathbf{c}} \wedge \mathcal{I}(l_{\mathbf{c}}(s)) \text{ and } v'_{\mathbf{c}}(s') = v_{\mathbf{c}}(s)[\mathcal{X}'_{\mathbf{c}} := 0] \text{ and } v'_{\mathbf{c}}(s') \models \mathcal{I}(l_{\mathbf{c}}(s')))$
2. Time transition:  $(s, \tau, s') \in T$  iff  $\forall_{\mathbf{c} \in Ag \cup \mathcal{E}} (l_{\mathbf{c}}(s) = l_{\mathbf{c}}(s'))$  and  $v_{\mathbf{c}}(s) \models \mathcal{I}(l_{\mathbf{c}}(s))$  and  $\text{succ}(v_{\mathbf{c}}(s)) \models \mathcal{I}(l_{\mathbf{c}}(s))$  and  $\forall_{\mathbf{c} \in Ag} (v'_{\mathbf{c}}(s') = \text{succ}(v_{\mathbf{c}}(s'))) \text{ and } (v'_{\mathcal{E}}(s') = \text{succ}(v_{\mathcal{E}}(s)))$ .

A path  $\pi$  in an abstract model is a sequence  $s_0 \xrightarrow{b_1} s_1 \xrightarrow{b_2} s_2 \xrightarrow{b_3} \dots$  of transitions such that for each  $i \leq 1$ ,  $b_i \in Act \cup \{\tau\}$  and  $b_1 = \tau$  and for each two consecutive transitions at least one of them is a time transition.

Given an abstract model one can define the indistinguishability relation  $\sim_{\mathbf{c}} \subseteq S \times S$  for agent  $\mathbf{c}$  as follows:  $s \sim_{\mathbf{c}} s'$  iff  $l_{\mathbf{c}}(s') = l_{\mathbf{c}}(s)$  and  $v_{\mathbf{c}}(s') = v_{\mathbf{c}}(s)$ .

### 3 SMT-Based Bounded Model Checking

In this section, we present an outline of the bounded semantics for WECKTLK and define an SMT-based BMC method for WECKTLK, which is based on the BMC encoding presented in [8]. As usual, we start by defining  $k$ -paths and  $(k, l)$ -loops. Next we define a bounded semantics, which is used for the translation to SMT.

**Bounded Semantics.** Let  $\mathcal{M}$  be a model, and  $k \in \mathbb{N}$  a bound. A  $k$ -path  $\pi_k$  is a finite sequence  $s_0 \xrightarrow{b_1} s_1 \xrightarrow{b_2} \dots \xrightarrow{b_k} s_k$  of transitions such that for each  $1 \leq i \leq k$ ,  $b_i \in \text{Act} \cup \{\tau\}$  and  $b_1 = \tau$  and for each two consecutive transitions at least one is a time transition. A  $k$ -path  $\pi_k$  is a *loop* if  $l < k$  and  $\pi(k) = \pi(l)$ . Note that if a  $k$ -path  $\pi_k$  is a loop, then it represents the infinite path of the form  $uv^\omega$ , where  $u = (s_0 \xrightarrow{b_1} s_1 \xrightarrow{b_2} \dots \xrightarrow{b_l} s_l)$  and  $v = (s_{l+1} \xrightarrow{b_{l+2}} \dots \xrightarrow{b_k} s_k)$ .  $\Pi_k(s)$  denotes the set of all the  $k$ -paths of  $\mathcal{M}$  that start at  $s$ , and  $\Pi_k = \bigcup_{s^0 \in \iota} \Pi_k(s^0)$ .

The bounded satisfiability relation  $\models_k$  which indicates  $k$ -truth of a WECKTLK formula in the model  $\mathcal{M}$  at some state  $s$  of  $\mathcal{M}$  is also defined in [8]. A WECKTLK formula  $\varphi$  is  $k$ -true in the model  $\mathcal{M}$  (in symbols  $\mathcal{M} \models_k \varphi$ ) iff  $\varphi$  is  $k$ -true at some initial state of the model  $\mathcal{M}$ .

The *model checking problem* asks whether  $\mathcal{M} \models \varphi$ , but the *bounded model checking problem* asks whether there exists  $k \in \mathbb{N}$  such that  $\mathcal{M} \models_k \varphi$ . The following theorem states that for a given model and a WECKTLK formula there exists a bound  $k$  such that the model checking problem ( $\mathcal{M} \models \varphi$ ) can be reduced to the bounded model checking problem ( $\mathcal{M} \models_k \varphi$ ).

**Theorem 1.** Let  $\mathcal{M}$  be the abstract model and  $\varphi$  a WECKTLK formula. Then, the following equivalence holds:  $\mathcal{M} \models \varphi$  iff there exists  $k \geq 0$  such that  $\mathcal{M} \models_k \varphi$ .

*Proof.* The theorem can be proved by induction on the length of the formula  $\varphi$  (for details one can see [8]).

**Translation to SMT.** Let  $\mathcal{M}$  be an abstract model,  $\varphi$  a WECKTLK formula, and  $k \geq 0$  a bound. The presented SMT encoding of the BMC problem for WECKTLK and for TRWIS is based on the SAT encoding of the same problem [10, 12], and it relies on defining the quantifier-free first-order formula:

$$[\mathcal{M}, \varphi]_k := [\mathcal{M}^{\varphi, \iota}]_k \wedge [\varphi]_{M, k}$$

that is satisfiable if and only if  $\mathcal{M} \models_k \varphi$  holds.

Let  $\mathbf{c} \in \text{Ag} \cup \{\mathcal{E}\}$ . The definition of the formula  $[\mathcal{M}, \varphi]_k$  assumes that

- each global state  $s \in S$  is represented by a valuation of a *symbolic state*  $\bar{w} = ((w_1, v_1), \dots, (w_n, v_n), (w_\mathcal{E}, v_\mathcal{E}))$  that consists of *symbolic local states* and each symbolic local state  $w_\mathbf{c}$  is a pair  $(w_\mathbf{c}, v_\mathbf{c})$  of individual variables ranging over the natural numbers, in which the first element represents a local state of the agent  $\mathbf{c}$ , and the second represents a clock valuation;

- each joint action  $a \in \text{Act}$  is represented by a valuation of a *symbolic action*  $\bar{a} = (a_1, \dots, a_n, a_\mathcal{E})$  that consists of *symbolic local actions* and each symbolic local action  $a_\mathbf{c}$  is an individual variable ranging over the natural numbers;

– each sequence of weights associated with the joint action is represented by a valuation of a *symbolic weights*  $\bar{d} = (d_1, \dots, d_{n+1})$  that consists of *symbolic local weights* and each symbolic local weight  $d_c$  is an individual variable ranging over the natural numbers.

The formula  $[\mathcal{M}^{\varphi,\iota}]_k$  encodes a rooted tree of  $k$ -paths of the model  $\mathcal{M}$ . The number of branches of the tree depends on the value of  $f_k : \text{WECTLK} \rightarrow \mathbb{N}$  which is the auxiliary function defined in [8]:

- $f_k(\text{true}) = f_k(\text{false}) = 0$ ;
- $f_k(p) = f_k(\neg p) = 0$ , where  $p \in \mathcal{PV}$ ;
- $f_k(\alpha \wedge \beta) = f_k(\alpha) + f_k(\beta)$ ;
- $f_k(\alpha \vee \beta) = \max\{f_k(\alpha), f_k(\beta)\}$ ;
- $f_k(\mathbf{EX}_I \alpha) = f_k(\alpha) + 1$ ;
- $f_k(\mathbf{EG}_I \alpha) = (k+1) \cdot f_k(\alpha) + 1$ ;
- $f_k(\mathbf{E}(\alpha \mathbf{U}_I \beta)) = k \cdot f_k(\alpha) + f_k(\beta) + 1$ ;
- $f_k(\overline{C}_I \alpha) = f_k(\alpha) + k$ ;
- $f_k(Y\alpha) = f_k(\alpha) + 1$  for  $Y \in \{\overline{K}_c, \overline{D}_I, \overline{E}_I\}$ .

The formula  $[\mathcal{M}^{\varphi,\iota}]_k$  is defined over  $(k+1) \cdot f_k(\varphi)$  different symbolic states,  $k \cdot f_k(\varphi)$  different symbolic actions, and  $k \cdot f_k(\varphi)$  different symbolic weights. Moreover, it uses the following auxiliary quantifier-free first-order formulae:

- $I_s(\overline{\mathbf{w}})$  - it encodes the state  $s$  of the model  $\mathcal{M}$ ;  $\mathbf{c} \in Ag \cup \mathcal{E}$ ;
- $H_{\mathbf{c}}(w_{\mathbf{c}}, w'_{\mathbf{c}})$  - it encodes equality of two local states, such that  $w_{\mathbf{c}} = w'_{\mathbf{c}}$  for  $\mathbf{c} \in Ag \cup \mathcal{E}$ ;
- $T_{\mathbf{c}}(w_{\mathbf{c}}, ((\bar{a}, \bar{d}), \bar{\delta}), w'_{\mathbf{c}})$  - it encodes the local evolution function of agent  $\mathbf{c}$ ;
- $\mathcal{A}(\bar{a})$  - it encodes that each symbolic local action  $a_{\mathbf{c}}$  of  $\bar{a}$  has to be executed by each agent in which it appears;
- $\mathcal{T}(\overline{\mathbf{w}}, ((\bar{a}, \bar{d}), \bar{\delta}), \overline{\mathbf{w}}') := \mathcal{A}(\bar{a}) \wedge \bigwedge_{\mathbf{c} \in Ag \cup \{\mathcal{E}\}} T_{\mathbf{c}}(w_{\mathbf{c}}, ((\bar{a}, \bar{d}), \bar{\delta}), w'_{\mathbf{c}})$ ;
- Let  $\pi_j$  denote the  $j$ -th *symbolic k-path*, i.e. the sequence of symbolic transitions:  $\overline{\mathbf{w}}_{0,j} \xrightarrow{(\bar{a}_{1,j}, \bar{d}_{1,j}), \delta_{1,j}} \overline{\mathbf{w}}_{1,j} \xrightarrow{(\bar{a}_{2,j}, \bar{d}_{2,j}), \delta_{2,j}} \dots \xrightarrow{(\bar{a}_{k,j}, \bar{d}_{k,j}), \delta_{k,j}} \overline{\mathbf{w}}_{k,j}$ . Then,  $\mathcal{D}_{a,b;c,d}^I(\pi_n)$  for  $a \leq b$  and  $c \leq d$  is a formula that:
  - for  $a < b$  and  $c < d$  encodes that the weight represented by the sequences  $\bar{d}_{a+1,n}, \dots, \bar{d}_{b,n}$  and  $\bar{d}_{c+1,n}, \dots, \bar{d}_{d,n}$  belongs to the interval  $I$ ,
  - for  $a = b$  and  $c < d$  encodes that the weight represented by the sequence  $\bar{d}_{c+1,n}, \dots, \bar{d}_{d,n}$  belongs to the interval  $I$ ,
  - for  $a < b$  and  $c = d$  encodes that the weight represented by the sequence  $\bar{d}_{a+1,n}, \dots, \bar{d}_{b,n}$  belongs to the interval  $I$ ,
  - for  $a = b$  and  $c = d$ , the formula  $\mathcal{D}_{a,b;c,d}^I(\pi_n)$  is true iff  $0 \in I$ .

Thus, given the above, we can define the formula  $[\mathcal{M}^{\varphi,\iota}]_k$  as follows:

$$[\mathcal{M}^{\varphi,\iota}]_k := \bigvee_{s \in \iota} I_s(\overline{\mathbf{w}}_{0,0}) \wedge \bigvee_{j=1}^{f_k(\varphi)} \overline{\mathbf{w}}_{0,0} = \overline{\mathbf{w}}_{0,j} \wedge \bigwedge_{j=1}^{f_k(\varphi)} \bigwedge_{i=0}^{k-1} \mathcal{T}(\overline{\mathbf{w}}_{i,j}, ((\bar{a}_{i,j}, \bar{d}_{i,j}), \bar{\delta}_{i,j}), \overline{\mathbf{w}}_{i+1,j})$$

where  $\overline{\mathbf{w}}_{i,j}$ ,  $\overline{a}_{i,j}$ , and  $\overline{d}_{i,j}$  are, respectively, symbolic states, symbolic actions, and symbolic weights for  $0 \leq i \leq k$  and  $1 \leq j \leq f_k(\varphi)$ . Hereafter, by  $\pi_j$  we denote the  $j$ -th symbolic  $k$ -path of the above unfolding, i.e., the sequence of transitions:

$$\overline{\mathbf{w}}_{0,j} \xrightarrow{(\overline{a}_{1,j}, \overline{d}_{1,j}), \overline{\delta}_{1,j}} \overline{\mathbf{w}}_{1,j} \xrightarrow{(\overline{a}_{2,j}, \overline{d}_{2,j}), \overline{\delta}_{2,j}} \dots \xrightarrow{(\overline{a}_{k,j}, \overline{d}_{k,j}), \overline{\delta}_{k,j}} \overline{\mathbf{w}}_{k,j}.$$

The formula  $[\varphi]_{\mathcal{M},k}$  encodes the bounded semantics of a WECKL formula  $\varphi$ , and it is defined on the same sets of individual variables as the formula  $[\mathcal{M}^{\varphi'}]_k$ . Moreover, it uses the auxiliary quantifier-free first-order formulae defined in [8].

Furthermore, following [8], our formula  $[\varphi]_{\mathcal{M},k}$  uses the following auxiliary functions  $g_l$ ,  $g_r$ ,  $g_\mu$ ,  $h_{\mathbf{U}}$ ,  $h_{\mathbf{G}}$  that were introduced in [11], and which allow to divide the set  $A \subseteq F_k(\varphi) = \{j \in \mathbb{N} \mid 1 \leq j \leq f_k(\varphi)\}$  into subsets needed for translating the subformulae of  $\varphi$ . Let  $0 \leq n \leq f_k(\varphi)$ ,  $m \leq k$ , and  $n' = \min(A)$ . The rest of translation is defined in the same way as in [8].

$$\begin{aligned} -[\text{true}]_k^{[m,n,A]} &:= \text{true}, [\text{false}]_k^{[m,n,A]} := \text{false}, \\ -[p]_k^{[m,n,A]} &:= p(\overline{\mathbf{w}}_{m,n}), \\ -[\neg p]_k^{[m,n,A]} &:= \neg p(\overline{\mathbf{w}}_{m,n}), \\ -[\alpha \wedge \beta]_k^{[m,n,A]} &:= [\alpha]_k^{[m,n,g_l(A,f_k(\alpha))]} \wedge [\beta]_k^{[m,n,g_r(A,f_k(\beta))]}, \\ -[\alpha \vee \beta]_k^{[m,n,A]} &:= [\alpha]_k^{[m,n,g_l(A,f_k(\alpha))]} \vee [\beta]_k^{[m,n,g_r(A,f_k(\beta))]}, \\ -[\mathbf{EX}_I \alpha]_k^{[m,n,A]} &:= \overline{\mathbf{w}}_{m,n} = \overline{\mathbf{w}}_{0,n'} \wedge (\overline{d}_{1,n'} \in I) \wedge [\alpha]_k^{[1,n',g_\mu(A)]}, \text{ if } k > 0; \text{false, otherwise,} \\ -[\mathbf{E}(\alpha \mathbf{U}_I \beta)]_k^{[m,n,A]} &:= \overline{\mathbf{w}}_{m,n} = \overline{\mathbf{w}}_{0,n'} \wedge \bigvee_{i=0}^k ([\beta]_k^{[i,n',h_{\mathbf{U}}(A,k,f_k(\beta))(j)]} \wedge \\ &(\sum_{j=1}^i \overline{d}_{j,n} \in I \wedge \bigwedge_{j=0}^{i-1} [\alpha]_k^{[j,n',h_{\mathbf{U}}(A,k,f_k(\beta))]})), \\ -[\mathbf{E}(\mathbf{G}_I \alpha)]_k^{[m,n,A]} &:= \overline{\mathbf{w}}_{m,n} = \overline{\mathbf{w}}_{0,n'} \wedge \left( (\sum_{j=1}^k \overline{d}_{j,n} \geq \mathbf{right}(I) \wedge \bigwedge_{i=0}^k (\sum_{j=1}^i \overline{d}_{j,n} \notin I \vee [\alpha]_k^{[i,n',h_{\mathbf{G}}(A,k)(j)]}) \vee (\sum_{j=1}^k \overline{d}_{j,n} < \mathbf{right}(I) \wedge \bigwedge_{i=0}^k (\sum_{j=1}^i \overline{d}_{j,n} \notin I \vee [\alpha]_k^{[i,n',h_{\mathbf{G}}(A,k)(j)]})) \right. \\ &\left. \wedge \bigvee_{l=0}^{k-1} (\overline{\mathbf{w}}_{k,n'} = \overline{\mathbf{w}}_{l,n'} \wedge \bigwedge_{i=l}^{k-1} (\neg D_{0,k;l,i+1}^I(\pi_{n'}) \vee [\alpha]_k^{[i,n',h_{\mathbf{G}}(A,k)(j)]}))), \right. \\ -[\overline{\mathbf{K}}_c \alpha]_k^{[m,n,A]} &:= (\bigvee_{s \in \iota} I_s(\overline{\mathbf{w}}_{0,n'})) \wedge \bigvee_{j=0}^k ([\alpha]_k^{[j,n',g_\mu(A)]} \wedge H_c(\overline{\mathbf{w}}_{m,n}, \overline{\mathbf{w}}_{j,n'})), \\ -[\overline{\mathbf{D}}_\Gamma \alpha]_k^{[m,n,A]} &:= (\bigvee_{s \in \iota} I_s(\overline{\mathbf{w}}_{0,n'})) \wedge \bigvee_{j=0}^k ([\alpha]_k^{[j,n',g_\mu(A)]} \wedge \bigwedge_{c \in \Gamma} H_c(\overline{\mathbf{w}}_{m,n}, \overline{\mathbf{w}}_{j,n'})), \\ -[\overline{\mathbf{E}}_\Gamma \alpha]_k^{[m,n,A]} &:= (\bigvee_{s \in \iota} I_s(\overline{\mathbf{w}}_{0,n'})) \wedge \bigvee_{j=0}^k ([\alpha]_k^{[j,n',g_\mu(A)]} \wedge \bigvee_{c \in \Gamma} H_c(\overline{\mathbf{w}}_{m,n}, \overline{\mathbf{w}}_{j,n'})), \\ -[\overline{\mathbf{C}}_\Gamma \alpha]_k^{[m,n,A]} &:= [\bigvee_{j=1}^k (\overline{\mathbf{E}}_\Gamma)^j \alpha]_k^{[m,n,A]}. \end{aligned}$$

The theorem below states the correctness and the completeness of the presented translation. It can be proved in a standard way by induction on the complexity of the given WECKL formula.

**Theorem 2.** *Let  $\mathcal{M}$  be a model, and  $\varphi$  a WECKL formula. For every  $k \in \mathbb{N}$ ,  $\mathcal{M} \models_k \varphi$  if, and only if, the quantifier-free first-order formula  $[\mathcal{M}, \varphi]_k$  is satisfiable.*

## 4 Experimental Results

In this section we experimentally evaluate the performance of our SMT-based BMC encoding for WECTLK over the TRWIS semantics.

The benchmark we consider is the *timed weighted generic pipeline paradigm* (TWGPP) TRWIS model [10]. The model of TWGPP involves  $n + 2$  agents:

- Producer producing data within certain time interval ( $[a, b]$ ) or being inactive,
- Consumer receiving data within certain time interval ( $[c, d]$ ) or being inactive within certain time interval ( $[g, h]$ ),
- a chain of  $n$  intermediate Nodes which can be ready for receiving data within certain time interval ( $[c, d]$ ), processing data within certain time interval ( $[e, f]$ ) or sending data.

The weights are used to adjust the cost properties of Producer, Consumer, and of the intermediate Nodes.

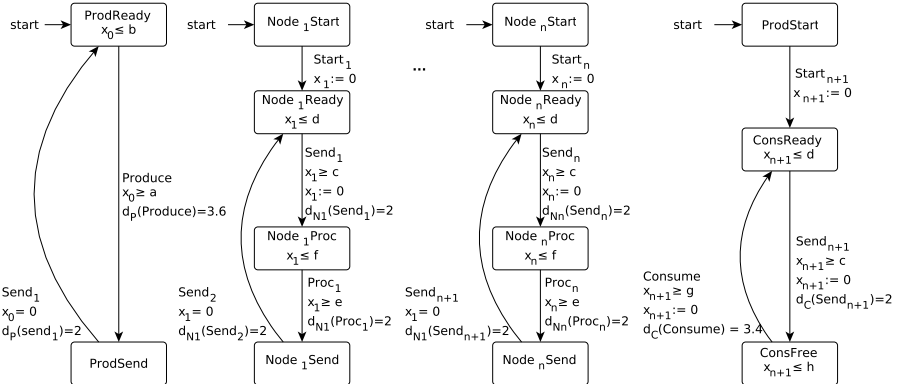


**Fig. 1.** The TWGPP system

Each agent of the scenario can be modelled by considering its local states, local actions, local protocol, local evolution function, local weight function, the local clocks, the clock constraints, invariants, and local valuation function. Fig. 1 shows the local states, the possible actions, and the protocol, the clock constraints, invariants and weights for each agent. Null actions are omitted in the figure.

Given Fig. 1, the local evolution functions of TWGPP are straightforward to infer. Moreover, we assume the following set of propositional variables:  $\mathcal{PV} = \{\text{ProdReady}, \text{ProdSend}, \text{ConsReady}, \text{ConsFree}\}$  with the following definitions of local valuation functions:

$$\begin{aligned} -\mathcal{V}_P(ProdReady-0) &= \{ProdReady\}, \mathcal{V}_P(ProdSend-1) = \{ProdSend\}, \\ -\mathcal{V}_C(ConsReady-0) &= \{ConsReady\}, \mathcal{V}_C(ConsFree-1) = \{ConsFree\}. \end{aligned}$$

Let  $Act = Act_P \times \prod_{i=1}^n Act_{N_i} \times Act_C$ , with  $Act_P = \{Produce, Send_1\}$ ,  $Act_C = \{Start_{n+1}, Consume, Send_{n+1}\}$ , and  $Act_{N_i} = \{Start_i, Send_i, Send_{i+1}, Proc_i\}$  defines the set of joint actions for the scenario. For  $\hat{a} \in Act$  let  $act_P(\hat{a})$  denotes an action of Producer,  $act_C(\hat{a})$  denotes an action of Consumer, and  $act_{N_i}(\hat{a})$  denotes an action of Node  $i$ . We assume the following local evolution functions:

$$\begin{aligned} -t_P(ProdReady, x_0 \geq a, \emptyset, \hat{a}) &= ProdSend, \text{ if } act_P(\hat{a}) = Produce \\ -t_P(ProdSend, true, \{x_0\}, \hat{a}) &= ProdReady, \text{ if } act_P(\hat{a}) = Send_1 \text{ and } act_{N_i}(\hat{a}) = Send_1 \\ -t_C(ConsStart, true, \{x_{n+1}\}, \hat{a}) &= ConsReady, \text{ if } act_C(\hat{a}) = Start_{n+1} \\ -t_C(ConsReady, x_{n+1} \geq c, \{x_{n+1}\}, \hat{a}) &= ConsFree, \text{ if } act_C(\hat{a}) = Send_{n+1} \text{ and } act_{N_n}(\hat{a}) = Send_{n+1} \\ -t_C(ConsFree, x_{n+1} \geq g, \{x_{n+1}\}, \hat{a}) &= ConsReady, \text{ if } act_C(\hat{a}) = Consume \end{aligned}$$

Finally, we assume the following two local weight functions for each agent:

$$\begin{aligned} -d_P(Produce) &= 4, d_P(send_1) = 2, d_C(Consume) = 4, d_C(send_{n+1}) = 2, \\ d_{N_i}(send_i) &= d_{N_i}(send_{i+1}) = d_{N_i}(Proc_i) = 2. \\ -d_P(Produce) &= 4000, d_P(send_1) = 2000, d_C(Consume) = 4000, \\ d_C(send_{n+1}) &= 2000, d_{N_i}(send_i) = d_{N_i}(send_{i+1}) = d_{N_i}(Proc_i) = 2000. \end{aligned}$$

The set of all the global states  $S$  for the scenario is defined as the product  $(L_P \times \mathbb{N}) \times \prod_{i=1}^n (L_i \times \mathbb{N}) \times (L_C \times \mathbb{N})$ . The set of the initial states is defined as  $\iota = \{s^0\}$ , where

$$s^0 = ((ProdReady-0, 0), (Node_1Ready-0, 0), \dots, (Node_nReady-0, 0), (ConsReady-0, 0)).$$

The system is scaled according to the number of its Nodes (agents), i.e., the problem parameter  $n$  is the number of Nodes. For any natural number  $n \geq 0$ , let  $D(n) = \{1, 3, \dots, n-1, n+1\}$  for an even  $n$ , and  $D(n) = \{2, 4, \dots, n-1, n+1\}$  for an odd  $n$ . Moreover, let

$$r(j) = d_P(Produce) + 2 \cdot \sum_{i=1}^j d_{N_i}(Send_i) + \sum_{i=1}^{j-1} d_{N_i}(proc_i)$$

Then we define *Right* as follows:

$$Right = \sum_{j \in D(n)} r(j).$$

We consider the following formulae as specifications:

- $\varphi_1 = \mathbf{EF}_{[0, Right]}(\text{ConsFree})$  - it states that there exists a path on which Consumer receives a data and the cost of receiving the data will be less than Right.
- $\varphi_2 = \mathbf{EF}_{[0, Right]}(\text{ConsFree} \wedge \mathbf{EG}(\text{ProdSend} \vee \text{ConsFree}))$  - it states that there exists a path on which Consumer receives a data and the cost of receiving the data is less than Right and from that point there exists a path on which always either the Producer has sent a data or the Consumer has received a data.
- $\varphi_3 = \overline{\mathbf{K}}_P(\mathbf{EF}_{[0, Right]}(\text{ConsFree} \wedge \mathbf{EG}(\text{ProdSend} \vee \text{ConsFree})))$  - it states that it is not true that Producer knows that there exists a path on which Consumer receives a data and the cost of receiving the data is less than Right and from that point there exists a path on which always either the Producer has sent a data or the Consumer has received a data.
- $\varphi_4 = \overline{\mathbf{K}}_P(\mathbf{EF}_{[0, Right]}(\text{ConsFree} \wedge \overline{\mathbf{K}}_C \overline{\mathbf{K}}_P(\mathbf{EG}(\text{ProdSend} \vee \text{ConsFree}))))$  - it states that it is not true that Producer knows that there exists a path on which Consumer receives a data and the cost of receiving the data is less than Right and at that point it is not true that Consumer knows that it is not true that Producer knows that there exists a path on which always either the Producer has sent a data or Consumer has received a data.

The number of the considered  $k$ -paths is equal to 1 for  $\varphi_1$ , 2 for  $\varphi_2$ , 3 for  $\varphi_3$ , and 5 for  $\varphi_4$ , respectively. The length of the witness is  $(n+1) \cdot 4$  for the formula  $\varphi_1$ , 9 if  $n=1$ , and  $(n+1) \cdot 4$  if  $n > 1$  for the formula  $\varphi_2$ ,  $2 \cdot n + 4$  if  $n \in \{1, 2\}$  and,  $2 \cdot n + 2$  if  $n > 2$  for the formula  $\varphi_3$ ,  $2 \cdot n + 2$  for the formula  $\varphi_4$ , respectively.

**Performance Evaluation.** We have performed our experimental results on a computer equipped with I7-3770 processor, 32 GB of RAM, and the operating system Arch Linux with the kernel 3.19.2. We set the CPU time limit to 3600 seconds. Our SMT-based BMC algorithm is implemented as standalone program written in the programming language C++. We used the state of the art SMT-solver Z3 [6] (<http://z3.codeplex.com/>).

For properties  $\varphi_1$ ,  $\varphi_2$ ,  $\varphi_4$ , and  $\varphi_4$  we have scaled up both the number of nodes and the weights parameters. The results are summarised on charts in Fig. 2, Fig. 3, Fig. 4, and Fig. 5. One can observe that our SMT-based BMC is not sensitive (Fig. 2, Fig. 4, Fig. 5) to scaling up the weights, but it is sensitive to scaling up the size of benchmark. More precisely, in order to calculate results for  $\varphi_1$  and for TWGPP with 1 node and the basic weights (**bwfor** short), the **bwmultiplied** by 1,000 our method uses 13.4 MB and the test lasts less than 0.1 seconds. In order to calculate results for  $\varphi_1$  and for TWGPP with 23 nodes and the **bwmultiplied** by 1,000 our method uses 236.1 MB and the test lasts 4510.0 seconds. The most interesting result which can be observed is for the formulae  $\varphi_2$ . In this case time usage for the **bwis** greater (9013.1 seconds) than for the **bwmultiplied** by 1,000 (570.9 seconds) for 11 nodes. In particular, in the time limit set for the benchmark, the SMT-based BMC is able to verify the formula  $\varphi_2$  for the **bwonly** for 11 nodes while for the **bwmultiplied** by 1,000 can handle 15 nodes.

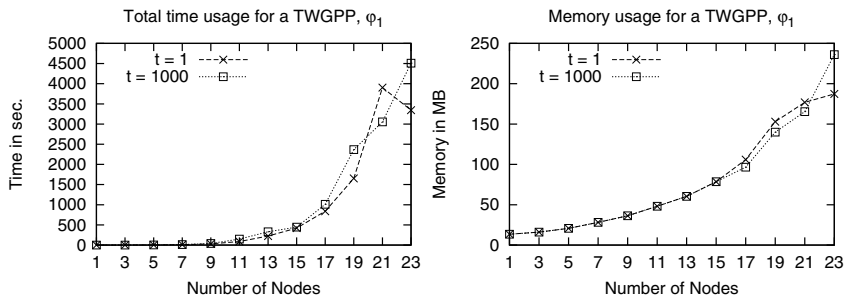


**Fig. 2.** Formula  $\varphi_1$ : Scaling up both the number of nodes and weights.

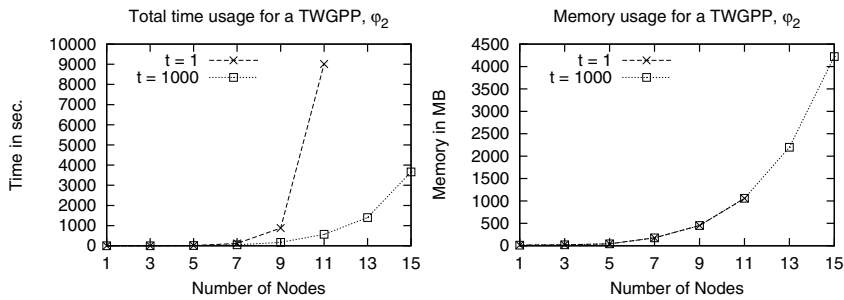


**Fig. 3.** Formula  $\varphi_2$ : Scaling up both the number of nodes and weights.

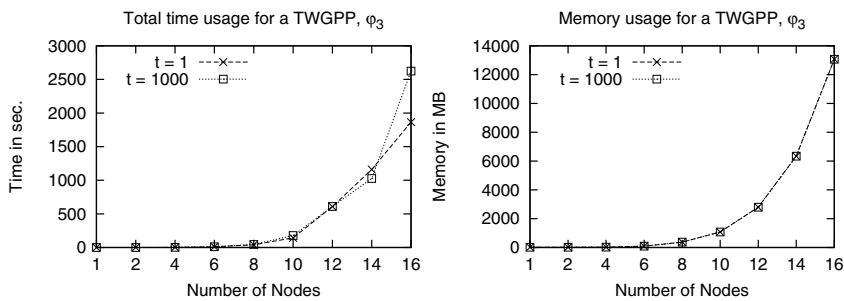


**Fig. 4.** Formula  $\varphi_3$ : Scaling up both the number of nodes and weights.

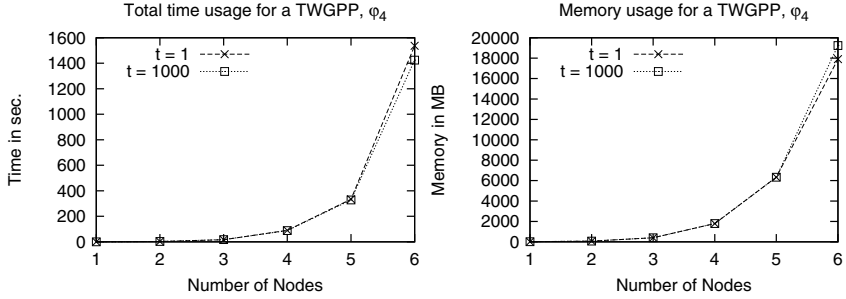


**Fig. 5.** Formula  $\varphi_4$ : Scaling up both the number of nodes and weights.

In the case of properties  $\varphi_3$  and  $\varphi_4$  we obtained similar results. Namely, in order to calculate results for  $\varphi_3$  and for TWGPP with 16 nodes and the  $\text{bw}$ , the  $\text{bw}$  multiplied by 1,000, our method uses 13074.2 (13072.0) MB and the test lasts 1864.4 (2624.5) sec. Next, in order to calculate results for  $\varphi_4$  and for TWGPP with 6 nodes and the  $\text{bw}$ , the  $\text{bw}$  multiplied by 1,000, our method uses 17904.5 (19240.9) MB and the test lasts 1536.9 (1424.4) sec.

In Tables 1 and 2 we present time usage, memory usage and the length of the witness for the formula  $\varphi_2$ .

**Table 1.** Formula  $\varphi_2$  for basic weights

n	time	memory	witness length
1	0.1	15.1	9
2	0.5	17.6	12
3	1.6	21.4	16
4	4.2	26.5	20
5	10.2	43.7	24
6	21.0	84.7	28
7	112.8	176.7	32
8	275.8	292.4	36
9	879.6	451.3	40
10	2284.4	707.9	44
11	9013.1	1056.5	48

**Table 2.** Formula  $\varphi_2$  for basic weights multiplied by 1,000

n	time	memory	witness length
1	0.2	14.7	8
2	0.8	17.5	12
3	1.8	21.6	16
4	5.7	27.1	20
5	12.5	43.3	24
6	25.6	86.5	28
7	47.6	177.1	32
8	105.1	290.8	36
9	172.5	452.1	40
10	290.2	705.3	44
11	570.9	1060.0	48
12	879.9	1557.1	52
13	1399.8	2198.9	56
14	2892.7	3078.3	60
15	3660.4	4222.0	64

## 5 Conclusions

We have proposed SMT-based BMC verification method for model checking WECTLK properties interpreted over the timed real-weighted interpreted systems. We have provided a preliminary experimental results showing that our method is worth interest. In the future we are going to provide a comparison of our new method with the SAT- and BDD-based BMC methods. The module will be added to the model checker VerICS([3]).

**Acknowledgments.** Partly supported by National Science Centre under the grant No. 2014/15/N/ST6/05079. The study is co-funded by the European Union, European Social Fund. Project PO KL “Information technologies: Research and their interdisciplinary applications”, Agreement UDA-POKL.04.01.01-00-051/10-00.

## References

1. Emerson, E.A.: Temporal and modal logic. In: van Leeuwen, J. (eds.) *Handbook of Theoretical Computer Science*, vol. B, chapter 16, pp. 996–1071. Elsevier Science Publishers (1999)
2. Fagin, R., Halpern, J.Y., Moses, Y., Vardi, M.Y.: *Reasoning about Knowledge*. MIT Press, Cambridge (1995)
3. Kacprzak, M., Nabialek, W., Niewiadomski, A., Penczek, W., Pólrola, A., Szerter, M., Woźna, B., Zbrzezny, A.: VerICS 2007 - a model checker for knowledge and real-time. *Fundamenta Informaticae* **85**(1–4), 313–328 (2008)
4. Levesque, H.: A logic of implicit and explicit belief. In: *Proceedings of the 6th National Conference of the AAAI*, pp. 198–202. Morgan Kaufman, Palo Alto (1984)
5. Lomuscio, A., Sergot, M.: Deontic interpreted systems. *Studia Logica* **75**(1), 63–92 (2003)
6. de Moura, L., Björner, N.S.: Z3: An efficient SMT solver. In: Ramakrishnan, C.R., Rehof, J. (eds.) *TACAS 2008. LNCS*, vol. 4963, pp. 337–340. Springer, Heidelberg (2008)
7. Wooldridge, M.: *An introduction to multi-agent systems*, 2nd edn. John Wiley & Sons (2009)
8. Woźna-Szcześniak, B.: SAT-Based bounded model checking for weighted deontic interpreted systems. In: Reis, L.P., Correia, L., Cascalho, J. (eds.) *EPIA 2013. LNCS*, vol. 8154, pp. 444–455. Springer, Heidelberg (2013)
9. Woźna-Szcześniak, B.: Checking EMTLK properties of timed interpreted systems via bounded model checking. In: Bazzan, A.L.C., Huhns, M.N., Lomuscio, A., Scerri, P. (eds.) *International Conference on Autonomous Agents and Multi-Agent Systems, AAMAS 2014*, Paris, France, May 5–9, pp. 1477–1478. IFAAMAS/ACM (2014)
10. Woźna-Szcześniak, B., Zbrzezny, A.M., Zbrzezny, A.: SAT-Based bounded model checking for weighted interpreted systems and weighted linear temporal logic. In: Boella, G., Elkind, E., Savarimuthu, B.T.R., Dignum, F., Purvis, M.K. (eds.) *PRIMA 2013. LNCS*, vol. 8291, pp. 355–371. Springer, Heidelberg (2013)
11. Zbrzezny, A.: Improving the translation from ECTL to SAT. *Fundamenta Informaticae* **85**(1–4), 513–531 (2008)
12. Zbrzezny, A.: A new translation from ECTL\* to SAT. *Fundamenta Informaticae* **120**(3–4), 377–397 (2012)

# SMT-Based Bounded Model Checking for Weighted Epistemic ECTL

Agnieszka M. Zbrzezny<sup>(✉)</sup>, Bożena Woźna-Szcześniak, and Andrzej Zbrzezny

IMCS, Jan Długosz University,  
Al. Armii Krajowej 13/15, 42-200 Częstochowa, Poland  
[{agnieszka.zbrzezny,b.wozna,a.zbrzezny}@ajd.czest.pl](mailto:{agnieszka.zbrzezny,b.wozna,a.zbrzezny}@ajd.czest.pl)

**Abstract.** We define the SMT-based bounded model checking (BMC) method for weighted interpreted systems and for the existential fragment of the weighted epistemic computation tree logic. We implemented the new BMC algorithm and compared it with the SAT-based BMC method for the same systems and the same property language on several benchmarks for multi-agent systems.

## 1 Introduction

The previous ten years in the area of multi-agent systems (MASs) have seen significant research in verification procedures, which automatically evaluate whether a MAS reaches its intended specifications. One of main techniques here is *symbolic model checking* [2]. Unfortunately, because of the agents' intricate nature, the practical applicability of model checking is firmly limited by the "state-space explosion problem" (i.e., an exponential growth of the system state space with the number of agents). To reduce this issue, various techniques, including the SAT- and BDD-based bounded model checking (BMC) [3,4], have been proposed. These have been effective in permitting users to handle bigger MASs, however it is still hard to check MASs with numerous agents and cost demands on agents' actions. The point of this paper is to help beat this inadequacy by employing SMT-solvers (i.e., *satisfiability modulo theories* tools for deciding the satisfiability of formulae in a number of theories) [1,5].

The fundamental thought behind bounded model checking (BMC) is, given a system, a property, and an integer bound  $k \geq 0$ , to define a formula (in the case of SAT-based BMC, this is a propositional logic formula; in the case of SMT-based BMC, this can be a quantifier-free first-order formula) such that the formula is satisfiable if and only if the system has a counterexample of length at most  $k$  violating the property. The bound is incremented until a satisfiable formula is discovered (i.e, the specification does not hold for the system) or a completeness threshold is reached without discovering any satisfiable formulae.

To model check the prerequisites of MASs, different extensions of temporal logics have been proposed. In this paper, we consider the existential fragment of

---

Partly supported by National Science Centre under the grant No. 2014/15/N/ST6/05079.

a weighted epistemic computation tree logic (WECKTLK) interpreted over WISs [6].

To the best of our knowledge, there is no work that considers SMT-based BMC methods to check multi-agent systems modelled by means of interpreted systems. Thus, in this paper we offer such a method. In particular, we make the following contributions. First of all, we define and implement an SMT-based BMC method for WECKTLK and for *weighted interpreted systems* (WISs) [6, 7]. Next, we report on the initial experimental evaluation of our SMT-based BMC methods. To this aim we use two scalable benchmarks: the *weighted generic pipeline paradigm* [7] and the *weighted bits transmission problem* [6]. Finally, we compare our prototype implementation of the SMT-based BMC method against the SAT-based BMC engine of [6, 8], the only existing technique that is suitable with respect to the input formalism and checked properties. The results show that the SMT-based BMC performs very good and is, in fact, sometimes significantly faster than the tested SAT-based BMC method.

The rest of the paper is organised as follows. In the next section we briefly present the theory of weighted interpreted systems and the WECKTLK language. In Section 3 we present our SMT-based BMC method. In Section 4 we experimentally evaluate the performance of our SMT-based BMC encoding. In Section 5, we conclude the paper.

## 2 Preliminaries

**WIS.** Let  $Ag = \{1, \dots, n\}$  be the non-empty and finite set of agents, and  $\mathcal{E}$  be a special agent that is used to model the environment in which the agents operate, and let  $\mathcal{PV} = \bigcup_{c \in Ag \cup \{\mathcal{E}\}} \mathcal{PV}_c$  be a set of propositional variables such that  $\mathcal{PV}_{c_1} \cap \mathcal{PV}_{c_2} = \emptyset$  for all  $c_1, c_2 \in Ag \cup \{\mathcal{E}\}$ . The *weighted interpreted system* (WIS) [6, 7] is a tuple  $(\{L_c, Act_c, P_c, V_c, d_c\}_{c \in Ag \cup \{\mathcal{E}\}}, \{t_c\}_{c \in Ag}, t_\mathcal{E}, \iota)$ , where  $L_c$  is non-empty and finite set of *local states* ( $S = L_1 \times \dots \times L_n \times L_\mathcal{E}$  denotes the non-empty set of all *global states*),  $Act_c$  is a non-empty and finite set of *possible actions* ( $Act = Act_1 \times \dots \times Act_n \times Act_\mathcal{E}$  denotes the non-empty set of *joint actions*),  $P_c : L_c \rightarrow 2^{Act_c}$  is a *protocol function*,  $V_c : L_c \rightarrow 2^{\mathcal{PV}_c}$  is a *valuation function*,  $d_c : Act_c \rightarrow \mathbb{N}$  is a *weight function*,  $t_c : L_c \times L_\mathcal{E} \times Act \rightarrow L_c$  is a (partial) *evolution function* for agents, and  $t_\mathcal{E} : L_\mathcal{E} \times Act \rightarrow L_\mathcal{E}$  is (partial) *evolution function* for the environment, and  $\iota \subseteq S$  is a set of initial global states.

Assume that  $l_c(s)$  denotes the local component of agent  $c \in Ag \cup \{\mathcal{E}\}$  in the global state  $s \in S$ . For a given WIS we define a *model* as a tuple  $M = (Act, S, T, V, d)$ , where the sets  $Act$  and  $S$  are defined as above,  $V : S \rightarrow 2^{\mathcal{PV}}$  is the valuation function defined as  $V(s) = \bigcup_{c \in Ag \cup \{\mathcal{E}\}} V_c(l_c(s))$ ,  $d : Act \rightarrow \mathbb{N}$  is a “joint” weight function defined as  $d((a_1, \dots, a_n, a_\mathcal{E})) = d_1(a_1) + \dots + d_n(a_n) + d_\mathcal{E}(a_\mathcal{E})$ , and  $T \subseteq S \times Act \times S$  is a transition relation defined as:  $(s, a, s') \in T$  (or  $s \xrightarrow{a} s'$ ) iff  $t_c(l_c(s), l_\mathcal{E}(s), a) = l_c(s')$  for all  $c \in Ag$  and  $t_\mathcal{E}(l_\mathcal{E}(s), a) = l_\mathcal{E}(s')$ ; we assume that the relation  $T$  is total, i.e. for any  $s \in S$  there exists  $s' \in S$  and a non-empty joint action  $a \in Act$  such that  $s \xrightarrow{a} s'$ .

For each agent  $\mathbf{c} \in Ag$ , the definition of the standard *indistinguishability* relation  $\sim_{\mathbf{c}} \subseteq S \times S$  is the following:  $s \sim_{\mathbf{c}} s'$  iff  $l_{\mathbf{c}}(s') = l_{\mathbf{c}}(s)$ . Finally, the following definitions of epistemic relations:  $\sim_{\Gamma}^E \stackrel{\text{def}}{=} \bigcup_{\mathbf{c} \in \Gamma} \sim_{\mathbf{c}}$ ,  $\sim_{\Gamma}^{C\text{def}} \stackrel{\text{def}}{=} (\sim_{\Gamma}^E)^+$  (the transitive closure of  $\sim_{\Gamma}^E$ ),  $\sim_{\Gamma}^D \stackrel{\text{def}}{=} \bigcap_{\mathbf{c} \in \Gamma} \sim_{\mathbf{c}}$ , where  $\Gamma \subseteq Ag$  are assumed.

**Syntax of WECTLK.** The WECTLK logic has been defined in [6] as the existential fragment of the weighted CTLK with cost constraints on *all* temporal modalities.

For convenience, the symbol  $I$  denotes an interval in  $\mathbb{N} = \{0, 1, 2, \dots\}$  of the form  $[a, \infty)$  or  $[a, b]$ , for  $a, b \in \mathbb{N}$  and  $a \neq b$ . Moreover, the symbol  $\mathbf{right}(I)$  denotes the right end of the interval  $I$ . Given an atomic proposition  $p \in \mathcal{PV}$ , an agent  $\mathbf{c} \in Ag$ , a set of agents  $\Gamma \subseteq Ag$  and an interval  $I$ , the WECTLK formulae are defined by the following grammar:  $\varphi ::= \mathbf{true} \mid \mathbf{false} \mid p \mid \neg p \mid \varphi \vee \varphi \mid \varphi \wedge \varphi \mid \mathbf{EX}_I \varphi \mid \mathbf{E}(\varphi \mathbf{U}_I \varphi) \mid \mathbf{EG}_I \varphi \mid \overline{K}_{\mathbf{c}} \varphi \mid \overline{D}_{\Gamma} \varphi \mid \overline{E}_{\Gamma} \varphi \mid \overline{C}_{\Gamma} \varphi$ .

$E$  (for some path) is the path quantifier.  $X_I$  (weighted neXt time),  $U_I$  (weighted until) and  $G_I$  (weighted always) are the weighted temporal modalities. Note that the formula “weighted eventually” is defined as standard:  $\mathbf{EF}_I \varphi \stackrel{\text{def}}{=} \mathbf{E}(\mathbf{true} \mathbf{U}_I \varphi)$  (meaning that it is possible to reach a state satisfying  $\varphi$  via a finite path whose cumulative weight is in  $I$ ).  $\overline{K}_{\mathbf{c}}$  is the modality dual to  $K_{\mathbf{c}}$ .  $\overline{D}_{\Gamma}$ ,  $\overline{E}_{\Gamma}$ , and  $\overline{C}_{\Gamma}$  are the dualities to the standard group epistemic modalities representing, respectively, distributed knowledge in the group  $\Gamma$ , everyone in  $\Gamma$  knows, and common knowledge among agents in  $\Gamma$ .

We omit here the definition of the bounded (i.e., the relation  $\models_k$ ) and unbounded semantics (i.e., the relation  $\models$ ) of the logic, since they can be found in [6]. We only recall the notions of  $k$ -paths and loops, since we need them to explain the SMT-based BMC. Namely, given a model  $M$  and a bound  $k \in \mathbb{N}$ , a  $k$ -path  $\pi_k$  is a finite sequence  $s_0 \xrightarrow{a_1} s_1 \xrightarrow{a_2} \dots \xrightarrow{a_k} s_k$  of transitions. A  $k$ -path  $\pi_k$  is a *loop* if  $l < k$  and  $\pi(k) = \pi(l)$ . Furthermore, let  $M$  be a model, and  $\varphi$  a WECTLK formula. The *bounded model checking* problem asks whether there exists  $k \in \mathbb{N}$  such that  $M \models_k \varphi$ , i.e., whether there exists  $k \in \mathbb{N}$  such that the formula  $\varphi$  is  $k$ -true in the model  $M$ .

### 3 SMT-Based BMC

In order to encode the BMC problem for WECTLK by means of SMT, we consider a quantifier-free logic with individual variables ranging over the natural numbers. Formally, let  $M$  be the model,  $\varphi$  a WECTLK formula and  $k \geq 0$  a bound. We define the quantifier-free first-order formula:  $[M, \varphi]_k := [M^{\varphi, \iota}]_k \wedge [\varphi]_{M, k}$  that is satisfiable if and only if  $M \models_k \varphi$  holds.

The definition of the formula  $[M, \varphi]_k$  is based the SAT encoding of [6], and it assumes that each state, each joint action, and each sequence of weights associated with a joint action are represented by a valuation of, respectively, a *symbolic state*  $\bar{w} = (w_1, \dots, w_n, w_{\mathcal{E}})$  consisting of *symbolic local states*  $w_{\mathbf{c}}$ , a *symbolic action*  $\bar{a} = (a_1, \dots, a_n, a_{\mathcal{E}})$  consisting of *symbolic local actions*  $a_{\mathbf{c}}$ , and a *symbolic weights*  $\bar{d} = (d_1, \dots, d_{n+1})$  consisting of *symbolic local weights*

$d_{\mathbf{c}}$ , where each  $w_{\mathbf{c}}$ ,  $a_{\mathbf{c}}$ , and  $d_{\mathbf{c}}$  are individual variables ranging over the natural numbers, for  $\mathbf{c} \in Ag \cup \{\mathcal{E}\}$ . Next, the definition of  $[M, \varphi]_k$  uses the auxiliary function  $f_k : WECTLK \rightarrow \mathbb{N}$  of [6] which returns the number of  $k$ -paths that are required for proving the  $k$ -truth of  $\varphi$  in  $M$ . Finally, the definition of  $[M, \varphi]_k$  uses the following auxiliary quantifier-free first-order formulae:  $I_s(\bar{w})$  - it encodes the state  $s$  of the model  $M$ ;  $p(\bar{w})$  - it encodes the set of states of  $M$  in which  $p \in \mathcal{PV}$  holds;  $H_{\mathbf{c}}(\bar{w}, \bar{w}') := w_{\mathbf{c}} = w'_{\mathbf{c}}$  for  $\mathbf{c} \in Ag$ ;  $T_{\mathbf{c}}(w_{\mathbf{c}}, (\bar{a}, \bar{d}), w'_{\mathbf{c}})$  - it encodes the local evolution function of agent  $\mathbf{c} \in Ag \cup \{\mathcal{E}\}$ ;  $\mathcal{A}(\bar{a})$  - it encodes that each symbolic local action  $a_{\mathbf{c}}$  of  $\bar{a}$  has to be executed by each agent in which it appears;  $\mathcal{T}(\bar{w}, (\bar{a}, \bar{d}), \bar{w}') := \mathcal{A}(\bar{a}) \wedge \bigwedge_{\mathbf{c} \in Ag \cup \{\mathcal{E}\}} T_{\mathbf{c}}(w_{\mathbf{c}}, (\bar{a}, \bar{d}), w'_{\mathbf{c}})$ . Let  $\pi_j$  denote the  $j$ -th *symbolic k-path*, i.e. the sequence of symbolic transitions:  $\bar{w}_{0,j} \xrightarrow{\bar{a}_{1,j}, \bar{d}_{1,j}} \bar{w}_{1,j} \xrightarrow{\bar{a}_{2,j}, \bar{d}_{2,j}} \dots \xrightarrow{\bar{a}_{k,j}, \bar{d}_{k,j}} \bar{w}_{k,j}$ , and let  $d_{i,j,m}$  denotes the  $m$ -th component of the symbolic joint weight  $\bar{d}_{i,j}$ . Then,

- $\mathcal{B}_k^I(\pi_j) := \sum_{i=1}^k \sum_{m=1}^{n+1} d_{i,j,m} < \text{right}(I)$  - it encodes that the weight represented by the sequence  $\bar{d}_{1,j}, \dots, \bar{d}_{k,j}$  is less than  $\text{right}(I)$ ;
- $\mathcal{D}_{a,b}^I(\pi_j)$  for  $a \leq b$  - if  $a < b$ , then it encodes that the weight represented by the sequence  $\bar{d}_{a+1,j}, \dots, \bar{d}_{b,j}$  belongs to the interval  $I$ , otherwise, i.e. if  $a = b$ , then  $\mathcal{D}_{a,b}^I(\pi_j)$  is true iff  $0 \in I$ ;
- $\mathcal{D}_{a,b;c,d}^I(\pi_j)$  for  $a \leq b$  and  $c \leq d$  - it encodes that the weight represented by the sequences  $\bar{d}_{a+1,j}, \dots, \bar{d}_{b,j}$  and  $\bar{d}_{c+1,j}, \dots, \bar{d}_{d,j}$  belongs to the interval  $I$ .

Given symbolic states  $\bar{w}_{i,j}$ , symbolic actions  $\bar{a}_{i,j}$  and symbolic weights  $\bar{d}_{i,j}$  for  $0 \leq i \leq k$  and  $0 \leq j < f_k(\varphi)$ , the formula  $[M^{\varphi,\iota}]_k$ , which encodes a rooted tree of  $k$ -paths of the model  $M$ , is defined as follows:

$$[M^{\varphi,\iota}]_k := \bigvee_{s \in \iota} I_s(\bar{w}_{0,0}) \wedge \bigwedge_{j=0}^{f_k(\varphi)-1} \bigwedge_{i=0}^{k-1} \mathcal{T}(\bar{w}_{i,j}, (\bar{a}_{i+1,j}, \bar{d}_{i+1,j}), \bar{w}_{i+1,j})$$

The formula  $[\varphi]_{M,k}$  encodes the bounded semantics of the WECTLK formula  $\varphi$ , it is defined on the same sets of individual variables as the formula  $[M^{\varphi,\iota}]_k$ , and it uses the auxiliary functions  $g_\mu$ ,  $h_k^U$ ,  $h_k^G$  of [9] that allow us to divide the set  $A \subseteq F_k(\varphi) = \{j \in \mathbb{N} \mid 0 \leq j < f_k(\varphi)\}$  into subsets necessary for translating the subformulae of  $\varphi$ .

Let  $[\varphi]_k^{[m,n,A]}$  denote the translation of  $\varphi$  at symbolic state  $\bar{w}_{m,n}$  by using the set  $A \subseteq F_k(\varphi)$ . The formula  $[\varphi]_{M,k} := [\varphi]_k^{[0,0,F_k(\varphi)]}$  is defined inductively with the classical rules for the propositional fragment of WECTLK and with the following rules for weighted temporal and epistemic modalities. Let  $0 \leq n \leq f_k(\varphi)$ ,  $m \leq k$ ,  $n' = \min(A)$ ,  $h_k^U = h_k^U(A, f_k(\beta))$ , and  $h_k^G = h_k^G(A)$ . Then,

$$\begin{aligned} - [\text{EX}_I \alpha]_k^{[m,n,A]} &:= \bar{w}_{m,n} = \bar{w}_{0,n'} \wedge \mathcal{D}_{0,1}^I(\pi_{n'}) \wedge [\alpha]_k^{[1,n',g_\mu(A)]}, \text{ if } k > 0; \text{false, else,} \\ - [\text{E}(\alpha \text{U}_I \beta)]_k^{[m,n,A]} &:= \bar{w}_{m,n} = \bar{w}_{0,n'} \wedge \bigvee_{i=0}^k ([\beta]_k^{[i,n',h_k^U(k)]} \wedge \mathcal{D}_{0,i}^I(\pi_{n'})) \wedge \\ &\quad \bigwedge_{j=0}^{i-1} [\alpha]_k^{[j,n',h_k^U(j)]}, \end{aligned}$$

$$\begin{aligned}
- [\mathbf{E}(\mathbf{G}_I \alpha)]_k^{[m,n,A]} &:= \overline{w}_{m,n} = \overline{w}_{0,n'} \wedge ((\neg \mathcal{B}_k^I(\boldsymbol{\pi}_n) \wedge \bigwedge_{i=0}^k (\neg \mathcal{D}_{0,i}^I(\boldsymbol{\pi}_{n'}) \vee \\
&\quad [\alpha]_k^{[i,n',h_k^G(k)]})) \vee (\mathcal{B}_k^I(\boldsymbol{\pi}_n) \wedge \bigwedge_{i=0}^k (\neg \mathcal{D}_{0,i}^I(\boldsymbol{\pi}_{n'}) \vee [\alpha]_k^{[i,n',h_k^G(k)]}) \wedge \\
&\quad \bigvee_{l=0}^{k-1} (\overline{w}_{k,n'} = \overline{w}_{l,n'} \wedge \bigwedge_{i=l}^{k-1} (\neg \mathcal{D}_{0,k;l,i+1}^I(\boldsymbol{\pi}_{n'}) \vee [\alpha]_k^{[i,n',h_k^G(k)]}))), \\
- [\overline{\mathbf{K}}_c \alpha]_k^{[m,n,A]} &:= (\bigvee_{s \in \iota} I_s(\overline{w}_{0,n'})) \wedge \bigvee_{j=0}^k ([\alpha]_k^{[j,n',g_\mu(A)]} \wedge H_c(\overline{w}_{m,n}, \overline{w}_{j,n'})), \\
- [\overline{\mathbf{D}}_\Gamma \alpha]_k^{[m,n,A]} &:= (\bigvee_{s \in \iota} I_s(\overline{w}_{0,n'})) \wedge \bigvee_{j=0}^k ([\alpha]_k^{[j,n',g_\mu(A)]} \wedge \bigwedge_{c \in \Gamma} H_c(\overline{w}_{m,n}, \overline{w}_{j,n'})), \\
- [\overline{\mathbf{E}}_\Gamma \alpha]_k^{[m,n,A]} &:= (\bigvee_{s \in \iota} I_s(\overline{w}_{0,n'})) \wedge \bigvee_{j=0}^k ([\alpha]_k^{[j,n',g_\mu(A)]} \wedge \bigvee_{c \in \Gamma} H_c(\overline{w}_{m,n}, \overline{w}_{j,n'})), \\
- [\overline{\mathbf{C}}_\Gamma \alpha]_k^{[m,n,A]} &:= [\bigvee_{j=1}^k (\overline{\mathbf{E}}_\Gamma)^j \alpha]_k^{[m,n,A]}.
\end{aligned}$$

The theorem below states the correctness and the completeness of the presented translation. It can be proven by induction on the length of the given WECTLK formula.

**Theorem 1.** *Let  $M$  be a model, and  $\varphi$  a WECTLK formula. For every  $k \in \mathbb{N}$ ,  $M \models_k \varphi$  if, and only if, the quantifier-free first-order formula  $[M, \varphi]_k$  is satisfiable.*

The proposed SMT-based BMC is based on the SAT-based BMC defined in [6]. The main difference between those two method is in the representation of symbolic states, symbolic actions, and symbolic weights. Thus, the main result is the generalisation of the propositional encoding of [6] into the quantifier-free first-order encoding.

## 4 Experimental Results

Here we experimentally evaluate the performance of our SMT-based BMC method for WECTLK over the WIS semantics. We compare our method with the SAT-based BMC [6, 8], the only existing method that is suitable with respect to the input formalism (i.e., weighted interpreted systems) and checked properties (i.e., WECTLK). We have computed our experimental results on a computer equipped with I7-3770 processor, 32 GB of RAM, and the operating system Arch Linux with the kernel 3.15.3. We set the CPU time limit to 3600 seconds. For the SAT-based BMC we used the PicoSAT solver and for the SMT-based BMC we used the Z3 solver.

The first benchmark we consider is the *weighted generic pipeline paradigm* (WGPP) WIS model [6]. The problem parameter  $n$  is the number of Nodes. Let  $Min$  be the minimum cost incurred by Consumer to receive the data produced by Producer, and  $p$  denote the cost of producing data by Producer. The specifications we consider are as follows:

$\varphi_1 = \overline{\mathbf{K}}_P \mathbf{EF}_{[Min, Min+1]} \mathbf{ConsReady}$  - it expresses that it is not true that Producer knows that always the cost incurred by Consumer to receive data is  $Min$ .

$\varphi_2 = \overline{\mathbf{K}}_P \mathbf{EF}(\mathbf{ProdSend} \wedge \overline{\mathbf{K}}_C \overline{\mathbf{K}}_P \mathbf{EG}_{[0, Min-p]} \mathbf{ConsReady})$  - it states that it is not true that Producer knows that always if it produces data, then Consumer knows that Producer knows that Consumer has received data and the cost is less than  $Min - p$ .

The size of the reachable state space of the WGPP system is  $4 \cdot 3^n$ , for  $n \geq 1$ . The number of the considered  $k$ -paths is equal to 2 for  $\varphi_1$  and 5 for  $\varphi_2$ , respectively. The lengths of the discovered witnesses for formulae  $\varphi_1$  and  $\varphi_2$  vary, respectively, from 3 for 1 node to 23 for 130 nodes, and from 3 for 1 node to 10 for 27 nodes.

The second benchmark of our interest is the *weighted bits transmission problem* (WBTP) WIS model [7]. We have adapted the local weight functions of [7]. This system is scaled according to the number of bits the  $\mathcal{S}$  wants to communicate to  $\mathcal{R}$ . Let  $a \in \mathbb{N}$  and  $b \in \mathbb{N}$  be the costs of sending, respectively, bits by Sender and an acknowledgement by Receiver. The specifications we consider are as follows:

$\phi_1 = \text{EF}_{[a+b, a+b+1]}(\text{recack} \wedge \bar{K}_{\mathcal{S}}(\bar{K}_{\mathcal{R}}(\bigwedge_{i=0}^{2^n-2}(\neg i))))$  - it expresses that it is not true that if an *ack* is received by  $\mathcal{S}$ , then  $\mathcal{S}$  knows that  $\mathcal{R}$  knows at least one value of the  $n$ -bit numbers except the maximal value, and the cost is  $a + b$ .

$\phi_2 = \text{EF}_{[a+b, a+b+1]}(\bar{K}_{\mathcal{S}}(\bigwedge_{i=0}^{2^n-1}(\bar{K}_{\mathcal{R}}(\neg i)))$  - it expresses that it is not true that  $\mathcal{S}$  knows that  $\mathcal{R}$  knows the value of the  $n$ -bit number and the cost is  $a + b$ .

The size of the reachable state space of the WBTP system is  $3 \cdot 2^n$  for  $n \geq 1$ . The number of the considered  $k$ -paths is equal to 3 for  $\phi_1$  and  $2^n + 2$  for  $\phi_2$ , respectively. The length of the witnesses for both formulae is equal to 2 for any  $n > 0$ .

**Performance Evaluation.** The experimental results show that the both BMC method, SAT- and SMT-based, are complementary. We have noticed that for the WGPP system and both considered formulae the SMT-based BMC is faster than the SAT-base BMC, however, the SAT-based BMC consumes less memory. Moreover, the SMT-based method is able to verify more nodes for both tested formulae. In particular, in the time limit set for the benchmarks, the SMT-based BMC is able to verify the formula  $\varphi_1$  for 120 nodes while the SAT-based BMC can handle 115 nodes. For  $\varphi_2$  the SMT-based BMC is still more efficient - it is able to verify 27 nodes, whereas the SAT-based BMC verifies only 25 nodes.

In the case of the WBTP system the SAT-based BMC performs much better in terms of the total time and the memory consumption for both the tested formulae. In the case of the formula  $\phi_2$  both methods are able to verify the same number of bits. For the WBTP the reason of a higher efficiency of the SAT-based BMC is, probably, that the lengths of the witnesses for both formulae is constant and very short, and that there is no nested temporal modalities in the scope of epistemic operators. For formulae like  $\phi_1$  and  $\phi_2$  the number of arithmetic operations is small, so the SMT-solvers cannot show its strength.

Further more we have noticed that the total time and the memory consumption for both benchmarks and all the tested formulae is independent from the values of the considered weights.

## 5 Conclusions

We have proposed, implemented, and experimentally evaluated SMT-based bounded model checking approach for WECTLK interpreted over the weighted interpreted systems. We have compared our method with the corresponding SAT-based technique. The experimental results show that the approaches are complementary, and that the SMT-based BMC approach appears to be superior for the WGPP system, while the SAT-based approach appears to be superior for the WBTP system. This is a novel and interesting result, which shows that the choice of the BMC method should depend on the considered system.

## References

1. Clark, B., Sebastiani, R., Sanjit, S., Tinelli, C.: Satisfiability modulo theories. In: *Handbook of Satisfiability*. Frontiers in Artificial Intelligence and Applications, vol. 185, chapter 26, pp. 825–885. IOS Press (2009)
2. Clarke, E.M., Grumberg, O., Peled, D.A.: *Model Checking*. The MIT Press (1999)
3. Jones, A.V., Lomuscio, A.: Distributed BDD-based BMC for the verification of multi-agent systems. In: Proc. AAMAS 2010, pp. 675–682. IFAAMAS (2010)
4. Męski, A., Penczek, W., Sreter, M., Woźna-Szczęśniak, B., Zbrzezny, A.: BDD- versus SAT-based bounded model checking for the existential fragment of linear temporal logic with knowledge: algorithms and their performance. *Autonomous Agents and Multi-Agent Systems* **28**(4), 558–604 (2014)
5. de Moura, L., Bjørner, N.S.: Z3: An efficient SMT solver. In: Ramakrishnan, C.R., Rehof, J. (eds.) TACAS 2008. LNCS, vol. 4963, pp. 337–340. Springer, Heidelberg (2008)
6. Woźna-Szczęśniak, B.: SAT-based bounded model checking for weighted deontic interpreted systems. In: Reis, L.P., Correia, L., Cascalho, J. (eds.) EPIA 2013. LNCS, vol. 8154, pp. 444–455. Springer, Heidelberg (2013)
7. Woźna-Szczęśniak, B., Zbrzezny, A.M., Zbrzezny, A.: SAT-based bounded model checking for weighted interpreted systems and weighted linear temporal logic. In: Boella, G., Elkind, E., Savarimuthu, B.T.R., Dignum, F., Purvis, M.K. (eds.) PRIMA 2013. LNCS, vol. 8291, pp. 355–371. Springer, Heidelberg (2013)
8. Woźna-Szczęśniak, B., Szczęśniak, I., Zbrzezny, A.M., Zbrzezny, A.: Bounded model checking for weighted interpreted systems and for flat weighted epistemic computation tree logic. In: Dam, H.K., Pitt, J., Xu, Y., Governatori, G., Ito, T. (eds.) PRIMA 2014. LNCS, vol. 8861, pp. 107–115. Springer, Heidelberg (2014)
9. Zbrzezny, A.: Improving the translation from ECTL to SAT. *Fundamenta Informatiae* **85**(1–4), 513–531 (2008)

# Dynamic Selection of Learning Objects Based on SCORM Communication

João de Amorim Junior<sup>(✉)</sup> and Ricardo Azambuja Silveira

PPGCC – UFSC, Florianópolis, Brazil

joao.amorim@iate.ufsc.br, ricardo.silveira@ufsc.br

**Abstract.** This paper presents a model to select Learning Objects in e-learning courses, based on multi-agent paradigm, aiming to facilitate the learning material reuse and adaptability on Learning Management Systems. The proposed model has a BDI multi-agent architecture, as an improvement of the Intelligent Learning Objects approach, allowing the dynamic selection of Learning Objects. As the first steps of our research, we implement a prototype to validate the proposed model using the JADEX BDI V3 platform. Thereafter, we extends the framework to allow the communication of the agents with SCORM standard resources, making possible to build enhanced dynamic learning experiences.

**Keywords:** Dynamic learning experience · Intelligent learning objects · SCORM

## 1 Introduction and Related Works

Adaptability and reuse are important aspects that contribute to improve learning process in virtual learning environments [1]. The former relates to different students' profiles and needs. An adaptable system increases the student understanding, taking into account its knowledge level and preferences [2,3,4]. The latter means that it is unnecessary to develop new resources if there are others related to the same learning purpose [4,5]. Some computational tools improve the teaching-learning process, i.e.: (1) Intelligent Tutoring Systems (ITS) - applications created for a specific domain, generally with few adaptability and interoperability [6]; (2) Learning Management Systems (LMS) - environments used to build online courses (or publishing material), allowing teacher to manage educational data [1], [7,8]; and (3) Learning Objects (LO) - digital artifacts that promotes reuse and adaptability of resources [9]. LO and LMS provide reusability, but they usually are not dynamically adaptable [8,9]. This article presents our research that seeks the convergence of these different paradigms for the development of intelligent learning environments and describes the mechanisms of an Intelligent Learning Objects' dynamic presentation model, based on communication with SCORM (Sharable Content Object Reference Model) resources [19, 20].

There are analogous studies that provides adaptability to learning systems. Some examples extend the LMS with distinct adaptive strategies, such as conditional jumps [8], Bayesian networks [3] or data mining [7]. Other researches are not integrated with

a LMS, and use diversified ways to adapt the learning to the students' style, i.e.: ITS [6], recommender system [2], genetic algorithm [10] and swarm intelligence [11].

Moreover, there are some similar works based on the Multi-Agent System (MAS) approach resulting on smarter applications [12,13]. Some of them combine LMS and MAS to make the former more adaptive [14], and another is a dynamically adaptive environment, based on agents that are able to identify the student cognitive profile [14]. These related works identify the student's profile applying questionnaires in the beginning of the course or by clustering the students according to their assessments performance. Additionally, we observe in these papers that the attachment of new LO to the system is not possible without teacher intervention. The educator needs to configure previously all the possible course paths for each student style, what could be hard and take so much time [3]. Further, the attaching of a new LO to the course involves modifying its structure, resulting in limited adaptability and reuse.

In order to produce more intelligent LO, we have proposed in previous researches the convergence between the LO and MAS technologies, called Intelligent Learning Objects (ILO) [15]. This approach makes possible to offer more adaptive, reusable and complete learning experiences, following the learner cognitive characteristics and performance. According to this approach an ILO is an agent capable to play the role of a LO, which can acquire new knowledge by the interaction with students and other ILO (agents information exchange), raising the potential of student's understanding. The LO metadata permits the identification of what educational topic is related to the LO [9]. Hence, the ILO (agents) are able to find out what is the subject associated with the learning experience shown to the student, and then to show complementary information (another ILO) to solve the student's lack of knowledge in that subject.

## 2 ILOMAS

The proposed model integrates MAS and LMS into an intelligent behavior system, resulting on the improvement of the related works, leading to dynamic LO inclusion. The objective of the new model called Intelligent Learning Object Multi-Agent System (ILOMAS) is to enhance the framework developed to create ILO based on MAS with BDI architecture [16], extending this model to allow the production of adaptive and reusable learning experiences taking advantage of the SCORM data model elements. The idea is to select dynamically ILO in the LMS according to the student performance, without previous specific configuration on the course structure. The proposed model achieves reuse by the combination of pre-existed and validated LO whose concept is the same of that the student needs to learn about, avoiding the building of new materials. Moreover, the course structure becomes more flexible, since it is unnecessary to configure all the possible learning paths for each student profile.

The solution's adaptability is based on the ability to attach new LO to the LMS (that was not explicitly added before) as soon as the system finds out that the student needs to reinforce its understanding on a specific concept. This is automatically identified through the verification of the student assessment performance (i.e.: grade), on each instructional unit, or by student choice, when the learner interacting with the LO.

It is important to clarify that the approach does not use student' learning profile (i.e.: textual, interactive [2]) as information to select LOs. The scope of this research is to consider only the learner performance results (grades, time of interaction, sequencing and navigation). The ILOMAS is composed by agents with specific goals, and capable of communicating and offering learning experiences to students in a LMS course, according to the interaction with these students, taking advantage of the SCORM standard's features [19]. The ILOMAS architecture needs two kinds of agents:

- LMSAgent – Finds out the subject that the student must learn about, and passes the control of the interaction with the student to a new ILOAgent. Its beliefs are data provided from the LMS database, i.e.: the topic that the student must learn about.
- ILOAgent – Searches for a LO on the repository (related to the topic obtained from the LMSAgent), and exhibits it to the student. Besides, monitors the interaction between the student and the LO, which means the analysis of the data received from the SCORM communication. Depending on the analyzed data (beliefs), the agent will deliberate the exhibition of another LO (course with dynamic content).

The JADEX BDI V3 (V3) platform was chosen to implement the agents based on the BDI architecture [12,13]. The design of ILOMAS includes the characteristics of e-learning courses deployed on LMS (as MOODLE [7]), which means an environment accessed mostly from Web Browsers. The Java Servlets and JSP technologies are the bases of the interface between the client side (student) and the server side (agents' environment), getting benefits of the V3 services communication structure [13]. A non-agent class based on the Facade design pattern [17] keeps the low coupling between the MAS layer and the external items (front-end and servlets).

A first prototype was developed and tested with emphasis on the MAS development, instead of visualization issues (such as LO formats or graphical user interfaces) [18]. The simulation of a learning situation resulted on a different LO retrieved from the repository. This new LO had the same subject as the previous LO shown. It was not explicitly defined in the database that the student should have watched this new LO (only the topic was defined, no specific LO), so the MAS obtained the related LO dynamically, taking into account the metadata elements declared in IEEE-LOM [9].

## 2.1 ILOMAS and SCORM Integration

The extension of ILOMAS to use the SCORM standard [19,20] raises reuse, dynamic sequencing, and interoperability on learning environments. The SCORM specification defines a set of API functions, which allows the communication among the student, the LO and the LMS. This API admits that the ILOMAS uses the data model elements to define the student's knowledge level, and to evaluate the status of the current experience. Some available elements are the learner's answers to quizzes (result), the elapsed time since the beginning of the interaction (latency), the weighting of the interaction status relative to others, and a description of the LO's objectives [19]. If the learner demonstrates difficult in some subject (i.e.: wrong answers in sequence on the SCORM quiz, or take a long time to interact with the LO without any progress), it is possible to make decisions based on the historical received data.

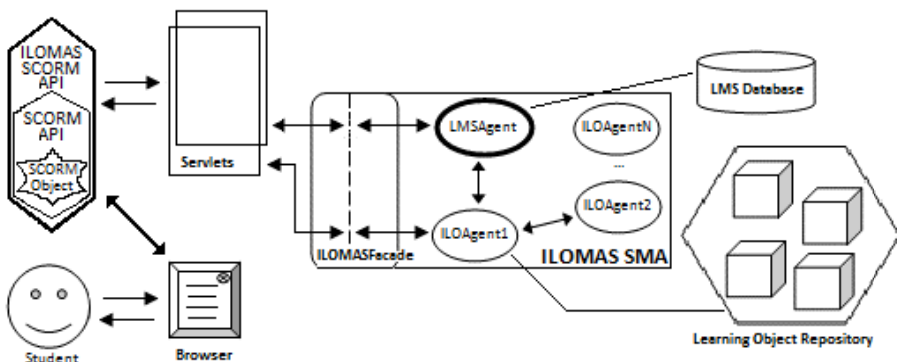


**Fig. 1.** ILOMAS SCORM Web architecture

The main desire defined to ILOAgent is to solve the student's lack of understanding about the subject. Thus, when the data received from SCORM points to a learner difficulty (error), the ILOMAS deliberation process (based on the JADEX engine [13]) dispatch the goal related with this objective. The ILOAgent's belief base stores the data received, and the deliberation process defines that the student needs to view a new (different) LO when the student selects an incorrect answer. This is the moment when the system achieves a dynamic learning situation, because a new LO not defined previously becomes part of the course structure. From the student's point of view (and even the teacher's point of view) the accessed object was just one, but with several contents (a larger LO composed dynamically by other smaller).

To validate this new version of the platform (SCORM integrated), we used some SCORM objects (on the version SCORM 1.2) about Social Security Laws (Public Law course). The learning interaction takes place in a custom LMS developed with limited features, only to test purposes. The implemented SCORM integration to ILOMAS was tested to reproduce distinct learning situations (Table 1): student that selects all the corrected answers (Student 1), another that misses all questions (Student 2), and one who increases understanding on the subject during interaction (Student 3). Each time that a student makes a mistake, the ILOMAS identifies the understanding problem and suggests another related LO to fill the learning gap (Fig. 2).

**Table 1.** ILOMAS SCORM preliminaries evaluation tests

Student	Quiz Errors	Previously Configured LO	New LO Offered	Dynamic Behavior
Student 1	0	1	0	No
Student 2	4	1	4	Yes
Student 3	1	1	1	Yes

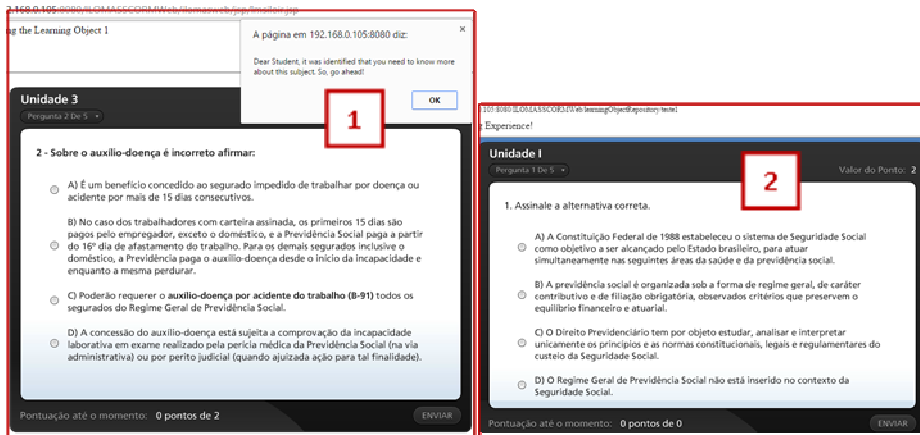


**Fig. 2.** The ILOMAS SCORM Web application execution: (1) The moment of the identification that the student needs another LO (wrong answer); (2) New LO exhibition

### 3 Conclusions and Future Work

This research resulted on a prototype implementation to verify the proposed model and its feasibility, followed by the execution of some evaluation tests. The SCORM API implementation gives to ILOMAS the ability of monitoring the overall communication between the LO and the learner, getting benefits of the SCORM data model element (i.e.: interaction status and time of the current learning session).

Future work leads to enhance the analysis of the received SCORM elements, taking into consideration the history of the student's experiences, and to explore all the SCORM data model elements in the process of determining if the learner needs to view a new LO. Another improvement would be the integration of ILOMAS with some MAS based recommender system for indexing and retrieving the related LO within the repository [21]. Finally, future work involves building a new plugin to integrate the ILOMAS inside the MOODLE LMS, and testing the application with different learning situations inside a LMS production instance, with real students.

### References

- Allison, C., Miller, A., Oliver, I., Michaelson, R., Tiropanis, T.: The Web in education. Computer Networks **56**, 3811–3824 (2012)
- Vesin, B., Klasnja-Milicevic, A., Ivanovic, M., Budimac, Z.: Applying recommender systems and adaptive hypermedia for e-learning personalization. Computing and Informatics **32**, 629–659 (2013). Institute of Informatics
- Bachari, E., Abelwahed, E., Adnani, M.: E-Learning personalization based on dynamic learners' preference. International Journal of Computer Science & Information Technology (IJCSIT) **3**(3) (2011)

4. Mahkameh, Y., Bahreininejad, A.: A context-aware adaptive learning system using agents. *Expert Systems with Applications* **38**, 3280–3286 (2011)
5. Caeiro, M., Llamas, M., Anido, L.: PoEML: Modeling learning units through perspectives. *Computer Standards & Interfaces* **36**, 380–396 (2014)
6. Santos, G., Jorge, J.: Interoperable Intelligent Tutoring Systems as Open Educational Resources. *IEEE Transactions on Learning Technologies* **6**(3), 271–282 (2013). IEEE CS & ES
7. Despotovic-Zrakic, M., Markovic, A., Bogdanovic, Z., Barac, D., Krco, S.: Providing Adaptivity in Moodle LMS Courses. *Educational Technology & Society* **15**(1), 326–338 (2012). International Forum of Educational Technology & Society
8. Komlenov, Z., Budimac, Z., Ivanovic, M.: Introducing Adaptivity Features to a Regular Learning Management System to Support Creation of Advanced eLessons. *Informatics in Education* **9**(1), 63–80 (2010). Institute of Mathematics and Informatics
9. Barak, M., Ziv, S.: Wandering: A Web-based platform for the creation of location-based interactive learning objects. *Computers & Education* **62**, 159–170 (2013)
10. Chen, C.: Intelligent web-based learning system with personalized learning path guidance. *Computers & Education* **51**, 787–814 (2008)
11. Kurilovas, E., Zilinskiene, I., Dagiene, V.: Recommending suitable scenarios according to learners' preferences: An improved swarm based approach. *Computers in Human Behavior* **30**, 550–557 (2014)
12. Wooldridge, M.: *An Introduction to MultiAgent Systems*, 2nd edn. John Wiley & Sons (2009)
13. Pokahr, A., Braubach, L., Haubeck, C., Ladiges, J.: *Programming BDI Agents with Pure Java*. University of Hamburg (2014)
14. Giuffra, P., Silveira, R.: A multi-agent system model to integrate Virtual Learning Environments and Intelligent Tutoring Systems. *International Journal of Interactive Multimedia and Artificial Intelligence* **2**(1), 51–58 (2013)
15. Silveira, R., Gomes, E., Vicari, R.: Intelligent Learning Objects: An Agent-Based Approach of Learning Objects. *IFIP – International Federation For Information Processing*, vol. 182, pp. 103–110. Springer-Verlag (2006)
16. Bavaresco, N., Silveira, R.: Proposal of an architecture to build intelligent learning objects based on BDI agents. In: XX Informatics in Education Brazilian Symposium (2009)
17. Gamma, E., Helm, R., Johnson, R., Vlissides, J.: *Design Patterns: Elements of Reusable Object-Oriented Software*. Addison-Wesley (1995)
18. de Amorim Jr., J., Gelaim, T.Á., Silveira, R.A.: Dynamic e-Learning content selection with BDI agents. In: Bajo, J., Hallenborg, K., Pawlewski, P., Botti, V., Sánchez-Pi, N., Duque Méndez, N.D., Lopes, F., Vicente, J. (eds.) PAAMS 2015 Workshops. CCIS, vol. 524, pp. 299–308. Springer, Heidelberg (2015)
19. SCORM 2004. Advanced Distributed Learning. <http://www.adlnet.org/scorm>
20. Gonzalez-Barbone, V., Anido-Rifon, L.: Creating the first SCORM object. *Computers & Education* **51**, 1634–1647 (2008)
21. Campos, R.L.R., Comarella, R.L., Silveira, R.A.: Multiagent based recommendation system model for indexing and retrieving learning objects. In: Corchado, J.M., Bajo, J., Kozlak, J., Pawlewski, P., Molina, J.M., Julian, V., Silveira, R.A., Unland, R., Giroux, S. (eds.) PAAMS 2013. CCIS, vol. 365, pp. 328–339. Springer, Heidelberg (2013)

# Sound Visualization Through a Swarm of Fireflies

Ana Rodrigues<sup>(✉)</sup>, Penousal Machado, Pedro Martins, and Amílcar Cardoso

CISUC, Department of Informatics Engineering, University of Coimbra,  
Coimbra, Portugal  
`{anatr,machado,pjmm,amilcar}@dei.uc.pt`

**Abstract.** An environment to visually express sound is proposed. It is based on a multi-agent system of swarms and inspired by the visual nature of fireflies. Sound beats are represented by light sources, which attract the virtual fireflies. When fireflies are close to light they gain energy and, as such, their bioluminescence is emphasized. Although real world fireflies do not behave as a swarm, our virtual ones follow a typical swarm behavior. This departure from biological plausibility is justified by aesthetic reasons: the desire to promote fluid visualizations and the need to convey the perturbations caused by sound events. The analysis of the experimental results highlights how the system reacts to a variety of sounds, or sequence of events, producing a visual outcome with distinct animations and artifacts for different musical pieces and genres.

**Keywords:** Swarm intelligence · Computer art · Multi-agent systems · Sound visualization

## 1 Introduction

Although sound visualization has been an object of study for a long time, the emergence of the computer, with graphic capabilities, allowed the creation of new paradigms and creative processes in the area of sound visualization. Most of the initial experiments were done through analogical processes. Since the advent of computer science, art has taken significant interest in the use of computers for the generation of automated images. In section 2, we present some of the main inspirations to our work including sound visualization, generative artworks, computer art and multi-agent systems.

Our research question relies on the possibility of developing a multi-agent model for sound visualization. We explore the intersection between computer art and nature-inspired multi-agent systems. In the context of this work, swarm simulations are particularly interesting because they allow the expression of a large variety of different types of behaviors and tend to be intuitive and natural forms of interaction.

In section 3 we present the developed project, which is based on a multi-agent system of swarms and inspired by the visual nature of fireflies. In the scope of our

work, visualization of music is understood as the mapping of a specific musical composition or sound into a visual language.

Our environment contains sources of light representing sound beats, which attract the fireflies. The closer a firefly is to the light, the more emphasized is its bioluminescence and higher is its chance of collecting energy (life). Using Reynolds' boids algorithm [6], fireflies interact with the surrounding environment by means of sensors. They use them to find and react to energy sources as well as to other fireflies. In section 4 we present an analysis and corresponding experimental results of the systems behavior to 5 different songs. Lastly, in section 5 we present our conclusions and further work to be done.

## 2 Related Work

Ernst Chladni studied thoroughly the relation between sound and image. One of his best-known achievements was the invention of Cymatics. It geometrically showed the various types of vibration on a rigid surface [5]. In the 1940s Oskar Fischinger made cinematographic works exploring the images of sound by means of traditional animation [4]. His series of 16 studies was his major success [4]. Another geometric approach, was made by Larry Cuba in 1978, but this time with digital tools. "3/78" consisted of 16 objects performing a series of precisely choreographed rhythmic transformations [2].

Complex and self-organized systems have a great appeal for the artistic practice since they can continuously change, adapt and evolve. Over the years, computer artifacts promoting emergent systems behaviors have been explored [1] [7]. Artists got fascinated with the possibility of an unpredictable but satisfying outcome. Examples of this include the work of Ben F. Laposky, Frieder Nake, Manfred Mohr, among many others [3].

## 3 The Environment

In this section we present a swarm-based system of fireflies and all of its interactions. In this environment, fireflies are fed by the energy of sound beats (rhythmic onsets). While responding to the surrounding elements of the environment, they search for these energies (see Fig. 1). The colors were chosen according to the

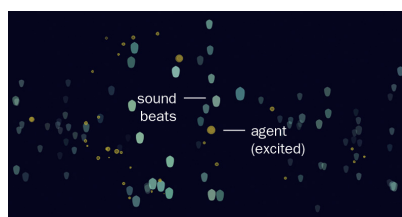


**Fig. 1.** Systems behavior and appearance example. Best viewed in color.

real nature of fireflies. Since they are visible at night, we opted for a dark blue in the background and a brighter one for the sound beats. As for bioluminescence, we used yellow.

The environment rules and behaviors, plus the visualization were implemented with Processing. The mechanism for extracting typical audio information was made with the aid of the Minim library, mainly because it contains a function for sound beat detection.

### 3.1 Sound (Energy Sources)

**Sound Analysis.** To visualize sound, a preliminary analysis is necessary. A sound is characterized by 3 main parameters: frequency, amplitude and duration. Frequency determines the pitch of the sound. Amplitude determines how loud the sound is. Duration can define the rhythm of music and also the instant in the music where sound beats happen.

We perform sound analysis prior to the visualization, in order to promote a fluid animation and convey the perturbations caused by sound events. We compute the main sound characteristics (pitch, volume, sound beats) and export them to a text file. Sound beats are detected note onsets. They are related to the temporal/horizontal position of a sound event.

Although the mechanism used to extract audio is not novel and remains simple, we think this approach is adequate to the goals of our system. It fits in the amount of expressiveness that we intend to represent in our visualization, as visual simplicity characterizes the fireflies natural environment

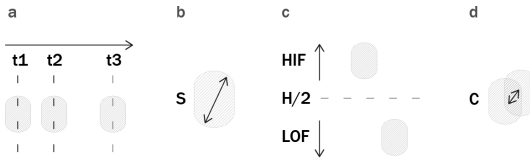


**Fig. 2.** Graphical representation of sound objects. a - Sound beats instants, b - Amplitude, c - Frequency, d - Collision.

**Sound's Graphic Representation.** After the sound analysis, all the properties of sound are mapped into graphical representations. Sound beats are mapped into instants ( $t_1, t_2, t_3, \dots$ ) which defined the objects horizontal position as shown in Fig. 2a. Each sound object has a pre-defined duration, meaning that it is removed from the environment at the end of its duration. Amplitude was translated into the objects size, i.e., the size is directly proportional to the amplitude (Fig. 2b). Lastly, frequency is mapped into the objects vertical position in the environment (Fig. 2c). High frequencies (HIF) are positioned on the top of screen and low frequencies (LOF) emerge in lower positions of the vertical axis. A fourth characteristic presented in the graphical representation of sound

objects is collision (Fig. 2d). This last one is not directly related to sound, only to sound object's physics. When a object collides with another one, a contrary force is applied between these two, separating them from each other.

### 3.2 Agents (Fireflies)

**Agent Behavior.** Because the sound beats are presented from the left to right, fireflies are initially born on the left side of the screen, vertically centered. Agents are provided with a specific vision towards the surrounding environment. A vision angle of  $30^\circ$  and a depth of 150 pixels were considered as optimum values (Fig. 3), because the agents could have a high amount of independence and resemble to their original behavior. Agents motion is based on the “Boids” algorithm. They walk randomly until they find something that may affect their behavior, such as source of light or other agents.

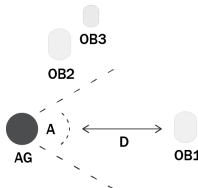


**Fig. 3.** Agent field of view: angle (A) and depth (D).

The closer they are to a source of light, the more attracted they get to it, meaning that there is a force of attraction towards it. Along with that, agents have a swarming behavior, meaning that neighbor agents can see each others and follow them through flocking behavior rules [6].

These rules were presented by Reynolds with a computational model of swarms exhibiting natural flocking behavior. He demonstrated how a particular computer simulation of boids could produce complex phenomena from simple mechanisms. These behaviors define how each creature behaves in relation to its neighbors: separation, alignment or cohesion [6].

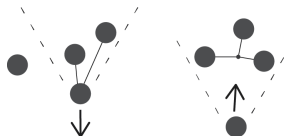


**Fig. 4.** Left image: separation. Right image: cohesion.

The swarming behaviors present in this system are: separation and cohesion (Fig. 4). Separation gives the agents the ability to maintain a certain distance

from others nearby in order to prevent agents from crowding together. Cohesion gives agents the ability to approach and form a group with other nearby agents [6]. No alignment force was applied. Alignment is usually associated with flocking behavior, like birds and fishes do. Swarm behavior – like the one found in bees, flies and our fireflies – does not imply alignment.

Additionally, the life and death of each agent is also determined by the way it interacts with the environment. The agent begins with an initial lifespan, losing part of its energy at each cycle. If the agent gets close to an energy source, it gains more energy and a longer lifespan; otherwise, it keeps losing its energy until it dies. There are no mechanisms for the rebirth of agents, as we intend to keep a clear visualization and understanding of interactions among agents.

**Agent's Graphic Representation.** Fireflies use bioluminescence to communicate and attract other fireflies. As an agent gradually approaches the light emitted by a sound object within its field of view, the more excited it gets and the more it emphasizes its bioluminescence (Fig. 5, left image). This will temporarily influence the agents size because it gets intermittent. The real agent size will be as big as the energy (Fig. 5, right image) that it has at a certain instant. When an agent dies, it disappears from the environment.



**Fig. 5.** Left image: agent approximation to an object (AG→OB). Right image: agent growth (E).

## 4 Results and Discussion

This section presents an analysis of the systems behavior in response to 4 different songs or melodic sequences (from track 1 to track 4). These tracks vary in rhythm, intensity and frequencies, allowing us to illustrate and highlight how the system reacts to different sound stimuli.

Unfortunately, conveying the overall feel of an animation<sup>1</sup> in a paper has its difficulties. To circumvent this issue and to ease our analysis, first we analyze a

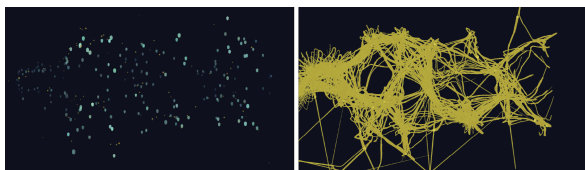


**Fig. 6.** The music that generated this response is characterized by a variety of intensity and big density of beats.

<sup>1</sup> A demonstration video can be found at <http://tinyurl.com/ky7yaql>.

complete visualization of the track so we can perceive the differences inside each one. Secondly, we present the trajectory made by the agents of the corresponding music to better analyze their behavior in the different tracks. We present only one example of those figures due to space constraints.

Track 1 corresponds to a piece with high density of beats and low contrast of intensities. This promotes a higher chance of having a longer lifespan. However, the low contrast of the intensities implies that they do not gather so much energy at once. Track 2 (Fig. 6), is also characterized by a high density of beats, but in this case the contrast in intensities make swarms gain more energy. Track 3 has a low contrast of frequencies and a balanced density of beats. For Last, Track 4 as opposed to almost all of the other examples so far described, has a strong contrast between high and low frequencies. Adding to this, the low density of beats results in a reduced lifespan for swarms as they have a short field of view.

From the observation of these patterns created by our system, we can conclude: (i) fireflies have a tendency to follow the pattern created by the sound beats as we could see in the example depicted in Fig. 6; (ii) there is a bigger concentration of fireflies in the sources that contain more energy; (iii) tracks with a lower contrast between frequencies promote a more balanced spread of the fireflies in the environment; (iv) tracks with a high density of beats give fireflies a longer lifespan because the agents have a narrow vision field and thus they can collect more energy even if it is in small pieces of it.

## 5 Conclusions and Future Work

We presented an environment to visualize audio signals. It was inspired by the visual nature of fireflies and based on a multi-agent system of swarms proposed by Reynolds. In this environment, sound is mapped into light objects with energy, which attract the virtual fireflies. When fireflies are close to light they gain energy and, as such, their bioluminescence is emphasized. The flocking behavior of the group emerges based on simple rules of interaction.

In real life the presented technique may be useful for people with low understanding of music to take part in musical events. In further work we will expand our system by introducing more sophisticated mechanisms for the sound analysis, which allow the representation of higher-level concepts and musical events. On the other hand, we also wish to explore alternative visual representations to offer the user a wider array of choices. Finally, a user study should be performed to assess the strengths and weaknesses of the different visualization variants and evaluate the system.

**Acknowledgments.** This research is partially funded by project ConCreTe. Project ConCreTe acknowledges the financial support of the Future and Emerging Technologies (FET) programme within the Seventh Framework Programme for Research of the European Commission, under FET grant number 611733.

## References

1. Barszczewski, P., Cybulski, K., Goliski, K., Koniewski, J.: Constellation (2013). <http://pangenerator.com>
2. Compart: Larry Cuba, 3/78 (nd). <http://tinyurl.com/k2y3vef>
3. Dietrich, F.: Visual intelligence: The first decade of computer art (1965–1975). Leonardo **19**(2), 159–169 (1986)
4. Evans, B.: Foundations of a visual music. Computer Music Journal **29**(4), 11–24 (2005)
5. Monoskop: Ernst Chladni (nd). [http://monoskop.org/Ernst\\_Chladni](http://monoskop.org/Ernst_Chladni)
6. Reynolds, C.W.: Steering behaviors for autonomous characters. In: Game Developers Conference, vol. 1999, pp. 763–782 (1999)
7. Uozumi, Y., Yonago, T., Nakagaito, I., Otani, S., Asada, W., Kanda, R.: Sjq++ ars electronica (2013). <https://vimeo.com/66297512>

# **Social Simulation and Modelling**

# Analysing the Influence of the Cultural Aspect in the Self-Regulation of Social Exchanges in MAS Societies: An Evolutionary Game-Based Approach

Andressa Von Laer, Graçaliz P. Dimuro<sup>(✉)</sup>, and Diana Francisca Adamatti

PPGCOMP, C3, Universidade Federal Do Rio Grande (FURG), Rio Grande, Brazil  
[{andressavonlaer,gracaliz,dianaada}](mailto:{andressavonlaer,gracaliz,dianaada}@gmail.com)@gmail.com

**Abstract.** Social relationships are often described as social exchanges, understood as service exchanges between pairs of individuals with the evaluation of those exchanges by the individuals themselves. Social exchanges have been frequently used for defining interactions in MAS. An important problem that arises in the context of social simulation and other MAS applications is the self-regulation of the social exchange processes, so that the agents can achieve/maintain the equilibrium of the exchanges by themselves, guaranteeing the continuation of the interactions in time. Recently, this problem was tackled by defining the spatial and evolutionary Game of Self-Regulation of Social Exchange Processes (GSREP), implemented in NetLogo, where the agents evolve their exchange strategies by themselves over time, performing more equilibrated and fair interactions. The objective of this paper is to analyse the problem of the self-regulation of social exchange processes in the context of a BDI-based MAS, adapting the GSREP game to Jason agents and introducing a cultural aspect, where the society culture, aggregating the agents' reputation as group beliefs, influences directly the evolution of the agents' exchange strategies, increasing the number of successful interactions and improving the agents' outcomes in interactions.

## 1 Introduction

As it is well known in social sciences, the acts, actions and practices that involve more than two agents and affect or take account of other agents's activities, experiences or knowledge states are called social interactions. Social interactions and, mainly, the quality of these interactions, are crucial for the proper functioning of the system, since, e.g., communication failure, lack of trust, selfish attitudes, or unfair behaviors can leave the system far of a solution. The application of the social interaction concept to enhancements of MAS's functionality is a natural step towards designing and implementing more intelligent and human-like populations of artificial autonomous systems. [13]

Social relationships are often described as social exchanges [1], understood as service exchanges between pairs of individuals with the evaluation of those

exchanges by the individuals themselves [16]. Social exchanges have been frequently used for defining social interactions in MAS [10, 15, 21]. A fundamental problem discussed in the literature is the regulation of such exchanges, in order to allow the emergence of equilibrated exchange processes over time, promoting the continuity of the interactions [12, 21], social equilibrium [15, 16] and/or fairness behaviour.<sup>1</sup> In particular, this is a difficult problem when the agents, adopting different social exchange strategies, have incomplete information on the other agents' exchange strategies, as in open societies [9].

In the literature (e.g., [9, 15, 21]), different models were developed (e.g., centralized/decentralized control, closed/open societies) for the social exchange regulation problem. Recently, this problem was tackled by Macedo et al. [12], by introducing the spatial and evolutionary *Game of Self-Regulation of Social Exchange Processes* (GSREP), where the agents, adopting different social exchange strategies (e.g., selfishness, altruism), considering both the short and long-term aspects of the interactions, evolve their exchange strategies along the time by themselves, in order to promote more equilibrated and fair interactions. This approach was implemented in NetLogo.

However, certain characteristics involved in social exchanges may be more appropriately modeled with cognitive agents<sup>2</sup>, such as *BDI Agents* (Belief, Desire, Intention) [4]. Also, taking into account the observations made by a society on the behavior of an agent  $ag$  in its past interactions, it is possible to qualify  $ag$ 's reputation [5, 6], which can be made available to the other agents who themselves have not interacted with that agent. These indirect observations can be aggregated to define any agent past behaviour based on the experiences of participants in the system [11]. Reputation can assist agents in choosing partners where there are other agents that can act so as to promote the disequilibrium of the social exchange processes in the society. Given the importance of this kind of analysis in many real-world applications, a large number of computational models of reputation have been developed (e.g., [23, 24]).

Then, this paper introduces an evolutionary and cultural approach of GSREP game for the JaCaMo [2] framework, considering also the influence of the agent society culture, so defining the Cultural-GSREP game. Observe that here are at least five basic categories of cultural knowledge that are important in the belief space of any cultural evolution model: situational, normative, topographic, historical or temporal, and domain knowledge [18]. In this paper, we explore just the normative category, and let the combination of other cultural aspects for further work. We consider a specific society's culture where the agents' reputations are aggregated as group beliefs [23], using the concept of artifacts [20]. Based on the idea that "the culture of a society evolves too, and its evolution may be faster than genetics, enabling a better adaptation of the agent to the environment" [19], we analyse the influence of the culture in the evolution of the

---

<sup>1</sup> We adopted the concept of fairness behaviour/equilibrium as in [17, 25].

<sup>2</sup> For discussions on the role of BDI agents in social agent-based simulation, see [14].

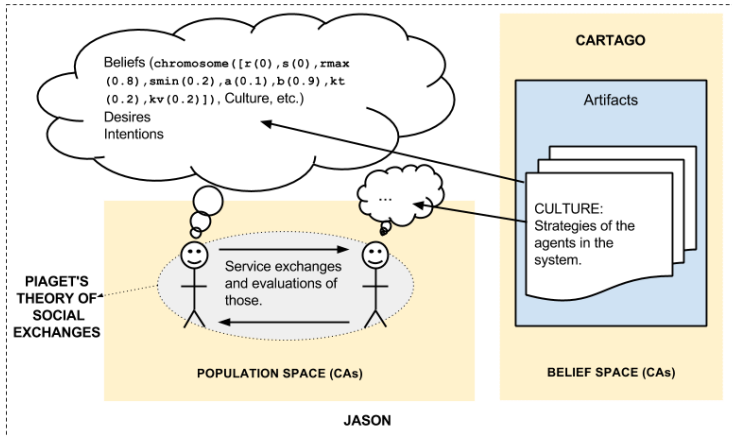


**Fig. 1.** An overview of the proposed model

agents' exchange strategies, the increase of the number of successful interactions and the improvement of the agents' outcomes in their interactions.<sup>3</sup>

## 2 The Cultural-GSREP Game

The Cultural-GSREP game is built on the spatial and evolutionary game of incomplete information presented in [12], for the self-regulation of social exchange processes, where agents evolve their strategies in order to maximize a *fitness* function by an evolutionary approach. In each simulation cycle, the fitness function evaluates the material result of the exchanges of an agent with its neighboring agents, getting influence by factors that characterize the exchange strategies and attitudes adopted by the agents.

For the agent belief learning process, the agent society's culture (consisted of a belief space common to all agents) may influence on the decision making in each single game (two-agent exchange). The addition of a belief space common to all agents involved in the system works as a focal point (Schelling Point) [22], serving as reference for agents, since the agents do not have knowledge about the other agents' exchange strategies. The belief space used in this paper is based on the work developed in [23].

Figure 1 shows an overview of the Cultural-GSREP game model, which is organized in two parts: the first is the social exchange game [12], where each single exchange occurs in two sequential stages with their respective evaluations

<sup>3</sup> We remark that the aim of the paper is not to introduce a novel method to evaluate reputation. On the contrary, we adopt a very simple method for analysing the reputation in order to show how this cultural aspect may influence the evolution of the self-regulation of social exchanges. For discussions on the perspectives of culture in a more general context see [8].

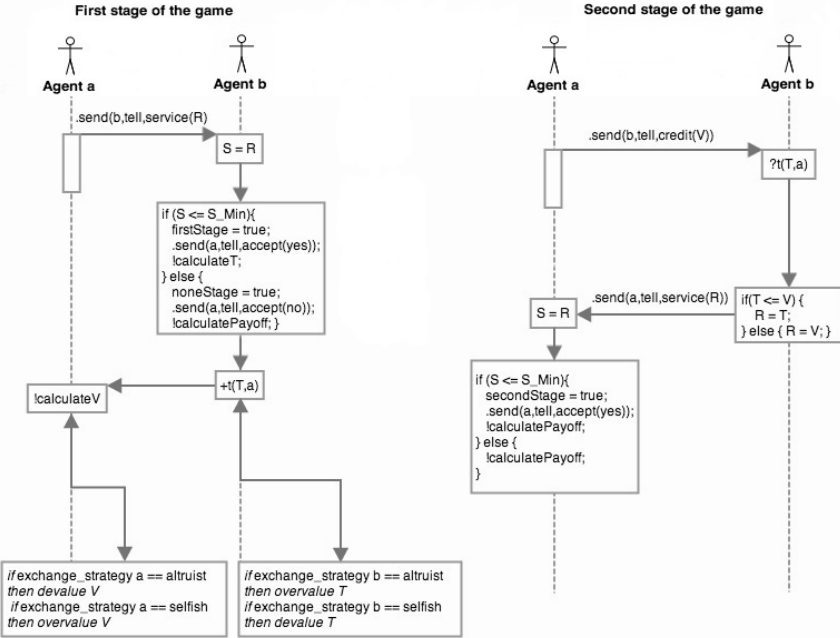


**Fig. 2.** Two stages of a single social exchange game (for selfishness/altruism exchange strategies)

by the agents themselves, and a fitness function helps to evolve the agents's exchange strategies; the second part is the creation of group beliefs (GBs) using artifacts, which forms the cultural level based on agents' reputations constructed over the exchanges experienced by the agents in the society. The model was implemented in Jason [3], using the concept of Agents & Artifacts [20] for the implementation of group beliefs in CArtAgO framework [2].<sup>4</sup>

### 3 The Game of Exchange Processes

Figure 2 shows the basic and simplified two-stage sequence of the first part of the model, where the exchanges between each two agents occur in a single exchange cycle.<sup>5</sup> In the first stage of the game, denoted by I, the agent  $a$  offers a service with some value of investment ( $R$ ) to the agent  $b$ , such that  $R \leq R_{\max}$ , where  $R_{\max}$  is the maximal investment value  $a$  is willing to have for a service performed for another agent. This yields a value of  $b$ 's satisfaction ( $S$ ) and debt ( $T$ ) for the service provided by  $a$ , which are directly related to  $a$ 's investment value.

<sup>4</sup> Note that shared artifacts are common in normative and organizational systems (see, e.g., [7]).

<sup>5</sup> The two-stage social exchange was inspired by Piaget's Theory of Social Exchanges.[16]

However, if  $b$  believes that the service offered by  $a$  provides less satisfaction than the minimal satisfaction ( $S_{\min}$ ) it is willing to accept, than  $b$  refuses  $a$ 's offer and this exchange stage does not occur. Supposing that  $b$  accepts the service provided by  $a$ , then, at the end of this stage, the agent  $a$  has a credit value ( $V$ ), that is, a credit related to the service it has previously performed to agent  $b$ .  $R$  and  $S$  are called material values, related to the performed exchanges.  $T$  and  $V$  are virtual values, related to future interactions, since they help the continuation of the exchanges.

The second stage, denoted by II, is similar to the first, but referring to a possible debt collection by agent  $a$ , when  $a$  charges  $b$  for a service in payment for its virtual value ( $V$ ) (the credit  $a$  has obtained from  $b$  in the stage I). The agent  $b$  has on its belief base a debt value ( $T$ ) and it then performs a service offer with an investment value ( $R$ ) to  $a$  (with  $R \leq R_{\max}$ ), which in turn generates a value of satisfaction ( $S$ ) for  $b$ 's offer, in case that it accepts such satisfaction value (i.e.,  $S \geq S_{\min}$ ), otherwise this exchange stage does not occur. After each 2-stage exchange between  $a$  and  $b$ , they calculate the material reward they received, using the payoff function  $p_{ab} : [0, 1]^4 \rightarrow [0, 1]$ :

$$p_{ab}(R_{I_{ab}}, R_{II_{ba}}, S_{I_{ba}}, S_{II_{ab}}) = \begin{cases} \frac{1 - R_{I_{ab}} + S_{II_{ab}}}{2} & \text{if } (R_{I_{ab}} \leq R_a^{\max} \wedge S_{I_{ba}} \geq S_b^{\min}) \wedge (R_{II_{ba}} \leq R_b^{\max} \wedge S_{II_{ab}} \geq S_a^{\min}) \\ \frac{1 - R_{I_{ab}}}{2} & \text{if } (R_{I_{ab}} \leq R_a^{\max} \wedge S_{I_{ba}} \geq S_b^{\min}) \wedge (R_{II_{ba}} > R_b^{\max} \vee S_{II_{ab}} < S_a^{\min}) \\ 0 & \text{if } (R_{I_{ab}} > R_a^{\max} \vee S_{I_{ba}} < S_b^{\min}) \wedge (R_{II_{ba}} > R_b^{\max} \vee S_{II_{ab}} < S_a^{\min}) \end{cases} \quad (1)$$

Observe that, according to Eq. (1), if both exchange stages I and II are successfully performed, then the agents' rewards are greater. On the contrary, if no stage occurs, i.e., the agent  $b$  refuses the service of agent  $a$  in the first stage I, the payoff is null.

### 3.1 Social Exchange Strategies in Beliefs

The agents evaluate the services according to their exchange strategies, e.g., an agent with selfishness strategy is more likely to devalue the received service and overvalue an offered service, which impacts on debt and credit values. The calculations of debts  $T$  and credits  $V$  are made using the debt and credit depreciation ( $\rho = d$ ) or overestimation ( $\rho = o$ ) factors  $k^{pt}, k^{ov} \in [0, 1]$ , respectively, characterizing each strategy, as follows:

$$\text{Depreciation: } T = (1 - k^{dt})S, V = (1 - k^{dv})R \quad (2)$$

$$\text{Overestimation: } T = S + (1 - S)k^{ot}, V = R + (1 - R)k^{ov} \quad (3)$$

Each agent has in its belief base an exchange strategy-based belief, called *chromosome belief*, which evolves along the time, by mutation plans. For example, the initial chromosome belief of an altruist agent is defined as:

```
chromosome([r(0), s(0), rmax(0.8), smin(0.2), e(0.1), g(0.9), kot(0.2), kdv(0.2)]),
```

where  $r(0)$  and  $s(0)$  are, respectively, the initial investment and satisfaction values, and the current parameters that represent its exchange strategy are:  $R$ ,  $R^{\max}$ ,  $S^{\min}$ ,  $k^t$  and  $k^v$ , where  $R \in [0; 1]$  is the value of investment,  $R^{\max} \in [0; 1]$  is the maximum value that the agent will invest,  $S^{\min} \in [0; 1]$  is the minimum

value of satisfaction that the agent accepts,  $k^{ot} \in [0; 1]$  and  $k^{dt} \in [0; 1]$  are, respectively, the debt overestimation and credit depreciation factors, as shown in Eqs. (2) and (3),  $e \in [0, 1]$  is the weight that represents the agent's tolerance degree when its payoff is less than of its neighboring agents (*envy degree*), and  $g \in [0, 1]$  represents the agent's tolerance degree when its payoff is higher than its neighboring agents' payoffs (*guilt degree*) [12, 25].

Analogously, the initial chromosome belief of a selfish agent is defined as:

```
chromosome([r(0), s(0), rmax(0.2), smin(0.8), e(0.9), g(0.1), kdt(0.2), kov(0.2)]).
```

To implement/evaluate the model, we consider five agents that perform the exchanges, each agent with a different initial exchange strategy, namely: altruism, weak altruism, selfishness, weak selfishness and rationality. The rational agent plays just for the Nash Equilibrium<sup>6</sup>, and then  $s_{\min} = e = g = k^t = k^v = 0$ .

### 3.2 The Fitness Evaluation

Given a neighborhood  $A = \{1, \dots, m\}$  of  $m$  agents, each agent  $i \in A$  plays the exchange game with the other  $m - 1$  neighboring agents  $j \in A$ , with  $j \neq i$ . In each simulation cycle, each agent  $i$  evaluates its local social exchange material results with each other neighboring agent  $j$ , using the local payoff function given in Eq. (1). The total payoff received by each agent is calculated after each agent has performed the two exchange stages with its entire neighborhood. For  $p_{ij}$  calculated by Eq. (1), the *total payoff allocation* of a neighborhood of  $m$  agents is given by

$$X = \{x_1, \dots, x_m\}, \text{ where } x_i = \sum_{j \in A, j \neq i} p_{ij}. \quad (4)$$

The agent  $i$  calculates its adaptation degree through its *fitness* function  $F_i : [0, 1]^m \rightarrow [0, 1]$ , whose definition, encompassing all types of exchange strategies, is:

$$F_i(X) = x_i - \frac{e_i}{(m-1)} \sum_{j \neq i} \max(x_j - x_i, 0) - \frac{g_i}{(m-1)} \sum_{j \neq i} \max(x_i - x_j, 0), \quad (5)$$

where  $X$  is the total payoff allocation of agent  $i$  (Eq. (4)),  $e_i$  and  $g_i$  are  $i$ 's envy and guilt degrees, respectively. To evaluate its *fitness*, the agent compares its current fitness with the previous one: if it exceeds the value of the previous fitness, then the current strategy is better than the previous one, and the agent makes an adjustment in the vector of probabilities, increasing the probability of the current strategy to be chosen again, increasing/decreasing the parameters of the chromosome belief defining its strategy.<sup>7</sup>

The probability vector of adjustments is in Table 1. There are 27 possible adjustments, e.g.,  $p_i^0$  is the probability of increasing  $R_i$ ,  $R_i^{\max}$  and  $S_i^{\min}$  (by a certain exogenously specified adjustment step), and  $p_i^5$  is the probability of increasing the value of  $R_i$ , keeping the value of  $R_i^{\max}$  and decreasing  $S_i^{\min}$ . The probability and strategy adjustment steps  $f_p$  and  $f_s$  determine, respectively, on which extent the probabilities of the probability vector and the values  $r_i$ ,  $r_i^{\max}$  and  $s_i^{\min}$  are increased or decreased.

<sup>6</sup> See [12] for a discussion on the Nash Equilibrium of the Game of Social Exchange Processes.

<sup>7</sup> The fitness function was based in [12, 25].

**Table 1.** The probability vector adjustment

	$R_i$	$R_i^{max}$	$S_i^{min}$		$R_i$	$R_i^{max}$	$S_i^{min}$		$R_i$	$R_i^{max}$	$S_i^{min}$
$p_i^0$	$\uparrow$	$\uparrow$	$\uparrow$	$p_i^9$	$=$	$\uparrow$	$\uparrow$	$p_i^{18}$	$\downarrow$	$\uparrow$	$\uparrow$
$p_i^1$	$\uparrow$	$\uparrow$	$=$	$p_i^{10}$	$=$	$\uparrow$	$=$	$p_i^{19}$	$\downarrow$	$\uparrow$	$=$
$p_i^2$	$\uparrow$	$\uparrow$	$\downarrow$	$p_i^{11}$	$=$	$\uparrow$	$\downarrow$	$p_i^{20}$	$\downarrow$	$\uparrow$	$\downarrow$
$p_i^3$	$\uparrow$	$=$	$\uparrow$	$p_i^{12}$	$=$	$=$	$\uparrow$	$p_i^{21}$	$\downarrow$	$=$	$\uparrow$
$p_i^4$	$\uparrow$	$=$	$=$	$p_i^{13}$	$=$	$=$	$=$	$p_i^{22}$	$\downarrow$	$=$	$=$
$p_i^5$	$\uparrow$	$=$	$\downarrow$	$p_i^{14}$	$=$	$=$	$\downarrow$	$p_i^{23}$	$\downarrow$	$=$	$\downarrow$
$p_i^6$	$\uparrow$	$\downarrow$	$\uparrow$	$p_i^{15}$	$=$	$\downarrow$	$\uparrow$	$p_i^{24}$	$\downarrow$	$\downarrow$	$\uparrow$
$p_i^7$	$\uparrow$	$\downarrow$	$=$	$p_i^{16}$	$=$	$\downarrow$	$=$	$p_i^{25}$	$\downarrow$	$\downarrow$	$=$
$p_i^8$	$\uparrow$	$\downarrow$	$\downarrow$	$p_i^{17}$	$=$	$\downarrow$	$\downarrow$	$p_i^{26}$	$\downarrow$	$\downarrow$	$\downarrow$

## 4 The Culture: Group Belief and Reputation Artifacts

The culture of the agent society is consisted of the group belief (GB) and the reputation artifacts. For the implementation in CArtAgO, these artifacts are firstly created by the *mediator* agent, which is also responsible for initiating the exchanges by sending a message to all agents to start the sequence of exchanges. The GB artifact stores the beliefs sent by agents after obtaining experience in exchanges and the reputation artifact creates the reputation of agents.

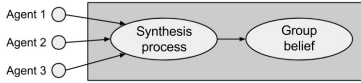
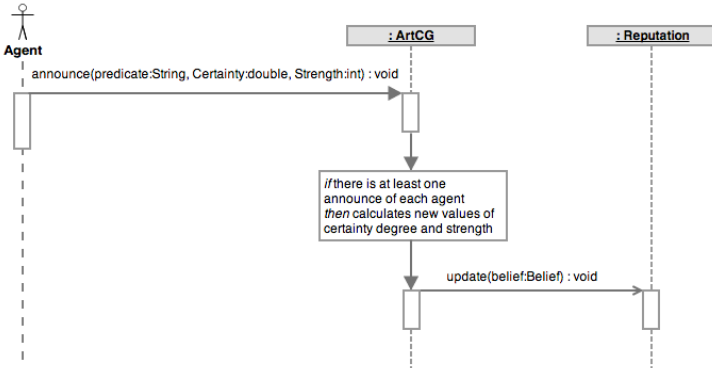
The beliefs that compose the artifacts are observable properties. The announcements are treated as interface operations, where some parameters are informed: the predicate announcement, the degree of certainty of a belief and a value of the strength of this certainty. The composition of a GB works as follows. The formation rules of individual beliefs lie within the agent minds. The rules that form the group beliefs (synthesis rules) are in an external entity to agents and the communication for the formation of GB is made through announcements sent to a component that aggregates it, forming a GB (see Fig. 3). The set  $A$  of all announces is defined by

$$A \stackrel{\text{def}}{=} \{< p, c, s > | p \in P, c \in [0..1], s \in \mathbb{N}\}, \quad (6)$$

where  $P$  is the set of all the predicates, and  $p$ ,  $c$  and  $s$  are, respectively, the predicate, the certainty degree and the strength degree of an announce. For example, in the announce `personality("selfish", bob)`, with certainty degree 0.8 and strength 6, the advertiser is quite sure that agent *bob* adopts a selfishness exchange strategy, based on 6 experiences it had in past exchanges with *bob*. See the method `announce` in Fig. 4.

Figure 5 shows the architecture of the artifact `ArtCG` of group beliefs, including the classes `AgentAnnounce`, `Belief` and the `announce` method, which corresponds to the announce operation of beliefs (Eq. (6)). When receiving an announce, the artifact adds it to a list of announces, and whenever there exists at least one equal announce from each agent present in the system, this announce becomes a reputation (see Fig. 4).

The `Belief` class function is to represent the group belief composed by the tuple: predicate, certainty degree and strength, and it implements a ToProlog interface, which allows its description in the form of a predicate.

**Fig. 3.** Group belief model**Fig. 4.** Predicate announcement

The **AgentAnnounce** class represents the announcements made by the agents and inherits its the **Belief** class, also adding the *advertiser* attribute that represents the agent that made the announce.

To create a reputation, the certainty and strength values are calculated by the synthesis process and the artifact **Reputation** is notified of the new belief group by the method **update**. If there is already a group belief with the same predicate in the artifact, then it updates such values, otherwise a new group belief is added.

In this paper, we consider a mixed society (composed of agents with five different exchange strategies), and, due to this fact, the adopted aggregation method is the weighted synthesis [23], where announcements are synthesized in order to seek a middle term between them, so not only benefiting a optimistic or pessimistic society. The function weighted synthesis  $sinpon_p$ , which gives the certainty degreec, the strength  $s$ , where  $|C_p|$  is the subset containing all the announcements of a predicate  $p$ , is given by:

$$sinpon_p = \langle p, c, s \rangle, \quad c = \frac{\sum_{a \in C_p} c_a s_a}{\sum_{a \in C_p} s_a}, \quad s = \frac{\sum_{a \in C_p} s_a}{|C_p|} \quad (7)$$

Then, in Fig. 2, to begin the second exchange stage between two agents  $a$  and  $b$ , the agent  $a$  charges the agent  $b$  for the service made in the first stage, and then it sends  $b$  the credit value  $V$  that it thinks itself worthy. Through a comparison between  $a$ 's credit value and the value  $R$  that  $a$  has invested in the

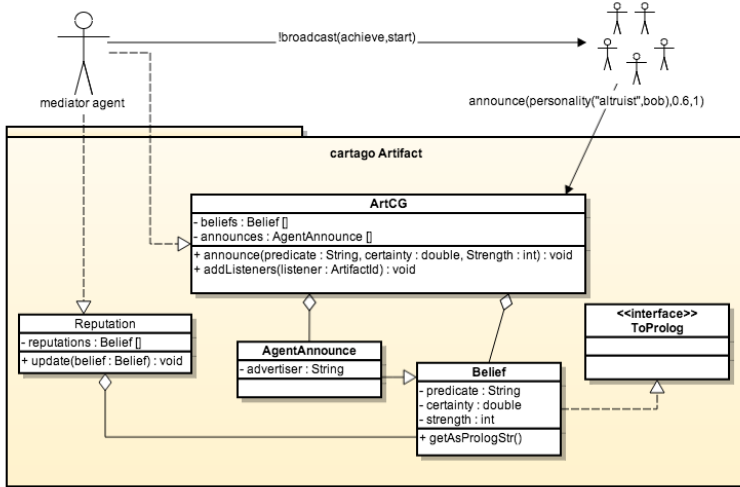


**Fig. 5.** Reputation diagram

first stage,  $b$  is able to draw a conclusion about the exchange strategy adopted by  $a$ :

- $R_a > V_a$ : if the value of investment used by  $a$  in the first stage is higher than the credit value it attributed itself,  $b$  concludes that  $a$  is altruist;
- $R_a < V_a$ : if the value of investment used by  $a$  in the first stage is lower than the credit value it attributed itself,  $b$  concludes that  $a$  is selfish;
- $R_a = V_a$ : If the value of  $a$ 's investment is equal to  $a$ 's credit value,  $b$  concludes that  $a$  is rational.

The agent  $b$  sends its conclusion about the strategy adopted by agent  $a$  to the group belief artifact `ArtCG`, using the `announce` method (Fig. 4), to form a reputation of the agent  $a$ . Once the reputation is formed in the `Reputation` artifact, it is added to the agents' beliefs, thus becoming a common group belief to all participants of the game.

Whenever there is a reputation that an agent  $i$  is selfish, the agents send a message informing the mediator agent, which sends a message to agent  $i$  saying that  $i$  can not participate in the next play. So,  $i$  fails to improve its fitness value, unless it modifies its strategy to enter into the game again, increasing its investment value  $R$  and the maximum investment value  $R_{max}$ , and decreasing its minimum satisfaction value  $S_{min}$ .

## 5 Simulation Analysis

An social exchange strategy is determined by how an agent behaves towards the exchanges proposed by other agents, by the way this agent determines the

**Table 2.** Initial Parameters of Exchange Strategies

Strategy	$r_{max}$	$s_{min}$	$g$	$e$	$k^{\rho t}$	$k^{\rho v}$
Altruism	0.8	0.2	0.9	0.1	$\rho = o$	$\rho = d$
Weak altruism	0.6	0.4	0.7	0.3	$\rho = o$	$\rho = d$
Selfishness	0.2	0.8	0.1	0.9	$\rho = d$	$\rho = o$
Weak selfishness	0.4	0.6	0.3	0.7	$\rho = d$	$\rho = o$
Rationality	0.2	0.2	0	0	0	0

amount of investment it wants to accomplish, and also by the guilt/envy degree when comparing its results with the other agents. As the overall results emerge over time, the agents become self-regulators of their exchange processes. The evaluated characteristics that define each strategy (which are critical in the evolution of the exchanges) are the maximum value that the agent intends to invest, the minimum value of satisfaction accepted when an agent receives a service proposal and the amount of investment it wants to accomplish. We adopted the initial parameters of the social exchange strategies shown in Table 2. The guilt and envy values related to the gain are null for the rational agent, therefore, the values  $g_{rac}$  and  $e_{rac}$  are defined as 0 (zero).

Two different scenarios were defined, one without considering the culture of the society, and the other with the group beliefs as a “culture” common to all agents, as explained in Section 4. In each scenario there are five agents, each with a different strategy, and each simulation was performed using 300 cycles, for a total of 20 simulations by scenario. In both scenarios, the system stabilizes before 300 cycles. For the lack of space, we present the detailed analysis just for the second scenario.

Considering the two exchange stages in Fig. 2, given  $m$  agents, each playing with  $m - 1$  agents, with zero, one, or two successful exchange stages in each two-agent interaction, then a cycle of a simulation is composed by  $m(m - 1) + w_1 + w_2 + \dots + w_m$  plays of stages of type I and/or II (successfully performed or not), where  $w_1$  is the number of agents that agent 1 has credit with after the first stage with all other agents (i.e., the number of successful exchanges for the agent 1) and analogously one defines  $w_2, \dots, w_m$ . In a single cycle, the number of exchanges of type I (successfully performed or not) is  $m(m - 1)$ , and the number of exchanges of type II (successfully performed or not) is  $w_1 + w_2 + \dots + w_m$ . Note that if all the exchanges of the type I have been successfully for all agents, then one cycle of a simulation presents  $2m(m - 1)$  exchanges of type I or II (successfully performed or not).

Figure 6 shows the simulation results in a range of 300 cycles.<sup>8</sup> Whenever the society culture is taken into account, the evolution of the agents’ strategies provided an increase in the number of two-stage successful exchanges, which starts with 8 and ends with 20 by the 50th cycle, with a decreasing in the number of non successful interactions to zero, in a short period of time. In comparison with the first scenario, this time was reduced in 44.45%. The average and standard deviation of the number of exchanges are shown in Table 3. In Fig. 7

---

<sup>8</sup> Each mark in the X-axis of 6 represents 10 cycles.

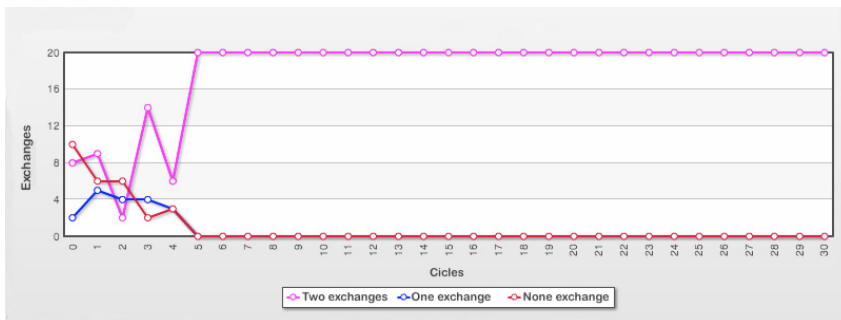


**Fig. 6.** Evolution of the number of exchanges, considering the culture

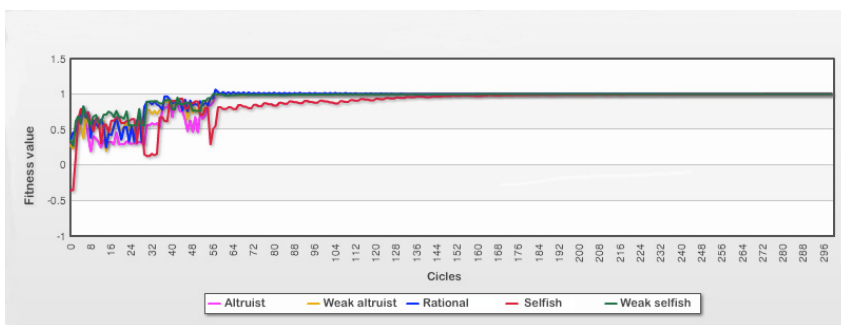


**Fig. 7.** Evolution of the Fitness value, considering the culture

we show the simulation of the evolution of the agents' fitness values in a period of 300 cycles.

Table 3 shows the number of two-stage exchanges, which was increased by 385.71 %. Table 5 shows the average value and standard deviation of the fitness values in the initial and final cycles of the simulations, considering the different exchange strategies. The increase in the fitness value of the altruist agent was 252.49 %, while for the weak altruist agent it was 258.20 %, for the rational agent it was 188.94 %, for the selfish agent it was 385.77 % and, finally, for the weak selfish agent it was 258.58 %. The strategy that showed lower growth was the rationality strategy, while the selfishness strategy had a higher evolution. In Table 4, we present the values of the overall average and the standard deviation of the global fitness value, showing an increasing of 584.26%.

In the case with culture, the increase in the number of two-stage exchanges was higher (385.71 %) than in the scenario without culture (171.73 %). Regarding the fitness values, in the scenario with culture only the Weak selfish strategy has not increased the average of the fitness value (343.95 % without culture and 258.58 % with culture). The others strategies showed largest increase in their fitness values, as shown in Table 6. Observe that, in both scenarios, the

**Table 3.** Number of exchanges

Average			
	Begin	End	
One-stage exchange	3.65	0.1	
Two-stage exchanges	2.8	13.6	
None exchange	8.65	0.1	
Standard deviation			
	Begin	End	
One-stage exchange	2.36809	0.44721	
Two-stage exchanges	3.17224	4.96726	
None exchange	3.32890	0.44721	

**Table 4.** Global fitness value

	Initial	Final
Global standard deviation	0.28005	0.01673
Global average	0.16701	0.97577

**Table 5.** Fitness value

Strategy	Average	
	Initial fitness	Final fitness
Altruist	0.27849	0.98170
Weak altruist	0.27411	0.98188
Rational	0.33743	0.975
Selfish	-0.33172	0.94797
Weak selfish	0.27673	0.99231
Standard deviation		
Strategy	Initial fitness	Final fitness
Altruism	0.02539	0.08101
Weak altruism	0.01128	0.07812
Rationality	0.00747	0.11180
Selfishness	0.02938	0.20056
Weak selfishness	0.12844	0.03437

**Table 6.** Increase of the fitness value

Strategy	Without the culture	With the culture
Altruism	164.32%	252.49%
Weak altruism	144.89%	258.20%
Rationality	71.79%	188.94%
Selfishness	297.05%	385.77%
Weak selfishness	343.95%	258.58%

rationality strategy was the one that showed lower growth in relation to the others, while selfishness strategies showed higher evolution.

## 6 Conclusion

In this paper, the GSREP game was adapted to a BDI-MAS society, using the Jason language, with the addition of group beliefs as the society “culture” common to all agents involved in the system, implemented as a CArtAgO artifact. We consider that the society culture is composed by the agents’ reputations. This BDI version of the game was called the Cultural-GSREP game. Then, we analysed and compared the simulation results considering two scenarios, just taking into account or not the culture.

The equilibrium of Piaget’s Social Exchange Theory is reached when occurs reciprocity in exchanges during the interactions. Our approach showed that with the evolution of the strategies the agents were able to maximize their adaptation values becoming self-regulators of exchanges processes and thereby contributing to increasing the number of successful interactions. All agents have evolved and contributed to the evolution of the society. Whenever the services offered are more fair (balanced), the greater is the number of successful interactions. Comparing the two scenarios, we conclude that the addition of the culture – the reputation as a focal point – in social exchanges had the expected influence on the evolution of the agents’s strategies and exchange processes, increasing the exchanges successfully performed and the fitness value in a shorter time.

Future work will consider the analysis of the final parameters of the strategies that emerged in the evolution process, and other categories of the cultural knowledge in the belief space, using belief artifacts in different scopes beyond the reputation, and creating different ways for the agents to reason about the group beliefs.

**Acknowledgments.** Supported by CNPq (Proc. No. 481283/2013-7, 306970/2013-9 and 232827/2014-1).

## References

1. Blau, P.: Exchange & Power in Social Life. Trans. Publish., New Brunswick (2005)
2. Boissier, O., Bordini, R.H., Hübner, J.F., Ricci, A., Santi, A.: Multi-agent oriented programming with JaCaMo. *Science of Computer Programming* **78**(6), 747–761 (2013)
3. Bordini, R.H., Hübner, J.F., Wooldridge, M.: Programming Multi-agent Systems in AgentSpeak Using Jason. Wiley Series in Agent Technology. John Wiley & Sons, Chichester (2007)
4. Bratman, M.E.: Intention, plans, and practical reason. Cambridge University Press (1999)
5. Castelfranchi, C., Falcone, R.: Principles of trust for MAS: cognitive anatomy, social importance and quantification. In: Intl. Conf. of Multi-agent Systems (ICMAS), pp. 72–79 (1998)
6. Castelfranchi, C., Falcone, R., Firozabadi, B., Tan, Y.: Special issue on trust, deception and fraud in agent societies. *Applied Artificial Intelligence Journal* **1**, 763–768 (2000)
7. Criado, N., Argente, E., Botti, V.: Open issues for normative multi-agent systems. *AI Communications* **24**(3), 233–264 (2011)
8. Dignum, V., Dignum, F. (eds.): Perspectives on Culture and Agent-based Simulations. Springer, Berlin (2014)
9. Dimuro, G.P., Costa, A.R.C., Gonçalves, L.V., Pereira, D.: Recognizing and learning models of social exchange strategies for the regulation of social interactions in open agent societies. *Journal of the Brazilian Computer Society* **17**, 143–161 (2011)
10. Grimaldo, F., Lozano, M.A., Barber, F.: Coordination and sociability for intelligent virtual agents. In: Sichman, J.S., Padget, J., Ossowski, S., Noriega, P. (eds.) COIN 2007. LNCS (LNAI), vol. 4870, pp. 58–70. Springer, Heidelberg (2008)
11. Huynh, T.D., Jennings, N.R., Shadbolt, N.R.: An integrated trust and reputation model for open multi-agent systems. *JAAMAS* **13**(2), 119–154 (2006)
12. Macedo, L.F.K., Dimuro, G.P., Aguiar, M.S., Coelho, H.: An evolutionary spatial game-based approach for the self-regulation of social exchanges in mas. In: Schaub, et al. (eds.) Proc. of ECAI 2014–21st European Conf. on Artificial Intelligence. Frontier in Artificial Intelligence and Applications, no. 263, pp. 573–578. IOS Press, Netherlands (2014)
13. Nguyen, N.T., Katarzyniak, R.P.: Actions and social interactions in multi-agent systems. *Knowledge and Information Systems* **18**(2), 133–136 (2009)
14. Padgham, L., Scerri, D., Jayatilleke, G., Hickmott, S.: Integrating BDI reasoning into agent based modeling and simulation. In: Proc. WSC 2011, pp. 345–356. IEEE (2011)

15. Pereira, D.R., Gonçalves, L.V., Dimuro, G.P., Costa, A.C.R.: Towards the self-regulation of personality-based social exchange processes in multiagent systems. In: Zaverucha, G., da Costa, A.L. (eds.) SBIA 2008. LNCS (LNAI), vol. 5249, pp. 113–123. Springer, Heidelberg (2008)
16. Piaget, J.: Sociological Studies. Routledge, London (1995)
17. Rabin, M.: Incorporating fairness into game theory and economics. *The American Economic Review* **86**(5), 1281–1302 (1993)
18. Reynolds, R., Kobti, Z.: The effect of environmental variability on the resilience of social networks: an example using the mesa verde pueblo culture. In: Proc. 68th Annual Meeting of Society for American Archeology, vol. 97, pp. 224–244 (2003)
19. Reynolds, R., Zanoni, E.: Why cultural evolution can proceed faster than biological evolution. In: Proc. Intl. Symp. on Simulating Societies, pp. 81–93 (1992)
20. Ricci, A., Viroli, M., Omicini, A.: The A&A programming model and technology for developing agent environments in MAS. In: Dastani, M., Seghrouchni, A.E.F., Ricci, A., Winikoff, M. (eds.) ProMAS 2007, vol. 4908, pp. 89–106. Springer-Verlag, Heidelberg (2008)
21. Rodrigues, M.R., Luck, M.: Effective multiagent interactions for open cooperative systems rich in services. In: Proc. AAMAS 2009, Budapest, pp. 1273–1274 (2009)
22. Schelling, T.C.: The strategy of conflict. Harvard University Press, Cambridge (1960)
23. Schmitz, T.L., Hübner, J.F., Webber, C.G.: Group beliefs as a tool for the formation of the reputation: an approach of agents and artifacts. In: Proc. ENIA 2012, Curitiba (2012)
24. Serrano, E., Rovatsos, M., Botía, J.A.: A qualitative reputation system for multiagent systems with protocol-based communication. In: AAMAS 2012, Valencia, pp. 307–314 (2012)
25. Xianyu, B.: Social preference, incomplete information, and the evolution of ultimatum game in the small world networks: An agent-based approach. *JASSS* **13**, 2 (2010)

# Modelling Agents’ Perception: Issues and Challenges in Multi-agents Based Systems

Nuno Trindade Magessi<sup>(✉)</sup> and Luís Antunes

GUESS/BioISI, Faculdade de Ciências, Universidade de Lisboa, Lisbon, Portugal  
[nmagessi@hotmail.com](mailto:nmagessi@hotmail.com), [xarax@ciencias.ulisboa.pt](mailto:xarax@ciencias.ulisboa.pt)

**Abstract.** In virtual agents modelling, perception has been one of main focus for cognitive modelling and multi-agent-based simulation. Research has been guided by the representation of human senses operations. In this sense, perception focus remains on the absorption of changes that occur in the environment. Unfortunately, scientific literature has not covered the representation of most of the perception mechanisms that are supposed to exist in an agent’s brain like for example ambiguity. In terms of multi-agent based systems, perception is reduced to a parameter forgetting the complex mechanisms behind it. The goal of this article is to point out that the challenge of modelling perception ought to be centred on the internal mechanisms of perception that occur in our brains, which increases the heterogeneity among agents.

## 1 Introduction

During the last decade, studies simulating virtual agents (VA) in multi-agent-based simulation (MABS) systems have tried to bring more realism into modelling the perception of environment. Researchers have been focused their efforts on improving perception models, and corresponding techniques.

Nevertheless, recent work [1, 25] has produced sophisticated theoretical models for reproducing the human senses like sight and hearing. The models were integrated then in a sustainable multi-sense perception system, in order to put together a perceptual system capable of approximately replicating the human sensory system. In fact, this is a keystone to use VAs to simulate how the senses of people work in order to capture a dynamic and nondeterministic environment [1]. The major problem of these proposals is to summarise perception into the operations of human senses.

Many of the psychological activities involved in perception, as well as the inherent mechanisms of the brain subsystems associated to it, have been overlooked. Is a VA sure about what it is capturing under this multiple senses frameworks? Is it reality? Clearly, the answer is no to both questions. The VA perception described in literature misses and does not represent the principal target of human perception: recognition.

This article proposes to discuss the challenges involved in perception, including the reproduction of all the mechanisms behind this cognitive process. The multi-senses framework represents only a small component of this huge and complex process that is perception. Perception goes beyond faithful representation of input sensors. As an

example, the article will focus on risk perception to demonstrate the challenge and what is involved in it.

Section 2 reviews the literature on modelling perception for virtual agents in a multi-agent-based system. Section 3 revisits the concepts behind perception. Section 4 discusses the principal main issues in the literature and presents the crucial challenges, that modelling perception will have in near future. Section 5 describes our vision for implementing perception and section 6 puts some conclusions forward.

## 2 Related Literature

Literature presents different standpoints about endowing VAs with perception for MABS. The most frequently used approach is to ensure that VAs have a generalised knowledge about the environment [2]. This approach does not allow us to use correctly perception in order to simulate realistic scenarios, because the VA is not certain about the veracity of what is capturing. The opposite case is the one in which agents take their decisions sustained on the collected data received through their multiple senses, having no knowledge about the environment, not even generic knowledge.

In between these extreme cases, we have agents that can perceive some information, have a conception of the environment around them and “act on their perception” [3]. In the case described by [4], agents have a graphical access to their environment. According the described concept of perception, agents choose which path on the graph is more feasible to achieve their target. There are several problems associated to this perspective. The main one is the assumption that environments are static, which raises difficulties in simulating complex scenarios. In this perspective, perception is incomplete and conceived in a very restricted form. Clearly, it is not adequate to use it for modelling realistic situations. Rymill and Dodgson have developed a method to simulate vision and attention of individuals in a crowd [5]. The simulation was done for open and closed spaces. Independently of the problems identified in the techniques to filter information from a highly dynamic environment, the issue remained that perception was incomplete and conceived in a very restricted form. Vision was modelled only as an input sensor and attention is its precedent on the cognitive process. Pelechano et al [6] made a debate about a simulator system for an evacuation scenario, but this system was inaccurate in representing real vision and consequently perception. Brooks [7] developed what he called creatures: a series of mobile robots operating without supervision in standard office environments. The intelligent system behind them was decomposed into independent and parallel activity producers, all of which interfaced directly to the world through perception and action, rather than interfacing to each other.

Other proposals, like [8], had built-in simulators to describe hearing. However olfactory perception is limited to a few published articles with no consistent simulator. And no study is known for simulating tactile senses. Steel et al [9] proposed and developed a cohesive framework to integrate, under a modular and extensible architecture, many virtual agent perception algorithms, with multiple senses available.

Their architecture allows the assimilation, in the sense of integration, of dynamic and distributed environments. They conceive perception according to an environment module, where information is extracted and transposed to the agent's memory. Clearly, they identify the brain as being outside the scope of perception and more related to memories. Kuiper et al [10] associated the vision process to perception and presented more efficient algorithms to process visual input, which were entirely implemented under the DIVAs (Dynamic Information Visualization of Agents systems) framework. Recently, Magessi et al [11] presented an architecture for risk perception. This architecture puts the main focus on the representativeness of perception as it is performed in reality by individuals. Vision and other senses are designated by input sensors and were considered as one component of this cognitive process.

## 3 Perception

### 3.1 Definition

Perception is one of the cognitive processes in the brain that precede decision making. Perception is the extraction, selection, organisation and interpretation of sensory information in order to recognise and understand the environment [12]. Perception is not restricted to passivity upon reception of input signals. Perception can suffer the influence of psychological, social and cultural dimensions [13]. Psychology influences perception through capabilities and cognitive factors. For example, one individual who suffers from a psychological disorder may have the notion that his/her perception may be being affected. Concerning the social dimension, the influence comes from the interaction among individuals in society, towards imitation or persuasion, for example. Learning, memory, and expectations can shape the way in which we perceive things [13, 14]. Perception involves these "top-down" effects as well as "bottom-up" methods for processing sensory input [14]. The "bottom-up" processing is basically low-level information that is used to build up higher-level information (e.g., shapes for object recognition). The "top-down" processing refers to recognition task in terms of what it was expected in a specific situation. It is a vital factor in determining where entities look like and knowledge that influence perception [23]. Perception depends on the nervous system complex functions, but subjectively it seems mostly effortless, because processing happens outside conscious awareness [10].

However, it is important to realise that if we want to have a more complete attention mechanism related to vision, the work must be conducted by the interaction of bottom-up factors based on image features and top-down guidance based on scene knowledge and goals. The top-down component could be understood as the epicentre of attention allocation when a task is at hand. Meanwhile, the bottom-up component acts as reaction mechanism of alert. It allows the system to discover potential opportunities or risks in order to stop threatening events. While the top-down process establishes coherence between the environment looked by agent and its goals or tasks, the bottom-up component has the intent of reproducing the alert mechanisms, warning about objects or places relevant to the agent.

### 3.2 The Perception Process

The perception process starts with a stimulus on body sensory organs [12]. These sensory organs transform the input energy into neural activity through transduction [12]. Then, neural signals are transmitted to the brain and therein processed [12]. The resulting mental re-creation of the distal stimulus is the percept. Perception is sometimes described as the process of constructing mental representations of distal stimuli using the information available in proximal stimuli.

People typically go through the following steps to form judgements: (i) first, when they face an unknown target, they ignite the interest for this target. This means that they activate their attention; (ii) second, people start to extract and select more information about the target. Incrementally, people find hints that they associated to similar experiences and those hints help them to interpret and categorise the target; (iii) in the third step, the hints become less efficient and selective. Thus, people try to look for more hints with the intent of confirming the categorisation of the target. Unfortunately, people also actively ignore and even distort hints that are against their initial perceptions. Perception becomes gradually selective and people finally achieve a judgment about the target.

Casual perception is one of fields with huge development nowadays [24]. It consists of “the relatively automatic, relatively irresistible perception of certain sequences of events as involving causation”. Normally, casual perception does not use conscious thoughts or reasoning. It is a kind of “launching effect” in which people perceive spontaneously.

### 3.3 Affordances

In [16], Gibson developed an interaction approach on perception and action, settled on information available in the environment. He refused the framing assumption of factoring external-physical and internal-mental processes. The interaction alternative is centred on processes of agent-situation interactions that come from ecological psychology and philosophy, namely situation theory [26, 27]. The concept of affordance for an agent can be defined as the conditions or constraints in the environment to which the agent is attuned. This broad view of affordances includes affordances that are recognised as well as affordances that are perceived directly.

Norman used the term affordances to refer just the possibilities of action that are perceivable by an individual [17]. He made the concept dependent on the physical capabilities of an agent and his/her individual goals, plans, values, beliefs, or past experiences. This means that he characterised the concept of affordance as relational, rather than subjective or intrinsic. In 2002, Anderson et al. [18] sought that directed visual attention, and not affordance, is the key responsible for the fast generation of many motor signals associated with the spatial characteristics of perceived objects. They discovered this by examining how the properties of an object affect an observer’s reaction time for judging its orientation.

### 3.4 Perception vs. Reality

For some individuals, the perceived environment, event or object can differ from what it is in reality. Their perception could put themselves far from what is in reality. An object could be perceived differently by each person. This phenomenon is commonly designated by perception gap [19]. This finding is patent in many psychological studies. For example, in the case of visual perception, there are individuals able to acknowledge the perception gap in their minds. Others may not recognise the shape shifting when the object changes. This happens when objects are ambiguous and multiple interpretations can be made on the perceptual level. So to reproduce human perception in VAs, the perception gap must be taken into account and reflected in the models.

## 4 Issues and Challenges

The agents' perception assumes a critical preponderance in defining their decision, which is then reflected in their behaviours, as social actors. Perception delivers information from the surrounding environment, which assists agents on their activities of planning and decision making [20]. In most approaches, the sensor systems architecture is represented, instead of the complete perception process. Most of the works are confined to relate the upstream part of the process. In some cases, for example the vision sense is not designed as part of the brain [8], which goes against the usual accounts from most of the relevant scientific areas involved. In most cases, the interpretation of information component, which is critical to the success of the process, is not described. The majority of the studies have the assumption that everything which was picked up by senses is reflected on the VA's knowledge [8]. This a strong assumption, which has no correspondence with reality. Interpretation is the goal activity of perception [14]. Grasping an object and having success on its recognition depends on the effectiveness and efficiency of interpretation. We must not forget that the main goal of perception is to produce a judgement about what was socially analysed. This judgement may or may not be stored in memory, depending of its relevance. This aspect is never mentioned in VA's literature. For example, Brooks [7], with his intelligent "Creatures" argues that perception is not necessary as central interface. This is not correct if we want to have robots acting like humans. The proof is on his own work, where he decomposed sensor data in many different sorts of processing, which proceed independently and in parallel, each affecting the "overall system". The "overall system" is in fact an example of spatial perception, ensured by the right extraction and selection of data input. The success of "Creatures" with multiple processes comes from the fact that perception is deeply rooted on his algorithm. However, the robots could not output the result that took them into action. Unfortunately, Brooks traces a direct and linear relation between input sensor and action. He omits representations and implicitly considers an action as decision, which is wrong because decision could result in action or not [16, 21]. This approach is overly simplistic, similarly to a common confusion between judgement (perception) and decision. People can only

perceive something if they have a representation of that thing, or from the parts that compose it, even if inchoate.

Other researchers assume that every perception even culminates in storing. However, memory should not be seen as passive, a simple storage of data collected by sensors. It must be seen under a dualistic perspective. VA memory should also have an influence on perception, because to perceive something we need to have the semantic knowledge in our semantic memory, for that object or event. Otherwise, VAs have to learn first, beside of accelerating recognition.

Clearly, the first challenge is to systematise all the perception process, including the missed activities or dimensions that have the incumbency to format agent's perception. The second challenge is to bring to Multi-Agent Based Systems the capacity to represent the interconnections among psychological, social and cultural dimensions involved in perception [11]. These dimensions and subsequent factors are the keystones for the dynamics of perception.

The third challenge, which is both ambitious and complex, is to establish the macro-micro link between a specific judgement and the neuro-physiological dimension of perception. Modelling perception of VAs cannot be trapped to upstream stage and moving on to the downstream stage of the process

## **5 Vision: Paths to Achieve Our Goals**

Taking into account the issues and challenges described above, it is important to figure out what would be the consequences if we improved perception modelling. The major consequence is to separate perception from decision in VAs, similarly to what happens in reality. This is determinant to understand many issues related to decision science, where in fact the relation between what we assimilate and decision is not linear. If we want to understand why a decision-maker took an incorrect decision we need to have clearly modelled his decision and perception processes. If the problem came from perception, it is relevant to pin down in which part of the process it occurred. This brings more heterogeneity to agents in multi-agent based systems.

Another important consequence is to understand if an agent perceived the reality surrounding him. Or instead, if he perceived something different from reality, when he took the decision.

In terms of improving perception modelling in robots, the strategy goes by the use of very simple cases, like the perception of a common figure which has associated ambiguity. For example, the Rubin Vase, which has two interpretations, either as a vase or as two faces. This can be done under pixel techniques, where the captured images allow robots to perceive some figure formats when a connection is established with their own semantic memory.

One of the common mistakes is to insist in capturing some kind of standard perception, common to all individuals. Of course, people have mechanisms in common for perception. However, perception is highly subjective, since it depends on the past experiences of each individual. These experiences and associated acquisition define his/her representation of an object, figure, event or environment. So, instead of

searching for (or defining) standard mechanisms of perception, we could replicate the perception of one individual. More specifically, to try to clone a specific person perception by using its own description of what this person is perceiving. In the Rubin Vase example, this means that one robot could recognise a vase and another could recognise faces. Everything depends on the forms (vases or faces) that were collected in the past by each robot and stored on their own semantic memory. In a case of multi-agent based system, the ambiguity of perception is present on the way that agents interpret the variations occurred in some parameters.

Another important key point about modelling perception is to build multidisciplinary teams to work on it. In this sense, the operational strategy must continue, refresh and fix the idea of [7] where Brooks developed multiple algorithms working in parallel to pursue perception. This strategy happens because a stimulus could not be transformed into a percept. Our claim is that an ambiguous stimuli may be transformed into multiple perceptions, experienced randomly, one at a time, in what is called "multi stable perception." [22] However, the same stimuli, or absence of them, may induce in different perceptions depending on the person's culture and previous experiences. After we integrate fundamental psychological insights in perception modelling and the advance of neuroscience brings us new inputs continuously, modelers will be able to substitute the developed algorithms by new ones, where these replicate what happens in real physiology. So, this vision clearly defends that is possible to build robots with perception similar to human beings if it focuses on a specific target and/or individual.

## 6 Conclusion

Part of VAs literature on perception is focused on building a multi agent simulator with a lot of features related to input sensors, instead of demanding the complete perception process. This article claims that this is not perception and the major challenge is to go forward in building a complete and holistic account of this cognitive process. Introducing psychological and physiological insights can ensure that virtual agents replicate better what happens in reality. In this sense, the challenge is to establish the macro-micro link for perception, from the physiological dimension to the final judgement.

## References

1. Ray, A.: Autonomous perception and decision-making in cyberspace. In: The 8th International Conference on Computer Science & Education (ICCSE), Colombo, Sri Lanka, April 26–28, 2013
2. Uno, K., Kashiyama, K.: Development of simulation system for the disaster evacuation based on multi-agent model using GIS. Tsinghua Science and Technology **13**(1), 348–353 (2008)

3. Shi, J., Ren, A., Chen, C.: Agent-based evacuation model of large public buildings under fire conditions. *Automation in Construction* **18**(3), 338–347 (2009)
4. Sharma, S.: Simulation and modelling of group behaviour during emergency evacuation. In: Proceedings of the IEEE Symposium on Intelligent Agents, Nashville, Tennessee, pp. 122–127, March 30–April 2, 2009
5. Rymill, S.J., Dodgson, N.A.: Psychologically-based vision and attention for the simulation of human behaviour. In: Proceedings of Computer Graphics and Interactive Techniques, Dunedin, New Zealand, pp. 229–236, November 29–December 2, 2005
6. Pelechano, N., Allbeck, J., Badler, N.: Controlling individual agents in high-density crowd simulation. In: 2007 ACM SIGGRAPH/Eurographics Symposium on Computer Animation, San Diego, California, pp. 99–108, August 2–4, 2007
7. Brooks, R.A.: Intelligence without representation. *Artificial Intelligence* **47**, 139–159 (1991)
8. Piza, H., Ramos, F., Zuniga, F.: Virtual sensors for dynamic virtual environments. In: Proceedings of 1st IEEE International Workshop on Computational Advances in Multi-Sensor Adaptive Processing (2005)
9. Steel, T., Kuiper, D., Wenkstern, R.: Virtual agent perception in multi-agent based simulation systems. In: IEEE/WIC/ACM International Conference on Web Intelligence and Intelligent Agent Technology (2010)
10. Kuiper, D., Wenkstern, R.Z.: Virtual agent perception in large scale multi-agent based simulation systems (Extended Abstract). In: Tumer, K., Yolum, P., Sonenberg, L., Stone, P. (eds.) Proc. of 10th Int. Conf. on Autonomous Agents and Multiagent Systems (AAMAS 2011), Taipei, Taiwan, pp. 1235–1236, May 2–6, 2011
11. Magessi, N., Antunes, L.: An Architecture for Agent's Risk Perception. *Advances in Distributed Computing and Artificial Intelligence Journal* **1**(5), 75–85 (2013)
12. Schacter, D.L., Gilbert, D.T., Wagner, D.M.: Psychology, 2nd edn. Worth, New York (2011)
13. Magessi, N., Antunes, L.: Modelling agents' risk perception. In: Omatu, S., Neves, J., Corchado Rodriguez, J.M., Paz Santana, J.F., Gonzalez, S.R. (eds.) *Distributed Computing and Artificial Intelligence. AISC*, vol. 217, pp. 275–282. Springer, Heidelberg (2013)
14. Bernstein, D.A.: Essentials of Psychology. Cengage Learning. pp. 123–124. ISBN 978-0-495-90693-3 (Retrieved March 25, 2011)
15. Gregory, R.: Perception. In: Gregory, R.L., Zangwill, O.L., pp. 598–601 (1987)
16. Gibson, J.: The theory of affordances. In: Shaw, R., Bransford, J. (eds.) *Perceiving, Acting, and Knowing* (1977). ISBN 0-470-99014-7
17. Norman, D.: Affordance, Conventions and Design. *Interactions* **6**(3), 38–43 (1999)
18. Anderson, S.J., Yamagishi, N., Karavia, V.: Attentional processes link perception and action. *Proceedings of the Royal Society B: Biological Sciences* **269**(1497), 1225 (2002). doi:10.1098/rspb.2002.1998
19. Ropeik, D.: How Risky Is It, Really? Why Our Fears Don't Always Match the Facts. McGraw Hill, March 2010
20. Steel, T., Kuiper, D., Wenkstern, R.Z.: Context-aware virtual agents in open environments. In: Proceedings of the Sixth International Conference on Autonomic and Autonomous Systems (ICAS 2010), Cancun, Mexico, March 7–13, 2010
21. Fine, K., Rescher, Nicholas: The Logic of Decision and Action. *Philosophical Quarterly* **20**(80), 287 (1970)

22. Eagleman, D.: Visual Illusions and Neurobiology. *Nature Reviews Neuroscience* **2**(12), 920–926 (2001). doi:10.1038/35104092. PMID: 11733799
23. Yabus, A.: “Eye movements and vision”, chapter Eye movements during perception of complex objects. Plenum Press, New York (1967)
24. Danks, D.: The Psychology of Causal Perception and Reasoning. In: Beebe, H., Hitchcock, C., Menzies, P. (eds.) *Oxford Handbook of Causation*. Oxford University Press, Oxford (2009)
25. Kurzweil, R.: *How to Create a Mind: The Secret of Human Thought Revealed*. Viking Books, New York (2012). ISBN 978-0-670-02529-9
26. Barwise, J., Perry, J.: *Situations and attitudes*. MIT Press/Bradford, Cambridge (1983)
27. Devlin, K.: Logic and information, pp. 49–51. Cambridge University Press (1991)

# Agent-Based Modelling for a Resource Management Problem in a Role-Playing Game

José Cascalho<sup>(✉)</sup> and Pinto Mabunda

Universidade dos Azores, Pólo de Angra do Heroísmo, Azores, Portugal  
jmc@uac.pt, pintomabunda@yahoo.com

**Abstract.** In this paper we present a prototype of a model created in the context of a resource management problem in Gaza, Mozambique. This model is part of a participatory approach to deal with a conflict of water supply. Farmers and cattle producers are added to a stylized environment and a conflict is modelled when cattle needs to access water and destroy farmers' harvest. To address the different behaviours of farmers and cattle producers, a BDI architecture is used to support the conflict simulation using a simple argument-based negotiation between proactive agents. This model is intended to be used as a support to a Role Playing Game (RPG) in the context of an interactive design assembled under the Netlogo tool environment.

**Keywords:** Agent-based modelling · BDI · Conflict management

## 1 Introduction

In Gaza, a province of Mozambique, a scenario of conflict exists between farmers and cattle producers. Both stakeholders need water and although the resource exists in abundance, the lack of planning to circumscribe an area for the cattle and a specific local for the agriculture, have been responsible for the increase the number of conflicts between these two activities. The cattle are usually abandoned in the fields near the river and, alone, these animals they follow an erratically trajectory to the water destroying cultivated fields near the river. Local authorities have difficult to deal with the problem because cattle producers argue that they have the right to have the cattle in lands that belong to community. Although cattle producers pay fines for the farmers' harvest losses, their behaviour seems not to change. Ancient practices are difficult to modify.

To address this problem, it was decided to follow the steps identified in the *companion modelling* approach [4]. With this approach we expect to promote an open debate inside the community and to help to find a participated solution that will help to overcome the problem. Although some solutions have been discussed between local authorities and population in general, the lack of investment and the difficulty to joint stakeholders to discuss the problem have delayed the implementation of a definite solution.

Role Playing Games (RPG) have been used for different proposes and one of them is the social learning. In fact, with RPG, it is possible to “reveal some

aspects of social relationships, allowing the direct observation of interactions among players” [1]. Players are the stakeholders in a problematic context. The use of RPG in these cases, is useful in certain phases of negotiation for different contexts, such as water, land-use and other resources (e.g. [8][6]).

In this project, the participatory approach is an essential feature for its own success. A RPG will be implemented supported by an agent-based model [5]. As described in the *companion approach*, we intend to add a board game in which the stakeholders can show along the game, how they decide in case of conflict. On the other hand, we are looking for some degree of autonomy in the agents created in the context of an agent-based modelling (ABM) approach. In fact, we want to add proactive agents, implementing an architecture that provides agents’ behaviour related to the personality traits that is possible to identify in the cattle producers and farmers because it gives us the possibility to generate unexpected events which are important in the context of a simulation [5]. The modelling of a real case-study led us to choose a BDI architecture [7] [10] to support the modelling of some of the decisions of the agents in conflict. This paper describes the first steps towards this implementation.

In the following section we will describe some of agent-based models used in simulation concerning resource management. Then, it is explained how conflicts are modelled in the context of the RPG and the implementation of the BDI agents’ architecture. In the last section the conclusions are presented.

## 2 Modelling Resource Management in ABM and Role Playing Games

The use of ABM to investigate environmental management must have as focus, the social interaction and the ecological dynamics. Agents represent stakeholders at an aggregated or individual level. Environment, which holds renewable resources, are defined as the landscape. These resources are typically modified by agents in the environment. One recurrent characteristics of these systems is the representation of space which usually contributes to the structure of interactions among agents. Different approaches can be used to create the model. In our case-study, the RPG was intentionally selected because it fits the desire to have a participatory approach that contributes to “social learning”. RPG is part of the modelling process in which stakeholders participate actively. On the other hand, ABM supports the interaction between stakeholders and leverage the knowledge about the context that is being modelled.

## 3 Modelling the Scenario for Farmers and Producers

In the following subsections we present the agents modelled as well as the main interactions between them, representing different stakeholders in conflict described. In the scenario implemented, two conflictual agents are provided with a simplified dialogue and in which different types of behaviour are identified.

It was assumed that the scenario could leverage our understanding of how the different stakeholders see the conflict. As already pointed out, a BDI architecture is used to support agents modelling in the ABM implementation. It is expected, as the RPG is implemented, the agents' model will be improved, adding beliefs, desires, rules and filters which underly the decisions observed in the real negotiation context.

### 3.1 The BDI Architecture and Conflict Resolution

A BDI architecture is used to support agents interactions along the conflict resolution. We are only interested to model the negotiation between a farmer and a producer about the price to pay for the loss in the farmer production.

D: des(get-payed-for-damaged);	D: des(pay-for-damaged);
B: bel(harvest-damaged, true,1); bel(respons-for damaged, #producer, #degree-certainty); bel(damage-patch-extension, #number-patch, #degree-certainty); bel(is-respons-pay, #money, #degree-certainty); bel(received-money-from-damage, false,1);	B: bel(harvest-damaged, true, #degree-certainty); bel(damage-patch-extension, #number-patch, #degree-certainty); bel(respons-for-damage, #number-patches, #degree-certainty); bel(is-responsible,true, #degree-certainty); bel(already-payed-for-damage,false,1); bel(pay-for-patch,10);
F:	F1: <i>if</i> (#degree-certainty < #threshold) <i>do</i> intention#1 <i>else do</i> intention#2
R: D(des(get-payed-for-damaged)) + B(bel(harvest-damaged, true,1)) → I(intention(get-payed-for-damaged))	R: D(des(pay-for-damaged)) + B(bel(is-responsible, true, #degree-certainty) + bel(already-payed-for-damage, false, 1)) (F1) → I(intention(pay-for-damage))
I: <i>get-payed-for-damaged</i> intention(get-payed-for-damaged): illocutionary act with info-seeking and negotiation steps.	I: <i>pay-for-damage</i> intention(pay-for-damage-1); intention(pay-for- damage-2): illocutionary act with negotiation steps;

**Fig. 1.** BDI architecture supporting the negotiation between farmers and producers.

The figure 1 shows a model for beliefs, desires and intentions of the agents inspired in [7]. The personality traits are related to decisions related to the intention to be executed. This mechanism in the architecture is implemented using a filter (F1) that defines the cases for which an agent selects one option. Notice that this process of decision depend upon the value of uncertainty of the beliefs. The rules are used to define which desires and beliefs activate which intentions. These rules are also part of the agent's trait. We adopt the model proposed by [9] for the dialogue protocol. Two protocols are used. One for information-seeking (info-seeking) and other for negotiation (negotiation). They are defined as simple request-response message sequences between two agents. While the former are used to ask for some information, the latter is used for exchange resources. In the case modelled, farmers ask to producers about their commitment to pay. Then they negotiate the value to pay in different contexts, as a result of successive agreements. The producers may have two different behaviours. They can assume that they agree with the farmer point of view or, otherwise, will have to negotiate. Although this is a very simple protocol, our goal was to test the



**Fig. 2.** The interaction environment in the Netlogo representing the conflict between the farmer and the cattle producer, represented by a link (blue line connecting the two agents).

model to understand if it could provide with an initial model in which farmers with different traits could be modelled and to address different behaviours to each one of these traits.

### 3.2 Experiment in Netlogo

Netlogo[11] has been used as a simulation platform aimed at supporting the realisation of (multi)agent-based simulations. It is a platform that provides a general purpose framework. A typical simulation consists in a cycle where agents, dubbed as turtles, are chosen to be performed an action, considering its situation and state. The stylised scenario and the easy and versatile interaction with the user (e.g. setting up different initial conditions) were the main reasons to select Netlogo.

**The Interface for the Participatory Approach.** The interface has two distinct goals. The first one is to provide a stylized environment in which stakeholders could identify the narrative space of the events described which are the farmers, the red human-shape agents and the producers, the blue human-shape agents. The latter is to foster autonomy to generate a simulation of events that create the conflictual situations which are intended to be studied. In the case-study, the river is identified as a blue area and the village where farmers and producers live, correspond to the yellow area. The green area along the right margin of the river is where the farmers have their cultivated areas. The interface is prepared to interact with users. As the game is played some of the actions are autonomous (e.g. the motion of the cattle to drink water). The red leaf-shape agents are the cultivated areas damaged by the cattle. The link between a farmer and a producer shows a conflict between them. The producer owns the cattle identified with the number 4 which damaged a large area of plantation that belongs to the farmer.

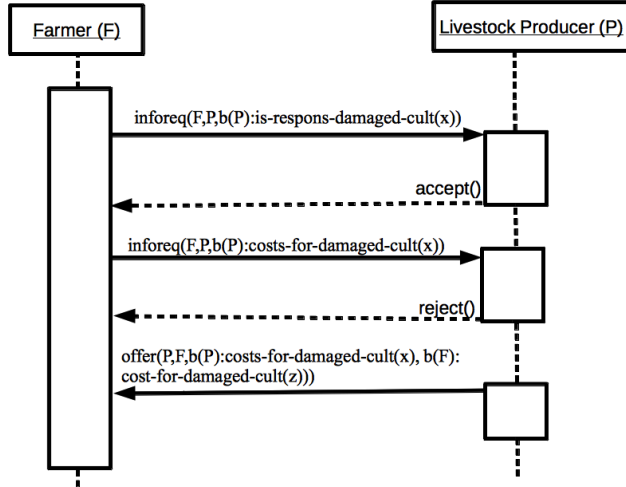


**Fig. 3.** The information-seeking messages sent by the farmer and the response of the producer.

**Interaction through the Conflict Resolution.** The figure 3 presents the sequences of messages exchanged by the farmers and the livestock producers. When a conflict is detected (i.e. a cultivated area of the farmer is damaged), the farmer invites the producer to negotiate. The messages sent by the farmer are information-seeking messages. The example shows that the producer wishes to negotiate the value to be payed by the damaged. Along the negotiation, the producer and farmer will try to agree into a final value. A maximum number of interactions along with thresholds concerning the limit values to achieve in negotiation i.e. beliefs in the context of negotiation (not showed in the figure 3), dictates the end of negotiations. The game in the context of the negotiation have uncertainties that might be identified as a result of the degree of certainty concerning beliefs and also the trait of the agents. Accepting conditions imposed by the farmer or not, will drive the producer to negotiate.

## 4 Conclusions

In this paper we present a prototype for an agent-based modelling in the context of conflict within a resource management in Gaza, Mozambique. To address this problem we chose the RPG approach. The following steps were made:

1. To create a stylized scenario where stakeholders could interact and to identify the situation of conflict;
2. To define a protocol of communication between agents in conflict. The propose of this protocol is to support the interaction of the simulation with the different stakeholders;

3. To provide a bdi-architecture to the agents in conflict. This architecture contributes to the definition of traits and improves the autonomy of the agents defined in the scenario.

This model will be used in the context of a RPG. A board game will be created and the stylized world in the simulated environment will support the game. The stakeholder decisions will be in part as result of game interaction and also based on the knowledge acquired along the steps of implementation of the model. The agents traits allow the RPG to interact with agents with different degree of autonomy. In scenarios where a social learning is a target (e.g. Sylvopast model [5]), a generation of contexts where unexpected events occurs are important to improve the learning and to foster the interaction between the stakeholders.

## References

1. Adamatti, D.F., et al.: A prototype using multi-agent-based simulation and role-playing games in water management. In: CABM-HEMA-SMAGET, 2005, Bourg-Saint-Maurice, Les Arcs. CABM-HEMA-SMAGET 2005, pp. 1–20. CDROM (2005)
2. Bandini, S., Manzoni, S., Vizzari, G.: Agent Based Modeling and Simulation: An Informatics Perspective. *Journal of Artificial Societies and Social Simulation* **12**(4), 4 (2009)
3. Barreteau, O., Bousquet, F., Attonaty, J.M.: Role-playing games for opening the black box of multi-agent systems: method and lessons of its application to Senegal River Valley irrigated systems. *Journal of Artificial Societies and Social Simulation* **4**(3) (2001)
4. Barreteau, O., et al.: Participatory approaches. In: Edmonds, B., Meyer, R. (eds.) *Simulating Social Complexity*, pp. 197–234. Springer, Heidelberg (2013)
5. Bousquet, F., et al.: Multi-agent systems and role games: collective learning processes for ecosystem management. In: Janssen, M.A. (ed.) *Complexity and Ecosystem Management: The Theory and Practice of Multi-agent Systems*, pp. 249–285. E. Elgar, Cheltenham (2002)
6. Briot, J.-P., et al.: A computer-based role-playing game for participatory management of protected areas: the SimParc project. In: *Anais do XXVIII Congresso da SBC*, Belém do Pará (2008)
7. Cascalho, J., Antunes, L., Corrêa, M., Coelho, H.: Characterising agents' behaviours: selecting goal strategies based on attributes. In: Klusch, M., Rovatsos, M., Payne, T.R. (eds.) CIA 2006. LNCS (LNAI), vol. 4149, pp. 402–415. Springer, Heidelberg (2006)
8. Cleland, D., et al.: REEFGAME as a Learning and Data-Gathering Computer-Assisted Role-Play Game. *Simulation Gaming* **43**, 102 (2012)
9. Hussain, A., Toni, F.: Bilateral agent negotiation with information-seeking. In: Proc. of the 5th European Workshop on Multi-Agent Systems (2007)
10. Luong, B.V., et al.: A BDI game master agent for computer role-playing games. In: Proceedings of the 2013 International Conference on Autonomous Agents and Multi-Agent Systems (AAMAS 2013), pp. 1187–1188 (2013)
11. Wilensky, U., Stroup, W.: Learning through participatory simulations: network-based design for systems learning in classrooms. In: Proceedings of Computer Supported Collaborative Learning (CSCL 1999). Stanford, CA, December 12–15, 1999

# An Agent-Based MicMac Model for Forecasting of the Portuguese Population

Renato Fernandes<sup>1(✉)</sup>, Pedro Campos<sup>2</sup>, and A. Rita Gaio<sup>3</sup>

<sup>1</sup> LIADD/INESC TEC, Faculdade de Ciências da Universidade do Porto,  
Porto, Portugal

[renato.fernandes@fc.up.pt](mailto:renato.fernandes@fc.up.pt)

<sup>2</sup> LIADD/INESC TEC, Faculdade de Economia da Universidade do Porto,  
Porto, Portugal

<sup>3</sup> Departamento de Matemática, Faculdade de Ciências da Universidade do Porto  
and Centro de Matemática da Universidade do Porto, Porto, Portugal

**Abstract.** Simulation is often used to forecast human populations. In this paper we use a novel approach by combining Micro-Macro (MicMac) models into an Agent-Based perspective to simulate and forecast the behavior of the Portuguese population. The models include migrations and three scenarios corresponding to three different expected economic growth rates. We conclude that the increase in the number of emigrants leads to a reduction of the Portuguese women that are in the fertile age. This justifies the decrease of births and therefore the general decrease of the total Portuguese Population.

**Keywords:** Agent-Based computational demography · Social simulation · MicMac model · Forecasting

## 1 Introduction

Agent-Based computational demography models (Billari et al. [4] Ferber [5]) can deal with complex interactions between individuals, constituting an alternative to mainstream modelling techniques. Conventional population projection methods forecast the number of people at a given age at a given point in time assuming that the members of a cohort are identical with respect to demographic behaviour. Different approaches include: macro simulation, based on policy interventions and other external events and conditions, and micro simulation, based on life courses of individual cohort members. Micro and Macro (MicMac) (Gaag et al. [6]) approaches offer a bridge between aggregate projections of cohorts. These are important contributes for the sustainability of the health care and pension systems, for example, as they are issues of current concern.

We construct an Agent-Based model, based on the MicMac approach, to simulate the behaviour of the Portuguese population, open to migrations. The notation and the main model components (fertility, mortality and migration) are firstly introduced. Then the iterative simulation process is created and a forecast for the Portuguese Population from 2011 to 2041 is presented.

## 2 Population Model

### 2.1 Fertility and Mortality

We start by establishing the notation and the main components of the model. The variables with  $A$  (resp.  $G$ ) refer to agent variables (resp. global variables). The indices  $a$ ,  $s$ ,  $k$  and  $y$  are used to denote age, sex, agent identification and year, respectively. Any variable indexed by  $a$ ,  $s$ ,  $k$ ,  $y$  represents the realization of the variable in the agent  $k$ , aged  $a$  years-old and of sex  $s$ , in the year  $y$ . A similar interpretation applies to any subset of these indices. The following variables are then defined:

- $A_{a,s,k,y}^{\text{Alive}}$  : vital status, taking the value 1 if the agent is alive and 0 otherwise
  - $G_{a,s,y}^{\text{Alive}}$  : number of living agents; clearly  $G_{a,s,y}^{\text{Alive}} = \sum_k A_{a,s,k,y}^{\text{Alive}}$ .
  - $G_y^{\text{MaleFreq}}$  : relative frequency of male agents, equal to  $\sum_a G_{a,M,y}^{\text{Alive}} / \sum_{a,s} G_{a,s,y}^{\text{Alive}}$
  - $G_{a,s,y}^{\text{Births}}$  : number of births of sex  $s$  given by female agents aged  $a$  years-old
  - $G_{a,y+1}^{\text{FertR}}$  : global fertility rate
  - $G_{a,s,y}^{\text{Deaths}}$  : number of deaths; it satisfies
- $$G_{a,s,y}^{\text{Deaths}} = \#\{A_{a,s,k,y}^{\text{Alive}} = 0 \wedge A_{a-1,s,k,y-1}^{\text{Alive}} = 1\}, \quad a \neq 0$$
- $$G_{0,s,y}^{\text{Deaths}} = \sum_a G_{a,s,y}^{\text{Births}} - G_{0,s,y}^{\text{Alive}}$$
- $G_{a,s,y+1}^{\text{MortR}}$  : global mortality rate.

Real data from the 2011 Portuguese Census is used as the base population, in a 2% size scale. The updating of the mortality and fertility rates is ensured by MicMac models, as in Gaag et al. [6]. The Mac part is ruled by the predictions obtained from Statistics Portugal [7], controlling the overall evolution of the variables. The Mic part is based on the results obtained from the previous year.

The controlling factor for the fertility (resp. mortality) rate is the expected mean fertility (resp. mortality) growth rate for the year  $y$ , denoted by  $G_y^{\text{FertEvo}}$  (resp.  $G_y^{\text{MortEvo}}$ ). Then

$$G_{a,y+1}^{\text{FertR}} = \frac{\sum_s G_{a,s,y}^{\text{Births}}}{G_{a,F,y}^{\text{Deaths}} + G_{a,F,y}^{\text{Alive}}} G_y^{\text{FertEvo}}, \quad G_{a,s,y+1}^{\text{MortR}} = \frac{G_{a,s,y}^{\text{Deaths}}}{G_{a,s,y}^{\text{Deaths}} + G_{a,s,y}^{\text{Alive}}} G_y^{\text{MortEvo}}.$$

Whenever the population size is very small, the mortality formula is replaced by  $G_{a,s,y+1}^{\text{MortR}} = G_{a,s,y}^{\text{MortR}} \times G_y^{\text{MortEvo}}$ .

The following random variables are created in order to achieve heterogeneity among the population of agents (division by 3 in the fractions ensures that its values lie between 0 and 1):

$$X_{a,y+1}^{\text{FertR}} \sim N(G_{a,y+1}^{\text{FertR}}, \sigma x_{a,y+1}^{\text{FertR}}), \quad \sigma x_{a,y+1}^{\text{FertR}} = \min\{0.02, \frac{G_{a,y+1}^{\text{FertR}}}{3}, \frac{1-G_{a,y+1}^{\text{FertR}}}{3}\}$$

$$X_{a,s,y+1}^{\text{MortR}} \sim N(G_{a,s,y+1}^{\text{MortR}}, \sigma x_{a,s,y+1}^{\text{MortR}}), \quad \sigma x_{a,s,y+1}^{\text{MortR}} = \min\{0.02, \frac{G_{a,s,y+1}^{\text{MortR}}}{3}, \frac{1-G_{a,s,y+1}^{\text{MortR}}}{3}\}.$$

The parameters described next are assigned to each agent:

$A_{a+1,k,y+1}^{\text{FertR}}$  : probability for a female agent to give birth in the year  $y+1$ ; it is given by  $x_{a+1,y+1}^{\text{FertR}} \in X_{a+1,y+1}^{\text{FertR}}$

$A_{a+1,s,k,y+1}^{\text{MortR}}$  : probability for an agent to die in the year  $y+1$ ; it is given by  $x_{a+1,s,y+1}^{\text{MortR}} \in X_{a+1,s,y+1}^{\text{MortR}}$ .

The evolution process is done according to the following steps:

- Step 1.** Increase simulation year by one and age every living agent by one.
- Step 2.** Give birth to new agents according to the fertility rates: randomly sample  $u_1, u_2$  from  $U(0, 1)$ ; if  $u_1 < A_{a,k,y}^{\text{FertR}}$  then a new agent is born; if  $u_2 < G_y^{\text{MaleFreq}}$  then set the agent to male sex, else set it to female.
- Step 3.** Randomly "kill" agents: randomly sample  $u_3$  from  $U(0, 1)$ ; if  $u_3 < A_{a,s,k,y}^{\text{MortR}}$ , set  $A_{a,s,k,y}^{\text{Alive}} = 0$ .
- Step 4.** Compute next year fertility and mortality parameters and male proportion rates and define each agent's fertility and mortality.

## 2.2 Migration

The Portuguese population is also affected by migrations, with a high amount of entries and exits, summing a total negative net migration. Our model also includes such process. Throughout,  $c$  is an index denoting a given country while  $c_0$  denotes Portugal.

$G_c^{\text{Health}}$  : health indicator with  $A_k^{\text{HealthW}}$  as its corresponding weight

$G_c^{\text{Safety}}$  : safety indicator with  $A_k^{\text{SafetyW}}$  as its corresponding weight

$G_{c,y}^{\text{Wage}}$  : wage indicator with  $A_k^{\text{WageW}}$  as its corresponding weight

$G_c^{\text{Pop}}$  : indicator for the Portuguese population size, with  $A_k^{\text{PopW}}$  as its corresponding weight

$G_c^{\text{Lang}}$  : indicator for the Portuguese language, with  $A_k^{\text{LangW}}$  as its corresponding weight

$G_c^{\text{Limit}}$  : emigration limits for country  $c$ , defined by the destination country

$G_c^{\text{ECCounter}}$  : emigration counter

The first four indicators range between 0 and 1. The used indicator must be the same for all countries and it is preferable that the data source is the same, because the same indicator may vary in different sources.  $G_c^{\text{Lang}}$  equals 1 if Portuguese is the native language and 0 otherwise. The wage indicator changes every year according to the country expected mean wage growth. Data were obtained from the UN and OECD databases [9], [8].

The above weights are assigned to each agent by a randomly sampled value from  $N(\mu, 0.75\mu)$ ;  $\mu$  for the first three and last weights are obtained from Balaz [3]. The value of  $A_k^{\text{PopW}}$  was based on findings from Anjos and Campos [2].

The gains of migrating also depend on the will to migrate, which is highly dependent on the age of the agent and its employment status. We define

- $G_{a,s}^{\text{EmpProp}}$  : proportion of employed individuals, obtained from the 2011 Portuguese rates of INE database [7]  
 $G^{\text{EcoGrow}}$  : expected economic growth for Portugal  
 $A_{a,s,k,y}^{\text{Emp}}$  : agent's employment status, coded -1 if employed and 1 otherwise.

Every year, and for each agent,  $A_{a,s,k,y}^{\text{Emp}}$  is obtained by randomly sampling  $u$  from  $U(0, 1)$ : if  $u < \left(G_{a,s}^{\text{EmpProp}} G^{\text{EcoGrow}}(y-y_0)\right)$ , the agent is employed; else it is unemployed. The variable  $A_k^{\text{EmpW}}$  is created as the weight for  $A_{a,s,k,y}^{\text{Emp}}$  and is sampled from  $N(\mu, 0.75\mu)$ , where  $\mu$  is chosen to fit the emigration data.

The Weibull distribution function  $W(x, \lambda, k)$  (and its derivative  $w(x, \lambda, k)$ ) is used to model the age effect on the will to emigrate. Its shape ( $\lambda$ )  $A_k^{\text{Shape}}$  and scale ( $k$ )  $A_k^{\text{Scale}}$  are estimated by statistical fitting. These values are also jittered for each agent, and three variables are created:  $A_k^{\text{X-axis}}$  (resp.  $A_k^{\text{Y-axis}}$ ) to perform dilatation of the function on the x-axis (resp. y-axis), and a third variable  $A_k^{\text{Base}}$  to define a base level for the will to emigrate.

For an agent  $k$ , its will to emigrate in the first year  $y_0$  of the simulation or when it becomes 18 years-old, is

$$A_{a,k,y_0}^{\text{Will}} = A_k^{\text{y-axis}} \times W(A_k^{\text{x-axis}} \times a; A_k^{\text{Shape}}, A_k^{\text{Scale}}) + A_k^{\text{Base}}$$

and is updated by

$$A_{a+1,k,y+1}^{\text{Will}} = A_k^{\text{y-axis}} \times w(A_k^{\text{x-axis}} \times a; A_k^{\text{Shape}}, A_k^{\text{Scale}}) + A_k^{\text{SuccessW}} \times A_{k,y}^{\text{Success}}.$$

The gain from emigration is then given by

$$A_{c,a,k,y}^{\text{Gain}} = \left( A_k^{\text{HealthW}} \times G_c^{\text{Health}} + A_k^{\text{SafetyW}} \times G_c^{\text{Safety}} + A_k^{\text{WageW}} \times G_{c,y}^{\text{Wage}} + A_k^{\text{PopW}} \times G_c^{\text{Pop}} + A_k^{\text{LangW}} \times G_c^{\text{Lang}} \right) \times A_{a,k,y}^{\text{Will}} , \text{ if } c \neq c_0$$

while the gain to remain in Portugal corresponds to

$$A_{c_0,a,k,y}^{\text{Gain}} = \left( A_k^{\text{HealthW}} \times G_{c_0}^{\text{Health}} + A_k^{\text{SafetyW}} \times G_{c_0}^{\text{Safety}} + A_k^{\text{WageW}} \times G_{c_0,y}^{\text{Wage}} + A_k^{\text{PopW}} \times G_{c_0}^{\text{Pop}} + A_k^{\text{LangW}} \times G_{c_0}^{\text{Lang}} \right) \times (1 - A_{a,k,y}^{\text{Will}}).$$

The emigration process is now done by the following steps:

**Step 1.** Initialize the emigration counter  $G_c^{\text{ECounter}}$  at 0

**Step 2.** Update each agent's  $A_{a,k,y}^{\text{Will}}$  and  $A_{c,a,k,y}^{\text{Gain}}$

**Step 3.** For each agent, determine its desired emigration destination

$$A_k^{\text{Dest}} = \arg \max_c \{A_{c,a,k,y}^{\text{Gain}}\}$$

restricted to  $G_{A_k^{\text{Dest}}}^{\text{ECounter}} < G_{A_k^{\text{Dest}}}^{\text{Limits}}$  and add 1 to the counter  $G_{A_k^{\text{Dest}}}^{\text{ECounter}}$

**Step 4.** Remove all agents with  $A_k^{\text{Dest}}$  different from Portugal.

As this mechanism needs some iterations to converge, the emigration amount in the first 6 years will be equal to that of 2011.

The immigration is exogenously defined by linear regressions on the countries with non-negative immigration rate in 2011 using OECD data since 2002 [8] and the age distribution of immigrants is fitted with UN data [9].

Finally, by defining

- $G_{c,y}^{\text{Immi}}$  : estimated amount of immigrants;
- $X^{\text{ImmiAge}}$  : Weibull distribution for the immigrants' age;
- $G_c^{\text{ImmiProp}}$  : male proportion of immigrants;
- $G_c^{\text{FertF}}$  : immigrants multiplying fertility factor, as in Adsera and Ferrer [1];
- $A_k^{\text{ImmiC}}$  : origin country of the immigrant agent k;

the immigration process is done according to:

- Step 1.** Create the immigrant agents as determined by  $G_{c,y}^{\text{Immi}}$  and define the origin country  $A_k^{\text{ImmiC}}$  accordingly;
- Step 2.** For each newly immigrant agent, set its age to a randomly sampled value  $x$  from  $X^{\text{ImmiAge}}$ ;
- Step 3.** For each newly immigrant agent k, randomly sample  $u$  from  $U(0, 1)$ ; if  $u < G_{A_k^{\text{ImmiC}}}^{\text{ImmiProp}}$  then set agent k as a male;
- Step 4.** For each immigrant agent k, define its birth and death parameters for the following year;
- Step 5.** For each immigrant agent k of age a and sex s, set  $A_{a,s,k,y}^{\text{BirthR}} = A_{a,s,k,y}^{\text{BirthR}} \times G_{A_k^{\text{ImmiC}}}^{\text{FertF}}$ .

### 3 Results

The results from the previously presented model for three different expected economic growth rates for Portugal,  $G^{\text{EcoGrow}} \in \{0.9, 1.0, 1.1\}$ , are now presented.

For each scenario, 300 simulations were considered for the period 2011-2041. The outputs of the model are: total population size, number of births, number of deaths and the total number of emigrants, by age and for each of the considered years. Totals across all ages (and subsequently their means) are obtained.

Whatever the economic scenario, the population size is expected to be a decreasing function with time. Moreover, the decrease is deepest when the economic growth rate attains the lowest value. This derives from the fact that economic growth plays a major role on the emigration decision and a decrease on this parameter would increase emigration. Such expectation is confirmed by fig 1.

In addition, although the economic does not directly affect the fertility rate, a decrease on this parameter leads to a faster decrease on the number of births over the years. This is most likely due to the fact that the primary age interval of the Portuguese emigrant population is within the women fertile ages. So the increase in the number of emigrants leads to a reduction of the Portuguese women that

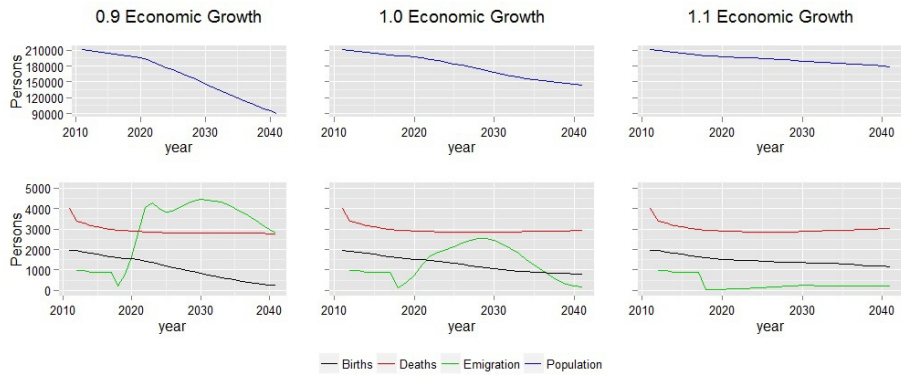


**Fig. 1.** Mean Population projection for different Economic Growth values

are in the fertile age. This justifies the decrease of births and further decreases the total Portuguese Population.

**Acknowledgments.** The first and second authors were partially financed by the FCT Fundação para a Ciéncia e a Tecnologia (Portuguese Foundation for Science and Technology) within project UID/EEA/50014/2013. The last author was partially supported by CMUP (UID/MAT/00144/2013), which is funded by FCT (Portugal) with national (MEC) and European structural funds through the programs FEDER, under the partnership agreement PT2020.

## References

1. Adsera, A., Ferrer, A.: Factors influencing the fertility choices of child immigrants in Canada. *Population Studies: A Journal of Demography* **68**(1), 65–79 (2014)
2. Anjos, C., Campos, P.: The role of social networks in the projection of international migration flows: an Agent-Based approach. Joint Eurostat-UNECE Work Session on Demographic Projections. Lisbon, April 28–30, 2010
3. Baláž, V., Williams, A., Fifeková, E.: Migration Decision Making as Complex Choice: Eliciting Decision Weights Under Conditions of Imperfect and Complex Information Through Experimental Methods. *Popul. Space Place* (2014)
4. Billari, F., Ongaro, F., Prskawetz, A.: Introduction: Agent-Based Computational Demography. Springer, New York (2003)
5. Ferber, J.: Multi-Agent Systems - An Introduction to Distributed Artificial Intelligence. Addison-Wesley Longman, Harlow (1999)
6. Gaag, N., Beer, J., Willekens, F.: MicMac Combining micro and macro approaches in demographic forecasting. Joint Eurostat-ECE Work Session on Demographic Projections. Vienna, September 21–23, 2005
7. INE: Statistics Portugal (2012). [www.ine.pt/en/](http://www.ine.pt/en/)
8. OECD: Organization for Economic Co-operation and Development (2015). [www.stats.oecd.org/](http://www.stats.oecd.org/)
9. UN: United Nations (2015). [www.data.un.org/](http://www.data.un.org/)

# **Text Mining and Applications**

# Multilingual Open Information Extraction

Pablo Gamallo<sup>1</sup>✉ and Marcos Garcia<sup>2</sup>

<sup>1</sup> Centro Singular de Investigación en Tecnologías de la Información (CITIUS), Universidade de Santiago de Compostela, Santiago de Compostela, Spain  
pablo.gamallo@usc.es

<sup>2</sup> Cilenis Language Technology, Santiago de Compostela, Spain  
marcos.garcia@cilenis.com

**Abstract.** Open Information Extraction (OIE) is a recent unsupervised strategy to extract great amounts of basic propositions (verb-based triples) from massive text corpora which scales to Web-size document collections. We propose a multilingual rule-based OIE method that takes as input dependency parses in the CoNLL-X format, identifies argument structures within the dependency parses, and extracts a set of basic propositions from each argument structure. Our method requires no training data and, according to experimental studies, obtains higher recall and higher precision than existing approaches relying on training data. Experiments were performed in three languages: English, Portuguese, and Spanish.

## 1 Introduction

Recent advanced techniques in Information Extraction aim to capture shallow semantic representations of large amounts of natural language text. Shallow semantic representations can be applied to more complex semantic tasks involved in text understanding, such as textual entailment, filling knowledge gaps in text, or integration of text information into background knowledge bases. One of the most recent approaches aimed at capturing shallow semantic representations is known as Open Information Extraction (OIE), whose main goal is to extract a large set of verb-based *triples* (or *propositions*) from unrestricted text. An Open Information Extraction (OIE) system reads in sentences and rapidly extracts one or more textual assertions, consisting in a verb relation and two arguments, which try to capture the main relationships in each sentence [1]. Wu and Weld [2] define an OIE system as a function from a document  $d$ , to a set of triples,  $(arg1, rel, arg2)$ , where  $arg1$  and  $arg2$  are verb arguments and  $rel$  is a textual fragment (containing a verb) denoting a semantic relation between the two verb arguments. Unlike other relation extraction methods focused on a predefined set of target relations, the Open Information Extraction paradigm is not limited to a small set of target relations known in advance, but extracts all types of (verbal) binary relations found in the text. The main general properties of OIE systems are the following: (i) they are domain independent, (ii) they rely on unsupervised extraction methods, and (iii) they are scalable to large amounts of text [3].

The objective of this article is to describe a heuristic-based OIE system, called ArgOE, which uses syntactic analysis to detect the argument structure of each verb, as well as a set of rules to generate the corresponding triples (or basic propositions) from each argument structure. In our work, an argument structure has a very broad sense, since it includes all those syntactic dependencies headed by a verb except specifiers, auxiliars, and adverbs. So, it includes all main clause constituents: subjects, objects, attributes, and prepositional phrases referring to locations, instrumentals, manners, causes, etc. So, there is no distinction between traditional arguments and adjuncts, both are used to build the argument structure.

Consider for example the sentence:

*In May 2010, the principal opposition parties boycotted the polls after accusations of vote-rigging.*

First, our OIE system detects the argument structure of the verb *boycotted* in this sentence: there is a *subject*, a *direct object*, and two prepositional phrases functioning as verb *adjunts*. Then, a set of basic rules transform the argument structure into a set of triples:

(“*the principal opposition parties*”, “*boycotted*”, “*the polls*”),  
 (‘*the principal opposition parties*”, “*boycotted the polls in*”, “*May*”),  
 (‘*the principal opposition parties*”, “*boycotted the polls after*”, “*accusations of vote-rigging*”)

ArgOE requires no training data, generates triples without any post-processing, and takes as input dependency parses in CoNLL-X format [4,5]. Given that such a dependency-based representation is provided by many robust parsers including multilingual systems, e.g., MaltParser [6] or DepPattern [7], ArgOE can be seen as a multilingual open information extractor. We will describe experiments of triples extraction performed on English, Portuguese, and Spanish text. ArgOE’s source code configured for English, Spanish, Portuguese, French, and Galician, as well as other resources are released under GPL license.

This article is organized as follows. Section 2 introduces previous work on OIE: in particular it describes different types of OIE systems. Next, in Section 3, the proposed method, ArgOE, is described in detail. Then, some experiments are performed in Section 4, where ArgOE system is compared against several systems and evaluated in several languages, including Portuguese. Finally, conclusions and future work are addressed in 5.

## 2 Related Work

The goal of an OIE system is to extract triples (*arg1*, *rel*, *arg2*) describing basic propositions from large amounts of text. A great variety of OIE systems has been developed in recent years. They can be organized in two broad categories: those systems requiring automatically generated training data to learn a classifier and those based on hand-crafted rules or heuristics. In addition, each system category

can also be divided in two subtypes: those systems making use of shallow syntactic analysis (PoS tagging and/or chunking), and those based on dependency parsing. In sum, we identify four categories of OIE systems:

- (1) **Training data and shallow syntax:** The first OIE system, TextRunner [8], belongs to this category. A more recent version of TextRunner, also using training data (even if hand-labeled annotated) and shallow syntactic analysis is R2A2 [9]. Another system of this category is WOE<sup>pos</sup> [2] whose classifier was trained with corpus obtained automatically from Wikipedia.
- (2) **Training data and dependency parsing:** These systems make use of training data represented by means of dependency trees: WOE<sup>dep</sup> [2] and OLLIE [10].
- (3) **Rule-based and shallow syntax:** They rely on lexico-syntactic patterns hand-crafted from PoS tagged text: ReVerb [11], ExtrHech [12], and LSOE [13].
- (4) **Rule-based and dependency parsing:** They make use of hand-crafted heuristics operating on dependency parses: ClauseIE [3], CSD-IE [14], KrakeN [15], and DepOE [16].

Our system belongs to the fourth category and, thus, is similar to ClauseIE and CSD-IE, which are the best OIE extractors to date according to the results reported in both [3] and [14]. However, these two systems are dependent on the output format of a particular syntactic parser, namely the Standford dependency parser [17]. In the same way, DepOE reported in [16], relies on a specific dependency parser, DepPattern [7], since it only operates on the by-default output given by this parser. ArgOE, by contrast, uses as input the standard CoNLL-X format and, then, does not depend on a specific dependency parser.

Another significant difference between ArgOE and the other rule-based systems is that ArgOE does not distinguish between arguments and adjuncts. As this distinction is not always clear and well identified by the syntactic parsers, we simplify the number of different verb constituents within the argument structure: all prepositional phrases headed by a verb are taken as verb complements, regardless of their degree of dependency (internal arguments or external adjuncts) with the verb. So, the set of rules used to generate triples from this simplified argument structure is smaller than in other rule-based approaches.

In addition, we make extraction multilingual. More precisely, our system has the following properties:

- Extraction of triples represented at different levels of granularity: surface forms and dependency level.
- Multilingual extraction based on multilingual parsing.

### 3 The Method

Our OIE method consists of two steps: detection of argument structures and generation of triples.

### 3.1 Step 1: Argument Structure Detection

For each parsed sentence in the ConLL-X format, all verbs are identified and, for each verb (V), the system selects all dependents whose syntactic function can be part of its argument structure. Each argument structure is the abstract representation of a clause. The functions considered in such representations are *subject* (S), *direct object* (O), *attribute* (A), and all complements headed by a preposition (C). Five types of argument structures were defined and used in the first experiments: SVO, SVC+, SVOC+, SVA, SVAC+, where “C+” means one or more complements. All these argument structures are correct syntactic options in our working languages: English, Portuguese, and Spanish. Table 1 shows English examples for each type of argument structure.

**Table 1.** Examples of argument structures extracted from our testing dataset.

Type	Example	Constituents
SVO	<i>A Spanish official offered what he believed to be a perfectly reasonable explanation for why the portable facilities weren't in service</i>	S=“A Spanish official”, V=“offered”, O=“what he believed to be a perfectly reasonable explanation for why the portable facilities weren't in service”
SVC <sub>1</sub> C <sub>2</sub>	<i>Output was reduced in 1996 after one of its three furnaces exploded</i>	S=“Output”, V=“was reduced”, C <sub>1</sub> =“in 1996”, C <sub>2</sub> =“after one of its three furnaces exploded”
SVOC	<i>These immigrants deserve consideration under the laws that were in place</i>	S=“These immigrants”, V=“deserve”, O=“consideration”, C=“under the laws”
SVA	<i>Koplowitz's next concert will be a more modest affair</i>	S=“Koplowitz's next concert”, V=“will be”, A=“a more modest affair”
SVAC	<i>Gallery hours are 11 a.m. to 6 p.m. daily</i>	S=“Gallery hours”, V=“are daily”, A=“11 a.m.”, C=“to 6 p.m.”

Within a sentence, it is possible to find several argument structures corresponding to different clauses. For instance, the SVO example in Table 1 represents the argument structure associated with the clause introduced by the verb *offered*, but there are three more clauses introduced by other verbs (in bold): *he believed to be a perfectly reasonable explanation for why the portable facilities weren't in service*, *what be a perfectly reasonable explanation for why the portable facilities weren't in service*, and *the portable facilities weren't in service*, giving rise to the different argument structures shown in Table 2.

**Table 2.** Argument structures extracted from the sentence *A Spanish official offered what he believed to be a perfectly reasonable explanation for why the portable facilities weren't in service*.

Type	Constituents
SV0	S=“A Spanish official”, V=“offered”, O=“what he believed to be a perfectly reasonable explanation for why the portable facilities weren't in service”
SV0	S=“he”, V=“believed to”, O=“be a perfectly reasonable explanation for why the portable facilities weren't in service”
SVA	S=“what”, V=“be”, A=“a perfectly reasonable explanation for why the portable facilities weren't in service”
SVA	S=“the portable facilities”, V=“weren't”, A=“in service”

The constituents of an argument structure are the full phrases or clauses playing different syntactic functions within the structure. Each constituent is built by finding all dependency paths from its head to all its (direct and indirect) dependents. For instance, consider the SVA example in Table 1. To build the full constituents, the first step is to identify the head word of each constituent: S=“concert”, V=“be”, A=“affair”. Then, each head is extended with all its dependency words by exploring the full dependency path and by taking into account the position in the sequence. This results in full phrases representing all constituents of the clause: S=“Koplowitz’s next concert”, V=“will be”, A=“a more modest affair”.

There is, however, an important exception in the process of building full constituents: namely, relative clauses. The constituents we generate do not include those clauses introduced by a verb modifying a noun. For instance, the SVOC example in Table 1 contains the constituent C=“under the laws”, extracted from the expression *under the laws that were in place*. In this case, the relative clause was not taken into account to generate the constituent C within the argument structure of the main verb *deserve*. However, relative clauses and their antecedents also introduce argument structures. In the same example, we identify a SVA argument structure from the chain “the laws that were in place”, where S=“the laws”, V=“were”, and A=“in place”. The main reason for removing relatives from constituents is to guarantee the generation of coherent and non over-specified propositions, as we will report in the next section.

Moreover, coordinatated conjunctions in verbal phrases are splitted into different argument structures, one for each coordinated verb. However, by taking into account the experiments performed in [3], coordinated phrases in the verb arguments are not processed.

Finally, notice that the argument structure SVO<sub>1</sub>O<sub>2</sub> (e.g. *John gave Mary a present*) is not considered here, since it is not a correct syntactic structure in Spanish (nor in the rest of latin languages). In order the system to be multilingual, we have defined only those argument structures that are shared by our working languages.

### 3.2 Step 2: Generation of Triples

One of the most discussed problems of OIE systems is that about 90% of the extracted triples are not concrete facts [1] expressing valid information about one or two named entities, e.g. “Obama was born in Honolulu”. However, the vast amount of high confident relational triples (propositions) extracted by OIE systems are a very useful starting point for further NLP tasks and applications, such as common sense knowledge acquisition [18], and extraction of domain-specific relations [19]. It follows that OIE systems are not suited to extract facts, but to transform unstructured texts into structured and coherent information (propositions), closer to ontology formats. Having this in mind, our objective is to generate propositions from argument structures, where propositions are defined as coherent and non over-specified pieces of basic information.

From each argument structure detected in the previous step, our OIE system generates a set of triples representing the basic propositions underlying the linguistic structure. We assume that every argument structure can convey different pieces of basic information which are, in fact, minimal units of coherent, meaningful, and non over-specified information. For example, consider again the sentence:

*In May 2010, the principal opposition parties boycotted the polls after accusations of vote-rigging.*

which gives rise to the following SVOC<sub>1</sub>C<sub>2</sub> argument structure:

**S**="the principal opposition parties" , **V**="boycotted" , **O**="the polls" ,  
**C**<sub>1</sub>="In May" ,  
**C**<sub>2</sub>="after accusations of vote-rigging"

An incoherent and over-specified extraction would generate from this structure the following odd propositions:

P<sub>1</sub>=("the principal opposition parties", "boycotted in", "May")  
P<sub>2</sub>=("the principal opposition parties", "boycotted after", "accusations of vote-rigging")  
P<sub>3</sub>=("the principal opposition parties", "boycotted the polls after accusations of vote-rigging in", "May")

Propositions P<sub>1</sub> and P<sub>2</sub> are incoherent extractions because the direct object constituent (O) is not optional and, then, may not be omitted from any proposition built from that argument structure. In addition, P<sub>3</sub> contains an over-specified relation constituted by several constituents of the argument structure. To ensure a correct extraction, we defined a set of simple rules allowing us to extract only those propositions that are considered as coherent and non over-specified. For this purpose, direct objects are never omitted and relations cannot contain more than one clause constituent. This way, the three coherent propositions generated from the above argument structure are the following:

P<sub>1</sub>=("the principal opposition parties", "boycotted", "the polls")  
P<sub>2</sub>=("the principal opposition parties", "boycotted the polls after", "accusations of vote-rigging")  
P<sub>3</sub>=("the principal opposition parties", "boycotted the polls in", "May")

As has been said, another restriction to avoid over-specification is to remove relative clause from the constituents. In the same way, that-clauses that are direct objects are never inserted in the relation so as to avoid long and over-specified relations.

Propositions are generated using trivial extraction rules that transform argument structures into triples. Table 3 shows the set of rules we used to extract triples from our five types of argument structures. As in the case of all current OIE systems, we only consider the extraction of verb-based triples. We took this

decision in order to make a fair comparison when evaluating the performance of our system against similar systems (see Section 4). However, nothing prevents us from defining extraction rules to generate several triples from non-verbal structures: noun-prep-noun, noun-noun, adj-noun, and verb-adverb dependencies.

**Table 3.** Rules applied on five argument structures to generate the corresponding triples

Argument Structure	Rules
SVO	<b>arg1=S, rel=V, arg2=O</b>
SVC+	for $i = 1$ to $n$ where $n$ is the number of Complements C: $C_i$ is descomposed in $\text{prep}_i$ and $\text{Term}_i$ <b>arg1=S, rel=V+prep<sub>i</sub>, arg2=Term<sub>i</sub></b>
SVOC+	if O is not a that-clause, then: <b>arg1=S, rel=V, arg2=O</b> for $i = 1$ to $n$ where $n$ is the number of Complements C: $C_i$ is descomposed in $\text{prep}_i$ and $\text{Term}_i$ <b>arg1=S, rel=V+O+prep<sub>i</sub>, arg2=Term<sub>i</sub></b>  if O is a that-clause, then: <b>arg1=S, rel=V, arg2=O</b> for $i = 1$ to $n$ where $n$ is the number of Complements C: $C_i$ is descomposed in $\text{prep}_i$ and $\text{Term}_i$ <b>arg1=S, rel=V+prep<sub>i</sub>, arg2=Term<sub>i</sub></b>
SVA	<b>arg1=S, rel=V, arg2=A</b>
SVAC+	<b>arg1=S, rel=V, arg2=A</b> for $i = 1$ to $n$ where $n$ is the number of Complements C: $C_i$ is descomposed in $\text{prep}_i$ and $\text{Term}_i$ <b>arg1=S, rel=V+A+prep<sub>i</sub>, arg2=Term<sub>i</sub></b>

The output of ArgOE does not offer confidence values for each extraction. As the system is rule-based, there is not probabilistic information to be considered. Finally, with regard to the output format, it is worth mentioning that most OIE systems produce triples only in textual, surface form. This can be a problem if triples are used for NLP tasks requiring more linguistic information. This way, in addition to surface form triples, ArgOE also provides syntax-based information, with PoS tags, lemmas, and heads. If more syntactic information would be required, it can be easily obtained from the dependency analysis.

## 4 Experiments

We conducted three experimental studies: with English, Spanish, and Portuguese texts. Preliminary studies were performed to select an appropriate syntactic parser as input of ArgOE. Two multilingual dependency parsers were tested:

MaltParser 1.7.1<sup>1</sup> and DepPattern 3.0<sup>2</sup>, which is provided with a format converter that changes the standard output of the parser into the CoNLL-X format. We opted for DepPattern as input of ArgOE because the tagset and dependency names of DepPattern is the same for all the languages it is able to analyze, and then, there is no need to configure and adapt ArgOE for each new language. The use of MaltParser with different languages would require implementing converters from tagsets and dependency names defined for a particular language to a common set of PoS tags and dependency names. Besides DepPattern, we also use two different PoS taggers as input of the syntactic analyzer: TreeTagger [20] for English texts and FreeLing [21] for Spanish and Portuguese. All datasets, extractions and labels of the two experiments, as well as a version of ArgOE configured for English, Spanish, Portuguese, French, and Galician, are freely available<sup>3</sup>.

#### 4.1 English Evaluation

We compare ArgOE against several OIE existing systems for English, namely TextRunner, ReVerb, OLLI, WOE<sup>parse</sup>, and ClausIE. In this experiment, we will report the results obtained by the best version of ClauseIE, i.e., without considering redundancy and without processing conjunctions in the arguments. Note that we are comparing four systems based on training data (TextRunner, ReVerb, OLLI, and WOE<sup>parse</sup>) against two rule-based methods: ClausIE and ArgOE.

The dataset used in the experiment is the Reverb dataset<sup>4</sup> manually labeled for the evaluation reported in [3]<sup>5</sup>. The dataset consists of 500 sentences with manually-labeled extractions for the five systems enumerated above. In addition, we manually labeled the extractions obtained from ArgOE for the same 500 sentences. To maintain consistency among the labels associated to the five systems and those associated to ArgOE, we automatically identified those triples extracted by ArgOE that also appear in, at least, one of the other labeled extractions. As a result, we obtained 355 triples extracted by ArgOE that were labeled by annotators of previous work. Then, the extractions of ArgOE were given to two annotators who were instructed to consider the 355 already labeled extractions as starting point. So, our annotators were required to study and analyze the evaluation criteria used by other annotators before starting annotating the rest of extracted triples. We also instructed the annotators to treat as incorrect those triples denoting incoherent and uninformative propositions, as well as those triples constituted by over-specified relations, i.e., relations containing numbers, named entities, or excessively long phrases (e.g., *boycotted the polls after accusations of vote-rigging in*). An extraction was considered as correct

---

<sup>1</sup> <http://www.maltparser.org/>

<sup>2</sup> <http://gramatica.usc.es/pln/tools/deppattern.html/>

<sup>3</sup> <http://172.24.193.8/ArgOE-epia2015.tgz> (anonymous version)

<sup>4</sup> <http://reverb.cs.washington.edu/>

<sup>5</sup> <http://www-mpi-inf.mpg.de/departments/d5/software/clausie>

if it was labeled as correct by both annotators. The two annotators agreed on 75% of extractions (Cohen's kappa  $k = 0,50$ ), which is considered a moderate agreement. In sum, we follow similar criteria to those defined in previous OIE evaluations [9].

The results of our evaluation are summarized in Table 4 and Figure 1. Table 4 shows the number of correct expressions extracted as well as the total number of extractions for each system. *Precision* is defined as the number of correct extractions divided by the number of returned extractions. *Recall* is estimated by identifying a pool of relevant extractions which is the total number of different correct extractions made by all the systems (this pool is our gold-standard). So, *recall* is the number of correct extractions made by the system divided by the total number of correct expressions in the pool (3,222).

**Table 4.** Number of correct extractions and total number of extractions in the Reverb dataset, according to the evaluation reported in [3] and our own contribution with ArgOE.

Systems	correct extractions	total extractions
texrunner	286	798
reverb	388	727
woe	447	1028
ollie	547	1242
argoe	582	1162
clausie	1706	2975

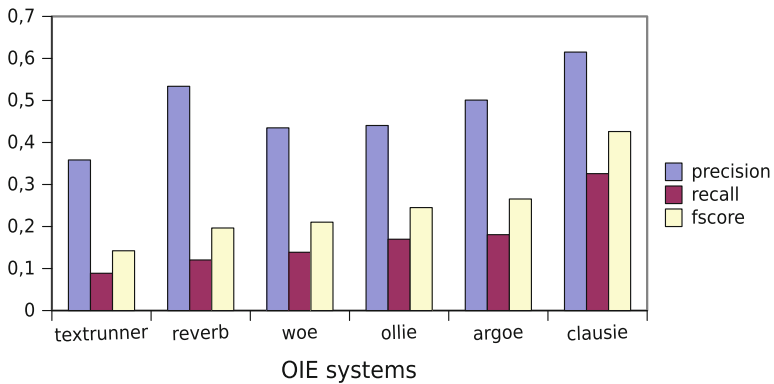


**Fig. 1.** Evaluation of six OIE systems

The results show that the two rule-based systems, ClausIE and ArgOE, perform better than the classifiers based on automatically generated training data. This is in accordance with previous work reported in [3,14]. Moreover, the four systems based on dependency analysis (ClausIE, ArgOE, OLLIE, and

WOE<sup>parse</sup>) improve over those relying on shallow syntax (TextRunner and ReVerb). And finally, ClausIE clearly outperforms the other systems, in terms of both precision and recall. A common problem for parse-based OIE systems is the large influence of parser errors. So, the quality of the parser can determine the quality of the OIE extractor. ClausIE uses the Standford Dependency Parser, while ArgOE uses DepPattern, and OLLIE the MaltParser. One possible reason for the comparably low precision of our system against ClausIE might be the lower parsing performance of DepPattern against the Standford Dependency Parser for the English language.

## 4.2 Spanish Evaluation

In this experiment, we compare ArgOE against the only OIE system that has been evaluated for other language than English: ExtrHech [12]. This is also a rule-based system, but it does not operate on dependency parsing but on shallow syntax (patterns of PoS tags). The Spanish dataset, called Raw Web<sup>6</sup>, contains 159 sentences randomly extracted with a web crawler from over 5 billion web pages in Spanish. Each extraction was labeled by two independent annotators. An extraction was considered as correct if it was labeled as correct by both annotators. They agreed on 81% of extractions (Cohen's kappa  $\kappa = 0,62$ ). Table 5 depicts the results obtained by the two systems on these sentences. Unfortunately, the extractions made by ExtrHech are not available, so it is not possible to create a pool of correct triples extracted by the two systems to measure recall. Only precision can be compared even if we were not able to unify the criteria given to our annotators with those defined in [12]. Notice that the precision of ArgOE is identical to that obtained for English (50%), which can be seen as an indirect evidence that the two parsers used by our system have similar performance.

**Table 5.** Precision of both ArgOE and ExtrHech on the Spanish dataset

Systems	correct extractions	total extractions	Precision (%)
argoe	107	214	50%
extrahech	-	-	55%

Most errors made by our OIE system come from three different sources: the syntactic parser, the PoS tagger, and the Named Entity Recognition module used by the PoS tagger. So, the improvement of our system relies on the performance of other NLP tasks.

## 4.3 Portuguese Evaluation

For this purpose, we selected 103 test sentences from a domain-specific corpus, called *CorpusEco* [22], containing texts on ecological issues. ArgOE was

<sup>6</sup> <http://www.gelbukh.com/resources/spanish-open-fact-extraction>

applied on the sentences and 190 triples was extracted. One annotator labeled the extracted triples and Table 6 shows the number of correct triples and precision achieved by the system. To the best of our knowledge, this is the first experiment that reports an OIE system working on Portuguese. Precision is again similar (53%) to that obtained in the previous experiments. Again, most errors are due to problems from the syntactic parser and PoS tagger.

**Table 6.** Precision of ArgOE on the Portuguese dataset

Systems	correct extractions	total extractions	Precision (%)
argoe	95	190	53%

## 5 Conclusion

We have described a rule-based OIE system to extract verb-based triples than takes as input dependency parsers in the CoNLL-X format. So, it may take advantage of efficient, robust, and multilingual syntactic parsers. Even if our system is outperformed by other similar rule-based methods, it reaches better results than those strategies based on training data. As far as we know, ArgOE is the first OIE system working on more than one language. In future work, we will include NLP modules to find linguistic generalizations over the extracted triples: e.g., co-reference resolution to link the arguments of different triples, and synonymy detection of verbs to reduce the open set of extracted relations and, then, to enable semantic inference.

**Acknowledgments.** This work has been supported by projects Plastic and Celtic, Innterconecta (CDTI).

## References

1. Banko, M., Cafarella, M.J., Soderland, S., Broadhead, M., Etzioni, O.: Open information extraction from the web. In: International Joint Conference on Artificial Intelligence (2007)
2. Wu, F., Weld, D.S.: Open information extraction using wikipedia. In: Annual Meeting of the Association for Computational Linguistics (2010)
3. Corro, L.D., Gemulla, R.: Clausie: clause-based open information extraction. In: Proceedings of the World Wide Web Conference (WWW-2013), Rio de Janeiro, Brazil, pp. 355–366 (2013)
4. Hall, J., Nilsson, J.: CoNLL-X shared task on multilingual dependency parsing. In: The Tenth CoNLL (2006)
5. Nivre, J., Hall, J., Kübler, S., McDonald, R., Nilson, J., Riedel, S., Yuret, D.: The CoNLL-2007 shared task on dependency parsing. In: Proceedings of the Shared Task Session of EMNLP-CoNLL 2007, Prague, Czech Republic, pp. 915–932 (2007)
6. Nivre, J., Hall, J., Nilsson, J., Chaney, A., Eryigit, G., Kübler, S., Marinov, S., Marsi, E.: Maltparser: A language-independent system for data-driven dependency parsing. Natural Language Engineering **13**(2), 115–135 (2007)

7. Gamallo, P., González, I.: A grammatical formalism based on patterns of part-of-speech tags. *Journal of Corpus Linguistics* **16**(1), 45–71 (2011)
8. Banko, M., Etzioni, O.: The tradeoffs between open and traditional relation extraction. In: ACL-08 (2008)
9. Etzioni, O., Fader, A., Christensen, J., Soderland, S., Mausam: Open information extraction: the second generation. In: International Joint Conference on Artificial Intelligence (2011)
10. Mausam, Schmitz, M., Soderland, S., Bart, R., Etzioni, O.: Open language learning for information extraction. In: EMNLP-12, pp. 523–534 (2012)
11. Fader, A., Soderland, S., Etzioni, O.: Identifying relations for open information extraction. In: EMNLP-11 (2011)
12. Zhilla, A., Gelbukh, A.: Comparison of open information extraction for English and Spanish. In: Dialogue 2014 (2014)
13. Xavier, C.C., Souza, M., de Lima, V.S.: Open information extraction based on lexical-syntactic patterns. In: Brazilian Conference on Intelligent Systems, pp. 189–194 (2013)
14. Bast, H., Haussmann, E.: Open information extraction via contextual sententence decomposition. ICSC 2013, 154–159 (2013)
15. Akbik, A., Loser, A.: Kraken: N-ary facts in open information extraction. In: Joint Workshop on Automatic Knowledge Base Construction and Web-scale Knowledge Extraction, pp. 52–56 (2012)
16. Gamallo, P., Garcia, M., Fernández-Lanza, S.: Dependency-based open information extraction. In: ROBUS-UNSUP Workshop at EACL-2012, Avignon, France (2012)
17. Klein, D., Manning, C.D.: Accurate unlexicalized parsing. In: ACL-03, pp. 423–430 (2003)
18. Lin, T., Mausam, Etzioni, O.: Identifying functional relations in web text. In: Conference on Empirical Methods in Natural Language Processing (2010)
19. Soderland, S., Roof, B., Qin, B., Xu, S., Mausam, Etzioni, O.: Adapting open information extraction to domain-specific relations. *AI Magazine* **31**(3), 93–102 (2010)
20. Schimd, H.: Improvements in part-of-speech tagging with an application to german. In: ACL SIGDAT Workshop, Dublin, Ireland (1995)
21. Padró, L., Stanilovsky, E.: Freeling 3.0: towards wider multilinguality. In: LREC 2012, Istanbul, Turkey (2012)
22. Zavaglia, C.: O papel do léxico na elaboração de ontologias computacionais: do seu resgate à sua disponibilização. In: Lingüística IN FOCUS - Léxico e morfofonologia: perspectivas e análises. Uberlândia: EDUFU, pp. 233–274 (2006)

# Classification and Selection of Translation Candidates for Parallel Corpora Alignment

K.M. Kavitha<sup>1,3(✉)</sup>, Luís Gomes<sup>1,2</sup>, José Aires<sup>1,2</sup>, and José Gabriel P. Lopes<sup>1,2</sup>

<sup>1</sup> NOVA Laboratory for Computer Science and Informatics (NOVA LINCS), Faculdade de Ciências e Tecnologia, Universidade Nova de Lisboa, 2829-516 Caparica, Portugal

[k.mahesh@campus.fct.unl.pt](mailto:k.mahesh@campus.fct.unl.pt), [luismsgomes@gmail.com](mailto:luismsgomes@gmail.com), [aires74@iol.pt](mailto:aires74@iol.pt), [gpl@fct.unl.pt](mailto:gpl@fct.unl.pt)

<sup>2</sup> ISTRION BOX-Translation & Revision, Lda., Parkurbis, 6200-865 Covilhã, Portugal

<sup>3</sup> Department of Computer Applications, St. Joseph Engineering College, Vamanjoor, Mangaluru 575 028, India  
[kavitham@sjec.ac.in](mailto:kavitham@sjec.ac.in)

**Abstract.** By incorporating human feedback in parallel corpora alignment and term translation extraction tasks, and by using all human validated term translation pairs that have been marked as *correct*, the alignment precision, term translation extraction quality and a bunch of closely correlated tasks improve. Moreover, such a labelled lexicon with entries tagged for correctness enables bilingual learning. From this perspective, we present experiments on automatic classification of translation candidates extracted from aligned parallel corpora. For this purpose, we train SVM based classifiers for three language pairs, English-Portuguese (EN-PT), English-French (EN-FR) and French-Portuguese (FR-PT). The approach enabled micro f-measure classification rates of 95.96%, 75.04% and 65.87% respectively, for the EN-PT, EN-FR and FR-PT language pairs.

## 1 Introduction

Annotated bilingual lexica with their entries tagged for (in)correctness can be mined to discover the nature of new term translation extractions and/or alignment errors. An automated classification system can then be trained when sufficient amount of positive and negative evidence is available. Such a classifier can facilitate and speed up the manual validation process of automatically extracted term translations, and contribute to make the human validation effort easier while augmenting the number of validated (rejected and accepted) bilingual entries in a bilingual term translation lexicon. Bionic interaction between linguists and highly precise machine classifiers in a continuous common effort, without loosing knowledge contributes to improve alignment precision and, at another level, translation quality. It is therefore important to have term translation extractions automatically classified prior to having them validated by human specialists.

In this paper, we assume sentence aligned parallel corpora for extracting term translations, constructing translation tables or obtaining that parallel corpora aligned at a subsentence grain [7, 13]. In this setting, translation correspondences are identified between term pairs by computing their occurrence frequencies or similarities within the aligned sentences rather than in the entire corpus.

In the completely unsupervised models based on parallel corpora, all the phrase pairs that are considerably consistent with the word alignment are extracted and gathered into a phrase table along with their associated probabilities [4, 19]. Naturally, the resulting table extracted from the alignment, with no human supervision, contains alignment errors. Moreover, many of the translations in the phrase table produced are spurious or will never be used in any translation [10]. A recent study shows that nearly 85% of phrases gathered in the phrase table can be reduced without any significant loss in translation quality [21].

A different approach [1], that deviates from this tradition acknowledges the need for blending the knowledge of language, linguistics and translation as relevant for research in Machine Translation [27]. The approach being semi-supervised and iterative takes privilege in informing the machine for not making the same kind of errors in subsequent iterations of alignment and extraction. In this partially supervised, iterative strategy, first a bilingual lexicon is used to align parallel texts [7]. New<sup>1</sup> term-pairs are then extracted from those aligned texts [1]. The newly extracted candidates are manually verified and then added to the existing bilingual lexicon with the entries manually tagged as *accepted* (Acc) and *rejected* (Rej). Iteration over these three steps (parallel text alignment using an updated and validated lexicon, extraction of new translation pairs and their validation) results in an improved alignment precision, improved lexicon quality, and in more accurate extraction of new term-pairs [7]. Human feedbacks are particularly significant in this scenario as incorporating them prevents alignment and extraction errors from being fed back into subsequent alignment and extraction iterations. The work described in this paper may be easily integrated in such a procedure.

Several approaches for extracting phrase translations prevail [1, 4, 8, 15]. However, it is important to have the extractions automatically classified prior to having them validated by human specialists. We view classification as a pre-validation phase that allows a first-order separation of correct entries from incorrect ones, so that the human validation task becomes lighter [11]. We extend our previous work by using a larger set of extracted translation candidates for the language pair EN-PT and by additionally adopting other extraction techniques [4, 15] and others not yet published. Experimental evaluations of the classifier for additional language pairs EN-FR and FR-PT are also presented. Further, the performance of the classifier with additional features is discussed.

In the Section 2, we provide a quick review of the related work. In the Section 3, we present the classification approach for selecting translation candidates and the features used. The data sets used, the classification results, and

---

<sup>1</sup> Not seen in the bilingual lexicon that was used for alignment.

their subsequent analysis are presented in Section 4. We conclude with Section 5 by reflecting a bit on the future work.

## 2 Selection of Bilingual Pairs

The translation selection process might be aimed from the perspective of improving the alignment precision and extraction quality or from the translation perspective itself [11, 24]. Nevertheless, different researchers have demonstrated varied views regarding the influence of alignment on translation quality, predominantly from the perspective of entries in a phrase table. It is shown that better alignment presents threefold benefit that includes the advantage of producing a phrase table of manageable size with fewer phrase pairs, a reduced decoding time in searching the phrase table for the most probable translation, and a better quality of word or phrase level translation [21]. However, it is also observed that the decreased alignment error rate does not necessarily imply a significant increase in the translation quality [6, 18, 26]. We reiterate that we aim at an improved alignment precision and extraction accuracy.

The task of selecting appropriate translation candidates may be cast as the problem of filtering spurious bilingual pairs from the associated tables<sup>2</sup> or as we view it, the learning phase (training) of a classifier that is then used for classifying the extracted bilingual pairs as ‘Accepted’ or ‘Rejected’ for further manual verification. Various filtering approaches have been proposed and used in selecting appropriate translations [1, 5, 10, 17, 22, 23, 28, 29].

### 2.1 Support Vector Machines in Selecting Bilingual Pairs

Ever since its introduction, the Support Vector Machine (SVM) [25] has been successfully adapted for various translation related machine learning tasks. Related applications include learning translation model for extracting word sequence correspondences (phrase translations) and automatic annotation of cognate pairs [3, 20].

The use of SVM based classifiers in selecting the translation candidates has been proposed earlier [2, 11, 14]. Common criteria for selection include translation coverage, source and target term co-occurrence and the orthographic similarity. Further, One-Class SVM has been used with the Mapping Convergence (MC) algorithm to differentiate the usable and useless phrase pairs based on the confidence scores assigned by the classifier [24]. While the focus is on translation quality and avoiding alignment errors, the classifier is trained with a corpus that comprises of only useful instances. All phrase pairs involved in best phrasal derivations<sup>3</sup> by the Oracle decoder are labeled as positive phrase pairs. Unlabelled examples of phrase pairs, however, are employed in addition to the positive examples in a semi-supervised framework<sup>4</sup> to improve the performance. We on

---

<sup>2</sup> Phrase table or a bilingual lexicon.

<sup>3</sup> One that maximises a combination of model score and translation quality metric.

<sup>4</sup> MC algorithm.

the other hand, view the selection of translation candidates as a supervised classification problem with labeled training examples for both the classes (positive and negative instances).

### 3 Classification Model

In the current section, we discuss the use of SVM based classifier in segregating the extracted translation candidates as accepted, ‘Acc’ or rejected, ‘Rej’. The classification task involves training and testing data representing bilingual data instances. Each bilingual pair is a data instance represented as a *feature vector* and a target value known as the *class label*<sup>5</sup>. We train the learning function with the scaled training data set, where each sample is represented as a feature vector with the label +1 (‘Acc’) or -1 (‘Rej’). The estimated model is then used to predict the class for each of the unknown data instance kept aside for testing, represented similarly as any sample in the training set, but with the class label 0. We use the Radial Basis Function (RBF) kernel:  $K(x_i, x_j) = e^{\gamma \|x-y\|^2}$ ; parameterised by  $(C, \gamma)$ , where  $C > 0$  is the penalty parameter of the error term and  $\gamma > 0$  is the kernel parameter.

#### 3.1 Features

Adequate feature identification for representing the data in hand is fundamental to enable good learning. An overview of the features used in our classification model is discussed in this section. We use the features derived using the orthographic similarity measures (strsim) and the frequency measures (freq) discussed in the section below as baseline ( $BL_{strsim+freq}$ ) for our experiments.

**Orthographic Similarity.** Two orthographic similarity measures based on edit distance are used to quantify the similarity between the terms in a bilingual pair: the Levenshtein Edit Distance [16] (Equation 1) and the Spelling Similarity measure [8] (Equation 2).

$$EditSim = 1.0 - \frac{EditDist(X, Y)}{Max(|X|, |Y|)} \quad (1)$$

where  $EditDist(X, Y)$  is the edit distance between the term X in first language and the term Y in second language.

$$SpSim(X, Y) = 1.0 - \frac{D(X, Y)}{Max(|X|, |Y|)} \quad (2)$$

where the distance function  $D(X, Y)$  is the  $EditDist$  discounting characteristic spelling differences that were learnt previously. In Equations 1 and 2,  $|X|$  represents the length of X and  $|Y|$  represents the length of Y.

---

<sup>5</sup> Positive and negative examples are respectively labeled as +1 and -1. Data to be classified is labeled 0.

We use the ‘*accepted*’ entries in the training dataset with  $\text{EditSim} \geq 0.65$  as examples to train SpSim and a dictionary containing the substitution patterns is learnt. For instance, the substitution pattern extracted from EN-PT cognate word pair ‘phase’ and ‘fase’ is (^ph’, ^f’), after eliminating all matched (aligned) characters, ‘a’ ⇔ ‘a’, ‘s’ ⇔ ‘s’ and ‘e’ ⇔ ‘e’. The caret (^), at the beginning of the aligned strings distinguishes that the pattern appears as a prefix.

**Frequency of Occurrence.** To represent the translational equivalence, based on the frequencies of the terms in a bilingual pair, two measures are used: the Dice association measure and the MinMaxRatio.

The Dice association measure for a pair of terms (X,Y) takes into account the frequency of the term X in the first language text,  $F(X)$ ; the frequency of the term Y in the second language text,  $F(Y)$ ; and the co-occurrence frequency of the terms in aligned segments of the parallel texts,  $F(X,Y)$  and is given by the equation,

$$\text{Dice}(X, Y) = \frac{2 * F(X, Y)}{F(X) + F(Y)} \quad (3)$$

Another measure that efficiently substitutes the individual frequencies  $F(X)$  and  $F(Y)$  is the minimum to maximum frequency ratio given by the equation,

$$\text{MinMaxRatio}(X, Y) = \frac{\text{Min}(F(X), F(Y))}{\text{Max}(F(X), F(Y))} \quad (4)$$

**Table 1.** The Similarity and Bad Ending Scores

Term <sub>EN</sub>	Term <sub>PT</sub>	EdSim	SpSim	BE <sub>sw</sub>	BE <sub>Pat<sub>R-A</sub></sub>
general indifference	indiferença geral	0.15	1.0	(0.00, 0.00)	(0.00, 0.00)
official	comercial	0.56	0.66	(0.00, 0.00)	(0.00, 0.00)
commitments	compromissos de crédito	0.29	0.24	(0.00, 0.00)	(0.00, 0.00)
limits of the	limites de a	0.54	0.82	(1.00, 1.00)	(1.00, 1.00)
impact on the	impacto em a indústria	0.39	0.47	(1.00, 0.00)	(1.00, 0.00)

**Bad Ends.** The bilingual pair ‘*limits of the* ⇔ *limites de a*’ instantiates a particular type of inadequate translation wherein, the term (on both sides) ends with a determiner following which a noun or a noun phrase is anticipated. It is the absence of the noun or a noun phrase after the determiner that makes the translation incomplete. By allowing this entry into the lexicon as a correct translation, we cannot refrain other entries ending with ‘o’, ‘os’, and so forth from accommodating the determiner’s position. We refer to such translations with inadequate endings as having bad ends (BE). To keep a check over such entries, we use a binary valued feature signifying whether a translation ends with a determiner (1) or not (0). This introduces two features, each representing the goodness of the translation endings on each side of the bilingual pair.

We use two different approaches to identify bad ends: one set of two features based on endings that are stop words ( $BE_{SW}$ ) and the other set of two features based on endings seen in the rejected, but not in the accepted training dataset ( $BE_{Pat_{R-A}}$ ). We consider only those endings that occur more than 5 times in the rejected but not in the accepted training dataset. To avoid the content words from being considered as bad ends, the term length is restricted to less than 5 characters.

**Translation Miscoverage.** A typical error observed in the extracted candidates represents the lack of parallelism with respect to content words. An example is the bilingual pair ‘*commitments*  $\Leftrightarrow$  *compromissos de crédito*’. For this pair to be considered as correct, ‘*crédito*’ needs to be translated either as ‘*lending*’ or as ‘*loan*’ in EN. So the correct term translation would be ‘*lending commitments*  $\Leftrightarrow$  *compromissos de crédito*’ or ‘*loan commitments*  $\Leftrightarrow$  *compromissos de crédito*’. Likewise, the bilingual pair ‘*union level*  $\Leftrightarrow$  *união*’ is incorrect because no translation exists for the English word ‘*level*’ on the right hand side.

To assess the bilingual candidates for parallelism, we introduce two features. We say that a translation candidate has translation gap with respect to the first language ( $gap_{L1}=1$ ) when the term in the first language does not have a translation in the second language in whole or in parts and vice versa. Lack of parallelism implies a gap in translation.

**Stemmed Coverage.** While looking for coverage, if the expressions on both sides are not covered by the lexicon, we set the features  $gap_{L1}$  and  $gap_{L2}$  to 0.5<sup>6</sup>. To deal with such situations reflecting our lack of support, we extract two features representing coverage using the stemmed training data. These features work in the same way as discussed above except that they look only at the word stems. To instantiate, while looking for coverage for the bilingual pair ‘*bronchitically*  $\Leftrightarrow$  *bronquiticamente*’, we use its stemmed version ‘*bronchit*  $\Leftrightarrow$  *bronquit*’, as the coverage is examined using the stemmed training and test datasets. If the training dataset contains the term ‘*bronchit*’ in EN and ‘*bronquit*’ in PT, then ( $gap_{L1}$ ,  $gap_{L2}$ ) would be (0.0, 0.0). This feature would find less gaps in translations that are indeed parallel, and thus decrease the number of false negatives (i.e., good translations that are classified as bad).

For identifying the translation gaps, we use the Aho-corasick set-matching algorithm that checks if the terms in the key-word tree<sup>7</sup> occur as (sub-)expressions in the bilingual pair to be validated and if they occur are accepted translations [9]. Similarly, to find the stemmed coverage, we use the stemmed training and test datasets, obtained using the Snowball stemmer. Here, each keyword tree is constructed using the stemmed part of the term. Translation

<sup>6</sup> A neutral value reflecting our lack of support in deciding whether to accept or to reject that pair.

<sup>7</sup> Constructed separately using the first and second language terms in the accepted bilingual training data.

gaps are identified using the Aho-corasick set-matching algorithm as mentioned previously.

## 4 Experimental Setup and Evaluation

We use the SVM based tool, LIBSVM<sup>8</sup> to learn the binary classifier, which tries to find the hyperplane, that separates the training examples with the largest margin. We scale the data in the range [0 1]. We perform a grid-search on RBF kernel parameters, ( $C, \gamma$ ) using cross-validation, so that the classifier can accurately predict unknown data (testing data).

### 4.1 Data Sets

The translation candidates used in our experiments were acquired using various extraction techniques applied on a (sub-)sentence aligned parallel corpora<sup>9</sup> [1, 4, 8, 15]. We experimented with 3 language pairs, EN-PT, EN-FR and FR-PT. The suffix array based phrase translation extraction technique was employed only for the language pair EN-PT and was excluded in extracting EN-FR and FR-PT bilingual pairs [1]. The statistics of the training and test datasets (validated bilingual lexicon) are as shown in Table 2. We set aside randomly 5% of the validated lexicon as the test set. We repeat experiments for comparing the experimental results related to the size of the training corpus by taking into account randomly extracted 50%, 75%, 80%, 90% and the entire 95% of the training set.

**Table 2.** Training and Testing Data Statistics

Data Sets		EN-PT			EN-FR			FR-PT		
		Accepted	Rejected	Total	Accepted	Rejected	Total	Accepted	Rejected	Total
Training	95%	853,452	575,951	1,429,403	362,017	51,054	413,071	372,306	78,754	451,060
	90%	768,105	518,356	1,286,461	342,963	48,370	391,333	352,711	74,609	427,320
	80%	682,761	460,761	1,143,522	304,856	42,996	347,852	313,521	66,319	379,840
	75%	640,088	431,963	1,072,051	285,803	40,308	326,111	293,926	62,174	356,100
	50%	426,725	287,976	714,701	181,009	26,871	207,880	195,952	41,449	237,401
Test	5%	44,920	30,312	75,232	19,053	2,687	21,740	19,595	4,145	23,740

### 4.2 Results

In the current section, we discuss the classification results and the performance of the classifier with respect to various features using the complete data set (95%) introduced in the Section 4.1 for each of the language pairs EN-PT, EN-FR and FR-PT.

<sup>8</sup> A library for support vector machines - Software available at <http://www.csie.ntu.edu.tw/~cjlin/libsvm>

<sup>9</sup> DGT-TM - <https://open-data.europa.eu/en/data/dataset/dgt-translation-memory>  
Europarl - <http://www.statmt.org/europarl/>

OPUS (EUconst, EMEA) - <http://opus.lingfil.uu.se/>

The Table 3 shows the precision ( $P_{Acc}$ ,  $P_{Rej}$ ), recall ( $R_{Acc}$ ,  $R_{Rej}$ ) and the accuracy of the estimated classifier in predicting each of the classes ( $Acc$  and  $Rej$ ) while using different features. Micro-average Recall ( $\mu_R$ ), Micro-average Precision ( $\mu_P$ ), and Micro-average f-measure ( $\mu_F$ <sup>10</sup>) are used to assess the global performance over both classes.

As might be seen from the Table 3, for EN-PT, substantial improvement is achieved by using the feature that looks for translation coverage on both sides of the bilingual pair. We observe an increase in  $\mu_F$  of 22.85% over the base line and 19.32% over a combination of the features representing baseline and bad ends. Best  $\mu_F$  is obtained when the stemmed<sup>11</sup> lexicon is used to look for stem coverage rather than the original lexicon. However, for EN-FR, training with stemmed lexicon did not show a meaningful improvement.

**Table 3.** Classifier Results using different features for EN-PT, EN-FR and FR-PT

Language Pairs	Features	$P_{Acc}$	$R_{Acc}$	$P_{Rej}$	$R_{Rej}$	$\mu_P$	$\mu_R$	$\mu_F$	Accuracy
EN-PT	BL <sub>strsim+freq</sub>	70.87	93.47	81.66	43.08	76.27	68.28	72.05	73.17
	BL+BE <sub>SW</sub>	76.50	88.47	77.76	59.73	77.13	74.10	75.58	76.89
	BL+BE <sub>Pat_R-A+Cov</sub>	98.93	92.41	89.75	98.52	94.34	95.47	94.90	94.87
	BL+BE <sub>Pat_R-A+CovSim</sub>	99.85	92.03	89.42	99.80	94.64	95.92	95.27	95.16
	BL+BE <sub>SW+CovSim</sub>	98.64	94.63	92.50	98.06	95.57	96.35	<b>95.96</b>	96.02
EN-FR	BL <sub>strsim+freq</sub>	90.67	98.45	71.89	28.17	81.28	63.31	71.18	89.76
	BL+BE <sub>SW</sub>	90.69	98.5	72.73	28.28	81.71	63.39	71.39	89.83
	BL+BE <sub>Pat_R-A+Cov</sub>	96.03	86.56	43.92	74.62	69.98	80.59	74.91	85.09
	BL+BE <sub>_Pat_R-A+Cov+SpSim</sub>	96.07	86.63	44.11	74.84	70.09	80.74	<b>75.04</b>	85.17
	BL+BE <sub>Pat_R-A+CovSim</sub>	91.10	98.25	71.98	31.93	81.54	65.09	72.39	90.05
	BL+BE <sub>Pat_R-A+CovSim+SpSim</sub>	91.34	98.23	73.04	33.98	82.19	66.11	73.26	90.29
FR-PT	BL <sub>strsim+freq</sub>	85.12	97.85	65.30	19.16	75.21	58.51	65.81	84.11
	BL+BE <sub>SW</sub>	85.12	97.83	65.05	19.13	75.09	58.48	65.75	84.09
	BL+BE <sub>SW+Cov</sub>	88.80	74.55	31.58	55.54	60.19	65.05	62.52	71.23
	BL+BE <sub>_Pat_R-A+Cov+SpSim</sub>	88.87	75.54	32.35	55.30	60.61	65.42	62.92	72.01
	BL+BE <sub>Pat_R-A+CovSim</sub>	85.12	97.83	65.05	19.13	75.09	58.48	65.75	84.09
	BL+BE <sub>Pat_R-A+CovSim+SpSim</sub>	85.13	97.87	65.54	19.18	75.34	58.53	<b>65.87</b>	84.13

FR-PT results are worse than the results obtained for other language pairs: the best  $\mu_F$  and accuracy of 65.87% and 84.13% respectively are obtained when we use a combination of features  $BL+BE_{Pat_{R-A}} + Cov_{Stm} + SpSim$ . However, the improvement is negligible (approximately ranging from 0.01% - 0.14%) against the baseline ( $BL_{strsim+freq}$ ) in every terms (precision, recall and micro f-measure) over both classes. This may be explained because the number of ‘single word - single word’ pairs is comparatively larger than for the other language pairs and the number of ‘multi-word - multi-word’ pairs is small (50,552 for the accepted). Approximately 250K French multi-words are paired with single Portuguese words and approximately 9K Portuguese multi-words are paired with single French words. Moreover, approximately 130K are single word pairs for this pair of languages which is quite different from the EN-PT scenario.

<sup>10</sup> Computed as discussed in [11].

<sup>11</sup> Stemmed using the snowball stemmer.

Also, patterns indicating bad ends that are stop words ( $BE_{SW}$ ) are substantially few in number with respect to FR-PT<sup>12</sup> and EN-FR<sup>13</sup> lexicon corpus as opposed to EN-PT<sup>14</sup>. This is because extractions for these language pairs use all of the techniques mentioned in section 4.1 except for the suffix array based extraction technique [1]. Hence EN-FR and FR-PT were much cleaner.

### 4.3 Classifier Performance by Training Set Size

We analyzed the impact of varying the size of training datasets on the improvement given by various features. Table 4 shows the results obtained using the features  $BL_{strsim+freq} + BE_{SW} + Cov$  (EN-PT) and  $BL_{strsim+freq} + BE_{Pat_{R-A}} + Cov + SpSim$  (EN-FR and FR-PT) respectively.

**Table 4.** Classifier Results for EN-PT, EN-FR and FR-PT by training set sizes

Language Pairs	Training Dataset	P <sub>Acc</sub>	R <sub>Acc</sub>	P <sub>Rej</sub>	R <sub>Rej</sub>	μ <sub>P</sub>	μ <sub>R</sub>	μ <sub>F</sub>	Accuracy
EN-PT	50%	<b>99.45</b>	92.22	89.59	<b>99.24</b>	<b>94.52</b>	<b>95.73</b>	<b>95.12</b>	<b>95.05</b>
	75%	99.21	92.32	89.68	98.90	94.45	95.61	95.02	94.97
	80%	99.04	92.38	89.73	98.67	94.39	95.53	94.95	94.91
	90%	98.74	92.38	89.69	98.25	94.22	95.32	94.76	94.74
	95%	98.38	<b>92.60</b>	<b>89.91</b>	97.74	94.15	95.17	94.65	94.67
EN-FR	50%	93.75	58.62	19.77	72.31	56.76	65.47	60.80	60.31
	75%	95.41	74.77	29.39	74.47	62.40	74.62	67.97	74.73
	80%	95.59	75.82	30.49	75.21	63.04	75.52	68.72	75.74
	90%	95.85	68.59	26.17	<b>78.94</b>	61.01	73.77	66.78	69.87
	95%	<b>96.07</b>	<b>86.63</b>	44.11	74.84	<b>70.09</b>	<b>80.74</b>	<b>75.04</b>	<b>85.17</b>
FR-PT	50%	88.68	67.57	27.86	<b>59.20</b>	58.27	63.39	60.72	66.11
	75%	88.62	75.05	31.59	54.45	60.11	64.75	62.34	71.46
	80%	88.76	75.29	31.99	54.93	60.38	65.11	62.65	71.74
	90%	88.43	79.29	<b>34.22</b>	50.95	<b>61.33</b>	65.12	<b>63.17</b>	<b>74.34</b>
	95%	<b>88.87</b>	<b>75.54</b>	32.35	55.30	60.61	<b>65.42</b>	62.92	72.01

Looking at the classification results for EN-PT using SVM and the training set, we observe that the larger the training set larger the recall ( $R_{Acc}$  is 92.6% against 92.22%) for the ‘Accepted’ class. Meanwhile, when we augment the training set we loose in precision from 99.45% to 98.38%. However, by augmenting the training set we augment the precision ( $R_{Acc}$  from 89.59% to 89.91%) for the ‘Rejected’ class, whereas the recall drops ( $R_{Rej}$  from 99.24% to 97.74%). As the training set is much larger than for other language pairs (95% of the corpus) we

<sup>12</sup> 5 in FR and 8 in PT; most frequent are ‘de’ in FR with 27 occurrences and ‘de’ in PT with 43 occurrences.

<sup>13</sup> 43 in EN and 15 in FR; most frequent are ‘to’ in EN with 210 occurrences and ‘pas’ in FR with 237 occurrences.

<sup>14</sup> 112 in EN and 86 in PT; most frequent are ‘the’ in EN with 27,455 occurrences and ‘a’ in PT with 22,242 occurrences.

do not necessarily gain much. Thus, precision and recall for EN-PT does evolve in a way, such that, while one augments the other tends to decrease, partially deviating from the trend observed in our earlier experiments [11]. It is possible that some sort of overfitting occurs.

Unlike EN-PT, for the language pairs EN-FR and FR-PT, with larger training sets the performance of the trained classifier improved. For the features listed in Table 3, best results were obtained with 95% and 90% of the training set.

#### 4.4 Classifier Trained on One Language Pair in Classifying Others

Motivated by the classifier performance for language pairs EN-PT, we conducted few more experiments: we trained the classifier using the full set of features on one language pair, and tested on the other. Training on EN-PT data and testing on EN-FR and FR-PT resulted in  $\mu_F$  of 55.64% and 54.99%, far below the baseline for EN-FR (a drop by approximately 15% from 71.18%) and FR-PT (a drop by approximately 11% against 65.81%) respectively. Training the system with EN-FR and testing on FR-PT did even worse, leading to a micro f-measure of 52.96%. Training on FR-PT data and testing on EN-FR, led to a  $\mu_F$  of 47.8%. This lets us to conclude that it does not make any sense to use a classifier trained on one language pair in classifying the data from other language pairs. The related results are shown in Table 5.

**Table 5.** Performance of Classifier trained on one language pair when tested on others.

Language Pairs (Test Set)	Classifier Trained	P <sub>Acc</sub>	R <sub>Acc</sub>	P <sub>Rej</sub>	R <sub>Rej</sub>	$\mu_P$	$\mu_R$	$\mu_F$	Accuracy
EN-FR	Train with EN-FR model	96.03	86.56	43.92	74.62	69.98	80.59	74.91	85.09
	Train with EN-PT model	89.07	88.55	22.02	22.93	55.55	55.74	55.64	80.44
	Train with FR-PT model	86.85	70.55	10.39	24.23	48.62	47.39	47.80	64.82
FR-PT	Train with FR-PT model	88.80	74.55	31.58	55.54	60.19	65.05	62.52	71.23
	Train with EN-PT model	85.71	59.66	21.74	52.98	53.73	56.32	54.99	58.49
	Train with EN-FR model	84.96	46.00	19.42	61.52	52.19	53.76	52.96	48.71

## 5 Conclusion

We have discussed the classification approach as a means for selecting appropriate and adequate candidates for parallel corpora alignment. Experimental results demonstrate the use of the classifiers on EN-PT, EN-FR and FR-PT language pairs under small, medium and large data conditions. Several insights are useful for distinguishing the adequate candidates from inadequate ones such as, lack (presence) of parallelism, spurious terms at translation ends and the base properties (similarity and occurrence frequency) of the translation pairs.

This work is motivated by the need for a system that evaluates the translation candidates automatically extracted prior to their submission for human

validation. Automatically extracted bilingual translations after human validation, are subsequently used for realigning parallel corpora and extracting new translations forming an indefinite cycle of iterations. Automatic classification prior to validation contributes to speed up the process of distinguishing the correct translations from naturally occurring alignment and extraction errors. The positive side effect is an enriched annotated lexicon suitable for machine learning systems such as bilingual morphology learning and translation suggestion tool, apart from its primary use as an aid in alignment, extraction and translation.

In future, the use of bilingual stem and suffix correspondences in classifying FR-PT and EN-FR word-to-word translations shall be studied [12]. Looking for coverage in word pairs might be cast as a morphological coverage problem that would enable us to classify word-to-word translations with high accuracy. Further, some experiments should be done on EN-FR and FR-PT using the suffix array based extractor [1]. Experiments must also be carried out to determine an optimal interval for the number of positive and negative bilingual lexicon entries in obtaining optimal classification results.

**Acknowledgments.** K. M. Kavitha and Luís Gomes acknowledge the Research Fellowship by FCT/MCTES with Ref. nos., SFRH/BD/64371/2009 and SFRH/BD/65059/2009, respectively, and the funded research project ISTRION (Ref. PTDC/EIA-EIA/114521/2009) that provided other means for the research carried out. The authors thank NOVA LINCS, FCT/UNL for providing partial financial assistance to participate in EPIA 2015, and ISTRION BOX - Translation & Revision, Lda., for providing the data and valuable consultation.

## References

1. Aires, J., Lopes, G.P., Gomes, L.: Phrase translation extraction from aligned parallel corpora using suffix arrays and related structures. In: Lopes, L.S., Lau, N., Mariano, P., Rocha, L.M. (eds.) EPIA 2009. LNCS, vol. 5816, pp. 587–597. Springer, Heidelberg (2009)
2. Aker, A., Paramita, M.L., Gaizauskas, R.J.: Extracting bilingual terminologies from comparable corpora. In: Proceedings of the 51st Annual Meeting for Computational linguistics, vol. 2, pp. 402–411 (2013)
3. Bergsma, S., Kondrak, G.: Alignment-based discriminative string similarity. In: Annual meeting-ACL, vol. 45, p. 656 (2007)
4. Brown, P.F., Pietra, V.J.D., Pietra, S.A.D., Mercer, R.L.: The mathematics of statistical machine translation: Parameter estimation. Computational linguistics **19**(2), 263–311 (1993)
5. Chen, B., Cattoni, R., Bertoldi, N., Cettolo, M., Federico, M.: The ITC-irst SMT system for IWSLT-2005, pp. 98–104 (2005)
6. Fraser, A., Marcu, D.: Measuring word alignment quality for statistical machine translation. Computational Linguistics **33**(3), 293–303 (2007)
7. Gomes, L.: Parallel texts alignment. In: New Trends in Artificial Intelligence, 14th Portuguese Conference in Artificial Intelligence, EPIA 2009, Aveiro, October 2009
8. Gomes, L., Pereira Lopes, J.G.: Measuring spelling similarity for cognate identification. In: Antunes, L., Pinto, H.S. (eds.) EPIA 2011. LNCS, vol. 7026, pp. 624–633. Springer, Heidelberg (2011)

9. Gusfield, D.: Algorithms on strings, trees, and sequences: computer science and computational biology. Cambridge Univ Pr., pp. 52–61 (1997)
10. Johnson, J.H., Martin, J., Foster, G., Kuhn, R.: Improving translation quality by discarding most of the phrasetable. In: Proceedings of EMNLP (2007)
11. Kavitha, K.M., Gomes, L., Lopes, G.P.: Using SVMs for filtering translation tables for parallel corpora alignment. In: 15th Portuguese Conference in Artificial Intelligence, EPIA 2011, pp. 690–702, October 2011
12. Kavitha, K.M., Gomes, L., Lopes, J.G.P.: Identification of bilingual suffix classes for classification and translation generation. In: Bazzan, A.L.C., Pichara, K. (eds.) IBERAMIA 2014. LNCS, vol. 8864, pp. 154–166. Springer, Heidelberg (2014)
13. Koehn, P., Hoang, H., Birch, A., Callison-Burch, C., Federico, M., Bertoldi, N., Cowan, B., Shen, W., Moran, C., Zens, R., et al.: Moses: open source toolkit for statistical machine translation. In: Proceedings of the 45th Annual Meeting of the ACL on Interactive Poster and Demonstration Sessions, pp. 177–180. ACL (2007)
14. Kutsumi, T., Yoshimi, T., Kotani, K., Sata, I., Isahara, H.: Selection of entries for a bilingual dictionary from aligned translation equivalents using support vector machines. In: Proceedings of PACLING (2005)
15. Lardilleux, A., Lepage, Y.: Sampling-based multilingual alignment. In: Proceedings of RANLP, pp. 214–218 (2009)
16. Levenshtein, V.I.: Binary codes capable of correcting deletions, insertions, and reversals. Soviet Physics Doklady **10**, 707–710 (1966)
17. Melamed, I.D.: Automatic evaluation and uniform filter cascades for inducing n-best translation lexicons. In: Proceedings of the Third Workshop on Very Large Corpora, pp. 184–198. Boston, MA (1995)
18. Och, F.J., Ney, H.: A systematic comparison of various statistical alignment models. Computational linguistics **29**(1), 19–51 (2003)
19. Och, F.J., Ney, H.: The alignment template approach to statistical machine translation. Computational Linguistics **30**(4), 417–449 (2004)
20. Sato, K., Saito, H.: Extracting word sequence correspondences based on support vector machines. Journal of Natural Language Processing **10**(4), 109–124 (2003)
21. Tian, L., Wong, D.F., Chao, L.S., Oliveira, F.: A relationship: Word alignment, phrase table, and translation quality. The Scientific World Journal (2014)
22. Tiedemann, J.: Extraction of translation equivalents from parallel corpora. In: Proceedings of the 11th NoDaLiDa, pp. 120–128 (1998)
23. Tomeh, N., Cancedda, N., Dymetman, M.: Complexity-based phrase-table filtering for statistical machine translation (2009)
24. Tomeh, N., Turchi, M., Allauzen, A., Yvon, F.: How good are your phrases? Assessing phrase quality with single class classification. In: IWSLT, pp. 261–268 (2011)
25. Vapnik, V.: The Nature of Statistical Learning Theory. Data Mining and Knowledge Discovery 1–47 (2000)
26. Vilar, D., Popovic, M., Ney, H.: AER: Do we need to “improve” our alignments? In: IWSLT, pp. 205–212 (2006)
27. Way, A., Hearne, M.: On the role of translations in state-of-the-art statistical machine translation. Language and Linguistics Compass **5**(5), 227–248 (2011)
28. Zens, R., Stanton, D., Xu, P.: A systematic comparison of phrase table pruning techniques. In: Proceedings of the 2012 Joint Conference on EMNLP and CoNLL, EMNLP-CoNLL 2012, pp. 972–983. ACL (2012)
29. Zhao, B., Vogel, S., Waibel, A.: Phrase pair rescoring with term weightings for statistical machine translation (2004)

# A SMS Information Extraction Architecture to Face Emergency Situations

Douglas Monteiro<sup>(✉)</sup> and Vera Lucia Strube de Lima

PUCRS, Faculdade de Informática, Programa de Pós-Graduação em Ciência da Computação, Porto Alegre, Brazil  
[dmmonteiro@gmail.com](mailto:dmmonteiro@gmail.com), [vera.strube@pucrs.br](mailto:vera.strube@pucrs.br)

**Abstract.** In disasters, a large amount of information is exchanged via SMS messages. The content of these messages can be of high value and strategic interest. SMS messages tend to be informal and to contain abbreviations and misspellings, which are problems for current information extraction tools. Here, we describe an architecture designed to address the matter through four components: linguistic processing, temporal processing, event processing, and information fusion. Thereafter, we present a case study over a SMS corpus of messages sent to an electric utility company and a prototype built with Python and NLTK to validate the architecture's information extraction components, obtaining Precision of 88%, Recall of 59% and F-measure (F1) of 71%. The work also serves as a roadmap to the treatment of emergency SMS in Portuguese.

**Keywords:** Information extraction · Short messages · Emergencies

## 1 Introduction

Currently, it is hard to imagine any line of business that does not use any textual information. Aside from the available content on the Internet, a large amount of information is generated and transmitted by computers and smartphones all over the world. Gary Miner *et al.* estimate that 80% of the information available in the world are in free text format and therefore not structured [7]. With such large amount of potentially relevant data, an information extraction system can structure and refine raw data in order to find and link relevant information amid extraneous information [3, 5]. This process is made possible by understanding the information contained in texts and their context, but this complex task face difficulties when processing informal languages, such as SMS messages or tweets [1, 6, 10].

Messages using the Short Message Service (SMS), as well as tweets, are widely used for numerous purposes, which makes them rich and useful data for information extraction. The content of these messages can be of high value and strategic interest, specially during emergencies<sup>1</sup>. Under these circumstances, the amount

<sup>1</sup> Also referred to as crisis events, disasters, mass emergencies and natural hazards by other researchers in the area.

of messages tends to increase considerably. However, users of these services write messages freely, with abbreviations, slangs and misspellings. Short messages tend to be brief, informal and to present similarities to speech.

In light of this, we propose an architecture to extract information from SMS messages exchanged during emergency situations. This Information Extraction architecture has as input a corpus of SMS messages and comprises four components: a linguistic processing component, a temporal processing component, an event processing component, and an information fusion component. The linguistic processing component preprocesses messages, handling with abbreviations and punctuation, sentence splitting, tokenization and stopword removal. The temporal processing component uses a set of rules and a list of temporal keywords to identify and classify temporal expressions. The event processing component is responsible for identifying events according to a set of domain-defined categories and provides additional information regarding situation awareness. As output, the architecture consolidates information so one can visualize strategic information in order to help the decision-making process. We built a prototype to validate the architecture and evaluated the information extraction taggers resulting in Precision of 88%, Recall of 59% and F-Measure (F1) of 71%.

This paper is organized in six sections, the first one being this introduction. In Section 2, we review related work on information extraction from short messages and its applications. In Section 3, we introduce the SMS information extraction architecture of messages sent during emergencies. Section 4 details the case study conducted to validate this architecture over a corpus built from SMS Messages sent by costumers to an electric utility company during emergencies. In Section 5, we discuss the evaluation performed over the prototype and the results obtained. Finally, in Section 6, we comment on challenges faced, as well as on future work.

## 2 Related Work

Corvey *et al.* introduce a system that incorporates linguistic and behavioral annotation on tweets during crisis events to capture situation awareness information [2]. The system filters relevant and tactical information intending to help the affected population. Corvey *et al.* collected data during five disaster events and created datasets for manual annotation. The authors linguistically annotated the corpus, looking for named entities of four types: person, name, organization and facilities. A second level of behavioral annotation assesses how community members tweet during crisis events. Tweets receive different and non-exclusive qualitative tags according to the type of information provided. Tweets containing situational awareness information are collected and tagged with macro-level (environmental, social, physical or structural) and micro-level (regarding damage, status, weather, etc.) information. The results indicated that, under emergencies, “users communicate via Twitter in a very specific way to convey information” [2]. Becoming aware of such behavior helped the framework’s machine learning classifier to achieve accuracy of over 83% using POS tags and bag of words. To classify location, they used Conditional Random Fields (CRFs)

with lexical and syntactic information and POS as features. The annotated corpus was divided into 60% for training and 40% for testing. They obtained an accuracy of 69% for the complete match and 86% for the partial match and recall of 63% for the complete match and 79% for the partial match.

Sridhar *et al.* present an application of statistical machine translation to SMS messages [11]. This research details on the data collection process and steps and resources used on a SMS message translation framework, which uses finite state transducers to learn the mapping between short texts and canonical form. The authors used a corpus of tweets as surrogate data and a bitext corpus from 40,000 English and 10,000 Spanish SMS messages, collected from transcriptions of speech-based messages sent through a smartphone application. Another 1,000 messages were collected from the Amazon Mechanical Turk<sup>2</sup>. 10,000 tweets were collected and normalized by removing stopwords, advertisements and web addresses. The framework processes messages segmented into chunks using an automatic scoring classifier. Abbreviations are expanded using expansion dictionaries and translated using a translation model based on sentences. The authors built a static table to expand abbreviations found in SMS messages, where a series of noisy texts have the corresponding canonical form mapped. For example, “4ever” is linked to the canonical form “forever”. Next, the framework segments phrases using an automatic punctuation classifier trained over punctuated SMS messages. Finally, the Machine Translation component uses a hybrid translation approach with phrase-based translation and sentences from the input corpus represented as a finite-state transducer. The framework was evaluated over a set of 456 messages collected in a real SMS interaction, obtaining a BLEU score of 31.25 for English-Spanish translations and 37.19 for Spanish-English.

Ritter *et al.* present TwiCAL, an open-domain event extraction and categorization system for Twitter [9]. This research proposes a process for recognizing temporal information, detecting events from a corpus of tweets and outputting the extracted information in a calendar containing all significant events. The authors focused on identifying events referring to unique dates. TwiCAL extracts a 4-tuple representation of events, including a named entity, an event phrase, and an event type. The authors trained a POS tagger and a NE tagger on in-domain Twitter data. To build an event tagger, they trained sequence models with a corpus of annotated tweets, and a rule-based system and POS to mark temporal expressions on a text. The open-domain event categorization uses variable models to discover types that match the data and discards incoherent types. The result is applied to the categorization of extracted events. The classification model is evaluated according to the event types created from a manual inspection of the corpus. The authors compared the results with a supervised Maximum Entropy baseline, over a set of 500 annotated events using 10-fold cross validation. Results achieved a 14% increase in maximum F1 score over the supervised baseline. A demonstration of the system is available at the Status Calendar webpage<sup>3</sup>.

---

<sup>2</sup> <https://www.mturk.com/>

<sup>3</sup> <http://statuscalendar.com>

Dai *et al.* present SoMEST (Social Media Event Sentiment Timeline), a framework for competitive intelligence analysis for social media and the architecture of a NLP tool combining NER, event detection and sentiment analysis [4]. This research presents an architecture to extract information from social media texts and the visualization of these information. The authors use Event Timeline Analysis (ETA) to detect events and display them in a timeline, highlighting trends or behaviors of competitors, consumers, partners and suppliers. Dai *et al.* also use Sentiment Analysis to measure human opinions from texts written in natural language, searching for the topic, its author, and if its a positive or negative opinion. The process comprises three phases: data collection, extraction and classification, and synthesis. From social media texts generated by customers, SoMEST focus on detecting events published from companies and opinions shared by customers. The extraction and classification phase consists of analyzing data and generating event extracts and opinion extracts, which are synthesized into a social media profile, unifying events and opinions linked to brands, services and products of a corporation into a period of time. The timeline displays a chronological order of the corporations events, the competitors events and changes in customers opinions.

Accordingly, as even IE systems built for different tasks may present similarities, we could understand common points in different IE architectures, mainly due to the nature of short text messages. From this learning, we could elaborate an information extraction architecture for SMS messages according to core components shared by most IE systems reviewed here, such as POS taggers, tokenization, and normalization, while adding other components to treat domain-specific characteristics.

### 3 SMS Information Extraction Architecture

SMS messages contain information that can be extracted, providing valuable resources to support decision-making under emergency situations. With this in mind, here, we detail the proposal for an architecture to extract information from messages under these circumstances. As seen in Figure 1, the proposed IE architecture takes as input a Corpus of SMS messages. Then, the linguistic processing component preprocesses each message and prepares them for Information Extraction. The temporal expression tagger component recognizes and tags all temporal information within the messages, while the event tagger identifies and tags domain-related events accordingly. The information fusion component displays the extracted information so as users of this system can interpret its results. The output of the system is the extracted information organized in a readable display, regarding the application. We detail each component in sections 3.1 to 3.4.

#### 3.1 Linguistic Processing Component

The linguistic processing component comprises a preprocessing module, including four steps: normalization, sentence splitting, tokenization, and stopword

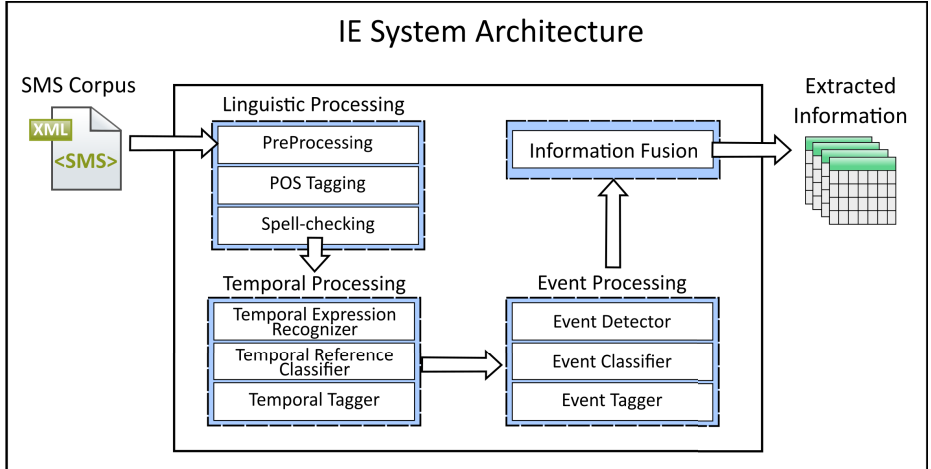


**Fig. 1.** IE Architecture overview

removal; and steps specifically designed for linguistic processing: POS tagging and spell-checking. The normalization step is responsible for adjusting the text while facing spelling variations, abbreviations, treating special characters and other features of the short message language. Next, the sentence splitting step divides each message into a list of sentences in order to process them individually. Every token is compared to a list of stopwords, which enables discarding unnecessary items and speeding up the process of information extraction.

Accordingly, the tokens are tagged with a part-of-speech tagger, which is trained with an annotated corpus of messages. The following step in the linguistic processing component comprises a Spell Checker, which makes use of an external dictionary to label untagged tokens and submits them to the POS tagger for revision. This component outputs a set of preprocessed sentences that serve as input for the temporal processing component.

### 3.2 Temporal Processing Component

The temporal processing component is responsible for applying regular expressions in order to identify temporal expressions related to events in SMS messages. Since temporal expressions are limited to a fixed set of syntactic patterns, most Temporal Expression Recognition systems make use of rule-based methods to recognize syntactic chunks [8].

Initially, the temporal expression recognizer uses a rule-based approach to identify variations of temporal references mentioned in the sentences. Despite the rule set being able to identify simple temporal expressions present in messages, rather complex expressions are still to be treated. For cases like “desde às 8h de domingo” (*since Sunday 8am*), the temporal expression recognizer counts on a list of temporal keywords, such as times of the day and days of the week to determine the extent of temporal expressions.

The temporal reference classifier analyzes the expression according to its lexical triggers and defines the type and value of the temporal expression. Finally, the component tags the temporal expression according to the TIMEX2 tag system provided by TimeML<sup>4</sup>.

### 3.3 Event Processing Component

The event processing component starts from the event detection step, which is responsible for finding relevant events in a sentence. This step counts on a set of rules to identify the event.

Since the proposed IE architecture aims to extract information from messages during emergencies situations, one can determine a certain set of categories of events to detect during this step. For instance, as discussed in Section 2, Corvey *et al.* proposed a situational awareness annotation level with the intention of understanding crisis events as a whole [2]. To address that matter, the authors define categories such as ‘Social Environment’, ‘Built Environment’ and ‘Physical Environment’. Each category has subcategories with specific information, such as ‘Crime’, ‘Damage’ or ‘Weather’.

Accordingly, in order to be executed, the event processing component requires a previous definition of a set of domain-related observable categories. Consequently, sentences that match any of these categories pass through a classification step which relates the event to the categories. This step makes use of a list of domain-related keywords. Then, the component can assign the correspondent tags to the event mention.

### 3.4 Information Fusion Component

This component groups and organizes all tagged information in a human understandable manner. All relevant information are “fused” to show the results of the IE application. As there may exist several ways to represent the results, this decision is linked to the intended purpose of their application. For instance, Ritter *et al.* [9], display their results in form of a calendar, where the respective events are shown. On the other hand, Dai *et al.* [4] present the Information Extraction results in a timeline, showing the progress of event mentions and the amount of associated opinions.

Given a set of tagged events and their corresponding temporal information, the relation between and event and when it occurred must be clearly expressed. An IE system built on this architecture must display the extracted information in a meaningful and relevant way to provide situation awareness and to aid decision-making during emergencies.

## 4 Case Study

In order to validate our proposal, we present a case study conducted over the IE Architecture. In this chapter, we detail our choices and decisions made.

---

<sup>4</sup> [http://www.timeml.org/site/publications/timeMLdocs/timeml\\_1.2.1.html](http://www.timeml.org/site/publications/timeMLdocs/timeml_1.2.1.html)

The input data for the process was organized from a set of 3,021 short messages received by an electric utility company. Clients notify the company when there is a power outage, sending short messages with the word “LUZ” (*light*) and the installation number (provided by the company). As observed in messages received, the company's clients use this communication channel to provide situation awareness information, which is currently not yet processed but could be of great help in services provision. It is important to extract information from these messages to deliver relevant and strategic information about emergencies so as to restore power to customers as quickly and safely as possible. The corpus was built in a XML format, comprising the messages and their delivery date. We split the corpus in a ‘learning corpus’, containing 2,014 messages; a ‘gold standard corpus’, containing 100 messages, to perform an evaluation of the prototypes taggers; a ‘test corpus’ to improve the prototype from the evaluation results.

We prototyped the architecture using Python<sup>5</sup> (version 2.7), mainly due to its ease of use, productivity and features for handling strings, lists, tuples and dictionaries, along with the Natural Language Toolkit (NLTK<sup>6</sup>) (version 3.0). NLTK provides some interesting features for Portuguese, like tokenizers, stemmers, Part-of-Speech taggers, and annotated corpora for training purposes. We highlight the main aspects of the components implementation as follows.

#### 4.1 Linguistic Processing

The component standardizes the text input. SMS messages contain many misspellings, as texters tend not to follow spelling and grammar rules, which led us to address this matter beforehand, covering the most common cases found on the learning corpus. Some variations are caused by different levels of literacy, besides idiosyncratic SMS language characteristics. In this step, we lowercased messages, removed commas, hyphens and special characters, such as ‘#’ and ‘@’, and unnecessary full stops, such as in zip codes or abbreviations. Each sentence undergoes a tokenization step, using whitespaces to mark word boundaries. The prototype uses `wordpunct_tokenize`<sup>7</sup> to split strings into lists of tokens. We built an external list containing 45 stopwords found on the learning corpus, as well as common word shortenings and phonetic abbreviations, such as “vc” and “q”.

The component uses MacMorpho<sup>8</sup>, a tagged training corpus with news in standard Brazilian Portuguese. However, the lack of a tagged corpus of texts in SMS language hampers the POS tagging step. Even though Normalization handles some misspellings, many words not written in standard Portuguese remain untagged. To address this matter, we used PyEnchant<sup>9</sup>, a spell checking library for Python, as a step to mitigate the spelling variation problem. We added the

---

<sup>5</sup> <https://www.python.org/>

<sup>6</sup> <http://www.nltk.org>

<sup>7</sup> <http://www.nltk.org/api/nltk.tokenize.html>

<sup>8</sup> <http://www.nilc.icmc.usp.br/macmorpho/>

<sup>9</sup> <https://pythonhosted.org/pyenchant>

Open Office<sup>10</sup> Brazilian Portuguese dictionary extension. The prototype only checks the spelling of untagged tokens. We also built an external list of domain-related words the POS tagger cannot resolve, like “transformador” (transformer) or “estouro” (burst), along with their corresponding POS tag, so the prototype can use this list to review untagged tokens.

## 4.2 Temporal Processing

Once tagged, messages proceed to temporal processing, which comprises the following steps: a Temporal Expression Recognizer, a Temporal Reference Classifier and a Temporal Tagger. There are two external resources associated with the component: a set of regular expressions and a list of lexical triggers.

From a linguistically processed message containing a time anchor, the Temporal Expression Recognizer must be able to identify and extract existing temporal information. For instance, the duration of an event, such as a power outage, may be of great importance to indicate the severity of the problem. A client may inform the existence of a natural disaster that causes a blackout that lasts for hours and affects an entire region.

We found many variations for the same temporal information like ‘10:30’, ‘10h30’, ‘10h30min’, and so on. In light of this, we resorted to a rule-based matcher, which relies on a set of regular expressions. Moreover, we added rules to identify days of the week and times of the day.

Since incoming messages express ongoing situations, the existing temporal expressions refer to past or present events. In order to identify more complex expressions like “desde ontem às 14h” (*since yesterday 2pm*), we built a list of lexical triggers, containing the most common temporal keywords found in the learning corpus and their corresponding TIMEX2 value, such as “ontem” (*yesterday*) with value ‘-1D’ (minus one day) and “noite” (*night*) with a time modifier ‘NI’. Tokens that correspond to words in the list are considered part of a temporal expression.

Each tagged temporal expression can contain a value and a modifier, according to its type, which, along with a time anchor (the delivery date), allows us to determine the beginning or duration of an event. For instance, the lexical trigger “amanhã” (*tomorrow*) has a type DATE and value ‘1D’, indicating one day must be added to the time anchor to determine the TIMEX value. The Temporal Expression Classifier verifies the list of lexical triggers to determine modifiers and values of each expression, considering first lexical triggers expressing largest periods of time. Duration expressions have precedence over dates and dates have precedence over times. Finally, the Tagger groups values and modifiers in a single form and assigns the corresponding time tag to the TEs.

## 4.3 Event Processing Component

To detect events, we focused on a verb-triggered rule-based approach to identify specific features that may be useful in the context, considering the urgency of

---

<sup>10</sup> <http://www.openoffice.org/>

the messages. From understanding the verb, its meaning and accessories, one can determine the structure of the sentence of which it is part. The prototype considers sentences in the following structure: Noun Phrase + Verb + Object. Both the Noun phrase and the Object can play semantic roles of agent and patient.

The prototype iterates through sentences looking for POS tags assigned during the linguistic processing in order to find verbs. After, the Event Detection step marks the boundaries of the event mention by greedy searching for nouns, prepositions, noun compounds, adjectives or pronouns on the surroundings of the verb. Verbs interspersed with other POS tags mark different event mentions, while adjectives and nouns (or noun compounds) mark the boundaries of event mentions.

Next, the prototype classifies the detected events. Through an extensive study of the learning corpus, we observed how clients communicate during emergencies as well as what they notify. Then, we listed the most relevant events and related words we found whilst defining the annotation standard. We defined three non-mutually exclusive categories of events, according to the observed events and thirteen notification types to provide situation awareness information. “Instalação” refers to messages containing information regarding the consumer unit (electrical installation), such as power outages, voltage drops and instabilities. “Rede” groups information about the electrical grid status and its components, such as short circuits or fallen utility poles. “Ambiente” comprises information regarding the environment that might affect the electrical grid, like fallen trees, storms and lightnings.

To properly classify the event, we split sentences and analyze separately noun phrases, verbs and objects, searching for domain-related words. The component depends on a list built from 83 words related to the notification types, collected from sources such as Dicionário Criativo<sup>11</sup> and Wordnet<sup>12</sup>. For instance, the sentence “caiu uma arvore na rede” (a tree fell over the power grid), is divided in two phrases: “caiu” (verb), and “uma arvore em rede” (object). Once verified, the Event Classifier considers that while the verb does not determine a notification type, the object notifies a notification type “Queda de Árvore”, due to the presence of the words “arvore” and “rede”. Finally, the Tagger groups all the information in a set of tags, according to its categories and notification types.

#### 4.4 Information Fusion

Once the information are already tagged, one can use different approaches to visualize and understand such data. Being aware of other possibilities that could be explored in a more extended study, we generated charts from tagged messages and their corresponding notification types, allowing the visualization of the application of the proposed model.

---

<sup>11</sup> <http://dicionariocriativo.com.br/>

<sup>12</sup> <http://wordnetweb.princeton.edu/>

We exported the output of the prototype to a spreadsheet containing messages and their corresponding notification types. Structured information can be more easily manipulated, in order to speed up the recognition and attendance of occurrences with more situation awareness.

## 5 Evaluation and Discussion

In order to evaluate the prototype's taggers, we elaborated a three-step plan comprising: confirming the model of categories and notification types; providing a gold standard - a manually annotated corpus considered as "definitive answer"; and comparing the prototypes results to the gold standard. Furthermore, we assessed the results of the Information Fusion component over the gold standard and the test corpus.

As some answers shall be provided by domain experts, we invited three judges with domain knowledge. They opined on the model of categories of events and temporal expressions and evaluated a set of 100 SMS according to this model. From their answers, we have composed the gold standard and compared it to the output of the IE prototype and obtained precision of 88%, recall of 59% and F-measure (F1) of 71%.

The prototype correctly identified relevant events, with 125 true positives over 16 false positives and 84 false negatives. The results indicate that the set of defined rules is accurate while detecting the events and temporal information mentioned in the gold standard corpus. However, a low recall score alerts us that there are other events, domain-related words and temporal information still uncovered by the model created.

Table 1 shows the hit percentage of the prototype when compared to the Gold Standard, as well as the amount of notifications found in the corpus. The prototype could not resolve mentions to "Wind" and "Rain" events. Analyzing the messages in the gold standard, we can see that some event mentions were not detected by the prototype as they omit verbs, like in "toda nossa comunidade sem luz devido muita chuva ventos fortes" (*our entire community without electricity because of a lot of rain and strong winds*). There were also problems in

**Table 1.** Hit Percentage by information type

Extracted Information	Prototype	Gold Standard	Percentage
Temporal Information	24	27	89%
Power Outage	86	88	98%
Downed Power Line	7	32	22%
Short Circuit	3	5	60%
Broken Power Pole	4	10	40%
Power Line Fire	5	7	71%
Fallen Tree	5	12	42%
Wind	0	4	0%
Rain	0	2	0%

differentiating “está” (*is*) and its popular contraction “tá” (absent in the training corpus) from “esta” (*this*) which compromised the detection of some events.

The temporal processing component behaved well over the gold standard. In fact, in one of the evaluated messages, the component tagged “15 minutos” (15 minutes) as a temporal expression, while the judges did not recognize it, showing that this understanding is not clear even for humans.

## 6 Considerations

During emergencies, any detail can help services provision. For that matter, SMS messages can be an important source of valuable information, as it is one of the most widely used means of communication. However, SMS messages are usually written in a proper language containing abbreviations, slangs and misspellings, which hamper their processing in their context of operation.

As observed in Section 2, even IE systems built for different tasks may present similarities. From this learning, we could propose an architecture for information extraction from SMS messages according to core components shared by most IE systems reviewed, while adding other components to treat domain-specific characteristics. The architecture comprises a linguistic processing component, which prepares messages for information extraction; a temporal processing component, which identifies and tags existing temporal information within messages; an event processing component, which detects and classifies events according to a list of domain-related categories; and an information fusion component that interprets information and displays them in a human-understandable manner.

To validate the architecture, we conducted a case study over a corpus of SMS messages sent to an electric utility company. We studied how users communicate during emergencies and defined categories of information that could aid services provision. We validated the architecture against a gold standard corpus built with the assistance of judges with domain knowledge. Among the tagging stages, we established a degree of severity (varying from 1 to 5) to distinguish the categories of events. We assessed the range of scores given by the judges, resulting in a kappa coefficient of 0.0013, *i.e.*, a poor level agreement, which led us to use fewer severity degrees.

As, to the best of our knowledge, there is no architecture to address this matter, especially for the Portuguese language, we expect this proposal to bring focus to this area and encourage other researchers to contribute to its improvement. IE systems built on this architecture may attend other electric utility companies or address other types of disasters or emergencies and other short messages, such as tweets. As improvement opportunities unveiled, we could mention resorting to a more appropriate tagged corpus trained over the SMS language. Such resource would decrease the number of untagged tokens, which in turn would increase the accuracy of the event detection step. However, to the present, we do not know of the existence of such resource for the Portuguese language.

For future work, we intend to continue our research, revising the Case Study results, and refine the prototype according to other approaches, such as machine

learning to automatize the categories definition step. Envisaged features comprise adding named entity recognition towards gathering geographic information, which was not considered during this stage of our work, but can be of great importance for services provision. Moreover, we intend to use temporal expressions to determine the start and duration of detected events. We will also assess the information fusion component results as well as alternatives to enhance it.

## References

1. Bernicot, J., Volckaert-Legrier, O., Goumi, A., Bert-Erboul, A.: Forms and functions of SMS messages: A study of variations in a corpus written by adolescents. *Journal of Pragmatics* **44***12*, 1701–1715 (2012)
2. Corvey, W.J., Verma, S., Vieweg, S., Palmer, M., Martin, J.H.: Foundations of a multilayer annotation framework for twitter communications during crisis events. In: 8th International Conference on Language Resources and Evaluation Conference (LREC), p. 5 (2012)
3. Cowie, J., Lehnert, W.: Information extraction. *Communications of the ACM* **39***1*, 80–91 (1996)
4. Dai, Y., Kakkonen, T., Sutinen, E.: SoMEST: a model for detecting competitive intelligence from social media. In: Proceedings of the 15th International Academic MindTrek Conference: Envisioning Future Media Environments, pp. 241–248 (2011)
5. Jurafsky, D., Martin, J. H.: Speech and language processing, 2nd edn. Prentice Hall (2008)
6. Melero, M., Costa-Juss, M.R., Domingo, J., Marquina, M., Quixal, M.: Holaaa!! writin like u talk is kewl but kinda hard 4 NLP. In: 8th International Conference on Language Resources and Evaluation Conference (LREC), pp. 3794–3800 (2012)
7. Miner, G., Elder, J.I., Hill, T., Nisbet, R., Delen, D.: Practical Text Mining and Statistical Analysis for Non-structured Text Data Applications. Elsevier, Burlington (2012)
8. Pustejovsky, J., Stubbs, A.: Natural Language Annotation for Machine Learning. O'Reilly Media, Inc. (2012)
9. Ritter, A., Etzioni, O., Clark, S., et al.: Open domain event extraction from twitter. In: Proceedings of the 18th ACM SIGKDD International Conference on Knowledge Discovery and Data Mining, pp. 1104–1112 (2012)
10. Seon, C.-N., Yoo, J., Kim, H., Kim, J.-H., Seo, J.: Lightweight named entity extraction for korean short message service text. *KSII Transactions on Internet and Information Systems (TIIS)* **5**–**3**, 560–574 (2011)
11. Sridhar, V.K.R., Chen, J., Bangalore, S., Shacham, R.: A Framework for translating SMS messages. In: Proceedings of COLING 2014, the 25th International Conference on Computational Linguistics: Technical Papers, pp. 974–983 (2014)

# Cross-Lingual Word Sense Clustering for Sense Disambiguation

João Casteleiro, Joaquim Ferreira da Silva<sup>(✉)</sup>, and Gabriel Pereira Lopes

NOVA LINCS FCT/UNL, 2829-516 Caparica, Portugal  
casteiroalves@gmail.com, {jfs,gpl}@fct.unl.pt

**Abstract.** Translation is one of the areas where word disambiguation must be solved in order to find out adequate translations for such words in the contexts where they occur. In this paper, a Word Sense Disambiguation (WSD) approach using Word Sense Clustering within a cross-lingual strategy is proposed. Available sentence-aligned parallel corpora are used as a reliable knowledge source. English is taken as the source language, and Portuguese, French or Spanish as the targets. Clusters are built based on the correlation between senses, which is measured by a language-independent algorithm that uses as features the words near the ambiguous word and its translation in the parallel sentences, together with their relative positions. Clustering quality reached 81% (V-measure) and 92% (F-measure) in average for the three language pairs. Learned clusters are then used to train a support vector machine, whose classification results are used for sense disambiguation. Classification tests showed an average (for the three languages) F-measure of 81%.

**Keywords:** Word Sense Disambiguation · Clustering · Parallel corpora · V-measure · F-measure · Support vector machine

## 1 Introduction

Word sense ambiguity is present in many words no matter the language, and translation is one of the areas where this problem is important to be solved. So, in order to select the correct translation, it is necessary to find the right meaning, that is, the right sense, for each ambiguous word. Although multi-word terms tend to be semantically more accurate than single words, multiword terms may also have some ambiguity, depending on the context.

Thus, a system for automatic translation, for example, from English to Portuguese, should know how to translate the word *bank* as *banco* (an institution for receiving, lending, exchanging and safeguarding money), or as *margem* (the land alongside or sloping down to a river or lake). As the efficiency and effectiveness of a translation system depends on the meaning of the text being processed, disambiguation will always be beneficial and necessary.

Approaches to tackle the issue of WSD may be divided in two main types: the supervised and the unsupervised learning. The former requires semantically

tagged training data. Although supervised approaches can provide very good results, the need for tagging may become a limitation: semantic tagging depends on more or less complex approaches and it may occur that tagging is not possible for some languages; and POS-tagging, if used, needs good quality taggers that may not exist for some languages. On the other hand, by working with untagged information, unsupervised approaches are more easily language-independent. However, the lack of tags may be a limitation to reach the same level of results as those achieved by supervised approaches.

One way to work around the limitations of both supervised and unsupervised approaches, keeping their advantages, is the use of a hybrid solution. We propose the use of a reliable and valid knowledge source, automatically extracted from sentence-aligned untagged bilingual parallel corpora.

In this paper we present a cross-lingual approach for Word Sense Clustering to assist automatic and human translators on translation processes when faced with expressions which are more complex, more ambiguous and less frequent than general. The underlying idea is that the clustering of word senses provides a useful way to discover semantically related senses, provided that each cluster contains strongly correlated word senses. To achieve our target we propose a semi-supervised strategy to classify words according to their most probable senses. This classification uses a SVM classifier which is trained by the information obtained in the process of the sense clustering. Clusters of senses are built according to the correlation between word senses taking into account the combinations of their neighbor words and the relative position of those neighbor terms; those combinations are taken as features, which are automatically extracted [1] from a sentence-aligned parallel corpora.

## 2 Related Work

Several studies that combine clustering processes with word senses and parallel corpora has been assessed by several authors in the past years. In [3], the authors present a clustering algorithm for cross-lingual sense induction that generates bilingual semantic resources from parallel corpora. These resources are composed by the senses of words of one language that are described by clusters of their semantically similar translations in another language. The authors proved that the integration of sense-clusters resources leads to important improvements in the translation process. In [4], the authors proposed an unsupervised method for clustering translations of words through point-wise mutual information, based on a monolingual and a parallel corpora. Comparing the induced clusters to reference clusters generated from WordNet, they demonstrated that their method identifies sense-based translation clusters from both monolingual and parallel corpora.

Brown et al. described in [5] a statistical technique for assigning senses to words based on the context in which they appear. By incorporating this method in a machine translation system, a significant reduction of the translation error rate was achieved. In [7], Diab addresses the problem of WSD from a multilingual

perspective, expanding the notion of context to encompass multilingual evidence. Given a parallel corpus and a sense inventory for one of the languages in the corpus, an approach to resolve word sense ambiguity in natural language was proposed. In [15], the authors present a method that exploits word clustering based on automatic extraction of translation equivalents, supported by available aligned wordnets. Apidianaki in [2] described a system for SemEval-2013 Cross-lingual WSD task, where word senses are represented by means of translation clusters in a cross-lingual strategy. The WSD method clusters the translations of target words in a parallel corpus using source language context vectors. These vectors are exploited in order to select the most appropriate translations for new instances of the target words in context.

With the goal of increasing the accuracy of WSD systems when faced with expressions that are more complex, ambiguous and less frequent than general, we propose the extension and changes of several works in the field [2–5, 7, 15]. It has differences from those mentioned above, since specific and validated bilingual lexicons, automatically extracted, are used to provide neighbor contexts enabling the calculation of the statistical correlation between senses, which is the basis to build sense clusters, therefore being a language independent approach.

### 3 System Description

#### 3.1 Dataset

The experiments performed to support the research presented in this article comply with the datasets presented in Table 1.

**Table 1.** Datasets of ambiguous words and possible senses for English-Portuguese (EN-PT), English-French (EN-FR) and English-Spanish (EN-SP)

Dataset	Source-Words (Ambiguous)	Target-Words (Senses)
EN-PT	15	94
EN-FR	15	70
EN-SP	15	83

Thus, by Table 1 we see that in the experiments performed to support this research, we used, for example, 15 English ambiguous words that could be translated in 94 different Portuguese words, each one having a meaning, that is a sense.

#### 3.2 The Gathering of Word Senses

The gathering of word senses consists of extracting meanings of words for a given ambiguous word. For this, we use the *ISTRION* (EN-PT; EN-FR; EN-SP) lexicon, which is a bilingual and strongly validated data source, resultant from

the project *ISTRION*<sup>1</sup>. This lexicon contains 810.000 validated entries for the English-Portuguese language pair, 380.000 for the English-French and 290.000 for the English-Spanish one. This knowledge was automatically extracted and manually validated. For each ambiguous word in the source language (eg. English) we get all different senses existing in the target language (eg. Portuguese, French, Spanish) by consulting the bilingual lexica database; see tables 2 and 3 containing an example for Portuguese and French respectively. These tables show a set of different senses for the same English word “sentence”, each one expressed in a word in the target language. According to the content of each table, the reader may predict that the senses could be divided in two semantically different groups (clusters): those signed with a “\*”, which are related to textual units; and those with a “+”, related to Court resolutions. Thus, one of the purposes of this approach is to build clusters of senses according to the semantic closeness among word senses.

**Table 2.** Example of the different senses for the ambiguous word “sentence” concerning the translation to Portuguese. Senses signed with a “\*” are textual units of one or more words. Those signed with a “+” are related to Court resolutions

Ambiguous Word (English)	Sense (Portuguese)
sentence	oração ( <i>clause</i> ) *
sentence	expressão ( <i>expression</i> ) *
sentence	frase ( <i>phrase</i> ) *
sentence	sentença ( <i>sentence</i> ) +
sentence	pena ( <i>penalty</i> ) +
sentence	condenação ( <i>condemnation</i> ) +

**Table 3.** Example of the different senses for the ambiguous word “sentence” concerning the translation to French. Senses signed with a “\*” are textual units of one or more words. Those signed with a “+” are related to Court resolutions

Ambiguous Word (English)	Sense (French)
sentence	condamnation ( <i>condemnation</i> ) +
sentence	jugement ( <i>sentence</i> ) +
sentence	phrase ( <i>phrase</i> ) *
sentence	peine ( <i>penalty</i> ) +
sentence	condamner ( <i>condemn</i> ) +

### 3.3 Feature Extraction

According to the authors in [10], local context features with bilingual words evidence starts from the assumption that incorporating knowledge from more than

<sup>1</sup> <http://citi.di.fct.unl.pt/project/project.php?id=97>

one language into the feature vector will be more informative than only using monolingual features . By using a sentence-aligned parallel corpora, the proposal we present in this paper confirms this principle. Thus, we use a sentence-aligned parallel corpora (composed by Europarl<sup>2</sup> and DGT<sup>3</sup>), from which we extract features from the neighbor context of the target pair (Ambiguous Word) \t (Sense N) that fall within a window of three words to the left and three words to the right of each word of the pair, discarding stop-words. Each target pair has a set of features where each one is a combination of one of the words in the window and its relative position. For a better understanding, let us take the example of the target pair “sentence” – “frase” and one of the sentence-pairs containing it, retrieved from the bilingual parallel corpora (EN \t PT): *Besides being syntactically well-formed, the sentence is correctly translated* \t *Para além de estar sintaticamente bem formada, a frase está corretamente traduzida.* Thus, the context words of the target pair “sentence” – “frase” in this sentence-pair are “Besides”, “syntactically”, “well-formed”, “correctly”, “translated”, “sintaticamente”, “bem”, “formada”, “corretamente” and “traduzida”, taking into account the limits of the window (three words to the left and three words to the right of each word of the pair). Following this, the corresponding features include a tag indicating the language and the relative position of the context word to the corresponding word of the target pair: “enL3\_Besides”, “enL2\_syntactically”, “enL1\_well-formed”, “enR1\_correctly”, “enR2\_translated”, “ptL3\_sintaticamente”, “ptL2\_bem”, “ptL1\_formada”, “ptR1\_corretamente” and “ptR2\_traduzida” —Recall that stop-words are discarded. “L” and “R” stands for Left and Right respectively.

However, for each target pair, there are usually several sentence-pairs retrieved from the bilingual parallel corpora (EN \t PT), containing that target pair. This means that probably several contexts will neighbor the same target pair, generating several features. In our approach, everytime a feature occurs in a sentence-pair, its frequency is incremented for the corresponding target pair. In other words, taking the feature “enL2\_syntactically”, it may have for example: 3 occurrences for target pair “sentence” – “frase” (meaning that the word “syntactically” occurs 2 positions left to the target word “sentence”, in 3 of the sentence-pairs containing this target pair); 2 occurrences for “sentence” – “oração”; 0 occurrences for “sentence” – “ pena”, etc..

We consider that, there is a tendency such that, the closer the relative position of the context word to the target word, the stronger the semantic relation between both words. So, in this approach a different importance is assigned to each feature, according to their relative positions. Thus, we use the criterion we called  $\sqrt[p]{f}$ , that is: for features whose relative position is  $p$ , the root of degree  $p$  is applied to frequency  $f$ , which is the number of times the feature occurs in the set of sentence-pairs containing the target pair. This criterion was chosen empirically as it showed good results after some experiments. Table 4 shows part of the feature extraction concerning the ambiguous word “sentence”.

---

<sup>2</sup> <http://www.statmt.org/europarl/>

<sup>3</sup> <http://ipsc.jrc.ec.europa.eu/?id=197>

**Table 4.** Feature extraction for the target pairs concerning the ambiguous word “sentence” (only a small part is shown)

Sense	Feature	Frequency	Final Assigned Value
oração	...	...	...
...	...	...	...
expressão	...	...	...
...	...	...	...
frase	enL3_Besides	1	$\sqrt[3]{1}$
frase	enL2_syntactically	3	$\sqrt{3}$
frase	enL1_well-formed	2	2
frase	enR1_correctly	3	3
frase	enR2_translated	3	$\sqrt{3}$
frase	ptL3_sintaticamente	2	$\sqrt[3]{3}$
frase	ptL2_bem	4	$\sqrt{4}$
frase	ptL1_formada	3	3
frase	ptR1_corretamente	2	2
frase	ptR2_traduzida	3	$\sqrt{3}$
frase	...	...	...
sentença	...	...	...
...	...	...	...
pena	...	...	...
...	...	...	...
condenação	...	...	...
...	...	...	...

For reasons of space, only values for some features of one of the target pairs (“sentence” – “frase”) are shown. Values in column *Final Assigned Value* contain the result of the application of  $\sqrt[3]{f}$  criterion on the values of column *Frequency*.

The information contained in all columns of Table 4, except *Frequency*, form a matrix which is the base for obtaining the Word Sense Clustering concerning the ambiguous word “sentence”. At the end of the feature extraction task we obtained 15 matrices per language pair, corresponding to each of the 15 ambiguous words used, as referred in Table 1.

### 3.4 Feature Reduction by Sense Correlation

As we have seen in the previous subsection, the number of features associated to each ambiguous word tend to be huge when compared to the number of senses which may correspond to just a few words as in the case of tables 2 and 3. So, considering the purpose of clustering the senses, we transform each of the previously obtained matrices into a new and more compact matrix of correlations (similarities) between each pair of senses. This is a  $N \times N$  symmetric matrix where  $N$  is the number of senses of the ambiguous word. Each line of this matrix corresponds to one of the senses now characterized by the correlation

between that sense and each of the  $N$  senses. Each correlation is given by (1), which is based on the Pearson's correlation coefficient.

$$\text{Corr}(S_i, S_j) = \frac{\text{Cov}(S_i, S_j)}{\sqrt{\text{Cov}(S_i, S_i)} \times \sqrt{\text{Cov}(S_j, S_j)}} \quad (1)$$

$$\text{Cov}(S_i, S_j) = \frac{1}{\|\mathcal{F}\| - 1} \sum_{F \in \mathcal{F}} \left( (f(S_i, F) - f(S_i, .)) \times (f(S_j, F) - f(S_j, .)) \right) \quad (2)$$

where  $F$  is an element of the feature set  $\mathcal{F}$  and  $f(S_i, F)$  stands for the *Final Assigned Value* (a column of Table 4) of feature  $F$  for sense  $S_i$ ;  $f(S_i, .)$  gives the average *Final Assigned Value* of the features for sense  $S_i$ , which is given by (3).

$$f(S_i, .) = \frac{1}{\|\mathcal{F}\|} \sum_{F \in \mathcal{F}} f(S_i, F) \quad (3)$$

Correlation given by (1) measures how semantically close are senses  $S_i$  and  $S_j$ . However, a qualitative explanation for this can be given through (2), rather than by (1). Thus, (2) shows that, for each feature  $F$ , two deviations are taken: one is given by the *Final Assigned Value* of feature  $F$  for sense  $S_i$ , subtracted from the average *Final Assigned Value* for  $S_i$ , that is,  $f(S_i, F) - f(S_i, .)$ ; the other one is obtained by the *Final Assigned Value* of the same feature  $F$  for sense  $S_j$ , subtracted from the average *Final Assigned Value* for  $S_j$ , that is,  $f(S_j, F) - f(S_j, .)$ . If both deviations have the same algebraic sign (+/−), the product will be positive, which means that both senses present *similar deviations* concerning feature  $F$ . And, if positive products happen for most of features resulting in high values, then there will be a strong positive covariance value ( $\text{Cov}(S_i, S_j)$ ), and therefore, a high correlation ( $\text{Corr}(S_i, S_j)$ ) — notice that (1) has the effect of just standardizing  $\text{Cov}(S_i, S_j)$  values, ranging from -1 to +1.

Still analyzing (2), if the partial sum of the positive products has a similar value to the partial sum of the negative ones (when deviations are contrary), then the correlation is close to 0, which means that the semantic closeness between both senses is very weak (or even null). In other words,  $\text{Corr}(S_i, S_j)$  gives close to +1 values, meaning a high correlation, when both senses tend to occur in the same contexts. If one of the senses occur in contexts where the other sense never occurs, and vice versa, then there is a negative correlation between them.

### 3.5 Finding Clusters

Our goal is to join similar senses of the same ambiguous word in the same cluster, based on the correlation matrix obtained as explained in Subsec. 3.4. To

create clusters we used the *WEKA* tool [8] with *X-means* [12] algorithm. With *X-means* the user does not need to supply the number of clusters, contrary to other clustering algorithms such as *k*-means or *k*-medoids. The algorithm returns the best solution for the correlation matrix presented as input. As a matter of fact, for the example of the ambiguous word “sentence”, regarding the Portuguese as the target language, it assigned the words “oração”, “expressão”, and “frase” to a cluster, while “pena” and “condenação” were assigned to another one. In other words, it returned the results expected that were presented in Table 2. With respect to the possible translations of the same ambiguous word “sentence” to French, the clusters were correctly formed too, according to the expected distribution shown in Table 3.

The results of the clustering phase for all ambiguous words gave rise to the evaluation presented in tables 5, 6 and 7.

## 4 Experiments and Results

### 4.1 Evaluation of the Clusters

In order to determine the consistency of the obtained clusters, all of them will be evaluated with V-measure and F-measure. V-measure introduces two criteria presented in [14]: homogeneity ( $h$ ) and completeness ( $c$ ). A clustering process is considered homogeneously well-formed if all of its clusters contain only data points which are members of a single class. Comparatively, a clustering result satisfies completeness if all data points that are members of a given class are elements of the same cluster. So, increasing the homogeneity of a clustering solution often results in decreasing its completeness. These two criteria run roughly in opposition. This measure will be used to evaluate the resulting clusters. The value of homogeneity varies between 1 and 0. In the perfectly homogeneous case, the homogeneity is 1. In an imperfect situation, it is 0, which happens when the class distribution within each cluster is equal to the overall class distribution.

Similarly to determination of the homogeneity, the results of the completeness also vary between 1 and 0. In the perfectly complete case, it is 1. In the worst case scenario, each class is represented by every cluster with distribution equal to the distribution of cluster sizes; consequently completeness is 0. V-measure is thus a measure for evaluating clusters, which studies the harmonic relationship between homogeneity and completeness. It is given by  $V\beta$  (see (4)) where  $\beta = 1$ , which is a value usually used. V-measure values varies between 1 and 0.

$$V\beta = \frac{(1 + \beta) \times h \times c}{(\beta \times h) + c} \quad F\beta = \frac{(1 + \beta)^2 \times Precision \times Recall}{(\beta^2 \times Precision) + Recall} \quad (4)$$

To establish a comparison between different criteria of clusters evaluation, we also compute F-measure [13], given by  $F\beta$  (see (4)) where  $\beta = 1$ , which is also a frequently used measure. As it is shown, this well known metric is based on both Precision and Recall measures. In this context, Precision is determined according

**Table 5.** English-Portuguese sense-clusters evaluation

Ambiguous Word	V-measure (Portuguese)	F-measure (Portuguese)
plant	1.0	1.0
train	0.81	0.96
motion	1.0	1.0
general	1.0	1.0
fair	0.45	0.81
sentence	1.0	1.0
cold	0.91	0.98
chair	1.0	1.0
break	0.51	0.86

**Table 6.** English-Spanish sense-clusters evaluation

Ambiguous Word	V-measure (Spanish)	F-measure (Spanish)
heart	1.0	1.0
plant	1.0	1.0
joint	1.0	1.0
motion	0.62	0.89
train	1.0	1.0
right	0.43	0.80
chair	1.0	1.0
sentence	1.0	1.0
break	0.51	0.86

to the following procedure: for each sense-cluster of a clustering, Precision is given by the size of the largest semantic group of senses contained in the cluster (the number of True Positives), divided by the size of the cluster (the sum of True Positives and False Positives); the average Precision of the clusters gives the Precision of the clustering. In order to calculate Recall, for each cluster of a clustering, this measure is given by the same number of True Positives, divided by the real size of the corresponding semantic group of senses (the sum of True Positives and False Negatives); the average Recall of the clusters is taken as the Recall of the clustering. As V-measure, F-measure also varies between 0 and 1, being the former the worst scenario and the latter the optimal.

Due to lack of space, tables 5, 6 and 7 contain the results of subset samples of the clusterings obtained for each of the 15 ambiguous English words regarding each target language. These tables show good results for sense-clusters for Portuguese, Spanish and French language, getting average V-measure and F-measure values of 0.81 and 0.92, respectively. Values tend to be higher for F-measure criterion. Tables also show that a significant part of the clustering were perfectly formed, that is, V-measure = 1.0 and F-measure = 1.0.

**Table 7.** English-French sense-clusters evaluation

Ambiguous Word	V-measure (French)	F-measure (French)
plant	1.0	1.0
motion	0.62	0.90
train	1.0	1.0
heart	0.51	0.86
joint	1.0	1.0
tank	1.0	1.0
fair	0.56	0.88
break	1.0	1.0
cold	0.62	0.90

However, for some target pairs existing in the bilingual lexica database, there were very few occurrences in the sentence-aligned parallel corpora, which prevents the accurate calculation of the correlation between senses. This is the reason why clustering results are relatively poor for some ambiguous words: for example “motion” for English-French and English-Spanish, among others, as shown in tables 5, 6 and 7.

#### 4.2 Classification — Assigning Sense Clusters to Ambiguous Words

To accomplish the classification process, potentially ambiguous sentences (containing ambiguous words) were extracted from a corpora that were not used in the learning stage, totaling 96 expressions. The purpose is to determine how the disambiguation system behaves when faced with a set of potentially ambiguous sentences. The classification task usually involves the use of two separate training and testing sets. The training phase is closely related with the stage of clustering achieved previously, since we used the acquired knowledge from clusters to train the system. Each cluster is encoded by the presence or absence of all features that belong to all clusters related with a particular ambiguous word, and a *target value* (i.e. the class label) corresponding to the sense cluster. In what concerns to the testing phase, our goal is to encode each testing sentence, extracted from a corpora which was not used in the training phase, and confront it with the training set. So, since each ambiguous word was taken to be translated to a target language, to encode each expression we analyze the presence or absence in the sentence of just the features from English used in the training set.

The classifier used was a support vector machine (LIBSVM) [6] with the Radial Basis Function (RBF) as kernel type, that allow to handle the case when the relation between class labels and attributes is non-linear.

#### 4.3 Classification Results

The results obtained with the application of SVM classifier were evaluated using F-measure [13], again given by  $F\beta$  (see (4)) where  $\beta = 1$ . All 96 ambiguous

sentences (containing ambiguous words) were classified and so, F-measure were calculated regarding each target language, as shown in Table 8. The fact that F-measure for French and Spanish did not reach the same value as for Portuguese (0.79 vs 0.85) is probably due to the fact that the EN-PT language pair lexicon used in the clustering process was considerably larger (810,000 entries) than the ones used for the other two language pairs (380,000 and 290,000), implying therefore a *better quality* training phase for that pair.

In order to have a baseline for comparison, the same tests described above were performed using the output of GIZA++ alignments on DGT [11], where the most probable sense is used to disambiguate each sentence: the results obtained were 0.43, 0.38 and 0.38 respectively for EN-PT, EN-FR and EN-SP pairs.

**Table 8.** Results for the assignment of sense-clusters to ambiguous words

Target Language	F-measure
French	0.79
Portuguese	0.85
Spanish	0.79

## 5 Conclusions and Future Work

In this paper, a language-independent WSD approach using Word Sense Clustering was proposed. Sentence-aligned parallel corpora revealed to be essential for achieving the objectives accomplished as it provided the neighbor contexts of ambiguous words, enabling the calculation of the statistical correlation between senses, and therefore the building of sense-clusters. The results obtained for sense clustering (V-measure and F-measure) allow us to conclude that the learned clusters are reliable sources of information, supporting the whole process of disambiguation. In the classification process, results were very positive for all language pairs tested, showing that *well-formed* sense clusters are a strong base for WSD.

As future work we would like to improve the approach by studying the optimal size of the neighbor context of the ambiguous words, which will require larger sentence-aligned parallel corpora, in order to keep, and gain, statistical representativeness. Future experiments will include ambiguous multi-words, for which this algorithm was also designed. The approach presented in this paper will enable us to build a semantic translation tagger that can be useful for translation aligners or other translation systems. It is also our intention to test our approach with existing datasets, used on cross-lingual WSD tasks of SemEval[9].

## References

1. Aires, J., Lopes, G.P., Gomes, L.: Phrase translation extraction from aligned parallel corpora using suffix arrays and related structures. In: Lopes, L.S., Lau, N., Mariano, P., Rocha, L.M. (eds.) EPIA 2009. LNCS, vol. 5816, pp. 587–597. Springer, Heidelberg (2009)
2. Apidianaki, M.: Cross-lingual word sense disambiguation using translation sense clustering. In: Proceedings of the 7th International Workshop on Semantic Evaluation (SemEval 2013), pp. 178–182. \*SEM and NAACL (2013)
3. Apidianaki, M., He, Y., et al.: An algorithm for cross-lingual sense-clustering tested in a MT evaluation setting. In: Proceedings of the International Workshop on Spoken Language Translation, pp. 219–226 (2010)
4. Bansal, M., DeNero, J., Lin, D.: Unsupervised translation sense clustering. In: Proceedings of the 2012 Conference of the North American Chapter of the Association for Computational Linguistics: Human Language Technologies, pp. 773–782. Association for Computational Linguistics (2012)
5. Brown, P.F., Pietra, S.A.D., Pietra, V.J.D., Mercer, R.L.: Word-sense disambiguation using statistical methods. In: Proceedings of the 29th annual meeting on Association for Computational Linguistics, pp. 264–270. Association for Computational Linguistics (1991)
6. Chang, C.C., Lin, C.J.: LIBSVM: a library for support vector machines. ACM Transactions on Intelligent Systems and Technology (TIST) **2**(3), 27 (2011)
7. Diab, M.T.: Word sense disambiguation within a multilingual framework. Ph.D. thesis, University of Maryland at College Park (2003)
8. Hall, M., Frank, E., Holmes, G., Pfahringer, B., Reutemann, P., Witten, I.H.: The weka data mining software: an update. ACM SIGKDD Explorations Newsletter **11**(1), 10–18 (2009)
9. Lefever, E., Hoste, V.: Semeval-2010 task 3: Cross-lingual word sense disambiguation. In: Proceedings of the 5th International Workshop on Semantic Evaluation, pp. 15–20. Association for Computational Linguistics (2010)
10. Lefever, E., Hoste, V., De Cock, M.: Five languages are better than one: an attempt to bypass the data acquisition bottleneck for WSD. In: Gelbukh, A. (ed.) CICLing 2013, Part I. LNCS, vol. 7816, pp. 343–354. Springer, Heidelberg (2013)
11. Och, F.J., Ney, H.: A systematic comparison of various statistical alignment models. Computational Linguistics **29**(1), 19–51 (2003)
12. Pelleg, D., Moore, A.W., et al.: X-means: Extending k-means with efficient estimation of the number of clusters. In: ICML, pp. 727–734 (2000)
13. Rijsbergen, V. (ed.): Information Retrieval, 2nd edn. Information Retrieval Group, University of Glasgow (1979)
14. Rosenberg, A., Hirschberg, J.: V-measure: a conditional entropy-based external cluster evaluation measure. EMNLP-CoNLL **7**, 410–420 (2007)
15. Tuflı̄ş, D., Ion, R., Ide, N.: Fine-grained word sense disambiguation based on parallel corpora, word alignment, word clustering and aligned wordnets. In: Proceedings of the 20th international conference on Computational Linguistics, p. 1312. Association for Computational Linguistics (2004)

# Towards the Improvement of a Topic Model with Semantic Knowledge

Adriana Ferrugento<sup>1(✉)</sup>, Ana Alves<sup>1,2</sup>, Hugo Gonçalo Oliveira<sup>1</sup>,  
and Filipe Rodrigues<sup>1</sup>

<sup>1</sup> CISUC, Department of Informatics Engineering,  
University of Coimbra, Coimbra, Portugal

`aferr@student.dei.uc.pt, {ana,hroliv,fmpr}@dei.uc.pt`

<sup>2</sup> Coimbra Institute of Engineering,  
Polytechnic Institute of Coimbra, Coimbra, Portugal

**Abstract.** Although typically used in classic topic models, surface words cannot represent meaning on their own. Consequently, redundancy is common in those topics, which may, for instance, include synonyms. To face this problem, we present SemLDA, an extended topic model that incorporates semantics from an external lexical-semantic knowledge base. SemLDA is introduced and explained in detail, pointing out where semantics is included both in the pre-processing and generative phase of topic distributions. As a result, instead of topics as distributions over words, we obtain distributions over concepts, each represented by a set of synonymous words. In order to evaluate SemLDA, we applied preliminary qualitative tests automatically against a state-of-the-art classical topic model. The results were promising and confirm our intuition towards the benefits of incorporating general semantics in a topic model.

**Keywords:** Topic model · Semantics · WordNet · SemLDA

## 1 Introduction

Topic models allow us to infer probability distributions over a set of words, called “topics”, which are useful for uncovering the main subjects in a collection of documents. They improve searching, browsing and summarization in such collections, and their application is not limited to text mining, as they revealed to be useful in fields such as computer vision [20] or bioinformatics [6].

Classic topic modelling algorithms, such as LDA [1], rely on the co-occurrences of surface words to capture their semantic proximity. They consider a surface word to be identical in different contexts and leverage on its co-occurrences with other words to differentiate topics. This fails to consider additional semantic knowledge on the words, which may, on one hand, exclude different senses of the same word from occurring in different topics and, on the other hand, lead to redundant topics, for instance with synonyms, that do not add information to the topic.

Whether it was during pre-processing [8], the generative process [18], or post processing [2], incorporating semantics into topic modeling emerged as an approach to deal with concepts rather than surface words. Since a word may have different meanings (e.g. *bank*) and since the same concept may be denoted by different words (e.g. *car* and *automobile*), these attempts exploit external semantic resources, such as WordNet [11] or, alternatively, follow a fully unsupervised approach, for instance, using word sense induction techniques [3]. In those approaches, topic distributions with synonymous and semantically similar words are unified in concept representations, such as synsets.

In order to improve current topic models, we propose a new model, SemLDA, which incorporates semantics in the well-known LDA model, using knowledge from WordNet. Similarly to other semantic topic models, the topics produced by SemLDA are sets of synsets, instead of words. The main difference is that SemLDA considers all possible senses of the words in a document, together with their probabilities. Moreover, it only requires a minimal intuitive change to the classic LDA algorithm.

The remaining of the paper is organized as follows: in Section 2, there is a brief enumeration of existing approaches to topic modelling; Section 3 introduces the proposed model in detail, with special focus on the differences towards the classic LDA. Section 4 reports on the performed experiments, with illustrative examples of the obtained topics and their automatic evaluation against the classic LDA. Finally, Section 5 draws some conclusions and future plans for this work.

## 2 Related Work

The first notable approach to reduce the dimensionality of documents was Latent Semantic Indexing (LSI) [5], which aimed at retaining the most of the variance present in the documents, thus leading to a significant compression of large datasets. Probabilistic Latent Semantic Indexing (pLSI) [9] later emerged as a variant of LSI, where different words in documents are modelled as samples from a simple mixture model where the mixture components are multinomial random variables that can be viewed as representations of “topics”. Nevertheless, pLSI was still not a proper generative model of documents, given that it provides no probabilistic model at the level of documents. Having this limitation in mind, Blei et al. [1] developed the Latent Dirichlet Allocation (LDA), a generalization of pLSI that is currently the most applied topic model. It allows documents to have a mixture of topics, given that it enables to capture significant intra-document statistical structure via the mixing distribution.

The single purpose of the previous models is to discover and assign different topics – represented by sets of surface words, each with a different probability – to the collection of documents provided. Those approaches have no concern with additional semantic knowledge about words, which can lead to some limitations in the generated topics. For instance, they might include synonyms, and thus be redundant and less informative. Alternative attempts address this problem using, for instance, WordNet [11], a lexical-semantic knowledge base of English.

WordNet is structured in synsets, which are groups of synonymous words that may be seen as concept representations of a language. Synsets may be connected according to different semantic relations, such as hypernymy (generalization) or meronymy (part-of).

In an attempt to include semantics in topic modelling and, at the same time, perform word sense disambiguation (WSD), Boyd-Graber and Blei [2] presented LDAWN, a modified LDA algorithm that includes a hidden variable for representing the sense of a word, according to WordNet. Each topic consists of a random walk through the WordNet hypernymy hierarchy, which is used to infer topics and their synsets, based on the words from documents. LDAWN was also applied to word sense disambiguation (WSD), although its authors accept the worse performance when compared with state-of-the-art WSD algorithms. One of the proposed solutions is to acquire local context to improve WSD, in the future. However, there is additional work towards the discovery of concept-based topics, not always relying in WordNet. For instance, LDA was used as a ground model to generate topics based on concepts of an ontology [4]; and a commonsense knowledge-based algorithm was used to transform documents into commonsense concepts, which were then clustered to generate the topics [17].

Despite some similarities, the model proposed in this paper differs from the previous in various ways. Instead of words, the produced topics are also distributions over concepts (synsets) and, similarly to LDAWN, it exploits WordNet and modifies the basic LDA by adding a sense variable. But SemLDA considers all possible senses of a word, with a distribution over all the synsets that include it. Indeed, we do not benefit from similar words in the same topic to improve WSD, as in LDAWN. Rather, we try to avoid it. This is why, in the future, our sense probabilities might be obtained from WSD. SemLDA is further explained in the next section.

### 3 Proposed Model

In order to consider the general semantics of a language during topic discovery, we propose SemLDA, a topic model that exploits external semantic knowledge, acquired from Princeton WordNet [11], a lexical-semantic knowledge base of English. SemLDA is based on the Latent Dirichlet Allocation model [1], but it introduces a new set of parameters  $\eta_{1:S}$ , where  $S$  is the number of synsets where the word occurs (one for each of its senses). The parameters correspond to the probabilities of each word belonging to a synset, which, in the current implementation, is obtained directly from the SemCor corpus [12] – in SemCor, words are manually annotated according their WordNet senses and, in WordNet, both synsets and word senses are ordered according to their frequencies in SemCor.

Given a corpus  $\mathcal{D} = \{\mathbf{w}^d\}_{d=1}^D$  of size  $|\mathcal{D}|$  and the probabilities of each word  $n$  in a synset  $s$ ,  $\eta_{s,n}$ , SemLDA estimates the most likely set of topics. Each document is represented by a distribution of topics,  $\theta$ , but, in contrast to the traditional LDA, a topic is represented as a distribution over the synsets in the vocabulary,  $\beta$ . This is a major difference because, in LDA, words are handled

according to the documents where they appear, regardless of their known semantics. In SemLDA, instead of just words, all the possible senses for each word are considered, although with different probabilities. We should notice that the more informative output (synsets) does not necessarily imply an increasing complexity in the topic representation. If needed, in order to have a comparable output to other topic models, a single word can be selected from each synset. When using WordNet, it makes sense to select the first word of a synset, which we recall to be the most frequently used to denote the concept.

The graphical model of SemLDA is displayed in Figure 1, where  $D$  is the number of documents in the corpus,  $K$  is the number of topics,  $N$  is the number of words in a document and  $S$  is the number of synsets of a given word. In this model, each word of a document,  $w_n$ , is drawn from a concept,  $c_n$ . This is represented by using the synset's distribution over words, parameterized by  $\eta$ , which we shall assume to be fixed. The concept  $c_n$  is determined by a discrete topic-assignment  $z_n$ , picked from the document's distribution over topics  $\theta$  and a topic distribution  $\beta$ . It follows the same reasoning as the LDA model, but includes a new layer corresponding to the concepts  $c_n$  that the words  $w_n$  express. The generative process of a document  $d$  under SemLDA is the following:

1. Choose topic proportions  $\theta|\alpha \sim Dir(\alpha)$
2. For each concept,  $c_n$ 
  - (a) Choose topic assignment  $z_n|\theta \sim Mult(\theta)$
  - (b) Choose concept  $c_n|z_n, \beta_{1:K} \sim Mult(\beta_{z_n})$
  - (c) Choose word to represent concept  $w_n|c_n, \eta_{1:S} \sim Mult(\eta_{c_n})$

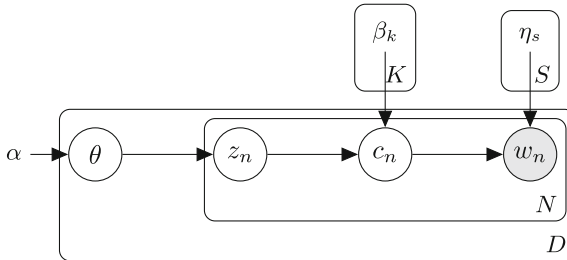


**Fig. 1.** Graphical model.

Our goal is thus to calculate, for every document, the posterior distribution over the latent variables,  $\theta, z_{1:N}, c_{1:N}$ . However, as in LDA, performing exact inference is intractable, so we need to use an approximate inference method. In this paper, we use variational inference to perform approximate Bayesian inference. The purpose of variational inference is to minimize KL divergence between the variational distribution  $q(\theta, z_{1:N}, c_{1:N})$  and the true posterior distribution  $p(\theta, z_{1:N}, c_{1:N}|w_{1:N})$ . A fully factorized (mean field) variational distribution  $q$ ,

of the form represented in equation 1, is employed, with  $\gamma$ ,  $\phi$  and  $\lambda$  as the variational parameters.

$$q(\theta, z_{1:N}, c_{1:N}) = q(\theta|\gamma) \left( \prod_{n=1}^N q(z_n|\phi_n)q(c_n|\lambda_n) \right) \quad (1)$$

KL minimization [10] is equivalent to maximizing the lower bound on the log marginal likelihood (equation 2) by using coordinate ascent.

$$\begin{aligned} \log p(w_{1:N}|\alpha, \beta_{1:K}, \eta_{1:S}) &= \log \int_{\theta} \sum_{z_{1:N}} \sum_{c_{1:N}} \frac{p(\theta, z_{1:N}, c_{1:N}, w_{1:N}|\Theta)q(\theta, z_{1:N}, c_{1:N})}{q(\theta, z_{1:N}, c_{1:N})} \\ &\geq \mathbb{E}_q[\log p(\theta, z_{1:N}, c_{1:N}, w_{1:N})] - \mathbb{E}_q[\log q(\theta, z_{1:N}, c_{1:N})] \\ &= \mathcal{L}(\gamma, \phi_{1:N}, \lambda_{1:N}|\Theta) \end{aligned} \quad (2)$$

The greek letter  $\Theta$  is used to denote the model's parameters  $\Theta = \{\alpha, \beta, \eta\}$ .

By optimizing  $\mathcal{L}$  w.r.t  $\gamma$ , we get the update the same update as in the classic LDA in [1], given by equation 3.

$$\gamma_i = \alpha_i + \sum_{n=1}^N \phi_{n,i} \quad (3)$$

The variational parameter  $\phi$  can be optimized by collecting only the terms in the lower bound that contain the parameter. Notice that this is a constrained maximization problem, since  $\sum_{k=1}^K \phi_{n,k} = 1$ , which is necessary for it to be a valid probability distribution. Hence, we need to include the necessary Lagrange multipliers, yielding equation 4.

$$\begin{aligned} \mathcal{L}_{[\phi]} &= \sum_{n=1}^N \sum_{i=1}^K \phi_{n,i} \left( \Psi(\gamma_i) - \Psi \left( \sum_{j=1}^K \gamma_j \right) \right) + \sum_{n=1}^N \sum_{j=1}^S \sum_{i=1}^K \lambda_{n,j} \phi_{n,i} \log \beta_{i,j} \\ &\quad - \sum_{n=1}^N \sum_{i=1}^K \phi_{n,i} \log \phi_{n,i} + \mu \left( \sum_{k=1}^K \phi_{n,k} - 1 \right) \end{aligned} \quad (4)$$

Setting the derivatives of  $\mathcal{L}_{[\phi]}$  w.r.t  $\phi$  to zero gives the update in equation 5.

$$\phi_{n,i} \propto \exp \left( \Psi(\gamma_i) - \Psi \left( \sum_{j=1}^K \gamma_j \right) + \sum_{j=1}^S \lambda_{n,j} \log \beta_{i,j} \right) \quad (5)$$

In order to optimize  $\mathcal{L}$  w.r.t  $\lambda$ , we again start by collecting only the terms in the bound that contain  $\lambda$ . Notice that this is also a constrained maximization problem, since  $\sum_{k=1}^S \lambda_{n,k} = 1$ . Hence, we need to also add the necessary Lagrange multipliers (see equation 6).

$$\begin{aligned} \mathcal{L}_{[\lambda]} &= \sum_{n=1}^N \sum_{j=1}^S \sum_{i=1}^K \lambda_{n,j} \phi_{n,i} \log \beta_{i,j} + \sum_{n=1}^N \sum_{j=1}^S \sum_{i=1}^{V_j} \lambda_{n,j} w_{n,i} \log \eta_{j,i} \\ &\quad - \sum_{n=1}^N \sum_{j=1}^S \lambda_{n,j} \log \lambda_{n,j} + \mu \left( \sum_{k=1}^S \lambda_{n,k} - 1 \right) \end{aligned} \quad (6)$$

Setting the derivatives of  $\mathcal{L}_{[\lambda]}$  w.r.t  $\lambda$  to zero gives the update in equation 7.

$$\lambda_{n,j} \propto \exp \left( \sum_{i=1}^K \phi_{n,i} \log \beta_{i,j} + \sum_{i=1}^{V_j} w_{n,i} \log \eta_{j,i} \right) \quad (7)$$

The variational inference algorithm iterates between the different updates presented until the convergence of the evidence lower bound. Since the parameters  $\alpha$  and  $\eta$  are assumed to be fixed, we only need to estimate  $\beta$ , for which a variational EM algorithm is used. In the E-step of the expectation-maximization algorithm, variational inference is used to find an approximate posterior for each document, as previously described. In the M-step, as in exact EM, we find maximum likelihood estimates of the parameters using the expected sufficient statistics computed in the E-step.

We start by collecting only the terms in the lower bound that contain  $\beta$ . Notice that this is a constrained maximization problem, since  $\sum_{k=1}^V \beta_{i,k} = 1$ , which is necessary to be a valid probability distribution. Hence, we also need to include the necessary Lagrange multipliers (see equation 8).

$$\mathcal{L}_{[\beta]} = \sum_{d=1}^D \sum_{n=1}^N \sum_{i=1}^K \sum_{j=1}^S \lambda_{n,j}^d \phi_{n,i}^d \log \beta_{i,j} + \sum_{i=1}^K \mu_i \left( \sum_{k=1}^S \beta_{i,k} - 1 \right) \quad (8)$$

Setting the derivatives of  $\mathcal{L}_{[\beta]}$  w.r.t  $\beta$  to zero gives the following update in equation 9, which is analogous to the update in standard LDA [1], but with the words  $w_{n,j}^d$  replaced by their probability in the  $j^{th}$  concept,  $\lambda_{n,j}^d$ .

$$\beta_{i,j} \propto \sum_{d=1}^D \sum_{n=1}^{N_d} \lambda_{n,j}^d \phi_{n,i}^d \quad (9)$$

## 4 Results and Evaluation

In this section, the experiments performed towards the validation of SemLDA are reported. The datasets used are described, some of the obtained synset-based topics are shown, and the evaluation metrics are presented. The latter were used to compare SemLDA with the classic LDA.

### 4.1 Datasets

Two freely available textual corpora were used in our experiments, namely: the Associated Press (AP) and the 20 Newsgroups dataset, both in English. AP is a large news corpus, from which we used only a part. More precisely, the sample data for the C implementation of LDA, available in David Blei's website<sup>1</sup>, which

---

<sup>1</sup> <http://www.cs.princeton.edu/~blei/lda-c/>

includes 2,246 documents. The 20 Newsgroups<sup>2</sup> is a popular dataset for experiments in text applications of machine learning techniques. It contains 20,000 documents, organized into 20 different newsgroups. Both datasets went through the same pre-processing phase, which included stop-word and numbers removal, as well as word lemmatization. For stop-word removal, we used the *snowball stop words* list<sup>3</sup>. Word lemmatization was based on the NLTK<sup>4</sup> WordNet reader.

## 4.2 Experiments

The experiments performed aimed at comparing the classic LDA algorithm [1] with SemLDA. An implementation of the classic algorithm, implemented in C, is available from Blei's website<sup>5</sup>. No changes were made to his code. We just had to pre-process the documents, generate a suitable input, and execute it.

For running SemLDA, extra work was needed. First, we retrieved all synsets from the SemCor 3.0 annotations<sup>6</sup>, and calculated their probability in this corpus. This is a straightforward task for those WordNet synsets that are in SemCor. But SemCor is a limited corpus and does not cover all words and senses in WordNet. To handle this issue, an extra pre-processing step was added, where all documents were reviewed and, when a word did not occur in SemCor, a new ‘dummy’ synset was created with a special negative id, and probability equal to the average probability of all the other synsets. This value was chosen to balance the unknown probabilities of dummy synsets according to the probabilities of the remaining synsets, and thus not favor any of them.

For each dataset, the SemLDA input file had the synsets retrieved from SemCor and the words that were in the documents, but not in SemCor. The only difference on the text pre-processing is the use of part-of-speech (POS) tagging, to consider only open-class words, namely nouns, verbs, adjectives and adverbs.

Instead of trial and error with different numbers of topics, we used a Hierarchical Dirichlet Process (HDP) [19] to discover the appropriate number of topics for each dataset. The results obtained suggested that the 20 Newsgroups dataset contains 15 topics and the AP corpus 24. After the pre-processing phase, each model was run for both datasets, with the  $\alpha$  parameter fixed at 0.5. Tables 1 and 2 illustrate the results obtained with the classic LDA and SemLDA, respectively for the 20 Newsgroups and for the AP corpus. For each topic discovered by the SemLDA presented, we tried to find an analogous topic by the classic LDA, in a sense that they share similar domains. For the sake of simplicity, we only show the top 10 synsets for each SemLDA topic, with their Synset ID, POS-tag, words and gloss. Underlined words are those present in SemCor and WordNet, whereas the others only appear in WordNet. For each LDA topic only the top 10 words are displayed.

---

<sup>2</sup> <http://qwone.com/~jason/20Newsgroups/>

<sup>3</sup> <http://snowball.tartarus.org/algorithms/english/stop.txt>

<sup>4</sup> <http://www.nltk.org/>

<sup>5</sup> <http://www.cs.princeton.edu/~blei/lda-c/>

<sup>6</sup> <http://web.eecs.umich.edu/~mihalcea/downloads.html#semcor>

**Table 1.** Illustrative (analogous) topics from 20 Newsgroups, obtained with the classic LDA (top) and with SemLDA (bottom).

LDA			
medical, health, use, patient, disease, doctor, cancer, study, infection, treatment			
Synset ID	POS	Words	SemLDA Gloss
14447908	N	health, wellness	A healthy state of well being free from disease.
3247620	N	drug	A substance that is used as a medicine or narcotic.
10405694	N	patient	A person who requires medical care.
10020890	N	doctor, doc, physician, MD, Dr., medico	A licensed medical practitioner.
14070360	N	disease	An impairment of health or a condition of abnormal functioning.
14239918	N	cancer, malignant neoplastic disease	Any malignant growth or tumor caused by abnormal and uncontrolled cell division.
47534	ADV	besides, too, also, likewise, as well	In addition.
14174549	N	infection	The pathological state resulting from the invasion of the body by pathogenic microorganisms.
1165043	V	use, habituate	Take or consume (regularly or habitually).
7846	N	person, individual, someone, somebody, mortal, soul	A human being.

The results show success on incorporating semantics into LDA. Topics are based on synsets and WordNet can be used to retrieve additional information on the concept they denote, including their definition (gloss), POS and other words with the same meaning. With both models, the top words of each topic are consistently nouns, which should transmit more content. The presented examples clearly describe very close semantic domains. They share many words and the other are closely related to each other (eg. *drug* and *treatment*, or *exchange* and *trading*). We call attention to topics where the same word is in different synsets (Table 2). While this might sometimes be undesirable, and a possible sign of incoherence, it also shows that the algorithm is correctly handling different senses of the same word. These situations should be minimized in the future, as we intend to acquire sense probabilities from word sense disambiguation (WSD) [14], instead of relying blindly in SemCor for this purpose. This will also minimize the number of dummy synsets.

We can say that the overall results are satisfying. Despite one or another less clear word association, we may say that we are moving towards the right direction. Still, to measure progress towards the classic LDA, we made an automatic evaluation of the coherence of the discovered topics.

### 4.3 Evaluation

Although, at a first glance, the results might seem promising, they were validated automatically, using metrics previously applied to the context of topic modelling, namely: pointwise mutual information (PMI) and topic coherence.

PMI is a measure of word association that, according to Newman et al. [15], is highly correlated with human-judged topic coherence. In this context, PMI

**Table 2.** Illustrative (analogous) topics from AP, obtained with the classic LDA (top) and with SemLDA (bottom).

LDA			
stock, market, percent, rate, price, oil, rise, say, point, exchange			
Synset ID	POS	Words	Gloss
8424951	N	<u>market</u>	The customers for a particular product or service.
13851067	N	<u>index</u>	A numerical scale used to compare variables with one another or with some reference number.
8072837	N	<u>market</u> , securities industry	The securities markets in the aggregate.
13342135	N	<u>share</u>	Any of the equal portions into which the capital stock of a corporation is divided and ownership of which is evidenced by a stock certificate.
79398	N	<u>trading</u>	Buying or selling securities or commodities.
3843092	N	<u>oil</u> , oil color, oil colour	Oil paint containing pigment that is used by an artist.
7167041	N	<u>price</u>	A monetary reward for helping to catch a criminal.
14966667	N	<u>oil</u>	A slippery or viscous liquid or liquefiable substance not miscible with water.
5814650	N	<u>issue</u>	An important question that is in dispute and must be settled.
13333833	N	<u>stock</u>	The capital raised by a corporation through the issue of shares entitling holders to an ownership interest (equity).

is calculated for each topic, based on the co-occurrence probabilities of every pair of its words. In our case, we used the 10 most probable words of each topic, which results in 45 different pairs. For both datasets, co-occurrence is computed from Wikipedia, which provides a large and wide-coverage source of text, completely independent from the datasets used and from WordNet. After comparing different approaches for evaluating topic coherence automatically, Newman et al. [16] concluded that PMI over Wikipedia provides a score that is very consistent with human judgements. See equation 10 for the PMI's formula, where  $p(w)$  is the probability of a word  $w$  (in our case, the number of Wikipedia articles using this word), and  $p(w_i, w_j)$  is the probability of words  $w_i$  and  $w_j$  co-occurring (in our case, the number of Wikipedia articles using both words). After computing PMI for all topics, we computed the average score for the full topic set.

$$PMI - Score(\mathbf{w}) = \frac{1}{45} \sum_{i < j} \log \frac{p(w_i, w_j)}{p(w_i)p(w_j)}, ij \in \{1 \dots 10\} \quad (10)$$

We recall that topics discovered by SemLDA are sets of synsets and not of surface words. Therefore, to enable a fair comparison with the classic LDA, before computing the PMI scores, we converted our topics to a plain word representation. For this purpose, instead of full synsets, we used only their first word. According to WordNet, this is the word most frequently used to denote the synset concept, in the SemCor corpus. For instance, the SemLDA topic in Table 2 becomes: *market*, *index*, *market*, *share*, *trading*, *oil*, *price*, *oil*, *issue*, *stock*. On the one hand, this representation limits the extent of our results, which are, in fact, synsets. On the other hand, by doing so, it might lead to duplicate words in the same topic, though corresponding to different senses.

*Coherence* measures the co-occurrence, within the modelled documents, of pairs of words in the same topic [13]. As in the PMI measure, the 10 most probable words of each topic are used. It is also calculated for each topic and, in the end, the average is computed for the full topic set. Assuming that, in every document, there is an explicit theme, by calculating this, we can analyze if the grouping of words is coherent, given their co-occurrence. This measure is very similar to PMI but, in some situations, it achieved higher correlation with human judges [13]. Equation 11 shows the formula of this measure, where  $D(v_m^{(t)}, v_l^{(t)})$  is the co-document frequency of two words, 1 is a smoothing count to avoid the logarithm of zero and  $D(v_l^{(t)})$  is the document frequency of a word.

$$C(t; V^{(t)}) = \sum_{m=2}^M \sum_{l=1}^{m-1} \log \frac{D(v_m^{(t)}, v_l^{(t)}) + 1}{D(v_l^{(t)})} \quad (11)$$

The results obtained with the two topic models, for both datasets, are presented in Table 3. Even if it was a close call, SemLDA outperformed the classic LDA. On both metrics, SemLDA had better scores in the AP corpus, which was the dataset originally used by Blei. For the 20 Newsgroups dataset, the topic coherence measure was very close with both models, whereas the PMI score was better for SemLDA. This confirms that we are heading towards a promising approach that, by exploiting an external lexical-semantic knowledge base, may improve the outcome of the classic LDA model. We should still stress that these are just preliminary results. The following steps are explained with further detail in the next section.

**Table 3.** Results obtained with the two evaluation metrics.

	<b>20 Newsgroups</b>		<b>AP</b>	
	PMI	Coherence	PMI	Coherence
LDA	$1.16 \pm 0.39$	$-32.89 \pm 19.77$	$1.12 \pm 0.31$	$-13.62 \pm 9.51$
SemLDA	$1.22 \pm 0.46$	$-35.4 \pm 17.65$	$1.43 \pm 0.26$	$-9.18 \pm 7.51$

## 5 Concluding Remarks

We have presented SemLDA, a topic model based on the classic LDA that incorporates external semantic knowledge to discover less redundant and more informative topics, represented as concepts, instead of surface words. We may say that we have been successful so far. The classic algorithm was effectively changed to produce topics based on WordNet synsets, which, after an automatic validation, shown to have comparable coherence to the original topics. Despite the promising results, there is still much room for improvement.

In fact, to simplify our task, we relied on some assumptions that should be dealt with in a near future and, hopefully, lead to improvements. For instance,

the  $\alpha$  parameter of LDA was simply set to a fixed value of 0.5. Its selection should be made after testing different values and assess their outcomes. We are also considering to add a Dirichlet prior over the variable concerning topics,  $\beta$ , so that it produces a smooth posterior and controls sparsity. Additional planned tests include the generation of topics considering just a subset of the open class words, for instance, just nouns, which might be more informative. Last but not least, we recall that we obtained the word sense probabilities directly from SemCor. While this corpus is frequently used in WSD tasks and should thus have some representativeness, this approach does not consider the context where the words occur. Instead of relying in SemCor, it is our goal to perform all-words WSD to the input corpora, and this way extract the probabilities of selecting different synsets, given the word context. This should also account for words that are not present in SemCor, and minimize the number of dummy synsets, with the averaged probabilities assigned.

Moreover, we should perform an additional evaluation of the results, not just through automatic measures, but possibly using people to assess the topic coherence. For instance, we may adopt the intruder test, where judges have to manually select the word not belonging to a topic (see [15]). It is also our intention to evaluate SemLDA indirectly, by applying it in tasks that require topic modelling, such as automatic summarization and classification.

We conclude by pointing out that, although the proposed model is language independent, it relies in language specific resources, especially the existence of a wordnet, besides models for POS-tagging and lemmatization. One of our mid-term goals is precisely to apply SemLDA to Portuguese documents. For such, we will use available POS-tagger and lemmatizers for this language, as well as one or more of the available wordnets (see [7] for a survey on Portuguese wordnets).

Since sense probabilities will soon be obtained from a WSD method, the unavailability of a SemCor-like corpus for Portuguese is not an issue.

**Acknowledgments.** This work was supported by the InfoCrowds project - FCT-PTDC/ECM-TRA/1898/2012FCT.

## References

1. Blei, D.M., Ng, A.Y., Jordan, M.I.: Latent dirichlet allocation. *Journal of Machine Learning Research* **3**, 993–1022 (2003)
2. Boyd-Graber, J., Blei, D., Zhu, X.: A topic model for word sense disambiguation. In: Proceedings of 2007 Joint Conference on Empirical Methods in Natural Language Processing and Computational Natural Language Learning (EMNLP-CoNLL), pp. 1024–1033. ACL Press, Prague, Czech Republic, June 2007
3. Brody, S., Lapata, M.: Bayesian word sense induction. In: Proceedings of 12th Conference of the European Chapter of the Association for Computational Linguistics. EACL 2009, pp. 103–111. ACL Press (2009)
4. Chemudugunta, C., Holloway, A., Smyth, P., Steyvers, M.: Modeling documents by combining semantic concepts with unsupervised statistical learning. In: Sheth, A.P., Staab, S., Dean, M., Paolucci, M., Maynard, D., Finin, T., Thirunarayanan, K. (eds.) ISWC 2008. LNCS, vol. 5318, pp. 229–244. Springer, Heidelberg (2008)

5. Deerwester, S.C., Dumais, S.T., Landauer, T.K., Furnas, G.W., Harshman, R.A.: Indexing by latent semantic analysis. *JASIS* **41**(6), 391–407 (1990)
6. Flaherty, P., Giaever, G., Kumm, J., Jordan, M.I., Arkin, A.P.: A latent variable model for chemogenomic profiling. *Bioinformatics* **21**(15), 3286–3293 (2005)
7. Gonçalo Oliveira, H., de Paiva, V., Freitas, C., Rademaker, A., Real, L., oes, A.S.: As wordnets do português. In: Simões, A., Barreiro, A., Santos, D., Sousa-Silva, R., Tagrin, S.E.O. (eds.) *Linguística, Informática e Tradução: Mundos que se Cruzam*, OSLA, vol. 7, no. 1, pp. 397–424. University of Oslo (2015)
8. Guo, W., Diab, M.: Semantic topic models: combining word distributional statistics and dictionary definitions. In: EMNLP, pp. 552–561. ACL Press (2011)
9. Hofmann, T.: Probabilistic latent semantic indexing. In: Proceedings of the 22nd annual international ACM SIGIR conference on Research and development in information retrieval, pp. 50–57. ACM (1999)
10. Jordan, M.I., Ghahramani, Z., Jaakkola, T.S., Saul, L.K.: An introduction to variational methods for graphical models. *Machine learning* **37**(2), 183–233 (1999)
11. Miller, G.A.: Wordnet: a lexical database for english. *Communications of the ACM* **38**(11), 39–41 (1995)
12. Miller, G.A., Chodorow, M., Landes, S., Leacock, C., Thomas, R.G.: Using a semantic concordance for sense identification. In: Proceedings of ARPA Human Language Technology Workshop. Plainsboro, NJ, USA (1994)
13. Mimno, D., Wallach, H.M., Talley, E., Leenders, M., McCallum, A.: Optimizing semantic coherence in topic models. In: Proceedings of the Conference on Empirical Methods in Natural Language Processing. EMNLP 2011, pp. 262–272. ACL Press (2011)
- 14.Navigli, R.: Word sense disambiguation: A survey. *ACM Computing Surveys* **41**(2), 1–69 (2009)
15. Newman, D., Bonilla, E.V., Buntine, W.: Improving topic coherence with regularized topic models. In: Advances in Neural Information Processing Systems, pp. 496–504 (2011)
16. Newman, D., Lau, J.H., Grieser, K., Baldwin, T.: Automatic evaluation of topic coherence. In: Human Language Technologies: The 2010 Annual Conference of the North American Chapter of the Association for Computational Linguistics. HLT 2010, pp. 100–108. ACL Press (2010)
17. Rajagopal, D., Olshevsky, D., Cambria, E., Kwok, K.: Commonsense-based topic modeling. In: Proceedings of the 2nd International Workshop on Issues of Sentiment Discovery and Opinion Mining, p. 6. ACM (2013)
18. Tang, G., Xia, Y., Sun, J., Zhang, M., Zheng, T.F.: Topic models incorporating statistical word senses. In: Gelbukh, A. (ed.) *CICLing 2014, Part I*. LNCS, vol. 8403, pp. 151–162. Springer, Heidelberg (2014)
19. Teh, Y.W., Jordan, M.I., Beal, M.J., Blei, D.M.: Hierarchical dirichlet processes. *Journal of the american statistical association* **101**(476) (2006)
20. Wang, C., Blei, D., Li, F.F.: Simultaneous image classification and annotation. In: IEEE Conference on Computer Vision and Pattern Recognition. CVPR 2009, pp. 1903–1910. IEEE (2009)

# RAPPORT — A Portuguese Question-Answering System

Ricardo Rodrigues<sup>1,2(✉)</sup> and Paulo Gomes<sup>1</sup>

<sup>1</sup> Centre for Informatics and Systems, University of Coimbra, Coimbra, Portugal  
[{rmanuel,pgomes}@dei.uc.pt](mailto:{rmanuel,pgomes}@dei.uc.pt)

<sup>2</sup> College of Education of the Polytechnic Institute of Coimbra, Coimbra, Portugal

**Abstract.** We present a question answering system for Portuguese that depends on *subject-predicate-object* triples extracted from sentences in a corpus. It is supported by indices that store triples, related sentences and documents. The system processes the questions and retrieves answers based on the triples.

For testing and evaluation purposes, we have used the CHAVE corpus, which has been used in multiple editions of CLEF. The questions from those editions were used to query and benchmark our system. In its current stage, the system has found the answer to 42% of the questions.

This document describes the modules that compose the system and how they are combined, providing a brief analysis on them, and also some preliminary results, as well as some expectations regarding future work.

**Keywords:** Question answering · Triple extraction · Portuguese

## 1 Introduction

When querying a system that provides or retrieves information about a given topic, with its contents in natural language, the user should not have to care about system specific details, such as:

- knowing the best keywords to get an answer to a specific question;
- using system specific syntax in order to interact with it;
- perusing the multiple documents that may contain the eventual answer;
- being limited by the questions someone has compiled before.

It is also possible that the information sources are not, or can not be, structured in such a way that can be easily accessed by more conventional techniques of information retrieval (IR) [2].

Most of these issues are addressed by question answering (QA) systems [22], which allow the user to interact with the systems by using natural language, and process documents whose contents are specified also using natural language.

In this context, we present a system that addresses QA for Portuguese, using triples extracted from sentences in a corpus, that are then used to present “short answers” (excerpts), alongside the sentences and documents they belong to.

In the remaining document, we briefly address the state of the art, describe the overall proposed approach and each of its modules, and draw some conclusions and reflections about future work.

## 2 Question Answering

Question answering, as in other subfields of IR, may include techniques such as: named entity recognition (NER) or semantic classification of entities, relations between entities, and selection of semantically relevant sentences, phrases or chunks [14], beyond the customary tokenization, lemmatization, and part-of-speech (POS) tagging. QA can also address a restricted set of topics, in a closed world domain, or forgo that restriction, operating in an open world domain.

Most approaches usually follow the framework shown in Fig. 1, where most of the processing stages are made on run-time (except for document indexing).

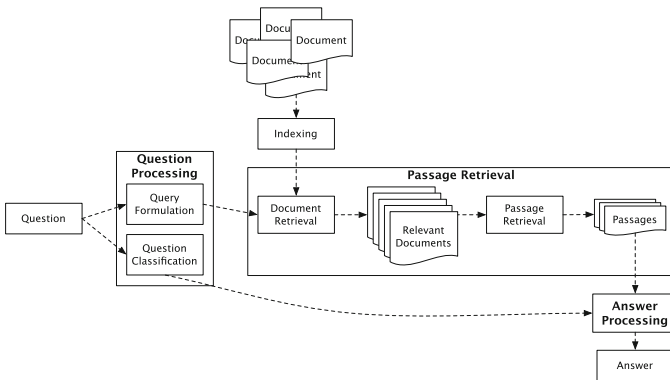


**Fig. 1.** A Typical Framework for a QA System (based on [10])

Regarding specific approaches to Portuguese, below is a list of the most relevant works whose results are compared against our work.

### 2.1 Esfinge

Esfinge [4] is a general domain question answering system that tries to take advantage of the great amount of information existent in the Web. Esfinge relies on pattern identification and matching. For each question, a tentative answer is created. For instance, a probable answer for a “What is X?” question will start

with “ $X$  is...”. Then this probable answer beginning is used to search the corpus, through the use of a search engine, in order to find possible answers that match the same pattern. In the following stages of the process, *n-grams* are scored and NER is performed in order to improve the performance of the system.

## 2.2 Senso

The Senso Question Answering System [19] (previously PTUE [17]) uses a local knowledge base, providing semantic information for text search terms expansion. It is composed of two modules: the solver module, that uses two components to collect plausible answers (the logic and the ad-hoc solvers); and the logic solver, that starts by producing a first-order logic expression representing the question and a logic facts list representing the text information and then looking for answers within the facts list that unify and validate the question logic form. There is also an *ad-hoc* solver for cases where the answer can be directly detected in the text. After all modules are used, the results are merged for answer list validation, to filter and adjust answers weight.

## 2.3 Priberam

Some of the most well known works on NLP and QA have been done at Priberam. Priberam’s QA System for Portuguese [1] uses a conservative approach, where the system starts by building contextual rules for performing morphological disambiguation, named entity recognition, etc.. Then it analyses the questions and divides them into categories. These same categories are applied to sentences in the source text. This categorization is done according to question patterns, answer patterns and question answering patterns (where pattern match between answer and question is performed).

## 2.4 NILC

Brazil’s Ncleo Interinstitucional de Lingstica Computacional (NILC) has built a summarization system to be used in the task of monolingual QA for Portuguese texts. NILC’s system uses a text summarizer that comprises three main processes: text segmentation, sentence ranking, and extract production [5] (associating sentences to a topic). The questions are then matched against the sentences, with the associated summaries being used to produce an answer.

## 2.5 RAPOSA

The RAPOSA Question Answering System [21] tries to provide a continuous on-line processing chain from question to answer, combining the stages of information extraction and retrieval. The system involves expanding queries for event-related or action-related factoid questions using a verb thesaurus automatically generated using information extracted from large corpora.

RAPOSA consists of seven modules more or less typical on QA systems: a *question parser*, a *query generator*, a *snippet searcher*, an *answer extractor*, *answer fusion*, an *answer selector*, and *query expansion*. It also deals with two categories of questions: definition questions and factoid questions.

## 2.6 QA@L<sup>2</sup>F

QA@L<sup>2</sup>F [13], the question-answering system from L<sup>2</sup>F, INESC-ID, is a system that relies on three main tasks: *information extraction*, *question interpretation* and *answer finding*.

This system uses a database to store information obtained by information extraction, where each entry is expected to represent the relation between the recognized entities. On a second step, the system processes the questions, creating SQL queries that represent the question and are run in the database. The retrieved records from the database are then used to find the wanted questions, through entity matching.

## 2.7 IdSay

IdSay: Question Answering for Portuguese [3] is an open domain question answering system that uses mainly techniques from the area of IR, where the only external information that it uses, besides the text collections, is lexical information for the Portuguese language.

IdSay starts by performing document analysis and then proceeding to entity recognition. After that, the system makes use of patterns to define the type of the question and expected answers. IdSay uses a conservative approach to QA, being its main stages: information indexing, question analysis, document retrieval, passage retrieval, answer extraction and answer validation.

## 3 The Proposed System — RAPPORT

Our system, RAPPORT, follows most of the typical framework for a QA system, while being an open domain system. It does, however, improves on some techniques that differ from other approaches to Portuguese.

One of the most differentiating elements is the use of triples as the basic unit of information regarding any topic, represented by a subject, a predicate and an object, and then using those triples as the base for answering questions. This approach shares also some similarities with open information extraction, regarding the storage of information in triples [7].

RAPPORT depends on a combination of four modules, addressing information extraction, storage, querying and retrieving. The basic structure of the system comprehends the following modules:

- triple extraction (performed offline);
- triple storage (performed offline);

- data querying (performed online);
- and answer retrieving (performed online).

Each of these modules are described next, specifying each of the main tasks.

### 3.1 Triple Extraction

The first module processes the contents of the corpus, picking each of the documents, identifying sentences and extracting triples. It includes multiple tasks, namely sentence splitting, chunking, tokenization, POS tagging, lemmatization, dependency parsing, and NER.

The sentence splitting, tokenization, POS tagging, and NER tasks are done using tools included in the *Apache OpenNLP toolkit*<sup>1</sup>, with some minor tweaks for better addressing the texts used. For instance, the system groups tokens that should be processed together — e.g., person names and dates — and, at the same time, it also splits composed tokens, such as it is the case of some Portuguese verbal conjugations and clitics — e.g., the preposition “*no*”<sup>2</sup> becomes “*em o*”. The model used in the chunker was also created for Portuguese (although following guidelines from OpenNLP), as there was no available pre-built model.

For the lemmatization process, *LemPORT* [18], a Portuguese specific lemmatizer was used. Another tool was used for dependency parsing, namely, *MaltParser* [16], with the model used by the parser being trained on Bosque 8.0<sup>3</sup> (available through Linguateca<sup>4</sup>). However, the output of MaltParser is further processed in order to group the tokens around the *main* dependencies, such as: subject, root (verb), and objects, among others.

Specifically regarding triple extraction, it is performed using two complementary approaches, both involving named entities, as a way of determining which triples are of use. The triples are defined by three fields: *subject*, *predicate*, and *object*. After the documents are split into sentences, each sentence is directly processed in order to extract named entities. Then, the sentences either are chunked or undergo tokenization, POS tagging and lemmatization before applying the MaltParser to identify the main dependencies. An algorithm describing the process is found in Alg. 1.

As can be noticed, only the triples with entities in the *subject* or in the *object* are further used. The triples extracted this way are then stored for future querying. Also, the predicate has the verb stored in its lemmatized form in order to facilitate later matches.

For clarification, in the triples that are based on the proximity between chunks, most of the predicates comprehend, but are not limited to, the verbs *ser* (to be), *pertencer* (to belong), *haver* (to have), and *ficar* (to locate). For instance, if two NP chunks are found one after another, and the first chunk contains a named entity, it is highly probable that it is further characterized by

---

<sup>1</sup> <http://incubator.apache.org/opennlp/>

<sup>2</sup> This corresponds to the combination of the preposition “in” with the article “the”.

<sup>3</sup> <http://www.linguateca.pt/floresta/BibliaFlorestal/completa.html>

<sup>4</sup> <http://www.linguateca.pt/>

```

Data: Corpus documents
Result: Triples
Read documents;
foreach document do
    Split sentences;
    foreach sentence do
        Tokenize, lemmatize, POS tag and dependency parse;
        Extract named entities;
        Get proximity chunks;
        foreach chunk do
            if chunk contains any entity then
                if neighbouring chunk has a specific type then
                    Create triple relating both chunks, depending on the
                    neighbouring chunk type and contents;
                end
            end
        end
    Get dependency chunks;
    foreach chunk do
        if chunk contains any entity and is a subject or an object then
            Create triple using the subject or object, the root, and
            corresponding object or subject, respectively;
        end
    end
end

```

**Algorithm 1:** Triple Extraction Algorithm

the second chunk. If the second chunk starts with a determinant or a noun, the predicate of the future triple is set to *ser*; if it starts with the preposition *em* (in), it is used the verb *ficar*; if it starts with the preposition *de* (of), it is used the verb *pertencer*; and so on.

As an example, the sentence “Mel Blanc, o homem que deu a sua voz a o coelho mais famoso de o mundo, Bugs Bunny, era alrgico a cenouras.”<sup>5</sup> yields three distinct triples: “{Bugs Bunny} {ser} {o coelho mais famoso do mundo}” and “{Mel Blanc} {ser} {o homem que deu a sua voz ao coelho mais famoso do mundo}”, both using the proximity approach, and “{Mel Blanc} {ser} {alrgico a cenouras}”, using the dependency approach.

### 3.2 Triple Storage

After triple extraction is performed, *Lucene*<sup>6</sup> is used for storing the triples, the sentences where the triples are found, and the documents that, by its turn, contain those sentences. For that purpose, three indices were created:

---

<sup>5</sup> In English, “Mel Blanc, the man who lent his voice to the world’s most famous rabbit, Bugs Bunny, was allergic to carrots.”.

<sup>6</sup> For Lucene, please refer to <http://lucene.apache.org>.

- the triple index stores the triples (subject, predicate and object), their id, and the ids of the sentences and documents that contain them;
- the sentence index stores the sentences' id (a sequential number representing its order within the document), the tokenized text, the lemmatized text and the documents' id they belong to;
- the document index stores the data describing the document, as found in CHAVE (number, id, date, category and author);

Although each index is virtually independent from the others, they can refer one another by using the ids of the sentences and of the documents. That way, it is easy to determine the relations between documents, sentences, and triples. These indices (mainly the sentence and the triple indices) are then used in the next steps of the present approach.

### 3.3 Data Querying

In a similar way to the annotation made to the sentences in the corpus, the questions are processed in order to extract tokens, lemmas and named entities, and identify their types, categories and targets.

For building the queries, the system starts by performing NER and lemmatizing the questions. The lemmas are useful for broadening the matches and results that could be found only by using directly the tokens. The queries are essentially made up of the lemmas found in the questions (including named entities and proper nouns). In those queries, all elements are, by default, optional, excluding the named entities. If no entities are present in the questions, proper nouns are made mandatory; by its turn, if there are also no proper nouns in the questions, it is the nouns that are used as mandatory keywords in the queries. For instance, in order to retrieve the answer to the question “*A que era alrgico Mel Blanc?*”<sup>7</sup>, the query will end up being defined by three words: “+Mel.Blanc a que ser alrgico”. We have opted for keeping all the lemmas because Lucene scores higher the hits with the optional lemmas, and virtually ignores them if they are not present.

The query is then applied to the sentence index — the system searches for sentences with the lemmas previously identified, with the verb as an optional term. When a match occurs, the associated triples are retrieved, along with the document data.

The triples that are related to the sentence are then processed, checking for the presence of question's entities in either the *subject* or the *object* of the triples, for selecting which triples are of interest.

### 3.4 Answer Retrieving

After a sentence matches a query, as stated before, the associated triples and document data are retrieved. As the document data is only used for better characterizing the answers, let us focus on the triples.

---

<sup>7</sup> In English, “What was Mel Blanc allergic to?”

When a sentence contains more than one triple, it is selected the triple which predicate matches the verb in the initial query. If that fails, it is selected the triple, as a whole, that best matches the query, accordingly to the Lucene ranking algorithm for text matches. After a triple is selected, if the best match against the query is found in the subject, the object is returned as being the answer. If, on the other hand, the best match is found against the object, it is the subject that is returned. An algorithm describing both the data querying and this process is found in Alg. 2.

**Data:** Question

**Result:** Answers

Create query using *named entities*, *proper nouns*, or *noun* as mandatory, and the remaining lemmas from the *question* as optional;

Run *query* against *sentence index*;

**foreach** *sentence hit* **do**

    Retrieve triples related to the sentence;

**foreach** *triple* **do**

**if** *subject* contains *named entities* from *question* **then**

            Add *object* to *answers* and retrieve sentence and document  
            associated with the triple;

**end**

**else if** *object* contains *named entities* from *question* **then**

            Add *subject* to *answers* and retrieve sentence and document  
            associated with the triple;

**end**

**end**

**end**

**Algorithm 2:** Answer Retrieval Algorithm

Continuing with the used example, given the correct sentence, of the three triples, the one that best matches the query is “{*Mel Blanc*} {*ser*} {*alrgico a cenouras*}”. Removing from the triple the known terms from que question, what remains must yield the answer: “[a] cenouras”. Besides that, as the named entity, *Mel Blanc*, is found in the subject of the triple, the answer is most likely to be found in the object.

## 4 Experimentation Results

For the experimental work, we have used the CHAVE corpus [20], a collection of the 1994 and 1995 editions — a total of 1456 — of newspapers “Pblico” and “Folha de So Paulo”, with each of the editions usually comprehending over one hundred articles, identified by *id*, number, date, category, author, and the text of the news article itself.

CHAVE was used in the Cross Language Evaluation Forum (CLEF)<sup>8</sup> QA campaigns as a benchmark — although in the lasts editions of the Multilingual QA Track at CLEF a dump of the Portuguese Wikipedia was also used.

---

<sup>8</sup> <http://www.clef-initiative.eu/>

Almost all of the questions used in each of the CLEF editions are known. It is also known the results of each of the contestant systems. The questions used in CLEF adhere to the following criteria [12]: they can be *list* questions, *embedded* questions, *yes/no* questions (although none was found in the questions used for Portuguese), *who*, *what*, *where*, *when*, *why*, and *how* questions, and definitions.

For reference, in Table 1 there is a summary of the best results (all answers considered) for the Portuguese QA task on CLEF from 2004 to 2008 (abridged from [6, 8, 11, 12, 23]), alongside with the arithmetic mean for each system comprehending the editions where they were contenders. At the end of the table, it is also shown the results of the proposed system.

**Table 1.** Comparison of the Results at CLEF 2004 to 2008

<b>Approach</b>	<b>Overall Accuracy (%)</b>					<i>Average</i>
	<b>2004</b>	<b>2005</b>	<b>2006</b>	<b>2007</b>	<b>2008</b>	
Esfinge	15.08	23.00	24.5	8.0	23.5	<i>18.82</i>
PTUE/Senso	28.54	25.00	—	42.0	46.5	<i>35.51</i>
Priberam	—	64.50	67.0	50.5	63.5	<i>61.34</i>
NILC	—	—	1.5	—	—	<i>1.5</i>
RAPOSA	—	—	13.0	20.0	14.5	<i>18.83</i>
QA@L <sup>2</sup> F	—	—	—	13.0	20.0	<i>16.5</i>
IdSay	—	—	—	—	32.5	<i>32.5</i>
RAPPORT	47.78	33.33	48.89	41.07*	37.78*	*

Although we are using the questions for Portuguese used in CLEF in those years, a major restriction applies: just the questions made upon CHAVE with known answers were selected, as made available from Linguateca. As such, we are using a grand total of 641 questions for testing our system.

Notice that the years of 2004, 2005 and 2006 have only 180 (out of 200) known questions each, with their answers found in CHAVE, and the other two years have the remaining, with 56 in 2007, and 45 in 2008. In those two last years, the majority of the questions had the answers found on the Portuguese Wikipedia instead of just CHAVE. As such, the results for 2007 and 2008 represent the overall accuracy (grouping CHAVE and Wikipedia) of the different systems in those years, and not just for questions over CHAVE — unfortunately, the values for CHAVE and Wikipedia were not available separately. That is the reason for omitting the average result of our system in Table 1, and signalling the results for the years 2007 and 2008.

For verifying if the retrieved triples contain the expected answers, the triples must contain (in the subject or in the object) the named entities found in the questions (or, in alternative, proper nouns, and, if that fails, just the remaining nouns), and also match in the subject or in the object the known answers from CHAVE (alongside the same document id).

Using the set of questions that were known to have their answers found on CHAVE, on a base line scenario, we were able to find the triples that answer

42.09% of the questions (274 in 641), grouping all the question from the already identified editions of CLEF, without a limit of triples for each question. (If the maximum retrieved triples per question is reduced to 10, the number of answered questions drops to 20.75%).)

On the answers that have not been found, we have determined that in a few cases the fail is due to questions depending on information contained in other questions or their answers. In other situations, the problem lies on the use of synonyms, hyponyms, hypernyms and related issues: for instance, the question focusing on a verb and the answer having a related noun, as in “*Who wrote Y?*” for a question and “*X is the author of Y.*”. There are certainly also many shortcomings in the creation of the triples, mainly on the chunks that are close together, as opposed to the dependency chunks, that should and must be addressed, in order to improve and create more triples. Furthermore, there are questions that refer to entities that fail to be identified as such by our system, an so no triples were created for them when processing the sentences.

## 5 Conclusions and Future Work

Although the proposed system currently only scores in an average place among the other systems, the use of triples seems to be a promising way of selecting the right and shorter answers to most of the questions addressed. However, there is a lot that can be improved.

Triples could be improved, namely those that are built from the relations of proximity between chunks, so the system is able to have a number of retrieved triples on par with the sentences that contain the answers (and the triples). Another boost to the approach would be to differentiate the queries accordingly to the types of the named entities found in the questions, and improve NER, both on questions an on corpus sentences.

It is also our intention to use synonyms, hyponyms, hypernyms, and other relations between tokens or lemmas, in order to expand and improve the queries made to the indices, which will increase the number of retrieved sentences — and the number of right triples would also increase — using a wordnet-like resource, such as Onto.PT [9].

We are currently studying a way of relating words of the same family, such as “*escritor*” (writer) and “*escrever*” (to write) that when lemmatized, or even stemmed, end up being put apart. That can be an issue in situations where the question uses a verb for characterizing the agent, and the candidate answer uses, for instance, an adjective (of the same family of the verb) to characterize the same agent. A solution may be a list of agents and corresponding verbs, applying a set of rules to the verbs in order to generate the corresponding agents.

Another aspect that should be considered is the use of coreference resolution [10] in order to improve the recall of triples by way of replacing, for instance, pronouns with the corresponding, if any, named entities, and hence increasing the number of usable triples.

We believe that expanding the queries using the above technics, and creating better model extract triples, can achieve better results in a short time span.

Finally, the next major goal is to use the Portuguese Wikipedia as a repository of information, either alongside CHAVE, to address the latter editions of CLEF, or by itself, as it has happened in Págico [15].

## References

1. Amaral, C., Figueira, H., Martins, A., Mendes, A., Mendes, P., Pinto, C.: Prib-eram's question answering system for Portuguese. In: Peters, C., et al. (eds.) CLEF 2005. LNCS, vol. 4022, pp. 410–419. Springer, Heidelberg (2006)
2. Baeza-Yates, R., Ribeiro-Neto, B.: Modern Information Retrieval. ACM Press, New York (1999)
3. Carvalho, G., de Matos, D.M., Rocio, V.: IdSay: question answering for Portuguese. In: Peters, C., et al. (eds.) CLEF 2008. LNCS, vol. 5706, pp. 345–352. Springer, Heidelberg (2009)
4. Costa, L.F.: Esfinge – a question answering system in the web using the Web. In: Proceedings of the Demonstration Session of the 11th Conference of the European Chapter of the Association for Computational Linguistics, pp. 410–419. Association for Computational Linguistics, Trento, Italy, April 2006
5. Filho, P.P.B., de Uzêda, V.R., Pardo, T.A.S., das Graças Volpe Nunes, M.: Using a text summarization system for monolingual question answering. In: CLEF 2006 Working Notes (2006)
6. Forner, P., et al.: Overview of the CLEF 2008 multilingual question answering track. In: Peters, C., et al. (eds.) CLEF 2008. LNCS, vol. 5706, pp. 262–295. Springer, Heidelberg (2009)
7. Gamallo, P.: An overview of open information extraction. In: Pereira, M.J.V., Leal, J.P., Simões, A. (eds.) Proceedings of the 3rd Symposium on Languages, Applications and Technologies (SLATE 2014). OpenAccess Series in Informatics, pp. 13–16. Schloss Dagstuhl – Leibniz-Zentrum für Informatik, Dagstuhl Publishing, Germany (2014)
8. Giampiccolo, D., et al.: Overview of the CLEF 2007 multilingual question answering track. In: Peters, C., Jijkoun, V., Mandl, T., Müller, H., Oard, D.W., Peñas, A., Petras, V., Santos, D. (eds.) CLEF 2007. LNCS, vol. 5152, pp. 200–236. Springer, Heidelberg (2008)
9. Gonçalo Oliveira, H.: Onto.PT: Towards the Automatic Construction of a Lexical Ontology for Portuguese. Ph.D. thesis, Faculty of Sciences and Technology of the University of Coimbra (2012)
10. Jurafsky, D., Martin, J.H.: Speech and Language Processing, 2nd edn. Pearson Education International Inc, Upper Saddle River (2008)
11. Magnini, B., et al.: Overview of the CLEF 2006 multilingual question answering track. In: Peters, C., Clough, P., Gey, F.C., Karlgren, J., Magnini, B., Oard, D.W., de Rijke, M., Stempfhuber, M. (eds.) CLEF 2006. LNCS, vol. 4730, pp. 223–256. Springer, Heidelberg (2007)
12. Magnini, B., et al.: Overview of the CLEF 2004 multilingual question answering track. In: Peters, C., Clough, P., Gonzalo, J., Jones, G.J.F., Kluck, M., Magnini, B. (eds.) CLEF 2004. LNCS, vol. 3491, pp. 371–391. Springer, Heidelberg (2005)
13. Mendes, A., Coheur, L., Mamede, N.J., Ribeiro, R., Batista, F., de Matos, D.M.: QA@L<sup>2</sup>F, first steps at QA@CLEF. In: Peters, C., Jijkoun, V., Mandl, T., Müller, H., Oard, D.W., Peñas, A., Petras, V., Santos, D. (eds.) CLEF 2007. LNCS, vol. 5152, pp. 356–363. Springer, Heidelberg (2008)

14. Moens, M.F.: Information Extraction: Algorithms and Prospects in a Retrieval Context. Springer-Verlag, Heidelberg (2006)
15. Mota, C.: Resultados Págicos: Participação, Resultados e Recursos. *Linguamática* **4**(1) (April 2012)
16. Nivre, J., Hall, J., Nilsson, J., Chanev, A., Eryigit, G., Kübler, S., Marinov, S., Marsi, E.: MaltParser: A language-independent system for data-driven dependency parsing. *Natural Language Engineering* **13**(2), 95–135 (2007)
17. Quaresma, P., Quintano, L., Rodrigues, I., Saias, J., Salgueiro, P.: The University of Évora approach to QA@CLEF-2004. In: CLEF 2004 Working Notes (2004)
18. Rodrigues, R., Gonçalo Oliveira, H., Gomes, P.: LemPORT: a high-accuracy cross-platform lemmatizer for Portuguese. In: Pereira, M.J.V., Leal, J.P., Simões, A. (eds.) Proceedings of the 3rd Symposium on Languages, Applications and Technologies (SLATE'14). OpenAccess Series in Informatics, pp. 267–274. Schloss Dagstuhl – Leibniz-Zentrum für Informatik, Dagstuhl Publishing, Germany (2014)
19. Saias, J., Quaresma, P.: The senso question answering approach to Portuguese QA@CLEF-2007. In: Nardi, A., Peters, C. (eds.) Working Notes for the CLEF 2007 Workshop. Budapest, Hungary (2007)
20. Santos, D., Rocha, P.: The key to the first CLEF in Portuguese: topics, questions and answers in CHAVE. In: Proceedings of the 5th Workshop of the Cross-Language Evaluation Forum, pp. 821–832. Springer-Verlag, Bath, September 2005
21. Sarmento, L., Oliveira, E.: Making RAPOSA (FOX) smarter. In: Nardi, A., Peters, C. (eds.) Working Notes for the CLEF 2007 Workshop. Budapest, Hungary (2007)
22. Strzalkowski, T., Harabagiu, S. (eds.): Advances in Open Domain Question Answering, Text, Speech and Language Technology, vol. 32. Springer-Verlag, Heidelberg (2006)
23. Vallin, A., et al.: Overview of the CLEF 2005 multilingual question answering track. In: Peters, C., et al. (eds.) CLEF 2005. LNCS, vol. 4022, pp. 307–331. Springer, Heidelberg (2006)

# Automatic Distinction of Fernando Pessoas' Heteronyms

João F. Teixeira<sup>1(✉)</sup> and Marco Couto<sup>2</sup>

<sup>1</sup> University of Porto, Porto, Portugal

jpfteixeira.eng@gmail.com

<sup>2</sup> HASLab / INESC TEC, University of Minho, Braga, Portugal

marcocouto90@gmail.com

**Abstract.** Text Mining has opened a vast array of possibilities concerning automatic information retrieval from large amounts of text documents. A variety of themes and types of documents can be easily analyzed. More complex features such as those used in Forensic Linguistics can gather deeper understanding from the documents, making possible performing difficult tasks such as author identification. In this work we explore the capabilities of simpler Text Mining approaches to author identification of unstructured documents, in particular the ability to distinguish poetic works from two of Fernando Pessoas' heteronyms: Álvaro de Campos and Ricardo Reis. Several processing options were tested and accuracies of 97% were reached, which encourage further developments.

**Keywords:** Authorship classification · Machine learning · SVM · Text mining

## 1 Introduction

With the dawn of Text Mining (TM) a massive amount of information was enabled to be retrieved automatically. It is intended to find and quantify even subtle correlations over a large amount of data. This way, a wide variety of themes (economics, sports, etc) with different levels of structure, could be analyzed with little effort. Many TM solutions have been employed in security and web text analysis (blogs, news, etc). TM has been used in sentiment analysis as for evaluating movie reviews to estimate acceptability [1]. Forensic Linguistics enhances TM by considering higher level features of text. Linguistic techniques are usually applied to legal and criminal contexts for problems such as document authorship, analysis and measure of content and intent.

The purpose of this study is to generate a small representation of a large corpus of poems, able to discern between authors or aliases. For this initial study we selected to classify the collection of poems by two of Fernando Pessoa's heteronyms. Ricardo Reis and Álvaro de Campos were chosen due to their contrasting themes and initial concerns relative to the model's accuracy for this kind of dataset.

To the best of our knowledge, there are no pattern recognition studies for alias distinction on poetic texts, therefore, no direct comparison of this work can be made. On the other hand, there is research on generic alias identification [2], however the objective is to find which aliases correspond to the same author and not to distinguish between personnas.

The author whose works we analyze is Fernando Pessoa [3], who wrote under several heteronyms or aliases. Each one had their own life stories and personal taste in writing style and theme.

Ricardo Reis is an identity of classical roots, when considering his poems' structure, theatricality and entities mentioned (ancient Greek and Roman references). He is fixated with death and avoids sorrow by trying to disassociate himself with anything in life. He seeks resignation and intellectual happiness.

Álvaro de Campos has a different personality, even presenting an internal evolution. Initially, he is shown to be a thrill seeker, mechanic enthusiast, and wishes to live the future. In the end, he feels defeated by time and devoided of the will to experience life. Consequently, he uses a considerable amount of interjections, in a weakly formatted writing style, with expressive punctuation.

The remaining of this document is structured as follows: In Section 2 the dataset is presented and described. Section 3 shows the methodology employed. Section 4 details the experimental approach, along with the result discussion. Section 5 the overall findings are presented along with possible future work.

## 2 Dataset

The dataset used in this work consists of the complete known poetic works<sup>1</sup> of *Ricardo Reis* (class RR) and *Álvaro de Campos* (class AC). Table 1 presents some statistics concerning the dataset.

**Table 1.** Class distribution

Class	# of entries	%	# of Words		# of Verses	
			Avg.	Std.	Min	Max
RR	129	54%	77.9	65.1	19	570
AC	108	46%	360.9	904.2	29	7857

## 3 Methodology

In this section, the steps taken and experimental approach followed are shown. First, we tested the classifier with the tokenized documents and we progressively introduced other pre-processing models, comparing their performance.

The SVM model was validated with 70% of the dataset using 5-fold cross-validation while the remaining 30% enabled to evaluate the generalization performance of the generated model, i.e., the voting result of the 5 fold models.

---

<sup>1</sup> Available at: <http://www.dominiopublico.gov.br>

### 3.1 Document Pre-processing

*S<sub>1</sub>-Tokenization.* Each document was turned into a sequence of word-level terms. Then, they were compacted into *bags-of-words* (BoW), disregarding their order, which is the most common document representation [4].

*S<sub>2</sub>-Casing Transformation.* After the tokenization, all words suffer a lower-case transformation, reducing the number of different terms. Here, we disregard the capitalization of the poems' first word at every verse, while inadvertently removing significance from capitalized names and some metaphoric references.

*S<sub>3</sub>-Length Filtering.* We remove from the token bags terms that contain below 4 or above 15 letters. The reason for this relates to the high probability of shorter words being irrelevant articles or connectors, leading to overfitting of the model, and not many Portuguese words have such large lengths. In fact, the average size of Portuguese words is 4.64 [5]. Nevertheless, removing words produces a more compact representation of the dataset and reduces possible dimensionality issues the classification model may experience with larger feature spaces.

*S<sub>4</sub>-Stemming.* Word Stemming also compacts document instances. This consists of removing word affixes, leaving only the root term. Generally, stemmers follow iterative replacement rules, some even dealing with irregular and rare terms. For this work, the Snowball Portuguese dictionary was used [6] [7].

*S<sub>5</sub>-Stopword.* Finally, we include stopword removal. This consists of ignoring all terms in a given dictionary. This might help the classifier focus on meaningful terms instead of considering articles, connectors and overall writing style. Also, specific unwanted words can be eliminated.

### 3.2 Occurrence Metrics

To evaluate if a word is distinctive for the classification task some methods based on its occurrence can be used. The following metrics were experimented:

*Binary Term Occurrence.* BTO identifies the number of documents in which a given term occurs. It provides little information thus is rarely used.

*Term Occurrence.* The TO metric provides the number of times a word occurs on each document of the collection. This can be viewed as a measure of significance of a given word for each document.

*Term Frequency.* The TF is a relative measure of the word occurrence considering the number of words in a document. Consequently, this can be misleading depending on the documents' length variability.

*TF-IDF.* is generally calculated as the product of TF and the Inverse Document Frequency (IDF) [8]. The IDF approach concerns the number of documents which contain a given term. A term that occurs frequently does not provide discriminative power and should be given less importance (lower weight) [9].

We used SVMs [10] that can linearly separate clusters of data on feature space, by maximizing the hyperspace boundary margin. The model was fed an array of occurrence metrics for the terms included after pre-processing.

Since the focus of this work was on Text Mining, the SVM model employed was relatively simple. A linear kernel with shrinking heuristics was used. It included a termination tolerance  $\varepsilon = 0.001$  and no penalty ( $C = 0$ ).

## 4 Experimental Results

### 4.1 Estimation Using Cross-Validation

In Section 3, we conduct several experiments in which the text pre-processing algorithms are incrementally included. These experiments considered the occurrence metric *tf-idf* since it is intuitively the most appropriate to compare the results of models trained with such different instance content. The accuracy of the experiments is  $S_1:93.35\%$ ,  $S_2:91.58\%$ ,  $S_3:90.44\%$ ,  $S_4:91.03\%$  and  $S_5:90.44\%$ .

With the length and stopword filtering several of the top scoring terms (SVM weights) were removed. However most of these were articles and connectors which could lead to model overfitting. Their removal only decreased slightly the accuracy. Along with stemming and the lowercase transformation, the number of attributes considered was reduced in more than half (8941 to 4398 terms).

The following experiments aim to evaluate the influence of different the occurrence metrics on the classification model. Table 2 presents the results of those experiments. The results show that the model using Term Occurrence based metrics (BTO, TO) performs worse than with frequency based metrics (TF, *tf-idf*) including misclassification rate balance.

We note that this comparison is not truly fair. The processing pipeline for the experiments was previously optimized for *tf-idf* thus, providing only a general comparison. The performances with these last two are very close and, therefore, the best method cannot be directly found.

**Table 2.** Occurrence Metrics Experiments (%)

Binary TO			TO			TF			TF-IDF		
Acc	F1 <sub>RR</sub>	F1 <sub>AC</sub>	Acc	F1 <sub>RR</sub>	F1 <sub>AC</sub>	Acc	F1 <sub>RR</sub>	F1 <sub>AC</sub>	Acc	F1 <sub>RR</sub>	F1 <sub>AC</sub>
80.74	84.91	73.33	68.71	77.39	49.01	91.03	91.89	89.80	90.44	91.58	88.73

### 4.2 Evaluation of Validation Setup

In this section, we considered, from the previous experiments, the pipelines with the two best performances and with BTO (baseline), while using the remaining 30% of the dataset. The results are shown on Table 3.

As expected, BTO maintained the low accuracy and obtained lower F1<sub>AC</sub>. The best two models kept the high accuracy, however, *tf-idf* managed to overcome the improvement of TF, from the validation phase, even if only by 3 instances. This suggests that, even though *tf-idf* presented lower validation results, it was somewhat underfitting. Either way, these comparative results were expected due to the consideration of term rarity metrics of *idf*.

### 4.3 Influence of Long Poems

Due to a large difference of length statistics between the two labels, we conducted further analysis. The documents were segmented into multiple instances such

**Table 3.** Testing Set Results (%)

Binary TO			TF			TF-IDF		
Acc	F1 <sub>RR</sub>	F1 <sub>AC</sub>	Acc	F1 <sub>RR</sub>	F1 <sub>AC</sub>	Acc	F1 <sub>RR</sub>	F1 <sub>AC</sub>
66,20	76,47	40,00	92,96	93,83	91,80	97,18	97,44	96,88

**Table 4.** Updated Class distribution

Class	# of entries	%	# of Words			# of Verses		
			Avg.	Std.	Min Max	Avg.	Std.	Min Max
RR	169	51%	63.5	27.0	3 161	11	4	1 17
AC	165	49%	240.8	150.0	29 521	30	145	5 54

that the portions had the maximum amount of verses equal to the previous mean for that class (plus a tolerance). Table 4 presents the updated class distribution.

For this experiment, the complete word processing pipeline and *tf-idf* scoring criteria were used (testing phase best results). For the cross-validation and testing steps, respectively, the accuracy was 96.58% and 96.04%; the F1<sub>RR</sub> was 96,64% and 96,15% and the F1<sub>AC</sub> was 96,49% and 95,92%.

The results show that imposing the upper bound on the number of verses per poem increased the accuracy of the model in the validation phase by around 5%. Apart from accuracy, the model should have really improved since the misclassification rates became more balanced.

It is safe to assume that longer poems might be more difficult to sort correctly into classes since they encompass more terms that can be highly influential to the *tf-idf* metric (through emphatic repetition, etc) which may not contribute positively for the accurate learning of attribute weights. Thus, this can affect poorly on the classification. On the other hand, the test results, in a way, contradict the analysis from the cross-validation. It performs slightly worse than the test experiment for *tf-idf*. As of this, we cannot provide an acceptable hypothesis as to which this occurs, rendering this analysis inconclusive.

## 5 Discussion and Conclusions

In this work we aimed to distinguish the authorship of poetic texts from two heteronyms of Fernando Pessoa, solely using basic Text Mining approaches. To our surprise, the methods were able to predict quite accurately (most over 70%, best ~97%), further verifying the a clear difference between the heteronyms.

This comes as a revelation mainly because, the author is, in fact, the same, despite having created these two personnas, and thus, the vocabulary and certain parts of writing style should be ubiquitous to the heteronyms.

Many of the best discerning words were related to writing style, including several possessive related terms for AC. However, obviously, some of the best terms were theme related keywords such as *grande* and *sentir*, referring to the

magnificence of feelings of AC, *cansaço*, *domingo* and *sonho* to the tiredness AC feels towards the end and recollections of the past; while RR tries to remain forever calm and avoids pain.

Among the settings tested, *tf-idf* demonstrated, as expected, the best balance and generated the highest accuracy for the testing set.

The change in accuracy for the shorter instance set was not conclusive. These results suggest that dividing the larger poems was either not that relevant or additional instances would be needed to confirm (accuracy already close to 100%).

Although our methodology produces good results, we intend to extend the study to the rest of the heteronyms to evaluate if this kind of simple analysis is still sufficient for discernibility. Additional relevant experiments and approaches could include the model's response to a few verses instead of large chunks or complete poems and word *n-grams* analysis for style traits identification.

We realized that, according to Zipf's law, both the highest and lowest frequent terms are less frequent in large documents. Thus, our approach could be improved concerning the enhancement of term relevance instead of only minding to frequency. This could be done by including a normalization term in the *tf-idf* formula [11].

## References

- Pang, B., Lee, L., Vaithyanathan, S.: Thumbs up?: sentiment classification using machine learning techniques. In: Proceedings of the ACL 2002 Conference on Empirical Methods in Natural Language Processing, EMNLP 2002, vol. 10, pp. 79–86. Association for Computational Linguistics, Stroudsburg (2002)
- Nirkhi, S., Dharaskar, R.V.: Comparative study of authorship identification techniques for cyber forensics analysis (2014). CoRR abs/1401.6118
- de Castro, M.G. (ed.): Fernando Pessoa's Modernity Without Frontiers: Influences, Dialogues, Responses. Tamesis Books, Woodbridge (2013)
- Sebastiani, F.: Machine Learning in Automated Text Categorization. ACM Comput. Surv. **34**(1), 1–47 (2002)
- Quaresma, P., Pinho, A.: Análise de frequências da língua portuguesa. In: Livro de Actas da Conferência Ibero-Americana InterTIC, pp. 267–272. IASK, Porto (2007)
- Porter, M.F.: Snowball: A language for stemming algorithms, October 2001. <http://snowball.tartarus.org/texts/introduction.html>
- Porter, M.F.: Snowball: Portuguese stemming algorithm. <http://snowball.tartarus.org/algorithms/portuguese/stemmer.html>
- Salton, G., Buckley, C.: Term-weighting Approaches in Automatic Text Retrieval. Inf. Process. Manage. **24**(5), 513–523 (1988)
- Robertson, S.: Understanding inverse document frequency: on theoretical arguments for IDF. Journal of Documentation **60**(5), 503–520 (2004)
- Vapnik, V.N.: An overview of statistical learning theory. Trans. Neur. Netw. **10**(5), 988–999 (1999)
- Singhal, A., Buckley, C., Mitra, M.: Pivoted document length normalization. In: Proceedings of the 19th Annual International ACM SIGIR Conference on Research and Development in Information Retrieval, SIGIR 1996, pp. 21–29. ACM, New York (1996)

# Social Impact - Identifying Quotes of Literary Works in Social Networks

Carlos Barata<sup>1,2(✉)</sup>, Mónica Abreu<sup>1</sup>, Pedro Torres<sup>2</sup>, Jorge Teixeira<sup>2,3</sup>,  
Tiago Guerreiro<sup>1</sup>, and Francisco M. Couto<sup>1</sup>

<sup>1</sup> Departamento de Informática, Faculdade de Ciências,  
Universidade de Lisboa, Lisbon, Portugal  
[cbarata7@gmail.com](mailto:cbarata7@gmail.com)

<sup>2</sup> SAPO Labs, Lisboa, Portugal

<sup>3</sup> LIACC, Universidade Do Porto, Porto, Portugal

**Abstract.** A non-neglectable amount of information shared in social networks has quotes to literary works that, most of the times, is not linked to the original work or author. Also, there are erroneous quotes that do not fully match the original work, for example by including synonyms and slang words. Moreover, users sometimes associate their quotes to the wrong author, which creates misleading information. This paper presents *Social Impact* framework as an approach to identify quotes in social networks and match them to the original literary works from a particular author. This framework was applied to two case-studies: *O Mundo em Pessoa* and *Lusica*. In the first case-study, *Social Impact* evaluation achieved 98% for precision measure and 59% for recall, whereas in the latter case-study it obtained 100% for precision and 53% of recall.

**Keywords:** Information retrieval · Information extraction · Web mining · Text mining · Pattern recognition

## 1 Introduction

Social networks emerged in last decade and changed the way we communicate, becoming essential tools in the human interaction. This happened possibly due to the fact that, at the distance of a click, lays the possibility to send and share content. As Kwak et al.[4] refers, this wide use of social networks provide a great interest of investigation in many areas like extraction and information analysis.

Most of the information shared in social networks such as Twitter and Facebook is in text format, and an interesting amount of such information (messages) contains quotes to literary works (e.g.: “Tudo vale a pena, quando a alma não é pequena - Fernando Pessoa”). Nevertheless, in a non-neglectable number of cases there is no reference to which text, book or literary work the quote is referred.

Due the fact that quotes may have incoherencies (e.g.: quote is different from the original text), the identification of the original text or author can be very challenging. These incoherencies have a higher presence on social networks

(against, for instance, opinion articles on news) because of particular characteristics of the network, namely: short messages or reduced context. The use of synonyms or typos are some of the most common causes for the lack of accuracy in the quotes published in social networks. One may think hash-tags can substantially reduce the complexity of this task, but unfortunately the usage of hash-tags on messages literary work is low as referred in [8] study. This study concluded that in Twitter, the ratio of hash-tags per tweet is between 4%(in Japanese language) to 25%(in German language) of the total tweets using them.

This paper presents *Social Impact* platform as an approach to this problem. The framework major goal is to identify quotes from literary work on social network messages, supported on *SocialBus*<sup>1</sup> and Apache Lucene systems. Evaluation was performed on two case-studies: *O Mundo em Pessoa* and *Lusica*.

## 2 Related Work

*Social Impact* platform is generically supported on two different technological blocks: *SocialBus*, a social network crawling and analysis platform, and Lucene, a high-scalable infrastructure for indexing and querying documents.

**SocialBus:** Social networks such as Twitter and Facebook provide APIs that allow access to public messages, within certain limits, giving the possibility of analysing such content for a variety of purposes, including quotes detection. We propose to use *SocialBus* platform[2, 7], a framework that collects and analyse data from Twitter and Facebook for a pre-defined set of users representative of the Portuguese community.

**Lucene:** is an open-source software<sup>2</sup> for text searching and indexing through a document indexation, coded in Java programming language and developed by Apache Software Foundation. According to Gospodnetic et al.[3] this framework works through the indexation of documents, information parsers and queries to consult and retrieve the indexed information. The result is a ranked list of documents ordered by relevance [1, 5, 6].

## 3 Social Impact Platform

*Social Impact* main objective is to find quotes in messages published in social networks and subsequently link them to their original literary work. This framework stores such data in a relation database and provides such data as RESTful APIs. More importantly, *Social Impact* architecture is abstract enough to be applied on different contexts and scenarios.

---

<sup>1</sup> <http://reaction.fe.up.pt/socialbus/>

<sup>2</sup> <http://lucene.apache.org/core/>

### 3.1 Architecture

The *Social Impact*'s structure is based on a Service-Oriented Architecture(SOA), broadly used in web applications, due to its standardisation approach. This architecture is represented in Figure 1 and it has three main layers, described below.

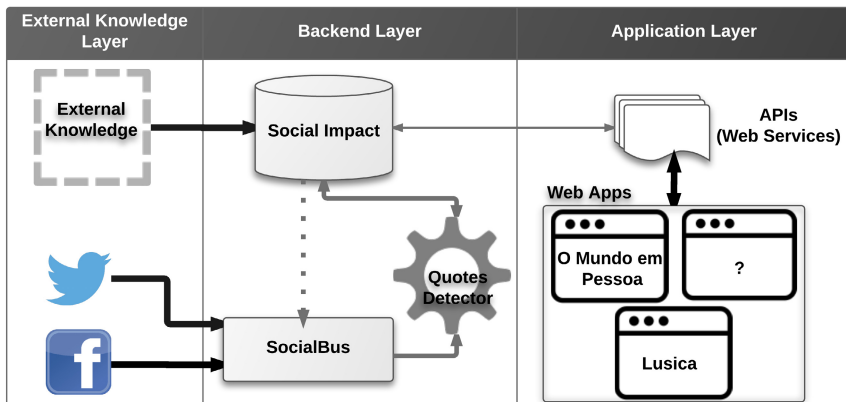


**Fig. 1.** *Social Impact* Global Architecture

**External Layer:** represents information and knowledge external to *Social Impact* platform and that somehow is collected into the system. The leftmost block, External knowledge, represents data specific to each case-study, including literary work (e.g.: poems from Fernando Pessoa<sup>3</sup>) or domain specific keywords used to narrow the search over *SocialBus* collected data (e.g.: poems or musics authors). The remain two blocks represent Twitter<sup>4</sup> and Facebook<sup>5</sup> APIs to feed *Social Impact* with data from social networks.

**Backend Layer:** is the core layer of *Social Impact*, and it is responsible for processing the messages coming from *SocialBus* and analyse them through the Quotes Detector, as well as store those messages and their subsequently generated meta-data on suitable a relational database (MySQL).

**Application Layer:** represents the interface with the potential applications using *Social Impact* platform. This layer comprehends a set of RESTful APIs that provides information previously processed in the Backend layer to the web applications.

<sup>3</sup> Data obtained from “Arquivo Pessoa” available at <http://arquivopessoa.net>

<sup>4</sup> <https://dev.twitter.com/rest/public>

<sup>5</sup> <https://developers.facebook.com>

### 3.2 Quotes Detector

Figure 2 presents a detailed diagram of the Quotes Detector module, with two essential flows of information:

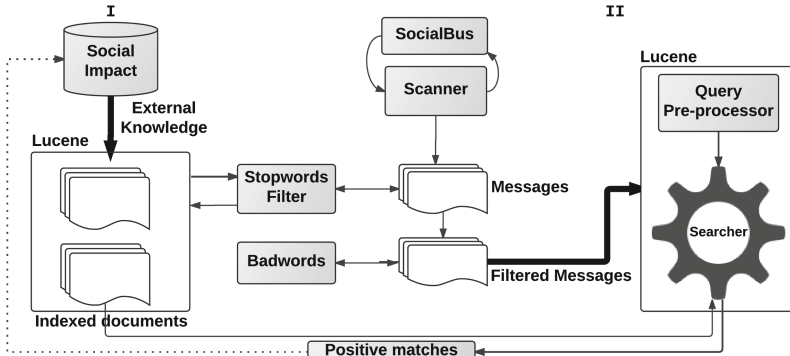


**Fig. 2.** Quotes detector workflow

**Pre-processing and Indexing External Knowledge:** represented in Figure 2 as “I” is imported only once and include, for instance, all the literary work from a particular author. Each of these documents (e.g.: a single poem) is submitted to Lucene engine, filtered through a stopwords filter and indexed.

**Identification and Indexing of Quotes** (refer to “II” in Figure 2) module is listening to *SocialBus* and imports new data as new messages arrive to *SocialBus*. Those messages are then filtered with a stopwords and a badwords (curse words) filter. Each filtered message is transformed into a lucene query syntax. The “Search” operation compares the indexed documents from *Social Impact* (External Knowledge) with each new message and retrieve, if the score is above a given threshold, the most relevant document (poem, music, etc.) as a positive match of a quote. Moreover, all tokens from the matched message are isolated and stored in the database.

## 4 Case Studies

**O Mundo em Pessoa**<sup>6</sup> is a web based project that aims to depict the presence of Fernando Pessoa poems on social networks, based on quotes to his literary. This project is based on *Social Impact* platform and it covers Fernando Pessoa work and from all his heteronyms. The list of terms used to narrow the messages crawling (refer to Section 3.1) contains the names of all Fernando Pessoa heteronyms. This project is supported on a Web Application that displays the identified quotes from Fernando Pessoa organized by timeframes, going from one

<sup>6</sup> <http://fernandopessoa.labs.sapo.pt/>

day to one month. For each quote, the user has the possibility to explore the number of social network users that publish that particular quote and access the original message, among other features.

*Lusica*<sup>7</sup> main purpose was study the lusophone music and its presence on the social networks, supported on *Social Impact* platform. There are two important aspects that differentiate “Lusica” from “Mundo em Pessoa”: (i) the domain is music instead of literary, and (ii) a large effort was put on the visualization of the information obtained from the quotes detection, through an interactive graph available online. “Lusica” external knowledge (refer to Figure 1) is based on the musics’ and albums’ titles from lusophone artists. Such information was obtained from LastFM APIs<sup>8</sup> (the list of lusophone artists) and from MusicBrainz service<sup>9</sup> (the albums and musics titles for each lusophone artist).

## 5 Results and Discussion

In this section will be displayed the results of the evaluation of *Social Impact* for both case studies. This evaluation aims to provide an overview of the system’s performance.

**Data Collection:** For evaluation purposes, we used a subset of data published between January 2014 and June 2014. Regarding *O Mundo em Pessoa*, from a set of 56.212 collected messages, only approximately 8% (4.720 messages) were identified as quotes (with Lucene score larger than 1,0). As expected, most of the collected messages are not classified as quotes, and this phenomenon can be explained by the fact that many of the collected messages are just references to Fernando Pessoa but are not actually a quote to his literary work. For *Lusica*, results are similar to *O Mundo em Pessoa*, with only less than 5% (7.628) of messages representing references to the songs’ artists, in a set of approximately 420.000 messages.

**Quotes Detector Evaluation:** Precision and recall metrics were calculated based on the following types of documents: True positive (TP): messages correctly classified as quotes; False positive (FP): messages incorrectly classified as quotes; True negative (TN): messages correctly classified as not quotes; False negative (FN): messages incorrectly classified as not quotes. Precision is measured as  $P = TP/(TP+FP)$  while recall is  $R = TP/(TP+FN)$ . Regarding recall, our assumption is that *SocialBus* filtered messages correspond to all representative messages for the specific domain of the case-study. Evaluation was performed manually on a sample of 200 randomly chosen messages for each of the case-studies. Regarding “Mundo em Pessoa”, the evaluation dataset was divided in 4 parts according to Lucene score and Twitter *versus* Facebook messages. Results for Twitter shown a precision of 19% and recall of 100% for low scores (between 0,5 and 1,0) and precision of 98% and recall of 100% for high scores (between

---

<sup>7</sup> <http://lusica.labs.sapo.pt/>

<sup>8</sup> <http://www.last.fm/api>

<sup>9</sup> [https://musicbrainz.org/doc/MusicBrainz\\_Identifier](https://musicbrainz.org/doc/MusicBrainz_Identifier)

1,0 and 2,0). Concerning Facebook, precision value for low scores was 100% and recall 21% while for high scores was precision was 96% and recall was 100%. The average precision for “Mundo em Pessoa” was  $P_{MundoemPessoa} = 98\%$ , while recall was  $P_{MundoemPessoa} = 59\%$ . In respect to “Lusica”, the same principle was followed, by selecting a sample of 200 messages and dividing them in two groups (Twitter messages with low and high Lucene score). Results shown a average precision value  $P_{Lusica} = 100\%$ , while recall was  $P_{Lusica} = 53\%$ .

**Execution Time:** the performance of *Social Impact* platform was also evaluated, measuring the execution time of processing a single message in a desktop with an Intel(R) Xeon(R) CPU E5405 @ 2.00GHz processor and 3GB of RAM memory. For *O Mundo em Pessoa* the results achieved an average time of execution of 0,01 seconds ( $\pm 0,002$ ). Regarding *Lusica*, the result obtained was an average execution time of 0,02 seconds ( $\pm 0,004$ ).

## 6 Conclusions

This paper presented an approach to find quotes of original literary work in shared messages on social networks. The proposed approach is supported on the *Social Impact* developed platform presented in this paper. This framework was applied to two distinct case studies: *O Mundo em Pessoa* and *Lusica*.

Evaluation shown that most of the collected messages from *SocialBus* are not classified as quotes (less than 8%) because they are just references to the author and do not contain any quotes. *Social Impact* evaluation achieved high precision values for both case-studies:  $P_{MundoemPessoa} = 98\%$  and  $P_{Lusica} = 100\%$ .

Future work includes: (i) to automatically set the threshold for the Lucene score based on machine learning approaches; (ii) improve the domain specific list of keywords using automatic approaches; (iii) use user feedback to fill missing information about authors and song lyrics; and (iv) apply *Social Impact* platform on other non-literary corpora, such as plagiarism detection.

**Acknowledgments.** This work was partially supported by SAPO Labs and FCT through the project PEst-OE/EEI/UI0408/2013 (LaSIGE), and by the European Commission through the BiobankCloud project under the Seventh Framework Programme (grant #317871). The authors would like to thank to Bruno Tavares, Sara Ribas and Ana Gomes from SAPO Labs, João Martins, Tiago Aparcio, Farah Mussa, Gabriel Marques and Rafael Oliveira from University of Lisbon and Arian Pasquali from Universidade de Porto for all their support, insights and feedback.

## References

1. Baeza-Yates, R., Ribeiro-Neto, B., et al.: Modern information retrieval, vol. 463. ACM press New York (1999)
2. Boanjak, M., Oliveira, E., Martins, J., Mendes Rodrigues, E., Sarmento, L.: Twitterecho: a distributed focused crawler to support open research with twitter data. In: Proceedings of the 21st WWW, pp. 1233–1240. ACM (2012)

3. Hatcher, E., Gospodnetic, O.: Lucene in action. Manning Publications (2004)
4. Kwak, H., Lee, C., Park, H., Moon, S.: What is twitter, a social network or a news media? In: Proceedings of the 19th WWW, pp. 591–600. ACM (2010)
5. Liu, B.: Web data mining. Springer (2007)
6. Manning, C.D., Raghavan, P., Schütze, H.: Introduction to information retrieval, vol. 1. Cambridge University Press, Cambridge (2008)
7. Oliveira, E.J.S.L.: TwitterEcho: crawler focado distribuído para a Twittosfera portuguesa. Master's thesis, Faculdade de Engenharia da Universidade do Porto (2010)
8. Weerkamp, W., Carter, S., Tsagkias, M.: How people use twitter in different languages. Proceedings of the Web Science (2011)

# Fractal Beauty in Text

João Cordeiro<sup>1,3(✉)</sup>, Pedro R.M. Inácio<sup>1,2</sup>, and Diogo A.B. Fernandes<sup>2</sup>

<sup>1</sup> Department of Computer Science, University of Beira Interior,  
Rua Marquês d'Ávila e Bolama, 6200-001 Covilhã, Portugal  
[{jpaulo,inacio}@di.ubi.pt](mailto:{jpaulo,inacio}@di.ubi.pt)

<sup>2</sup> Instituto de Telecomunicações, Av. Rovisco Pais, 1 - Torre Norte,  
1049-001 Lisboa, Portugal  
[diogoabfernandes@gmail.com](mailto:diogoabfernandes@gmail.com)

<sup>3</sup> INESC – TEC, University of Porto,  
Rua Dr. Roberto Frias, 378, 4200-465 Porto, Portugal  
[jpcc@inescporto.pt](mailto:jpcc@inescporto.pt)

**Abstract.** This paper assesses if text possesses fractal properties, namely if several attributes that characterize sentences are self-similar. In order to do that, seven corpora were analyzed using several statistical tools, so as to determine if the empirical sequences for the attributes were Gaussian and self-similar. The Kolmogorov-Smirnov goodness-of-fit test and two Hurst parameter estimators were employed. The results show that there is a fractal beauty in the text produced by humans and suggest that its quality is directly proportional to the self-similarity degree.

**Keywords:** Self-similarity in text · Statistical linguistic studies

## 1 Introduction

Since the advent of the *World Wide Web*, an increasing number of users insert text from a multitude of sources, namely from newly created web pages, news in electronic newspapers, blogs, product reviewing, and social networks. This opened new opportunities for linguistic studies and the need for new applications to intelligently deal with all this text and to make sense out of it.

The question of automatically and effectively assessing the *quality* of a text remains unanswered. In general, an experienced human reader can judge the complexity and quality of a given text, a task not so easily attained with computational means. The human reader can not only determine if phrases are grammatically correct, but also figure out the lexicon degree and the structural and rhetorical combination of words, sentences, and ideas. There are aesthetic principles in the way of writing, yielding different types of texts. The spectrum ranges from almost telegraphic accretions, posted in Twitter, up to nobel prize winning novels. The goal of this study covers the topic of the text quality referred herein by looking after the mathematical principles underlying it.

This paper discusses a series of experiments conducted to find out if the text produced by humans exhibits a statistical property known as *self-similarity*. Self-similarity is a property of fractals, and it refers to the possibility of parts of a

(mathematical) object to be similar to its parts. In the case of self-similarity, it refers more specifically to the fact that the statistical properties of the object look the same independently of the scale from which it is observed.

This paper presents our initial findings on the self-similar properties of text. Its main contributions are twofold: (i) it is shown that the sequences, constructed by measuring several attributes of text blocks produced by humans, are self-similar, suggesting also that the self-similarity degree is related with the quality of the text; and (ii) the way the analysis is performed defines the basic foundations for future research on the intersection of these two fields.

## 2 Related Work

To the best of our knowledge, no other work has been involved in the determination of self-similarity in text and how it can be used for characterization assessment of general aesthetic principles. However, there are a number of related works with similar goals. For example, McCarthy and Jarvins [9] compared different methods to determine lexical diversity (LD) in text.

The LD index measures the vocabulary diversity of a given text segment and is usually calculated by dividing the number of tokens by the number of types (the number of unique tokens in a segment of text), also known as the *token-type* proportion. As it depends on the considered text segment length, it is not used directly to compute the LD index. Instead, a number of strategies have been proposed [6,9], some of them being based on the division of a text in fixed segments of  $n$  tokens. The LD index has been used to assess the writing skills of a subject in a variety of studies, namely in children language skills measurements, English second language acquisition, Alzheimer's onset, and even speaker socioeconomic status [7,8].

*Forensic linguistic analysis* [10] is a recent field with diverse applications, such as plagiarism detection [1], authorship identification [12], cybercrime and terrorism tracking [10], among others. The work in this field is based on the use of a number of text characteristics in different levels of analysis like morphological, lexical, syntactical, and rhetorical [1,12]. These textual characteristics necessarily exhibit different self-similar properties that suggest investigation. The findings presented in this work are a first step toward that objective, specifically at the lexical level.

## 3 Self-Similarity and Statistical Tools

In this paper, fractality is studied for values representing attributes of text. It does not concern any particular visual interpretation of the text, in which some artifact is repeated as we graphically zoom in or out. It refers to an interpretation for the statistical behavior of the aforementioned values (*e.g.*, the number of words or non-words in a sentence). Self-similarity refers to the property of a stochastic process that looks statistically identical for any (aggregation) scale from which it is observed from. It is typical to define a (discrete-time) self-similar

process  $\{X(t)\}_{t \in \mathbb{N}}$  as the one that fulfills the condition that  $X(t) \stackrel{d}{=} a^{-H} X(at)$ , where  $\stackrel{d}{=}$  denotes equality in all finite-dimensional distributions,  $a \in \mathbb{N}$  and  $0 < H < 1$  is the *Hurst parameter*, also referred to as the *self-similarity degree* or the *Hurst exponent*. The most widely known example of a self-similar process is the fractional Brownian motion (fBm), which has a Gaussian distribution. Its *first order differences process*, denoted as fractional Gaussian noise (fGn) is often useful too, since many natural or artificial processes occur in this form. Thus, when performing self-similarity analysis, it is typical to assess whether the empirical values are consistent with sampling a Gaussian variable. In this work, the Kolmogorov-Smirnov goodness-of-fit test [3] was used for that purpose.

There are several methods for estimating the Hurst parameter from empirical data, most of them based on repeatedly calculating a given statistic (*e.g.*, variance or maximum value) for the original process and for a finite number of aggregated processes. The Hurst parameter estimators used in this study were the well-known Variance Time (VT) and Rescaled Range Statistics (RS) estimators. The statistical tools mentioned herein are all implemented in the open-source *TestH* tool [4]. It accepts files containing raw values separated by space or newline, normalizes them, and outputs the estimated values of the Hurst parameter and the p-value concerning the Kolmogorov-Smirnov goodness-of-fit test.

When the Hurst parameter is 0.5, the process is *memoryless* and each occurrence is completely independent of any past or future occurrences. For values of the Hurst parameter ranging from 0 to 0.5, the process is *anti-persistent* or *short-range dependent*, while for values between 0.5 and 1, the process is said to be *persistent* or *long-range dependent*. There are many examples of long-range dependent processes in natural and artificial processes (*e.g.*, the water level in rivers [5]). Prior from starting this work, our expectation was that the text was self-similar with Hurst parameter larger than 0.5 and that the degree of self-similarity was perhaps related with the quality of the text.

Our base unit to construct processes of text attributes is a block of 100 words, meaning that all the sequences analyzed in the scope of this work refer to *attributes per 100 tokens*. If a self-similar structure is embedded in the data, then the statistical behavior of these attributes is the same (apart from scaling) for each block of tokens, or for any number of them. Additionally, it is an indication that human writing is done in bursts, which means that blocks with higher counts in some attribute are probably followed by other blocks with higher counts also, and vice-versa.

## 4 Data and Experimentation

Five different types of English-written corpora were analyzed in the performed experiments. Each corpus was prepared identically before being submitted for testing. There are essentially three major genres that stand out: *Literature*, *News Stories*, and *Blogs*. In order to strengthen the validation of the main hypothesis, it was also decided to include a text corpus generated randomly from the words of the English language. Below, follows a more detailed description of each corpus:

**The Blogs Corpus:** Also known as the *Blog Authorship Corpus* [11], is a massive collection of 681K blog posts, gathered from 19320 users, from the blogger.com website. These blogs cover a wide range of subjects like *Advertising*, *Biotechnology*, *Religion*, *Science*, among others. It contains a total of 38 different subjects, with 300 million words (844 MB). There are three user age clusters: 13-17 years (8240 users), 23-27 years (8066 users) and 33-48 years (2944 users);

**The News Corpus:** This corpus is formed by a huge set of news stories, automatically collected from the web. An amount of 4.2 MB of text was randomly selected from the set. The news stories were collected for several main subjects, namely *Politics*, *Economics*, *Finance*, *Science*, among others;

**The Literature Corpus:** The (i) complete work of Shakespeare and the (ii) set of books (66) from the Bible<sup>1</sup> was selected for this corpus type;

**The Random Corpus:** A corpus of similar size was randomly generated in order to validate the proposed self-similarity measure. Each word was randomly taken from the English vocabulary, according to a uniform<sup>2</sup> distribution.

The aim of this study is to know whether certain text characteristics exhibit self-similarity properties by resorting to the estimation of the Hurst parameter. The test herein described was designed to determine self-similarity in time series, performing a large number of measurements of attributes over time. Here, the origin of the several time series is a corpus consisting of a considerable amount of text. Thus, the experience had to be drawn to meet two principles: the (i) set of the textual attributes to be measure and the (ii) reading structure of the text in order to achieve a number of significant measurements.

**Definition of Attributes:** For the first principle we have considered six lexical features that are measured for a given block (amount) of text: the number of ( $A_0$ ) non-words; ( $A_1$ ) small words ( $|w| < 3$ ); ( $A_2$ ) medium words ( $3 \leq |w| < 7$ ); ( $A_3$ ) long words ( $|w| > 6$ ); ( $A_4$ ) sentences; and ( $A_5$ ) the lexical diversity.

**Reading Structure:** To satisfy the second principle we have decided to divide the text in sequential blocks with equal number of words. It was decided to choose the block size near to an average paragraph length, assuming five sentences per paragraph with each one having an average length of 20 words [2]. In previous studies of this kind, researchers usually take text chunks of this length [6,9]. Below is one such block of 100 tokens:

```
The guy's license plate was a little obvious" 68CONVT". I mean, you can see that
it's a convertible please, because the top was down. Anyway, I stared straight
ahead. but could hear that low throaty rumble next to me. Suddenly, I felt tears
prickling in my eyes. It dawned on me that I was suffering from the maliblues.
What will happen at Hot August Nights? Those muscle cars cruise nightly and rev
and rev and rev. I'm thinking I should get a medical bracelet with maliblues
```

---

```
(~W, |W|<3, 3=<|W|<6, |W|>=6, #Sentences, Lex. Div.) ---> (18, 16, 51, 15, 8, 67)
```

<sup>1</sup> We have chosen the English translation version from King James.

<sup>2</sup> In the future a Zipfian law will be considered.

## 5 Results

Each corpora (Section 4) was processed to produce the necessary sequences of numbers representing the time series to be analyzed. Given the attributes and block size, these sequences consisted of integer numbers larger than 0 and smaller than 100. After being input to the TestH tool, they were normalized and the VT and RS estimators were applied to the resulting process. The p-value for the  $\sqrt{n}D$  statistic was also calculated, via the application of the Kolmogorov-Smirnov goodness-of-fit statistical test available in the tool. Note that the values

**Table 1.** Results obtained on seven corpora regarding six attributes.

Corpora	<b>A<sub>0</sub>:</b> num. non words			<b>A<sub>1</sub>:</b> num. words < 3 chars			<b>A<sub>2</sub>:</b> num. words 3-6 chars		
	VT	RS	KS	VT	RS	KS	VT	RS	KS
Blogs 13-17	0.73778	0.86064	0.20301	0.70702	0.83312	0.27614	0.72485	0.83613	0.27614
Blogs 23-27	0.76648	0.86895	0.10449	0.81549	0.83606	0.34726	0.75532	0.81676	0.34726
Blogs 33-48	0.84432	0.85356	0.09445	0.83969	0.86252	0.11157	0.86863	0.84596	0.07483
News	0.63524	0.78496	0.01202	0.46540	0.81174	<b>0.00491</b>	0.73615	0.85698	<b>0.00351</b>
Bible	0.53201	0.83720	0.19772	0.65733	0.79622	0.19772	0.88749	0.81389	<b>0.00688</b>
Shakespeare	0.64795	0.84271	0.01136	0.63140	0.75893	0.03116	0.57925	0.78148	0.02035
Random	0.28842	0.46262	<b>0.00432</b>	0.68364	0.51305	0.97693	0.57995	0.46603	0.03807
Corpora	<b>A<sub>3</sub>:</b> num. words > 6 chars			<b>A<sub>4</sub>:</b> num. sentences			<b>A<sub>5</sub>:</b> Lexical Diversity (LD)		
	VT	RS	KS	VT	RS	KS	VT	RS	KS
Blogs 13-17	0.71949	0.86469	0.69745	0.76482	*VOR	0.43729	0.76005	0.82502	0.32957
Blogs 23-27	0.81764	0.88098	0.65178	0.82454	*VOR	0.40002	0.76380	0.81367	0.13147
Blogs 33-48	0.88160	0.92609	0.28191	0.81082	0.88063	0.66304	0.81663	0.82250	0.18178
News	0.75006	0.87849	0.03398	0.66815	*VOR	0.99286	0.64356	0.77951	0.25809
Bible	0.80095	0.84375	0.07482	0.81976	0.89219	0.59353	0.87111	0.86753	<b>0.00039</b>
Shakespeare	0.69241	0.75295	0.14385	0.66554	0.90009	0.29770	0.69826	0.81306	<b>0.00000</b>
Random	0.60186	0.40670	0.03351	0.26403	0.47593	0.67707	0.29526	0.46444	<b>0.00495</b>

\*VOR: Estimated value out of range.

in the KS column (table 1) suggest that the sequences seem to be coming from Gaussian processes, with only seven cases rejecting the null hypothesis if the significance level is set to 0.01 (bold values). This is interesting, and we will explore if it may be the consequence of the *central limit theorem*, verifying if the attributes are the result of the sum of several independent and identically distributed variables.

For the three age sub-sets of the blogs corpus, we can see that the VT and RS values improve consistently in almost all attributes, and this difference was very marked in the  $A_3$  and  $A_5$  attributes for the VT estimator. This shows well that, even within the same genre, more mature and possibly more experienced authors produce text with an higher degree of self-similarity. The estimated values of the Hurst parameter are consistently larger for RS.

In the literary corpora, we have a significant difference between text from Shakespeare and the Bible. In the latter, self-similarity values are much higher for most of the attributes and in particular for the lexical diversity ( $A_5$ ). Moreover, Shakespeare text reveals a low self-similarity in all attributes, with the exception for the RS estimator in  $A_4$ . The news genre did not reveal high self-similarity for most attributes. There are, however higher parameter values, for the attributes  $A_1$ ,  $A_2$ , and  $A_3$ , which suggests strong self-similarity in the lexicon used. The low values obtained in the randomly generated corpus (Random) allow us to put in perspective the values obtained for the other corpora. This reveals a phenomenon of self-similarity in the human writing process.

## 6 Conclusions and Future Work

The paper shows that there is fractal beauty in text. It is naturally not a property that is consciously included by the authors of the text, which makes the results even more surprising. They suggest that there might be a relation between what is perceived as text quality and the self-similarity degree, although a more complete (more attributes) and exhaustive (more corpora) analysis is required.

Future research work includes the assessment of self-similarity and goodness-of-fit for more attributes and a larger number of different corpus. It should also focus on a more detailed pre-processing of the data, which allows to address the potential lacks of stationarity in large corpus. Gaussianity will also be tested using the Chi-squared goodness-of-fit test, for consistency purposes. The RS will be replaced by the DFA estimator in the future, since the later is known to be more reliable than the aforementioned one. Our efforts will be directed towards finding the (mathematical) explanations behind our initial findings. We intend also to explore self-similarity on different levels of linguistic attributes.

**Acknowledgments.** This work is financed by the FCT – Fundação para a Ciência e a Tecnologia (Portuguese Foundation for Science and Technology) within project UID/EEA/50014/2013.

## References

1. Alzahrani, S., Naomie, S., Ajith, A.: Understanding plagiarism linguistic patterns, textual features, and detection methods. *IEEE Transactions on Systems, Man, and Cybernetics, Part C: Applications and Reviews* **42**(2), 133–149 (2012)
2. Cordeiro, J., Dias, G., Cleuziou G.: Biology Based Alignments of Paraphrases for Sentence Compression. Workshop on Textual Entailment (ACL-PASCAL) (2007)
3. Corder, G.W., Foreman, D.I.: Nonparametric Statistics for Non-Statisticians: A Step-by-Step Approach. Wiley, New Jersey (2009)
4. Fernandes, D.A.B., Neto, M., Soares, L.F.B., Freire, M.M., Inácio, P.R.M.: A tool for estimating the hurst parameter and for generating self-similar sequences. In: Proceedings of the 46th Summer Computer Simulation Conference 2014 (SCSC 2014), Monterey, CA, USA (2014)
5. Hurst, H.: Long-Term Storage Capacity of Reservoirs. *Transactions of the American Society of Civil Engineers* **116**, 770–799 (1951)
6. Koizumi, R.: Relationships Between Text Length and Lexical Diversity Measures: Can We Use Short Texts of Less than 100 Tokens? *Vocabulary Learning and Instruction* **1**(1), 60–69 (2012)
7. Malvern, D., Richards, B., Chipere, N., Durán, P.: Lexical diversity and language development: Quantification and assessment. Houndsill, NH (2004)
8. McCarthy, P., Jarvis, S.: A theoretical and empirical evaluation of vocd. *Language Testing* **24**, 459–488 (2007)

9. McCarthy, P., Jarvis, S.: MTLD, vodc-D, and HD-D: A validation study of sophisticated approaches to lexical diversity assessment. *Behavior Research Methods* **42**(2), 381–392 (2010)
10. Olsson, J., Luchjenbroers, J: Forensic linguistics. A&C Black (2013)
11. Schler, J., Koppel, M., Argamon, S., Pennebaker, J.W.: Effects of Age and Gender on Blogging. AAAI Spring Symposium: Computational Approaches to Analyzing Weblogs **6**, 199–205 (2006)
12. Stamatatos, E.: A survey of modern authorship attribution methods. *Journal of the American Society for Information Science and Tech.* **60**(3), 538–556 (2009)

# How Does Irony Affect Sentiment Analysis Tools?

Leila Weitzel<sup>1(✉)</sup>, Raul A. Freire<sup>2</sup>, Paulo Quaresma<sup>3</sup>, Teresa Gonçalves<sup>3</sup>,  
and Ronaldo Prati<sup>2</sup>

<sup>1</sup> Universidade Federal Fluminense, Niterói, RJ, Brazil  
[leila.weitzel@gmail.com](mailto:leila.weitzel@gmail.com)

<sup>2</sup> Universidade Federal Do ABC, Santo André, SP, Brazil  
[{f.raul,ronaldo.prati}@ufabc.edu.br](mailto:{f.raul,ronaldo.prati}@ufabc.edu.br)

<sup>3</sup> Universidade de Évora, Évora, Portugal  
[{pq,tcg}@uevora.pt](mailto:{pq,tcg}@uevora.pt)

**Abstract.** Sentiment analysis applications have spread to many domains: from consumer products, healthcare and financial services to political elections and social events. A common task in opinion mining is to classify an opinionated document into a positive or negative opinion. In this paper, a study of different methodologies is conducted to rank polarity as to better know how the ironic messages affect sentiment analysis tools. The study provides an initial understanding of how irony affects the polarity detection. From the statistic point of view, we realize that there are no significant differences between methodologies. To better understand the phenomenon, it is essential to apply different methods, such as SentiWordNet, based on Lexicon. In this sense, as future work, we aim to explore the use of Lexicon based tools, thus measuring and comparing the attained results.

**Keywords:** Social media · Irony · Sarcasm · Opinion mining · Polarity detection

## 1 Introduction and Motivation

Sentiment analysis and opinion mining are very growing topics of interest over the last few years due to the large number of texts produced through Web 2.0. A common task in opinion mining is to classify an opinionated document as a positive or a negative opinion. A comprehensive review of both sentiment analysis and opinion mining as a research field for Natural Language Processing (NLP) is presented in Pang and Lee [1]. The demand for applications and tools to accomplish sentiment classification tasks has attracted the researchers' attention in this area. Hence, sentiment analysis applications have spread to many domains: from consumer products, healthcare and financial services to political elections and social events. Sentiment classification is commonly categorized in two basic approaches: machine learning and lexicon-based. Machine learning approach uses a set of features, usually some function of the vocabulary frequency, which are learned from annotated corpora or labelled examples. The lexicon-based approach uses lexicon to provide the polarity, or semantic orientation, for each word or phrase in the text. Despite the considerable amount of research,

the classification of polarity is still a challenging task; mostly because it involves a deep understanding of explicit and implicit information conveyed by language structures. Henceforth, irony or sarcasm has become an important topical issue in NLP. Irony writing is common in opinionated user generated content such as blog posts and product reviews. As a whole, irony is an activity of saying or writing in such a way that the textual meaning of what is said is the opposite of what is meant. According to Rioff et al. [2] ironic message typically conveys a negative opinion using only positive words. In this paper, we present a study of different methodologies to classify polarity to better know how the ironic messages affect tools of sentiment analysis.

The classifications were carried out by Machine Learning Algorithms (mainly Support Vector Machine – SVM and Naïve Bayes Classifier). We aim to find out how irony affects the sentiment classification. Therefore, our research main question is: What is the best methodology able to boost performance classification?

The outline of this paper is as follows: In section 2, we present the related works. Section 3 explores the background in which this research is established. Section 4 presents our methodology, and Section 5 and 6 provides our results and main conclusions.

## 2 Related Work

In [3] the authors presented a semi-supervised approach for identification of sarcasm on two different data sets a collection of 5.9 million tweets collected from Twitter, and a collection of 66000 product reviews from Amazon. Using the Mechanical Turk, they created a gold standard sample in which each sentence was tagged by 3 annotators, obtaining F-scores of 0.78 on the product reviews dataset and 0.83 on the Twitter dataset. Tayal et al [4] proposed two algorithms, one to identify a sarcastic tweet and other to perform polarity detection on political sarcastic tweets. The main goal is to analyze and predict who will win the 2014 Indian Central Government Election based on sarcastic tweets. They came to the conclusion that using a supervised approach and their proposed algorithm, they will be able to achieve their goal. They found out that sarcastic tweets can predict election results in an efficient level.

## 3 Background

The Web 2.0 is the ultimate manifestation of User-Generated Content (UGC) systems. The UGC can be virtually about anything including politics, products, people, events, etc. One of highlights is the Twitter. Twitter constitutes a very open social network space, whose lack of barriers to access, e.g., even non-registered users are able to use Twitter to track breaking news on their chosen topics, from “World Economic Crisis” to “European Football Championship”, for instance. Twitter social networkers communicate with each other by posting tweets allowing for a public interactive dialogue. On Twitter, users often post or update short messages referred to as tweets, describing one’s current status within a limit of 140 characters [5]. Beyond merely displaying news and reports, the Twitter itself is also a large platform where different opinions are presented

and exchanged. The interest that users (companies, politicians, celebrities) show in on-line opinions about products and services and the potential influence such opinions wield is something that vendors of these items are paying more and more attention to. Thus, it is important for correct identification of users opinions expressed in written text. In the general area of sentiment analysis, irony and sarcasm play a role as an interfering factor that can flip the polarity of a message. According to Macmillan English Dictionary (2007), irony is “a form of humor in which you use words to express the opposite of what the words really mean”. This mean that it is the activity of saying or writing the opposite of what you mean. Unlike a simple negation, an ironic message typically conveys a negative opinion using only positive words or even intensified positive words [2]. As humans, when we communicate with one another, we have access to a wide range of spoken and unspoken figures that help create the intended message and ensure that our audience will understand what we are saying. Some of these figures include body language, hand gestures, inflection, volume, and accent. Hence, the challenge for Natural Language Processing (NLP) is: how to recognize sarcasm and gauge the appropriate sentiment of any given statement.

## 4 Methodology

### 4.1 Data Description and Corpus Generation

This research focuses on document-level irony detection on English Twitter datasets. The text content of Twitter is usually ambiguous and rich of acronym slang and fashion word. And, apart from the plain text, a tweet can contain others elements such as hashtags which are tags assigned by the user to identify topic (e.g. #Obama) or sentiment (#angry, #sarcasm); hyperlinks (typically a bitly URL, i.e., a URL shortening service), emoticons (it is a pictorial representation of a facial expression), references to other users (@<user>), and etc. In our experiments, the tweets were extracted by means of a Java package developed in-house, used for streaming posts [6]. We gathered about ten thousand tweets. Sarcastic tweets were collected using previously selected hashtags {sarcasm, irony, lying, moresarcasm, notcool, notreally, notsarcasm, somuchsarcasm}. These hashtags were used as an indicator of ironic or sarcastic tweets. An example is < I just love all the support I get from my mom. #sarcasm > or like this <I love my highspeed internet connection #moresarcasm>. Our assumption is that the best judge of whether a tweet is intended to be sarcastic or not is the author of the tweet, expressed by his hashtags.

### 4.2 Preprocessing of Data

The semi-automatic cleaning of the corpus is done to address concerns about corpus noise. Firstly, we removed: Tweets starting with “RT” because they refer to a previous tweets, e.g., <RT@iFraseSincera: © #Sarcasm... http://t.co/MkFuO4JKa >; posts that contain only user name and link e.g. <@ZarethPanther @Ambybutt. #sarcasm http://t.co/zw2ieHVUGN>; Tweets that have less than 3 words e.g. <Price is low. #sarcasm>; tweets that are meaningless, e.g. <@smackalalala yeah, oooooo yeap

#Sarcasm>. We also removed special characters (\$, %, &, #, etc.); punctuation marks (full stops, commas etc); all hashtags words and emoticons (smiley). We applied automatic filtering to remove duplicates tweets, and tweets that are written in other idioms. Afterwards, we manually classify the ironic posts in order to ensure that all messages are truly ironic or sarcastic. We gathered about 10000 tweet, after the pre-processing step, the sample size was about 7628 tweets, where 3288 are positive, 3600 are sarcastic and 740 are neutral.

### 4.3 Set of Experiments

As aforesaid, we used two different approaches in our experiment. The first method was **SUPPORT VECTOR MACHINE CLASSIFIER (SVM)** with: wrapper class called Library for Support Vector Machines (LIBSVM with default kernel RBF, i.e., Gaussian kernel) [7]; and the second classifier was **NAIVE BAYES MULTINOMIAL (NBM)** which is a learning algorithm that is frequently employed to tackle text classification problems. Our motivation to test multiple classifiers also stemmed from related work, which mostly test more than one classifier. We use the Weka [8] (Waikato Environment for Knowledge Analysis) where, each document (row or a tweet) is called as instance and each feature (term) is called as attribute. The SVM classifier requires that each data instance be represented as a vector of real numbers. Thus in order to set a vectorial input data, we use an unsupervised Weka build-in function called StringToWordVector (that converts string attributes into a set of attributes representing word occurrence), with the following parameters: IDF and TF transform (to show how important a word is to a document in a collection or corpus). All tokens were converted to lowercase before being added to the dictionary. The minimum frequency of each term was restricted to five due to tweet size (up to 140 characters). We also removed stopwords and no stemmer algorithm was used. The classification is based on unigrams of words. Then, the resulting model has 7628 instance and 1502 attributes. All test modes are based on a stratified ten-fold cross-validation; this means that the data is randomly partitioned into 10 equal-sized parts. Thus, each attribute selection method is applied ten times on sub samples of the training set. This validation method reduces the variability of the classification. After finding the best parameters and build the final model, the adopted classifiers were applied on the test set. We also considered the metrics: (i) Precision (also called positive predictive value), (ii) Recall (also known as sensitivity) and (iii) F-measure as a main measure to evaluate the performance of classifier methodologies. All these metrics are generally accepted at Information Retrieval approaches as evaluation performance methods. It is, by far, the most widely performance metrics used in IR. Others measure were also considered, such as: True-positive (TP) and False-Positive (FP) rate (also known respectively as Sensitivity and Specificity measures), ROC area (The area under the ROC curve is a measure of how well a parameter can distinguish features), and Kappa statistic (The kappa coefficient measures pairwise agreement among a set of coders making category judgments).

## 5 Classification Results

The predictive performances of the models can be seen in Table 1. Table 2 shows the accuracy and the kappa coefficient. We have not obtained a reasonable model, which means we have not achieved a small number of misclassification errors (Relative Absolute Error is about 34%). The simple mean of ROC area is about 87%, which indicates a good performance of the models in terms of AUC. The Accuracy rates (equal to 79%) and Kappa (equal to 66%) point out that there is a moderate statistical dependence between the attributes and the classes. The best performance was achieved by **NBM** algorithm according to Precision (86%), F-measure (83%) and ROC curve Area (95%). However, the rates TP (84%) and Recall (84%) of the **SVM** were better than the **NBM**. On can see that there is a considerable number of TPs, but, nonetheless, there is not a small number of FPs (16% - incorrectly identified), mainly if we only consider the irony category.

**Table 1.** The main results.

Methods	TP Rate	FP Rate	Precision	Recall	F-Measure	ROC Area	Category
<b>SVM</b>	80%	13%	82%	80%	81%	83%	positive
	<b>84%</b>	<b>16%</b>	80%	<b>84%</b>	82%	84%	irony
	55%	6%	58%	55%	57%	74%	neutral
	78%	13%	78%	78%	78%	82%	weighted avg.
<b>NBM</b>	83%	15%	81%	83%	82%	93%	positive
	80%	10%	<b>86%</b>	80%	<b>83%</b>	<b>95%</b>	irony
	65%	7%	58%	65%	61%	90%	neutral
	79%	12%	80%	79%	80%	94%	weighted avg.
	82%	12%	82%	82%	82%	87%	weighted avg.

**Table 2.** Correct Classified Instances (Accuracy) and Kappa statistic.

	<b>SVM</b>	<b>NBM</b>
<b>Kappa</b>	64%	<b>66%</b>
<b>Accuracy</b>	78%	<b>79%</b>

## 6 Conclusions

Individuals post messages in the internet using e-mail, message boards and websites like Facebook and Twitter. These forms of contact are highly integrated in everyday life. With the proliferation of reviews, ratings, recommendations and other forms of online expression, online opinion has turned into a kind of virtual currency for

businesses willing to market their products, identify new opportunities and manage their reputations. Despite the considerable amount of research, the classification of polarity is still a challenging task; mostly since it involves a deep understanding of explicit and implicit information conveyed by language structures. Henceforth, irony or sarcasm has become an important topical issue in NLP, mostly because irony (or sarcasm) flips the polarity of the message. Hence, this paper investigated how irony affects tools of sentiment analysis. The classifications were conducted with Support Vector Machine and Naïve Bayes Classifier. The results and conclusions of the experiments raise remarks and new questions. A first remark to be made is that all experiments are performed with English texts. Consequently, the result cannot directly be generalized to other languages. We believe that the results in other languages are different are likely, for instance, to have more structured languages such as Brazilian Portuguese. Another interesting observation is whether very similar results are obtained when the experiments are carried out on data from a different method. From statistic point of view, there are no relevant differences between methodologies, for example, the total accuracy ranges between 78 and 79% and kappa from 64 to 66%, in spite of the inherently ambiguous nature of irony (or sarcasm) that makes hard to be analyzed, not just automatically but often for humans. Our work indicate that the NBM and SVM were reasonably able to detect irony in twitter messages. Bearing in mind that our research deals with only one type of irony that is common in tweets. The study provides us an initial understanding of the how irony affects the polarity detection. To better understand the phenomenon, it is essential to apply different methods, such as polarity given by SentiWordNet, based on Lexicon. In this sense, for future work, we aim to explore the use Lexicon-based tools and thus measure and compare the obtained results.

## References

1. Pang, B., Lee, L.: Opinion Mining and Sentiment Analysis. *Found. Trends Inf. Retr.* **2**, 1–135 (2008)
2. Platt, J.C.: Fast training of support vector machines using sequential minimal optimization. In: *Advances in Kernel Methods*, pp. 185–208. MIT Press (1999)
3. Weitzel, L., Aguiar, R.F., Rodriguez, W.F.G., Heringer, M.G.: How do medical authorities express their sentiment in twitter messages? In: *2014 9th Iberian Conference on Information Systems and Technologies (CISTI)*, pp. 1–6 (2014)
4. Miller, G.A.: WordNet: a lexical database for English. *Commun. ACM* **38**, 39–41 (1995)
5. Weitzel, L., Quaresma, P., Oliveira, J.P.M.D.: Measuring node importance on twitter microblogging. In: *Proceedings of the 2nd International Conference on Web Intelligence, Mining and Semantics*, pp. 1–7. ACM, Craiova (2012)
6. Chang, C.-C., Lin, C.-J.: LIBSVM: A library for support vector machines. *ACM Trans. Intell. Syst. Technol.* **2**, 1–27 (2011)
7. Hall, M., Frank, E., Holmes, G., Pfahringer, B., Reutemann, P., Witten, I.H.: The WEKA data mining software: an update. *SIGKDD Explor. Newsl.* **11**, 10–18 (2009)

# Author Index

- Abdelwahab, Omar 238  
Abelha, António 116, 122  
Abreu, Mónica 789  
Adamatti, Diana Francisca 673  
Aires, José 723  
Al-Rifaie, Mohammad Majid 201  
Alkabani, Yousra 493  
Almeida, Ana 27  
Alvelos, Filipe 143  
Alves, Ana 759  
Amaral, Filipe 433  
Analide, Cesar 33  
Andres, Emmanuel 110  
Anselma, Luca 79  
Antunes, Francisco 181  
Antunes, Luís 687  
Araujo, Rodrigo L. 262  
Artikis, Alexander 128  
Baccan, Davi 402  
Bacci, Davide 54  
Badr-El-Den, Mohamed 298  
Baía, Luís 560  
Bamidis, Panagiotis D. 128  
Barata, Carlos 789  
Barbosa, Helio J.C. 262  
Barbosa, Vítor 143  
Bedour, Hassan 493  
Belo, Orlando 597  
Benmimoune, Lamine 110  
Bento, Carlos 181  
Bernardino, Heder S. 262  
Bhatia, Ajay 67  
Billis, Antonis S. 128  
Blackwell, Tim 201  
Bodnarova, Agata 313  
Boissier, Olivier 624  
Bonisoli, Andrea 103  
Boughaci, Dalila 298  
Branco, Paula 513  
Bryson, Joanna J. 292  
Bydžovská, Hana 425  
Campos, Pedro 702  
Cano, Alberto 305  
Cardoso, Amílcar 664  
Carneiro, Davide 15  
Carneiro, João 3  
Cascalho, José 696  
Casteleiro, João 747  
Castelli, Mauro 213  
Cavadas, Bruno 513  
Cavique, Luís 584  
Chessa, Stefano 54  
Christensen, Anders Lyhne 189  
Cimler, Richard 313  
Cordeiro, João 796  
Correia, Luís 189, 250  
Correia, Marco 41, 376, 480  
Correia, Sara 340  
Cortez, Paulo 535  
Costa, Ernesto 226  
Costa, Paulo 487  
Costa, Pedro Maurício 169  
Costa, Vera 169  
Couto, Francisco M. 789  
Couto, Marco 783  
Cruz, Jorge 41, 376, 480  
Cruz, Lúcia P. 353  
Cruz-Correia, Ricardo 91  
Cunha, Bernardo 457  
da Silva, Joaquim Ferreira 747  
da Silva Soares, Anderson 274  
Damásio, Carlos Viegas 363  
de Amorim Junior, João 658  
de Brito, Maiquel 624  
De Felice, Matteo 213  
de Lima, Vera Lucia Strube 735  
de Paula, Lauro Cássio Martins 274  
Dias, Cláudia Camila 91  
Dias, Ricardo 433  
Dias, Teresa Galvão 169  
Dimuro, Graçaliz P. 673  
Dolezal, Rafael 313  
Faria, Ana Raquel 27  
Faria, Brígida Mónica 445  
Fernandes, Diogo A.B. 796

- Fernandes, Kelwin 535  
 Fernandes, Renato 702  
 Ferreira, Luís Miguel 445  
 Ferro, Erina 54  
 Ferrugento, Adriana 759  
 Figueiredo, Lino 27  
 Fonseca, Carlos M. 280  
 Fontes, Tânia 169  
 Fortunati, Luigi 54  
 Franco, Andrea 41  
 Freire, Raul A. 803  
 Fuad Muhammad 603
- Gaio, A. Rita 702  
 Gallicchio, Claudio 54  
 Gama, João 501  
 Gamallo, Pablo 711  
 Garcia, Marcos 711  
 Gatta, Roberto 103  
 Gaudl, Swen E. 292  
 Gerevini, Alfonso E. 103  
 Géryk, Jan 578  
 Ghodous, Parisa 110  
 Gomes, Luís 723  
 Gomes, Paulo 771  
 Gomes, Rui 181  
 Gonçalves, Ivo 280  
 Gonçalves, Ramiro 27  
 Gonçalves, Ricardo 611  
 Gonçalves, Teresa 803  
 Guerreiro, Tiago 789
- Hajjam, Amir 110  
 Hajjam, Mohamed 110  
 Hammad, Sherif 493  
 Hanke, Sten 54  
 Henriques, Rui 326  
 Hübner, Jomi F. 624  
 Husakova, Martina 313
- Ibarguren, Igor 572  
 Inácio, Pedro R.M. 796  
 Ivanov, Vadim 388
- Javaheri Javid, Mohammad Ali 201
- Katzouris, Nikos 128  
 Kavitha, K.M. 723  
 Kitchin, Diane 103
- Knobbe, Arno 525  
 Knorr, Matthias 388, 611  
 Korabecny, Jan 313  
 Kreiner, Karl 54  
 Krejcar, Ondrej 313  
 Krenek, Jiri 313  
 Kropf, Johannes 54  
 Kuca, Kamil 313  
 Kumar, Suman 67
- Lau, Nuno 433, 445, 457  
 Leite, João 388, 611  
 Lemes, Cristiano Inácio 91  
 Lenca, Philippe 547  
 Leon, Miguel 286  
 Lopes, Gabriel Pereira 747  
 Lopes, José Gabriel P. 723  
 Lourenço, Nuno 226  
 Lowrance, Christopher J. 238
- Mabunda, Pinto 696  
 Macedo, Luis 402  
 Machado, José 116, 122  
 Machado, Penousal 664  
 Madeira, Sara C. 326  
 Magessi, Nuno Trindade 687  
 Mago, Vijay Kumar 67  
 Manzoni, Luca 213  
 Marques, Nuno Cavalheiro 584  
 Marreiros, Goreti 3  
 Martinho, Diogo 3  
 Martins, Bruno 590  
 Martins, Constantino 27  
 Martins, Pedro 664  
 Marwan Muhammad 603  
 Mazzei, Alessandro 79  
 Mazzini, Nicola 103  
 McCluskey, Thomas Leo 134  
 Melo, Fernando 590  
 Meshcheryakova, Olga 480  
 Micheli, Alessio 54  
 Mills, Rob 250  
 Monteiro, Douglas 735  
 Moreira, António Paulo 445, 487  
 Moura, João 363  
 Muguerza, Javier 572
- Najman, Lukas 313  
 Neves, António J.R. 433  
 Neves, José 15  
 Novais, Paulo 3, 15

- Oliveira, Bruno 597  
 Oliveira, Hugo Gonçalo 759  
 Oliveira, Sérgio 122  
 Osborn, Joseph Carter 292
- Palumbo, Filippo 54  
 Parodi, Oberdan 54  
 Pedrosa, Eurico 457  
 Pereira, Artur 457  
 Pereira, Francisco B. 226  
 Pereira, Luís Moniz 414  
 Pereira, Sérgio 513  
 Pereira, Sónia 116  
 Pérez, Jesús María 572  
 Petry, Marcelo 445  
 Pimenta, André 15  
 Pinheiro, David 305  
 Pinto, Andry 487  
 Portela, Filipe 116, 122  
 Prati, Ronaldo 803
- Quaresma, Paulo 803
- Racakova, Veronika 313  
 Rebelo, Carla 525  
 Rebelo de Sá, Cláudio 525  
 Reis, Luís Paulo 445  
 Respício, Ana 143  
 Rezk, Nesma M. 493  
 Rezoug, Abdellah 298  
 Ribeiro, Rita P. 501  
 Rocha, Miguel 340  
 Rodrigues, Ana 664  
 Rodrigues, Filipe 759  
 Rodrigues, Pedro Pereira 91  
 Rodrigues, Ricardo 771  
 Rosado, José 469  
 Rossetti, Rosaldo J.F. 157  
 Rua, Fernando 122
- Santos, Manuel F. 116, 122  
 Santos, Vítor 469  
 Saptawijaya, Ari 414  
 Sbruzzi, Elton 402
- Silva, Álvaro 122  
 Silva, Ana M. 501  
 Silva, Fábio 33  
 Silva, Fernando 189  
 Silva, Filipe 469  
 Silva, João 433  
 Silva, Paulo 181  
 Silva, Sara 280  
 Silveira, Ricardo Azambuja 658  
 Soares, Carlos 525  
 Somarakis, Vassiliki 134  
 Soulas, Julie 547  
 Sousa, Pedro A.C. 376, 480
- Talha, Samy 110  
 Tavares, José Pedro 157  
 Teixeira, João F. 783  
 Teixeira, Jorge 789  
 Tiple, Pedro 584  
 Torgo, Luís 560  
 Torres, Pedro 789
- Valentini, Vincenzo 103  
 Vallati, Mauro 103, 134  
 Vanneschi, Leonardo 213  
 Ventura, Sebastián 305  
 Vieira, Susana M. 353  
 Vilarinho, Cristina 157  
 Vinagre, Pedro 535  
 Vinga, Susana 353  
 Von Laer, Andressa 673  
 Vozzi, Federico 54
- Weitzel, Leila 803  
 Woźna-Szcześniak, Bożena 651
- Xiong, Ning 286
- Yampolskiy, Roman V. 238
- Zanin, Massimiliano 376  
 Zbrzezny, Agnieszka M. 638, 651  
 Zbrzezny, Andrzej 638, 651  
 Zimmer, Robert 201